



सत्यमेव जयते

INDIAN AGRICULTURAL  
RESEARCH INSTITUTE, NEW DELHI.

28125/136  
ॐ

I. A. R. I. 6.

MGIPC—S1—6 AR/54—7-7-54—10,000.







THE  
LONDON, EDINBURGH, AND DUBLIN  
PHILOSOPHICAL MAGAZINE  
AND  
JOURNAL OF SCIENCE.

CONDUCTED BY

SIR OLIVER JOSEPH LODGE, D.Sc., LL.D., F.R.S.  
SIR JOSEPH JOHN THOMSON, O.M., M.A., Sc.D., LL.D., F.R.S.  
JOHN JOLY, M.A., D.Sc., F.R.S., F.G.S.  
RICHARD TAUNTON FRANCIS, F.R.S.E.

AND

WILLIAM FRANCIS, F.L.S.

---

"Nec araneorum sane textus ideo melior quia ex se fila gignunt, nec noster vilior quia ex alienis libamus ut apes." JUST. LIPS. *Polit. lib. i. cap. l. Not.*

---

VOL. X.—SEVENTH SERIES.

JULY—DECEMBER 1930.

---

28125/136  
LONDON:

TAYLOR AND FRANCIS, RED LION COURT, FLEET STREET.

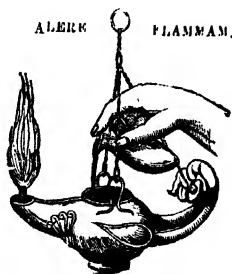
SOLD BY SMITH AND SON, GLASGOW;—HODGES, FIGGIS, AND CO., DUBLIN;—  
AND VEUVÉ J. BOYVHAU, PARIS.

“Meditationis est perscrutari occulta; contemplationis est admirari perspicua . . . . Admiratio generat quæstionem, quæstio investigationem, inuestigatio inventionem.”—*Hugo de S. Victore.*

---

—“Cur spirent venti, cur terra dehiscat,  
 Cur mare turgescat, pelago cur tantus amaror,  
 Cur caput obscura Phœbus ferrugine condant,  
 Quid toties diros cogat flagrare cometas,  
 Quid pariat nubes, veniant cur fulmina cœlo.  
 Quo micet igne Iris, superos quis conciat orbes  
 Tant vario motu.”

*J. B. Pinelli ad Mazonium.*



# CONTENTS OF VOL. X.

## (SEVENTH SERIES).

### NUMBER LXII.—JULY 1930.

	Page
Mr. D. Burnett on the Reflexion of Long Electromagnetic Waves from the Upper Atmosphere.....	1
Dr. E. J. Irons on the Fingering of Wind Instruments .....	16
Dr. E. C. Stoner on the Magnetic and Magneto-thermal Properties of Ferromagnetics .....	27
Mr. R. Walsh on the Inductive Ratio Arms in Alternating Current Bridge Circuits .....	49
Prof. H. R. Robinson and Mr. C. L. Young on the Influence of Chemical State on X-Ray Absorption Frequencies .....	71
Mr. F. J. Garrick on Studies in Coordination.—Part I. Ion Hydrates. A Correction .....	76
Mr. F. J. Garrick on Studies in Coordination.—Part II. Ion Ammoniates .....	77
Dr. J. Dougall on Newton's Law of Gravitation in an Infinite Euclidean Space .....	81
Prof. S. S. Bhatnagar and Messrs. R. N. Mathur and R. S. Mal on Magnetism and Molecular Structure.—Part I. The Magnetic Susceptibilities of some Liquid Organic Isomers .....	101
Mr. C. E. Wright: Note on the Potential and Attraction of Rectangular Bodies .....	110
Mr. E. Thomas and Prof. E. J. Evans on the Isotope Effect in Neon Lines .....	128
Mr. E. W. B. Gill on the Distribution of Electric Forces in Spaces traversed by Electrons .....	134
Mr. C. O. Pringle on some Observations on Movements of Particles in Kundt's Tube. (Plate I.).....	139
Prof. V. A. Bailey and Mr. W. E. Duncanson on the Behaviour of Electrons amongst the Molecules $\text{NH}_3$ , $\text{H}_2\text{O}$ , and $\text{HCl}$ .....	145
Dr. S. C. Bradford: Contribution to the Kinetic Theory of Vaporization.—III. The Vapour Pressure of Solutions .....	160
Dr. L. G. H. Huxley on the Corona Discharge in Nitrogen .....	185
Drs. F. W. Gray and J. Farquharson on Diamagnetism and Submolecular Structure .....	191

### NUMBER LXIII.—AUGUST.

Dr. W. Hume-Rothery on the Lattice Constants of the Elements..	217
Dr. R. D. Rusk on the Glow Discharge in Hydrogen .....	244
Messrs. L. G. Carpenter and L. G. Stoodley on the Specific Heat of Mercury in the Neighbourhood of the Melting-Point .....	249
Mr. N. N. Pal on the Dielectric Polarization of Liquid Mixtures and Association.—Part I. ....	265
Dr. J. Thomson on the Mechanism of the Electrodeless Discharge..	280
Mr. E. H. Synge on a Modification of Michelson's Beam Interferometer .....	291

	Page
Messrs. A. C. Law and G. Mutch on the Absorption in Hydrogen Gas of Hydrogen Positive Rays .....	297
Mr. Mata Prasad on an X-Ray Investigation of the Crystals of Azobenzene .....	306
Mr. L. Page on Three-Dimensional Periodic Orbits in the Field of a Non-Neutral Dipole .....	314
Mr. R. S. Bradley on Polymolecular Films .....	323
Mr. A. L. Hodges on an Automatic Recording Waterproof Tester..	327
Prof. J. A. Crowther and Mr. L. H. H. Orton on the Absorption of X-Rays in Gases and Vapours.—Part I. Gases.....	329
Mr. A. E. Knowler on the Measurement of the Sound Transmission of a Partition .....	342
Prof. S. Chapman on the Annual Variation of Upper Atmospheric Ozone .....	345
Mr. E. H. Syngé on a Design for a very large Telescope.....	353
Notices respecting New Books:—	
Mr. R. F. Deimel's Mechanics of the Gyroscope .....	360
Sir J. Jeans's The Universe around Us .....	361
Mr. A. S. C. Lawrence's Soap Films .....	361
Mr. L. A. Coles's An Introduction to Modern Organic Chemistry.	362
Mr. A. B. Coble's Algebraic Geometry and Theta Functions ..	363
Dr. R. Crookall's Coal Measure Plants .....	363
Drs. P. Haas and T. G. Hill's An Introduction to the Chemistry of Plant Products. Vol. II. Metabolic Processes .....	364
Dr. J. W. Smith's The Effects of Moisture on Chemical and Physical Changes .....	364
Monsieur P. J. Richard's La Gamme—Introduction à l'étude de la musique .....	365
Sir Oliver Lodge's Beyond Physics .....	366
Proceedings of the Geological Society:—	
Mr. F. A. Bannister exhibited lantern-slides to demonstrate the Identification of Minerals in Thin Sections of Rocks by X-Ray Methods .....	368

#### NUMBER LXIV.—SEPTEMBER.

Prof. S. Chapman on Ozone and Atomic Oxygen in the Upper Atmosphere.....	369
Prof. L. D. Mahajan on the Effect of the Surrounding Medium on the Life of Floating Drops .....	383
Dr. L. Simons on the Space Distribution of X-Ray Photoelectrons from a Solid Film .....	387
Mr. J. C. Jacobsen on the Capture of Electrons by Swift $\alpha$ -particles.	401
Mr. J. C. Jacobsen: Note on Photographic Counting of $\alpha$ -particles.	413
Dr. R. A. Houstoun on the Visibility of Radiation and Dark Adaptation .....	416
Dr. R. A. Houstoun and Mr. J. F. Shearer on Weber's Law and Visual Acuity .....	433
Prof. A. C. Banerji on some Problems of Nuclear Physics treated according to Wave-Mechanics .....	450
Mr. A. F. Dufton on the Reduction of Observations .....	465
Messrs. D. Solomon and W. Morris-Jones on an X-Ray Investigation of the Lead-Antimony Alloys .....	470
Mr. J. H. Bruce on the Corona Discharge in Hydrogen .....	476
Mr. F. H. Schofield on the Heat-loss from a Plate embedded in an Insulating Wall .....	480

	Page
Prof. J. C. McLennan and Messrs. J. F. Allen and J. O. Wilhelm on Electrical Conductivity Measurements at Low Temperatures..	500
Mr. H. E. Hurst on Reducing Observations by the Method of Minimum Deviations .....	511
Miss E. A. Nelson on the Effect of Stratification on the Gravity Gradient and the Curvature of the Level Surface.....	513
Notices respecting New Books:—	
Dr. Fisher's Statistical Methods for Research Workers .....	517
Dr. E. G. Richardson's The Acoustics of Orchestral Instru- ments and of the Organ .....	517
Monsieur L. de Broglie's Ondes et Corpuscules.....	518
Monsieur L. de Broglie's Mécanique Ondulatoire .....	518
Monsieur L. de Broglie's Wave Mechanics .....	518
Dr. B. L. Worsnop's X-rays .....	519
Mr. R. W. James's X-ray Crystallography .....	519
Mr. J. Buckingham's Matter and Radiation, with particular reference to the Detection and Uses of the Infra-Red Rays..	519
Prof. E. N. da C. Andrade's The Mechanism of Nature: Being a simple approach to Modern Views on the Structure of Matter and Radiation .....	520

## NUMBER LXV.—OCTOBER.

Dr. W. de Groot: Some Remarks on the Analogy of certain Cases of Propagation of Electromagnetic Waves and the Motion of a Particle in a Potential Field .....	521
Mr. G. A. Tomlinson on Further Experiments on the Cohesion of Quartz Fibres .....	541
Mr. E. Ower on a Micromanometer of High Sensitivity .....	544
Dr. W. F. Ehret and Mr. R. D. Fine on the Crystal Structure in the System Copper-Bismuth. (Plate II.) .....	551
Mr. F. K. V. Koch on the Interaction of Molecules with the Silver Ion .....	559
Mr. J. B. Coleman on a Theorem in Determinants .....	564
Mr. A. F. Dufton on Graphic Statistics: Per mille Paper .....	566
Mr. W. J. Davies and Prof. W. J. Evans on the Electrical Con- ductivities of Dilute Sodium Amalgams at various Temperatures.	569
Mr. M. Söderman on some Precision Measurements in the Soft X-ray Region. (Plates III. & IV.).....	600
Mr. A. E. Bate on (i.) The End-corrections of an Open Organ Flue- pipe; and (ii.) the Acoustical Conductance of Orifices.....	617
Mr. F. L. Uffelman on the Expansion of Metals at High Temper- atures .....	633
Mr. W. A. Wood on the X-Ray Study of some Tungsten Magnet Steel Residues. (Plate V.) .....	659
Messrs. J. A. Ratcliffe and F. W. G. White on the Electrical Pro- perties of the Soil at Radio Frequencies.....	667
Dr. J. R. Ashworth on the Relations of the Magnetic and Thermal Constants of Ferromagnetic Substances ..	681
Mr. H. V. Lowry: A Note on Approximation Curves for a Fourier Series .....	695
Mr. E. Howells on the Statistical Theory of Para- and Diamag- netism .....	698
Dr. F. C. Chalklin on some Series in the Extreme Ultra-Violet Spark Spectra of Copper .....	711
Dr. W. G. Shilling and Mr. A. E. Laxton on the Effect of Temper- ature on the Viscosity of Air.....	721

## P L A T E S.

- I. Illustrative of Mr. C. O. Pringle's Paper on Some Observations on Movements of Particles in Kundt's Tube.
  - II. Illustrative of Dr. W. F. Ehret and Mr. R. D. Fine's Paper on the Crystal Structure in the System Copper-Bismuth.
  - III. & IV. Illustrative of Mr. M. Söderman's Paper on some Precision Movements in the Soft X-Ray Region.
  - V. Illustrative of Mr. W. A. Wood's Paper on an X-Ray Study of some Tungsten Magnet Steel Residues.
  - VI. & VII. Illustrative of Dr. D. H. Black and Mr. R. H. Nisbet's Paper on the Conduction of Electricity in Liquid Dielectrics
  - VIII.-X. Illustrative of Mr. J. Thewlis's Paper on the Orientation of Rolled Aluminium.
  - XI. Illustrative of Mr. J. S. Forrest's Paper on the Glow Discharge at the Active Electrode of an Electrolytic Rectifier.
  - XII. Illustrative of Mr. R. H. Sloane's Paper on the Fracture of Discharge-Tubes.
-

THE  
LONDON, EDINBURGH, AND DUBLIN  
PHILOSOPHICAL MAGAZINE  
AND  
JOURNAL OF SCIENCE.

---

[SEVENTH SERIES.]

---

JULY 1930.

---

- I. *The Reflexion of Long Electromagnetic Waves from the Upper Atmosphere.* By D. BURNETT, M.A., B.Sc., B.A.,  
*Carnegie Teaching Fellow in the University of Aberdeen* \*.

THE problem of the reflexion of electromagnetic waves from the upper atmosphere has been considered mathematically by Macdonald† in an idealized form, viz., when the earth is a perfectly conducting sphere surrounded by an atmosphere made up of two parts, each homogeneous in itself, separated by a spherical surface concentric with the earth. His solution is satisfactory for short and medium wave-lengths, but not for the very long waves now employed, as the approximations which he makes are not valid in this case unless in the immediate neighbourhood of the transmitter; whereas modern ideas of the constitution of the upper atmosphere suggest that Macdonald's idealized atmosphere will most closely represent the effect of the actual atmosphere in the case of very long waves, so that it is of some importance to get a solution for this case.

The various correcting factors required in Macdonald's result can be found by considering the second approximations, and these might be useful for getting more accurate results for moderate wave-lengths; but it has been found that only a slightly greater range of validity is obtained for very long

\* Communicated by the Author.

† Proc Roy. Soc. A, cviii. p. 52 (1925).



## P L A T E S.

- I. Illustrative of Mr. C. O. Pringle's Paper on Some Observations on Movements of Particles in Kundt's Tube.
  - II. Illustrative of Dr. W. F. Ehret and Mr. R. D. Fine's Paper on the Crystal Structure in the System Copper-Bismuth.
  - III. & IV. Illustrative of Mr. M. Söderman's Paper on some Precision Movements in the Soft X-Ray Region.
  - V. Illustrative of Mr. W. A. Wood's Paper on an X-Ray Study of some Tungsten Magnet Steel Residues.
  - VI. & VII. Illustrative of Dr. D. H. Black and Mr. R. H. Nisbet's Paper on the Conduction of Electricity in Liquid Dielectrics
  - VIII.-X. Illustrative of Mr. J. Thewlis's Paper on the Orientation of Rolled Aluminium.
  - XI. Illustrative of Mr. J. S. Forrest's Paper on the Glow Discharge at the Active Electrode of an Electrolytic Rectifier.
  - XII. Illustrative of Mr. R. H. Sloane's Paper on the Fracture of Discharge-Tubes.
-

THE  
LONDON, EDINBURGH, AND DUBLIN  
PHILOSOPHICAL MAGAZINE  
AND  
JOURNAL OF SCIENCE.

---

[SEVENTH SERIES.]

---

JULY 1930.

---

- I. *The Reflexion of Long Electromagnetic Waves from the Upper Atmosphere.* By D. BURNETT, M.A., B.Sc., B.A.,  
*Carnegie Teaching Fellow in the University of Aberdeen* \*.

THE problem of the reflexion of electromagnetic waves from the upper atmosphere has been considered mathematically by Macdonald† in an idealized form, viz., when the earth is a perfectly conducting sphere surrounded by an atmosphere made up of two parts, each homogeneous in itself, separated by a spherical surface concentric with the earth. His solution is satisfactory for short and medium wave-lengths, but not for the very long waves now employed, as the approximations which he makes are not valid in this case unless in the immediate neighbourhood of the transmitter; whereas modern ideas of the constitution of the upper atmosphere suggest that Macdonald's idealized atmosphere will most closely represent the effect of the actual atmosphere in the case of very long waves, so that it is of some importance to get a solution for this case.

The various correcting factors required in Macdonald's result can be found by considering the second approximations, and these might be useful for getting more accurate results for moderate wave-lengths; but it has been found that only a slightly greater range of validity is obtained for very long

\* Communicated by the Author.

† Proc Roy. Soc. A, cviii. p. 52 (1925).

waves—for example, with a wave-length of 19 km., Macdonald's result for the first reflected wave is correct up to angular distances of  $5^\circ$  from the transmitter, and the inclusion of the correcting factors gives results up to about  $7^\circ$ . Beyond this point accurate values cannot be found, on account of the asymptotic character of some of the correcting factors; the magnitude of the error can be reduced to a certain minimum value and no further, and the method can be used only when this minimum value is sufficiently small.

Macdonald has also given, in the second part of the paper quoted\*, a method of dealing with the cases to which his first method is inapplicable, but it involves the calculation of a large number of integrals, and for very long waves the amount of arithmetic involved seems to be very great; moreover, a factor  $M_k$  is assumed constant, and certain other approximations are made which are probably not accurate for very long waves. The method given below, analogous to that used by Macdonald in his discussion of the diffracted wave†, obtains an *exact* result, and the amount of computation required to get numerical values is not excessive, unless near the transmitter—especially as most of the quantities which have to be calculated are functions of the wave-length and of the electric constants of the earth and atmosphere, but not of the distance from the transmitter, and once they are found the results for all distances can quickly be calculated. It has already been noticed that Macdonald's solution is valid near the transmitter, so that the two methods together give a complete solution, except possibly for a band of intermediate distances, and the width of this band can be reduced only by increasing considerably the arithmetic involved in the second method. No solution has yet been obtained suitable for calculating results at these intermediate distances.

It is assumed in the analysis that the earth is perfectly conducting; but the modification required to take account of finite conductivity can easily be made‡, and calculation has shown that this effect is small—much less than the possible error in present-day experimental work,—so that it can be neglected in the meantime.

The quantity tabulated is the amplitude of the magnetic force in the diffracted wave plus a wave reflected once from the upper atmosphere, expressed as a fraction of the

\* *Loc. cit.* p. 70.

† *Proc. Roy. Soc. A*, xc. p. 50 (1914).

‡ *Cf. H. M. Macdonald, Proc. Roy. Soc. A*, xcii. p. 493 (1916).

amplitude at the same point due to the same transmitter in free space. The diffracted wave is calculated from Macdonald's formula\*, with the addition of a correction noted by Watson †, which affects the phase of the result. Macdonald uses the approximation

$$P_n(\cos \theta) = J_0\{(2n+1) \sin \frac{1}{2}\theta\}, \quad (n \text{ large}),$$

which is valid only when  $n\theta^3$  is negligibly small. Laplace's approximation, however, viz.,

$$P_n(\cos \theta) = \sqrt{\frac{2}{\pi(n+\frac{1}{2}) \sin \theta}} \cos \left\{ (n+\frac{1}{2})\theta - \frac{\pi}{4} \right\},$$

is adequate, and the correction to Macdonald's result is easily made. The corrected value, with his notation, is

$$\begin{aligned} \frac{\bar{\psi}}{\psi_0} &= 4\pi^{1/2} \left( z_0^{1/3} \sin \frac{\theta}{2} \right)^{1/2} \left( \cos \frac{\theta}{2} \right)^{-3/2} e^{\pi i/12 + 2iz_0 \left( \sin \frac{\theta}{2} - \frac{\theta}{2} \right)} \\ &\times \sum (3x_k)^{-2/3} e^{-(3x_k)^{2/3} z_0^{1/3} \cdot \frac{1}{2}\theta \cdot e^{\pi i/6}}. \end{aligned}$$

### *The Reflected Waves.*

Macdonald's solution for a perfectly conducting spherical earth (radius  $r_0$ ) surrounded by an ideal atmosphere, as explained above, is in the form

$$\psi = \psi_{00} + \sum_{k=1}^{k=\infty} \psi_{0k},$$

where  $\psi = r_0 \sin \theta$  times the magnetic force on the surface at an angular distance  $\theta$  from the source ;

$\psi_{00}$  represents the direct (diffracted) wave ;

and  $\psi_{0k}$  represents a wave which has been reflected  $k$  times from the upper atmosphere.

The value found for  $\psi_{0k}$  is

$$\begin{aligned} ik^{-1} r_0^{-2} 3^{-1/3} z_0^{1/3} \pi^{1/2} \sum_{n=0}^{n=\infty} (2n+1)^{3/2} (\sin \theta)^{1/2} \\ \sin \left\{ (n+\frac{1}{2})\theta - \frac{\pi}{4} \right\} \left( \frac{w_1}{w_0} \right)^k \frac{w_0'^{k-1}}{w_0'^{k+1}} M_k^k, \end{aligned}$$

\* *Loc. cit.* (1914).

† *Proc. Roy. Soc. A*, xciv. p. 83 (1918).

and so, if  $|\zeta_{11}|$  and  $|\zeta_1|$  are not small,

$$\rho z_{11}^{-1/3} \zeta_{11}^{1/3} = z_1^{-1/3} \bar{\zeta}_1^{1/3}$$

approximately, in the neighbourhood of a root, from the asymptotic expansions of the Bessel functions. But in the lower half of the  $\nu$  plane  $\frac{\pi}{2} < \arg \zeta_{11}^{1/3} < \pi$  and  $-\frac{\pi}{2} < \arg \bar{\zeta}_1^{1/3} < 0$ , and the above relation cannot be satisfied. Since

$$\frac{K_{2/3}(\zeta e^{-\pi i})}{K_{1/3}(\zeta e^{-\pi i})} = 1 - \frac{1}{6\zeta} \dots$$

asymptotically, it can be inferred that there is no root in that part of the lower half plane for which  $6|\zeta_{11}|$  and  $6|\bar{\zeta}_1|$  are of order greater than unity. If  $|\zeta_{11}|$  is small,

$$\zeta_{11}^{1/3} \frac{K_{2/3}(\zeta_{11} e^{-\pi i})}{K_{1/3}(\zeta_{11} e^{-\pi i})} = \frac{(\frac{1}{2} e^{-\pi i})^{-2/3}}{(\frac{1}{2} e^{-\pi i})^{-1/3}} = 2^{1/3} e^{-\pi i/3},$$

approximately, while if  $|\bar{\zeta}_1|$  is small,

$$\bar{\zeta}_1^{1/3} \frac{K_{2/3}(\bar{\zeta}_1 e^{\pi i})}{K_{1/3}(\bar{\zeta}_1 e^{\pi i})} = 2^{1/3} e^{-\pi i/3}.$$

Hence, if there is a root near  $\zeta_{11}=0$ ,  $\arg \bar{\zeta}_1^{1/3} \frac{K_{2/3}(\bar{\zeta}_1 e^{\pi i})}{K_{1/3}(\bar{\zeta}_1 e^{\pi i})}$  must be approximately  $\frac{\pi}{3}$  at it, which is seen to be impossible in the lower half plane; and similarly there can be no root near  $\zeta_1=0$  in the lower half plane.

It follows that the integral is equal to  $2\pi i$  times the sum of the residues at the zeros of  $w_0$ , and these have already been calculated by Macdonald\*. To find the residues let

$$\frac{1}{\zeta_0^{4/3} K_{2/3}^2(\zeta_0 e^{-\pi i})} = \sum_{k=0}^{k=\infty} \left\{ \frac{A_k}{\nu - \nu_k} + \frac{B_k}{(\nu - \nu_k)^2} \right\},$$

where  $\nu = \nu_0, \nu_1 \dots$  are the zeros of  $\zeta_0^{2/3} K_{2/3}(\zeta_0 e^{-\pi i})$ ; then

$$B_k = \text{Lt.}_{\nu=\nu_k} \left\{ \zeta_0^{2/3} K_{2/3}(\zeta_0 e^{-\pi i}) \right\}^2 = \frac{z_0}{2\nu_k} \left\{ \frac{1}{\zeta_0^{2/3} K_{1/3}(\zeta_0 e^{-\pi i})} \right\}_{\nu=\nu_k}^2,$$

which, if  $\zeta = x e^{-\pi i/2}$ , becomes

$$\frac{z_0}{2\nu_k} \frac{e^{2\pi i/3}}{x_k^{4/3} K_{2/3}^2(x_k e^{-3\pi i/2})} = - \frac{z_0^{2/3}}{3^{2/3} x_k^2 K_{2/3}^2(x_k e^{-3\pi i/2})}.$$

\* *Loc. cit.* p. 54 (1914).

Also 
$$A_k = \text{Lt.}_{\nu=\nu_k} \frac{\partial}{\partial \nu} \frac{(\nu - \nu_k)^2}{\zeta_0^{4/3} K_{2/3}^2(\zeta_0 e^{-\pi i})},$$

which, after some simplification, reduces to

$$\frac{2z_0^{1/3}}{3^{4/3}} \frac{e^{\pi i/3}}{x_k^{8/3} K_{1/3}^2(x_k e^{-3\pi i/2})},$$

and so

$$B_k = -\frac{1}{2}(3x_k)^{2/3} z_0^{1/3} e^{-\pi i/3} A_k = -\nu_k A_k.$$

Hence

$$\begin{aligned} \psi_{01} &= -3^{-1/3} z_0^{-1/6} (2\pi)^{1/2} \kappa (\sin \theta)^{1/2} e^{\pi i/4 - i z_0 \theta} \\ &\quad \int_{-\infty}^{\infty} d\nu \left(1 + \frac{\nu}{z_0}\right)^{3/2} \frac{e^{-i\nu \theta} \cdot M_1 \frac{w_1}{\bar{w}_1}}{\zeta_0^{4/3} K_{2/3}^2(\zeta_0 e^{-\pi i})} \\ &= -3^{-1/3} z_0^{-1/6} (2\pi)^{3/2} \kappa (\sin \theta)^{1/2} e^{3\pi i/4 - i z_0 \theta} \\ &\quad \sum_{k=0} A_k (f - \nu f')_{\nu=\nu_k}, \end{aligned}$$

where 
$$f = \left(1 + \frac{\nu}{z_0}\right)^{3/2} M_1 \frac{w_1}{\bar{w}_1} e^{-i\nu \theta}$$

and 
$$\frac{f'}{f} = \frac{3}{2z_0} \frac{1}{1 + \frac{\nu}{z_0}} + \frac{1}{M_1} \frac{\partial M_1}{\partial \nu} + \frac{\bar{w}_1}{w_1} \frac{\partial}{\partial \nu} \frac{w_1}{\bar{w}_1} - i\theta.$$

Therefore

$$\psi_{01} = 3^{-1/3} z_0^{-1/6} (2\pi)^{3/2} \kappa (\sin \theta)^{1/2} e^{-\pi i/4 - i z_0 \theta} \sum \nu_k A_k f_k(E_k + i\theta),$$

where

$$E_k = \frac{1}{\nu} - \frac{1}{M_1} \frac{\partial M_1}{\partial \nu} - \frac{\bar{w}_1}{w_1} \frac{\partial}{\partial \nu} \frac{w_1}{\bar{w}_1},$$

omitting the term

$$\frac{3}{2z_0} \frac{1}{1 + \frac{\nu}{z_0}},$$

which is much smaller than the others.  $E_k$  is independent of  $\theta$ . Also

$$\begin{aligned} A_k &= \frac{2}{3} \left(\frac{z_0}{3}\right)^{1/3} \frac{e^{\pi i/3}}{x_k^{8/3} K_{1/3}^2(x_k e^{-3\pi i/2})} \\ &= \frac{2}{3} \left(\frac{z_0}{3}\right)^{1/3} \frac{e^{\pi i/3}}{x_k^{8/3}} \left[ \frac{2 \sin \frac{\pi}{3}}{\pi \{I_{-1/3}(x_k e^{-3\pi i/2}) - I_{1/3}(x_k e^{-3\pi i/2})\}} \right]^2 \\ &= \frac{2}{\pi^2} \left(\frac{z_0}{3}\right)^{1/3} \frac{e^{\pi i/3}}{x_k^{8/3}} \frac{1}{\{J_{-1/3}(x_k) + J_{1/3}(x_k)\}^2}, \end{aligned}$$

using the definitions of the K and I functions\*. Hence, if the Hankel function

$$H_{1/3}(x) = H e^{ia},$$

so that

$$J_{1/3}(x) = H \cos \alpha, \quad J_{-1/3}(x) = H \cos \alpha + \frac{\pi}{3},$$

$$A_k = \frac{2}{3\pi^2} \left(\frac{z_0}{3}\right)^{1/3} \frac{e^{\pi i/3}}{x_k^{2/3}} \frac{1}{H_k^2 \cos^2 \alpha_k + \frac{\pi}{6}}$$

and 
$$\nu_k A_k = \left(\frac{z_0}{3}\right)^{2/3} \frac{1}{\pi^2 x_k^2} \frac{1}{H_k^2 \cos^2 \alpha_k + \frac{\pi}{6}},$$

so that

$$\begin{aligned} \psi_{01} &= 12 \cdot \pi^{-1/2} \kappa z_0^{1/2} e^{-\pi i/4 - iz_0 \theta} \left( \sin \frac{\theta}{2} \cos \frac{\theta}{2} \right)^{1/2} \\ &\quad \sum \frac{f_k}{(3x_k)^2 H_k^2 \cos^2 \alpha_k + 30} (E_k + i\theta) \\ &= 12 \pi^{-1/2} \kappa z_0^{1/2} e^{-3\pi i/4 - iz_0 \theta} \left( \sin \frac{\theta}{2} \cos \frac{\theta}{2} \right)^{1/2} \\ &\quad \sum C_k e^{2\zeta_1 - i\nu_k \theta} (E_k + i\theta) \end{aligned}$$

where

$$C_k = \left[ \frac{\left(1 + \frac{\nu}{z_0}\right)^{3/2} M_1}{(3x)^2 H^2 \cos^2 \alpha + 30} \cdot \frac{v_1}{w_1} e^{\pi i/2 - 2\zeta_1} \right]_{\nu=\nu_k}$$

is independent of  $\theta$ .

If 
$$\psi_0 = -i\kappa \cos^2 \frac{1}{2} \theta \cdot e^{-2iz_0 \sin \frac{1}{2} \theta}$$

is the value of  $\psi$  at the same point due to the same oscillator in free space,

$$\begin{aligned} \frac{\psi_{01}}{\psi_0} &= 12 \pi^{-1/2} \cdot z_0^{1/2} e^{-\pi i/4 - iz_0(\theta - 2 \sin \frac{1}{2} \theta)} \left( \sin \frac{\theta}{2} \right)^{1/2} \left( \cos \frac{\theta}{2} \right)^{-3/2} \\ &\quad \sum_{k=0} C_k e^{2\zeta_1 - i\nu_k \theta} (E_k + i\theta). \end{aligned}$$

*Calculation of  $C_k$  and  $E_k$ .*

The values of  $x_0, x_1, x_2, \dots$ , the zeros of  $K_{2/3}(x e^{-3\pi i/2})$ , are

$$\begin{aligned} x_0 &= 6.854, & x_1 &= 3.902, & x_2 &= 7.05, & x_3 &= 10.20, \\ x_4 &= 13.34, & x_5 &= 16.49, \dots \end{aligned}$$

\* Cf. Watson's 'Bessel Functions,' chap. iii.

The quantities  $H$  and  $\alpha$  are tabulated in Watson's 'Bessel Functions' for values of  $x$  up to 16; thereafter at a root  $x = x_k$ ,

$$H = \sqrt{\frac{2}{\pi x}} \quad \text{and} \quad \alpha = 150^\circ.$$

Also

$$2\nu_k = (3x_k)^{2/3} z_0^{1/3} e^{-\pi i/3}, \quad (3\xi_1)^{2/3} = 2z_1^{-1/3}(\nu - z_1 + z_0), \quad (1)$$

$$\frac{w_1}{\bar{w}_1} = \frac{K_{1/3}(\xi_1 e^{-\pi i})}{K_{1/3}(\bar{\xi}_1 e^{\pi i})} = \frac{\xi_1^{-1/2} e^{\pi i/2 + \zeta_1} \left\{ 1 + \frac{5}{72\xi_1} + \frac{5.77}{2.72^2 \xi_1^2} \dots \right\}}{\bar{\xi}_1^{-1/2} e^{-\pi i/2 + \bar{\zeta}_1} \left\{ 1 + \frac{5}{72\bar{\xi}_1} + \frac{5.77}{2.72^2 \bar{\xi}_1^2} \dots \right\}},$$

if  $|\xi_1|$  is not too small\*, and this, after simplification becomes

$$\frac{w_1}{\bar{w}_1} = e^{2\zeta_1 - \pi i/2} \left\{ 1 + \frac{5}{36\xi_1} + \frac{50}{72^2 \xi_1^2} \dots \right\}.$$

Further,

$$M_1 = - \frac{\rho \frac{w_{11}'}{w_{11}} - \frac{w_1'}{w_1}}{\rho \frac{w_{11}'}{w_{11}} - \frac{\bar{w}_1'}{\bar{w}_1}},$$

and the two quantities in the numerator are nearly equal, so that a fairly accurate determination of  $\frac{w_{11}'}{w_{11}}$  and  $\frac{w_1'}{w_1}$  is required. For the smallest values of  $k$  the asymptotic expansions of the Bessel functions are not sufficiently accurate, and the ascending series have to be used; but when  $k$  is greater than one the asymptotic series have been found to be adequate. If  $w$  is the same function of  $\zeta$  as  $w_1$  is of  $\xi_1$  and  $w_{11}$  of  $\xi_{11}$ , the asymptotic series is given by

$$\begin{aligned} -\frac{w'}{w} &= 3^{1/3} z^{-1/3} \xi^{1/3} \frac{K_{2/3}(\xi e^{-\pi i})}{K_{1/3}(\xi e^{-\pi i})} \\ &= \left(\frac{3\xi}{z}\right)^{1/3} \frac{1 - \frac{7}{72\xi} - \frac{7.65}{2.72^2 \xi^2} - \frac{7.65.209}{6.72^3 \xi^3} \dots}{1 + \frac{5}{72\xi} + \frac{5.77}{2.72^2 \xi^2} + \frac{5.77.221}{6.72^3 \xi^3} \dots} \\ &= \left(\frac{3\xi_1}{z_1}\right)^{1/3} \left\{ 1 - \frac{1}{6\xi} - \frac{5}{72\xi^2} - \frac{5}{72\xi^3} \dots \right\} \end{aligned}$$

on expanding.

\* For the asymptotic expansions employed see Watson's 'Bessel Functions,' chap. vii.



At the first two poles ( $k=0$  and  $k=1$ ),  $K_{2/3}(\xi e^{-\pi i})$  and  $K_{1/3}(\xi e^{-\pi i})$  must be expressed in terms of  $I_{\pm 2/3}(\xi e^{-\pi i})$  and  $I_{\pm 1/3}(\xi e^{-\pi i})$ , and hence as series of ascending powers of  $\xi$ . Hence

$$C_k = \left[ \frac{\left(1 + \frac{\nu}{z_0}\right)^{3/2} M_1}{(3x)^2 H^2 \cos^2 \alpha + 30^c} \frac{w_1}{w_1} e^{\pi i/2 - 2\xi_1} \right]_{\nu=\nu_k}$$

can be calculated without any great difficulty,  $\nu_k$  and  $\xi_1$  being determined by the above expressions (1).

In order to find  $E_k$  it is necessary to calculate  $\frac{1}{M_1} \frac{\partial M_1}{\partial \nu}$  and  $\frac{\bar{w}_1}{w_1} \frac{\partial}{\partial \nu} \frac{w_1}{\bar{w}_1}$ ; the former is the most laborious part of the whole calculation, as it depends on the difference of quantities which are nearly equal, and requires very great accuracy in the early stages of the arithmetic to ensure a small error in the result.

$\frac{\partial}{\partial \nu} \frac{w_1}{\bar{w}_1}$  is readily found from the asymptotic series already given for  $\frac{w_1}{\bar{w}_1}$ , viz.,

$$e^{2\xi_1 - \pi i/2} \left\{ 1 + \frac{5}{36\xi_1} + \frac{50}{72^2\xi_1^2} \dots \right\},$$

and so

$$\begin{aligned} \frac{\bar{w}_1}{w_1} \frac{\partial}{\partial \nu} \frac{w_1}{\bar{w}_1} &= \frac{\partial \xi_1}{\partial \nu} \left\{ 2 - \frac{5}{36\xi_1^2} \dots \right\} \\ &= 2 \left( \frac{3\xi_1}{z_1} \right)^{1/3} \left\{ 1 - \frac{5}{72\xi_1^2} \dots \right\}, \end{aligned}$$

since

$$(3\xi_1)^{2/3} = 2 \cdot z_1^{-1/3} \cdot (\nu - z_1 + z_0).$$

The term  $\frac{5}{72\xi_1^2}$  is negligible in the calculations below except at the first pole ( $k=0$ ), where it has a small effect.

To find  $\frac{1}{M_1} \frac{\partial M_1}{\partial \nu}$ , let

$$N = \rho \frac{w_{11}'}{w_{11}} - \frac{w_1'}{w_1} \quad \text{and} \quad D = \rho \frac{w_{11}'}{w_{11}} - \frac{\bar{w}_1'}{\bar{w}_1},$$

so that

$$M_1 = -\frac{N}{D} \quad \text{and} \quad \frac{1}{M_1} \frac{\partial M_1}{\partial \nu} = \frac{1}{N} \frac{\partial N}{\partial \nu} - \frac{1}{D} \frac{\partial D}{\partial \nu}.$$

Now if  $|\xi|$  is not too small,

$$\frac{w'}{w} = -\left(\frac{3\xi}{z}\right)^{1/3} \left\{ 1 - \frac{1}{6\xi} - \frac{5}{72\xi^2} - \frac{5}{72\xi^3} \dots \right\},$$

so that

$$\frac{\partial}{\partial \nu} \frac{w'}{w} = - \left( \frac{1}{3z^2 \zeta} \right)^{1/3} \left\{ 1 + \frac{1}{3\zeta} + \frac{25}{72\zeta^2} + \frac{5}{9\zeta^3} \dots \right\},$$

where, as usual with such series, the best approximation is obtained by stopping at the term next before the smallest.

In the example given below the values of  $\frac{1}{N} \frac{\partial N}{\partial \nu}$  and  $\frac{1}{D} \frac{\partial D}{\partial \nu}$  calculated from these asymptotic series are adequate, unless at the first two poles ( $k=0$  and  $k=1$ ); in these cases  $\frac{K_{2/3}(\zeta e^{-\pi i})}{K_{1/3}(\zeta e^{-\pi i})}$  must be calculated from the ascending series, and  $\frac{\partial}{\partial \nu} \frac{w'}{w}$  can then be deduced as follows.

$$\text{Since} \quad \frac{\partial}{\partial z} z^{2/3} K_{2/3}(z) = -z^{2/3} K_{1/3}(z),$$

$$\frac{\partial}{\partial \zeta} \zeta^{2/3} K_{2/3}(\zeta e^{-\pi i}) = \zeta^{2/3} K_{1/3}(\zeta e^{-\pi i}),$$

and therefore

$$\begin{aligned} \frac{\partial}{\partial \zeta} \frac{\zeta^{2/3} K_{2/3}(\zeta e^{-\pi i})}{\zeta^{1/3} K_{1/3}(\zeta e^{-\pi i})} &= \frac{\zeta K_{1/3}^2(\zeta e^{-\pi i}) - \zeta K_{2/3}^2(\zeta e^{-\pi i})}{\zeta^{2/3} K_{1/3}^2(\zeta e^{-\pi i})} \\ &= \zeta^{1/3} \left\{ 1 - \frac{K_{2/3}^2(\zeta e^{-\pi i})}{K_{1/3}^2(\zeta e^{-\pi i})} \right\}. \end{aligned}$$

Hence

$$\frac{\partial}{\partial \nu} \frac{w'}{w} = - \left( \frac{3\zeta}{z} \right)^{2/3} \left\{ 1 - \frac{K_{2/3}^2(\zeta e^{-\pi i})}{K_{1/3}^2(\zeta e^{-\pi i})} \right\},$$

and

$$\begin{aligned} \frac{\partial N}{\partial \nu} &= \left( \frac{3\zeta_1}{z_1} \right)^{2/3} \left\{ 1 - \frac{K_{2/3}^2(\zeta_1 e^{-\pi i})}{K_{1/3}^2(\zeta_1 e^{-\pi i})} \right\} \\ &\quad - \rho \left( \frac{3\zeta_{11}}{z_{11}} \right)^{2/3} \left\{ 1 - \frac{K_{2/3}^2(\zeta_{11} e^{-\pi i})}{K_{1/3}^2(\zeta_{11} e^{-\pi i})} \right\} \\ \frac{\partial D}{\partial \nu} &= \left( \frac{3\zeta_1}{z_1} \right)^{2/3} \left\{ 1 - \frac{K_{2/3}^2(\zeta_1 e^{+\pi i})}{K_{1/3}^2(\zeta_1 e^{+\pi i})} \right\} \\ &\quad - \rho \left( \frac{3\zeta_{11}}{z_{11}} \right)^{2/3} \left\{ 1 - \frac{K_{2/3}^2(\zeta_{11} e^{-\pi i})}{K_{1/3}^2(\zeta_{11} e^{-\pi i})} \right\}. \end{aligned}$$

In the case tabulated below  $|\zeta_1| = 3.9004$  and  $|\zeta_{11}| = 3.2180$  at the second pole, and the values found for  $\frac{\partial}{\partial \nu} \cdot \frac{w_1'}{w_1}$  are

$\cdot 001456 + \cdot 002555i$  from the asymptotic series, and  $\cdot 001436 + \cdot 002600i$  from the ascending series; the corresponding values of  $\frac{1}{M_1} \frac{\partial M_1}{\partial \nu}$  ( $w_{11}'/w_{11}$  being calculated from the ascending series) are  $\cdot 0191 - \cdot 0437i$  and  $\cdot 0185 - \cdot 0447i$ , and  $E_k$  is found to be  $\cdot 169 - \cdot 233i$  from the first and  $\cdot 169 - \cdot 232i$  from the second and more accurate value.

The following values of  $C_k$ ,  $E_k$ ,  $\zeta_{1k}$ , and  $\nu_k$  have been calculated for the case when  $r_0$ =radius of the earth = 6367.4 km.,  $r_1$ =6467.4 km. (*i. e.*, the height of the reflecting surface above the surface of the earth is 100 km.),  $\lambda$ =18,750 m.,  $K'/K$ = $\cdot 99$ , and when the earth is supposed perfectly conducting. The values given are believed to be sufficiently accurate to give  $\left| \frac{\psi_{01}}{\psi_0} \right|$  correct to the second decimal place for values of  $\theta$  greater than  $10^\circ$ .

	$k=0.$	$k=1.$	$k=2.$
$ C_k .$	$\cdot 0325$	$\cdot 00475$	$\cdot 00171$
$\arg C_k.$	$-12^\circ 8'$	$-75^\circ$	$-93^\circ 58'$
$E_k.$	$\cdot 0570 - \cdot 2394i$	$\cdot 169 - \cdot 232i$	$\cdot 262 - \cdot 268i$
$2\zeta_{1k}.$	$2.93 - 5.87i$	$7.80 - 10i$	$10.35 + 5.34i$
$i\nu_k.$	$9.014 + 5.204i$	$28.73 + 16.59i$	$42.63 + 24.61i$
	$k=3.$	$k=4.$	$k=5.$
$ C_k .$	$\cdot 00092$	$\cdot 000582$	$\cdot 000406$
$\arg C_k.$	$-102^\circ 21'$	$-108^\circ 24'$	$-111^\circ 43'$
$E_k.$	$\cdot 320 - \cdot 291i$	$\cdot 367 - \cdot 309i$	$\cdot 405 - \cdot 326i$
$2\zeta_{1k}.$	$12.18 + 10.90i$	$13.62 + 16.50i$	$14.89 + 22.22i$
$i\nu_k.$	$54.54 + 31.49i$	$65.22 + 37.66i$	$75.12 + 43.37i$

These values being known,  $\frac{\psi_{01}}{\psi_0}$  is given by the formula

$$\frac{\psi_{01}}{\psi_0} = 12\pi^{-1/2} z_0^{1/2} \left( \sin \frac{\theta}{2} \right)^{1/2} \left( \cos \frac{\theta}{2} \right)^{-3/2} e^{-\pi i/4 - i z_0 (\theta - 2 \sin \theta/2)} \cdot S,$$

where

$$S = \sum_{k=0}^{k=\infty} C_k e^{2\zeta_1 k - i\nu_k \theta} (E_k + i\theta) = \sum_k u_k.$$

When  $\theta = 10^\circ$ ,

$$u_6 = \cdot 0010 - \cdot 0002 i \quad \text{and} \quad \sum_{k=0}^{k=5} u_k = \cdot 0009 - \cdot 0032 i;$$

when  $\theta = 11^\circ$  or more the contribution of  $u_6$  to  $S$  is almost negligible. The value for  $S$  got from the first six poles may therefore be slightly in error when  $\theta = 10^\circ$ , and in order to get it accurately the constants for the next pole  $k=6$  would have to be calculated; but when  $\theta > 10^\circ$ , the constants given are sufficient. When  $\theta > 20^\circ$ , the whole of the effective part of  $S$  is contributed by the first pole, and the arithmetic is comparatively light. The values found

for  $\frac{\psi_{01}}{\psi_0}$  are:—

$\theta.$	$10^\circ.$	$11^\circ.$	$12^\circ.$	$13^\circ.$	$14^\circ.$	$15^\circ.$	$16^\circ.$
$\left  \frac{\psi_{01}}{\psi_0} \right .$	$\cdot 31 (?)$	$\cdot 33$	$\cdot 36$	$\cdot 38$	$\cdot 40$	$\cdot 41$	$\cdot 43$
$\left  \frac{\psi_{01}}{\psi_0} \right .$	$-146^\circ 19'$	$-141^\circ 29'$	$-141^\circ 15'$	$-146^\circ 6'$	$-153^\circ 4'$	$-167^\circ 55'$	$+176^\circ 15'$

$\theta.$	$17^\circ.$	$18^\circ.$	$19^\circ.$	$20^\circ.$	$22^\circ.$	$25^\circ.$
$\left  \frac{\psi_{01}}{\psi_0} \right .$	$\cdot 45$	$\cdot 45$	$\cdot 45$	$\cdot 44$	$\cdot 42$	$\cdot 37$
$\left  \frac{\psi_{01}}{\psi_0} \right .$	$+154^\circ 54'$	$+130^\circ 52'$	$113^\circ 14'$	$69^\circ 53'$	$-7^\circ 5'$	$-151^\circ 16'$

The values of  $\frac{\psi_{01}}{\psi_0}$  from  $\theta=3^\circ$  to  $\theta=7^\circ$  have been calculated from Macdonald's solution, corrected when necessary by the addition of terms got by including second approximations; these, and the values of  $\frac{\psi_{00}}{\psi_0}$  for the diffracted wave, obtained from the formula given in the beginning of this paper, are tabulated below, along with the value of  $\left| \frac{\psi_{00} + \psi_{01}}{\psi_0} \right|$  found from them, this being the intensity of the measured signal when only one reflected wave is present. The values of  $\left| \frac{\psi_{00}}{\psi_0} \right|$  are added for comparison.

$\theta$ .	$3^\circ$ .	$3^\circ 20'$ .	$3^\circ 40'$ .	$4^\circ$ .	$4^\circ 20'$ .	$4^\circ 40'$ .	$5^\circ$ .
$\frac{\psi_{01}}{\psi_0}$ .	0.01 -0.01 <i>i</i>	0.01 +0.02 <i>i</i>	-0.02 +0.02 <i>i</i>	-0.03 -0.01 <i>i</i>	-0.02 -0.04 <i>i</i>	0.02 -0.05 <i>i</i>	0.05 -0.03
$\frac{\psi_{00}}{\psi_0}$ .	1.76 -0.23 <i>i</i>	1.71 -0.27 <i>i</i>	1.66 -0.31 <i>i</i>	1.62 -0.35 <i>i</i>	1.57 -0.39 <i>i</i>	1.51 -0.43 <i>i</i>	1.46 -0.47 <i>i</i>
$\left  \frac{\psi_{00} + \psi_{01}}{\psi_0} \right $ .	1.79	1.74	1.67	1.63	1.61	1.60	1.59
$\left  \frac{\psi_{00}}{\psi_0} \right $ .	1.77	1.73	1.69	1.66	1.62	1.57	1.54
$\theta$ .	$5^\circ 20'$ .	$5^\circ 40'$ .	$6^\circ$ .	$6^\circ 20'$ .	$6^\circ 40'$ .	$7^\circ$ .	
$\frac{\psi_{01}}{\psi_0}$ .	0.07 +0.00 <i>i</i>	0.07 +0.04 <i>i</i>	0.04 +0.08 <i>i</i>	0.02 +0.10 <i>i</i>	-0.02 +0.10 <i>i</i>	-0.07 +0.10 <i>i</i>	
$\frac{\psi_{00}}{\psi_0}$ .	1.40 -0.51 <i>i</i>	1.35 -0.55 <i>i</i>	1.29 -0.59 <i>i</i>	1.22 -0.62 <i>i</i>	1.16 -0.66 <i>i</i>	1.09 -0.69 <i>i</i>	
$\left  \frac{\psi_{00} + \psi_{01}}{\psi_0} \right $ .	1.56	1.51	1.42	1.35	1.27	1.18	
$\left  \frac{\psi_{00}}{\psi_0} \right $ .	1.50	1.46	1.42	1.37	1.34	1.29	

Values of  $\frac{\psi_{01}}{\psi_0}$  for  $\theta > 10^\circ$  have already been given.

The corresponding values of  $\left| \frac{\psi_{00} + \psi_{01}}{\psi_0} \right|$  and  $\left| \frac{\psi_{00}}{\psi_0} \right|$  are as follows :—

$\theta.$	$10^\circ.$	$11^\circ.$	$12^\circ.$	$13^\circ.$	$14^\circ.$	$15^\circ.$	$16^\circ.$
$\left  \frac{\psi_{00} + \psi_{01}}{\psi_0} \right .$	1.05(?)	1.06	1.06	1.03	0.99	0.95	0.91
$\left  \frac{\psi_{00}}{\psi_0} \right .$	0.96	0.87	0.77	0.69	0.61	0.54	0.48
$\theta.$	$17^\circ.$	$18^\circ.$	$19^\circ.$	$20^\circ.$	$22^\circ.$	25	
$\left  \frac{\psi_{00} + \psi_{01}}{\psi_0} \right .$	0.88	0.81	0.76	0.73	0.64	0.23	
$\left  \frac{\psi_{00}}{\psi_0} \right .$	0.42	0.37	0.33	0.29	0.22	0.15	

The values of  $\left| \frac{\psi_{00} + \psi_{01}}{\psi_0} \right|$  at  $7^\circ$  and  $10^\circ$  may be in error by a unit in the second decimal place; it is believed that the others are correct. The graph of  $\left| \frac{\psi_{00} + \psi_{01}}{\psi_0} \right|$  suggests that between  $\theta = 7^\circ$  and  $\theta = 10^\circ$  the signal intensity falls to a minimum between  $8^\circ$  and  $9^\circ$ , and then rises to the value 1.06 at  $10^\circ$ , but it would be advantageous to obtain values at these intermediate distances by some other method.

I have to acknowledge my indebtedness to Prof. H. M. Macdonald for much help and encouragement in the preparation of this paper.

## II. *The Fingering of Wind Instruments.*

By ERIC J. IRONS, *Ph.D.* \*

### 1. *Introductory.*

IN 1924 Paris <sup>(1)</sup> derived a formula for the free periods of a stopped pipe having two Helmholtz resonators on the side, and it may be noted that if in his equation (26) we make the volumes of the resonators infinite by putting  $n_s=0$ , we obtain an expression for the resonant frequencies of a stopped pipe having two side holes.

More recently Richardson <sup>(2)</sup>, guided by impedance principles, has discussed the theory of fingering on the woodwind, and has made some measurements on flutes and clarinets. Basing his argument upon the approximation (due to Steinhausen <sup>(3)</sup>) that when two side holes are open the instrument may be considered as one pipe extending from the mouth to the first hole and another pipe extending from this hole to the second hole (at which an antinode is supposed to form), Richardson has, in effect, considered the system as a shortened pipe with only one hole open at a time.

The theory of the present paper renders possible the calculation of the pitch of the note emitted by an instrument when any number of side holes are open.

### 2. *Theoretical.*

In a former paper <sup>(4)</sup> a simple proof was given of Webster's <sup>(5)</sup> formula

$$Z_1 = \beta/\sigma \cdot \frac{Z_2 \cos kl - (\beta/\sigma) \sin kl}{Z_2 \sin kl + (\beta/\sigma) \cos kl} \quad \dots \quad (1)$$

for the impedance,  $Z_1$ , at one end of a tube of length  $l$  † and area of cross-section  $\sigma$  in terms of the impedance,  $Z_2$ , at the other end, and  $\beta$  the product of the elasticity of the gas and  $k$  ( $=2\pi n/a$  in the usual notation).

For the purposes of calculation it is convenient to write (1) in the form

$$Z_1 = \frac{Z_2 - (\beta/\sigma) \tan kl}{1 + (\sigma/\beta) Z_2 \tan kl} \quad \dots \quad (1.1)$$

\* Communicated by the Author.

† It is to be understood throughout the paper that the length of a column of gas is its geometrical length together with any appropriate end-correction or corrections.

If, now, we suppose the impedance  $Z_2$  at  $x=l$  to be zero, and that  $l$  is so small that  $kl$  may be written for  $\tan kl$ , it follows that

$$Z_1' = -(\beta/\sigma)kl = -\beta k/c, \quad \dots \quad (2)$$

where  $c$  is the conductance of the resulting short channel or orifice.

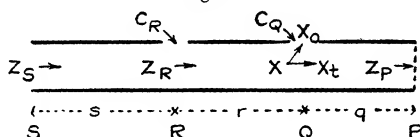
Next consider the system shown in fig. 1. The impedance at Q due to the air in the tube of length  $q$  is, by (1.1), equal to

$$\frac{Z_p - (\beta/\sigma) \tan kq}{1 + (\sigma/\beta) Z_p \tan kq} = M \text{ (say).}$$

The impedance of the orifice at Q is, by (2), equal to

$$-\beta k/c_Q = N \text{ (say).}$$

Fig. 1.



Following the principle enunciated by Rayleigh<sup>(6)</sup> we shall assume the air in the neighbourhood of Q to be incompressible, so that a volume displacement  $X$  arriving at Q will give rise to volume displacements  $X_0$  and  $X_t$  through the orifice and down the tube QP respectively, such that  $X = X_0 + X_t$ . Since at any instant the excess pressure  $p_Q$  on the incompressible volume of gas near Q is constant throughout that volume,  $X/p_Q = X_0/p_Q + X_t/p_Q$ , or, with Webster's notation, where impedance is defined as the ratio  $p/X$ ,  $1/Z_Q = 1/N + 1/M$ , which determines  $Z_Q$ .

$Z_R$  may be shown in an exactly similar manner to be given by

$$1/Z_R = \frac{1 + (\sigma/\beta) Z_Q \tan kr}{Z_Q - (\beta/\sigma) \tan kr} - c_R/\beta k.$$

Finally, the impedance at S is given by

$$Z_S = \frac{Z_R - (\beta/\sigma) \tan ks}{1 + (\sigma/\beta) Z_R \tan ks}.$$

If the tube is resonating to a source at S (the source being such as to make S an antinode)\*, it follows that a very small

\* As, for example, in an organ pipe or flute. For an instrument of the clarinet type S is a node and for resonance  $Z_S = \infty$ .



excess pressure  $p_s$  will give rise to a very large volume displacement  $X_s$ , so that  $Z_s = p_s/X_s = 0$ , in the absence of friction. From a knowledge of the dimensions of the system, it follows that the resonant frequency may be calculated by the method of successive approximations. Furthermore, the method is applicable to any number of side holes\*.

When only one side hole is open the problem lends itself to graphical treatment in a similar manner to Paris's formula<sup>(1)</sup> for a stopped pipe having one Helmholtz resonator on the side.

Disregarding  $c_R$  (fig. 1) and equating  $Z_R$  to zero gives  $Z_Q - (\beta/\sigma) \tan kr = 0$  or, substituting the value of  $Z_Q$ ,

$$(\sigma/\beta) \cot kr = -c_Q/\beta k + \frac{1 + (\sigma/\beta) Z_P \tan kq}{Z_P - (\beta/\sigma) \tan kq}.$$

If the tube is open at P,  $Z_P = 0$  and

$$-1/(\cot kr + \cot kq) = k\sigma/c_Q; \quad . \quad . \quad . \quad (3)$$

or, if it is closed,  $Z_P = \infty$  and

$$-1/(\cot kr - \tan kq) = k\sigma/c_Q. \quad . \quad . \quad . \quad (4)$$

Let the frequency of the pipe, when no side holes are open, be  $n_0$  and define a variable  $f$  such that  $f = r/(r+q)$ , when (3) and (4) will become

$$\frac{-1}{\cot \pi \cdot \frac{n}{n_0} \cdot f + \cot \pi \cdot \frac{n}{n_0} \cdot (1-f)} = \frac{\pi}{L} \cdot \frac{n}{n_0} \cdot \frac{\sigma}{c} \quad . \quad . \quad . \quad (3.1)$$

and

$$\frac{-1}{\cot \frac{\pi}{2} \cdot \frac{n}{n_0} \cdot f - \tan \frac{\pi}{2} \cdot \frac{n}{n_0} \cdot (1-f)} = \frac{\pi}{2L} \cdot \frac{n}{n_0} \cdot \frac{\sigma}{c}, \quad . \quad . \quad (4.1)$$

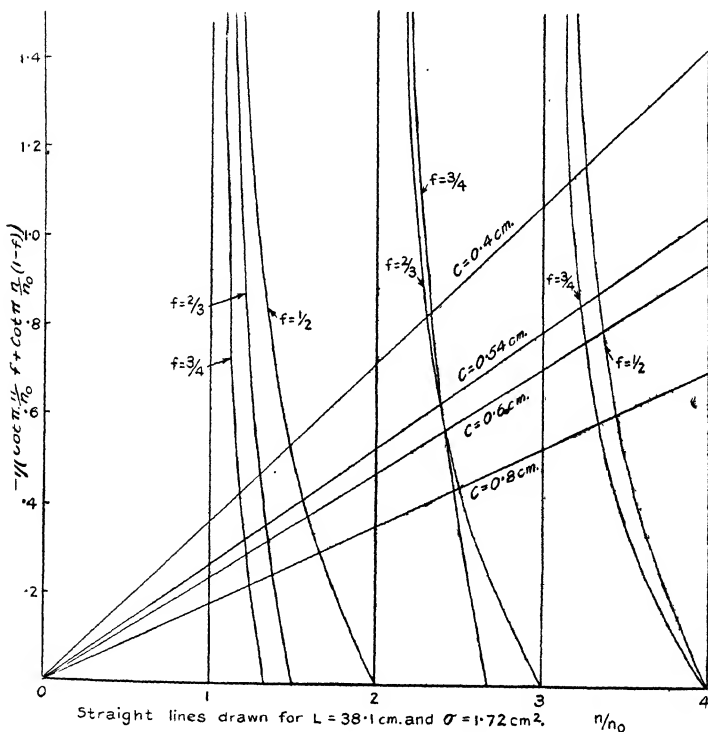
where  $L$  is the total length of the pipe and the subscript of  $c$  is dropped.

Plotting values of the left-hand sides of (3.1) and (4.1) against  $n/n_0$  for various values of  $f$  gives rise to the curves

\* The method of taking the impedances of an open and a closed pipe as  $-(\beta/\sigma) \tan kl$  and  $+(\beta/\sigma) \cot kl$  respectively (where impedance is defined by  $p/X$ ); adding the impedances of the component parts in series (or by a "parallel" rule for side holes); and equating to zero for resonance is, as the results of the present paragraph show, applicable in general only where the number of tubes does not exceed two<sup>(4 & 7)</sup>. See also Hanson<sup>(6)</sup>. Richardson's theory<sup>(2)</sup> as it stands cannot therefore be extended to include more than the one side hole which he has treated.

of figs. 2 and 3 respectively; and plotting values of the right-hand sides for a given hole in a given instrument against  $n/n_0$  gives rise to the series of straight lines in the same figures. The intersections of the curves and the straight lines determine the resonant frequencies in terms of  $n_0$ . It is to be noted that the curves—as distinct from

Fig. 2.

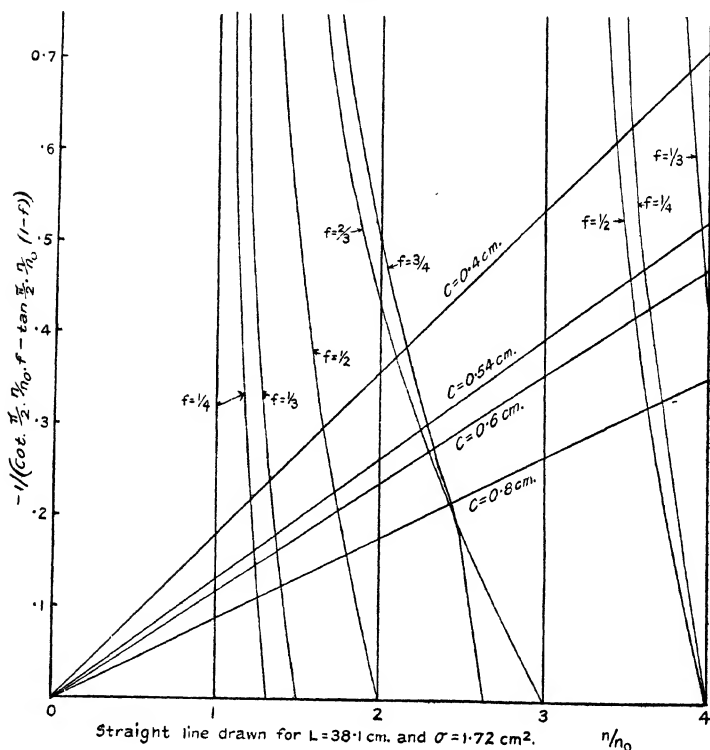


the straight lines—will serve for any instrument for which the value of  $n_0$  is known.

Equation (4.1) and fig. 3 are here given to explain experiments with an instrument having an “antinodal” mouth and stopped end. The same equation and diagram will serve to illustrate the properties of instruments of the clarinet type having a “nodal” (reed) mouth and open end if, in terms of fig. 1,  $f$  is redefined as equal to  $q/(r+q)$ .

It is of theoretical interest to note from figs. 2 and 3 the values of the frequencies indicated for the instances in which  $c$  is very large (equivalent to nearly opening the tube) and very small (equivalent to practically no side opening), and to compare these values with those derived from the corresponding "stationary wave-diagrams" for the pipe.

Fig. 3.



It would appear that when  $c$  is large the longer portion of the tube governs the frequency; this is to be expected as, *ceteris paribus*, energy is proportional to the square of the frequency, and therefore inversely proportional to the square of the length.

### 3. Practical.

The preceding theory has been used to calculate the notes emitted by a flageolet having various holes open, but before

describing the results obtained it will be necessary to refer to a

### *Preliminary Investigation.*

The end correction at the end of an unflanged cylindrical pipe is well known to approximate to 0.6 times the radius of the pipe<sup>(9)</sup>, but the mouth correction is a more indefinite quantity and does not appear to have received the attention it deserves. To obtain a value for the mouth correction of the instrument to be used and to trace its variation (if any) with frequency, an auxiliary mouth-piece, of similar structure to that of the flageolet, was made to excite various lengths of closed and open tube into resonance. We have for a closed pipe,  $L = a/4n - C$  (where  $L$ ,  $C$ ,  $a$ , and  $n$  represent tube-length, mouth correction, velocity of sound, and frequency respectively), and for an open pipe,  $L = a/2n - C$ , where  $L$  now represents the geometrical length of the pipe together with 0.6 times its radius. Plots of  $L$  against  $1/n$  (fig. 4) are sensibly rectilinear, from which it follows that, to within the limits of the present experimental error ( $n$  being determined by a sonometer),  $C$  is constant. Fig. 4 also shows that the correction is approximately the same whether the tube is open or closed, and is equal to 2.1 cm., which is 2.8 times the tube radius\*. A careful comparison of the frequencies obtained when the actual flageolet was sounded (with its side holes closed), firstly when open and secondly when closed by a tightly-fitting brass stop protruding 0.3 cm. into the tube, also yielded a value of the mouth correction equal to 2.1 cm., which value was accordingly adopted in the calculations which follow. This measurement is a delicate one, a slight error in one of the pitches involved making a considerable difference in the value of the mouth correction.

The mean of the three values of  $a$  determined from fig. 4

\* The following calculation serves to show that this correction is of the right order. It has been stated by Cavaillé-Coll<sup>(10)</sup> that the total of the mouth and the open end corrections for a square pipe is twice the distance ( $b$ ) from the side containing the lip to the back of the pipe. The radius of the circle having the same area as the cross-section of the pipe is given by  $b^2 = \pi r^2$ , so that the total of the corrections for a cylindrical pipe should be about  $2b = 2\sqrt{\pi} \cdot r = 3.5 \cdot r$ , which compares favourably with the  $(2.8 + .6) \cdot r$  above.

A similar result has been obtained for the mouth correction of a cylindrical organ pipe (see forthcoming paper on Constrictions in Organ Pipes).

and the above experiment was 350 metres/sec., which is reasonable figure having regard to temperature effects\*.

Fig. 4.

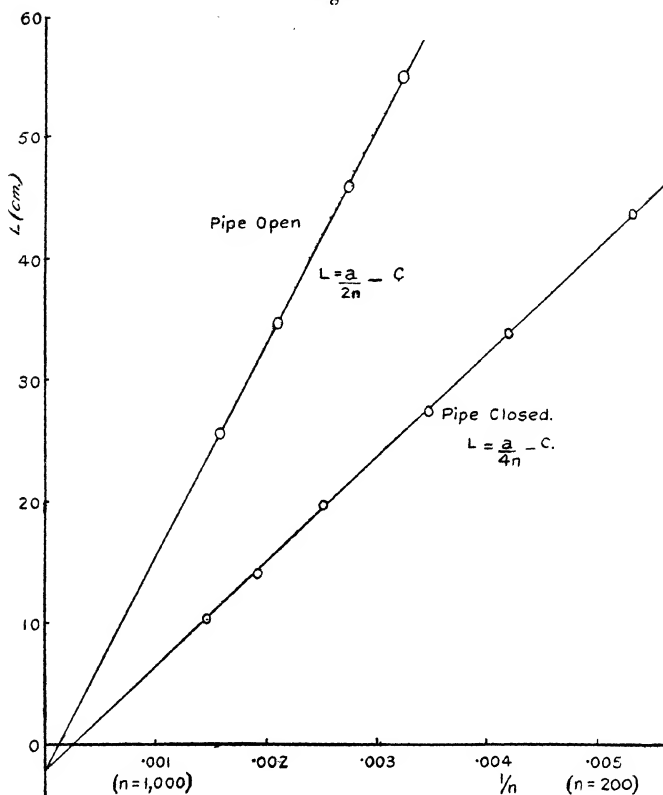
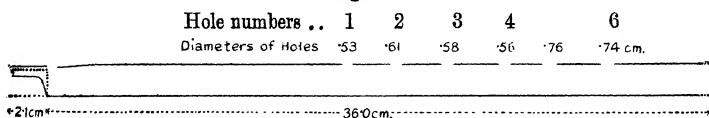


Fig. 5.



### *Investigation of Tones emitted by Flageolet.*

Fig. 5 is a scale drawing of the flageolet, and, following Mason's<sup>(11)</sup> procedure (derived from theoretical reasoning in

\* The air in an instrument is partly expired air, and the chief difference between this and inspired air is that 5 per cent. of the oxygen by volume in inspired air is replaced by  $\text{CO}_2$ .

connexion with acoustical filters), the lengths of the constituent air-columns were measured from opposite the centres of the side holes.

We shall, for lack of more precise data, follow Rayleigh and take the conductance of an orifice in a thin wall as equal to its diameter, although it has been found that for smaller wave-lengths and somewhat larger holes in a cap closing a tube the conductances exceed this value <sup>(7), (12)</sup>.

The note emitted by the instrument depends on the blowing pressure, and the values tabulated below (Table I.) are for the normal frequencies, *i. e.*, those frequencies which are compatible with the formulæ  $a=4nL$  and  $a=2nL$  for a closed and an open pipe respectively. The theoretical values were obtained by successive approximations using four-figure tables.

TABLE I.  
Frequencies of Notes emitted by Flageolet.

Side holes open (fig. 5).	Open pipe ( $Z_P=0$ , fig. 1).		Closed pipe ( $Z_P=\infty$ , fig. 1).		$F_1$ .	$F_2$ .
	Obs.	Cal.	Obs.	Cal.		
1	913	920	830	827	946	
123456	861	855	862	855	946	876
23456	769	763	770	763	829	777
2	724	712	766	762	829	
3456	691	679	690	679	732	688
3	664	652	708	708	732	
456	618	608	598	608	648	617
4	594	590	537	541	648	
56	567	565	554	563	595	570
5	563	560	534	545	595	
6	507	509	489	498	538	

*Investigation with Auxiliary Whistle.*

To investigate more fully the notes emitted when only one side hole is open, the auxiliary mouth-piece already mentioned was fitted with a tube of the same cross-section and length as the flageolet. A shorter tube, of length equal to the open end correction of the first tube, terminating in a solid cap, was used to close the first tube when desired; in this manner the "length" of the tube was unaltered. Side holes of diameter equal to 0.54 cm. were bored in the

tube at distances equal to  $\frac{1}{4}$ ,  $\frac{1}{3}$ ,  $\frac{1}{2}$ ,  $\frac{2}{3}$ , and  $\frac{3}{4}$  of its corrected length from the ("corrected") mouth end. The lower notes emitted under different blowing pressures when each side hole was open in turn are tabulated in Table II. (in terms of the fundamental frequencies of the tube  $n_0$ ) for the instances in which the tube was open and closed by the cap.

Straight-line plots of the right-hand sides of equations (3.1) and (4.1) for  $c=0.54$  cm. and  $L=38.1$  cm. were made on figs. 2 and 3, and the theoretical values of  $n/n_0$  were read off. From the symmetry of equation (3.1) it will be seen that the same notes should be emitted when  $f=\frac{1}{4}$  or  $\frac{3}{4}$ , or when  $f=\frac{1}{3}$  or  $\frac{2}{3}$ .

TABLE II.

Frequencies of Notes emitted by Auxiliary Whistle.  
(Given as the ratio of the frequency of the note to that of the fundamental of the pipe with no side holes open.)

$f$ .	Open pipe.		Closed pipe.	
	Obs.	Cal.	Obs.	Cal.
$\frac{1}{4}$ .....	{ 1.20* 2.37 3.18	1.22	1.24*	1.22
		2.39	3.61	3.60
		3.22		
$\frac{1}{3}$ .....	{ * 2.33	1.35	1.34*	1.36
		2.38	3.83	3.96
$\frac{1}{2}$ .....	{ 1.54 3.17	1.57	1.76	1.73
		3.32	3.62	3.52
$\frac{2}{3}$ .....	{ 1.38 2.35	1.35	2.20	2.24
		2.38		
$\frac{3}{4}$ .....	{ 1.23 2.37 3.16	1.22		
		2.39	2.21	2.28
		3.22		

\* Obtained with difficulty.

#### 4. Discussion of Results obtained with :

##### A. The Flageolet.

As an approximation let us first suppose that the note emitted by an instrument is governed solely by the distance between the mouth and the first open hole, and that this distance represents half a wave-length. Frequencies calculated on this assumption are tabulated under  $F_1$  in Table I., and although they follow the general trend of the results it will be noted that the approximation is not a good one.

As a nearer approximation let us, in those instances in which more than one hole is open, follow Richardson<sup>(2)</sup>, and consider the resonance system to consist of two pipes with one side hole (*cf.* § 1); the results then obtained are tabulated under  $F_2$  (Table I.), and compare very favourably with the observed values—especially where the “ventilation” at the end of the flageolet remote from the mouth is good. It would, in fact, appear that there is little, if anything, to be gained by considering the impedance beyond the second open hole, so that equation (3), having due regard to the interpretation of  $L$ , represents very nearly the behaviour of the flageolet. In consequence, figs. 2 and 3 assume a new importance as summarizing in a graphical manner all that we require to know concerning the tones such an instrument emits.

### B. *Auxiliary Whistle.*

A certain amount of difficulty was experienced in determining the results recorded in Table II., inasmuch as the blowing pressure had to be regulated to a nicety, the mouth-piece did not receive expert voicing, and the tones proper to the pipe with a side hole open were liable to be masked by the overtones to be expected if there had been no side hole—the presence of a hole at an antinode facilitating the production of these overtones. Special difficulty was experienced in obtaining the lowest notes when the side hole was near the mouth. Taken altogether the results appear to indicate that the theory is capable of predicting the frequencies of overtones as far as tested (*i. e.*, up to  $n/n_0=4$ ), and shows that they are not, in general, harmonic.

As a final application of our graphical solution let us follow Richardson and consider how a given note may be flattened by fingering and cross-fingering.

We will suppose that on a given instrument we have holes, the distances between which are as represented in fig. 6, and that we require to flatten very slightly the note obtained by playing the instrument as in 1. This may be done by :—

(1) Partially covering hole A (fingering) and thus reducing its conductance, which, in terms of fig. 3, means that the gradient of the straight line for that hole is increased, so that  $n/n_0$  is decreased.

(2) Covering hole B as in fig. 6, 2 (cross-fingering). Before we cover B,  $f=\frac{3}{4}$ ,  $L=8x$ , and  $n_0=a/16x$ ; after we cover B,

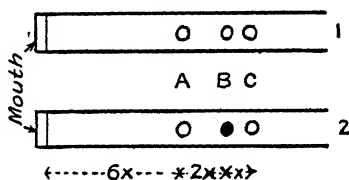


$f = \frac{2}{3}$ ,  $L = 9x$ , and  $n_0 = a/18x$ . Let us suppose that the conductance of hole A is 0.54 cm., so that the effect of the alteration of  $L$  on the straight line (fig. 2) is the same as increasing the value of  $c$  to about 0.61 cm. (*vide* equation (3.1)). From fig. 2 we find that the frequency before B is covered is  $1.22a/16x$ , and after it is covered it is  $1.36a/18x$ , so that covering B flattens the note in the ratio  $(1.36/18) \div (1.22/16)$ , *i. e.*, by about 1 per cent. of the frequency. In general the reduction would be greater, but this example is convenient as regards explanation in terms of fig. 3.

### 5. Conclusion.

The observations indicate that the "impedance theory" is capable of predicting the frequencies of the tones emitted by the flageolet to within one or two per cent., and to

Fig. 6.



indicate the trend of the results obtained with the auxiliary whistle. The impedance of a conical horn being known<sup>(4)</sup>, it is possible to extend the argument to instruments having that form, and, in fact, it is to be expected that the theory may lead to the better understanding of a number of musical instruments.

In conclusion, I wish to thank Prof. C. H. Lees and Dr. E. G. Richardson for their interest in this paper, and to express my indebtedness and thanks to Mr. B. C. Fleming-Williams, a senior student, for his able assistance with the frequency measurements.

### References.

- (1) Paris, *Phil. Mag.* xlviii. p. 769 (1924).
- (2) Richardson, 'The Acoustics of Orchestral Instruments' (Appendix). (Arnold, 1929.)
- (3) Steinhäusen, *Ann. d. Phys.* xlviii. p. 693 (1915).
- (4) Irons, *Phil. Mag.* ix. p. 346 (1930).
- (5) Webster, *Proc. Nat. Acad. Sci.* v. p. 275 (1919).
- (6) Rayleigh, 'Theory of Sound,' ii. p. 66. (Macmillan, 1926).

- (7) Irons, *Phil. Mag.* vii. p. 873 (1929).
  - (8) Hanson, *Proc. Phys. Soc.* xlix. p. 43 (1929), and Discussion.
  - (9) See, *e. g.*, Irons, *Phil. Mag.* v. p. 580 (1928), and references therein.
  - (10) Cavallé-Coll, *Comptes Rendus*, l. p. 176 (1860).
  - (11) Mason, *Bell System Tech. Journ.* iv. p. 258 (1927).
  - (12) Bate, *Phil. Mag.* ix. p. 23 (1930).
- 

III. *The Magnetic and Magneto-thermal Properties of Ferromagnetics.* By EDMUND C. STONER, *Ph.D.* (Cambridge), *Reader in Physics at the University of Leeds*.\*

*Introduction.*

THE theory of para- and ferromagnetism associated with the names of Langevin and Weiss has been remarkably successful in correlating a wide range of experimental facts. Langevin's treatment applies to a system of molecules whose mutual magnetic interaction can be neglected, and each of which possesses a magnetic moment which can assume any orientation with respect to an applied field. Weiss extended the theory by assuming that the molecules were acted on by a molecular field,  $NI$ , proportional to the intensity of magnetization,  $I$ , in addition to the external field. This hypothesis leads to an expression for the variation of susceptibility with temperature ( $\chi = \frac{C}{T - \theta}$ ), which is found to hold experimentally for many paramagnetics; it indicates the conditions under which spontaneous magnetization will occur, as in ferromagnetics; and it leads to curves for the variation of "quasi-saturation" magnetization with temperature below the Curie point, which agree approximately with those observed. The Weiss theory, however, is formal, for the molecular field is such that it cannot be of magnetic origin, and until recently no satisfactory suggestion was made as to how the effects attributed to it could arise.

The main contribution of the quantum theory, before the advent of the recent quantum mechanics, was in connexion with the calculation of the magnetic moments of the elementary carriers (atoms, ions, or molecules) from the experimental data. Whereas the classical theory indicates that the magnetic moment can assume any orientation with respect to an applied field, the quantum theory indicates that the magnetic moment can only assume certain discrete

\* Communicated by Prof. R. Whiddington, F.R.S.

values in the field direction. These values depend on the spectral state of the carrier, and can be determined when this is known. The appropriate modification of the Langevin treatment is readily made, and a considerable amount of theoretical and experimental work has been done on this part of the subject\*. Although many interesting points of detail remain unexplained, on the whole it may be said that the agreement between the magnetic moments deduced from susceptibility measurements on paramagnetics, and those deduced from spectroscopic observations, are in very satisfactory agreement.

For normal paramagnetics, such as salts, the nature of the carriers is usually fairly certain. In ferromagnetics, on the other hand, it is not known whether the carriers are electrons, atoms, ions, or groups of these. From the extensive magnetic data, it is reasonable to suppose that a fairly definite decision could be arrived at, but at present different lines of attack on the problem seem to lead to entirely different conclusions. For this reason it seems desirable to derive some of the more important quantum theory formulæ bearing on ferromagnetism, as these are necessary in any discussion of the significance of experimental results. The new mechanics is not here involved, and while there is nothing essentially new in the formulæ, no explicit derivation of some of them seems to have been given.

A fundamental advance in the theory of para- and ferromagnetism has been made by Heisenberg, who has shown that the interchange of electrons in atoms, which is characteristic of quantum mechanics, is capable, under certain conditions, of giving rise to those effects which have been partially correlated by the molecular field hypothesis. Even with the particularly simple model which is taken, the calculations are of considerable complexity, and the final results are only to be regarded as approximate. It is, however, the general nature of the results which is of importance. Here, again, it seems desirable to put these results in a form in which their relation to the experimental data is as clearly shown as possible; or, since experimental results have usually been considered with reference to the Weiss theory, to show the relation between the Heisenberg and Weiss theories.

In this paper, then, various theoretical formulæ for ferromagnetics will be derived, and they will be put in such a form as to facilitate comparison with experiment. The

\* For a summary and discussion, see E. C. Stoner, *Phil. Mag.* viii. p. 250 (1929).

experimental results are briefly considered, and the conclusions that can be drawn from them as to the interpretation of ferromagnetic phenomena are discussed.

*The Variation of Magnetization with Temperature  
above and below the Curie Point.*

In deriving expressions for the variation of susceptibility above the Curie point, and for the variation of magnetization below, it will be assumed that the carriers in the ferromagnetic are the same in both ranges, and that they all have the same magnetic moment. (Such modifications as may be necessary can readily be made.) When the carriers are regarded as quantized systems, the magnetic moment  $\mu$  is equal to  $jg\mu_B$ , where  $j$  is the quantum number giving the total angular momentum in Bohr units,  $g$  is the Landé splitting factor (equal to the ratio of the magnetic to the mechanical moment), and  $\mu_B$  is the Bohr unit magneton. Before giving the quantum treatment, the classical formulæ will be set down, so that corresponding expressions may be easily compared. To avoid confusion, a list of the symbols (other than those well established) used is given:—

- $\mu$  Magnetic moment of carrier. (For a quantum system  $\mu = jg\mu_B$ , this being the maximum moment in the field direction.)
- $\bar{\mu}$  Mean resolved magnetic moment of carriers.
- $\mu_B$  Bohr unit magneton.
- $\mu_W$  Weiss unit magneton ( $\mu_B = 4.97 \mu_W$ ).
- $M_B, M_W$  Bohr and Weiss magneton values per gram molecule ( $M_W = 1123.5$ ).
- $L$  Number of molecules per gram molecule ( $M_B = L\mu_B$ ;  $M_W = L\mu_W$ ).
- $I$  Intensity of magnetization (unit volume).
- $\sigma$  Specific intensity of magnetization (unit mass).
- $\sigma_0$  Saturation value of  $\sigma$ .
- $\sigma_M$  Saturation moment per gram molecule ( $\sigma_M = L\mu$ ).
- $H_i$  Molecular field.
- $H_e$  External field.
- $H$  Total field.
- $N$  Weiss molecular field constant ( $H_i = NI$ ).
- $p$  Magnetic moment in Weiss magnetons (calculated classically).
- $a = \mu H/kT$ .
- $M$  Molecular weight.

## CLASSICAL THEORY.

The Langevin expression for the magnetization is

$$\bar{\mu}/\mu = \sigma/\sigma_0 = \coth a - 1/a. \quad . \quad . \quad . \quad (1)$$

For  $a$  small

$$\bar{\mu}/\mu = a/3 - a^3/45. \quad . \quad . \quad . \quad . \quad (1a)$$

For  $a$  large

$$\bar{\mu}/\mu = 1 - \frac{1}{a} + 2e^{-2a}. \quad . \quad . \quad . \quad . \quad (1b)$$

The hypothesis of the molecular field is introduced in a second equation,

$$\begin{aligned} a &= \frac{\mu H}{kT} = \frac{\mu H_e}{kT} + \frac{\mu NI}{kT} \\ &= \frac{\mu H_e}{kT} + \frac{\mu N}{kT} \frac{\rho L \bar{\mu}}{M} \\ &= \frac{\mu H_e}{kT} + \frac{\sigma_M^2 N \rho}{MRT} \frac{\bar{\mu}}{\mu}. \quad . \quad . \quad . \quad . \quad (2) \end{aligned}$$

*Curie Point.*—In the absence of an external field ( $H_e=0$ ) spontaneous magnetization can occur if the slope of the straight line given by (2) is less than the slope of the tangent at the origin of (1),

$$\begin{aligned} \frac{MRT}{\sigma_M^2 N \rho} &< \frac{1}{3}, \\ T &< \frac{N \rho \sigma_M^2}{3MR}. \end{aligned}$$

The Curie temperature is therefore given by

$$\theta = \frac{N \rho \sigma_M^2}{3MR}. \quad . \quad . \quad . \quad . \quad (3)$$

*Paramagnetism.*—Above the Curie point an expression for the susceptibility may readily be obtained from the above equations; the expression will hold if  $a$  is small; the temperature must not be too close to the Curie temperature,

$$\chi_M = \frac{M\sigma}{H_e} = \frac{\sigma_M^2/3R}{T-\theta} = \frac{C_M}{T-\theta}. \quad . \quad . \quad . \quad (4)$$

For the Weiss magneton value,

$$p = \frac{\sigma_M}{M_w} = \frac{1}{M_w} \sqrt{3RC_M} = 14.07 \sqrt{C_M}. \quad . \quad . \quad (5)$$

For a normal paramagnetic obeying the Weiss-Curie law,  $p$  is obtained directly from the experimental results, which give  $\chi$  and  $\theta$ , for the Curie constant  $C_M$  is the product of  $\chi_M$  and  $T - \theta$ . Although the Weiss magneton is not a fundamental unit, magneton values  $p$  are still frequently used, partly for historical reasons, and partly because the  $p$  values are convenient numbers and can be derived simply and uniquely from experimental results. The experimental behaviour of a paramagnetic is summarized by the values of  $p$  and  $\theta$ ; the usual procedure in dealing with quantized systems is to calculate the theoretical value of  $p$ , and to compare this with that found experimentally.

*Ferromagnetism.*—Below the Curie point the quasi-saturation magnetization at any temperature may be found by extrapolation to zero field of the magnetization observed in high fields, and by various other methods. The theoretical value of this spontaneous magnetization may be obtained by eliminating  $a$  between the equations

$$\sigma/\sigma_0 = \coth a - 1/a,$$

$$\frac{\sigma}{\sigma_0} = \frac{MRT}{\sigma_M^2 \rho N} a = \frac{T}{\theta} \cdot \frac{a}{3} \quad \dots \quad (6)$$

The result may be expressed as

$$\sigma/\sigma_0 = f(T/\theta), \quad \dots \quad (7)$$

where the function may be found graphically.

The variation of the magnetization near the Curie point may be found analytically by making use of the approximation (1 a). (Near the Curie point,  $a$  may be regarded as small.)

$$\sigma/\sigma_0 = a/3 - a^3/45. \quad \dots \quad (1 a)$$

Substituting for  $\sigma/\sigma_0$  from (6),

$$\frac{a}{3} \left( 1 - \frac{T}{\theta} \right) = \frac{a^3}{45},$$

$$a = \sqrt{15 \left( 1 - \frac{T}{\theta} \right)}. \quad \dots \quad (8)$$

As long as  $T$  is not much less than  $\theta$ , the value of  $\sigma/\sigma_0$  is given by the first term in (1 a), so that

$$\frac{\sigma}{\sigma_0} = \frac{a}{3} = \sqrt{\frac{5}{3} \left( 1 - \frac{T}{\theta} \right)}. \quad \dots \quad (9)$$

If  $(\sigma/\sigma_0)^2$  is plotted against  $(T/\theta)$ , the slope of the tangent at the Curie point ( $T/\theta=1$ ) is  $-\frac{5}{3}$ ,

$$\left[ \frac{d(\sigma/\sigma_0)^2}{d(T/\theta)} \right]_{T/\theta \rightarrow 1} = -\frac{5}{3}. \quad (10)$$

At very low temperatures ( $T/\theta \rightarrow 0$ ),

$$\sigma/\sigma_0 = 1 - 1/a.$$

Substituting  $\frac{1}{3} \frac{T}{\theta} \frac{\sigma_0}{\sigma}$  for  $\frac{1}{a}$  from (6),

$$\frac{T}{\theta} = 3 \left[ \frac{\sigma}{\sigma_0} - \left( \frac{\sigma}{\sigma_0} \right)^2 \right]; \quad (11)$$

$$\left[ \frac{d(T/\theta)}{d(\sigma/\sigma_0)} \right]_{T/\theta \rightarrow 0} = 3 - 6 \left( \frac{\sigma}{\sigma_0} \right) \doteq -3,$$

$$\left[ \frac{d(\sigma/\sigma_0)}{d(T/\theta)} \right]_{T/\theta \rightarrow 0} \doteq -\frac{1}{3}. \quad (12)$$

Some of the expressions derived above have been given by Debye\*, who has shown in particular that the variation in magnetization near absolute zero given by the Langevin theory is incompatible with Nernst's heat theorem, as the entropy tends to an infinite value.

The main quantitative characteristics of the "classical" theoretical curve for the variation of magnetization with temperature are summarized by (10) and (12). The intermediate parts can be obtained with sufficient accuracy graphically, so that a satisfactory comparison with the experimental results may be made.

### QUANTUM THEORY.

Quantized systems with a moment  $\mu = jg\mu_B$  can assume moments in the field direction equal to  $mg\mu_B$ , where  $m$  has the values  $j, j-1, j-2 \dots -j$ . (It may here be noted that for free electrons, and atoms or ions in S states,  $g=2$ . For electrons, and doublet atoms or ions,  $j=\frac{1}{2}$ .) The quantum analogue of the Langevin equation is

$$\frac{\bar{\mu}}{\mu} = \frac{\sigma}{\sigma_0} = \frac{1}{jg} \left( \sum_{-j}^{+j} e^{mg\hbar} mg \right) / \left( \sum_{-j}^{+j} e^{mg\hbar} \right), \quad (13)$$

where  $\hbar$  is written for  $\frac{\mu_B H}{kT}$ .

\* P. Debye, 'Handbuch der Radiologie,' vi. (1925); *Ann. der Phys.* lxxxix. p. 1154 (1926).

The Weiss equation, as before, is

$$\begin{aligned} a &= \frac{\mu H_e}{kT} + \frac{\mu NI}{kT} \\ &= \frac{\mu H_e}{kT} + \frac{\sigma_M N \rho}{MRT} \frac{\bar{\mu}}{\mu}. \quad \dots \quad (14) \end{aligned}$$

Curie Point.—Expanding the exponentials in (13),

$$\begin{aligned} \frac{\bar{\mu}}{\mu} &= \frac{1}{j} \sum_{-j}^{+j} m \left( 1 + mgh + \frac{(mgh)^2}{2!} + \dots \right) / \sum_{-j}^{+j} (1 + mgh + \dots) \\ &= \frac{1}{j} \sum_{-j}^{+j} \left( m^2 gh + m^4 \frac{(gh)^3}{3!} + \dots \right) / \sum_{-j}^{+j} \left( 1 + \frac{(mgh)^2}{2!} \dots \right). \quad (15) \end{aligned}$$

The following sums are required:—

$$\left. \begin{aligned} \sum_{-j}^{+j} 1 &= 2j+1, \\ \sum_{-j}^{+j} m^2 &= \frac{1}{3} j(j+1)(2j+1), \\ \sum_{-j}^{+j} m^4 &= \frac{1}{15} j(j+1)(2j+1)(3j^2+3j-1). \end{aligned} \right\} \dots \quad (16)$$

Taking the first approximation (corresponding to  $\bar{\mu}/\mu = a/3$  in the classical case),

$$\begin{aligned} \frac{\bar{\mu}}{\mu} &= \frac{1}{j} \frac{j(j+1)(2j+1)gh}{3(2j+1)} \\ &= \frac{gh(j+1)}{3} \\ &= \frac{g\mu_B H(j+1)}{3kT} = \frac{(jg\mu_B)H}{3kT} \cdot \frac{j+1}{j} = \frac{a}{3} \cdot \frac{j+1}{j}. \quad (17) \end{aligned}$$

Spontaneous magnetization can occur when the slope of the line (14) with  $H_e=0$  is less than the slope of the tangent at the origin to (13), given by (17),

$$\begin{aligned} \frac{MRT}{\sigma_M^2 N \rho} &< \frac{j+1}{3j}, \\ T &< \frac{j+1}{3j} \frac{N \rho \sigma_M^2}{MR}, \\ \theta &= \frac{j+1}{3j} \frac{N \rho \sigma_M^2}{MR} \dots \dots \dots (18) \end{aligned}$$



The minimum value of  $\frac{j+1}{3j}$  is  $\frac{1}{3}$  (corresponding to the classical theory); the maximum for  $j=\frac{1}{2}$  is 1.

*Paramagnetism.*—Above the Curie point, and with  $a$  small, following the same procedure as before,

$$\begin{aligned}\chi_M &= \frac{L\bar{\mu}}{H_e} = \frac{L^2(jg\mu_B)^2 j+1}{3R(T-\theta)j} = \frac{\sigma_M^2/3R}{T-\theta} \cdot \frac{j+1}{j} \\ &= \frac{C_M}{T-\theta} \dots \dots \dots (19)\end{aligned}$$

If the values of  $j$  and  $g$  are known, the value of  $C_M$  can be calculated. It is convenient, however, for the reasons already given, to obtain an expression for  $p$  in terms of  $j$  and  $g$ .

From (5),

$$\begin{aligned}p &= \frac{1}{M_w} \sqrt{3RC_M} = \frac{1}{M_w} Ljg\mu_B \sqrt{\frac{j+1}{j}} \\ &= \frac{M_B}{M_w} g \sqrt{j(j+1)} \\ &\doteq 5g \sqrt{j(j+1)} \dots \dots \dots (20)\end{aligned}$$

This is the well-known expression which has been used so extensively for paramagnetics.

In general there is no simple convenient expression for (13). For  $j=\frac{1}{2}$ ,  $g=2$ ,  $\mu=\mu_3$ ,

$$\begin{aligned}\frac{\bar{\mu}}{\mu} &= \frac{\sigma}{\sigma_0} = \frac{1}{2j} (e^h - e^{-h})(e^h + e^{-h}) \\ &= \tanh(\mu_B H/kT) = \tanh a \dots \dots \dots (21) \\ &= a - a^3/3 + \dots \dots \dots (21a)\end{aligned}$$

*Ferromagnetism.*—As in the classical case, the curve giving  $\sigma/\sigma_0$  as a function of  $T/\theta$  may be obtained by graphical elimination of  $a (=jg\mu_B H/kT)$  between equations (13) and (14). The curve lies above the classical curve over the whole range, the relative magnetization for a given value of  $T/\theta$  being greater. For temperatures near the Curie point an analytical procedure may be followed by taking the second approximation for  $\sigma/\sigma_0$  from (15). From (15), making use of (16), there results, after reduction,

$$\frac{\bar{\mu}}{\mu} = \frac{\sigma}{\sigma_0} = \frac{j+1}{3j} a - \frac{j+1}{3j} \cdot \frac{2j^2+2j+1}{30j^2} a^3 \dots \dots (22)$$

From (14) for  $H_e=0$ , using (18), the second equation is

$$\frac{\bar{\mu}}{\mu} = \frac{T}{\theta} \cdot \frac{j+1}{3j} a. \quad (23)$$

Combining these equations,

$$\begin{aligned} \frac{j+1}{3j} a \left(1 - \frac{T}{\theta}\right) &= \frac{j+1}{3j} \cdot \frac{2j^2 + 2j + 1}{30j^2} a^3, \\ a &= \sqrt{\left\{ \frac{30j^2}{2j^2 + 2j + 1} \left(1 - \frac{T}{\theta}\right) \right\}}. \quad (24) \end{aligned}$$

Using the first term approximation in (22),

$$\left(\frac{\sigma}{\sigma_0}\right)_{T/\theta \gg 1} = \sqrt{\left\{ \frac{10}{3} \frac{(j+1)^2}{j^2 + (j+1)^2} \left(1 - \frac{T}{\theta}\right) \right\}}. \quad (25)$$

The quantum expression corresponding to (10) is

$$\left[ \frac{d(\sigma/\sigma_0)^2}{d(T/\theta)} \right]_{T/\theta \gg 1} = -\frac{10}{3} \frac{(j+1)^2}{j^2 + (j+1)^2}. \quad (26)$$

This has a minimum (numerical) value (for  $j \rightarrow \infty$ ) of  $5/3$  and a maximum (for  $j = \frac{1}{2}$ ) of 3. At very low temperatures, for this same limiting case

$$\frac{\sigma}{\sigma_0} = \tanh a = \frac{e^a - e^{-a}}{e^a + e^{-a}} \doteq 1 - 2e^{-2a}. \quad (27)$$

Since  $a$  becomes very large as  $T/\theta \rightarrow 0$ ,

$$\left[ \frac{d(\sigma/\sigma_0)}{d(T/\theta)} \right]_{T/\theta \rightarrow 0} = 0. \quad (28)$$

In general a limiting value for  $\sigma/\sigma_0$  as  $T/\theta$  approaches zero may be found by taking the first two terms in the expansion of (13),

$$\begin{aligned} \left(\frac{\sigma}{\sigma_0}\right)_{a \gg 1} &= \frac{1}{j} \frac{j e^{jgh} + (j-1) e^{(j-1)gh} + \dots}{e^{jgh} + e^{(j-1)gh} + \dots} \\ &\doteq \left(1 - \frac{j-1}{j} e^{-gh}\right) (1 - e^{-gh}) \\ &= 1 - \frac{1}{j} e^{-gh}. \end{aligned}$$

Since  $h = \mu_B H / kT$ ,  $gh = gj\mu_B H / jkT = \frac{a}{j}$ ,

$$\left(\frac{\sigma}{\sigma_0}\right)_{a \gg 1} = 1 - \frac{1}{j} e^{-a/j}, \quad (29)$$

in agreement with (27) for  $j = \frac{1}{2}$ .

	Quantum Theory.	
	General.	$j=\frac{1}{2} \quad g=2. \quad \frac{1}{2} \frac{1}{g}$
<i>Paramagnetism.</i> $\theta$  $p=14.07 \sqrt{C_M}$  $\frac{\sigma}{\sigma_0} \quad (\alpha \leq 1)$  $\frac{\sigma}{\sigma_0} \quad (\alpha \geq 1)$	$\frac{1}{3} \cdot \frac{N \rho \sigma_M^2}{MR}$	$\frac{N \rho \sigma_M^2}{MR}$
	$\frac{\mu}{\mu_W}$	$\frac{\mu_N}{\mu_W} \sqrt{3} = 8.6$
	$\coth a - \frac{1}{a}$	$\tanh a$
	$\frac{a}{3} - \frac{a^3}{45}$	$a - \frac{a^3}{3}$
	$1 - \frac{1}{a} + 2e^{-2a}$	$1 - 2e^{-2a}$
<i>Ferromagnetism.</i> $\frac{\sigma}{\sigma_0} \quad \left( \frac{T}{\theta} \rightarrow 1 \right)$ $\left[ \frac{d(\sigma/\sigma_0)^2}{d(T/\theta)} \right]_{T/\theta \rightarrow 1}$ $\left[ \frac{d(\sigma/\sigma_0)}{d(T/\theta)} \right]_{T/\theta \rightarrow 0}$	$\sqrt{\left\{ \frac{10}{3} \frac{(j+1)^2}{j^2 + (j+1)^2} \left( 1 - \frac{T}{\theta} \right) \right\}}$	$\sqrt{\left\{ 3 \left( 1 - \frac{T}{\theta} \right) \right\}}$
	$-\frac{5}{3}$	$-3$
	$-\frac{1}{3}$	$0$

The slope of the tangent for  $T/\theta=0$  will in all cases be zero.

The main formulæ for para- and ferromagnetism which have been derived in this section are collected together in Table I.

*The Change in Specific Heat at the Curie Point.*

The essential postulate of Weiss that there is a pseudo-magnetic field  $NI$  in ferromagnetics may also be stated, as he has pointed out, in the form that the energy associated with magnetization in ferromagnetics is large and negative, being equal to  $-\frac{1}{2}NI^2$  per unit volume. The specific heat associated with the change in this "magnetic" energy is given by

$$\begin{aligned} S &= - \frac{d}{dT} \frac{1}{2} \left( \frac{NI^2}{\rho} \right) \\ &= - \frac{1}{2} N \rho \frac{d\sigma^2}{dT} \dots \dots \dots (30) \end{aligned}$$

For the "magnetic" specific heat per gram molecule  $S_M$ ,

$$\begin{aligned} S_M &= - \frac{1}{2} N \rho M \frac{d\sigma^2}{dT} \\ &= - \frac{1}{2} N \rho M \sigma_0^2 \frac{d}{dT} \left( \frac{\sigma}{\sigma_0} \right)^2 \\ &= - \frac{1}{2} \frac{N \rho \sigma_M^2}{M \theta} \frac{d(\sigma/\sigma_0)^2}{d(T/\theta)} \dots \dots \dots (31) \end{aligned}$$

From the values for  $\theta$  in Table I. this gives

$$\text{Classical Theory} \dots S_M = - \frac{3R}{2} \frac{d(\sigma/\sigma_0)^2}{d(T/\theta)}, \dots \dots \dots (32)$$

$$\text{Quantum Theory} \dots S_M = - \frac{3jR}{2(j+1)} \frac{d(\sigma/\sigma_0)^2}{d(T/\theta)} \dots \dots \dots (33)$$

Above the Curie point,  $\theta$ , the spontaneous magnetization becomes zero, and the decrease  $\Delta S_M$  in specific heat on passing through  $\theta$  is equal to  $S_M$  calculated from the value of  $\frac{d(\sigma/\sigma_0)^2}{d(T/\theta)}$  just below the Curie point.

$$\text{Classical Theory} \dots (\Delta S_M)_{T=\theta} = \frac{5R}{2}, \dots \dots \dots (34)$$

$$\text{Quantum Theory... } (\Delta S_M)_{T=0} = \frac{5R}{2} \frac{j^2 + j}{j^2 + j + \frac{1}{2}} \quad \dots (35)^*$$

For the purposes of this calculation it has been supposed that one carrier of moment  $\mu$  (or  $jg\mu_B$ ) is associated with each molecule (or atom). Taking  $R = 2$ , the values of  $\Delta S_M$  for various values of  $j$  in calories per gram molecule are shown in Table II. The classical formula corresponds to  $j \rightarrow \infty$  in the quantum formula.

TABLE II.

Change in Specific Heat at the Curie Point in  
Calories per Gram Molecule.

$j$ .....	$\frac{1}{2}$	1	$3/2$	2	$5/2$	3	$\rightarrow \infty$
$\Delta S_M$ .....	3	4	4.41	4.61	4.73	4.8	5

Unless the treatment has to be essentially modified in the light of the Heisenberg theory, the indications are that if the decrease in the gram atomic heat is less than 3 (as for nickel), there must be less than one independent carrier per atom; and that if the decrease—attributable to the magnetic change only—is greater than 5 (as for iron), there must be more than one quasi-independent carrier per atom.

### *Heisenberg's Theory of Ferromagnetism.*

In his theory Heisenberg† investigates the effect of interchange interaction in a lattice consisting of similar atoms, each atom containing one electron free to orientate itself. The magnetization is attributed to these electrons, the remainder of the atom having no magnetic effect. (This assumption is perhaps somewhat artificial; but the interaction of atoms having one electron in excess of a closed configuration will presumably be similar to that of atoms which have one electron less than the number required to complete a group‡. These correspond more closely to the atoms (or ions) of the ferromagnetic elements, in which the *d*-group of electrons is incomplete.) It is shown that if the interaction integral is positive, spontaneous magnetization

\* This formula is quoted by J. Dorfmann and I. Kikoin, *Zeits. für Phys.* liv. p. 289 (1929).

† W. Heisenberg, *Zeits. für Phys.* xlix. p. 619 (1928).

‡ Cf. J. E. Lennard-Jones, *Trans. Faraday Soc.* xxv. p. 683 (1829).

may occur below a critical temperature, the model having the salient characteristics of a ferromagnetic. Before considering certain points in the treatment in greater detail, the results will be written down in a form which enables them to be compared with those from previous theories. Since the carriers are electrons, the equations are most usefully compared with (13) and (14) in their simplest forms (13 in the form 21). Heisenberg's results may be expressed by the equations

$$\bar{\mu}/\mu = \sigma/\sigma_0 = \tanh a, \quad . \quad . \quad . \quad (36)$$

$$a = \frac{\mu H_e}{kT} + \frac{1}{2} \left( \beta - \frac{\beta^2}{z} \right) \frac{\bar{\mu}}{\mu} + \frac{\beta^2}{4z} \left( \frac{\bar{\mu}}{\mu} \right)^2, \quad . \quad . \quad (37)$$

where

$$\beta = zJ_0/kT,$$

$z$  = number of neighbours surrounding each atom.  
( $z=8$  for a cube-centred lattice,  $z=12$  for a face-centred lattice),

$J_0$  = interaction integral.

When the external field is zero the Weiss equation

$$a = \frac{N\rho\sigma_m^2}{MRT} \frac{\bar{\mu}}{\mu}$$

is replaced by

$$a = \frac{1}{2} \left( \beta - \frac{\beta^2}{z} \right) \frac{\bar{\mu}}{\mu} + \frac{\beta^2}{4z} \left( \frac{\bar{\mu}}{\mu} \right)^2$$

Substituting  $I_0$  for  $\rho\sigma_m/M$ , and  $\mu/k$  for  $\sigma_m/R$ , and  $zJ_0/kT$  for  $\beta$ , the constant  $NI_0$  of the Weiss theory (giving the maximum molecular field) is replaced by

$$\frac{1}{2\mu} \left[ zJ_0 \left\{ 1 - \frac{J_0}{kT} + \frac{J_0}{2kT} \left( \frac{\bar{\mu}}{\mu} \right)^2 \right\} \right], \quad . \quad . \quad (39)$$

a quantity which varies with the magnetization and with the temperature.

Following the same treatment as before, spontaneous magnetization occurs for

$$\frac{1}{2} \left( \beta - \frac{\beta^2}{z} \right) > 1. \quad . \quad . \quad . \quad (40)$$

This is a maximum when  $\beta = \frac{z}{2}$ , so that, as a necessary condition,

$$z \geq 8.$$

In general the limiting values of  $\beta$  for which spontaneous magnetization will occur are given by the roots of the equation

$$\beta^2 - 4\beta z + 2z = 0.$$

$$\begin{aligned}\beta &= \frac{1}{2} \{ z \pm \sqrt{z^2 - 8z} \} \\ &= \frac{z}{2} \left\{ 1 \pm \sqrt{1 - \frac{8}{z}} \right\},\end{aligned}$$

giving

$$T = \frac{2J_0}{k \left\{ 1 \pm \sqrt{1 - \frac{8}{z}} \right\}} \quad \dots \quad (41)$$

As the temperature decreases from a high value, spontaneous magnetization will set in when

$$T = \frac{2J_0}{k \left\{ 1 - \sqrt{1 - \frac{8}{z}} \right\}},$$

increase to a maximum roughly at

$$T = \frac{2J_0}{k},$$

then decrease, and disappear when

$$T = \frac{2J_0}{k \left\{ 1 + \sqrt{1 - \frac{8}{z}} \right\}}.$$

In the limiting case when  $z=8$  the two values of  $T$  are equal, and spontaneous magnetization will just not occur, or taking into account the higher terms, will be restricted to the neighbourhood of the Curie point. In any case the range in which spontaneous magnetization occurs will be small. The behaviour of actual ferromagnetics is, of course, widely different from that indicated by the Heisenberg equations in their present form.

*The Change in Specific Heat at the Curie Point.*—Below the Curie point, in the absence of an external field, the part of the energy dependent on the magnetization per gram atom is given by

$$(E_A)_1 = -RT \left\{ \frac{1}{4} \left( \beta - \frac{2\beta^2}{z} \right) \left( \frac{\bar{\mu}}{\mu} \right)^2 + \frac{\beta^2}{8z} \left( \frac{\bar{\mu}}{\mu} \right)^4 \right\} \dots \quad (42)$$

From this and the equations for the magnetization (36) and (37), the part of the specific heat associated with the magnetization may be determined. Fowler and Kapitza\* conclude that the change at the Curie point will be roughly

$$\Delta S_A = \frac{3}{2} R. \quad . \quad . \quad . \quad . \quad . \quad (43)$$

They reach this conclusion, however, by making use of some approximations which do not seem justifiable. In the neighbourhood of the Curie point the term in  $(\bar{\mu}/\mu)^4$  may be neglected, and there results for the change in specific heat

$$\begin{aligned} \Delta S_A &= -R\theta \left[ \frac{1}{4} \beta \left( 1 - \frac{2\beta}{z} \right) \right] \left\{ \frac{d}{dT} \left( \frac{\sigma}{\sigma_0} \right)^2 \right\}_{T=\theta} \\ &= -R \left[ \frac{1}{4} \beta \left( 1 - \frac{2\beta}{z} \right) \right] \left\{ \frac{d(\sigma/\sigma_0)^2}{d(T/\theta)} \right\}_{T=\theta}. \end{aligned}$$

Making use of (36) and (37),

$$\Delta S_A = 3R \left[ \frac{1}{4} \beta \left( 1 - \frac{2\beta}{z} \right) \right]. \quad . \quad . \quad . \quad . \quad (44)$$

Fowler and Kapitza state that the factor in square brackets is approximately  $\frac{1}{2}$ . From the equations (41), however,

$$\beta_{T=\theta} = \frac{z}{2} \left\{ 1 - \sqrt{1 - \frac{8}{z}} \right\}.$$

Substituting in (44),

$$\Delta S_A = \frac{3}{2} R \left[ \frac{z}{8} \left\{ 1 - \sqrt{1 - \frac{8}{z}} \right\} \left( \sqrt{1 - \frac{8}{z}} \right) \right]. \quad (45)$$

This gives the results

$$\begin{aligned} z=8, \quad \Delta S_A &= 0, \\ z=12, \quad \Delta S_A &= \frac{3}{2} R \left[ \frac{1}{2} (\sqrt{3} - 1) \right] = \cdot 55 R. \end{aligned}$$

Such agreement with experiment as is given by (43) thus completely disappears.

*Energy Distribution of States.*—The lack of agreement between theory and experiment in respect both of magnetization and the change in specific heat can be traced to the occurrence of terms in  $\beta^2$  in (37). In discussing the magnetization, Heisenberg suggests that the failure of the theory for lower temperatures is possibly due to the special assumptions made as to the energy distribution of

\* R. H. Fowler and P. Kapitza, Proc. Roy. Soc. cxxiv. p. 1 (1929).



states corresponding to a particular value for the number of unpaired electrons.

While it is unnecessary here to outline the whole treatment—for which Heisenberg's paper or that of Fowler and Kapitza should be consulted—it seems desirable to indicate briefly how the  $\beta^2$  terms arise. The nomenclature of the papers referred to will be followed as far as possible.

Let  $2n$  be the number of atoms, each with one electron free to orientate itself,  $J_0$  the interchange interaction integral. The atoms are treated as hydrogen-like, but  $J_0$  must be positive (it is negative for two hydrogen atoms in the ground state) in order that the corresponding energy may be negative when the spins are parallel. Each atom is surrounded by  $z$  neighbours. Each electron has a spin of  $\frac{1}{2}$  and a magnetic moment of 1 in Bohr units. Each arrangement of  $(n-s)$  pairs of electrons (with zero resultant spin) and  $2s$  unpaired electrons corresponds to a term with a resultant moment  $s$ . Using the suffix  $\sigma$  to refer to this partition, that is to

$$2 + 2 + 2 \dots (n-s) \text{ times}; 1 + 1 + 1 \dots 2s \text{ times},$$

it may be shown that the number of such arrangements, or terms, is  $f_\sigma$  where

$$f_\sigma = \frac{2n!}{(n+s)!(n-s)!} - \frac{2n!}{(n+s+1)!(n-s-1)!}, \quad (46)$$

and the mean energy depending on interchange interaction is  $E_\sigma$  where

$$E_\sigma = -z \frac{s^2 + n^2}{2n} J_0. \quad (47)$$

The energy of these terms will be distributed about this mean value, and the mean square deviation  $\Delta_\sigma^2$  may further be shown to be

$$\Delta_\sigma^2 = z J_0^2 \frac{(n^2 - s^2)(3n^2 - s^2)}{4n^3}. \quad (48)$$

It is here that the particular assumption is made that the distribution is Gaussian, and that the number of terms with energies between  $E_\sigma + x$  and  $E_\sigma + x + dx$  is

$$\frac{f_\sigma}{\sqrt{2\pi\Delta_\sigma}} e^{-\frac{1}{2}x^2/\Delta_\sigma^2} dx.$$

In the summand of the partition function there then appears the factor

$$\exp \{E_\sigma/kT + \Delta_\sigma^2/(2k^2T^2)\}. \quad (50)$$

The stable state of magnetization is obtained by finding the value for which the summand is a maximum, with the result given by (36) and (37), the  $\beta^2$  terms in (37) coming from the  $\Delta_\sigma^2$  term in (50).

The equations (48) and (49) imply that some of the states corresponding to a spin  $s$  ( $s < n$ ) will have an energy less than that for  $s=n$ . Expressed in another way this means that states of small magnetization are assumed possible for which the energy is less than that corresponding to saturation magnetization. Since  $\Delta_\sigma=0$  for  $s=n$  from (48), and  $f_\sigma=1$  from (46), the most probable state giving an energy equal to that for saturation will correspond to a magnetization less than the saturation value. This illustrates, by the consideration of a special case, how the variation of magnetization with temperature—already discussed—is linked up with the energy deviations and their assumed distribution.

The difficulty seems to be inherent in the group theory method of treating the crystal as a whole. The root mean square deviation is always small compared with the energy. When  $s$  is small, for example,

$$E_\sigma = -znJ_0/2, \quad \text{and} \quad \sqrt{\Delta_\sigma^2} = J_0 \sqrt{3nz}/4.$$

On the other hand, the deviation will in general be large compared with  $kT$ , and it is this which gives the  $\beta^2$  terms their importance at the lower temperatures. It should be noted, however, as shown by the consideration of the specific heat change, that it is not only at lower temperatures that the  $\beta^2$  terms are in disagreement with experiment.

*Modified Treatment* \*.—Instead of the crystal being treated as a whole, it may be regarded for approximate purposes as an assembly of atoms. The electron free to orientate itself in each atom can set itself parallel or antiparallel to the direction of magnetization of the crystal. The energy in these two settings is  $\pm \frac{zJ_0}{z} \frac{\bar{\mu}}{\mu}$ . The expression then obtained for the magnetization is

$$\begin{aligned} \frac{\bar{\mu}}{\mu} &= \tanh \frac{zJ_0}{2kT} \frac{\bar{\mu}}{\mu} \quad . \quad . \quad . \quad . \quad (51) \\ &= \tanh \frac{\beta}{2} \frac{\bar{\mu}}{\mu}. \end{aligned}$$

\* E. C. Stoner, Proc. Leeds Phil. Soc. ii. p. 56 (1930).

The result is formally the same as that given by the Weiss theory, modified for the quantum  $j=\frac{1}{2}$  case, the molecular field constant being interpreted as  $zJ_0/2\mu l_0$ . While the rigour of the treatment is perhaps open to question, it does show in a simple way how interchange interaction may give rise to molecular field effects, and the difficulties which arise in dealing with energy fluctuations of a crystal are evaded. Moreover, as will be indicated in the next section, this equation is in close agreement with the present results of ferromagnetics.

### *Experimental Results on Ferromagnetics\*.*

The fundamental problems of ferromagnetism are those connected with the nature of the carriers and of the molecular field, and a large number of the experimental results on ferromagnetics are of secondary importance from this point of view. In this section some of the results which are of importance in connexion with the theories which have been discussed will be very briefly summarized, and their significance will be indicated.

*Gyromagnetic Effect.*—The experiments on the gyromagnetic effect show conclusively that in ferromagnetics at ordinary temperatures the ratio of the magnetic to the mechanical moment of the carriers is 2, both moments being measured in Bohr units. This, taken by itself, is consistent with the view that the carriers are (1) free electrons, (2) atoms or ions in S states, or (3) electrons in atoms or ions free to change their orientation. When atoms are in S states, the moment is entirely due to the spin moment  $s$  of the electron; the third possibility differs from the second in that the atom or ion may have an "orbital" moment, but that this is assumed to be ineffective magnetically owing to some kind of " $l$  interlocking" of the different atoms.

*Variation of "Spontaneous magnetization" with Temperature below the Curie Point.*—When  $(\sigma/\sigma_0)$  is plotted against  $(T/\theta)$  the curves for iron, cobalt, and nickel differ little from each other, and lie well above the curve given by the Langevin-Weiss theory. The results of Weiss and Forrer† for nickel are probably the most accurate. The experimental curve has been carefully compared by Tyler‡ with those given by

\* For references see E. C. Stoner, 'Magnetism and Atomic Structure,' 1926, and 'Magnetism,' 1930 (Methuen).

† P. Weiss and R. Forrer, *Ann. de Phys.* v. p. 153 (1923).

‡ F. Tyler, *Phil. Mag.* ix. p. 1026 (1930).

the modified Weiss theory for the various quantum cases ; it is in good agreement with the curve corresponding to  $j=\frac{1}{2}$ , and is quite definitely incompatible with the classical curve, or the quantum curves for higher values of  $j$ . The experimental curve lies slightly below the theoretical for  $T/\theta \rightarrow 0$  and slightly above for  $T/\theta \rightarrow 1$ ; these discrepancies may be of significance, but they are small, and the conclusion can be drawn that to a close approximation the experimental results for the three ferromagnetic elements correspond to magnetic carriers for which  $j=\frac{1}{2}$ . The conclusion as to the carriers is the same as that to be derived from a consideration of a gyromagnetic effect. The form of the magnetization temperature curve is incompatible with the Heisenberg formula, obtained by treating the crystal as a whole, but agrees with that obtained by the modified treatment of the interchange interaction, in which the atoms in the crystal are regarded as separate systems ; this suggests that if the "whole crystal" method is used, the treatment of fluctuations requires considerable modification

*Change of Specific Heat at the Curie Point.*—If the carriers are identified as electrons, and there are  $f$  of these per atom. the change in the gram atomic specific heat at the Curie point will be

$$\Delta S_A = \frac{3}{2} Rf = 3f. \quad . \quad . \quad . \quad . \quad (52)$$

This follows from the "quantized" Weiss theory (eq. 35) or from the interchange interaction theory, as expressed by (51), but not from the original Heisenberg formula, which leads to (45).

Now  $f$  is obtainable directly from the value of the saturation magnetization. If  $p$  is the atomic moment (from saturation) expressed in Weiss units, since the electron moment corresponds to 5 Weiss units

$$f = \frac{p}{5}. \quad . \quad . \quad . \quad . \quad . \quad (53)$$

If there is no change in the number of "magnetic electrons" between low temperatures and the Curie point, the same value for  $f$  should be obtained from (52) and (53). The results for iron and nickel are shown in Table III.

The agreement in the  $f$  values derived in the two ways can leave little doubt that the carriers are electrons (or more precisely that it is the spin moment of electrons which is effective) ; it also shows that the number of

magnetic electrons changes very little, if at all, between low temperatures and the Curie point.

*Thermoelectric Properties.*—Dorfmann and Jaanus\* have recently measured carefully the thermoelectric power of nickel against platinum over a range of temperatures. Their results show that there is a fairly sudden change in the Thomson coefficient for nickel at the Curie point. They have interpreted this as indicating that there is a change in the specific heat of the conduction electrons; and if this view is taken, the magnitude is such that the whole change in the specific heat of nickel at the Curie

TABLE III.

Number of Magnetic Electrons per atom from  
Low Temperature Magnetization and Change  
in Specific Heat.

			<i>f.</i>	
	<i>p.</i>	$\Delta S_A$ .	<i>p</i> /5.	$\Delta S_A$ /3.
Ni .....	3	1.7	0.60	0.57
Fe .....	11	6.8	2.20	2.27

point can be attributed to the change in that of the conduction electrons. It is doubtful whether this interpretation can be maintained; but in any case other considerations † show that the ferromagnetism cannot be due to electrons which are free in the Sommerfeld sense, and the results do not necessarily conflict with the view that ferromagnetism is to be traced to electrons “in atoms” as in Heisenberg’s theory.

*Susceptibility above the Curie Point.*—The possible significance of the temperature variation of susceptibility above the Curie point has been discussed elsewhere ‡. It will be

\* J. Dorfmann, R. Jaanus, and I. Kikoin, *Zeits. für Phys.* liv. pp. 277 & 289 (1929).

† F. Bloch, *Zeits. für Phys.* lvii. p. 545 (1929); E. C. Stoner, *Proc. Leeds Phil. Soc.* ii. p. 50 (1930).

‡ E. C. Stoner, *Proc. Leeds Phil. Soc.* i. p. 55 (1926).

sufficient here to consider some of the values for iron. If there are  $f$  magnetic electrons per atom (that is,  $f$  effectively independent spin moments) the value of  $f$  can be calculated in terms of  $p_A$ , the magneton value per atom, calculated as in (5). Writing  $p_e$  for the magneton value per electron,

$$p_A^2 = f \times p_e^2.$$

Using (20),

$$p_A^2 = f \times \{5g \sqrt{j(j+1)}\}^2$$

$$= f \times (5\sqrt{3})^2,$$

$$f = \frac{1}{3} \left( \frac{p_A}{5} \right)^2.$$

In Table IV. are given the values of  $f$ , so calculated for various states of iron.

TABLE IV.

Values of  $f$  from Paramagnetic Susceptibility.

	$p_A$ .	$f$ .
Fe $\beta_1$ .....	20.9	5.8
$\beta_2$ .....	17.4	4.0
$\gamma$ .....	28.2	10.6
$\delta$ .....	7.05	0.7

It is hardly possible to suppose that the number of quasi-independent effective spin moments per atom could change in this manner, and that the number could be as large as 10. The only possible conclusion seems to be that above the Curie point the orbital moments  $l$  may play a part as well as the  $s$  moments, and the magnetization may then be said to be due to ions (or atoms) as carriers rather than to individual electrons in them. This point of view has already been put forward\* and will not be further discussed here.

The experimental evidence as a whole supports the view that the carriers in ferromagnetics are electrons in atoms, the interchange interaction electrons of Heisenberg's theory.

\* E. C. Stoner, Phil. Mag. viii. p. 250 (1929).

The detailed results of that theory are not in agreement with the observations on ferromagnetics. The observations do, however, agree well with the formal formulæ given by the quantum modification of the Weiss theory for the  $j = \frac{1}{2}$  case, and by a slight change in the treatment of the interaction theory it may be shown that the Weiss molecular field constant is very simply related to the interaction integral.

### *Summary.*

Formulæ for the variation of magnetization with field and temperature are derived, using the quantum modification of the formal Weiss theory of ferromagnetism. These are put into such a form as to facilitate comparison with experiment. The more important are collected in a table. Expressions for the change in specific heat at the Curie point are also given.

The Heisenberg interchange interaction theory is discussed. It leads to a satisfactory interpretation of the molecular field, but gives quantitative results which cannot be reconciled with experiment for the variation of spontaneous magnetization with temperature and for the change in specific heat. This is due to difficulties in the treatment of "fluctuations." If the crystal, instead of being treated as a whole, is regarded as an aggregate of atomic systems, a result is obtained which is formally similar to that of Weiss, modified for the quantum  $j = \frac{1}{2}$  case, the molecular field constant  $N$  being replaced by  $zJ_0/2\mu I_0$ .

The gyromagnetic ratio and the variations of magnetization with temperature indicate that magnetization in ferromagnetics is due to the change of orientation of electrons. The saturation magnetization and the change in specific heat lead to the same value for the number of effective electrons per atom. This indicates that the number of these electrons varies little up to the Curie point. Above the Curie point the variation of susceptibility with temperature leads to magnetic moments per atom which cannot be entirely attributed to the electron spin moments ( $s$ ), but must be partly due to the orbital moments ( $l$ ). Below the Curie point, all the experimental results are compatible with the view that the primary magnetic characteristics are due to the interchange interaction electrons, whose spin moments only are magnetically effective.

IV. *Inductive Ratio Arms in Alternating Current Bridge Circuits.* By R. WALSH, B.Sc. (International Telephone and Telegraph Laboratories Incorporated, Hendon.)\*

INTRODUCTION.

**I**N the practice of alternating current measurement the Wheatstone net is perhaps the most widely used of all devices, and in the course of many years of development the Wheatstone Bridge has been made an instrument of high precision. The chief difficulties which have been encountered in obtaining high accuracy have been concerned with the stray capacities in the circuit and the balance of the ratio arms.

This paper gives a theoretical account of a new type of ratio arms assembly intended to give high stability and high accuracy, which it is hoped will contribute to practical bridge design by rendering more simple the questions of construction and maintenance.

To avoid confusion of terms, it is here convenient to define the various forms of inductively-wound coils that enter into this investigation. They may be distinguished as follows:—

- (a) An “inductance coil” is any coil so wound as to possess inductive impedance between its terminals.
- (b) A “transformer” comprises two or more windings which serve the purpose of providing electromagnetic coupling between two or more independent circuits.
- (c) A “retardation coil” or “retard coil” is a coil of high impedance. It may have divisions in its windings. It has a high ratio between its alternating current impedance and its direct current resistance.

The difficulties of making non-inductive ratio arms are well known, and a large amount of work has been done both as regards the nature of the windings and the method of construction.

The present method departs radically from classical practice in that the bridge ratio is determined by reactive impedances, these being in the form of bifilar windings on a single core.

The essential ideas connected with the use of such highly balanced coils for bridge measurements have been investigated by A. D. Blumlein.

\* Communicated by R. Appleyard.



## 1. THEORETICAL CONSIDERATIONS.

1.10. *Ratio Arms and the Bridge Network.*

In the simple case of a Wheatstone net the condition of balance is

$$\frac{Z_{AB}}{Z_{BC}} = \frac{Z_1}{Z_2}$$

(see fig. 1 a). Therefore, at balance, the ratio between the impedance  $Z_1$  and  $Z_2$ , that is, in general between the standard and the unknown, is determined by the ratio between the two adjacent arms  $Z_{AB}$  and  $Z_{BC}$ . This applies equally well for non-reactive resistances and for complex impedances.

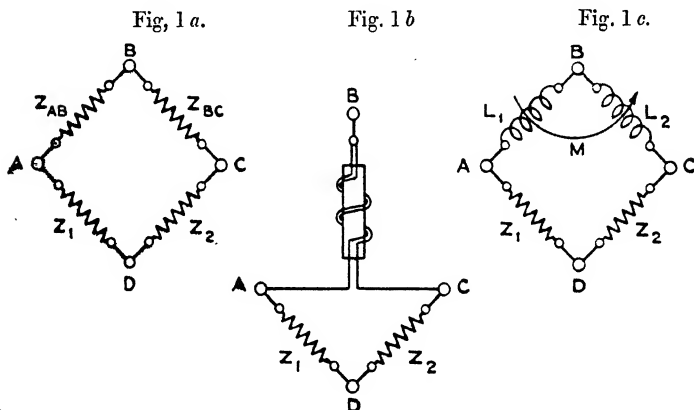


Fig. 1 a.—Wheatstone bridge network.

Fig. 1 b.—Bridge network with inductive ratio arms.

Fig. 1 c.—Simplified arrangement of bridge arms.

1.11. *Retard Coil as Ratio Arms.*

If the windings of a retard coil are used to provide the impedances  $Z_{AB}$  and  $Z_{BC}$  there will be a mutual inductance  $M$  between the arms  $AB$  and  $BC$ , in addition to their self-impedances.

The arrangement will then be as shown in fig. 1 b, and this can be represented more clearly as in fig. 1 c.

The balance conditions for such a network are given by the generalized solution of the Wheatstone net\*. For the purpose of discussion, however, it is more convenient to use

\* B. Hague, 'Alternating Current Bridge Methods,' p. 51.

a well-known transformation in order to remove the complications\* due to the mutual inductance between the arms AB and BC.

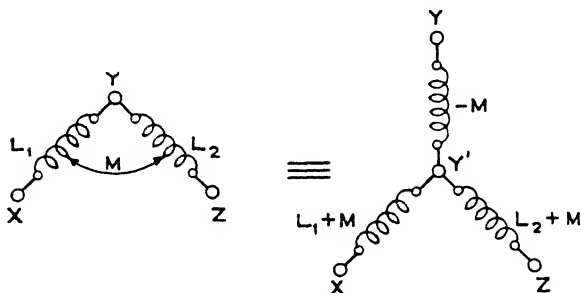
### 1.12. Equivalent Ratio Arms without Mutual Inductance.

The following transformation provides a network which may be considered as exactly equivalent to the original, but which contains no mutual inductance.

The transformation is shown below.

The above transformation (see Hague, 'Alternating Current Bridge Methods,' p. 50) may be directly applied to the Wheatstone net previously shown, which then becomes as in fig. 3.

Fig. 2.



Transformation for mutual inductance.

In practice the impedances

$$R_1 + j\omega(L_1 + M) \quad \text{and} \quad R_2 + j\omega(L_2 + M)$$

will be complicated by the presence of an effective resistance term due to iron losses and eddy current losses in the coil windings, but it is not necessary to introduce these considerations into the discussion, because they may be eliminated by considering  $M$  to be a complex quantity. This is indeed a necessity of the transformation given above, if the equivalent of the two circuits is to hold for practical inductance coils. The present mode of treating the network of the inductance coil windings is, however, adequate to deal with the principal

\* R. Appleyard, "The Solutions of Net-work Problems by Determinants," Proc. Phys. Soc. Lond. xxiv. pt. 4 (June 15, 1912).

sources of error, and further analysis will not be attempted in this paper.

The conditions for balance in a Wheatstone Bridge, *i. e.*, for zero potential difference between points A and C, may be defined solely in terms of the impedance of the four arms AB, BC, CD, and DA, and, therefore, the impedance  $-j\omega M$  which has appeared in the arm B'D will have no influence in determining the point of balance of the bridge.

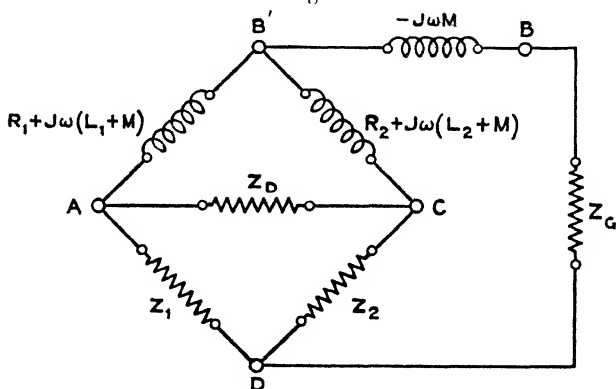
Since at the point of balance

$$\frac{Z_{AB'}}{Z_{B'C}} = \frac{Z_{AD}}{Z_{CD}},$$

the ratio of  $Z_{AD}$  to  $Z_{CD}$  will depend on the ratio of the two impedances

$$R_1 + j\omega(L_1 + M) \quad \text{and} \quad R_2 + j\omega(L_2 + M).$$

Fig. 3.



Bridge network with mutually inductive ratio arms.

This is exactly the same result as would be obtained by considering a bridge network (fig. 1a) having arms AB and BC composed of separate impedances, in the case of the usual types of ratio arms, having the values given above.

The above reasoning shows how two impedances in adjacent arms of a bridge, and having mutual inductance between them, will determine the ratio of the two remaining arms when the bridge is balanced.

In order to use such an arrangement to make accurate measurements, it must be possible rigidly to control the ratio between the two impedances

$$R_1 + j\omega(L_1 + M) \quad \text{and} \quad R_2 + j\omega(L_2 + M).$$

In order that a bridge made on this principle should be useful in practice, it is necessary that this ratio should be accurately an integer and that it should be as nearly as possible wholly real.

In the further discussion the general case outlined above will be dealt with as two cases—one in which the ratio between the bridge arm impedance is 1 : 1, and the other in which this ratio is  $n : 1$ , where  $n$  is an integer.

In considering a Wheatstone net to be used as a measuring instrument, there is another important aspect which will be affected when inductive windings with mutual inductance between them are substituted for the normal resistance ratio arms, namely, sensitivity. This quality of the bridge network is affected by the values of the impedances of all the branches of the structure, and therefore the presence of the impedance  $-j\omega M$  in the generator arm (see fig. 3) must be considered.

If the ratio of the impedance of the Arms AB' and B'C is theoretically exact, then the potential difference occurring between A and C may be considered as due to an inaccuracy in the ratio of the other two arms AD and CD. The value of this potential difference will, moreover, depend on the degree of the above inaccuracy and the current flowing into the bridge at B' and D. Thus, in order to make the potential difference as large as possible for a given departure in the ratio  $Z_{CD}$  to  $Z_{AD}$  from its true balance value, the current into the bridge should be made as large as possible. If no limit is imposed on the value of this current by the conditions of measurement, it will depend on the value of the impedance of the bridge network between the terminals B and D.

In the case of a bridge (fig. 1 *a*) with independent impedances

$$R_1 + j\omega(L_1 + M) = Z_{AB} \quad \text{and} \quad R_2 + j\omega(L_2 + M) = Z_{BC}$$

as ratio arms, the impedance of the bridge network between the terminals B and D will be

$$\frac{Z_{AB} \cdot Z_{BC}}{Z_{AB} + Z_{BC}} + \frac{Z_1 \cdot Z_2}{Z_1 + Z_2},$$

whereas with a retard coil giving equivalent values for the impedance of the ratio arms the value will be

$$\frac{R_1 \cdot R_2}{R_1 + R_2} + \frac{Z_1 \cdot Z_2}{Z_1 + Z_2},$$

owing to the fact that the parallel opposing inductance of the windings of the retard coil is zero.

Since  $\frac{R_1 \cdot R_2}{R_1 + R_2}$ , the D.C. resistance of the coil windings in parallel, will be a small quantity, it will be seen that the impedance of the bridge circuit between terminals B and D will be considerably less when a retardation coil is used in place of the usual resistances.

On the other hand, if the current to be supplied to the bridge (fig. 3) by the generator is limited by the conditions of measurement, then the sensitivity of the bridge will depend on the current in the detector for a given unbalance potential across AC. Current may flow from A to C by three paths, directly through the detector circuit, *via* the point B' or *via* the point D. In order that the maximum proportion may take the direct route, the series aiding impedance of the windings AB', B'C of the retardation coil should be as high as possible. Owing to the bifilar method of winding these coils, there is a limit to the impedance to which they can be wound; moreover, it is important, as will be seen later, that the direct-current resistance of the windings be kept as low as possible. Compromise must therefore be made in designing coils for this purpose between the requirements imposed by the questions of balance and sensitivity.

It will be seen that the impedance of the equivalent ratio arms formed by the coil windings depends on the frequency of the testing current employed. Therefore the design of the coil must be adapted to the frequency range within which it will be required to work. If the impedance to be measured is small, or if an unequal ratio bridge is to be used, the impedance which the bridge circuit presents to the generator will be small, and the input to the bridge should be by means of a transformer of suitable ratio in order to secure the maximum efficiency.

The transformation given in Section 1.11 may also be used to make clear the action of a retardation coil when used to provide an unequal ratio.

If, in fig. 3,  $L_2 = n^2 L_1$ , then the two arms of the equivalent bridge network will have impedances

$$R_1 + \omega L_1 + \omega n \sqrt{L_1}^2$$

and

$$R_2 + n^2 \omega L_1 + \omega n \sqrt{L_1}^2,$$

and these reduce to

$$R_1 + j\omega L_1(1+n)$$

and

$$R_2 + j\omega n L_1(1+n),$$

and it may be seen that, if  $R_2$  is made equal to  $nR_1$ , the total impedance of the arms will be in the ratio  $n : 1$ .

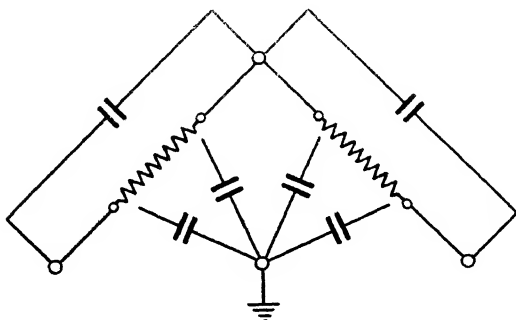
Thus, to secure a bridge ratio of  $n : 1$ , it is necessary to provide a coil whose windings have self inductances in the ratio  $n^2 : 1$  and resistances in the ratio  $n : 1$ .

### 1.20. Effect of Stray Capacities.

One of the principal sources of error in bridges employing resistance ratio arms is that due to the shunting effect of stray capacities on the ratio arms.

These capacities may be either directly in shunt on either arm or they may be to other parts of the bridge or to earth, in which case they act indirectly across the arms.

Fig. 4.



Stray capacities in ratio arms.

The current shunted off through these capacities will be proportional to the e.m.f. across them, which in the case of equal resistance ratio arms will be  $\frac{1}{2} RI$ , where  $R$  is the resistance of each arm, and  $I$  is the current into the bridge.

In the case of retardation coil ratio arms the effect of stray capacities may be examined by the aid of the transformed circuit shown in fig. 5, remembering that the point  $B'$  is inaccessible and all capacities must act at the point  $B$ .

Putting in a capacity acting across the  $BC$  arm, fig. 6 is obtained.

Assuming that the coil gives an impedance ratio of  $n : 1$ , then the e.m.f. across the condenser  $C$  is

$$\begin{aligned} E &= -j\omega(n+1)IM_2 + I\{R_2 + j\omega(L_2 + M)\} \\ &= -j\omega(n+1)InL_1 + I\{R_2 + j\omega(n^2L_1 + nL_1)\}. \end{aligned}$$

Since

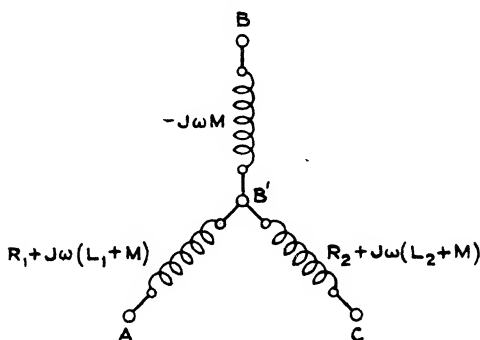
$$M = nL_1 \quad \text{and} \quad L_2 = n^2L_1.$$

Hence

$$E = IR_2.$$

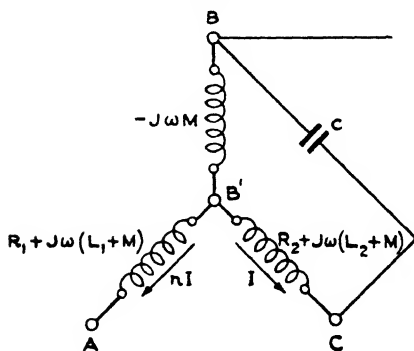
Thus the e.m.f. across the condenser, and consequently the magnitude of its shunting effect, depends on the D.C. resistance of the windings of the retard coil.

Fig. 5.



Transformed circuit for ratio arms.

Fig. 6.



Capacity shunting ratio arms.

### 1.21. Effect of Leakage Coefficient K.

To determine the effect of the leakage coefficient  $K$  in the case of a coil wound to give an unequal ratio, the following assumptions are made:—

- (1) The coil consists of  $(n+1)$  identical windings.
- (2) The mutual inductance between any pair of sections is the same, and is  $KL_1$ , where  $L_1$  is the inductance of any section.

This arrangement is as in fig. 7 a.

The equivalent star network may then be represented as is fig. 7 b.

Taking account of assumption (2) above, the value of  $L_2$  is given by

$$nL_1 \{1 + (n-1)K\}.$$

Fig. 7 a.

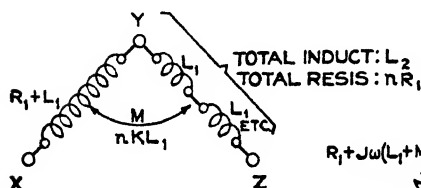


Fig. 7 b.

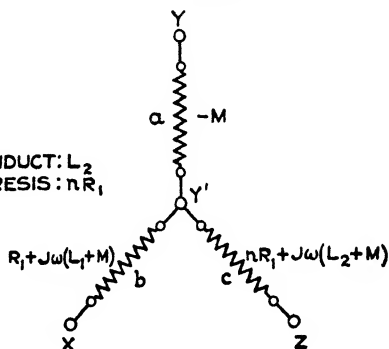


Fig. 7 a.—Network for unequal ratio arms.

Fig. 7 b.—Resolved network for unequal ratio arms.

Therefore the network is completely determined, the branch impedance being as below :—

- (a)  $-j\omega nKL_1$ ,
- (b)  $R_1 + j\omega L_1(1 + nK)$ ,
- (c)  $nR_1 + j\omega nL_1 \{1 + (n-1)K\} + j\omega nKL_1$ .

The ratio of the bridge-arm impedances, therefore, is

$$\begin{aligned} \frac{R_1 + j\omega L_1(1 + nK)}{nR_1 + j\omega \{1 + (n-1)K + K\}nL_1} \\ = \frac{R_1 + j\omega L_1(1 + nK)}{n \{R_1 + j\omega L_1(1 + nK)\}} \\ = \frac{1}{n}. \end{aligned}$$



Therefore the leakage factor  $K$  does not introduce any error into the impedance ratio of the coil.

### 1.30. The Unity Ratio Case.

Referring to fig. 3, a unity ratio Wheatstone net may be obtained by writing  $L_1 = L_2 = M$ .

Errors may arise from two principal causes, namely, unbalances in the coil itself and capacities between the coil and the rest of the bridge circuit.

The errors in the coil itself may arise from unbalances in the self inductances in the halves of the winding, or from internal skew capacities affecting the symmetry of the winding.

The errors arising in the coil itself are complex in nature, and the following treatment deals only with the simplest factors.

In general it is sufficient to say that if these inherent unbalances in the coil are not small enough to neglect altogether—that is to say, if they cause the impedances of the two arms to differ by more than a few parts in a million—then some means would be necessary for their adjustment, and the resulting ratio arm assembly would have little advantage over resistive arms.

As a matter of interest it may be pointed out that an adjustment of retard coil ratio arms may be made by means of a resistance slide wire to balance the direct current resistance of the windings, and a variable condenser connected from the extremity of one of the arms to a point in the generator arm, which is connected to the mid-point of the retard coil through 500 ohms. This expedient is, however, not really practicable, and would introduce undesirable complications.

It may be assumed for the time being that coils may be so constructed that the inherent unbalance of the two halves is within the limits of 10 parts in a million. The direct current resistance unbalance of the windings can be reduced to 0.01 ohm, so that the errors due to this cause are negligible.

In this case the effect of external capacities may be determined at once. Referring to the fig. 3 above, and assuming a unity ratio bridge, the circuit conditions when a single external capacity exists can be shown, as in fig. 8.

Considering the bridge at the point of balance, the voltage across the condenser  $C$  is

$$-2I_1j\omega L + (R + 2j\omega L)I_1 = V.$$

$$V = RI.$$

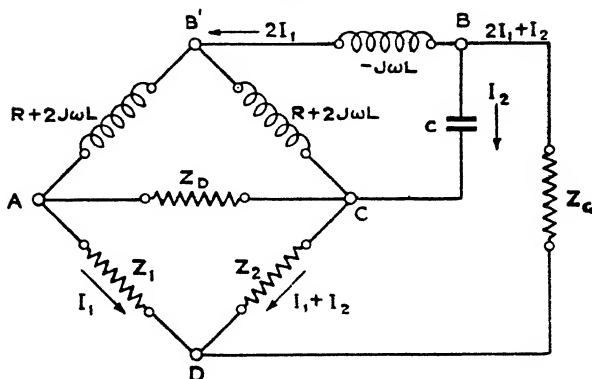
Also at balance, since A and C are at the same potential

$$I_1 Z_1 = (I_2 + I_1) Z_2,$$

and hence

$$\begin{aligned} \frac{Z_1}{Z_2} &= 1 + \frac{I_2}{I_1} \\ &= 1 + \frac{V}{Z_c I_1}, \end{aligned}$$

Fig. 8.



Capacity shunting one ratio arm.

where  $Z_c$  is the impedance of the condenser

$$= 1 + \frac{j\omega CR I_1}{I_1}.$$

$$\begin{aligned} \therefore \frac{Z_1}{Z_2} &= 1 + j\omega CR \\ &= 1 + jp \quad (\text{say}). \end{aligned}$$

If, then, values be assumed for  $Z_1$  and  $Z_2$ , the percentage errors in measurement may be calculated by substitution in the equation arrived at above.

### 1.31. Errors due to Capacity C Bridged Across One Ratio Arm.

$$\frac{Z_1}{Z_2} = 1 + jp \quad \text{from above.}$$

Put

$$Z_1 = R_1 + jX_1,$$

$$Z_2 = R_2 + jX_2.$$

Then  $R_1 + jX_1 = R_2 + jX_2 + jpR_2 - pX_2$ .

$$\therefore R_1 = R_2 - pX_2$$

$$\text{and } X_1 = X_2 + pR_2;$$

and writing  $Q$  for  $\frac{X_2}{R_2}$ ,

$$R_1 = R_2(1 - pQ) \quad \text{and} \quad X_1 = X_2\left(1 + \frac{p}{Q}\right).$$

Substituting values for  $p$  and  $Q$ , the percentage errors in any particular case may be evaluated.

These figures may be used to show that the measurement of effective resistance is subject to greater errors when the time constant of the impedance is high, while the measurement of reactance is least accurate for impedances of low-phase angle. This, however, is not a fault particular to the type of bridge here described; it is present in nearly all inductance measurements.

#### 1.40. The Unequal Ratio Case.

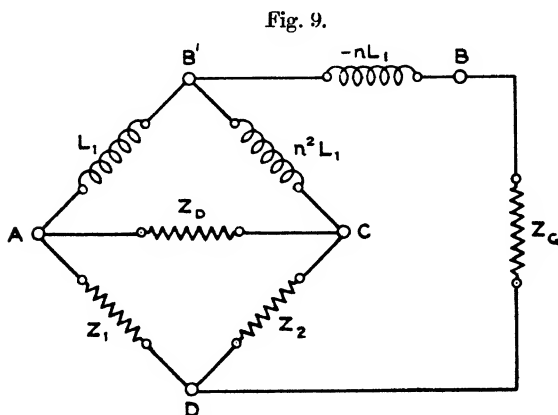
Referring again to fig. 3, we have

$$L_2 = n^2 L_1 \quad \text{and} \quad M = \sqrt{L_1 L_2} = n L_1.$$

It may also be arranged that

$$R_2 = n R_1;$$

then the equivalent bridge network without mutual inductance may be shown thus:—



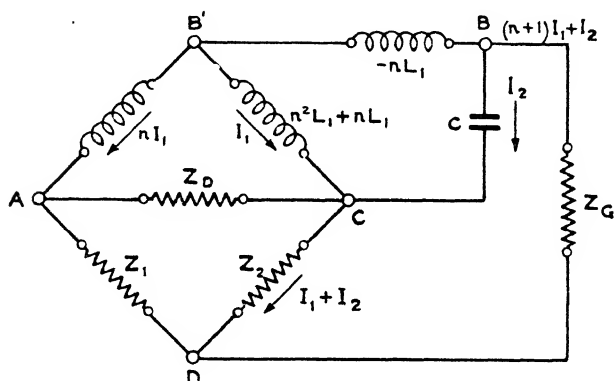
Equivalent bridge network.

The inductance of the two halves of the windings of the coil are in the ratio  $n^2:1$ . Therefore the number of turns on the two halves of the coil must be in the ratio  $n:1$ —namely, the same ratio as that of the required bridge ratio.

#### 1.41. Errors due to Capacity Bridged Across One Ratio Arm.

Assuming that the inherent unbalances in the coil do not appreciably affect the ratio, the effect of external capacities may be shown as follows:—

Fig. 10.



External capacities in unequal ratio arms.

The voltage across the condenser C is

$$-(n+1)nj\omega L_1 I_1 + nR_1 + n(n+1)j\omega L_1 I_1 = V.$$

$$\therefore V = nR_1 I_1.$$

Also at balance the points A and C are at the same potential.

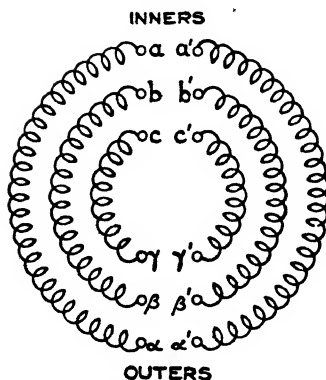
$$\therefore nI_1 Z_1 = Z_2 (I_1 + I_2).$$

$$\therefore \frac{Z_1}{Z_2} = \frac{I_1}{n} \left( 1 + \frac{I_2}{I_1} \right)$$

$$= \frac{1}{n} + \frac{I_2}{nI_1}.$$

$$\begin{aligned}
 \therefore \quad \frac{Z_1}{Z_2} &= \frac{1}{n} + \frac{V}{Z_c n I_1} = \frac{1}{n} + \frac{n I_1 R_1}{Z_c n I_1} \\
 &= \frac{1}{n} + \frac{R_1}{Z_c} \\
 &= \frac{1}{n} \left( 1 + n \frac{R_1}{Z_c} \right) \\
 &= \frac{1}{n} (1 + n R_1 j \omega C) \\
 &= \frac{1}{n} (1 + j n p).
 \end{aligned}$$

Fig. 11.



Multifilar windings.

It follows from the above that the errors calculated for the unity ratio cases will apply for the case of  $n : 1$  ratio when they are multiplied by  $n$ . That is,

$$R_1 = \frac{R_2}{n} (1 - p n Q),$$

$$X_1 = \frac{X_2}{n} \left( 1 + \frac{p n}{Q} \right).$$

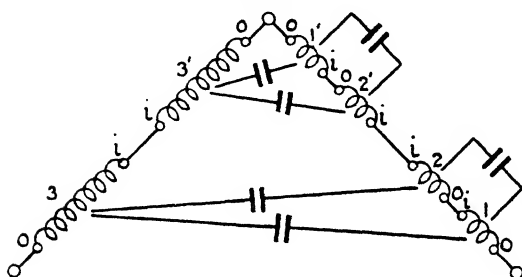
#### 1.50. Windings of a Retard Coil to give a 2 : 1 Ratio.

The distribution of the windings on a 2 : 1 ratio coil is indicated in fig. 11.

The winding consists of two sections of trifilar wire. The two possible methods of making the connexions are as below :—

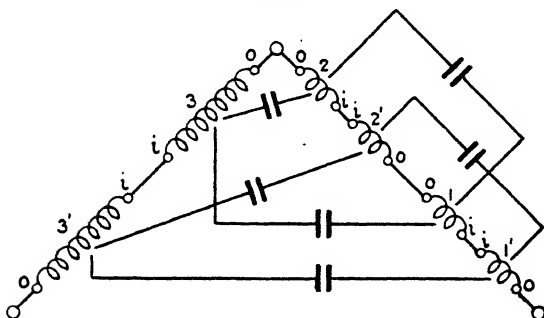
1. Join  $c, c'$  ;  $a, a'$  ;  $b, b'$  ; also  $\alpha, \beta$  ;  $\gamma, \alpha'$  ;  
then the winding is divided in 2 : 1 ratio at the point  $\gamma, \alpha'$ .
2. Join  $c, c'$  ;  $\alpha', \alpha$  ;  $a', B'$  ;  $\beta, a$  ; also  $b, b'$  ;  
then the winding is divided in 2 : 1 ratio at the point  $\gamma', \alpha'$ .

Fig. 12.



Arrangement No. 1 for capacities of windings.

Fig. 13.



Arrangement No. 2. for capacities of windings.

The above diagrams show the distribution of the major capacities corresponding to the two possible methods of making the connexions in a 2 : 1 ratio coil wound with trifilar wire in two sections.

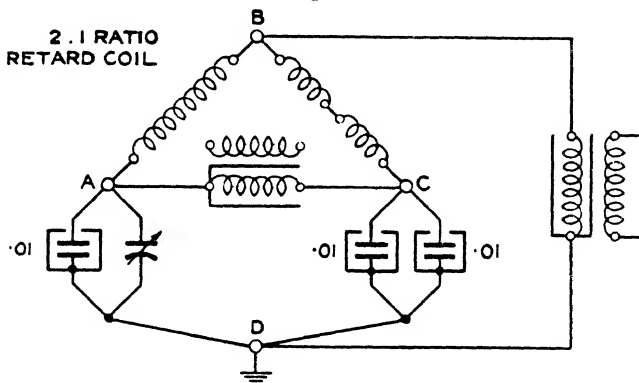
## 1.51. Accuracy of 2 : 1 Ratio Coil.

The exactness of the impedance ratio is checked in the following manner:—

A bridge is set up as shown in fig. 14, and the unbalances between each of the three fixed condensers and the other pair in parallel is measured on the air-condenser. If the ratio of the bridge arms is exactly 2 : 1, then the sum of these unbalances should be zero.

The error in the ratio can be determined from a consideration of the figures obtained from this test. In practice it is found that of the two arrangements of connexions mentioned above arrangement No. 1 is the better, and by using it a

Fig. 14.



Arrangement for checking the accuracy of 2 : 1 ratio arms.

2 : 1 ratio may be obtained which is accurate to about 1 in 1000.

It is realized that, owing to the multiplicity of windings and the unavoidable skewness of the capacities, the same accuracy cannot be expected from unequal ratios as from unity ratio coils; but since for all the most precise work a unity ratio bridge would be used, this is not of great importance.

## 1.60. Shielding\*.

The construction of the coil does not allow the ratio arms to be shielded from one another, as is usual in shielded bridges, and instead the ratio arms form a single unit in a common shield.

\* G. A. Campbell, "The Shielded Balance," 'Electrical World' (1904).

The rest of the shielding of a bridge circuit is also affected and generally simplified by the presence of the retard coil ratio arms in consequence of their property of suppressing the effect of capacities shunted across them.

The detailed treatment of the retard coil, both in its design and its relation to the shielding of the bridge, depends on the particular purpose for which it is intended.

Certain typical cases will therefore be discussed in some detail.

## 2. APPLICATION.

### 2.10. Impedance Bridges.

The coil to be used for impedance bridges will depend on the nature of the impedances to be measured and the frequency at which the bridge is to be used.

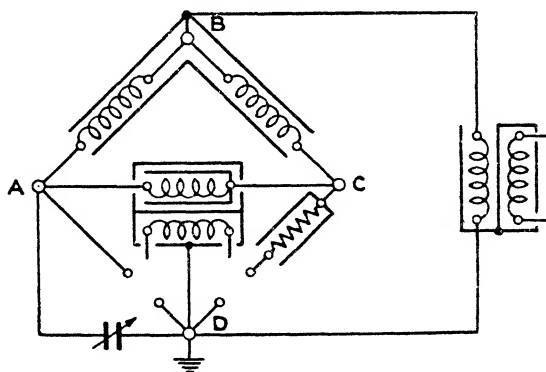
Referring to paragraph 1.11 the equivalent series impedance of the windings of the retard coil in the bridge network is

$$R_1 + R_2 + j\omega(L_1 + L_2 + 2M),$$

and this should be made approximately double the mean value of the impedance to be measured, provided this is not small compared with the impedance of the detector.

2.11. A suitable shielding scheme\* for such a bridge is shown below if the measurements may be made with one end of the unknown to earth.

Fig. 15.



Shielded impedance bridge.

\* An account of a complete shielding scheme for an impedance bridge will be found in a paper by M. G. Fergusson, "Shielded Impedance Bridge," *Bell Technical Journal*, vi. p. 142 (1927).



2.12. Such a bridge may be constructed so that the capacity unbalance across the ratio arms does not exceed 1000 mmf.

Referring to paragraph 1.31, we may now assume the following values:—

$$C = 1000 \text{ mmf.},$$

$$R = 10\omega \times 10 \text{ ohms},$$

$$\omega = 10,000,$$

$$\frac{X_2}{R_2} = 200,$$

then the error in resistance reading due to the capacity  $C$  is

$$100pQ \text{ per cent.}$$

$$= 100\omega CR \frac{X_2}{R_2} \text{ per cent.}$$

$$= 100 \times 10,000 \times 1000 \times 10^{-12} \times 10 \times 200$$

$$= 2 \text{ per cent.},$$

and the error in reactance reading

$$= 100 \frac{p}{Q} \text{ per cent.}$$

$$= 5 \times 10^{-5} \text{ per cent.}$$

The above would correspond to the measurement of a high-phase angle inductance coil. If, on the other hand, a value of  $Q=1$  were taken, the errors would be

$$\text{Error in } R_2 = 0.01 \text{ per cent.},$$

$$\text{Error in } X_2 = 0.01 \text{ per cent.}$$

## 2.20. *Capacity Bridges.*

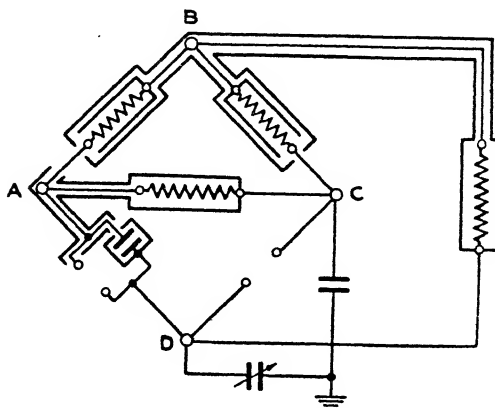
The shielding of a type of equal ratio comparison bridge for the measurement of capacity is shown below (omitting the earthing screen) when resistance ratio arms are used.

The shielding of the AD and CD arms is comparatively simple in the case of a capacity bridge, and a suitable arrangement with retard coil ratio arms is shown in fig. 17.

Such a bridge, in addition to making accurate measurements of mutual capacity in the usual way, may be used for measurements of direct capacity in a manner which requires one reading only to be taken.

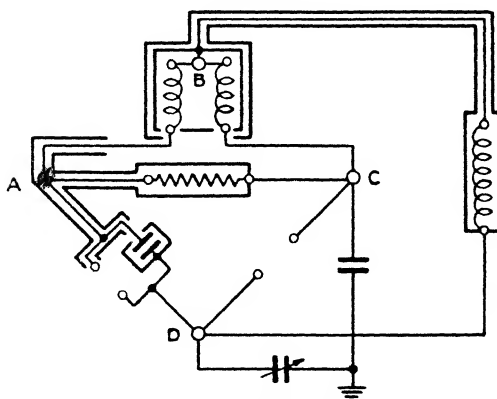
For example, in the case of a three-terminal system, as in fig. 18, if it is required to measure the direct capacity  $C_{bc}$ , the conductors A, B, and C would be connected respectively to the B, C, and D corners of the bridge (see fig. 16), so that

Fig. 16.



Shielded bridge with resistance ratio arms.

Fig. 17.



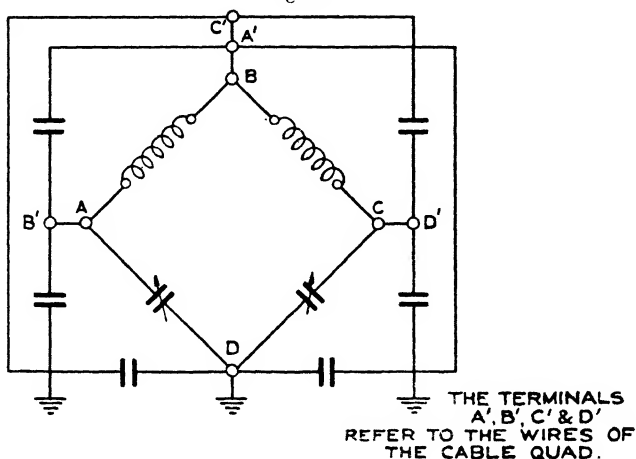
Shielded bridge with mutually inductive ratio arms.

the capacity  $C_{ab}$  is shunted by the ratio arms, and the capacity  $C_{ac}$  is across a diagonal of the bridge.

This method gives very good results provided that  $C_{be}$  is

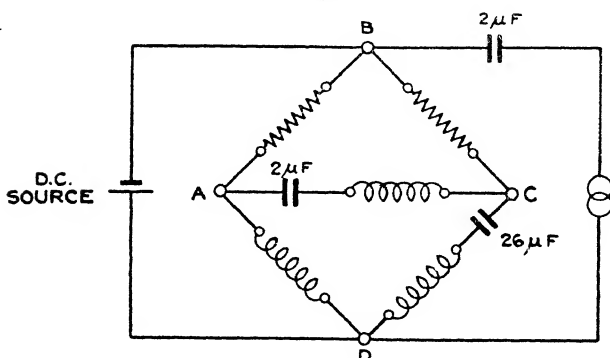
not small compared with  $C_{ab}$  and that it is not required to find the conductance of  $C_{be}$ , since in the latter case errors of upwards of 10 per cent. will often be found.

Fig. 18.



Measurement of direct capacity.

Fig. 19.



Bridge for alternating current measurements with superimposed direct current.

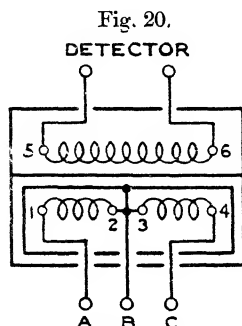
2.30. It is sometimes necessary to use superimposed direct current while making A.C. measurements, as in the bridge circuit shown in fig. 19.

In this case there is difficulty in securing large values of direct current in the impedance tested if the usual 1000 ohm ratio arms are used on the A.C. bridge. This provides another example of the use of retardation coils, as they would very materially increase the efficiency of such a bridge from the D.C. point of view, the power loss being about 1/100 of that encountered when ratio arms of 1000 ohms are used.

#### 2.40. *Incorporation of a Detector Winding.*

An alternative form of inductive winding used as ratio arms exists in the form of the "hybrid coil" or three winding transformer.

This type of coil can be used to provide the input winding and the ratio arms.



Incorporated detector winding.

It is possible to apply the type of winding described in this paper to improve the balance obtained on such a coil.

Similarly, a detector winding may be added to the usual windings described in the preceding pages, thus avoiding the necessity for an output transformer to the bridge. In this case the detector winding would be separated from the ratio arm windings by a complete electrostatic screen. The success of this arrangement depends on the completeness of this screen, and in any case such additional windings tend to disturb the exact balance obtained with the bifilar windings alone. This arrangement is shown in fig. 20, above.

### 3. *RÉSUMÉ OF PRINCIPLE AND ADVANTAGES.*

The essential points in the production of retard coil ratio arms are the use of a toroidal core and multifilar windings. The material of the core should have high permeability, in

order that the direct current resistance of the windings may be as low as possible.

The advantages of the use of these coils may be summarized.

The ratio arms assembly can be made a compact unit which easily fits into any shielding scheme; moreover, the use of retard coil ratio arms often simplifies the shielding.

By correct design of the coil, the sensitivity of the bridge can be made higher than with resistance ratio arms when the sensitivity depends on the current which can be drawn from a given generator.

When the current through the unknown impedance is specified, the sensitivity is approximately the same as with resistive ratio arms.

The measurement of impedances at frequencies between 5,000 and 20,000 is rendered much easier, as the effect of small capacities, which is so great with resistive ratio arms, is reduced by the use of retardation coils.

Retardation coil ratio arms are very stable, since their balance is not affected by temperature effects, and it has been found that they can be more safely relied on than the best resistance ratio arms; they are, too, more easily constructed when high quality ratio arms are required, and the cost is probably less when the degree of balance required is better than 1 in 1000.

Most of the coils made up so far for experimental purposes have been wound on a silicon steel core, although a successful experiment was made with iron dust in the case of a coil for a carrier frequency bridge. The high permeability of permalloy suggests that this material would be excellent as a core material for high quality retardation coil ratio arms.

The advantages of permalloy as a core material would lie in the ability to secure a sufficiently high inductance with low D.C. resistance, and in the very good value of the coupling factor obtained on such a core.

In conclusion, while the adaptation of such coils to precision apparatus is still in the experimental stage, it is believed that they will find a wide application in high frequency alternating current measurements.

The author wishes to express his indebtedness to the International Standard Electric Corporation for permission to publish this paper.

V. *The Influence of Chemical State on Critical X-Ray Absorption Frequencies.* By Prof. H. R. ROBINSON, F.R.S., and C. L. YOUNG, B.Sc.\*

ALTHOUGH X-ray spectral terms are dependent mainly on nuclear charge, it has been known for some years that they are slightly displaced by changes in the state of chemical combination of the atom. The smallness of the effect is sufficiently well indicated by the length of time which elapsed before its discovery. It was first observed for X-ray absorption edges in 1920, and for emission lines in 1924. There is now an extensive literature of experimental work on this subject, much of which has been summarized in Siegbahn's 'Spectroscopy of X-rays' and in Lindh's 'Report' †. Finally, Aoyama, Kimura, and Nishina have succeeded in accounting quantitatively for the magnitudes of the displacements in certain cases ‡.

In view of well-known difficulties—particularly in connexion with the complex fine structure of absorption edges, which is still far from completely understood—it is desirable that the problem should be attacked from as many sides as possible. It is clearly one which lends itself to experimental investigation by the magnetic spectroscopy of the photoelectrons ejected from an element and its compounds by a primary X-radiation of suitable frequency. The details of this method, as applied to the determination of X-ray energy levels, are given fully in an earlier paper §.

Briefly, the element or compound under examination is made the "target" of a bombardment by homogeneous X-radiation. Pencils of the resulting secondary cathode rays are defined by a suitable slit system, and guided and focussed by a uniform magnetic field in such a manner that they produce accurately measurable traces on a photographic plate. The measurements lead to the value

\* Communicated by the Authors.

† Lindh, *Phys. Zeitschr.* xxviii. p. 92 (1927).

‡ Aoyama, Kimura, and Nishina, *Zeitschr. f. Physik*, xlv. p. 810 (1927).

§ Robinson, *Proc. Roy. Soc. A*, civ. p. 455 (1923).

of the product  $rH$ , where  $H$  is the magnetic field strength and  $r$  the radius of curvature of the path of the electron, which is arranged to be perpendicular to  $H$ . From  $rH$  the kinetic energy  $W$  of the electron may readily be deduced; for small velocities it is given very nearly by  $k(rH)^2$ , where  $k$  is a constant which is known in terms of fundamental atomic constants. Then if  $\nu_1$  is the frequency of the primary X-radiation, and  $\nu_a$  the critical absorption frequency of the atomic level under investigation, we have  $\nu_a = \nu_0 - k(rH)^2/h$ , or  $\nu_a = \nu_0 - A(rH)^2$  where  $A$  is another known constant.

If  $\nu_a + \Delta\nu_a$  is the frequency of a neighbouring level, and  $r - \Delta r$  the corresponding value of  $r$ , we have

$$\Delta r = \frac{\Delta\nu_a}{2AH^2r} = \frac{r\Delta\nu_a}{2(\nu_0 - \nu_a)} \quad (1)$$

In comparing two neighbouring levels, we have to measure accurately the distance between the corresponding lines on the photographic plate; with our apparatus this distance is almost exactly  $2\Delta r$ .  $\Delta r/\Delta\nu_a$  may therefore be taken as a measure of the "dispersion." If  $\Delta\nu_a$  is the displacement produced in a given level by a change in the chemical state of the atom,  $\Delta\nu_a$  is always small—of the order 1 Rydberg unit, or less. High dispersion is therefore essential.

There are obvious practical objections against increasing  $r$  above 5–10 cm. If  $\nu_0 - \nu_a$  is made very small, another practical difficulty arises, as a result of the rapid falling off of the photographic efficiency of slow electrons with diminishing velocity. Theoretically the practical difficulties may be overcome, and the dispersion increased almost indefinitely, by introducing a suitable combination of retarding and accelerating fields along the trajectories of the electrons. This plan, however, has the not uncommon defect of being simpler in conception than in execution.

In 1926 one of us, with Mr. A. M. Cassie, applied the method of magnetic spectroscopy to the problem of these displacements produced by change in chemical state, using a fairly soft primary radiation (copper  $K\alpha$ ). There are, however, other difficulties, besides those directly due to the low photographic efficiency of the electrons, in the

\* Cf. Ledrus, *Comptes Rendus*, clxvi, p. 383 (1923).

investigation of regions of the photographic plate corresponding to small values of  $\nu_0 - \nu_a$ . These are principally difficulties arising from the continuous background of scattered and straggled electrons, and from the ease with which slow electrons are diffused by irregularities in the target surface. For these reasons, although the experiments of 1926 were sufficiently good to show the displacements in question, it was not possible to obtain photographs which could be measured with sufficient accuracy to warrant publication.

We have recently, in the course of other work, been able to develop a satisfactory technique for slower electrons than those previously recorded, and to measure the displacements with much greater accuracy. Using copper  $K\alpha_1$  as primary X-radiation (frequency = 592.8 Rydberg units ( $\nu/R$ )), we have been able to measure the difference between the K level of chromium in the metallic state and as hydroxide. This involves the photography of electrons with energies just under 2000 electron-volts—which we have so far found to be near the practical limit at which we can work without excessively long exposures and without resorting to the use of Schumann plates.

According to the measurements of Lindh\*, the level values are :—

Chromium, element, K edge,  $\nu/R = 440.99$ .

$\text{Cr}(\text{OH})_3$            ,,           K edge,  $\nu/R = 441.95$ .

Taking 5 cm. as radius of curvature of the paths of the secondary cathode rays, and assuming that the same values of  $\nu/R$  are applicable in our experiments, this difference would correspond to a shift of just over 0.03 cm. on the photographic plate (Eqn. 1 above). This is not large, but it is many times greater than our errors of measurement on a good line, and would not be difficult to detect in the normal course of our experiments.

In order to make the test as rigorous as possible, we modified the experimental procedure in such a way as to eliminate possible errors in setting the photographic plate or in measuring the absolute distances of the lines from the fiducial line. The K lines of  $\text{Cr}(\text{OH})_3$  and metallic

\* Lindh, *Zeitschr. f. Physik*, xxxi. p. 210 (1925).



chromium were photographed on the same plate in successive exposures, the plate being kept fixed in the plate-holder while the target was changed, and different halves of the plate being exposed in the two cases. The normal and displaced K lines are thus obtained in positions which enable the displacement to be measured with the greatest possible accuracy, and with no possibility even of minor errors which might conceivably occur through minute shrinkage or expansion of the photographic emulsion during manipulation. In controlling experiments it was shown, by reversing the order of the portions of the photographic plates used to record the lines of the element and the hydroxide respectively, that there was no sensible error due to any possible lack of symmetry in the apparatus.

The result of the measurements on metallic chromium is :— $rH=153.2$  cm. gauss ; equivalent  $\nu/R$  calculated 153.0 Rydberg units. Hence K critical frequency for metallic chromium  $= (592.8 - 153.0) = 439.8$  Rydberg units, in good agreement with Lindh's value. These two values are not strictly comparable, as the calculation involves fundamental atomic constants which are not known with sufficient accuracy. For this reason, we have not attempted to measure the absolute energy of the line with any very high accuracy. The difference between this and the line for  $\text{Cr}(\text{OH})_3$  has, however, been measured with great care. Errors in the fundamental constants and systematic errors in our measurements do not appreciably vitiate the values obtained for small differences of this kind.

We find, as the mean of measurements on a number of plates, obtained with different magnetic fields, that the K line of  $\text{Cr}(\text{OH})_3$  is displaced, relative to that of the element, in the sense indicated by the X-ray spectroscopic results. In other words, the secondary cathode rays emerge from the K level of the chromium atom in the compound with appreciably smaller velocities than those from the K level of the element. This in itself is very satisfactory in view of recent evidence of the extreme complexity of the absorption edges even of elements. We find, however, instead of Lindh's difference of 0.96 Rydberg unit, about half this value. In round figures, the mean of our measurements gives  $\Delta\nu_a/R=0.5$  Rydberg unit with a probable error—fairly generously estimated—of

$\pm 0.15$  unit. It is therefore practically certain that the displacement as measured by corpuscular spectrometry is appreciably less than that obtained by Lindh with the X-ray spectrometer. Further work on this is desirable, as such a difference, if it is real, must be significant.

We cannot, of course, be quite certain that our chromium hydroxide target remained unchanged throughout an exposure; it seems at least possible that the surface layers, which alone are effective, become dehydrated during an intense X-ray bombardment *in vacuo*. Lindh's results do not include a value for the K edge of chromium in  $\text{Cr}_2\text{O}_3$ . In an earlier paper Coster\* has given a value for the oxide, but no measurement for the element, so no data are available for the direct comparison of the levels. So far as can be judged from a comparison of results which are common to Lindh and Coster, there is not likely to be a large difference between the K levels in the oxide and the hydroxide respectively. Dehydration therefore does not appear to afford a plausible explanation of the discrepancy.

We have two photographs, taken with relatively large magnetic fields, which also show the "fluorescent" corpuscular lines, due to the internal conversion of the K energy of the excited chromium atoms. The effects here are more complicated, as more than one level is involved, but there is definite evidence of displacements of the fluorescent lines in compounds. The displacements are of the same order of magnitude as those of the secondary cathode rays, but we have not yet made sufficiently accurate measurements to enable us to communicate any definite results in these regions.

Much of the material used in this work was purchased by means of a grant from the Government Grant Committee of the Royal Society, for which we desire to make acknowledgment. The metallic chromium used was in the form of a thin plating on copper, for which we are indebted to the Research Department of the Metropolitan-Vickers Electrical Company.

\* Coster, *Zeitschr. f. Physik*, xxv. p. 83 (1924).

VI. *Studies in Coordination. Part I.—Ion Hydrates.*

A Correction. By F. J. GARRICK, B.A.\*

IN the author's paper under the above title (Phil. Mag. ix. p. 131, 1930) one of the equations used is incorrect. This is equation (7), p. 139, and should read as follows:—

$$F_E = p \cdot \frac{\partial E}{\partial r} = -\frac{2zep}{r^3} + \sum_{k=1}^{k=(n-1)} p^2/s_k^4 \cdot 3(1 + \cos^2 \theta) \cos \theta.$$

TABLE I.

Ion.	<i>n</i> .	<i>r</i> .	$-\phi_E$ .	$-\phi_{R_1}$ .	$-\phi_{R_2}$ .	$-\phi$ .
Na <sup>+</sup> .....	{ 4	2.05	132	27	1	104
	{ 6	2.19	138	21	3	114
	{ 8	2.44	120	9	9	102
K <sup>+</sup> .....	{ 6	2.54	106	21	1	84
	{ 8	2.73	101	15	3	83
Rb <sup>+</sup> .....	{ 6	2.67	96	20	0	76
	{ 8	2.84	95	15	2	78
Cs <sup>+</sup> .....	{ 6	2.88	83	16	0	67
	{ 8	3.02	85	13	1	71
	{ 12	3.34	77	7	23	47
Mg <sup>2+</sup> .....	{ 4	1.64	631	141	9	481
	{ 6	1.78	606	93	26	487
	{ 8	2.03	494	34	54	406
Ca <sup>2+</sup> .....	{ 6	2.05	454	99	6	349
	{ 8	2.23	417	62	21	334
Sr <sup>2+</sup> .....	{ 6	2.17	402	92	4	306
	{ 8	2.33	385	65	13	307
Ba <sup>2+</sup> .....	{ 6	2.37	332	66	1	265
	{ 8	2.49	339	43	7	289
	{ 12	2.73	326	35	174	117

The effect of the error is small ; most of the values for *r* in Table III. of the paper are slightly too large, but the values of  $-\phi$  are for the most part nearly correct. The present note gives the revised results (Table I.).

It will be seen that the conclusions reached in the former paper hold good in every case except that of Rb<sup>+</sup>, for which

\* Communicated by the Author.

it now appears that the coordination number is definitely 8, in agreement with Sidgwick's Rule. The agreement between this rule and the theory is now complete, as shown.

Ion.	Coord. No. (found).	Coord. No. (Sidgwick Rule).
Na, K, Mg, Ca .....	6	6
Rb, Cs, Sr, Ba .....	8	8

Inorganic Chemistry Dept.,  
The University,  
Leeds.

VII. *Studies in Coordination.* Part II.—*Ion Ammoniates.*  
By F. J. GARRICK, B.A.\*

IN previous papers † it was shown that the electrostatic theory of coordination as there developed led to coordination numbers for ion hydrates in agreement with the general covalency rule of Sidgwick. In the present paper this theory is extended to amino-compounds. The necessary data are as follows :—

1. *Force Constants.*

Rankine and Smith ‡ give for  $\text{NH}_3$  and Ne  $\pi\omega^2 = 0.640$  and  $0.417$  respectively. This, with the assumptions made in paper I., gives

$$\frac{\sigma_{\text{NH}_3}^{(\nu)}}{\sigma_{\text{Ne}}^{(\nu)}} = 1.24.$$

From this, with the generalized diameters of Ne and various ions as given in paper I., the force constants are derived in the usual way.

\* Communicated by the Author.

† Garrick, Phil. Mag. (Jan. 1930); see also the correction published later (*suprà*, p. 76). These two papers will be referred to as I. and I. (a) respectively.

‡ Rankine and Smith, Phil. Mag. xlii. p. 601 (1921).

2. *Electrical Constants.*

The permanent dipole moment (P) of the ammonia molecule is given by Jona \* as  $1.44 \times 10^{-18}$  E.S.U. The deformability ( $\alpha$ ) is obtained from the index of refraction of ammonia gas for visible frequencies (Landolt-Börnstein) by the relation

$$\frac{n^2-1}{n^2+2} \cdot \frac{M}{d} = \frac{4}{3} \pi N \alpha,$$

and is found to be  $2.21 \times 10^{-24}$ . Using these data, the calculation is carried out exactly as described in the previous papers. The results are shown in the Table, where the symbols have the same significance as before:—

Ion.	$n$ .	$r$ .	$-\phi_E$ .	$\phi_{R_1}$ .	$\phi_{R_2}$ .	$-\phi$ .
Na <sup>+</sup> ..	{ 4	2.26	105	23	1	81
	{ 6	2.41	111	18	3	90
	{ 8	2.69	97	8	8	81
K <sup>+</sup> .....	{ 6	2.70	89	18	1	70
	{ 8	2.91	85	13	4	68
Rb <sup>+</sup> .....	{ 6	2.83	81	17	1	63
	{ 8	3.02	80	13	3	64
Cs <sup>+</sup> .....	{ 6	3.04	70	14	0	56
	{ 8	3.19	72	12	1	59
	{ 12	3.52	68	7	4	57
Mg <sup>2+</sup> .....	{ 4	1.73	607	141	10	456
	{ 6	1.91	543	79	32	434
	{ 8	2.22	420	23	56	341
Ca <sup>2+</sup> .....	{ 4	2.02	411	115	2	294
	{ 6	2.17	415	90	9	316
	{ 8	2.39	365	51	27	287
Sr <sup>2+</sup> .....	{ 6	2.28	371	88	5	278
	{ 8	2.48	340	55	18	267
Ba <sup>2+</sup> .....	{ 6	2.48	306	70	2	234
	{ 8	2.63	301	52	10	239
	{ 12	2.93	279	23	22	231

From the Table the favoured coordination numbers are found to be as follows:—Mg<sup>2+</sup>, 4; Na<sup>+</sup>, K<sup>+</sup>, Ca<sup>2+</sup>, and Sr<sup>2+</sup>, 6; Rb<sup>+</sup>, Cs<sup>+</sup>, and Ba<sup>2+</sup>, 8. These numbers agree with the coordination numbers of the elements according to Sidgwick's Rule with two exceptions, namely Mg<sup>2+</sup> and

\* Jona, *Phys. Zeits.* xx. p. 14 (1919).

$\text{Sr}^{2+}$ , whose coordination numbers are 6 and 8 respectively. A direct appeal to observation is useless; in solution the ammines of these ions are too much dissociated for their formulæ to be determined, while in dealing with solid ammines it is necessary to know their crystal structure. Even where it can be shown that the crystalline ammine has an ion lattice with all the ammonia present as a complex cation, the results of the present theory would not be rigidly applicable, because the ammonia molecules will be polarized differently, since the electric field to which they are subjected in the lattice is not simply that of the central ion of the complex. According to the work of Biltz and his collaborators\* the magnesium halides form no definite ammines higher than the diamine; further addition of ammonia leads to mixed crystal formation, while both calcium and strontium halides form octammines and barium a decammine. These have very different properties from the stable hexammines like  $\text{NiCl}_2 \cdot 6\text{NH}_3$ , which are known to have a lattice of the  $\text{CaF}_2$  type in which the positive ion is a complex cation, say  $[\text{Ni}(\text{NH}_3)_6]^{2+}$ .

#### *Ammines in Solution.*

Comparing the values for  $-\phi$  given in the Table with those given for hydrates in I. (a), it will be seen that the latter are always the greater, implying that in solution the ammines should be unstable and form hydrates. This is in agreement with observation for the elements considered. But since ammonia, while having a smaller permanent moment than water, has a greater polarizability, it is clear that, with increasing charge and decreasing size of the central ion,  $-\phi$  for the ammine must increase more rapidly than  $-\phi$  for the hydrate. Thus the ratio  $\frac{\phi \text{ Ammine}}{\phi \text{ Hydrate}}$  expressed as a percentage varies from 79 to 83 per cent. for the alkali metals, while for the smaller divalent ions,  $\text{Mg}^{2+}$ ,  $\text{Ca}^{2+}$ , and  $\text{Sr}^{2+}$ , it is between 93 and 95 per cent. This corresponds to the fact that in ammoniacal solutions of salts of Ca, etc., some slight ammine formation appears to take place; in solutions of alkali metal salts there is no trace of ammine formation. The force constants of trivalent ions are unknown, so that the theory cannot be applied to them; but it is clear that the ratio  $\frac{\phi \text{ Ammine}}{\phi \text{ Hydrate}}$  will be still

\* Biltz, *Zeits. für Anorg. Chem.* cxxx. p. 93 (1923).

greater in this case and may even be greater than unity, so that trivalent ions should form ammines fairly stable in solution were it not that in most cases the ion only exists in acid solution, being removed from neutral or alkaline solutions either by the precipitation of a very insoluble hydroxide (*e. g.*  $\text{Al}^{3+}$ ,  $\text{Fe}^{3+}$ ) or by the formation of a complex anion ( $\text{AlO}_2^-$ ). But it seems quite plausible to explain the stable ammines of  $\text{Cr}^{3+}$  and  $\text{Co}^{3+}$  on the electrostatic basis.

In addition to the ammines of trivalent ions, there is another group of ammines more or less stable in solution. These are ammines in which the coordination number is less than the usual, which do not correspond to the solid ammine in formula, and in which the central ion is not of inert-gas type. Thus Ag and Cu halides in the solid state form sesqui- or tri-ammines, which according to Biltz (*loc. cit.*) are to be regarded as molecule-ammines. In solution, however, they form stable diamines. Again, a number of divalent elements like Cu, Ni, Zn form solid hexamine salts, as would be expected, but their ammines in solution are tetrammines. To account for their formation and stability it may be supposed that they are really hydrato-ammines—tetrammine-dihydrates for the divalent ions and diammine-tetrahydrates for the univalent ions. Such mixed compounds would normally have  $-\phi$  values intermediate between those for hexamine and hexahydrate, so that one or other of these would be the most stable form. But a mixed complex of unsymmetrical space structure would exert a resultant electric field at the central ion due to the different dipole moments of the two kinds of molecule.  $\phi_E$  would then include an additional term due to the polarization of the central ion, and if the latter were sufficiently polarizable the additional term could be of sufficient magnitude to make the mixed compound more stable than either hexamine or hexahydrate. Now the ions in the transitional periods, which have incomplete or "18" shells, are much more polarizable than the corresponding ions of inert-gas type (see, *e. g.*, the refractivity data of Fajans and Joos\*), and it is precisely these ions which form the abnormal ammino-ions of the type under consideration.

Inorganic Chemistry Department,  
The University, Leeds.

---

\* Fajans and Joos, *Zeits. für Physik*, xxiii. p. 1 (1924).

VIII. *Newton's Law of Gravitation in an Infinite Euclidean Space.* By JOHN DOUGALL, M.A., D.Sc., F.R.S.E.\*

*Introduction.*

IT appears to be at present a generally accepted belief among physicists and astronomers that an infinite Euclidean spatial world, in which the average density of matter over a large region has approximately the same value everywhere, and in which Newton's Law of Gravitation holds universally, cannot be regarded as a possibility, being inconsistent with the observed finiteness of interstellar gravitational fields.

The following paper contains a criticism of the grounds on which this belief is founded, leading to a conclusion definitely adverse to the prevailing view.

The point on which the whole question turns is the fact that Newton's Law, as ordinarily stated, is ambiguous unless the field considered is finite. If we are dealing with infinite space, the law must in general be supplemented by some convention or definition, analogous to the specification of the order of the terms in a conditionally convergent series which is to be summed.

The definition adopted in the present paper is so simple and natural as to seem almost inevitable. But it is not the definition assumed, or rather implied, in the ordinary theory, and the results to which it leads differ sufficiently from those usually obtained to affect very materially the decision on the question at issue. It is shown, in fact, on the basis of the new definition, that it is perfectly consistent with the Newtonian law of the inverse square of the distance for matter to be distributed in an infinite Euclidean space in such a way that :—

- (a) the average density of the matter within any very large spherical volume is approximately constant, though the density itself may vary within wide limits, while nevertheless
- (b) the gravitational intensity at every point of space is finite, and
- (c) the difference of potential between any two points whatever is likewise finite. *i. e.*, less than an assignable number independent of the choice of points.

\* Communicated by the Author.



A considerable part of the paper is taken up with the determination of a set of conditions which, if satisfied by the distribution of matter, are sufficient to ensure the results just mentioned. Subject to these conditions, it is found that Poisson's equation

$$\nabla^2 V = 4\pi\rho$$

connecting the potential  $V$  with the density  $\rho$  of matter assumes the modified form

$$\nabla^2 V = 4\pi(\rho - \bar{\rho}),$$

where  $\bar{\rho}$  is the constant average density—that is to say, the limit, for  $p$  tending to infinity, of the quotient of the mass within any sphere of radius  $p$ , and fixed centre, by the volume of the sphere.

No conditions to be satisfied at infinity by the potential  $V$  are required. These are replaced by the condition that  $V$  is everywhere finite. It is well known that this condition, combined with the differential equation and the usual suppositions as to continuity, *defines*  $V$ , in the sense that if one solution exists, any other can only differ from it by a constant.

The modification of Poisson's equation suggests—and indeed, if it is accepted, almost necessitates—a corresponding modification of the equations of General Relativity. The change would have quite inappreciable effects in all the ordinary applications, but—so far, at least, as a first approximation is concerned—it would remove an outstanding difficulty with respect to the behaviour of the Einsteinian potentials at infinity and thus, incidentally, detract materially from the plausibility of the current theory of the finiteness of space.

### *Newton's Law and Infinite Space—Einstein's View.*

§ 1. The purpose for which Newton's Law is used is to define the force acting on a hypothetical particle of unit mass placed at any assigned point of the field. In practical applications to the astronomy of the solar system it is always assumed that the only attracting masses which need be taken into account are the masses belonging to the system itself, the total effect due to external masses being considered negligible; and the assumption appears to be abundantly justified by results.

Does the success of this hypothesis allow us to draw any conclusions regarding the distribution of matter in space as a whole? Is the stellar universe “a finite island in the

infinite ocean of space\*,” or should we believe rather that “however far we might travel through space we should find everywhere an attenuated swarm of fixed stars of approximately the same kind and density”?

These questions have attracted much attention within recent years on account of their bearing on the General Theory of Relativity.

Thus Einstein †, following Seeliger, came to the conclusion—but on grounds which we are going to try to prove inadequate—that an infinite Euclidean space in which Newton’s Law holds throughout, and in which the average density of matter is everywhere broadly the same, is definitely incompatible with the finiteness of gravitational forces and potential differences in space, as attested by the finiteness and even comparative smallness of the relative velocities of the stars. He turned therefore to the “finite island” theory but, finding it impossible to make his potentials satisfy the conditions at infinity which this theory seems to impose, he finally cut the knot by introducing into the gravitational equations a “cosmological term” that allowed him to abolish the infinitude of space altogether.

Weyl ‡ accepts the view that space is finite, but not quite on the same grounds as Einstein. His objection to the infinitude of space would lose its force altogether if Poisson’s equation were modified as suggested above.

§ 2. In coming to their decision about Newton’s Law, Einstein and Weyl rely upon the supposed fact that the law of the inverse square carries with it as a consequence Poisson’s equation, or the practically equivalent proposition known as Gauss’s Theorem. Einstein’s argument is in effect as follows §: by Gauss’s Theorem, the average normal attraction over the surface of a sphere =  $4\pi$  (Mass within sphere  $\div$  area of surface). On the supposition of a finite average density of matter, the mean intensity at the surface would therefore obviously become infinite with the radius of the sphere, which is contrary to observation, so that Newton’s Law cannot hold in a roughly uniform world.

\* A. Einstein, ‘Relativity: the Special and the General Theory’ (translated by R. W. Lawson), chap. xxx.

† A. Einstein, ‘Kosmologische Betrachtungen . . .,’ *Sitzungsber. d. Pr. Ak. d. Wiss.* (1917) (translated in the ‘Principle of Relativity’ by W. Perrett and G. B. Jeffery).

‡ H. Weyl, ‘Space—Time—Matter’ (translation by H. L. Brose), pp. 275–279.

§ A. Einstein, ‘Relativity: the Special and the General Theory,’ p. 106.

On the premises assumed, the conclusion indubitably follows. What we question is the correctness of Gauss's Theorem, for an infinite field. But before the nature of the objection can be explained, it is necessary to go back to first principles and examine what Newton's Law, in this general case, really means.

*Definition Supplementary to Newton's Law.*

§ 3. It is implied in Newton's Law that the effects of the various masses in the field on the intensity at a given point are *additive*, so that the rectangular components of the intensity are to be found by algebraic summation (or integration) of the components due to the separate masses. No difficulty arises in the summation process so long as the total volume occupied by the masses is finite; but the same cannot be said when they extend to an infinite distance, for the series which gives any component contains both positive and negative terms, and the sum of the terms of either type is in general infinite.

To see this we need only consider the simple case of a spherical shell of uniform density. The intensity at the centre due to either of two hemispheres into which the shell may be imagined to be divided is a constant multiple of the thickness of the shell, and therefore becomes infinite when the outer radius is indefinitely increased. Nevertheless the intensity at the centre (and indeed at any point in the hollow of the shell) is rigorously *nil*. There is, as it were, an interference effect between the fields due to the two shells taken separately.

Hence, before we can begin to speak at all about the intensity of field due to a distribution of masses extending to infinity, it is absolutely essential to *define the order* in which the masses are to be taken when we are calculating the component intensities at an assigned point by summation of the effects of individual masses. The natural and obvious course is—to speak somewhat vaguely for the moment—to take the masses in the order of their nearness. We therefore give the following:—

**DEFINITION A :** *The gravitational intensity at a point P in a field containing masses extending to infinity is to be found by calculating by Newton's Law the intensity due to the matter contained within a sphere of radius  $p$  having the point P for its centre, and then taking the limit of the result when  $p$  is made to tend to infinity.*

The limit of course may or may not exist, but it will be seen from the examples given below that it does exist in an important class of cases, among which, so far as one can see, the case of the actual physical universe may very possibly be included.

*Possible Failure of Gauss's Theorem.—Examples.*

§ 4. *Ex. 1.*—The simplest possible case is that in which the density is uniform. For a sphere of uniform density the intensity at the centre is *nil*. If the radius is  $p$ , the limit of the value of the intensity for  $p$  tending to infinity is therefore also *nil*. Hence the definition just given makes the intensity zero everywhere; and a potential  $V$  exists, namely  $V = \text{constant}$ .

It may be noted, in verification of the statement in the Introduction, that this value of  $V$  gives  $\nabla^2 V = 4\pi(\rho - \bar{\rho})$ , not  $= 4\pi\rho$ .

We may also test Gauss's Theorem by this case. Take any closed surface  $S$ . The intensity at the surface is 0. The integral of the normal intensity is therefore also 0, which is certainly not equal to  $4\pi \times \text{mass within } S$ . Hence, assuming *Def. A*, Gauss's Theorem is incorrect when the field is infinite.

§ 5. For an infinite field, the definition of the intensity at a given point must involve a limit in some way or other, but of course many alternatives to *Def. A* are possible. The alternative next in naturalness to *Def. A* would differ from it only in having the centre of the sphere  $p$  at an arbitrary fixed point instead of at the point where the intensity is to be found. Subject to convergence conditions, this alternative definition would lead to Gauss's Theorem and the ordinary theory. Take for example once more the simple case of constant density. Choose the radius  $p$  so large that the surface  $S$  is entirely within the varying sphere. Denote the normal force at a point of  $S$  due to the matter within  $p$  by  $N_p$ . As in the usual proof, a particle of mass  $m$  within  $S$  contributes  $4\pi m$  to the surface integral of  $N_p$ , but a particle outside  $S$ , though still within  $p$ , contributes nothing. Hence

$$\iint N_p dS = 4\pi (\text{mass within } S).$$

Since a uniform spherical shell exerts no force at a point in the hollow of the shell,  $N_p$  does not change as  $p$  increases,

so that it tends to its limit uniformly over  $S$ , and we therefore have

$$\iint N \, dS = 4\pi \text{ (mass within } S),$$

which is Gauss's theorem ; and from this Poisson's equation follows at once.

Note that, with Def. A, the sphere  $p$  varies from point to point of  $S$ , so that this method could not be applied.

At a superficial glance it may seem that the usual proof of Gauss's Theorem should hold good whether the field is finite or not, irrespective of any supplement to the law to meet the case of the field being infinite. For the proof is: an internal mass  $m$  contributes  $4\pi m$ , but an external mass nothing, to the surface integral, and the integral must therefore be equal to  $4\pi$  (total internal mass).

The fallacy lies, of course, in the assumption that a process (such as change in the order of integration or summation) which is legitimate for finite integrals and sums can also be applied without question to infinite integrals and series. Thus, if  $F(P, Q) \, dm$  denotes the inward normal force at a point  $P$  of the surface  $S$ , due to the element of mass  $dm$  at any point  $Q$  outside  $S$ , the above "proof" takes for granted that

$$\iint \left[ \int F(P, Q) \, dm \right] dS = \int \left[ \iint F(P, Q) \, dS \right] dm ;$$

the argument being that—since for a fixed  $dm$  (outside  $S$ ) we have

$$\iint F(P, Q) \, dS = 0,$$

so that the integrand on the right, and therefore the integral on the right, vanishes—therefore the integral on the left (exists and) vanishes. But the simple example given at the end of § 4 shows that the inference may be quite erroneous.

It may be worth observing also that if the above argument were sound, we should be proving a definite property of the gravitational intensity before we had even defined it.

§ 6. The example considered in §§ 4, 5—density constant throughout infinite space—is certainly trivial, but it is sufficient to bring out clearly the essential points of difference between the ordinary theory and the one now being proposed. According to the latter, when  $\rho$  is constant, a particle, no matter where situated, is not attracted at all. According to the theory which starts from Poisson's equation, the simplest value of the potential is

$$V = \frac{2\pi}{3} \rho (x^2 + y^2 + z^2),$$

and the force on a given particle depends on the choice of an arbitrary origin at which the force shall vanish; and there is obviously no upper bound to the differences of potential which occur.

If we take the view that no point of space is to be privileged above another, there seems to be no question which theory is to be preferred.

§ 7. *Ex. 2.*—Let  $\rho$  be everywhere constant as before, except for a spherical cavity with centre O and radius  $a$ . For any point P we can always take the radius  $p$  large enough to include the cavity. If this were filled up, the intensity at P would be zero; the actual force, if P is outside the cavity, is therefore a repulsion from O of amount  $\frac{4}{3}\pi\rho a^3/OP^2$ ; and the potential at any point is that due to a sphere of radius  $a$ , centre O, and density  $(-\rho)$ . In this example also, the equation for the potential is

$$\nabla^2 V = 4\pi(\rho - \bar{\rho}).$$

§ 8. *Ex. 3.*—Let  $\rho = \cos(lx + my + nz + \alpha)$ , where  $x, y, z$  are rectangular coordinates and  $l, m, n, \alpha$  are constants. For the calculations we may work with  $\rho = e^{i(lx + my + nz)}$ , or, by simply changing the axes, with  $\rho = e^{ikz}$ , where  $k = \sqrt{l^2 + m^2 + n^2}$ .

To calculate the component intensities  $I_x, I_y, I_z$  at P( $x, y, z$ ) when  $\rho = e^{ikz}$ , we surround P with a sphere of radius  $p$ , at any point ( $x+X, y+Y, z+Z$ ) of which the density is  $\rho(x+X, y+Y, z+Z)$  or  $e^{ikz} \cdot e^{ikZ}$ . We then have, denoting by  $I_z(p)$  the  $z$ -intensity from the sphere  $p$ ,

$$I_z(p) = e^{ikz} \iiint_p e^{ikZ} (Z/R^3) dX dY dZ,$$

where  $R \equiv \sqrt{X^2 + Y^2 + Z^2},$

and the subscript  $p$  indicates that the volume integral is taken through the sphere  $X^2 + Y^2 + Z^2 = p^2$ .

Changing to polar coordinates  $R, \theta, \phi$  we find

$$\begin{aligned} I_z(p) &= e^{ikz} \iiint_p e^{ikR \cos \theta} \cos \theta \sin \theta dR d\theta d\phi \\ &= e^{ikz} \cdot 2\pi \int_0^\pi \sin \theta d\theta \int_0^p e^{ikR \cos \theta} \cos \theta dR \\ &= e^{ikz} \cdot 2\pi \int_0^\pi \sin \theta d\theta (e^{ikp \cos \theta} - 1)/ik \end{aligned}$$

$$\begin{aligned}
 &= e^{ikz} \cdot 2\pi \left\{ \frac{e^{ikp} - e^{-ikp}}{ikp} - 2 \right\} / ik \\
 &= (4\pi/ik) \left\{ (\sin kp)/(kp) - 1 \right\} e^{ikz}.
 \end{aligned}$$

By Def. A (§ 3) the intensity  $I_x$  at P is the limit of  $I_x(p)$  when  $p \rightarrow \infty$ . Hence

$$I_x = (4\pi i/k) e^{ikz}.$$

On writing down the expressions for  $I_x(p)$  and  $I_y(p)$  it will be seen at once that they vanish; thus

$$I_x = I_y = 0.$$

The field is therefore derivable from the potential  $(-4\pi/k^2) e^{ikz}$ .

The quantity of matter in the sphere  $p$  is

$$\begin{aligned}
 &e^{ikz} \iiint_p e^{ikz} dX dY dZ \\
 &= e^{ikz} (4\pi/k^3) (\sin kp - kp \cos kp)
 \end{aligned}$$

which is of order  $p$ .

The corresponding results for  $\rho = \cos(lx + my + nz + \alpha)$  are obtained from these at once by taking the real parts, and changing  $k$  into  $\sqrt{(l^2 + m^2 + n^2)}$ , and  $kz$  into  $lx + my + nz + \alpha$ .

The example does not immediately apply to gravitation, since negative densities occur. But this defect is remedied in a moment by adding a constant  $A$  to the given  $\rho$ , where  $A$  is any positive number not less than 1. By § 4, this makes no change in the intensity or in the potential at any point.

The total quantity of matter in the sphere  $p$  will now be

$$\frac{4}{3} \pi p^3 A + \text{the term of order } p \text{ already found,}$$

so that the mean density  $\bar{\rho}$  is  $A$ .

Thus, for

$$\rho = A + e^{ikz},$$

the potential  $V$  is

$$(-4\pi/k^2) e^{ikz};$$

so that

$$\begin{aligned}
 \nabla^2 V &= 4\pi e^{ikz} \\
 &= 4\pi(\rho - \bar{\rho}),
 \end{aligned}$$

as in the simpler examples already given.

It is obvious that a density represented by the sum of a finite number of terms of the above type,

$$A + \cos(lx + my + nz + \alpha),$$

each multiplied by a positive constant, will again give a finite potential  $V$  satisfying the equation

$$\nabla^2 V = 4\pi(\rho - \bar{\rho}).$$

Clearly a distribution of considerable generality could be built up in this way, and it might be interesting to attempt to carry the investigation further on these lines, from the point of view of a Fourier integral representing the density. But the analysis would be very delicate, and we can obtain all we want in a much more elementary way, as in the succeeding paragraphs.

*Problem—Potential given, Density required.*

§ 9. Before taking up the final problem of determining the potential (when it exists) of a given distribution of matter, we shall first consider the simpler case when it is the potential that is given, and it is required to determine the distribution of matter which—always on the basis of the definition of § 3—will produce this potential.

Suppose that we are given a function  $u$  of  $x, y, z$  which is finite and continuous throughout all space (so that there is an assignable positive number  $\mu$  which the numerical value of  $u$  never exceeds), and which has first and second derivatives possessing these same properties.

We shall calculate the potential due to a distribution of matter with density

$$\rho' = \frac{\partial^2 u}{\partial x^2} + \frac{\partial^2 u}{\partial y^2} + \frac{\partial^2 u}{\partial z^2}.$$

In general it will turn out that this value of  $\rho'$  takes negative values as well as positive, but we shall get over the difficulty by the same artifice as in § 8. Following the method already used there, we calculate the component intensity  $I_z(p)$  at  $(x, y, z)$  due to the density  $\rho'(x+X, y+Y, z+Z)$  throughout the sphere  $X^2 + Y^2 + Z^2 = p^2$ .

Write  $u$  simply for

$$u(x+X, y+Y, z+Z),$$

and  $\nabla^2 u$  for

$$\frac{\partial^2 u}{\partial X^2} + \frac{\partial^2 u}{\partial Y^2} + \frac{\partial^2 u}{\partial Z^2}.$$



Then 
$$I_z(p) = \iiint_p \nabla^2 u(Z/R^3) dX dY dZ.$$

We now apply Green's Theorem, in the form

$$\iiint (\alpha \nabla^2 \beta - \beta \nabla^2 \alpha) dX dY dZ = \iint \left( \alpha \frac{\partial \beta}{\partial \nu} - \beta \frac{\partial \alpha}{\partial \nu} \right) dS,$$

taking  $\alpha = Z/R^3$ ,  $\beta = u$ , to the field obtained from the sphere  $p$  by cutting out an infinitesimal concentric sphere of radius  $\epsilon$ .

From the conditions imposed on  $u$ , we have, over the surface of the sphere  $\epsilon$ ,

$$\beta = u(x, y, z) + \left( X \frac{\partial}{\partial x} + Y \frac{\partial}{\partial y} + Z \frac{\partial}{\partial z} \right) u(x, y, z)$$

+ a remainder of order  $\epsilon^2$ ; and

$$\frac{\partial \beta}{\partial \nu} = -\frac{1}{\epsilon} \left( X \frac{\partial}{\partial x} + Y \frac{\partial}{\partial y} + Z \frac{\partial}{\partial z} \right) u(x, y, z)$$

+ a remainder of order  $\epsilon$ .

Hence, when  $\epsilon \rightarrow 0$ , the limit of

$$\begin{aligned} & \iint \left( \alpha \frac{\partial \beta}{\partial \nu} - \beta \frac{\partial \alpha}{\partial \nu} \right) dS_\epsilon \\ &= \text{Lt} \iint \left\{ (Z/\epsilon^3)(-Z/\epsilon) - Z(2Z/\epsilon^4) \right\} \frac{\partial}{\partial z} u(x, y, z) dS_\epsilon \\ &= -4\pi \frac{\partial}{\partial z} u(x, y, z). \end{aligned}$$

Thus, noting that  $\nabla^2 \alpha = 0$ , we find

$$I_z(p) = -4\pi \frac{\partial}{\partial z} u(x, y, z) + \iint \left( \frac{Z}{R^3} \frac{\partial u}{\partial R} + \frac{2Z}{R^4} u \right) dS_p.$$

Since  $u$  is finite, the part of the surface integral arising from the second term is of order  $1/p$  and vanishes in the limit when  $p \rightarrow \infty$ .

The remaining part

$$\begin{aligned} &= \frac{1}{p^3} \iint Z \frac{\partial u}{\partial R} dS_p \\ &= \frac{1}{p^3} \iint u \frac{\partial Z}{\partial R} dS_p + \frac{1}{p^3} \iiint_p Z \nabla^2 u dX dY dZ, \end{aligned}$$

by Green's Theorem.

The first term on the right is again of order  $1/p$ , so that, making  $p \rightarrow \infty$ , we have

$$I_z = -4\pi \frac{\partial}{\partial z} u(x, y, z),$$

provided

$$\lim_{p \rightarrow \infty} \frac{1}{p^3} \iiint_p Z \nabla^2 u \, dX \, dY \, dZ = 0. \quad \dots \quad (1)$$

Since

$$\iiint_p \nabla^2 u \, dX \, dY \, dZ = \iint \frac{\partial u}{\partial R} \, dS_p,$$

which is of order  $p^2$ , the average density of the matter in the sphere  $p$  tends to 0 when  $p \rightarrow \infty$ . But, as already indicated, we may add to the density a constant positive term  $A$ , large enough to ensure that the sum is nowhere negative; the density  $\rho$  is now  $A + \rho'$ , so that  $\rho' = \rho - A$ , or (since  $A$  is now evidently the mean density)  $\rho' = \rho - \bar{\rho}$ .

Thus, provided  $u$  satisfies the condition (1), as well as the conditions stated near the beginning of this § 9, the gravitational field calculated directly from Newton's Law in accordance with Def. A for a density

$$\rho = \bar{\rho} + \frac{1}{4\pi} \left( \frac{\partial^2 u}{\partial x^2} + \frac{\partial^2 u}{\partial y^2} + \frac{\partial^2 u}{\partial z^2} \right)$$

has for its potential the function  $u(x, y, z)$ . The constant  $\bar{\rho}$  is the limiting mean density of matter in any indefinitely increasing sphere with fixed centre, and the equation satisfied by the potential is

$$\frac{\partial^2 u}{\partial x^2} + \frac{\partial^2 u}{\partial y^2} + \frac{\partial^2 u}{\partial z^2} = 4\pi(\rho - \bar{\rho}).$$

### *Sufficient Conditions for Finite Potential.*

§ 10. We now come to our main problem, viz., to determine sufficient conditions that a given distribution of matter should produce a potential which is everywhere finite, and to obtain an analytical expression for the potential when these conditions are satisfied—again on the understanding that the intensity is calculated from Newton's Law as in Def. A.

Let the density at  $(x, y, z)$  be  $\rho(x, y, z)$ . It will be assumed that  $\rho$  and its first derivatives are continuous throughout, the analysis being thus considerably shortened.

With the notation already used in §§ 8, 9 we have

$$I_z(p) = \iiint_p \rho(x+X, y+Y, z+Z) (Z/R^3) dX dY dZ.$$

Ignoring explicit reference to  $x, y, z$  for the moment, put

$$\iiint_p \rho(x+X, y+Y, z+Z) Z dX dY dZ = f(p);$$

then

$$\iint \rho(x+X, y+Y, z+Z) Z dS_p = \frac{\partial}{\partial p} f(p) = f'(p),$$

and

$$I_z(p) = \int_0^p f'(R) dR/R^3.$$

Hence

$$\begin{aligned} I_z(q) - I_z(p) &= \int_p^q f'(R) dR/R^3 \\ &= f(q)/q^3 - f(p)/p^3 + 3 \int_p^q f(R) dR/R^4. \end{aligned}$$

Suppose now that  $f(R)/R^3 \rightarrow 0$  when  $R \rightarrow \infty$ ; or rather, with closer restriction, that for all values of  $R >$  some fixed value  $R_0$  we have

$$|f(R)| < MR^{3-s}, \quad \dots \quad (2)$$

where  $M$  and  $s$  are fixed positive numbers.

It obviously follows that  $I_z(q) - I_z(p)$  can be made as small numerically as we please, by taking  $p$  large enough and  $q > p$ . In other words  $\lim_{p \rightarrow \infty} I_z(p)$  exists, *i. e.*, the density  $\rho$  gives rise to intensities which are everywhere finite.

§ 11. Suppose next that the mean density within the sphere  $p$ , viz.

$$\iiint_p \rho(x+X, y+Y, z+Z) dX dY dZ / \frac{4}{3} \pi p^3,$$

tends, when  $p \rightarrow \infty$ , to a limit  $\bar{\rho}$ , independent of  $x, y, z$ ; and consider the integral

$$E_p = - \iiint_p \{ \rho(x+X, y+Y, z+Z) - \bar{\rho} \} (1/R) dX dY dZ.$$

If we write

$$\iiint_p \{ \rho(x+X, y+Y, z+Z) - \bar{\rho} \} dX dY dZ = \psi(p).$$

then

$$E_p = - \int_0^p \psi'(R) dR/R;$$

and

$$\int_p^q \psi'(R) dR/R = \psi(q)/q - \psi(p)/p + \int_p^q \psi(R) dR/R^2.$$

Suppose that, when  $R > R_0$ ,

$$|\psi(R)| < M_1 R^{1-s_1}, \quad . \quad . \quad . \quad . \quad . \quad (3)$$

where  $M_1, s_1$  are fixed positive numbers.

Then, as in the similar case of § 10,  $\lim_{p \rightarrow \infty} E_p$  exists; we shall denote it by  $E(x, y, z)$ .

§ 12. Write

$$\rho_1(x, y, z) \quad \text{for} \quad \rho(x, y, z) - \bar{\rho}.$$

Returning to § 10, we have, by one form of Green's Theorem, noting that

$$\iiint_p \bar{\rho} (dR^{-1}/dZ) dX dY dZ = 0,$$

$$\begin{aligned} I_z(p) &= - \iiint_p \rho(x+X, y+Y, z+Z) (dR^{-1}/dZ) dX dY dZ \\ &= - \iiint_p \rho_1(x+X, y+Y, z+Z) (dR^{-1}/dZ) dX dY dZ \\ &= \iiint_p R^{-1} (\partial \rho_1 / \partial Z) dX dY dZ - \iint_n R^{-1} \rho_1 dS_p, \end{aligned}$$

where  $n$  is the  $z$ -direction cosine of the normal to  $S_p$ . We can replace the surface integral by the volume integral

$$\frac{1}{p} \iiint_p \frac{\partial}{\partial Z} \rho_1(x+X, y+Y, z+Z) dX dY dZ;$$

and clearly

$$\partial \rho_1 / \partial Z = \partial \rho_1 / \partial z.$$

We therefore have

$$I_z(p) = \frac{\partial}{\partial z} \left\{ \iiint_p (\rho_1/R) dX dY dZ - \frac{1}{p} \iiint_p \rho_1 dX dY dZ \right\}.$$

Integrate this equation from  $z_0$  to  $z$ , keeping  $x, y$  constant. Thus

$$\int_{z_0}^z I_z(p) dz = \left| \begin{array}{l} \iiint_p (\rho_1/R) dX dY dZ \\ -(1/p) \iiint_p \rho_1 dX dY dZ \end{array} \right|_{x, y, z_0}^{x, y, z}$$

Now let  $p \rightarrow \infty$ . If the numbers  $M$  and  $s$  of § 10 are fixed throughout the field,  $I_z(p)$  tends *uniformly everywhere* to its limit  $I_z$ , so that

$$\int_{z_0}^z I_z(p) dz \rightarrow \int_{z_0}^z I_z dz.$$

As for the other side of the equation, we have already postulated, at § 11 (3), that

$$(1/p) \iiint_p \rho_1 dX dY dZ \rightarrow 0.$$

Hence

$$\begin{aligned} \int_{z_0}^z I_z dz &= \lim_{p \rightarrow \infty} \left| \iiint_p (\rho_1/R) dX dY dZ \right|_{x, y, z_0}^{x, y, z} \\ &= -E(x, y, z) + E(x, y, z_0), \end{aligned}$$

from § 11. Thus

$$I_z = -\frac{\partial E}{\partial z};$$

and similarly,

$$I_x = -\frac{\partial E}{\partial x}, \quad I_y = -\frac{\partial E}{\partial y},$$

so that the field has the potential  $E$ .

### *Deduction of the Modified Poisson's Equation.*

§ 13. We now come to the final step of the analysis, the investigation of the differential equation for the potential.

For finite systems, we have Poisson's equation

$$\nabla^2 E = 4\pi\rho.$$

For the infinite systems under consideration, and of course as a special case for finite systems also, it will now be shown that the corresponding equation is

$$\nabla^2 E = 4\pi(\rho - \bar{\rho}),$$

where  $\bar{\rho}$  is (§ 11) the mean density over the whole of space (so that  $\bar{\rho} = 0$  for finite systems).

This equation is the same as

$$\begin{aligned}\frac{\partial I_x}{\partial x} + \frac{\partial I_y}{\partial y} + \frac{\partial I_z}{\partial z} &= -4\pi(\rho - \bar{\rho}) \\ &= -4\pi\rho_1, \text{ say,}\end{aligned}$$

where (§ 10)

$$I_z = \lim_{p \rightarrow \infty} I_z(p),$$

with

$$I_z(p) = - \iiint_p \rho(x+X, y+Y, z+Z) (dR^{-1}/dZ) dX dY dZ;$$

here we may, as at the beginning of § 12, write  $\rho_1$  instead of  $\rho$  without changing the value of the integral.

For convenience in calculating the derivative  $\partial I_z/\partial z$ , this integral will now be modified by cutting out from the field of integration a small sphere of radius  $\epsilon$  round  $(x, y, z)$  as centre. Thus

$$I_z = \lim_{p \rightarrow \infty, \epsilon \rightarrow 0} I_z(p, \epsilon),$$

where  $I_z(p, \epsilon)$  only differs from  $I_z(p)$  by the excision of the volume of the sphere  $\epsilon$ , and  $p, \epsilon$  go to their limits independently; and we write

$$I_z(p, \epsilon) = - \iiint_{p, \epsilon} \rho_1(x+X, y+Y, z+Z) (dR^{-1}/dZ) dX dY dZ.$$

This gives

$$\frac{\partial}{\partial z} I_z(p, \epsilon) = - \iiint_{p, \epsilon} \frac{\partial \rho_1}{\partial Z} \frac{\partial R^{-1}}{\partial Z} dX dY dZ,$$

since  $\partial \rho_1 / \partial z = \partial \rho_1 / \partial Z$ .

We may not infer at once that

$$\lim_{p \rightarrow \infty, \epsilon \rightarrow 0} \frac{\partial}{\partial z} I_z(p, \epsilon)$$

exists, and is equal to  $\partial I_z/\partial z$ . Some such analysis as the following is first necessary.

By Green's Theorem we have

$$\begin{aligned}\frac{\partial}{\partial z} I_z(p, \epsilon) &= \iiint_{p, \epsilon} \rho_1 \frac{\partial^2 R^{-1}}{\partial Z^2} dX dY dZ \\ &= \left| \iint_{\epsilon} \frac{Z}{R} \rho_1 \frac{\partial R^{-1}}{\partial Z} dS \right|_p.\end{aligned}$$

Put

$$J_z(p, \epsilon) = \iiint_{p, \epsilon} \rho_1(x+X, y+Y, z+Z)(d^2R^{-1}/dZ^2) dX dY dZ.$$

We first specify sufficient conditions that  $J_z(p, \epsilon)$  may tend to a limit  $J_z$ , and that uniformly as regards  $z$ , when  $p$  and  $\epsilon$  tend to their limits.

We have

$$J_z(p, \epsilon) = \iiint_{p, \epsilon} \rho_1(x+X, y+Y, z+Z)(3Z^2 - R^2)/R^5 dX dY dZ.$$

Write

$$\left( \iiint_p \rho_1(x+X, y+Y, z+Z)(3Z^2 - R^2) dX dY dZ \right) = \chi(p).$$

Then

$$\iint \rho_1 \cdot (3Z^2 - R^2) dS_p = \chi'(p),$$

and

$$\begin{aligned} J_z(q, \epsilon) - J_z(p, \epsilon) &= \int_p^q \chi'(R) dR/R^5 \\ &= \chi(q)/q^5 - \chi(p)/p^5 + 5 \int_p^q \chi(R) dR/R^6. \end{aligned}$$

Assume

$$|\chi(R)| < M_2 R^{5-s_2}, \quad \dots \dots \dots (4)$$

when  $R > R_0$ , where  $M_2$  and  $s_2$  are positive numbers independent of  $x, y, z$ ; not an onerous condition, seeing that  $\chi(R)$  is of order not higher than  $R^5$ , even if  $\rho_1$  is subjected only to the condition of finiteness.

Then  $J_z(q, \epsilon) - J_z(p, \epsilon)$  clearly  $\rightarrow 0$  as  $p$  and  $q \rightarrow \infty$ , and that uniformly with respect to  $z$ ; the uniform convergence at the  $\epsilon$  end is easily proved on replacing  $\rho_1(x+X, y+Y, z+Z)$  by the sum of  $\rho_1(x, y, z)$  and a remainder term of the first order as in Taylor's Theorem, and changing to polar co-ordinates.

Hence  $J_z(p, \epsilon)$  tends, uniformly as to  $z$ , to a limit, say  $J_z(x, y, z)$  or  $J_z$ .

Return now to the equation

$$\begin{aligned} \frac{\partial}{\partial z} J_z(p, \epsilon) &= J_z(p, \epsilon) \\ &- \left[ \iint \frac{Z}{R} \rho_1(x+X, y+Y, z+Z) \frac{\partial R^{-1}}{\partial Z} dS \right]_p^p. \end{aligned}$$

The contribution to the last term of this equation from the  $\epsilon$  surface is

$$-\iint \frac{Z}{R} \rho_1 \frac{Z}{R^3} dS_\epsilon.$$

Call this  $t_\epsilon$ ; its limit, when  $\epsilon \rightarrow 0$ , is  $-\frac{4\pi}{3} \rho_1(x, y, z)$ .

From the  $p$  surface the last term of the equation gives

$$\frac{1}{p^3} \iint \frac{Z}{R} \rho_1(x+X, y+Y, z+Z) Z dS_p,$$

which, by Green's Theorem, is equal to

$$\begin{aligned} & \frac{1}{p^3} \iiint_p \frac{\partial}{\partial Z} (Z \rho_1) dX dY dZ \\ &= \frac{1}{p^3} \iiint_p \rho_1 dX dY dZ + \frac{1}{p^3} \frac{\partial}{\partial z} \left( \iiint_p Z \rho_1 dX dY dZ \right). \end{aligned}$$

It will be shown that the two terms on the right will disappear from the final result. Write them briefly as  $T_1 + (\partial/\partial z)T_2$ ; it has already been postulated that  $T_1$  (§ 11) and  $T_2$  (§ 10)  $\rightarrow 0$  when  $p \rightarrow \infty$ .

Resuming all the terms of the equation for  $(\partial/\partial z)I_z(p, \epsilon)$ , we have now

$$\frac{\partial}{\partial z} I_z(p, \epsilon) = J_z(p, \epsilon) + t_\epsilon + T_1 + \frac{\partial}{\partial z} T_2.$$

Hence, integrating from  $z_0$  to  $z$ , we get

$$\left[ I_z(p, \epsilon) - T_2 \right]_{z_0}^z = \int_{z_0}^z \left\{ J_z(p, \epsilon) + t_\epsilon + T_1 \right\} dz.$$

Now let  $p$  and  $\epsilon$  tend to their limits. We have seen that  $J_z(p, \epsilon) \rightarrow J_z$ ,  $t_\epsilon \rightarrow -\frac{4\pi}{3} \rho_1(x, y, z)$ ,  $T_1 \rightarrow 0$ ,  $T_2 \rightarrow 0$ ,  $I_z(p, \epsilon) \rightarrow I_z$ ; and all, the first three in particular, uniformly as to  $z$ . Thus

$$I_z - I_{z_0} = \int_{z_0}^z \left\{ J_z - \frac{4}{3} \pi \rho_1(x, y, z) \right\} dz,$$

and, by differentiation,

$$\frac{\partial I_z}{\partial z} = J_z - \frac{4}{3} \pi \rho_1(x, y, z).$$



A single step more gives us the result we seek. For we have, from the definition of  $J_z(p, \epsilon)$ ,

$$\begin{aligned} & J_x(p, \epsilon) + J_y(p, \epsilon) + J_z(p, \epsilon) \\ &= \iiint_{p, \epsilon} \rho_1(x+X, y+Y, z+Z) \\ & \quad \left( \frac{\partial^2 R^{-1}}{\partial X^2} + \frac{\partial^2 R^{-1}}{\partial Y^2} + \frac{\partial^2 R^{-1}}{\partial Z^2} \right) dX dY dZ \\ &= 0. \end{aligned}$$

Hence, taking the limits, we have

$$J_x + J_y + J_z = 0,$$

and therefore

$$\frac{\partial I_x}{\partial x} + \frac{\partial I_y}{\partial y} + \frac{\partial I_z}{\partial z} = -4\pi\rho_1(x, y, z),$$

or finally (§ 12)

$$\frac{\partial^2 E}{\partial x^2} + \frac{\partial^2 E}{\partial y^2} + \frac{\partial^2 E}{\partial z^2} = 4\pi(\rho - \bar{\rho}),$$

the result required.

#### *Interpretation of Conditions for Finite Potential.*

§ 14. The conditions (3), (2), (4) have an obvious and interesting dynamical interpretation. To speak in the broadest possible terms, they may be regarded as stating that—

- (i.) The average density of matter is the same round every point of space;
- (ii.) Every point is a centre of inertia;
- (iii.) Every axis is a principal axis of inertia.

It is a curious fact, on which a little reflexion might not be wasted, that these are just the sort of conditions which, on the basis of Newtonian dynamics, we should expect to be fulfilled if the present distribution and motion of matter have arisen, in consequence of some initial disturbance, from a primæval uniform distribution at rest in infinite Euclidean space.

Further, on the assumption that gravitation is propagated with a finite velocity, say  $c$ , it is clear that matter at a greater spatial distance than  $cT$  would have no effect,  $T$  being the

distance in time of the original disturbance. In these circumstances, the Newtonian gravitational intensity could hardly be defined in any other way than in Def. A, modified of course for "retardation."

### *Application to Relativity.*

§ 15. The chief point of interest about the suggested modification of Poisson's equation is doubtless its bearing upon the General Theory of Relativity, an essential step in the usual presentation of which is the proof that Einstein's equations reduce in a first approximation to the ordinary equations of Newtonian dynamics, including in particular Poisson's equation  $\nabla^2 V = 4\pi\rho$ . If the latter equation is to be replaced by  $\nabla^2 V = 4\pi(\rho - \bar{\rho})$ , it would seem reasonable to make a corresponding change in the equations of relativity, *i. e.* in the set of equations \*

$$G_{\mu\nu} - \frac{1}{2}g_{\mu\nu}G = -8\pi T_{\mu\nu}.$$

The natural change to make is to replace  $T_{\mu\nu}$  by  $T_{\mu\nu} - \bar{T}_{\mu\nu}$ , where  $\bar{T}_{\mu\nu}$  is some tensor of the second order, connected with the matter in the field. The tensor  $\bar{T}_{\mu\nu}$  should be in some sense a mean, or smoothed-out, form of  $T_{\mu\nu}$ , but, of course, we cannot define it literally as the mean of  $T_{\mu\nu}$ , since the mean value of a tensor is not itself a tensor. A constant multiple of  $g_{\mu\nu}$  might serve.

For our purpose one condition is essential. If, with Eddington, we assume the proper density  $\rho$  to be given by

$$\rho = T,$$

$T$  being the invariant  $g^{\mu\nu}T_{\mu\nu}$ , then we must impose on  $\bar{T}_{\mu\nu}$  the condition

$$\bar{T} = \bar{\rho},$$

where  $\bar{T} = g^{\mu\nu}\bar{T}_{\mu\nu}$ , and  $\bar{\rho}$  is the mean density, which we assume to exist, and which will be given as the limit of the ratio of the integrals

$$\begin{aligned} & \int \sqrt{-g\rho} \, dx_1 \, dx_2 \, dx_3 \, dx_4 \\ \text{and} \\ & \int \sqrt{-g} \, dx_1 \, dx_2 \, dx_3 \, dx_4, \end{aligned}$$

\* The notation and units are essentially those of Eddington's 'Mathematical Theory of Relativity.'

taken over a region of space-time increasing indefinitely in every direction from any assigned origin.

We shall then have the usual first approximation to the metric of space-time in the form

$$ds^2 = (1 + 2V) dx_4^2 - (1 - 2V)(dx_1^2 + dx_2^2 + dx_3^2);$$

but the equation for  $V$  will now be

$$\nabla^2 V = 4\pi(\rho - \bar{\rho}).$$

The point to be emphasized is that this equation may have a solution which is finite *everywhere*, so that the above approximation to  $ds^2$  is no longer of merely local application, but may hold good throughout the whole of space-time.

From this point of view, the curvatures represented by the gravitational tensor are not related directly to the energy tensor itself, but to its deviation from uniformity. The mean curvature has one sign where there is matter, and the opposite sign where there is none. On the large scale, the deviations from flatness balance each other, so that *space-time on the whole is approximately Galilean throughout*, and in particular space is roughly Euclidean to infinity.

Since  $\bar{\rho}$  is excessively minute—Hubble estimates the mean density of matter at  $1.5 \times 10^{-31}$  gr. per c.c.—the ordinary applications within the solar system are not interfered with.

### *Summary.*

Newton's Law of the inverse square must be supplemented before it can be applied to a distribution of matter extending to infinity. The procedure which seems most natural leads to a modification of Poisson's equation which, though unimportant for ordinary applications, is of considerable significance cosmologically, since it allows the possibility of a gravitational potential and intensity everywhere finite, even when the distribution of matter is of broadly uniform character throughout all space. A similar modification is suggested for the equations of General Relativity. The main effect of this would be that the world would be macroscopically Galilean, so that space would be Euclidean instead of having a small constant positive curvature as in Einstein's theory.

IX. *Magnetism and Molecular Structure.*—Part I. *The Magnetic Susceptibilities of some Liquid Organic Isomers.*  
By Prof. S. S. BHATNAGAR, D.Sc.(Lond.), F.Inst. Phys.,  
RAM NARAIN MATHUR, M.Sc., and RAM SAHAI MAL,  
M.Sc.\*

THE relation between magnetic susceptibilities and chemical constitution of organic compounds has been considerably investigated. Henrichsen<sup>(1)</sup> showed that the "magnetization numbers" of organic compounds can be calculated additively from the values for the component atoms. Besides other substances, he tried some isomeric compounds and found that the values of the magnetic susceptibilities for the normal and iso compounds were always the same. And the values for ortho, meta, and para compounds should also be the same according to his views. Again, according to Meyer<sup>(2)</sup>, the isomeric substances have, at least to a first approximation, no difference in their "magnetization numbers." Meslin<sup>(3)</sup> also determined the specific magnetic susceptibility of a large number of organic compounds, and compared his results with those of Plücker, Faraday, Becquerel, Quincke, and Henrichsen. The only isomeric substances in his tables of data are butyl and iso-butylalcohols, and the latter is a little more diamagnetic than the former. The influence of chemical constitution on magnetic properties was also extensively studied by Pascal<sup>(4)</sup>. His general results confirm Henrichsen's<sup>(5)</sup> observations that the magnetic properties of organic liquids are additive in character, *i. e.*, the molecular susceptibility  $x_M = \sum a x_A + \lambda$  where  $a$  is the number of atoms of susceptibility,  $x_A$  and  $\lambda$  is a constitutive constant depending on the nature of the linkages between the atoms. The values of  $x_A$  should therefore be the same for isomeric substances.

But when we examine the physical properties of organic isomers, we find that their densities, boiling-points, surface-tensions, refractive indices, and viscosities are never exactly the same. According to Perkin<sup>(6)</sup>, even their molecular magnetic rotations are different. The experiments of Krishnan<sup>(7)</sup>, Rama Krishna Rao<sup>(8)</sup>, and others on the scattering of light show that their depolarization

\* Communicated by the Author.

factors are not the same. Stewart<sup>(9)</sup> examined them by the X-ray diffraction ionization method and found different results for them. Sogani<sup>(10)</sup> and Krishnamurti<sup>(11)</sup> also observed differences between the X-ray diffraction liquid haloes of isomeric molecules. Even the ultra-violet absorption spectra<sup>(12)</sup> and the Raman spectra<sup>(13)</sup> of the isomeric xylenes and the primary and secondary alcohols show that isomerides are distinguishable from each other. In view of these facts it became interesting to examine the isomers regarding their magnetic properties on a sensitive magnetic balance and to see whether these properties can be co-related with their other physical properties and with the views expressed in previous papers from this laboratory<sup>(14)</sup> on the subject of electronic isomers.

### *Experimental.*

The apparatus employed during this investigation is similar to Bauer and Piccard's<sup>(15)</sup> U-tube apparatus (Method I.) with this difference, that the sides of both the reservoir and the tube, except near the two ends, are made double-walled. Readings for any temperature of the liquid under investigation are taken by circulating water from a thermostat, electrically maintained at the desired temperature, in the outer jackets around the tube and the reservoir. Before taking readings water is allowed to flow till the liquid under investigation attains the desired constant temperature. The portion of the narrow tube in between the pole-pieces is not double-walled. And, in order to prevent any variation in temperature at the meniscus, it is necessary that the atmosphere around it should be at about the same temperature. The portion of the narrow tube from a little above the meniscus was therefore surrounded by a small glass condenser through which water, at the same temperature as that passing through the rest of the apparatus, was circulated.

Again, as in Bauer and Piccard's apparatus, the reservoir could be moved up and down by means of a fine screw. But on applying magnetic field, the actual rise or fall of the meniscus was observed by a microscope. As the differences between the deflexions of the meniscus for the isomeric liquids are very small, a micrometer eyepiece was used. In doing the actual experiments, it was also observed that very small changes in the position of the

narrow tube and the meniscus in the field affect the results. It was, therefore, necessary to put the tube every time after cleaning in exactly the same position. A brass plate was therefore fixed to the top of the pole-pieces of the electromagnet, and a hole was bored in it so that the narrow tube could just pass through it. This served to check any big change in the position of the tube in the field. To avoid small displacements, a fine cross-mark was etched on the narrow tube, and its position was noticed by a fixed microscope and kept the same. For every reading the meniscus was brought to the same position in the field by raising or lowering the reservoir by means of a fine screw, and every precaution was taken to ensure that the readings for isomerides and water are always taken in the same position of the tube and the meniscus in the field. Scrupulous care was also taken in cleaning the tube and the bottle to prevent any sticking of the liquid, and a constant current was passed in the electromagnet. The values of the magnetic susceptibility  $x$  were calculated by the equation

$$x = \frac{2\theta g}{H^2} + x \frac{\rho_0}{\rho},$$

where

$x$  = specific susceptibility of the liquid,

$x_0$  = specific susceptibility of air ( $210 \times 10^{-7}$ ),

$\rho_0$  = density of air,

$\rho$  = density of the liquid, and

$\theta$  = displacement of the meniscus.

The apparatus was standardised with respect to water ( $x = -7.25 \times 10^{-7}$ ).

#### *Estimation of the Purity of Substance investigated.*

The differences between the susceptibilities of isomerides are of very small order, and it is therefore absolutely necessary that the substances investigated be quite pure. As water is a very common impurity in some of the substances used, its absence was made sure of by four or five tests. Absence of iron was also carefully tested for. Very elaborate precautions were taken in purifying the

substances. The difficulty chiefly arose from the isomerides being associated with each other, and great care had to be taken in separating them. As the methods of purification and estimation are different in each case, they are given below briefly and separately for the substances investigated.

(a) *Alcohols*.—Kahlbaum's pure propyl and isopropyl and Merck's extra pure butyl alcohols were taken. A very large amount of work on the purification of alcohols has been done by Brunel, Crenshaw and Tobin<sup>(16)</sup>, Wildermann<sup>(17)</sup>, Young and Fortey<sup>(18)</sup>, Andrews<sup>(19)</sup>, etc. And Kahlbaum and Merck's pure specimens further purified, according to the observations of workers named above, were used. In order to test for the impurities, the specimens were estimated volumetrically by the process of acetylation of the hydroxyl group by acetic anhydride. The results obtained, within the limits of experimental error, showed that the substances are quite pure. Absence of one isomeride in the other was also made sure of. Normal alcohol on oxidation gave aldehyde only, whereas the iso-alcohols gave acetone and no aldehyde. Any mixing of iso and tertiary isomerides was then tested for by means of their iodides (Meyer and Jacobsen's test).

(b) *Cresols*.—Merck's extra pure specimens were taken. In order to purify them they were distilled at their boiling-points. In the case of meta-cresol, it was cooled before distilling to 15° C. to remove all traces of ortho and para varieties, since they are solid at this temperature. Any mixing of ortho and para cresols was then tested for by means of their nitroso derivatives (Nolting and Kohn, vol. xvii. p. 351).

(c) *Nitro-toluenes*.—Same as for cresols.

(d) *Chloro-phenols*.—Kahlbaum's pure specimens further purified by distilling them at their boiling-points were used.

Physical constants like density, boiling-point, melting-point (where possible), and refractive index were also determined carefully for the substances investigated, and a comparison of our values with those given by other careful workers showed that the specimen used are quite pure.

*Experimental Results.*

The substances given in this investigation are all diamagnetic, but some of them have got double bonds in their structural formulæ to which the role of paramagnetism has been assigned by Pascal. It was also observed by us that the readings in some cases vary with temperature, and it was for this reason that the values for the different isomers have been taken at the same temperature. In the Table below are given the values at 34° C. except for ortho and para chlorophenol, for which the values are at

TABLE I.

Substance.	$x \times 10^7$
N-propyl alcohol .....	— 7.94
Iso-propyl alcohol .....	— 8.14
N-butyl alcohol .....	— 8.25
Iso-butyl alcohol .....	— 8.35
Tertiary butyl alcohol .....	— 8.40
Ortho-cresol .....	— 6.81
Meta-cresol .....	— 6.69
Para-cresol* .....	— 6.73
O-nitro toluene .....	— 5.61
M-nitro toluene .....	— 5.52
O-chlorophenol .....	— 5.20
P-chlorophenol .....	— 5.10

\* Although its melting-point is 37° C., it can be kept liquid at 34° C. for a considerable time (*cf.* Perkin, J. C. S. vol. lxix. p. 1182, 1896).

45° C. The values have been calculated according to the formula given before, and are referred to water with  $x = -7.25 \times 10^{-7}$ .

*Discussion of Results.*

It is clear from the preceding table that the values of  $x$  for isomerides are somewhat different. Sometimes the differences between these values are very small, for example, in the case of butyl and iso-butyl alcohols. But a series of experiments carried out in these special cases brought to our notice the interesting fact that the



differences were always in the same direction and real. Although Henrichsen (*loc. cit.*) and Meyer \* found no change in the susceptibilities of isomerides, Meslin † has observed that the value of  $\alpha$  for iso-butyl alcohol is greater than that for butyl alcohol. Pascal<sup>(20)</sup> has also observed at one place that there is a small increase in the diamagnetism in passing from a primary to a secondary and thence to a tertiary compound. His values for ethyl butyl iso-, butyl and tertiary butyl ketones come out to be  $-7.10 \times 10^{-7}$ ,  $-7.17 \times 10^{-7}$  and  $-7.20 \times 10^{-7}$ , respectively. The values of  $\alpha$  for the isomerides in the above stray observations, therefore, change in the same direction as observed by us. Again, if we examine the three values given above by Pascal for ethyl butyl ketones, we find that the values for secondary and tertiary isomerides are near together while a much larger difference exists between the value for primary and secondary isomerides. We have also examined the three isomerides of butyl alcohol, and we find that our values also for the secondary and tertiary isomerides are near together while a comparatively larger difference exists between the values for primary and secondary isomerides.

Again, according to the empirical equation<sup>(20)</sup> developed in previous papers from this laboratory, the value of the molecular magnetic susceptibility  $\alpha_M$  is given by  $\alpha_M = -2.85 \times 10^{10} \times k(r_1)^2$  where  $r_1$  is the radius of the molecule and  $K$  is a constant depending on the number of electrons and atoms in the molecule. The values of this constant for isomeric substances will therefore be the same. Now according to the approximate methods of calculation used before, the values of the radii of two isomeric molecules will be the same. But it is apparent that on account of different constitutive forces the radii will always differ by a small amount. And, therefore, even according to the above equation, there should always be some difference between the values of  $\alpha_M$  for isomeric substances as observed by us.

In order to get an idea of these constitutive forces attempts have been made by several workers to compare physical properties of compounds, especially organic, with their molecular constitution. Considerable discussion has centred round the relations between the boiling-points

\* *Loc. cit.*† *Loc. cit.*

molecular volumes, and molecular constitution. Most of the properties of organic substances like molecular volume, molecular magnetic rotation, molecular refractivity, etc., have been shown to be additive in character with some constitutive factors. The magnetic susceptibilities of organic substances are also additive in character with certain constitutive factors. In the light of the above observations and those given in the introduction, it was

TABLE II.

Substance.	Boiling-point.	Depolarization factor, $v \times 100$ .	Molecular volume.	Molecular magnetic susceptibility, $\chi_M \times 10^6$ .	Molecular magnetic rotation.
N-propyl alcohol .	97.3	7.1	81.3	-47.70	3.768
Iso-propyl alcohol	82.31	5.0	82.3	-48.91	4.019
N-butyl alcohol ..	117.42	9.3	101.8	-61.13	4.79 (calc.)
Iso-butyl alcohol.	107.81	7.3	102.1	-61.87	4.936
Tertiary alcohol ..	82.22	4.1	102.4*	-62.24	5.122
O-cresol. ....	190.8	..	121.5	-73.62	13.382
M-cresol .....	202.0	..	123.2	-72.32	12.776
P-cresol .....	201.0	..	123.5	-72.75	12.869
O-nitrotoluene ..	219.0	82	142.3	-76.94	10.806
M-nitrotoluene ..	230.6	83	144.0	-75.70	
O-chlorophenol ..	173.0	..	..	-66.83	
P-chlorophenol ..	217.0	..	..	-65.54	

\* Horstmann, Graham-Otto's 'Lehrbuch der Chemie,' vol. i. 3, 375.

considered that it might be possible to trace some similarity between the magnetic and other properties of isomerides. The data have therefore been collected together in the above table. The values of molecular magnetic rotations have been taken from Perkin's† papers. The values of the boiling-points are those carefully determined by us. The values of  $r$  for orange incident light, except in the case of nitro-toluenes, have been taken from

† *Loc. cit.*

Krishnan's \* data and the values of molecular volumes have been taken from Lossen's<sup>(21)</sup> data.

An examination of the above table shows the following significant relations :—

(1) The values of  $x_M$  for aliphatic isomerides increase in the order primary—secondary—tertiary, and, as given before, the difference between the values for tertiary and secondary is much less than that between the values for secondary and primary isomerides.

(2) In the case of aromatic isomerides the value of  $x_M$  for ortho is maximum. And the values for meta and para, like their other physical properties, are near together.

(3) In every group the isomeride having a larger value of the molecular magnetic rotation has also a larger value of the molecular magnetic susceptibility.

(4) In every group the isomeride of a higher boiling-point has got a lower magnetic susceptibility.

(5) In the case of primary, secondary, and tertiary alcohols, the one with a larger molecular volume has also a larger magnetic susceptibility, but in the case of aromatic isomerides, on the other hand, ortho having the smallest molecular volume, has got the largest magnetic susceptibility.

(6) According to Krishnan (*loc. cit.*) within the same series of compounds, increased symmetry causes more perfect polarization. In a group of isomerides, therefore, the values of the depolarization factor  $v$  can be taken as a measure of the anisotropy of the molecule. And we find, in all the groups of isomerides for which the values of  $v$  are available, that the more anisotropic the molecule, the smaller its magnetic susceptibility. The values of  $v$  have also been measured for the three isomeric xylenes, and the value is least for the isomeride, which, according to all the above observations, has got maximum susceptibility. Further, the true anisotropy of the molecule is given by the value of  $v$  in the gaseous state. And we find that the above relation between  $x_M$  and  $v$  holds as well with the values of  $v$  for vapours of organic isomers, as observed by Ganesan<sup>(22)</sup> and by Rama Krishna Rao (*loc. cit.*).

\* *Loc. cit.*

An explanation of the above facts will be given shortly when more data are available. But it might be pointed out here that, in the case of isomerides, not only the nature and number of the atoms are the same, but the number and nature of the valency bonds remain unaltered. The only difference that has occurred is a change in the spatial arrangement of groups of atoms constituting the molecule and its consequent effect on the orientation of molecules with respect to one another. And, therefore, in order to give a complete explanation of the influence of position isomerism on magnetic susceptibilities, it is necessary to consider the effect of changes in spatial arrangements of various groups constituting the molecule. From this standpoint, a large number of solid and liquid isomerides, including optical isomers,—are being investigated.

### References.

- (1) *Ann. Phys. Chem.* xxii. pp. 121, 123 (1884) ; *ibid.* xxxiv. pp. 180–221 (1888).
- (2) *Akad. Wiss. Wien. Sitz. Ber.* cxiii. 2 a, pp. 1007–1017 (1904).
- (3) *Compt. Rend.* cxl. pp. 237–239 (1905).
- (4) *Compt. Rend.* clvi. pp. 323–325 (1913).
- (5) *Loc. cit.*
- (6) *J. C. S.* xlv. p. 575 (1884) ; *ibid.* lxix. p. 1236 (1896).
- (7) *Phil. Mag.* [6] l. p. 697 (1925).
- (8) *Ind. Journ. Phys.* ii. p. 61 (1927).
- (9) *Physical Review*, xxx. pp. 889–899 (1929).
- (10) *Ind. Journ. Phys.* i. 358 (1926–27).
- (11) *Ind. Journ. Phys.* ii. p. 355 (1927–28).
- (12) Savard, *Ann. Chim.* x. pp. 287–350 (1929).
- (13) Ganesan and Venkateswaran, *Ind. Journ. Phys.* iv. p. 209 (1929) ; *Kohlrausch. Naturwiss.* xvii. pp. 366–367 (1929) ; Czapsaka, *Compt. Rend.* clxxxix. pp. 32–33 (1929).
- (14) *Phil. Mag.* (7) v. pp. 536–545 (1928) ; *ibid.* (7) vi. pp. 217–233 (1928) ; *Journ. Ind. Chem. Soc.* vi. p. 303 (1929). (In the last paper a correction has also been applied to the values given in the second paper.)
- (15) *Journ. de Phys.* i. p. 97 (1920).
- (16) *J. A. C. S.* xlii. p. 561 (1921) ; *ibid.* xlv. p. 1334 (1923).
- (17) *Zeit. physik. Chem.* xiv. p. 232 (1894).
- (18) *J. C. S.* lxxxi. p. 723 (1902).
- (19) *J. A. C. S.* xxx. p. 353 (1908).
- (20) Pascal, *Comptes Rendus*, cxlix. pp. 342–345 (1909).
- (21) *Annalen der Chemie*, ccliv. p. 42.
- (22) *Phil. Mag.* (6) xlix. p. 1219 (1925).

University Chemical Laboratories,  
University of the Punjab,  
Lahore (India).

X. *Note on the Potential and Attraction of Rectangular Bodies.* By C. E. WRIGHT\*.

§ 1. *Introduction.*

THE evaluation of the mutual potential of two extended bodies presents considerable difficulty unless the shape of the bodies is especially simple. For the needs of astronomy the case of widely-separated bodies has been discussed to an adequate degree of approximation. There are also very many elegant theorems on the attraction of ellipsoids and of nearly spherical bodies: in general these are not susceptible of simple numerical evaluation.

The case of *similarly oriented* rectangular bodies is amenable to straightforward methods, and numerical values can be obtained without excessive labour. As the results do not seem to be readily accessible, some discussion of this case is here attempted.

§ 2. *Notation and Method.*

The bodies concerned are rods, rectangular laminæ, and rectangular solids (cuboids). Since the densities of these bodies and the constant of gravitation (or force) can be supplied at will from consideration of "dimensions," these will be omitted. The coordinates of the geometric centre of one body relative to that of the other appear in the formulæ deduced. Hence it will be clear that whether attraction or repulsion is concerned, the *signs* of the component forces and couples can be determined from the configuration; and so in numerical values these signs are omitted.

The centre of the first body is taken at an origin of rectangular coordinates  $(O, x, y, z)$ . The coordinates of the centre of the second body will be denoted by  $(\xi, \eta, \zeta)$ , and through this point  $(O')$  is drawn a system  $(O', x', y', z')$  parallel to  $(O, x, y, z)$  and similarly oriented. The dimensions of the bodies, in the most general case considered, are  $(2a, 2b, 2c)$ ,  $(2a', 2b', 2c')$  respectively, parallel to  $Ox, Oy, Oz$ . The value of the mutual potential,

$$V = \Sigma \Sigma \frac{mm'}{r},$$

\* Communicated by the Author.

is then given by the integral

$$\int_{-a}^{+a} \int_{-a'}^{+a'} \int_{-b}^{+b} \int_{-b'}^{+b'} \int_{-c}^{+c} \int_{-c'}^{+c'} \frac{dx dx' dy dy' dz dz'}{\{(\xi + x' - x)^2 + (\eta + y' - y)^2 + (\zeta + z' - z)^2\}^{\frac{3}{2}}}.$$

This, and most of the corresponding integrals which arise later, may be simplified by a method which depends essentially on the fact that the limits of integration are constant, and which has been employed in the consideration of a mathematically similar problem (Phil. Mag., June 1929, p. 940).

Writing

$$\xi + x' - x = u, \quad \eta + y' - y = v, \quad \zeta + z' - z = w,$$

integration with respect to  $x'$  and  $-x$  may each be represented by integration with respect to  $u$ , and similarly for the other pairs. With

$$P^2 = u^2 + v^2 + w^2$$

the result becomes

$$V = - \iiint \iiint \frac{(du)^2 (dv)^2 (dw)^2}{P}.$$

Disregarding sign for the moment, let this integral be represented by (112233). It will be found that all the integrals represented by omission of any number (up to five inclusive) of the digits in the above symbol will represent mutual (or simple) potentials for the cases indicated. But, further, they also yield the force components of one body on the other. To see this, in the general case take  $Z$  the force component of the first body on the second, in the direction  $Oz$ . This is given by

$$\pm \frac{\partial V}{\partial \xi} = \pm \frac{\partial}{\partial w} [V],$$

provided that the differentiation takes place on the general integral, and afterwards substitution takes place for *all* the variables  $(x, x', y, y', z, z')$ . But  $\frac{\partial V}{\partial w}$  may be symbolized by (11223·), with some distinctive notation for the sixfold substitution, say (11223·)<sub>6</sub>.

The integral (11223·) thus admits of two interpretations:—

- (a) Let the variables be  $x, x', y, y', z$ , so that,  $u, v$  being as before,  $w = \xi - z$ . Then  $\pm(11223\cdot)$  is the mutual potential of a rectangular solid and a plate in the  $x'y'$  plane.
- (b) Let  $x, x', y, y', z, z'$  all occur ( $w = \xi + z' - z$ ), and let substitution for all six take place. This is the case considered above.

Similar results hold for some of the other cases, as noted below.

### § 3.

This method of integration does not permit the deduction of the couple components by means of virtual work, since continuous angular change is not provided for. Direct evaluation reduces partially to integrals of the class considered above. Thus N, the component about  $Oz$ , of the couple exerted on the body with centre  $(\xi, \eta, \zeta)$  is given by the integral of  $\pm\{(\eta + y')u - (\xi + x')v\}/P^3$  or of  $(yu - xv)/P^3$  since

$$(\eta + y' - y)u - (\xi + x' - x)v \equiv 0.$$

But taking the integrations in convenient order,

$$\int \frac{v dv}{P^3} = -\frac{1}{P},$$

and substituting in the sixfold integral gives

$$\pm N = \int x(1233) dx - \int y(1233) dy,$$

and similarly for L and M.

### § 4.

The results for the various cases are brought up to the point at which numerical substitution may be employed. Since as many as nine parameters ( $a$  etc.,  $a'$  etc.,  $\xi$  etc.) may remain, such interest as the problem contains would not justify further general consideration. But a sufficient numerical view can be given when all the dimensions are the same ( $a = a' = b = b' = c = c'$ , except such as vanish). Let  $\phi(u, v, w)$  be any integral, and write

$$\xi = 2\lambda a, \quad \eta = 2\mu a, \quad \zeta = 2\nu a,$$

and let  $\phi$  become  $\psi(\lambda, \mu, \nu)$ . Substitution for  $x$  (or  $x'$ ) gives then

$$\pm \{ \psi(\lambda + \frac{1}{2}, \mu, \nu) - \psi(\lambda - \frac{1}{2}, \mu, \nu) \},$$

or a central difference of  $\psi$  with respect to  $\lambda$ . Hence a tabulation for  $\psi$  at unit intervals would lead, by differencing, to the numerical values required. In practice it is found that this method gives sufficient values for the construction of reasonably accurate diagrams.

### § 5.

When the distance between the bodies is relatively large, expansion of the integrands in ascending powers of  $x' - x$  etc. may be employed as in the well-known general method. The result of integration of a term involving  $(x' - x)^p$  yields a factor

$$A_{p+2} \equiv \frac{2}{(p+1)(p+2)} \{ (a' + a)^{p+2} - (a' - a)^{p+2} \}$$

if  $p$  is even (including  $p=0$ ), and zero if  $p$  is odd. For the special case of equal dimensions, the integral of  $(x' - x)^p (y' - y)^q (z' - z)^r$

$$= \frac{2^{p+q+r+9} a^{p+q+r+6}}{(p+1)(p+2)(q+1)(q+2)(r+1)(r+2)}$$

or zero, the finite value requiring  $p, q, r$  all even.

### § 6. Evaluation of the Integrals.

$$(1) \quad \int \frac{du}{P} = \log(u + P), \quad . \quad . \quad . \quad . \quad . \quad (A)$$

$$(11) \quad \iint \frac{(du)^2}{P} = u \log(u + P) - P, \quad . \quad . \quad . \quad (B)$$

$$(12) \quad \iint \frac{du dv}{P} = v \log(u + P) + u \log(v + P) + w \tan^{-1} \frac{wP}{uv}, \quad (C)$$

$$(112) \quad \iiint \frac{(du)^2 dv}{P} = uv \log(u + P) + uw \tan^{-1} \frac{wP}{uv} + \frac{1}{2}(u^2 - w^2) \log(v + P) - \frac{1}{2}vP, \quad (D)$$



$$(123) \quad \iiint \frac{du dv dw}{P} \\ = \sum_{u, v, w} \left[ wv \log(u + P) + \frac{1}{2} u^2 \tan^{-1} \frac{uP}{vw} \right], \quad \dots \quad (E)$$

$$(1122) \quad \iiint \frac{(du)^2 (dv)^2}{P} \\ = \frac{1}{2} u(v^2 - w^2) \log(u + P) \\ + \frac{1}{2} v(u^2 - w^2) \log(v + P) \\ + uvw \tan^{-1} \frac{wP}{uv} + \frac{1}{2} w^2 P - \frac{1}{6} P^3, \quad (F)$$

$$(1123) \quad \iiint \frac{(dw)^2 dv dw}{P} \\ = uvw \log(u + P) \\ + \frac{1}{2} (u^2 w - \frac{1}{6} w^3) \log(v + P) \\ + \frac{1}{2} (u^2 v - \frac{1}{6} v^3) \log(w + P) \\ + \frac{1}{6} u^3 \tan^{-1} \frac{uP}{wv} + \frac{1}{2} uv^2 \tan^{-1} \frac{vP}{uw} \\ + \frac{1}{2} uw^2 \tan^{-1} \frac{wP}{uv}, \quad \dots \quad (G)$$

$$(11223) \quad \iiint \frac{(du)^2 (dv)^2 dw}{P} \\ = \frac{1}{6} uw(3v^2 - w^2) \log(u + P) \\ + \frac{1}{6} vw(3u^2 - w^2) \log(v + P) \\ + \frac{1}{24} (6u^2 v^2 - u^4 - v^4) \log(w + P) \\ + \frac{1}{6} uw^3 \tan^{-1} \frac{vP}{uw} + \frac{1}{6} vu^3 \tan^{-1} \frac{uP}{vw} \\ + \frac{1}{2} uvw^2 \tan^{-1} \frac{wP}{uv} + \frac{1}{12} Pw^3 \\ - \frac{1}{8} (u^2 + v^2) Pw, \quad \dots \quad (H)$$

$$(112233) \quad \iiint \frac{(du)^2 (dv)^2 (dw)^2}{P} \\ = \frac{1}{24} \Sigma (6u^2 v^2 - u^4 - v^4) w \log(P + w) \\ + \frac{1}{6} \Sigma u^3 vw \tan^{-1} \frac{uP}{vw} + \frac{1}{60} \Sigma (u^4 - 3u^2 v^2). \quad \dots \quad (K)$$

In these integrations terms arise which will clearly give zero result on substitution. Such terms have been omitted and hence cross-differentiation of the various integrals will not always give results in complete agreement; but complete differentiation should always restore the integrand  $P^{-1}$ .

For numerical work it may be noted that (after substitution of limits)  $u, v, w$  are built up by mere addition from  $\xi, a, a'$ ;  $\eta, b, b'$ ; and  $\zeta, c, c'$ : hence the tabulation of the integrals as functions of  $u, v, w$  will be effective. The forms which require tabulation reduce, in fact, to  $\log(u + P)$  and  $\tan^{-1} uP/vw$ ; these are symmetrical in two of the variables, and the surfaces of equal values are given, for

$$\log(u + P) = K,$$

by the confocal paraboloids of revolution

$$v^2 + w^2 = e^K(e^K - 2u),$$

and for the function

$$\tan^{-1} uP/vw = \beta,$$

by the quartic cones

$$u^2(u^2 + v^2 + w^2) = w^2v^2 \tan^2 \beta.$$

Both these functions also satisfy

$$\left\{ \frac{\partial^2}{\partial u^2} + \frac{\partial^2}{\partial v^2} + \frac{\partial^2}{\partial w^2} \right\} \phi = 0.$$

## § 7.

Some of the results arising directly from the integrals in § 6 will now be considered in a little detail, and in the next paragraph some numerical results will be given.

(A)  $\log(u + P)$ ;  $u = \xi - x$ ,  $v = \eta$ ,  $\zeta = w$  gives the potential of a uniform rod at any point in space.

(B) With substitution  $u = \xi + x' - x$ ,  $v = \eta$ ,  $w = \zeta$  gives the mutual potential of two parallel rods. The force components (always the force exerted on the second body by the first) are given numerically by values

$$X = \frac{\partial B}{\partial \xi} = \frac{\partial B}{\partial u} = (A)_{x, x'}$$

(the notation indicating substitution for  $x$  and  $x'$  in the

function (A) and substitution of limits for these variables. Thus (A)<sub>x, x'</sub> here stands for

$$\log \left[ (\xi + x' - x) + \{(\xi - x' + x)^2 + \eta^2 + \zeta^2\}^{\frac{1}{2}} \right]_{x=-a}^{+a} \Big|_{x'=-a'}^{+a'},$$

whilst for the potential of a rod, (A) stands for

$$\log \left[ (\xi - x) + \{(\xi - x)^2 + \eta^2 + \zeta^2\}^{\frac{1}{2}} \right]_{x=-a}^{+a}$$

and so in all similar cases as indicated, § 2, end),

$$Y = \frac{\partial B}{\partial v} = \left( \frac{v}{u + P} \right)_{x, x'}, \quad Z = \left( \frac{w}{u + P} \right)_{x, x'}.$$

(C) With variables  $x, y$  this gives the potential, at any point in space, of a uniform rectangular plate; the intensity components follow in the usual way\*.

If variables  $x, y'$  are used, the mutual potential of two rods at right angles is derived from the same integral, and the components of force are given by

$$X = (\pm) \log(v + P), \quad Y = \log(u + P),$$

$$Z = \pm \frac{\partial C}{\partial w} = \pm \left[ \frac{wv}{w^2 + v^2} + \frac{wu}{w^2 + u^2} + \tan^{-1} \frac{wP}{uv} \right].$$

(D) Substitution  $x, x', y$  gives the mutual potential of a rectangle and a rod parallel to one of its edges. The force components are

$$X = \pm (12 \cdots \cdots)_3, \quad Y = (11 \cdots \cdots)_3,$$

$$Z = \pm \frac{\partial}{\partial w} (112 \cdots \cdots) = \pm \left[ w \log(u + P) - u \tan^{-1} \frac{wP}{uv} - \frac{uvw}{v^2 + w^2} - \frac{1}{2} \frac{(u^2 - w^2)(2v - P)}{u^2 + w^2} \right],$$

with triple substitution.

(E) Substitution  $x, y, z$  gives the potential of a rectangular solid at a point. The force components are

$$\pm (23 \cdots \cdots)_3, \quad \pm (13 \cdots \cdots)_3, \quad \pm (12 \cdots \cdots)_3.$$

\* When a simple potential arises from the integral, a suitable factor evidently gives the mutual potential of the body concerned (centre at origin) and a uniform sphere or spherical shell with centre at  $(\xi, \eta, \zeta)$ .

When the substitution is  $x, y, z'$  the mutual potential of a rectangle and a rod perpendicular to its plane arises. The force components are as before, except for the substitution.

(F) The substitution is for  $(x, y, x', y')$ , and gives the mutual potential of two rectangular plates in parallel planes. The force components are

$$\begin{aligned} & (122\cdots)_4, \quad (112\cdots)_4, \quad \text{and} \quad \pm \frac{\partial F}{\partial w} \\ & = \pm \left[ \frac{1}{2} \frac{uw(v^2 - w^2)}{P(u + P)} + \frac{1}{2} \frac{vw}{P} \cdot \frac{u^2 - w^2}{v + P} \right. \\ & \quad - uw \log(u + P) - vw \log(v + P) \\ & \quad \left. + \frac{u^2 v^2 w}{P} \left\{ \frac{1}{u^2 + w^2} + \frac{1}{v^2 + w^2} \right\} + \frac{1}{2} \frac{w(P^2 + w^2)}{P} \right]. \end{aligned}$$

(G) Substitution  $x, x', y, z$  gives the mutual potential of a solid and a rod parallel to one of its edges.

Substitutions  $(x, x', y', z)$  or  $(x, x', y, z')$  give mutual potentials of rectangular laminæ with planes at right angles. The force components are derivable from

$$(123\cdots)_4, \quad (113\cdots)_4, \quad (112\cdots)_4,$$

with corresponding substitution in the several cases.

(H) Substitution  $x, x', y, y'$  and  $(z \text{ or } z')$  gives mutual potential of rectangular solid and lamina whose plane is parallel to a face of the solid. The force components are derived from

$$(1223\cdots)_5, \quad (1123\cdots)_5, \quad (1122\cdots)_5,$$

with the proper substitutions.‡

(K) The mutual potential of similarly oriented rectangular solids. The force and couple components are indicated in §§ 2, 3 respectively.

## § 8.

Short tables of the functions  $\log_e \{\lambda + (\lambda^2 + \mu^2)^{\frac{1}{2}}\}$  (Table I.) and  $\tan^{-1} \frac{(1 + \alpha^2 + \beta^2)^{\frac{1}{2}}}{\alpha\beta}$  (Table II.) are included for use in numerical evaluations. As examples, the case of equal parallel rods is considered in some detail.

TABLE I.

Values of  $10^7 \log_e \{\lambda + (\lambda^2 + \mu^2)^{\frac{1}{2}}\}$ .

$\lambda$ .	$\mu=1$ .	$\mu=2$ .	$\mu=3$ .	$\mu=4$ .
0	0	6931472	10986122	13862943
	8818736	11743590	14260624	16337608
	14436354	15745207	17237573	18675061
	18184464	18879103	19799858	20794415
	20947125	21367826	21972245	22676678
5	23124382	23403782	23824079	24338873
	24917797	25115935	25422476	25810575
	26441206	26588675	26821012	27121920
	27764722	27878596	28060236	28299297
	28934439	29024948	29170586	29364522
10	29982228	30055854	30175086	30335254
	30931021	30992062	31091391	31225718
	31797853	31849269	31933247	32047407
	32595724	32639617	32711517	32809664
	33334774	33372678	33434912	33520147
15	34023065	34036123	34110505	34185188
	34667109	34696193	34744112	34810068
$\lambda$ .	$\mu=5$ .	$\mu=6$ .	$\mu=7$ .	$\mu=8$ .
0	16094378	17916903	19459101	20794415
	18081279	19576639	20882857	22041182
	19994731	21192095	22278738	23269079
	21782627	22729711	23623408	24461660
	23421062	24169045	24900813	25606533
5	24908114	25502455	26102407	26695851
	26254109	26731330	27225803	27725886
	27474198	27862168	28272836	28696102
	28584211	28903717	29247809	29608150
	29598785	29865226	30156208	30465011
10	30530733	30755550	31003874	31270434
	31390983	31582746	31796526	32028061
	32188757	32353948	32539511	32742046
	32931809	33075392	33237697	33416007
	33626667	33752483	33895455	34053392
15	34278842	34389900	34516668	34657358
	34893013	34991708	35104776	35230769

TABLE I. (contd.).  
 Values of  $10^7 \log_e \{\lambda + (\lambda^2 + \mu^2)^{\frac{1}{2}}\}$ .

$\lambda$ .	$\mu=9$ .	$\mu=10$ .	$\mu=11$ .	$\mu=12$ .
0	21972245	23025851	23978952	24849066
	23081082	24024191	24886794	25681437
	24176572	25012751	25787262	26508111
	25246746	25982580	26673499	27323730
	26282026	26926203	27539599	28123567
5	27275671	27837968	28380864	28903717
	28223696	28714099	29193890	29661184
	29124459	29552515	299276506	30393874
	29978097	30352532	30727613	31100516
	30785981	31114519	31446981	31780537
10	31550249	31839586	32135040	32433927
	32273465	32529319	32792687	33061105
	32958367	33185581	33421130	33662801
	33607706	33810360	34021763	34239956
	34224144	34405670	34596075	34793640
15	34810201	34973482	35145579	35324995
	35368219	35515683	35671773	35835188
$\lambda$ .	$\mu=13$ .	$\mu=14$ .	$\mu=15$ .	$\mu=16$ .
0	25649493	26390572	27080501	27725702
	26417967	27104252	27746675	28350480
	27181949	27814328	28409915	28972653
	27937178	28517360	29067402	29590070
	28679823	29210204	29716533	30200551
5	29406627	29890131	30355002	30802137
	30114990	30554880	30980854	31393132
	30802949	31202690	31592392	31972127
	31469215	31832284	32188757	32538004
	32113026	32442829	32768750	33089927
10	32734101	33033878	33331952	33627323
	33332533	33605313	33878105	34149847
	33908709	34157275	34407183	34657358
	34463228	34690108	35218222	35149880
	34996834	35204308	35414890	35627530
15	35510367	35700475	35894236	36090705
	36004723	36179280	36357873	36539622



From the integral B, with  $u = \xi + x' - x$  and limits  $-a$  to  $+a$  for  $x$  and  $x'$ , together with the substitution  $w = \zeta = 0$  (evidently permissible in this case), the following values arise : —

*Mutual Potential.*

$$\epsilon V = 2a\Delta^2 [\lambda \log_e \{\lambda + (\lambda^2 + \mu^2)^{\frac{1}{2}}\} - (\lambda^2 + \mu^2)^{\frac{1}{2}}].$$

*Force.*

$$\epsilon X = \Delta^2 \log_e \{\lambda + (\lambda^2 + \mu^2)^{\frac{1}{2}}\},$$

$$\epsilon Y = \Delta^2 \frac{1}{\lambda + (\lambda^2 + \mu^2)^{\frac{1}{2}}} = \frac{1}{\mu} \Delta^2 (\lambda^2 + \mu^2)^{\frac{1}{2}}.$$

*Couple.*

$$\epsilon N = 2a^2 \left[ \frac{\lambda}{\mu} \Delta^2 (\lambda^2 + \mu^2)^{\frac{1}{2}} - \Delta^2 \log_e \{\lambda + (\lambda^2 + \mu^2)^{\frac{1}{2}}\} \right].$$

Here  $\epsilon = \pm 1$ , chosen to make the values positive in general; and the differences refer to  $\lambda$  only.

Tables for the potential and force components are given below.

TABLE III.

Values of

$$10^7 \epsilon V / 2a \equiv 10^7 \Delta^2 [\lambda \log_e \{\lambda + (\lambda^2 + \mu^2)^{\frac{1}{2}}\} - (\lambda^2 + \mu^2)^{\frac{1}{2}}].$$

$\lambda$ .	$\mu=0$ .	$\mu=1$ .	$\mu=2$ .	$\mu=3$ .
0	$\infty$	9343200	4902876	3303450
	$\infty$	7168828	4440323	3143839
	5232478	4578161	3552120	2771748
	3397984	3208242	2792795	2362279
	2526712	2447442	2249170	2006083
5	2009410	1973171	1865477	1720045
	1682761	1651165	1586774	1434595
	1429324	1418828	1387721	1315962
	1253272	1243466	1215403	1172595
	1113420	1106523	1086631	1055758
10	1001657	996673	982070	959112
	910358	906672	895561	878074
	834297	831405	822886	809248
	769982	767710	760899	750192
	714908	713079	707870	698956
15	664210	665675	661199	654163



TABLE III. (*contd.*).

Values of

$$10^7 eV/2a \equiv 10^7 \Delta_\lambda^2 [\lambda \log_e \{\lambda + (\lambda^2 + \mu^2)^{\frac{1}{2}}\} - (\lambda^2 + \mu^2)^{\frac{1}{2}}].$$

$\lambda$ .	$\mu=4$ .	$\mu=5$ .	$\mu=6$ .	$\mu=7$ .
0	2487218	1993408	1662840	1426156
	2415658	1955646	1640609	1412019
	2232373	1853818	1578834	1371918
	2000342	1714096	1489603	1312066
	1770028	1562242	1386564	1239925
5	1563348	1415379	1280764	1162484
	1391138	1281711	1179177	1084839
	1241355	1163768	1085440	1010581
	1119669	1061143	1000755	941204
	1016661	972280	935206	877540
10	929531	895255	848137	820099
	855224	828309	798629	766600
	791270	769819	745856	720584
	735784	718467	698827	687644
	687280	673079	656841	639172
15	644577	632819	619441	604404

---

$\lambda$ .	$\mu=8$ .	$\mu=9$ .	$\mu=10$ .	$\mu=11$ .
0	1248380	1109972	999170	908466
	1238835	1103237	994242	904757
	1211458	1083741	979886	893888
	1169572	1053409	947278	876614
	1117561	1014910	928084	854020
5	1059841	971056	894190	827376
	1000068	924448	857378	797956
	940919	877128	819229	766910
	884179	830618	780938	735221
	831664	785864	743413	703662
10	779409	743519	707245	672864
	736424	703832	672828	642937
	693680	666898	640371	614412
	655402	632660	609873	587356
	620420	601061	581401	561764
15	588459	571836	554848	537736

Values of

TABLE III. (*contd.*).

$$10^7 \epsilon V / 2a \equiv 10^7 \Delta_\lambda^2 [\lambda \log_e \{\lambda + (\lambda^2 + \mu^2)^{\frac{1}{2}}\} - (\lambda^2 + \mu^2)^{\frac{1}{2}}].$$

$\lambda$ .	$\mu=12$ .	$\mu=13$ .	$\mu=14$ .	$\mu=15$ .	$\mu=16$ .
0	832852	768852	713984	666420	624120
	829989	766596	712172	664948	623581
	821570	759944	706833	660592	619987
	808091	749235	698180	653513	614122
	799282	734971	686596	643978	606185
5	769017	717792	672510	632311	596418
	745213	698206	656399	618057	585102
	719746	677250	638791	605656	572517
	693357	655073	620102	587371	558954
	666687	632458	600764	571626	544711
10	640230	609720	581319	554684	529970
	614363	587265	561676	537619	515015
	589347	565304	542355	520705	500006
	565320	543190	523480	503804	484482
	542424	525086	505126	487416	471604
15	520683	503095	486937	471449	455380

TABLE IV.

$$\text{Values of } 10^7 \epsilon X \equiv 10^7 \Delta_\lambda^2 \log_e \{\lambda + (\lambda^2 \pm \mu^2)^{\frac{1}{2}}\}.$$

$\lambda$ .	$\mu=0$ .	$\mu=1$ .	$\mu=2$ .	$\mu=3$ .
0	0	0	0	0
	$\infty$	3191118	810500	297553
	2876820	1874508	867720	414664
	1177830	985449	645174	389898
	645384	585404	452767	320553
5	408223	383842	329803	253437
	281708	270006	239412	199861
	206192	199893	182821	159312
	157483	153799	143568	128874
	124226	121928	115446	105850
10	100504	98996	94698	88195
	82987	81961	79001	74449
	69687	68961	66859	63586
	59347	58821	57287	54875
	51152	50759	49614	47802
15	44542	44247	43375	41986

TABLE IV. (*contd.*).Values of  $10^7 \epsilon X \equiv 10^7 \Delta_\lambda^2 \log_e \{\lambda + (\lambda^2 \pm \mu^2)\}$ .

$\lambda$ .	$\mu=4$ .	$\mu=5$ .	$\mu=6$ .	$\mu=7$ .
0	0	0	0	0
	137312	73449	44280	27875
	218099	125556	77838	51211
	237091	149461	98284	67265
	220068	151383	105924	75811
5	190493	141057	104535	78198
	160357	125906	98027	76363
	133968	110076	89309	72060
	112152	95439	80030	66574
	94493	82626	71185	60733
10	80268	71698	63128	55014
	68775	62476	55994	49667
	59432	54722	49758	44529
	51774	48194	44353	40968
	45442	42680	39674	36275
15	40161	38010	35609	33105

---

$\lambda$ .	$\mu=8$ .	$\mu=9$ .	$\mu=10$ .	$\mu=11$ .
0	0	0	0	0
	18870	13347	9780	7374
	35316	25316	18731	14231
	47708	34894	26206	20137
	55555	41635	31858	25835
5	59283	45620	35634	27239
	59820	47262	37715	30410
	58166	47125	38399	31509
	55189	45754	38030	31739
	51526	43616	36920	31309
10	47617	41052	35334	30412
	43732	38314	33471	29204
	40024	35563	31483	27810
	36576	32901	29469	26319
	33429	30381	27498	24808
15	30546	28039	25611	23310

TABLE IV. (*contd.*).Values of  $10^7 \epsilon X \equiv 10^7 \Delta_\lambda^2 \log_e \{\lambda + (\lambda^2 + \mu^2)\}$ .

$\lambda$ .	$\mu=12$ .	$\mu=13$ .	$\mu=14$ .	$\mu=15$ .	$\mu=16$ .
0	0	0	0	0	0
	5697	4492	3604	2934	2605
	11055	8753	7044	5753	4756
	15782	12584	10183	8356	6936
	19687	15841	12917	10662	8895
5	22683	18441	15178	12617	10591
	24777	20404	16939	14314	12000
	26048	21693	18216	15173	13118
	26621	22455	19052	16372	13954
	26631	22736	19490	16791	14537
10	26212	22643	19617	17049	14872
	25482	22256	19473	17075	15013
	24541	21657	19129	16917	14989
	23471	20913	18633	16615	14872
	22329	20073	18033	16197	14475
15	21162	19177	17392	15709	14258

TABLE V.

Values of  $10^7 \epsilon Y \equiv \frac{10^7}{\mu} \Delta_\lambda^2 (\lambda^2 + \mu^2)^{\frac{1}{2}}$ .

$\lambda$ .	$\mu=1$ .	$\mu=2$ .	$\mu=3$ .	$\mu=4$ .
0	8284272	2360680	1081851	614528
	4076408	1781456	936653	564812
	1043553	923826	646053	447084
	346182	447303	400900	322476
	150860	232221	245309	223539
5	78291	131809	154334	154271
	45623	80821	101057	107942
	28846	52734	68871	77148
	19375	36159	48662	56429
	13631	25807	35481	42215
10	9949	19032	26581	32246
	7482	14422	20383	25101
	5766	11181	15949	19873
	4538	8840	12699	15974
	3636	7106	10268	13014
15	2955	5796	8416	10732

TABLE V. (*contd.*).

Values of  $10^7 \epsilon Y \equiv \frac{10^7}{\mu} \Delta^2 (\lambda^2 + \mu^2)^{\frac{1}{2}}$ .

$\lambda$ .	$\mu=5$ .	$\mu=6$ .	$\mu=7$ .	$\mu=8$ .
0	396078	275875	203051	155644
	374252	265051	197106	152120
	319284	236426	180887	142299
	252770	198750	158316	128095
	191543	160414	133690	111801
5	142477	126474	110217	95387
	105787	98719	89616	80159
	79160	76987	72429	66771
	59986	60331	58511	55404
	46122	47660	47418	45960
10	35993	38017	38640	38210
	28496	30639	31700	31891
	22869	24949	26200	26747
	18584	20520	21819	22557
	15278	17039	18310	19133
15	12693	14275	15477	16324

---

$\lambda$ .	$\mu=9$ .	$\mu=10$ .	$\mu=11$ .	$\mu=12$ .
0	123078	99751	82475	69324
	120860	98288	81471	68613
	114588	94104	78578	66551
	105263	87756	74119	63335
	94164	79987	68546	59246
5	82502	71554	62338	54600
	71196	63088	55929	49790
	60822	55041	49659	44938
	51652	47683	43758	40027
	43749	41136	38362	35587
10	37049	35422	33529	31518
	31426	30498	29264	27851
	26732	26289	25540	24584
	22823	22711	22311	21800
	19567	19675	19522	19167
15	16850	17100	17119	16953

TABLE V. (contd.).

Values of  $10^7 \epsilon Y = \frac{10^7}{\mu} \Delta_\lambda^2 (\lambda^2 + \mu^2)^{\frac{1}{2}}$ .

$\lambda$ .	$\mu=13$ .	$\mu=14$ .	$\mu=15$ .	$\mu=16$ .
0	59084	50955	44395	39024
	58567	50570	44102	38798
	57058	49442	43242	38131
	54684	47652	41869	37061
	51624	45322	40065	35644
5	48088	42592	37928	33951
	44234	39609	35563	32056
	40394	36507	33069	30033
	36566	33401	30534	27951
10	32908	30380	28030	25867
	29489	27507	27612	23827
	26348	24823	23319	21867
	23501	22349	21169	20010
	20244	20095	19194	18272
15	18664	18056	17378	16661
	16642	16223	15727	15178

### § 9. Extensions to other Inverse Power Laws.

Let  $I$  be any integral in which  $w$  does not occur as a variable of integration. Replace  $w^2$  by  $\alpha$ . Then  $\text{Lt}_{\alpha \rightarrow 0} \left( \frac{\partial}{\partial \alpha} \right)^s I$  gives the result corresponding to  $I$  in the case of attraction proportional to  $r^{-(2+2s)}$ . Deduction for odd powers of  $r$  would require the initial integration of  $(u^2 + v^2 + \alpha)^{-1}$  or for the law  $r^{-1}$ , of  $\log(u^2 + v^2 + \alpha)$ . The most general case of the kind requires the evaluation of

$$\iiint \iiint Q (du)^2 (dv)^2 (dw)^2$$

with the values

$$Q = (u^2 + v^2 + w^2 + \alpha)^{-\frac{1}{2}},$$

$$(u^2 + v^2 + w^2 + \alpha)^{-1}, \text{ and } \log(u^2 + v^2 + w^2 + \alpha)$$

with subsequent differentiations with respect to  $\alpha$ .

Blackheath.

18 Dec., 1929.

XI. *The Isotope Effect in Neon Lines.* By ELFED THOMAS, B.Sc., and Prof. E. J. EVANS, D.Sc., *University College of Swansea* \*.

THE isotope effect in the line spectra of some elements has been examined by Aronberg †, Harkins ‡, Merton §, Perete-Montamat ||, McLennan and Ainslie ¶, and by Schüler and Wurm \*\*. During the past three years investigations have been carried out at Swansea on the structure and width of spectrum lines, and the present work on the neon lines was submitted to Prof. A. Fowler, who informed us of the important investigation which had been carried out by Nagaoka and Mishima †† on the same problem. The results of the present investigation confirm those of Nagaoka and Mishima, who found that every strong neon line was accompanied by a weaker companion situated on the lower wave-length side of the strong line. When, however, the experimental values of the separations of the lines are compared, it is seen that the agreement is not complete.

In the present experiments the source of light was an ordinary spectrum tube containing neon, which was connected to the secondary terminals of an induction coil. An approximately parallel beam of light from the capillary portion of the tube was directed towards the Fabry-Perot interferometer by means of a lens, and the fringes focussed on the slit of a Hilger constant deviation spectroscope. When the spectrum tube was immersed in liquid air, it was found that the bright circular fringes were accompanied by much fainter ones, which had slightly lower wave-lengths than the bright fringes. The distances apart between the faint and bright fringes could not be measured accurately with the micrometer eyepiece at our disposal, and it was therefore decided to photograph the fringes. Various exposures were

\* Communicated by Prof. E. J. Evans.

† Aronberg, *Proc. Nat. Acad. Sci.* iii. p. 710 (1917). *Astr. Journ.* xlvii. p. 96 (1918).

‡ Aronberg and Harkins, *Journ. Am. Chem. Soc.* xlii. p. 1328 (1920).

§ Merton, *Proc. Roy. Soc.* xvi. p. 388 (1920); xcix. p. 87 (1921); c. p. 84 (1921).

|| Perete-Montamat, *Thèse* (Paris, 1928).

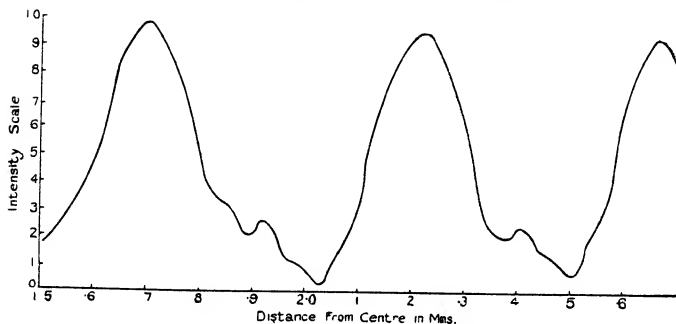
¶ McLennan and Ainslie, *Proc. Roy. Soc.* ci. p. 342 (1922).

\*\* Schüler and Wurm, *Naturwiss.* xv. p. 971 (1927).

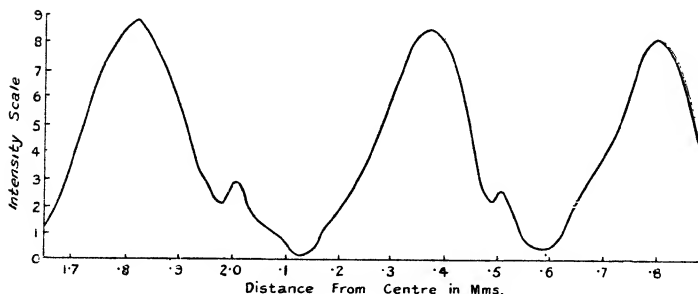
†† Nagaoka and Mishima, 'Proceedings of the Imperial Academy,' v. No. 5 (1929).

given ranging from 0.5 to 20 minutes, the longer exposures in order to bring out the faint companions of the weak neon lines. The intensity of the faint companion according to eye estimation, is from a fifth to a tenth that of its bright companion, but the relative intensity on the photographic plates depends on the exposure and on the intensity of

CURVE I.— $\lambda$  6717.22 ;  $e = 3.0$  cm.



CURVE II.— $\lambda$  6163.73 ;  $e = 2.5$  cm.



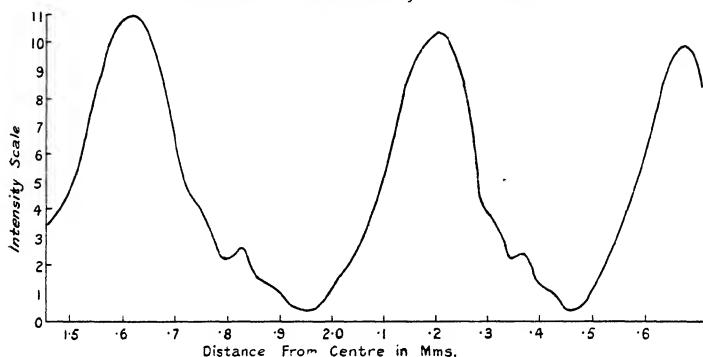
the neon line examined. The intensity distribution across the fringes was measured by means of a Cambridge microphotometer. Typical examples of the measurements are given in Curves I., II., III. and IV., which show the intensity distribution across the fringes of the 6717, 6164, 6030, and 5882 neon lines. These curves show the presence of the faint companions whose intensities are approximately about one-fourth that of their brighter companions.



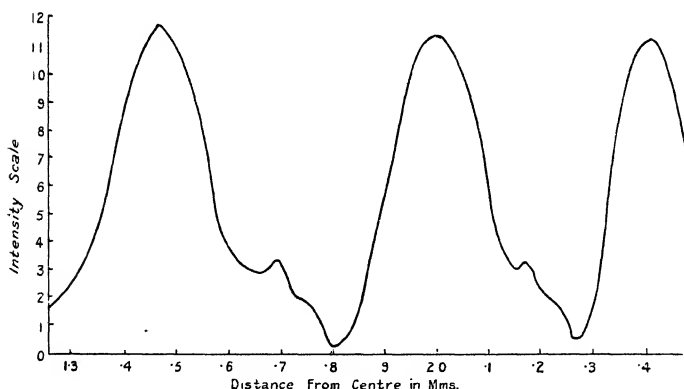
Let  $e$  = distance between the plates of the interferometer.  
 Then path difference for rays passing through normally =  $2e$ .  
 Let rays inclined at an angle  $\theta_1$  produce a ring of order  $m_1$ .  
 Then

$$\frac{2e}{\lambda} \cos \theta_1 = m_1. \quad . \quad . \quad . \quad . \quad . \quad (1)$$

CURVE III.— $\lambda 6030.2$  ;  $e = 2.5$  cm.



CURVE IV.— $\lambda 5882.06$  ;  $e = 3.0$  cm.



The next ring further out from the centre will be represented by

$$\frac{2e}{\lambda} \cos \theta_2 = m_1 - 1, \quad . \quad . \quad . \quad . \quad . \quad (2)$$

and

$$\frac{2e}{\lambda} \cos \theta_f = m_1 - f, \quad . \quad . \quad . \quad . \quad (3)$$

where  $f$  is a fraction less than unity.

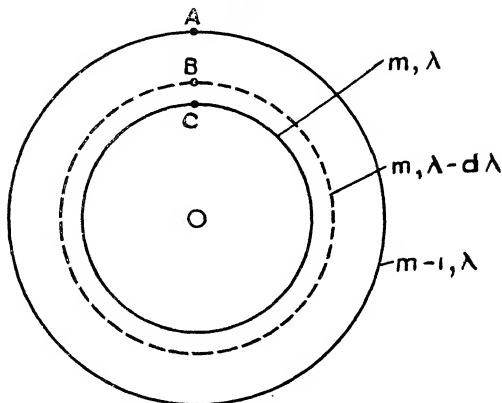
From equations (1), (2), and (3),

$$\frac{2e}{\lambda} (\cos \theta_1 - \cos \theta_2) = 1$$

and

$$\frac{2e}{\lambda} (\cos \theta_1 - \cos \theta_f) = f.$$

Fig. 1.



Expanding  $\cos \theta$  and neglecting higher power than  $\theta^2$ , it can be shown that

$$f = \frac{\theta_f - \theta_1}{\theta_2 - \theta_1} \cdot \frac{\theta_f + \theta_1}{\theta_2 + \theta_1}.$$

In fig. 1 let A and C represent the  $m$ th and  $(m-1)$ th order fringes of the stronger component  $\lambda$ , and let B represent the  $m$ th order of the faint component  $\lambda - d\lambda$ . The fraction

$$\begin{aligned} f &= \frac{OB - OC}{OA - OC} \cdot \frac{OB + OC}{OA + OC} \\ &= \frac{BC}{AC} \cdot \frac{OB + OC}{OA + OC}. \end{aligned}$$

Now

$$m(\lambda - d\lambda) = (m - f)\lambda$$

and .

$$d\lambda = \frac{f}{m} \cdot \lambda,$$

where  $m$  is very nearly equal to  $\frac{2e}{\lambda}$ . Therefore

$$d\lambda = \frac{f\lambda^2}{2e}$$

and

$$\frac{d\nu}{\nu} = \frac{f\lambda}{2e} \quad \text{where} \quad \nu = \frac{1}{\lambda}.$$

In this manner the separation  $d\lambda$  of the faint component from its brighter companion was calculated for about twenty neon lines in the visible spectrum, and the results are given in Table I. The values of  $d\lambda$  obtained by Nagaoka and Mishima are shown in column VII. of this table.

### *Experimental Results.*

Table I. includes all the strong neon lines in the region of the spectrum investigated, and it is seen that every strong line is accompanied by a fainter companion. In addition, the value of  $\frac{d\nu}{\nu}$  for the lines belonging to each Paschen series is constant within experimental error. The mean values of  $\frac{d\nu}{\nu} \times 10^8$  for the series  $1s_2-2p_m$ ,  $1s_3-2p_m$ ,  $1s_4-2p_m$ , and  $1s_5-2p_m$  are 437, 367, 367, and 370 respectively, and are practically constant for the last three series. An examination of the table shows that the values of  $d\lambda$  obtained in the present experiments are for the first series about 15 per cent. lower on the average than those given by Nagaoka and Mishima, and for the last three series about 10 per cent. higher.

Neon, which has an atomic weight of 20.20, has been shown by Aston to consist of a mixture of two isotopes of atomic weights 20.0 and 22.0 in the ratio of 9:1. For an atom consisting of a nucleus with one electron theory shows

that  $\nu \propto \frac{Mm}{M+m}$  where  $M$  is the mass of the nucleus of the

atom, and  $m$  the mass of the electron. It therefore follows that the wave-lengths of the spectrum lines emitted by Ne(22) should be lower than those emitted by Ne(20),

TABLE I.

Series (Paschen).	Wave- length of line. $\lambda$ .	Distance apart of mirrors. $e$ cm.	Fraction $f$ .	$\frac{d\nu}{\nu} \times 10^3$ .	$\frac{d\lambda}{\lambda}$ in Å.U.	$\frac{d\lambda}{\lambda}$ in Å.U. Nagaoka and Mishima.
$1s_2 - 2p_1$	5852	2.5 3.0	0.382 0.456	447 445	-0.0261 -0.0259	-0.0279
$1s_2 - 2p_2$	6599	2.5 3.0	0.329 0.396	434 436	-0.0286 -0.0287	-0.0341
$1s_2 - 2p_4$	6678	2.5 3.0	0.325 0.392	434 436	-0.0289 -0.0290	-0.0342
$1s_2 - 2p_5$	6717	2.5 3.0	0.324 0.390	435 436	-0.0292 -0.0293	-0.0361
$1s_2 - 2p_6$	6930	3.0	0.376	434	-0.0301	
$1s_3 - 2p_2$	6164	3.5 2.5	0.414 0.298	364 367	-0.0224 -0.0226	-0.0197
$1s_3 - 2p_5$	6266	3.5 3.0	0.407 0.358	364 373	-0.0228 -0.0233	-0.020
$1s_3 - 2p_7$	6533	3.5	0.392	366	-0.0239	-0.0218
$1s_4 - 2p_2$	6030	2.5	0.301	363	-0.0219	-0.0207
$1s_4 - 2p_3$	6074	3.0	0.358	363	-0.0220	-0.0213
$1s_4 - 2p_4$	6096	3.0	0.357	363	-0.0221	-0.0208
$1s_4 - 2p_6$	6305	3.0	0.351	369	-0.0233	-0.0205
$1s_4 - 2p_7$	6383	3.0	0.350	372	-0.0238	-0.0216
$1s_4 - 2p_8$	6507	3.0	0.344	373	-0.0243	-0.0230
$1s_5 - 2p_2$	5882	3.5	0.436	367	-0.0215	-0.0197
$1s_5 - 2p_4$	5945	3.5	0.430	365	-0.0217	-0.0198
$1s_5 - 2p_5$	5976	3.5	0.434	371	-0.0221	-0.0202
$1s_5 - 2p_3$	6143	2.5 3.0	0.307 0.369	377 377	-0.0232 -0.0232	-0.0208
$1s_5 - 2p_7$	6217	3.5	0.414	368	-0.0229	-0.0209
$1s_5 - 2p_9$	6334	2.5 3.0	0.291 0.351	369 371	-0.0234 -0.0235	-0.0212
$1s_5 - 2p_9$	6402	3.0	0.350	373	-0.0239	-0.0217
$1s_5 - 2p_{10}$	7032	3.5	0.368	370	-0.0260	-0.0254

and, in addition, it is to be expected from the composition of ordinary neon, that the Ne(22) lines should be faint as compared with the Ne(20) lines. The faint lines measured

in the present experiments satisfy both these conditions, but the value of  $\frac{d\nu}{\nu}$  found experimentally is greater than that calculated from the above formula. Let  $\nu$  be the wave-number of a particular line for Ne(20) having a nuclear mass  $M$ , and  $\nu_1$  the wave-number of the corresponding line for Ne(22) of nuclear mass  $M_1$ , then

$$\frac{\nu_1 - \nu}{\nu} = \frac{d\nu}{\nu} = \frac{m(M_1 - M)}{M(M_1 + m)} = \text{constant}.$$

Putting into the equation the values of  $m$ ,  $M$ , and  $M_1$ , it is found that  $\frac{d\nu}{\nu} = 247.4 \times 10^{-8}$ . The mean values of  $\frac{d\nu}{\nu}$  determined experimentally are  $437 \times 10^{-8}$  for the series  $1s_2 - 2p_m$ , and  $368 \times 10^{-8}$  for the series  $1s_3 - 2p_m$ ,  $1s_4 - 2p_m$ ,  $1s_5 - 2p_m$ . The simple theory, however, does not apply to atoms possessing more than one electron.

The authors wish to thank Prof. A. Fowler, F.R.S., for the kind interest he has taken in this investigation.

## XII. Distribution of Electric Forces in Spaces traversed by Electrons. By E. W. B. GILL, B.Sc., M.A., Fellow of Merton College, Oxford\*.

1. **I**N the past ten years considerable use has been made of the so called "force free" spaces in measurements of critical potentials of gases. In these experiments a stream of electrons moves from a hot filament  $F$  to a grid  $G_1$ , which is kept at a potential  $V$  above the filament. The grid  $G_1$  is close to the filament, so most of the electrons do not collide with molecules of gas in passing from  $F$  to  $G_1$ . After passing through  $G_1$  the electrons move in a large space between  $G_1$  and another electrode or grid  $G_2$  which is at the same potential as  $G_1$ . The experiments are interpreted on the hypothesis that the electrons between  $G_1$  and  $G_2$  move with constant velocity, except in so far as they collide with gas molecules; and the arrangement is thus supposed to enhance the effects of electrons moving with the velocity corresponding to the potential  $V$ .

\* Communicated by Professor Townsend, F.R.S.

A typical example of this method occurs in the investigations made by Horton and Davies\* of the critical potentials of neon. The electrons passed through a hole in an electrode  $G_1$  and were received on another electrode  $G_2$ , 1.5 cm. from  $G_1$ . Both these electrodes were at the same potential  $V$  relative to the filament. The discharge was prevented from spreading laterally by a magnetic field, and spectroscopic and electrical observations were made on the gas between the two electrodes.

The authors say "For the purpose of determining the limiting electron velocity required to produce the particular lines in the spectrum it was necessary that the bombarding electrons should suffer no change of velocity throughout the space viewed by the spectroscope except such changes as result from collisions. To secure this condition the grid and anode were maintained at the same potential." While in another paper† they say "Since there is no potential difference between the gauges the detection of ionization depends upon the diffusion of positive ions out of this space." The minimum electron velocity they observed for a glow was about 20 volts.

It is quite clear that the authors regarded the electric force in the space between the electrodes  $G_1$  and  $G_2$  as being zero or negligible.

The same underlying idea is present in experiments of Franck and Hertz in which electrons entered a large metal box with gauze sides through which they diffused, and also in experiments where the electrons were projected into a large space between two grids differing in potential by a small fraction of a volt. Although the experiments quoted were made some years ago the "force free" space is still in use as a recent letter to 'Nature' indicates ‡.

2. It does not seem that sufficient consideration has been given to the effect of the space charge in the "force free space." When there is no current traversing the space between  $G_1$  and  $G_2$  the potential at any point is the same as at the boundary, but when electrons enter the space this is no longer the case; and as the effect of this charge has not been completely investigated it is of interest to consider to what extent the field is disturbed under the simplest conditions. The actual field depends on the current and can be calculated quite easily for plane parallel electrodes if the electrons are

\* Phil. Mag., June 1921, p. 921.

† Phil. Mag., May 1920, p. 596.

‡ 'Nature,' March 22, p. 460 (1930).

moving in a vacuum or through a gas at such a low pressure that collisions are rare.

3. The calculation of the electric field due to the distribution of electrons is similar to the well-known theory of Langmuir and Child.

Let the potential of the filament be zero and let the two grids be at  $V$ . The effect of the negative charge on the electrons is to reduce the potentials in the space between the grids to values less than  $V$ . If the grids are parallel planes whose area is large compared with the distance between them, the equipotential surfaces will be planes parallel to the grids.

Fig. 1.

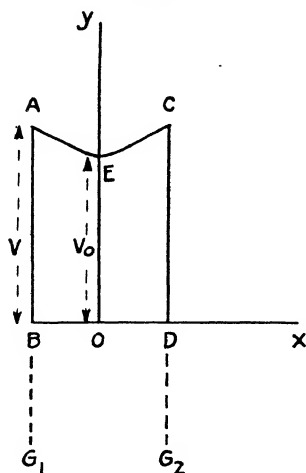


Fig. 1 represents the distribution of potential along a line normal to the grids; AB and CD are equal to  $V$  the grid potentials, BD is the distance between them, and EO the minimum potential  $V_0$  in the space between them.

Let  $v$  be the potential at a plane distant  $x$  from the plane OE where the potential is a minimum, and let the electrons move across the space between the grids from left to right in fig. 1.

Let  $n$  be the number of electrons per cu. cm., and  $u$  the velocity of the electrons at the plane  $x$ ; the direction of motion being perpendicular to the planes.

And let  $i$  be the current per sq. cm. of the plane  $x$ ,  $e$  and  $m$  the charge and mass of an electron.

The quantities  $v$ ,  $n$ , and  $u$  are functions of  $x$ , but in the steady motion which is considered  $i$  is a constant independent of  $x$ .

The kinetic energy of the electron is

$$\frac{1}{2}mu^2 = ev, \quad . \quad . \quad . \quad . \quad . \quad (1)$$

also the current  $i$  is

$$i = neu, \quad . \quad . \quad . \quad . \quad . \quad (2)$$

while the potential  $v$  is given by

$$\frac{d^2v}{dx^2} = 4\pi ne, \quad . \quad . \quad . \quad . \quad . \quad (3)$$

whence

$$\frac{d^2v}{dx^2} = \frac{a}{\sqrt{v}} \text{ where } a = 4\pi i \sqrt{\frac{m}{2e}}.$$

Integrating this equation gives

$$\left(\frac{dv}{dx}\right)^2 = 4a(\sqrt{v} - \sqrt{V_0}), \quad . \quad . \quad . \quad . \quad (4)$$

since  $V_0$  is the minimum value of  $v$ .

A second integration gives, since  $v = V_0$  when  $x = 0$ ,

$$\sqrt{\sqrt{v} - \sqrt{V_0}} \{ \sqrt{v} + 2\sqrt{V_0} \} = \frac{3}{2} \sqrt{a} x. \quad . \quad . \quad (5)$$

If  $OD = d$ , then when  $x = d$ ,  $v = V$ , so that the following equation for  $V_0$  is obtained from equation (5):

$$\frac{3}{4} ad^2 = (\sqrt{V} - \sqrt{V_0})(\sqrt{V} + 2\sqrt{V_0})^2 \quad . \quad . \quad (6)$$

Replacing  $a$  by its numerical value the following expression is obtained for the current:

$$i = \frac{2.33 \times 10^{-6} (\sqrt{V} - \sqrt{V_0})(\sqrt{V} + 2\sqrt{V_0})^2}{d^2}, \quad (7)$$

$i$  being in amperes per sq. cm.,  $V$  and  $V_0$  in volts, and  $d$  in cm.

The consideration that  $v = V$  at both grids proves that  $OB = OD$ , so that  $O$  is midway between the grids and the distribution curve is symmetrical about  $OE$ . Equation (7) thus gives the potential  $V_0$  at the middle point of a "force free space" of length  $2d$  across which a current  $i$  flows, the electrodes being at a potential  $V$  above the filament. Equation (5) gives the actual distribution of field.

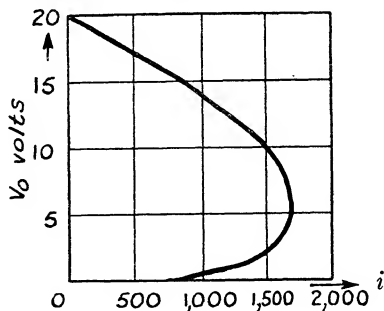
4. The effect of the space-charge is seen most simply by tabulating the currents which give various values of  $V_0$  for



some assigned value of  $V$ . Fig. 2 gives the values of the potentials  $V_0$  midway between two grids, one centimetre apart, each at a potential of 20 volts above the filament for different currents  $i$  per sq. cm.

It will be observed that there are quite large effects due to very small currents. Thus it only requires 180 microamps. per sq. cm. to cause a drop of one volt in the "force free space," while about 500 microamps. gives a drop of 3 volts, and so on. A further interesting result is that if the current exceed a certain value (830 microamps. per sq. cm. in this case) there are two possible distributions of potential. For example, one milliamp. per sq. cm. may cause the potential at the middle to drop to either 13.7 or .4 volts. (The possibility

Fig. 2.



Potential  $V_0$  midway between 2 grids 1 cm. apart each at 20 volts, above the filament for different currents,  $i$ .  
( $i$  current in microamps per sq. cm.)

of two alternative distributions is not confined to gas free spaces, as they can be obtained experimentally in cases where a discharge passes through a gas at low pressure in which positive ions produced by collision are also present.) The maximum current which can traverse the space is just under 1.7 milliamps. per sq. cm., and this reduces the potential at the middle to 5 volts.

It is easily seen from equation (7) that for a given current the distortion of the field increases if either the grid potentials are reduced or the distance between the grids is increased.

5. The preceding theory only applies rigidly to large electrodes and to currents distributed uniformly over the surface, in which cases the electrons move normally to the

electrodes and there is no electric force perpendicular to their motion. In general it is impossible to calculate the effect of the space-charge, but the preceding investigation indicates approximately the effect in many experiments. Very similar calculations made by Langmuir for infinite electrodes have been found to be in good agreement with measurements made with two electrode valves. It is, unfortunately, rare in accounts of experiments on critical potentials to find the currents given in anything except arbitrary units, so that it is impossible to say to what extent the energies of the electrons were affected by the force due to the space-charges; but as hot filaments are generally used as the source of electrons, it may be concluded that the emission currents were certainly more than a few microamperes and were therefore large enough to cause considerable changes in the field of force.

The gas-free space considered is, of course, the most favourable for lack of distortion by space-charge. If gas is present the electrons move with less velocity and the space-charge effect is considerably increased and is much greater than that indicated by the preceding calculations.

The general conclusion to be drawn therefore from these calculations is that the velocities of the electrons traversing force free spaces are generally less than the velocities with which they are projected through the first grid.

I am indebted to Prof. Townsend for advice and criticism.

---

XIII. *Some Observations on Movements of Particles in Kundt's Tube.* By C. O. PRINGLE, B.Sc., Dept. of Physics, Queen's University, Belfast\*.

[Plate I.]

**D**URING an attempt to reproduce the results obtained by Andrade and Lewer † with an electrically-operated Kundt's tube, some phenomena have been observed to which attention does not yet appear to have been drawn.

The note used, of frequency about 900 per second, was generated by a valve oscillator and amplified by a power

\* Communicated by Prof. W. B. Morton, M.A.

† Andrade and Lewer, 'Nature,' cxxiv. p. 724 (1929).

valve followed by a 2-valve "push-pull" amplifier before being applied to the tube through a loud-speaker unit, the cone of which was replaced by a cork disk which just fitted into the end of the tube without touching the glass. The current through the unit was measured by a thermocouple, and had a maximum of about 20 milliamps. When the tube was working on maximum power the effect produced was not quite so strong as that which can be obtained with a Kundt's tube of the ordinary type when the vibrating rod is stroked vigorously.

Silica and cork-dust have been found to give best results. The silica was prepared in the laboratory by the action of sulphuric acid on powdered glass and fluorspar\*, and was not so fine as the commercial product. The latter, however, did not give satisfactorily any of the results obtained.

Using cork-dust in a glass tube  $\frac{3}{4}$  in. in diameter, a number of disks were obtained at an antinode. Of these, the central one was similar to that photographed by Andrade and Lewer. The others were less dense, those nearer the antinode being more like the central one, those further away becoming merely partial rings round the upper part of the inside of the tube. These disks and rings, when first formed, have a spacing approximately the same as that of the secondary striæ in the bottom of the tube; they do not remain stationary, however, but tend to close in and merge into each other or into the central disk.

With comparatively large quantities of silica in the tube some of the antinodal ripples may extend to the top of the tube, forming "solid" disks of almost stationary particles. Several of these disks are formed at first, but all but one or two break down in a few seconds as the dust is carried to the nodes. There is a continual fall of particles from each side of a disk into the bottom of the tube, and in the disk a corresponding rise of particles from the bottom of the tube. Plate I., *a*, shows two of these disks and the antinodal ripples on each side. These disks are possibly of the type obtained by Cook†. They can be obtained easily by a method corresponding to his, namely, by inserting a smaller tube, of diameter  $\frac{1}{2}$  in., containing silica into the end of a 1-in. diameter Kundt's tube, as shown at *b* in

\* "Silicon," Thorpe's Dict. App. Science, vi. p. 84 (1926).

† Cook, 'Nature,' cxviii. p. 157 (1926).

Plate I. Another print (Plate I., c) from the same photograph shows more clearly the disks at the two antinodes. A closer view of the disks in this tube is given in Plate I., d. In this photograph three disks are shown, and between the second and third from the right-hand side is another disk in the act of breaking down.

The disks in the small tube are steadier and more permanent than those in the larger tube, especially when the end of the tube is tightly closed.

If a sliding stop is used there is a gradual movement of the disks towards that end of the tube. This is accompanied by a breakdown of each disk as it approaches the node and the formation of new disks at the antinodes, so long as there is enough silica present.

Cork-dust in this secondary tube gives the light disks and rings of the type mentioned above at each antinode, but in a smaller tube, of diameter  $\frac{3}{8}$  in., cork-dust gives the "solid" disks.

In addition to the streaks \* due to particles vibrating in a line parallel to the axis of the tube, which in the apparatus used were mainly microscopic, streaks are obtained from particles vibrating in a plane perpendicular to the length of the tube, and such streaks are found in all directions in this plane. They are found when very small quantities of cork-dust or silica are present, and are of different lengths up to about 5 mm. The particles from which they arise have not all the same frequency of oscillation; some have a frequency which may be that of the note supplied, others have a much lower frequency, and in some cases their motion can easily be followed by the eye. Occasionally these short bright lines remain steady for a few seconds, but more often they move up and down, or along the tube near the walls, or shoot from side to side across the tube until they collide with another particle. In Plate I., e, some stationary streaks of this type are indicated by arrows. This photograph was taken from slightly above the tube, and the particles forming partial striæ in the bottom of the tube therefore appear as if a short distance up the wall of the tube.

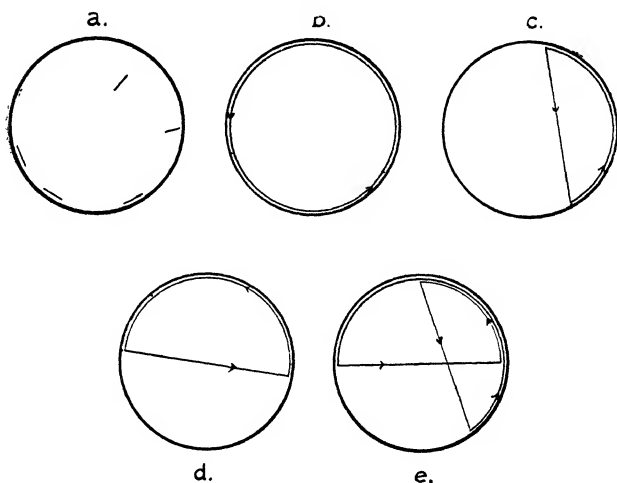
Fig. 1a is a diagram of the cross-section of the tube showing some of the positions which may be taken up by the streaks.

\* Andrade and Lewer, *loc. cit.*; Carrière, *Journal de Physique*, x. p. 198 (1929).

The microscope reveals some particles which have simultaneously both this type of vibration at low frequency and a vibration parallel to the axis at a much greater frequency. These appear as small rectangles of light.

A particle may also move in a small circular orbit giving a ring of light, or two such particles may have intersecting orbits giving intersecting rings. These two particles do not collide until disturbed by the approach of another particle. These circular paths are only visible in a microscope, but can be found easily near the end of an

Fig. 1.



Cross-sections of tube, with paths of particles.

antinodal ripple or near a larger particle in the bottom of the tube; they only exist when there is a very small quantity of dust in the tube.

With small quantities of dust in the tube, particles have been observed moving round the inside of the tube in circles, the planes of which are perpendicular to the axis of the tube. Such an orbit is shown diagrammatically in fig. 1 b. If there are so few particles that collisions are rare, a single particle may make a large number of complete circuits of the tube at a rate of about 2 per second. The particles appear to be thrown up from the bottom of

the tube, from between ripples if there is enough dust present to form ripples. Two particles may travel round the tube in opposite directions in orbits just far enough apart to prevent collisions. If two such particles meet they either move off along the wall of the tube or fall into the bottom, where they may again take up the above motion. When very few particles are present some have been observed to move with a longitudinal drift imposed on the above motion, giving a spiral the pitch of which is the same as the spacing of the ripples. With larger quantities of dust the particles start up the walls and collide with other particles, and it is suggested that it is such particles which form the disks obtained by Andrade and Lewer.

Particles have also been observed tracing an orbit which lies in a plane perpendicular to the axis of the tube, and which consists not of a complete circle, but of an arc and chord. The chord may be of any length up to a diameter of the tube, and may have any inclination to the horizontal. A particle may trace out this orbit a large number of times before being displaced. This type of orbit is indicated in figs. 1 c and 1 d, and it may also be traversed by a particle which is itself in oscillation in the plane perpendicular to the axis of the tube, as described above. A particle may also change from one orbit to another and back to the first, giving the more complex path (fig. 1 e). Observations were made in which such a path was traced out up to six times.

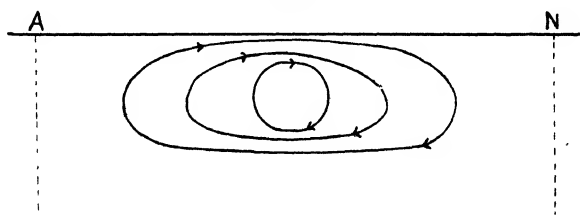
When a quantity of cork-dust is placed at the antinode nearest to the sounding-disk in the tube, and the stop is so far along the tube that there are several antinodes, some very fine dust is carried to the second antinode. This dust moves in a manner which indicates the presence of a current of air from antinode to node near the walls of the tube, and from node to antinode in the centre of the tube. The existence of this current was proved on theoretical grounds by Lord Rayleigh \*.

The particles can be observed moving up the centre of the tube towards the antinode, and some can be seen rising into the upper part of the tube, where they move back again near the wall, falling as they approach the node and retracing the path. Fig. 2 is a diagram showing the

\* Rayleigh, *Phil. Trans.* clxxv. part 1, p. 1 (1884,

general position of these paths. This motion has also been observed with single particles of silica when there are only a few particles in the tube. The orbit never has a length equal to the full distance from antinode to node, but varies in length from about two-thirds of this distance down to a size where it is almost circular and situated half way between antinode and node. A single particle has been observed to make up to four or five complete circuits of this type, each being of about one second in duration, before it was disturbed by collision with another particle. In the

Fig. 2.



Orbital motion of particles, indicating presence of air-currents.

lower half of the tube in this case the tendency of the particles to form ripples and the greater concentration of particles appear to prevent the formation of such orbits.

The writer is greatly indebted to Mr. J. Wylie, B.A., who suggested this work, and has given valuable assistance during its progress. He also desires to thank other members of the staff of the Department for their help at various times.

### *Key to Plate.*

- a.* Two solid disks with antinodal ripples in a  $\frac{3}{4}$ -in. diameter tube.
- b.* A secondary tube,  $\frac{3}{8}$  in. in diameter, inserted into the end of a 1-in. diameter Kundt's tube giving disks at two antinodes.
- c.* The antinodal disks shown more clearly than in *b*: same photograph as *b*.
- d.* The disks in the secondary tube, viewed obliquely.
- e.* Short streaks of light due to strongly illuminated vibrating particles: only the one against the middle arrow shows clearly in the reproduction. (Magnification,  $\times 1.05$ ).

XIV. *On the Behaviour of Electrons amongst the Molecules  $NH_3$ ,  $H_2O$ , and  $HCl$ .* By V. A. BAILEY, M.A., D.Phil. (Oxon), F.Inst.P., Associate Professor of Physics, University of Sydney, and W. E. DUNCANSON, B.Sc., Science Research Scholar, University of Sydney\*.

1. **T**HE easy familiarity with which some chemists and physicists discuss the electrical properties of molecules when considering chemical combination or the motion of electricity in gases is apt to be misleading, as there are several of these properties about which little is known.

For molecules which have a negligible power of combining with electrons, the most successful and unimpeachable methods of investigation are those used by J. S. Townsend and his collaborators; but with molecules like  $NH_3$  and  $HCl$ , which can capture electrons comparatively frequently, there have not been, until recently†, any methods for determining their behaviour towards slow electrons which are at all comparable with the former in reliability and the wealth‡ of information which can be derived from them.

In this communication we describe how these recent methods may be used to determine the four quantities  $u$ ,  $L$ ,  $\lambda$ ,  $h$  for electrons moving in the gases  $NH_3$ ,  $H_2O$ , and  $HCl$  under the action of uniform electric fields, where

$u$  is the velocity of agitation of an electron,

$L$  its mean free path at 1 mm. pressure of the gas,

$\lambda$  its fractional loss of energy at a collision with a molecule, and

$h$  is the probability of its becoming attached at a collision.

\* Communicated by the Authors.

† V. A. Bailey, *Phil. Mag.*, July 1923, p. 213; October 1925, p. 825.  
V. A. Bailey and J. D. McGee, *Phil. Mag.*, December 1928, p. 1073.  
V. A. Bailey, *Phil. Mag.*, April 1930, pp. 560 and 625.

‡ The methods of Ramsauer and Mayer give information only about the apparent sizes of molecules, and that of Cravath could determine only the coefficients of attachment  $\alpha$ .

*Phil. Mag.* S. 7. Vol. 10. No. 62. July 1930.

L



## 2. Description of the Methods.

These four quantities can be calculated \* by means of the following formulæ :—

$$\left. \begin{aligned} u &= 1.15 \times 10^7 \sqrt{k} \text{ cm./sec.}, \\ L &= 8 \times 10^{-9} W \sqrt{k/(Z/p)} \text{ cm.}, \\ \lambda &= 1.86 \times 10^{-14} W^2/k, \\ h &= 7 \times 10^{-16} (\alpha/Z) W^2, \end{aligned} \right\} \dots \dots (1)$$

where  $p$  is the pressure of the gas, in mm. of mercury,

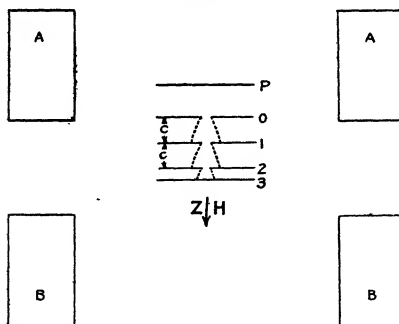
$Z$  the electric intensity, in volts/cm.,

$k$  the mean energy of agitation of an electron in terms of that of a molecule at  $15^\circ \text{C.}$ ,

$\alpha$  the probability of attachment of an electron in moving unit distance in the direction of  $Z$ , and

$W$  is the mean drift velocity of an electron, in cm./sec.

Fig. 1.



The apparatus used to determine  $k$ ,  $\alpha$ , and  $W$  is simply represented by fig. 1. Five parallel disks P, 0, 1, 2, 3 are kept at the potentials necessary to produce the uniform field  $Z$  throughout the space in which the electrons move, the disks 0, 1, and 2 containing parallel and superposed

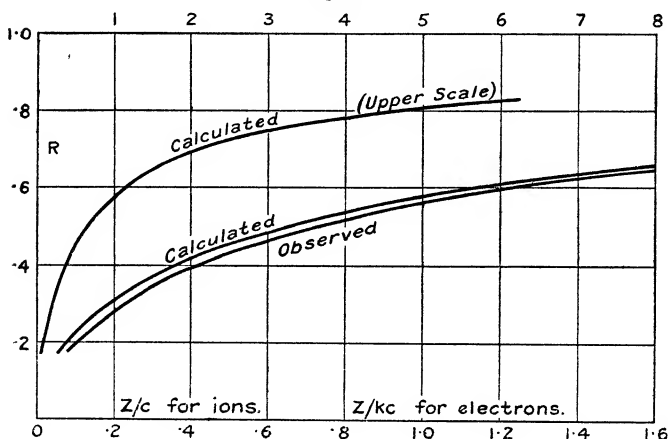
\* *Vide* J. S. Townsend, 'Motion of Electrons in Gases' 1925 (O.U. Press), and V. A. Bailey, Phil. Mag., October 1925, p. 843.

slits each 4 mm. wide and respectively 1.5, 6.2, and 7.2 cm. long. The intervals  $c$  between these electrodes can be varied between the values 2 and 4 cm.

Electrons are emitted by P under the action of ultra-violet light, and finally reach the electrodes 1, 2, and 3 in relative proportions which depend on the nature and pressure of the gas in the apparatus as well as on the values of  $Z$  and  $c$ .

The mutual ratios of the currents to these three electrodes are measured, and from these measurements the ratios  $S_1$  and  $S_2$  are determined, where  $S$  is the fraction of

Fig. 2.



the stream which passes through the slit of the electrode that it approaches.

If the streams are composed entirely of negative *ions*, then  $S_1$  and  $S_2$  each become equal to a fraction  $R$ , which is known in terms of the ratio  $Z/c$  and is represented by the curves in fig. 2.

But when the streams contain both electrons and ions this is not so, and the values of  $S_1$  and  $S_2$  are then used to calculate the quantity

$$a = S_1 \left( \frac{R - S_2}{R - S_1} \right).$$

Its value  $a_1$  corresponding to a set of values of  $c$ ,  $p$ , and  $Z$ , and its value  $a_n$  corresponding to a homologous set  $nc$ ,  $np$ ,

$nZ$  are determined, and the points with coordinates  $(x, y)$  are plotted, where

$$x = n^2 \quad \text{and} \quad y = \log_{10} a_n.$$

The straight line \* determined by these points has its slope equal to  $\alpha c/2.3$ , and its intercept on the  $y$ -axis equal to  $\log_{10} R(Z/kc)$ , therefore the value of  $\alpha$  can be deduced from the slope, and that of  $k$  can be deduced from the intercept by using the curves in fig. 2.

To measure  $W$  a uniform magnetic field of intensity  $H$  and parallel to  $Z$  is produced by means of the coils A and B shown in fig. 1, and is adjusted to a value  $H_0$  at which  $S_2$  becomes equal to  $R$ . The velocity of drift may then be calculated by means of the formula †,

$$W = \frac{Z}{H_0} \sqrt{k-1} \times 10^8. \quad . \quad . \quad . \quad . \quad . \quad (2)$$

since  $k$  is now known.

### 3. Use with $NH_3$ .

This gas was generated by heating a mixture of pure  $NH_4Cl$  and  $CaO$  to about  $190^\circ C$ . in an evacuated flask, dried by means of  $KOH$ , twice fractionally distilled from the solid form in liquid-air traps, and finally stored in flasks containing small quantities of  $P_2O_5$ .

The observed values of  $(\log_{10} a + 1)$  and of  $H_0$  (in gauss) corresponding to various sets of values of  $c$ ,  $p$ , and  $Z$  are shown in Table I., each being the mean of at least two observations. Since  $k$ ,  $\alpha/p$ , and  $W$  are functions of the ratio  $Z/p$  alone, the observations are arranged in groups each of which corresponds to a given value of  $Z/p$ .

The values of  $\alpha/p$  deduced from these numbers, and given in the eighth column, are in excellent agreement with the values found in an earlier ‡ investigation of  $NH_3$ .

The numbers deduced for  $k$  with the help of the calculated § distribution curve in fig. 2 are also in good agreement with those previously || obtained, but the values of  $k$  shown in the ninth column are those determined by means

\* V. A. Bailey and J. D. McGee, *loc. cit.* p. 1077.

† V. A. Bailey, *Phil. Mag.*, April 1930, p. 566.

‡ V. A. Bailey and J. D. McGee, *loc. cit.* fig. 9.

§ Obtained by means of a simple calculation which neglects the effect of diffusion to the edges of the slits.

|| V. A. Bailey and J. D. McGee, *loc. cit.* fig. 8.

of the more reliable distribution curve obtained from observations † on pure hydrogen.

TABLE I.

NH<sub>3</sub>.

Z/p.	c.	p.	Z.	$\log_{10} \frac{\alpha}{1.1}$	H <sub>0</sub> .	H <sub>0</sub> /Z.	$\alpha/p$ .	k.	W × 10 <sup>-5</sup> .
4.....	3	1.5	6	.740	604	101	—	1.50*	6.9
6.....	2	1.33	8	—	510	64	—	1.55*	12.4
	3	2.00	12	.785	720	60			
8.....	2	.50	4	—	(255)	(64)	.006	4.3	31
	2	1.00	8	.732	476	59			
	3	1.50	12	—	708	59			
	4	2.00	16	.715	915	57			
10.....	2	.60	6	—	(450)	(75)	—	—	49
	2	.80	8	—	560	70			
	3	1.20	12	—	825	69			
12.....	2	.33	4	.173	340	85	.06	30	65
	4	.67	8	.121	670	84			
	2	.67	8	.326	640	80			
	4	1.33	16	.255	—	—			
16.....	2	.25	4	.104	368	92	.13	50	76
	4	.50	8	.021	755	94			
	2	.50	8	.190	726	91			
	4	1.00	16	.033	—	—			
24.....	2	.17	4	.107	354	88	.21	56	84
	4	.33	8	.017	708	89			
	2	.33	8	.163	702	88			
	4	.67	16 (-	.007)	—	—			
32.....	4	.37	12	—	990	82	.20	57	92
	2	.25	8	.176	650	81			
	4	.50	16	.046	—	—			

\* These values of  $k$  are obtained from the values of  $S_1$  as if no ions were present.

It may be seen from Table I. that the values of  $\alpha/p$  obtained with the values 2 and 4 of  $Z/c$  are in good agreement, a test of the method which was also satisfied in the former work on NH<sub>3</sub>, where the two values of  $Z/c$  were 4 and 8.

The quantities  $k$  and  $\alpha/p$  are represented as functions of  $Z/p$  by curves in figs. 3 and 4 respectively.

† See for example V. A. Bailey, *Phil. Mag*, October 1925, p. 835.

In order to provide a test of the method for obtaining  $W$ , the values of the ratio  $H_0/Z$  are given in the seventh column of the table, as the formula (2) shows that this ratio must remain constant for a given value of  $Z/p$ . The numbers show that this rule is closely followed.

Another useful test consists in determining the values of  $S_1$  with the magnetic field  $H_0$  applied and comparing them with the corresponding values of  $S_2$  as in Table II.

Fig. 3.

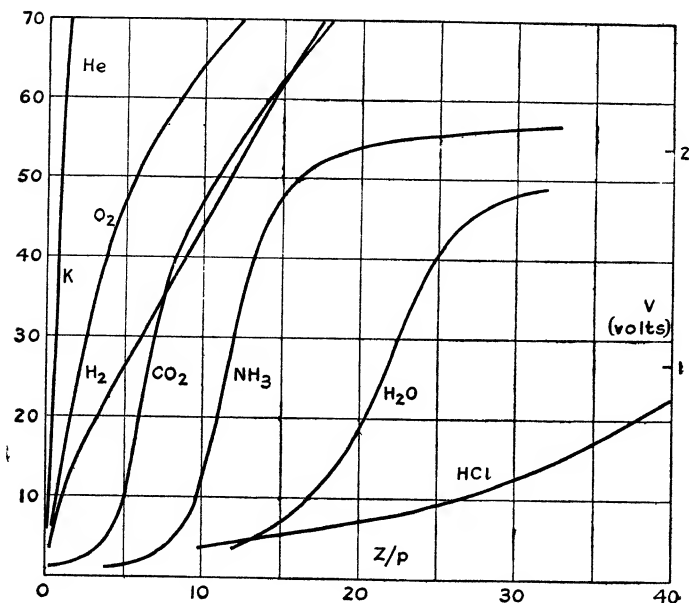
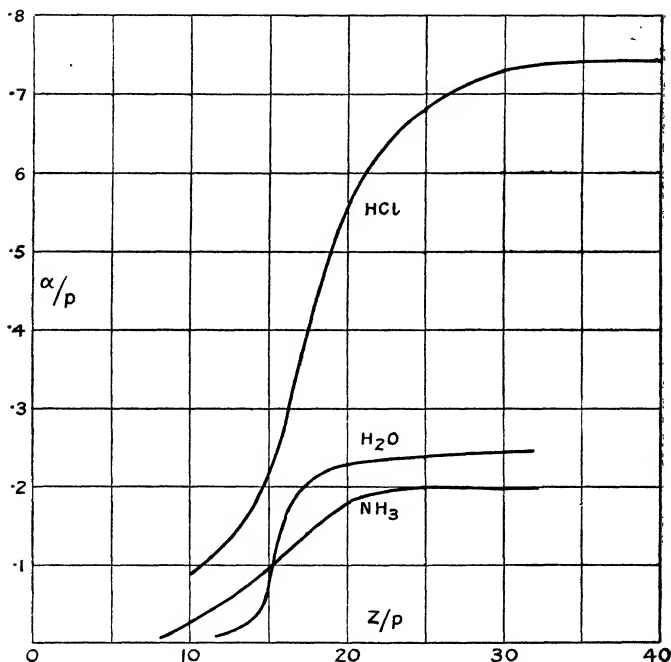


TABLE II.

$Z/p$ .	$c$ .	$p$ .	$Z$ .	$H_0$ .	$S_1$ .	$S_2$ .	$R$ .
8	3	1.5	12	—	.531	.541	
"	"	"	"	708	.770	.780	.780
16	4	.5	8	—	.180	.392	
"	"	"	"	755	.692	.690	.690
24	2	.333	8	—	.207	.379	
"	"	"	"	702	.773	.780	.780

In each instance the theoretical relation  $S_1=S_2=R$  is well satisfied, despite the large difference between  $S_1$  and  $S_2$ , which exists in the absence of a magnetic field with the higher values of  $Z/p$ . For example, with  $c=4$  cm.,  $p=.5$  mm.,  $Z=8$  volts/cm. the values of  $S_1$  and  $S_2$  were  $.180$  and  $.392$  respectively; the magnetic field necessary to increase the value of  $S_2$  to that of  $R$  (namely  $.690$ ) was found to have the value  $755$  gauss; in the presence of this field the value of  $S_1$  was then observed to be  $.692$ .

Fig. 4.

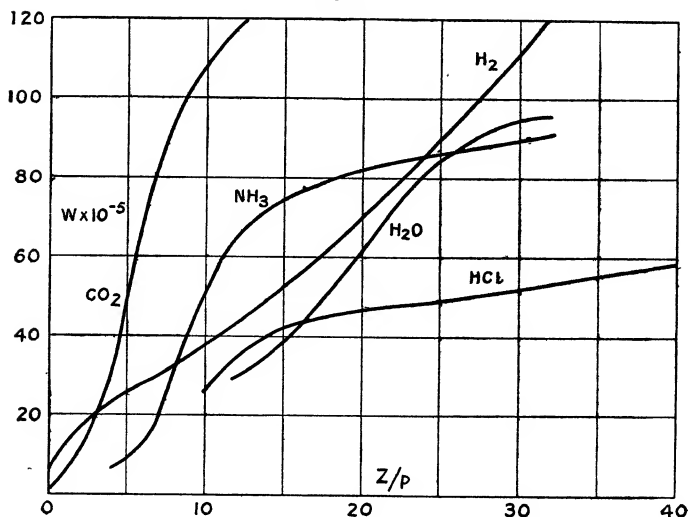


This test in general would only be satisfied if the electrons attained a steady state before passing through the first slit, and if no notable number of positive ions were generated by collisions between electrons and molecules.

The values of  $W$  calculated by means of (2) are given in the last column of Table I., and are also represented by a curve in fig. 5.

A few observations of  $W$  were also made by means of Townsend's method, in which the stream is deflected through a known angle by means of a transverse magnetic field. With the ratio  $Z/p$  equal to 4 and 6 the values of  $W$  so determined were independent of the pressure and in agreement with those given in Table I. This is to be expected if permanent ions are absent. For the values 8 and 16 of  $Z/p$  the numbers for  $W$  were notably lower than those in Table I., which is consistent with the conclusion that the streams contain a large proportion of ions under these conditions.

Fig. 5.



The values of  $u$ ,  $L$ ,  $\lambda$ , and  $h$  for  $NH_3$ , deduced from these results by means of the formulæ (1), are given in Table V. together with  $V$ , the energy of an electron expressed in volts. For the purpose of comparison with other molecules the quantities  $L$ ,  $\lambda$ , and  $h$  are expressed as functions of  $u$  by curves in figs. 6, 7, and 8 respectively.

#### 4. Use with $H_2O$ .

The gas was evaporated from distilled water in an evacuated glass bulb, its pressure being determined by means of a manometer filled with paraffin oil. This

Fig. 6.

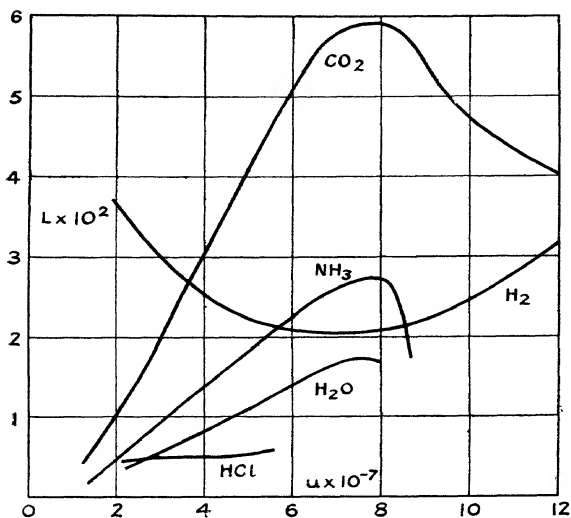
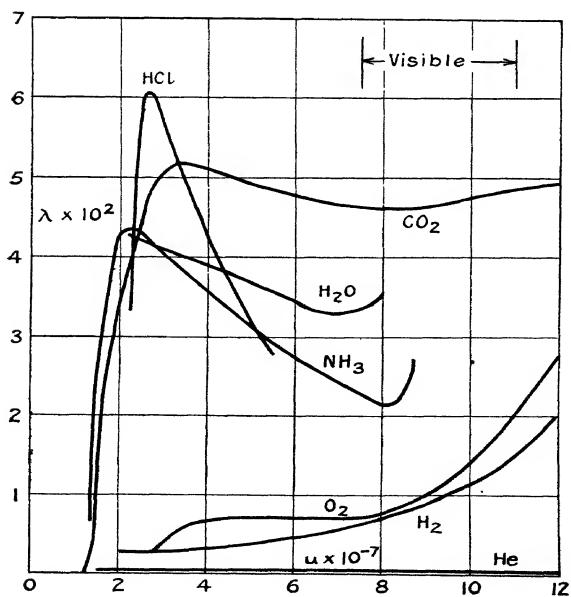


Fig. 7.



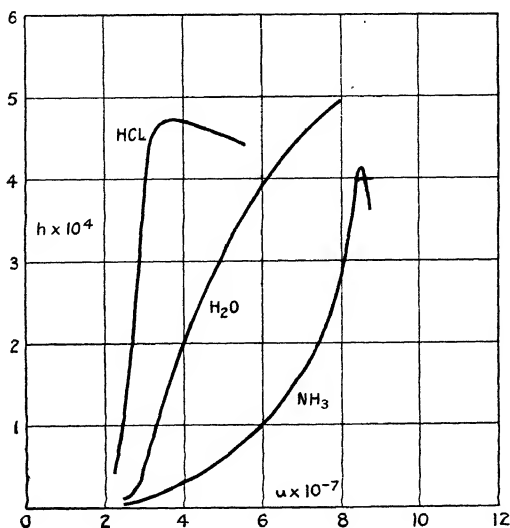


manometer was standardized by means of hydrogen at a pressure which could be measured with a mercury manometer.

The experimental results are set out in Table III. (which is similar to Table I.), the value of  $Z/c$  being 4 throughout.

For values of  $Z/p$  near 15 the conditions are somewhat critical, on account probably of the extremely rapid increase of  $\alpha/p$  with  $Z/p$ . Hence the values of  $\alpha/p$ ,  $k$ , and

Fig. 8.



W for  $Z/p$  equal to 14 and 15 are not as accurate as those for the other values given. A more precise exploration of this region would require some improvements in the apparatus used which it has not yet become convenient to make.

The numbers under  $H_0/Z$  show that this ratio remains constant for a given value of  $Z/p$  as required by the theory.

The values of  $u$ ,  $L$ ,  $\lambda$ , and  $h$  are given in the second part of Table V., and the curves representing  $k$ ,  $\alpha/p$ ,  $W$ ,  $L$ ,  $\lambda$ , and  $h$  are shown in figs. 3 to 8.

TABLE III.



Z/p.	c.	p.	Z.	$\log_{10}^a \frac{a}{+1}$	H <sub>0</sub> .	H <sub>0</sub> /Z.	$\alpha/p$ .	k.	W × 10 <sup>-5</sup> .
12.....	2	.67	8	.769	453	57	.015	3.2	27
	3	1.00	12	.757	668	56			
	4	1.33	16	.742	905	57			
14.....	2	.57	8	.643	429	54	.022	6.8	44
	3	.86	12	—	661	55			
	4	1.14	16	.620	—	—			
15.....	2	.53	8	.623	476	60	.07	7.0	41
	3	.80	12	—	731	61			
	4	1.07	16	.527	—	—			
16.....	2	.50	8	.586	507	63	.17	7.2	39
	3	.75	12	.456	789	66			
	4	1.00	16	.358	—	—			
20.....	2	.40	8	.402	557	70	.23	17	56
	3	.60	12	—	870	72			
	4	.80	16	.154	—	—			
24.....	2	.33	8	.218	580	72	.23	40	84
	3	.50	12	.149	905	75			
	4	.67	16	.015	—	—			
32.....	2	.25	8	.192	569	71	.25	49	96
	3	.38	12	.130	882	73			
	4	.50	16	.029	—	—			

### 5. Use with HCl.

This gas was prepared by removing the air from a glass bulb containing a normally-boiling solution of HCl, roughly drying the evaporated gas over strong sulphuric acid, and fractionally distilling it by means of several liquid-air traps, the first of which contained a small quantity of sulphuric acid. The purified gas was then stored in a glass reservoir which also contained a little sulphuric acid.

The experimental results are set out in Table IV. which is similar to Tables I. and III., but with Z/c equal to 2.

The values of *k* and  $\alpha/p$  are in fair agreement with those obtained previously \* by means of a different instrument and a different method.

\* V. A. Bailey and A. J. Higgs, Phil. Mag., Feb. 1929, p. 281.

But it was more difficult to determine  $H_0$  accurately with this gas than with  $NH_3$  and  $H_2O$ , on account of the large proportion of ions in the streams and the low values of  $k$  and  $Z$ . At the higher pressures the intensity of the ultra-violet light appreciably affected the observed values of  $H_0$ , which may be due to the effect of self-repulsion of the ions on the divergence of the stream ; consequently the intensity of the light was kept as small as possible.

It can be seen from the numbers in the seventh column of Table IV. that the ratio  $H_0/Z$  is not as constant for a

TABLE IV.

HCl:

$Z/p$ .	$c$ .	$p$ .	$Z$ .	$\log_{10} a$ +1	$H_0$ .	$H_0/Z$ .	$\alpha/p$ .	$k$ .	$W \times 10^{-5}$ .
10.....	$\left\{ \begin{array}{l} 2 \\ 3 \\ 4 \end{array} \right.$	$\left\{ \begin{array}{l} .40 \\ .60 \\ .80 \end{array} \right.$	$\left\{ \begin{array}{l} 4 \\ 6 \\ 8 \end{array} \right.$	$\left\{ \begin{array}{l} .617 \\ .603 \\ .533 \end{array} \right.$	$\left\{ \begin{array}{l} 248 \\ — \\ — \end{array} \right.$	$\left\{ \begin{array}{l} 62 \\ — \\ — \end{array} \right.$	$\left\{ \begin{array}{l} .09 \\ .09 \\ .09 \end{array} \right.$	$\left\{ \begin{array}{l} 3.4 \\ 3.4 \\ 3.4 \end{array} \right.$	$\left\{ \begin{array}{l} 25 \\ 25 \\ 25 \end{array} \right.$
15.....	$\left\{ \begin{array}{l} 2 \\ 4 \end{array} \right.$	$\left\{ \begin{array}{l} .27 \\ .53 \end{array} \right.$	$\left\{ \begin{array}{l} 4 \\ 8 \end{array} \right.$	$\left\{ \begin{array}{l} .504 \\ .356 \end{array} \right.$	$\left\{ \begin{array}{l} 201 \\ 457 \end{array} \right.$	$\left\{ \begin{array}{l} 50 \\ 57 \end{array} \right.$	$\left\{ \begin{array}{l} .22 \\ .22 \end{array} \right.$	$\left\{ \begin{array}{l} 5.9 \\ 5.9 \end{array} \right.$	$\left\{ \begin{array}{l} 44 \\ 44 \end{array} \right.$
20.....	$\left\{ \begin{array}{l} 2 \\ 4 \end{array} \right.$	$\left\{ \begin{array}{l} .20 \\ .40 \end{array} \right.$	$\left\{ \begin{array}{l} 4 \\ 8 \end{array} \right.$	$\left\{ \begin{array}{l} .438 \\ .144 \end{array} \right.$	$\left\{ \begin{array}{l} 213 \\ 522 \end{array} \right.$	$\left\{ \begin{array}{l} 53 \\ 65 \end{array} \right.$	$\left\{ \begin{array}{l} 56 \\ 56 \end{array} \right.$	$\left\{ \begin{array}{l} 6.6 \\ 6.6 \end{array} \right.$	$\left\{ \begin{array}{l} 45 \\ 45 \end{array} \right.$
30.....	$\left\{ \begin{array}{l} 2 \\ 4 \end{array} \right.$	$\left\{ \begin{array}{l} .13 \\ .27 \end{array} \right.$	$\left\{ \begin{array}{l} 4 \\ 8 \end{array} \right.$	$\left\{ \begin{array}{l} .310 \\ .056 \end{array} \right.$	$\left\{ \begin{array}{l} 267 \\ — \end{array} \right.$	$\left\{ \begin{array}{l} 67 \\ — \end{array} \right.$	$\left\{ \begin{array}{l} .73 \\ .73 \end{array} \right.$	$\left\{ \begin{array}{l} 12 \\ 12 \end{array} \right.$	$\left\{ \begin{array}{l} 50 \\ 50 \end{array} \right.$
40.....	$\left\{ \begin{array}{l} 2 \\ 4 \end{array} \right.$	$\left\{ \begin{array}{l} .10 \\ .20 \end{array} \right.$	$\left\{ \begin{array}{l} 4 \\ 8 \end{array} \right.$	$\left\{ \begin{array}{l} .200 \\ .007 \end{array} \right.$	$\left\{ \begin{array}{l} 310 \\ 830 \end{array} \right.$	$\left\{ \begin{array}{l} 78 \\ 104 \end{array} \right.$	$\left\{ \begin{array}{l} .74 \\ .74 \end{array} \right.$	$\left\{ \begin{array}{l} 22 \\ 22 \end{array} \right.$	$\left\{ \begin{array}{l} 60 \\ 60 \end{array} \right.$

given value of  $Z/p$  as it is with the other two gases, but it is probable that the numbers corresponding to the lower pressures are correct within about 20 per cent. Should the necessity arise it would be possible to attain greater accuracy.

The values of  $u$ ,  $L$ ,  $\lambda$ , and  $h$  are given in the last part of Table V., and the curves representing  $k$ ,  $\alpha/p$ ,  $W$ ,  $L$ ,  $\lambda$ , and  $h$  are shown in figs. 3 to 8.

### 6. Discussion of Results.

The results for several other gases are also shown in these figures, as it is of interest to consider the values of some of the above quantities for the different molecules

and to indicate properties of molecules which may be related to the variations of these quantities with the energy of the electrons.

The curves for  $k$  (as in fig. 3) are of three types, the first corresponding to the gases \* He, Ne, A, the second to  $H_2$ ,  $N_2$ ,  $O_2$ , NO, CO, and the third to  $CO_2$ ,  $NH_3$ ,  $H_2O$ , HCl,  $N_2O$ ,  $C_2H_4$ ,  $C_5H_{12}$ . These groups of molecules are in

TABLE V.

$Z/p$ .	V volts.	$u \times 10^{-7}$ cm./sec.	$L \times 100$ cm.	$\lambda \times 100$ .	$h \times 10^4$ .
$NH_3$ .					
4.....	·055	1·40	·17	·62	—
6.....	·06	1·43	·21	1·83	—
8.....	·17	2·49	·67	4·27	·03
10.....	·45	4·02	1·37	3·54	·32
12.....	1·11	6·29	2·38	2·61	1·2
16.....	1·85	8·12	2·70	2·15	3·1
24.....	2·05	8·57	2·09	2·34	4·1
32.....	2·11	8·67	1·73	2·73	3·7
$H_2O$ .					
12.....	·14	2·21	·37	4·23	·06
14.....	·21	2·72	·48	4·18	·19
16.....	·32	3·37	·63	4·00	1·3
20.....	·70	4·98	1·07	3·69	3·0
24.....	1·37	7·00	1·65	3·28	4·5
32.....	1·81	8·04	1·69	3·52	5·0
HCl.					
10.....	·14	2·24	·41	3·3	·4
15.....	·20	2·64	·51	6·0	1·7
20.....	·26	3·04	·49	5·6	4·1
30.....	·45	4·02	·49	4·2	4·7
40.....	·83	5·46	·56	2·8	4·4

order of increasing complexity, and also behave differently in regard to the absorption of light. The first group is extremely transparent to light of all wave-lengths down to the lower limit of the ultra-violet region; the second

\* J. S. Townsend, *loc. cit.* M. F. Skinner and J. V. White, *Phil. Mag.*, Oct. 1923, p. 630. H. L. Brose, *Phil. Mag.*, Sept. 1925, p. 536. J. Bannon and H. L. Brose, *Phil. Mag.*, Nov. 1928, p. 817. J. D. McGee and J. C. Jæger, *Phil. Mag.*, Dec. 1928, p. 1107.

(excepting CO) absorbs light notably only in the ultra-violet region; and the third is known\* to have strong absorption-bands in the infra-red region.

Similar remarks may be made about the curves for the fraction  $\lambda$  (as in fig. 7); but a more interesting fact about them is the correspondence between the magnitudes of  $\lambda$  for any gas and its light-absorption. If the light-frequency  $\nu$  is given in terms of the electronic energy by Einstein's relation  $h\nu = \frac{1}{2}mu^2$ , then the larger values of  $\lambda$  correspond to values of  $\nu$  in the neighbourhood of strong absorption-bands, and the smaller values of  $\lambda$  correspond to regions of small light-absorption †.

The larger values of  $\lambda$  are of the order of 6 per cent., which is roughly the same as the average order of the fractional change of frequency in the Raman effect. A closer examination of the relation between  $\lambda$  and the absorption and scattering of light requires much more complete information about the light-intensities involved than is now available.

The curves for the mean free path  $L$  (in fig. 6) have similar forms for the molecules  $\text{CO}_2$ ,  $\text{NH}_3$ , and  $\text{H}_2\text{O}$ . With each of these  $L$  increases to a maximum value as the velocity  $u$  increases, and a similar but smaller change occurs for  $\text{HCl}$ . It is interesting to notice that the largest value of  $L$  obtained by these methods, namely 16 mm. in argon, is 800 times as large as the smallest value, namely .02 mm. in  $\text{NH}_3$ .

The curves for  $\alpha/p$  (in fig. 4) also show a mutual resemblance for the gases  $\text{NH}_3$ ,  $\text{H}_2\text{O}$ , and  $\text{HCl}$ , each increasing with  $Z/p$  from a low to a maximum value. The experiments of Skinker‡ and White appear to indicate that  $\text{N}_2\text{O}$  behaves similarly. But for air,  $\text{O}_2$ , and  $\text{NO}$  the experiments show a diminution of  $\alpha/p$  with increasing  $Z/p$ .

The curves for the probability of attachment  $h$  (in fig. 8) all show large increases§ of  $h$  with the velocity  $u$  of an electron which collides with one of the molecules  $\text{NH}_3$ ,  $\text{H}_2\text{O}$ , and  $\text{HCl}$ . On comparing this with the curves for the mean free path  $L$  (in fig. 6), it is seen that in colliding with one of these molecules an electron is more liable

\* No absorption data have been found for the gas  $\text{C}_5\text{H}_{12}$ .

† Thus the blueness of the sky and the redness of the setting sun correspond to the decrease of  $\lambda$  for air from .05 to .003 over the visible spectrum from short to long waves.

‡ M. F. Skinker and J. V. White, *loc. cit.*

§ *E. g.* for  $\text{NH}_3$  the increase is at least a hundredfold.

to remain attached the further it penetrates into the molecule. The same rule applies to the "molecule" of air, and to  $O_2$ ,  $NO$ , and  $N_2O$  as far as can be judged from the available evidence.

On the other hand, for the four molecules air,  $NH_3$ ,  $H_2O$ , and  $HCl$  the probability of an electron of a given energy becoming attached increases with the apparent size of the molecule.

The rapid diminution of  $h$  with  $u$  for  $NH_3$ ,  $H_2O$ , and  $HCl$  suggests the possibility that, at still lower velocities than those shown,  $h$  may be so small that the streams of negative electricity will be composed almost entirely of free electrons. As mentioned in Section 3, this possibility has been verified\* for  $NH_3$ , but no opportunity has yet occurred to examine it for  $H_2O$  and  $HCl$ .

It is probable that the properties investigated here are also related to chemical properties of the molecule (*e.g.*, the heat of formation), but no reliable conclusions are possible until a much larger number of kinds of molecules has been studied.

Recently A. Cravath† has published an account of a method for measuring  $\alpha/p$  which makes use of an ingenious device (also independently conceived by Van der Graaf) for collecting most of the electrons in a mixed stream of negative particles. He has not yet succeeded in obtaining consistent results with it, but it appears to promise success when suitably modified.

## 7. Summary.

The problem of determining the statistical behaviour of electrons amongst molecules, to which they may become attached, has now been solved for those conditions where ionization by collision is absent and where the negative ions are permanent. The methods used and their application to the gases  $NH_3$ ,  $H_2O$ , and  $HCl$  are described in some detail, and are found to give consistent results for the energy of agitation of electrons, their velocity of drift, and their probability of attachment to molecules per unit distance of drift.

\* It should be mentioned that Wahlin has also found few ions accompanying a stream of electrons through  $NH_3$  with low values of  $Z/p$ .

† A. Cravath, *Phys. Rev.*, April 1929.

From these quantities have been deduced the values of the mean free path  $L$  of an electron in each gas, the fraction  $\lambda$  of its own energy which is lost and the probability  $h$  of its becoming attached when it collides with a molecule.

The results obtained from these and other experiments appear to show that  $\lambda$  bears some relation to the light-absorbing power of the molecule, and that the probability  $h$  for a given kind of molecule varies considerably with the energy of the electron, generally increasing with its penetration into the molecule.

In conclusion we wish to acknowledge our indebtedness to Mr. J. D. McGee for his valuable assistance in the designing and standardizing of the coils used for producing the magnetic fields.

#### XV. *Contribution to the Kinetic Theory of Vaporization.*—

III. *The Vapour Pressure of Solutions.* By SAMUEL CLEMENT BRADFORD, D.Sc., *The Science Museum, London, S.W. 7* \*.

IN previous papers † Maxwell's theory of the distribution of molecular velocities, which regarded molecules merely as hard, perfectly elastic spheres, has been amplified to take into account the effects of molecular attraction. An expression was thus obtained for the vapour pressure of a pure liquid in terms of molecular attraction, volume, and motion only, and the vapour pressures calculated from this formula agreed remarkably with the observed values for every liquid examined. In the second paper it was suggested that the theory should be capable of extension to the case of solutions of salts in water. This has now been done, and, in spite of the more complicated conditions, the theory gives results almost equally as good for solutions as for pure liquids. This remarkable agreement is evidence that the so-called failure of the classical dynamics is due not to any inherent defect in the method, but to the omission on the part of mathematicians to allow for the mutual attractions of moving particles in close proximity to one another.

\* Communicated by the Author.

† Phil. Mag. xlviii. p. 936 (1924); 1. p. 1147 (1925).

(i.) *The Vapour Pressure of a Pure Liquid.*

Let us consider a pure liquid in contact with its vapour only, and maintained at constant temperature in a thermostat under ordinary laboratory conditions, so that any heat abstracted from the liquid by the escaping vapour will be supplied immediately by the enclosure, while any heat gained by the vapour will be given up to the surroundings.

Although the molecules of the liquid are not spherical in shape, they will be in continuous motion, and their rapid rotational velocity will maintain a clear spherical space around the centre of rotation of each molecule. As the molecules are electrically neutral, they will repel in some orientations and attract in others ; but, as the duration of the attractive encounters is greater, the effect of the attractions will preponderate over that of the repulsions.

Let  $\delta$  be the mean of the nearest distances of approach of the centres of two molecules during a considerable number of encounters. If we consider a space element  $dv$  at a definite position relative to a given molecule, the molecules with their centres within  $dv$  will be continually changing their position and attractive forces. During a sufficient interval of time, any point within  $dv$  will have been occupied by a molecular centre as often as any other point, and the average force at that point will be the same as at any other point. In measuring the vapour pressure of liquids we are concerned not with instantaneous values, but with average values, during a considerable interval of time. It seems legitimate, therefore, to consider the average values of the molecular forces within a given space element. The space element  $dv$  may be situated at any distance from an attracted molecule equal to, or greater than,  $\delta$ .

The average value of the attraction\* between two molecules whose centres are at a distance  $r$  has been shown to be approximately

$$f = \frac{c}{\lambda}, \quad . \quad . \quad . \quad . \quad . \quad . \quad . \quad . \quad (i)$$

where

$$c = \frac{6K\delta^4}{\pi n^2}, \quad . \quad . \quad . \quad . \quad . \quad (\text{ii})$$

\* Edser, "Molecular Attraction and the Physical Properties of Liquids," Brit. Assoc. 4th Report on Colloid Chemistry, p. 40 (1922).





An equal amount of work must be done by the molecule in escaping completely from the surface to infinity, so that, neglecting the small attraction of the vapour, the total work done by a particle of liquid in passing into the vapour is

$$W = \frac{\pi c n}{3\delta^4} = \frac{2K}{n} \quad \dots \quad \text{(vii)}$$

Giving  $n$  its value  $\frac{\rho}{M} \times 6.23 \times 10^{23}$ ,  $\rho$  being the density of the liquid and  $M$  its molecular weight, we have

$$W = 3.21 \times 10^{-24} \frac{MK}{\rho} \quad \dots \quad \text{(viii)}$$

The vapour of the liquid is formed by the particles that strike the surface of the liquid with sufficient velocity normal to the surface to accomplish the work  $W$  and escape from the liquid.

The number of such particles is determined by Maxwell's law of the distribution of molecular velocities, bearing in mind that the particles in the interior of the liquid are moving under the influence of molecular forces.

The number of particles in unit volume of the liquid that have velocities whose vertical components lie between  $u$  and  $u + du$  is

$$\frac{n_s}{\sqrt{\pi} V_{ps}} e^{-\frac{u^2}{V_{ps}^2}} \cdot du, \quad \dots \quad \text{(ix)}$$

where  $n_s$  is the concentration of the liquid particles and  $V_{ps}$  Maxwell's most probable speed of the particles. Therefore the number of particles per unit volume, having velocities normal to the surface between  $u$  and  $u + du$ , that strike the surface from below is

$$\frac{n_s}{V_{ps} \sqrt{\pi}} e^{-\frac{u^2}{V_{ps}^2}} \cdot u du. \quad \dots \quad \text{(x)}$$

But of these, only those having velocities normal to the surface equal to, or greater than, a certain critical velocity  $s$  will be able to escape from the attraction of the liquid and pass into the vapour. The total number of such particles is

$$\int_s^\infty \frac{n_s}{V_{ps} \sqrt{\pi}} e^{-\frac{u^2}{V_{ps}^2}} \cdot u du = \frac{n_s V_{ps}}{2\sqrt{\pi}} \cdot e^{-\frac{s^2}{V_{ps}^2}} \quad \dots \quad \text{(xi)}$$

Now the total number of particles from the vapour that strike the same area of the surface is

$$\int_0^\infty \frac{n_s}{V_{pl}\sqrt{\pi}} e^{-\frac{u^2}{V_{pl}^2}} \cdot u \, du = \frac{n_l V_{pl}}{2\sqrt{\pi}}, \quad \dots \quad (\text{xii})$$

where  $n_l$  is the concentration of the vapour and  $V_{pl}$  Maxwell's constant for the vapour phase.

The greater attraction of the liquid ensures that all particles striking the surface from above return to the liquid. In equilibrium, the number of particles escaping from the liquid must be equal to the number returning, so that from (xi) and (xii)

$$\frac{n_s V_{ps}}{2\sqrt{\pi}} \cdot e^{-\frac{s^2}{V_{ps}^2}} = \frac{n_l V_{pl}}{2\sqrt{\pi}}$$

or 
$$n_l = n_s \frac{V_{ps}}{V_{pl}} e^{-\frac{s^2}{V_{ps}^2}} \dots \dots \dots (\text{xiii})$$

Previously, in attempting to apply Maxwell's law of the distribution of molecular velocities to systems of attracting particles, the mistake has been made of assuming that the most probable speeds of the particles in such a system will be the same as in a perfect gas at the same temperature. Since, however, the particles attract one another, it follows from the definition of a force that the speeds in a system of attracting particles cannot be the same as in a medium composed of inert particles. That is to say, the law of the equipartition of energy applies only to perfect gases. Therefore  $V_{ps}$  is not equal to  $V_{pl}$ , and it is necessary to make allowance for the effect of the forces of attraction. Since we may assume that the forces are distributed in magnitude and direction according to the laws of probability, we may write

$$V_{ps} = \lambda V_{pl}, \quad \dots \dots \dots (\text{xiv})$$

where  $\lambda$  is a function of the forces of attraction in the medium.

If  $v_l$  be the volume occupied by the number  $N$  of molecules in a gramme molecule of the given substance in the vapour state, and  $v_s$  the volume of the same number of molecules in the liquid condition, then, allowing for the volume occupied by the molecules,

$$n_l = \frac{N}{v_l - b_l} \quad \text{and} \quad n_s = \frac{N}{v_s - b_s},$$



From equations (viii) and (xviii) we have, therefore,

$$p = 81.84 \frac{T\lambda}{\phi_s} e^{-\frac{2.414 \times 10^{-8} KM}{\lambda^2 \rho T}} \quad \dots \quad (\text{xix})$$

It has been shown that the cohesion  $K$  can be calculated with considerable accuracy from Edser's equation (iii), in which  $\delta$  is given by the formula

$$\delta = \left( \frac{3.24M}{2.016\rho_m} \right)^{1/3} \times 10^{-8}, \quad \dots \quad (\text{xx})$$

$\rho_m$  being the density of the liquid near the freezing-point. Writing

$$\delta' = \delta \times 10^8 \quad \text{and} \quad \frac{M}{\rho} = v_s,$$

the pressure of the vapour becomes

$$p = 81.84 \frac{T\lambda}{\phi_s} e^{-\frac{9.6658v_s}{\lambda^2 T \delta'}}.$$

This applies to a non-associated liquid. Should the liquid be associated, its molecular weight would be  $A.M$ , where  $A$  is the degree of association and  $M$  the molecular weight of the unassociated substance, so that the molecular and co-volume of an associated liquid become  $Av_s$  and  $A\phi_s$  respectively. Similarly, the average molecular diameter becomes  $A^{1/3}\delta$ . It should be noticed that  $A$  is not an arbitrary factor, but represents the actual physical state of the liquid. Therefore the vapour pressure in atmospheres of an associated liquid is

$$p = 81.84 \frac{T\lambda}{A\phi_s} e^{-\frac{9.6658v_s A^{2/3}}{\lambda^2 T \delta'}} \quad \dots \quad (\text{xxi})$$

or

$$p = 81.84 \frac{T\lambda}{A\phi_s} e^{-\frac{2.416K'v_s A^{2/3}}{\lambda^2 T}}, \quad \dots \quad (\text{xxii})$$

where  $K' = K \times 10^{-8}$ .

This formula assumes that for every particle, associated or unassociated, which approaches the surface of a liquid with a velocity normal to the surface equal to, or greater than, the critical velocity  $s$ , a single particle is communicated to the vapour. The assumption is not entirely without

justification. But the complete analysis would require a knowledge of the actual values of the attractions of the associated and unassociated particles, and at present these data are lacking. However, when  $A$  is small, the expression (xxi) is sufficiently accurate, as Table II. shows. The values of  $\phi_s$  are given approximately by the relation

$$\phi_s = v - \frac{S'^3}{4}. \quad \dots \dots \dots \text{(xxiii)}$$

In the equation (xxi) the value of the variable  $\lambda$  remains to be determined. This function, which is the ratio of the most probable speed of the particles in the given liquid to that in a perfect gas, was considered by Kleeman, who calculated its value for  $\text{CO}_2$  at  $40^\circ$  and 112 atmospheres pressure to be 1.6. Actually this is near the figure that the present writer has found for water under ordinary conditions.

TABLE I.

Liquid.	$t$ .	$K \times 10^{-8}$ .	$\lambda$ .
<i>n</i> -Hexane .....	$18^\circ$	11.47	1.270
Toluene .....	$18^\circ$	21.18	1.390
Mercury .....	$200^\circ$	599.0	1.915

What is needed, however, is a direct method of deducing  $\lambda$  from the physical condition of the liquid. In previous papers a relation between  $\lambda$  and the density of the liquid was obtained that worked very well for a variety of organic liquids. But for water the relation was not so good, and it seemed desirable to endeavour to trace a direct relation between  $\lambda$  and the cohesion of the liquid.

Three liquids were selected as being unlikely to be much associated. Their cohesions were calculated from Edser's formula (iii), and the values of  $\lambda$  necessary to make the calculated vapour pressures fit the observed figures were determined. The values of  $K$  and  $\lambda$  are given in Table I.

Putting

$$\lambda - 1 = y,$$

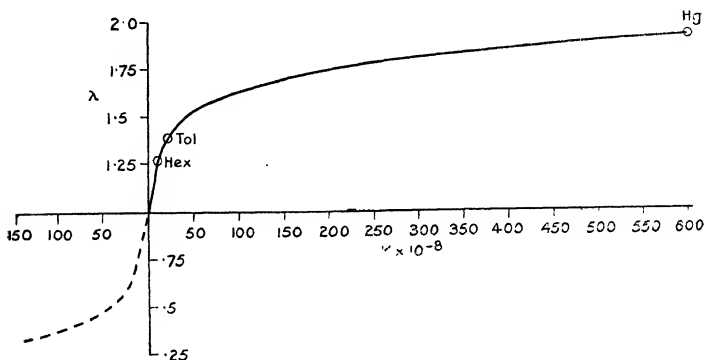
the relation between  $K$  and  $y$  was assumed to be of the form

$$K = ay + by^3 + cy^5,$$

which gives  $\lambda=1$  for  $K=0$ , the condition corresponding to a perfect gas. The coefficients were determined from the data in Table I., and the equations became

$$K' = 42.16y - 64.7y^3 + 952y^5. \quad \dots (xxiv)$$

The relation between  $\lambda$  and  $K$  is expressed graphically in the following curve:—



Either the equation or the curve can be used to find the value of  $\lambda$  from which to calculate the vapour pressure of a pure liquid from the formula (xxi), as has been done in Table II. Although the equation (xxiv) must still be regarded as approximate, the agreement between the observed and calculated values of the vapour pressures shows that the cohesion of the medium has such an effect on the most probable speed of the particles as has been supposed, and that, when this is allowed for, the kinetic theory is sufficient to explain the vapour pressures of liquids.

If the calculated value of the vapour pressure does not agree exactly with the observed value, association is indicated, and a value of  $A$  can be determined that will give a figure for the cohesion  $K$ , which, together with the corresponding value of  $\lambda$ , leads to the observed value of the vapour pressure. It will be seen that the necessary values of the association agree very well with those calculated by more empirical methods by Ramsay and Shields\*. It will be noticed that, in certain cases, the use of equation (xxiv) gives a very slightly lower value of the association factor at lower temperatures for the same liquid.

\* J. C. S. lxiii. p. 1089 (1893).

This suggests that in reality the curve should rise a very little more quickly. The effect of this would be to give a rather higher value of  $\lambda$ , say about 1.63 for water, so that the association would work out at about 3.00 with  $K=65.2$ . This is, perhaps, a more likely value. The equation (xxiv) may be said to be fairly definite for the region between  $\lambda=1.275$ ,  $K=11.75 \times 10^8$ , and  $\lambda=1.44$ ,  $K=28.07 \times 10^8$ , which covers most of the liquids in the table. Beyond the latter point the curve is only approximate.

These calculations are also of interest in showing that Edser's formula (iii) written in the form

$$K = \frac{4S}{A^{1/3}\delta},$$

with the introduction of an association factor, provides, for the first time, an accurate method of calculating the cohesion of a liquid. Previous methods of estimating this quantity have given values varying between wide limits, such as from 1.710 to 3.570 for toluene, 1.919 to 7.140 for acetic acid, and 3.645 to 17.300 for water. Unless a really accurate method of determining the cohesion of a liquid were available, there could be no hope of calculating its vapour pressure.

### (ii.) *The Surface Tension of a Solution.*

Before proceeding to extend equation (xxi) to the case of a solution, it is interesting to develop a formula for the surface tension of a solution. If we neglect, for the time being, the change in concentration in the surface layers, the surface tension of a solution may be determined very simply by Gauss's method.

The surface tension of a liquid is equal to half the work  $W$  done per unit area of a surface  $AB$  in separating the liquid below  $AB$  from that above it.

Let  $\delta_1$  and  $\delta_2$  be the least distances of approach of the liquid molecules  $M_1$  and solute molecules  $M_2$  respectively,  $c_1$  and  $c_2$  the corresponding coefficients of attraction, and  $n_1$  and  $n_2$  the concentrations of the particles :

- (1) The work done in removing to infinity the solution that is at a distance below  $AB$  greater than  $\delta$ .
- (1a) Work due to mutual attraction of the solvent molecules  $M_1$ .

The attraction exerted by all the solvent molecules  $M_1$



TABLE

Substance.	Molecular weight M.	Temperature °C. t.	Density $\rho$ .	Molecular volume v.	$\delta'$ .	Co-volume $\phi$ .
Acetone.....	58.05	56	0.710	81.76	4.679	57.14
		20	0.778	73.3		48.68
Aniline .....	93.04	184	0.867	107.31	5.253	71.07
		54.8	0.990	93.98		57.74
Benzene .....	78.05	80.5	0.810	96.36	5.192	66.09
		55	0.841	92.8		62.53
Carbon disulphide .....	76.12	46.8	1.221	62.19	4.618	35.77
Carbon tetrachloride ...	153.8	76.4	1.489	103.29	5.313	65.80
		25	1.585	97.03		59.54
Chlorobenzene .....	112.5	131	0.985	126.9	5.417	87.16
		25	1.101	102.18		62.44
Chloroform .....	119.51	61.2	1.414	84.46	4.994	53.32
		35	1.459	81.91		50.77
Ethyl ether .....	74.08	34.8	0.698	106.13	5.277	69.39
		25.3	0.707	104.78		68.04
		-20.5	0.753	97.3		60.99
		-75	0.818	90.56		53.82
Ethyl iodide.....	152.88	72.5	1.830	83.55	5.000	52.30
		20.4	1.934	79.04		47.79
Nitrobenzene .....	123.06	209	1.031	122.62	5.473	81.63
		100	1.125	109.87		68.88
<i>n</i> -Hexane .....	86.12	20	0.6595	130.58	5.905	79.10
		25	0.6559	131.30		79.80
Phosphorus trichloride.	137.42	77.4	1.471	93.04	5.026	61.30
Pyridine .....	75.05	114.5	0.882	89.73	4.911	63.12
Toluene.....	92.06	109.4	0.780	118.13	5.383	79.14
		26	0.860	107.05		68.06
Water .....	18.02	100	0.958	18.8	3.095	11.50
		18	0.9986	18.045		10.633
Mercury .....	200.6	200	13.113	15.298	2.88	9.33
		17.5	13.552	14.802		8.83

## II.

Surface-tension S.	$K \times 10^{-8}$ .	$\lambda$ .	Association A.		Vapour pressure P.			
			From vapour pressure.	R. & S.	Calculated.		Observed.	
					Atmo- spheres.	mm.	Atmo- spheres.	mm.
19.4	15.69	1.332	1.18		1.02		1.00	
23.1	18.09	1.360	1.30	1.26		181		180
24.3	17.51	1.354	1.185	1.05	0.994		1.00	
39.5	28.07	1.440	1.23			4.09		4
20.7	15.49	1.330	1.09	1.01	0.998		1.00	
23.8	17.9	1.358	1.075			332		327
27.3	21.84	1.396	1.27	1.07 at 32°	1.01		1.00	
20.2	15.03	1.324	1.035	1.01 at 46°	0.987		1.00	
25.4	18.96	1.368	1.026			117		116
19.0	14.0	1.312	1.007		0.995		1.00	
32.9	23.9	1.412	1.05	1.03		12		12
21.8	16.64	1.346	1.13		1.04		1.00	
24.8	19.14	1.370	1.12			307		308
15.9	12.03	1.280	1.005	0.99	0.994		1.00	
16.7	12.62	1.291	1.009			536		540
21.5	16.22	1.340	1.015			67		67
28.5	21.1	1.390	1.073			0.9		0.9
22.3	16.88	1.347	1.18	0.96	1.02		1.00	
28.1	21.38	1.392	1.163	1.01 at 46°		109		108
21.2	14.50	1.318	1.22	1.13 at 156°	1.005		1.00	
29	19.27	1.371	1.33	0.93 at 78.4°		21.4		21
17.41	11.75	1.275	1.005			118		120
16.93	11.47	1.270	1.00			153		153
21.9	17.09	1.350	1.061	1.02 at 32°	1.01		1.00	
25.2	19.88	1.377	1.10	0.93 at 46°	.997		1.00	
19.5	14.47	1.318	1.005		1.01		1.00	
28.4	21.1	1.388	1.00			29.4		29
58.92	54.56	1.540	2.45	2.66	.994		1.00	
72.82	67.75	1.568	2.68	3.68 at 20°		15.7		15.48
431.2	599	1.915	1.00			17.2		17.2
547.2	792	1.970	0.884			0.00106		0.00106

above AB on a molecule of solvent  $M_1$  at a distance  $x$  below AB where  $x > \delta_1$

$$= \frac{2\pi c_1 n_1}{35x^5}$$

from (iv).

The work done in removing this molecule to infinity

$$= \frac{2\pi c_1 n_1}{35} \int_x^\infty \frac{dx}{x^5} = \frac{\pi c_1 n_1}{70x^4}.$$

Describe two planes parallel to AB at distances  $x$  and  $x+dx$  below AB. Unit area of the layer between these planes will comprise  $n_1 dx$  molecules of solvent. The work of removing these molecules to infinity

$$= \frac{\pi c_1 n_1}{70x^4} n_1 dx.$$

Therefore the work of removing to infinity the whole of the solvent molecules originally at a distance  $\delta_1$  or more below AB

$$\begin{aligned} &= W_{1a} = \frac{\pi c_1 n_1^2}{70} \int_{\delta_1}^\infty \frac{dx}{x^4} \\ &= \frac{\pi c_1 n_1^2}{210\delta_1^3} \dots \dots \dots \quad (\text{xxv}) \end{aligned}$$

(1b) Work due to the attraction of solute molecules  $M_2$  above AB on solvent molecules  $M_1$  below AB.

Describe two planes parallel to AB at distances  $\xi$  and  $\xi+d\xi$  above AB. Molecules of solute whose centres are between these planes will exert on a solvent molecule  $M_1$  a resultant attraction

$$\begin{aligned} &= \frac{2\pi c_1^{1/2} c_2^{1/2} n_2 d\xi}{(x+\xi)^6} \int_0^{\pi/2} \cos^6 \theta \sin \theta d\theta \\ &= \frac{2\pi c_1^{1/2} c_2^{1/2} n_2 d\xi}{7(x+\xi)^6}. \end{aligned}$$

The attraction exerted on  $M_1$  by all the solute molecules above AB

$$= \frac{2\pi c_1^{1/2} c_2^{1/2} n_2}{7} \int_0^\infty \frac{d\xi}{(x+\xi)^6} = \frac{2\pi c_1^{1/2} c_2^{1/2} n_2}{35x^5}.$$

The work done in removing this solvent molecule to infinity

$$= \frac{2\pi c_1^{1/2} c_2^{1/2} n_2}{35} \int_0^\infty \frac{dx}{x^5} = \frac{\pi c_1^{1/2} c_2^{1/2} n_2}{70x^4}.$$

Describe two planes parallel to AB at distances  $x$  and  $x + dx$  below AB. The number of solvent molecules per unit area between those planes is  $n_1 dx$ . The work per unit area of AB in removing to infinity the whole of the solvent molecules below AB originally at a distance  $\delta_{12}$  or more below AB

$$\begin{aligned} &= W_{1b} = \frac{\pi c_1^{1/2} c_2^{1/2} n_1 n_2}{70} \int_{\delta_{12}}^{\infty} \frac{dx}{x^4} \\ &= \frac{\pi c_1^{1/2} c_2^{1/2} n_1 n_2}{210 \delta_{12}^3}, \quad . . . . . \text{(xxvi)} \end{aligned}$$

where  $\delta_{12}$  is the nearest distance of approach of a solute and solvent particle.

- (1c) Similarly the work due to the attraction of solvent molecules  $M_1$  above AB in removing solute molecules  $M_2$  below AB to infinity

$$= W_{1c} = \frac{\pi c_1^{1/2} c_2^{1/2} n_1 n_2}{210 \delta_{12}^3}, \quad . . . \text{(xxvii)}$$

and

- (1d) The work due to the attraction of solute molecules  $M_2$  above AB in removing solute molecules  $M_2$  below AB to infinity

$$= W_{1d} = \frac{\pi c_2 n_2^2}{210 \delta_2^3} . . . . . \text{(xxviii)}$$

- (2) To find the work done per unit area of AB in removing to infinity the solution at a distance  $x$  below AB where  $x < \delta$ .

- (2a) Mutual attraction of solvent molecules.

The attraction exerted by all the solvent molecules AB on a solvent molecule at distance  $x < \delta$  below AB

$$= \pi c_1 n_1 \left\{ \frac{1}{5\delta_1^5} - \frac{x^2}{7\delta_1^7} \right\} . . . \text{(xxix)}$$

from (v).

The work of removing this molecule to a distance  $\delta_1$  from AB

$$\begin{aligned} &= \pi c_1 n_1 \int_x^{\delta_1} \left( \frac{1}{5\delta_1^5} - \frac{x^2}{7\delta_1^7} \right) dx \\ &= \pi c_1 n_1 \left( \frac{\delta_1 - x}{5\delta_1^5} - \frac{\delta_1^3 - x^3}{21\delta_1^7} \right). \end{aligned}$$



(2 c) Similarly the work due to the attraction of solvent molecules above AB on solute molecules below

$$= W_{2c} = \frac{9\pi c_1^{1/2} c_2^{1/2} n_1 n_2}{140 \delta_{12}^3}, \quad . \quad . \quad . \quad (\text{xxxiv})$$

and

$$W_{2c} = \frac{\pi c_1^{1/2} c_2^{1/2} n_1 n_2}{70 \delta_{12}^3} \quad . \quad . \quad . \quad (\text{xxxv})$$

(2 d) Likewise the work due to the attraction of solute molecules above AB on solute molecules below

$$= W_{2d} = \frac{9\pi c_2 n_2^2}{140 \delta_2^3}, \quad . \quad . \quad . \quad (\text{xxxvi})$$

and

$$W_{2d} = \frac{\pi c_2 n_2^2}{70 \delta_2^3} \quad . \quad . \quad . \quad (\text{xxxvii})$$

The surface tension is half the sum of all these  $W$ 's. Writing  $\delta_{12} = \delta_1^{1/2} \delta_2^{1/2}$  approximately, we get

$$S_{12} = \frac{\pi}{24} \left( \frac{c_1^{1/2} n_1}{\delta_1^{3/2}} + \frac{c_2^{1/2} n_2}{\delta_2^{3/2}} \right)^2, \quad . \quad . \quad (\text{xxxviii})$$

or from (ii),

$$S_{12} = \frac{(K_1^{1/2} \delta_1^{1/2} + K_2^{1/2} \delta_2^{1/2})^2}{4}; \quad . \quad (\text{xxxix})$$

from which we have, by (iii),

$$K_2 = \frac{4(S_{12}^{1/2} - S_1^{1/2})^2}{\delta_2} \quad . \quad . \quad . \quad (\text{xl})$$

This formula gives a method of determining the cohesion of the solute particles in a solution from the surface tensions of the pure solvent and the solution.

### (iii.) *The Vapour Pressure of a Solution.*

From previous work it will be seen that the attraction of the solvent on a particle of solute at a distance  $x$  below the surface of the solution would be

$$\pi c_1 n_1 \left\{ \frac{1}{5 \delta_1^5} - \frac{x^2}{7 \delta_1^7} \right\} + \frac{2\pi c_1 n_1}{35 x^5} \quad . \quad . \quad . \quad (\text{xli})$$

To determine the attraction of the solute molecules on an escaping molecule of solvent; let P be the centre of a molecule of solvent at a distance  $x$  below the surface AB of the solution, where  $x > \delta_{12}$ ,  $\delta_{12}$  being the average of the

nearest distances of approach of solvent and solute molecules. The attraction of the solute molecules in the solution is taken as equal and opposite to the attraction that would be exerted by a similar number and distribution of solute molecules above the surface AB.

Molecules of solute in this imaginary mass of solution above AB, whose centres would be between two planes parallel to AB at distances  $\xi$  and  $\xi + d\xi$  above AB, would exert on P a resultant attraction equal to

$$\frac{2\pi c_1^{1/2} c_2^{1/2} n_2 d\xi}{(x + \xi)^6} \int_0^\pi \cos^6 \theta \sin \theta d\theta = \frac{2\pi c_1^{1/2} c_2^{1/2} n_2 d\xi}{7(x + \xi)^6}.$$

The attraction per unit area on P by all the molecules of of solute whose centres would be above AB would be

$$\frac{2\pi c_1^{1/2} c_2^{1/2} n_2}{7} \int_0^\infty \frac{d\xi}{(x + \xi)^6} = \frac{2\pi c_1^{1/2} c_2^{1/2} n_2}{35x^5}. \quad (\text{xlii})$$

When the distance below AB of the escaping molecule becomes less than  $\delta_{12}$ , that part above AB of a sphere with radius  $\delta_{12}$  described around P will contain no centres of attracting molecules of solute. These may now be considered to have their centres within the portions above AB of two spheres with radii  $r$  and  $r + dr$  described around P. The resultant attraction on P by all the molecules of solute whose centres would be between these spheres would be

$$\begin{aligned} & \frac{2\pi c_1^{1/2} c_2^{1/2} n_2 dr}{r^6} \int_0^{\cos^{-1}(\frac{x}{r})} \cos \theta d\theta \\ &= \frac{\pi c_1^{1/2} c_2^{1/2} n_2 dr}{r^6} \left(1 - \frac{x^2}{r^2}\right), \end{aligned}$$

and the total attraction on the solvent molecule at P by all the solute molecules whose centres would be above AB would be

$$\pi c_1^{1/2} c_2^{1/2} n_2 \int_{\delta_{12}}^\infty \left(\frac{1}{r^6} - \frac{x^2}{r^8}\right) dr = \pi c_1^{1/2} c_2^{1/2} n_2 \left\{ \frac{1}{5\delta_{12}^5} - \frac{x^2}{7\delta_{12}^7} \right\}. \quad (\text{xliii})$$

Therefore the total work done by the solvent molecule at P in escaping to the surface of the solution

$$\begin{aligned} &= \frac{2\pi c_1 n_1}{35} \int_{-\infty}^{-\delta_1} \frac{dx}{x^5} + \frac{2\pi c_1^{1/2} c_2^{1/2} n_2}{35} \int_{-\infty}^{-\delta_{12}} \frac{dx}{x^5} + \pi c_1 n_1 \\ &\quad \times \int_{-\delta_1}^0 \left( \frac{1}{5\delta_1^5} - \frac{x^2}{7\delta_1^7} \right) dx + \pi c_1^{1/2} c_2^{1/2} n_2 \end{aligned}$$

$$\times \int_{-\delta_{12}}^0 \left( \frac{1}{5\delta_{12}^5} - \frac{x^2}{7\delta_{12}^7} \right) dx = \frac{\pi}{6} \left( \frac{c_1 n_1}{\delta_1^4} + \frac{c_1^{1/2} c_2^{1/2} n_2}{\delta_{12}^4} \right). \quad \dots \quad (\text{xliv})$$

An equal amount of work must be done by the solvent molecule in escaping completely from the surface to infinity, so that the total work done by a particle of solvent in passing from the solution into the vapour

$$= W = \frac{\pi}{3} \left( \frac{c_1 n_1}{\delta_1^4} + \frac{c_1^{1/2} c_2^{1/2} n^2}{\delta_{12}^4} \right). \quad \dots \quad (\text{xlv})$$

The next step is complicated by the difficulty that although particles of one kind obey Maxwell's law of the distribution of molecular velocities, as modified by the introduction of  $\lambda$ , when there are two kinds of particles of different masses and attractive forces, neither set will obey Maxwell's law exactly. In the first place the different masses of the particles will involve different values of the most probable speed at a given temperature for each set of particles. Secondly, the attraction of the medium on the two sets of particles with different fields of force will be different. This will modify the most probable speeds of each set. And finally, the most probable speeds of either set will be upset by encounters between the two sets of particles.

It may not be impossible to allow for these reactions, but in a preliminary study, in which there are a number of such difficulties, it is permissible to assume that the deviations from Maxwell's law will not be great.

We have, therefore, from (xiii) the number of solvent particles that escape from the solution is

$$n_t = \frac{n_1}{n_1 + n_2} \cdot n_s \frac{V_{ps}}{V_{pl}} \cdot e^{-\frac{s^2}{V_{ps}^2}}, \quad \dots \quad (\text{xlvi})$$

where  $n_s$  is the total number of molecules in unit co-volume of the solution.

As before, if  $v_l$  is the volume occupied by the number  $N$  of molecules in a gram molecule of solvent in the vapour state, and  $v_s$  is the volume of  $N$  molecules of solution in the liquid condition,

$$n_t = \frac{N}{v_l - b_l} = \frac{N}{\phi_l},$$

since the effective volume in which the molecules may move is the co-volume, and

$$n_s = \frac{N}{v_s - b_s} = \frac{N}{\phi_s},$$



where  $\phi_l$  is the co-volume of solvent vapour and  $\phi_s$  that of the solution ;

$$\therefore \phi_l = \frac{n_1 + n_2}{n_1} \cdot \frac{\phi_s}{\lambda} \cdot e^{\frac{s^2}{\lambda^2 V p l^2}},$$

giving

$$\phi_l = \frac{n_1 + n_2}{n_1} \cdot \frac{\phi_s}{\lambda} \cdot e^{\frac{7.52 \times 10^{15} W}{\lambda^2 T}}, \quad \dots \quad (\text{xlvi})$$

or from (xlv)

$$\phi_l = \frac{n_1 + n_2}{n_1} \cdot \frac{\phi_s}{\lambda} \cdot e^{\frac{7.52 \times 10^{15} \cdot \pi \left( \frac{c_1 n_1}{\delta_1^4} + \frac{c_1^{1/2} c_2^{1/2} n_2}{\delta_{12}^4} \right)}{\lambda^2 T}};$$

and since

$$p = 81.84 \frac{T}{\phi_l},$$

$$\therefore p = 81.84 \frac{n_1 T \lambda}{(n_1 + n_2) \phi_s} e^{-\frac{7.882 \left( \frac{c_1 n_1}{\delta_1^4} + \frac{c_1^{1/2} c_2^{1/2} n_2}{\delta_{12}^4} \right) \times 10^{15}}{\lambda^2 T}}. \quad \dots \quad (\text{xlviii})$$

For purposes of calculation it is convenient to express  $n_1$  and  $n_2$  in terms of grams. Let  $w_1$  and  $w_2$  be the weights of solvent and solute taken respectively, and let  $\rho_{12}$  be the density of the solution.

The volume of the solution is

$$\frac{w_1 + w_2}{\rho_{12}}.$$

The number of molecules of solvent in  $w_1$  grams of solvent is

$$\frac{w_1}{M_1} \times 6.23 \times 10^{23},$$

where  $M_1$  is the molecular weight of the solvent.

Therefore the number of molecules of solvent in 1 c.c. of solution is

$$n_1 = \frac{w_1 \rho_{12}}{M_1 (w_1 + w_2)} \times 6.23 \times 10^{23}. \quad \dots \quad (\text{i})$$

Similarly

$$n_2 = \frac{w_2 \rho_{12}}{M_2 (w_1 + w_2)} \times 6.23 \times 10^{23}, \quad \dots \quad (\text{ii})$$

$M_2$  being the molecular weight of the solute.

From (xxxvii) we have

$$S_{12}^{1/2} = \pm \frac{\sqrt{\pi}}{2\sqrt{6}} \left( \frac{c_1^{1/2} n_1}{\delta_1^{3/2}} + \frac{c_2^{1/2} n_2}{\delta_2^{3/2}} \right). \quad \text{. . . (lii)}$$

Also from (ii) and (iii) we have

$$c_1^{1/2} = \frac{2\sqrt{6}}{\sqrt{\pi}} \cdot \frac{S_1^{1/2} \delta_1^{3/2}}{n}, \quad \text{. . . . (liii)}$$

where  $n$  corresponds to the number of molecules in the pure solvent and is given by the equation

$$n = 6.23 \times 10^{23} \frac{\rho_1}{M_1}, \quad \text{. . . . (liv)}$$

$\rho_1$  being the density of the solvent.

Therefore from (lii) and (liii)

$$c_2^{1/2} = \pm \frac{2\sqrt{6}}{\sqrt{\pi}} \frac{\delta_2^{3/2}}{n_2} \left( S_{12}^{1/2} - \frac{n_1}{n} S_{11}^{1/2} \right). \quad \text{. . . (lv)}$$

Substituting in (xlix), and writing

$$\delta_1 = \partial_1 \times 10^8,$$

$$\delta_2 = \partial_2 \times 10^8,$$

we get

$$p = 81.84 \frac{w_1 M_2 T \lambda}{(w_1 M_2 + w_2 M_1) \phi_s} \times e^{-\frac{9.665 M_1 S_1^{1/2} \{ S_1^{1/2} w_1 \rho_1 (\partial_2^{1/2} - \partial_1^{1/2}) + S_{12}^{1/2} (w_1 + w_2) \rho_1 \partial_1 \}}{\rho_1^2 \partial_1 \partial_2^{1/2} \lambda^2 T (w_1 + w_2)}}; \quad \text{. . . (lvi)}$$

or, if the solvent is associated,

$$p = \frac{81.84 w_1 M_2 T \lambda}{(w_1 M_2 + w_2 A M_1) \phi_s} \times e^{-\frac{9.665 A^{2/3} M_1 S_1^{1/2} \{ S_1^{1/2} w_1 \rho_1 (\partial_2^{1/2} - A^{1/6} \partial_1^{1/2}) + S_{12}^{1/2} (w_1 + w_2) \rho_1 A^{1/6} \partial_1^{1/2} \}}{(w_1 + w_2) \rho_1^2 \partial_1 \partial_2^{1/2} \lambda^2 T}}. \quad \text{. . . (lvii)}$$

In this equation  $\phi_s$  is determined by the relation

$$\phi_s = v_{12} - \frac{\partial_{12}^3}{4}, \quad \text{. . . . (lviii)}$$

in which

$$v_{12} = \frac{M_{12}}{\rho_{12}},$$

$M_{12}$  being the molecular weight of the solution and equal to

$$M_{12} = \frac{n_1 A M_1 + n_2 M_2}{n_1 + n_2},$$

giving

$$v_{12} = \frac{(w_1 + w_2) A M_1 M_2}{(w_1 M_2 + w_2 A M_1) \rho_{12}}, \quad \dots \quad (\text{lix})$$

and  $\bar{d}_{12}$  is the average of the nearest distances of approach of all the particles in the solution. This is determined as follows.

The number of encounters of the solvent molecules between themselves is proportional to  $n_1^2$ , those of the

TABLE  
Vapour pressure at 18° of some salt solutions  
100 grams of water making

	$w_1$ .	$w_2$ .	$M_1$ .	$M_2$ .	$t$ .	$\rho_1$ .	$\rho_{12}$ .	$v_s$ .	$\bar{d}_1$ .
H <sub>2</sub> O .....	—	—	18.02	—	18	0.9986	—	48.360	3.079
NaCl .....	100	17.64	18.02	58.46	18	0.9986	1.1087	44.725	3.079
NaI .....	100	17.64	18.02	149.92	18	0.9986	1.1269	42.702	3.079
KCl .....	100	17.64	18.02	74.56	18	0.9986	1.0978	46.445	3.079
KNO <sub>3</sub> ...	100	17.64	18.02	101.11	18	0.9986	1.0970	47.763	3.079
AgNO <sub>3</sub> ...	100	17.64	18.02	169.89	18	0.9986	1.1402	47.442	3.079

solute molecules among themselves to  $n_2^2$ , and those between the solvent and solute molecules to  $2n_1n_2$ . Therefore the average value of  $\bar{d}_{12}$  is

$$\left( \frac{n_1 \bar{d}_1^{1/2} + n_2 \bar{d}_2^{1/2}}{n_1 + n_2} \right)^2$$

or

$$\bar{d}_{12} = \left( \frac{w_1 A^{1/6} M_2 \bar{d}_1^{1/2} + w_2 A M_1 \bar{d}_2^{1/2}}{w_1 M_2 + w_2 A M_1} \right)^2 \dots \quad (\text{lx})$$

In using this formula to calculate the vapour pressure of an aqueous solution, it must be borne in mind that the effect of dissolving a substance in water will be to alter

the cohesion of the liquid. It is possible, therefore, that the state of aggregation of the water molecules will be affected. In the absence of a means of determining this effect accurately it must be neglected, but it cannot be expected that the calculated values of the vapour pressure will be quite accurate. In Table III. the value of the association factor for water was taken throughout as 2.68, the value found for water at 18° as shown in Table II.

In this table the values of  $\delta$  were calculated from the formula

$$\delta = \left( \frac{3.24Mb}{2.016} \right)^{1/3} \times 10^{-8}, \quad . \quad . \quad . \quad (1x)$$

### III.

containing 17.64 grams of salt dissolved in 15 per cent. solutions.

$\delta_2$	$\delta_s$	$\phi_s$	$S_1$	$S_{12}$	$K_{12} \times 10^{-8}$	$\lambda$	Vapour pressure in mm.	
							Calculated.	Observed.
—	—	31.94	72.66	—	67.75	1.568	15.7	15.5
3.789	4.232	25.772	72.66	77.41	73.16	1.579	12.1	13.63
4.304	4.299	27.835	72.66	74.03	68.88	1.568	14.1	14.93
4.148	4.283	26.796	72.66	76.00	70.97	1.575	13.1	14.1
4.382	4.308	27.813	72.66	74.40	69.12	1.569	13.7	14.6
4.148	4.292	27.675	72.66	74.70	69.67	1.571	14.07	—

which is probably more accurate than (xx); but, as the values obtained are slightly smaller, they were multiplied by 1.037 to bring them into line with those calculated from formula (xx), from which the values of  $\lambda$  had been deduced.

Considering the greater complexity of the conditions in mixed substances, it will be seen that the agreement between the observed and calculated values of the vapour pressures is fairly good. Actually the calculated values depend to an appreciable extent on the magnitude of the association factor  $A$  chosen for water. If this factor had been taken as 3.00, as suggested previously, with the corresponding values of  $\lambda$ , the vapour pressures of the solutions in Table III.

would work out at 13.56, 14.36, 13.53, 13.86, and 13.85 respectively.

These results must be regarded as preliminary only. It is important to be able to plot the  $\lambda : K$  curve more accurately. The analysis is interesting, however, as indicating a new development of the kinetic theory that is capable of wide application, *e. g.*, to the viscosity of liquids, conduction of heat by liquids, the solution of liquids in liquids, etc. It is particularly noteworthy that the negative part of the  $\lambda : K$  curve may correspond to the motion of negatively-charged particles, whose velocity must be less than that of moving particles not subject to the action of a repulsive force. As a particular case, an electron rotating in an orbit and passing near another electron at certain intervals of time, which may or may not be regular, would have its velocity retarded.

The general conclusion from these results is that moving particles of matter may not be treated as if they were isolated from the attractions and repulsions of adjacent particles: the definition of force requires that the velocities of such particles are affected by the action of the forces exerted on them by neighbouring particles or systems of forces, or, in other words, the law of equipartition of energy is not of general application.

Thus the mean kinetic energy of a mechanical system becomes

$$U = \frac{1}{2} \Lambda^2 kT \quad . \quad . \quad . \quad . \quad . \quad (lxii)$$

for each degree of freedom instead of  $\frac{1}{2}kT$  as has been assumed previously; and if  $\Lambda$  is less than unity, the energy of such a system is less than  $\frac{1}{2}kT$ .

Returning to the particular case of the kinetic theory of solutions, it will be remembered that, in a previous paper\*, it was shown that when the molecular fields of the solute and solvent are taken into account, the solubilities of substances generally, whether solid, liquid, or gaseous, can be accounted for, and that, when substances are arranged in the order of their solubilities, they are in the order of every other property of solutions, which, therefore, must also be due to the interaction of molecular forces.

In the same paper it was shown, in particular, that the observed increases in the depression of the freezing-point of aqueous solutions of salts below that due to a "normal" solute are caused by the enhanced cohesions of the solutions,

\* Phil. Mag. xliv. p. 897 (1922).

resulting from the greater molecular fields of the solutes, and can be calculated from the surface tensions of the solutions.

In view of the analysis in the present paper, it will be seen that the basic assumption of the dissociation theory of solution, *i. e.*, that the reduction of the vapour pressure, elevation of the boiling-point, and depression of the freezing-point of solutions is proportional only to the number of molecules present, is incorrect. The observed values of these various properties of solutions are dependent partly on the fewer number of solvent molecules present, that is, on the number of solute molecules contained in the solution; but they are also affected by the changes in volume and cohesion that are due to the added solute particles. When these additional factors are taken into consideration, the observed values of these properties are completely accounted for.

Instead, therefore, of being obliged to choose the "dissociation" of a substance in solution to fit the observed vapour pressure, etc., the properties of solutions can be calculated from the attractions of the particles and the densities of the liquids.

In this connexion it is interesting to calculate the actual forces of attraction between the particles in, *e.g.*, a 15 per cent. solution of potassium nitrate at 18°. If the molecules of potassium nitrate were dissociated, the force between the ions would be

$$f = \frac{(4.7 \times 10^{-10})^2}{r^2} \\ = \frac{2.21 \times 10^{-19}}{r^2} \text{ dyne.}$$

Supposing the ions to be  $1 \times 10^{-7}$  cm. apart, the force would be

$$f = 2.21 \times 10^{-5} \text{ dyne.} \quad . \quad . \quad . \quad . \quad . \quad (a)$$

From (xl), (ii), and (li) we find that the observed surface tension of such a solution corresponds to an actual force between the molecules of potassium nitrate of

$$f = \frac{6.24 \times 10^{-67}}{r^8} \text{ dyne}$$

or, at a distance of  $1 \times 10^{-7}$  cm., of

$$f = 6.24 \times 10^{-11} \text{ dyne.} \quad . \quad . \quad . \quad . \quad . \quad (b)$$

Thus the force between dissociated particles at this distance would be of the order of a million times as great, and would

decrease only in proportion to the square of the distance instead of to the eighth power. Measurement of the surface tension of the solution is sufficient to show that such forces do not exist within it.

In conclusion the writer wishes to express his indebtedness to Miss M. J. Humphries for much kind help with the somewhat laborious calculations.

### *Summary.*

Maxwell's theory of the distribution of molecular velocities has been amplified to take into account the effect of molecular attraction. The extended theory has been applied to obtain expressions for the vapour pressures of a pure liquid and of a solution in terms of molecular attraction, motion, and volume only. The agreement between the calculated and observed values is so close as to indicate that the vapour pressures of liquids are actually dependent on these factors alone. This is particularly interesting in connexion with the theory of solutions, as it becomes unnecessary any longer to assume an hypothetical dissociation of salt molecules in solution to account for the greater reductions of the vapour pressures, depressions of the freezing-point, etc., of solutions of these substances.

The vapour pressure of a pure liquid is given by the formula

$$p = 81.84 \frac{T\lambda}{A\phi_s} e^{-\frac{9.665MA^{2/3}}{T\lambda^2\rho}},$$

and that of a solution by

$$p = 81.84 \frac{M_2 w_1 T \lambda}{(A M_1 w_2 + M_2 w_1) \phi_s} \times e^{-\frac{9.665 A^{2/3} M_1 S_1^{1/2} \{S_1^{1/2} \rho_{12} w_1 (\partial_2^{1/2} - A^{1/6} \partial_1^{1/2}) + S_{12} \rho_1 (w_1 + w_2) A^{1/6} \partial_1^{1/2}\}}{T \partial_1 \partial_2^{1/2} \lambda^2 \rho_1 (w_1 + w_2)}},$$

where

$T$  is the absolute temperature ;

$\lambda$  is the ratio of the total average velocity of the molecules in the liquid under the given circumstances to that in a perfect gas ;

$A$  is the actual state of aggregation of the molecules in the given liquid ;

$\phi$  is the co-volume of the liquid ;

S its surface tension, the subscripts 1 and 2 indicating solvent and solute respectively ;

M its molecular weight ;

$\rho$  its density ;

$w_1$  and  $w_2$  the weights of solvent and solute in a solution ; and

$\partial \times 10^{-8}$  the nearest distance of approach of the centres of the molecules of the liquid.

It has been shown that the total average velocity of the molecules in a liquid cannot be the same as that in a perfect gas, for the reason that they are under the influence of strong forces. The ratio of these two velocities,  $\lambda$ , is dependent on the cohesion of the liquid, and the relation between  $\lambda$  and the cohesion K of the liquid has been shown to be determined by the equations

$$\left. \begin{aligned} K \times 10^{-8} &= 42 \cdot 16y - 64 \cdot 7y^3 + 952y^5, \\ \lambda &= 1 + y. \end{aligned} \right\}$$

Obviously the method is capable of wide application, and its success in this particular case indicates that the so-called classical dynamics may yet be found to be sufficient to explain phenomena for which, in the past, it had been supposed to be inadequate.

XVI. *The Corona Discharge in Nitrogen.* By L. G. H. HUXLEY, M.A., D.Phil., Lecturer and Demonstrator at the Electrical Laboratory, Oxford \*.

IN a former paper † I have described experiments on the corona discharge in helium and neon, in which especial precautions were taken to secure the purity of the gas in the apparatus.

It was considered desirable to investigate also the corona discharge in a diatomic gas, and experiments which I have made with nitrogen are described below.

2. The apparatus was that used in the experiments on helium and neon, so that it is unnecessary to repeat in detail the description which has already been given (*loc. cit.*).

\* Communicated by Prof. J. S. Townsend, F.R.S.

† Phil. Mag. v. p. 721, April 1928.



It consisted essentially of coaxial cylindrical electrodes contained in a clear quartz envelope. The outer cylinder was a nickel tube 4.6 cm. in diameter and 12 cm. long, with guard-rings of the same diameter. The inner electrode was a nickel wire 1.65 mm. in diameter fixed along the axis of the outer tube by quartz supports.

Electrical connexions were made to the electrodes and guard-rings, and were brought through the quartz envelope by air-tight seals.

A second piece of apparatus was constructed identical with the first, with the exception of the central wire, which had a diameter of 3.16 mm.\*

3. Pure nitrogen was obtained by heating pure sodium azide in a vacuum, and was stored in a glass flask.

To remove traces of mercury vapour the nitrogen passed through two traps cooled in liquid air, before entering the apparatus. The pressure of the gas was measured by a McLeod gauge from which mercury vapour was prevented from entering the apparatus by a third trap cooled in liquid air. The whole could be exhausted by a mercury vapour pump connected to the gauge, the arrangement being that used in the experiments on helium and neon.

Before making measurements it was necessary to drive impurities from the electrodes and the walls of the envelope. This was effected by introducing pure nitrogen into the apparatus and then heating the quartz to a high temperature with blow-pipes, at the same time passing a heavy discharge between the electrodes. The impurities which were evolved were removed with the nitrogen on exhausting the apparatus. This process was repeated many times, and when all impurities had been removed it was found that consistent results were obtained, which could be easily repeated.

In these experiments the gas was examined spectroscopically by means of a high-frequency discharge through the gas in the quartz tubes.

4. Measurements were then made of the potentials between the electrodes required to start discharges and to maintain currents through the gas over a range of pressures.

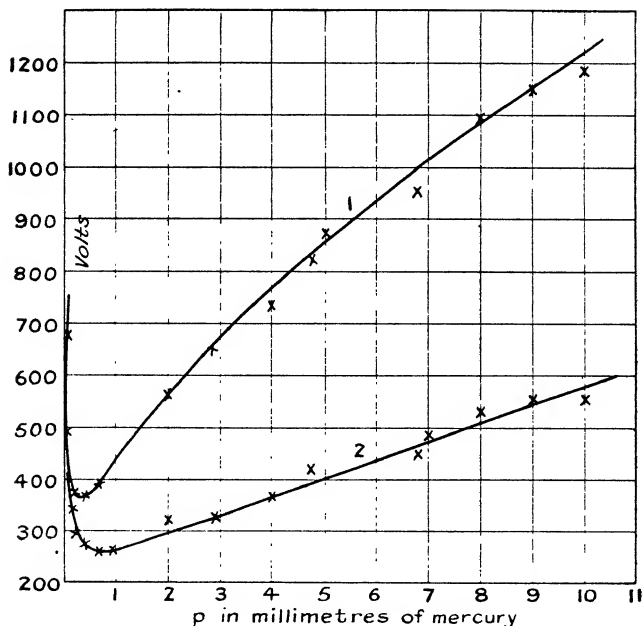
\* In the experiments on the monatomic gases the wire was 2 mm. in diameter in the second apparatus. This was replaced by one of larger diameter.

The source of potential was a battery of small accumulators, and the potentials were measured by a standard voltmeter in series with a suitable resistance. The currents were measured by a sensitive galvanometer.

The results are most conveniently expressed in the form of curves, showing the potentials required to start a discharge as a function of the pressure of the gas.

The curves given in fig. 1 represent the results obtained

Fig. 1.



Starting potentials for wire 1.65 mm. diameter.

Curve 1. Wire positive.

„ 2. „ negative.

with the apparatus in which the wire (inner cylinder) was 1.65 mm. in diameter. Curve 1 gives the voltages required to start discharges when the wire was at a positive potential relative to the outer cylinder, and curve 2 the voltages when the wire was negatively charged.

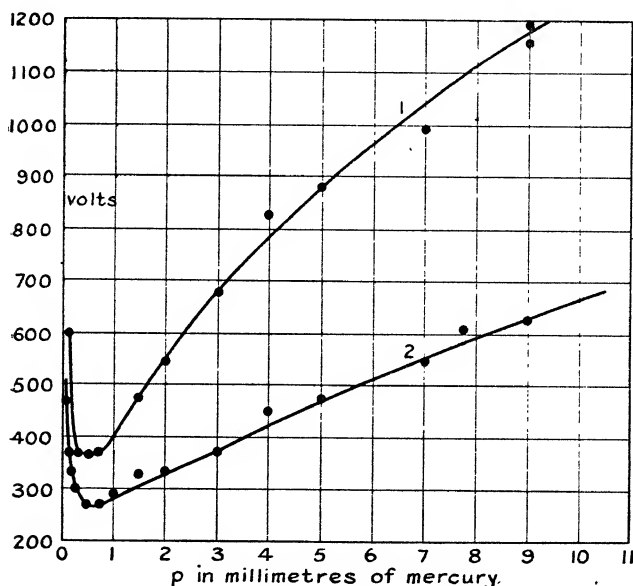
It will be seen that over the range of pressures investigated a discharge occurs more easily with the wire at a

negative potential than at a positive potential, and that both curves have well-defined minima.

In fig. 2 similar curves are given for the second apparatus (inner cylinder 3.16 mm. diameter).

5. The results of the experiments are in agreement with Townsend's theory\*, which shows that in a corona discharge the following relation exists between the diameter

Fig. 2.



Starting potentials for wire 3.16 mm. diameter.

Curve 1. Wire positive.

„ 2. „ negative.

of the wire, the electric force  $X_1$  at its surface, and the pressure  $p$  :—

$$aX_1 = f(ap)$$

provided the region of ionization in the gas does not extend to the outer electrode.

This is shown by the curve, given in fig. 3, showing the experimental values of the product  $aX_1$  plotted as a

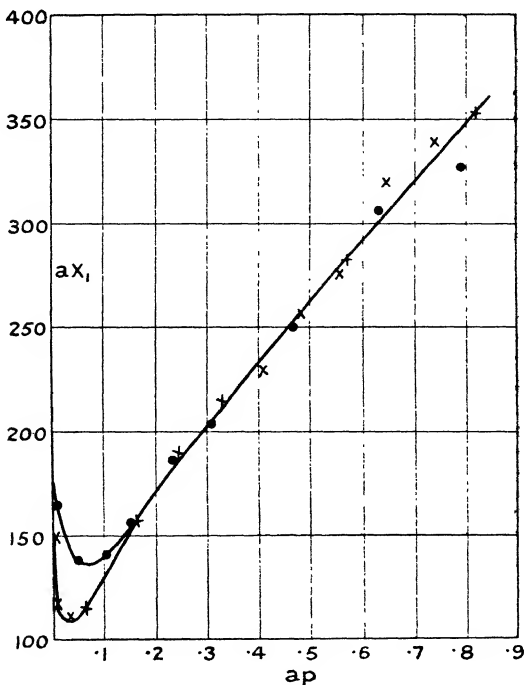
\* 'Electricity in Gases,' p. 369.

function of the product  $ap$  for each apparatus for discharges in which the wires were at positive potentials.

The force  $X_1$  is in volts per centimetre,  $a$  in centimetres, and  $p$  in millimetres of mercury.

The points corresponding to the smaller (1.65 mm.) and larger (3.16 mm.) values of  $a$  are indicated by crosses and circles respectively.

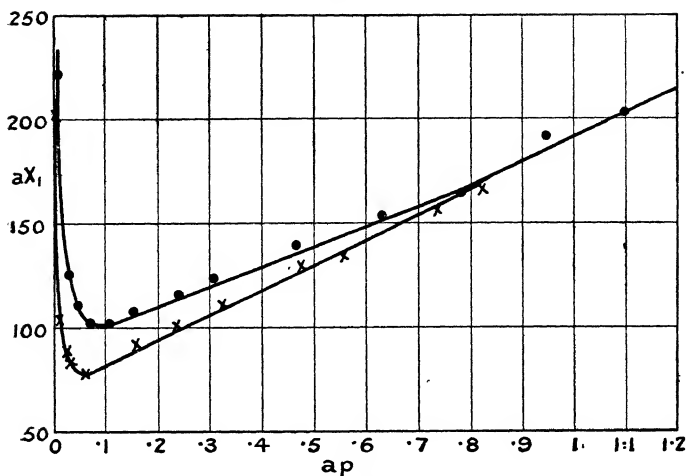
Fig. 3.



$aX_1$  as a function of  $ap$  wires positive,  
 Points marked X for wire 1.65 mm. diameter.  
 " " O " 3.16 " "

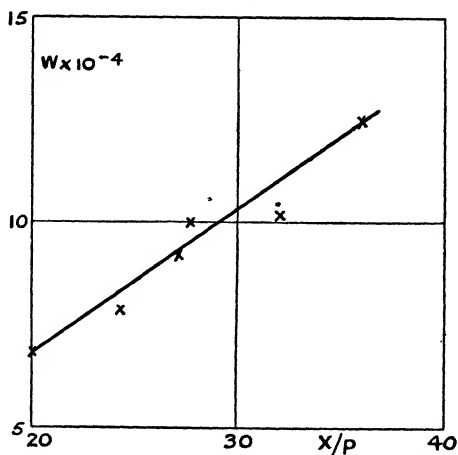
All the points lie on a single smooth curve, except at the minimum, where a divergence occurs. This indicates that at these pressures the region in which the gas is ionized extends to the outer electrode. In fig. 4 the corresponding results are shown for the wires when at negative potentials.

Fig. 4.



$aX_1$  as a function of  $ap$  wires negative.  
 Points marked X for wire 1.65 mm. diameter.  
 " " O " 3.16 " "

Fig. 5.



The velocities  $W$ , of positive ions in nitrogen in the direction of the electric force  $X_1$  as a function of  $X/p$ .  
 $W$  in centimetres per second,  $X$  in volts per centimetre,  $p$  in millimetres of mercury.

6. The velocities of the positive ions in the direction of the electric force were calculated from the potentials required to maintain various currents through the gas. The formula for the velocity in terms of the potential and the current has been given by Townsend \*. This method is the same as that adopted in the experiments with monatomic gases †.

The velocities thus obtained for nitrogen are shown by the curve figure 5 for values of  $X/p$  from 20 to 36, being the average force in the space between the electrodes in volts per centimetre, and  $p$  the gas pressure in millimetres of mercury. The velocity  $W$  is given by the formula

$$W = 3.5 \times 10^3 \times X/p.$$

If this formula held for small values of  $X/p$  the velocity under a volt per cm. in nitrogen at atmospheric pressure would be 4.6 cm. per sec.

.

XVII. *Diamagnetism and Sub-Molecular Structure.* By FRANCIS W. GRAY, M.A., D.Sc., Senior Lecturer in Chemistry, Aberdeen University, and JOHN FARQUHARSON, B.Sc., Ph.D., Carnegie Research Scholar ‡.

VAN VLECK, Nat. Acad. of Sciences Proc. (Amer.) xii. pp. 662-670 (1926), by an application of the new quantum mechanics has derived an expression for the diamagnetic susceptibility of a gram atom.

L. Pauling, Roy. Soc. Proc. A, cxiv. pp. 181-211 (1927), has obtained the same expression, also by the aid of the new quantum mechanics. Pauling gives

$$\chi = \frac{-Ne^2}{6mc^2} \sum_{\kappa} \overline{r_{\kappa}^2}$$

(for S states and completed groups and subgroups), where

$\chi$  = the diamagnetic susceptibility of a gram atom,

$N$  = Avogadro's number,

$m$  = mass of an electron and  $e$  = its charge,

$c$  = velocity of light,

\* J. S. Townsend, Phil. Mag. (6) xxviii. p. 83 (1914).

† L. G. H. Huxley, *loc. cit.* p. 731.

‡ Communicated by the Authors.

$r_\kappa$  = distance of the  $\kappa$ th electron from the nucleus,

$\overline{r_\kappa^2}$  = time average of  $r_\kappa^2$ ,

$\Sigma_\kappa$  means that summation extends over all the electrons in the atom.

Further, wave mechanics gives an expression for  $\overline{r_\kappa^2}$  in terms of the quantum numbers, and we have

$$\chi = -2.010 \times 10^{-6} \Sigma_\kappa \frac{n_\kappa^4}{(Z - S_{M\kappa})^2} \left[ 1 - \frac{3l_\kappa(l_\kappa + 1) - 1}{5n_\kappa^2} \right],$$

where

$n$  = total quantum number,

$l = k - 1$  (where  $k$  = the old azimuthal number),

$S_{M\kappa}$  = screening number,

$Z$  = charge of nucleus.

Pauling's method enables us to obtain theoretical values for the diamagnetic susceptibilities of free atoms or ions, and it is of very great importance that we should have such standard values for use in the interpretation of diamagnetic quantities observed in the laboratory. For a given nuclear charge and a given number of circum-nuclear electrons Pauling's value is the upper limit.

Any experimentally derived value, being obtained from substances in which the ions or atoms cannot be said to be free, must be less than Pauling's value and variable according to the nature of the substance, and therefore unsuitable as a standard. Such experimental values have hitherto been used as standards of reference, and this has been a most unsatisfactory feature of diamagnetic investigation.

We find, for example, that values for the atomic susceptibilities of the halogens have been given by Pascal and by Joos (Pascal, "L'additivité des propriétés diamagnétiques" (1913), and Joos, *Zeit. f. Phys.* xix. p. 347 (1923), and xxxii. p. 835 (1925).)

PASCAL:—

	F.	Cl.	Br.	I.
Observed directly from elements...	6.3	20.1 (Pascal)	30.6 (Pascal) 30.6 (Honda)	45.9 (Owan) 44.4 (Honda)
Observed indirectly from compounds.	6.3 (Pascal)	19.9 (Pascal)	30.4 (Pascal)	44.6 (Pascal)

Joos:—

F <sup>-1</sup> .	Cl <sup>-1</sup> .	Br <sup>-1</sup> .	I <sup>-1</sup> .
10.8	19.5	38.3	57.5

The values by these two authorities agree, at least qualitatively, for the neutral atom, except in the case of chlorine, where either the value of Joos must be raised or that of Pascal must be lowered before complete consistence can be obtained.

All these numbers and other values for diamagnetism in this paper require to be multiplied by  $10^{-6}$ .

### *Valency Bonds.*

The present discussion deals with the relation of diamagnetism to two kinds of valency bonds.

1. *Covalency Bonds* such as we have in  $\text{Cl}_2$ , which may be regarded as



where  $\text{Cl}^{+1}$  is  $\text{Cl}^{+7}$  surrounded by six electrons, and  $\text{Cl}^{-1}$  is  $\text{Cl}^{+7}$  surrounded by eight electrons (octet).

In  $\text{Cl}^{+1} - \text{Cl}^{+1}$  the pair of electrons in the bond are shared by two octets and are in a state of oscillation to and fro between the two atoms,  $\text{Cl}^{+1}$  and  $\text{Cl}^{+1}$ , interchanging positions whereby there is a fluctuation of angular momentum.

In  $\text{Cl}^{+1}\text{Cl}^{-1}$  the bond pair are both in the octet of  $\text{Cl}^{-1}$ , and only one of the constituent atoms has an octet.

There may be said to be a balance between the two conditions  $\text{Cl}^{+1}\text{Cl}^{-1}$  and  $\text{Cl}^{+1} - \text{Cl}^{+1}$ .

The first condition represents a purely heteropolar molecule, the second a purely homopolar.

2. *Electrovalency Bonds* such as we have in  $\text{KCl}$ , which may be regarded as  $\text{K}^{+1}\text{Cl}^{-1}$  or  $\text{K}^{+1} - \text{Cl}^{+1}$ , where  $\text{K}^{+1}$  is  $\text{K}^{+9}$  surrounded by eight electrons (octet),  $\text{Cl}^{-1}$  is  $\text{Cl}^{+7}$  surrounded by eight electrons (octet), and  $\text{Cl}^{+1}$  is  $\text{Cl}^{+7}$  surrounded by six electrons.

In  $\text{K}^{+1} - \text{Cl}^{+1}$  the pair of electrons in the bond are not shared by two octets (unlike the case of  $\text{Cl}_2$ ), but are in a state of oscillation to and fro between the two atoms  $\text{K}^{+1}$  and  $\text{Cl}^{+1}$ , interchanging positions, whereby there is a fluctuation of angular momentum.

In  $\text{K}^{+1}\text{Cl}^{-1}$  the bond pair are both in the octet of  $\text{Cl}^{-1}$  and both the constituent atoms have an octet.

There may be said to be a balance between the two conditions  $\text{K}^{+1}\text{Cl}^{-1}$  and  $\text{K}^{+1} - \text{Cl}^{+1}$ .

The first condition represents a purely heteropolar molecule, the second a purely homopolar.

Octet formation for both atoms of the molecule is most readily obtained, on the one hand, with  $\text{Cl}_2$  in the last



condition, *i. e.*, in  $\text{Cl}^{+1}-\text{Cl}^{+1}$ , and, on the other hand, with KCl in the first condition, *i. e.*, in  $\text{K}^{+1}\text{Cl}^{-1}$ .

Thus, the covalency bond favours the homopolar condition, the electrovalency bond the heteropolar.

The difference between the two types of bonds is more one of degree than of kind.

In the electrovalency bond one of the constituent atoms either contains a non-sharing octet, as  $\text{K}^{+1}$  in  $\text{K}^{+1}-\text{Cl}^{+1}$ , or no octet at all, as  $\text{H}^{+1}$  in  $\text{H}^{+1}-\text{Cl}^{+1}$ .

In the covalency bond both the constituent atoms either contain sharing octets, as in  $\text{Cl}^{+1}-\text{Cl}^{+1}$ , or no octets at all, as in  $\text{H}^{+1}-\text{H}^{+1}$ .

In this view of a single bond, of whatever type, there are always concerned two electrons, which may be called simply valency electrons.

Some molecules contain both types of bonds, *e. g.*,

Bonds.			
$\text{H}_2\text{O}_2$ .....	Hydrogen-oxygen.	Electrovalency.	More heteropolar.
	Oxygen-oxygen.	Covalency.	More homopolar.
$\text{KClO}_3$ ...	Potassium-oxygen.	Electrovalency.	More heteropolar.
	Chlorine-oxygen.	Covalency.	More homopolar.

The activation of covalency produces a greater depression of diamagnetism (greater fluctuation of angular momentum) than the activation of electrovalency.

It is usually easy formally to represent a diamagnetic molecule as derived from a neutral group of ions—that is, a group of positive and negative ions for which the algebraic sum of the charges is zero.

In the present discussion we consider the diamagnetic changes brought about by the coming closer together of the widely separated ions of the *neutral group* first to form *the molecule*, and afterwards, by an imaginary forced merging of the ionic nuclei, to form a *single merger atom*.

For example, the *neutral group*  $\text{K}^{+1}+\text{Cl}^{-1}$  gives *the molecule* KCl and the *merger atom* Kr.

As the inner levels of the neutral group are completely filled, the formation of the merger atom involves the raising of the quantization of several of the electrons with a corresponding rise of diamagnetism. On the other hand, this rise is counteracted by a fall due to the larger nucleus of the merger atom, the result being that the final diamagnetism may differ little from the original value. For example :

$$\text{K}^{+1} + \text{Cl}^{-1} = 45.7, \quad \text{Kr} = 42,$$

$$\text{K}^{+1} + \text{Br}^{-1} = 70.7, \quad \text{Xe} = 66.$$

Similar results may be obtained from a neutral group containing neutral atoms. For example :

$$\begin{aligned} 2A &= 43.0, & \text{Kr} &= 42, \\ A + \text{Kr} &= 63.5, & \text{Xe} &= 66. \end{aligned}$$

There are cases, however, where the difference is considerable. For example :

$$3\text{H}^{+1} + \text{N}^{-3} = 22 \quad \text{and} \quad \text{Ne} = 5.7.$$

Here the circumnuclear electrons in  $\text{N}^{-3}$  and Ne are the same in number, configuration, and quantization. The lower diamagnetism in Ne is due entirely to the amount by which the nuclear charge in Ne is greater than in  $\text{N}^{-3}$ .

Similarly for

$$4\text{H}^{+1} + \text{C}^{-4} = 50 \quad \text{and} \quad \text{Ne} = 5.7.$$

For the purpose of the present paper it is of special interest to examine the relation of the experimental molecular diamagnetism to the theoretical values for the neutral group, on the one hand, and for the merger atom on the other.

When the ions only approach near enough to one another to give the molecule any change in diamagnetism may be regarded as taking place mainly in the outer layers, the inner layers remaining almost unchanged.

The diamagnetism of a diatomic molecule is the resultant of three parts :—(1) the diamagnetism of electrons under the influence of one nucleus, (2) the diamagnetism of electrons under the influence of the other nucleus, (3) the diamagnetism and weak paramagnetism of electrons under the influence of both nuclei. The first two parts form the diamagnetism of the unchanged cores; the third part is the magnetism of the remaining or surplus or valency electrons, any one of which does not belong to one nucleus more than to the other, but may be said to be influenced by a virtual nucleus which lies between the real nuclei and is the vector sum of these.

Thus in a diatomic molecule there are in general three nuclei (two real and one virtual).

In the formation of the molecule from the ionic group, then, if there is no rise of quantization, any change in diamagnetism should be in the direction of a depression, and this conclusion is supported by experimental results. This depression, according to its amount, may be attributed (1) to the distortion of the electronic orbits, or (2) to the

activation of valency together with distortion. The distortion loss may be regarded as small compared with the valency loss.

The valency loss is of two-fold origin. It is partly due to the amount by which the virtual nucleus is greater than either of the real nuclei, and partly to the development of a weak form of paramagnetism independent of temperature. This paramagnetism may be explained by the fluctuation of angular momentum arising from the interchange occurring in the Heitler-London activation of valency.

In this view, when a diatomic molecule is being formed, we see a virtual nucleus assuming control over certain of the electrons originally controlled by only one or the other of the two real nuclei, and along with this there is the development of weak paramagnetism.

According to the amount of the diamagnetic depression different molecules show different stages in the development of this new control. The virtual nucleus is building up a set of levels of its own. We have in the molecule the first beginnings of a gradual growth, round the virtual nucleus, of a structure which finally culminates in the merger atom in which the virtual nucleus has become real. In the earlier stages of this development the new structure consists of electrons derived from the outer layers of the original atoms or ions with diamagnetic depression. In the later stages, however, after the supply of electrons from the outer layers of the original atoms has become exhausted, the new growth takes place at the expense of electrons from inner layers, and a point is reached where there must be a rise of quantization with a corresponding rise of diamagnetism. This diamagnetic rise cancels part of the depression of the earlier stages and also part of the depression due to the amount by which the virtual nucleus exceeds either of the real nuclei. In the course of this process, therefore, the diamagnetism first falls down to a minimum and then rises, and ultimately, when the merger atom is formed, attains a value that may not differ much from the original.

We expect, then, the molecular diamagnetism to be always less than that of the neutral group, and to be sometimes less than that of the merger atom also. A very great depression usually brings the molecular diamagnetism below that of the merger atom, and in any case points to great fluctuation of angular momentum and a decidedly homopolar nature.

In the case of methane the diamagnetic depression is so great that there is indicated a large interchange effect and

homopolar character. In passing from the molecule to the merger atom, there is involved a diamagnetic rise due to a rise of quantization and a diamagnetic fall due to a rise in the nuclear charge. The latter effect must be greater than the former, since methane lies diamagnetically between the neutral group and the merger atom. The diamagnetic difference between  $4\text{H}^{+1} + \text{C}^{-4}$  (50) and Ne (5.7) shows that in this case the diamagnetic depression due to rise of nuclear charge is very great.

Table I. (p. 198) contains numerical values illustrating the above discussion.

In the paper mentioned above Pauling has given diamagnetic susceptibilities for sets of ions having the same number of circumnuclear electrons as He, Ne, Ar, Kr, Xe, and  $\text{Cu}^{+1}$ ,  $\text{Ag}^{+1}$ ,  $\text{Au}^{+1}$ . But, in addition to these, we require ions for which the number of circumnuclear electrons is different from any of Pauling's numbers, and it is important to inquire to what extent these other ions are suitable for the interpretation of molecular diamagnetism.

In a recent paper (Phys. Rev. xxxi. p. 587, 1928) Van Vleck has developed an expression for atomic susceptibility which may be put simply thus: —

$$\chi = P_x + P_y - D,$$

where  $D$  is the pure diamagnetism the expression for which is that given by Pauling.

$P_x$  is paramagnetism dependent on temperature, the value for which is large compared with  $P_y$  or  $D$ ; and  $P_y$  is a weak form of paramagnetism, independent of temperature.

The constituent groups of circumnuclear electrons present in Pauling's ions are in every case complete, consisting of two  $s$  electrons, six  $p$  electrons, ten  $d$  electrons, or fourteen  $f$  electrons. Each of these completed groups gives a  $^1\text{S}_0$  state, and therefore displays pure diamagnetism. The value of the resultant spin and that of the resultant orbital angular momentum are both zero; therefore the paramagnetic moment is zero and  $P_x = 0$ . Also, there is no fluctuation of angular momentum to give any  $P_y$ . Accordingly, Pauling's expression for  $D$  gives the atomic susceptibility, and Pauling's values are admissible as standards to be used in the interpretation of molecular diamagnetism.

In the case of Pauling's ions the spin and the orbital angular momentum are *both* zero, but a zero value for  $P_x$  may be obtained under certain conditions when the *resultant* of the spin and the angular momentum is zero, *i. e.*, when

$J=0$ . This may be the case with sub-groups containing two  $p$  electrons, four  $d$  electrons, and six  $f$  electrons. These

TABLE I.  
The Diamagnetism of

<i>the neutral group of widely separated ions.</i>		<i>the molecule obtained by combining the ions.</i>		<i>the merger atom obtained by an imaginary forced merging of the nuclei.</i>
$H^{+1}H^{-1}$	8			
or $H^0+H^0$	4·83	$H_2$	4·71	He 1·54
$2H^{+1}-O^{-2}$	12·6	$H_2O$	12·96	Ne 5·7
$3H^{+1}+N^{-3}$	22	$NH_3$	17·05	Ne 5·7
$4H^{+1}+C^{-4}$	50	$CH_4$	12·2	Ne 5·7
$2H^{+1}+O^{-2}+O^0$	19·79	$H_2O_2$	16·73	A 21·5
$H^{+1}+Cl^{-1}$	29	$HCl$	23·05	A 21·5
$H^{+1}+Br^{-1}$	54	$HBr$	31·45	Kr 42
$H^{+1}+I^{-1}$	80	$HI$	49·29	X 66
$K^{+1}+Cl^{-1}$	45·7	$KCl$	36·15	Kr 42
$K^{+1}+Br^{-1}$	70·7	$KBr$	48·12	X 66
$K^{+1}+I^{-1}$	96·7	$KI$	63·9	(Hf 87)
$4H^{+1}+N^{-3}+Cl^{-1}$	51	$NH_4Cl$	35·71	Ni 15
$4H^{+1}+N^{-3}+Br^{-1}$	76	$NH_4Br$	46·71	Pd 52
$4H^{+1}+N^{-3}+I^{-1}$	102	$NH_4I$	69·48	
$K^{+1}+Cl^{+5}+3O^{-2}$	60·21	$KClO_3$	40·7	
$K^{+1}+Br^{+5}+3O^{-2}$	68·24	$KBrO_3$	52·3	
$K^{+1}+I^{+5}+3O^{-2}$	82·18	$KIO_3$	63·1	
$H^{+1}+I^{+5}+3O^{-2}$	65·48	$HIO_3$	50·41	
$K^{+1}+Cl^{+7}+4O^{-2}$	68·3	$KClO_4$	44·6	
$K^{+1}+I^{+7}+4O^{-2}$	84·1	$KIO_4$	72	
$H^{+1}+I^{+7}+4O^{-2}$	67·4	$HIO_4$	56·55	
$2I^{+5}+5O^{-2}$	118·36	$I_2O_5$	79·4	
$I^{+1}+Cl^{-1}$	86·27	$ICl$	54·54	
$I^{+3}+3Cl^{-1}$	127·53	$ICl_3$	90·16	

yield various possible terms, the lowest of which are multiplets of which the triplet  ${}^3P_{0,1,2}$  in the  $p$  sub-group is an example. In each case the multiplet is normal and the deepest component is that with  $J$  equal to zero.

If the multiplet interval is large, it is possible to deal with

each component separately, and the normal state is that with  $J=0$ , for which  $P_x=0$  being equal to

$$Ng^2J(J+1)\beta^2/3kT,$$

where  $\beta$  is a Bohr magneton and the other letters have the usual significance. On the other hand,  $P_y$  does not vanish, and with these quotas of electrons the atomic diamagnetism is a value calculated by Pauling's method, but diminished by an amount equal to  $P_y$ .

Again, if the multiplet interval is narrow, the components cannot be considered separately and  $P_x$  does not vanish, being equal to

$$N[4S(S+1)+L(L+1)]\beta^2/3kT,$$

where       $S$  is the resultant spin,

$L$  is the resultant angular momentum,

and       $\beta$  is a Bohr magneton.

On the other hand, some of the ions specially interpolated for the purpose of the present discussion do contain sub-groups that yield, in their deepest state, values for  $J$  differing from zero. Of these doubtful sub-groups some seem to have little claim to consideration, whilst for others, where the multiplet component separation is wide, the possibility should be kept in mind that they may be in a state somewhat higher than the deepest. This possibility should be considered in connexion with those sub-groups containing quotas complementary to the quotas two  $p$ , four  $d$ , and six  $f$  electrons, namely, four  $p$ , six  $d$ , and eight  $f$  electrons. These give the same multiplets in their stable state as the complementary quotas, but inverted. The deepest state does not give  $J$  equal to zero.

Accordingly, for the widely separated atoms or ions of the neutral group, i. e., *before the formation of the molecule*, Pauling values for the atomic diamagnetism may be used for a  $^1S_0$  state without any correction, but when there is a multiplet and  $J=0$ , then, although Pauling's values may still be used, they should be subjected to a reduction.

On the other hand, *after the formation of the molecule* all the atomic diamagnetisms are subject to a depression, whether the free atoms and ions are in  $^1S_0$  or in multiplet states, and even when the molecule is in a  $^1\Sigma$  state.

It is the object of the present research to investigate this depression, which is partly due to fluctuation of angular momentum.

In the present discussion the following values from Pauling's paper are utilized :—

$F^{-1}$	$Cl^{+7}$	$Cl^{-1}$	$Br^{+7}$	$Br^{-1}$	$I^{+7}$	$I^{-1}$
8.1	1.2	29	6.0	54	17	80
$O^{-2}$	$N^{+5}$	$N^{-3}$	$C^{+4}$	$C^{-4}$		
12.6	0.11	22.0	0.15	50		
$Na^{+1}$	$K^{+1}$	$Rb^{+1}$				
4.2	16.7	35				
$H^{-1}$	$H^0$					
8	2.415					

It is assumed that the atomic susceptibility of  $H^{+1}$  is zero. In the treatment of halogen compounds, however, values are required for the valency stages  $+1$ ,  $+3$ , and  $+5$ , in addition to the stages  $-1$  and  $+7$  given above, between which it has been necessary for us to interpolate the three missing quantities. We remove the two outermost electrons in  $I^{-1}$  to obtain  $I^{+1}$ . To calculate the smaller diamagnetism of the new ion we must not assume that the core, from which the outermost pair is detached, is the same as the ion  $I^{+1}$ , formed after the pair is removed. When the core changes to the new ion the orbits shrink to smaller dimensions. Accordingly, to obtain the diamagnetism of  $I^{+1}$  we must adopt one of two courses. We may calculate the diamagnetism of the pair, using a larger screen-number than that assigned to the pair when part of  $I^{-1}$ , and subtract the diamagnetism so obtained from the value for  $I^{-1}$ ; or we may calculate  $I^{+1}$  afresh, using for each layer screen-numbers less than those assigned to  $I^{-1}$ . The values shown below have been obtained by the first method.

In order to work out the values it is necessary to have suitable screening numbers. For the ion with charge  $-1$  Pauling gives only two screening numbers for the four outer pairs of electrons—one for the three pairs with azimuth number 2, and one for the single pair with azimuth number 1. In the process of stripping the electrons away a pair at a time to get the successive steps already referred to, use has been made here of four screening numbers, one for each of the steps

$$-1 \rightarrow +1 \rightarrow +3 \rightarrow +5 \rightarrow +7.$$

Both the susceptibility of the pair removed and the corresponding screening number must diminish as the

process proceeds. By keeping these requirements in view, and using Pauling's screening numbers as a guidance, it has been possible to carry out the required interpolations.

The method has been applied to other atoms in addition to the halogens. Some of the results are shown in Tables II., III., and IV.

TABLE II.

Diamagnetic increment obtained when a pair of electrons is added to the given ion to yield the ion to the right. Below each diamagnetic increment is placed the Hund symbol for the layer in which the pair is situated.

$C^{+4}$	$C^{+2}$	$C^0$	$C^{-2}$	$C^{-4}$
4.68	5.50	10.68	29	
2s	2p	2p	2p	
$N^{+5}$	$N^{+3}$	$N^{+1}$	$N^{-1}$	$N^{-3}$
2.93	3.15	5.27	10.54	
2s	2p	2p	2p	
$O^{+6}$	$O^{+4}$	$O^{+2}$	$O^0$	$O^{-2}$
2.01	2.00	3.10	5.41	
2s	2p	2p	2p	
$F^{+7}$	$F^{+5}$	$F^{+3}$	$F^{+1}$	$F^{-1}$
1.46	1.42	2.03	3.12	
2s	2p	2p	2p	
$Cl^{+7}$	$Cl^{+5}$	$Cl^{+3}$	$Cl^{+1}$	$Cl^{-1}$
4.51	5.21	7.27	10.81	
3s	3p	3p	3p	
$Br^{+7}$	$Br^{+5}$	$Br^{+3}$	$Br^{+1}$	$Br^{-1}$
7.74	9.35	12.72	18.19	
4s	4p	4p	4p	
$I^{+7}$	$I^{+5}$	$I^{+3}$	$I^{+1}$	$I^{-1}$
10.68	12.85	16.74	22.74	
5s	5p	5p	5p	

*Magnetism of Valency Electrons.*

Table II. shows the increment of diamagnetism when a pair of electrons is added to any given ion to obtain an ion with two more circumnuclear electrons.



Table III. shows the effective nucleus acting on each electron of the pair referred to.

We have the following relationships between the diamagnetic increments and between the effective nuclei.

In passing down a column of the diagram for C, N, O, F, we see that the quantum numbers of all the pairs of electrons are the same and the diamagnetism of the pair diminishes,

TABLE III.

## Effective Nucleus.

Each electron of the pair of electrons added to the given ion to obtain the ion to the right is acted on by the effective nucleus shown below.

$C^{+4}$	$C^{+2}$	$C^0$	$C^{-2}$	$C^{-4}$
3.8	2.96	2.12	1.29	
$N^{+5}$	$N^{+3}$	$N^{+1}$	$N^{-1}$	$N^{-3}$
4.8	3.91	3.03	2.14	
$O^{+6}$	$O^{+4}$	$O^{+2}$	$O^0$	$O^{-2}$
5.8	4.91	3.95	2.98	
$F^{+7}$	$F^{+5}$	$F^{+3}$	$F^{+1}$	$F^{-1}$
6.8	5.82	4.87	3.93	
$Cl^{+7}$	$Cl^{+5}$	$Cl^{+3}$	$Cl^{+1}$	$Cl^{-1}$
8.59	7.45	6.31	5.17	
$Br^{+7}$	$Br^{+5}$	$Br^{+3}$	$Br^{+1}$	$Br^{-1}$
11.60	10.16	8.72	7.28	
$I^{+7}$	$I^{+5}$	$I^{+3}$	$I^{+1}$	$I^{-1}$
15.4	13.7	12.0	10.3	

and collateral with this there is an increase in the effective nucleus.

For example :—

	$C^{+2}$	$N^{+3}$	$O^{+4}$	$F^{+5}$
Diamagnetic increments .....	5.495	3.15	2.003	1.223
Hund symbol for pair of electrons ...	$2p$	$2p$	$2p$	$2p$
Effective nucleus .....	2.96	3.91	4.91	5.82

If we add to the given ion not only a pair of electrons but also a positive ion, then the diamagnetism of the pair (which now may be called valency diamagnetism) will be less than before, but the relative order of the values will remain the same as in Table II.

Table II. provides a means of estimating the change in diamagnetism caused by a change in valency bonds. For example, if two  $N^{+3}$  valency bonds (each containing two

TABLE IV.

Ionic Diamagnetic Susceptibilities.

$C^{+4}$	$C^{+2}$	$C^0$	$C^{-2}$	$C^{-4}$
0.15	4.83	10.32	21.00	50
$N^{+5}$	$N^{+3}$	$N^{+1}$	$N^{-1}$	$N^{-3}$
0.11	3.04	6.19	11.46	22
$O^{+6}$	$O^{+4}$	$O^{+2}$	$O^0$	$O^{-2}$
0.08	2.09	4.09	7.19	12.6
$F^{+7}$	$F^{+5}$	$F^{+3}$	$F^{+1}$	$F^{-1}$
0.063	1.52	2.95	4.98	8.10
$Cl^{+7}$	$Cl^{+5}$	$Cl^{+3}$	$Cl^{+1}$	$Cl^{-1}$
1.20	5.71	10.92	18.19	29.0
$Br^{+7}$	$Br^{+5}$	$Br^{+3}$	$Br^{+1}$	$Br^{+1}$
6.00	13.74	23.09	35.81	54.00
$I^{+7}$	$I^{+5}$	$I^{+3}$	$I^{+1}$	$I^{-1}$
17.00	27.68	40.53	57.27	80.00

electrons) are changed to three  $N^{+5}$  valency bonds, then there is an increase of diamagnetism amounting to

$$(2.93 + 3.15 + 5.27) - (3.15 + 5.27)$$

or 2.93 diminished by an amount depending on the atom sharing the bond with nitrogen, and by an amount depending on the interchange effect.

In the diagram for F, Cl, Br, and I there is an important difference from C, N, O, and F.

In passing down a column of the F, Cl, Br, I diagram, the level of the electronic pair rises, with the result that,

although the increasing effective nuclei should cause a diminishing diamagnetic increment, yet the increasing quantum numbers bring about a predominating increase in the increment. Accordingly, in passing down a column of the diagram for F, Cl, Br, and I there is (contrary to what we see with C, N, O, F) an increasing diamagnetic increment and a corresponding increasing valency diamagnetism.

In the case of some substances, such as ammonia, the difference between the diamagnetism of the neutral group and that of the molecule is not great enough to warrant the assumption of much loss from the interchange effect, and the depression is to be ascribed mostly to increase of the effective nucleus. On the other hand, there are substances such as methane where the depression is so great that it cannot be explained without a large fluctuation of angular momentum due to the interchange effect.

In selecting suitable ions, account has to be taken not only of the electronic groups within the ions themselves, but also of the interionic valency groups containing the surplus electrons, and in doubtful cases preference should be given to groups the quotas of which are suitable with respect to their values for resultant spin and resultant orbital angular momentum.

Of the ions or atoms given in Table IV., all have zero values for these quantities except those in columns 3 and 4. Those in column 3,  $C^0$ ,  $N^{+1}$ ,  $O^{+2}$ ,  $F^{+3}$ ,  $Cl^{+3}$ ,  $Br^{+3}$ , and  $I^{+3}$ , if the multiplet intervals are assumed wide enough, have zero value for  $J$ , *i.e.* for the resultant of the spin and the orbital angular momentum, and the atomic susceptibility is that given by the Pauling formula diminished by an amount due to high-frequency paramagnetism.

In the ions in column 4, *i.e.* those next to the last in each row, namely  $C^{-2}$ ,  $N^{-1}$ ,  $O^0$ ,  $F^{+1}$ ,  $Cl^{+1}$ ,  $Br^{+1}$ , and  $I^{+1}$ , the incomplete outer shell is a  $p$  layer containing four electrons, and therefore complementary to the non-paramagnetic quota of two electrons. These ions will, therefore, in the isolated state display paramagnetism unless they are considered to be in a state somewhat higher than the deepest.

In studying each diamagnetic molecule, the procedure adopted in the present paper is to consider the suitability of various trial structures. The constituent parts of each structure are ions or cores selected from the list given above.

A structure may be rejected because the number of surplus electrons is unsuitable for distribution among the bonds, or because theoretically a paramagnetic moment has to be

assigned to the outer group of one or more of the constituent cores.

The first structure to be studied in each case is that containing the ions of the neutral group. The amount by which the molecular diamagnetism is less than that of the neutral group gives some indication of the homopolar character of the substance. Then a structure is considered containing smaller ions than those of the neutral group, and the magnetism is estimated of the surplus or valency electrons, two of which are assigned to each bond. A compound may contain both homopolar and heteropolar bonds. The first show small diamagnetism or, it may be, paramagnetism; the second show less reduced diamagnetism.

The diamagnetism of an ion when acting as a core is somewhat larger than when in the isolated state. Again, the above strictures regarding the paramagnetism of certain ions refer to isolated particles, and certain ionic values are used in this discussion to which exception might be taken if the ions were isolated.

### *Applications of the above Theory.*

#### Water and Ammonia.

Trial structure.	Theoretical sum of ionic diamagnetisms.	Experimental molecular susceptibility.	Number of surplus electrons.	Diamag. of surplus electrons.
$2\text{H}^{+1} + \text{O}^{-2}$ .....	12.6	12.96	0	(0.36)
$2\text{H}^{+1} + \text{O}^0$ .....	7.19	.....	2	5.77
$2\text{H}^{+1} + \text{O}^{+2}$ .....	4.09	.....	4	8.87
$3\text{H}^{+1} + \text{N}^{-3}$ .....	22	$17.05 \pm 0.41$	0	-5
$3\text{H}^{+1} + \text{N}^{-1}$ .....	11.46	.....	2	5.59
$3\text{H}^{+1} + \text{N}^{+1}$ .....	6.19	.....	4	10.86
$3\text{H}^{+1} + \text{N}^{+3}$ .....	3.04	.....	6	14.01

For water the given experimental figure is the very reliable and generally accepted value, and for ammonia the value measured by Farquharson using strong aqueous solutions. The value for ammonia gas in agreement with this would be about 18, whereas 19 is usually given.

Water is quite exceptional in having an experimental molecular susceptibility that shows no depression below that of the neutral group. There is a very slight rise instead. Water has been so thoroughly investigated experimentally

that doubt seems to be suggested rather regarding the theoretical value of  $O^{-2}$ , which is probably too low. In any case, should there turn out to be really a depression in the case of water, then it seems likely that this depression would be small compared with that in ammonia, which again shows a much smaller depression than methane. The very great lowering in methane, which is confirmed by methyl substitution products, indicates that the fluctuation of angular momentum in the interchange process has a far greater effect in methane than in ammonia or water, where any depression is mainly due to change of effective nucleus.

The structure suggested for water contains oxygen in the form  $O^{+2}$ , which is assigned the value 4.09, which, however, should be subjected to a reduction, as explained above. If this is done, the exceptional character of water is made still more marked.

The second structure in water and the second and third in ammonia are rejected because there are not enough surplus electrons for the bonds.

The two bonds in water require at least four valency electrons, *i. e.* two for each bond; similarly, ammonia requires at least six valency electrons, two for each of its three bonds. The second structure in each case also receives less favour for another reason: theory assigns a paramagnetic moment to both  $O^0$  and  $N^{-1}$  in the isolated condition, unless in a state somewhat higher than the lowest.

On the other hand, ions with larger positive charges than those shown in the above table would give unnecessarily large numbers of surplus electrons. Accordingly, the most suitable structures seem to be  $2H^{+1} + O^{+2}$  for water and  $3H^{+1} + N^{+3}$  for ammonia. The valency diamagnetism is then 8.87 in water and 14.01 in ammonia. These values may be compared with the increments 3.098 + 5.412 or 8.15 for  $O^{+2}$  and 3.15 + 5.27 + 10.54 or 18.96 for  $N^{+3}$  (see Table II.).

The suggestion has sometimes been made that for a molecule the atoms of water are at the corners of a triangle and not in one straight line, the atoms of ammonia at the corners of a tetrahedron, and the atoms of methane at the corners of a pyramid with four-sided base. This suggestion is favoured by considerations of dielectric capacity and other properties.

In the present structure, there is a single bond (corresponding to a pair of electrons) in each of two of the sides of the water triangle, the third side being unoccupied,

and there is a single bond in each of three of the edges of the ammonia tetrahedron, the other three edges being unoccupied.

The above structures for water and ammonia have octets round the oxygen and nitrogen atoms, some of the electrons of the octet forming bonds.

### *Hydrogen Peroxide.*

The experimental molecular diamagnetism of hydrogen peroxide is  $16.73 \pm 0.20$  (measured in this laboratory by Farquharson).

If an octet is supposed to be round each oxygen atom, the choice for hydrogen peroxide seems to be between two structures, for which the following are the diamagnetic details:—

Diamagnetisms.						
	Cores.	Three bonds.	Two H—O bonds.	One O—O bond.	Average of two H—O bonds.	
$\begin{array}{c} \text{O}^{+2} - \text{O}^{+2} \\   \quad   \\ \text{H}^{+1} \text{ H}^{+1} \end{array} \dots$	8.18	8.55	6.20	2.35	3.10	
$\begin{array}{c} \text{H}^{+1} \\ \diagdown \\ \text{O}^{+4} - \text{O}^0 \\ \diagup \\ \text{H}^{+1} \end{array}$	9.28	7.45	5.10	2.35	2.55	

When the two H—O bonds are attached to *different*  $\text{O}^{+2}$  cores, the bond magnetisms are given by  $3.1 + 3.1$  or  $6.2$  (see Table II.), subjected to appropriate reduction. When they are attached to the *same*  $\text{O}^{+4}$  core, the values are given by  $2.00 + 3.10$  or  $5.10$ , subjected to appropriate reduction. Although the O—O bond works out as the same for both structures, the first formula receives the greater support from the present measurements because, by it, it is clearer that the H—O bond is more heteropolar than the O—O bond.

In the above no reduction has been made in the diamagnetic increments of Table II. Probably any required reduction would be slight, but, even so, it would go to diminish still further the diamagnetic difference between the two kinds of bonds.

As pointed out already, from the fact that water appears not to show a depression below the neutral group, we conclude that the given theoretical value of the atomic susceptibility of  $\text{O}^{-2}$  is probably too low. If it were higher,

water would show a depression, and in hydrogen peroxide the difference between the two kinds of bonds would be more distinct.

The first arrangement shown above suits the dielectric capacity better than a structure with all four ions in the same straight line:  $H^{+1}-O^{+2}-O^{+2}-H^{+1}$ .

Again, hydrogen peroxide is not formed by the oxidation of water, but by the reduction of oxygen. So it must not be thought that the molecular structure of hydrogen peroxide can be built up by merely taking the water triangle (having  $2H^{+1}$  and  $O^{+2}$  at the three corners) and attaching an oxygen atom to the outside of the  $O^{+2}$  corner. A more suitable and a simpler structure is the one given above, which also agrees with the formation of peroxides such as  $BaO_2$ .

*The Chloride, Bromide, and Iodide of Ammonium.*

The following molecular diamagnetisms were determined by Farquharson:—

$NH_4Cl.$	$NH_4Br.$	$NH_4I.$	
$35.71 \pm 0.47$	$46.71 \pm 0.36$	$69.48 \pm 0.22$	
$NH_3.$	$HCl.$	$HBr.$	$HI.$
$17.05 \pm 0.41$	$23.05 \pm 0.20$	$31.45 \pm 0.15$	$49.29 \pm 1.36$

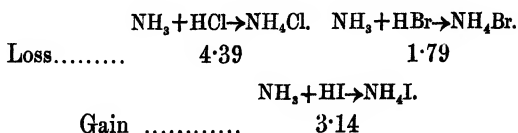
The values for the salts were determined from measurements on the solids, and those for ammonia and the hydrogen halides from very concentrated aqueous solutions. The value for ammonia gas in agreement with the above would be about 18, and that for hydrogen chloride gas about 24.2, whereas the value usually given for ammonia gas is 19 and that calculated for hydrogen chloride gas by Mott Smith from argon and  $Cl^{-1}$  is 24.65 (Phys. Rev. xxxii. p. 821, 1928).

The confirmation thus obtained for the above values for  $NH_3$  and  $HCl$  from concentrated solutions, and the small experimental errors, encourage us to place in these numbers a confidence which may reasonably be extended to those for  $HBr$  and  $HI$  also.

For each of the above the molecular diamagnetism is less than the value for the corresponding neutral group, the following depressions being shown:—

$NH_3.$	$HCl.$	$HBr.$	$HI.$
4.95	5.95	22.55	30.71

A further diamagnetic change appears when ammonia and hydrogen halide unite to form ammonium halide :—



By adding together the appropriate losses we obtain the total depression displayed on the formation of each salt :—



When the total depression is large the greater part occurs in the formation of hydrogen halide, only a small change occurring in the formation of ammonia and in the union of ammonia and hydrogen halide.

The very large depressions in HBr and HI, and the small ones in HCl and NH<sub>3</sub>, indicate a large interchange effect and homopolar nature in HBr and HI, and a small interchange effect and more heteropolar nature in HCl and NH<sub>3</sub>. This explanation also surmounts a difficulty encountered if we ascribe similar structures to all the hydrogen halides and try to reconcile the molecular diamagnetisms.

The diamagnetic data may be explained by representing the reactions thus :—

		Core change.	Valency change.	Net result
$\begin{array}{c} \text{H}^{+1} \backslash \\ \text{H}^{+1} - \text{N}^{+3} + \text{H}^{+1} - \text{Cl}^{+1} \\ \text{H}^{+1} / \end{array} \rightarrow \begin{array}{c} \text{H}^{+1} \backslash \\ \text{H}^{+1} - \text{N}^{+5} - \text{H}^{+1} - \text{Cl}^{+1} \\ \text{H}^{+1} / \end{array}$		fall 2·93	fall 1·46	fall 4·39
$\begin{array}{c} \text{H}^{+1} \backslash \\ \text{H}^{+1} - \text{N}^{+3} + \text{H}^{+1} - \text{Br}^{+1} \\ \text{H}^{+1} / \end{array} \rightarrow \begin{array}{c} \text{H}^{+1} \backslash \\ \text{H}^{+1} - \text{N}^{+5} - \text{H}^{+1} - \text{Br}^{+1} \\ \text{H}^{+1} / \end{array}$		fall 2·93	rise 1·14	fall 1·79
$\begin{array}{c} \text{H}^{+1} \backslash \\ \text{H}^{+1} - \text{N}^{+3} + \text{H}^{+1} - \text{I}^{+1} \\ \text{H}^{+1} / \end{array} \rightarrow \begin{array}{c} \text{H}^{+1} \backslash \\ \text{H}^{+1} - \text{N}^{+5} - \text{H}^{+1} - \text{I}^{+1} \\ \text{H}^{+1} / \end{array}$		fall 2·93	rise 6·07	rise 3·14

The core change is calculated from the ionic values in Table IV. The valency change is calculated from the core change and the experimental net result is shown in the last column.

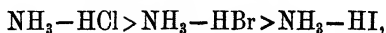
The homopolar relations of the hydrogen halides are as follows :—





the bond magnetisms being  $-4.86$ ,  $+4.36$ , and  $+7.98$  respectively.

Similarly, for the homopolar nature of the bond between ammonia and hydrogen halide we have



the bond magnetisms being  $+1.46$ ,  $-1.14$ , and  $-6.07$  respectively. Note, however, that among the hydrogen halides HI has the most homopolar bond, whereas among the ammonium halides  $\text{NH}_4\text{I}$  has the most heteropolar molecular bond.

The above relative order of the polar characters remains the same, whether we adopt the structure  $\text{H}^{+1}-\text{X}^{+1}$  for hydrogen halide or one with a multiple bond.

The use of the single bond involves the core  $\text{X}^{+1}$  for which, in the isolated state at least, there is a paramagnetic moment unless the ion is in a state somewhat higher than the lowest. Structures with multiple bonds would give non-paramagnetic cores, but as the use of the core  $\text{X}^{+1}$  as a part of a molecule does not seem to be without some reasonable grounds, it is preferable to adopt the single bond.

The relative order for the polar character of the hydrogen halides agrees with the conclusions of Pauling (Proc. Nat. Acad. Sc. Amer. xiv. pp. 359-362, 1928), and with those of London.

*Hydrochlorides of Hydroxylamine, Hydrazine,  
and Monomethylamine.*

The molecular diamagnetisms in this table were determined in this laboratory by Farquharson.

Substance.	Molecular diamagnetism.	Rise in dia- magnetism on substitution of group in $\text{NH}_4\text{Cl}$ .	Diamagnetism lost or gained on substitution.		
			Lost in bonds.	Gained in bonds.	Gained in cores.
$\text{NH}_4\text{Cl}$ .....	$35.71 \pm 0.47$				
$\text{NH}_2\text{OH}\cdot\text{HCl}$ ...	$42.45 \pm 0.39$	6.74	$\text{N}^{+5}-\text{H}^{+1}$ 7.77	$\text{O}^{+2}-\text{H}^{+1}$ 3.10 $\text{O}^{+2}-\text{N}^{+5}$ 7.32	$\text{O}^{+2}$ 4.09
$\text{NH}_2\text{NH}_2\cdot\text{HCl}$ ...	$40.90 \pm 0.27$	5.19	$\text{N}^{+5}-\text{H}^{+1}$ 7.77	two $\text{N}^{+3}-\text{H}^{+1}$ 6.20 $\text{N}^{+3}-\text{N}^{+5}$ 3.72	$\text{N}^{+3}$ 3.04
$\text{NH}_2\text{CH}_3\cdot\text{HCl}$ ...	$44.55 \pm 0.39$	8.84	$\text{N}^{+5}-\text{H}^{+1}$ 7.77	three $\text{C}^{+4}-\text{H}^{+1}$ 5.01 $\text{C}^{+4}-\text{N}^{+5}$ 11.45	$\text{C}^{+4}$ 0.15

The three substituted ammonium salts are regarded as obtained from  $\text{NH}_4\text{Cl}$  by the substitution of  $\text{OH}$ ,  $\text{NH}_2$ , and  $\text{CH}_3$  respectively, the substituted groups containing the ions  $\text{O}^{+2}$ ,  $\text{N}^{+3}$ , and  $\text{C}^{+4}$ . This allows for octet formations round the O, N, and C atoms. The diamagnetisms put for the cores  $\text{O}^{+2}$ ,  $\text{N}^{+3}$ , and  $\text{C}^{+4}$  are those given in Table IV.

The diamagnetisms for the bonds  $\text{N}^{+5}-\text{H}^{+1}$ ,  $\text{O}^{+2}-\text{H}^{+1}$ ,  $\text{N}^{+3}-\text{H}^{+1}$ , and  $\text{C}^{+4}-\text{H}^{+1}$  were obtained from the increments of Table II., which were subjected to appropriate reductions estimated from the magnetic properties of water, ammonia, and methane.

The diamagnetisms for the remaining bonds were obtained by difference from the total experimental rise of diamagnetism observed in each of the three substitutions.

Thus we have for the bonds  $\text{O}^{+2}-\text{N}^{+5}$ ,  $\text{N}^{+3}-\text{N}^{+5}$ ,  $\text{C}^{+4}-\text{N}^{+5}$ :—the bond diamagnetisms 7.32, 3.72, 11.45; depression below increment of Table II. (rise 1.91), 6.82, 17.55; relation of homopolar natures of bonds  $< <$ .

Thus it appears, with regard to homopolar nature, that the bonds of  $\text{O}^{+2}$ ,  $\text{N}^{+3}$ , and  $\text{C}^{+4}$  with  $\text{N}^{+5}$  occupy the same relative position as their bonds with  $\text{H}^{+1}$ .

From a superficial comparison of the molecular diamagnetisms the hydrochloride of hydrazine does not appear to lie magnetically between those of hydroxylamine and monomethylamine. However, by contrasting the corresponding bonds we have found that the hydrazine salt does occupy an intermediate place.

The substitution of methyl in place of a hydrogen atom of ammonium involves the displacement of one of the  $\text{N}^{+5}-\text{H}^{+1}$  bonds, and it is the one with the highest diamagnetism, namely the 10.54 of Table II. reduced to 7.77 by the activation of valency.

If it is desired to introduce a second methyl group, the four bonds of  $\text{N}^{+5}$  are again all occupied before substitution, and the  $\text{N}^{+5}-\text{H}^{+1}$  bond to be displaced must again be the one of the highest value, namely 10.54 reduced to 7.77. Accordingly, it is not surprising to find that sometimes successive substitutions of the methyl group in the same ammonium halide give a constant rise of diamagnetism, namely about 8.8 per substituted methyl. In certain cases, however, there is obtained a diamagnetic rise beyond 8.8, which will be discussed in the next section.

#### *The Methyl Substitution Derivatives of Ammonium.*

The molecular diamagnetisms in this table were determined in this laboratory, all by Farquharson except the

methyl derivatives of ammonium bromide and of ammonium iodide, which were by Dakers.

Substance.	Molecular diamagnetism.	Difference.	Difference per methyl.
$\text{NH}_4\text{Cl}$ .....	$35.71 \pm 0.47$		
$\text{NH}_2(\text{CH}_3)\text{HCl}$ .....	$44.55 \pm 0.39$	8.84	8.84
$\text{NH}(\text{CH}_3)_2\text{HCl}$ .....	$53.32 \pm 0.28$	8.77	8.77
$\text{N}(\text{CH}_3)_3\text{HCl}$ .....	$64.27 \pm 0.51$	10.91	10.91
$\text{NH}_4\text{Br}$ .....	$46.71 \pm 0.36$		
$\text{N}(\text{CH}_3)_4\text{Br}$ .....	$87.21 \pm 0.46$	40.50	10.1
$\text{NH}_4\text{I}$ .....	$69.48 \pm 0.22$		
$\text{N}(\text{CH}_3)_4\text{I}$ .....	$105.0 \pm 0.91$	35.52	8.88

The substitution of the first methyl group in  $\text{NH}_4\text{Cl}$  produces the same addition of diamagnetism as that of the second methyl, and four times this addition is obtained by the substitution of all the four methyl groups in  $\text{NH}_4\text{I}$ , the average per methyl being the same in the two cases.

If it is supposed that in  $\text{NH}_4\text{Br}$  the addition in diamagnetism obtained by the addition of the first three methyls is  $26.4$  or  $3 \times 8.8$ , then that for the fourth methyl must be  $14.10$  or  $8.8 + 5.3$ .

The corresponding change in  $\text{NH}_4\text{Cl}$  for the third methyl is  $10.91$  or  $8.8 + 2.11$ , and for the fourth methyl  $8.8 + x$ .

The magnetisms of the molecular bonds in the ammonium halides are  $\text{NH}_4\text{Cl} + 1.46$ ,  $\text{NH}_4\text{Br} - 1.14$ , and  $\text{NH}_4\text{I} - 6.07$ .

Difference.....			4.93	4.93
Difference.....	2.60	+	4.93	7.53

The substitution of methyl in  $\text{NH}_4\text{Br}$  raises the diamagnetism by  $5.3$ , whereas the difference in the molecular bonds in  $\text{NH}_4\text{I}$  and  $\text{NH}_4\text{Br}$  is  $4.93$ . Again substitution in  $\text{NH}_4\text{Cl}$  causes a rise of  $2.11 + x$ . If we put this equal to  $7.53$ , then  $x$  would be  $5.42$ , or about the same as in the fourth substitution in  $\text{NH}_4\text{Br}$ .

The condition of wide polar difference in the molecular bonds of the ammonium halides, in which the bond is most heteropolar in the iodide and least in the chloride, is changed by substitution of methyl into a state in which the chloride

and the bromide are nearly as heteropolar in their molecular bond as the iodide.

The very small diamagnetic addition 8·8, yielded by the substitution of methyl when there is no other addition, is consistent with the very small molecular diamagnetism of methane in which there is displayed a very large fluctuation of angular momentum. The diamagnetic depression below the value for the neutral group is very great for methane, 37·8, compared with that for ammonia, 4·95.

*The Chloride, Bromide, and Iodide of Potassium.*

The molecules KCl, KBr, and KI have the experimental diamagnetisms  $36\cdot15 \pm 0\cdot36$ ,  $48\cdot12 \pm 0\cdot85$ , and  $63\cdot9 \pm 0\cdot25$  respectively. These figures were measured in this laboratory by Farquharson.

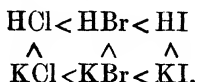
For each of these the molecular diamagnetism is less than the value for the corresponding neutral group, the following depressions being shown :—KCl 9·55, KBr 22·58, KI 32·8.

Compare these with the depressions for the hydrogen halides :—HCl 5·95, HBr 22·55, HI 30·71.

For the hydrogen halides we have already suggested that the fluctuation of angular momentum is very slight in HCl, great in HBr and largest in HI.

Similarly, for the potassium salts the fluctuation is moderate in KCl, larger in KBr, and largest in KI.

The homopolar relations are



For structures with single bonds K—Cl, K—Br, K—I, the bond magnetisms are  $-1\cdot26$ ,  $+4\cdot39$ ,  $+10\cdot07$ .

*The Halogenates and Perhalogenates of Potassium.*  
*Iodic Acid, Periodic Acid, and Iodine Pentoxide.*

These substances have the following experimental molecular diamagnetisms :—

KClO <sub>3</sub> .	KBrO <sub>3</sub> .	KIO <sub>3</sub> .	HIO <sub>3</sub> .
$40\cdot7 \pm 0\cdot47$	$52\cdot3 \pm 0\cdot49$	$63\cdot1 \pm 0\cdot50$	$50\cdot41 \pm 0\cdot30$
KClO <sub>4</sub> .	KIO <sub>4</sub> .	HIO <sub>4</sub> .	I <sub>2</sub> O <sub>5</sub> .
$44\cdot6 \pm 0\cdot22$	$72\cdot0 \pm 0\cdot30$	$56\cdot55 \pm 0\cdot75$	$79\cdot4 \pm 0\cdot89$

Further, HIO<sub>3</sub>.I<sub>2</sub>O<sub>5</sub> gave  $130\cdot6 \pm 1\cdot40$ .

These experimental values were measured in this laboratory by Farquharson, who also carried out a number of other experiments on these substances. The whole of this section will be treated more fully in a subsequent paper.

*The Change from Halide to Halogenate.*

The change in molecular diamagnetism in passing from KCl to KClO<sub>3</sub> is a rise of 4.55 (36.15 to 40.7); in passing from KBr to KBrO<sub>3</sub> a rise of 4.18 (48.12 to 52.3); in passing from KI to KIO<sub>3</sub> a fall of 0.8 (63.9 to 63.1).

When we bear in mind that three oxygen atoms have been added in each case, it is very remarkable that the molecular diamagnetism has been increased by so small an amount in the first two cases and that there is actually a diminution in the third case.

This striking result suggests that the halogen atom in each case undergoes a very large diminution in its diamagnetism caused by the casting off of electrons.

This diminution counteracts to a very large extent the increase due to the addition of three oxygen atoms.

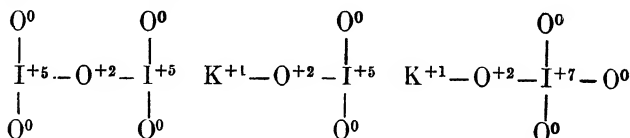
We must reckon also with the change in valency diamagnetism.

*The Change from Halogenate to Perhalogenate.*

Here the alteration in molecular diamagnetism is not less remarkable than that just described. In passing from KClO<sub>3</sub> to KClO<sub>4</sub> there is a rise of 3.9 (40.7 to 44.6), and from KIO<sub>3</sub> to KIO<sub>4</sub> a rise of 8.9 (63.1 to 72.0).

The changes brought about in these two cases obviously cannot be represented by the mere addition of one oxygen atom; there is probably an alteration in the halogen ion.

The following illustrate the structures used in the next section of the discussion:—



We have preferred to use simple structures like these with single bonds, although they involve the use of cores of which O<sup>0</sup> is typical, rather than to use more complicated structures with multiple bonds, even if these allowed the use of cores less liable to be impure diamagnetically in the isolated state.

The following table shows the diamagnetic relations of the halides, halogenates, and perhalogenates :—

Halide to halogenate. Neutral group.		Diamagnetism of neutral group.	Experi- mental molec. sus.	Difference.	
KCl	$K^{+1} + Cl^{-1}$	45·7	36·15	—	9·55
KClO <sub>3</sub>	$K^{+1} + Cl^{+5} + 3O^{-2}$	60·21	40·7	—	19·51
		rise 14·51		fall 9·96	net rise 4·55
KBr	$K^{+1} + Br^{-1}$	70·7	48·12	—	22·58
KBrO <sub>3</sub>	$K^{+1} + Br^{+5} + 3O^{-2}$	68·24	52·3	—	15·94
		fall 2·46		rise 6·64	net rise 4·18
KI	$K^{+1} + I^{-1}$	96·7	63·9	—	32·8
KIO <sub>3</sub>	$K^{+1} + I^{+5} + 3O^{-2}$	82·18	63·10	—	19·08
		fall 14·52		rise 13·72	net fall 0·80
HI	$H^{+1} + I^{-1}$	80	49·29	—	30·71
HIO <sub>3</sub>	$H^{+1} + I^{+5} + 3O^{-2}$	65·48	50·41	—	15·07
		fall 14·52		rise 15·64	net rise 1·12
Halogenate to perhalogenate.					
KClO <sub>3</sub>	$K^{+1} + Cl^{+5} + 3O^{-2}$	60·21	40·7	—	19·51
KClO <sub>4</sub>	$K^{+1} + Cl^{+7} + 4O^{-2}$	68·30	44·6	—	23·70
		rise 8·09		fall 4·19	net rise 3·90
KIO <sub>3</sub>	$K^{+1} + I^{+5} + 3O^{-2}$	82·18	63·10	—	19·08
KIO <sub>4</sub>	$K^{+1} + I^{+7} + 4O^{-2}$	84·10	72·00	—	12·10
		rise 1·92		rise 6·98	net rise 8·9
HIO <sub>3</sub>	$H^{+1} + I^{+5} + 3O^{-2}$	65·48	50·41	—	15·07
HIO <sub>4</sub>	$H^{+1} + I^{+7} + 4O^{-2}$	67·40	56·55	—	10·85
		rise 1·92		rise 4·22	net rise 6·14

The simplest structure of I<sub>2</sub>O<sub>5</sub> contains six single bonds which show a paramagnetism of +8·81. This marked homopolar character is retained in the internal bonds of the complex anion of iodic acid.

The hydration of one molecule of I<sub>2</sub>O<sub>5</sub> gives two molecules of iodic acid which contain eight bonds which show a diamagnetism of -8·52. The three iodine-oxygen bonds of each acid molecule have their homopolar character masked by the strong heteropolar nature of the fourth bond—the one connecting to the simple cation.

The magnetic relations of the complete hydration are as follows :—

	$\text{H}_2\text{O}$	+	$\text{I}_2\text{O}_5 \rightarrow 2\text{HIO}_3$	Diamagnetic rise.
Mol. sus. ....	-12.96		-79.4    -100.82	8.46
Bonds .....	2		6            8	
Bond magnetisms ...	-8.87		+8.81    -8.52	8.46

The rise in diamagnetism on hydration is therefore due to the formation of bonds of marked heteropolar nature. The hydration takes place in stages, thus :—

			Diamagnetic rise.
	$\text{H}_2\text{O} + 3\text{I}_2\text{O}_5$	$\rightarrow 2(\text{HIO}_3 \cdot \text{I}_2\text{O}_5)$	10.06
	$2\text{H}_2\text{O} + 2(\text{HIO}_3 \cdot \text{I}_2\text{O}_5)$	$\rightarrow 6\text{HIO}_3$	15.34
Total result...	$3\text{H}_2\text{O} + 3\text{I}_2\text{O}_5$	$\rightarrow 6\text{HIO}_3$	25.40 or $3 \times 8.46$

*Magnetisms of Bonds of Halogenates and Perhalogenates.*

	$\text{KClO}_3$	$\text{KBrO}_3$	$\text{KIO}_3$	$\text{HIO}_3$
Number of bonds .....	4	4	4	4
Magnetism of bonds ...	+0.18	-3.39	-0.25	-4.26

	$\text{KClO}_4$	$\text{KIO}_4$	$\text{HIO}_4$
Number of bonds .....	5	5	5
Magnetism of bonds ...	-1.04	-12.64	-13.89

A contrast of the  $\text{KIO}_3$  and  $\text{HIO}_3$  shows that the single bond attached to  $\text{H}^{+1}$  is more heteropolar than that to  $\text{K}^{+1}$ ; and the same holds for  $\text{KIO}_4$  and  $\text{HIO}_4$ .

The iodine-oxygen bonds are very homopolar, but the chlorine-oxygen bonds are more so. Accordingly, the three internal bonds in the complex anion are more homopolar in the chlorate than in the iodate of potassium. A similar contrast is obtained with  $\text{KClO}_4$  and  $\text{KIO}_4$ , and with  $\text{KClO}_3$  and  $\text{KBrO}_3$ . On the other hand,  $\text{KBrO}_3$  does not lie magnetically between  $\text{KClO}_3$  and  $\text{KIO}_3$ .

The weakening of the homopolar nature of the halogen-oxygen bond, caused by the raising of the positive valency of the halogen, is displayed by a contrast of  $\text{KClO}_3$  and  $\text{KClO}_4$ , of  $\text{KIO}_3$  and  $\text{KIO}_4$ , and of  $\text{HIO}_3$  and  $\text{HIO}_4$ . Indeed, the diamagnetism of the bond is so strong in the periodates that the more homopolar aspect of  $\text{I}_2\text{O}_5$  is changed into one more heteropolar.

Chemistry Department,  
Aberdeen University.

[The Editors do not hold themselves responsible for the views expressed by their correspondents.]



a.



b.



c.



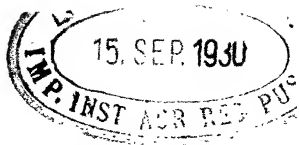
d.



e.







THE  
LONDON, EDINBURGH, AND DUBLIN  
PHILOSOPHICAL MAGAZINE  
AND  
JOURNAL OF SCIENCE.

---

[SEVENTH SERIES.]

---

AUGUST 1930.

---

XVIII. *The Lattice Constants of the Elements.*  
By WILLIAM HUME-ROTHERY, M.A., Ph.D.\*

(1) INTRODUCTION.

EVER since the introduction of the methods of X-ray crystal analysis, great interest has been aroused by the problem of the factors affecting the interatomic distances, and lattice constants of the different structures. Attention has been concentrated chiefly upon the interatomic distances in salts, and particularly in the alkali halides, and for these W. L. Bragg<sup>(1)</sup> has deduced a series of atomic or "ionic radii," which give consistent results when applied to the halides, and which can in many places be applied to more complicated structures. Recently Pauling<sup>(2)</sup> has used the principles of the new quantum mechanics to deduce ionic radii for the rock-salt type of structure, and the values obtained are in good agreement with those of W. L. Bragg, and explain certain abnormalities which are found when the structure involves the "contact" of like ions, instead of the more usual "contact" of oppositely-charged ions. In the method used by Pauling, the electrons in the outermost shell of the ions are treated as though they were in quantized orbits surrounding a nucleus of charge ( $Ze-s$ ), where  $Z$

\* Communicated by Prof. W. L. Bragg, F.R.S.

is the atomic number of the ion, and “ $s$ ” is the so-called screening constant, to allow for the effect of the inner shells of electrons.

For the interatomic distances in metallic crystals detailed investigations have been made by Goldschmidt<sup>(3)</sup>, who has emphasized the importance of the coordination number—*i. e.*, the number of atoms surrounding the particular atom under consideration. The majority of the metallic elements have structures with coordination number 12 (face-centred cubic, and hexagonal close-packed structures), or 8 (body-centred cubic), and Goldschmidt has deduced a series of “atomic radii” for metallic crystals in which the coordination number is 12. In cases where the element crystallizes with a different structure, the appropriate “atomic radius” is deduced from an alloy of the metal in which the structure has coordination number 12. These methods are open to the criticism that rather indiscriminate use is made of both solid solutions and intermetallic compounds, and since almost all the metals concerned are of variable valency, it is by no means certain that the atoms (or ions) are always in the same state in the different structures.

Up to the present, however, the atomic or ionic radii have been given as more or less empirical constants, and little is known of the laws which connect them with the atomic structures. In the present paper we shall describe some relations which have been found in this connexion for the interatomic distances in the crystals of the elements and shall discuss their significance. The only previous reference which has been found to work of this kind is a paper by Davey<sup>(4)</sup>, describing a law of atomic radii, according to which the ratio of the atomic radii of any two members of a given group in the Periodic Table (say chromium and tungsten in Group VI.) is the same as the ratio of the atomic radii of the corresponding members of another group (say vanadium and tantalum in Group V.). As we shall see later, this law is not strictly true in all cases, although it is accurate for some groups, but it is curious that it was not investigated further.

## (2) GENERAL CONSIDERATIONS.

In order to appreciate the laws underlying the lattice constants, it is advisable to consider briefly what is to be expected on theoretical grounds. It is well known that

the atoms of the different elements are built up in such a way that, as we go down the Periodic Table, each step results in the addition of one unit charge to the nucleus, and one extra-nuclear electron in order to keep the atom as a whole neutral. The extra-nuclear electrons in the *free atoms* then arrange themselves into definite shells characterized by the principal and subsidiary quantum numbers, and the periodic relations are the result of the fact that as each shell of electrons becomes completely filled, a new shell begins, and the process repeats itself. The presence of both the A and the B sub-groups, and of the rare-earth elements, is due to the fact that in the shells of higher quantum number, groups of 8 or 18 electrons have a provisional stability, and later expand into completed group of 18 or 32 electrons respectively. The result of this process is that the *free atoms* of the elements of any one sub-group have, except occasionally with high quantum numbers, the same number of electrons in the outermost shell (valency electrons), and, except as regards the first Short Period, they have the same number of electrons in the outermost shell but one. Thus all the alkali metal atoms have one-valency electron surrounding a shell of 8, except in the case of lithium, where the one-valency electron surrounds a completed shell of 2 electrons. Similarly in a group such as VI. A., the atoms of the three metals, chromium, molybdenum, and tungsten, each have 2-valency electrons surrounding an incomplete group of 12 in the outermost shell but one.

In the crystals of the solid elements it seems reasonable to suppose that it is the valency electrons which are responsible for the cohesive forces, except in Group O (the inert gases), where no such electrons are available. We have therefore to distinguish between those electrons responsible for the binding forces, and those which remain attached wholly to one atom or "ion." For convenience we shall denote by  $n$  the principal quantum number of the outermost shell of electrons remaining attached to the atomic cores or ions; since these electrons are attached to one atom only in the crystal, the values of  $n$  will be the same as those of the free atoms. Thus, in the alkali group,  $n=1, 2, 3 \dots$  for lithium, sodium, potassium. With the metals of variable valency in the middle of the long periods, it does not, of course, necessarily follow that the number of electrons in the outermost shell of the atomic

core or ion in the solid crystal is the same as that in the corresponding shell of the free atom.

We may first consider the nature of the repulsive forces which hold the atoms apart, and it seems reasonable to suppose that these will be determined principally by the outermost shell of electrons remaining attached to the atomic cores. In so far as these repulsive forces depend upon the symmetry, or the number of electrons in the outermost shell, they may be expected to be of a similar nature in the elements of any one sub-group, and to be a function of the quantum numbers  $n$ . The forces will not, however, be the same as those for the corresponding quantum numbers of a hydrogen atom, for the charge on the nucleus ( $Ze$ ) must be taken into account, since increase in  $Z$  decreases the "size" of an electron shell of given quantum number. The magnitude of the effect may of course depend upon the screening action of the inner electrons, as considered in the work of Pauling.

The nature of the attractive forces is however less certain. It has been shown by the present author <sup>(1)</sup> that in the later B sub-groups (Groups IV., V., VI., and VII. B) there is a tendency for the element to crystallize so that each atom has  $(8-N)$  neighbours, where  $N$  is the number of the group. This was interpreted as meaning that each atom completes an octet of electrons by sharing one electron with each of its neighbours, and it was suggested that the metallic bond of the normal metals was of a similar nature, except that one electron had to serve for more than two atoms. For the attractive forces the following alternatives appear possible:—(1) The valency electrons may move in quantized orbits in which the attraction is towards the nuclei of charge  $Ze$ , probably modified by the screening effect of the inner electrons. (2) The electrons may be attracted towards the ion as a whole (*e.g.* towards  $\text{Na}^+$ ,  $\text{Ca}^{++}$ , etc.), but may still move in quantized orbits; this is simply an extreme case of (1). (3) The electrons may be attracted towards the ions as a whole, but move freely between the atoms instead of in quantized orbits as in (2). (4) The valency electrons may form a lattice of the static type proposed by Lindemann <sup>(6)</sup>, or the more dynamic type of Lennard-Jones <sup>(9)</sup>.

Since the interatomic distance ( $d$ ) in the crystal is that at which the attraction and repulsion balance one another, we shall expect that, in any one sub-group,  $d$  will be given

by an expression in which  $Z$  exerts a continuous effect to make the distance smaller, whilst  $n$  appears as a discontinuous factor, making the distance larger as the successive shells of electrons are built up. This expectation is fulfilled in the *Law of the Sub-Groups* described in the next section. It is, however, desirable to take into account the temperature at which the interatomic distance shall be measured, and we have here adopted the policy of comparing the distances at one-half the characteristic temperature. The correction for expansion is, however, negligible except in the alkali and alkaline-earth sub-groups, and for  $\gamma$  iron.

### (3) THE LAW OF THE SUB-GROUPS.

The first law concerning the interatomic distances may be expressed in the following form:—

*In any one sub-group of the Periodic Table, provided that the Co-ordination Number remains constant, the interatomic distance  $d$  is given by the relation*

$$\frac{d}{n} = \left( \frac{1}{aZ} \right)^x,$$

where  $n$  is the principal quantum number of the outermost shell of electrons remaining attached to the ions ;

$Z$  is the atomic number ;

$x$  is a constant which is the same for groups with the same number of electrons in the outermost shell of the atomic core or ion ;

$a$  is a second constant which in some groups may be connected with the valency.

In the case of those groups in which the atomic cores contain an outer group of 8 electrons (the inert-gas group, the alkali and alkaline-earth groups, and the titanium sub-group) the value of  $x$  is very nearly  $\frac{1}{3}$ , so that the law here becomes approximately  $\frac{d^3}{n^3} = \frac{1}{aZ}$ .

But as the outer group of 8 electrons develops into an 18 group, the value of  $x$  increases to about 0.39–0.40. This law implies that if  $\log \frac{d}{n}$  be plotted against  $\log Z$ , a straight line will be obtained, and figs. 1 and 2 show how

well this is established. The only point to be noted here is that, in Group IV., the elements carbon and silicon give values of  $d$  lying on the straight line through the titanium family, in spite of the fact that the coordination numbers are different, being 4 for carbon and silicon, and 12 for the

Fig. 1.

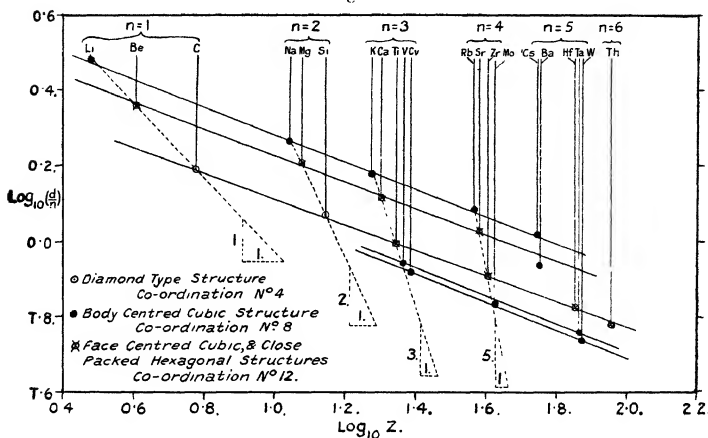
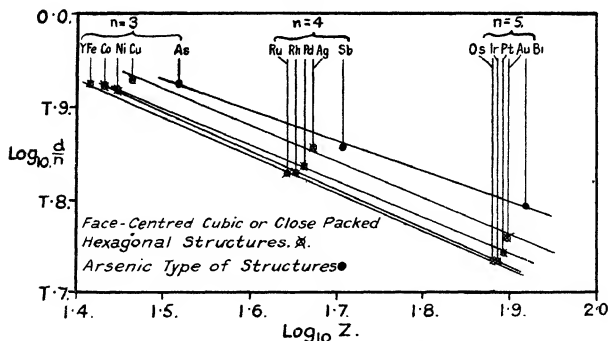


Fig. 2.



titanium sub-group. The significance of this is discussed later. The law suggested by Davey (*loc. cit.*) would require all the lines to be exactly parallel, but it can be seen that this is not strictly true. In the next section we shall discuss the accuracy with which the law holds.

Space does not enable a detailed review to be given of the experimental data which have been employed, but, in

general, use has been made of the data in the International Critical Tables, and those collected by Elam<sup>(8)</sup>, except where these values have been corrected by later and more accurate work. The principal exceptions in this connexion are the results of Simon and Vohsen<sup>(9)</sup>, Posnjak<sup>(10)</sup>, Clark<sup>(11)</sup>, and Ebert and Hartman<sup>(12)</sup> for the alkali and alkaline-earth metals, of Nazza and Nasini<sup>(13)</sup> for nickel, and of Natta and Nasini<sup>(14)</sup> for solid xenon\*.

In order to reduce the interatomic distances to those at one-half the characteristic temperatures, the values of the latter have been taken from the paper by Biltz<sup>(15)</sup>, whose data were recalculated by Lewis<sup>(16)</sup>. Use was also made of a paper by Allen<sup>(17)</sup>, and in one or two cases it was necessary to estimate the characteristic temperature by interpolation on the periodic curve given by Biltz.

For the coefficients of expansion, the values given in the International Critical Tables were used. In some cases the coefficient is not given for low temperatures, and here the tendency is for the results to be over-corrected, when the characteristic temperatures are very low, and the values estimated for the alkali and alkaline-earth metals may be in error by  $\cdot 01$  Å. on this account. The only metal for which any real doubt exists is  $\gamma$ -iron, for which the experimental value for the interatomic distance is  $2\cdot 566$  Å. at  $1373^\circ$  K., and the estimated value at one-half the characteristic temperature is  $2\cdot 52$  Å., but cannot be looked upon as entirely reliable. In one or two cases where the coefficients of expansion were not available, these were estimated from those for metals occupying neighbouring places in the Periodic Table. The corrections introduced in this way are, however, negligible except for the alkali and alkaline-earth groups, and for  $\gamma$ -iron. The calculations have been carried out by means of four-figure logarithms, the fourth figure being dropped at the finish.

The majority of the elements crystallize in the diamond type, body-centred cubic, face-centred cubic, or close-packed hexagonal structures, in which each atom has four, eight, or twelve neighbours at an equal distance, which is taken as the inter-atomic distance. There are, however, some metals with the close-packed hexagonal structure, but with an axial ratio  $a/c = 1\cdot 59$ , or slightly less than that

\* For molybdenum the lattice constant, according to Davey<sup>(18)</sup>, is  $a = 3\cdot 14$ , and the value  $3\cdot 41$  given in Elam's paper is apparently a misprint.



corresponding to close-packed spheres. In such cases we give the values  $a$  and  $b$  of the major and minor axes of the oblate spheroid, to the close packing of which the structure corresponds, and we take the inter-atomic distance as that given by the value of  $a$ . The reason for this is that in the case of cobalt, which crystallizes both in a face-centred cubic form and in a close-packed hexagonal structure of axial ratio 1.59, it is the value of  $a$  which agrees with the interatomic distance in the face-centred cube. This point is discussed later.

### 1. Group I. A. *The Alkali Metals.*

As can be seen from fig. 1, all five alkali metals lie approximately on one straight line, in spite of the fact that in lithium the underlying ion contains a group of only two electrons, whereas, in all the other metals, the outer shell of the ion contains a group of eight. This is in many ways rather striking, and supports the conclusion of Pauling that completed shells of electrons are spherically symmetrical. Taking the group as a whole, the equation deduced from the graph is

$$\frac{d}{n} = \left( \frac{1}{.01637Z} \right)^{.362} = \frac{4.435}{Z^{.362}},$$

and Table I shows the agreement between the calculated and observed values. The maximum error here is .05 Å. Close examination shows, however, that the last four alkali metals lie on a very much better straight line, indicating that lithium is not exactly equivalent to the remaining four, and this, of course, is only to be expected, since a group of two electrons can hardly behave in exactly the same way as one of eight. For the last four alkali metals the equation is

$$\frac{d}{n} = \left( \frac{1}{.0157Z} \right)^{.344} = \frac{4.175}{Z^{.344}},$$

and Table II. shows the agreement between the calculated and observed values. The maximum error is now only .03 Å., and owing to the uncertainty of the coefficients of expansion there is an error of .01 Å. in the reduction of the interatomic distances for rubidium and caesium to one-half the critical temperature, in addition to any error in the experimental values. The error is thus of the order 0.6 per cent

TABLE I.

Metal.	Calculated interatomic distance.	Interatomic distance at $\frac{1}{2}$ characteristic temp.	Error.
Lithium .....	2.98	3.02	— .04
Sodium .....	3.72	3.67	+ .05
Potassium .....	4.58	4.54	+ .04
Rubidium .....	4.80	4.85-4.86	— .05
Cæsium .....	5.20	5.22-5.23	— .02

TABLE II.

Metal.	Calculated interatomic distance.	Interatomic distance at $\frac{1}{2}$ characteristic temp.	Error.
Sodium .....	3.66 Å.	3.67	— .01
Potassium .....	4.55 Å.	4.54	+ .01
Rubidium .....	4.82 (4)	4.85-4.86	— .03-.04
Cæsium .....	5.26 (4)	5.22-5.23	+ .03-.04

### 2. Group II. A. The Alkaline-earth Metals.

The equation deduced from the graph is here

$$\frac{d}{n} = \left( \frac{1}{.02265Z} \right)^{.35} = \frac{3.765}{Z^{.35}}$$

TABLE III.

Metal.	Calculated interatomic distance.	Interatomic distance at $\frac{1}{2}$ critical temperature.		Error.
Beryllium .....	2.32	a. 2.29	c.p. hexag.	+ .03
		b. 2.25		
Magnesium.....	3.16	3.20	c.p. hexag.	— .04
Calcium .....	3.96	3.91-3.92	f.c. cube.	+ .04-.05
Strontium .....	4.22	4.26	f.c. cube.	— .04
Barium .....	4.60 for face- centred cube.	4.32	b.c. cube.	Body-centred cubic.

and Table III. shows the agreement between the calculated and observed values, the accuracy being of the order

1 per cent. In this group barium has the body-centred cubic structure with coordination number 8, and therefore lies markedly off the straight line referring to the other members.

### 3. Group III. A.

This group cannot be examined because the structures of the later members have not been determined. The position of aluminium is discussed later (Section 8).

### 4. Group IV. A.

We have already mentioned that in this group the values for carbon and silicon lie almost on the same straight line as those for the titanium sub-group, in spite of the difference in coordination number. Taken as a whole, the group shows the worst agreement with the straight-line law, but examination shows that the error is due almost entirely to the value for thorium, and that if this metal be omitted, the remaining five elements are almost exactly on a straight line, as can be seen from fig. 1. The equation for this line is

$$\frac{d}{n} = \left( \frac{1}{\cdot 0465(6)Z} \right)^{\cdot 345} = \frac{2\cdot 882}{Z^{\cdot 345}},$$

and Table IV. shows the agreement between the observed and calculated values. As in Group II., we take the  $a$  value for the inter-atomic distance in the close packed

TABLE IV.

Element.	Structure.	Calculated value of $d$ .	$d$ at $\frac{1}{2}$ charact. temp.	Error.
Carbon .....	Diamond type.	1.55	1.54	+ .01
Silicon .....	Diamond type.	2.32	2.35	— .03
Titanium .....	c.p. hex. $\frac{a}{c} = 1.59$	2.98	$a = 2.95$ $b = 2.90$	+ .03
Zirconium ....	„ „	3.23	$a = 3.23$ $b = 3.17$	0
Hafnium .....	c.p. hex. $\frac{a}{c} = 1.62$	3.30	$a = b = 3.32$	— .02
Thorium .....	f.c. cube.	3.66	3.59	+ .07

hexagonal structures with axial ratio 1.59 (see p. 224). The value for thorium lies distinctly off the straight line given for other elements, and the reason for this is discussed later (pp. 235, 236). The effect of the coordination number in this group is discussed in Section 6, in which it is shown that, to a higher degree of accuracy, the close-packed hexagonal metals titanium, zirconium, and hafnium probably form one straight line, from which carbon, silicon, and thorium diverge owing to differences in crystal structure, and in the number of electrons in the outermost shell of the core, and to a systematic deviation from the law for very large values of  $Z$ .

#### 5. Group V. A. (*Body-centred Cubic.*)

In this group data are only available for vanadium and tantalum, so that the straight line law cannot be tested. The straight line through the two points gives the equation

$$\frac{d}{n} = \left( \frac{1}{.0628Z} \right)^{.368} = \frac{2.769}{Z^{.368}}.$$

#### 6. Group VI. A. (*Body-centred Cubic.*)

The three metals chromium, molybdenum, and tungsten give a very good straight line corresponding to the equation

$$\frac{d}{n} = \left( \frac{1}{.0675Z} \right)^{.376} = \frac{2.755}{Z^{.376}}.$$

TABLE V.

Metal.	Calculated interatomic distance.	Interatomic distance at $\frac{1}{2}$ critical temperature.	Error.
Chromium .....	2.50	2.49	+ .01
Molybdenum ...	2.70	2.72	— .02
Tungsten .....	2.73	2.73	0

Table V. shows the agreement between the observed and calculated values.

#### 7. Group VII. A.

The only metal investigated in this group is manganese, which has complex structures for its different allotropic forms. The straight-line law cannot therefore be tested.

8. *Group VIII. (a). Iron, Ruthenium, Osmium.*

In this group the position is obscured by the fact that ruthenium and osmium have close-packed hexagonal structures with coordination number 12, whilst the face centred allotropic form of iron, with the same coordination number, is stable only at very high temperatures, and the correction for expansion becomes considerable and speculative, although the error is not likely to be more than  $\cdot 02$  or  $\cdot 03$  Å. The close-packed hexagonal structures have axial ratio 1.59, and both major and minor axes of the oblate spheroid are given in Table VI., which shows the agreement with value calculated from the equation

$$\frac{d}{n} = \left( \frac{1}{\cdot 05998Z} \right)^{.404} = \frac{3.116}{Z^{.404}}.$$

TABLE VI.

Metal.	Calculated interatomic distances.	Interatomic distances at $\frac{1}{2}$ characteristic temp.	Error.
Iron ( $\gamma$ ) .....	2.51	? 2.52?	—0.01?
Ruthenium.....	2.70	$\left\{ \begin{array}{l} a=2.69 \\ b=2.64 \end{array} \right\}$	+0.01
Osmium.....	2.71	$\left\{ \begin{array}{l} a=2.71 \\ b=2.66 \end{array} \right\}$	0

As in the case of beryllium the straight line has been drawn to give the best agreement with the value of  $a$  in the close-packed hexagonal structure. The errors are negligible.

9. *Group VIII. (b).*

The equation in this case is

$$\frac{d}{n} = \left( \frac{1}{\cdot 05689Z} \right)^{.418} = \frac{3.314}{Z^{.418}},$$

and the straight line law is fulfilled almost exactly, as can be seen from Table VII.

TABLE VII.

Metal.	Calculated interatomic distances.	Interatomic distances at $\frac{1}{2}$ characteristic temp.	Error.
$\alpha$ Cobalt .....	2.51	2.51 face-centred cube	0.00
$\beta$ Cobalt .....	...	$\left\{ \begin{array}{l} a=2.51 \\ b=2.46 \end{array} \right\}$ hex. c.p.	
Rhodium .....	2.70	2.70 f.c. cube	0.00
Iridium .....	2.70	2.70 f.c. cube	0.00

## 10. Group VIII. (c).

The equation here is

$$\frac{d}{n} = \left( \frac{1}{.05808Z} \right)^{.39} = \frac{3.035}{Z^{.39}},$$

and the straight-line law is fulfilled almost exactly as can be seen from Table VIII.

TABLE VIII.

Metal.	Calculated interatomic distance.	Interatomic distance at $\frac{1}{2}$ characteristic temp.	Error.
Nickel .....	2.48	2.48	0.00
Palladium .....	2.73	2.73	0.00
Platinum .....	2.77	2.76	+0.01

## 11. Group I.B.

The equation here is

$$\frac{d}{n} = \left( \frac{1}{.05105Z} \right)^{.393} = \frac{3.219}{Z^{.393}},$$

and the agreement with the straight-line law is not so good as in the preceding groups, the error being as much as 1 per cent., as can be seen from Table IX.

TABLE IX.

Metal.	Calculated interatomic distance.	Interatomic distance at $\frac{1}{2}$ characteristic temp.	Error.
Copper .....	2.57	2.55	+0.02
Silver .....	2.84	2.87	-0.03
Gold .....	2.89	2.87	+0.02

12. *Groups II. B and III. B.*

In these groups the crystal structures are irregular so that the law cannot be tested, and as the author has previously suggested (5) the evidence is that, in some cases, the metals are not fully ionized in the solid crystal. Thus indium and thallium are probably only singly ionized, and so have much larger interatomic distances than the preceding univalent metals silver and gold.

13. *Group IV. B. (Diamond Structure.)*

In Group IV., as we have already explained, carbon and silicon give  $\frac{d}{n}$  values which fit on to the line for the titanium sub-group, in spite of the difference in co-ordination number. The four elements with the diamond type of structure (carbon, silicon, germanium, and grey tin) do form a rough straight line, and the equation for this is

$$\frac{d}{n} = \left( \frac{1}{\cdot 0515Z} \right)^{\cdot 40} = \frac{3 \cdot 275}{Z^{\cdot 40}}$$

which gives 1.60, 2.28, 2.46, and 2.74 Å. as compared with the experimental values of 1.54, 2.35, 2.43, and 2.79 for carbon, silicon, germanium, and grey tin respectively. The agreement is thus approximate only, and this, of course, is to be expected, since we have three different electronic groupings in the underlying ions—2 for carbon, 8 for silicon, and 18 for germanium, and grey tin.

The straight line through the two points for germanium and grey tin with the (18) group of electrons corresponds to the equation

$$\frac{d}{n} = \left( \frac{1}{\cdot 0588Z} \right)^{\cdot 33} = \frac{2 \cdot 571}{Z^{\cdot 33}}.$$

If the experimental values for germanium and grey tin be plotted in fig. 1, it will be found that they lie distinctly below the straight line given by the elements of Group IV. A.

14. *Group V. B. (Arsenic, Antimony, Bismuth.)*

These elements crystallize so that each atom has three close neighbours, and thus satisfy the (8-N) rule indicating

a simple co-valent bond. The law of the sub-groups is, however, still satisfied, the equation being

$$\frac{d}{n} = \left( \frac{1}{\cdot 04753Z} \right)^{\cdot 323} = \frac{2\cdot 569}{Z^{\cdot 323}},$$

and as can be seen from Table X. and fig. 2, a very fair straight line is obtained.

TABLE X.

Metal.	Calculated interatomic distance.	Interatomic distance $d$ , at $\frac{1}{2}$ characteristic temp.	Error.
Arsenic .....	2.49	2.51	—02
Antimony .....	2.89	2.86	+03
Bismuth .....	3.08	3.09	—01

We shall consider later (p. 242) the very interesting relations found for the second distances of approach in these structures.

### 15. Group VI. B. (*Selenium, Tellurium.*)

In this group only two members have been investigated so that the linear relation cannot be tested. The structures are such that each atom has two close neighbours, and four at a greater distance, so that the (8-N) rule is fulfilled, indicating simple covalent bonds. For the closest distance of approach ( $d$ ), the straight line through the two points corresponds to the equation

$$\frac{d}{n} = \left( \frac{1}{\cdot 0944Z} \right)^{\cdot 21}.$$

The slope is thus markedly different from all the preceding groups, and the reason for this is clearly that in Group VI. B each atom has six valency electrons and shares two with each of two neighbours, so that four of the valency electrons remain attached to each atomic core, and the repulsive forces are no longer the result of the  $n$  electrons alone.

### 16. Group O. (*Inert Gases.*)

The structures of krypton and xenon have now been determined, and it is interesting to note that the line



through the two points which are thus available has almost exactly the same slope as that for the alkali, alkaline earth, and titanium sub-groups in which the underlying ions have the inert gas structure. The straight line for the inert gas group deduced from these two values gives the equation

$$\frac{d}{n} = \left( \frac{1}{\cdot 02735Z} \right)^{.318} = Z^{-.348}.$$

(4) THE VARIATIONS OF THE CONSTANT  $x$ .

TABLE XI.

Group.	Value of $x$ .
O .....	.348
I. A .....	.344*
II. A .....	.35
IV. A .....	.345
V. A .....	.368
VI. A .....	.376
VIII. (a) .....	.404
VIII. (b) .....	.418
VIII. (c) .....	.39
I. B .....	.393
IV. B .....	.33†
V. B .....	.323
VI. B .....	.21

In Table XI. are summarized the values for the constant  $x$  in the equations  $\frac{d}{n} = \left( \frac{1}{aZ} \right)^x$  for the different groups. It will be seen that these are constant at 0.34–0.35 for the four groups with the inert gas type of ion, and that this constant value is very nearly  $\frac{1}{3}$  (0.33). The value of  $x$  then increases steadily to a maximum of 0.418 in Group VIII. *b*. Close examination reveals certain additional minor regularities. Thus the slope of the line through germanium and grey tin is 0.33, and is identical with that through copper and silver. The value 0.39 given for Group I. B is higher than this, because the line is drawn so as to include the value for gold. These differences are clearly due to the difference in the screening effects caused

\* Taken from the equation for the last four alkali metals.

† Taken from the line through germanium and grey tin.

by the filling up of the inner quantum shells which takes place during the rare earth elements.

(5) THE VARIATION OF THE CONSTANT  $a$ .

In Table XII. are summarized the values of the constant  $a$  in the equations  $\frac{d}{n} = \left(\frac{1}{aZ}\right)^r$  for the different groups, the figures after each group giving the coordination number, which, of course, affects the value of  $a$ . It will be noted that in Groups II. A and IV. A which have the same coordination number, the values of  $a$  are almost as 1 : 2,

TABLE XII.

Group.	Value of $a \times 10^2$
O (12) .....	2.74
I. A (8) .....	1.57
II. A (12) .....	2.27
IV. A (12) .....	4.66
V. A (8) .....	6.28
VI. A (8) .....	6.75
VIII. $a$ (12) .....	6.00
VIII. $b$ (12) .....	5.69
VIII. $c$ (12) .....	5.81
I. B (12) .....	5.11
IV. B (4) .....	5.88
V. B complex .....	4.74
VI. B complex .....	9.44

suggesting that in the early A groups, the value of  $a$  is proportional to the valency, provided that the coordination number remains the same. If this were so we should expect that on plotting  $\log \frac{d}{n}$  for the metals of Groups I. A, II. A, and IV. A against  $\log Z$ ,  $\log 2Z$ , and  $\log 4Z$  respectively, all the metals with the same coordination number should lie on the same straight line. For the metals with coordination number 12 in Groups II. A and IV. A this condition is satisfied to an approximation, but, on the other hand, barium, with the body-centred cubic structure, lies distinctly above the straight line corresponding to the alkali metals, the difference being equivalent to about 0.3 Å. From this we may conclude that the constant  $a$  is not strictly proportional to the valency.

## (6) THE EFFECT OF COORDINATION NUMBER AND CRYSTAL STRUCTURE.

Before discussing the significance of the laws described above, it is advisable to consider briefly what evidence the equations give for the effect of coordination number and structure upon the interatomic distances. We shall here confine ourselves solely to the evidence from the elements, and shall not deal with the figures obtained from alloy structures.

We have already seen that in Group II., the straight line obtained for the first four members would give the value of  $d$  for barium with coordination number 12 as 4.60 Å., as compared with the experimental value 4.32 Å. for the body-centred structure with coordination number 8. This gives the ratio

$$d(12) : d(8) = 1.06 : 1.$$

In this group the equation is subject to a comparatively large error of from .03 to .04 Å., so that the extreme possible values for  $d(12)$  are 4.56 and 4.64, the corresponding values of the ratio  $d(12) : d(8)$  being 1.05 : 1 and 1.07 : 1. This means that the change from coordination number 12 to coordination number 8 results in a contraction of  $5\frac{1}{2}$  per cent., which is considerably greater than that deduced by Goldschmidt from his work on alloy structures.

The second case in which we can compare the same effect is that of iron, which crystallizes in both body-centred and face-centred forms, but here we meet with the difficulty in reducing the value for iron from that obtained at very high temperatures. If we allow an error of  $\pm .02$  Å. in our value 2.52 Å., we have the value for  $d(12)$  as lying between 2.50 Å. and 2.54 Å., whilst  $d(8)$  from the experimental data is 2.475 Å., so that the extreme values for the ratio  $d(12) : d(8)$  are 1.01 and 1.025. This is of the same order as the change deduced by Goldschmidt, *but it is, of course, subject to the assumption that the iron atom is in the same state in both structures*, which in the opinion of the present author is improbable. This difficulty does not arise in the case of barium, for the whole of the evidence is that this element is divalent in the crystal. But although the data for iron may to some extent be affected by a change in the state of the atom, a very marked difference would have to occur in order to increase the ratio to the value 1.06 deduced for

the values for barium. On the other hand, in the case of chromium the value of  $d$  in the body-centred cubic modification is 2.49 Å., and, in the close-packed hexagonal structure, 2.71 Å., so that the ratio  $d(12) : d(8) = 1.09 : 1$ . This is even greater than the ratio deduced for barium, so that the evidence is that the ratio is not constant in the different groups.

This conclusion is confirmed by the fact, which we have already mentioned, that in Group IV. the points for carbon and silicon lie very nearly on the straight line for the titanium sub-group, in spite of the difference in co-ordination number. Careful examination shows that titanium, zirconium, and hafnium form a slightly better straight line if carbon and silicon be omitted, the equation in this case being

$$\frac{d}{n} = \left( \frac{1}{.04685Z} \right)^{.34},$$

which gives 1.54, 2.31, 2.97, 3.23, and 3.31 Å. for the values of  $d$  in carbon, silicon, titanium, zirconium, and hafnium as compared with the experimental values 1.54, 2.35, 2.95, 3.23, and 3.32 Å. respectively. But the difference between this and the previous equation for the group as a whole is very slight. It will be noted that the greatest difference ( $-.04$  Å.) is shown by silicon, so that it is possible that the almost negligible difference for carbon is due to opposing effects of change in coordination number, and change in the number of electrons in the outermost shell of the atomic core. But there is no doubt that, in this case, the change from coordination number 4 to one of 12 affects the value of  $d$  by only about 1 per cent., and is much less important than the number of electrons in the outermost shell of the ion, as is shown by the comparatively large errors ( $.05$ – $.07$  Å.) if the values are plotted for the four elements carbon, silicon, germanium, and grey tin, which have the same crystal structure, but different numbers of electrons in the outermost shell. The significance of this is discussed later. The conclusion is opposed to that of Goldschmidt, and, in the opinion of the author, this is probably due to the fact that, in the alloy structures considered by this worker, the atoms were not always in the same state.

There is, however, no doubt that the value for thorium deviates from the straight line given by the other members

of the group, and this is probably due to the gradual breakdown of the law for high values of  $Z$  (see (8)), whilst it is also perhaps possible that the direct comparison of the face-centred cubic and close-packed hexagonal structures is not strictly justified. We have assumed so far that those two structures can be compared directly, since they both have the same coordination number, but it is unlikely that the structures are exactly equivalent, since, if it were just a matter of chance which structure was formed, we should expect many metals to crystallize in both forms, whereas, actually, cobalt and chromium are the only metals which show this type of allotropy. Apart from this, we have, as explained previously, compared the distance in the face-centred cubic structures with the  $a$  values in the close-packed hexagonal structures of axial ratio 1.59, and this is, of course, rather arbitrary. In Group II. A close examination shows that the line through the points for beryllium and magnesium with close-packed hexagonal structures lies above that for the face-centred cubic metals of the same group, so that it is possible that the two are not really directly comparable.

To summarize, the evidence is that change in coordination number does not cause the same percentage contraction in the different groups, and that in Group IV. the effect of coordination is comparatively slight.

### (7) RELATIONS IN THE PERIODS.

In the preceding sections we have seen how, in each subgroup, the interatomic distances are given simply by

equations of the type  $\frac{d}{n} = \left(\frac{1}{aZ}\right)^x$ , but except for noting

that the value of  $a$  was roughly doubled in passing from Group II. A to IV. A, we have not attempted to show how the different lines are related. This problem is much more complicated owing to the fact that in passing along *any one period* the coordination numbers and the numbers of electrons in the outer shells of the ions change, whereas in passing down any one sub-group these factors in general remain unaltered. It has, however, been possible to trace some very interesting relations.

(a) *In the First Short Period the interatomic distance is, to an approximation, simply inversely proportional to the*

*atomic number.* Thus, assuming the experimental value  $a=2.29$  Å. for beryllium ( $Z=4$ ), we should expect the values of  $d$  for lithium ( $Z=3$ ) and carbon ( $Z=6$ ) to be  $\frac{2.29 \times 4}{3} = 3.05$  Å., and  $\frac{2.29 \times 4}{6} = 1.53$  Å., as compared with the experimental values 3.02 Å. and 1.54 Å. The difference in the case of lithium is in the direction to be expected from the different coordination numbers, whilst as we have already shown in (6) the evidence is that the coordination number has little effect in Group IV.

This relation is of interest in two ways. In the first place, considered purely empirically, it enables us to generalize the three equations for Groups I. A, II. A, and IV. A. Thus if we assume the experimental value for beryllium, we can calculate the values for lithium and carbon from the fact that in the First Short Period  $d \sim \frac{1}{Z}$ , and then, knowing that the three straight lines connecting  $\log \left( \frac{d}{n} \right)$  and  $\log Z$  have approximately the same slope of about 0.35, we can in effect calculate the interatomic distances in all the elements of those three sub-groups, except barium, by assuming only two constants. A very satisfactory degree of generalization is thus obtained, although there is some loss of accuracy owing to the fact that lithium does not lie exactly on the straight line for the other alkali metals.

In the second place, this relation confirms the conclusion that, when the screening effects due to inner shells of electrons are absent, the interatomic distance is simply inversely proportional to the atomic number. This can readily be seen from fig. 1, where it will be noted that the points for lithium, beryllium, and carbon lie on a straight line inclined at  $45^\circ$  to the axes.

(b) *In the Second, Third, and Fourth Periods* some very curious relations exist, and, although these are really included in the Law of the Sub-Groups, and the relation (a) above, it may be well to point them out directly. As we have shown above, the data indicate that the coordination number has comparatively little effect in Group IV. A, so that the value for silicon can be compared directly with that of magnesium, whilst, later, comparison

can be made between titanium and calcium, and between zirconium and strontium, where the coordination number is 12 throughout. On the other hand, the values for the alkali metals are not necessarily strictly comparable with these, since we have shown that a contraction occurs in Group II. A, when the structure changes from coordination number 12 to 8, and the same may be expected in Group I. A.

The curious fact now emerges that, whilst in the First Period, on passing from Group II. A to IV. A, the interatomic distance varies as  $\frac{1}{Z}$ , in the Second Period it varies as  $\frac{1}{Z^2}$  and, in the Third Period as  $\frac{1}{Z^3}$ .

This implies that the lines in fig. 1 connecting the first few elements in any one period make angles whose tangents are 1, 2, and 3 in the first three periods, and this is indicated in fig. 1, but for accuracy it is necessary to redraw the figure to a suitable scale, and if this be done it will be found that the relation is satisfied with quite remarkable accuracy in passing from Group II. to Group IV., although not always so accurately from Group I to Group II.

Thus in the Second Period the interatomic distances in sodium, magnesium, and silicon are 3.67, 3.20, and 2.35, or as 1.56 : 1.36 : 1. The inverse squares of the atomic numbers are as  $\frac{1}{11^2} : \frac{1}{12^2} : \frac{1}{14^2} = 1.62 : 1.36 : 1$ .

In the Third Period, the interatomic distances in potassium, calcium, and titanium are 4.54, 3.91, and 2.95, or as 1.54 : 1.33 : 1. The inverse cubes of the atomic numbers are as  $\frac{1}{19^3} : \frac{1}{20^3} : \frac{1}{22^3} = 1.55 : 1.33 : 1$ .

On the other hand, in the Fourth Period the interatomic distances do not vary as  $\frac{1}{Z^4}$ , but nearly as  $\frac{1}{Z^5}$ , although the agreement is not so good as in the previous Periods. The interatomic distances in rubidium, strontium, and zirconium are 4.85, 4.26, and 3.23 Å., or as 1.50 : 1.32 : 1, whilst the inverse fifth power of the atomic numbers are as  $\frac{1}{37^5} : \frac{1}{38^5} : \frac{1}{40^5}$  or 1.48 : 1.29 : 1. In the

Fifth Period, the fact that barium has a different coordination number from the other alkaline earth metals prevents a comparison from being made\*. There is, however, no doubt that, as we proceed from Group I. to Group V., the interatomic distances vary almost exactly as  $\frac{1}{Z}$ ,  $\frac{1}{Z^2}$ , and  $\frac{1}{Z^3}$  in the first three Periods, and almost as  $\frac{1}{Z^5}$  in the Fourth

Period. All these relations are, of course, contained in the Law of the Sub-Groups and the relation (a) above, since these enable us to fix the positions of the three lines for Groups I., II., and IV. A. but the exact whole numbers involved in the terms  $\frac{1}{Z}$ ,  $\frac{1}{Z^2}$ ,  $\frac{1}{Z^3}$  and  $\frac{1}{Z^5}$  are of great interest, and are clearly connected with the screening effect, the jump from  $\frac{1}{Z^3}$  to  $\frac{1}{Z^5}$  coinciding with the building up of an (18) group in the inner shells of electrons.

It has not yet been found possible to extend the generalization beyond Group IV., and the reason for this is clearly that the outermost shell of the ion no longer contains the same number of electrons.

## (8) DISCUSSION.

The discovery of such clear quantum relations for the lattice constants of the elements is of interest, since it indicates how the quantum numbers of atomic structure may be introduced directly into problems connected with the solid state. The following points may now be discussed briefly.

### 1. *The Accuracy of the Law of the Sub-Groups.*

Reference to the previous tables shows that the divergences from the linear relations between  $\log d/n$  and  $\log Z$ , correspond to differences which rarely exceed 1 per cent., and which, in many sub-groups, are less than  $\frac{1}{2}$  per cent. of

\* The slope of the line through barium and caesium is almost exactly 10, indicating a variation as  $\frac{1}{Z^{10}}$  in this period, but the gradient is here very steep so that accuracy is lost.



the values of  $d$ . The deviations are, however, to some extent systematic, and may be classed as follows:—

(a) Except in Group IV., the effect of coordination number is important, and cannot be allowed for by a simple proportionality factor.

(b) The number of electrons in the outermost shell of the ion is important, and completed groups of 2, 8, and 18 electrons are not exactly comparable.

(c) There is a general tendency for the calculated values to be too small in the second short Period (Na, Mg, Si), and too great with very large values of  $Z$  (Th, Au).

It is clear, therefore, that the equation will eventually have to contain secondary quantum numbers or other correction factors. It is, however, thought undesirable to attempt to introduce correction terms of this kind until either it has been possible to place the law on a theoretical basis, which indicates the correction factor, or until the lattice constants are known to within  $\cdot 005$  Å. at corresponding temperatures for a number of groups, a condition which is not yet satisfied. At present, therefore, absolute agreement with the experimental values cannot be claimed, but in view of the fact that only the principal quantum number is being used in these equations, an error of from  $\frac{1}{2}$  per cent. to 1 per cent. in the different groups must be considered as satisfactory.

## 2. *The Meaning of the Law*

It is possible to account for an equation of the type  $\frac{d}{n} = \left(\frac{1}{aZ}\right)^x$  if we assume an attractive force varying as the inverse square of the distance, and a repulsive force varying as an inverse higher power, with a proportionality factor involving  $n$  and  $Z$ . In apparent agreement with this is the approximate doubling of the constant  $a$  in passing from Group II. A to IV. A, suggesting an attraction proportional to the charge on the ion. It seems improbable that this line of approach is correct for the following reasons: (1) There is no such contraction or passing from Group I. B to IV. B. (2) The value of  $d$  for barium is not given exactly by the equation for the alkali group with the constant  $a$  doubled. (3) The relations in the first short Period where the distance is simply inversely proportional

to the atomic number do not support the view that the charge on the ion is directly responsible for the contraction in passing from Group I. to Group IV. (4) Any explanation on these lines would, by the conventional analysis, require the compressibilities of the different elements in one sub-group to vary as  $d^4$ , and this is not the case.

In this connexion reference may be made to a paper by Thomas <sup>(19)</sup> on the calculation of atomic fields. In this work the atomic quantum numbers are not introduced, but the atom is treated as a nucleus surrounded by an atmosphere of electrons. The equations obtained are of such a nature that, if two atoms of atomic numbers  $Z_1$  and  $Z_2$  are compared, the expression for the potential at a distance  $a_1$  from the centre of the first atom is simply related to that at a distance  $d_2$  in the second atom, provided that  $\frac{d_2}{d_1} = \left(\frac{Z_1}{Z_2}\right)^{\frac{1}{3}}$ . There is a curious similarity between this conclusion and the simplified form of the Law of the Sub-Groups  $\frac{d}{n} = \left(\frac{1}{aZ}\right)^{\frac{1}{3}}$ , where the inverse cube root of the atomic number is again found.

### 3. *The Relations for the Group IV. Elements.*

We have already seen that the values for carbon and silicon give points lying on the straight line through the titanium-zirconium group in spite of the difference in co-ordination number. This is of particular interest in view of the fact that titanium, although it has a close-packed structure, shows the phenomenon of a minimum electrical resistance at 112° C., an effect which is characteristic of many of the elements of the B sub-groups, which obey the (8-N) rule indicating the presence of simple covalent bonds in the crystal. The existence of a minimum electrical resistance is quite to be expected in those structures which are the result of covalent electronic bonds where each valency electron is shared between two atoms, since, on raising the temperature, we may expect that electrons will first be liberated with a fall in resistance, but that this effect will be counterbalanced by the steadily increasing amplitudes of the atomic vibrations, which increase the resistance in the usual way. But the occurrence of the effect in a metal with the normal close-packed structure is much more striking, and appears to indicate

that we have a continuous transition from the purely covalent type of bond in those elements obeying the (8-N) rule, through the intermediate linkage found for titanium, to the purely metallic bond in the normal metals. This supports the author's previous suggestion that the covalent and the metallic linkages are really of the same nature, and differ only in that a valency electron is shared between two atoms in a covalent structure, but serves for more than two atoms in a metal.

#### 4. *The Inert Gas Group.*

One of the rather unexpected results in connexion with the interatomic distance in the elements is that the inert gases argon and xenon give smaller values of  $d$  (3.84 Å. and 4.37 Å.) than those for the following alkali metals potassium (4.56 Å.) and caesium (5.22 Å.). At first it might be expected that the interatomic distances would be greater in the inert gases, because (a) the atomic numbers are less than those of the following alkali metals, and (b) the very low melting-points of the inert gases indicate a weak kind of binding. The probable explanation of this is that in the inert gases the atom is neutral, and has no valency electrons which can be shared. In the crystal of the alkali metal, on the other hand, the *ions* are bound together by the shared electrons, and, whilst this linkage is more stable thermally, the mutual repulsion of the positive ions makes the equilibrium distance greater.

#### 5. *The Position of Aluminium.*

We have already noted that lack of experimental data prevents the law of the Sub-Groups being tested for Group III. A. If the isolated value for aluminium be inserted in fig. 1, it will be found that the value of  $d$  appears to be too high to fit in with the regular decrease from Group I. to Group IV. This suggests that aluminium is not fully ionized in the metallic crystal, and this conclusion is supported by many other facts such as the very small increase (8°) in melting-point in passing from magnesium to aluminium, irregularities in the sequence of photo-electric threshold frequencies, electrical conductivities per atom, etc.

#### 6. *The Second Distances of Approach in the Arsenic Group.*

In the arsenic type of structure, each atom has three close, and three more distant, neighbours, and we have

already seen that, for the closest distances of approach, a very good straight line is formed when  $\log \frac{d}{n}$  is plotted against  $\log Z$ , the slope of this line being 0.32. If the second distances of approach ( $d^1$ ) are plotted in the same way, a distinctly poor agreement with the linear law is found, and the slope of the best straight line through the three points is  $-0.46$ , i. e., very much greater than in all the previous cases. These abnormalities are clearly due to the fact that in the Group V. Elements, each atom has five valency electrons of which only three are shared in order to complete the octet; thus leaving two unshared valency electrons attached to each ion. It seemed possible therefore that the unshared valency electrons were responsible for the repulsive zones which caused the second distances of approach, and the interesting fact was then found that if  $\log Z$  were plotted, not against  $\log \frac{d^1}{n}$ , but against  $\log \left( \frac{d^1}{n+1} \right)$ —where  $(n+1)$  gives the quantum number of the valency electrons—not merely was a much better straight line obtained, but the slope was  $-0.33$ , or almost exactly the same as that of the  $\log \frac{d}{n} / \log Z$  curves for the closest distance of approach. If this is not a mere coincidence, it clearly suggests that the two different sets of interatomic distances are due to the two distinct shells of electrons, and this will, of course, explain why the two distances become more nearly equal as we pass from arsenic to bismuth, since the ratios  $\frac{n}{n+1}$  approach unity as  $n$  becomes greater. But in Group VI. B (selenium and tellurium), where there are four unshared electrons per atom, this kind of relation does not hold.

#### 9. ACKNOWLEDGMENTS.

The author must express his gratitude to Professor F. Soddy, F.R.S., for kindly giving laboratory accommodation which enables him to work in Oxford. He must also thank Professor W. L. Bragg, F.R.S., and Professor F. A. Lindemann, F.R.S., for much stimulating discussion in connexion with the preparation of this paper, and must gratefully acknowledge his indebtedness to the Armourers'

and Brasiers' Company for election to a Research Fellowship.

### References.

- (1) W. L. Bragg, *Phil. Mag.* ii. p. 258 (1926).
- (2) Pauling, *J. Amer. Chem. Soc.* xlix. p. 765 (1927); *Proc. Roy. Soc. A*, cxiv. p. 181 (1927).
- (3) Goldschmidt, *Z. Phys. Chem.* cxxxiii. p. 397 (1928); also *Faraday Soc. Trans.* xxv. p. 253 (1929).
- (4) Davey, *Phys. Rev.* xxiii. p. 318 (1924).
- (5) Hume-Rothery, *Phil. Mag.* ix. p. 65 (1930).
- (6) Lindemann, *Phil. Mag.* xxix. p. 127 (1915).
- (7) Lennard-Jones and Woods, *Proc. Roy. Soc. A*, cxx. p. 727 (1928).
- (8) Elam, *J. Inst. Metals* (1929).
- (9) Simon and Vohsen, *Z. Phys. Chem.* cxxxiii. p. 165 (1928).
- (10) Posnjak, *J. Phys. Chem.* xxxii. p. 354 (1928).
- (11) Clark, *J. Amer. Chem. Soc.* li. p. 1709 (1929).
- (12) Ebert and Hartman, *Z. Anorg. Chem.* clxxix. p. 418 (1929).
- (13) Nazza and Nasini, *Phil. Mag.* vii. p. 301 (1929).
- (14) Natta and Nasini, '*Nature*,' cxxv. p. 457 (1929).
- (15) Biltz, *Z. Elektrochem.* xvii. p. 676 (1911).
- (16) Lewis, '*A System of Physical Chemistry*,' iii. p. 63.
- (17) Allen, *Proc. Roy. Soc.* xciv. p. 100 (1917).
- (18) Davey, *Phys. Rev.* xxv. p. 756 (1925).
- (19) Thomas, *Proc. Camb. Phil. Soc.* xxiii. p. 542 (1927).

The Old Chemistry Department,  
The University Museum, Oxford,  
May 1930.

### XIX. *Glow Discharge in Hydrogen.*

By Dr. R. D. RUSK, *Mt. Holyoke College* \*.

IT has been suggested by Richardson and Tanaka † that the glow which they obtained by a discharge in hydrogen at pressures below one-tenth of a millimetre is most probably caused by resonance of neutral molecules, because it has little or no relation to the distribution of the electric field. They also suggest that the glow probably arises as a result of excitation by radiation rather than by electron impact. Some measurements of the space potential have been made by Bramley ‡ in the region between the hot filament and the cold anode both for the striated and non-striated discharges. In the latter instance the potential distribution was found to be quite

\* Communicated by the Author.

† *Proc. Roy. Soc. A*, cvi. (1924).

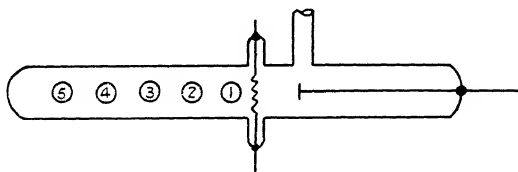
‡ *Phys. Rev.* xxvi. (1925).

uniform except for the sharp drop at the cathode and a slight indication of a reverse field. In the present experiment these measurements of potential were extended into the region back of the hot filament and away from the anode.

The apparatus and method followed were essentially those of Bramley, except that different sets of readings were taken with both fixed and movable electrodes. The cold exploring electrode consisted in every instance of about a millimetre of number 26 platinum wire extending from the sealed tip of a glass tube.

The experimental tube, as shown in fig. 1, was two and a half centimetres in diameter, and the filament and anode were placed fifteen millimetres apart near the centre of the tube, which was about twenty centimetres long. The filament was an ordinary coated platinum wire, and the

Fig. 1.



The experimental tube with exploring electrodes.

anode was a ring of nickel wire. Measurements of the potential with the fixed electrodes were made in five positions at varying intervals along the tube.

Of particular interest were the values of the potential near the filament and toward the extremity of the glow. Fig. 2 shows the electrode current plotted logarithmically, according to the method of Langmuir, for two points inside the glow, and fig. 3 shows typical curves for a point in the extreme edge of the glow. The results indicated a sharp rise of potential near the filament similar to that on the anode side of the filament, then a slightly decreasing but nearly constant potential along the glow to the farther edge, where the drop in potential was rapid. The unmistakable bend-points in the curves indicate the applicability of the Langmuir method in the present instance.

In fig. 4 the volt-ampere characteristics of the exploring electrode are shown for three successive points in the glow. Outside of the glow the branch of the curve for negative

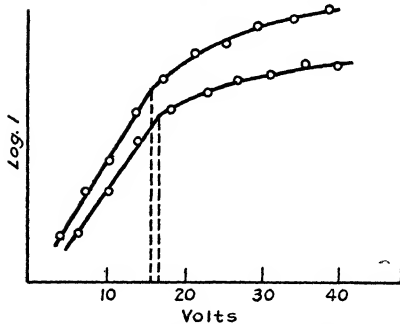
potentials (*i. e.*, positive ion current) became inappreciable, indicating that though there was a plentiful supply of positive ions in the glow there were few if any outside, although negatives were plentiful outside. From this it would appear that the glow is not due only to resonance of neutral molecules. As is well known, the necessary

FIG. 2.



Electrode potentials in glow.

FIG. 3.

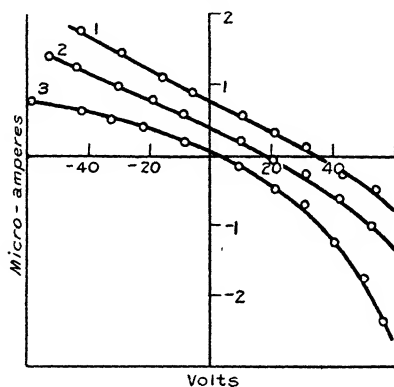


Electrode potentials in extreme edge of glow.

condition for the maintenance of an arc discharge is a sufficient density of positive ions to give the necessary positive space-charge near the cathode, by which means the requisite positive ion bombardment and cathode drop are maintained. Some information on this point was obtained by striking an arc between a second filament and plate placed in the tube, so that they were illuminated

directly by the glow from the first filament and plate. Under such conditions arcs could always be struck at potentials equal to the least potential at which the arc could normally be maintained because of the abundance of positive ions in the glow of the first arc. Just outside the glow, where electrons were still numerous, it was not possible to do this. If excited molecules were present in any abundance they were scarcely subject to cumulative action, or lower voltages would have resulted. Positive ions unquestionably were plentiful.

Fig. 4.



Volt-ampere characteristics of exploring electrode.

It has been noted by McCurdy\* from the equation for the electron current to the cold exploring electrode when the velocity distribution is Maxwellian that

$$V = \frac{3}{2 \tan \theta},$$

where  $V$  is the average energy of the electrons in volts and  $\theta$  is the angle of inclination of the lower portion of the curve. A consideration of fig. 3, again, shows that the slope of the curve representing a higher potential (nearer the filament) would indicate greater electron energy providing the ratio of positives to negatives did not change appreciably. Actually, however, the number of positives must decrease from the filament to the edge of the glow, where it becomes negligible. The points of zero current

\* Phil. Mag. xlviii. (1924).



for the volt-ampere characteristic curves in each instance indicate that the potential of zero current was lower than the potential of the surrounding space, and decreased with increasing distance from the filament for the points measured, in the order indicated on the diagram. Hence the exploring electrode was surrounded by a positive ion space charge-sheath, which was less effective with increasing distance from the filament in keeping electrons from reaching the electrode. This resulted in a decrease in the potential of zero current as represented, and if electron energies did not increase with increasing distance from the filament, certainly the ratio of electrons to positives did increase.

Potentials up to eighty volts were applied to the anode. At high filament temperatures a two volt variation of the anode potential would at times produce as much as a ten cm. variation in the length of the glow. With lower filament temperatures, at which the glow was more diffuse and its edges less sharply defined, the reverse was true, and comparatively large variations in the potential produced only a small variation in the extent of the glow. The latter is presumably the effect mentioned by Richardson and Tanaka.

The steep potential gradient behind the filament indicates that electrons not pulled toward the anode would be accelerated in the reverse direction, producing both excitation and ionization. Beyond a certain limiting distance inelastic collisions would reduce the electron energy below that necessary to maintain the glow. Weakness of the Balmer lines indicated dissociation was slight at the lower voltages.

In conclusion, the space potential rose sharply behind the filament to nearly the value of the anode potential and dropped again sharply at the extremity of the glow. Electrons accelerated into this region would produce ionization and excitation, and at the higher potentials would seem to be more responsible for the glow than excitation by radiation. The abundance of positive ions in the glow supports the view. At lower potentials positive ions were still present, but ionization was less intense in proportion to excitation, and hence the glow was less affected by changes of potential.

Mr. Wesley Stein of North Central College made a number of the measurements.

XX. *The Specific Heat of Mercury in the Neighbourhood of the Melting-Point.* By L. G. CARPENTER, B.A., B.Sc., and L. G. STOODLEY, B.Sc., University College, Southampton\*.

### *Introduction.*

IF a monatomic solid be considered at a temperature so high that the variation of its energy content with temperature may be calculated from classical mechanics,  $C_v$ , its atomic heat at constant volume, should be  $3R$ . It is assumed that each atom may be considered as an harmonic oscillator, its energy being expressible in terms of the squares of its positional and momentum coordinates.

As a matter of fact at high temperatures many (presumably) monatomic solids show values of  $C_v$  which exceed  $3R$ . The cause of this excess has been the subject of some speculation. It has been suggested that the excess is due to the variation of the energy of free electrons with temperature, to the variation of rotational energy of atoms with temperature, to premature melting caused by the presence of impurities which lower the melting-point, or to the fact that at high temperatures, when the amplitude of atomic oscillation is large, the oscillations are no longer harmonic.

The object of the work described in this paper was to obtain additional knowledge of  $C_v$  for mercury of a high degree of purity at temperatures slightly below the melting-point (where but few observations had been made). The results obtained experimentally are, of course, values of  $C_p$ , the atomic heat at constant pressure. The results have therefore been corrected to obtain  $C_v$ , although, as a matter of fact, the exact value of this correction is doubtful, mainly owing to a lack of accurate data on the expansion coefficient of solid mercury.

### *Apparatus and Method of Experiment.*

The apparatus employed was of the well-known Nernst type, and does not call for any very detailed description. The calorimeter itself consisted of a hollow cylinder of length 8 cm., diameter 4.5 cm., and wall-thickness about  $\frac{1}{4}$  mm., which was turned out of a solid piece of mild steel.

\* Communicated by the Authors.

The top of the calorimeter was closed by a thin screw-on lid, in the centre of which was a hole which took a thin hollow steel tube of length 6 cm., and internal diameter 7 mm. This tube was closed at the bottom, and had a flange at the top which was hard-soldered to the lid. Thus, when the lid of the calorimeter was screwed on, there was a central cylindrical cavity, open at the top and leading into the calorimeter to a depth of 6 cm. The capacity of the calorimeter was about 95 c.c. and the weight of the steel 41.56 gms. In order to protect the mercury from possible contamination by the steel, a thin hard coat of bakelite varnish was applied to the inside of the calorimeter. The calorimeter (which was covered with a case of thin silver foil) was suspended by silk threads inside a pyrex-tube, which could be highly exhausted by means of a mercury vapour pump. Interchange of heat by radiation between the calorimeter and its surroundings was minimized by highly polished silver radiation shields. The pyrex-tube was immersed in a bath of methylated spirit, cooled with liquid air, and contained in a large Dewar vessel. The bath was vigorously stirred by means of a mechanical stirrer. Energy was supplied to the calorimeter electrically by means of a platinum coil which also served as a platinum thermometer, the measurement of energy input being made by means of carefully calibrated ammeter and voltmeter, and the resistance of the platinum thermometer measured by a Callendar-Griffith bridge. The platinum coil, which played the double rôle of heating coil and resistance thermometer, was wound non-inductively on a former of copper foil, 4 mm. in diameter, insulated by silk and bakelite varnish, and inserted in the central cavity. Thermal contact with the walls of the central steel tube was obtained by using the eutectic alloy of bismuth and lead (which melts at 125° C.) as a cement, the alloy being poured in when molten.

The platinum coil was connected by means of copper leads of 44 S.W.G., each 4 cm. in length, to stout copper wires of 22 S.W.G., which passed out of the pyrex-vessel and led to the Callendar-Griffith bridge. The considerations which determined the gauge and length of the copper leads and platinum coil were as follows:—

The leads had to be of such length and diameter that the heat-leak from the calorimeter due to their presence was not greater than a specified magnitude. On the other

hand, the electrical resistance of the leads had to be such that the heat generated in them, while energy was being supplied electrically to the calorimeter, should be small compared with the heat generated in the calorimeter coil itself. Lastly, the resistance of the platinum coil had to be such that it was measurable with the bridge available, at the highest temperature (*i.e.*, resistance) at which the calorimeter was to be used. Considerations of heat-leakage settled the leads as being 4 cm. long and of 44 S.W.G. copper, as mentioned above. This value of lead resistance necessitated a coil resistance of at least that corresponding to 1 metre of 44 S.W.G. platinum. As, however, the resistance of 1 metre of 44 S.W.G. platinum at 100° C., which was the temperature of the steam-point calibration, was too great to be measured with the Callendar-Griffith Bridge available, this resistance was partly compensated by winding 60 cm. of similar wire on the same former, and connecting this coil in the compensating side of the bridge. As a result, the resistance of the thermometer coil used as a heating coil was still that due to 1 metre of 44 S.W.G. platinum, while its effective resistance as a thermometer was that due to 40 cm. of wire. This corresponded to 11 ohms at 100° C., and was measurable with the bridge available. The calorimeter, considered as a platinum thermometer, was calibrated at the steam-point, the ice-point, and at the melting-point of mercury, and the usual Callendar formula for the platinum thermometer employed. Below - 40° C., however, the platinum scale requires correction. This was done, using the results of Van Dusen\* and of Loomis†, who have investigated the platinum thermometer at low temperatures. The heat capacity of the calorimeter, when filled with mercury, was determined in the usual manner, the rise of temperature due to a measured amount of electrical energy being determined by resistance measurements, correction being made for the slight loss of heat which occurs during the input period.

When measuring the heat capacity of the mercury and calorimeter over the range -90° C. to -40° C., the time of heat input was usually 4 minutes, the current being about 300 milliamps, and the voltage about 4.5 volts. The resulting temperature rise was of the order of 1½° C. In order to calculate the specific heat of the mercury it

\* *Am. Chem. Soc. Journ.* xlvii. p. 326 (1925).

† *Am. Chem. Soc. Journ.* xlvii. p. 851 (1925).

was of course necessary to know the heat capacity of the calorimeter alone. To this end a separate set of experiments was carried out to determine the specific heat of the steel, which contributed about 80 per cent. of the total heat capacity of the calorimeter, the specific heats of the small quantities of platinum, silver foil, solder, etc., used in its construction being taken from tables. Over the range of temperatures covered in this research the heat capacity of the calorimeter was 12 per cent. of the heat capacity of the mercury it contained.

### *Purification of the Mercury.*

It has already been stated that a possible explanation of the increase of  $C_v$  above  $3R$  near the melting-point is to attribute it to the presence of impurities, which lower the melting-point, so that some fusion takes place below the melting-point of the pure substance. Thus, the apparent rise of the specific heat would be due in reality to the effect of latent heat of fusion. Such an effect has, in fact, been observed by Dickinson and Osborne\* in some precision experiments made by them on the specific heat of ice.

In the present research, therefore, it was resolved to use mercury of a high degree of purity, and, further, to compare the results with those obtained with mercury of a less degree of purity. The two samples of mercury used were called the P and D samples respectively. In order to obtain the P sample of mercury the following procedure was adopted.

A quantity of mercury was taken from a laboratory stock which had been passed in the form of a fine spray five times through 20 per cent. nitric acid, and, after washing with water, distilled once *in vacuo*. The mercury was then agitated with a 2 per cent. solution of potassium cyanide by sucking air through the mixture, small quantities of sodium peroxide being added twice a day. This removed the bulk of any noble metals present†. After washing, the mercury was shaken well with a mixture consisting of equal volumes of 9N sulphuric acid and a cold-saturated solution of potassium permanganate. Shaking was continued until the pink colour disappeared,

\* Bureau of Standards, Bull. xii. p. 49 (1915).

† Bettel, Chem. News, xevii. p. 158 (1908).

the solution then being renewed. This method also is said to remove any base metals present \*. After renewing the solution about ten times the mercury was separated from the white precipitate which had formed, and was washed, dried, and filtered through a pinhole. It was then subjected to two distillations in a current of air under a reduced pressure of 30 millimetres, in order to remove final traces of the base metals, and to eliminate the noble metals. Hulett † states that, starting with a saturated solution of silver, not more than 0.03 parts in a million remain after two such distillations.

After the experiments were finished the P sample was taken from the calorimeter and sent to Messrs. Adam Hilger for a spectroscopic examination. Their report was as follows :—"Antimony, iron, magnesium, calcium, and silicon—a trace. Zinc, cadmium, arsenic, bismuth, lead, silver, boron, and carbon were specially sought, with negative results. A minute trace of tin may have been present, but the indication was so faint as not to be conclusive."

The D sample was taken from the laboratory stock mentioned above, and was used without further purification. Its treatment, therefore, consisted in having been passed five times through 20 per cent. nitric acid, washed, and then distilled *in vacuo*.

### *The Experimental Results.*

Previous determinations of the specific heat of mercury have been made by Koref ‡, Pollitzer §, Simon ||, Russell ¶, and Barnes and Cooke \*\*. In Table I. are given the values of  $C_p$  obtained by the present authors; the range of temperature is from  $197.6^\circ$  abs. to  $285.15^\circ$  abs. In fig. 1 have been plotted our results for the P sample of mercury in a graph which extends from  $190^\circ$  to  $250^\circ$  abs., together with such results of Koref, Pollitzer, and Simon as lie in this range. It is not convenient to plot, on a single graph,

\* Russell, Evans, and Rowell, *Chem. Soc. Journ.* cxxviii. p. 1872 (1926).

† *Phys. Rev.* xxxiii. p. 307 (1911).

‡ *Ann. d. Physik*, xxxix. p. 49 (1911).

§ *Zeits. Elektrochem.* xix. p. 513 (1913).

|| *Ann. d. Physik*, lxxviii. 3, p. 241 (1922).

¶ *Phys. Zeits.* xiii. p. 59 (1912).

\*\* *Phys. Rev.* xvi. p. 65 (1903).

our results together with all the results of other observers, as, on the rather small scale which would have to be used, the points would be too crowded. On fig. 1, therefore, a curve has been drawn which best represents our results from the lowest temperature at which we worked ( $197^{\circ}\cdot6$

TABLE I.

Absolute Temperature.	Atomic Heat (at constant pressure).
197·6	6·41
199·4	6·495
201·1	6·50
207·5	6·495
208·05	6·515
208·6	6·59
209·9	6·55
212·9	6·505
214·45	6·515
217·6	6·60
218·9	6·68
222·9	6·65
227·4	6·72
229·2	6·79
229·65	6·755
231·0	6·755
231·0	6·74
232·4	6·738
232·7	6·785
233·8	6·755
234·23	Melting-point.
236·5	6·80
285·15	6·70

abs.) to the melting-point ( $234^{\circ}\cdot2$  abs.). On fig. 2, which extends from  $100^{\circ}$  to  $300^{\circ}$  abs., the curve so obtained has been plotted, together with the results of all other observers who made determinations in this range. A curve which best represents our results from the melting-point to  $300^{\circ}$  abs. has been drawn, and the points obtained for the

Fig. 1.

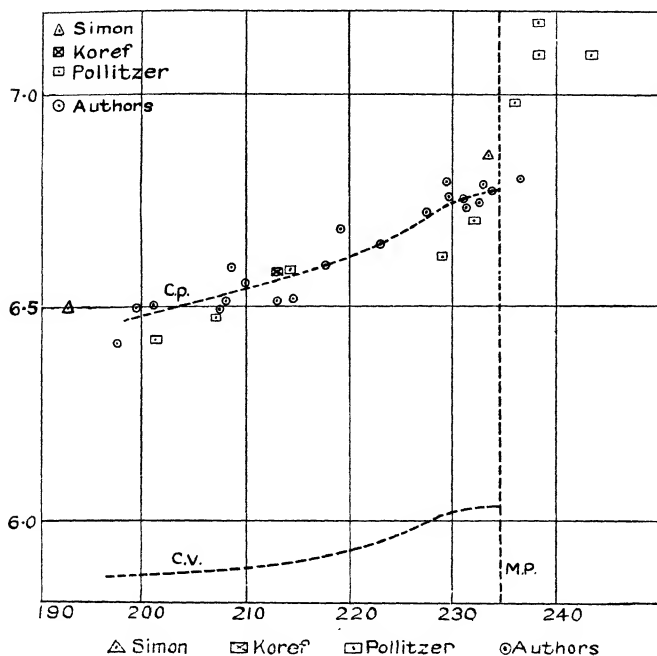
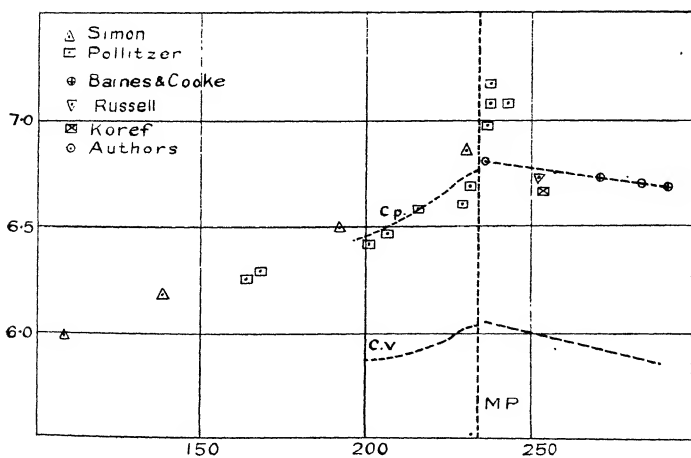


Fig. 2.





liquid by Russell, Koref, Pollitzer, and by Barnes and Cooke have been plotted for comparison.

It is particularly satisfactory to notice that the line joining our two values for the liquid at  $236^{\circ}.5$  abs. and  $285^{\circ}.15$  abs. agrees very closely indeed with the line joining the two points for the liquid obtained by Barnes and Cooke, whose work was of a very high order of accuracy. Hence we feel confident that no serious systematic error is to be found in our own work. We estimate that our experimental arrangements were such as to give the true value of  $C_p$  within 1 per cent. This estimate is confirmed by the fact that on fig. 1, on which all our results for the solid have been plotted, the greatest divergence of points from the average curve we have drawn is 1 per cent., while the average deviation is considerably less. The values of  $C_p$  have, as a matter of fact, been computed to about 1 part in 700 in Table I., but an experimental accuracy of this order is not claimed. As to the results for the D sample, they were identical with those for the P sample within the limits of experimental accuracy. At the melting-point itself, indeed, the values obtained for the P and D samples were the same within two parts in 700, but, of course, the closeness of this agreement was probably partly accidental.

#### *The $C_p - C_v$ Correction.*

The difference between the specific heats at constant pressure and at constant volume is given (in mechanical units) by the expression

$$C_p - C_v = \frac{\alpha^2 VT}{\kappa},$$

where  $\alpha$  is the coefficient of cubical expansion,  $V$  is the molecular volume,  $T$  the absolute temperature, and  $\kappa$  the compressibility. For mercury in the liquid state the values of  $\alpha$  and  $\kappa$  have been determined with considerable accuracy by Bridgman\*. The value of  $V$ , the molecular volume, at each temperature  $T$  is also known with sufficient accuracy for our purpose. Values of  $C_p - C_v$  for various temperatures of liquid mercury have therefore been calculated from Bridgman's data, and by subtraction from the  $C_p$  curve the  $C_v$  curve has been obtained, and plotted

\* Am. Acad. Proc. xlvii. p. 347 (1911).

on fig. 2. The situation with regard to solid mercury is much less satisfactory. The compressibility is indeed known from Bridgman's work, being about  $3.37 \times 10^{-6}$  cm.<sup>2</sup>/kgm., but there is considerable uncertainty as to the expansion coefficient. According to Dewar \* the coefficient of cubical expansion of mercury over the range from  $-188^{\circ}7$  C. up to the melting-point is  $0.887 \times 10^{-4}$ , while Grunmach † gives  $1.23 \times 10^{-4}$  for the same coefficient over the range  $-80^{\circ}$  C. to the melting-point.

As Bridgman remarks (*loc. cit.*) Grunmach used a dilatometer method in which he made no correction for the effect of the glass envelope, and the value he obtained by this method for the change of volume on freezing is certainly wrong. Bridgman himself gives a value of  $1.45 \times 10^{-4}$  (which is the mean of two determinations  $1.25$  and  $1.65 \times 10^{-4}$ ) for the region just below the melting-point, which value, though extremely rough, he considers is probably as good as that of either Dewar or Grunmach. The empirical correction  $C_p - C_v = aT^2$  has been employed by Pollitzer ‡ and by Simon ‡ for mercury, with  $a = 21 \times 10^{-5}$ . This formula gives  $C_p - C_v = 0.753$  calorie per gram atom at the melting-point. Assuming that this value is actually correct, and taking Bridgman's value for the compressibility of the solid, viz.,  $3.37 \times 10^{-6}$  cm.<sup>2</sup>/kgm., the coefficient of cubical expansion would be  $1.8 \times 10^{-4}$ . This is higher than the values of either Dewar, Grunmach, or Bridgman, and is equal to the value for the liquid immediately above the melting-point. It is therefore almost certainly too high, since the expansion coefficient of an element immediately above the melting-point is probably always greater than the coefficient of expansion immediately below the melting-point. For the only three elements for which data is to be found in the Landolt-Börnstein's tables, viz., phosphorus, sodium, and potassium, the expansion coefficients of the liquid phase are greater than those of the solid phase by about 34 per cent., 13 per cent., and 17 per cent. respectively. Thus the expansion coefficient of solid mercury at the melting-point may be taken as less than  $1.8 \times 10^{-4}$ , and the  $C_p - C_v$  correction is therefore less than 0.753 at this temperature.

\* Roy. Soc. Proc. lxx. p. 237 (1902).

† *Phys. Zeits.* iii. p. 133 (1902.)

‡ *Loc. cit.*

As, however, the real value is not known, the correction has been calculated from  $C_p - C_v = 21 \times 10^{-5} T^{\frac{3}{2}}$ , and the  $C_v$  curve inserted on figs. 1 and 2. Nevertheless, we emphasize the fact that 6.02, the value of  $C_v$  at the melting-point shown on the curves, is almost certainly too low. A more accurate determination of the expansion coefficient of solid mercury is obviously highly desirable, and is being carried out in this laboratory.

In order that the values obtained from our smoothed curves may be readily available to anyone who may be interested in the exact numerical values which we consider

TABLE II.

Absolute Temperature.	$C_p$ .	$C_v$ .
200 solid.....	6.47	5.875
210 „ .....	6.54	5.90
220 „ .....	6.62	5.93
225 „ .....	6.68	5.97
230 „ .....	6.75	6.01
234 „ .....	6.77	6.02
240 liquid .....	6.79	6.04
250 „ .....	6.76	6.00
260 „ .....	6.74	5.96
270 „ .....	6.72	5.93
280 „ .....	6.70	5.88
290 „ .....	6.68	5.82

most probable, they are set out in Table II. It should be remembered that, while the exact value of  $C_p$  for the solid is doubtful on account of the uncertain  $C_p - C_v$  correction, the value of  $C_v$  for the liquid is much more reliable, since it depends only on our measurements (which are in good agreement with those of Russell \* and Barnes and Cooke \*) and on the direct and trustworthy determinations of  $\alpha$  and  $\kappa$  by Bridgman.

#### *Discussion of Results.*

In this section of the paper we will discuss the validity of the experimental results obtained, so as to provide a

\* *Loc. cit.*

foundation of fact for whatever theoretical speculation may subsequently be possible.

The purity of the mercury may first be considered. Messrs. Adam Hilger's analysis, though not quantitative, may be taken as showing that the amount of impurity in our P sample was certainly small. The specific heats obtained with the D sample were, however, the same as those obtained with the P sample. Assuming that the additional treatment of the P sample resulted in a higher degree of purity, there are two possible explanations:—

1. The mercury was so pure that the effect of any residual impurity was not detectable with our apparatus. In this case the slope of our curve is not due to impurity.
2. The P sample was fairly pure, and the D sample much less so, but the effect of the impurity remains constant until practically the last trace has disappeared. In this case the slope of our curve is due to impurity.

Alternative 2 seems definitely much less probable than alternative 1. We therefore conclude that the shape of the curve near the melting-point is not due to impurity.

It has been found by some observers (*e.g.*, Griffiths\*—in the case of sodium) that the specific heat of a metal depends on the previous heat treatment of the specimen. In the case of the present experiments the points on the curve were obtained on several different days, the mercury being allowed to melt between one set of observations and the next. The temperature ranges of the various sets of observations overlapped, but no systematic difference was found between the observations obtained on different days, although the time of freezing and amount of cooling were varied. Hence it is not probable that the results were vitiated by want of annealing.

Comparing our results with those of other observers, it is evident from fig. 1 that our  $C_p$  curve lies between those of Simon and Pollitzer, being about 1 per cent. lower than the former, and 1 per cent. higher than the latter, and agrees closely with Koref's value for  $213.6^\circ$  abs., which, however, is a mean atomic heat over the range from  $195.9^\circ$  to  $231.3^\circ$  abs. Since only two observations of Simon lie within the

\* Roy. Soc. Proc. lxxxix. p. 561 (1914).

temperature range of the present experiments, it is not possible to deduce what slope he would ascribe to the curve in the immediate neighbourhood of the melting-point. Pollitzer's results, on the other hand, show a sudden and steep rise about  $4^{\circ}$  below the melting-point. In view, however, of the fact that he made only two determinations in the neighbourhood of the melting-point, and of the rather erratic nature of his results, no great weight need be attached to it. It can therefore fairly be said that the results of the present experiments are in good general agreement with those of other observers, and give considerably more detailed information as to the shape of the specific-heat curve in the immediate neighbourhood of the melting-point.

The value of  $C_p$  measured at the melting-point is 6.77; if we subtract the  $C_p - C_v$  correction of  $21 \times 10^{-5} T^{\frac{3}{2}}$  used by Pollitzer, the corresponding value of  $C_v$  is 6.02. It has already been pointed out, however, that this value of  $C_v - C_c$  is almost certainly too high, since it involves assuming a value of the expansion coefficient for the solid as large as that for the liquid. Hence, at the melting-point,  $C_p$  is at least equal to 6.02, and in all probability is higher\*. It seems therefore that at the melting-point  $C_c$  exceeds the value of 5.95.

It is evident from our measurements that above about  $210^{\circ}$  abs. the slope of the curve begins to increase, although Debye's equation would lead one to expect it to become more nearly parallel to the axis of temperature and asymptotic to 5.95. It might, perhaps, be argued that this increase of  $C_v$  is only apparent, and is in fact due to an unexpected increase of  $C_p - C_c$  in this region, caused by increase of  $\alpha$  or decrease of  $\kappa$  or both. This view, however, is hardly tenable. It is unlikely that  $\alpha$  suddenly increases in the neighbourhood of the melting-point, and in the case of sodium, where such an effect has been specially sought†, it has been found to be absent.  $\kappa$ , on the other hand, may be expected to increase rather than decrease as the melting-point is approached. This is shown, for example, by some

\* A rough estimate of how much higher can be made if we assume the expansion coefficient of the solid to be of the order of 10 per cent. less than that of the liquid—which seems a reasonable assumption to make in view of the values in the case of sodium, potassium, and phosphorus. This would reduce  $C_p - C_v$  by about 20 per cent. and increase the value of  $C_v$  at the melting-point to about 6.17.

† Griffiths, Phys. Soc. Proc. xxvii. p. 477 (1915).

measurements on tungsten made by Geiss, and quoted by Zwikker\*.

The specific-heat curve becomes nearly parallel to the axis of temperature in the immediate neighbourhood of the melting-point. Of the reliability of the experimental evidence on this point there can be no doubt. As has already been stated, the results for the D sample of mercury were identical with those of the P sample within the limits of experimental accuracy; further, a preliminary set of determinations was made with the P sample, in which a variable source of error (which was subsequently determined and eradicated) made the results rather erratic. Nevertheless, the mean curve given by these preliminary determinations also became horizontal in the immediate neighbourhood of the melting-point. In fact, it was substantially identical with the curve recorded in this paper.

It may therefore be concluded that the curve representing the specific heat of mercury as a function of temperature in the neighbourhood of the melting-point exceeds the value that would be expected on the basis of an extrapolation from the value at lower temperatures made in accordance with Debye's theory. Further, the value of  $C_v$  at the melting-point in all probability exceeds 5.95; and, finally, the curve in the immediate neighbourhood of the melting-point is not concave upwards, but becomes more nearly parallel to the axis of temperature as the melting-point is approached.

#### *Some Theoretical Considerations.*

The excess of the atomic heat of metals above  $3R$  at high temperatures has been treated by several writers. So far as we are aware, the effect has been observed up to the present only in the case of metallic elements. It is true that White† has argued that the phenomenon is a general one, and is not confined to metals. He supports this view by quoting measurements he made on certain silicates, for which  $C_v$  departs from Debye's curve at high temperatures. As, however, in no pure silicate on which he experimented did  $C_v$  actually exceed 5.95, his thesis requires to be supported by further evidence.

The fact that in metals  $C_v$  exceeds  $3R$  at high temperatures has generally been explained in terms of one of two

\* *Zeits. f. Physik*, lii. 9-10, p. 668 (1928).

† *Nat. Acad. Sci. Proc.* iv. p. 343 (1918).

hypotheses, of which the first is that it is attributable to anharmonic oscillations of atoms, and the second is that it is the result of the participation of the free electrons in the thermal energy of the atomic lattice. The first hypothesis has been enunciated by Lindemann\* in a paper in which (having shown that Honda's† theory, which attributes the effect to atomic rotations in the solid state, is untenable) he remarks that a simple application of Taylor's Theorem shows that the restoring force on a displaced atom in the lattice is elastic for small displacements, but does not remain so for large displacements. Hence the mean potential energy equals the mean kinetic energy at low temperatures, but may exceed it near the melting-point. It is evident that, if the average potential energy of oscillations of the atoms in a gram atom of metal is to exceed the average kinetic energy (*i.e.*, exceed  $\frac{3}{2}$  R.T.), the restoring force on a displaced atom must increase more slowly than in a linear proportion to the displacement. The dependence of the average potential energy on the relation between restoring force and displacement has been treated by Tolman‡, who shows, for instance, that if the restoring force varies as the  $n$ th power of the displacement, then the average potential energy of an oscillator will be  $\frac{kT}{n+1}$  per degree of freedom, giving, of course, the familiar  $\frac{k}{2}T$  per degree of freedom for the simple harmonic oscillator. Braunbek§, also, has made use of the conception of anharmonic oscillations near the melting-point to explain the anomalous increase of  $C_v$ ; while Waller||, considering the case of a one-dimensional lattice, has worked out the conditions under which the atomic heat at constant volume of such a lattice should exceed R.

The specific heat of a solid consisting of anharmonic oscillators has also been treated by Born and Brody¶, in accordance with the quantum theory, but Schrödinger\*\* has shown that their results can equally well be obtained by the use of classical mechanics.

\* Phil. Mag. xlv. p. 1119 (1923).

† Phil. Mag. xlv. p. 189 (1923).

‡ 'Statistical Mechanics,' p. 76 (Chemical Catalog. Co., 1927).

§ Zeits. f. Physik, xxxviii. 6-7, p. 549 (1926).

|| Ann. d. Physik, lxxxiii. 2, p. 163 (1927).

¶ Zeits. f. Physik, vi. 2, p. 132 (1921).

\*\* Zeits. f. Physik, xi. 3, p. 170 (1922).

Turning now to the second hypothesis, viz., that the effect is due to the participation of free electrons in the thermal energy of the atomic lattice, we find that a considerable use has been made of it by Eastman\* and others in America. These investigators have examined the excess of  $C_v$  over  $3R$  for a large number of metals, and claim that it is the greater the more electro-positive the metal. This correlation is, however, not very well marked, and Eastman†, indeed, admits that the hypothesis of anharmonic oscillations is particularly well suited to explain the relatively rapid increase of specific heat which is found in some substances in the immediate neighbourhood of the melting-point, but he considers that the effect of the free electrons is also present over the whole range of high temperatures. Now, Sommerfeld‡ has recently estimated, by the aid of Fermi-Dirac statistics, the contribution which free electrons should make to the specific heat, if one free electron per atom is assumed. He arrives at the result

$$(C_v)_{\text{electrons}} = \pi^2 \frac{mk}{h^2} \left( \frac{8\pi}{3n} \right)^{\frac{2}{3}} RT,$$

in which  $m$  is the mass of an electron,  $k$  is Boltzmann's constant,  $h$  Planck's constant, and  $n$  is the number of free electrons per cubic centimetre, which is assumed to be equal to the number of atoms per cubic centimetre. The free electrons are treated as a gas, and their interaction with the atomic cores of the lattice is neglected. The application of this formula to solid mercury at its melting-point gives

$$(C_v)_{\text{electrons}} = 0.04 \text{ cal./gram. mol./deg.}$$

If this is subtracted from our value of  $C_v$  at the melting-point, viz., 6.02 (which is, as we have already emphasized, a lower limit), the contribution of atomic oscillations to  $C_v$  would be 5.98, a value which is, of course, to our order of accuracy, experimentally indistinguishable from the limiting value of Debye's theory, 5.95. Although Sommerfeld's theory, which perhaps cannot be expected to yield more than order of magnitude, might possibly suffice to explain our value of  $C_v$  at the melting-point, without having recourse to the hypothesis of anharmonic oscillations, yet,

\* Am. Chem. Soc. Journ. xlv. p. 1184 (1924).

† *Loc. cit.*

‡ *Zeits. f. Physik*, xlvii. 1-2, p. 1 (1928).



as it stands, it does not explain the shape of the  $C_v$  curve, in particular the rise at about  $210^\circ$  abs., and the subsequent tendency at the melting-point to parallelism with the axis of temperature.

The explanation, if it is to be found solely in terms of electrons, is no doubt connected with the interaction of the electrons with the atomic cores, which has been taken into account by Bloch \*. If the interaction of the increasingly disordered lattice with the electrons is the cause of the observed phenomena, it seems that such an effect must also be present in the liquid state. Whether the anomalous rise of  $C_v$  is due to anharmonic vibrations or to the effect of electrons, or to both these causes acting together, it is clear that it must be associated with large atomic vibrations and with atomic disorder, since these phenomena are characteristic of an approach to the melting-point. It is well known that at higher temperatures atomic oscillations are to some extent anharmonic, and, indeed, as Debye has pointed out, if it were not so, the coefficient of expansion of solids would be zero. Having granted, then, that near the melting-point atoms will depart from simple harmonic motion, it is difficult to resist the conclusion that such departure will affect the specific heat. The exact extent of this contribution cannot at present be determined, but, in our opinion, it certainly exists.

Investigations on other substances are in progress in this laboratory in order to elucidate the matter.

### *Summary.*

Observations of the specific heat of pure mercury have been made over a range of  $200^\circ$  to  $285^\circ$  abs., which includes the melting-point ( $234^\circ$  abs.). The results have been reduced to give values of  $C_v$ , the atomic heat at constant volume, though, owing to lack of accurate data on the expansion coefficient, the reduction is somewhat doubtful.

The shape of the  $C_v$  curve is significant in that it shows an increase of slope in the neighbourhood of  $210^\circ$  abs., followed by a subsequent flattening. The curve is certainly not concave upwards at the melting-point.

The significance of the results obtained is discussed with regard to the relative contributions of free electrons and of anharmonic atomic oscillations.

\* *Zeits. f. Physik*, lii. 7-8, p 555 (1928).

Our thanks are due to Professor Lindemann, who suggested this investigation, to Professor Stansfield, in whose laboratory it was carried out, and to the Department of Scientific and Industrial Research, who made it possible for one of us (L. G. Stoodley) to engage in the work.

16th April, 1930.

---

*XXI. The Dielectric Polarization of Liquid Mixtures and Association.*—Part I. *By* N. N. PAL, *M.Sc., Research Scholar, Dacca University* \*.

ABSTRACT.

THE paper describes an investigation, by the heterodyne heat method, of the dielectric polarization of mixtures of nitrobenzene and benzene and of nitrobenzene and carbon tetrachloride, of various concentrations and at various temperatures. The results are discussed on the basis of Debye's dipole theory and the assumption of molecular association.

---

*Introduction.*

IT is well known that the Debye expression for the dielectric constant of a medium consisting of electrically polar molecules fails in the case of liquids, though the agreement is generally very good in the case of vapours.

We explain this failure on the assumption that in the liquid state the polar molecules do not all exist in the same simple form, but that a considerable fraction of the total number combine to form more complicated structures. We have independent experimental evidence in favour of this existence of association, and one would generally expect that the molecules with large electrical moment would naturally show this tendency to associate to a marked degree.

The nature of this association is, however, not very clearly understood; Debye † has suggested an electrical theory of association, much on the same lines as his theory of dissociation, and has shown that the general qualitative nature of the phenomena can in some cases be explained from this standpoint. It is clear, however, that more data regarding the

\* Communicated by Prof. S. N. Bose, M.Sc.

† Debye in Marx's '*Handbuch der Radiologie*,' vi. (1925).

various influences of dilution and temperature on the so-called association have to be collected and compared with the theory before it can be regarded as satisfactorily established. The measurements of dielectric constants of binary mixtures, consisting of a polar and a non-polar liquid, may be expected to give valuable data regarding the nature of association, as we can thus vary the concentration of the polar molecules.

This aspect of the problem does not seem to have attracted much attention; most of the work done on the dielectric constants of polar liquids (except those of Lange\* and Williams and Mathews†) have been with a view to determine the permanent electric moment of the individual molecules, and for this purpose the general tendency has been to concentrate on the values of the dielectric constants of mixtures at large dilutions rather than a careful determination of the general behaviour.

It is with an aim to examine more closely the nature of the association that this work has been taken up. The programme of work has been to take mixtures of different non-polar solvents and to examine carefully the influence of temperature and concentration, as well as the action of the solvent in each case.

The present paper, which forms Part I. of the series, describes a detailed study of the dielectric polarization of nitrobenzene in solutions of carbon tetrachloride and benzene at different concentrations and at various temperatures, and an attempt is made to correlate the general features of the results obtained with the electrical theory of association.

### *Experimental Procedure.*

The measurements of dielectric constants were made by a heterodyne beat arrangement similar to that used by Zahn‡ in the case of gases. The general arrangement of the apparatus will be clear from fig. 1. As this method of measurement is now sufficiently well known, we need mention here only those points which are specially important in this connexion.

As pointed out by Zahn, the accurate determination of the dielectric constants mainly depends upon a careful calibration of the condenser system. Great importance has, therefore, been attached to the calibration of the condenser system, which consists of the variable condenser 500 m.m.F., a

\* Lange, *Zeits. f. Phys.* Bd. 33 (1925).

† Williams and Mathews, *Zeits. Phys. Chem.* cxxx. (1927).

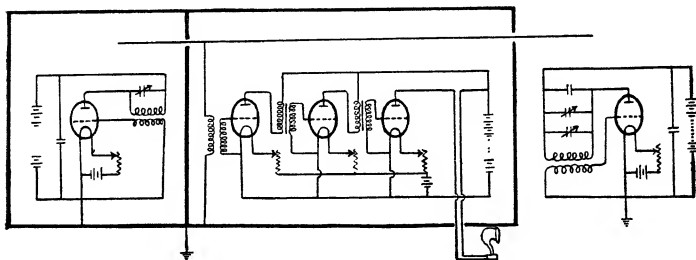
‡ C. T. Zahn, *Phys. Rev.* xxiv. (1920).

vernier condenser 25 m.m.F., and the cell condenser, all placed in parallel. One division of the scale attached to the variable condenser corresponds to  $\frac{1}{2}$  m.m. F., while that of the vernier one reads  $1/25$  m.m.F. The calibration of the bigger condenser has been carefully made by a fixed air condenser specially prepared for the purpose, and that of the vernier one by a neutrodyne condenser. Every condenser was carefully shielded, and final adjustments of the condenser were made from a distance by means of a long glass rod. In fact, the method was very sensitive for the present purpose.

The measurements were done by electric waves of 1200 kilocycles. Marconi P.M. 4 valves were used to produce the continuous oscillations, while Cossor valves were employed in the amplifying circuit.

The cell condenser is a cylindrical gold-plated brass condenser with about 1.5 mm. separation between the

Fig. 1.



cylinders and is similar to that used by Zahn. The two cylinders are held together and insulated by means of two small glass pieces (fig. 2). The condenser is mounted in a glass tube fitted up with a glass-stoppered mouth.

The oscillations were observed to be steady only after half-an-hour's run, as was evident from the constancy of the beat note between the fork (electrically maintained) and the loud speaker. Readings were always taken when this secondary beat note became steady, for then the cell condenser had assumed the temperature of the bath.

The capacity of the cell condenser under any circumstances was measured by the method of substitution, except when with the higher concentration of nitrobenzene its capacity was greatly increased and went outside the limit of the variable condenser. The cell capacity under these conditions was determined by measuring the effective capacity of the cell and an auxiliary fixed condenser placed in series. Of

course, the original sensitiveness is to some degree diminished, but it is recovered to a great extent by making the fixed condenser as great as the variable one. In the particular experiment one of 450 m.m.F. was used, which was carefully shielded, preserved from external heat, and calibrated in position. The cell capacity thus measured was corrected for the lead capacity, which was determined by preparing an imitation lead and measuring its capacity. The contribution from the glass pieces was calculated to be very small.

The liquids used were Merck's extra pure; they were shaken with calcium chloride, kept over night and after

Fig. 2.

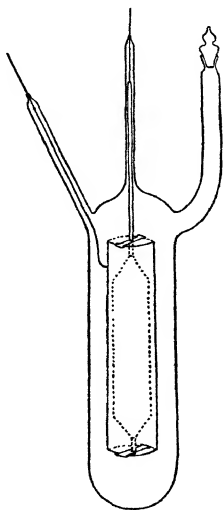
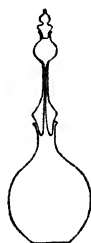


Fig. 3.



The cell condenser and the sp. gr. bottle.

decantation twice distilled, the distillate being received in a vessel provided with a side tube containing calcium chloride. The purpose was to obtain samples pure and free from moisture. Solutions were made by mixing known weights of two components. The process of weighing and mixing was made in stoppered flasks, so that there was evaporation only when the solution was being transferred from one vessel to another. Owing to the large capacity of the cell (100 c.c.), this, however, did not appreciably affect the concentration or the measurement.

A water bath in a large glass vessel was used, care being taken to maintain the constant level of the bath and to dip

the condenser in the bath up to the same point, for although the condenser was shielded on account of its outside cylinder being earthen, a slight effect of the level of the bath upon the capacity was noticed. The density bottle was suspended in the bath by a network of threads.

The density measurements were made simultaneously with the dielectric constant measurements in the same bath by a gravity bottle fitted up with a special type of mouth (fig. 3). The error in the density measurements seems to be not greater than 5 in 10,000.

### Discussions and the Results.

According to Debye \* P, the molar dielectric polarization of a perfectly miscible binary liquid mixture, is given by

$$P = \frac{\epsilon - 1}{\epsilon + 2} \cdot \frac{M_1 C_1 + M_2 C_2}{\rho},$$

where  $\epsilon$  and  $\rho$  are the dielectric constant and the density of the mixture.  $M_1$ ,  $M_2$  and  $C_1$ ,  $C_2$  are the molecular weights and molar fraction concentrations of the non-polar and the polar liquids respectively.

P can also be assumed as equal to  $P_1 C_1 + P_2 C_2$ , where  $P_1$  denotes the contribution to the total polarization of the non-polar solvent, and may be put equal to

$$\frac{\epsilon_1 - 1}{\epsilon_1 + 2} \cdot \frac{M_1}{\rho_1},$$

and  $P_2$ , the polarization due to the polar solute. Since these molecules of the second kind have dipole moments, we can further split it up into two portions, first, the induced polarization A, which is generally taken to be the optical value extrapolated to zero-frequency, and a part  $P_3$ . In the absence of association, according to the simple Debye theory,

$P_3$  can be expressed in the form  $\frac{B}{T}$ , where  $B = \frac{4\pi N \mu^2}{3 \cdot 3k}$ ,

$\mu$  being the electrical moment of the molecule.

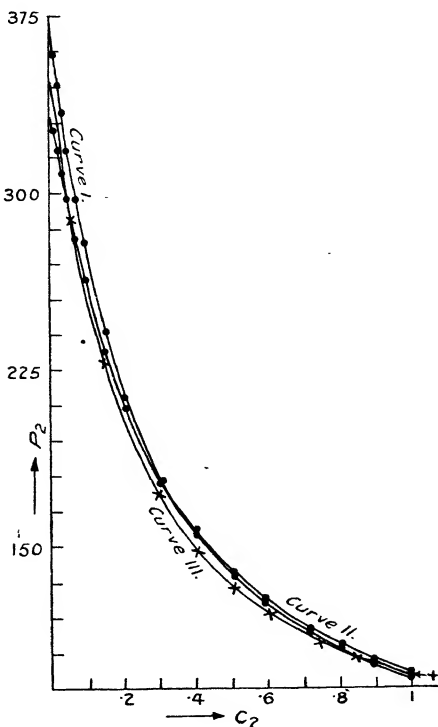
A determination of B therefore enables us to calculate the electric moment of the dipole molecule. The presence of association, on the other hand, is revealed by the variation of  $P_3$  with concentration even at any fixed temperature.

On the assumption that the increase in dilution or the rise of temperature will favour dissociation, we can try to interpret the variation of  $P_3$  with increasing dilution as an indication

\* Debye in Marx's 'Handbuch der Radiologie,' vi. (1925).

of the presence of a greater number of unassociated molecules. In the particular case of nitrobenzene the dilution increases  $P_2$  continuously, as will be seen in Curve I. and from Tables I. and II. (pp. 272-274), and hence we can conclude that the association tends to generate complex molecules of lesser moments.

CURVE I.



Curve I. For nitrobenzene at 10° C. with  $\text{CCl}_4$  as solvent.

Curve II. " at 50° C.

Curve III. " at 27° C. with benzene as solvent.

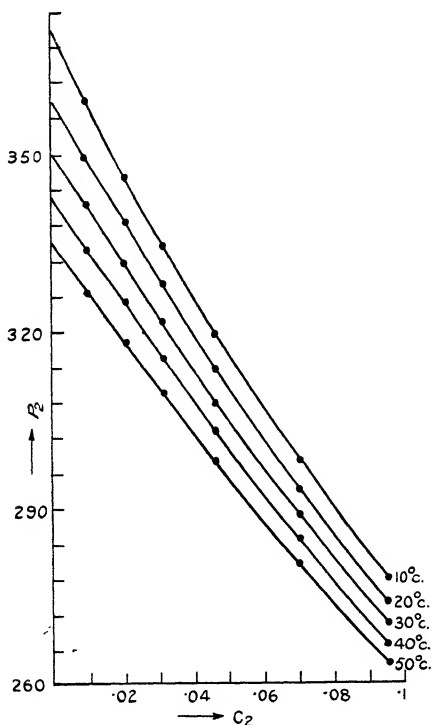
If we assume, as suggested by Debye\*, that association consists in the formation of double molecules with zero moment in this particular case, which will be easily understood if we regard the molecules as having an elongated

\* Debye in Marx's 'Handbuch der Radiologie,' vi. (1925).

shape, which tend to form mutually compensated pairs, we can regard the polarization  $P_2$  as consisting of contributions from  $n_1$  undissociated molecules and  $n_2$ , the rest, being dissociated molecules. Then  $P_2$  can be written as

$$P_2 = n_1 A' + n_2 \left( A' + \frac{B'}{T} \right) = (n_1 + n_2) A' + n_2 \frac{B'}{T}.$$

CURVE II.



Polarization curves for nitrobenzene with  $\text{CCl}_4$  as solvent.

In the above formula, we assume that both the dissociated as well as the undissociated molecules have the same induced polarization, whereas it is only the dissociated molecules which contribute a further portion in the dielectric polarization by an orientation which evidently can be calculated and expressed in terms of the usual kinetic theory basis as in the



TABLE I.

## Nitrobenzene and Benzene.

 $t = 27^\circ \text{C}$ .  $n$ , number of nitrobenzene mols. per c.c.

$$= \frac{\rho C_2}{M_1 C_1 + M_2 C_2} \cdot N.$$

$C_2$	$\rho$	$\epsilon$	P.	$n/N \times 10^4$	$P_2$	$B \times 10^{-2}$ with $A = 33$ .
0	·8707	2·275	26·73	0		
·0624	·8919	3·708	42·98	6·882	287·1	762
·1475	·9243	5·811	56·39	16·11	227·8	584·4
·2984	·9806	10·064	70·03	32·0	171·8	416·4
·4088	1·019	13·55	76·38	43·20	148·1	345·3
·5105	1·052	16·92	80·74	53·19	132·5	298·5
·6132	1·085	20·56	84·35	62·99	120·7	263·1
·7478	1·126	25·60	88·37	75·43	109·2	228·6
·8437	1·155	29·70	90·90	84·01	102·8	209·4
1	1·196	33·0	94·73	97·21	94·73	185·2

TABLE II.

## Nitrobenzene and Carbon Tetrachloride.

$C_2$	$t^\circ \text{C}$	$\rho_0$	$\epsilon_0$	P.	$n/N \times 10^4$	$P_2$	$B \times 10^{-2}$
0	10	1·6133	2·245	27·967	0		
	20	1·5940	2·224	27·966			
	30	1·5747	2·203	27·962			
	40	1·5555	2·183	27·972			
	50	1·5362	2·163	27·977			
·009851	10	1·6094	2·460	31·230	1·033	358·9	922·3
	20	1·5903	2·428	31·134	1·020	349·2	
	30	1·5712	2·398	31·061	1·008	341·7	935·4
	40	1·5520	2·368	30·982	·996	333·7	
	50	1·5328	2·339	30·910	·983	326·4	947·7
·02101	10	1·6047	2·709	34·645	2·201	345·7	884·9
	20	1·5859	2·666	34·490	2·175	338·3	
	30	1·5669	2·625	34·350	2·149	331·6	904·8
	40	1·5479	2·585	34·212	2·123	325·1	
	50	1·5289	2·546	34·075	2·097	318·5	922·2
·03193	10	1·6006	2·931	37·748	3·344	334·2	852·5
	20	1·5818	2·906	37·541	3·304	327·7	
	30	1·5628	2·853	37·344	3·265	321·5	874·2
	40	1·5438	2·802	37·154	3·225	315·6	
	50	1·5248	2·752	36·958	3·185	309·5	893·1

TABLE II. (*cont.*)  
Nitrobenzene and Carbon Tetrachloride.

C <sub>2</sub> .	t° C.	$\rho_0$ .	$\epsilon_0$ .	P.	$n/N \times 10^4$ .	P <sub>2</sub> .	B $\times 10^{-2}$ .
·04686	10	1·5946	3·314	41·615	4·903	319·2	809·9
	20	1·5759	3·240	41·338	4·846	313·2	
	30	1·5571	3·170	41·078	4·788	307·7	832·3
	40	1·5383	3·106	40·860	4·730	303·0	
	50	1·5196	3·042	40·615	4·673	297·8	855·3
·07064	10	1·5849	3·900	47·034	7·382	297·8	749·4
	20	1·5665	3·796	46·703	7·296	293·2	
	30	1·5481	3·698	46·386	7·211	288·7	774·8
	40	1·5295	3·606	46·094	7·124	284·5	
	50	1·5108	3·520	45·827	7·037	280·8	800·4
·09586	10	1·5745	4·549	51·930	10·00	277·92	693·1
	20	1·5566	4·408	51·550	9·89	273·95	
	30	1·5385	4·276	51·191	9·77	270·21	718·7
	40	1·5203	4·154	50·863	9·66	266·80	
	50	1·5022	4·046	50·602	9·54	264·06	746·3
·1527	10	1·5516	6·101	60·520	15·89	241·13	589·0
	20	1·5342	5·877	60·183	15·71	238·93	
	30	1·5169	5·674	59·880	15·53	236·94	617·9
	40	1·4995	5·485	59·592	15·35	235·06	
	50	1·4823	5·313	59·335	15·18	233·37	647·2
·2098	10	1·5285	7·795	66·880	21·76	213·43	510·6
	20	1·5118	7·486	66·647	21·52	212·32	
	30	1·49517	7·197	66·412	21·28	211·02	539·4
	40	1·4783	6·934	66·209	21·05	210·03	
	50	1·4618	6·687	65·994	20·81	209·06	568·7
·3103	10	1·4873	10·950	74·530	31·99	178·02	410·4
	20	1·4720	10·465	74·421	31·66	177·67	
	30	1·4565	10·026	74·343	31·33	177·41	437·6
	40	1·4411	9·621	74·267	30·99	177·17	
	50	1·4255	9·235	74·182	30·66	176·90	464·8
·4039	10	1·4494	14·197	79·477	41·41	155·50	346·7
	20	1·4350	13·543	79·506	40·99	155·56	
	30	1·4205	12·928	79·528	40·58	155·62	371·5
	40	1·4060	12·359	79·546	40·17	155·66	
	50	1·3916	11·853	79·593	39·76	155·78	396·6
·5001	10	1·4099	17·755	83·268	50·94	138·54	298·6
	20	1·3962	16·919	83·420	50·44	138·85	
	30	1·3825	16·123	83·549	49·95	139·10	321·5
	40	1·3689	15·406	83·690	49·46	139·39	
	50	1·3553	14·742	83·831	48·97	139·60	344·3
·5917	10	1·3726	21·39	86·113	59·90	126·23	263·8
	20	1·3597	20·29	86·299	59·34	126·55	
	30	1·3468	19·28	86·483	58·77	126·80	284·2
	40	1·3341	18·37	86·666	58·22	127·10	
	50	1·3213	17·55	86·871	57·66	127·51	305·3

TABLE II. (*cont.*)

Nitrobenzene and Carbon Tetrachloride.

$C_2$	$t^\circ \text{C.}$	$\rho_0$	$\epsilon_0$	P.	$n/N \times 10^4$	$P_2$	$B \times 10^{-2}$
7166	10	1.3224	26.48	89.128	71.93	113.31	227.3
	20	1.3106	25.06	89.375	71.29	113.66	
	30	1.2989	23.78	89.622	70.65	114.00	245.5
	40	1.2872	22.66	89.895	70.02	114.38	
	50	1.2754	21.70	90.218	69.37	114.84	264.4
8046	10	1.2882	30.40	90.882	80.33	106.16	207.1
	20	1.2770	28.78	91.186	79.64	106.54	
	30	1.2658	27.33	91.502	78.94	106.93	224.0
	40	1.2546	26.00	91.819	78.24	107.32	
	50	1.2434	24.88	92.183	77.54	107.78	241.5
8936	10	1.2539	34.71	92.480	88.73	100.16	190.1
	20	1.2433	32.79	92.810	87.98	100.53	
	30	1.2327	31.16	93.174	87.23	100.94	205.9
	40	1.2221	29.69	93.548	86.48	101.36	
	50	1.2115	28.47	93.972	85.73	101.83	222.3
1	10	1.2135	39.98	94.116	98.66	94.12	173.0
	20	1.2035	37.56	94.451	97.85	94.45	
	30	1.1935	35.46	94.805	97.03	94.80	187.3
	40	1.1836	33.67	95.180	96.22	95.18	
	50	1.1736	32.03	95.566	95.41	95.57	202.1

Debye theory. On the assumption that  $(n_1 + n_2) A_1'$  can be calculated by extrapolation of the optical value, we get

$$P_3 = n_2 \frac{B'}{T}.$$

The number  $n_2$  of the dissociated molecules, however, is now a function of the concentration as well as the temperature, and we can take  $P_3 T$  to be proportional to the number of dissociated molecules at any dilution and temperature and a variation of  $P_3 T$  as an indication of the variation of association.

There is, however, one difficulty in calculating  $P_3$  which is generally overlooked. The value of  $A$  is generally taken to be, in all concentrations usually made, equal to the value at optical frequency, though specially in the case of polar molecules it is open to grave objections. The polar liquids are generally known to possess characteristic absorption-frequencies in the long wave-length regions, generally for wave-lengths of the order of a few metres, and an extrapolation over these critical frequencies seems scarcely theoretically justifiable.

We have, therefore, tried a different tentative calculation, and as the result seems encouraging, we venture to put forward the considerations, which are as follows:—

If, tentatively, we assume that the number of dissociated molecules at any dilution is given by a formula

$$n = N_0 e^{-\epsilon/KT},$$

where  $\epsilon$  is of the nature of an energy threshold which determines association, and if, further, we assume that approximately the threshold value  $\epsilon$  is determined by the residual electrical attraction between the dipoles, we can take

$$\epsilon \propto \frac{1}{Dr^2},$$

where  $D$  is the dielectric constant of the solvent, and  $r$  the average distance between the dipoles. Now, the average distance  $r$  can be taken to vary as  $\frac{1}{n^{1/3}}$ ;

$$\therefore \epsilon = \frac{\alpha' n^{2/3}}{D}.$$

The polarization  $P_2$  will approximately be of the form

$$P_2 = A + \frac{BN}{T} e^{-\frac{\alpha' n^{2/3}}{DKT}},$$

or

$$\log(P_2 - A) = \log\left(\frac{BN}{T}\right) - \frac{\alpha' n^{2/3}}{DKT}.$$

It is found from Tables III. and IV. (pp. 276–278), as also from the Curve III., that remarkably enough, if the concentration be greater than .1, the dielectric constant of the mixture of nitrobenzene and benzene or nitrobenzene and carbon tetrachloride can be represented accurately by the formula

$$\log(P_2 - 62) = \log \beta - \alpha n^{2/3}.$$

We have also found that the value of the ratio of  $\alpha$  in the two cases varies almost inversely as the dielectric constants of the solvents. The values for lower concentrations, however, seem definitely to disagree with the above formula.

A comparison with the electrolytic dissociation theory will seem here not wholly out of place. It is well known that for binary electrolytes Ghose's formula, which is based on considerations very similar to the above, agrees very well with experiments; at high dilutions, however, there are slight discrepancies which can, on the other hand, be completely accounted for by the Debye-Hückel theory.

TABLE III.

Nitrobenzene with Benzene as solvent.

$(n/N)^{2/3} \times 10^2$ .	$\log_e (P_2 - 62)$ .	$\log_e (P_2 - 62) + a(n/N)^{2/3}$ .
·7798	5·4165	5·815
1·374	5·1108	5·812
2·172	4·6990	5·809
2·653	4·4545	5·810
3·047	4·2556	5·812
3·411	4·0725	5·815
3·846	3·8544	5·818
4·132	3·7087	5·819
4·555	3·4883	5·814

$a = 51·07 N^{2/3}$ .

TABLE IV.

Nitrobenzene with Carbon Tetrachloride as solvent.

(1) 10° C.

$(n/N)^{2/3} \times 10^3$ .	$\log_e (P_2 - 62)$ .	$\log_e (P_2 - 62) + a(n/N)^{2/3}$ .
2·201	5·6935	
3·645	5·6480	
4·817	5·6065	5·861
6·218	5·5499	5·878
8·168	5·4630	5·895
10·0	5·3750	5·904
13·62	5·1882	5·909
16·79	5·0201	5·909
21·71	4·7538	5·903
25·78	4·5380	5·903
29·60	4·3378	5·905
32·98	4·1625	5·908
37·26	3·9380	5·910
40·11	3·7880	5·910
43·86	3·6418	5·911
46·0	3·4695	5·904

$a = 52·81 \cdot N^{2/3}$ .

TABLE IV. (*cont.*).

Nitrobenzene with Carbon Tetrachloride as solvent.

(2) 20° C.

$(n/N)^{2/3} \times 10^3$ .	$\log_e (P_2 - 62)$ .	$\log_e (P_2 - 62) + a(n/N)^{2/3}$ .
2.184	5.6602	
3.617	5.6215	
4.780	5.5824	5.833
6.170	5.5263	5.849
8.105	5.4433	5.870
9.926	5.3563	5.876
13.514	5.1756	5.883
16.67	5.0126	5.885
21.56	4.7508	5.880
25.61	4.5386	5.880
29.41	4.3419	5.882
32.77	4.1675	5.883
37.04	3.9447	5.884
39.88	3.7969	5.885
42.62	3.6516	5.883
45.74	3.4798	5.876

$$a = 52.38 \cdot N^{2/3}.$$

(3) 30° C.

2.166	5.6337	
3.588	5.5970	
4.741	5.5590	5.805
6.120	5.5042	5.822
8.041	5.4237	5.841
9.850	5.3386	5.850
13.41	5.1644	5.860
16.547	5.003	5.861
21.41	4.7485	5.858
25.44	4.5390	5.858
29.22	4.3451	5.861
32.567	4.1722	5.861
36.82	3.9513	5.860
39.64	3.8052	5.861
42.37	3.6620	5.860
45.49	3.4904	5.850

$$a = 51.87 \cdot N^{2/3}.$$

TABLE IV. (*cont.*)

Nitrobenzene with Carbon Tetrachloride as solvent.

(4) 40° C.

$(n/N)^{2/3} \times 10^3$ .	$\log_e (P_2 - 62)$ .	$\log_e (P_2 - 62) + a(n/N)^{2/3}$ .
2.148	5.6046	
3.559	5.5726	
4.703	5.5358	5.777
6.071	5.4848	5.796
7.977	5.4049	5.814
9.771	5.3220	5.824
13.31	5.1536	5.836
16.42	4.997	5.838
21.260	4.7460	5.836
25.27	4.5396	5.835
29.03	4.3489	5.837
32.36	4.1759	5.836
36.60	3.9585	5.835
39.41	3.8137	5.834
42.13	3.6726	5.833
45.24	3.5019	5.823

$$a = 51.31 \cdot N^{2/3}.$$

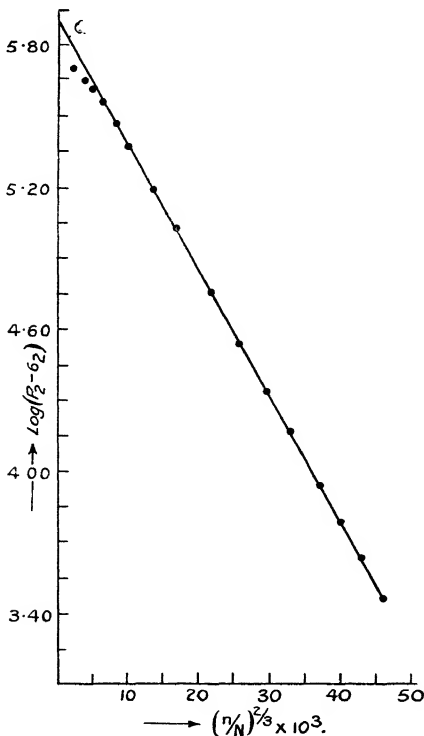
(5) 50° C.

2.131	5.5775	
3.529	5.5472	4
4.664	5.5114	5.749
6.022	5.4630	5.769
7.911	5.3882	5.791
9.694	5.3086	5.802
13.21	5.1437	5.815
16.300	4.9909	5.818
21.10	4.7440	5.818
25.10	4.5410	5.817
28.83	4.3516	5.818
32.15	4.1823	5.817
36.37	3.9673	5.816
39.17	3.8239	5.816
41.89	3.6842	5.814
44.99	3.5137	5.803

$$a = 50.87 \cdot N^{2/3}.$$

Perhaps a more rigorous calculation on the same lines will explain the discrepancies at lower dilutions (the deviations are in the same sense in the two cases), as well as have the above simple formula as a limiting case for strong concentrations.

CURVE III.



For nitrobenzene with carbon tetrachloride as solvent at 10° C.

It is admitted, however, that it is rather premature to lay too much stress on this single case of nitrobenzene, and the author intends to collect more data about the different polar liquids to test the empirical formula.

The work already done, however, seems to point definitely towards the electrical origin of association in polar liquids.



TABLE V.  
Moment of Nitrobenzene molecule.

Solvent.	$t^{\circ}\text{C.}$	$P_0 \text{ c.c.}$	$(P_0 - A)T$ $\times 10^{-2}$	Calc. $\mu \times 10^{18}$	Solvent.	Author.	$\mu \times 10^{23}$ .
Carbon tetra- chloride	10	373	956	3.92	Benzene	Lange	3.86
	20	359.3	956	3.92	CS <sub>2</sub>		
	30	350.3	961	3.94	CS <sub>2</sub>	Williams* & Ogg	3.89
	40	343	970	3.95	Hexane		
	50	335.3	976	3.96	Benzene	Williams† & Schwingel	3.90
Benzene	27	351	954	3.916	CCl <sub>4</sub>	Author	3.94 3.92
					Benzene		

$$A = 33.$$

\* Williams and Ogg, Am. Ch. Soc. Jour. January 1928.

† Williams and Schwingel, Am. Ch. Soc. Jour. 1. February 1928.

The author takes this opportunity of expressing his deepest gratitude to Professor S. N. Bose for his inspiring guidance and kind interest in the work.

University of Dacca,  
Ramna, Dacca,  
Bengal.

XXII. *On the Mechanism of the Electrodeless Discharge.*  
By JOHN THOMSON, M.A., B.Sc., Ph.D., Lecturer in  
*Physics in the University of Reading* \*.

*Introductory.*

THE purpose of the present communication is to give a brief account of a simple theory of the discharge with external electrodes. It is not suggested that the treatment is either conclusive or exhaustive, but the expressions which emerge from the analysis are sufficient to explain many phenomena characteristic of this type of discharge. They also suggest possible lines of experimental attack. An application of the Tesla Coil transformer to the production of high-tension high-frequency oscillations is also discussed. The writer has been able, by this means, to obtain "electrodeless" discharges at relatively high gas pressures.

\* Communicated by the Author.

The mechanism of the self-sustained discharge between metallic electrodes maintained at constant potentials is not yet clearly understood. The presence of the electrodes associated with the constant difference of potential between them causes the "life" of a gas ion to be very short indeed. This difficulty may in part be removed by the use of high-frequency alternating potentials; it may be almost entirely removed by applying the high-frequency oscillations to the discharge-tube by means of external electrodes. Under these circumstances ions produced in the discharge can only disappear owing to recombination or to diffusion to the walls, and consequently a self-sustained discharge will take place when the rate of formation of the ions is just more than sufficient to compensate for these losses. As a result it is unnecessary to postulate any ionizing mechanism beyond that due to collisions between electrons and molecules. The bulk of the electrons produced in this way remain in the field; they are not neutralized at an electrode after a relatively short "life." Hence the controversy which still exists concerning the action of the positive ions need not concern us.

*Conditions for the Ionization of a Gas by a High-frequency Field.*

Making the simplest possible assumptions, suppose a free electron to move under the action of an alternating electric field  $E \cos \omega t$ ; then

$$m \frac{d^2 x}{dt^2} = E e \cos \omega t;$$

whence, if  $x=0=\frac{dx}{dt}$ , when  $t=0$ ,

$$\frac{dx}{dt} = \frac{E}{\omega} \frac{e}{m} \sin \omega t,$$

and

$$x = \frac{E}{\omega^2} \frac{e}{m} (1 - \cos \omega t).$$

The assumption that  $\frac{dx}{dt}=0$  at  $t=0$  is, of course, an approximation; but since the velocity of agitation of an electron is of the order  $10^5$  cm./sec. at room temperature, and since the velocity producing ionization is of the order  $10^8$  cm./sec., the former may easily be neglected in comparison with the

latter. Relativity corrections have also been neglected for similar reasons.

The electron will have acquired sufficient energy to ionize a gas molecule colliding with it at time  $t$ , if

$$\frac{1}{2}m\left(\frac{E}{\omega} \frac{e}{m} \sin \omega t\right)^2 > Ve, \quad . . . . (1)$$

where  $V$  is a gas constant related to the ionizing potential of the molecule. This is our first condition for ionization. The second condition must limit in some way or another the distance travelled by the electron while acquiring an ionizing velocity. For, should the electron collide inelastically with a molecule before attaining this velocity, or, conversely, should it not collide with a molecule until it had lost this velocity, then ionization would not in general occur. Writing this condition in the most general way to include the possibilities of a discharge at very low gas pressures,

$$\frac{Ee}{\omega^2 m} [2n+1+(-1)^{n+1} \cos k\pi] < L \quad \text{if } k < \frac{1}{2}, \quad . (2)$$

$$\frac{Ee}{\omega^2 m} [2n+1+(-1)^{n+1} \cos k\pi] > L \quad \text{if } k > \frac{1}{2}, \quad . (3)$$

where  $\omega t = (n+k)\pi$ ,  $n$  is an integer,  $k$  is fractional, and  $L$  is a quantity proportional to the mean free path of the electron. These conditions state that when the electron is about to collide inelastically with a molecule it shall be moving with the ionizing velocity. Condition (2) applies to the case where the speed of the electron is increasing, condition (3) to the case where the speed is decreasing. The limiting values of  $k$  are supposed to be determined from condition (1).

At low pressures yet another condition becomes operative. If  $L$  for the electron is greater than the length of the discharge-tube, then, in order that the electrons should not be absorbed by the glass, the amplitude of the oscillations performed must be less than a certain length related in some way to the length of the tube, *i. e.*,

$$\frac{E}{\omega^2} \frac{e}{m} < l. \quad . . . . (4)$$

These four conditions are in themselves sufficient to define the electric field  $E$  and pulsatace  $\omega$ , suitable for the production of ions at any pressure. However, as the pressure is varied, the four conditions vary in relative importance. For example, if the gas considered is air in

a tube 20 cm. long, and the pressure is greater than a certain minimum which is certainly less than 0.1 mm. of mercury, the fourth condition is of no importance,  $L$  being certainly less than  $l$ . Again, for frequencies less than  $10^7$  per sec., and so long as  $L$  is less than about 40 cm.,  $\omega t$  must be less than  $\pi/2$ , as defined by (1). Therefore, under these circumstances, conditions (2) and (3) may be written

$$\frac{E}{\omega^2} \frac{e}{m} (1 - \cos \omega t) < L. \quad (2')$$

But to say that  $L$  is less than 40 cm. is to say that the pressure is greater than a minimum as yet undefined, but certainly less than 0.1 mm. in air. Hence, unless the pressure is very low or the frequency of the impressed voltage very high, our conditions simplify to the eminently workable form

$$\frac{1}{2} \frac{E^2}{\omega^2} \frac{e}{m} \sin^2 \omega t > V \quad (1')$$

and

$$\frac{Ee}{\omega^2 m} (1 - \cos \omega t) < L. \quad (2')$$

If  $\omega t$  is eliminated between these two conditions, remembering that  $\omega t < \pi/2$ , the resulting condition is

$$E > \frac{V}{L} + \frac{L\omega^2}{2e/m}. \quad (5)$$

Write  $\omega = 2\pi\nu$ , where  $\nu$  is the frequency of the oscillation, and  $L = K/p$ , where  $p$  is the gas pressure; then

$$E > \frac{Vp}{K} + \frac{4\pi^2\nu^2 K}{2pe/m}. \quad (5')$$

Now consider  $p/K$  as a variable  $x$ , and assume approximate values for the other constants. Let  $\nu = 10^7$ ,  $V = 2 \cdot 10^9$ , and, since the velocities of the electrons are small compared with the velocity of light, let  $\frac{e}{m} = \frac{e}{m_0} = 1.8 \cdot 10^7$ ; then

$$E > Vx + \frac{2\pi^2\nu^2}{ex/m},$$

or

$$E > 2 \cdot 10^8 \left( 10x + \frac{1}{2x} \right).$$

Write

$$E = 2 \cdot 10^8 \left( 10x + \frac{1}{2x} \right); \quad (6)$$

then equation (6) should represent with fair accuracy the mode of variation with the gas pressure of the electric field of frequency  $10^7$  per sec. necessary to produce ions by electronic collision. Going back to condition (5), and writing it as an equality, the mode of variation of the electric field with the frequency is obtained.

*Conditions for the Maintenance of a Discharge.*

If the ions did not recombine or diffuse to the walls, the four conditions already given would be sufficient to define the fields and frequencies necessary for a discharge. If, however, the rate of destruction of the ions due to diffusion is represented by  $\beta n$ , where  $n$  is the number of ions per c. c. at time  $t$ , and the rate of destruction due to recombination by  $\gamma n^2$ , while the ions are being formed at rate  $\alpha n$ , then

$$\frac{dn}{dt} = (\alpha - \beta)n - \gamma n^2,$$

whence

$$n = \frac{\alpha - \beta}{\gamma + (\alpha - \beta - \gamma)e^{-(\alpha - \beta)t}};$$

and when  $t = \infty$ ,

$$n = \frac{\alpha - \beta}{\gamma}.$$

Hence, for a discharge to take place  $\alpha - \beta$  must be very great relative to  $\gamma$ . The rate of recombination will not be a function of the gas pressure, nor will the rate of diffusion. Hence equation (6) will exhibit the mode of variation with the pressure of the field necessary to maintain the discharge: but the absolute value of  $E$  will not be given by the equation unless the losses due to diffusion and recombination are small. Townsend\* states that there is no appreciable recombination in a high-frequency discharge, basing his conclusion on the experimental fact that the field necessary to produce a discharge is independent of the current. Recombination or some equivalent process must of course take place if the discharge is to be luminous.

Kirchner†, in an important paper on the subject of the high-frequency discharge, has given accurate curves showing the variation of the "maintainance potential" with the pressure. The discharge-tube which he used was furnished with internal electrodes, but under the conditions of his

\* *Comptes Rendus*, clxxvi. p. 55 (1928).

† *Ann. d. Physik*, lxxvii. p. 287 (1925).

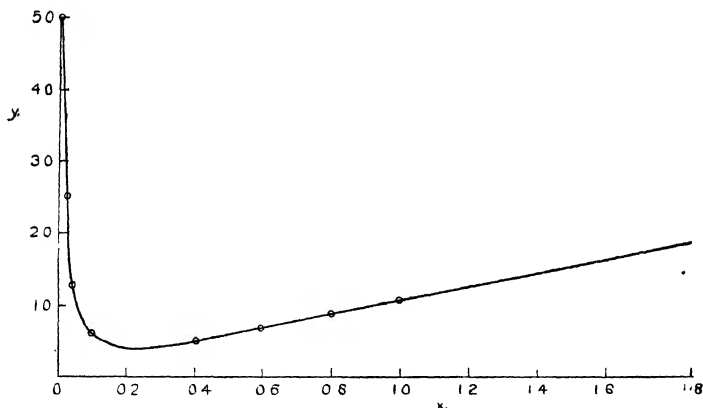
experiments these merely increased the rate of destruction of the ions. Otherwise (with certain restrictions as to electrode distances) the theory given above may be applied to his results. A striking confirmation of equation (6) is obtained.

Fig. 1 shows the curve

$$y=10x+\frac{1}{2x}$$

Fig. 2 is a reproduction of two figs. from Kirchner's paper. Fig. 2 (a) exhibits the mode of variation of the potential necessary to maintain the discharge with the pressure in the gas oxygen, while fig. 2 (b) shows similar curves for air.

Fig. 1.



If the discharge is maintained by means of metallic rings surrounding the tube, the field due to the applied E.M.F. will not be uniform even when there is no electron current flowing. If there is a potential difference  $P$  between the rings at any instant, then the mode of variation of the electric field along the common axis of the rings is indicated in fig. 3, the distance between the rings measured along the axis being  $d$ , and the radius of the rings in this case being  $d/3$ . It will be observed that the maximum field in the region between the rings may be considerably greater than the mean field  $P/d$ . The components of the electric field are given by elliptic integrals, and a consideration of these has shown that the maximum variation in the resultant field takes place along the axis.

In the case of a discharge with external electrodes it is therefore not admissible to consider the electric field

Fig. 2 (a).

Oxygen.

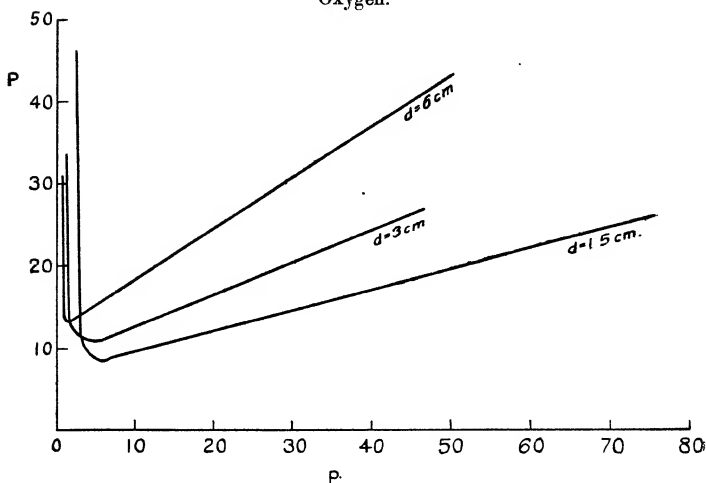
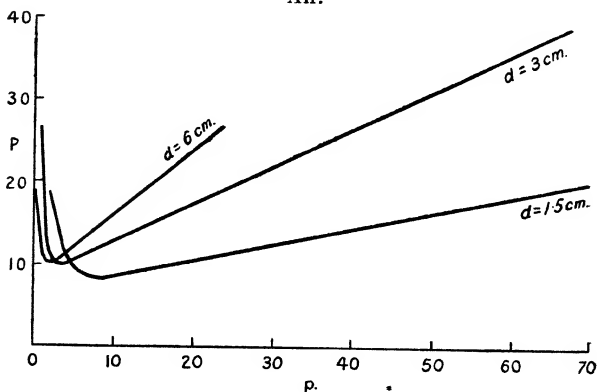


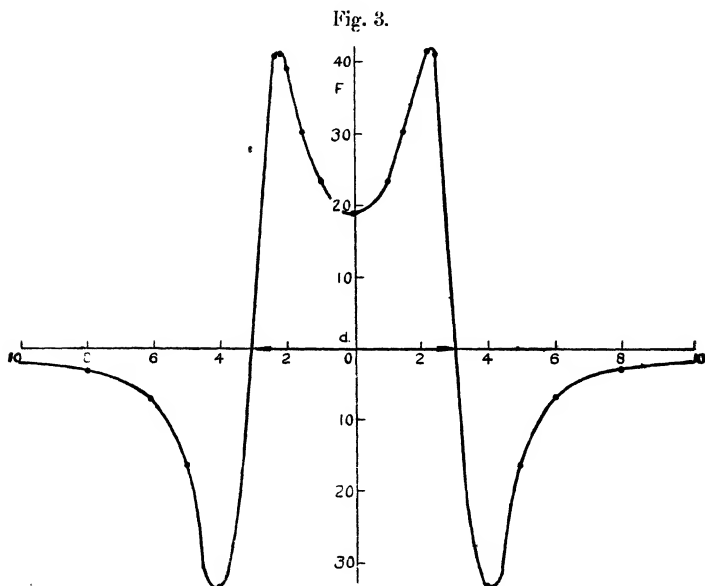
Fig. 2 (b).

Air.



producing ionization as the mean field, but a first approximation to the field will be obtained by dividing the peak potential difference by the distance between the rings.

In the case of a discharge with internal electrodes the variation of the field along the axis is not so marked, and the mean field will give a better approximation to the ionizing field. It is to be expected that the passage of any considerable current through the gas will further disturb the electrostatic distribution of potential.



If, as a first approximation, we assume  $E = P/d$ , where  $P$  is the peak potential difference between the electrodes, and  $d$  their distance apart, then equation (6) becomes

$$P = 2 \cdot 10^8 d \left( 10x + \frac{1}{2x} \right),$$

and when  $x$  is large the curve becomes a straight line whose gradient is proportional to  $d$ . This is also indicated unequivocally by Kirchner's curves. The fact that the potential difference between the electrodes producing a discharge is a linear function of the distance between the electrodes has also been noted by Townsend, Gutton, and others, and has led them to draw analogies between the high-frequency discharge and the positive column of a "straight" discharge.



Returning to the condition (5'), and writing the limiting equation

$$P = V \frac{pd}{K} + \frac{2\pi^2 \nu^2 K d}{p e/m}, \quad \dots \dots (7)$$

P has a minimum value given by

$$\left. \begin{aligned} P_m &= 2V \frac{pd}{K} \\ \text{when} \quad p_m^2 &= \frac{2\pi^2 \nu^2 K^2}{V e/m} \end{aligned} \right\} \dots \dots (8)$$

Kirchner's values for the constants involved should be fairly accurate when the distance between the electrodes is reasonably large, and so we take his curve for  $d=3$  cm., the gas being air,  $\nu=3.5 \cdot 10^7$  per sec.,  $P_m=4.6 \cdot 10^9$  e.m.u.,  $p_m=3 \cdot 10^{-3}$  cm. of mercury. Substituting in equations (8) we find  $V=4$  volts,  $K=2 \cdot 10^{-3}$ , whence  $L=200$  cm. when  $p=.0001$  mm. At this pressure the mean free path of the electron in air as calculated from the kinetic theory of gases is about 400 cm. Hence equation (7) not only predicts the experimental curve, but gives at least the correct order for the constants involved. Possibly the agreement between experiment and theory would be closer if accurate data were available for the discharge with external electrodes. The agreement obtained appears to indicate that the rate of destruction of ions at this frequency is negligible.

#### *Condition for a Discharge at any Pressure.*

From condition (1) no discharge can take place at any pressure whatsoever unless

$$\frac{E^2}{\nu^2} > \frac{8\pi^2 V}{e/m} \dots \dots (9)$$

Now Kirchner finds that with  $\nu=3.5 \cdot 10^7$  the minimum E is of the order  $1.5 \cdot 10^9$  e.m.u. Assuming  $V=2.6 \cdot 10^9$  for the gas, which was neon,

$$\frac{E^2}{\nu^2} \doteq 2 \cdot 10^3,$$

while

$$\frac{8\pi^2 V}{e/m} \doteq 10^4.$$

Again the quantities are of the correct order of magnitude. If cumulative ionization takes place (and in neon this is very probable),  $V$  might easily be one-fifth of the assumed value. Kirchner's values for  $E$  are maintainance values. The fields required to start a discharge he finds unreliable, but about three times the maintainance values (in the case of air). Hence it may be supposed that for the discharge to start, the electron must first fall through a potential comparable with the ionization potential. When the discharge is once started, however, the probability of cumulative ionization occurring is great, and the value of  $V$  in our equations diminishes greatly. This is equivalent to saying that the ionization efficiency of the electrons varies with the electron density. Apart altogether from such conjectures, it may be seen that equation (9) correctly predicts the possibility of a discharge with potential differences smaller than the ionizing potential of the gas.

*Variation of the Maintainance Potential with the Frequency.*

The equation (7) suggests that as the frequency of the applied E.M.F. increases the potential necessary to produce a discharge also increases. It must be observed, however, that at high gas pressures the term  $\frac{2\pi^2\nu^2 Kd}{pe/m}$  is relatively unimportant, unless  $\nu$  is very large indeed. As has already been shown, the variation of  $P$  is then given approximately by

$$P = V \frac{pd}{K}.$$

Also, the losses due to diffusion of the electrons will depend in some way on the frequency of the E.M.F. It might be suggested that the greater the amplitude of their free oscillations the greater the losses would be. This would obviously be the case with internal electrodes. But the amplitude varies inversely as the square of the frequency, and consequently it might be expected that the greater the frequency the smaller the diffusion losses would be. It is therefore suggested that the complete expression for the discharge potential ought to contain a factor  $\phi(\nu)$  such that it decreases as  $\nu$  increases—i. e.,

$$P = \phi(\nu) \left[ V \frac{pd}{K} + \frac{2\pi^2\nu^2 Kd}{pe/m} \right]. \quad (7')$$

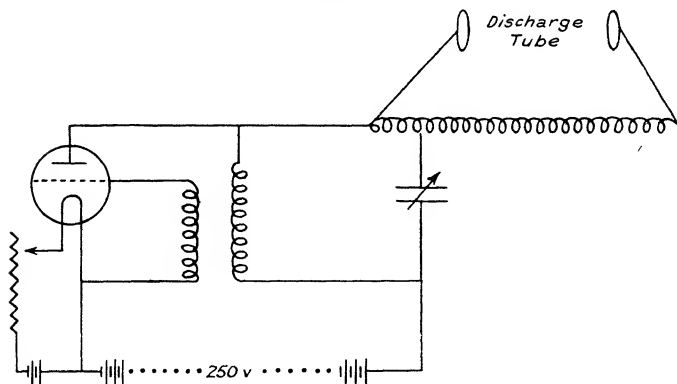
This is also suggested by the condition (4).

Summarizing the results of the preceding discussion, it may be said that the high-frequency discharge may obviously be maintained by the ionization produced only by electronic collisions. The equations and conditions derived from this hypothesis are sufficient to explain the mode of variation of the maintenance potential with the pressure. The magnitudes of the gas constants obtained from them are at least of the correct order. Also, while the mode of variation of the maintenance potential with the frequency is not given by the simple equation derived, other considerations at least indicate how the experimental facts might be explained.

*The Application of the Tesla Transformer to the Production of High-Frequency Discharges.*

The circuit employed by the writer is shown in fig. 4. Large alternating currents of approximate frequency  $10^6$

Fig. 4.



were produced by means of four Marconi T15 valves in parallel. This current was sent through the bottom four or five turns of a Tesla Coil. The latter contained about 130 turns of stout copper wire of radius 15 cm., the turns being about 1 cm. apart. Peak voltages of about 4000 were obtained across the whole coil. By means of a variable condenser in the oscillating circuit the applied frequency could be varied. Exceedingly sharp resonance was obtained with the Tesla Coil, and consequently a small variation in the capacity controlled the potential applied to the discharge-tube without seriously altering the frequency. In this way

discharges were obtained at pressures ranging from 0.01 mm. to 10 mm. The remarkable striations examined by Richards \* were observed. This appears to be a very suitable method for the production of high potentials at a frequency of a million per second.

Physics Department,  
The University of Reading,  
March 24th, 1930.

---

XXIII. *A Modification of Michelson's Beam Interferometer.* By E. H. SYNGE †.

THE present limitations to Michelson's Beam Interferometer are of a mechanical nature. The length of a rigid metal beam, which is light enough to be carried on the structure of a moving telescope, cannot be increased indefinitely; and the resolving power of the apparatus is thus limited by purely mechanical difficulties.

It seems possible to escape altogether from these limitations by substituting two small cœlostats, arranged in a certain way, for the massive moving telescope frame and metal beam of Michelson's arrangement. A modification of the apparatus on these lines will be discussed in the present paper.

The essential feature of the arrangement suggested is the relative position of the two cœlostats. When these are placed so that their axes (which, of course, are polar axes) form part of the same geometrical right line, it is evident that their reflecting surfaces can be set so as to form part of the same plane, and, when so set, the two cœlostats virtually form part of one large cœlostat. If a long base-line is desired the cœlostats must clearly be placed on a hill-side with a north-south slope equal to the latitude. At the Equator this becomes a north-south alignment on the same level.

Once it is seen that we can in this way form what, for the purpose of stellar interferometry, is virtually one large cœlostat of almost unlimited size, it becomes obvious that the two cœlostats can be used, in conjunction with a fixed

\* Phil. Mag. ii. p. 508 (1926).

† Communicated by the Author.

telescope, to obtain a resolving power which is proportional to the distance between the cœlostats multiplied by the cosine of the declination of the star under consideration. Accessory plane mirrors must, of course, be employed, these being adjusted so that the two beams from the star, which are reflected by the two cœlostats, ultimately pass down the sides of the fixed telescope, and arrive together in the centre of its focal plane, with equality of optical path-lengths, as measured from any arbitrary wave-front in space. Thinking of the two cœlostats as parts of one large cœlostat, we see at once that if there is this equality at any moment there will be equality at every moment. If the cœlostats are not quite in correct alignment a continually increasing retardation of one beam upon the other will indicate what further adjustments must be made.

For stars of a different declination there must obviously be a rearrangement of the accessory plane mirrors, and the apparatus should be designed so that such rearrangement can be carried out readily. Where the base-line is long the simplest plan would perhaps be the following:—The telescope can be moved along a rail which is parallel to the axes of the cœlostats, *i. e.*, is a polar axis. As it moves it preserves its direction. The telescope is fitted with two mirrors, corresponding to the inner mirrors of Michelson's arrangement, the line joining the centres of these mirrors being parallel to the common axis of the cœlostats. Each cœlostat has two plane mirrors near it, which can be adjusted to throw a beam from the cœlostat in any direction. For any given declination these mirrors are arranged so that each of the two beams strikes the corresponding mirror attached to the telescope at the proper angle to bring it ultimately to the focal centre. Care is taken that the two beams have no rotation with respect to one another as they pass into the telescope. That is, each cœlostat shows the same field, in the same orientation, if used independently with the telescope. An approximate equalization of path-lengths is obtained by moving the telescope along the rail, final equalization being effected by similar methods to those used by Michelson.

In comparing such an arrangement of cœlostats with the present form of Beam Interferometer the following points may be noted:—

(1) The optical principles are exactly the same. The resolving power is not, however, proportional to the

distance between the *cœlostats*, but to this distance multiplied by the cosine of the declination of the star.

(2) The stellar diameters which can be measured are north-south diameters, and no others. This, as a rule, will be of very little consequence.

(3) The stars very near the celestial poles cannot be dealt with.

(4) The practical limits to the resolving power, apart from atmospheric or other disturbances, depend on latitude and local topography. At the Equator these limits recede almost indefinitely.

Since the ultimate possibilities of the arrangement seem to depend almost entirely on the effect of atmospheric or mechanical disturbances, it may be of interest to consider these in some way which will help us to estimate how far they are likely to impose practical limits on the distance between the two *cœlostats*. To understand the effect of such disturbances upon the fringes it is necessary, in the first place, to be quite clear about the optical principles which are involved in Michelson's use of plane mirrors to increase the resolving power. This matter is, perhaps, not treated with sufficient fulness in the text-books. Everything is no doubt contained in the general principle which is invoked in Schuster and Nicholson's '*Optics*' (3rd edition, pp. 167 F, G). But not every reader is likely to see immediately how this principle leads to the observed phenomena. Indeed, to what else but some difficulty or obscurity in the connexion, can one ascribe the singular fact that Michelson's brilliant idea lay neglected for thirty years after he had published it in 1890, obtaining no recognition whatever until he had himself carried it into effect experimentally?

Anyone who is not perfectly clear as to the formation of the fringes will probably find it worth while to work out the matter at length. The slits need not be taken, where they would be situated in practice, after the various reflexions. It is immaterial to the result where they are placed, and the writer, at all events, finds it more easy to follow the rays when the slits are placed immediately above the pair of distant mirrors in Michelson's arrangement.

Turning to the disturbing factors: mechanical disturbances will probably be quite negligible if two *cœlostats* are used. Any slight effects of this kind should be lost in the atmospheric disturbances, which are our real

concern. As regards these: if we take Michelson's symmetrical arrangement, with the telescope directly pointed at a star, and suppose that slits,  $S_1$  and  $S_2$ , are opened above the distant pair of mirrors, and that these slits are narrow, and if we assume that no disturbances between the slits and the focus of the telescope need be reckoned with, it appears that the alterations in the fringes may be occasioned in two ways, which can be dealt with separately. (1) The wave-front at one slit,  $S_2$ , may have a retardation or advance on the wave-front at the other slit,  $S_1$ . (2) The wave-front at  $S_2$  may be inclined at some angle  $\theta_2$  to the norm-plane which would represent the wave-front in ideally calm conditions of the atmosphere, while the wave-front at  $S_1$  may be inclined at an angle  $\theta_1$  to the same plane, and  $\theta_1$  and  $\theta_2$  will not, in general, be equal to one another.

Of these two irregularities, (2) does not produce any displacement of the fringes, but only changes their intensity. Provided that there is no retardation of a wave-front at one slit on the corresponding wave-front at the other slit, the central fringe, for white light, will remain fixed in the centre of the focal plane, no matter what  $\theta_1$  and  $\theta_2$  may be, so long as the fringes are visible at all. This seems remarkable at first sight, and yet it is really self-evident; for, no matter what  $\theta_1$  and  $\theta_2$  may be, those diffracted rays from  $S_1$  and  $S_2$  which reach the central point of the focal plane are of exactly equal optical length, as measured from  $S_1$  and  $S_2$  to that point. Under the supposed circumstances, these rays will therefore form the centre of the central white fringe at the point in question. Possibly the remark made by several writers, that the steadiness of the fringes is inadequately explained by the theory, is due to an insufficient recognition of this point.

The displacement of the fringes is entirely due to the factor (1). There will be a displacement from bright to dark for every half wave-length of retardation which the wave-front at one slit has with respect to that at the other.

We may now consider how far the motion of the fringes is likely to depend on the length of the base-line; and it will be well to form some kind of working conception of the atmospheric disturbances. Taking, as before, the symmetrical arrangement of Michelson, with a moving telescope, and neglecting certain variations which would occur

in a calm atmosphere, we will consider a point  $p$  above one of the distant mirrors, and fixed relatively to the telescope, which, of course, supplies our frame of reference. A plane  $P$ , drawn through  $p$ , will represent the wave-front of a star for ideally calm conditions of the atmosphere, and if the telescope is pointed directly towards the star this plane will cut the axis of the telescope at right angles. If the atmosphere is not perfectly calm the wave-fronts for various instants will be represented by a group of undulating surfaces drawn through  $p$ . In the simplest case the plane  $P$  will be the mean, or norm, of this group, and no matter how far the two mirrors may be distant from one another, we may assume that, for this case, the wave-fronts will not depart from the norm by more than a certain amount which attains a maximum at quite a small distance from  $p$ . The case resembles somewhat that of the undulating surface of the sea, and would probably answer to the actual phenomena for the atmosphere, if the disturbances had no sort of coherence—if they were not caused by any definite travelling bands of air.

To obtain a better approximation to the facts it will be necessary to consider the norm of the wave-fronts as being no longer a fixed plane  $P$ , but an undulating surface  $P'$ , moving with a larger, slower motion than that of the wave-fronts with respect to it. We might pass on to a further approximation, and consider the norm of  $P'$  at various instants. But for our purposes it will probably be sufficient to think of the wave-fronts drawn through  $p$  as undulating rapidly about a surface  $P'$ , which itself has a large and comparatively slow motion. We have to deal with the superposition of these effects. As regards the motion of  $P'$ , this effect is likely to increase both in range and in rapidity as we proceed further from  $p$ . But the motion should have a certain steadiness. Its rate of change should not vary rapidly. The various methods used by Michelson to equalize the path-lengths might be adequate to counteract it. But a more powerful method would consist in carrying the beams through closed pipes containing air, the pressure of which could be altered at will by some means which would not produce currents of air in the pipes. For instance, a narrow rubber tube might be laid in the pipe, and the increase or decrease of pressure inside the tube would be conveyed to the air outside it in the pipe with little disturbance. Some device for continu-



ously altering the pressure at varying rates, the operator simply controlling the rate, would probably make it possible to deal with the most rapid motion  $P'$  might have under ordinary circumstances. It should be added that, although the motion of  $P'$  would tend to increase with increase of base-line, the former increase would certainly not be proportional to the latter. And after a certain, not very great, distance, the motion of  $P'$  would probably reach its maximum. As regards the rapid small undulations about  $P'$ , it is clear, on the assumptions made, that these should produce no more rapid displacement of the fringes when the mirrors are very distant than when they are comparatively close.

From these considerations one seems justified in expecting that atmospheric disturbances, under favourable conditions, will not impose any limit on the length of base-line which may be used. Everything that has been said is, of course, applicable without essential change to the case of two cœlostats. If these were very far apart it would certainly be desirable to conduct the beams the whole way from the cœlostats to the telescope through partially evacuated pipes. Michelson mentions an experiment\* in which he conducted beams in opposite directions round a circuit of a mile in partially evacuated pipes, and obtained fringes which were capable of accurate measurement to one hundredth part of a fringe. With the much less accuracy which is necessary, or possible, in the case of the stellar interferometer, it seems that beams might be satisfactorily conducted through pipes of many times this length; and it is not inconceivable that, at the Equator, results might be obtained with two cœlostats over a base-line a thousand times as great as would be practicable with the Beam form of apparatus.

From the foregoing discussion it might appear that the reflecting surfaces of the two cœlostats must necessarily be adjusted to form part of one plane. But this is not an essential condition. It depends on the arrangement of the accessory mirrors. Indeed, siderostats could probably be substituted for the cœlostats with advantage. The most convenient plan might even be to replace the cœlostats by two small reflecting telescopes, mounted equatorially. In each of these a small convex parabolic

\* A. A. Michelson. 'Studies in Optics,' p. 164.

mirror would be substituted for the Cassegrain hyperbolic reflector. Narrow parallel beams would thus be obtained which would be reflected along the polar axes, supposing this part of the instruments to be made hollow, as has been done in some telescopes. With this arrangement the principal telescope might be greatly reduced in size, as can easily be seen, the general principle invoked by Schuster and Nicholson still holding good for the optical theory. The collinearity of the polar axes, considered as geometrical lines, of the two other instruments, is of course an essential condition in all cases, whether coelostats, or siderostats, or subsidiary telescopes are in question.

---

XXIV. *Absorption in Hydrogen Gas of Hydrogen Positive Rays.* By A. C. LAW, M.A., and G. MUTCH, M.A.\*

*Introduction.*

ACCORDING to the theory of the absorption of electrified particles positive rays are absorbed by electron collisions, and have, like  $\alpha$ -rays, a definite range. On the other hand early experiments with non-homogeneous positive rays showed there was considerable absorption for rays of all energies; the absorption was exponential and did not vary much with the energy of the rays. Wien †, Königsberger and Kutschewski ‡, Ruchardt §, and Conrad ¶ have studied this problem, and found values for the absorption coefficient in various cases. It should be noted that these experiments, with the exception of one by Ruchardt and that by Conrad, were made with non-homogeneous rays.

Wien found, by using a thermo-element, that the absorption coefficient of positive rays in hydrogen gas was not proportional to the pressure. Conrad showed that most of the diminution in intensity of positive rays passing through hydrogen at the order of pressures and velocities

\* Communicated by Prof. G. P. Thomson.

† W. Wien, *Ann. der Phys.* xxiii. p. 485 (1907); xlviii. p. 1089 (1915); lxx. p. 1 (1923).

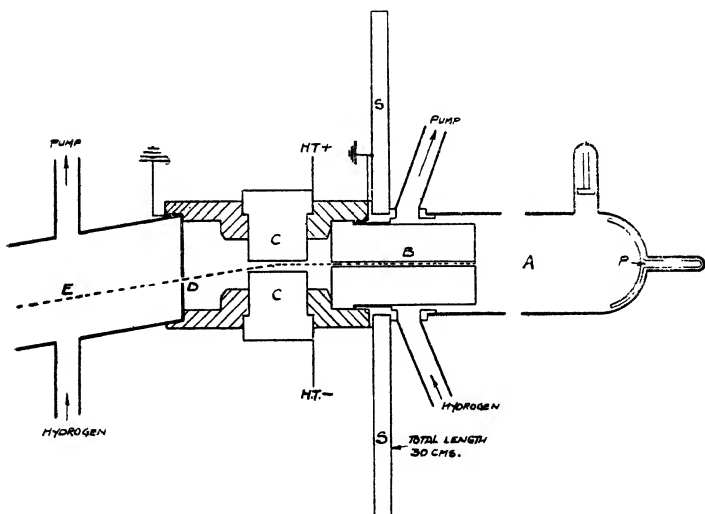
‡ Königsberger and Kutschewski, *Ann. der Phys.* xxxvii. p. 161 (1912).

§ E. Ruchardt, *Ann. der Phys.* lxxi. p. 377 (1923).

¶ R. Conrad, *Zeit. für Phys.* xxxv. p. 73 (1925); xxxviii. p. 465 (1926).

here considered, as measured by his apparatus, was caused by spreading. Further, Conrad determined experimentally that the spreading exponent for hydrogen positive rays in hydrogen was directly proportional to the pressure. In a preliminary experiment by one of the authors, using non-homogeneous rays and employing a method as described below for homogeneous rays, the absorption was found to be exponential, but no definite relation could be obtained between absorption coefficient and pressure of the hydrogen gas or the velocity of the rays. To simplify the problem it was decided to use homogeneous positive rays.

Fig. 1.



### *Apparatus.*

Fig. 1 is a sketch of the apparatus.

The positive rays are produced in the discharge-tube A, and pass through a hole 2 mm. in diameter, 7.75 cm. long, in the cathode B, which is made of Swedish iron. The length of the cathode is such that the positive rays have reached a steady state before entering the deflecting chamber. A magnetic shield S of stalloy stampings is built up round the cathode to prevent the magnetic field deflecting the positive rays into the cathode itself. The rays then pass between two magnetic pole-pieces C (3 cm.  $\times$

1.5 cm.), which can be utilized also for an electric field by suitably connecting to a battery, since the pole-pieces are mounted in an ebonite cylinder. Knowing the dimensions of the apparatus and the strengths of the magnetic and electric fields, a portion of the positive ray parabola of known energy can be made to pass through the slit D in an aluminium earthed disk. The slit is so placed that the mean deflexions are: magnetic 1.636 cm., electric 0.825 cm. The distance from the end of the fields to the aluminium disk is 3.5 cm. A small glass slide, coated with willemite, is fixed in the aluminium disk in the quadrant adjoining the slit, so that by reversing the magnetic field the positive ray parabola can be observed, and the one corresponding to the hydrogen atoms chosen by altering the field strengths. In the other two quadrants there are holes, so that the pressure is the same on both sides of the disk. The resulting beam of positive rays, which is fairly homogeneous, passes along an observation chamber E, where the absorption is measured. The far side of E is painted dull black inside, and baked before assembly. This prevents the reflexion of the light of the beam.

The discharge-tube and observation chamber are exhausted by a mercury diffusion-pump backed by a water-pump, mercury vapour being prevented from entering by a suitable trap. Hydrogen gas can be allowed to enter either chamber at will. A pyrex glass shield, P, at the anode end of the discharge-tube prevents the end of the tube being melted by the intense cathode ray bombardment.

### *Method.*

A photographic method is used to get the intensities of the positive ray-beam at different points along its course, and from these the absorption is found. The experiments of Königsberger and Kutschewski showed that within fairly wide limits of pressure and velocity the velocity of the positively charged atoms is not appreciably altered by their passage through the gas. So it was assumed here that the intensity of the light emitted at any point in the beam was proportional to the number of positively charged atoms present at that point.

A photograph of the light originating in the beam is taken with a camera having a lens of numerical aperture 2

and a movable plate-holder, so that a series of photographs can be taken on the same plate by exposing successive strips of it. Fast plates (650 H. and D.), which are "backed" to prevent reflexion, are used in order to reduce the time of exposure to three hours.

A characteristic curve for the photographic plate is constructed, showing the relation between the intensity of the light incident on the plate and the density of the image. From the density of the image of the beam and the characteristic curve the intensity of the light emitted along the positive ray-beam can be calculated, and hence the absorption found.

The method of constructing the characteristic curve for the plate is as follows:—An optical wedge is placed in front of the brightest part of the beam, with its gradation at right angles to the axis of the positive ray-beam. A photograph of this part of the beam is then taken. A series of such exposures is taken on the same plate, the wedge being moved a known distance for each one. The time of exposure for these and also for the whole beam is three hours. The whole photographic plate, with the latent image of the beam and those for the characteristic curve, is developed, due precautions being taken to get uniform development. The density of the darkest part of each image on the plate for the characteristic curve is measured by a photometer, and a curve plotted between the density of the image and  $10^{-kx}$ , where  $k$  is the wedge-constant and  $x$  is the distance the wedge has been moved from zero position for that image. Fig. 2 shows a curve so obtained. Now the intensity of the light passing through the wedge is given by  $I_x = I_0 10^{-kx}$ , so that actually fig. 2 gives the relation between the density of the photographic image and the intensity, in arbitrary units, of the light which made it.

The only variable factor affecting the amount of blackening of the plate is the intensity of the light falling on it. For accuracy in constructing the intensity-density curve it is essential that the intensity photographed should not alter except by movement of the optical wedge. It is impossible in practice to keep the discharge-tube under constant conditions for three hours, neither is it possible to obtain exactly the same conditions from day to day. In these experiments it is assumed that, providing the voltage applied to the discharge-tube and the current through

it remain constant, the intensity of the beam of positive rays is the same. This assumption is justified by the fact that the points obtained lie on a smooth curve of the expected shape, as in fig. 2. This is confirmed too by the

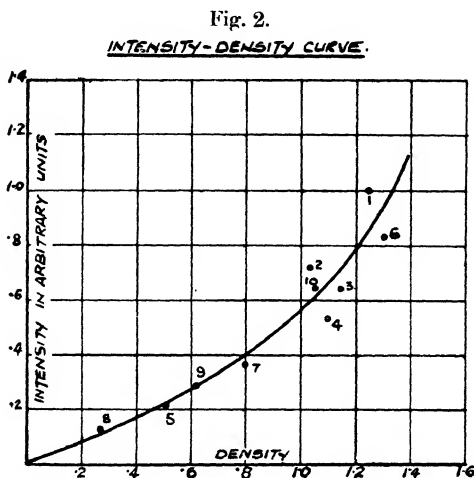


TABLE I.

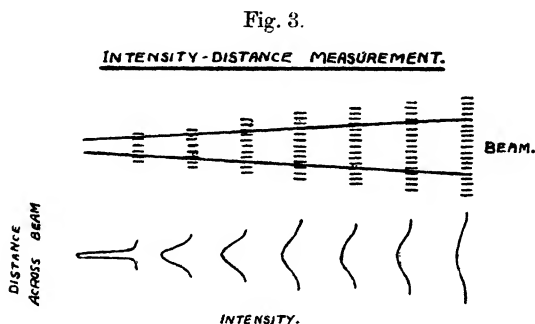
Photograph.	Pressure mm./1000 of Hg.	Current. milliamps.	Spark gap. cm.	Wedge. cm.	Density of image.
1 .. . . .	9 to 12	2	0.53	0	1.25
2.....	9 to 13	2	.53	0.3	1.028
3 .....	10 to 18	2	.54	0.5	1.145
4.....	10 to 18	2	.53	0.7	1.11
5.....	12 to 19	2	.53	1.7	0.515
6.....	12 to 20	2	.48	0.2	1.30
7.....	12 to 21	1.9	.48	1.1	0.80
8.....	12 to 20	2	.54	2.3	0.27
9.....	13 to 19	2	.53	1.4	0.62
10.....	10 to 19	1.9	.54	0.5	1.05

fact that similar results are obtained using the intensity-density curve when the densities of the photograph of the beam cover the whole range of the curve or only part of it.

The results from which fig. 2 is constructed are given in Table I. All these exposures were made on one plate.

By measuring the density at any point of the photographic image of the beam, and using the intensity-density curve, the intensity of the light emitted at the corresponding point of the beam is obtained. The density of the photographic image is measured at small intervals across it, *i. e.*, at right-angles to the direction of the beam, and these densities are converted to intensities as above. Intensity of the light is then plotted against distance across the beam. The resulting curve is, as it were, a cross-section in intensity of the beam at that distance along the beam. Fig. 3 shows the type of curve obtained at various distances.

The areas of these curves are proportional to the light incident on the plate at these distances along the beam.



They are not, however, proportional to the total light emitted from the corresponding sections in the beam of positive rays. Owing to the obliquity of the rays of light from the ends of the beam the corresponding densities are too small. If a ray of light makes an angle  $\theta$  with the axis of the lens of the camera at its centre  $O$ ,  $r$  is the distance of the point  $P$  in the beam considered from  $O$ ,  $d$  is the perpendicular distance from  $O$  to the beam, and  $A$  the area of the lens, the solid angle subtended by the lens at  $P$  is  $A \sin(90 - \theta)/r^2$  or  $A \cos \theta/r^2$ . Hence the total amount of light from an element  $\delta x$  of the beam at  $P$ , which passes through the lens and goes to form an image, is  $I_x \delta x A \cos \theta/r^2$ , and the intensity of the image will be proportional to this, *i. e.*, to  $I_x \delta x A \cos^3 \theta/d^2$ , since  $\frac{d}{r} = \cos \theta$ . Hence the measured intensity of the light at a point in the

beam will be less than the true intensity in the ratio  $\cos^3\theta$  to 1.

The distance from the beam to the lens is 36 cm., and the magnification of the image is 0.149. The photographs obtained of the beam are about 4.5 cm. long and 0.25 cm. to 0.4 cm. wide.

### *Experimental Results.*

Table II gives the results of the experiment.

TABLE II.  
Atomic Rays (Protons).

Pressure mm./1000 Hg.	Intensity in arbitrary units.									
Distance along photo.	0.25	0.75	1.25	1.75	2.25	2.75	3.25	cm.		
9	258	214	222	244	233	130				
10	494	487	503	494	424	363	265			
20	732	636	646	565	535	482	324			
30	413	265	234	177	146	167				
Distance along photo.	0	0.3	0.6	0.9	1.2	1.5	1.8	2.1	2.4	2.7 cm.
15	723	744	798	726	766	736	677	657	597	539

The energy of the positive rays was 10,800 volts.

Fig. 4 shows the results contained in Table II graphically.

### *Discussion.*

It will be seen that the absorption of homogeneous positive rays by hydrogen is definitely not exponential. On the contrary, most of the beams show a sharp decrease of intensity, which seems to indicate the existence of a range for the particles. It is important to note, however, that the method of the experiment breaks down when the velocity of the particles changes appreciably, so that no definite conclusion can be drawn as to the length of the range, but the experimental results can be compared in a general way with the results given by theory.

When Thomson's formula\* for the range of an electrified particle was applied to these results the range calculated

\* 'Conduction through Gases,' p. 376.

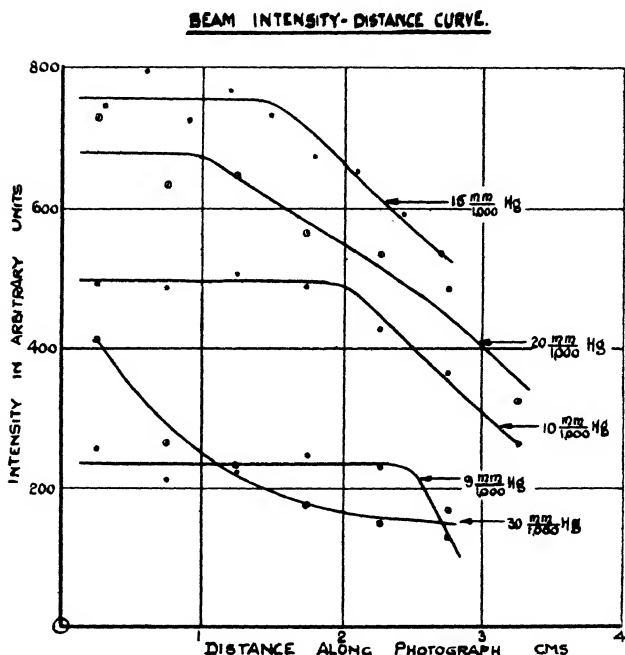


was much greater than the range found by experiment. Bohr's formula\* for hydrogen breaks down completely when applied to atoms of the velocity here considered.

Now Henderson's theory †, as modified by Fowler ‡, gives

$$\frac{dT}{dx} = - \frac{2\pi e^4 N}{mV^2} \log_e \frac{4P}{\lambda},$$

Fig. 4.



where  $T$  is the Kinetic Energy ;  $e$  is charge on an electron ;

$N$  is number of electrons per unit volume ;  $m$  is mass of an electron ;

$V$  is velocity of the atomic rays ;  $P$  is the energy of the ray in E.S.U.

$\lambda$  is the first resonance potential.

\* Bohr, Phil. Mag. xxv. p. 10, and xxx. p. 581.

† Henderson, Phil. Mag. xlv. p. 680.

‡ Fowler, Camb. Phil. Soc. xxi. p. 521.

Taking  $\lambda=10$  volts, and protons of 10,800 volts energy gives

$$\text{Range} = \frac{880}{p}.$$

The authors find for rays of 10,800 volts energy a marked drop in the intensity of the beam at a distance  $d$  on the photographic plates as obtained from fig. 4 and tabulated below.

TABLE III.

mm. $p$ 1000 Hg.	$d$ on plates, cm.	$d$ 0.149 cm.	$d$ $x=0.149^{+5}$ cm.	$px$ .
9 .....	2.4	16.1	21.1	190
10 .....	2.0	13.4	18.4	184
20 .....	1.0	6.7	11.7	234
30 .....	<0.5	<3.3	<8.3	<249
15 .....	1.5	10	15	225

$x$  is the actual distance the beam has travelled from the middle of the electric and magnetic deflecting fields where the energy is measured to that point where a marked drop in the intensity of the beam occurs.

Taking a mean value of  $px$  as 216, this theory also gives too long a range. This being so, the method of experiment breaks down. But it is clearly the case that the absorption of positive rays is due to a gradual stopping.

These results are not inconsistent with the results obtained by Königsberger and Kutschewski. They found that with rays of velocity  $2.3 \times 10^8$  cm. per second the change of velocity in passing through 16 cm. of hydrogen at  $3 \times 10^{-3}$  mm. of mercury did not exceed 0.5 per cent. A calculation based on Henderson's formula gives the change of velocity as 0.46 per cent. under the same conditions.

#### General Conclusions.

1. The absorption is not exponential. Hence it is not a case of the removal of particles by sudden stoppage or large angle scattering.

2. It follows that the decrease in velocity must be gradual and an important factor.

3. This prevents the method from giving quantitative results.

4. The distance at which a rapid decrease in luminosity occurs is probably the place at which the energy is so reduced that the emitting power is seriously diminished.

5. The diminution in velocity predicted by Henderson's formula does not seem enough to account for the observed diminution in luminosity. This is not surprising in view of the failure of the formula for  $\alpha$ -rays. A factor of 2, which is needed in the latter case, would make the results plausible.

The authors desire to express their thanks to Prof. G. P. Thomson for suggesting this problem, for many helpful suggestions, and for his continued interest in it, and their appreciation of the technical assistance given by Mr. C. G. Fraser and his staff in the Natural Philosophy Department of the University of Aberdeen.

XXV. *An X-ray Investigation of the Crystals of Azobenzene.* By MATA PRASAD \*.

THE crystal structure of azobenzene has been studied by Becker and Jancke †. They examined the substance in the state of a compressed powder by a method that combined that of Bragg and of Debye and Scherrer, and found the dimensions of the unit cell to be

$$a = 12.50 \text{ \AA.}, \quad b = 5.28 \text{ \AA.}, \quad c = 8.38 \text{ \AA.}, \quad \beta = 116^\circ,$$

the axial ratio being

$$a : b : c = 2.370 : 1 : 1.590.$$

They found the density of the crystals to be 1.235. These data indicate that the unit cell contains two molecules.

Bragg examined the crystals by the Ionization Spectrometer method, and concluded that the unit cell contains four molecules ‡.

Crystals of azobenzene, ( $\text{C}_6\text{H}_5-\text{N}=\text{N}-\text{C}_6\text{H}_5$ ), were prepared by the slow evaporation of the solution in alcohol of the substance. They are rod-like in appearance. The

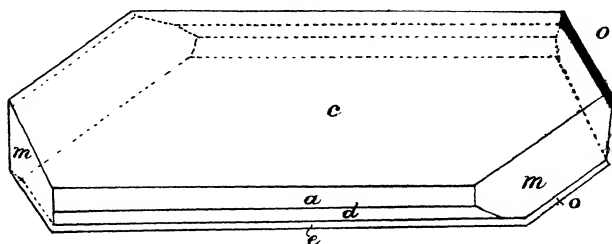
\* Communicated by Sir W. H. Bragg, K.B.E., F.R.S.

† *Zeit. Phys. Chem.* xcix. p. 242 (1921).

‡ 'X-rays and Crystal Structure,' 5th edition, p. 251.

$c$  (001) face is a flat face; other predominant faces observed are  $d$  ( $20\bar{1}$ ) and  $m$  ( $110$ ). In some crystals faces  $k$  ( $021$ ),  $o$  ( $11\bar{1}$ ), and  $e$  ( $40\bar{3}$ ) are also present. The shape of the crystal is shown in fig. 1.

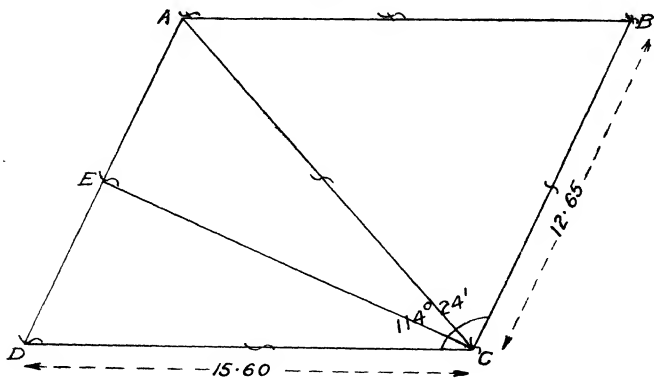
Fig. 1.



The crystallographic measurements of the crystals indicate that they belong to the monoclinic prismatic class. The axial ratio found by crystallographers is

$$a : b : c = 2.1076 : 1 : 1.3312^*.$$

Fig. 2.



In the present investigation the crystals were examined by the rotating crystal method. With a Shearer gas-tube containing an anti-cathode made of copper the rotation photographs about the three axes were taken; the dimensions of the cell were found to be (see fig. 2).

$$a = 12.65 \text{ \AA.}, b = 6.06 \text{ \AA.}, c = 15.60 \text{ \AA.}, \text{ and } \beta = 114^\circ 24'.$$

\* Cf. Groth, *Chemische Krystallographie*, v. p. 60.

The axial ratios are

$$a : b : c = 2.087 : 1 : 2.574.$$

The *c* axis is twice that found by Becker and Jancke.

The crystals of azobenzene are volatile ; on exposure to air they become smaller ; and the setting was often spoiled during the time of exposure ; hence considerable difficulty was found in taking good rotation photographs. But with a Shearer's tube well set it was found that a good rotation photograph could be taken in about 15 minutes and an oscillation photograph in about 8-10 minutes.

In order to examine further the doubling of the *c* axis, and to compare the intensity of reflexion from various planes, the oscillation photographs about the *a* and *b* axes were taken in as short a time as possible. The indices of the spots appearing on the plate were worked out by means of Bernal's method of analysis \*. The following tables give the indices of the planes observed, together with a rough idea of their relative intensities. The method adopted in estimating the intensity of the spot was that used by Robertson †, *i. e.*, by comparing the  $K\alpha$  (copper) reflexion spot of weaker planes with the  $K\beta$  reflexions of the stronger planes. The symbols used carry the same meaning as in Robertson's paper †, and are repeated here for the sake of clearness.

v.s. = very strong.

w.m. = weak medium.

s. = strong.

w. = weak.

m.s. = medium strong.

v.w. = very weak.

m. = medium.

It will be seen from the nature of reflexions from planes (*ool*) that they are very weak when *l* is odd ; probably the error in Becker and Jancke's determination of the *c* axis arose on this account. The plane (001) observed in the oscillation photograph about the *b* axis was much weaker than the  $\beta$  spot of the plane (002), which was very strong.

Table I. shows that the planes (*hol*) are halved when *h* is odd and there are no other general halvings. This halving corresponds to the space-group  $C_{2h}^1$  or  $C_{2h}^5$  with  $\overline{m}$  lattice. The space-group  $C_{2h}^5$  requires that, in addition

\* Proc. Roy. Soc. A, cxiii. p. 117 (1926).

† Proc. Roy. Soc. A, cxviii. p. 712 (1928).

to the halving mentioned above, the planes (010) should also be halved. It is probable in this case that the plane (010) is halved and that (020) is a very weak plane, and hence did not appear; the space-group therefore is  $C_{2h}^5$ . This probability is the greater because crystals of tolane, which is isomorphous with azobenzene, have been examined by Miss K. Yardley by the ionization spectrometer and the plane (010) has been found to be halved. The author is much indebted to Miss Yardley for supplying him with her data on tolane. The author has examined tolane by the photographic method, and the results of this

TABLE I.

Axial planes.	Planes ( <i>hol</i> ).		Planes ( <i>okl</i> ).	Planes ( <i>hko</i> ).
001 w.	201 v.s.	402 s.	011 m.s.	110 v.s.
002 v.s.	202 v.s.	403 s.	012 v.s.	120 w.m.
003 w.	203 v.s.	404 s.	013 s.	130 m.
004 v.s.	204 v.w.	405 v.w.	014 s.	220 m.
005 v.w.	205 v.w.	40 $\bar{1}$ w.m.	015 v.w.	320 m.
006 m.	206 m.	40 $\bar{2}$ s.	016 w.	420 m.s.
007 v.w.	207 m.	40 $\bar{3}$ m.	017 v.w.	520 w.
008 w.m.	20 $\bar{2}$ v.s.	40 $\bar{6}$ s.	018 v.w.	210 m.
200 v.s.	20 $\bar{3}$ v.s.	40 $\bar{7}$ m.s.	021 w.	310 w.m.
	20 $\bar{4}$ v.s.	40 $\bar{8}$ s.	022 w.m.	410 s.
	20 $\bar{5}$ v.s.	40 $\bar{9}$ m.	023 w.	230 w.m.
	20 $\bar{6}$ v.w.	60 $\bar{4}$ w.	024 v.w.	330 w.m.
	20 $\bar{7}$ v.w.		025 v.w.	
	20 $\bar{8}$ m.		026 v.w.	
			031 v.w.	

investigation will shortly be communicated in another paper.

The number of molecules in the unit cell required by the space-group  $C_{2h}^5$  is four. The number of molecules calculated from the dimensions of the cell and the density of the crystals being also four, the molecules in the cell are asymmetric. The elements of symmetry of the cell are, in accordance with the space-group, a glide plane of symmetry parallel to the (*ac*) plane and screw-axes parallel to the *b* axis\*.

\* Cf. Astbury and Yardley, Phil. Trans. A, ccxxiv. pp. 221-257.

TABLE II.

Planes (*hkl*).

111 s.	121 w.m.	211 v.s.	221 s.	311 s.	321 s.	411 m.	421 w.m.
112 v.s.	122 w.m.	212 m.s.	222 w.m.	312 s.	322 w.	412 s.	422 w.
113 v.s.	123 w.m.	213 m.s.	223 m.	313 w.m.	323 w.m.	413 w.m.	423 w.m.
114 v.s.	124 w.m.	214 m.s.	224 m.	314 m.s.	324 m.	414 v.w.	424 m.
115 m.s.	125 w.	215 m.s.	225 w.m.	315 w.	325 w.	415 w.	425 w.
116 m.	126 w.m.	216 m.s.	226 w.m.	316 w.m.	326 w.	416 m.	427 v.w.
117 v.w.	127 v.w.	217 w.	227 w.m.	317 m.s.	327 v.w.	417 m.	421 v.w.
118 v.w.	133 w.m.	218 v.w.	232 v.w.	318 s.	333 v.w.	418 m.	423 v.w.
111 v.s.	121 w.m.	211 m.s.	233 v.w.	319 w.m.	321 m.	419 v.w.	516 w.
112 v.s.	122 w.m.	212 v.s.	221 w.	311 w.	322 w.m.	411 w.	612 w.
113 v.s.	123 v.w.	213 m.	222 m.	312 m.	323 w.m.	412 m.	
114 m.	124 w.	214 m.s.	223 w.	313 m.	324 w.	413 m.	
115 v.w.	125 m.	215 v.w.	224 w.	314 s.		414 m.s.	
117 v.w.	132 w.m.	216 m.s.	231 v.w.	315 v.w.			
	133 v.w.			316 w.m.			

In fig. 2, if A and C are joined, the length of the side AC is 15.51 Å., which is very nearly equal to the length of the side CD. Therefore EC is nearly at right angles to AD. Hence if ADFG (fig. 3) be taken as the boundary, in the (010) plane, of a cell which will be twice as large as the unit cell, the new cell will be nearly orthogonal.

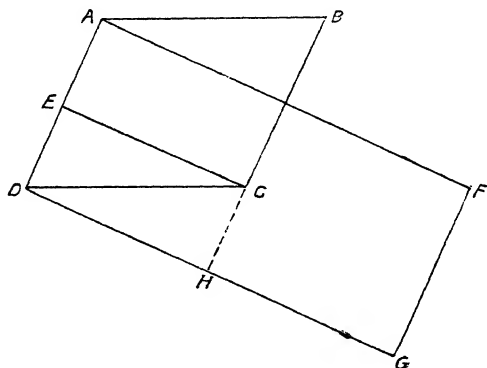
The dimensions of the cell will then be

$$a=12.65 \text{ Å.}, \quad b=6.06 \text{ Å.}, \quad c=28.4 \text{ Å.}, \quad \text{and } \beta=90^\circ$$

(very nearly),

and the cell will contain eight molecules. The indices of the planes given in Tables I. and II. can easily be found in

Fig. 3.



terms of the new coordinates. The plane  $(hkl)$  will become  $(h'k'l')$ , where

$$h' = h,$$

$$k' = k,$$

$$\text{and } l' = 2l + h.$$

It is then interesting to find, as the following tables show, that  $(h'k'l')$  and  $(h'k'\bar{l}')$  have not only the same spacings, very nearly, but also correspond similarly in regard to intensities.

It is fairly safe to infer that the molecule of azobenzene lies so that its long dimension is generally parallel to one of the coordinate axes. It is somewhat premature to attempt other deductions until the reflexions have been measured not only relatively but absolutely. This ex-



tension of the investigation will be carried out as soon as possible.

In conclusion, I wish to express my sincere thanks to Sir William Bragg, F.R.S., for suggesting the work and taking a great interest in the investigation. My thanks are also due to Dr. Shearer and Dr. Muller for guidance in the technique of X-ray methods as applied to crystal structure; to Mr. Bernal for giving me helpful and valuable sugges-

TABLE III.

Axial planes.		(hol) planes.	
002	w.	202	v.s.
004	v.s.	204	v.s.
006	w.	206	v.s.
008	v.s.	208	v.s.
0010	v.w.	2010	v.w.
0012	m.	2012	v.w.
0014	v.w.	2014	m.
0016	w.m.	2016	m.
(012)	m.s.	400	s.
(014)	v.s.	402	w.m.
(016)	s.	408	s.
(018)	s.	4010	s.
(0110)	v.w.	4012	s.
(0112)	w.	4014	v.w.
(0114)	v.w.	602	w.
(0116)	v.w.		
022	w.		
024	w.m.		
026	w.		
028	v.w.		
0210	v.w.		
0212	v.w.		
032	v.w.		

tions from time to time; and to the authorities of the Royal Institution, who gave me the opportunity to carry on this investigation.

### Summary.

The structure of the azobenzene crystal has been examined. The dimensions of the unit cell are

$$a = 12.65 \text{ \AA.U.}; b = 6.06 \text{ \AA.U.}; c = 15.60 \text{ \AA.U.}; \beta = 114^\circ 24'$$

TABLE IV.  
Other Planes.

111 v.s.	11 $\bar{1}$ s.	210 v.s.	
113 v.s.	11 $\bar{3}$ v.s.	212 m.	21 $\bar{2}$ m.s.
115 v.s.	11 $\bar{5}$ v.s.	214 m.s.	21 $\bar{4}$ m.s.
117 v.s.	11 $\bar{7}$ v.s.	216 v.s.	21 $\bar{6}$ m.s.
119 m.	11 $\bar{9}$ m.s.	218 m.	21 $\bar{8}$ m.s.
1111 v.w.	11 $\bar{1}$ m.	2110 m.s.	21 $\bar{1}$ 0 m.s.
	11 $\bar{1}$ 3 v.w.	2112 v.w.	21 $\bar{1}$ 2 w.
1115 v.w.	11 $\bar{1}$ 5 v.w.	2114 m.s.	21 $\bar{1}$ 4 v.w.
121 w.m.	12 $\bar{1}$ w.m.	220 s.	
123 w.m.	12 $\bar{3}$ w.m.	222 m.	22 $\bar{2}$ w.m.
125 w.m.	12 $\bar{5}$ w.m.	224 w.	22 $\bar{4}$ m.
127 v.w.	12 $\bar{7}$ w.m.	226 m.	22 $\bar{6}$ m.
129 w.	12 $\bar{9}$ w.	228 w.	22 $\bar{8}$ w.
1211 m.	12 $\bar{1}$ 1 w.m.	2210 w.	22 $\bar{1}$ 0 w.m.
	12 $\bar{1}$ 3 v.w.		22 $\bar{1}$ 2 w.m.
131 m.		232 w.m.	23 $\bar{2}$ v.w.
135 w.m.	13 $\bar{5}$ w.m.	234 v.w.	23 $\bar{4}$ v.w.
137 v.w.		410 s.	
311 s.	31 $\bar{1}$ s.	412 m.	41 $\bar{2}$ w.m.
313 w.m.	31 $\bar{3}$ w.m.	414 s.	41 $\bar{4}$ v.w.
315 w.	31 $\bar{5}$ m.s.	416 w.	41 $\bar{6}$ w.
317 m.	31 $\bar{7}$ w.	418 m.	41 $\bar{8}$ m.
319 m.	31 $\bar{9}$ w.m.	4110 m.	41 $\bar{1}$ 0 m.
3111 s.	31 $\bar{1}$ 1 m.s.	4112 m.s.	41 $\bar{1}$ 2 m.
3113 v.w.	31 $\bar{1}$ 3 s.		41 $\bar{1}$ 4 v.w.
3115 w.m.	31 $\bar{1}$ 5 w.m.	420 w.	
321 s.	32 $\bar{1}$ w.	422 w.m.	42 $\bar{2}$ w.m.
323 m.	32 $\bar{3}$ w.m.	424 m.s.	42 $\bar{4}$ m.
325 m.	32 $\bar{5}$ m.	426 v.w.	42 $\bar{6}$ w.
327 w.m.	32 $\bar{7}$ w.	4210 v.w.	42 $\bar{1}$ 0 v.w.
329 w.m.	32 $\bar{9}$ w.	517 w.	
3211 w.	32 $\bar{1}$ 1 v.w.	525 w.	612 w.
333 w.m.	33 $\bar{3}$ v.w.		

The cell contains four molecules. A remarkable feature is the nearly complete symmetry about the (20 $\bar{1}$ ) plane, both in respect to the geometrical relations and to the intensities of reflexion by corresponding planes.

Davy-Faraday Laboratory,  
Royal Institution, London,

and  
Royal Institute of Science, Bombay.

XXVI. *Three-Dimensional Periodic Orbits in the Field of a Non-Neutral Dipole.* By LEIGH PAGE\*.

ABSTRACT.

(1) The periodic orbits of an electron moving in the field of a stationary electric doublet which has a positive charge associated with it are investigated by the Newtonian dynamics.

(2) Special cases of orbits on a cone and orbits on a sphere are treated.

(3) The Hamilton-Jacobi method is applied to the problem, the energy being expressed as a function of the phase integrals. The motion is shown to be completely non-degenerate.

THE two dimensional periodic orbits of an electron in a plane through the axis of a stationary electric dipole have been investigated by D. Wrinch† and M. A. Higab‡. The first author considers the case of a neutral dipole and shows that the only periodic orbit is a semi-circle in which the angle  $\theta$  made by the radius vector with the axis of the doublet oscillates between the values  $-\pi/2$  and  $\pi/2$ . The second author treats the more general case of a doublet which has associated with it a positive charge, and finds orbits which surround the doublet (in particular, circular orbits) as well as orbits which do not.

The object of the present contribution is to discuss the three-dimensional periodic orbits of an electron in the field of an electrical doublet of moment  $m\lambda/e$  with which is associated a positive charge  $m\mu/e$ ,  $m$  and  $e$  representing the mass and charge respectively of the electron.

Using polar coordinates  $r, \theta, \phi$ , where  $\theta$  is the angle which the radius vector makes with the axis of the dipole and  $\phi$  the azimuth, the equations of motion are

$$\ddot{r} - r\dot{\theta}^2 - r\sin^2\theta\dot{\phi}^2 = -\frac{\mu}{r^2} - \frac{2\lambda\cos\theta}{r^3}, \quad . \quad . \quad (1)$$

$$\frac{1}{r} \frac{d}{dt}(r^2\dot{\theta}) - r\sin\theta\cos\theta\dot{\phi}^2 = -\frac{\lambda\sin\theta}{r^3}, \quad . \quad . \quad (2)$$

$$\frac{1}{r\sin\theta} \frac{d}{dt}(r^2\sin^2\theta\dot{\phi}) = 0. \quad . \quad . \quad . \quad (3)$$

\* Communicated by the Author.

† Phil. Mag. xliii. p. 993 (1923).

‡ Ibid. vii. p. 783 (1929).

Integrating (3)

$$r^2 \sin^2 \theta \dot{\phi} = h, \quad . \quad . \quad . \quad . \quad . \quad . \quad (4)$$

and using (4) to eliminate  $\dot{\phi}$  from (2) the latter equation can be integrated, giving

$$r^4 \dot{\theta}^2 = a^2 + 2\lambda \cos \theta - \frac{h^2}{\sin^2 \theta}. \quad . \quad . \quad . \quad (5)$$

Next  $\phi$  and  $\theta$  may be eliminated from (1) by means of (4) and (5), and the resulting equation integrated. This gives

$$\dot{r}^2 = -2w + \frac{2\mu}{r} - \frac{a^2}{r^2}. \quad . \quad . \quad . \quad . \quad . \quad (6)$$

The constants  $\mu, \lambda, h, a, w$  have the following physical dimensions:—

$$\mu = \frac{L^3}{T^2}, \quad \lambda = \frac{L^4}{T^2}, \quad a = h = \frac{L^2}{T}, \quad w = \frac{L^2}{T^2}.$$

From (4) it is clear that  $h$  represents the azimuthal momentum per unit mass. To find the significance of  $w$  we form the energy equation from (4), (5), (6):

$$\frac{1}{2}(\dot{r}^2 + r^2 \dot{\theta}^2 + r^2 \sin^2 \theta \dot{\phi}^2) - \frac{\mu}{r} - \frac{\lambda \cos \theta}{r^2} = -w. \quad . \quad (7)$$

Evidently  $w$  is the negative of the total energy per unit mass. Periodic orbits are possible only for positive values of  $w$ . It will be shown later that  $a^2$  must be positive as well.

### *Equations of the Orbit.*

We can describe the orbit in the general case as the curve of intersection of two surfaces

$$F(r, \theta) = 0, \quad G(\theta, \phi) = 0.$$

To obtain the first put  $u \equiv 1/r$ ,  $x \equiv \cos \theta$ , and eliminate the time between (5) and (6). We find

$$\frac{-du}{\sqrt{-2w + 2\mu u - a^2 u^2}} = \frac{dx}{\sqrt{2\lambda f(x)}}, \quad . \quad . \quad . \quad (8)$$

where

$$f(x) \equiv \left( \frac{a^2}{2\lambda} + x \right) (1 - x^2) - \frac{h^2}{2\lambda}. \quad . \quad . \quad . \quad (9)$$

In order that the motion in  $u$  shall be periodic, the expression under the radical on the left-hand side of

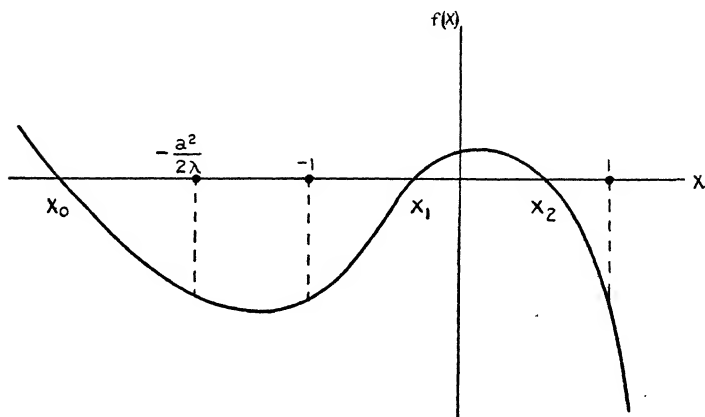
(8) must be positive only for values of  $u$  lying between two positive libration limits  $u_1$  and  $u_2$ . Hence  $a^2$  must be positive as well as  $w$ . The libration limits are

$$u_1 = \frac{1}{a^2} (\mu - \sqrt{\mu^2 - 2a^2w}), \quad u_2 = \frac{1}{a^2} (\mu + \sqrt{\mu^2 - 2a^2w}). \quad (10)$$

For these to be real, it is necessary that  $2a^2w \leq \mu^2$ , the case of equality being that in which the libration limits coincide, and the motion is therefore confined to the surface of a sphere.

For the motion in  $\theta$  to be periodic the function  $f(x)$  must be positive for values of  $x$  lying between two real roots  $x_1$  and  $x_2$  which satisfy the conditions

$$-1 \leq x_1 < x_2 \leq 1.$$



These roots mark the extreme values which  $\cos \theta$  is capable of assuming.

We note that

$$f(-\infty) = \infty, \quad f\left(-\frac{a^2}{2\lambda}\right) = f(-1) = f(1) = -\frac{h^2}{2\lambda},$$

$$f(\infty) = -\infty.$$

Therefore  $f(x)$  has one real root  $x_0$  less than the smaller of the two quantities  $-a^2/2\lambda$  and  $-1$ . If the other roots are real so that the motion is physically possible, the graph of the function is as indicated in the figure.

The function  $f(x)$  is a maximum for

$$x_m = \frac{1}{6\lambda} (\sqrt{a^4 + 12\lambda^2} - a^2), \quad . \quad . \quad . \quad (11)$$

which is always positive and less than unity. If the function vanishes at its maximum  $x_1$  and  $x_2$  coincide, and the motion is limited to the surface of a circular cone. It is clear from (9) that for any admissible values of  $a^2$  and  $\lambda$  the roots  $x_1$  and  $x_2$  are real and within the prescribed limits for all values of  $h$  ranging in absolute value from 0 up to a maximum

$$h_m = 2\lambda \left\{ \left( \frac{a^2}{2\lambda} + x_m \right) (1 - x_m^2) \right\}.$$

If  $\lambda$  is small, approximate values of the roots are

$$\begin{aligned} x_0 &= -\frac{a^2}{2\lambda} \left( 1 + 4\lambda^2 \frac{h^2}{a^6} \dots \right), \\ x_1 &= -\sqrt{1 - \frac{h^2}{a^2}} + \lambda \frac{h^2}{a^4} + 2\lambda^2 \frac{h^2}{a^6} \frac{1 - \frac{5}{4} \frac{h^2}{a^2}}{\sqrt{1 - \frac{h^2}{a^2}}} \dots, \\ x_2 &= \sqrt{1 - \frac{h^2}{a^2}} + \lambda \frac{h^2}{a^4} - 2\lambda^2 \frac{h^2}{a^6} \frac{1 - \frac{5}{4} \frac{h^2}{a^2}}{\sqrt{1 - \frac{h^2}{a^2}}} \dots \end{aligned} \quad (12)$$

Let us put

$$\begin{aligned} v &\equiv u - \frac{u_1 + u_2}{2}, & b &\equiv \frac{u_2 - u_1}{2}; \\ y &\equiv x - \frac{x_1 + x_2}{2}, & -y_0 &\equiv x_0 - \frac{x_1 + x_2}{2}, & c &\equiv \frac{x_2 - x_1}{2}; \end{aligned}$$

$b$  and  $c$  representing the amplitudes of  $u$  and  $x$  respectively. Then the integral of (8) is

$$\begin{aligned} \alpha - \sin^{-1} \frac{v}{b} &= \frac{\alpha}{\sqrt{2\gamma y_0}} \left[ \left( 1 + \frac{3}{16} \frac{c^2}{y_0^2} \dots \right) \sin^{-1} \frac{y}{c} \right. \\ &\quad \left. + \left( 1 - \frac{3}{8} \frac{y}{y_0} \dots \right) \frac{\sqrt{c^2 - y^2}}{2y_0} \right], \quad . \quad (13) \end{aligned}$$

where  $\alpha$  is a constant of integration.

To get the relation between  $\theta$  and  $\phi$  we eliminate  $r$  and  $t$  between (4) and (5). This gives

$$d\phi = \frac{h dx}{(1-x^2)\sqrt{2\lambda f(x)}}. \quad (14)$$

Integrating we have

$$\begin{aligned} \phi - \phi_0 = & \frac{h}{\sqrt{8\lambda y_0}} \left\{ \left[ 1 + \frac{1}{2} \frac{1+\bar{x}}{y_0} + \frac{3}{8} \frac{(1+\bar{x})^2}{y_0^2} \dots \right] \right. \\ & \times \frac{1}{\sqrt{(1+\bar{x})^2 - c^2}} \sin^{-1} \left\{ \frac{1+\bar{x}}{c} - \frac{(1+\bar{x})^2 - c^2}{c(1+\bar{x}+y)} \right\} \\ & + \left[ 1 - \frac{1}{2} \frac{1-\bar{x}}{y_0} + \frac{3}{8} \frac{(1-\bar{x})^2}{y_0^2} \dots \right] \frac{1}{\sqrt{(1-\bar{x})^2 - c^2}} \\ & \left. \sin^{-1} \left\{ \frac{(1-\bar{x})^2 - c^2}{c(1-\bar{x}-y)} - \frac{1-\bar{x}}{c} \right\} - \frac{3}{4y_0^2} \sin^{-1} \frac{y}{c} \dots \right\}, \quad (15) \end{aligned}$$

where  $\bar{x} \equiv (x_1 + x_2)/2$ .

The period  $P_r$  of  $r$  is obtained at once from (6). We have

$$P_r = \oint \frac{dr}{\sqrt{-2w + \frac{2\mu}{r} - \frac{a^2}{r^2}}} = \frac{2\pi\mu}{(2w)^{3/2}}. \quad (16)$$

Certain special types of motion are of interest. These may be classified as follows:—

(a)  $\phi$  constant. The motion is limited to a plane through the axis of the dipole. This case has been discussed in detail by Higab (*loc. cit.*).

(b)  $\theta$  constant. The orbit lies on the surface of a right circular cone whose axis coincides with the axis of the dipole.

(c)  $r$  constant. The motion is confined to the surface of a sphere. Cases (b) and (c) will now be investigated in detail.

#### *Motion on the Surface of a Cone.*

For this type of motion the roots  $x_1$  and  $x_2$  of  $f(x)$  coincide with the value (11) for which the function is a maximum. So the angle of the cone is given by

$$\cos \theta = x = \frac{1}{6\lambda} (\sqrt{a^4 + 12\lambda^2} - a^2), \quad (17)$$

for a specified value of  $a$ . Solving for  $a^2$  and determining  $h$  from (9)

$$a^2 = \lambda \frac{1-3x^2}{x}, \quad h^2 = \frac{\lambda}{x} (1-x^2)^2. \quad (18)$$

As  $a^2$  must be positive and both  $a^2$  and  $h^2$  finite,

$$\cos^{-1} \frac{1}{\sqrt{3}} \leq \theta < \frac{\pi}{2}.$$

Consequently the angle  $\theta$  of the cone must lie between  $54^\circ.8$  and  $90^\circ$ .

Eliminating the time between (4) and (6) the differential equation of the orbit is found to be

$$\frac{-du}{\sqrt{-2w+2\mu u^2-a^2u^2}} = \frac{\sin^2 \theta}{h} d\phi, \quad . \quad . \quad (19)$$

of which the integral is

$$\frac{1}{r} = \frac{1}{a^2} [\mu + \sqrt{\mu^2 - 2a^2w} \cos \{ \sqrt{1-3 \cos^2 \theta} (\phi - \phi_0) \}], \quad (20)$$

where

$$a^2 = \lambda \frac{1-3 \cos^2 \theta}{\cos \theta}, \quad w \leq \frac{\mu^2}{2a^2}.$$

This is the equation of an ellipse with rotating apsides inscribed on the surface of the cone, the focus being at the origin. If we develop the cone on a plane, using the polar coordinates  $r$  and  $\alpha$ ,

$$\alpha = \phi \sin \theta,$$

and the equation of the developed orbit is

$$\frac{1}{r} = \frac{1}{a^2} [\mu + \sqrt{\mu^2 - 2a^2w} \cos \{ (\sin \theta)^{-1} \sqrt{1-3 \cos^2 \theta} (\alpha - \alpha_0) \}] \quad . \quad . \quad . \quad (21)$$

The semi-major axis  $A$  of the ellipse is  $\mu/2w$  and the period of  $r$  is

$$P_r = 2\pi \frac{A^{3/2}}{\sqrt{\mu}},$$

which is identical with Kepler's third law of planetary motion.

The mean period of revolution is evidently

$$P_\phi = P_r \sqrt{1-3 \cos^2 \theta}, \quad . \quad . \quad . \quad (22)$$

so  $P_\phi < P_r$  for all admissible values of  $\theta$ .

As an example of motion on the surface of cone assume  $\mu = 10$ ,  $\lambda = 8$ ,  $\theta = 60^\circ$ . Then  $h = 3$ ,  $a = 2$ , and taking  $w = 4.5$ ,

$$\frac{1}{r} = 2.5 + 2 \cos \frac{1}{2}(\phi - \phi_0),$$



the radius vector oscillating between the minimum value  $2/9$  and the maximum  $2$ . For  $r$  to go through a cycle of values two revolutions are necessary. The periods are

$$P_r = \frac{20\pi}{27}, \quad P_\phi = \frac{10\pi}{27}.$$

The pseudo-elliptical orbit degenerates into a circle under the following circumstances:—

$$(1) \quad w = \frac{\mu^2}{2a^2} = \frac{\mu^2}{2\lambda} \frac{\cos \theta}{1 - 3 \cos^2 \theta}.$$

The orbit is a circle of radius

$$r = \frac{\lambda}{\mu} \frac{1 - 3 \cos^2 \theta}{\cos \theta}. \quad (23)$$

For each admissible value of  $\theta$  there is one and only one circular orbit, the radius of the circle increasing from  $0$  to  $\infty$  as  $\theta$  varies from  $54^\circ.8$  to  $90^\circ$ . For a given  $\theta$  the period  $P_\phi$  is less for the circular orbit than for any other orbit. If  $w$  has its maximum value  $12.5$  in the numerical example cited above, the orbit is a circle of radius  $0.4$  and period  $2\pi/25$ .

$$(2) \quad \mu = 0.$$

In this case  $\theta$  can be only  $\cos^{-1} \frac{1}{\sqrt{3}}$ , but the radius of the circle may have any value. No other type of periodic orbit on the surface of a cone is possible under this condition. The period  $P_\phi$  is

$$P_\phi = \frac{2\pi r^2}{3^{1/4} \sqrt{\lambda}}. \quad (24)$$

#### *Motion on the Surface of a Sphere.*

For the motion to take place on the surface of a sphere  $u_1$  must equal  $u_2$ . Therefore  $2a^2w = \mu^2$  and

$$r = \frac{1}{u} = \frac{a^2}{\mu} = \frac{\mu}{2w}, \quad (25)$$

showing that this type of motion is impossible if  $\mu = 0$  except for the circular orbit previously considered.

The equation of the orbit is given in differential form by (14) and in integrated form by (15),  $\cos \theta$  oscillating between the roots  $x_1$  and  $x_2$  of  $f(x)$  as the electron progresses around the axis of the doublet. The motion is similar to that of the apex of a top acted on by the torque due

to gravity, although retrograde motion is impossible, since it is clear from (4) that for  $h$  not equal to zero  $\dot{\phi}$  can never vanish or change sign. Consequently the orbit always meets the limiting parallels of latitude tangentially. Since  $x_1 + x_2 > 0$  it follows from (4) that the revolution is more rapid when  $\theta$  is minimum than when  $\theta$  is maximum.

The period of  $\theta$  is obtained at once from (5). It is

$$P_\theta = \frac{r^2}{\sqrt{2\lambda}} \oint \frac{dx}{f(x)} \\ = \frac{2\pi r^2}{\sqrt{2\lambda y_0}} \left( 1 + \frac{3}{16} \frac{c^2}{y_0^2} \dots \right). \quad (26)$$

Substituting the approximate values of the roots given by (12) and using (25)

$$P_\theta = \frac{2\pi\mu}{(2w)^{3/2}} \left\{ 1 + 3 \frac{\lambda^2 w^2}{\mu^4} \left( 1 - 10 \frac{wh^2}{\mu^2} \right) \dots \right\} \\ = \frac{2\pi r^{3/2}}{\sqrt{\mu}} \left\{ 1 + \frac{3}{4} \frac{\lambda^2}{\mu^2 r^2} \left( 1 - 5 \frac{h^2}{\mu r} \right) \dots \right\}. \quad (27)$$

When  $\theta$  goes through a cycle of values we see from (15) that  $\phi$  increases by

$$\Delta\phi = \frac{\pi h}{\sqrt{2\lambda y_0}} \left\{ \frac{1}{\sqrt{(1+\bar{x})^2 - c^2}} \left[ 1 + \frac{1}{2} \frac{1+\bar{x}}{y_0} + \frac{3}{8} \frac{(1+\bar{x})^2}{y_0^2} \dots \right] \right. \\ \left. + \frac{1}{\sqrt{(1-\bar{x})^2 - c^2}} \left[ 1 - \frac{1}{2} \frac{1-\bar{x}}{y_0} + \frac{3}{8} \frac{(1-\bar{x})^2}{y_0^2} \dots \right] - \frac{3}{4y_0^2} \dots \right\} \\ \dots (28)$$

The mean azimuthal angular velocity is then

$$\bar{\phi} = \frac{\Delta\phi}{P_\theta}.$$

In terms of the approximate values of the roots (12)

$$\bar{\phi} = \frac{\sqrt{\mu}}{r^{3/2}} \left\{ 1 - \frac{3}{4} \frac{\lambda^2}{\mu^2 r^2} \left( 1 + 2 \frac{h}{\sqrt{\mu} r} - 5 \frac{h^2}{\mu r} \right) \dots \right\}. \quad (29)$$

Therefore the mean period of revolution  $P_\phi$  is related to  $P_\theta$  by the equation

$$P_\phi = P_\theta \left\{ 1 + \frac{3}{2} \frac{\lambda^2 h}{(\mu r)^{5/2}} \dots \right\}, \quad (30)$$

indicating that  $P_\phi > P_\theta$ .

To illustrate this type of motion take  $\mu = 10$ ,  $\lambda = 8$  as before, and let  $h^2 = 24$ ,  $w = 50/24$ . Then  $r = 2.4$ ,  $a^2 = 24$ , and

$$f(x) = -x^3 - \frac{3}{2}x^2 + x = -x(x - \frac{1}{2})(x + 2).$$

So

$$x_0 = -2, \quad x_1 = 0, \quad x_2 = \frac{1}{2},$$

and  $\theta$  oscillates from  $60^\circ$  to  $90^\circ$ . Moreover,

$$y_0 = \frac{9}{4}, \quad c = \bar{x} = \frac{1}{4},$$

and from (26) and (30)

$$P_\theta = 6.032(1 + .0023 + \dots) = 6.046$$

$$P_\phi = 6.046(1 + .17 + \dots) = 7.1.$$

### Hamilton-Jacobi Method of Solution.

The Hamilton-Jacobi equation, obtained at once from the energy equation (7), is

$$\frac{1}{2} \left\{ \left( \frac{\partial S}{\partial r} \right)^2 + \frac{1}{r^2} \left( \frac{\partial S}{\partial \theta} \right)^2 + \frac{1}{r^2 \sin^2 \theta} \left( \frac{\partial S}{\partial \phi} \right)^2 \right\} - \frac{\mu}{r} - \frac{\lambda \cos \theta}{r^2} = -w. \quad (31)$$

The variables are easily separated and the phase integrals calculated. They are

$$I_\phi = 2\pi h,$$

$$I_\theta = 2\pi(a - h) - \frac{\pi \lambda^2}{2a^3} \left( 1 - 3 \frac{h^2}{a^2} \right) \dots, \quad (32)$$

$$I_r = 2\pi \left( \frac{\mu}{\sqrt{2w}} - a \right),$$

where the constants of separation  $h$  and  $a$  have the same significance as the constants designated by the same letters in the previous treatment of the motion. Evidently  $h$  is a function of  $I_\phi$  alone,  $a$  of  $I_\phi$  and  $I_\theta$ , and  $w$  of the three phase integrals.

If

$$I \equiv I_r + I_\theta + I_\phi$$

elimination of  $h$  and  $a$  gives for the energy expressed as a function of the phase integrals

$$H = -w = -\frac{2\pi^2 \mu^2}{I^2} + \frac{16\pi^6 \mu^2 \lambda^2}{I^3 (I_\theta + I_\phi)^3} \left\{ 1 - 3 \frac{I_\phi^2}{(I_\theta + I_\phi)^2} \right\} \dots \quad (33)$$

up to terms in  $\lambda^4$ . The fundamental frequencies may be obtained by differentiating  $H$  partially with respect to the  $I$ 's. The periods given in the earlier part of the paper have been checked from the frequencies so obtained. Evidently the motion for finite  $\lambda$  and  $\mu$  is completely non-degenerate.

Sloane Physics Laboratory.

Yale University.

November 11, 1929.

XXVII. *On Polymolecular Films.* By R. S. BRADLEY\*.

SEVERAL cases are known in which a vapour adsorbs on a solid surface to give a film several layers in thickness. Lehner† obtained thick films of water on platinum, glass, and quartz. Frazer, Patrick, and Smith‡ criticized Lehner's work on the grounds that the walls were etched by acids. They found no adsorption of toluene on a plane surface. Smits§, however, has obtained polymolecular layers of mercuric iodide on glass 500 molecules thick at 300° C., and J. W. Smith|| thick layers of water and benzene on amalgamated platinum (as smooth as possible). Since the range of surface forces is small, the formation of such films must be due to interaction between adsorbed molecules. In this paper interaction caused by electric polarization will be studied.

Landé and R. Lorenz¶ have considered the case of an electric doublet forming an electrical image in a solid surface. If the dipole makes an angle  $\theta$  with the normal to the surface, the energy of the doublet in the field of its electrical image is

$$\frac{-\mu^2}{2r^3} (3 + \cos 2\theta),$$

where  $\mu$  is the strength of the dipole and  $r$  is its distance from the surface. Adopting a treatment slightly different from Landé and Lorenz's,  $dN$  the number of mols. per c.c.

\* Communicated by the Author.

† Lehner, J. C. S. 1927, p. 272.

‡ Frazer, Patrick, and Smith, J. Phys. Chem. xxxi. p. 897 (1927).

§ Smits, J. C. S. 1928, p. 2045.

|| J. W. Smith, J. C. S. 1928, p. 2045.

¶ Landé and Lorenz, *Zeit. Anorg. Chem.* cxxv. p. 47 (1922).

at a distance  $r$ , whose axes make an angle  $\theta$  with the surface normal is

$$\left( e^{\frac{\mu^2}{2kT r^3} (3 + \cos 2\theta)} \right) d(\cos 2\theta).$$

Hence  $N_r$ , the number of molecules per c.c. at a distance  $r$ , is

$$N_r = C e^{3b} \int_{-1}^{+1} e^{b\lambda} d\lambda,$$

where

$$b = \frac{\mu^2}{2kT r^3} \quad \text{and} \quad \lambda = \cos 2\theta.$$

Hence

$$N_r = N_\infty e^{3b} \frac{\sinh b}{b},$$

while the number of molecules adsorbed per sq. cm. is

$$\int_{a/2}^{\infty} N_\infty \left( e^{3b} \frac{\sinh b}{b} - 1 \right) dr,$$

where  $a$  is the diameter of a dipole. It is clear that, instead of giving a thick film, the concentration of adsorbed molecules diminishes approximately exponentially with the distance. The calculation neglects the polarization at optical frequencies of the adsorbed molecules, and the interaction between the various adsorbed molecules and their electrical images in the surface.

The problem is, of course, a three-dimensional one. The point charges should be replaced by a Fourier development after the method of Ewald. Such a method has been applied by Kornfeld\* to determine the energy of a dipole lattice. The thick film may be replaced by a static model of a dipole lattice with a fading polarization from the surface upwards. This, however, makes the calculation extremely difficult, and in this paper only the case of a dipole chain will be considered.

The dipole next to the surface is taken as completely oriented by the surface forces, and of fixed net permanent moment independent of temperature. Built up on this is a dipole chain. Each dipole forms an induced charge on the surface, which acts in the case of a conductor as if it were the mirror image of the dipole. For a dielectric of constant  $K$  the image has a moment

$$\mu \left( \frac{K-1}{K+1} \right)^{\frac{1}{2}}.$$

\* *Zeit. für Physik*, xxii. p. 27 (1924).

Consider  $n$  dipoles of diameter  $a$ . Let the force on the  $p$ th dipole be  $F_p$ , let  $\mu_s$  be the net moment of the  $s$ th dipole, and  $\alpha$  the polarizability.

Then

$$F_p - \sum_{s=1}^{s=p-1} \left[ \frac{2\mu_s}{(p-s)^3 a^3} + \frac{2\mu_s}{(p+s-1)^3 a^3} \right] + \sum_{s=p+1}^{s=n} \left[ \frac{2\mu_s}{(s-p)^3 a^3} + \frac{2\mu_s}{(p+s-1)^3 a^3} \right] + \frac{2\mu_p}{(2p-1)^3 a^3} = 0.$$

Here the terms containing  $p+s-1$  are due to the images in the conductor. Also

$$\mu_s = \mu L\left(\frac{\mu F_s}{kT}\right) + \alpha F_s,$$

where  $L(x)$  is the Langevin function

$$= \coth x - \frac{1}{x} = \frac{x}{3} - \frac{x^3}{45} \quad \text{for small } x,$$

$$= 1 - \frac{1}{x} + 2e^{-2x} \quad \text{for large } x.$$

We shall take the case

$$\frac{\mu F}{kT} > 1,$$

and use the second expansion. Hence,

$$\begin{aligned} F_p - \sum_{s=2}^{s=p-1} \frac{1}{a^3} \left[ \frac{1}{(p-s)^3} + \frac{1}{(p+s-1)^3} \right] & \left[ 2\mu \left( 1 - \frac{kT}{\mu F_s} \right) + \lambda \alpha F_s \right] \\ - \sum_{s=p+1}^{s=n} \frac{1}{a^3} \left[ \frac{1}{(s-p)^3} + \frac{1}{(p+s-1)^3} \right] & \left[ 2\mu \left( 1 - \frac{kT}{\mu F_s} \right) + \lambda \alpha F_s \right] \\ - \frac{1}{(2p-1)^3 a^3} \left[ 2\mu \left( 1 - \frac{kT}{\mu F_p} \right) + \lambda \alpha F_p \right] & - \frac{2\mu + 2\alpha F_1}{a^3} \left( \frac{1}{(p-1)^3} + \frac{1}{p^3} \right) = 0. \end{aligned}$$

It is useful to note that

$$\frac{1}{1^3} + \frac{1}{2^3} + \frac{1}{3^3} \dots \frac{1}{x^3} = 1.202 - \frac{1}{2x^2} + \frac{1}{2x^3} - \frac{1}{4x^4} \dots$$

These  $n$  equations determine the  $n$  unknowns  $F$ . They become linear when, as a first approximation,  $1 - \frac{kT}{\mu F}$  is written as 1. Hence the first approximation is

$$F_p = \frac{\Delta_p}{\Delta},$$

where  $\Delta$  is the determinant formed by the coefficients of the  $F$ 's on the left-hand side, and  $\Delta_p$  is the determinant formed by replacing the coefficients of  $F_p$  in  $\Delta$  by the constants terms of each linear equation

$$AF_p + BF_1 + CF_3 + \dots = \text{constant}.$$

The second approximation is then obtained by giving  $1 - \frac{kT}{\mu F_p}$  the values  $1 - \frac{kT\Delta}{\mu\Delta_p}$ , giving

$$F_p = \frac{\Delta'_p}{\Delta'}.$$

The energy of the  $p$ th dipole is then

$$-\mu F_p L \left( \frac{\mu F_p}{kT} \right) - \frac{1}{2} \alpha F_p^2 + \frac{2\lambda}{(n-1)a^{n-1}}.$$

The last term is due to the repulsive forces, and acts merely between adjacent dipoles. Its evaluation is uncertain, but it may be computed for water (the example chosen below) from Lennard-Jones' forces constants for neon\* on the assumption of a neon-like sheath for the pseudo-atom water, and it is relatively small.

The solution of the determinants is laborious, and we shall consider only the case of three layers. We take  $a$  for the liquid film to be the same as for water, where X-ray diffraction suggests a similar partial orientation;  $\mu = 1.7 \cdot 10^{-18}$  and the molecular refraction = 3.7. The difference between the total energies of chains of three and two molecules will give the energy required to remove the surface molecule from a chain of three molecules, and this is the latent heat of evaporation, per molecule, of a film of three molecules.

\* Lennard-Jones, P. R. S. cix. p. 476 (1925).

In the case of water at 25° C. we find for a layer of three molecules (E.S.U.)

$$F_3 = 1.61 \cdot 10^5, \quad F_2 = 2.85 \cdot 10^5, \quad F_1 = 3.13 \cdot 10^5;$$

whilst for a layer of two molecules

$$F_2 = 1.625 \cdot 10^5, \quad F_1 = 2.69 \cdot 10^5.$$

This gives for the latent heat of evaporation of the film of three molecules the value 8,600 cal. per gram mol., which agrees well with Lehner's figures for

$$\frac{-Rd \log_e P_\phi}{d\left(\frac{1}{T}\right)} = L_\phi,$$

$\phi$  being the number of layers, viz.,

$$\begin{array}{ll} \text{at } 25^\circ \text{ C.} & \phi = 5, \quad L = 9100, \\ & \phi = 10, \quad L = 10,530. \end{array}$$

The University, Leeds.  
April 1930.

## XXVIII. Automatic Recording Waterproof Tester.

By A. L. HODGES\*.

SOME few years ago the writer had to develop a device that would record accurately the time it took water to seep through various fabrics and papers. The result was a very satisfactory piece of apparatus which is shown in the accompanying drawing.

In comparing samples for waterproof qualities it was found absolutely necessary to condition them all alike before testing. The conditioning used by the writer was to confine the samples in a space at laboratory temperature for 24 hours with a vessel having a free water surface.

For thin samples the large drop of water shown in fig. 1 was found to be all that was necessary. For thicker ones the water head shown in fig. 2 was used.

The operation of the device is simple. The water is placed on the sample and the clock started. When the

\* Communicated by the Author.



water seeps through to the salt and wets it (a very quick process as the amount of salt is small) the electrical circuit is completed. The lamp lights up and the pen is pulled to one side. The current, however, being about an ampere, quickly dries the salt and shuts itself off. When the water seeps through again the pen, of course, repeats. In the drawing the record shows a breakdown time of five hours, and a first seepage time of two hours, a second seepage of one hour.

Thus the device is capable of showing automatically not only the breakdown time but the various successive

Fig. 2.

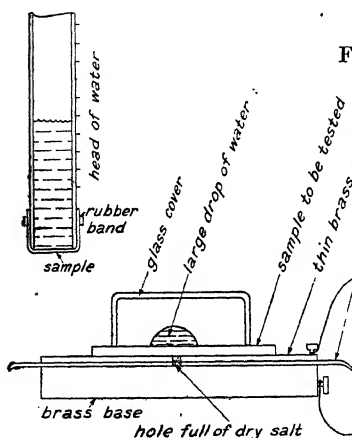
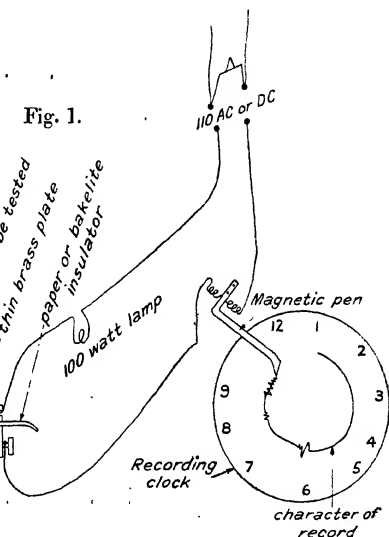


Fig. 1.



seepage times of samples. It is thought that, if the device were to come into general use, specifications and a standard scale could be arranged for it, so that the waterproof qualities of a material could be placed on a standard basis, and an understandable one. However, no attempt has so far been made to have the device manufactured, and as the materials necessary are in general available in all laboratories, it was thought that publication might result in trial by others, or at least in criticisms of value.

XXIX *On the Absorption of X-Rays in Gases and Vapours.*—Part I. *Gases.* By J. A. CROWTHER, M.A., Sc.D., F.Inst.P., Professor of Physics in the University of Reading, and L. H. H. ORTON, B.Sc., Wantage Scholar, University of Reading\*.

THE research described in this and subsequent papers consists in the measurement of the absorption of X-rays in a number of gases and vapours, and of the ionization produced by this absorption. A similar series of experiments was made by one of the writers† rather more than twenty years ago. The radiation used in the earlier experiments was the heterogeneous radiation from an ordinary X-ray tube. The absorption measurements were therefore of little real significance, and no conclusions of value as to the relation between absorption and ionization can be drawn from them. In spite of this there has been, as far as we are aware, no subsequent redetermination of these quantities on an extensive scale, though a few scattered observations have been recorded, and the values obtained in the early paper are still quoted in the standard books of tables. In the circumstances it was felt that a re-survey of the problem, using radiation of definite wavelength, was highly desirable. Accurate data are frequently required for practical purposes, and, in addition, it was hoped that some information might emerge on the interesting subject of the energy relations involved in the production of ions in gases by X-rays. The portion of the work now published deals with the measurements made on selected gases.

### §1. *Experimental Details.*

Owing to the rapidity with which the absorption of X-rays varies with the wave-length, absorption measurements are only significant if made on radiation which is homogeneous to a fairly high degree. No practicable amount of "filtration" will produce a beam sufficiently homogeneous for the purpose‡, and it is necessary to have recourse to a crystal reflexion method. In order to avoid

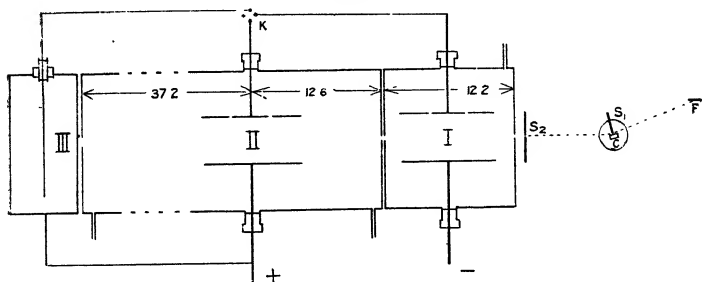
\* Communicated by Prof. J. A. Crowther, Sc.D.

† J. A. Crowther, Proc. Roy. Soc. A, lxxxii. p. 103 (1909).

‡ J. A. Crowther, Brit. Journ. Rad. ii. p. 175 (1929).

too greatly attenuating the reflected beam, the crystal (a large-rock salt crystal which had been thoroughly tested in previous experiments) was mounted as shown in fig. 1, following a suggestion originally due to Seeman. A lead screen  $S_1$  with a vertical straight edge makes contact with the vertical face of the crystal C, both screen and crystal being mounted on a turntable the axis of rotation of which coincides with the line along which the screen meets the crystal. The screen is then moved back slightly, leaving a gap of approximately one millimetre between its vertical edge and the crystal. This forms the first limiting slit of the reflected pencil; the second slit  $S_2$ , adjusted to a width of about 1 mm., is placed so that the line  $S_2C$  makes with the face of the crystal an angle equal to the glancing

Fig. 1.



angle for  $\text{Cu.K}_\alpha$  radiation. The distance  $S_2C$  was made equal to the distance between the focal spot  $F$  of a Shearer tube fitted with a copper anticathode and the axis of rotation  $C$ , each distance being 7 cm. The preliminary settings were made optically, and the final settings by photographic methods. The arrangement had not sufficient resolving power to separate the two  $\alpha$  components, but a photograph taken at the extreme end of the apparatus *i. e.*, 70 cm. from the crystal, showed that the radiation coming through the three chambers consisted of a well-defined beam with sharp edges and rather less than 1 mm. in width.

The Shearer tube was excited with a current of 6 ma. at a potential of 40,000 volts. Potentials of this order were required in order to produce radiation of sufficient intensity for accurate measurement. Some "general" radiation will thus be reflected to the slit  $S_2$  in the second order

spectrum. An analysis of the radiation from the tube showed, however, that the amount of such radiation was completely negligible. As an additional test, however, the mass absorption of the radiation in aluminium was measured with the apparatus, using sheets of sufficient thickness to absorb up to  $\frac{2}{3}$  of the radiation. The coefficient so obtained, 48.7, agreed closely with the value given by the recent experiments of Allen \*, for the absorption of  $K_{\alpha}$  radiation of copper in aluminium.

The beam after passing the slit  $S_2$  passed axially through two cylindrical brass chambers, I. and II. (fig. 1), entering and leaving the chambers through narrow rectangular windows covered with thin cellophane of thickness 0.05 mm. Both chambers were made vacuum-tight, and could be evacuated to any desired pressure by a Hyvac pump, the pressures being measured by mercury manometers. Each chamber was fitted with a pair of parallel plate electrodes of aluminium. The collecting plate of the system was 3.8 cm. wide and was surrounded by a guard-ring of 2.5 cm. width to ensure uniformity of field across the collecting area. The distance between the electrodes was 3 cm. It was calculated that this distance was sufficient to ensure complete absorption of the photo-electrons ejected by the X-ray beam at the lowest pressures used. The final ionization chamber, III., which remained at atmospheric pressure throughout, was of the paper electrode type, investigated by Treloar †.

Chambers I. and III. always contained air. The gas under investigation was contained in chamber II. This vessel was made sufficiently long (49.8 cm.) to produce an easily measurable absorption of the radiation by the gas under observation.

Chamber I. was permanently connected to a Wilson tilted electroscope working at a sensitivity of about 100 divisions per volt. The collecting plates of II. and III. were connected to a high insulation key, so that either of them could be connected either to the electroscope or to earth. The high potential electrodes were so arranged that the charge collected by chamber I. was opposite in sign to that collected by either II. or III. The usual precautions for screening the apparatus both from stray radiation and from electrostatic disturbances were taken.

\* S. J. Allen, *Phys. Rev.* xxviii. p. 907 (1926).

† Treloar, *J. Brit. Inst. Rad.* ii. p. 188 (1929).

§ 2. *Measurement of Absorption.*

All measurements were made by a balance method, originally described by one of the authors\*. It has been shown that in an ionization chamber of the type of chamber I. the ionization produced by a beam of X-rays is directly proportional to the pressure of the gas in the chamber. Thus, by adjusting the pressure, it is possible to adjust the ionization current through I. to any known fraction of its value at normal atmospheric pressure. Suppose, now, that the collecting systems of I. and III. are connected to the electroscope, that of II. being earthed. Since the charges collected are opposite in sign, it will be possible to adjust the pressure in I. so that the resultant charge on the gold leaf is zero when the X-rays are passing through both chambers. The system may then be said to be balanced. Let  $p_1$  be the pressure at which a balance is obtained when II. is evacuated, and  $p_1'$  the smaller pressure required for a balance with the chamber II. full of gas. Then  $p_1'/p_1$  is clearly the ratio of the intensities of the radiation in III. with the chamber II. full and empty, and thus measures the absorption of the column of gas. If  $\lambda$  is the linear coefficient of absorption for the gas  $p_1'/p_1 = e^{-d\lambda}$  where  $d$  is the length of chamber II.

This method eliminates most of the errors incidental to the measurement of small ionization currents with a sensitive electroscope. The balance is clearly independent of fluctuations in intensity of the radiation (a source of considerable uncertainty in X-ray work); it is independent of fluctuations in the sensitivity of the electroscope; and has the additional merit that slight defects in insulation do not affect the balance point, although they reduce the sensitivity of the method. In practice, with radiation of the intensity available in these experiments, it was possible to balance the system with certainty to about 1 mm. of pressure. As the smallest pressure used in I. was about 25 cm. this should give an accuracy rather better than  $\frac{1}{2}$  per cent. on an individual reading.

In practice corrections have to be applied for the varying absorption of the radiation in chamber I., for the absorption of the radiation by the residual gas in II., and for the slight change in pressure in III., which being at atmospheric pressure changes with the barometer. These

\* Crowther, *Phil. Mag.* xiv. p. 653 (1907).

corrections are of the order of a few per cent. It is also more convenient to express the results in terms of the mass absorption coefficient,  $\mu$ , rather than the linear coefficient. It can easily be shown that if  $\mu$  is the mass coefficient of absorption of the gas in II., and  $\rho$  its density at N.T.P.,  $\mu_a$  and  $\rho_a$  the same coefficients for air,  $d_1$  the length of chamber I. (12.2 cm.), and  $d_2$  the length of chamber II. (49.8 cm.)

$$\frac{p_1}{p_3} \frac{p_3'}{p_1'} = \epsilon - [\mu \rho d_2 (\frac{p_2}{\theta} - \frac{p_2'}{\theta'}) + \mu_a \rho_a d_1 (\frac{p_1}{\theta} - \frac{p_1'}{\theta'})] \frac{\theta_0}{\Pi},$$

where  $p_1, p_i$  are the balance pressures in I. and III. with II., full of gas at a pressure  $p_2$  and absolute temperature  $\theta$ , the symbols with the dash affixed referring to the same quantities with chamber II. at a low pressure;  $\theta_0$  and  $\Pi$  being the standard temperature and pressure.

The mass coefficient of absorption for air can be determined by using air in chamber II.  $\mu$  thus becomes equal to  $\mu_a$ , and we have an equation with a single unknown. The value so obtained can then be used in the correcting term for other gases. The term involving  $\mu_a$  is only of the order of 3 per cent., so that an error in  $\mu_a$  would not affect the other values appreciably.

### §3. Measurement of the Ionization.

The ionization of the various gases has been measured relative to air under the same conditions of pressure and temperature. The collecting electrodes of chambers I. and II. were connected to the electroscope, that of III. being earthed, and the pressures adjusted so that the gold-leaf remained at rest when the tube was excited. A balance was obtained first with the chamber II. filled with the air, and again when the air had been replaced by the gas under experiment. The ionization in II. is directly proportional to the pressure of the air in I. which is required to balance it. The result is clearly independent of the dimensions of the chambers, and of the intensity of the radiation.

The ionization of the gas in II., however, varies with its temperature and pressure, and for convenience, all the observations were reduced to normal temperature and pressure. Correction is also required for the absorption of the radiation in passing from the collecting system in I. to that in II., since this absorption varies with the nature

of the gas in II. and the pressure of the air in I. (The absorption of the cellophane windows, being constant, does not enter into the calculation.) The path of the radiation was reckoned from the centre of the collecting electrode in I. to the centre of the collecting electrode in II., *i. e.*, 6.1 cm. in air in I., and 12.6 cm. in the gas in II. Since the absorption coefficients are known the correction can readily be calculated. It varies according to the nature of the gas in II. from about 15 per cent. to 30 per cent.

### *Preparation of the Gases.*

As far as possible preparations were chosen which could be carried out *in vacuo*. In this case the whole system could be evacuated to a low pressure and the complete elimination of air ensured. When this was not possible the apparatus was washed out repeatedly with the gas; the chamber being evacuated between each filling.

*Air.*—The air used both in I. and II. entered the chamber through long tubes packed with soda-lime to remove water vapour and carbon dioxide.

*Carbon dioxide.*—This gas was obtained from a cylinder. The first portions of the gas from the cylinder were discarded. The gas was dried by calcium chloride.

*Nitrogen.*—Prepared from sodium nitrite and ammonium chloride. The gas was purified by passing through a mixture of concentrated sulphuric acid and potassium bichromate, potassium hydroxide, and soda-lime, and was dried by calcium chloride and phosphorus pentoxide.

*Oxygen.*—Prepared by the action of heat on pure crystalline potassium permanganate. It was then passed over solid potassium hydroxide to remove traces of carbon dioxide, and dried by phosphorus pentoxide.

*Ethylene.*—Prepared by the action of phosphoric acid on absolute alcohol.

*Hydrogen sulphide.*—Prepared by the action *in vacuo* of water on a mixture of barium sulphide and magnesium chloride, and dried by phosphorus pentoxide.

Nitric oxide was also prepared but was found to attack the insulation so rapidly that measurements were impossible.

### § 4. *Experimental Results.*

The results obtained are given in Table I. The first column gives the value assumed in our calculations for the density of the gas at standard temperature and pressure.

The second column gives the measured mass coefficient,  $\mu$ , of absorption of the gas for the copper  $K_{\alpha}$  radiation. It clearly includes both the true absorption and the scattering. The third column gives the volume ionization of the gas relative to air, that is to say, it gives the ratio of the ionization produced in a given volume of the gas by a given beam of X-rays to the ionization produced by the same beam in an equal volume of air under the same conditions of temperature and pressure. The final column of the table, which is deduced from the previous column, gives the ratio of the ionization of a given mass of the gas to that of an equal mass of air. It thus corresponds to the mass absorption coefficient. The absorption coefficient is an absolute value; the ionization values are all relative to air.

It will be desirable, at this point, to discuss the probable accuracy of the results given in Table I. It has been

TABLE I.

	$\rho_0$	$\mu$	$I_v$	$I_m$
Air.....	·001293	9·46	1·000	1·000
N <sub>2</sub> .....	·001254	7·43	0·743	0·766
O <sub>2</sub> .....	·001429	11·14	1·438	1·301
CO <sub>2</sub> .....	·001965	9·30	1·530	1·006
C <sub>2</sub> H <sub>4</sub> .....	·001254	4·32	0·508	0·524
H <sub>2</sub> S .....	·001538	82·7	14·96	12·58

$\rho_0$ =density at N.T.P.;  $\mu$ =mass absorption coefficient;  $I_v$ =relative ionization for equal volumes;  $I_m$ =relative ionization for equal masses.

mentioned that the balance pressure can be fixed with certainty to about 1 mm. of mercury. With the pressures usually employed this should give an accuracy of at least  $\frac{1}{2}$  per cent. in the values for the balance pressures. The relative ionization depends only on the ratio of the balance pressures and should, therefore, have the same order of accuracy. In point of fact, repeated observations of the relative ionization made with different samples of the same gas did not, as a rule, vary by more than  $\frac{1}{2}$  per cent. from the mean value. The values given in the table are the mean of at least four independent experiments. They should, therefore, be correct to at least  $\frac{1}{2}$  per cent.

The absorption measurements were not quite so satisfactory. It will be seen from the equation in § 2 that



the coefficient of absorption involves the difference between the logarithms of two balance pressures. With some of the less absorbent gases the change in the balance pressure produced by evacuating the gas from chamber II. did not amount to more than 30 per cent. of the original pressure. Discrepancies of the order of 2 or 3 per cent. may therefore be expected between different independent determinations of  $\mu$ , and variations from the mean of this order of magnitude were in fact found. The values given in the table are usually the means of at least four independent determinations. They should be accurate as far as the first place of decimals. The second decimal figure is probably not significant.

### § 5. *The Total Ionization in Different Gases.*

If a beam of homogeneous X-rays is of such intensity that it produces in a layer of gas having a mass per unit area  $dm$  an amount of ionization equal to  $I_m dm$ , the total ionization produced by the complete absorption of the radiation in the gas will be  $I_m \int_0^{\infty} e^{-\tau m} dm$  or  $\frac{I_m}{\tau}$ ; where  $\tau$  is the mass coefficient of true absorption. Our experiments give us the relative values of  $I_m$  for different gases, and the values of  $\mu$  the mass absorption coefficient, including the scattering. We have not been able to find any reliable data on the scattering coefficient for copper  $K_\alpha$  radiation. For the heterogeneous radiation from a fairly soft X-ray tube it is known that the mass coefficient of scattering,  $\sigma$ , is of the order of 0.2, and is approximately the same for all elements of low atomic number. These results are in agreement with the classical theory of scattering. There is no reason to suppose that the scattering, from elements of low atomic number, increases rapidly with the wave-length, though it is known to increase with the atomic number when the latter is large. Unless the value 0.2 is a gross underestimate, the scattering is such a small fraction of the whole absorption that its exact value becomes of no importance. In the calculations which follow we have assumed that the mass coefficient of scattering for each of the gases used has the value 0.2 and that  $\tau$  can be calculated by subtracting this amount from the coefficient  $\mu$ .

The values so obtained for the total ionization in the different gases are given in the first column of Table II.,

the value for air being again taken as unity. (It may be noted that the values so obtained hardly differ by more than the experimental error from those which would be obtained if the scattering correction were ignored completely.) For comparison we give in the second column the values collected by Stuhlman\* for the relative total ionization produced in the same gases by the complete absorption of a beam of  $\alpha$ -rays from radium. The agreement between the two columns is extraordinarily close, and seems to show quite conclusively that the relative total ionization produced in a gas is independent of the nature of the ionizing agent, even for agents as widely different as  $\alpha$ -rays and X-rays.

§ 6. *The average Energy spent per Ion in different Gases.*

The coefficient T, which we have called the relative total ionization, is a measure of the total number of ions produced in the different gases by the complete absorption of the same amount of X-ray energy. Its reciprocal,  $1/T$ , thus measures the average energy spent in producing a pair of ions in the different gases. The values are, of course, not absolute but are relative to that for air, which is taken as unity. It is interesting therefore to compare the values of  $1/T$ , which measure the average energy absorbed in the production of a pair of ions, with the ionization potential P, which measures the smallest amount of energy which will produce a pair of ions. In fact, it was the primary object of our experiments to obtain the data which would enable us to make this comparison, and our choice of gases was governed by this consideration.

Unfortunately, the ionization potentials for the majority of gases available for our experiments do not appear to be known with any great accuracy. The first ionization potential for nitrogen seems to be well established and is given, in the International Critical Tables, as  $16.7 \pm 0.3$  volts. This summarises most of the more reliable experiments sufficiently well. The value for oxygen was originally taken as 15.5 volts, but Mackay† obtained strong evidence for the production of some ionization in oxygen at 12.5 to 12.8 volts. This lower value is confirmed by Smyth‡

\* Stuhlman, Intern. Critical Tables, vi. p. 122.

† Mackay, Phil. Mag. xlv. (1923); Phys. Rev. xxii. (1924).

‡ Smyth and Stueckelberg, Phys. Rev. xxxii. p. 779 (1928)

by comparing directly the ionization potential in oxygen with that of argon. He states that the ionization potential of oxygen is certainly lower than 15 volts, probably even less than 13 volts. The International Critical Tables adopt the value 12.8 volts for the lowest ionization potential of oxygen, and this is the value we have accepted on the authority of Morris\*, whose values for other gases seem to be in excellent agreement with the best data. The values for carbon dioxide and sulphuretted hydrogen rest entirely on the observations of Mackay†, as we have been unable to trace any other measurements of the ionization potentials of these gases. Hydrogen and helium, whose ionization potentials are particularly accurately known, could not, unfortunately, be used in our experiments, as the absorption produced by a 50 cm. column of either of these gases would be far too small to be measured. The values adopted for P, the first ionization potential, are given in the third column of Table II.

It will be seen at once that the total ionization is greatest for gases for which the minimum ionization potential is the least. In fact, the total ionization is not far from being inversely proportional to the minimum ionization potential. The product  $P.T$  is given in the last column of the table. For four of the five gases used (oxygen, carbon dioxide, ethylene, and sulphuretted hydrogen) the product  $P.T$  cannot be said to differ from a mean value, 14.4, by more than the possible uncertainties in the values of  $P$ . This implies that for any one of these gases the average energy absorbed in forming a pair of ions is closely proportional to the minimum energy required to form a pair of ions in the gas. The value of the product for nitrogen is definitely higher than for the other gases, the difference being definitely greater than the possible experimental error. A large amount of work has been published on the ionization potentials of nitrogen, and there seems no reasonable cause to doubt that its value lies between the limits given in Table II. The value for nitrogen is thus the most certain of all the values.

These results raise some interesting points. It is sometimes supposed that the whole of the energy absorbed in a gas is utilized in producing ionization. In this case,

\* Morris, Phys. Rev. xxxii. p. 456 (1928).

† *Loc. cit.*

neglecting the ionization produced at critical potentials above the minimum ionization potential, the average energy spent in forming a pair of ions would be very nearly equal to the minimum ionization potential. A theory of the production of ionization by collisions between high-speed particles ( $\alpha$ - or  $\beta$ -rays) and gaseous molecules, put forward originally by Sir J. J. Thomson\*, developed by Bohr †, and finally corrected by Fowler ‡, suggests that the average energy spent in producing a pair of ions in this way in a gas with a single ionization potential should be equal to  $4/3$  times the ionization potential. If ionization also takes place at higher critical potentials allowance has to be made for the extra energy required for this process. It is generally believed that the large majority of the ions are

TABLE II.

	T.	T <sub>a</sub> .	P.	P.T.
Air .....	1.000	1.00	—	—
N <sub>2</sub> .....	0.982	0.98	16.7 ± .3	16.4
O <sub>2</sub> .....	1.103	1.13	12.8	14.1
CO <sub>2</sub> .....	1.024	1.02	14.3	14.6
C <sub>2</sub> H <sub>4</sub> .....	1.179	1.22	12.2	14.4
H <sub>2</sub> S .....	1.410	—	10.4	14.7

T=relative total ionization from X-ray measurements.

T<sub>a</sub>=relative total ionization for  $\alpha$ -rays.

P=minimum ionization potential in volts.

formed at the minimum potential §, and that the correction is quite small. It could, of course, easily be calculated if the percentage of ions formed at each potential were known. Neglecting this correction it follows that on either view the ratio of P.T to the energy, E, absorbed should be constant; the ratio P.T/E being unity on the first supposition and  $\frac{3}{4}$  on Fowler's theory. It should, therefore, be constant for all gases, except in so far as modification is required by the effect of the higher critical potentials, if this effect is appreciable.

\* J. J. Thomson, Proc. Phys. Soc. xxvii. p. 96 (1914).

† N. Bohr, Phil. Mag. xxx. p. 581 (1915).

‡ R. H. Fowler, Proc. Camb. Phil. Soc. xxi. p. 531 (1923).

§ H. D. Smyth, Roy. Soc. Proc. A, civ. p. 121 (1923); A, cv. p. 116 (1924).

The results given in Table II. would thus appear to be in general agreement with the predictions of the theory were it not for the fact that the value of the product  $P.T$  for nitrogen is *greater* by some 15 per cent. than the mean value for the other gases employed. The average energy spent in producing a pair of ions in nitrogen is thus less than that for the other gases. The approximately constant value for  $P.T$  given by these other gases must be less than the value,  $\frac{3}{4}$ , indicated by Fowler's theory.

The value of the fraction is, of course, reduced if ionization takes place at higher ionizing potentials, that is to say, if the electron is ejected from a lower level in the molecule. Experiments made with comparatively low velocity electrons indicate that the fraction of the ions produced at the higher levels is small, but this would not necessarily be true for the electrons generated by the absorption of X-rays. Both nitrogen and oxygen are known to have several ionization potentials above the minimum value, and no doubt the same applies to the other gases in the list, although no observations of such potentials appear to have been recorded.

Let  $k$  be the fraction of the absorbed energy  $E$  (measured in volts) utilized in producing ions with the expenditure of the minimum amount of work, *i. e.*, at the minimum ionization potential  $P$ , and  $k_n$ , the fraction absorbed in producing ionization at a higher potential  $P_n$ . The total number of ions produced is given by

$$T = k \frac{E}{P} + \sum k_n \frac{E}{P_n}; \quad \frac{P.T}{E} = k + \sum k_n \frac{P}{P_n}.$$

If the higher terms are negligible and there is no loss of energy by processes other than that of ionization, the value of  $k$  should, as Fowler has shown, be equal to  $\frac{3}{4}$ .

The lack of constancy in the product  $P.T$  can be explained by assuming that the energy converted at the higher potentials is appreciable, and differs for different

gases, that is to say that the term  $\sum k_n \frac{P}{P_n}$  must be taken into account. If, however, the difference between the value of this term for nitrogen and for, say oxygen, amounts to as much as 15 per cent. the term itself must be fairly large, even for nitrogen, as there is no such marked difference in the ratios  $P/P_n$  for the higher ionization

potentials as would lead one to suppose that the difference between the terms is likely to be a large fraction of either. If the work spent in producing ions at the higher potentials is comparable with that utilized at the minimum potential, the average value of the energy spent per ion will be appreciably greater than the value (22.3 volts for nitrogen) calculated from Fowler's formula on the assumption that the higher potentials can be neglected, and may quite conceivably be as high as the values suggested (35 volts-42 volts) \* by direct thermal measurements on the energy of X-radiation.

On the other hand, it is also conceivable that energy may be lost by the X-ray beam or by the resultant photoelectrons in ways not concerned with the production of ionization, the amount so lost varying with the nature of the gas. It may be significant that nitrogen is the one gas in the table which has no electron affinity. The lower efficiency of the ionization process in these other gases may be connected with their power to attract and capture electrons. The further discussion of these points, however, is not directly involved in the subject matter of the present series of investigations, and is reserved for a separate communication.

### *Summary.*

The coefficient of absorption of copper  $K_{\alpha}$  radiation has been measured for a number of gases. The ionization produced in these gases by a beam of constant intensity has been compared with that in air under the same conditions.

The total ionization produced by the complete absorption of the radiation (relative to that in air) has been calculated. The values so obtained are found to approximate closely to the values obtained for the relative ionizations produced by the total absorption of  $\alpha$  radiation.

The average energy expended by X-rays in producing a pair of ions in the gas is found to be approximately proportional to the minimum ionization potential of the gas for oxygen, carbon dioxide, ethylene, and hydrogen sulphide, but is about 15 per cent. smaller for nitrogen.

\* Kulenkampff, *Ann. der Phys.* vi. p. 97 (1923). Crowther and Bond, *Phil. Mag.* vi. p. 401 (1928).

The fraction of the X-ray energy absorbed utilized in producing ionization is approximately constant for the majority of the gases investigated, but is about 15 per cent. greater for nitrogen.

Department of Physics,  
University of Reading,  
June 1930.

XXX. *On the Measurement of the Sound Transmission of a Partition.* By A. E. KNOWLER, M.Sc., A.Inst.P.\*

IN the Watson † method of measuring sound transmission through a partition a parallel beam of sound is directed towards the partition and the sound intensities on either side are compared. The basis of the Sabine ‡ method of measuring sound transmission is the measurement of reverberation, both in the source room, and in that on the other side of the partition. This paper describes a third method.

Suppose two rooms, A and B, to be separated by an incompletely soundproof partition. Then, if a moving-coil loud-speaker be placed in A and the current through it reduced until the sound is just audible in B, the intensity in the room A is given below by

$$I_A = \frac{4Ki_1^2}{va_A},$$

where

$I_A$  is the sound intensity in A.

$K$  is the constant in the equation  $E = Ki^2$ ,  $E$  being the rate of emission of acoustic energy from the loud-speaker and  $i$  the current.

$i_1$  is the current for minimum audibility in B.

$v$  is the velocity of sound in air.

$a_A$  is the absorbing power of the surfaces in A.

If the loud-speaker now be placed in B and the current reduced until the sound is just audible in the same room, we have

$$I_B = \frac{4Ki_2^2}{va_B}.$$

\* Communicated by the Director of Building Research, Department of Scientific and Industrial Research.

† F. R. Watson, *Phys. Rev.* vol. v. pp. 125-132 (1916).

‡ W. C. Sabine, 'Collected Papers on Acoustics,' p. 237.

The reduction of the wall in transmission units is given by

$$10 \log_{10} \frac{4Ki_1^2}{va_A} - 10 \log_{10} \frac{4Ki_2^2}{va_A} \\ = 10 \log_{10} i_1^2 - 10 \log_{10} i_2^2 - 10 \log_{10} a_A + 10 \log_{10} a_B.$$

Similarly, if the experiment be repeated, starting with the observer in A the reduction is given by

$$10 \log_{10} i_3^2 - 10 \log_{10} i_4^2 - 10 \log_{10} a_B + 10 \log_{10} a_A.$$

Any difference between the absorbing power of the two rooms can thus be eliminated, the reduction of the wall being given by

$$10 (\log_{10} i_1 + \log_{10} i_3 - \log_{10} i_2 - \log_{10} i_4)$$

In this analysis the energy lost by transmission through the bounding surfaces is considered small compared with the total energy.

Since the observer is absent from each room in turn, the total absorbing power of each room changes. A slab of absorbing material is therefore introduced to compensate for the absence of the observer.

The transmission of a  $4\frac{1}{2}$ -inch brick wall set in cement mortar has been measured by this method. The transmission laboratory consists of three rooms, the centre one of which is separated from those on either side by test partitions. Shunts of values  $\frac{1}{2}$ ,  $\frac{1}{5}$ ,  $\frac{1}{10}$ ,  $\frac{1}{10}$ ,  $\frac{1}{10}$ ,  $\frac{1}{10}$ , and a sliding resistance were used to control the current, which was measured with a thermal milliammeter.

The tone used was a "howling tone" of frequency  $600 \pm 50$ . Each result given below is the mean of at least six values. To illustrate the variation of the individual values among themselves the following set is quoted: 43.55, 40.34, 43.58, 42.42, 34.70, 38.30. The experiments were spread over several days. Results found on separate days are placed on separate lines.

Observer 1.		Observer 2.	
Room A.	Room B.	Room A.	Room B.
44.0	41.4	44.4	30.6
44.0	45.8	41.8	35.4
41.2	44.6	44.2	48.4
40.8	41.6	42.0	42.2
	46.0		36.2
40.8	55.2	38.0	42.6
	44.0		46.0
41.8	43.2	43.4	37.2
	44.4		
Means ...	42.1	42.3	39.8
	45.1		



The mean of these four values is  $42.4 + 0.4$  T.U. Davis and Littler\*, for a  $4\frac{1}{2}$ -inch Fletton brick partition measuring 5 ft.  $\times$  4 ft. and set in lime mortar, found a value of approximately 44.5 T.U.

The discrepancy between the results of the two observers in room B may be explained by the fact that room B admits a good deal of extraneous noise, while room A is comparatively well insulated. Listening tests in room B are, therefore, more difficult and less accurate. For listening tests made in the quiet room the two observers agree to within 0.2 T.U.

Further tests were made on a fibre-board partition fixed to 3-in.  $\times$   $1\frac{1}{2}$ -in. battens on 2 ft. 0 in. vertical and 2 ft. 6 in. horizontal centres. Each result given below is the mean of six values. Experiments were spread over a period of several days.

Observer 1.		Observer 2.	
Room A.	Room B.	Room A.	Room B.
22.5	20.2	22.5	21.2
22.5	23.1	21.9	21.0
21.3	21.5	21.0	20.4
21.9	20.6	21.2	20.5
21.5	19.8	21.0	20.5
20.8	20.4	20.9	20.9
<hr/>			
Means ...	21.8	20.9	21.4
			20.8

The mean of these values is  $21.2 \pm 0.2$  T.U. The value found by Davis and Littler for a 5-ft.  $\times$  4-ft. partition of the same fibre board was 18.3 T.U.

When the position of the source and of the observer was changed, the variation among the readings was no greater than that due to the experimental error when the positions are fixed. Extreme positions were included in these experiments.

The variation of the loud-speaker "constant" over the range of energy input used was negligible.

The method has the advantage that it can readily be applied to the measurement of the sound transmission of the walls in existing buildings. The whole apparatus could readily be made portable.

\* Davis and Littler, *Phil. Mag.*, June 1929.

XXXI. *On the Annual Variation of Upper-Atmospheric Ozone.* By S. CHAPMAN\*.

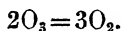
1. **T**HE annual mean ozone content of the atmosphere, expressed in terms of the thickness of the equivalent layer of pure ozone at normal temperature and pressure, increases with latitude from about 2 mm. at the equator to about 3.25 at Abisko (68° N.). It undergoes a well-marked annual variation, increasing in range from zero at the equator to about 1.5 mm. at Abisko: in each hemisphere the maximum occurs nearly at the vernal equinox (perhaps slightly after, according to the present observations) and the minimum nearly at the autumnal equinox. North of 50° latitude the variation has not been observed through the winter months.

Thus the ozone content  $C$  can be expressed very approximately by the formula

$$C = C_0 + C_1 \cos \theta, \quad . \quad . \quad . \quad . \quad (1)$$

where  $\theta$  denotes time measured, at the rate  $2\pi$  per year, from the epoch of maximum  $C$  (the vernal equinox);  $C_0$  denotes the annual mean content, and  $2C_1$  the annual range, apart from irregular fluctuations.  $C$  decreases during the summer half-year, most rapidly at midsummer, and increases during the winter half-year. These changes show that processes of decay and formation of ozone are going on at unequal rates during the year. At present the nature of both these processes is unknown.

2. It has recently been suggested that the main process in the decay of ozone is the normal thermal decomposition, according to the formula



The reaction only takes place if the colliding molecules possess energy of activation. If  $n$  is the number of ozone molecules per c.c., the number which disappear by this reaction per second may be denoted by  $kn^2$ ; the recombination coefficient  $k$  varies with the absolute temperature  $T$  approximately as  $e^{-26,000/RT}$ , according to C. N. Hinshelwood†, and its values at  $T=300^\circ$ ,  $400^\circ$ ,  $500^\circ$  are roughly  $1.7 \cdot 10^{-25}$ ,  $10^{-20}$ ,  $6.8 \cdot 10^{-18}$ , rapidly increasing with temperature.

\* Communicated by the Author.

† 'Kinetics of Chemical Change in Gaseous Systems,' p. 61 (on the basis of Clement's experiments); the value of  $E$ , and consequently of  $k$ , is somewhat uncertain.

*Phil. Mag.* S. 7. Vol. 10 No. 63. August 1930. 2 A

The temperature in the layer where the ozone is densest (about 45 km.) is not definitely known, but there are good reasons for believing it to be at least  $300^{\circ}$ . The value of  $n$  at about 45 km. height may be calculated roughly by supposing the total ozone content to be spread uniformly through a layer 10 km. thick; thus the annual mean value of  $n$  increases from about  $5.5 \cdot 10^{12}$  at the equator to about  $8 \cdot 10^{12}$  at Abisko. If  $T=300^{\circ}$  at this level,  $kn^2=11$  (at Abisko), and in half a year ( $1.58 \cdot 10^7$  seconds) the total decrease of  $n$  by thermal decomposition would be relatively small; even if  $T=373^{\circ}$  or  $100^{\circ}$  C., when  $k=8.5 \cdot 10^{-22}$ , thermal decomposition is not very important. If, however,  $T$  rises to  $400^{\circ}$ , though only for a part of each day, thermal decomposition must play a large part in the equilibrium and changes of the ozone.

3. In a recent paper\* I have given a tentative theory of these changes, assuming that  $T$  is sufficiently below  $400^{\circ}$  for it to be possible to neglect the thermal decomposition. It has, however, been suggested that  $T$  may be high enough for the decay to occur chiefly by this means, and that the rapid decay in the ozone content during the summer may be due to the greater temperature which may then be supposed to exist in the ozone layer. This hypothesis, which at first sight is attractively simple, is here examined.

4. The equation of change of  $n$  is

$$\frac{dn}{dt} = \Delta - kn^2, \quad . \quad . \quad . \quad . \quad . \quad (2)$$

where  $t$  is measured in seconds, and the rate of increase of  $n$ ,  $dn/dt$ , is expressed as the difference between  $\Delta$ , which denotes the rate of production of ozone, per c.c. per sec., and the rate of disappearance,  $kn^2$ , by thermal decomposition; it is unnecessary at present to consider how the ozone is produced, and  $\Delta$  may include a portion due to convection or diffusion, from outside, into the volume-element considered, as well as a part due to new production of ozone by dissociation of oxygen molecules into atoms, and their subsequent attachment to other oxygen molecules.

The ozone content of the atmosphere undergoes no perceptible diurnal variation, but this is not necessarily true of  $\Delta$ ,  $T$ , and  $k$ ; however, in considering the annual variation,

\* Mem. Roy. Meteor. Soc. iii. No. 26 (1930): an abstract is given in Gerland's *Beiträge zur Geophysik*, xxiv. pp. 66-68 (1929).

it is legitimate to ignore any such daily variations, and to use the daily mean values of  $\Delta$  and  $k$ ; the symbols  $n$ ,  $\Delta$ , and  $k$  are to be interpreted in this sense.

It is convenient to transform the time variable  $t$  to  $\theta$ , given (§ 1) by

$$\frac{\theta}{2\pi} = \frac{t}{365\frac{1}{4} \cdot 86,400}, \quad \dots \quad (3)$$

where the denominator on the right denotes the number of seconds in a year.

Let

$$k = k_0 \{1 + \phi(\theta)\}, \quad \dots \quad (4)$$

$$\Delta = \Delta_0 \{1 + \psi(\theta)\}, \quad \dots \quad (5)$$

where  $\phi$  and  $\psi$  are annually-periodic functions with zero mean value, so that  $k_0$ ,  $\Delta_0$  are the annual mean values of  $k$  and  $\Delta$ . If the rate of production of ozone is constant,  $\psi(\theta) = 0$ , but this will not be assumed.

Let the dependent variable  $n$  in (2) be transformed to  $\nu$ , where

$$\nu = n/n_0 \quad \dots \quad (6)$$

and

$$n_0 = \sqrt{(\Delta_0/k_0)}; \quad \dots \quad (7)$$

$n_0$  is clearly the steady value which  $n$  would attain if  $k$  and  $\Delta$  had their annual mean values through the year, without variation, because then, by (2),  $dn/dt$  would be zero. Hence  $\nu$  is the ratio of the actual value of  $n$  at any epoch, to this hypothetical steady value.

If  $k$  were constantly equal to  $k_0$ , and if, at time  $t=0$ ,  $n$  having the value  $n_0$ , the production of new ozone ceased, the decay of  $n$  would occur according to the equation

$$n = \frac{n_0}{1 + k_0 n_0 t}; \quad \dots \quad (8)$$

thus after a time  $t_0$  given by

$$k_0 n_0 t_0 = 1, \quad \dots \quad (9)$$

the ozone would be halved; this time  $t_0$  may be called the half-life of the ozone in these circumstances. Let its value expressed in years be  $s$ , so that,  $t_0$  being expressed in seconds,

$$t_0 = 365\frac{1}{4} \cdot 86,400s. \quad \dots \quad (10)$$

4. Expressed in terms of  $\nu$  and  $\theta$ , (2) becomes

$$2\pi s \frac{d\nu}{d\theta} = 1 + \psi(\theta) - \nu^2 \{1 + \phi(\theta)\}. \quad \dots \quad (11)$$

Now  $\nu$  is proportional to  $C$ , and therefore, by (1), may be written in the form

$$\nu = a_0 + a_1 \cos \theta. \quad (12)$$

Substituting for  $\nu$  from this equation, we obtain the following equation involving the unknown quantities  $\phi$ ,  $\psi$ , and  $s$ :

$$\begin{aligned} -2\pi s a_1 \sin \theta = 1 + \psi(\theta) - \{a_0^2 + 2a_0 a_1 \cos \theta \\ + a_1^2 \cos^2 \theta\} \{1 + \phi(\theta)\}, \end{aligned} \quad (13)$$

or

$$\begin{aligned} \{a_0^2 + \tfrac{1}{2}a_1^2 + 2a_0 a_1 \cos \theta + \tfrac{1}{2}a_1^2 \cos 2\theta\} \{1 + \psi(\theta)\} \\ = 1 + \psi(\theta) + 2\pi s a_1 \sin \theta. \end{aligned} \quad (14)$$

We suppose that if  $\phi$  and  $\psi$  are expanded in Fourier's series, without constant terms (since their mean values, by definition, are zero), *i. e.*,

$$\phi(\theta) = f_1 \sin \theta + g_1 \cos \theta + f_2 \sin 2\theta + g_2 \cos 2\theta + \dots \quad (15)$$

$$\psi(\theta) = p_1 \sin \theta + q_1 \cos \theta + p_2 \sin 2\theta + q_2 \cos 2\theta + \dots \quad (16)$$

Then equating the constant terms, and the coefficients of the various harmonics, on the two sides of (14), we have

$$a_0^2 + \tfrac{1}{2}a_1^2 + a_0 a_1 g_1 = 1, \quad (17)$$

$$2a_0 a_1 + g_1(a_0^2 + \tfrac{3}{4}a_1^2) + a_0 a_1 g_2 = q_1, \quad (18)$$

$$f_1(a_0^2 + \tfrac{1}{4}a_1^2) + a_0 a_1 f_2 = 2\pi s a_1 + p_1, \quad (19)$$

and so on.

### 5. At Abisko

$$a_1/a_0 = C_1/C_0 = 0.75/3.25 = 3/13;$$

hence for latitudes up to  $68^\circ$ ,

$$a_1/a_0 \leq 3/13.$$

Consequently  $a_1^2$  is small compared with  $a_0^2$ , and will be neglected in (17)–(19). Further, since  $k$  and  $\phi$  increase with  $T$ , which must undergo a simple annual variation, the main terms in (14) must be those of the first harmonic ( $f_1, g_1$ ), and the later coefficients will be of small magnitude; moreover, the maximum of  $T$  and  $\phi$  must occur at or near midsummer, *i. e.*, at  $\theta = \frac{1}{2}\pi$  approximately, since  $\theta$  is measured from an epoch at or near the vernal equinox. Hence  $f_1$  is positive and  $g_1$  is small compared with it: as also are  $f_2, g_2, \dots$ . Thus, in (17)–(19) any terms in which  $g_1, f_2, g_2, \dots$  are multiplied by the rather small factor  $a_1$  may be neglected in a first approximation. Thus (17) reduces to  $a_0^2 = 1$  or

$$a_0 = 1. \quad (20)$$

The interpretation of this result is that, to the present degree of approximation (a few per cent.), the annual mean value of  $n$ , which is  $n_0 a_0$ , is equal to  $n_0$ , the steady value corresponding to the annual values of  $\Delta$  and  $k$ .

6. Using (20), and making the approximations already indicated, (19) becomes

$$2a_1 + g_1 = q_1, \quad . \quad . \quad . \quad . \quad . \quad (21)$$

$$f_1 = 2\pi s a_1 + p_1. \quad . \quad . \quad . \quad . \quad (22)$$

The annual variations of  $n$ ,  $k$ , and  $\Delta$  are all zero at the equator, and increase with latitude, and therefore the same will be true of  $a_1, f_1, g_1, p_1, q_1$ . It is convenient to consider the values corresponding to Abisko, where  $a_1 = 3/13$ .

7. If the maximum of  $T$  and  $k$  is supposed to occur exactly three months after that of  $n$  or  $C$ , *i. e.*, at  $\theta = \frac{1}{2}\pi$ , then  $g_1 = 0$ . In this case (21) indicates that  $q_1 = 2a_1$ , *i. e.*, whatever the value of  $f_1$  (which determines the proportionate variation of  $k$ ) the rate of *production* of the ozone must undergo a proportionate variation at least twice as great as that of  $n$  or  $C$ . The variation is exactly twice as great if  $p_1 = 0$ , otherwise it is  $\sqrt{(p_1^2 + q_1^2)}$  which exceeds  $q_1$  or  $2a_1$ .

The variation of  $\Delta$  represented by the terms  $q_1 \cos \theta$  is of a rather improbable kind, because, whatever the value of  $p_1$ , it implies a great inequality between the values of  $\Delta$  in spring and autumn, the ratio being  $(1 + q_1)$  to  $(1 - q_1)$ , or, at Abisko, 19 : 7. It is difficult to see why, in spring, ozone should be produced nearly thrice as rapidly as in autumn, whether the production is due to ultra-violet radiation or to corpuscular action.

But if  $k$  has its maximum at the summer solstice, and is equal at the two equinoxes, as supposed, then the necessity for this conclusion, on the basis of the equation (2), is easily seen; for at the equinoxes  $n$  is stationary, and therefore production and destruction just balance; but in spring  $n$  is much greater than in autumn, and the same is true *a fortiori* of the rate of destruction of ozone,  $kn^2$ ; consequently, the rate of production in spring must much exceed the autumn rate.

8. This is so improbable as to preclude the hypothesis here being examined, if it were certain that the annual variation of  $T$  and  $k$  is symmetrical about the solstices. If, however, the maximum of  $T$  and  $k$  can occur a month after

the solstice, that is, about four months after the epoch of maximum ozone (though this would be somewhat surprising), the difficulty would largely disappear, and  $q_1$  can be zero, *i.e.*, the rate of production of ozone can have an annual variation symmetrical with respect to the solstices, as would be expected. For then, by (21),

$$g_1 = -2a_1 = -6/13 \text{ (at Abisko)} = -0.46.$$

Now, if  $\alpha$  is the lag of the maximum of  $T$  and  $k$  after the solstice (expressed in angle, so that  $30^\circ$  corresponds to one month),  $g_1 = -f_1 \tan \alpha$ ; if  $\alpha = 30^\circ$ ,  $g_1 = -0.58f_1$ , and since  $f_1$  can be nearly unity if  $T$  in winter sinks to a value for which  $k$  is much smaller than its summer maximum, the value  $g_1 = -0.46$  is not an unlikely one.

9. The equation (22) has not so far been used: if the value  $a_1 = 3/13$ , appropriate to Abisko, is inserted, it becomes

$$f_1 = 1.45s + p_1.$$

This enables an upper limit to be imposed on  $s$ , because  $f_1$  and  $p_1$  cannot exceed 1, and whatever their sign, therefore,  $f_1 - p_1$  cannot exceed 2. Hence

$$0 < s < 2/1.45 = 1.38 \text{ year} = 15\frac{1}{2} \text{ months.}$$

Since

$$s = 3.16 \cdot 10^{-8} t_0 = 3.16 \cdot 10^{-8} / k_0 n_0 = 4 \cdot 10^{-21} / k_0,$$

for Abisko, taking  $n_0 = 8 \cdot 10^{12}$ , this indicates that  $k_0$  must be at least equal to  $2.9 \cdot 10^{-21}$ , which corresponds to a temperature of about  $385^\circ \text{ K}$ . This is the lower limit of  $T$  for which the present hypothesis can fit the observed annual variation, and this limit corresponds to  $f_1 = 1$ ,  $p_1 = -1$ ; these values are actually not compatible with (20), because if  $f_1 = 1$ ,  $p_1 = 1$ , then  $g_1 = q_1 = 0$ ; ignoring this difficulty, however, we note that  $p_1 = -1$  implies that the production of new ozone is zero at midsummer and has twice the mean value at midwinter (terms in  $\psi$  of higher period than the first are here neglected), which is improbable though perhaps not impossible. Until more is known about the mode of production of the ozone and about its annual variation, it is impossible, however, to make the lower limit of  $T$  more precise.

10. The increase of  $C_0$  (§ 1) with increasing latitude demands a corresponding increase of  $n_0$  or  $\sqrt{(\Delta_0/k_0)}$ ; this may be due to an increase in  $\Delta_0$ , or a decrease in  $k_0$ ; or to both these causes. If the ozone production is due to ultra-violet radiation,  $\Delta_0$  would be expected to decrease with the

latitude ( $\lambda$ ), approximately as  $\cos \lambda$ ; if so,  $k_0$  must decrease in proportion to  $(\cos \lambda)/n_0^2$ , *i.e.*, from the equator to Abisko, in the ratio 1 to 0.14 or 7 to 1; if at Abisko  $p_1=0$ , so that  $k_0$  (§ 9) is at least  $5.8 \cdot 10^{-21}$ , and  $T=390^\circ$ , then at the equator  $k_0$  must at least equal  $4 \cdot 10^{-20}$  corresponding to  $T=420^\circ$  approximately.

The corresponding value of  $\Delta_0$  is  $k_0 n_0^2$  or  $2.6 \cdot 10^6$ , which is a lower limit. If production occurs only during the hours of sunlight, the mean rate during the period of production must be at least twice this, *i.e.*,  $5 \cdot 10^6$ , or, in a layer 10 km. thick,  $5 \cdot 10^{12}$ . This is about one-tenth the number of O atoms which could be produced (at the equator) by the dissociation of oxygen molecules by the sun's ultra-violet radiation, if the effective radiation lies in the band 1300–1800 Å., assumed to have the energy corresponding to the spectrum of a black body at 6000°, and assuming also that each quantum of this radiation dissociates an oxygen molecule; these assumptions are, of course, doubtful.

11. The results of the preceding discussion may be summarized as follows:—

(i.) Annual mean values and annual ranges of  $T$  and  $k$  can be assigned which will account for the observed annual variation of ozone, and its observed distribution in latitude, without assuming any annual variation in the rate of production of the ozone. In this case it is indispensable that the maximum of  $T$  and  $k$  shall occur after the summer solstice by about a month, so that the interval between the maxima of the ozone and the temperature is about four months

This mode of variation of  $T$  is somewhat improbable, because the high atmosphere has but little heat capacity and would be expected to adjust its temperature rapidly to the amount of solar radiation received at any time; thus the maximum temperature should occur very nearly at the solstice, or even, possibly, a little before (if the high temperature in the ozone layer is due to absorption of solar radiation by ozone), because the ozone content is diminishing during the summer. If, however, the temperature at 45 km. is partly determined by large-scale convection, a lag of maximum temperature after the solstice may be possible.

(ii.) If the maximum of  $T$  (and  $k$ ) occurs at the solstice, so that  $T$  and  $k$  have equal values at the two equinoxes, the observed annual ozone variation requires (on the hypothesis



expressed by (2)) that the rate of production of new ozone shall be much greater in spring than in autumn. This is considered improbable.

The preceding discussion must remain inconclusive until more exact knowledge is attained as to the temperature of the ozone layer. The existing determinations of the height of the ozone layer indicate that half the ozone is below 50 km., and therefore we are concerned mainly with the temperatures at below this level.

The temperatures originally calculated by Gowan for this region are  $270^{\circ}$  or less; I understand that later calculations give higher values, but these are not yet published. Whipple\* has deduced from the density distribution of the upper atmosphere, calculated by Lindemann and Dobson from meteor data, that the temperature rises from  $220^{\circ}$  at 30 km. to  $380^{\circ}$  at 50 km.; he has also inferred the same value,  $380^{\circ}$ , for the temperature at about 56 km., from observations of the abnormal audibility of sounds from gunfire during the summer of 1928†. These inferences are, however, admittedly very uncertain, and it seems rather improbable that the temperature gradient should be so very rapid in this 20-km. layer; the temperature at the level 30 km. is known by actual observation to be about  $220^{\circ}$ . The highest estimates of the temperature between 40 and 50 km. are near the point where the thermal decomposition of ozone rises to importance, according to the present laboratory data, which also, unfortunately, are somewhat uncertain. It is therefore very desirable to confirm or disprove these estimates, and also, if possible, to determine whether the temperature undergoes annual and diurnal variations (and, if so, with what amplitudes and phases); a diurnal variation would be of great importance if it raised the temperature to about  $400^{\circ}$  even for only a short part of the day; it may be remarked, however, that if there is an appreciable daily variation it is unlikely that the annual maximum of temperature will lag by so much as a month after midsummer. I understand that observations of the abnormal propagation of sound do not suggest any diurnal variation of temperature at about 50 km.

\* 'Nature,' Aug. 28, 1926.

† Gerland's *Beiträge zur Geophysik*, xxiv. p. 75 (1929).

XXXII. *A Design for a very large Telescope.**By E. H. SYNGE\*.*

RESULTS which were formerly looked upon as requiring the construction of a very large curved surface are obtained in Michelson's method of stellar interferometry by the superposition of reflexions from small surfaces. It seems possible to extend this idea to the purpose of light-gathering, instead of resolving, power.

A form of telescope will be suggested in which a number of moderate-sized parabolic reflectors perform the functions of a single very large reflector. Theoretically, at least, this form of telescope could be made to give virtually the same degree of resolution as a telescope with a single large reflector, of surface area equal to the combined areas of the assemblage of small reflectors. But to do this it would have to be made and adjusted with very great refinement, and with the best atmospheric conditions which are met with in the temperate latitudes this refinement would be wasted. It seems that  $\cdot 6''$  may be taken as the minimum angular diameter of the photographic image of a star, which can be obtained by any of the large telescopes in the United States; and in the case of a very large telescope (from 3 or 4 metres in aperture upwards) it is improbable that the best visual image can be much less than the photographic. This limit is imposed by the minimum of atmospheric disturbance over the area; and if a very large telescope is designed for use in that area, so that under the steadiest atmospheric conditions to be met with it will give a photographic image of approximately  $\cdot 6''$ , there is no advantage in carrying refinements of design and construction any further.

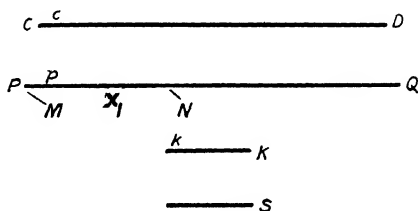
There is a considerable gain in simplicity in limiting the discussion to a telescope which will obtain this result, but does not aim at a greater theoretical efficiency; and we will first discuss the design with this limitation. Afterwards we can consider the possible use of a higher theoretical efficiency, and how this could be obtained.

The design consists essentially in the assemblage of a number of similar reflecting telescopes pointed in the same direction, the images from which are ultimately superimposed in the focal plane of another reflector or lens S, the

\* Communicated by the Author.

resultant image containing the aggregate light of all. If the assemblage contains  $n^2$  reflectors each of 1 metre aperture, it will be shown that the resultant image of the field is virtually identical with that which would be formed by a single reflector  $n$  metres in diameter and having a focal length whose ratio to aperture is slightly greater than this ratio in the case of S. The field is indeed more restricted, and some light is lost by additional reflexions and transmission through a lens. But there are many compensating advantages.

The diagram below shows a schematic cross-section of the arrangement.



The  $n^2$  parabolic reflectors are arranged within a circle of which PQ is a cross-section.  $n^2$  corresponding Cassegrainian reflectors are represented by CD. The whole assemblage forms a sort of "battery" of  $n^2$  1-metre telescopes, all pointing in the same direction. S is a large lens, or reflector, of, say, 1 metre in diameter. K is the cross-section of an assemblage of  $n^2$  collimating lenses, each of a little less than  $\frac{1}{n}$  metre in diameter and set together

as closely as possible. I is the image of the field formed by  $p$ , a parabolic reflector at the left-hand side of the assemblage, the rays incident on  $p$  being reflected, first, to the Cassegrain reflector  $c$ , then emerging through a hole in  $p$ , whence they are reflected by a plane mirror M to I. We are only concerned with a limited area of I, in the centre of the field, the remainder being cut out by a diaphragm or the walls of a tube. The rays after passing through their foci at I are reflected by a parallel plane mirror N into  $k$ , one of the collimating lenses at K. M and N are adjusted so that I or, to speak more accurately, its reflexion, is in the focal plane of  $k$ , and the rays will consequently emerge from  $k$  as parallel beams, and, striking S, will form an

image of the field in the focal plane of S. It can easily be seen that this image is a magnification by a little more than  $n$  diameters of the image of the field which would be formed if S were used directly as an objective. The parallel beams incident on  $p$  have, in fact, been converted into parallel beams issuing from  $k$ , and the latter have somewhat less than  $\frac{1}{n}$  the diameter of the former. There will, therefore, according to the general law which governs such reductions, be a corresponding increase in all angular divergencies.

We have dealt with one parabolic reflector  $p$  and the rays which fall upon it. A precisely similar arrangement is made in the case of every other member of the assemblage. To any other parabolic reflector  $p'$  corresponds a Cassegrain reflector  $c'$ , two plane mirrors  $M'$  and  $N'$ , and a collimating lens  $k'$ , which ultimately conduct the rays incident upon  $p$  to an image in the focal plane of S. This image of the field is precisely similar to that formed by the rays coming from  $p$ , and if the apparatus is properly adjusted, will be directly superposed on it. Owing to the "boiling" effect of atmospheric disturbances, we may consider that there are no special phase relations between the two superposed images, the resultant effect being simply additive. The  $n^2$  parabolic mirrors at PQ will thus form  $n^2$  identical superposed images of the field in the focal plan of S, the resultant image containing, at all events near the centre of the field, all the light which is incident upon the  $n^2$  parabolic mirrors, except the fraction which is lost in the reflexions and in transmission through the lenses. Except for this loss, the image of the field will be virtually identical in all respects with that which would be formed by an objective  $n$  metres in diameter, and having a slightly greater ratio of focal length to aperture than S. This is true, however, only within a limited region near the centre of the field, and we have still to consider how large this region may be. We need not consider curvature of the image-surface at I as this can be compensated for elsewhere.

If the parallel beam which emerges from the collimating lens  $k$  is the full breadth of the lens, it is clear that, if there is to be no loss of light, only the point in the exact centre of the field will be properly provided for. The images will deteriorate as we pass outwards from the centre. It

would probably be best that the parallel beams emergent from  $k$ , and the other collimating lenses, were a little less in width than the lenses, and thus the images should be equally good over a small region in the centre of the field. We may take that portion of I, from which a tolerably good image can be obtained, as a circle of about one-half the diameter of the collimating lens, there being some deterioration towards the boundary of this circle. If  $k$

is a little less than  $\frac{1000}{n}$  mm. in diameter, and if we take

10 mm. in the image I as equivalent to a minute of arc of the field, the effective field would be some  $\frac{50}{n}$  minutes of arc

in diameter, or 5 minutes of arc when  $n=10$ . The dimensions of the effective field can be increased by increasing the size of S, and hence of  $k$ . Thus, if S were 2 metres instead of 1 metre in diameter, the effective field would be 10 minutes of arc in diameter. The field could also be increased if there were an assemblage of lenses, instead of reflectors, at PQ. Indeed, there would be many advantages in having objective lenses instead of mirrors here. The writer has limited himself to reflectors only because the expense of an assemblage of 1 metre lenses would probably be prohibitive. The best results of all, and the largest effective field, could probably be obtained, if expense were not in question, by an assemblage of lenses at PQ and a large doublet lens at S. In the case of reflectors the focal lengths of  $p$  (diagram, p. 354) should be made as short as possible. If S were a reflector, it might be more convenient that it should face in the opposite direction, with, of course, a corresponding modification of the arrangement of the plane mirrors and collimating lenses. Many other modifications would probably suggest themselves to anyone constructing an actual instrument. The aim of the present paper is only to suggest the general method in broad outline.

As regards the arrangement of the plane mirrors, care would be taken that the mirrors and diaphragms, or tubes, which served one beam should not cut across the path of any other beam. It is necessary, also, that the light from one beam should not enter any collimating lens but that designed for it. As well, therefore, as a diaphragm at I, delimiting the field, there should be a diaphragm near I, which would cut out all light except what would enter the

proper lens. There does not seem to be any particular difficulty about these details, as one has the widest latitude in all the arrangements. It may be remarked also that there need not be any members of the assemblage PQ near the centre of PQ. They could be arranged in an annular form if this were more convenient for the arrangement of the plane mirrors.

All the component parts would, of course, be carried on a lattice metal framework. This could be made tubular, and air circulated through it, so that there would be no differential temperature effects. If necessary, there could also be provision for temperature compensation in the frame. So far as the effect of temperature is concerned, a composite telescope of this kind should be much superior to one with a single very large reflector, supposing this could be constructed of equivalent size. The superiority would be still more marked as regards weight and convenience, for the weight of such a telescope would tend to increase as the square of the equivalent aperture, while that of an ordinary telescope would increase as the cube.

Hitherto we have considered the case of a composite telescope in which we could look upon the beams contributed by the various members of the assemblage PQ as quite independent of one another. It was merely necessary to make the adjustments so that the  $n^2$  images in the focal plane of S were exactly superposed on one another. In spite of any appearance of complexity in the arrangement, there was so much latitude in planning the details that there did not seem to be formidable difficulties of any kind in constructing such an instrument, even of a very large size with light-gathering capacity quite beyond anything possible in the case of a telescope with a single large reflector. But the difficulties would become much more formidable if the attempt were made to construct such a telescope, which would yield the full resolving power of its equivalent aperture. To justify the consideration of such a telescope, it seems necessary to turn our attention to the question of atmospheric disturbances, and see whether we must take  $\cdot 6''$ , or thereabouts, as a definite limit to the photographic resolution, or whether we might hope, in any cases, to pass beyond it.

In the lower atmosphere, and up to a considerable height, there are, in most places, days of almost complete calm ;

but meteorologists seem to be in agreement that, in the temperate latitudes, there is a perpetual west wind at a very great height, blowing with a velocity of 60 miles per hour, or upwards. This constant wind, which is connected with the rotation of the earth, seems quite sufficient to account for the limit of  $\cdot 6''$ , which corresponds with the calmest conditions of the lower atmosphere. If we wish to pass beyond this limit, we must therefore find some latitude where there is no such strong constant wind at great heights. At the Equator the Krakatoa dust revealed a constant *East wind* of about 60 miles an hour, at a great height. We might, therefore, fairly expect to find a zone between the Equator and the temperate latitudes where the winds in the higher atmosphere were much less strong, and probably indeterminate in direction, with occasional periods of almost complete calm. One would expect the same thing in the Polar regions, for any winds depending on the rotation of the earth must become indeterminate in direction as we approach the Poles. We know, indeed, that there are periods of almost complete calm in the Antarctic regions. C. G. Simpson in 'The Meteorology of the British Antarctic Expedition, 1910-13,' vol. i. p. 133, records occasions when the smoke from Mount Erebus (4000 metres) "rose so vertically that no direction could be assigned to it. This means that the air through a great thickness was for all practical purposes absolutely still; and yet this phenomenon was observed four times in twelve months." He also mentions one occasion when a balloon was sent up, and an instrument detached when it had risen 4000 metres. The balloon ascended almost vertically, and after 25 minutes the instrument was seen to fall within 100 metres of its starting-point. There do not seem to be any reasons why this state of almost absolute stillness should not extend to the very highest portion of the atmosphere in these latitudes. So that, both here and, possibly, also in a zone in the tropical or subtropical latitudes, there may be a few days in the year when a resolving power far in excess of anything practicable in the United States could be brought into play. It is not, therefore, of merely theoretical interest to show that the type of telescope suggested is available for a great resolving power, and that, if the workmanship and adjustments are perfect enough, the various beams can be made to combine in such a way that

the effect is not merely additive, but that they should yield the full resolving power of the equivalent aperture.

Let us first suppose that the arrangement of the parabolic reflectors (or lenses) at PQ is exactly similar to the arrangement of collimating lenses at K. Thus the collimating lens corresponding to any given member of the assemblage at PQ occupies precisely the same relative position in the arrangement at K as the member in question in the arrangement at PQ. We may suppose that the members of the assemblage at PQ, and also the collimating lenses, are all set together as closely as possible, and that the beams issuing from the latter have the full breadth of the lenses, which means, of course, that we confine ourselves to the consideration of a star directly on the axis of the instrument. The adjustments are assumed to be of such accuracy that the path-lengths of the  $n^2$  beams are all optically equal when they meet in the focus of S.

Under these circumstances it can be seen that the total beam which proceeds from K to S is virtually the same as would be obtained by converting (by any ordinary system of lenses or reflectors) the beam incident upon a single reflector, of area equal to the combined areas of the assemblage at PQ, into a parallel beam of the breadth of S.

The diffracted rays of the  $n^2$  constituent beams which proceed from L to S, in fact, tend to combine and cancel one another out. One can apply to the consideration of the question the very general argument which Schuster and Nicholson use in connexion with Michelson's stellar interferometer.

What has been said refers only to a star on the axis of the telescope. To make the instrument available for a larger field, it would be necessary that the beams issuing from the collimating lenses at L should not have the full breadth of the lenses. The members of the assemblage at PQ would, then, not be arranged as closely together as possible; but the diameter of any member of the assemblage should bear to the distance between its centre and the centre of any other member the same ratio as is borne by the diameter of a beam emerging from a collimating lens to the distance between the centres of the two collimating lenses corresponding to the two members of the assemblage at PQ, which are in question.

Thus, theoretically, at least, over a limited field, it



appears possible to obtain the full resolving power of the equivalent aperture ; although it is unnecessary to enlarge on the refinements of workmanship which would be needed to secure this in practice, in the case of a very large telescope.

When the writer had nearly completed the present paper, he came upon a suggestion by E. E. Fournier D'Albe \* for a " composite telescope " which at first seemed to him to be essentially the same as that developed above. From the context, however, it appeared that Dr. Fournier D'Albe looked upon the resolving power as dependent upon the focal length of the constituent lenses or reflectors ; and this the present writer did not understand. But what finally convinced him that Dr. Fournier D'Albe must have had some quite different idea in view was the fact that his suggestion was put forward as the converse of a suggestion for a searchlight or beacon in which a large number of very small carbon arcs were to be used with a corresponding number of small reflectors. Now, the converse of the idea which has been developed in the present paper is obtained by placing a *single* carbon arc of ordinary size in the focus of S. A beam with very small angular divergence will then emerge from the assemblage PQ.

Quite apart from the possibilities of the arrangement suggested for telescopic purposes, a useful application of it might indeed be found—with some obvious modifications—in a searchlight or beacon of very small angular divergence, and hence of great intensity at a distance.

### XXXIII. *Notices respecting New Books.*

*Mechanics of the Gyroscope.* By R. F. DEIMEL. (The Macmillan Co., New York. Price 17s. net.)

THIS work, the latest addition to the Engineering Science Series, edited by Prof. D. C. Jackson, of the Massachusetts Institute, and Prof. E. R. Hedrick, of the University of California, has been primarily written to provide an introduction to the study of gyroscopic phenomena and the numerous and varied applications in modern engineering. The first three chapters of the book are entirely mathematical, and deal with plane motion, motion in space, dynamical laws, and the general equations of rotation : numerous exercises are introduced, some fully worked out, others

\* E. E. Fournier D'Albe, 'The Moon Element,' p. 88 (1924).

with hints as to the methods of solution. In the remaining chapters, the author gives a clear and concise treatment of typical gyroscopic devices: a detailed description of the behaviour of gyro-compasses and their use in automatic steering—the three graphs at the end of the ninth chapter show in a striking way the superiority of gyro-pilot steering—and the theory of gyro-stabilizers, the one invented by Schlick a quarter of a century ago and the active type of stabilizer introduced by Sperry. Prof. Deimel's book can be cordially recommended as a preparation for the study of the more advanced texts and the discussion of the new problems, such as the whirling of shafts, which have arisen with the introduction of high-speed machinery.

*The Universe around Us.* By Sir JAMES JEANS. (Cambridge University Press, Fetter Lane, London, E.C. 4. Price 12s. 6d. net.)

IN writing this book, Sir James Jeans had in mind the needs of the reader with no special scientific knowledge, and, dispensing with mathematical analysis, has given an able survey of recent astronomical advances, especially the researches of Prof. Shapley and Dr. Hubble on globular clusters and spiral nebulae, whose distances are measured in millions of light years, and the equally remarkable researches in the structure of the atom. It was a remark of Pascal's that "Man should learn to estimate the earth and the heavens. Then let him take some small creature and observe its minute structure: has he found the least thing in Nature? I will show him a depth beyond. Not only this world but all that we can conceive of the world may exist within the limits of an atom. He who reflects after this manner will realize that he is supported between two infinities: he will contemplate in reverent silence the wonders of which he is a part."

In discussing the internal constitution of the stars, the author introduces the hypothesis that the central regions may properly be described as in the liquid state, and for the source of stellar energy the hypothesis of the annihilation of matter. Of particular interest are the fine photographs of nebulae, planetary, galactic, and extra-galactic, taken at the Mount Wilson and Yerkes Observatories, the series of three Lowell Observatory photographs of Saturn, and the photographs of the tracks of  $\alpha$  and  $\beta$  particles taken by Prof. C. T. R. Wilson and Mr. P. M. S. Blackett.

*Soap Films.* By A. S. C. LAWRENCE. (G. Bell and Sons, Ltd., York House, Portugal Street, Kingsway, London, W.C. 2. Price 12s. 6d. net.)

THE author has drawn on his wide experience in the Royal Institution, where he acted as Assistant to the late Sir James Dewar, and has produced a very complete account of the

*Phil. Mag.* S. 7. Vol. 10. No. 63. August 1930      2 P

preparation, manipulation, and behaviour of soap films. In a Foreword, Sir William Bragg commends this book, which is not only a record of practically acquired knowledge, but a detailed summary of the researches on films carried out during the last thirty or forty years. References are given to the earlier work of Reinold and Rücker, the numerous experimental results obtained by Dewar, and to the latest work of McBain, P. V. Wells, and others. Mr. Lawrence has repeated some of Perrin's experiments and has written an interesting account of stratified films and the theories of the constitution of the black film. Four important papers referred to in the text were published in the 'Philosophical Magazine': Lord Rayleigh, on thin oil films on water (this study having a direct bearing on the nature of soap films); Johonnott, two papers on the thickness of the black film; Narayan and Subrahmanyam, on the surface-tensions of sodium oleate solutions; and de Noüy's researches on soap solutions at extreme dilution. The author summarizes much of the experimental work of Freundlich on the determination of surface-tension and on solutions with threadlike colloid particles, and Lascary's investigations of the lowering of the surface-tension of water by the sodium salts of the fatty acid series. A considerable number of graphs and tables of numerical data are given in the book; the preparation of pure oleic acid is described in an Appendix, followed by a table of measurements of the thickness of soap films. The beautiful photographic plates of soap films, especially the coloured microphotographs of stratified films forming the frontispiece, add much to the value of this book.

*An Introduction to Modern Organic Chemistry.* By L. A. COLES, B.Sc., A.I.C. [Pp. xv+452, with illustrations and 77 figures.] (London: Longmans, Green & Co., 1929. Price 7s. 6d.)

THE requirements of the examination for Higher School Certificates and of other examinations of this standard are covered by this book. It combines theory and practice; a large number of experiments, which have been selected with care, are described in detail. The book is divided into three parts. The first deals with the properties and reactions of ethyl alcohol and acetic acid, and is largely experimental. The second part is concerned with aliphatic compounds, and introduces considerations with regard to molecular structure and molecular changes during reactions. The third deals similarly with aromatic compounds. The principal stages in the development of organic chemistry are summarized in a final historical chapter.

Type of two sizes is used, the smaller size being intended to be passed over at a first reading. Questions are given at the end of each chapter. In spite of a few errors, which should be corrected in a second edition, the book can be recommended as suitable for school use.

*Algebraic Geometry and Theta Functions.* By ARTHUR B. COBLE. American Mathematical Society Colloquium Publications, vol. x. [Pp. vii + 282.] (New York: American Mathematical Society, 1929. Price \$3.00. English agents: Bowes & Bowes, Cambridge.)

THIS monograph contains, in amplified form, the Colloquium Lectures delivered at Amherst in September, 1928, under the title "The determination of the tritangent planes of the space sextic of genus four."

The first two chapters are introductory and give an outline of those topics in algebraic geometry and theta functions which are necessary to the understanding of later applications. The succeeding three chapters deal with the geometrical applications of the functions of genus two, genus three, and of Abelian modular functions of genus four respectively. The final chapter, on theta relations of genus four, gives Schottky's solution of the tritangent plane problem when the sextic lies on a quadric cone.

Schottky, with the theta relations as a starting point, defines a few sets of points in terms of theta modular functions of genera two, three, and four. The author's method is to develop the properties of discrete sets of points in projective spaces, congruent to each other under regular Cremona transformations. Such sets have associated groups which are isomorphic with theta modular groups. The two methods of treatment are correlated by means of a theorem proved in this volume that the sets defined by Schottky are transformed under period transformation of the moduli into sets congruent to the original set under Cremona transformation.

As a summary of the work which has been done in combining theta function theory with algebraic geometry the volume is excellent. The type and general arrangement are worthy of commendation.

*Coal Measure Plants.* By R. CROOKALL, Ph.D. [Pp. 80, with frontispiece and 39 plates.] (London: Edward Arnold & Co., 1929. Price 12s. 6d. net.)

FOSSIL plants provide the best and sometimes the only criteria by which different coalfields may be correlated with one another, and serve also in some instances to correlate individual seams. Dr. Crookall, who is palæobotanist to the Geological Survey of Great Britain, has written this book to serve as a brief introduction to the palæobotany of the British Coal Measures; it is not written primarily for the specialist, but it is intended for the use of students of botany, geology, and mining, and of amateur naturalists.

After a general introduction dealing with types of fossilization and plant divisions in the Coal Measures, brief descriptive notes are given on 240 of the more common and characteristic British

**Coal Measure plants.** Rare forms have been included only where they are characteristic. Figures of all these plants are given in the excellent series of plates.

This book should do much to facilitate the identification of species by the non-specialist. Amateur collectors have in the past contributed considerably to the subject, but the complicated nomenclature is perhaps responsible for interest fading. It is to be hoped that Dr. Crookall's work will help to remedy this state of affairs. Some useful practical hints to collectors are given in an appendix.

*An Introduction to the Chemistry of Plant Products.* Vol. II. *Metabolic Processes.* By PAUL HAAS, D.Sc., Ph.D., and T. G. HILL, D.Sc., A.R.C.S. Second Edition. [Pp. viii + 220, with 12 figures.] (London: Longmans, Green & Co., 1929. Price 10s. 6d. net.)

THE second volume of Haas and Hill's *Chemistry of Plant Products* deals with metabolic processes in the living plant. The subjects dealt with include the synthesis of carbohydrates, of fats and of proteins, respiratory processes, and growth. The increasing importance of these subjects and the large amount of research done on them since the publication of the first edition in 1922 have necessitated much revision and rewriting. This task the authors have carried out with marked success, and no work of importance up to the date of publication has been omitted. The treatment throughout is clear and concise, and full references are given to original papers. A subject-index is given, but not an author's index.

*The Effects of Moisture on Chemical and Physical Changes.* By J. W. SMITH, B.Sc., Ph.D. (Text-Books on Physical Chemistry.) [Pp. xii + 235, with 44 figures.] (London: Longmans, Green & Co., 1929. Price 15s. net.)

AN extensive literature has accumulated on the influence of intensive drying on chemical and physical properties. No connected account of the work which has been done on this subject has hitherto been available. Dr. Smith's book therefore fills an important gap.

After a general historical survey, which includes references to the effects of traces of water-vapour on chemical reaction dating back as far as 1780, the effects on chemical changes are considered. These are discussed in the order: gaseous reactions, solid-gas reactions, reactions between solids, reactions in non-aqueous solvents, the decomposition of solids and miscellaneous effects. To the more important reactions, such as carbon monoxide-oxygen and hydrogen-chlorine, a whole chapter is devoted. The experimental procedures are frequently given at some length,

and the different theories which have been proposed to account for the phenomena are summarized. The effects of intensive drying on physical properties are then considered in detail. All investigations up to 1929 have been included.

As a compilation the work is excellent, but a more critical discussion of the material, both on the experimental and on the theoretical sides, would have been of value. The experimental evidence is not all of the same weight, and conclusions are apt to be misleading if this is not expressly pointed out.

Many theories have been put forward to explain the various phenomena. No one theory has gained universal acceptance, and it is probable that no single theory is applicable to every case. A critical discussion and inter-comparison of the several theories would have added to the value of the work. Students of physical chemistry will be greatly indebted, nevertheless, to Dr. Smith for his account of the work which has been done; full references to original papers are given throughout, so that these can always be referred to for further details.

*La Gamme—Introduction à l'étude de la musique.* Par P. J. RICHARD. [Pp. 231.] (Librairie Scientifique, Hermann et Cie, Paris. Price 28 fr.)

MONSIEUR RICHARD wrote this book primarily for the benefit of his daughter, who was studying music, in order to give her and other students a clearer knowledge of the fundamental facts of the subject. It is an account of the various musical scales, and it is treated very lucidly, the fundamental likenesses between the scales being plainly indicated.

The first chapter introduces Arithmetic and Algebra. This groundwork illuminates acoustical facts occurring in the other chapters of the book. Thus, students of music, when they follow the course laid out in this book, ought clearly to understand the various symbols.

The next four chapters are given up to a full explanation of the various scales adopted in Europe, ending with a table of comparison between four of them, including the scale of Pythagoras.

Chapter V. is devoted to the Physical significance of the scales and such properties of sound as pitch or frequency, intensity, and quality. Simple harmonic motion is expounded graphically, and the place of partials, natural and artificial, is also illustrated.

The method of modulation and transposition is explained with reference to the various scales, and the discrepancies emphasized.

Various musical instruments are described, a chapter being devoted to the organ-pipe. In every case the laws of vibration, transverse and longitudinal, are stated and discussed. The notes of the scales which occur as partials in the different cases are shown on the systems in which they appear.

The book ends with a note of regret that modern music seems to be degenerating into a jumble of noises without any attention being paid to discord or concord.

The subject is dealt with in a very competent manner, the illustrations are sufficient and clear, and the whole arrangement is good.

*Beyond Physics.* By Sir OLIVER LODGE. [Pp. 172.] (George Allen & Unwin. Price 5s.)

AT a period when doubt is so much abroad that uncertainty has been elevated into a principle, it is well that we have among us one who is not only not afraid to examine the wide problems that lie beyond physics, and in particular the age-old questions of the nature of life and mind, but who also has an intellect sufficiently comprehensive to formulate a general plan and an unrivalled mastery of graphic phrase to expound it. Sir Oliver Lodge brings to the discussion of the relationship between spirit and matter an experience of things physical and spiritual which is not to be matched. In physics he combines a profound knowledge of the old with a keen appreciation of the new, while his professional acquaintance with the properties of matter has progressively strengthened his faith in a common basis for the material and the non-material. Anything which he has to say on a subject of such fundamental importance as the nature of life is properly addressed to a very wide public, but it is, perhaps, of particular interest to physicists to follow the bold arguments by which Sir Oliver makes the latest and most revolutionary aspects of physical theory the basis for a general scheme of psychical reality, and amalgamates the problems of the propagation of light and the purpose of life into one.

The fundamental substance—for Sir Oliver calls it a “continuous substance”—of Sir Oliver’s scheme is the ether of space, a conception which has undergone many vicissitudes, as can be seen from Professor Whittaker’s ‘History.’ Sir Oliver freely acknowledges that the old “mechanical or engineering ether” as he calls it, with one of his happy phrases that condense many ideas into a few words, is extinct, but he has a vivid conception of a medium “far less familiar but more accommodating” in its place. This conception is more or less intuitive, a matter of direct apprehension: Sir Oliver alludes to certain sources of information not accessible to the physicist as such, but does not invoke them in his exposition. “I postulate, then, as the one all-embracing reality on the physical side, the Ether of Space. And I conceive that in terms of that fundamental physical entity everything else in the material universe will have to be explained.” It is the

first step that is likely to prove one of the most difficult for the sceptical physicist who has replaced the sceptical chymist of Robert Boyle. Sir Oliver's conception of the ether is astonishingly vivid. It has for him that quality of reality which makes it a suitable medium for the expression of his ideas ; as Faraday, no doubt, " saw " his lines of force, so Lodge sees the ether. There is no doubt that any genius progressing along difficult and unexplored paths must have some brilliant torch of this nature to illumine his way, and if it enables him to advance towards the truth it needs no other defence. Although he may not be able to hand it to certain others, this limitation of its usefulness does not, and should not, prevent all benefiting by any discoveries made by its light.

Sir Oliver's ether is a difficult conception. He speaks of it as containing ultra-microscopic vortices circulating or spinning with the velocity of light, and elsewhere of variety of circulatory movement, and of a constitutional turbulent or rotational velocity of the ether. It is hard to think of a vortex motion denoted by one fixed linear velocity, nor, in spite of his insistence on it, does this turbulent velocity seem essential to Sir Oliver's scheme. Elsewhere it appears that ether and space are almost synonymous, yet we have to imagine discontinuities, hollows, in it to represent particles. Sir Oliver's position may well be that the conception of the ether, being the key to the whole life problem, is likely to remain obscure, and, perhaps, not amenable to close analysis, for some time, and that he puts forward this ether as a pictorial, and not necessarily self-consistent aid, rather than as an entity subject to mathematical laws : he may contend that a vividly apprehended ether is a nearer approach to reality than a system of equations without humanity. Such a view would command assent in many quarters.

Having made the ether a plausible reality to any but the most censorious and cynical reader, Sir Oliver proceeds to expound the elements of wave mechanics, and more particularly the connexion between the group velocity—corresponding to particle velocity—and the wave velocity in the hypothetical dispersive medium of de Broglie and Schrödinger. In this discussion he displays to the full that critical acumen and incisive phrase, that gift for illuminating analogy, which make all his physical work so stimulating. For many the dispersion waves, or constituent waves, are provisional mathematical fictions, and it would appear that to Schrödinger himself they are little more, but it is of fundamental importance to Sir Oliver's thesis that they should be an abiding reality and " the substratum of everything." They direct, he points out, but leave no experimentally accessible record, and have no energy of their own. " Are not," he asks boldly, " these the



kind of assertions which we have been constantly making about life?" His far-reaching hypothesis is that these ether waves are the physical basis of life and mind. For the development of the new theory, and the daring arguments by which it is supported, we must refer readers to the book itself.

The critic may say that the conception of the ether put forward is not self-consistent, and that the argument depends entirely upon analogies. It seems to us a sufficient answer that in an attempt to solve, or to adumbrate a solution of, a fundamental question of such magnitude and difficulty minor contradictions cannot be avoided, and that beyond analogy and direct apprehension there are no weapons available. We commend this extraordinarily acute and persuasively-written book to all who take an interest in what lies outside and beyond physics.

E. N. DE C. A.

#### XXXIV. *Proceedings of Learned Societies.*

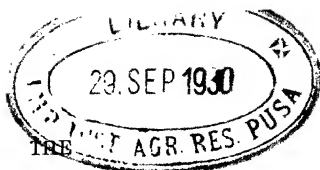
##### GEOLOGICAL SOCIETY.

[Continued from vol. ix. p. 1200.]

May 14th, 1930.—Prof. E. J. Garwood, M.A., Sc.D., F.R.S.,  
President, in the Chair.

Mr. F. A. BANNISTER exhibited lantern-slides to demonstrate the identification of minerals in thin sections of rocks by X-ray methods. Laue photographs of supposed nepheline in small phenocrysts in kenyte from Mount Kenya were shown, and compared with a Laue photograph of a nepheline-crystal from Monte Somma, Vesuvius. These photographs confirm the presence in kenytes of nepheline as phenocrysts. This problem, suggested by Mr. W. Campbell Smith, illustrates the use of X-ray methods for identification of minerals in thin sections, where the separation for chemical analysis of the constituents which are being examined is too difficult: this work is in a preliminary stage. For phenocrysts not oriented so favourably, Laue photographs are in some cases to be supplemented by oscillation photographs. The information recorded on X-ray photographs is considerable. In addition to determining minerals, the mutual orientation of two individual crystals may be obtained, the twin-law (if any) deduced, and accurate values for the axial ratios and unit cell-sides calculated. Photographs have been obtained for crystals of the order of 0.1 mm. in diameter. For the ground-mass of some finer-grained rocks the powder method would probably yield a solution.

[*The Editors do not hold themselves responsible for the views expressed by their correspondents.*]



LONDON EDINBURGH AND DUBLIN

# PHILOSOPHICAL MAGAZINE

AND

# JOURNAL OF SCIENCE.

---

[SEVENTH SERIES.]

---

SEPTEMBER 1930.

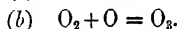
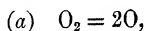
---

XXXV. *On Ozone and Atomic Oxygen in the Upper Atmosphere.* By S. CHAPMAN, F.R.S.\*

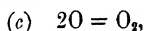
1. **I**N a recent paper† I have given a tentative theory of the equilibrium and annual changes of the ozone which exists in the upper atmosphere; the ozone was, for simplicity, treated as if all of it was situated in a uniform layer of the atmosphere, 10 km. thick, between 40 and 50 km. height. The object of the present paper is to consider how, at greater heights, the concentration of ozone, and also of atomic oxygen, is likely to vary.

Any quantitative discussion of these matters is bound to involve speculative assumptions and estimates, but some interesting qualitative considerations, which are scarcely open to doubt, may be developed.

In the first place, the *production* of ozone almost certainly requires the dissociation of molecular oxygen ( $O_2$ ) into atomic oxygen (O), and the subsequent attachment of the oxygen atoms to oxygen molecules, according to the equations



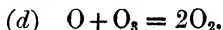
Some of the O atoms may, however, revert to  $O_2$  molecules, according to the reaction



\* Communicated by the Author.

† *Memoirs Roy. Meteor. Soc.* iii. No. 26, pp. 103-125 (1930).

while others may combine with ozone and thus again cause reversion to molecular oxygen, *i.e.*,

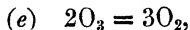


The reactions (*b*), (*c*), in which two particles combine to form a single molecule, will in general occur only in three-body collisions, the participation of a third particle being necessary in order that the conditions of conserved momentum and energy may be fulfilled; the third particle may be an atom or molecule of any kind.

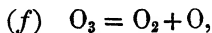
As the density of the atmosphere diminishes, the chance of a third body taking part in a collision of any given kind diminishes in the same ratio, so that the interval between the genesis of an O atom and its combination with an O<sub>2</sub> molecule or another O atom in an effective three-body collision must be correspondingly lengthened. Thus the free life of the O atoms increases with height, and the ratio of O atoms to O<sub>3</sub> molecules must likewise increase, except in so far as convective mixing restores uniformity. At very great heights recombination must be so slow that the proportion of O atoms to O<sub>2</sub> molecules will become large, and whereas at lower levels the reaction (*b*) must be far more frequent than (*c*), because of the large excess of O<sub>2</sub> molecules there present as compared with O atoms, at high levels the reactions (*c*) will be the more frequent—that is, most of the oxygen atoms revert directly to molecular oxygen, and few of them form ozone.

The green line in the spectrum of the aurora, both polar and non-polar, affords direct evidence of the permanent existence of atomic oxygen (in the neutral state) in some stratum of the upper atmosphere.

The *disappearance* of ozone may occur by the reaction (*d*), in conjunction with atomic oxygen, or by the reaction



which is supposed to be the mode of purely thermal decomposition of ozone, or by dissociation in the manner inverse to (*b*), *viz.*,



thus giving rise to atomic oxygen. The last reaction requires the communication of energy to the ozone molecule; this may be effected either by unusually violent collisions with other molecules of any kind, or by the action of sunlight. Radiation in the band  $\lambda$  2300–2900 is absorbed by ozone, and is believed to bring about this dissociation;

it is by this and other ozone absorption-bands in the solar spectrum that the existence, amount, and height of the ozone in the earth's atmosphere are detected and measured.

The *production* of atomic oxygen by the process (*f*) may at particular levels be greater than by the process (*a*), but the latter is the more fundamental; if it ceased, and O atoms were formed only from ozone, the amount of ozone would slowly diminish.

The reciprocal reactions (*f*) and (*b*) form a cyclic process, and if every O atom formed by (*f*) reverted to  $O_3$  by (*b*), the combined number of O atoms and  $O_3$  molecules would remain constant; but actually the number must diminish by the reactions (*c*), (*d*), and (*e*), so that unless there were replenishment by the formation of new O atoms direct from  $O_2$ , not from  $O_3$ , the number of O atoms and  $O_3$  molecules would steadily diminish to zero.

The formation of O atoms from  $O_2$  may occur either by absorption of ultra-violet sunlight, in the band  $\lambda$  1300–1800, or by bombardment of the atmosphere (as during auroræ) by corpuscles from without; probably both actions occur, though at the equator sunlight is likely to be the chief agent. In this case, and elsewhere so far as dissociation by sunlight is concerned, the formation of O atoms either from  $O_2$  or  $O_3$  will proceed by day but not by night, and a daily variation in the numbers of O atoms and  $O_3$  molecules per c. c. will arise. During the night the atomic oxygen can only decrease, while the ozone may either decrease or increase. The daily variation of the atomic oxygen will necessarily decrease with height, owing to the increasing free life of each atom.

These general considerations, while indicating certain definite conclusions, cannot give numerical results for the O and  $O_3$  concentrations at actual heights, on the basis merely of present observed data. The ozone observations indicate the total amount of ozone in each square cm. column of atmosphere, and also the mean height of the ozone; but they cannot without further assumptions indicate the detailed distribution of the ozone, especially at high levels, where the absolute density, whatever the relative concentration, must be very low. Hence the numerical development of the discussion, in the former paper and also here, is necessarily of a speculative character.

2. Let  $n_1$ ,  $n_2$ ,  $n_3$ ,  $n$  respectively denote the number per c. c. of O atoms,  $O_2$  and  $O_3$  molecules, and of air molecules, at height  $h$ . Also let the number of reactions per c. c. per sec.

at this height of the types (b), (c), (d), (e) be denoted respectively by

$$K_{12}n_1n_2, \quad K_{11}n_1^2, \quad k_{13}n_1n_3, \quad k_{33}n_3^2,$$

where the large  $K$ 's refer to the three-body collisions mentioned in § 1, and are proportional to the density of the air, *i. e.*, to  $n$ ; thus  $K_{12} \equiv k_{12}n$ ,  $K_{11} \equiv k_{11}n$ . The small  $k$ 's are independent of the density, but may depend on the temperature; this dependence is likely to be small over the range of temperatures involved, and will not be considered here.

3. Let the intensity of the radiations in the bands  $\lambda$  1300–1800 and  $\lambda$  2300–2900, at height  $h$ , be respectively denoted by  $I_2$ ,  $I_3$ , and let the absorption per cm. of air traversed be denoted by  $\sigma_2n_2I_2$ ,  $\sigma_3n_3I_3$  in the two cases, being proportional to the numbers of the absorbing molecules and to the intensity of the radiation. Then  $I_2$  and  $I_3$  satisfy the differential equations

$$a_2 \equiv \frac{dI_2}{dh} = \sigma_2n_2I_2, \quad . \quad . \quad . \quad . \quad . \quad (1)$$

$$a_3 \equiv \frac{dI_3}{dh} = \sigma_3n_3I_3. \quad . \quad . \quad . \quad . \quad . \quad (2)$$

The numbers  $a_2$  and  $a_3$  are proportional to the number of  $O_2$  or  $O_3$  molecules dissociated per c. c. per second, and by suitable choice of the units in which  $I_2$  and  $I_3$  are measured they will actually equal the number of molecules dissociated; it will be supposed that the units are so chosen. For example, if each quantum dissociates one molecule, then the intensities of the two bands must be measured, not in ordinary energy units, but in numbers of quanta of their respective wavelengths; if, however, only one quantum in  $\nu_2$  or  $\nu_3$  is effective for dissociation, then  $I_2$  and  $I_3$  must be measured in units equal to  $\nu_2$  or  $\nu_3$  quanta respectively.

The density of the atmosphere, and therefore also  $K_{11}$ ,  $K_{12}$ , varies as  $\exp(-h/H)$ , where  $H$  depends on the temperature and mean molecular weight of the constituents; so long as the composition is nearly uniform  $n_2$  will vary in like manner. It cannot be assumed, however, that  $n_1$  or  $n_3$  vary in this way, nor do they sensibly affect the mean molecular weight, or  $H$ , so long as  $O$  and  $O_3$  are rare constituents of the air. This is true as regards  $O_3$  even in the layer of maximum ozone density.

So long as  $n_2$  varies as  $\exp(-h/H)$ , and  $H$  is constant, (1) can be integrated, giving

$$I_2 = (I_2)_\infty \exp\{-\mu H \exp(-h/H)\}, \quad . \quad . \quad (3)$$

where  $\mu \equiv \sigma_2 n_2 \exp(h/H)$  and is therefore constant;  $(I_2)_\infty$  is the value of  $I_2$  outside the earth's atmosphere. Also

$$a_2 = \sigma_2 n_2 I_2 = \mu I_2 \exp(-h/H) \\ = \mu (I_2)_\infty \exp\{-(h/H) - \mu H \exp(-h/H)\}. \quad (4)$$

At great heights this increases downwards approximately as  $\exp(-h/H)$ , or proportionally to  $n_2$ ; this is in the region of small absorption, where  $I_2$  has nearly its maximum value  $(I_2)_\infty$ . As we descend, the second term in the index of the exponential becomes important, and  $a_2$  rises to a maximum, after which it tends rapidly to zero.

Though  $n_3$ , unlike  $n_2$ , cannot be assumed to vary as  $\exp(-h/H)$ , it is clear that at great heights  $I_3$  must be nearly constant, and  $a_3$  proportional to  $n_3$ ; since most of the radiation in the Hartley band ( $\lambda$  2300–2900) is ultimately absorbed,  $I_3$  must tend to zero within or at the base of the ozone layer, and therefore in the lower part of this layer  $a_3$  decreases downwards more rapidly than in proportion to  $n_3$ .

4. It will provisionally be supposed that the amounts of O and  $O_3$  in each element of air are determined solely by the processes of dissociation and reaction occurring in the element, and are unaffected by convection and diffusion. Then the equations of change of  $n_1, n_2, n_3$  by day are as follows:—

$$\frac{dn_1}{dt} = 2N_2 + N_3 - n_1(2K_{11}n_1 + K_{12}n_2 + k_{13}n_3), \quad (5)$$

$$\frac{dn_2}{dt} = N_3 - N_2 - K_{12}n_1n_2 + K_{11}n_1^2 + 3k_{23}n_3^2 + 2k_{13}n_1n_3, \quad (6)$$

$$\frac{dn_3}{dt} = -N_3 + K_{12}n_1n_2 - 2k_{33}n_3^2 - k_{13}n_1n_3, \quad (7)$$

where

$$N_2 \equiv a_2 \cos(\pi t/t_0), \quad N_3 \equiv a_3 \cos(\pi t/t_0); \quad (8)$$

here  $a_2$  and  $a_3$  are taken to denote the numbers of  $O_2$  or  $O_3$  molecules dissociated per c. c. per sec. at noon, while  $N_2$  and  $N_3$  are the corresponding numbers at time  $t$  reckoned forward or backward from noon;  $t_0$  denotes the duration of sunlight. The daily variation represented by (8) represents the facts only roughly, but sufficiently well for the present purpose.

The equations of change of  $n_1, n_2, n_3$  at night are obtainable from (5)–(7) by omitting the  $N$ 's.

For simplicity we will in the first instance consider the conditions above the equator at the equinoxes, so that  $t_0$  represents half a day or, in seconds,

$$t_0 = 4 \cdot 32 \cdot 10^4. \quad . \quad . \quad . \quad . \quad . \quad (9)$$

Since  $n_1$  and  $n_3$  do not increase or decrease indefinitely, but maintain nearly constant values (especially near the equator), the average values of  $(dn_1/dt)$  and  $(dn_3/dt)$  must be zero; hence also the daily average values of the right-hand sides of (5) and (7) must be zero. The average daily values of  $N_2$  and  $N_3$  may be expressed as  $\lambda n_2$ ,  $\mu n_3$ , where  $\lambda$  and  $\mu$  tend to constant limiting values with increasing height; *e.g.*,  $\lambda$  and  $\mu$  are approximately  $\sigma_2 I_2/\pi$  and  $\sigma_3 I_3/\pi$ . Consequently, the  $n$ 's referring to daily mean values, we have

$$2\lambda n_2 + \mu n_3 = n_1(2K_{11}n_1 + K_{12}n_2 + k_{13}n_3), \quad . \quad . \quad (10)$$

$$K_{12}n_1n_2 = \mu n_3 + 2k_{33}n_3^2 + k_{13}n_1n_3. \quad . \quad . \quad (11)$$

Now the  $n$ 's of every kind must ultimately decrease with increasing height; hence on the right of (11) the last two terms, which contain  $n_3$  multiplied by other  $n$ 's, must ultimately become small compared with the term  $\mu n_3$ , and at sufficiently great heights we must have approximately

$$n_3 = (k_{12}/\mu)n_1n_2n. \quad . \quad . \quad . \quad . \quad (12)$$

Thus  $n_3/n$  must decrease upwards proportionately to  $n_1n_2$ , *i.e.*, the proportion of ozone to the other molecules must decrease rapidly; presumably in this region there will be a corresponding decrease of temperature, if ozone be the main cause of the high temperature in the upper atmosphere.

On the left-hand side of (10) the term  $2\lambda n_2$  must ultimately outweigh the term  $\mu n_3$ , because at sufficiently great heights the ratio of the latter to the former is  $K_{12}n_1n_2/2\lambda n_2$  or  $k_{12}n_1/2\lambda$ . Likewise the term  $K_{12}n_1n_2$  on the left, which is of the same order as  $\mu n_3$ , may be omitted. Hence  $2\lambda n_2$  must ultimately tend to equality with  $2K_{11}n_1^2 + k_{13}n_1n_3$ , and the latter term is negligible at sufficiently great heights. Thus (10) approximates to

$$2\lambda n_2 = 2K_{11}n_1^2 = 2k_{11}n_1^2n, \quad . \quad . \quad . \quad (13)$$

or

$$n_1 = \sqrt{\{(\lambda/k_{11})(n_2/n)\}}. \quad . \quad . \quad . \quad (14)$$

Since  $n_1$  must itself decrease upwards, the proportion  $n_2/n$  of molecular oxygen in the air must necessarily diminish. But  $n_1/n_2$ , the proportion of atomic to molecular oxygen, must increase upwards, because

$$n_1/n_2 = \sqrt{\{\lambda/(k_{11}nn_2)\}}, \quad . \quad . \quad . \quad (15)$$

which tends to infinity with increasing height—that is, the oxygen at great heights must tend to be completely dissociated.

The heights at which the limiting equations (12) and (14) become approximately true are unfortunately very uncertain, because the values of the  $k$ 's and of  $\lambda, \mu$  are unknown. An attempt will be made, however, to gain some idea as to their order of magnitude, on the basis of the theory given in the former paper already cited.

5. It was provisionally supposed that at the level  $h_m$  of maximum ozone density the most important reaction is (b), and that

$$K_{12}n_2 > 6 \cdot 10^{-3}.$$

The conception there tentatively arrived at regarding the processes in the layer where the  $O_3$  concentration is greatest is as follows:—during the day O atoms are formed, mainly by dissociation of  $O_3$  (since  $a_3$  much exceeds  $a_2$ ), but their increase is limited by their rapid combination with  $O_2$  to re-form  $O_3$ ; thus the approximate value of  $n_1$  by day is

$$\frac{a_3}{K_{12}n_2} \cos \pi \frac{t}{t_0} \dots \dots \dots (16)$$

At sunset the O atoms that are left ((16) not being quite accurate in representing them as zero) recombine rapidly, so that  $n_1$  varies as  $\exp(-K_{12}n_2t)$ ; in less than 7 minutes they are reduced to one-tenth their sunset value, and therefore during most of the night there is practically no atomic oxygen. Thus the daily dissociation of  $O_3$  and  $O_2$  is only temporary, and soon after sunset its effects have almost disappeared. The maximum loss of ozone, near noon, is  $a_3/K_{12}n_2$ , and since the daily variation of  $n_3$  is shown by observation to be small, probably less than  $\frac{1}{10}n_3$ , a lower limit (as above stated) for  $K_{12}n_2$  can be deduced.

The daily dissociation of  $O_2$  and  $O_3$  does not directly determine the mean value of  $n_3$ , but does so in an indirect way, because the O atoms formed by the sunlight do not all form ozone on recombination; a few of them participate in the reactions (c) and (d), and it is through these reactions that the equilibrium of  $n_3$ , and its slow annual variation, (north or south of the equator) are mainly determined. Nevertheless, the values of  $N_3$  and  $K_{12}n_2$ , which are the chief factors determining the amount  $n_1$  of atomic oxygen existing during each day, thereby govern the number of the reactions (c) and (d). The reaction (e) also affects the ozone equilibrium, but reasons are given (*l.c.*) for believing its influence to be very slight.



From a consideration of the annual variation of  $n_3$  very tentative estimates of  $k_{13}(=8.10^{-20})$  and  $K_{11}(=8.10^{-18})$  at the level  $h_m$  were deduced. Moreover,  $n_2$  being approximately  $10^{16}$  at this level, it follows that  $K_{12} > 6.10^{-19}$ . These numbers are quoted as possibly indicating the order of magnitude of the recombination coefficients, though they are admittedly uncertain. The value of  $k_{33}$  is estimated (from chemical data) as about  $2.10^{-25}$  at  $300^\circ \text{K}$ , or  $10^{-20}$  at  $400^\circ \text{K}$ .

6. Let

$$\sigma_2 I_2 \equiv \alpha_2, \quad \sigma_3 I_3 \equiv \alpha_3, \quad . \quad . \quad . \quad (17)$$

so that

$$a_2 = \alpha_2 n_2, \quad a_3 = \alpha_3 n_3; \quad . \quad . \quad . \quad (18)$$

$\alpha_2$  and  $\alpha_3$  increase upwards, but only to finite limiting values  $\sigma_2(I_2)_\infty$ ,  $\sigma_3(I_3)_\infty$ . Taking

$$a_2 = 2.10^6, \quad a_3 = 5.10^9$$

at level  $h_m$ , where

$$n_2 = 10^{16}, \quad n_3 = 8.10^{12} \text{ about,}$$

we have

$$\alpha_2 = 2.10^{-10}, \quad \alpha_3 = 6.10^{-4}$$

at  $h_m$ .

7. The equation of daily variation of  $O_3$  is (7), which, by use of (8) and (18), may be written in the form

$$\frac{d \log n_3}{dt} = -\alpha_3 \cos \frac{\pi t}{t_0} + \frac{K_{12} n_1 n_2}{n_3} - 2k_{33} n_3 - k_{13} n_1. \quad (19)$$

At the level  $h_m$  the last two terms are negligible compared with the others on the right, and this must persist for some distance above  $h_m$ , so that the equation will be used in the approximate form

$$\frac{d \log n_3}{dt} = -\alpha_3 \cos \frac{\pi t}{t_0} + \frac{K_{12} n_1 n_2}{n_3} . . . . \quad (20)$$

This holds during the day ( $t = -\frac{1}{2}t_0$  to  $t = \frac{1}{2}t_0$ ); during the night the term containing  $\alpha_3$  is absent. Since  $n_3$  and  $\log n_3$  do not indefinitely increase with time, but (at the equator, where there is no annual variation) merely undergo a daily cycle, the integral of  $d \log n_3 / dt$  over a whole day must be zero. Hence

$$\frac{2t_0}{\pi} \alpha_3 = \int \frac{K_{12} n_1 n_2}{n_3} dt, \quad . \quad . \quad . \quad (21)$$

where the integral on the right is extended over the whole 24 hours ( $2t_0$ ); or, what is equivalent,

$$\alpha_3 = \pi \left[ \frac{K_{12}n_1n_2}{n_3} \right], \quad . \quad . \quad . \quad . \quad . \quad (22)$$

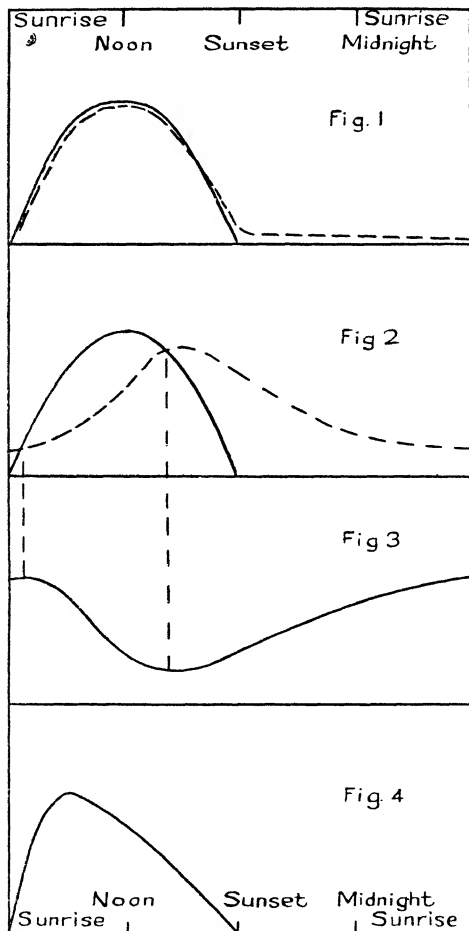
where the square brackets denote that the daily mean value of the enclosed expression is intended. Thus, the daily mean value of  $K_{12}n_1n_2/n_3$ , being equal to  $\alpha_3$ , must with increasing height tend to the finite limit  $\sigma_3(I_3)$ .

Ozone is formed only by the reaction (b), and the term  $K_{12}n_1n_2/n_3$  on the right of (14) may be termed the (ozone-) "production" term; the term  $-\alpha_3 \cos(\pi t/t_0)$  may be called the (ozone-) dissociation term. The dissociation curve, representing the variations of this term throughout the day, is here taken to be of the same form at all heights (though this is not strictly true), and its amplitude increases with height to a finite limit. The "production" curve, representing the daily variation of  $K_{12}n_1n_2/n_3$ , must enclose an area equal to that of the dissociation curve, since  $n_3$  and  $\log n_3$  are periodic in a day (at least at the equator, where there is no annual variation). At the level  $h_m$  the two curves are as shown in fig. 1, the production (shown by a dotted line) almost balancing the dissociation (shown by a full line) at all times.

The factor  $K_{12}n_2$  in the production term decreases upwards as  $\exp(-2h/H)$  so long as the  $O_2$  concentration in the air remains fairly constant; since  $H$  is about 8.5 km., this exponential decreases approximately in the ratio 10 to 1 for each 10 km. change of level. Thus, taking  $h_m$  to be 45 km., at 55 km.  $\exp\{(h_m - h)/H\}$  is 0.1, at 65 km. it is 0.01, and at 80 km. it is about 0.0003. The corresponding change in  $K_{12}n_2$  greatly affects the form of the production curve. At night ozone is formed at the expense of O at the rate  $K_{12}n_1n_2$ , so that the O disappears at least as rapidly as  $\exp(-K_{12}n_2t_0)$ . At the level  $h_m$  nine-tenths of the O remaining at sunset has disappeared in less than 7 minutes; 10 km. higher the same decrease will take 10 times longer—that is, in 70 minutes or less. At 80 km. only a small fraction of O will have disappeared, *by formation of ozone*, even by the following dawn; this fraction is  $1 - \exp(-K_{12}n_2t_0)$ , or  $K_{12}n_2t_0$  itself when this is small. Taking  $K_{12}n_2 = 6.10^{-3}$  at  $h_m$ , at 80 km. only about 80 per cent. of the O left at sunset has become transformed into  $O_3$  by dawn.

During the night  $n_1$  decreases (owing to this and also to other reactions), while  $n_3$  increases; hence  $K_{12}n_1n_2/n_3$  decreases for both reasons. The night-time increase in  $n_3$

must be balanced by an equal day-time decrease, and *vice versa* for the O. Thus  $K_{12}n_1n_2/n_3$  increases by day, though not necessarily throughout the whole daylight period; indeed, the night-time increase of  $n_3$  or  $\log n_3$  must continue for a



short time after dawn, before the dissociation has increased sufficiently to balance the new production.

At the level  $h_m$  we have estimated  $\alpha_3$  as  $6 \cdot 10^{-4}$  at 80 km., and above  $h_m$  it will be somewhat greater. At dawn at these levels  $n_3$  is greater than at sunset by not less than

$K_{12}(n_1)_{\text{dawn}}n_2t_0$ , since  $n_1$  has its least value at dawn; hence  $(n_3)_{\text{dawn}} \geq K_{12}(n_1)_{\text{dawn}}n_2t_0$ , and  $(K_{12}n_1n_2/n_3)_{\text{dawn}} \leq 1/t_0$ , i. e.,  $1/(4 \cdot 32 \cdot 10^4)$ , or  $0 \cdot 23 \cdot 10^{-4}$ ; this is much less than  $\alpha_3$ . From this value it sinks slightly further to a minimum shortly after sunrise; very soon, however, as  $O_3$  (and  $O_2$ ) become dissociated, increasing  $n_1$  and decreasing  $n_2$ ,  $K_{12}n_1n_2/n_3$  begins to rise to a maximum which must be attained somewhat before sunset, when again the production of  $O_3$  gains on the dissociation. From these considerations, and the equality of area of the two graphs, it follows\* that the production graph at these high levels must be somewhat like the dotted curve in fig. 2. The maximum of  $K_{12}n_1n_2/n_3$  must be not much less than  $\alpha_3$ .

The curve giving  $n_3$  itself is determined, apart from an arbitrary constant, by the curves of fig. 2, and is as shown in fig. 3. The form of  $\alpha_3 n_3 \cos(\pi t/t_0)$  during the day is given in fig. 4. The curves of figs. 2-4 probably tend towards a limiting form with increasing height.

The area of fig. 4 represents the total daily dissociation of ozone according to the equation

$$\frac{dn_3}{dt} = -\alpha_3 n_3 \cos \frac{\pi t}{t_0} + K_{12}n_1n_2, \quad \dots \quad (23)$$

omitting the smaller terms on the right (*cf.* 20). This area may be expressed as  $2t_0 A \alpha_3 [n_3]$ , where  $[n_3]$  denotes the mean value of  $n_3$  throughout the whole 24 hours, and  $A$  is a constant which would be  $1/\pi$  if  $n_3$  were constant, and which is probably not much different from this—say between  $\frac{1}{4}$  and  $\frac{1}{2}$ —when  $n_3$  has the form shown (apart from an undetermined additive constant) by fig. 3. Since the integral of  $K_{12}n_1n_2$  throughout the day, that is  $2t_0 K_{12} [n_1]n_2$ , must equal the area of fig. 4, we have

$$\frac{[n_3]}{[n_1]} = \frac{K_{12}n_2}{A\alpha_3}, \quad \dots \quad (24)$$

a result already suggested, though not proved, by (22).

In (24)  $\alpha_3$  increases with height to a finite limit, while  $K_{12}n_2$  decreases proportionately to  $\exp(-2h/H)$  so long as the oxygen-nitrogen ratio does not depart much from its normal value. Thus,  $[n_3]/[n_1]$  must decrease at least as rapidly as  $\exp(-2h/H)$ . At the level  $h_m$ ,  $[n_3]$  is about  $8 \cdot 10^{12}$ , while  $[n_1]$  is approximately  $(1/\pi)(n_1)_{\text{noon}}$ ; probably

\* The complete variation of  $n_2$  and  $n_3$  can be worked out by quadratures, but in view of the uncertainty as to the numerical values of certain of the factors involved this is at present scarcely worth while.

$(n_1)_{\text{noon}}$  is not more than  $\frac{1}{10}n_3$ ; taking it to be equal to  $\frac{1}{10}n_3$ , or  $8.10^{11}$ ,  $[n_3]/[n_1]$  will be about  $10\pi$  at this level; but the real value can be determined only when the daily variation of the ozone content of the atmosphere can be measured. If  $[n_3]/[n_1]$  is  $10\pi$  at 45 km., then at 80 km. it will be less than 0.01.

Owing to the rapid upward decrease of  $[n_3]/[n_1]$  the neglected terms in (19) are still less important than at the latter level, so that the above argument needs no revision on their account.

8. By adding (5) and (7) we obtain the equation governing the variation of  $n_1 + n_3$ , namely,

$$\frac{d(n_1 + n_3)}{dt} = 2(N_2 - K_{11}n_1^2 - k_{13}n_1n_3 - k_{33}n_3^2); \quad (25)$$

this is independent of the processes (b) and (f)—that is, of the dissociation and formation of ozone. This equation holds during daylight; at night the term  $N_2$  must be omitted. The ratio of the term  $k_{33}n_3^2$  to the term  $K_{11}n_1^2$ , at the level  $h_m$ , appears (*l. c.*) to be negligible; at greater heights it varies approximately as  $(k_{33}/K_{11})\{[n_3]/[n_1]\}^2$ —that is, proportionately to  $\exp(-3h/H)$ ; thus  $k_{33}n_3^2$  can be neglected at all heights above  $h_m$ . The ratio of the term  $k_{13}n_1n_3$  to  $K_{11}n_1^2$  will vary approximately as  $\exp(-h/H)$  above  $h_m$ ; at  $h_m$ , according to the very tentative estimates mentioned at the end of § 5, the daily mean value of the ratio is about  $\frac{1}{3}$  (taking  $[n_3]/[n_1]$  as  $10\pi$ , and  $k_{13}/K_{11}$  as  $\frac{1}{100}$ ), so that at 80 km. it will be about  $\frac{1}{200}$ ; at and above 80 km., therefore,  $k_{13}n_1n_3$  can be neglected, so that (25) reduces to

$$\begin{aligned} \frac{d(n_1 + n_3)}{dt} &= 2(N_2 - K_{11}n_1^2) & (h > 80 \text{ km.}) \\ &= 2 \left\{ \alpha_2 n_2 \cos \frac{\pi t}{t_0} - K_{11}n_1^2 \right\}. \quad (26) \end{aligned}$$

Hence, as in § 7, since the daily variation of  $n_1 + n_2$  is cyclic,

$$[n_1^2] = \frac{1}{\pi} \frac{\alpha_2 n_2}{K_{11}} = \frac{1}{\pi} \frac{\alpha_2 n_2}{k_{11} n}, \quad (27)$$

writing  $K_{11} = k_{11}n$ , where  $k_{11}$  is independent of the air density. The right-hand side of (27) varies with height owing both to  $\alpha_2$ , which increases upwards to a finite limit, and to  $n_2/n$ , though the latter is nearly constant so long as only a small fraction of the oxygen is dissociated, and so long as the oxygen-nitrogen ratio is maintained uniform by

convective mixing; the latter may be effective up to 100 km. or more. Thus, at and somewhat above 80 km.,  $[n_1^2]$  probably varies only slightly with height; its magnitude can scarcely be estimated at present, but if the values of  $\alpha_2 n_2$  ( $2 \cdot 10^6$ ) and  $K_{11}$  ( $8 \cdot 10^{-18}$ ) tentatively estimated for the level  $h_m$  are adopted, we get  $[n_1]^2 = 8 \cdot 10^{23}$  approximately, or, at levels where  $n_1$  does not vary much throughout the 24 hours (as is the case above 80 km.),  $[n_1] = 3 \cdot 10^{11}$ , the same as the estimated mean value of  $n_1$  at level  $h_m$ .

So long as  $[n_1]$  is varying slowly with height it follows from § 7 that  $[n_3]$  varies as  $\exp(-2h/H)$ ; at 80 km., taking  $[n_3]/[n_1]$  as 0.01, as estimated, we have  $[n_3] = 3 \cdot 10^9$ . At this level  $n_2$  will be of order  $10^{14}$ , so that there only a small fraction of the oxygen exists in the atomic form or as ozone. At 120 km., however, where  $n_2$  is of order  $10^{12}$ , the value  $3 \cdot 10^{11}$  for  $[n_1]$  represents a considerable proportion of dissociated oxygen (at this level the ozone concentration has become very small,  $n_3$  being less than  $10^5$ ).

9. The estimates of  $n_2$  which have been quoted in § 8 are based on the assumption that the oxygen-nitrogen ratio is maintained nearly constant by convective mixing; this need not be very rapid in order to counteract the rate of diffusive separation, which is slow until great heights are attained. The mixing will also affect the distribution of atomic oxygen and ozone, tending to make it more uniform; thus, it will tend to make the ozone decrease upwards less rapidly than has been estimated in § 7. If interchange between different levels, by mixing or diffusion, were absent, the atomic oxygen would remain nearly constant in absolute density ( $n_1$ ) over a wide range of height, its relative concentration therefore increasing upwards; convective mixing must tend to make the concentration more nearly uniform, thus increasing  $n_1$  in the lower levels at the expense of the upper ones. The extent to which this tendency is effective will depend on the relation between the rate of interchange of air between different levels by mixing, the rate at which the light atomic oxygen rises by diffusion, and the rate at which the atomic-oxygen density at any level tends, by dissociation or recombination, to the equilibrium value determined by (21); the first of these rates is entirely unknown, the second increases with height, while the third decreases with height. To prove the last of these statements it is only necessary to consider the total number of oxygen atoms formed in a day at level  $h$  by dissociation; this is  $2 \int N_2 dt$ , or (taking  $\alpha_2 n_2 = 2 \cdot 10^6$  at level  $h_m$ )  $(2t_0/\pi) \cdot 2 \cdot 10^6 \exp \{(h_m - h)/H\}$ .

that is,  $5 \cdot 10^{10} \exp \{ (h_m - h)/H \}$ , or  $\frac{1}{6} [n_1] \exp \{ (h_m - h)/H \}$ , according to the above estimate of  $[n_1]$ . Thus, at 80 km., for example, where the exponential factor is about  $\frac{1}{35}$ , it would take 330 days to attain the equilibrium value of  $[n_1]$  if originally there were no atomic oxygen and if, during these 330 days, there were no reactions removing the oxygen atoms. Thus it is clear that a departure from the equilibrium state, by convective mixing or diffusion, would be restored only very slowly, at and above 80 km., by dissociation and recombination.

Owing to our ignorance of the degree of convective mixing it is impossible to form any definite conclusion as to the precise value of  $[n_1]$  at any level above 80 km., but, as we ascend, diffusion must become relatively more important, and this will tend to make atomic oxygen predominate over molecular nitrogen and oxygen. If, above some high level such as 120 km., convective mixing ceases, the state at higher levels will be intermediate between the distributions corresponding to purely diffusive and purely reactive equilibrium; according to the former,  $n_1$  would vary with height approximately in proportion to  $\exp(-h/2H)$ , corresponding to the fact that the atomic weight of oxygen is roughly half the mean molecular weight of air, while  $n_2$  would vary nearly as  $\exp(-h/H)$ —that is, as  $n_1^2$ . The equilibrium between dissociation and recombination, given by (21) as  $n_2 \propto n_1^2 n$ , implies a more rapid rate of decrease of  $n_2/n_1$  with height than would correspond to diffusive equilibrium. The actual state at very high levels, assuming hydrogen, helium, and atomic nitrogen to be absent, will be one in which the fractional concentration of molecular oxygen diminishes upwards somewhat more rapidly than would correspond with an undissociated mixture of molecular nitrogen and oxygen in diffusive equilibrium. There is, however, no apparent reason why atomic nitrogen should not be present as well as atomic oxygen, and according to Slipher and Sommer there is definite evidence for this in the auroral spectrum\*.

10. While the foregoing discussion is unavoidably speculative in so far as it involves numerical estimates, two main conclusions stand out as highly probable. The existence of ozone implies a mechanism which will form atomic oxygen by dissociating oxygen molecules; this mechanism is almost certainly, at least in part, ultra-violet radiation, which will be absorbed gradually as it passes through the highest

\* V. M. Slipher and M. A. Sommer, *Naturwiss.* xvii. p. 802 (1929).

atmospheric strata, there dissociating oxygen. At sufficiently great heights recombination will be slow, so that little ozone will be formed, and atomic oxygen will accumulate; and it will rise by diffusion until (in the absence of hydrogen and helium), together with atomic nitrogen, it becomes the chief atmospheric constituent. On the other hand, as we descend the oxygen atoms will more and more readily attach themselves to oxygen molecules, to form ozone. These, in brief, are the reasons which render it likely that (1) the ozone concentration diminishes rapidly with height above the level of maximum concentration, and especially above the level at which convective mixing is important, and (2) the atomic oxygen concentration increases upwards until it exceeds that of molecular oxygen.

---

XXXVI. *The Effect of the Surrounding Medium on the Life of Floating Drops.* By L. D. MAHAJAN, M.Sc., Professor of Physics, Mohindra College, Patiala\*.

IN a previous paper† the author gave some general accounts of the "Liquid Drops on the same Liquid Surface." The author has now tried to find out if there is any effect of the surrounding medium on the life of the liquid drops floating on the same liquid surface. Several gases and liquids have been tried, and their densities, viscosities, and surface-tensions found at various temperatures. It is found that the nature of the surrounding medium affects the life of the floating drops. Calmness of the weather and viscosity of the surrounding medium have an effect on the life of the drops.

*Method.*

A very fine nozzle was attached to the jet-end of the burette. The liquid was dropped from the burette through the nozzle on the surface of the same liquid, kept in a shallow dish. The nature of the surrounding medium was varied by simply changing the surrounding medium, air, into some other gases, or some light liquids (lighter than the liquid used to form the drops) at room-temperature or at high

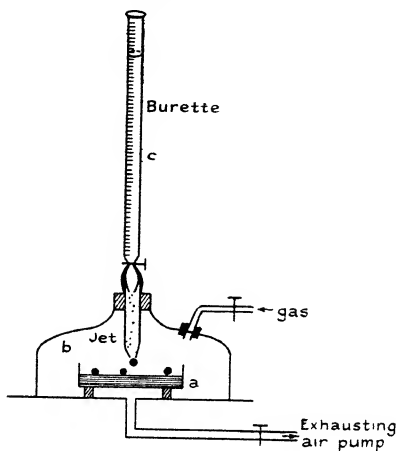
\* Communicated by the Author.

† J. B. Seth, C. Anand, and L. D. Mahajan, "Liquid Drops on the same Liquid Surface," *Phil. Mag.* vii. pp. 247-253 (Feb. 1929).



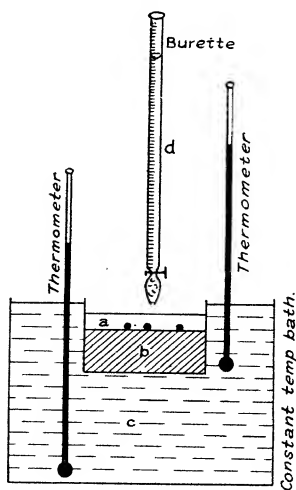
temperature. Fig. 1 represents the method when the surrounding medium is some gas instead of air, and fig. 2

Fig. 1.



*a*, shallow dish containing water; *b*, vessel containing  $\text{CO}_2$ ;  
*c*, burette containing water.

Fig. 2.



*a*, olive oil; *b*, water; *c*, constant temp. bath;  
*d*, burette containing water.

represents the method when the surrounding medium is some light liquid instead of air.

The observations in the following Table were taken :—

No.	Liq. of Drops.	Surrounding Medium.	Mean Life of a Drop.	Viscosity of the Surr. Med.
			sec.	
1.	Water .....	Air .....	·5	$1·84 \times 10^{-4}$
2.	„ .....	Carbon dioxide...	·5	$1·9 \times 10^{-4}$
3.	„ .....	Petrol .....	4·0	·02
4.	„ .....	Olive-oil at 80° C.	13·5	·083
5.	„ .....	„ „ „ 60° C.	45·0	·19
6.	„ .....	„ „ „ 50° C.	76·0	·43
7.	„ .....	„ „ „ 20° C.	180·0	·95
1.	Boys' Soap Solution	Air .....	4·5	$1·84 \times 10^{-4}$
2.	„ „ „	CO <sub>2</sub> .....	4·5	$1·9 \times 10^{-4}$
3.	„ „ „	Petrol .....	12·5	·02
1.	Aniline .....	Air .....	3·0	$1·84 \times 10^{-4}$
2.	„ .....	CO <sub>2</sub> .....	3·0	$1·9 \times 10^{-4}$
3.	„ .....	Water .....	8·0	·01

A curve, for the case of water-drops, is drawn (fig. 3) showing the relation between the mean life of the drop and the viscosity of the surrounding medium. The form of the curve shows that, as the viscosity of the surrounding medium increases, the life of the drop also increases in the same manner.

### *Discussion.*

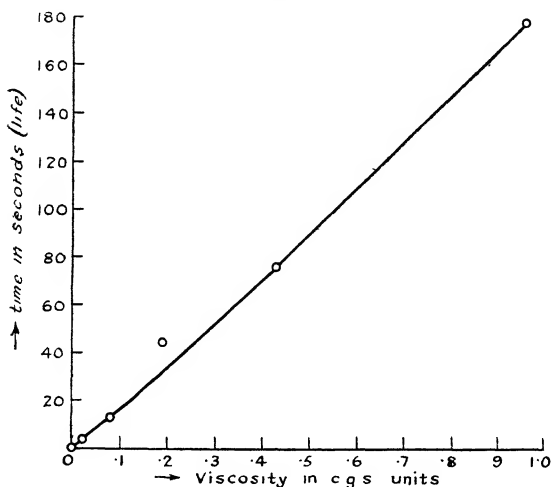
Under ordinary circumstances, at the room-temperature neither water nor olive-oil is able to form good drops; but when the medium surrounding the drops is changed to some more viscous substance the life of the drop is greatly increased. Then the drop becomes very stable. The stability increases as the viscosity of the surrounding medium increases. This fact is quite evident from the experimental results tabulated above and the curve shown in fig. 3. Hence the more viscous the surrounding medium the stabler the drops are and the longer the life they have. The density and the surface-tension of the surrounding medium have no effect on the life of the floating drops.

### 386 *Effect of Surrounding Medium on Life of Floating Drops.*

This shows that the effect of the surrounding medium is caused by the cushions of the surrounding medium formed in between the drop and the free liquid surface. The more viscous the surrounding medium, the stronger the layer which tends to prevent the drop from combining or mixing with the free liquid surface.

The above theory is supported by another important fact, namely, that it is very difficult to get water-drops floating on the water surface if the surrounding air (surrounding medium) is disturbed, for this tends to remove the cushion away from beneath the water-drop floating on the water surface. Moreover, it is also observed in this case that the

Fig. 3.



surrounding air (surrounding medium) should be free from dust particles. The second condition is fulfilled if the water be splashed continuously for about twenty minutes before the actual experiment is performed.

#### *Conclusion.*

Further experiments are being performed to find out the actual mathematical relation between the life of a floating drop and its properties, which the author hopes to give in a future paper.

Physics Laboratory,  
Mohindra College, Patiala.  
March 31, 1930.

XXXVII. *The Space Distribution of X-Ray Photoelectrons from a Solid Film.* By LEWIS SIMONS, D.Sc., Reader in Physics, Birkbeck College (University of London) \*.

IN a recent work Auger and Perrin † have investigated the hypothesis that the probability of photoelectric ejection at an angle  $\xi$  to the electric vector of a plane polarized wave is proportional to  $\cos^2 \xi$ . Wentzel ‡ has deduced this result from the view point of wave mechanics. It has been verified in the case of the emission of photoelectrons from gases by Auger §. At the outset it must be stated, however, that the phenomenon is complicated by the asymmetry produced in what would otherwise be a longitudinally symmetrical distribution by considerations such as the transfer of momentum from the incident quantum to the photoelectron and the interaction of the magnetic force in the wave-front upon it ||. These effects will be small in comparison with the major one, and their influence on the lateral asymmetry required by the "cosine squared" law for a plane polarized wave will be correspondingly small.

The angular distribution of photoelectrons from solids has been investigated by Watson ¶. In this case magnetic spectra were obtained of the photoelectrons ejected at various angles to the wave-front of homogeneous X-rays incident upon metal foils. The photographic records show that the maximum velocity of ejection of the photoelectrons is the same in all directions. This is an important conclusion from the point of view of the validity of Einstein's photoelectric equation, also as in the case of gases the emitted particles preponderate in a direction a little forward of that given by the probability law. Watson makes this direction about  $80^\circ$  to the forward direction of the beam. In a more recent paper Watson and Van der Akker \*\* have gone farther in demonstrating photographically the way in which the numbers of K, L, M, etc. photoelectrons fall off with respect to one another with increasing obliquity of the unpolarized beam upon the radiator. The general nature

\* Communicated by the Author.

† P. Auger and P. Perrin, *C. R.* clxxx. p. 1742 (1925); *Jour. de Physique*, viii. 2, p. 93 (1927).

‡ G. Wentzel, *Zeit. f. Physik*, xl. p. 574 (1926). Cf. Beck, *loc. cit.* xli. p. 443 (1927).

§ Auger, *Jour. de Physique*, ix. 7, p. 225 (1928).

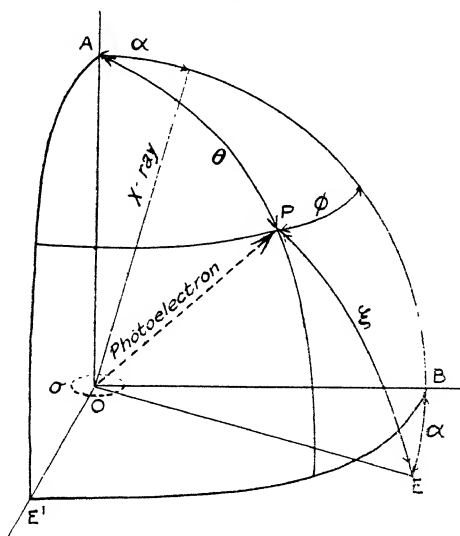
|| Carrelli, 'Nature,' June 1st, 1929, p. 836.

¶ E. C. Watson, *Phys. Rev.* xxx. p. 479 (1927).

\*\* *Proc. Roy. Soc. A*, cxxvi. p. 138 (1929).

of their results will be referred to later. The probability law, however, could hardly be investigated by Watson's method. In passing it should be noticed that this probability law, together with Einstein's photoelectric law, would require, not only that the maximum velocity of ejection should be independent of direction, but also that all unscattered photoelectrons of minor velocities should have the same spatial distribution as the most rapid ones. In the work described below the method of the retarding electric field has been used. The angle of incidence of X-rays upon

Fig. 1.



a thin gold film has been varied and the photoelectric currents measured in the ordinary manner. The author believes that he has succeeded in verifying the probability law, and other interesting results have been obtained.

In fig. 1 let us suppose that the fixed surface  $\sigma$  at  $O$  emits electrons in all directions, under the influence of a plane polarized ray making an angle  $\alpha$  to  $OA$ , the normal to  $\sigma$ , and lying in the plane  $AOB$ . Let  $OE$  represent the direction of the electric vector in the wave-front. The direction of ejection of the electron  $OP$  makes an angle  $\xi$  with the direction of the electric vector in the light producing it. The angles  $\theta$  and  $\phi$  define the direction of  $OP$ .

Regard the problem as of the same type as for gas molecules flying through a surface element  $\sigma$ . The electrons moving in the direction OP with a velocity  $v$  would fill a cylinder of base  $\sigma$  and height  $v \cos \theta$  in 1 sec. Similarly, all the electrons of any velocity moving in the direction OP would in 1 sec. fill a similar cylinder of height  $\cos \theta \Sigma v$ . Confining our attention, however, to electrons of one velocity, we may say that the number passing per sec. through a small aperture  $d\omega$  of which OP is axis is proportional to  $\cos \theta d\omega$  or to

$$\sin \theta \cos \theta d\theta d\phi. \quad . \quad . \quad . \quad . \quad . \quad (i.)$$

Supposing, now, there is an added probability which is independent of other factors and of the velocity, viz. the probability of ejection in the direction OP is proportional to  $\cos^2 \xi$ , then the number of electrons passing through the aperture will now be proportional to  $\sin \theta \cos \theta \cos^2 \xi d\theta d\phi$ . Now, in the spherical triangle APE,

$$\cos \xi = -\sin \alpha \cos \theta + \cos \alpha \sin \theta \cos \phi; \quad \text{. . . (ii.)}$$

hence P, the number of electrons passing per second through a given conical aperture with OA as axis and of semi-vertical angle  $\bar{\theta}$ , which we may call the gathering angle, will be given by

$$P_{\bar{\theta}} \propto \int_0^{\bar{\theta}} \int_0^{2\pi} \sin \theta \cos \theta (-\sin \alpha \cos \theta + \cos \alpha \sin \theta \cos \phi)^2 d\theta d\phi. \quad \text{--- (iii.)}$$

If  $\alpha=0$ , then  $P_{d\theta}$ , the probability of photoelectron emission between angles  $\theta$  and  $\theta+d\theta$  to the ray, will be given by the usual expression

$$P_{d\theta} \propto \sin^2 \theta \cos \theta d\theta, \quad . \quad . \quad . \quad . \quad (iv.)$$

whilst generally

$$P_{\bar{\theta}} \propto \sin^4 \bar{\theta} (1 + \sin^2 \alpha) + 4 \sin^2 \alpha \sin^2 \bar{\theta} \cos^2 \bar{\theta}$$

when we are dealing with emission within a cone of semi-vertical angle  $\bar{\theta}$ , the ray making an angle  $\alpha$  to the axis of the cone.

The following cases are important to this work, viz. :

if  $\bar{\theta} = 0$ , then  $P_{\bar{\theta}} = 0$ ,

$$,, \bar{\theta} = \frac{\pi}{2}, ,, P_{\pi/2} \propto (1 + \sin^2 \alpha).$$

In this latter case we are dealing with the emission of electrons from the element  $\sigma$ , lying in the diametral plane

of a hemisphere, to the hemispherical space around it, the ray being inclined at an angle  $\alpha$  to the axis of symmetry of the hemisphere. Twice as many particles would emerge when the ray is glancing along the surface ( $\alpha = \frac{\pi}{2}$ ) as when the ray is normal to  $\sigma$  ( $\alpha = 0$ ). There has not been introduced any question as to the absorption of the particles in the material from which they emerge, nor of any momentum and energy interchange between the effective quantum and the electron.

Conditions of the experimental work must now be considered briefly in order to show that the above limiting values of  $\theta$  are valid, as otherwise it would be necessary to consider a much fuller analysis of a difficult mathematical problem which would involve an exact knowledge of the distribution amongst velocities of the particles and the relation between the retarding potential and the effective semivertical angle  $\bar{\theta}$ \*.

It has already been shown by the writer that the surface of a thin metallic film irradiated by X-rays is the source of two distinct groups of electrons†. The more rapid group consists of the primary photoelectrons, whilst the well-marked slower and more copious stream is probably produced by some secondary action. A Maxwell distribution in speeds exists amongst members of the slower group, for which the most probable speed was determined to be of the order 3 electron volts. The character of the curve was independent of the wave-length of the incident X-rays and of the metal emitting. When a retarding potential below -15 volts or an accelerating potential above +15 volts was applied to the film little, if any, changes in current could be observed. A typical curve representing current leaving the film against applied potential is shown in fig. 2. The fast group was named  $\beta$  and the slower group  $\delta$ -rays. In interpreting the curve it was assumed that the maximum ordinate gave a measure of the number of electrons of both types leaving the film per sec. and the smallest ordinate the number of the  $\beta$  type. Rudberg has recently extended these observations in the soft X-ray region and justified the writer's conclusions‡, his soft X-rays being about 100 times the wave-length of those employed in the above research. The fact that

\* Cf. O. W. Richardson's thermionic problem; for a summary see Lorentz, 'Lectures on Theoretical Physics, I,' p. 171 (1927).

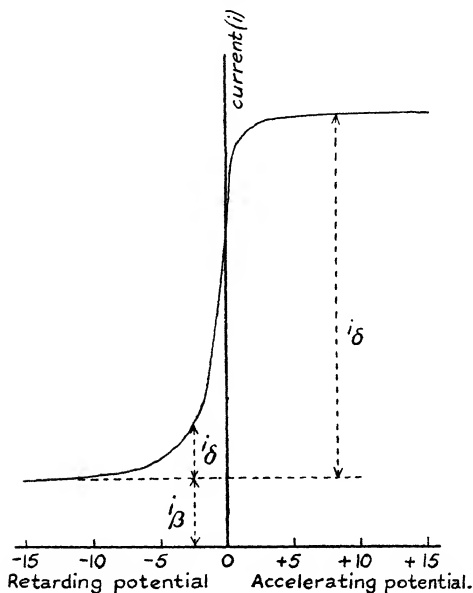
† Phil. Mag. xlv. p. 473 (1924).

‡ E. Rudberg, Proc. Roy. Soc. A, cxx. p. 385 (1928).

Rudberg was able to bake out a fair part of the  $\delta$  current in some cases, and also that Farnsworth\* has stated that the whole of the  $\delta$  current is due to surface gas films, does not invalidate any conclusions concerning the directional relationships between the incident X-rays and the photoelectrons, whatever be the source of the latter.

In the light of the above, consider now the experimental arrangements adopted in this work. Let the small circular element of the film  $\sigma$  emitting electrons be mounted at the

Fig. 2.



centre of an extended conducting plane near to, and parallel to which is another conducting plane. An accelerating or retarding potential can be applied between the two. Assuming that a retarding potential of  $-15$  volts has an insignificant influence upon the  $\beta$ -rays, but completely returns all the  $\delta$ -rays to the plane from which they emerge, then the effective angle  $\bar{\theta}_\beta$  of the conical aperture from which the  $\beta$ -rays pass from  $\sigma$  to the opposite extended plane remains practically  $\pi/2$ , whilst  $\bar{\theta}_\delta$ , the corresponding angle for the  $\delta$ -rays, is zero, as none get across. As the angle of incidence

\* Phys. Rev. xxxi. p. 413 (1928).



$\alpha$  of the X-rays on the surface  $\sigma$  is now varied, we have :—  
Retarding potential of 15 volts : all  $\delta$ -rays stopped, no influence on  $\beta$  rays :

$$\begin{aligned}\bar{\theta}_\delta &= 0; & I_\delta &= 0; \\ \bar{\theta}_\beta &= \pi/2; & I_\beta &\propto (1 + \sin^2 \alpha).\end{aligned}$$

Again, if the potential difference between the plates is zero, both the  $\beta$ - and the  $\delta$ -particles will be unaffected. Assuming tentatively that the  $\delta$  particles have the same fundamental distribution as the  $\beta$ -particles, then for this case we have :—  
No potential difference between the plates : no influence on either  $\delta$  or  $\beta$  rays :

$$\begin{aligned}\bar{\theta}_\delta &= \pi/2; & I_\delta &\propto (1 + \sin^2 \alpha); \\ \bar{\theta}_\beta &= \pi/2; & I_\beta &\propto (1 + \sin^2 \alpha);\end{aligned}$$

providing such curves are drawn for various settings of  $\alpha$ . This would show that for a given setting of  $\alpha$  it is legitimate to subtract the *total* ionization current when the potential difference between the plates is zero from that when it is 15 volts retarding (say). The result is a measure of the  $\delta$ -current. The constant of proportionality is the same throughout. Or otherwise the difference between maximum and minimum ordinates of curves drawn in fig. 2 gives the  $\delta$ -current, whilst the minimum ordinate gives the  $\beta$ -current. As a matter of fact, the potential difference between the plates was not zero as above, but an accelerating potential of +15 volts was applied for the maximum ordinate. Probably the effect of this is to create artificially the conditions of an infinite plane for the  $\delta$ -particles, most of which have so small a proper velocity of emission.

#### *The Polarization of the X-ray Beam.*

The above considerations are for a plane polarized beam. In experimental work the complete polarization of an X-ray beam cannot be accomplished. An ordinary X-ray beam cannot be employed in consequence of its partial polarization. Arguing from the principle of the incoherence of independent monochromatic light trains, Auger and Perrin\* have assumed that completely unpolarized monochromatic light may be regarded as two phase independent beams of equal intensity polarized at an angle of  $\pi/2$  to each other. Indeed, it is only by making such an assumption, together with the  $\cos^2 \xi$  law already quoted, that the obvious lateral symmetry of the ejected electrons about an unpolarized ray may be deduced.

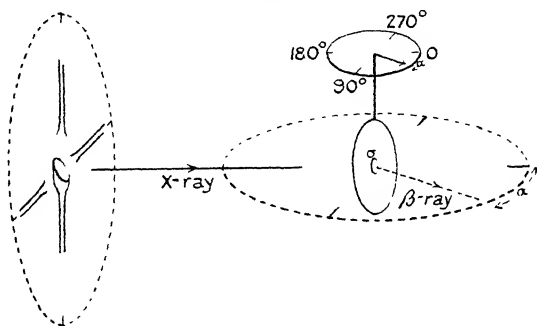
\* *Journ. de Phys.* viii. p. 93 (Feb. 1927).

The scheme adopted therefore in these experiments was to take every instrumental reading for each of four settings of the X-ray tube corresponding to four directions of the cathode ray stream separated by angles of  $\pi/2$  to each other. The mean of the four readings was taken to be the effect of a perfectly unpolarized beam.

Fig. 3 shows the schematic arrangement of apparatus. The axis of the X-ray tube could be moved in a vertical plane about the anticathode as centre. The plane of the disk emitting electrons was vertical. This could be rotated about a fixed vertical diameter, thus varying  $\alpha$  (fig. 1).

Let us now choose two arbitrary directions at right angles to each other, both lying in the plane of the wave-front. These directions, according to the above, will correspond to the directions of the equal electric vectors in the unpolarized

Fig 3.

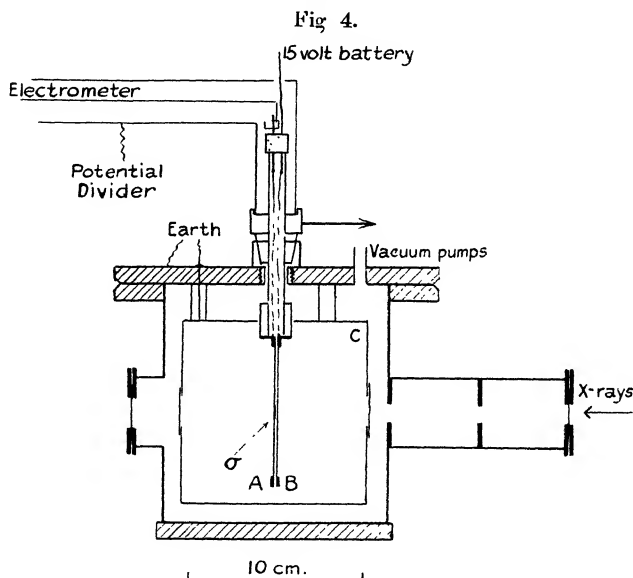


X-ray beam, the one (OE, fig. 1) lying in the plane of the paper, and the other, OE', perpendicular to it. As the ray moves through a given angle  $\alpha$  to the normal OA, the direction OE also moves through an angle  $\alpha$ , but OE' remains unaffected. When  $\alpha=0$ , i. e., when the ray is normal to the disk, one-half of the observed effects will be due to either polarity. The half due to OE' will remain unaffected for any variation of  $\alpha$ , whilst that due to OE should alter with  $\alpha$ , according to the expression given above.

#### *Description of Apparatus.*

Geometrical accuracy and the elimination of spurious X-ray effects were the chief factors governing the design of the apparatus. Fig. 4 shows a section to scale. The disk  $\sigma$  was made by sputtering gold in air on to celluloid 0.003 inch in thickness. From the large uniform piece a

small circular piece 1.2 cm. in diameter was cut by needle-point spring compasses. The colour of the film was pale blue by transmitted white light, and estimating from the mass of an ordinary gold leaf, the gold of the film was probably not more than  $10^{-6}$  cm. in thickness. A piece of silk gauze was stretched taut on the brass ring A, the mesh of the gauze being closed with a thin mixture of pure graphite and sugar solution, and when dry the disk was laid exactly on the middle of this, gold film uppermost, and a little of the conducting solution was carried just over the edge of the disk, making contact with the gold and thereby



giving a continuous conducting plane surface. At B we have an exactly similar brass ring with a piece of silk gauze stretched over it. In this case the mesh was left open, but the fibres were rendered conducting by being carefully smoked with a paraffin lamp. This gauze has a mesh of 37 per cm. and weighs  $0.033 \text{ gm. cm.}^{-2}$ . The two planes A and B were mounted accurately parallel to each other, their distance apart being about 0.15 cm. The mounting was such that when they were turned by the conical head shown, the centre point of  $\sigma$  remained stationary. Leads were carried up through a brass tube; that from A went to the Wilson electrometer, and from B to a 15-volt battery. By

means of the little lug shown at the top, any cross connexion could be made. The contact point of the electrometer was accurately central on this lug, ensuring that there would be no change in the electrostatic capacity of the system when it was rotated. A thin aluminium accurately made vessel C, smoked within and provided with conducting gauze windows, surrounded the planes A and B. This was earthed, and served the purpose of limiting the space around the working system. The X-ray beam was limited by suitable lead stops, so that the disk was only just immersed in it. Details of the X-ray tube, the null method of recording, etc., will be found in the author's paper quoted above.

#### *Heterogeneous X-ray Beam used.*

The photoelectrons were liberated from the gold by the heterogeneous beam from an ordinary Coolidge radiator pattern X-ray tube. The experiments were embarked upon primarily for the purpose of studying the mode of production of the  $\delta$ -rays. It has already been stated that the distribution curves for these were practically independent of the wave-lengths used, and as a compromise had to be made amongst many factors for securing a workable speed for taking readings, it was felt that the added complexity in using any method at this stage for securing homogeneity was unjustified. The disk  $\sigma$  had to be small, in order that the plates A and B may be regarded as infinite; B must be near to A to secure a uniform field; this increases the capacity, and as the potential difference between them was kept constant by hand during observation of the leaf system, it will be seen that long runs were impossible.

#### *Experimental Results.*

The currents below (Table I.), which are in arbitrary units and without any corrections, were taken for settings of  $\alpha$  in all four quadrants. An angle of  $45^\circ$ , for example, between the X-rays and the normal to the film was taken as physically equivalent to one of  $315^\circ$ , providing every mean reading is the result of four settings of the X-ray tube to eliminate polarization as has already been described. The  $\beta$ -currents were obtained with a retarding potential of  $-15$  volts between A and B; the  $\delta$ -currents, by subtracting the corresponding  $\beta$ -currents from those obtained with an accelerating potential of  $+15$  volts between A and B. Angles between  $65^\circ$  and  $115^\circ$  for the X-rays on the film could not be employed, as within this range the X-rays would have fallen upon the supporting brass rings.

It is not proposed, at this stage, to attempt to apply any experimental corrections to the above results, such as, for example, the increasing area of carbon immersed in the beam for increasing obliquity of the X-rays on the film giving a corresponding increase in the photoelectric current from the carbon. More serious corrections, by far, are involved by the varying absorption of the fast and slow photoelectrons in the film itself, varying degrees of scattering of these rays, and the recoiling effects. The plan has been rather to make a best fit of the results on to the three curves: (i.)  $I=A$ , corresponding to the theoretical emission due to the electric vector  $OE'$  (fig. 1), as the current due to this remains constant for variations of  $\alpha$ ; (ii.)  $I=A(1 + \sin^2 \alpha)$ ,

TABLE I.

Currents due to completely unpolarized X-rays.

Angle between normal to film and X-rays.	Mean value of $\beta$ -current.	Mean value of $\delta$ -current.	
0°	181	517	Electrons from face of emergence of X-rays.
22°·5 (337°·5)	194	544	
45° (315°)	217	579	
65° (295°)	237	615	
115° (245°)	243	671	Electrons from face of incidence of X-rays.
135° (225°)	216	625	
157°·5 (202°·5)	186	572	
180°	180	536	

corresponding to currents due to the electric vector  $OE$ , which, if Auger and Perrin's results be true, should vary in this manner, as shown above; and (iii.) any residues there may be over.

The curves drawn in the manner described are seen in fig. 5. The two upper quadrants are for the  $\delta$  or slow rays (column 3, Table I.). The lower two quadrants the  $\beta$  or fast rays (column 2 of the table). The two right-hand quadrants represent the figures for the two types of rays from the emergence side of the X-rays on the film, the two left-hand quadrants the corresponding rays from the incidence side. The angle indicated is  $\alpha$ , that between the X-rays and the





and (v.). This might easily be interpreted either as a volume and area effect respectively, or, in other words,  $\xi$  favoured and ( $\xi$  and normal) favoured respectively.

In the paper referred to above by Watson and Van der Akker the interesting conclusion is arrived at that the probability distribution laws differ for photoelectrons from various levels, and a theoretical suggestion due to Oppenheimer is mentioned that the space distribution of the K- and  $L_1$ -electrons follows the  $\cos^2 \xi$  law, whilst that of the  $L_{II}$ - and  $L_{III}$ -electrons follows the law  $a_{(v)} + b_{(v)} \cos^2 \xi$ ,  $a$  and  $b$  being constants depending on the frequency. Now, if this latter be substituted in expression (iii.), it will be seen that two independent sets of particles would arise, the first following the distribution law already quoted, viz.,

$$\propto (1 + \sin^2 \alpha);$$

the second, constant and independent of  $\alpha$  for a constant value of  $\bar{\theta}$ . In practice this would amount to an emission from a plane and from a transparent volume respectively, as already shown, and diffusion need not be introduced for interpreting the curves. One conjectures, therefore, that the plane and the volume are in some way identifiable with the atomic configurations from which the photoelectrons originate.

#### *Deductions from Curves. (Fig. 5.)*

If the method described above for drawing the curves of fig. 5 is valid, then from these and the data from which they are drawn, we deduce the following:—

The total number of  $\beta$ -electrons is approximately the same from both sides of the film.

There is greater diffusion amongst those going forward with the X-rays than amongst those travelling opposite to the X-rays producing them

All the  $\beta$ -rays coming from the "incidence" side of the film obey the theoretical considerations given above, suggested by Auger and Perrin.

It is suggested that that factor in the X-rays responsible for the production of the  $\beta$ -rays is very strongly absorbed. The majority of the  $\beta$ -rays are produced at the surface of the film upon which the X-rays are incident. This would account for the greater diffusion of those  $\beta$ -rays that emerge from that surface of the film remote from the X-ray tube. Absorption of this nature has recently been suggested by O. W. Richardson \* in dealing with the soft X-ray region.

\* Proc. Roy. Soc. A, cxix. p. 531 (1928).



An alternative suggestion to the above is that the admixture of the Compton recoiling electrons in the stream of  $\beta$ -rays moving forward in the same direction as the X-rays producing them somewhat masks the distribution given by the  $\cos^2 \xi$  law. No preponderance in number emerging from this side of the film is apparent; but even, according to the Compton theory, the number of electrons taking part in the modified scattering would be very small for a substance of such high atomic weight as gold. The same general principles seem to govern the emission of the slow  $\delta$ -particles.

A larger fraction of those moving forward with the X-rays than of those moving in the reverse direction have a uniform radial distribution.

On the other hand, we should expect a greater general diffusion of these slow particles; this is apparent even for those moving in the reverse direction to the X-rays.

If the  $\delta$ -particles are produced in a secondary manner, as many experiments suggest, the fact that such large fractions of both  $\beta$ - and  $\delta$ -rays obey the  $\cos^2 \xi$  law points to the conclusion that the electric vector operates on the electron after its expulsion from the parent atom, for otherwise it is very difficult to see why the distribution of  $\delta$ -particles should be of any other type than a uniformly radial one.

The total number of  $\delta$ -particles moving backwards exceeds the number moving forwards for all angles of incidence, *e. g.*, for normal incidence of X-rays there are 4 per cent. more moving backwards than forwards with the X-rays, which increases to 9 per cent. for the largest angle of incidence used. This observation is not without precedent, for it agrees with certain experiments of W. Seitz\*, whilst Stenberger's work on back diffusion of primary electrons† of high speed falling on metals indicates the complexity of this subject. He, too, picks out a special slow group of particles always present and independent of the speed of the primary particles producing them, and limits the group to 36 volts. In the present work this group is taken to be marked by a maximum of about 45 volts *resultant* velocity.

Arguing, then, that any secondary effects, such as diffusion, multiple ionization, etc., disturbing the ideal distribution of particles from an infinitely thin layer would, in a thicker layer, most probably tend ultimately to produce a uniform spherical distribution, these experiments have then analysed

\* *Phys. Zeit.* xxv. p. 546 (1924).

† *Ann. d. Phys.* lxxxvi. 6, p. 825 (1928).

the particle stream from a very thin film due to a polarized beam into the two portions—those that, after production, have suffered a further disturbance and those that have not. The former portion have a uniform radial distribution; the latter portion are distributed as to their number according to the law which is both classical and modern. Einstein's law and most theories of atomic structure require that the photo-electric velocities shall not be influenced by direction of emission.

We conclude, then, that the number of particles moving in a given direction times their average energy measures the square of the resolved part in that direction of the amplitude of the electric vector of the ray, or, as stated by Auger and Perrin, the probability of ejection of a particle in a given direction is proportional to the square of the cosine of the angle between this direction and that of the electric vector in the light producing it.

---

XXXVIII. *On the Capture of Electrons by Swift  $\alpha$ -particles.*  
By J. C. JACOBSEN \*.

IT was found by Henderson† that  $\alpha$ -particles, when passing through different substances, changed their charge by capture and loss of electrons. The matter was examined in more detail by Rutherford‡. A beam of  $\alpha$ -particles was sent through a screen of mica into an evacuated chamber, and the charge of the  $\alpha$ -particles measured by deflexion in a magnetic field. On a zinc-sulphide screen, which was placed at the other end of the chamber, two beams were observed—the main beam, which is due to  $\alpha$ -particles which have left the mica-leaf with a double charge, and the midway beam, due to  $\alpha$ -particles which have captured an electron. At low velocities neutral  $\alpha$ -particles were also observed. It was further found that an  $\alpha$ -particle in passing through a substance changes its charge so rapidly that, for a given velocity of the  $\alpha$ -particle, a state of equilibrium is established between the number of double-charged and single-charged  $\alpha$ -particles. When this is the case, a mean free path  $\lambda_2$  and  $\lambda_1$  may be introduced for double-charged and single-charged  $\alpha$ -particles respectively. When  $N_2$  and

\* Communicated by Prof. N. Bohr, Ph.D.

† Proc. Roy. Soc. cii. p. 496 (1923).

‡ Phil. Mag. xlvii. p. 277 (1924).

$N_1$  are the number of double-charged and single-charged  $\alpha$ -particles, it can be easily shown that

$$\frac{N_1}{\lambda_1} = \frac{N_2}{\lambda_2}.$$

A determination of  $\lambda_1$  in a gas can be carried out by measuring the decrease in  $N_1$  when the deflexion-chamber is filled with the gas to a suitable pressure. If  $\lambda_1$  is the mean free path referred to atmospheric pressure, the number  $N_p$  of single-charged  $\alpha$ -particles is given by

$$N_p = N_1 e^{-\frac{pl}{76\lambda_1}} \quad (p \text{ in cm.}), \quad . \quad . \quad . \quad (1)$$

where  $l$  may be called the effective length of the deflexion-chamber. On account of the finite width of the beam this is somewhat smaller than the geometrical length. For  $\alpha$ -particles with a velocity  $0.94 v_0$  the result was  $\lambda_1 = 0.011$  mm. in air. It was further found that for a given velocity of the  $\alpha$ -particles the ratio  $N_2:N_1$  was nearly the same for the substances celluloid, mica, and silver. This could be shown by interposing a thin sheet of the substance to be examined on the inner side of the mica-leaf; when the sheet is sufficiently thin the velocity of the  $\alpha$ -particles is not changed, while, on the other hand, the thickness is sufficient to set up a new equilibrium state between single- and double-charged  $\alpha$ -particles. These results showed a remarkable similarity between the ratio of the probabilities for capture and loss in elements of widely differing atomic numbers. From general considerations, however, we are led to expect that for elements of very small atomic number this ratio is decidedly smaller than in heavier substances\*. Indeed, from simple mechanical considerations it follows that for small nuclear charges the chance of collisions leading to capture—which claim the interaction of at least three particles—is exceedingly small compared with the chances for capture in atoms, where the presence of the nucleus has a considerable influence on the result of a collision between the  $\alpha$ -particle and the electron. The problem has been treated in detail by Thomas†, from whose calculations it follows that for swift  $\alpha$ -particles the probability of capture in hydrogen would be about  $10^4$  times smaller than in air.

The main object of the present investigation was to examine the capture of electrons in hydrogen. Experiments were made with air also, because the interpretation of

\* Cf. Bohr, *Zs. f. Phys.* xxxiv. p. 142 (1925).

† Thomas, *Proc. Roy. Soc.* cxiv. p. 561 (1927).

the results with hydrogen must be carried out by comparison with a gas. The apparatus was similar to that employed by Rutherford. The  $\alpha$ -particles entered the deflexion-chamber through a mica window. The slit which defined the beam of  $\alpha$ -particles had a width of 0.41 mm. The scintillations were counted with a Watson "holoscopic" objective together with a low-power eyepiece; a rectangular aperture in the eyepiece limited the field of view to a width of 2.2 mm. Close to the aperture in the eyepiece rotating sector disks could be placed, which cut down the number of scintillations in the ratio 1:2, 1:4, and 1:8. The pole-pieces of the magnet were circular, with a diameter of 146 mm., the deflexion of the main beam of  $\alpha$ -particles was 18 mm. In a few experiments photographic counting of the  $\alpha$ -particles was employed. The velocity of the  $\alpha$ -particles in the experiments here referred to was 0.89 of the initial velocity of the  $\alpha$ -particles from RaC'. The active sources were platinum wires with radium active deposit. The technique used in photographic counting is given in a subsequent paper\*.

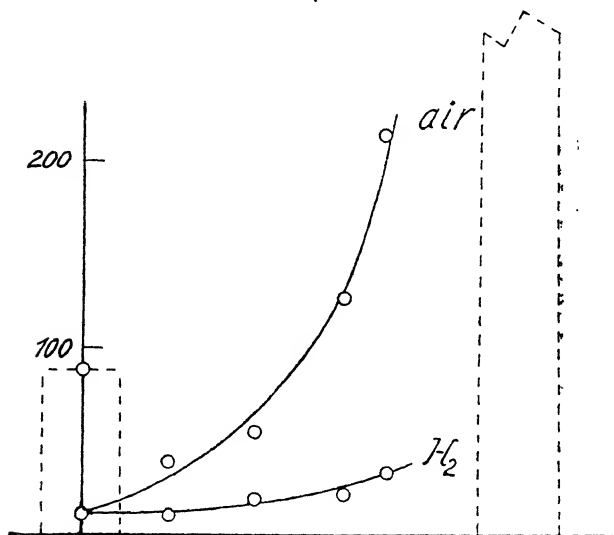
It can be demonstrated quite simply that the probability of capture in hydrogen is several times smaller than that in air. Suppose that with vacuum in the apparatus singly charged and doubly charged  $\alpha$ -particles are present in numbers  $N_1$  and  $N_2$ . When gas is admitted at a suitable pressure  $N_1$ , and when capture takes place also  $N_2$ , will decrease. At the same time a continuous distribution of scintillations appears between the main beam and the midway beam, because when an  $\alpha$ -particle changes its charge on its way through the apparatus the deflexion for an  $\alpha$ -particle originally single charged becomes larger, and that for one originally doubly charged becomes smaller. Roughly speaking the processes  $\text{He}^{++} \rightarrow \text{He}^+$  and  $\text{He}^+ \rightarrow \text{He}^{++}$  contribute by the same amount to the continuous distribution when the relation  $N_1 : N_2 = \lambda_1 : \lambda_2$  is fulfilled, so that the number of scintillations in the continuous distribution must be smaller in hydrogen than in air, if capture does not take place in hydrogen. If the pressure of hydrogen and of air is so adjusted that  $N_1$  has decreased in the same ratio in the two gases, the number to be expected in hydrogen will be about half of that in air.

This was found to be the case. The result of an experiment is shown in fig. 1, where the position and strength of the midway beam are indicated by dotted lines on the left side, while the dotted lines on the right indicate the position of the main beam. With vacuum in the apparatus

\* See p. 413.

$N_1 : N_2$  was about 1 : 150. The pressure of air and hydrogen was chosen such that  $N_1$  had decreased in the same ratio (about 1 : 10). The necessary pressure was determined previously. It is seen that with air the number of scintillations in the continuous distribution is from 2 to 3 times higher than with hydrogen. This means that the contribution to the continuous background from capture is much smaller in hydrogen than in air, since the contribution due to loss is the same in the two gases. A preliminary account of this result has been given previously\*.

Fig. 1.



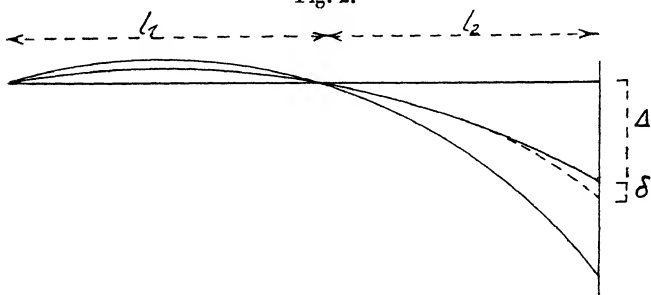
This experiment shows, in a qualitative way, that the probability of capture is several times smaller in hydrogen than in air. After this had been found, an attempt was made to obtain quantitative information by a calculation of the number of  $\alpha$ -particles in the continuous distribution as a function of the pressure; it was hoped to get in this way an upper limit for the probability of capture in hydrogen. It was soon found that agreement between calculation and experiment could only be expected when the countings were carried out on the midway beam or close to it. This is due to the fact that with vacuum in the apparatus a "background" is already present between the main and the

\* 'Nature,' June 19 (1926).

midway beam. The origin of this is not clear; it disappears when the magnetic field is cut off, so it must be due to an inhomogeneity in the velocity of the  $\alpha$ -particles, originating in some way from the source itself or from the passage through the mica-leaf. With a field of view of width 2.2 mm., which was employed throughout, the number of scintillations in the background was generally about 10 per cent. of  $N_1$ . When a gas is admitted into the apparatus the background will change in a manner which is difficult to estimate, especially close to the main beam; only in the close vicinity of the midway beam can a correction be carried out with some accuracy.

The method which was finally adopted consisted in determining the change in the number of scintillations with increasing pressure, first with the microscope focussed on the midway beam, then with the microscope moved 2.2 mm.

Fig. 2.



(width of the field of view) towards the main beam. The two positions will be denoted by I. and II. in the following pages.

The apparatus is shown schematically on fig. 2. It is assumed that the path of an  $\alpha$ -particle which moves without changing its charge is circular throughout its whole length. When  $R$  is the radius of the circle, the deflexion is given by

$$\Delta = \frac{l_2(l_1 + l_2)}{\sqrt{4R^2 - (l_1 + l_2)^2} - l_2^2}.$$

Suppose now that a singly charged  $\alpha$ -particle loses its electron at a distance  $x$  from the ZnS screen, so that it moves through a distance  $l_1 + l_2 - x$  with a single charge and a distance  $x$  with a double charge. The change  $\delta$  in the deflexion of the  $\alpha$ -particle can be calculated as the distance between two circles with radii  $R$  and  $\frac{1}{2}R$  (fig. 3).



If capture takes place there is added a number  $n_2$  of  $\alpha$ -particles which have captured an electron at distances from the mica-leaf such that they come inside the field of view. If  $y_1$  is the value of  $y$  in (3) which corresponds to  $\delta=1.1$  mm., the probability that an  $\alpha$ -particle, which has left the mica-leaf with a double charge, comes inside the field of view is the product of (1) the probability  $\frac{y_1}{\lambda_2}$  that the  $\alpha$ -particle captures an electron between  $y=0$  and  $y=y_1$ ; (2) the probability that such an  $\alpha$ -particle reaches the ZnS screen without losing its electron; this is given approximately by

$$\frac{1}{2} \left( e^{-\frac{l-x_1}{\lambda_1}} + e^{-\frac{l-y_1}{\lambda_1}} \right).$$

For  $n_2$  we thus get

$$n_2 = N_2 \cdot \frac{y_1}{\lambda_2} \cdot \frac{1}{2} \left( e^{-\frac{l-x_1}{\lambda_1}} + e^{-\frac{l-y_1}{\lambda_1}} \right).$$

The number of  $\alpha$ -particles which come into the field of view is thus, without capture

$$n_1 = N_1 e^{-\frac{l-x_1}{\lambda_1}}, \quad . \quad . \quad . \quad . \quad . \quad (4)$$

with capture

$$n_1 + n_2 = N_1 e^{-\frac{l-x_1}{\lambda_1}} \left\{ 1 + \frac{y_1}{L} \cdot \frac{1}{2} \left( 1 + \frac{y_1 - x_1}{\lambda_1} \right) \right\}, \quad (5)$$

where

$$L = \frac{N_1}{N_2} \lambda_2.$$

If, now, we put  $\lambda = \bar{\lambda} \cdot \frac{76}{p}$ , the number of  $\alpha$ -particles is obtained as a function of the pressure. The values for the constants used in the final experiments were  $\Delta=8.6$  mm.,  $l_1=9.2$  cm.,  $l_2=7.0$  cm.,  $2R=133$  cm.

In fig. 4 are shown the results of the measurements in hydrogen and air. The abscissa is the pressure in cm. Hg, the ordinate  $\log_e$  of the number of scintillations. Different experiments are brought to the same scale by putting  $N_1=100$ . It appears that within the experimental error the number of single-charged  $\alpha$ -particles decreases exponentially with increasing pressure.

For hydrogen the value of  $\bar{\lambda}_1$  ( $\lambda_1$  referred to atmospheric pressure) is determined from (4). The result is

$$\bar{\lambda}_1 = 6.8 \cdot 10^{-3} \text{ cm. (760 mm., } 25^\circ \text{ C.)}.$$

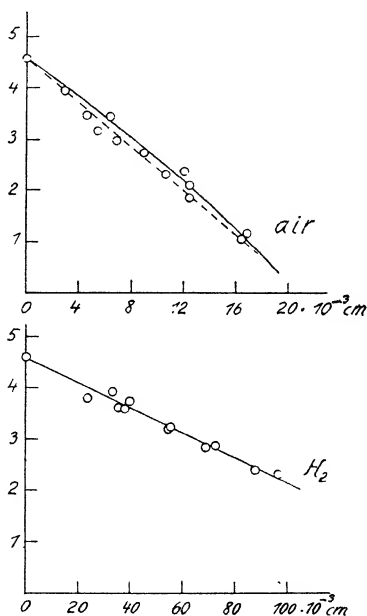


For air we use (5). This formula contains two variables, namely,  $\lambda_1$  and  $L$ . If it is assumed—and this will be tested later—that  $N_1 : N_2 = \lambda_1 : \lambda_2$ , then  $L = \lambda_1$  and  $\bar{\lambda}_1$  can be found by trial. The formula fits the measurements for

$$\bar{\lambda}_1 = 0.60 \cdot 10^{-3} \text{ cm. (760 mm., } 25^\circ \text{ C.)}$$

The curve given by (5), which is shown as a full line on fig. 3, is slightly concave. The deviation from a straight

Fig. 4.



line (dotted curve) is, however, small compared with the experimental errors, so that the experiments are equally well represented by the simple exponential formula (4). If this formula is used, the result is

$$\bar{\lambda}_1 = 0.75 \cdot 10^{-3} \text{ cm.}$$

It appears from the analysis given here that in determinations of the mean free path for loss a correction is required if capture takes place. In the case here considered the correction amounts to 20 per cent.

It is unsatisfactory, however, that this correction cannot be derived from the experiments, but appears only as the result of a calculation; and further, that the assumption  $N_1 : N_2 = \lambda_1 : \lambda_2$  which was made for air has not been tested. The deviation from a simple exponential curve, which is indicated by (5), is so small that it cannot be utilized. The experiments were therefore continued with the microscope in position II. As before, the number of scintillations was determined as a function of the pressure in hydrogen and in air.

The results showed a difference between hydrogen and air which was well beyond the experimental error, and which afforded a test of the validity of the assumption  $N_1 : N_2 = \lambda_1 : \lambda_2$  for air.

The calculation of the number of  $\alpha$ -particles to be expected can be carried out as follows:—As mentioned above, position II. was obtained by moving the microscope 2.2 mm. (width of field of view) from the midway beam towards the main beam. When a singly charged  $\alpha$ -particle changes its charge at a distance  $x$  from the ZnS-screen, put

$$\begin{aligned} x &= x_1 \text{ corresponding to } \delta = 1.1 \text{ mm.} \\ x &= x_2 \quad \quad \quad \text{,,} \quad \quad \quad \delta = 2.2 \quad \text{,,} \\ x &= x_3 \quad \quad \quad \text{,,} \quad \quad \quad \delta = 3.3 \quad \text{,,} \end{aligned}$$

When a doubly charged  $\alpha$ -particle changes its charge at a distance  $y$  from the mica leaf, put

$$\begin{aligned} y &= y_1 \text{ corresponding to } \delta = 1.1 \text{ mm.} \\ y &= y_2 \quad \quad \quad \text{,,} \quad \quad \quad \delta = 2.2 \quad \text{,,} \\ y &= y_3 \quad \quad \quad \text{,,} \quad \quad \quad \delta = 3.3 \quad \text{,,} \end{aligned}$$

The values of  $x$  and  $y$  are calculated from (2), (2a), (3), and (3a). The contribution from the midway beam is given by

$$n_1 = \frac{N_1}{\lambda_1} e^{-\frac{l-x_2}{\lambda_1}} (x_3 - x_1) \dots \dots \dots (6)$$

The contribution from the main beam cannot be given in finite terms, partly because some of the  $\alpha$ -particles here considered change their charge twice. The probability that a doubly charged  $\alpha$ -particle changes its charge first at a distance from the mica-leaf between  $y$  and  $y+dy$  and next at a distance from the ZnS screen between  $x+dx$  and  $x$ , is given by

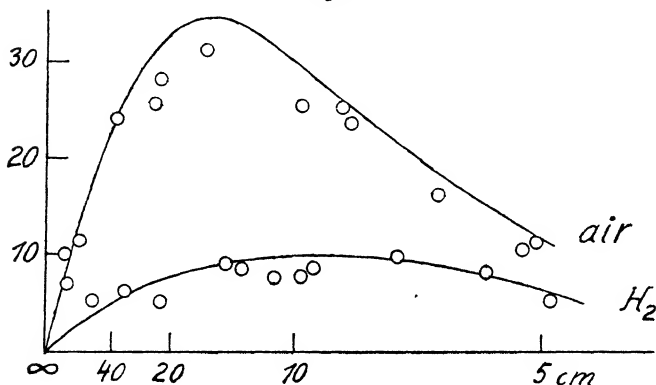
$$\frac{dy}{\lambda_2} e^{-\frac{l-y-x}{\lambda_1}} \frac{dx}{\lambda_1}; \dots \dots \dots (7)$$

$y$  may here vary from 0 to  $y_3$ ,  $x$  from 0 to  $x_3$ ; when  $y_3 \geq y > y_1$ , the factor  $\frac{dx}{\lambda_1}$  has to be omitted. The calculation was carried out by a numerical integration, the path of the  $\alpha$ -particle being divided into intervals of about 1 cm.

The results of the measurements are shown in fig. 5 for hydrogen and air. The abscissa is the actual mean free path  $\lambda_1$  given by  $\lambda_1 = \lambda \frac{76}{p}$ ; the ordinate the number of scintillations. The results from different experiments are brought to the same scale by putting  $N_1 = 100$ .

The curves drawn are those found by the calculation indicated above. For hydrogen only the contribution

Fig. 5.



from the midway beam was taken into account. The curve for hydrogen thus represents the number to be expected when no capture takes place. For  $\bar{\lambda}_1$  was used the value found previously  $\bar{\lambda}_1 = 6.8 \cdot 10^{-3}$  cm. For air was used  $\bar{\lambda}_1 = 0.60 \cdot 10^{-3}$  cm.,  $\bar{\lambda}_2 = \bar{\lambda}_1 \cdot \frac{N_2}{N_1}$ .

Considering the approximate character of the calculation, the results obtained from it fit the experiments fairly well. As already mentioned, two general assumptions were used in the calculations, namely: (1) that in hydrogen the probability of capture can be neglected for the purpose of this calculation, (2) that the equilibrium state between single- and double-charged  $\alpha$ -particles is the same for mica and for air for the same velocity of the  $\alpha$ -particles.

The agreement between calculation and experiment is sufficient to show the validity of these assumptions.

The number of  $\alpha$ -particles plotted on fig. 5 are not those actually counted. As mentioned previously, with the microscope in position II. scintillations are seen already with vacuum in the apparatus. A correction for this was carried out under the assumption that with a gas in the apparatus the "vacuum background" would change in the same ratio as the midway beam. The following figures, which are taken from an experiment with hydrogen, give an idea of the magnitude of the correction :—

$p \cdot 10^4$ cm.	I.	II.	Correction.	$n_1$
0	1.00	14.6	—	—
24	0.576	13.2	-8.4	4.8
48	0.316	12.4	-4.6	7.8
52	0.286	11.7	-4.2	7.5
105	0.080	8.1	-1.2	6.9

$p$  is the pressure. The figures under I. give the fraction of the midway beam which is left at the corresponding pressures calculated from  $\bar{\lambda}_1 = 6.8 \cdot 10^{-8}$  cm. Column II. gives the number of scintillations per minute, corresponding to  $N_1 = 100$ ; the actual value of  $N_1$  in the experiment was 700. The correction at  $p = 24 \cdot 10^{-3}$  cm. is taken to be  $0.576 \times 14.6 = 8.4$  etc. The correction turns out to be so large that the experimental accuracy is chiefly limited by it, especially at low pressures. The countings in position II. with hydrogen were carried out chiefly to get some idea of an upper limit for the probability of capture in hydrogen. From the results in fig. 5 it can be shown that  $\lambda_2$  in hydrogen must be at least ten times larger than in air when the pressure is so adjusted that  $\lambda_1$  is the same in the two gases. This limit is very far from the value for  $\lambda_2$  given by Thomas's calculation. The experimental accuracy is so small, however, that no quantitative test of the theory seems possible.

The value of  $\bar{\lambda}_1$  in hydrogen can be calculated by a simple application of the Thomson ionization theory. The experiments give the mean free path of a helium ion in an atmosphere of hydrogen. Since the probability of capture depends on the relative velocity only,  $\bar{\lambda}_1$  may be considered as the average distance between ions produced by a molecule of hydrogen, which moves through an atmosphere of helium ions. For swift  $\alpha$ -particles the electrons in the hydrogen molecule are further considered as free.

In the theory it is assumed that a collision between an atom and a swiftly-moving electrified particle results in ionization when the energy given to an electron during the collision is higher than the ionization energy. The number of ions per cm. is given by

$$A_w = \frac{2\pi e^2 E^2 N n}{m V^2} \left( \frac{1}{W} - \frac{1}{Q_0} \right),$$

where

$$Q_0 = \frac{2mM^2V^2}{(m+M)^2};$$

$E$ ,  $M$ , and  $V$  are charge, mass, and velocity for the moving particle,  $e$  and  $m$  charge and mass for the electron,  $W$  the ionization energy for the particular electron.

In the case here considered  $W = 54.5$  volts, for an electron  $Q_0 = \frac{1}{2}mV^2$ , for a hydrogen nucleus  $Q_0 = 2mV^2$ .

By introducing  $e = 4.774 \cdot 10^{-10}$ ,  $N = 2.76 \cdot 10^{19}$ ,  $n = 1$ , we obtain for an electron

$$A'_w = \frac{1.78 \cdot 10^6}{\eta} \left( \frac{1}{54.5} - \frac{1}{\eta} \right),$$

where  $\eta$  is the energy, expressed in volts, of an electron which moves with the velocity of the  $\alpha$ -particle. For a proton we obtain

$$A''_w = \frac{1.78 \cdot 10}{\eta} \left( \frac{1}{54.5} - \frac{1}{4\eta} \right).$$

The number of ions per cm. produced by two electrons and two protons is thus

$$A_w = \frac{7.12 \cdot 10^6}{\eta} \left( \frac{1}{54.5} - \frac{5}{8\eta} \right) = \frac{1}{\bar{\lambda}_1}.$$

For  $\alpha$ -particles with velocity  $0.89 \cdot 2.19 \cdot 10^9$  cm.,  $\eta$  is 825 volts, which gives

$$\bar{\lambda}_1 = 6.5 \cdot 10^{-3} \text{ cm.}$$

The experimental value for  $\bar{\lambda}_1$  is  $6.2 \cdot 10^{-3}$  cm. (76 cm.,  $0^\circ\text{C}$ ). The well-known difficulty in determinations of the number of ions produced by  $\alpha$ - and  $\beta$ -particles, that part of the ionization is of secondary origin, is not present here, where the number of primary ions is determined directly.

My thanks are due to Professor Bohr for continuous interest throughout the work.

XXXIX. *Note on Photographic Counting of  $\alpha$ -particles.*

By J. C. JACOBSEN\*.

FOR the direct counting of single  $\alpha$ -particles only the scintillation method has proved of value. The various methods which have been developed for counting by electrical means all suffer from the disadvantage that counting cannot be carried out in the presence of  $\gamma$ -radiation. A photographic method would at first sight seem promising, and a large number of investigations have been carried out on this subject. Kinoshita† found that when  $\alpha$ -particles were sent perpendicular to a photographic plate the relation between blackening and number of  $\alpha$ -particles was represented by a curve which went through the zero point. This is an important result, since it proves that the photographic effect of  $\alpha$ -particles is not cumulative. It was further found that proportionality existed between blackening and number of  $\alpha$ -particles when the blackening was small.

In spite of these results the photographic method of counting has apparently never been used for quantitative work. The method seems promising at first sight, partly because a much larger number of  $\alpha$ -particles can be counted than by the scintillation method, and partly because the result of an experiment is preserved, so that a counting can be repeated.

In the experiments which are reported here the photographic method and the scintillation method were used with the same apparatus and under nearly identical conditions. The  $\alpha$ -particles were sent through a mica-leaf into an evacuated chamber which was placed between the pole-pieces of a magnet. To the other end of the chamber either a zinc-sulphide screen or a plate-holder could be attached. The plate-holder could be moved without letting air into the apparatus, so that four exposures could be made on the same plate close to one another. For further details of these experiments the reader is referred to a foregoing paper‡.

The plates used were Hauff lantern-plates. The developer was Rodinal 1 : 40, time of development 1 minute at a temperature of 15° to 17° C. After fixation the plates were washed in distilled water and dried; a microscope cover-glass was attached with Canada balsam to protect the plate. The determination of the blackening was carried out by direct

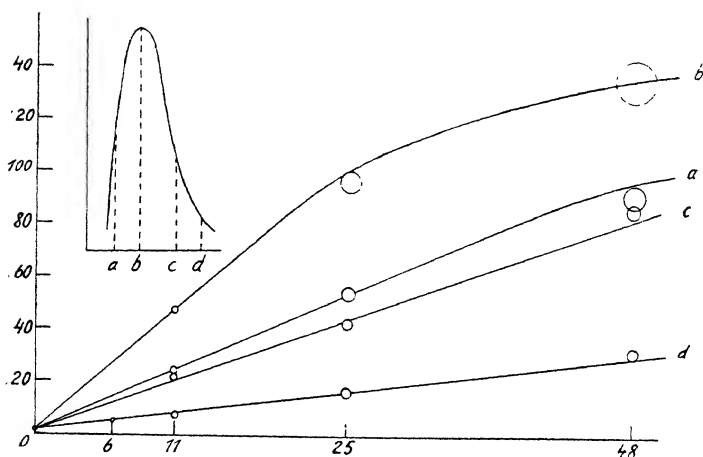
\* Communicated by Prof. N. Bohr, Ph.D.

† Proc. Roy. Soc. lxxxiii. p. 432 (1910).

‡ See p. 401.

counting of the grains. An image of the plate was thrown on a ground-glass plate with a linear magnification of about 1500; the light source was a pointolite lamp. By lead-pencil lines the ground-glass plate was divided into squares with sides of 3 cm. length; the number of squares, in which the grains were counted, varied from 2 to 40, according to the density of the plate and the accuracy which was aimed at. The fine screw of the microscope had to be moved continuously during the counting to search out the grains in different depths in the gelatine.

On the figure are shown the results of an experiment. The countings were carried out on a beam of double-charged  $\alpha$ -particles. The source was a glass tube closed by a mica-



leaf, which contained radium emanation. The geometrical width of the beam was about 2 mm. Four exposures were made on the same plate, with exposure times 6, 11, 25, and 48 minutes, with vacuum in the apparatus. The countings on this plate were carried out chiefly to test the proportionality between number of  $\alpha$ -particles and number of grains. On the figure to the left is shown the distribution of blackening inside the beam. Four points, *a*, *b*, *c*, and *d*, were selected on the beam, where the countings were carried out. Since the activity of the source may be considered as constant, the number of grains in the four exposures for each of the points *a*, *b*, *c*, and *d* should be in the ratio 6 : 11 : 25 : 48, when the number of grains is proportional to the number of  $\alpha$ -particles. On the figure the number of grains in each of the

squares of the ground-glass plate mentioned above is plotted against the time of exposure. The radius of the circle surrounding each point gives the statistical mean error, determined by the number of grains actually counted. It is seen that proportionality exists so long as the number of grains is smaller than about 80 per square; this corresponds to 200,000 grains per square millimetre. The fog on the plate was 2.0 grains per square, or 5000 per square millimetre, shown as the point where the curves meet. The range of the  $\alpha$ -particles in this experiment was about 2 cm.; it seems a reasonable assumption that the number of grains produced by one  $\alpha$ -particle cannot differ much from unity, but no attempt was made to obtain an estimate of this quantity.

From this and other similar experiments it was concluded that the photographic counting presents no real difficulties, in so far as proportionality exists between number of grains and number of  $\alpha$ -particles within certain limits. The chief difficulty is the fogging of the plates, and this in fact gives a very serious limitation to the method. The number of grains per square millimetre of the fog was generally about 5000; this means that the smallest number of  $\alpha$ -particles which can be determined with any accuracy is about 10,000 per square millimetre. In most experiments where a small fraction of the total number of  $\alpha$ -particles has to be counted this is far beyond what can be obtained with reasonable quantities of radioactive substances. The fog can be partly eliminated by treating the plate with chromic acid, but the smallest number of grains which has ever been obtained was 2000 per square millimetre.

Another serious limitation is given by the fact that the photographic effect ceases when the velocity of the  $\alpha$ -particles is below a certain limit. This point was not examined in detail, but an orientating experiment, where the velocity of the  $\alpha$ -particles was 0.3 times the velocity of the  $\alpha$ -particles from RaC, showed that the sensitivity was so small that no practical use could be made of the method. It is very unfortunate that the photographic action ceases at about the same velocity of the  $\alpha$ -particles as that at which the counting of scintillations begins to present serious difficulties.

With the experimental arrangement used any action of  $\beta$ -rays was eliminated, since the rays had to travel a distance of 15 cm. through a magnetic field of about 5000 gauss before reaching the plate. The photographic action of  $\gamma$ -rays seems to be exceedingly small; with a  $\gamma$ -ray activity of 150 millicurie-hours at a distance of 15 cm. no increase of the fog could be detected.



In the experiments here mentioned the  $\alpha$ -particles were sent perpendicular to the plate. In another series of experiments grazing incidence was used. In this way tracks are obtained consisting of a number of grains; it was hoped in this way to obtain a distinction between grains produced by  $\alpha$ -particles and grains belonging to the fog. It was soon found that such a distinction cannot be carried out with any certainty. The reason for this is that the number of grains in each track varies very much; tracks containing 10 grains were frequently observed, but, judging from the fog of the plate, tracks containing only one grain were present at the same time in a considerable number.

### *Summary.*

The conditions necessary to carry out photographic counting of  $\alpha$ -particles have been investigated.

Quantitative work is possible with swift  $\alpha$ -particles when the number lies between 10,000 and 200,000 per square millimetre of the plate.

## *XL. The Visibility of Radiation and Dark Adaptation. By R. A. HOUSTOUN, D.Sc., Lecturer on Physical Optics in the University of Glasgow\*.*

§ 1. **T**HE relative visibility of the different colours of the spectrum at high intensities has been measured with very great care in America. First of all we had the determination of H. E. Ives,<sup>†</sup> then the determinations of W. W. Coblentz and W. H. Emerson,<sup>‡</sup> of E. P. Hyde, W. E. Forsythe, and F. E. Cady §, and of K. S. Gibson and E. P. Tyndall ||. The results are in good agreement, and when graphed against the wave-length are not unlike the probability curve, though the general opinion has been that they have no connexion with the latter. I should, however, have been surprised if the distribution had been a symmetrical probability curve with respect to  $\lambda$ , for then it would have been skew with reference to  $\nu$  or  $1/\lambda$ , and there

\* Communicated by the Author.

† Phil. Mag. xxiv. p. 853 (1912).

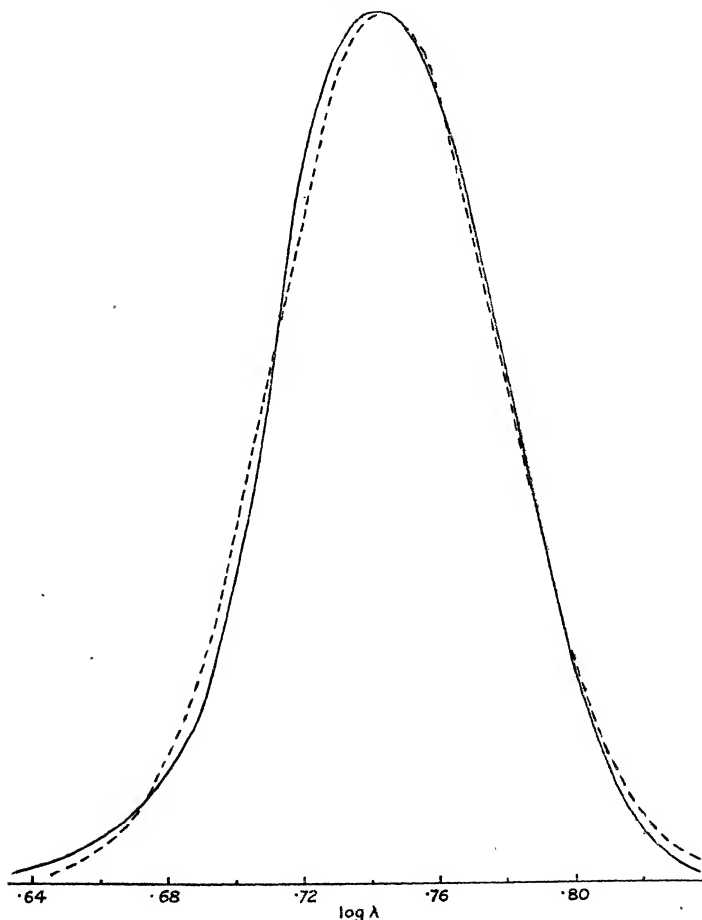
‡ Bull. Bur. Stds., xiv. p. 167 (1918).

§ Astrophys. Journ. xlviii. p. 65 (1918).

|| Bur. Stds. Sci. Papers, No. 475 (1923).

is no reason why the variation in the properties of the molecules of the photochemical substance dissociated by the light should favour the one system of measurement

Fig. 1.



rather than the other. If, however, we graph the results against  $\log \lambda$  or  $\log \nu$ , or the logarithm of any power of  $\lambda$ , the shape of the curve is always the same; it seems, then, to express only a property of the eye itself. In fig. 1 I have

graphed the values of the relative visibility recommended by Gibson and Tyndall as a result of a consideration of their own work and the work of their predecessors, taking  $\log \lambda$  as abscissa. The values are shown by the full line and the dotted curve is a probability curve fitted to them by trial and error. The fit is an extremely good one.

Hecht\* has determined the relative visibility of the colours of the spectrum for an intensity not much above the threshold of visibility, so little above the threshold that the spectrum appeared monochromatic, and he found that the curve representing the mean result for 48 observers had the same form as that represented in fig. 1, but that it was displaced  $48 \mu\mu$  towards the blue end of the spectrum. His curve is thus also a probability curve when expressed in terms of  $\log \lambda$ .

The question arises as to the shape of the curve at intermediate intensities. This has been investigated so far only by A. König†, but on account of his great experience the results are very valuable. They show that, as the intensity is increased, the shape of the curve remains approximately constant, that it moves at first slowly, then more rapidly, and finally slowly again across into the position for high intensities. There are two characteristic conditions of the eye involved, and the change takes place from the one to the other. König matched different parts of the spectrum with a constant intensity in the green, and gives his results in slit-widths. The weak part of the investigation is the measurement of the energy distribution in the spectrum of the gas-flame employed as source. This he was not in a position to do himself. He also omits to make the slit-width correction. Nutting‡ has, however, done this, and gives the results directly as visibility, making them comparable with the results of the investigators already mentioned in this paper. I have graphed Nutting's results as a function of  $\lambda$ , and determined the positions of the maximum for the different intensities. They are given in the following table:—

	S.	A.	B.	C.	D.	E.	F.	G.	H.
Log intensity .....	4.4 ?	3.4	2.6	1.8	0.4	1.0	1.6	2.2	2.8
Maximum.....	503 $\mu\mu$	505	507	508	515	535	540	542	544

\* Journ. Gen. Physiol. v. p. 1 (1922).

† 'Collected Works,' p. 144.

‡ Bull. Bur. Stds. vii. p. 238 (1911).

The letter is König's name for the intensity, and the intensity is given in terms of his arbitrary unit. This unit is the "brightness of a surface of magnesium oxide distant 1 metre from a 0.1 cm.<sup>2</sup> surface of platinum at its melting point as seen through a diaphragm of area equal to 1 sq. mm." This area of platinum should give 2.0 international candles, so the objective brightness of the surface would be 0.2 millilambert. The intensity of illumination of the retina is obtained by multiplying this result by the area of the pupil in sq. mm., and is then said to be expressed in photons, a unit introduced by Troland. König's unit of intensity should thus equal one-fifth photon. We have assumed that magnesium oxide diffuses the incident light perfectly according to the cosine law, but the correction to be applied here does not seem to have ever been determined with accuracy, and, in any case, there is reason to believe that the value given by König for his unit is very far wrong. The intensity *F* was determined both by König and a colleague, apparently by viewing two fields rapidly one after the other, and the values 36.9 and 54.9 found respectively. In order to have a round number I have adopted the value antilog 1.6.

The positions of the maxima given in the table are rough determinations. The end values 544  $\mu\mu$  and 503  $\mu\mu$  do not agree with the values of Gibson and Tyndall and of Hecht, namely, 555  $\mu\mu$  and 507  $\mu\mu$ . An agreement might be obtained by repeating Nutting's calculation in the light of the recent data and a careful study of the whole question, but this is in the meantime deferred. The change takes place principally between C and F. The equation to the dotted curve in fig. 1 is

$$e^{-\frac{(\log \lambda - \log 555)^2}{2 \times 0.034^2}}.$$

The equation to Hecht's curve is, consequently,

$$e^{-\frac{(\log \lambda - \log 507)^2}{2 \times 0.034^2}}.$$

Within the limits of experimental error König's intermediate curves can be obtained by superposing his end ones and altering the ratio of the maximum ordinates of each. What the exact ratio should be for each intensity is difficult to determine. It may be shown, by trial, that the shift of the maximum is roughly proportional to the

ratio of the maximum ordinates, *i. e.*, if the ratio is 9 to 1, the maximum shifts one-tenth of the distance from one to the other of the characteristic positions. From the preceding results we consequently obtain the following table, in which the two lower rows give the ratio of the components present in the mixture.

	S.	A.	B.	C.	D.	E.	F.	G.	H.
Log intensity .....	4.4	3.4	2.6	1.8	0.4	1.0	1.6	2.2	2.8
Low .....	1	.95	.90	.88	.71	.22	.10	.05	0
High .....	0	.05	.10	.12	.29	.78	.90	.95	1

§ 2. Let us now approach the problem from another standpoint. König and Brodhun determined the least perceptible increase of intensity  $\Delta I$  for various values of  $I$ , and expressed the results in curves giving  $\Delta I/I$ , *i. e.*,  $\Delta(\log I)$  in terms of  $\log I$ . In a recent paper\* I suggested that, instead of  $\Delta(\log I)$ , it was better to graph the reciprocal of this quantity in terms of  $\log I$ . The ordinates are then great when the sensibility of the eye to increase of intensity is great, and there is the additional advantage that we are able to attach a special meaning to the area of the curve. For let  $S$  denote the magnitude of the sensation. Then the rate of increase of sensation with  $\log I$  is given approximately by

$$\frac{dS}{d(\log I)} = \frac{k}{\Delta(\log I)},$$

where  $k$  is a constant of proportionality. Hence

$$S = \int \frac{k d(\log I)}{\Delta \log I},$$

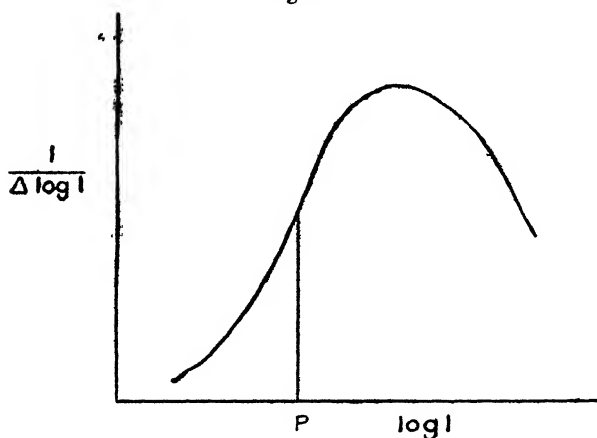
and if the area of the curve is represented in fig. 2. the sensation at  $P$  is represented by the area to the left of the ordinate. The result holds, no matter what the shape of the curve is. But the interesting feature is that the curve is a probability curve, *i. e.*, it is of the same nature as the curve we have used to represent the visibility throughout the spectrum. This was shown in the former paper by graphing the mean of König and Brodhun's data for white, for  $605 \mu\mu$ , and for  $470 \mu\mu$ .

In addition to these wave-lengths, König and Brodhun made observations at  $670 \mu\mu$ ,  $575 \mu\mu$ ,  $505 \mu\mu$ , and  $430 \mu\mu$ , and they state, with reference to their data, that both

\* Phil. Mag. viii. p. 520 (1909).

observers were in good agreement, and that the results were the same at all wave-lengths except at low intensities, when there was a divergence between the three more and the three less refrangible wave-lengths. This deviation started at 50 on the intensity scale for König and at 10 on the intensity scale for Brodhun. In view of this statement the best method of summarizing their results seems to be to take the mean of their values for all wave-lengths and graph its reciprocal. This has been done in the case of fig. 3 for König and of fig. 4 for Brodhun. The abscissæ are the logarithms of the intensity; the latter is measured on the scale already referred to. The ordinates are

Fig. 2.



$(I - \Delta I) / \Delta I$  or simply  $I / \Delta I$ , as the difference between these two expressions can be neglected except for the lowest intensity. When the results fall into two groups, the mean of each is plotted separately; in this case the greater ordinate refers to the blue end of the spectrum. In each figure a Gaussian curve has been fitted by trial and error to the data.

It was stated in my former paper that König and Brodhun did not correct their data for the variation in the aperture of the pupil. This is erroneous; the observations were made with a uniform aperture of 1 sq. mm. area, and hence required no correction. This information is not given in their paper on the subject, but in a paper written

by König\* ten years later, and has been overlooked by Hecht.

Fig. 3.

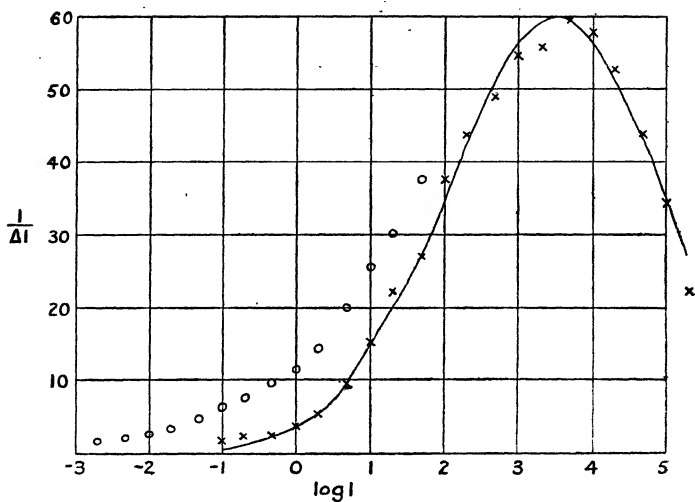
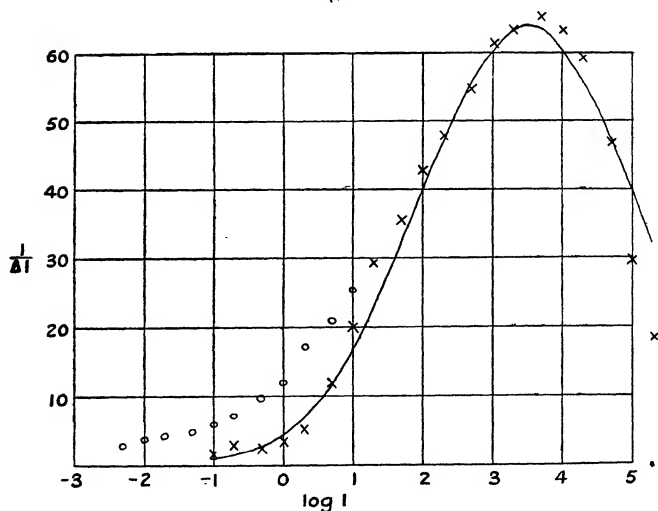


Fig. 4.



\* 'Collected Works,' p. 381.

It is obvious, from figs. 3 and 4, that the Gaussian curve fits the data for the red end of the spectrum well considering the difficulties of the observations; but there is a deviation for the blue end of the spectrum. Let us confine our attention at present to the red end. The Gaussian curve in fig. 3 is represented by

$$e^{-\frac{(\log I - 3.5)^2}{2 \times 1.45^2}}.$$

Thus in the red end of the spectrum the sensation of brightness is given by

$$\int_{-\infty}^{\log I} e^{-\frac{(\log I - 3.5)^2}{2 \times 1.45^2}} d(\log I).$$

It was suggested in the former paper that the percipient elements of the retina had different intensity thresholds, that the sensation of brightness was proportional to the number of elements active, and that the increase in sensation was due to more elements coming over the threshold as the intensity increased. Let us suppose now that each element has its own wave-length, and that the complete distribution is given by

$$e^{-\frac{(\log I - 3.5)^2}{2 \times 1.45^2}} - \frac{(\log \lambda - \log 555)^2}{2 \times 0.034^2} d(\log I) d(\log \lambda).$$

If monochromatic light of a range  $d(\log \lambda)$  is incident upon the photochemical substance, it liberates electrons of a range of velocities given by the quantum relation, and we suppose that certain only of the percipient elements are susceptible to electrons of this velocity. There is no product term in the index of the exponential, and consequently no correlation between variation with  $\log I$  and with  $\log \lambda$ ; the one change is quite independent of the other. If we adhere to the former assumption, namely, that the sensation of brightness is proportional to the number of percipient elements, both the variation with intensity in the red and the variation with wave-length at high intensities are fully explained. The question now arises as to the explanation of the Purkinje effect, *i. e.*, the shift of the maximum of the visibility curve towards the blue with decrease in intensity.

The figures on p. 420 represent only the relative values of the two components which we found necessary to represent this shift. As König used the same unit of intensity in his work on the visibility curve and on Weber's law, it is



easy to calculate the absolute value of the high-intensity component. It should simply be proportional to

$$\int_{-\infty}^{\log I} e^{-\frac{(\log I - 3.5)^2}{2 \times 1.47^2}} d(\log I).$$

This has been done in the following table:—

	C.	D.	E.	F.	G.	H.
Log I. ....	1.8	0.4	1.0	1.6	2.2	2.8
High .....	5	17	42	96	180	311
Low .....	37	42	12	11	9	0

The row marked "High" gives numbers proportional to the maximum ordinate of the high-intensity component at the different intensities in question, and the row marked "Low" numbers proportional to the maximum ordinate of the low-intensity curve, calculated by means of the former table of ratios. The result is only approximate, and values are not given for the three lowest intensities S, A, and B, as they would be worthless altogether.

Let us return now to the consideration of fig. 3. The circles are the mean of König's results for 505  $\mu\mu$ , 470  $\mu\mu$ , and 430  $\mu\mu$ . Let us say that they represent 470  $\mu\mu$ . Now at 470  $\mu\mu$  the high-intensity component has 0.091 of its maximum value and the low-intensity component about 0.67 of its maximum value. The quotient of the second of these quantities by the first is 7.4. If we multiply the low-intensity row in the preceding table by 7.4 and add it to the high-intensity row, we obtain numbers representative of the sensation at 470  $\mu\mu$  for the intensities in question, and if we differentiate the result with respect to  $\log I$  we ought to obtain the curve represented by the circles in fig. 3. As a matter of fact, the addition of the low-intensity curve brings in the necessary correction in the right direction, of the right order of magnitude, and at the right place. But that is all we can say. The want of agreement is not due, I think, to the cumulative effect of the various approximations I have made, but to the uncertainty of the observations, and to a difference in the degree of dark adaptation in the data under comparison.

In any case the deviation at low intensities in the blue in König and Brodhun's observations on Weber's law is due to the same cause as the Purkinje effect, and it must be

possible to bring it into numerical relation with the latter ; and the formulæ employed above seem to be the best way of doing this, whatever may be thought of the theoretical views which have led to the construction of the formulæ.

§ 3. It is customary to suppose that vision at high intensities is due to the cones. These form the photopic mechanism, whereas at low intensities vision is due to the rods which form the scotopic mechanism. This view is referred to as the duplicity hypothesis ; it is due to Von Kries, and finds wide, but not universal, support. The Purkinje effect is caused by the shift from the one mechanism to the other.

It seems to me an unnecessary complication to postulate a second mechanism. When we go into the dark, the rods do not begin to function at once, according to the duplicity theory. Time must be allowed for dark adaptation, a process which does not affect the cones to the same degree. The rods therefore exist in two states. Thus, to explain two conditions of the eye we assume two mechanisms, one of which has two states. It is obviously simpler to assume one mechanism with two states.

§ 4. The view has been advanced by Hecht that the photochemical substance in the retina is dissociated by exposure to light, and recombines in the dark according to the equation for a bimolecular reaction. The two states of the scotopic mechanism referred to above are consequently characterized by a difference in the quantity of photochemical substance available. Let  $a$  be the concentration of the dissociated substance at the instant  $t=0$ , when dark adaptation starts, and  $a-x$  the concentration at time  $t$ . Then

$$\frac{d}{dt}(a-x) = -k(a-x)^2,$$

whence

$$k = \frac{x}{at(a-x)}.$$

Let  $I$  denote the intensity at the visual threshold. Then Hecht assumes that in the periphery of the retina  $a-x$  is proportional to  $\log I$ , while in the fovea it is proportional to  $I-c$ , where  $c$  is a constant. A different law is necessary in the second case, because the extent of foveal dark

adaptation is so very much less; here the threshold diminishes only to about one-eighth of its initial value, whereas in the former case it diminishes to a ten-thousandth of its initial value. But there is no physical reason given for the difference in the law in the two cases; the structure of rods and cones is not so different that we would expect them to obey two radically different laws. Moreover the numerical examples which he gives, one for each case, do not appear to support his contention. If we take the figures for peripheral dark adaptation\*, and calculate the value of  $k$  as shown in the table, we do not get agreement;  $k$  rises to a maximum in the middle of the range, and then diminishes to less than half its maximum value, giving a mean of 0.0130 as against 0.0143 as stated in the paper, where the details of the calculation are not shown. If we add 0.45 to  $a-x$ ,  $k$  becomes more nearly constant, the values being, in order, 0.104, 0.119, 0.112, 0.125, 0.134, 0.108, 0.098, 0.092, 0.057; but we have no theoretical justification for doing this, and there is still the rise in the middle and the descent at the end, which gives rise to the surmise that this is the wrong type of formula altogether.

$t$ , time.	$a-x$ , log of threshold intensity.	$x$ .	$k = \frac{x}{a(a-x)}$ .
0 min. ....	4.41	0	—
2 .....	4.00	0.41	$1162 \times 10^{-5}$
5 .....	3.40	1.01	1347
8.5 .....	2.97	1.44	1293
12 .....	2.47	1.94	1485
20 .....	1.78	2.63	1676
31 .....	1.51	2.90	1405
39.5 .....	1.34	3.07	1315
45 .....	1.27	3.14	1246
72 .....	1.27	3.14	779

If we take the figures for foveal dark adaptation†, and work out the values for  $k$ , we obtain the results in the following table, which gives a mean value of  $k$  equal to 0.00222:—

\* Journ. Gen. Physiol. ii. p. 499 (1920).

† Journ. Gen. Physiol. iv. p. 113 (1921).

$t$ , time.	$I_t$ , threshold intensity corrected for pupil.	$a-x$ .	$x$ .	$k = \frac{x}{at(a-x)}$ .
0 sec.	39.8	33.3	0	—
9.3 ....	25.7	19.7	13.6	$223 \times 10^{-5}$
22.2 ....	15.8	9.8	23.5	324
52.4 ....	11.5	5.5	27.8	283
128.9 ....	9.5	3.5	29.8	198
188.9 ....	7.57	1.57	31.73	321
377.9 ....	7.28	1.28	32.02	199
618.9 ....	6.62	0.62	32.68	256
917.9 ....	6.30	0.30	33.00	360
1209.9 ....	5.50	-0.50	33.8	-168

This time there is no systematic deviation, but the values exhibit a considerable amount of irregularity, one of them being negative. Still the agreement is good, considering the difficulties of the experiment. But, taking the two cases together, it does not appear probable that dark adaptation is due to the recombination of a photochemical substance.

It is doubtful whether the equation for a bimolecular reaction applies to the molecules of the photochemical substance under the conditions in which they exist in the rods and cones. Also we obtain the same measure of agreement with the equation in the case of the opening of the pupil of the eye in the dark. This has been measured very carefully by Reeves \*, and the following table gives the mean of his results for seven observers. The first column gives time in seconds and the second the diameter of the pupil in millimetres. The eye was light-adapted; at  $t=0$  the illumination was shut off, and the numbers show the rate at which the eye opened in the dark. I have applied the same procedure as in Hecht's treatment of foveal dark adaptation, taken the difference of the diameter and a constant, namely 7.7 mm., put the result equal to  $a-x$ , and calculated

$$\frac{x}{t(a-x)},$$

which should be proportional to  $k$  for each value of  $d$ . The results are shown in the third and sixth columns.

\* Psych. Rev. xxv. p. 340 (1918).

The agreement is as good as in the other two cases, and it has never been suggested that the recombination of a photochemical substance is the cause of this change. Consequently, there is the less reason for supposing that it is the cause of dark adaptation.

$t$	$x$	$t(a-x)^{-1}$	$t$	$x$	$t(a-x)^{-1}$
0 sec.	2.8	—	9 ...	6.2	0.252
0.5 ...	3.1	0.130	15 ...	6.5	.205
1.0 ...	3.5	.167	29 ...	6.8	.153
1.5 ...	3.9	.193	60 ...	7.2	.147
3 ...	4.7	.211	180 ...	7.5	.130
5 ...	5.5	.245	300 ...	7.6	.160

§ 5. A totally different explanation is suggested by the experiments of Dreser and Wölfflin\*. They injected strychnine under the skin, and found a distinct increase of one-fourth or one-fifth in the amplitude of accommodation. The rate of adaptation appeared also to be increased. Now strychnine favours conduction between the nerve-endings. The impulse has to cross synaptic junctions in the outer and inner reticular layers of the retina on its way to the brain. Dark adaptation may consequently be due to the nerve-endings making better contact in the reticular layers.

A suggestive experiment is recorded by Adrian and Matthews† on the eye of the conger-eel. In the eels they experimented on the optic nerve is about 15 mm. long, and the retina contains both rods and cones, differing little from the mammalian retina. The number of fibres in the optic nerve is, however, considerably less, about 10,000. The eye and optic nerve were removed from the head, and the nerve placed upon two electrodes. These were connected to a capillary electrometer, the deflexions of which were magnified by a three-valve amplifier and recorded on cinematograph film. When the retina was exposed to light, the action-current in the nerve-fibres recorded itself as a series of oscillations on the film. The action-current did not start immediately the image was focussed on the retina; there was an interval, the latent period, between the starting signal and the commencement of the current.

\* Graefe's *Arch. für Ophthalm.* lxx. p. 302 (1907).

† Journ. of Physiol. lxx. p. 273 (1928).

When four disks of light, each 0.22 mm. in diameter, set at equal distances on a circle of 1 mm. diameter, were focussed on the retina, they gave a shorter latent period than when one alone was focussed. But there was no shortening when the diameter of the circle was raised to 2-3 mm. Then a strychnine solution was applied to the retina, and the latent period for the four areas when the diameter was 2-3 mm. became much shorter than for any one singly. The interaction of the different areas obviously took place in the retina, since the eye was separated from the brain, and it was greatly increased by the action of strychnine. Thus, since strychnine increases lateral conduction and dark adaptation, it is probable that the latter is due to a better forward conduction.

It is a mistake to regard the retina as a mosaic of receptors leading by independent pathways to the different fibres of the optic nerve. No doubt there is a closer connexion to one particular fibre, but the same fibre is open to the spread of excitation from other parts of the synaptic layers. The system seems to adjust itself automatically to the best way of coping with the image. If the latter is a bright one, with plenty of detail, the receptors work independently; if it is dim. they work in groups.

§ 6. The most interesting example of this automatic adjustment is Ricco's law of foveal vision. This law states that, if the image of a uniformly bright disk is thrown on the retina, and the brightness is diminished until the disk is just visible, the total quantity of light received on the image is constant, provided that the angle subtended by the disk does not exceed one or two degrees.

The table below gives observations verifying the law, as yet unpublished, obtained by Mr. James F. Shearer and myself five years ago. The first column gives the angle subtended at the eye by the radius of the object, expressed in minutes. The next column gives the quantity of light entering the pupil of the eye, in each case expressed in arbitrary units. Each result is the mean of three observations. The eye was very thoroughly dark adapted. If the law holds, this column should be constant, and it will be observed that the constancy holds up to an angle of about 6 degrees. It was found during the experiments, that a point-source was just visible, when it gave as much

light as one-tenth candle at 1 kilometre. The third column gives the degree of illumination of the retina in photons calculated on this basis. For the purpose of the calculation the area of the pupil was assumed to be 45 square millimetres.

Angle subtended by radius of disk, in minutes.	Quantity of light falling on image, in arbitrary units.	Intensity of illumina- tion, in photons.
0.175.....	2.25	174
.35 .....	3.23	43.4
.70 .....	3.91	10.9
1.40 .....	2.35	2.72
2.80 .....	3.42	0.680
5.59 .....	2.74	0.170
13.76 .....	3.81	0.0280
21.84 .....	3.08	0.0112
43.67 .....	2.47	0.0028
349.4 .....	3.19	0.000044
699 .....	11.3	—
1000 .....	30.8	—

The figures are very striking. They show that, though the area on the retina increased four million times, the quantity of light incident on it necessary to produce excitation remained substantially the same.

In making the measurements a Fullolite lamp was placed outside a small hole in the window of a light-tight room. The rays from this hole diverged on to a large ground-glass screen, the distance of which from the hole could be varied. A circular aperture was placed in front of this screen and viewed by the observer, while the screen was moved towards the aperture until the image disappeared. The observer usually sat at about a distance of 2 metres from the aperture, and the hole at the window was capable of a wide range of variation. At the point of extinction form-vision goes; the observer does not see a disk, but is conscious of a luminous something extending over an area.

§ 7. Hecht explains the Purkinje effect by assuming that both rods and cones are excited by the same photo-chemical substance, but that it is immersed in media of different refractive index in the two cases. The displacement is then to be ascribed to the operation of Kundt's law. Kundt in 1874 dissolved substances that produced absorption bands, using different solvents, and found that the position of the band varied with the

solvent. He came to the conclusion that the greater the refraction and dispersion of the solvent, the further was the band displaced towards the red, and his conclusion has persisted in the literature of the subject until this day under the name of Kundt's law, in spite of the fact that it was not borne out by subsequent investigation. The band moves as often the one way as the other, and generally there is a marked change in intensity and shape, in comparison with which the shift in position can be neglected. This has been shown in a striking manner by Georg. J. Katz \*. Hence I am dubious about the validity of the explanation, and it is not relevant unless the rods are percipient elements; but it has the merit of tackling the problem in a physical manner.

I suggest the following alternative explanation:—Let us suppose that the photochemical substance has, under standard conditions, an extremely narrow absorption band. In the eye, owing to variations in density, action of surface forces, etc., no two molecules are in the same condition. These narrow curves are, consequently, distributed about a mean according to the laws of statistics, and their resultant is shaped like a probability curve. Hence the shape of the visibility curve at high intensities.

To get the shape at low intensities, consider the quantum relation

$$h\nu = \frac{1}{2}mv^2,$$

and suppose it applicable to the case of high intensities.  $\nu$  is the frequency of the incident light, and  $v$  the velocity with which the electron impinges on the percipient element. Let us suppose that at low intensities the electron has to do a certain amount of work  $W$  to reach the same place. Then the final velocity  $v$  is caused by a different frequency  $\nu'$ , according to the equation

$$h\nu' = W + \frac{1}{2}mv^2.$$

By subtraction

$$h(\nu' - \nu) = Wh \quad \text{or} \quad \nu' - \nu = W/h,$$

that is, at the low intensity all frequencies are increased by the same amount  $W/h$ .

§ 8. When a surface is illuminated by a beam of, for example, red light, there are three kinds of unit involved in the measurement of the degree of illumination. First

\* Inaug.-diss., Erlangen (1898).



of all there is the energy per sq. cm. per sec., as it would be indicated by a thermopile. Then there is the intensity in metre-candles; this could be obtained by placing a rod in front of the surface and throwing a second shadow by means of a standard candle. The result follows, on balancing the shadows, according to the principle of the shadow photometer, although the somewhat difficult operation of heterochromatic photometry is involved. The intensity of the illumination in metre-candles determines the objective brightness of the surface. Subjective brightness, the sensation of brightness, is another matter. Equality of sensation can be determined by a photometer, but the absolute measurement of sensation cannot be effected in this way. We must fall back on the number of just perceptible increments between the degree of sensation in question and the threshold value.

In their celebrated paper on Weber's law, König and Brodhun raise the question as to whether any numerical value can be given to the sensation of brightness. Suppose we have equally bright red and blue surfaces. Then we would expect the sensation of brightness which they excite to be measured by the same number. But according to the measurements of König and Brodhun, a greater number of steps is required to reach zero sensation from the blue surface than from the red surface.

I think there is here a confusion of thought. We ought to expect agreement only if the just perceptible increments are measured by a light-adapted eye. If we consider the point P in fig. 2, the area to the left of the ordinate through P measures the sensation for the value of  $\log I$  in question. When the eye becomes dark-adapted, this area increases, and at the same time the area on the right decreases, the total area remaining constant, since the number of nerve-fibres is fixed anatomically.

In fig. 2 the quantity  $I$  is measured in photometric units. If the light is not monochromatic, and the distribution of the energy over the different wave-lengths is known,  $I$  can be calculated from a knowledge of the visibility function, but only for one state of adaptation of the eye. The diagram has a meaning only for one state of adaptation. If the latter alters, the visibility function alters, and points on the axis of abscissæ shift relatively to one another, unless the light is monochromatic or approximately monochromatic.

XLI. *Weber's Law and Visual Acuity.* By R. A. HOUSTOUN, D.Sc., and JAMES F. SHEARER, M.A., B.Sc.,  
Lecturers in the University of Glasgow \*.

§ 1. IF  $I$  is the brightness of a surface and  $\Delta I$  its least perceptible increment Dr. Houston showed recently†, from the results of König and Brodhun, that when  $I/\Delta I$  was graphed as a function of  $\log I$  it formed a Gaussian probability curve, and stated that investigations would be set on foot to test the matter further. The present paper describes some of these investigations.

König and Brodhun found that their results were independent of the wave-length of the light employed, except at low intensities, where there was a difference between the two halves of the spectrum. This has been shown in a previous paper to be due to "rod vision" coming into play. We therefore did not resolve the light spectrally, but merely passed it through filters.

As source of light we employed principally a 220-volt Pearl Osram lamp; this was used up to 250 volts. A similar 125-volt lamp was used occasionally up to 250 volts, and the brightness was regulated in each case by altering the current through the lamps. This was found preferable to using neutral filters. The candle-power of these lamps was determined in terms of an 8 C.P. lamp on a long photometer bench for a wide range of currents, using a wedge photometer with red, green, and blue filters. Observations were then made at lower currents with a special photometer, in which the surface of the lamp itself was used as one of the comparison surfaces, being compared directly with a white paper surface which could be illuminated by lamps at various distances. By this means the candle-power of the lamp could be measured through a range of from 1 to  $10^7$ .

After preliminary experiments with a half-shadow polarimeter the following different arrangements were tried:—

(1) A Wollaston prism was mounted on the prism table of a spectrometer the telescope of which was fitted with a rotating nicol eyepiece. The image then consisted of two rectangles plane polarized at right-angles to one another,

\* Communicated by the Authors.

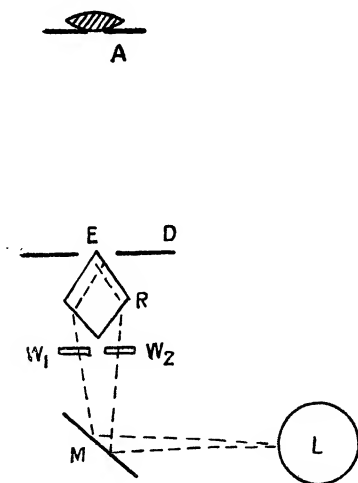
† Phil. Mag. viii. p. 520 (1929).

and the slit-width was regulated so that these rectangles touched one another sharply. Their intensities were altered by turning the nicol. This arrangement was abandoned because the magnification and definition of the eyepiece were not satisfactory.

(2) The same apparatus was used with an ordinary eyepiece, and the intensities were altered by rotating a nicol in front of the slit.

(3) An aperture A of diameter 2 mm. was fitted with a magnifying lens (fig. 1), and through it the eye of the

Fig. 1.



observer looked down at the sharp edge E of a glass rhomb R. The beams of light from the two faces of this rhomb came from the surface of the lamp L through neutral wedges  $W_1$  and  $W_2$  after reflexion by a mirror M. The angles of the prism and the distances were calculated so that the beams diverging from E came from the same part of the surface of the lamp. D is a diaphragm with a circular hole in it. Thus the eye saw a half-shadow field the intensities of which could be altered by moving the wedges. The sides of the rhomb were about 3 cm. in length, the circular hole was of 1 cm. radius, and the distance AE about 12 cm.

(4) This is the same arrangement as (2) with a plate polarizer substituted for the slit nicol. This plate polarizer consisted of two glass plates mounted in front of the telescope object-glass, with their surfaces making an angle of  $30^\circ$  with the axis of the telescope. They could be rotated about this axis by a rack-and-pinion motion. The light from the Wollaston prism was in this case only partially polarized. The plate polarizer transmitted more light and gave a better definition than a nicol. It was calibrated by means of the slit nicol.

The power of the eye to discriminate differences in intensity fluctuates considerably from time to time, and the object of using so many different arrangements was to study the conditions necessary for constant results. These are the sharpness of the dividing line, perfectly uniform illumination of the two fields, the size of the fields, and the mechanical arrangement for altering the relative intensity. With the third arrangement it was possible to alter the size of the field. The following table shows the effect of doing this :—

Angle subtended by radius . . . .	2.39°	1.55°	0.78°	0.39°	0.19°	.009°
Least perceptible increment . . . .	9.5	6.4	3.6	7.9	13.4	22

The field consisted of two semicircular disks, and the upper row shows the angle subtended by the radius of the field in degrees. The lower row gives  $\Delta I/I$  measured in per cent. for each field, the result in each case being the mean of four determinations by J.F.S. for red light at the intensity of maximum sensibility. It decreases to a minimum at  $0.78^\circ$  and increases for smaller fields. The surround was the same in each case, dark but not absolutely black.

The fourth arrangement gave the best results. With this apparatus it was possible to start with the slit slightly too narrow, focus the narrow band between the two fields very sharply, then widen the slit until it just disappeared. At some points there was then a trace of overlapping and at others a slight shadow, but there was always a section where the junction was perfect, and it was here that the observations were made.

In making the observations the apparatus was adjusted until one half of the field was the darker, and the reading taken. It was then adjusted until the other half was darker, and the reading taken again. The least perceptible increment was calculated from half the difference of these readings.

We give some results in the following tables :—

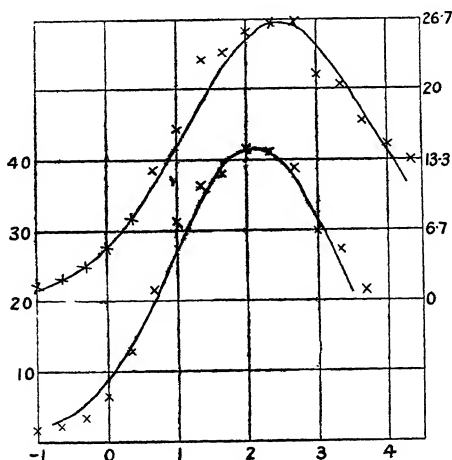
I.		II.		III.		IV. V.	
Inten- sity.	R.A.H. Red.	Inten- sity.	R.A.H. Red.	Inten- sity.	J.F.S. Red.	R.A.H. Red. Blue.	
2.86	0.59	1.1	1.7	2.33			1.54
1.36	3.42	1.5	3.0	.67			2.03
1.86	7.77	0.0	6.7	1.00	1.62	1.3	3.01
0.36	15.7	0.5	12.0	.33	2.10	2.0	4.44
0.86	22.1	1.0	13.1	.67	3.46	3.1	6.02
1.36	23.3	1.5	17.0	0.00	6.75	5.0	7.46
1.86	25.8	2.0	18.8	.33	12.8	7.7	10.1
2.36	20.8	2.5	20.1	.67	21.5	12.3	12.9
2.86	18.8	3.0	14.5	1.00	31.2	16.2	17.1
3.36	16.1	3.5	12.5	.33	36.2	22.8	21.2
3.68	13.8	3.9	9.2	.67	38.0	23.5	29.4
				2.00	41.7	25.6	29.9
				.33	41.1	26.1	32.5
				.67	38.5	26.4	29.4
				3.00	30.0	21.3	27.9
				.33	27.1	20.4	22.6
				.67	21.4	17.2	
				4.00		14.9	
				.33		13.4	

Of these series I. was taken by arrangement 2, series II. and III. by arrangement 3, and series IV. and V. by arrangement 4. In the case of I., IV., and V. the image consisted of two vertical rectangles each  $14^{\circ} \times 65'$  which touched on a long side, in the case of IV. it was a disk the radius of which subtended  $0.78^{\circ}$  at the eye, and in the case of II. it was a much larger disk. I. is the mean of nine determinations, II. of eighteen, III. of eighteen, and IV. and V. of ten each. The most presentable of the results, III. and IV., are graphed in fig. 2.

As our object was to determine the variation of the least perceptible increment with intensity, and as the values vary irregularly from day to day, it was our practice to take two readings for every intensity at one sitting, starting from one end of the range and working to the other. In

series I., II., and III. the observer did not read the scales himself, and his eye was highly but not perfectly dark adapted at the low end. On considering the matter it seemed to us that the eye should be in the same state for all readings if they were to be comparable. In series IV. and V., therefore, the observer set the current, read the scale of the polarizer, and entered up the current himself, all by the aid of a two-volt lamp in, of course, a darkened room. We considered that these operations would bring the eye into the same condition before every pair of readings.

Fig. 2.



The four principal brightness levels are regarded as 0.001 ml. for exteriors at night, 0.1 ml. for interiors at night, 10 ml. for interiors in daylight, and 1000 ml. for exteriors in daylight. This corresponds to 3.5, 1.5, 1.5, and 3.5 on the above intensity scale.

It is the logarithm of the intensity in photons that is entered in the tables. The relative value of the candle-power of the lamp at different currents was known from the calibration-curve of the lamp, and to find absolute values it was necessary to standardize one particular current. This was done in the following manner:—An 8 C.P. carbon lamp was measured in terms of a Hefner lamp at its rated voltage. The reflexion coefficient of a certain kind of white paper was determined in terms of the reflexion

coefficient of a fresh magnesium oxide surface for perpendicular incidence, and found to be 78 per cent. of the latter. The paper was then assumed to reflect in this direction 0.75 times as much light as a perfectly diffusing surface. In arrangements 2 and 4 a piece of clear glass was set up in front of the eyepiece with its surface at  $45^\circ$  to the axis of the latter, so that the eye saw both the field by transmission and the white paper illuminated by the 8 C.P. lamp by reflexion side by side. Suppose now that the brightness of both halves of the field is to be 1 millilambert. Viewed through the glass they will be dimmed each to a different extent. The brighter half will then be 0.98 millilambert. The distance of the lamp from the paper was adjusted so that the brightness of the reflected image of the latter had this value, incidence and reflexion being normal, and the current adjusted until paper and field were equally bright. Thus the current is standardized.

There is, however, a pitfall here which shows the necessity for introducing the new unit, the photon. The millilambert is an objective unit of brightness. It is always the same, no matter what the diameter of the pupil is. Now, the subjective brightness varies with the area of the pupil. It is the latter which is measured in photons. The eye-ring of the spectrometer did not fill the aperture of the pupil at any of the intensities used in the experiments, and when the comparison was made the beam from the white paper filled the full aperture of the latter. To obtain the subjective brightness at the current in question we have to multiply by the area of the pupil for this brightness. This was taken from Reeves' data, and assumed to be 23 sq. mm. When the comparison was made the white paper had thus an apparent objective brightness of 0.98 millilambert and a subjective brightness of  $0.98 \times 23$  photons. It is subjective brightnesses which are balanced. To find the objective brightness of the half of the field in question it would be necessary to divide this product by the cross-sectional area of the other beam. But the objective brightness of the field is not required. When the glass plate is removed, the subjective brightness of the field becomes 23 photons at the current in question. Arrangement 3 was standardized in a different manner.

Some workers prefer to measure objective brightness of a surface in metre-candles, a brightness of ten metre-candles being equal to one millilambert. The millilambert

is to be preferred, however, as a unit of brightness, since the metre-candle is strictly speaking a unit of illumination. The millilambert suffers from the disability that we are unaware how far magnesium oxide fulfils the requirements of a perfectly diffusing surface.

It will be observed that the maxima of our two best curves lie at antilogs 2.1 and 2.45, say a mean of 2.3. How much of the difference is real we are as yet unable to say; the results are by different observers with different apparatus standardized in different ways, the standardization involving the difficult process of heterochromatic photometry. Now, the maxima of König and Brodhun's curves lie at 3.5 on their scale of intensities. To change their unit to log photons it seems that we must subtract 1.2.

We cannot reconcile this with the definition of their unit. The latter is the brightness of a magnesium oxide surface illuminated by one-tenth of a Violle standard at a distance of 1 metre and viewed through a 1 sq. mm. artificial pupil. The brightness of the surface is therefore 0.2 millilambert. In their work on Fechner's law they used an aperture of 1 sq. mm. area. So their unit was one-fifth photon. Thus the maxima of their curves should lie at  $3.5 - \log 5 = 2.8$ , and there is a discrepancy of 0.5 between their results and ours. The Violle standard was difficult to work with, and the standardization of their field was done apparently by viewing the standard and the field one after the other, not simultaneously with the comparison surfaces touching. This is not an accurate method.

The value of König's unit has already been considered by Blanchard\* and by Hecht†. Blanchard made a determination of  $\Delta I/I$  for white light for a part of the range, and decided that, if his contrast sensibility was the same as König's, the latter's unit should be multiplied by 0.004 to bring it to photons. Hecht arrives at the same conclusion in another way. He divides 0.2 photon by 50, which he takes as the normal pupil aperture at this intensity; this gives 0.004. The position of the maximum is thus at  $3.5 + \log 0.004 = 1.1$ . Blanchard did not reach the maximum in his determination, so we do not know that his contrast sensibility is the same as König's. Since König

\* Phys. Rev. xi. p. 81 (1918).

† Journ. Gen. Physiol. vii. p. 235 (1924-25).




worked with an aperture of 1 sq. mm., there is no justification for bringing in the factor 50 as Hecht does ; moreover, for the intensity in question the factor should be nearer 35 than 50.

In comparing series IV. and V. for red and blue it will be noticed that the maxima occur at the same place, but that the maximum sensibility is higher for blue. This second result is doubtful, because the point was not specifically investigated. The eye may have been in a more sensitive condition when the blue observations were made. To be certain on this point it would be necessary to take the red and blue readings alternately on the same days.

It will be noticed that at low intensities the sensibility in the blue is higher. This is due to so-called rod vision coming into play. In taking V. the eye was intentionally kept in the same state of partial dark adaptation throughout. If the eye is carefully dark adapted  $I/\Delta I$  becomes greater throughout this region, and it is also possible to observe at much lower intensities. For example, at antilog  $-1$  photons  $I/\Delta I$  is 3.0 under the conditions of the experiment. On observing immediately after entering the room from daylight it is 3.5 ; after 10 minutes in the dark it was 2.4, and after another 20 minutes it was 1.6. After another 10 minutes it was possible to observe down to approximately antilog  $-5$  photons. There is doubt, however, about the exact value of this limit, as it was obtained by extrapolating the calibration curve.

§ 2. Experiments investigating the relation between visual acuity and intensity of illumination have been carried out by Uhthoff (1886, 1890), König (1897), and others, but the results obtained by König\* are so comprehensive, and the range of illumination he used was so great, that the more recent researches may be regarded as merely corroborating his work.

As object he employed Snellen's test figure  in various sizes, painted in black on a white background, and he altered the illumination by (1) using different sources—a candle, a petroleum lamp, and an electric arc, (2) varying the distance of the source from the object, and (3) interposing neutral glasses between the source and object. When working with white light he took as his unit of

\* *Sitzungsber. d. Akad. d. Wissensch. zu Berlin*, p. 559 (1897)

illumination that which was produced by a Hefner lamp at a distance of 1 metre.

He made the observations himself, and assumed that his eye had unit acuity if it could approximately recognize the open side of the figure when the latter was at such a distance that it subtended an angle of  $5'$ , and the lines and spaces each subtended  $1'$ . His values are thus higher than if expressed in ophthalmologist's units, which may be regarded as the reciprocal of the angle subtended in minutes by the breadths of the lines and spaces when they are clearly distinguishable. It was in order to avoid fatigue that he renounced certainty in favour of approximation, and he gave the factor  $\frac{3}{4}$  for the conversion of his results to ophthalmologists' units.

To investigate the effect of colour he cut out the black test figures and pasted them on red, green, or blue paper. The light from the above-mentioned sources was then made to pass through glasses of the appropriate colour before falling on the object.

Unfortunately, he did not state definitely his unit of intensity in these latter cases. He exhibited his results as four curves (one for each colour), showing the variation of the acuity with the logarithm of the illumination, and regarded each curve as made up of three straight lines, the one for low values having a low gradient, the intermediate one being fairly steep, and the one for high values being almost flat. Since he stated that if the curves for the colours had been plotted for the same unit of intensity as for white the four intermediate lines would have been coincident, we have been able to reduce all his results to absolute units with fair accuracy, and they are shown in the following table. His unit of intensity for white is equivalent to 0.072 millilamberts if we assume the reflexion coefficient of his paper to have been 0.8, and his units for red, green, and blue, derived as explained above, are 0.0072, 0.00018, and 0.000018 millilamberts respectively. In the table the log of the intensity  $I$  has been expressed in log photons. König did not use an artificial pupil in this work, so the area of the pupil at each intensity has been calculated from the data of Reeves.

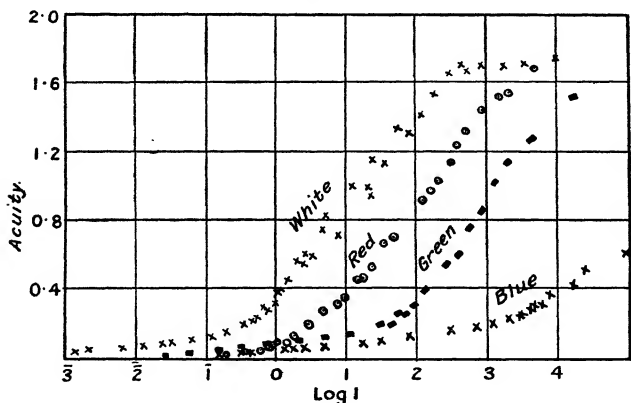
As the observations were very numerous they have been averaged in threes for white, in fives for red, in threes for green, and in fours for blue :—

White.		Red.		Green.		Blue.	
Log I.	Acuity.	Log I.	Acuity.	Log I.	Acuity.	Log I.	Acuity.
3.124	0.038	2.26	0.023	4.41	0.016	4.23	0.022
.32	.046	.55	.034	.76	.034	.52	.031
.81	.065	.74	.044	3.16	.050	.625	.032
2.09	.072	.85	.060	.49	.061	3.13	.049
.36	.084	.95	.074	.88	.081	.235	.054
.49	.095	1.03	.094	2.15	.088	.415	.062
.77	.101	.15	.095	.37	.101	.67	.069
1.045	.126	.26	.127	.70	.115	2.19	.092
.28	.147	.47	.192	1.04	.128	.47	.099
.56	.201	.68	.275	.505	.188	.88	.126
.64	.214	.87	.319	.63	.195	1.46	.155
.71	.226	.97	.344	.75	.246	.83	.176
.79	.293	0.16	.451	.86	.257	0.09	.199
.84	.277	.23	.463	.97	.302	.27	.226
.955	.325	.38	.527	0.10	.391	.42	.232
0.02	.386	.57	.664	.415	.550	.48	.251
.06	.395	.67	.700	.615	.595	.61	.280
.17	.449	1.08	.913	.75	.741	.67	.300
.315	.565	.22	.971	.91	.845	.77	.311
.385	.545	.31	1.027	1.12	1.025	.88	.361
.42	.605	.49	1.137	.32	1.131	1.22	.422
.50	.596	.58	.242	.68	.267	.63	.516
.66	.744	.68	.331	2.23	.516	.99	.607
.71	.821	.93	.452				
.89	.693	2.15	.528				
1.08	1.000	.30	1.538				
.30	0.994	.69	.686				
.34	0.939						
.38	1.146						
.54	1.116						
.73	1.333						
.89	.313						
2.05	.420						
.25	.532						
.46	.650						
.64	1.695						
.73	.672						
.94	.693						
3.22	.686						
.525	.708						
.99	1.750						

Fig. 3 expresses the results in graphical form, the axes being in their correct positions for white, but the other curves are displaced one, two and four units of the log I scale to the right respectively to avoid superposition. It will be noticed that the blue curve extends further to the left than the green and that the green extends further to the left than the red. This is due to "rod vision" coming into operation.

Before attempting to explain König's results we thought it better to verify them for the case of white light. As test-object we chose the simplest possible—viz., a series of parallel lines, the widths of the lines and the intervening spaces being equal.

Fig. 3.



Among various preliminary attempts may be mentioned one which utilized the rhomb and sliding apparatus described above. A series of pairs of parallel lines separated by spaces of the same width as the lines, with the widths increasing from pair to pair, was drawn and photographed so that they all appeared on the one negative. The latter was placed just over the rhomb, and the intensity of the beam was changed until each pair in turn was just resolvable. The values of log I were obtained from those of the currents through the lamp. But this was abandoned in favour of the following arrangement:—

Two positives, one dense and "contrasty" and the other thin, were prepared of a drawing of a large number of

parallel lines. One of them was set up in front of a Fullo-lite lamp, the current through which could be varied and noted; and for different values of the current, and consequently of the intensity, the observer moved nearer to or farther from the object until the lines just appeared separate. His distance from the object was measured by means of a tape which was fixed in a convenient position, and this distance was proportional to his acuity at that intensity. The latter was determined in millilamberts and in photons from the calibration curve of the lamp, in much the same way as has been described earlier. An artificial pupil was not used, but one of a series of prepared apertures was always in position in front of the object, so that the angle subtended by the diameter of the "available" object was constant—approximately  $2^\circ$ .

Then the other positive was used as the object, and the series of observations repeated. The whole arrangement was characterized by extreme simplicity, the one source and the one object being used throughout for each test.

The results obtained are shown in the following table, each value being the mean of six observations. The acuity is taken as the reciprocal of the angle subtended by the breadth of a line or the breadth of a space in minutes, and I is expressed in photons in log I.

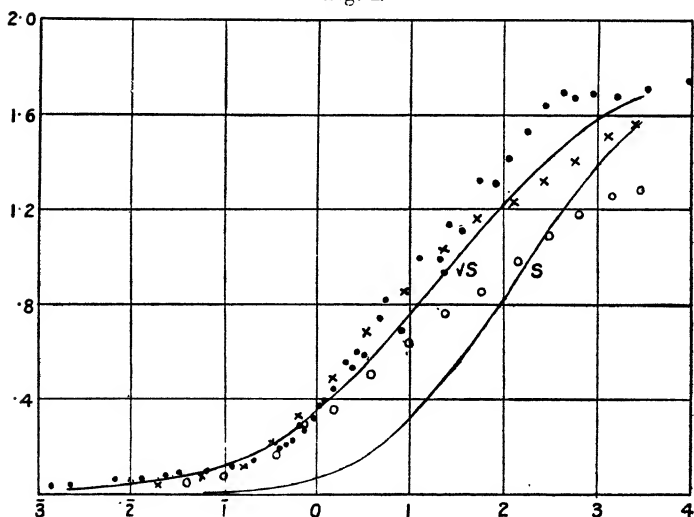
---

Dense Positive.		Thin Positive.	
Log I.	Acuity.	Log I.	Acuity.
3.44	1.564	3.48	1.280
.13	.517	.17	.260
2.79	.413	2.82	.179
.46	.329	.49	.097
.13	.241	.17	0.984
1.72	.174	1.76	.858
.35	.036	.39	.764
0.96	0.856	.00	.642
.54	.687	0.58	.508
.16	.502	.18	.345
1.80	.341	1.84	.292
.51	.230	.56	.171
.19	.126	2.99	.087
2.75	.079	.60	.054
.27	.051		

---

The results are shown graphically in fig. 4. On the same diagram König's results for white light are plotted as black disks for the purpose of comparison. König's intensity was the intensity of the white part of the test-object, ours the average intensity of the whole test-object, and the agreement of his results with the results for our dense object would be improved by shifting all our results 0.2 to the right. It is also obvious that the units of acuity have not been equivalent, for the agreement would be improved by increasing our ordinates by one eighth. König's curve has a corner near the top which ours lack.

Fig. 4.



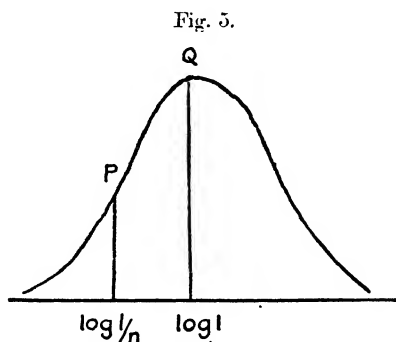
This may be due to his object being contrastier than ours, but the point requires further investigation.

Let us now consider the theoretical interpretation of the results. König describes his curves as being composed of three straight lines. This is hardly accurate, and gives us no clue as to the mechanism. Hecht suggested that the acuity is proportional to the number of percipient elements per unit area in the retina, and in a former paper Houstoun put forward the view that instead of this quantity we should take the number of percipient elements per unit length modified by a contrast factor. Since we are assuming that the sensation of brightness  $S$  is proportional

to the number of percipient elements stimulated, this would mean that the acuity should be proportional to  $\sqrt{S}$  modified by a contrast factor or to  $\sqrt{S}$  alone if the contrast factor is left out.

This hypothesis was tested in fig. 5 of the previous paper just referred to without success, owing to using the commonly accepted value of König's intensity unit, which we have found to be wrong. Let us now test it in the light of our own results. The observations on acuity were all made by J. F. Shearer. He also made the observations recorded in the lower curve of fig. 2. The integral curve corresponding to the latter, that is  $y = \int_{-\infty}^x e^{-\frac{x^2}{2}} dx$ , has been

entered on fig. 4, choosing a suitable scale of ordinates.



It represents  $S$  for Mr. Shearer's eye. Alongside is graphed  $\sqrt{S}$ , and it will be observed it fits the "dense" results reasonably well. It is also obvious that  $S$  does not fit the results.

In order to introduce the effect of contrast suppose that the brightness of the transparent strips is  $I$ , and that the black strips transmit one  $n$ th of the light incident upon them. Let us suppose that the intensity of light falling upon the black strips is, to begin with,  $I$ , and the intensity of light falling upon the clear strips is  $I/n$ . Then the whole test object appears one uniform hue. Throughout the area involved the elements are stimulated up to the level  $P$  in fig. 5. Increase the intensity in the clear strips to the level  $I$ . Then the additional elements represented by the area  $PQ$  come into action, and it is upon them alone that

the discrimination of detail depends. As the intensity rises this area moves across the curve. It has a constant breadth,  $\log n$ . It is the root of this area which determines the number of active elements per unit-length, and we suggest that the acuity is proportional to this quantity. In the case of a very contrasty test object  $\log n$  is large numerically, and the area to the left of P may be neglected.

By proceeding on these lines the difference between our "dense" and "thin" results may be explained, but a detailed discussion of this part of the work is postponed until we have more observations at our disposal. No matter what further results accrue it is clear that our hypotheses enable us to connect successfully the hitherto unrelated fields of acuity and intensity discrimination.

§ 3. We have suggested that the brightness of the image of a surface is proportional to the number of nerve-fibres stimulated by that image, and that each nerve-fibre transmits impulses only at a constant rate. This requires that if point sources are unequally bright one must stimulate more fibres than the other; is this consistent with the process of image formation by the eye?

The stars have been graded from ancient times into six classes, and are recognized as point sources. Thus a point is capable of six different brightnesses. This question seemed worthy of detailed investigation, so an artificial star was formed by setting up a circular hole of diameter one-tenth millimetre in the window of a light-tight room, and focussing the image of the filament of a half-watt lamp outside the room on this hole. The latter was viewed by an observer inside the room, from a distance of 4 metres, while an assistant decreased the intensity of the image by putting resistance in series with the lamp. This resistance was increased in steps, each step being adjusted to produce a just perceptible diminution in the brightness of the image. It will be noticed that in this method of experimenting the observer sees nothing but the point source, and we have to consider nothing but the area directly involved; spatial induction is eliminated. Observations were made both with the unfiltered light of the lamp and also with Wratten tricolour filters in front of the hole. To the degree of accuracy attained in the experiments the hole could be regarded as infinitely small.

When white or red light was used extinction was reached in about 16 or 17 steps from the highest intensity. At the



highest intensity the image had a definite area of irregular outline, its breadth subtended perhaps 3 or 4 mm. at the eye, and it had streamers; only for the last six steps was it a point. The last step was colourless. Over the last six steps with red the intensity increased one hundred times, and the increase in the logarithm of the intensity was approximately the same from each step to the one above it; the other colours gave similar results, though not quite so regular. Thus the steps correspond roughly to the magnitudes of the stars, for an average star of the first magnitude is just about one hundred times as bright as one of the sixth, and the stars of each magnitude are approximately two and one-half times as bright as those of the next fainter.

The image of a point on the retina is not a point but an Airy disk surrounded by rings. With a pupil of 4 mm. and yellow light the radius of the first dark ring subtends  $0.61'$ , and the radii of the second and third dark rings subtend respectively  $1.12'$  and  $1.62'$ .  $0.839$  of the total light goes to form the central disk,  $0.071$  to form the first bright ring, and  $0.028$  to form the second bright ring. Now, while the pupillary diameter during the observations was considerably greater than 4 mm., owing to other aberrations there would be no gain in definition; so we may take the above distribution of light in the image as fairly accurate. We notice at once that the average density of illumination over the central disk is twenty-eight times the average density of illumination over the first bright ring.

A point source is just visible when it gives as much light as one-tenth candle at 1 kilometre. Let us suppose that the light is distributed uniformly over the Airy disk in the retina. Then the same image would be formed if we assumed that the object was a disk the radius of which subtended  $0.61'$  and the laws of geometrical optics strictly held. If the brightness of a small area is  $B$  lamberts, and its area is  $S$ , it radiates as much light in the direction of the normal as a source of  $BS/\pi$  candles. We have thus

$$\frac{BS}{\pi} = \frac{1}{10},$$

$$S = \pi \left( \frac{0.61\pi \times 10^5}{60 \times 180} \right)^2 \text{ cm.}^2,$$

$$= 988 \text{ cm.}^2,$$

and

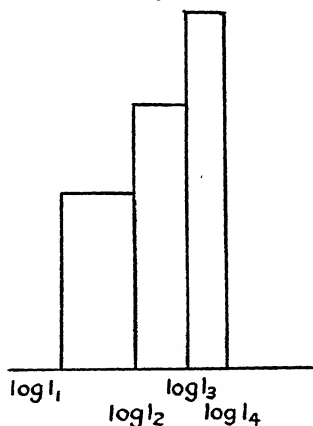
$$B = 0.318 \text{ millilamberts.}$$

The maximum area of the pupil of the eye is about 45 sq. mm. Hence the brightness of the image on the retina is  $45 \times 0.318 = 14.3$  photons.

This may be taken as the average intensity of illumination of the Airy disk at the limit of visibility. It is a comparatively high illumination. At this intensity four-tenths of the cones are above the threshold. The Airy disk covers five or six cones and the first bright ring about fourteen. Hence at the limit of visibility two cones on the disk should be above the threshold.

If we increase the intensity by six just perceptible steps, *i. e.*, raise it to the limit when the image ceases to appear

Fig. 6.



a point, the intensity of illumination on the disk goes up to 1430 photons, and on the first bright ring to 51 photons. At these intensities four-fifths and two-fifths of the cones respectively are above the threshold, *i. e.*, about ten should be stimulated.

The calculation is only approximate, but it shows that the increase in brightness of a point source can be quite reasonably explained on the assumption that each step in intensity is due to an additional nerve-fibre going into action.

§ 4. When  $I / \Delta I$  is graphed as a function of  $\log I$  the area of the curve to the left of any intensity represents the sensation at that intensity. It may be shown that this

holds not only for the limit, when  $\Delta I$  is infinitesimal, but also for the case of finite steps. For (fig. 6) let  $I_2 - I_1$  be the just appreciable increase in intensity when the intensity is  $I_1$ , let  $I_3 - I_2$  be the just appreciable increase when the intensity is  $I_2$ , and so on. At the points whose abscissæ are  $\log I_1$ ,  $\log I_2$ , etc., erect ordinates equal to

$$\frac{1}{\log I_2 - \log I_1}, \quad \frac{1}{\log I_3 - \log I_2}, \quad \frac{1}{\log I_4 - \log I_3}, \text{ etc.,}$$

and complete the rectangles as shown. Then their areas are equal. By definition the sensation increases by one unit from  $I_1$  to  $I_2$  and by one unit from  $I_2$  to  $I_3$ . Thus each rectangle corresponds to one unit of sensation. If we wish to be rigorously accurate the smoothed curves we have hitherto dealt with should be replaced by a stepped curve as shown in fig. 6. But the accuracy attainable in the experimental work is not sufficient to make this refinement necessary.

**XLII.** *On some Problems of Nuclear Physics treated according to Wave-Mechanics.* By A. C. BANERJI, M.A. (Cantab.), M.Sc. (Cal.), Professor of Mathematics, Allahabad University\*.

**I**N a previous paper† the author treated the problem of scattering of  $\alpha$ -particles by light (not heavy) atoms according to Schrödinger's form of wave-mechanics, and showed that the assumption of the law of force,

$$F = \frac{2Ze^2}{r^2} \left(1 - \frac{r_0}{r}\right),$$

leads to results which are in good agreement with experimental data. In the present paper an attempt has been made to extend the same consideration to some problems of nuclear physics. It is first necessary to give a brief survey of these problems.

According to modern theories of atomic structure, all atoms are composed of protons and electrons. The electrons are arranged in definite shells about the nucleus, according

\* Communicated by Dr. M. N. Saha, F.R.S.

† Phil. Mag. ix. p. 273 (1930).

to the principles successively elaborated by Bohr\*, Stoner and Mainsmith, and Pauli. The nucleus, whose dimension is of the order  $10^{-13}$  cm., consists of an excess of protons, the electrons acting as binding material. We have to explain why, in spite of the preponderance of positive particles, the nucleus does not ordinarily explode. The assumption is made (Rutherford and Chadwick, Bieler †, and Debye ‡ and Hardemeier) that the usual repulsive forces between positively-charged particles change into attractive forces when the distance between them is of the order  $10^{-13}$  cm. The assumption of these attractive forces gives a general explanation of abnormal scattering, and Rutherford and Thibaud § have attempted to explain the origin of nuclear  $\gamma$ -rays on the assumption of these forces. But more problems on the principle of nucleus construction have been suggested by the investigations of Aston || on the packing effect of atoms. Possibly successive theoretical treatment of these problems will enable us to evolve the principles of nuclear construction (Kern-auf-bau-prinzip); hence it will be profitable to give a brief account of the problems suggested by Aston's experimental results.

Aston showed that, even if the weight of oxygen nucleus be taken as 16, the weight of the other nuclei differ markedly from whole numbers. To take the simplest case—the weight of the H-atom is found to be 1.00778, while the weight of the neutral H-particle (or neutron) in the nucleus is found to be unity. The reality of this neutron is rendered very plausible because we have got isotopes like  $\text{Li}_6$  and  $\text{Li}_7$ , the different isotopes of Kr, which differ in weight exactly by unity on the oxygen scale. Since the nuclear charges are exactly the same, we have to suppose that the isotope  $\text{Li}_7$  is simply  $\text{Li}_6$  with a neutron attached to it. Hence we come to the following interesting problem:—According to Bohr's theory, the electron can be at best at a distance of  $10^{-9} \times 5.32$  cm. from the proton (Bohr's first orbit); it cannot approach nearer. The mass is 1.00778 (proton + electron). But in the nucleus a new proton-electron combination is formed in which the distance is  $< 10^{-13}$  cm., resulting in a loss of mass of amount .00724 from the proton. It has been pointed out that .00724 =  $\alpha$ , where  $\alpha$  = Sommer-

\* See 'Atomic Structure and Spectral Lines,' by Sommerfeld.

† Proc. Camb. Phil. Soc. xxi. p. 686 (1923).

‡ Phys. Zs. xxvii. p. 181.

§ Journ. de Phys. vi. p. 82 (1925).

|| Proc. Roy. Soc. cxxiii. p. 383.

feld's fine structure constant  $\frac{2\pi e^2}{ch}$ ; hence in such a close combination the system loses the energy  $Mac^2 + mc^2$ , where  $M$ =mass of the proton,  $m$ =mass of the electron. The existing theories (Bohr, Schrödinger, Dirac) seem incapable of explaining this fact.

We can also refer to the explanation of the packing effect observed in the formation of other heavier nuclei; but these problems can be tackled only after the neutron problem has been successfully solved.

### *Radioactivity.*

In finding out the principles of nuclear construction, our knowledge of the phenomena of radioactivity will be a great guiding factor. It is well known that the phenomenon of spontaneous disintegration cannot be explained from mechanical principles. Recently Gamow\* and Gournay and Condon† suggested explanations from the wave-mechanical point of view which have been further elucidated by von Laue‡, Kudar, Th. Sexl, Möller, and Born.

From the works of Rutherford, Chadwick, and Bieler, it transpires that, if we plot the value of the potential from the centre of the atom outwards, it starts from negative infinity in the centre, passes through the zero value and rises to a steep positive maximum value, and gradually falls down to zero asymptotically (*vide* curve A).

This steep maximum of potential prevents the constituents in the inside from getting out, thus preventing explosion, and is known as the potential barrier. But, according to wave-mechanics, the  $\alpha$ -particle is a wave, and though as a particle it cannot jump over the barrier unless it has an amount of energy which is never observed, as a wave it can occasionally get over the barrier. Gamow worked out the rate of leakage of the  $\alpha$ -particle wave, and identified the process with the radioactive process of disintegration. He was thus able to offer a general explanation of the Geiger-Nutall relationship, connecting life with velocity of emission; but subsequent more rigorous work by von Laue, Kudar, Sexl, and Möller§ has shown that the agreement is not as good as was at first

\* Gamow, *Zs. f. Phys.* li. p. 204 (1928); lii. p. 501 (1929); liii. p. 601 (1929).

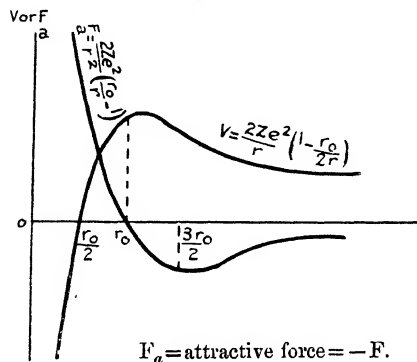
† Gournay and Condon, 'Nature,' cxxii. p. 439 (1928).

‡ Laue, *Zs. f. Phys.* lii. p. 726 (1929). Kudar, *Zs. f. Phys.* liii. pp. 61, 95 (1929). Sexl, *Zs. f. Phys.* liv. p. 445 (1929). Möller, *Zs. f. Phys.* lv. p. 451 (1929). Born, *Zs. f. Phys.* lviii. p. 306 (1929).

§ *Locc. citt.*

supposed. In particular, none of these workers have been able to show why  $\alpha$ -particles emerge with *discrete positive* values.

CURVE A.



### Origin of Nuclear $\gamma$ -Rays and Cosmic Rays.

The success of the law  $V = 2e^2Z\left(\frac{1}{r} - \frac{r_0}{2r}\right)$  in explaining the main results of scattering by light elements encourages the belief that it may also give us some clue regarding the origin of nuclear  $\gamma$ -rays. Recently some lively controversy has taken place on this question.

### Methods of Measuring the Wave-length of the $\gamma$ -Ray Spectrum\*.

It is necessary to know how far the wave-lengths of the  $\gamma$ -rays have been correctly determined. The method which has been universally used by Ellis, M. de Broglie, Black, Meitner, and others† is that of photo-electric ionization. As the  $\gamma$ -ray which originates from the nucleus traverses the atom, it is absorbed by the electrons in the K, L<sub>I</sub>, L<sub>II</sub>, L<sub>III</sub>, ... layers. Hence, in the resulting  $\beta$ -ray spectrum the known differences K-L<sub>I</sub>, K-L<sub>II</sub>, L<sub>I</sub>-L<sub>II</sub> occur, and from an analysis of them it is possible to find out the frequency of the original  $\gamma$ -ray. The wave-lengths have been directly

\* See 'Handbuch der Experimental Physik'—XV. Radioaktivitat, pp. 47, 56, 57.

† See Ellis and Wooster, Proc. Camb. Phil. Soc. 1925, p. 849. Ellis, Proc. Camb. Phil. Soc. 1924, p. 376. Black, Proc. Roy. Soc. 1924, p. 633; Proc. Camb. Phil. Soc. 1925, p. 838.

determined by Thibaud\*, using ruled glass gratings at glancing-angle. The results of Thibaud are in fair agreement with those of the earlier workers.

L. Meitner† showed from such analysis that the  $\gamma$ -ray emission follows a process of radioactive disintegration, and does not precede it, as has been formerly thought. An example will suffice: RadAct (atomic No. 90) breaks up with ejection of  $\alpha$ -rays. It has also got a  $\gamma$ -ray activity. Analysis of  $\gamma$ -rays, according to the methods sketched above, shows that the  $\gamma$ -ray spectrum excites  $\beta$ -rays with characteristic energy-level differences of the atomic No. 88, and not of 90. Hence it is concluded that the  $\gamma$ -ray emission takes place after ejection of  $\alpha$ -rays. After the ejection the atomic shells are rearranged, according to the displacement law of Fajans and Soddy, as they would be in the element 88; and as the  $\gamma$ -ray traverses the atom, the  $\beta$ -rays are excited with the characteristic energy-level differences of element No. 88. Ellis‡ has established the same fact in the case of a  $\beta$ -ray transformation.

The emission of  $\gamma$ -rays is therefore due to some rearrangement in the nucleus after either the  $\alpha$ - or the  $\beta$ -ray has left it, and is therefore unconnected with the main causes leading to disintegration. It is still an open question whether they are due to the vibration of electrons, protons,  $\alpha$ -particles, or some neutral particles which are supposed to exist in the nucleus. Ellis§ has shown that the different  $\gamma$ -rays are homogeneous at least one in a thousand, *i. e.*, they are almost monochromatic; and from this and certain other arguments Kuhn|| concludes that they cannot be due to the vibrations of electrons, but are due to vibrations of heavier particles, the proton or the  $\alpha$ -particle, as otherwise, owing to radiation damping, the line would be drawn into a broad band.

The damping factor due to radiation is

$$\alpha = \frac{8\pi^2 e^2 \nu^2}{3c^3 m},$$

where  $m$  = mass of the vibrating particle

\* Thibaud, *Journ. de Phys.* vi. p. 82 (1925); 'Handbuch der Physik,' xxiii. chap. ii. D.

† Meitner, *Zs. f. Phys.* xxvi. p. 169 (1924); 'Handbuch der Physik,' xxii. chap. ii. D.

‡ Ellis and Wooster, *Proc. Camb. Phil. Soc.* xxii. p. 844 (1924).

§ See the recent discussion in *Proc. Roy. Soc.* cxxiii. p. 353.

|| Kuhn, *Zs. f. Phys.* xliii. p. 56; xliv. p. 32.

Since  $\nu = 3 \times 10^{21}$  for  $\gamma$ -rays,  $\alpha$  would be too large, unless  $m$  were large. The half-breadth of the emitted line would be too great.

At present we may suppose that the  $\gamma$ -ray emission is due to any one of the following causes :—

(1) The  $\alpha$ -particle or any charged positive particle may be describing quantum orbits with definite energy values about the nucleus. The  $\gamma$ -rays may be due to change of levels as in the optical spectrum.

Ellis has established the presence of discrete energy levels in the  $\gamma$ -spectrum of Ra B and Ra C, but the data are yet too fragmentary.

(2) The  $\gamma$ -ray spectrum may be similar to vibration or rotation spectra of molecules. The outer  $\alpha$ -particle and the nucleus may be rotating about the common C.G. like a molecular dipole, and give rise to  $\gamma$ -rays ; or it may be due to similar processes in discrete entities like  $\alpha$ - $\alpha$ , neutron-neutron oscillating in the field of the nucleus.

We have only explored the possibility No. 1. Let the potential energy be given by

$$V = \frac{2e^2Z}{r} \left(1 - \frac{r_0}{2r}\right). \quad . \quad . \quad . \quad . \quad . \quad (1)$$

Case I. :

When discrete *quantized negative* values of energy are observed.

The Schrödinger equation is now

$$\nabla^2 \psi + \frac{8\pi^2 M}{h^2} \left( E - \frac{2e^2 Z}{r} + \frac{e^2 Z r_0}{r^2} \right) \psi = 0. \quad . \quad . \quad (2)$$

Put \*  $\psi = R \cdot \theta \cdot \Phi$ , and the equation in R is

$$\frac{d^2 R}{dr^2} + \frac{2}{r} \frac{dR}{dr} + \left\{ \frac{8\pi^2 M E}{h^2} - \frac{16\pi^2 M Z e^2}{h^2 r} + \frac{8\pi^2 e^2 M Z r_0}{h^2 r^2} - \frac{k(k+1)}{r^2} \right\} R = 0. \quad (2A)$$

Putting  $R = e^{i\alpha_1 r} \cdot S$ , where the negative value of  $\alpha_1$  is to be taken, we have

$$\frac{d^2 S}{dr^2} + \left( \alpha_1 + \frac{2}{r} \right) \frac{dS}{dr} + \left( \frac{\alpha_0}{r} + \frac{b_0}{r^2} \right) S = 0, \quad . \quad . \quad (2B)$$

\* See 'Wave Mechanics,' by H. T. Flint, chap. iii.



where

$$\left. \begin{aligned} \frac{1}{4}a_1^2 &= -\frac{8\pi^2 ME}{h^2}, \\ a_0 &= a_1 - \frac{16\pi^2 MZe^2}{h^2}, \\ b_0 &= -k(k+1) + \frac{8\pi^2 e^2 MZr_0}{h^2}. \end{aligned} \right\} \dots \dots (3)$$

Our equation now reduces to

$$f\left(r\frac{d}{dr}\right)S + \frac{1}{r}g\left(r\frac{d}{dr}\right)S = 0, \dots \dots (4)$$

where

$$\begin{aligned} f(z) &= a_1 z + a_0, \\ g(z) &= z^2 + z + b_0. \end{aligned}$$

Let  $\alpha_1$  be one of the roots of

$$z^2 + z + b_0 = 0,$$

so that

$$\begin{aligned} \alpha_1 &= -\frac{1}{2} + \frac{1}{2}\sqrt{1-4b_0} \\ &= -\frac{1}{2} + \sqrt{\left(k+\frac{1}{2}\right)^2 - \frac{8\pi^2 e^2 MZr_0}{h^2}}. \end{aligned}$$

One of the series will terminate after  $n_r$  terms if

$$a_1(\alpha_1 + n_r) + a_0 = 0,$$

from which we get, after substituting the values of  $a_1, a_0, \alpha_1$ , the discrete quantized values of E:

$$E = -\frac{8\pi^2 e^4 Z^2 M}{h^2} \frac{1}{\left\{ \left(n_r + \frac{1}{2}\right) + \sqrt{\left(k + \frac{1}{2}\right)^2 - \frac{8\pi^2 e^2 MZr_0}{h^2}} \right\}^2} \dots \dots (5)$$

The quantity

$$\frac{8\pi^2 e^2 MZ}{h^2} r_0 = \frac{r_0}{\frac{am}{2MZ}}, \dots \dots (6)$$

where  $a$  = radius of the Bohr orbit  $= \frac{h^2}{4\pi^2 e^2 m}$ ,

$m$  = mass of the electron,

$M$  = mass of the  $\alpha$ -particle

$$\frac{am}{2MZ} = \frac{3.66 \times 10^{-13}}{Z} \text{ cm.}$$

For RadAct,  $Z=90$ , this equals  $4 \times 10^{-15}$  cm.

As  $r_0$  is certainly of the order  $10^{-13} \sim 10^{-12}$  cm.\*,

$$\frac{r_0}{am} = n_0^2,$$

$$\frac{1}{2MZ}$$

where  $n_0$  is a quantity of the order of 10 to 12.

Hence we have

$$E = -4RhZ^2 \left( \frac{M}{m} \right) \left\{ \frac{1}{n_r + \frac{1}{2} + \sqrt{(k + \frac{1}{2})^2 - n_0^2}} \right\}^2, \quad (7)$$

where  $R$  is the Rydberg's constant, and for real values of  $E$  ( $k + \frac{1}{2}$ ) must be greater than  $n_0$ .

If we use Dirac's form, the half-values will probably disappear, and moreover if we put  $n_r=0$ , we get

$$E = - \frac{4RhZ^2 \left( \frac{M}{m} \right)}{k^2 - n_0^2}, \quad k > n_0. \quad (7A)$$

We have

$$\nu = RhZ^2 \left( \frac{M}{m} \right) \left[ \frac{1}{k^2 - n_0^2} - \frac{1}{k'^2 - n_0^2} \right], \quad (8)$$

where  $k' \geq k$ .

If we take

$$k = n_0 + 1, \quad k' = n_0 + 2,$$

$$\nu = 4RhZ^2 \frac{M}{m} \frac{2n_0 + 3}{(4n_0 + 4)(2n_0 + 1)} \quad (8A)$$

$$= RhZ^2 \frac{M}{m} \frac{1}{n_0 + 1} \quad \text{approximately.}$$

Since  $\frac{M}{m} = 4 \times 1836$ , these rays become about 600 times

harder than the K-spectrum of the element, and even if they exist, they can only be compared to the cosmic rays. Hence we cannot explain the ordinary nuclear  $\gamma$ -ray spectrum on the basis of the existence of negative energy values. Wave-lengths of cosmic rays have been estimated by Millikan to range from  $\cdot 004$  cm. to  $\cdot 00013 \times 10^{-8}$  cm. (about 1000 times harder than  $\gamma$ -rays) from the values of absorption-coefficients. The relation of absorption-coefficients to wave-length, which is the basis of Millikan's measurements of wave-lengths, is,

\* See discussion in Proc. Roy. Soc. cxxiii. p. 353.

however, not definitely settled. Klein and Nishina\* have worked out a new formula of dispersion from Dirac's theory according to which the wave-length may be several times smaller than hitherto thought. The negative energy values, however, afford a clue to the origin of cosmic rays which may be identified as those arising from vibrations in the intra-nuclear space.

### Case II.:

When discrete *quantized positive* values of energy are observed.

We take the Schrödinger equation in the form

$$\nabla^2 \Psi = -\frac{4\pi i M}{h} \frac{\partial \Psi}{\partial t} - \frac{8\pi^2 M}{h^2} V \Psi = 0. \quad (9)$$

Put

$$\Psi = e^{-\frac{\mu}{2}t} \cdot e^{\frac{2i\pi E}{h}t} \psi. \quad (10)$$

We get

$$\nabla^2 \psi + \frac{8\pi^2 M}{h^2} (E - V) \psi + \frac{i \cdot 2\pi M \mu}{h} \psi = 0. \quad (9A)$$

Putting the value of  $V$ , we have

$$\nabla^2 \psi + \frac{8\pi^2 M}{h^2} \left( E - \frac{2Ze^2}{r} + \frac{Ze^2 r_0}{r^2} \right) \psi + \frac{i \cdot 2\pi M \mu}{h} \psi = 0. \quad (9B)$$

Put

$$\psi = R \cdot \theta \cdot \Phi,$$

and the equation in  $R$  is found to be

$$\frac{d^2 R}{dr^2} + \frac{2}{r} \frac{dR}{dr} + \left\{ \frac{8\pi^2 M E}{h^2} + \frac{i \cdot 2\pi M \mu}{h} - \frac{16\pi^2 Z M e^2}{h^2} \cdot \frac{1}{r} \right. \\ \left. + \frac{8\pi^2 M Z e^2 r_0}{h^2} \cdot \frac{1}{r^2} - \frac{k(k+1)}{r^2} \right\} R = 0. \quad (9C)$$

Put

$$R = e^{\frac{1}{2}(a_1 + ip)r} \cdot S.$$

We have

$$\frac{d^2 S}{dr^2} + \left( a_1 + ip + \frac{2}{r} \right) \frac{dS}{dr} + \left( \frac{a_0}{r} + \frac{b_0}{r^2} \right) S = 0. \quad (9D)$$

\* Klein and Nishina, *Z. f. Phys.* lii. p. 853; 'Nature,' Sept. 15, 1928.

where

$$\left. \begin{aligned} \frac{1}{4}(p^2 - a_1^2) &= \frac{8\pi^2 M E}{h^2}, \\ a_1 p &= -\frac{4\pi M \mu}{h}, \\ a_0 &= a_1 + ip - \frac{16\pi^2 M Z e^2}{h^2}, \\ b_0 &= -k(k+1) + \frac{8\pi^2 M Z e^2 r_0}{h^2}. \end{aligned} \right\} \quad \cdot \quad \cdot \quad (11)$$

Our equation now reduces to

$$f\left(r \frac{d}{dr}\right) S + \frac{1}{r} g\left(r \frac{d}{dr}\right) S = 0, \quad \cdot \quad \cdot \quad \cdot \quad (9 \text{ E})$$

where

$$\begin{aligned} f(Z) &= (a_1 + ip)Z + a_0, \\ g(Z) &= Z^2 + Z + b_0. \end{aligned}$$

Let  $\alpha_1$  be one of the roots of

$$Z^2 + Z + b_0 = 0,$$

so that

$$\begin{aligned} \alpha_1 &= -\frac{1}{2} + \frac{1}{2} \sqrt{1 - 4b_0} \\ &= -\frac{1}{2} + \sqrt{\left(k + \frac{1}{2}\right)^2 - \frac{8\pi^2 e^2 M Z r_0}{h^2}}. \quad \cdot \quad \cdot \quad (12) \end{aligned}$$

The series will terminate after  $n_r$  terms if

$$(a_1 + ip)(\alpha_1 + n_r) + a_0 = 0$$

or

$$a_1 + ip = \frac{16\pi^2 e^2 M Z}{h^2} \frac{1}{n_r + \frac{1}{2} + \sqrt{\left(k + \frac{1}{2}\right)^2 - \frac{8\pi^2 e^2 M Z r_0}{h^2}}}. \quad (12)$$

In order that the above equation may be possible,  $\frac{8\pi^2 e^2 M Z r_0}{h^2}$  must be greater than  $(k + \frac{1}{2})^2$  or  $r_0 > f_0(k + \frac{1}{2})^2$ ,

where

$$f_0 = \frac{h^2}{8\pi^2 e^2 M Z} = \frac{am}{2MZ}.$$

Then we have from (12), after some calculations,

$$a_1 = \frac{16\pi^2 e^2 M Z}{h^2} \frac{n_r + \frac{1}{2}}{(n_r + k + 1)(n_r - k) + \frac{r_0}{f_0}}, \quad \cdot \quad (13)$$

$$p = -\frac{16\pi^2 e^2 MZ}{h^2} \frac{\sqrt{\frac{r_0}{f} - (k + \frac{1}{2})^2}}{(n_r - k)(n_r + k + 1) + \frac{r_0}{f_0}}. \quad (14)$$

For the quantized discrete values of  $E$  we get

$$\begin{aligned} E &= \frac{8\pi^2 MZ^2 e^4}{h^2} \frac{\left\{ \frac{r_0}{f_0} - (k + \frac{1}{2})^2 - (n_r + \frac{1}{2})^2 \right\}}{\left\{ (n_r + k + 1)(n_r - k) + \frac{r_0}{f_0} \right\}^2} \\ &= 4R\hbar Z^2 \left( \frac{M}{m} \right) \frac{\left\{ \frac{r_0}{f_0} - (k + \frac{1}{2})^2 - (n_r + \frac{1}{2})^2 \right\}}{\left\{ (n_r + k + 1)(n_r - k) + \frac{r_0}{f_0} \right\}^2}, \quad (15) \end{aligned}$$

where  $R$  is Rydberg's constant.

We get also

$$\mu = \frac{8\pi E}{h} \frac{(n_r + \frac{1}{2}) \sqrt{\frac{r_0}{f_0} - (k + \frac{1}{2})^2}}{\frac{r_0}{f_0} - (k + \frac{1}{2})^2 - (n_r + \frac{1}{2})^2}. \quad (16)$$

$E$  is positive when  $r_0 > f_0 \{ (k + \frac{1}{2})^2 + (n_r + \frac{1}{2})^2 \}$ .

If we put  $n_0 = 0$ , we get discrete quantized *positive* energy values, provided  $r_0 > f_0 [ (k + \frac{1}{2})^2 + \frac{1}{4} ]$ .

If we now take

$$\frac{r_0}{f_0} = n_0^2 + \frac{1}{4} \quad \text{approximately,}$$

we get

$$E = 4R\hbar Z^2 \left( \frac{M}{m} \right) \frac{1}{[n_0^2 - (k + \frac{1}{2})^2]} \quad \text{approximately.}$$

When  $k < n_0$ , the frequency is given by

$$\nu = 4RZ^2 \left( \frac{M}{m} \right) \left[ \frac{1}{n_0^2 - (k + \frac{1}{2})^2} - \frac{1}{n_0^2 - (k' + \frac{1}{2})^2} \right].$$

If  $n_0$  is sufficiently large, and  $k'$  and  $k$  are taken as 1 and 2 respectively, we get

$$\nu = 4RZ^2 \left( \frac{M}{m} \right) \cdot \frac{4}{n_0^4} \quad \text{approximately.}$$

We come within the  $\gamma$ -ray region if we take  $n_0 = 10$ , which is not an improbable value\*.

\* Rutherford has used as large a quantum number as 30 for accounting for  $\gamma$ -rays on the Debye-Hardemeir theory. See *Volta Centenary Volume*.

This type of solution has been obtained by Thibaud \*, using the elementary Bohr theory. He gets

$$\nu = 4RZ \left( \frac{M}{m} \right) \left[ \frac{1}{n_0^2 - k^2} - \frac{1}{n_0^2 - k'^2} \right],$$

where  $k' < k$  and  $k, k' < n_0$ . He shows that this formula accounts in a fairly satisfactory way for the nuclear  $\gamma$ -ray of RadAct.

The energy of  $\alpha$ -rays emitted from radioactive bodies varies in range from  $6.6 \times 10^{-6}$  erg ( $\alpha$ -rays from Ur) to  $1.4 \times 10^{-5}$  erg ( $\alpha$ -rays from ThC) †. But the energy of  $\gamma$ -rays is much less than this, *e.g.* in RadAct the wave-length of  $\gamma$ -rays varies from  $40 \times 10^{-11}$  cm. to  $400 \times 10^{-11}$  cm., corresponding to energy-values  $5 \times 10^{-7}$  erg to  $5 \times 10^{-8}$  erg ‡. This is easily explained on the theory given here. The energy of the  $\alpha$ -particle is

$$\frac{R/Z^2}{n_0^2 - (k + \frac{1}{2})^2} \cdot \frac{M}{m} = \frac{1.24 \times 10^{-3}}{n_0^2 - (k + \frac{1}{2})^2} \text{ erg},$$

$$Z = 90 \text{ for RadAct.}$$

If we put  $k=0$  and  $n_0=14$ , the energy becomes  $6.6 \times 10^{-6}$  erg; for  $n_0=9$ ,  $E=1.40 \times 10^{-5}$  erg. So the order of energy of  $\alpha$ -rays is of the same dimensions as is actually observed. The energy of  $\gamma$ -rays is then for the transition  $k' \rightarrow k$ ,  $1 \rightarrow 2$  of the order  $4 \times 10^{-8}$  erg, *i. e.* of the same order as is observed for the softest  $\gamma$ -rays. For transitions involving larger values of  $k$ , the energy becomes of the same order as of the harder  $\gamma$ -rays.

The above results, viz. existence of discrete and quantized positive energy values, of  $\alpha$ -rays within the potential barrier, and agreement in the order of dimensions of the calculated energy values for  $\alpha$ -particles and nuclear  $\gamma$ -rays with those actually observed, are distinctly new.

In Tables I. to VI. I have tried to account for the nuclear  $\gamma$ -rays of six elements: RaB, RaC, — ThC + C', MesTh 2, RadAct, Act X; the data have been taken from the 'Handbuch der Experimental Physik,' xv. p. 56.

In the first column are given the wave-lengths in Siegbahn units, viz.  $10^{-11}$  cm. The second column gives the energy

\* Thibaud, *Compt. Rend.* clxxxi. p. 857 (1925).

† See Emskog, *Zs. Phys.* lii. p. 207.

‡ See 'Handbuch der Experimental Physik'—XV. Radioaktivität, pp. 56-57.

$h\nu$  in ergs. In the third column values of  $P$  as deduced from observations are given, where

$$P = \frac{(n_0^2 - k^2)(n_0^2 - k'^2)}{k^2 - k'^2}$$

The values of  $n_0$ ,  $k$ , and  $k'$  have been chosen by trial. In the last column calculated values of  $P$  from trial values of  $n_0$ ,  $k$ , and  $k'$  are given.  $Z$  stands for atomic number.

TABLE I.  
Radium B,  $Z=81$ .

X. E.	Ergs.	Values of P deduced from observations.	$n_0=19$ .	Calculated values of P.
230.3	$8.5 \times 10^{-8}$	$1.22 \times 10^4$	$k=5, k'=4$	$1.29 \times 10^4$
62.7	$3.1 \times 10^{-7}$	$.34 \times 10^4$	$k=6, k'=1$	$.33 \times 10^4$
59.9	$3.3 \times 10^{-7}$	$.32 \times 10^4$	$k=6, k'=0$	$.32 \times 10^4$
50.7	$3.9 \times 10^{-7}$	$.27 \times 10^4$	$k=7, k'=3$	$.28 \times 10^4$
47.5	$4.1 \times 10^{-7}$	$.25 \times 10^4$	$k=7, k'=2$	$.25 \times 10^4$
44.7	$4.4 \times 10^{-7}$	$.24 \times 10^4$	$k=7, k'=1$	$.23 \times 10^4$
41.6	$4.7 \times 10^{-7}$	$.22 \times 10^4$	$k=7, k'=0$	$.23 \times 10^4$
34.9	$5 \times 10^{-7}$	$.21 \times 10^4$	$k=8, k'=0$	$.21 \times 10^4$
26.2	$7.5 \times 10^{-7}$	$.14 \times 10^4$	$k=9, k'=3$	$.14 \times 10^4$
25.6	$7.7 \times 10^{-7}$	$.13 \times 10^4$	$k=9, k'=2$	$.13 \times 10^4$

TABLE II.  
Radium C,  $Z=81$ .

X. E.	Ergs.	Values of P deduced from observations.	$n_0=19$ .	Calculated values of P.
44.9	$4.3 \times 10^{-7}$	$.24 \times 10^4$	$k=7, k'=2$	$.25 \times 10^4$
37.1	$5.3 \times 10^{-7}$	$.20 \times 10^4$	$k=8, k'=4$	$.21 \times 10^4$
31.7	$6.2 \times 10^{-7}$	$.17 \times 10^4$	$k=8, k'=1$	$.17 \times 10^4$
28.8	$6.8 \times 10^{-7}$	$.15 \times 10^4$	$k=9, k'=4$	$.15 \times 10^4$
20.2	$9.2 \times 10^{-7}$	$.11 \times 10^4$	$k=10, k'=3$	$.10 \times 10^4$
13.1	$1.5 \times 10^{-6}$	$.69 \times 10^3$	$k=12, k'=7$	$.70 \times 10^3$
10.9	$1.8 \times 10^{-6}$	$.58 \times 10^3$	$k=12, k'=4$	$.58 \times 10^3$
9.9	$2 \times 10^{-6}$	$.52 \times 10^3$	$k=13, k'=8$	$.53 \times 10^3$
8.66	$2.1 \times 10^{-6}$	$.50 \times 10^3$	$k=13, k'=7$	$.50 \times 10^3$
6.94	$2.8 \times 10^{-6}$	$.37 \times 10^3$	$k=14, k'=8$	$.37 \times 10^3$
5.56	$3.5 \times 10^{-6}$	$.30 \times 10^3$	$k=14, k'=1$	$.30 \times 10^3$

TABLE III.  
Thorium C + C', Z=81.

X. E.	Ergs.	Values of P deduced from observations.	$n_0=19.$	Calculated values of P.
303	$6.5 \times 10^{-8}$	$1.6 \times 10^4$	$k=4, k'=3$	$1.73 \times 10^4$
85.4	$2.2 \times 10^{-7}$	$.47 \times 10^4$	$k=5, k'=1$	$.50 \times 10^4$
58.6	$3.3 \times 10^{-7}$	$.32 \times 10^4$	$k=6, k'=0$	$.32 \times 10^4$
52.9	$3.7 \times 10^{-7}$	$.28 \times 10^4$	$k=7, k'=3$	$.28 \times 10^4$
48.8	$4.0 \times 10^{-7}$	$.26 \times 10^4$	$k=7, k'=2$	$.25 \times 10^4$
47.7	$4.1 \times 10^{-7}$	$.25 \times 10^4$	$k=7, k'=1$	$.23 \times 10^4$
44.3	$4.4 \times 10^{-7}$	$.24 \times 10^4$	$k=7, k'=0$	$.23 \times 10^4$
42.3	$4.9 \times 10^{-7}$	$.21 \times 10^4$	$k=8, k'=4$	$.21 \times 10^4$
23.8	$8.2 \times 10^{-7}$	$.13 \times 10^4$	$k=9, k'=2$	$.13 \times 10^4$
18.8	$1.1 \times 10^{-6}$	$.95 \times 10^3$	$k=10, k'=1$	$.95 \times 10^3$
4.7	$4.2 \times 10^{-6}$	$.25 \times 10^3$	$k=15, k'=8$	$.25 \times 10^3$

TABLE IV.  
Mesothorium 2, Z=90.

X. E.	Ergs.	Values of P deduced from observations.	$n_0=19.$	Calculated values of P.
214	$8.9 \times 10^{-8}$	$1.4 \times 10^4$	$k=3, k'=0$	$1.45 \times 10^4$
95.6	$2.1 \times 10^{-7}$	$.59 \times 10^4$	$k=5, k'=2$	$.58 \times 10^4$
67.2	$2.9 \times 10^{-7}$	$.43 \times 10^4$	$k=6, k'=3$	$.42 \times 10^4$
38.8	$5.1 \times 10^{-7}$	$.24 \times 10^4$	$k=7, k'=2$	$.15 \times 10^4$
36.5	$5.3 \times 10^{-7}$	$.23 \times 10^4$	$k=7, k'=1$	$.23 \times 10^4$
26.7	$7.3 \times 10^{-7}$	$.17 \times 10^4$	$k=8, k'=1$	$.17 \times 10^4$
13.5	$1.5 \times 10^{-6}$	$.83 \times 10^3$	$k=11, k'=5$	$.84 \times 10^3$
12.7	$1.6 \times 10^{-6}$	$.78 \times 10^3$	$k=11, k'=4$	$.79 \times 10^3$

TABLE V.  
Radio-actinium, Z=90.

X. E.	Ergs.	Values of P deduced from observations.	$n_0=19.$	Calculated values of P.
41.1	$4.8 \times 10^{-7}$	$.26 \times 10^4$	$k=7, k'=2$	$.25 \times 10^4$
43.8	$4.5 \times 10^{-7}$	$.28 \times 10^4$	$k=7, k'=3$	$.28 \times 10^4$
48.6	$4 \times 10^{-7}$	$.31 \times 10^4$	$k=6, k'=0$	$.32 \times 10^4$
63	$3.1 \times 10^{-7}$	$.40 \times 10^4$	$k=6, k'=3$	$.42 \times 10^4$



TABLE V. (*cont.*).Radio-actinium,  $Z=90$ .

X. E.	Ergs.	Values of P deduced from observations.	$n_0=19$ .	Calculated values of P.
82.8	$2.4 \times 10^{-7}$	$.52 \times 10^4$	$k=5, k'=1$	$.5 \times 10^4$
123	$1.6 \times 10^{-7}$	$.78 \times 10^4$	$k=5, k'=3$	$.74 \times 10^4$
201	$9.7 \times 10^{-7}$	$1.28 \times 10^4$	$k=5, k'=4$	$1.29 \times 10^4$
232	$8.4 \times 10^{-7}$	$1.47 \times 10^4$	$k=3, k'=0$	$1.45 \times 10^4$
282	$7.0 \times 10^{-8}$	$1.77 \times 10^4$	$k=4, k'=3$	$1.73 \times 10^4$
390	$5.0 \times 10^{-8}$	$2.48 \times 10^4$	$k=3, k'=2$	$2.51 \times 10^4$

TABLE VI.

Actinium X,  $Z=88$ .

X. E.	Ergs.	Values of P deduced from observations.	$n_0=17$ .	Calculated values of P.
86	$2.3 \times 10^{-7}$	$.53 \times 10^4$	$k=4, k'=1$	$.52 \times 10^4$
80.4	$2.4 \times 10^{-7}$	$.50 \times 10^4$	$k=4, k'=0$	$.49 \times 10^4$
79	$2.5 \times 10^{-7}$	$.48 \times 10^4$	$k=5, k'=3$	$.47 \times 10^4$
62	$3.2 \times 10^{-7}$	$.38 \times 10^4$	$k=5, k'=2$	$.36 \times 10^4$
46	$4.3 \times 10^{-7}$	$.28 \times 10^4$	$k=6, k'=3$	$.26 \times 10^4$

It is to be seen that in most cases the agreement is extremely good. We expect, in each case, that if all the intermediate values of  $k$  and  $k'$  are to be allowed, a much larger number of  $\gamma$ -rays should exist. Such a number is not observed. Probably there may be a selection principle restricting the transitions from  $k' \rightarrow k$ , or certain weak  $\gamma$ -rays have not yet been observed. It may be pointed out that  $k$  has been chosen in place of  $k+n_r$ , and such transitions as  $k'=3$  to  $k'=7$  denote changes in the total quantum number. I hope to treat the problem further from the standpoint of Dirac's theory of the electron on a future occasion.

I have great pleasure in thanking my colleague Prof. M. N. Saha, F.R.S., of the Physics Department of the Allahabad University, for much help and many suggestions in preparing this paper.

Department of Mathematics,  
Allahabad University.  
Dec. 10, 1929.

# XLIII. *The Reduction of Observations.*

By A. F. DUFTON, M.A., D.I.C. \*

1. **I**N the reduction of observations, the possibilities of a graphical solution are not always realized. The determination of the function  $R=46.3465+0.181600\ t$  (with a mean deviation of  $2.4 \times 10^{-4}$ ) from observations with values of  $t$  ranging from 14 to 28, which would appear at first sight beyond the scope of a graph, is a typical example †.

In a recent paper on "Reducing Observations by the Method of Minimum Deviations" ‡, Dr. Rhodes calls attention to the necessity for methods alternative to that of Least Squares and discusses the fitting of a parabola to a series of points. The method he describes is stated to be simpler than that of Edgeworth but undoubtedly more laborious than that of Least Squares.

It may perhaps be of interest to show the application of a simple graphic method to Dr. Rhodes' data, which are reproduced below.

2. This method, which was briefly described in 'Nature' two years ago §, is for the determination of a linear function of  $X$  approximating to  $Y$  for a range of corresponding values ( $X, Y$ ). The plotted values are divided into two classes by the median of  $X$  and the required straight line divides each class into equal numbers.

In the description given in 'Nature,' the straight line is unique when the number of values of ( $X, Y$ ) is  $4n+2$  or  $4n+3$ . In other cases, to avoid ambiguity, the following procedure is suggested: when there are  $4n+1$  values, include the median in each class into which it divides the values; when there are  $4n$  values, include the two "medians" in each class.

3. In the problem of the parabola stated by Dr. Rhodes, if the required equation is

$$y=a+b(x+c)^2,$$

it follows that  $\Delta=2b(n+c),$

where  $\Delta=\frac{1}{2}(y_{(n+1)}-y_{(n-1)})$

$$\text{or} \quad y_{(n+\frac{1}{2})}-y_{(n-\frac{1}{2})}.$$

\* Communicated by the Director of Building Research, Department of Scientific and Industrial Research.

† Proc. Phys. Soc. xliii. p. 103 (1930).

‡ Phil. Mag. ix. p. 974 (1930).

§ 'Nature,' cxxi. p. 866 (1928).

and a linear function of  $\Delta$  approximating to  $n$  can be determined as in fig 1.

$x$ ( $=n$ )	$y$	$\Delta$
-8	28	
$-7\frac{1}{2}$		-67
-7	-39	-34
$-6\frac{1}{2}$		-1
-6	-40	19
$-5\frac{1}{2}$		39
-5	-1	$31\frac{1}{2}$
$-4\frac{1}{2}$		24
-4	23	$17\frac{1}{2}$
$-3\frac{1}{2}$		11
-3	34	1
$-2\frac{1}{2}$		-9
-2	25	3
$-1\frac{1}{2}$		15
-1	40	9
$-\frac{1}{2}$		3
0	43	$-5\frac{1}{2}$
$\frac{1}{2}$		-14
1	29	$-14\frac{1}{2}$
$1\frac{1}{2}$		-15
2	14	$-8\frac{1}{2}$
$2\frac{1}{2}$		-2
3	12	-15
3		-28
4	-16	-13
$4\frac{1}{2}$		2
5	-14	-15
$5\frac{1}{2}$		-32
6	-46	-26
$6\frac{1}{2}$		-22
7	-68	11
$7\frac{1}{2}$		44
8	-24	

The graph shows that when  $\Delta=0$ ,  $n=-\frac{1}{2}$ , so that the value of  $c$  is  $\frac{1}{2}$ .

The parabola, therefore, is

$$y = a + b(x + \frac{1}{2})^2$$

and a linear function of  $(x + \frac{1}{2})^2$  approximating to  $y$  can be determined as shown in fig. 2.

The function is

$$y = 33 - 1.7(x + \frac{1}{2})^2,$$

which is the parabola required.

Fig. 1.

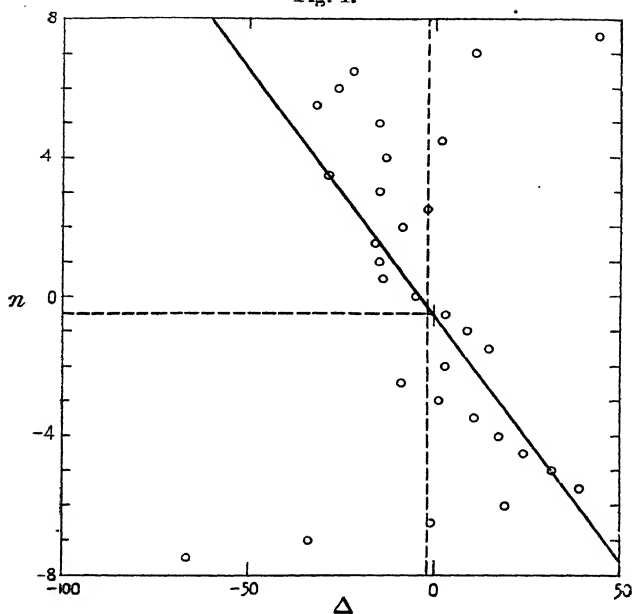
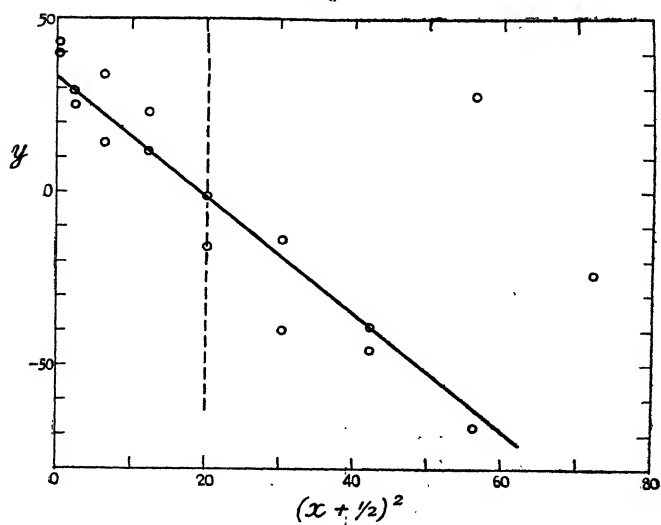
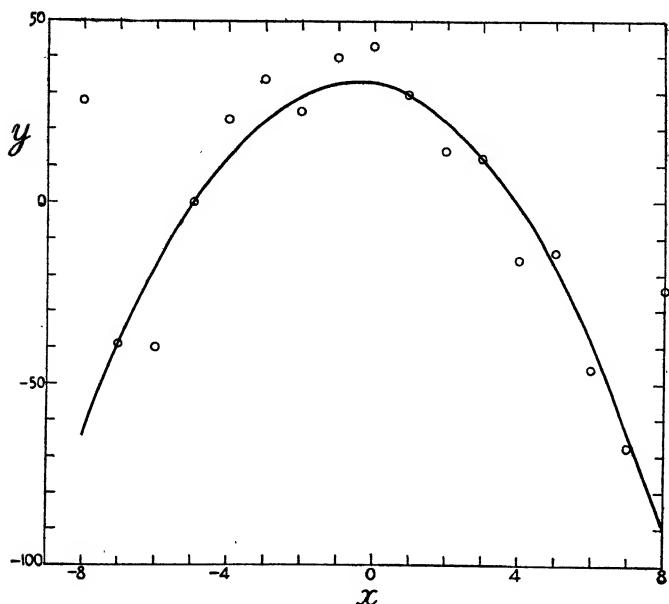


Fig. 2.



This parabola is shown with the original data in fig. 3. The mean deviation of  $y$  from the parabola is 15.4, which may be compared with 17.2 from the "least square" parabola and with the minimum value of 15.3.

Fig. 3.



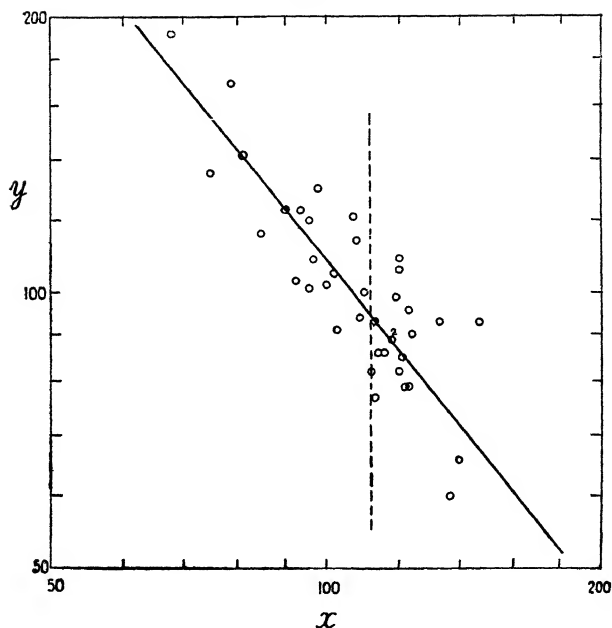
4. The second of Dr. Rhodes' examples deals with the fitting of the curve  $y=Bx^a$  to the following data :—

$x$ .	$y$ .	$x$ .	$y$ .
68	192	102	105
75	135	103	91
79	169	107	121
81	141	108	114
85	116	109	94
90	123	110	100
93	103	112	82
94	123	113	77
96	123	113	93
96	101	114	86
97	109	116	86
98	130	118	89
100	102	118	89

## DATA (cont.).

$x$ .	$y$ .		$x$ .	$y$ .
119	99		123	96
120	106		124	90
120	109		133	93
120	82		137	60
121	85		140	66
122	79		147	93
123	79			

Fig. 4.



A graph on logarithmic paper (fig. 4) shows that on each side of the straight line joining the points (90, 123) and (113, 93) there are nine points on each side of the median  $x=112$ .

The points (90, 123) and (113, 93) lie on

$$y = 30.953x^{-1.2285},$$

which is the curve required.

The mean deviation of  $y$  from this curve is 10.2, which may be compared with the minimum value of 10.1.

5. The examples discussed illustrate incidentally the expedience of anamorphosis: by a suitable transformation the fitting of a curve to a series of points is reduced to the simpler problem of fitting a straight line to a corresponding series. In each case the graphical solution compares favourably with that obtained by the method of Minimum Deviations.

Building Research Station,  
Garston, Herts.

**XLIV. An X-Ray Investigation of the Lead-Antimony Alloys.** By D. SOLOMON, B.Sc. (Wales) and W. MORRIS JONES, M.A., M.Sc., F.Inst.P. (Department of Physics, University College of Swansea) \*.

#### *Introduction.*

THE equilibrium diagram of the lead-antimony system, and the physical properties of the alloys, have occupied the attention of many workers. The most recent investigations are those of R. S. Dean<sup>(1)</sup>, Broniewski and Sliwowski<sup>(2)</sup>, and Stephens<sup>(3)</sup>.

Dean<sup>(1)</sup>, by thermal analysis and microscopic examination of lead alloys of low antimony content, found that antimony is soluble in solid lead up to between 2 per cent. and 3 per cent. by weight of antimony at the eutectic temperature of 247° C. In a further paper, Dean, Hudson, and Fogler<sup>(4)</sup> measured the electrical conductivities, at various temperatures, of lead alloys of low antimony content, and concluded that the solid solubility of antimony in lead varies from 2.45 per cent. at the eutectic temperature to .8 per cent. at room temperature. They added a note to the effect that the alloy containing .8 per cent. of antimony breaks down, and the solubility of antimony in lead may be brought at least as low as .5 per cent. antimony.

Later work, in 1928, of Broniewski and Sliwowski<sup>(2)</sup>, who examined the complete system, agrees with that of previous investigators as to the absence of definite compounds, but shows evidence of two solid solutions in the neighbourhood of the two constituent elements, of about 8 atomic per

\* Communicated by W. Morris Jones, Senior Lecturer in Physics, University College, Swansea.

cent. (13 per cent. by weight) of lead in antimony, and 2 atomic per cent. (1.2 per cent. by weight) of antimony in lead.

E. Stephens<sup>(3)</sup>, working in this laboratory, has examined the galvanomagnetic effects in the lead-antimony alloys, and the curves obtained by him, being continuous and containing no irregularities, offer no evidence for the formation of solid solutions or compounds.

Since the alloys made and annealed by Stephens<sup>(3)</sup> were at hand, an investigation of their crystal structures was undertaken, as a knowledge of the structures would be of interest, and should also serve to identify the phases of the system.

### *Method of Experiment.*

The crystal structures were examined by the X-ray powder method. The precautions taken to ensure accuracy of measurement have been described in previous papers<sup>(5)</sup>. The copper target used gave rise to two radiations,  $K_{\alpha}$  and  $K_{\beta}$ , the latter being absorbed, as far as possible, by a thin filter of nickel.

TABLE I.  
Antimony.

Radiation.	Plane.	Intensity.	Observed $d/n$ .	Calculated $d/n$ .
$K_{\alpha}$ .....	100 (2)	St.	3.103	3.111
$K_{\alpha}$ .....	211	M.	2.636	2.637
$K_{\alpha}$ .....	110 (2)	M.	2.250	2.250
$K_{\alpha}$ .....	221	M.	2.154	2.159
$K_{\alpha}$ .....	111	W.	1.874	1.880
$K_{\alpha}$ .....	320	M.	1.771	1.755
$K_{\alpha}$ .....	100 (4)	W.	1.557	1.555
$K_{\alpha}$ .....	210 (2)	W.	1.417	1.416
$K_{\alpha}$ .....	332	W.	1.370	1.385
$K_{\alpha}$ .....	431	W.	1.259	1.261
$K_{\alpha}$ .....	100 (5)	V.W.	1.244	1.245
$K_{\alpha}$ .....	432	V.W.	1.196	1.203

*Structure* :—Face-centred rhombohedral.  
*Dimension of unit cell* :— $a_0 = 6.235$  Å.U.  
*Angle of rhombohedron* =  $87^{\circ} 24'$ .



*Results.*

To obtain the crystal structures of the system, powder photographs were taken of the two metals (lead and antimony), and of the alloys 70 per cent. antimony 30 per cent. lead, and 20 per cent. antimony 80 per cent.

TABLE II.

Alloy of 70 per cent. Antimony and 30 per cent. Lead.

Radiation.	Plan.	Intensity.	Observed $d/n$ .	Calculated $d/n$ .
*K $\alpha$ .....	100 (2)	St.	3.101	3.111
K $\alpha$ .....	111	M.	2.840	2.846
*K $\alpha$ .....	211	M.	2.636	2.637
K $\alpha$ .....	100 (2)	M.	2.457	2.465
*K $\alpha$ .....	110 (2)	W.	2.245	2.250
*K $\alpha$ .....	221	W.	2.149	2.159
K $\beta$ .....	110 (2)	V.W.	1.745	1.743
*K $\alpha$ .....	111	W.	1.869	1.880
*K $\alpha$ .....	320	W.	1.765	1.755
K $\alpha$ .....	110 (2)	M.	1.746	1.743
*K $\alpha$ .....	100 (4)	W.	1.549	1.555
K $\alpha$ .....	131	M.	1.486	1.484
*K $\alpha$ .....	210 (2)	W.	1.417	1.416
*K $\alpha$ .....	332	W.	1.375	1.385
*K $\alpha$ .....	431	W.	1.255	1.261
K $\alpha$ .....	100 (4)	V.W.	1.237	1.232
K $\alpha$ .....	331	W.	1.129	1.129
K $\alpha$ .....	120 (2)	W.	1.101	1.099
K $\alpha$ .....	112 (2)	W.	1.009	1.006
K $\alpha$ .....	151	W.	.949	.947
K $\alpha$ .....	110 (4)	V.W.	.870	.871
K $\alpha$ .....	531	W.	.834	.833

Mixture of face-centred cubic lattice, dimensions :— $a_0 = 4.93$  Å.U. ; and a face-centred rhombohedral lattice, dimensions :— $a_0 = 6.240$  Å.U., and angle of rhombohedron  $87^\circ 24'$ .

Note :—The lines of the face-centred rhombohedral lattice of antimony are denoted by \*.

lead, the results being tabulated in Tables I. to IV. The first column states the quality of the copper radiation ; the second, the Miller indices of the reflecting planes ; the third, the intensities of the lines on the photograph ;

the fourth, the plane spacings obtained from measurements on the film ; and the fifth, the calculated spacings for the structure found.

Antimony is known to have a face-centred rhombohedral structure. The side of the unit cell deduced in the present investigation is  $a_0 = 6.235 \text{ \AA.U.}$ , and the angle of the rhomb  $87^\circ 24'$ . The result is identical with the value found by Morris Jones and Howells<sup>(6)</sup>, and closely agrees also with that found by Persson and Westgren<sup>(7)</sup>.

Table II. gives the spacings from the powder photograph of the alloy 70 per cent. antimony 30 per cent. lead. The

TABLE III.

Lead.

Radiation.	Plane.	Intensity.	Observed $d/n$ .	Calculated $d/n$ .
$K_{\alpha}$ .....	111	M.	2.840	2.846
$K_{\alpha}$ .....	100 (2)	M.	2.461	2.465
$K_{\beta}$ .....	110 (2)	V.W.	1.747	1.743
$K_{\alpha}$ .....	110 (2)	St.	1.742	1.743
$K_{\alpha}$ .....	131	St.	1.486	1.484
$K_{\alpha}$ .....	111 (2)	M.	1.423	1.423
$K_{\alpha}$ .....	100 (4)	W.	1.229	1.232
$K_{\alpha}$ .....	331	M.	1.130	1.129
$K_{\alpha}$ .....	120 (2)	M.	1.102	1.099
$K_{\alpha}$ .....	112 (2)	M.	1.005	1.006
$K_{\alpha}$ .....	151	M.	.948	.947
$K_{\alpha}$ .....	110 (4)	W.	.870	.871

Structure :—Face-centre cubic.

Dimension of unit cell :— $a_0 = 4.93 \text{ \AA.U.}$

lines on the film show that the crystal structure of the alloy consists of a mixture of the face-centred rhombohedral lattice of antimony and the face-centred cubic lattice of lead, the lattice constants being the same as those for pure antimony and pure lead. The atomic diameter of antimony is  $2.80 \text{ \AA.U.}$ , and that of lead  $3.80 \text{ \AA.U.}$  An expansion of the antimony cell would, therefore, be expected if lead was soluble to any extent in solid antimony. The results give no measurable change in the size of the antimony cell—hence the solution of lead in antimony

is very small, and does not exceed .5 per cent. by weight of lead.

Lead has a face-centred cubic lattice, earlier investigation giving the edge as  $a_0=4.91$  Å.U. Powder photographs of Phebus and Blake <sup>(8)</sup>, however, resulted in the determination  $a_0=4.93$  Å.U. In the present investigation the side of the lattice was calculated to be  $a_0=4.93$  Å.U.

TABLE IV.

Alloy of 80 per cent. and Lead 20 per cent. Antimony.

Radiation.	Plane.	Intensity.	Observed $d/n$ .	Calculated $d/n$ .
*K $\alpha$ .....	100 (2)	M.	3.107	3.111
K $\alpha$ .....	111	M.	2.848	2.846
*K $\alpha$ .....	211	W.	2.650	2.637
K $\alpha$ .....	100 (2)	M.	2.455	2.465
*K $\alpha$ .....	110 (2)	W.	2.246	2.250
*K $\alpha$ .....	221	W.	2.149	2.159
K $\beta$ .....	110 (2)	V.W.	1.747	1.743
*K $\alpha$ .....	111	V.W.	1.870	1.880
*K $\alpha$ .....	320	W.	1.761	1.755
K $\alpha$ .....	110 (2)	St.	1.747	1.743
*K $\alpha$ .....	100 (4)	W.	1.553	1.555
K $\alpha$ .....	131	St.	1.490	1.484
K $\alpha$ .....	111 (2)	M.	1.427	1.423
*K $\alpha$ .....	332	V.W.	1.377	1.385
*K $\alpha$ .....	431	V.W.	1.257	1.261
K $\alpha$ .....	100 (4)	W.	1.235	1.232
K $\alpha$ .....	331	M.	1.133	1.129
K $\alpha$ .....	120 (2)	M.	1.104	1.099
K $\alpha$ .....	151	M.	.950	.947
K $\alpha$ .....	110 (4)	W.	.872	.871
K $\alpha$ .....	531	M.	.834	.833
K $\alpha$ .....	100 (6)	M.	.822	.822

Mixture of a face-centred cubic lattice, dimensions:— $a_0=4.93$  Å.U., and a face-centred rhombohedral-lattice, dimensions:— $a_0=6.240$  Å.U., and angle of rhombohedron  $87^\circ 24'$ .

Note:—The lines of the face-centred rhombohedral lattice of antimony are denoted by \*.

The results obtained from the powder photograph of the alloy 80 per cent. lead 20 per cent. antimony are given in Table IV.

An examination of the spacings deduced from this film shows a mixture of the lattice spacings of pure lead and pure antimony, the size of the lattice in each case being unchanged. Thus, the X-ray analysis offers no evidence for the formation of a solid solution at the lead end of the equilibrium diagram.

Table II., which shows that in alloy 70 per cent. antimony 30 per cent. lead the lead lattice is unchanged, also indicates this result. If any solid solution of antimony in lead exists, therefore, at room temperature, the solubility cannot be more than about .5 per cent. by weight of antimony.

The present work shows that there are no definite compounds in the lead-antimony system of alloys, and that if lead is soluble in antimony, or antimony in lead, the degree of solubility of either metal in the other is very small at room temperature; and in no case does it exceed .5 per cent. by weight.

These results agree with Dean's <sup>(1)</sup> work on the lead end of the equilibrium diagram, but do not confirm the existence of the solid solutions found at both ends by Broniewski and Sliwowski <sup>(2)</sup>.

As the atomic diameters of lead and antimony are 3.80 Å.U. and 2.80 Å.U. respectively, the solid solution of 13 per cent. by weight of lead in antimony, and the solid solution of 1.2 per cent. by weight of antimony in lead, should produce measurable changes in the size of the respective unit cells.

No such changes were observed in the present investigation, the structures obtained being those of antimony and lead.

### *References.*

- (1) J. Ann. Chem. Soc. xlv. p. 1683 (1928).
- (2) *Revue de Met.* xxv. p. 392 (1928).
- (3) Phil. Mag., April 1930.
- (4) Ind. and Engin. Chem. p. 1246 (1925).
- (5) Phil. Mag. vii. (Jan. 1929).
- (6) Phil. Mag. (May 1930).
- (7) *Zeit. für Phys. Chem.* cxxxvi. p. 208 (Sept. 1928).
- (8) Phys. Rev. (ii.) xxv. p. 107 (1925).

XLV. *Corona Discharge in Hydrogen.*  
*By J. H. BRUCE, B.A., Balliol College, Oxford \*.*

1. **T**HE study of the corona discharge yields data bearing on problems of theoretical interest in connexion with the motion of positive ions, and this paper contains an account of experiments which I have made on the discharge between coaxial cylinders in hydrogen at low pressures.

2. The apparatus used by Huxley in his researches on helium and neon† was used in these experiments. It consisted of two quartz tubes each containing a nickel cylinder 4·6 cm. in diameter and 12 cm. long, with guard-rings 8 cm. long. A nickel wire 1·65 mm. in diameter was fixed along the axis of one cylinder and a wire 3·16 mm. in diameter along the axis of the other cylinder. The pressure-gauge and the pump for exhausting the apparatus were connected to the quartz cylinders through mercury vapour taps cooled with liquid air. The hydrogen was prepared by the electrolysis of barium hydrate and admitted to the apparatus through heated palladium. The apparatus was heated and washed out several times with fresh gas, while a high-frequency discharge was passed between the electrodes. This process was repeated until all traces of impurities were removed.

3. The starting-potentials for discharges between the wires and the cylinders are shown in fig. 1, in which the ordinates are the starting-potentials measured in volts and the abscissæ the pressures in mm. of mercury.

It will be observed that at pressures above that corresponding to the minimum starting-potential, the discharge passes more readily when the wire is negative than when it is positive, while at lower pressures the positive discharge passes more readily than the negative. The positive and negative discharges differ greatly in character, the positive consisting of a glow distributed uniformly along the wire, while the negative is generally concentrated at various parts of the wire. In the positive discharge the current increases continuously with the applied potential when the pressure is large, while the negative discharge is disruptive.

\* Communicated by Prof. J. S. Townsend, F.R.S.

† Phil. Mag. v. p. 74 (1928).

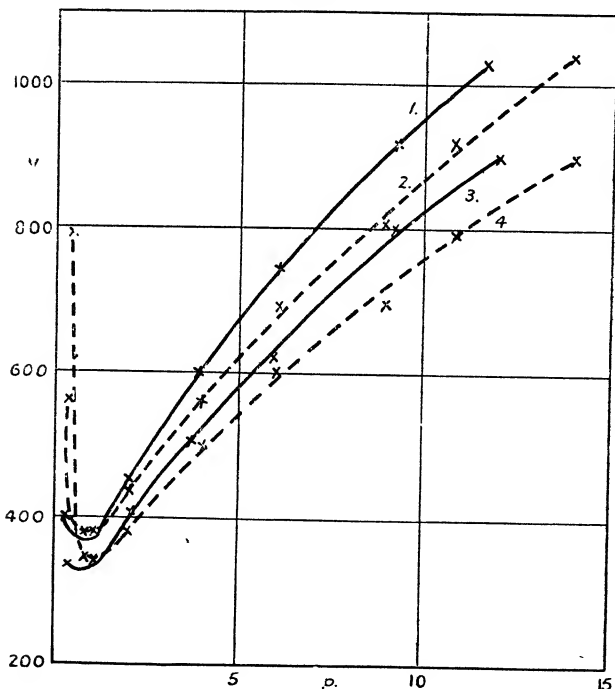
The electric force  $X$  at the surface of the wire required to start a discharge is found from the potential difference between the electrodes.

The relation

$$aX = f(ap),$$

where  $a$  is the radius of the wire and  $p$  is the pressure of the gas, is found to hold except at the lower pressures (as with

Fig. 1.

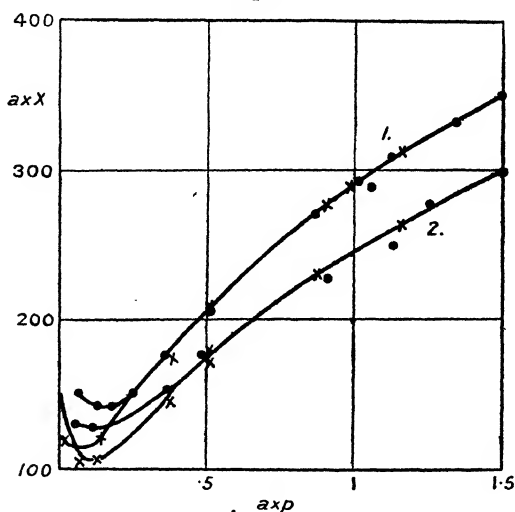


Potential required to start a discharge between the wire and the cylinder, as a function of the pressure. Curves 1 and 3 refer to the wire 3.16 mm. in diameter, curves 2 and 4 to the wire 1.65 mm. in diameter. Curves 1 and 2 refer to positive discharges and curves 3 and 4 to negative discharges.

other gases). In fig. 2  $aX$  is represented as a function of  $ap$ , the ordinates being  $aX$  measured in volts and the abscissæ the product  $ap$ ,  $a$  being measured in cm. and  $p$  in mm. of mercury.

Impurities, when present in small quantities, lower the starting-potentials; in large quantities they raise them and make them ill defined, the current being maintained by a lower potential than is required to start it. This effect is specially marked when the wire is negative; thus, when the tube containing the wire 3.15 mm. in diameter was being cleaned out, the values found for the starting-potentials were those given in the second column of the following table. The potentials required to maintain the current were those given in the third column. This potential was nearly con-

Fig. 2.



$aX$  as a function of  $ap$ . Points marked with crosses refer to the wire 1.65 mm. in diameter, those with circles to the wire 3.15 mm. in diameter. In curve 1 the wire is positive, in curve 2 it is negative.

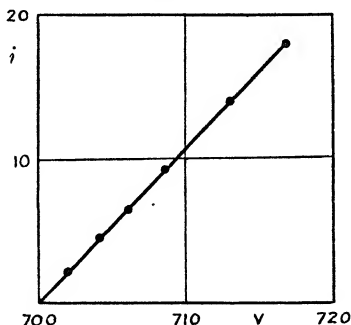
stant for currents ranging from about 1 microampere to about 100 microamperes.

$p$ .	Starting potential.	Potential to maintain current.
8.35 mm. ....	790 volts.	700 volts.
6.5. „ ....	665 „	610 „
3.6 „ ....	515 „	485 „

4. The current in pure hydrogen between the wire and cylinder when the wire was positive was measured for various

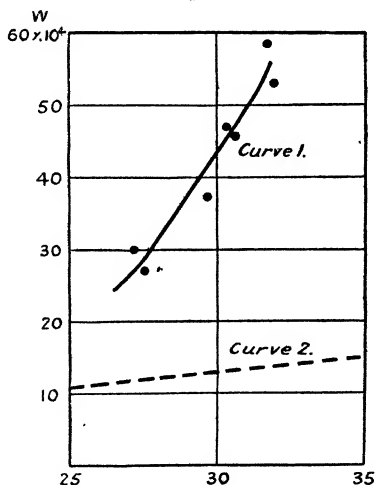
values of the applied potential. A curve giving the current as a function of the applied potential is shown in fig. 3, where the abscissæ ( $V$ ) are the applied potential in volts and the ordinates ( $i$ ) are the currents in microamperes.

Fig. 3.



Relation between current  $i$  and applied potential  $V$ .

Fig. 4.



Velocities of the positive ions in the direction of the electric force as a function of  $X/p$ . The ordinates are  $W$  in cm. per sec. and the abscissæ  $X/p$ ,  $X$  being in volts per cm. and  $p$  in mm. of mercury.

5. The velocity  $W$  of the positive ions in the direction of the electric force may be found from a formula of



Townsend's\*, from the curve fig. 3. The values of  $W$  in terms of the ratio  $X/p$  thus obtained are given by curve 1 of fig. 4,  $X$  being the mean electric force in the space between the cylinders and  $p$  the pressure.

For small values of  $X/p$  it is known that  $W$  is proportional to  $X/p$ , and the velocity under a force of 1 volt per cm. at 1 mm. pressure is given by Van de Graaff† as 4300 cm. per sec. If the ratio of  $W$  to  $X/p$  were constant and equal to 4300  $X/p$  for all values of  $X/p$ , the velocities for values of  $X/p$  from 25 to 35 would be given by curve 2 of fig. 4.

It will be seen that as  $X/p$  is increased  $W$  increases very rapidly. Thus the increases in  $W$  found by Huxley‡ in the monatomic gases are equally present in hydrogen.

In conclusion I wish to thank Professor Townsend for his constant advice and criticism.

XLVI. *The Heat-loss from a Plate embedded in an Insulating Wall.* By F. H. SCHOFIELD, B.A., B.Sc., *Physics Department, National Physical Laboratory, Teddington, Middlesex* §.

#### ABSTRACT.

A MATHEMATICAL treatment of the two-dimensional problem of the steady flow of heat from a rectangular isothermal plate embedded in an insulating wall with rectangular isothermal boundaries. The use of measurements of the electrical resistance of sheet metal as a means for checking and extending the theoretical results is described, and consideration is given to the three-dimensional case of a finite plate within a finite wall as the basis of a simplified apparatus for testing thermal insulators.

#### I. Introduction.

THIS problem arises in connexion with the design of apparatus for measuring the thermal conductivity of heat-insulating materials. Theoretically the best type of apparatus for this purpose is one in which the specimen

\* Phil. Mag. xxviii. p. 83 (1914).

† Phil. Mag. vi. p. 210 (1928).

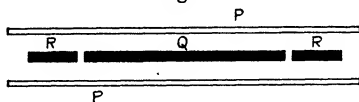
‡ *Loc. cit.*

§ Communicated by the Author.

takes the form of a spherical shell, having a constant source of heat applied internally and means for measuring the steady gradient of temperature maintained between the inner and outer surfaces. A method of this description has, in fact, been used\*, and lends itself to the case of powders or other materials readily adaptable to the spherical form; but where, as is often the case, the material is made up in the form of a flat slab, it becomes necessary to adopt another form of apparatus. One commonly used for the purpose† (see fig. 1) consists of an electrically-heated plate (Q) and guard-ring (R) sandwiched between two layers of the test material, the whole being contained between the water-cooled plates (PP).

The use of the guard-ring is based on the analogy of Kelvin's electrometer; but whereas in the electrical case the plate R must be at a constant potential which is easily adjusted to equality with that of Q, it is not possible in the thermal case to do more than adjust the heat supply to Q and R, so that the contiguous edges of the plates show,

Fig. 1.



on the average, as small a difference of temperature as possible. The heat transfer due to any temperature difference between the hot plate and guard-ring is inversely proportional to the width of the gap between them, and can therefore be reduced by increasing this width. On the other hand, an increased width means a departure from normal flow near the edges of the plate, and a resulting uncertainty as to its "effective" area.

It is proposed to consider whether it is feasible, without serious loss of accuracy, to simplify the apparatus by dispensing with the guard-ring and using a single hot plate. For this purpose account must be taken of the departures from normal flow due to the edges, thickness, and corners of the plate. The treatment below is strictly two-dimensional; but, when taken in conjunction with similar experimental work in three-dimensions, would appear to give the desired heat-loss to a fair degree of accuracy.

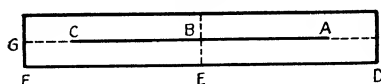
\* Nusselt, *Forsch. Ver. d. Ing.* 1909, pp. 63, 64.

† See, e. g., Poensgen, *Zs. d. Ver. Deutsch. Ing.* lvi. p. 1653 (1912), or Special Report No. 35 of Food Investigation Board (H.M. Stationery Office, 1929).

II. *Edge Effect of Thin Plate.*

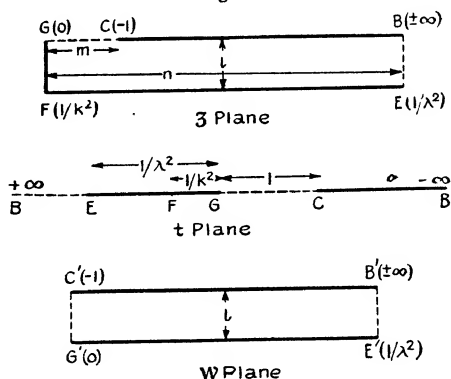
First consider a thin plate of section ABC (fig. 2) surrounded by insulation, with an isothermal boundary DEFG, etc., the whole being infinitely broad in the plane perpendicular to the paper. The flow lines BE and CG, from the

Fig. 2.



centre and edge of the plate respectively, will be straight, and hence it is only necessary to treat the rectangle EFGB. This can be done on the lines previously adopted by the author\* in a similar case, by means of the Christoffel-Schwarz transformation. Since we shall require to deal also with the case in which the length of the rectangle becomes infinite, it is convenient to use a transformation which will allow of the deduction of this case from that of the finite rectangle. Such a transformation is represented in fig. 3. Here the linear dimensions of the  $z$  and  $w$  planes

Fig. 3.



are as indicated, and the lettering in brackets represents the lengths of the corresponding points along the real axis in the  $t$  plane. We follow also the convention previously adopted of showing the boundary isothermals and flow lines as full and dashed lines respectively.

\* Phil. Mag. v. p. 567 (1928).

For the transformation from the  $z$  to the  $t$  plane we have

$$\frac{dz}{dt} = \frac{A}{(t)^{1/2}(t-1/k^2)^{1/2}(t-1/\lambda^2)^{1/2}}.$$

By the substitution  $t=r^2/k^2$  this yields on integration \*

$$z = P \operatorname{sn}^{-1} k(t)^{1/2}, \lambda/k\} + Q.$$

If  $G$  is the origin and  $GF$  the real axis in the  $z$  plane, we have  $Q=0$  and  $P=l/K$ , and hence by inversion

$$\operatorname{sn}\{zK/l, \lambda/k\} = k(t)^{1/2}. \quad (1)$$

The constants  $\lambda$  and  $k$  are given in terms of the linear dimensions  $l$ ,  $m$ , and  $n$  by means of the following relations derived from (1):

$$\frac{l}{n} = \frac{K}{K'} (\operatorname{mod} \lambda/k), \quad (2)$$

$$\begin{aligned} ik &= \operatorname{sn}\{imK/l, \lambda/k\} \\ &= i \frac{\operatorname{sn}}{\operatorname{cn}} \left\{ \frac{mK}{l}, \left(1 - \frac{\lambda^2}{k^2}\right)^{1/2} \right\}. \quad (3) \end{aligned}$$

Similarly, for the transformation from the  $w$  to the  $t$  plane,

$$\frac{dw}{dt} = \frac{B}{(t)^{1/2}(t+1)^{1/2}(t-1/\lambda^2)^{1/2}}.$$

Hence, by substituting  $(t+1)=r^2$ , and calling  $C'$  the origin, and  $C'G'$  the real axis in the  $w$  plane,

$$\operatorname{sn}\left\{\frac{wK}{l}, \frac{\lambda}{(1+\lambda^2)^{1/2}}\right\} = (t+1)^{1/2}. \quad (4)$$

Now eliminating  $t$  and  $k$ , except when it appears in the modulus, between (1), (3), and (4),

$$\begin{aligned} \operatorname{sn}\left\{\frac{zK}{l}, \frac{\lambda}{k}\right\} &= i \operatorname{cn}\left\{\frac{wK}{l}, \frac{\lambda}{(1+\lambda^2)^{1/2}}\right\} \\ &\quad \times \frac{\operatorname{sn}}{\operatorname{cn}}\left\{\frac{mK}{l}, \left(1 - \frac{\lambda^2}{k^2}\right)^{1/2}\right\}. \quad (5) \end{aligned}$$

Then, since  $\lambda$  and  $k$  are known in terms of  $l$ ,  $m$ , and  $n$ , it is clear that equation (5) gives the coordinates  $(x+iy)$  of any point of the  $z$  plane in terms of the coordinates  $(u+iv)$  of the corresponding point of the  $w$  plane, and so gives the distribution of flow lines and isothermals of the former plane

\* Since the integral is to be inverted, it is here written  $\operatorname{sn}^{-1}$  in place of Legendre's  $F$ .

in terms of the rectilinear distribution of the latter. The calculation of the distribution would involve the troublesome process of splitting (5) into real and imaginary parts\*. However, it will be shown below that, provided the semi-length of the plate ( $n-m$ ) is somewhat greater than the thickness ( $l$ ) of the insulation, the distribution in a finite rectangle corresponds closely with that in an infinite rectangle. The latter may be calculated as follows:—Putting  $\lambda=0$ ,  $n$  becomes infinite and equation (5) reduces † to

$$\sin(z\pi/2l) = i \cos(w\pi/2l) \sinh(m\pi/2l). \quad (6)$$

Here the imaginary axes are infinite, *i.e.*, axis of  $y$  in the  $z$  plane and  $v$  in the  $w$  plane, and in order to bring the case into line with others to be dealt with below, it is convenient to turn the axes in both planes through a right angle. Equation (6) then reads

$$\sinh(z\pi/2l) = \cosh(w\pi/2l) \sinh(m\pi/2l). \quad (7)$$

The complete distribution of flow lines and isothermals may be calculated from (7) by use of tables or graphs ‡ of trigonometric functions of a complex variable. Thus for the intersection of any flow line ( $u=\text{constant}$ ) with any isothermal ( $v=\text{constant}$ ), the real and imaginary parts of  $\cosh[(u+iv)\pi/2l]$  could be read off and, after multiplying by the constant  $\sinh(m\pi/2l)$ , the inverse sinh-function would give the coordinates  $x$  and  $y$ . Alternatively (7) can be split into real and imaginary parts and solved for  $x$  and  $y$  respectively. This would yield:

$$\frac{\cosh^2(u\pi/2l) \cos^2(v\pi/2l)}{\cosh(x\pi/l) - 1} + \frac{\sinh^2(u\pi/2l) \sin^2(v\pi/2l)}{\cosh(x\pi/l) + 1} = \frac{1}{2 \sinh^2(m\pi/2l)} \quad (8)$$

$$- \frac{\cosh^2(u\pi/2l) \cos^2(v\pi/2l)}{1 + \cos(y\pi/l)} + \frac{\sinh^2(u\pi/2l) \sin^2(v\pi/2l)}{1 - \cos(y\pi/l)} = \frac{1}{2 \sinh^2(m\pi/2l)} \quad (9)$$

\* See method suggested in previous paper, p. 570.

†  $K(\text{mod } 0) = \pi/2$ ,  $\text{sn}(u, 0) = \sin u$ ,  $\text{cn}(u, 0) = \cos u$ ,  $\text{sn}(u, 1)/\text{cn}(u, 1) = \tanh u/\text{sech } u = \sinh u$ . See, *e.g.*, Dixon's 'Elliptic Functions,' p. 69 (Macmillan & Co.).

‡ Johnston, Proc. Phys. Soc. xxiii. p. 344 (1911); Kennelley's 'Tables of Complex Hyperbolic and Circular Functions.' Also 'Chart Atlas' of same (Harvard Univ. Press, 1914).

These equations are quadratics in  $\cos(y\pi/l)$  and  $\cosh(x\pi/l)$  respectively, and taking a value of  $m=l$  we have calculated the points of intersection of the flow lines  $u=l/4, 2l/4, 3l/4, \dots$  with the isothermals  $v=l/4, 2l/4, 3l/4, \dots$ . The result is shown on the left-hand side of fig. 4. For purposes of comparison, on the right hand of fig. 4 is shown the distribution when the boundary GF is moved to infinity. This case was originally treated by Clerk-Maxwell\* without the aid of the Christoffel-Schwarz transformation, but the data can readily be obtained from equation (7). Thus, transferring the origin in the  $z$  plane to C, so that  $z$  is replaced by  $(z' + m)$ , we have

$$\begin{aligned}\cosh(w\pi/2l) &= \sinh\{(z' + m)\pi/2l\} \div \sinh(m\pi/2l) \\ &= \sinh(z'\pi/2l) \coth(m\pi/2l) + \cosh(z'\pi/2l); \end{aligned}$$

so that, when  $m$  is infinite,

$$\cosh(w\pi/2l) = e^{z'\pi/2l}. \quad (10)$$

Hence by taking the logarithms and splitting into real and imaginary parts,

$$y = (2l/\pi) \tan^{-1} \{\tanh(u\pi/2l) \tan(v\pi/2l)\}, \quad (11)$$

$$\begin{aligned}x' &= (l/\pi \log \{\cosh^2(u\pi/2l) \cos^2(v\pi/2l) \\ &\quad + \sinh^2(u\pi/2l) \sin^2(v\pi/2l)\}). \quad (12)\end{aligned}$$

Comparing the two halves of fig. 4, it will be observed that the effect of moving the boundary GF to infinity only produces a slight displacement in the lines of flow from the plate, and that in each case the spacing of the isothermals and flow lines becomes practically normal at a short distance from the edge. Since the effect of the edge dies rapidly away, it is clear that the total heat-loss from a finite rectangle of moderate length will not differ greatly from that of the same length of an infinite rectangle. The difference between the two cases can be calculated as follows:—

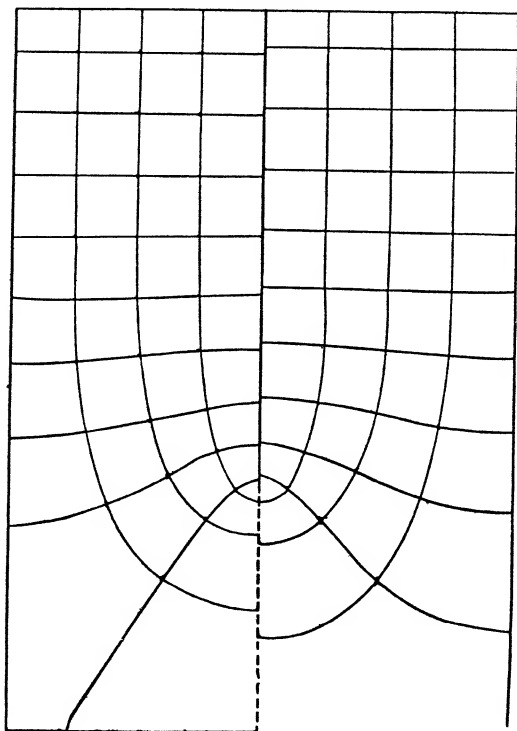
The total heat flow across a strip of width  $l$  and length BC (see fig. 3,  $z$  plane) is equal to the flow across a strip of the same width and length B'C' in the  $w$  plane, where the flow is entirely normal. If there were no edge at C, so that the side of the rectangle extended indefinitely in the direction BC, the flow from BC would also be normal. Hence we

\* 'Electricity and Magnetism,' i. para. 195 and fig. xi.

may regard the effect of the edge on the heat-flow across the strip as adding a length  $X$ , which is given by

$$\begin{aligned} X &= B'C' - BC \\ &= m - l \{ K'/K (\text{mod } \lambda/k) - K'/K (\text{mod } \lambda/(1+\lambda^2)^{1/2}) \}. \quad (13) \end{aligned}$$

Fig. 4.



The corresponding effect of the edge in the case of a rectangle extending to infinity in the direction  $CB$  (fig. 3) is obtained by putting  $\lambda=0$ . Hence

$$\begin{aligned} [X]_{n=\infty/2} &= m - (2l/\pi) \text{Lt}_{\lambda=0} [\log 4k/\lambda - \log 4(1+\lambda^2)^{1/2}/\lambda] \\ &= m - (2l/\pi) \text{Lt}_{\lambda=0} [\log k], \end{aligned}$$

or substituting for  $k$  the value given by (3) and the footnote to (6),

$$[X]_{n=\infty/2} = m - (2l/\pi) \log \sinh (m\pi/2l). \quad (14)$$

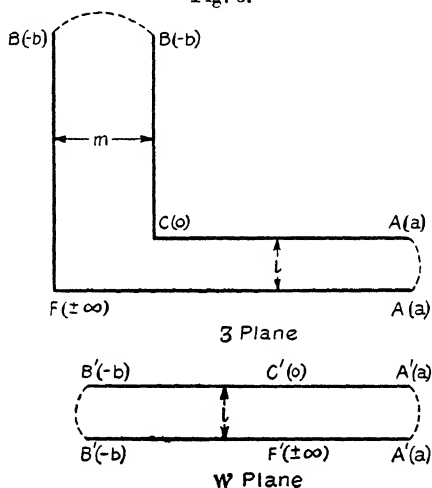




III. *Comparison of Thin and Square Edge.*

In the preceding section it was shown that the disturbing effect of a thin edge rapidly dies away. The effect in the case of a thick plate might be expected to be even more restricted. To obtain a more precise idea of the limits of disturbance, we may compare the extreme cases of an infinitely thin and infinitely thick plate. For the latter a convenient transformation\* is that shown in fig. 5. Here the two boundary flow lines are wholly at infinity,

Fig. 5.



and are shown as curved dashed lines, following the convention previously used by the author. The transformation yields

$$dz/dt = M(t)^{1/2}(t-a)^{-1}(t+b)^{-1}, \quad \dots \quad (16)$$

$$dw/dt = N(t-a)^{-1}(t+b)^{-1}. \quad \dots \quad (17)$$

Integrating, we have

$$z = \frac{2M}{(a+b)} \left\{ (b)^{1/2} \tan^{-1} \left( \frac{t}{b} \right)^{1/2} - (a)^{1/2} \tanh^{-1} \left( \frac{t}{a} \right)^{1/2} \right\} + P, \quad \dots \quad (18)$$

$$w = \frac{N}{(a+b)} \log \frac{(t-a)}{(t+b)} + Q. \quad \dots \quad (19)$$

\* For the particular purpose required here this transformation is perhaps more convenient than that given in Jeans's 'Electricity and Magnetism' (4th edition), p. 277.

If the origins are C and C' and the real axes are CA and C'A' in the respective planes,

$$l = \frac{M\pi a^{1/2}}{(a+b)}, \quad m = \frac{M\pi b^{1/2}}{(a+b)}, \quad P=0 \quad . \quad . \quad (20)$$

$$l = \frac{N\pi}{(a+b)}, \quad Q = -\frac{N}{(a+b)} \log\left(-\frac{a}{b}\right), \quad . \quad (21)$$

and (18) may be written

$$z = + (2m/\pi) \tan^{-1}(t/b)^{1/2} - (2l/\pi) \tanh^{-1}(t/a)^{1/2}. \quad (22)$$

Now the spacing of the flow lines or flux density at any point  $(x, 0)$  along the real axis is given by

$$\frac{\partial u}{\partial x} = \frac{N}{M(t)^{1/2}} = \left(\frac{a}{t}\right)^{1/2} \quad . \quad . \quad . \quad (23)$$

At an infinite distance along the  $x$ -axis  $\partial u/\partial x = 1$ . If we wish to find the position of a point P of coordinates  $(p, 0)$ , such that the flux density at this point differs by a certain amount, say 1 per cent. from its final value of 1 at infinity, we express  $p$  in terms of  $(a/t)^{1/2}$ , for which the value 1.01 is then substituted. Thus

$$p = (2l/\pi) \tanh^{-1}(1/1.01) - (2m/\pi) \tan^{-1}(l/m \times 1.01). \quad (24)$$

For the thin plate we have from (7), putting  $y$  and  $v=0$ ,

$$\sinh(x\pi/2l) = \cosh(u\pi/2l) \sinh(m\pi/2l), \quad . \quad (25)$$

and hence by differentiation

$$\cosh(x\pi/2l) = -\sinh(m\pi/2l) \sinh(u\pi/2l) [\partial u/\partial x]. \quad (26)$$

On eliminating  $u\pi/2l$  between (25) and (26),

$$\sinh^2(x\pi/2l) - \cosh^2(x\pi/2l) [\partial x/\partial u]^2 = \sinh^2(m\pi/2l).$$

$$\therefore \cosh(x\pi/2l) = \cosh(m\pi/2l) \div [1 - (\partial x/\partial u)^2]^{1/2}. \quad (27)$$

$x$  is measured from G (fig. 3), and hence, if  $p$  is the distance from the edge C at which  $\partial u/\partial x = 1.01$ , we have

$$p + m = \frac{2l}{\pi} \cosh^{-1} \left\{ \frac{\cosh(m\pi/2l)}{0.1404} \right\} \quad . \quad . \quad (28)$$

Comparing the formulæ (24) and (28), we have the following values for the thin edge and square edge.

TABLE II.

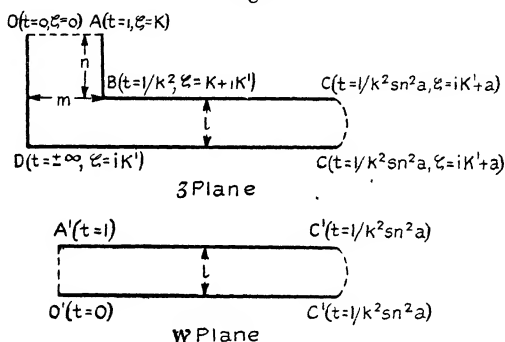
$p$  is the distance from the edge beyond which the flux density is within 1 per cent. of its final value.

$m/l$ .	$p/l$ .	
	Thin edge.	Square edge.
0	1.69	1.69
0.5	1.37	1.34
1.0	1.28	1.19
2.0	1.25	1.10
3.0	1.25	1.08
$\infty$	1.25	1.06

#### IV. Edge Correction for Thick Plate.

It is clear from the argument above that a plate of finite thickness may, if of moderate length, be assumed to be

Fig. 6.



infinitely long. This case, of an infinitely long thick plate (figs. 6 or 8), has already been treated by Cockcroft\*, but for our present purpose it is convenient to develop an alternative solution, using for the  $z$ -plane transformation one already employed by the author†. We treat one half of the figure as divided by the line of symmetry  $AO$  (see fig. 6),  $2n$  being the thickness of the plate. Then, as already shown, the several dimensions are given by

$$\frac{m}{l} = \frac{2K}{\pi} \left\{ \frac{\operatorname{sn} a \operatorname{dn} a}{\operatorname{cn} a} - Z(a) \right\}, \quad \dots \quad (29)$$

\* Journ. Inst. Elect. Eng. lxi. p. 403 (1928).

† Loc. cit. pp. 578-580 and 591.

$$\frac{n}{l} = \frac{2K'}{\pi} \left\{ \frac{\operatorname{sn} a \operatorname{dn} a}{\operatorname{cn} a} - Z(a) \right\} - \frac{a}{K}. \quad (30)$$

$$BC = \frac{l}{\pi} \log \left\{ \frac{\operatorname{sn} 2a \Theta(2a)}{\Theta(0)} \right\} - m \left( 1 - \frac{a}{K} \right) - \frac{l}{\pi} \operatorname{Lt}_{\epsilon=0} [\log \operatorname{sn} \epsilon]. \quad (31)$$

Here the infinite length BC is obtained by putting  $t=1/k^2 \operatorname{sn}^2(a+\epsilon)$  and taking the limit for  $\epsilon=0$ .

For the transformation from the  $w$  to the  $t$  plane

$$dw/dt = Pt^{-1/2}(t-1)^{-1/2}(t-1/k^2 \operatorname{sn}^2 a)^{-1}, \quad (32)$$

which, on integration and evaluation of the constants,  $O'$  being the origin and  $O'C'$  the real axis in the  $w$  plane, gives

$$w = \frac{l}{\pi} \log \left\{ \frac{t^{1/2} - k \operatorname{sn} a + \operatorname{dn} a (t-1)^{1/2}}{-t^{1/2} - k \operatorname{sn} a + \operatorname{dn} a (t-1)^{1/2}} \times \frac{t^{1/2} k \operatorname{sn} a + 1}{t^{1/2} k \operatorname{sn} a - 1} \right\}. \quad (33)$$

To obtain the infinite length  $O'C'$ , we proceed in the manner already adopted for the  $z$  plane :

$$O'C' = \operatorname{Lt}_{\epsilon=0} \left[ \frac{l}{\pi} \log \left\{ \frac{1 - k^2 \operatorname{sn} a \operatorname{sn}(a+\epsilon) + \operatorname{dn} a \operatorname{dn}(a+\epsilon)}{-1 - k^2 \operatorname{sn} a \operatorname{sn}(a+\epsilon) + \operatorname{dn} a \operatorname{dn}(a+\epsilon)} \times \frac{\operatorname{sn} a + \operatorname{sn}(a+\epsilon)}{\operatorname{sn} a - \operatorname{sn}(a+\epsilon)} \right\} \right],$$

which can be shown to reduce to

$$O'C' = \frac{l}{\pi} \log \left\{ \frac{2 \operatorname{dn} a}{k^2 \operatorname{sn} a \operatorname{cn} a} \right\} - \frac{l}{\pi} \operatorname{Lt}_{\epsilon=0} [\log \operatorname{sn} \epsilon]. \quad (34)$$

We may consider the effect of the edge as follows:— If the heat flow from AB and BC had been normal, it would have been equivalent to the flow across a strip of width  $l$  and length  $(BC + nl/m)$ . Actually the flow from AB plus BC is equal to the normal flow across a strip of width  $l$  and length  $O'C'$ , since the latter is the length in the  $w$  plane equivalent to AB plus BC in the  $z$  plane. Hence the effect of the edge is equivalent to the addition, to a strip of width  $l$ , of a length  $X$  given by

$$\begin{aligned} X &= O'C' - BC - nl/m \\ &= \frac{l}{\pi} \log \left\{ \frac{2 \operatorname{dn} a \Theta(0)}{k^2 \operatorname{sn} a \operatorname{cn} a \operatorname{sn} 2a \Theta(2a)} \right\} + m \left( 1 - \frac{a}{K} \right) - \frac{nl}{m}. \end{aligned} \quad (35)$$

The problem treated above involves three finite dimensions, and its solution as given by equations (29), (30), and (35) may be checked by degenerating it to obtain the solutions for three marginal cases, each involving two finite dimensions.

*Case 1:  $n/l=0$ .*

This is obtained by putting  $k=1$ , which gives the following degenerations:

$$K=\infty, \quad K'=\pi/2, \quad \operatorname{sn} a=\tanh a, \quad \operatorname{cn} a=\operatorname{dn} a=\operatorname{sech} a,$$

$$Z(a)=(\tanh a - a/K), \quad \Theta(2a)/\Theta(0)=\cosh 2a;$$

so that

$$m/l=2a/\pi,$$

$$n/l=0,$$

$$\begin{aligned} X &= m + \frac{l}{\pi} \log \left( \frac{2}{\tanh a \tanh 2a \cosh 2a} \right), \\ &= m - (2l/\pi) \log \sinh (m\pi/2l), \quad . \quad . \quad . \quad (36) \end{aligned}$$

which agrees with (14) above.

*Case 2:  $m/l=\infty$ .*

This is obtained by putting  $k=1$  and  $a=K-\beta$ , where  $\beta$  is a finite quantity,  $K$  of course being infinite. Then

$$Z(K-\beta)=\beta/K=0,$$

$$\frac{\operatorname{sn}(K-\beta) \operatorname{dn}(K-\beta)}{\operatorname{cn}(K-\beta)} = \frac{\operatorname{cn} \beta}{\operatorname{sn} \beta \operatorname{dn} \beta} = \frac{1}{\tanh \beta};$$

so that

$$\frac{m}{l} = \frac{2K}{\pi} \left( \frac{1}{\tanh \beta} - \frac{\beta}{K} \right) = \infty,$$

$$\frac{n}{l} = \frac{1}{\tanh \beta} - 1,$$

and hence

$$\tanh \beta = l/(n+l)$$

or

$$\beta = \frac{1}{2} \log \left( \frac{2l+n}{n} \right).$$

In dealing with the expression for  $X$ , we have

$$\frac{\operatorname{dn}(K-\beta)}{\operatorname{sn}(K-\beta) \operatorname{cn}(K-\beta)} = \frac{\operatorname{dn} \beta}{\operatorname{sn} \beta \operatorname{cn} \beta} = \frac{1}{\tanh \beta},$$

$$\Theta(2K-2\beta)/\Theta(0)=\cosh 2\beta,$$

and hence

$$\begin{aligned} X &= \frac{l}{\pi} \log \left\{ \frac{2}{\tanh \beta \tanh 2\beta \cosh 2\beta} \right\} + m \left( 1 - \frac{K - \beta}{K} \right) \\ &= \frac{2l}{\pi} \log \left( \frac{1}{\sinh \beta} \right) + \frac{2l\beta}{\pi \tanh \beta} \\ &= \frac{2l}{\pi} \log \left( \frac{2l+n}{l} \right) + \frac{n}{\pi} \log \left( \frac{2l+n}{n} \right), \quad . . . . (37) \end{aligned}$$

which agrees with J. J. Thomson's \* solution for this marginal case.

Case 3:  $n/l = \infty$ .

This is obtained by putting  $k=0$ , which gives

$$\operatorname{sn} a = \sin a, \quad \operatorname{cn} a = \cos a, \quad \operatorname{dn} a = 1, \quad Z(a) = 0, \quad \Theta(2a)/\Theta(0) = 1,$$

$$K = \pi/2, \quad K' = \log(4/k) = \infty;$$

so that

$$m/l = \tan a,$$

$$n/l = (2K'/\pi) \tan a - a/K = \infty.$$

From these two latter

$$\frac{nl}{m} = \frac{2l}{\pi} K' - \frac{2l^2}{m\pi} \tan^{-1} \left( \frac{m}{l} \right),$$

$$m \left( 1 - \frac{a}{K} \right) = \frac{2m}{\pi} \left[ \frac{\pi}{2} - \tan^{-1} \left( \frac{m}{l} \right) \right] = \frac{2m}{\pi} \tan^{-1} \left( \frac{l}{m} \right).$$

Further,

$$\begin{aligned} \frac{l}{\pi} \log \frac{2 \operatorname{dn} a \Theta(0)}{k^2 \operatorname{sn} a \operatorname{cn} a \operatorname{sn} 2a \Theta(2a)} &= \frac{l}{\pi} \log \frac{1}{k^2 \sin^2 a \cos^2 a} \\ &= \frac{2l}{\pi} \log \left( \frac{4}{k} \right) + \frac{2l}{\pi} \log \left( \frac{m^2 + l^2}{4ml} \right). \end{aligned}$$

Hence,

$$X = \frac{2l}{\pi} \left\{ \log \left( \frac{l^2 + m^2}{4lm} \right) + \frac{m}{l} \tan^{-1} \frac{l}{m} + \frac{l}{m} \tan^{-1} \frac{m}{l} \right\}, \quad (38)$$

which agrees with J. J. Thomson's † solution for this marginal case.

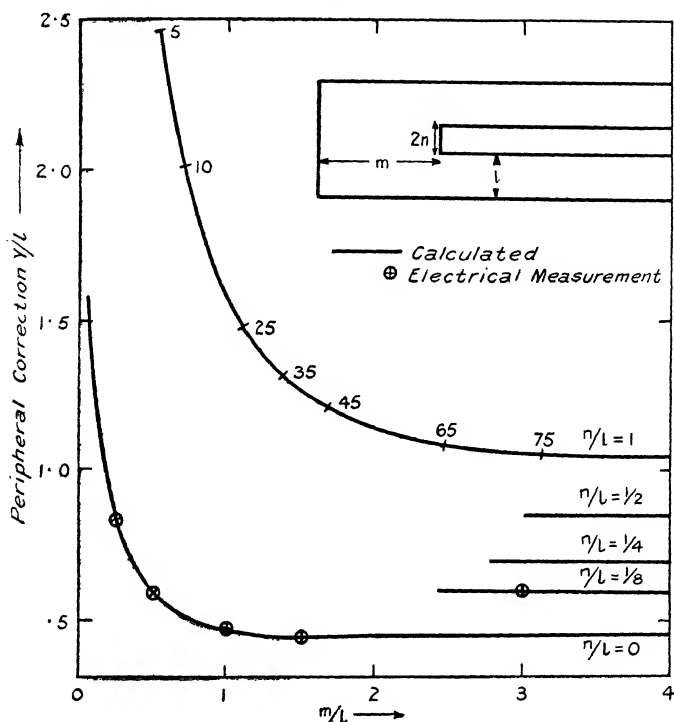
\* *Loc. cit.* p. 219.

† *Loc. cit.* p. 222, or see form given in Jeans's 'Electricity and Magnetism' (4th edition), p. 277.

## V. Calculation of "Edge" or "Peripheral" Correction.

For the purpose of calculation from equations (29), (30), and (35) use may be made of the tables of  $\Theta$  and allied functions due to Greenhill and Hippisley\*. The equation (35) gives the correction (X) for the "edge" proper, *i.e.*, the total heat-flow less that which would be given by the normal flow from AB plus BC (fig. 6). Since we

Fig. 7.



are concerned mainly with comparatively thin plates, it is convenient to use a correction, which may be called the "peripheral correction," representing the total heat-flow less the normal flow from BC only. This peripheral correction (Y) is obtained from (35) by omission of the last

\* 'Smithsonian Mathematical Formulæ and Tables of Elliptic Functions' (Publication No. 2672, Washington, 1922).

term, and can be expressed as follows, in the notation used in the tables, the argument  $r$  being equal to  $90a/K$ :

$$\frac{Y}{l} = \frac{1}{\pi} \log \left\{ \frac{2(k')^{3/2} C(r) D(r)}{k^2 A(r) B(r) A(2r)} \right\} + \frac{m}{l} \left( 1 - \frac{r}{90} \right). \quad (39)$$

When  $2r$  is greater than  $90^\circ$ ,  $A(2r)$  is replaced by  $B(s)$ , where  $s = 2r - 90$ .

Similarly, equations (29) and (30) become

$$\frac{m}{l} = \frac{2K}{\pi} \left\{ \frac{A(r)C(r)}{B(r)D(r)} - E(r) \right\}, \quad . \quad . \quad . \quad (40)$$

$$\frac{n}{l} = \frac{2K'}{\pi} \left\{ \frac{A(r)C(r)}{B(r)D(r)} - E(r) \right\} - \frac{r}{90}. \quad . \quad . \quad (41)$$

If, for example, we wish to obtain for a constant  $n$  the variation of  $Y$  with  $m$ , we can from (40), using any modulus  $k$ , get the value of  $r$  to give the required value for  $n/l$ , and hence calculate  $m/l$  and  $Y/l$ . This has been done for the case  $n=l$  with the result shown in fig. 7, the figures written against the curve being the respective angles of modulus. It will be seen that the value of the correction is rapidly asymptotic to its final value, given by equation (37), for an infinite value of  $m$ . The curve for the thin plate ( $n/l=0$ ), calculated for (14), is even more rapidly asymptotic.

## VI. *Electrical Determination of Effect of shape, etc.*

It has been pointed out in a former paper \* that the effect on the flow of heat of shape and other complexities of structure may be determined by measurements based on electrical analogy. Thus, in the case of three-dimensional problems, the measurement of the capacity of an air-condenser of the correct shape or of the resistance of an electrolyte contained within cells reproducing the appropriate boundary conditions can be made to give the required information. In the paper referred to, two-dimensional cases were treated by the simple plan of measuring the resistance of a sheet of metal cut to the required shape.

The main difficulty in carrying out this plan consists in so attaching the electrodes as to reproduce accurately the boundary conditions. Theoretically the electrodes should be of negligible resistance, as compared with the sheet, and make perfect contact with it along the desired lines. The

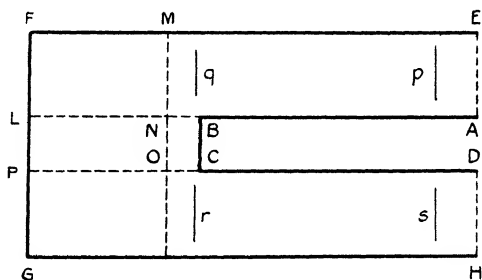
\* J. H. Awbery and F. H. Schofield, "Effect of Shape on Heat-loss through Insulation" (5th Internat. Congress on Refrigeration, 1928).



lines in question may correspond either with the boundary isothermals or the boundary flow lines—since in any particular problem the two sets of lines are interchangeable—the choice being made so as to reduce to a minimum the errors due to failure to comply with the ideal requirements set out above.

If we take as an example the heat-flow from a thick plate to a rectangular isothermal boundary, a semi-section of which is shown in fig. 8, the isothermals ABCD and EFGH are seen to be of considerable length, and any failure to attach electrodes accurately and in good contact along them, particularly near BC, would be likely to give rise to serious error. Inverting the problem, however, the electrodes could be attached along the lines EA and DH, which are comparatively short and are situated in a region of normal flow.

Fig. 8.



The resistance of the sheet between these lines is then directly proportional, instead of inversely proportional as in the other case, to the required heat-flow.

In the experiments previously described, the metal sheet consisted of thin lead foil, which allowed of the making of very rapid measurements of moderate accuracy. For our present purpose the attempt has been made to increase considerably the accuracy, and to this end a number of modifications have been introduced. Brass sheet was used, 1.6 mm. in thickness, so as to reduce errors due to inequalities of a very thin sheet, and about  $40 \times 120$  cm. in area. The contacts at EA and DA were made by clamping the brass sheet between heavy copper bars with an interleaving of lead foil. The resistance measurements were made by comparing the potential drop on the strip and on a standard resistance in series with it, a steady current of 10 amps. being passed through the two. The usual precautions were adopted of

taking readings before and after reversals of the current and potential leads. The potential contacts were needle-points resting on the lines  $p$  and  $s$ , taken at such a distance from the electrodes that a traverse of the lines showed variations of E.M.F. not exceeding 0·1 per cent. After a measurement of resistance, taken from the mean of a number of readings across the potential lines, had been made, the strip was cut through on a line parallel to FG and the process repeated. Finally, after the measurement for the line through M (near BC), cuts were made along BN and CO and the normal resistance of the sides was determined between the respective pairs of potential lines  $pg$  and  $rs$ . Throughout the experiments the temperature of the sheet was measured by means of a thermocouple soldered to a thin copper disk which could be pressed on to the sheet. A number of readings were taken along the central flow line, and the mean temperature so obtained was used to reduce all resistance values to a common temperature.

The results of the determinations of edge correction for a thin plate (see fig. 2, or fig. 8 with  $BC=0$ ) are given in the following Table, together with the theoretical values calculated from equation (14):—

TABLE III.  
Edge Correction for Thin Plate.

$m/l$ .	$X/l$ by	
	Electrical measurement.	Calculation.
$\infty$	—	0·442
1·5	0·447	0·447
1	0·470	0·470
0·5	0·587	0·590
0·25	0·822	0·831

It will be seen that there is a good agreement between the experimental and theoretical values. The former were obtained as the differences between two comparatively large quantities, and the maximum error, of the order of 1 per cent., shown in the above Table is only equivalent to an uncertainty of about 1 part in 1000 on the resistance measurements.

An example of the use of resistance measurements on a sheet of metal to determine corrections not amenable to calculation is afforded by the following case:—Suppose a hot plate ABCD (fig. 8) to be surrounded by two slabs of

material ALFE and HGPD, the conductivity of which is required, and that it is not convenient to cut the slab material so as to fill with it the gap LBCP. It is proposed to ascertain the effect of inserting into the gap material of somewhat different conductivity. Taking relative dimensions such as might be met with in practice, viz., 5 cm. for EA ( $l$ ), 1.25 cm. for BC ( $2n$ ), 15 cm. for LB ( $m$ ), and 15 cm. for AB, a specimen was made up of this size in sheet brass 0.6 cm. thick. After measurement of its resistance, as above described, the area LBCP was milled out to about  $\frac{3}{4}$  and then  $\frac{1}{2}$  of its previous thickness, corresponding to the thermal conductivity of this portion, being respectively 25 and 50 per cent. greater than that of the remainder. The reverse case of a material of less conductivity than the rest could be reproduced by milling away the whole of the strip except LBCP, but as a simpler plan, though one of less accuracy, a sheet of tinned iron was taken with an extra thickness, lightly soldered along the edges, over the area in question. The results of the experiments are given in the Table below.

TABLE IV.

Peripheral Correction for Fig. 8 when Area LBCP  
is  $t$  times the Thickness of Remainder.

$t$ .	$Y_t \div l$ .	
	Electrical measurement.	Equation (42).
$\infty$	—	<b>0.442</b>
2	0.54 <sub>3</sub>	0.51 <sub>7</sub>
1	0.58 <sub>5</sub>	<b>0.592</b>
0.69	0.63 <sub>9</sub>	0.65 <sub>9</sub>
0.44	0.70 <sub>5</sub>	0.78 <sub>3</sub>

For purposes of comparison a theoretical estimate of the correction may be attempted. Thus, calling  $Y_t$  the peripheral correction when the thickness of LBCP is  $t$  times that of the remainder, we have  $Y_1$  given generally by equation (35), or where, as in the present case, LB is large, by equation (37). Further, when  $t = \infty$ , corresponding to the case of a perfect thermal insulator in the gap LBCP, it is clear that the correction becomes identical with that for a thin edge, and is, therefore, given by equations (14) or (15), as the case may be. Hence we try the following simple formula for the case taken above, in which  $Y_\infty = 0.442l$  and  $Y_1 = 0.592l$ :

$$Y_t = Y_\infty + (Y_1 - Y_\infty)/t. \quad . \quad . \quad . \quad (42)$$

It will be seen that there is a rough agreement between the formula and experiment. In the case of the interpolated value the divergence would be near its maximum for the position taken, and for most cases of interpolation, *i. e.*, with the space LBCP having a material of less conductivity than the rest, the formula (42) could apparently be used with sufficient accuracy for practical purposes.

## VII. Application of Results to Finite Rectangular Plate.

In considering the bearing of the two-dimensional results given above on the problem of a finite rectangular plate contained within a finite wall, reference may be made of the experiments of Langmuir, Adams, and Meikle\*. By measuring the resistance of an electrolyte of the appropriate shapes they were able to make an analysis of the corrections applicable to the case of one rectangular parallelopiped contained within another, the gap between the two being constant. It was shown that the departure from normal flow was divisible into two parts, namely, the two-dimensional edge corrections and the three-dimensional corner corrections. As regards the former, it is interesting to note that the correction for a thin edge was given as 0.93, as against the theoretical value of 0.940 † found in the present investigation, while for a square edge the value was 0.54, as against the theoretical value of 0.558 ‡. The correction for the total eight corners was relatively small, being given as 0.357 for a thin plate and 1.27 for a thick plate. For a single plate embedded in a uniform thickness of insulation the formulæ of Langmuir could be used, or, as an alternative for the edge corrections, those given in this paper. Such an apparatus could very well be employed for testing thermal insulators, but would have the disadvantage that the four end plates FG (fig. 8) would have to be maintained strictly isothermal with the main plates FE and GH, *e. g.*, by water-cooling. However, by increasing the overlap of the main plates so that the length LB(*m*) becomes considerably greater than the length EA(*l*), the edge correction becomes independent of *m*, and the need for accurate temperature control of the end plates becomes less important.

Thus it has been shown above for a moderately thin plate that, if the overlap *m* and the semi-width (*a*/2) of the plate are each of the order of 2*l* the peripheral correction Y

\* Trans. Electrochem. Soc. xxiv. p. 53 (1913).

† *I. e.* twice the value shown in line 3 of Table III.

‡ Jeans, 'Electricity and Magnetism,' p. 279.

will be given by (37). The correction  $X$  for the four short square edges, each of length  $2n$ , would be given by (38), and, assuming the corner correction to be unaltered, we should have for the complete shape-factor  $S$ ,

$$S = (2a^2/l) + (8a Y/l) + 8n X/l + 0.35 l.$$

Taking the following as a numerical example, viz., 40 cm. for the side  $a$  of the plate, 6 cm. for the thickness  $l$  of the insulation, 1.5 cm. for  $2n$  the thickness of the plate, and 18 cm. for the overlap  $m$ , we should find that  $Y$  was 0.592  $l$  and  $X$  0.762  $l$ , and hence

$$S = 533 + 189 + 5 + 2.$$

We observe that the fourth, or three-dimensional, term of the equation is very small, and that a large error in its coefficient could be tolerated without appreciably affecting the total.

As to the construction of the hot plate, the usual procedure of clamping an electric heater between thick metal plates could be followed, but in view of the increased flux-density towards the edges (see fig. 4), it would be as well to have independent heating elements for the marginal and central portions of the plate. By this device, and the use of plates of sufficient thickness and conductivity, it should be possible to secure a reasonable uniformity of temperature over the hot plate.

In conclusion, the author wishes to acknowledge the assistance received from Mr. C. R. Barber, Junior Observer at the National Physical Laboratory, in the electrical measurements and calculations.

**XLVII. *Electrical Conductivity Measurements at low Temperatures.*** By Prof. J. C. McLENNAN, *F.R.S.*, J. F. ALLEN, *M.A.*, and J. O. WILHELM, *M.A.*\*

**D**URING the course of an investigation on superconductivity, a number of elements, alloys, and compounds were examined which did not show this phenomenon over the temperature range available. The substances on which the measurements were made do not fall into any definite group. The measurements represent, however, the result of following up various lines of attack which suggested themselves during the investigation.

\* Communicated by the Authors.

It has been found \* that alloys composed of a superconductor and an element of the fifth group have a higher superconducting point than that of the superconductor alone. With this in mind, various metals alloyed with those of the fifth group were examined in the hope that their superconducting point which existed would be raised sufficiently so as to fall within our temperature range. These alloys were Ag-Bi, Cu-Bi, Cd-Bi, Mn-Bi, Ag-Sb, Cd-Sb, Cu-As, and Au-As. The radioactive element Po was also examined. It was expected that this substance would show signs of superconductivity, since it degenerates into an isotope of lead. The rare earth elements Ce and La were then studied, since their position in the periodic table of the elements lies close to several of the superconductors. Also alloys of these rare earth metals with lead were examined in order to determine their effect on its superconductivity.

The discovery of the superconductivity of CuS by Meissner † recently led us to examine other common sulphides, namely, PbS, AgS, FeS, and Bi<sub>2</sub>S<sub>3</sub>. The result of the investigation on PbS showed that it became superconducting at 4°·2 K. This was the only sulphide to show the phenomenon. Other substances Cd-Zn, Ag-Cl<sub>2</sub>, and a Heusler alloy were also examined.

Various methods were used in the preparation of samples for measurement. Many of the alloys were made by fusion in a pyrex tube, the molten mixture then being strained through glass wool and allowed to solidify in a capillary tube. When the glass was cracked off, current and potential leads of fine copper wires were soldered or fastened with copper clips to the rod thus formed. Other substances of higher melting-point were fused and cast in a carbon tube resistance furnace. Several metals such as Ce, La, and the Heusler alloys were in the form of blocks or large rods, from which small rods suitable for measurement were sawn. The results obtained are given in Tables I. to XX. and plotted in figs. 1 to 5.

#### I.—Ag-Bi, Cu-Bi, Cd-Bi, Mn-Bi.

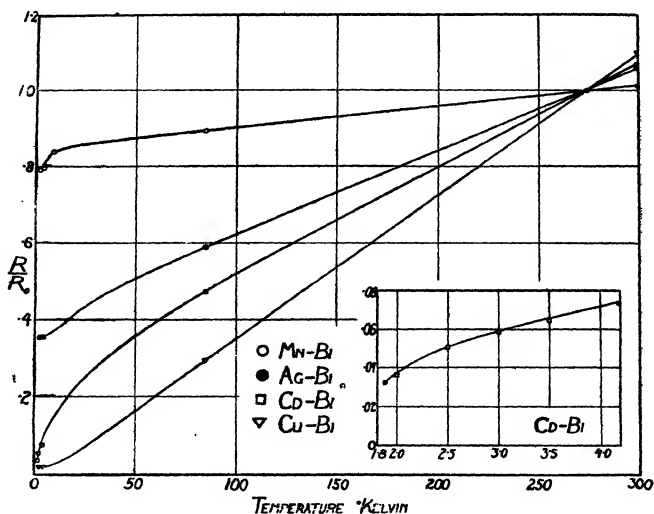
The first three of these were prepared in pyrex tubes and the fourth, Mn-Bi, being of higher melting-point was

\* McLennan, Allen, and Wilhelm, Trans. Roy. Soc. Can. xxiv. Sect. III. (1930).

† Meissner, *Zeit. für Phys.* lviii. p. 570 (1929).

fused in a carbon furnace. Ag-Bi, Cd-Bi, and Mn-Bi are eutectic alloys, while Cu-Bi is a solid solution. Ag and Cu were expected to show signs of superconductivity on being alloyed with Bi since Au-Bi is known to be a superconductor. However, at a temperature of  $1^{\circ}9\text{K.}$ , none of the alloys had become superconducting. Cd, which was at one time thought to be superconducting, was also expected to exhibit this phenomenon on alloying with Bi. The alloy, however, does not, although its curve bends down sharply towards the temperature axis as though

Fig. 1.



it would become superconducting between  $1^{\circ}0$  and  $1^{\circ}5\text{K.}$  The Mn-Bi also shows quite a pronounced drop in resistance near the low-temperature end of the curve, and a further extension of the curve down to lower temperatures might prove it to become superconducting. The readings for these alloys are given in Tables I., II., III., and IV. and curves for them are plotted in fig. 1.

## II.—Ag-Sb, Cd-Sb, Cu-As, Au-As.

These again were all eutectics with the exception of Cd-Sb, which was a 60 per cent. Sb alloy. Being alloys containing a member of the fifth group of elements, it was

TABLE I.—Mn—Bi.

T° K.	R (microhms).	R/R <sub>0</sub> .
300	1303	1.015
273	1285	1.000
85	1149	.894
9	1067	.838
4.2	1027	.799
2.0	1020	.794

TABLE II.—Ag—Bi.

T° K.	R (microhms).	R/R <sub>0</sub> .
300	3581	1.060
273	3380	1.000
85	1990	.589
4.2	1199	.354
2.0	1190	.352

TABLE III.—Cd—Bi.

T° K.	R (microhms).	R/R <sub>0</sub> .
300	2055	1.070
273	1920	1.000
85	910	.474
4.2	142	.0739
3.5	125	.0652
3.0	113	.0589
2.5	98	.0510
2.0	70	.0635
1.9	64	.0345
1.88	60	.0325

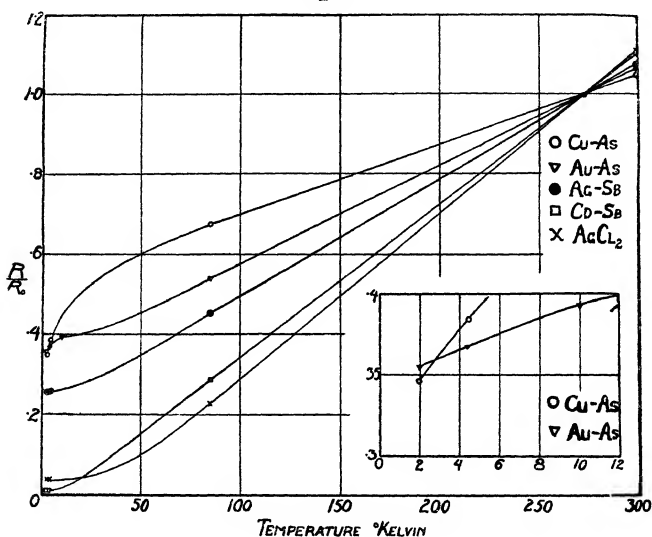
TABLE IV.—Cu—Bi.

T° K.	R (microhms).	R/R <sub>0</sub> .
300	513	1.103
273	465	1.000
85	138	.296
4.2	8	.0172
1.9	8	.0172



expected that some of them might exhibit superconductivity. Ag-Sb and Cd-Sb were prepared in pyrex, Cu-As in a carbon furnace, and Au-As in a quartz tube. Difficulty was experienced in obtaining the Au-As alloy, since the As sublimed at a much lower temperature than the Au melted. However, by melting the gold and dropping some crystals of As on the molten metal an alloy was successfully obtained. Neither of the Sb alloys showed any tendency to lose their resistance at very low temperatures, but both of the As alloys exhibited sharp

Fig. 2.



drops at the lower end of the resistance curves. This indicated that if lower temperatures were available, they might be found superconducting. It is, of course, impossible to predict the onset of the superconducting state, since the transition usually takes place within a few hundredths of a degree and the shape of the curve above the transition-point is no real criterion for superconductivity. The measurements obtained from these alloys are given in Tables V. to VIII. and plotted in fig. 2.

### III.—Ce, La, Pb-Ce, Pb-La.

The results of observations made on these substances are given in Tables X. to XIII. and plotted in fig. 3. The

TABLE V.—Cu-As.

T° K.	R (microhms).	R/R <sub>0</sub> .
300 <sup>o</sup>	1314	1.051
273	1250	1.000
85	840	.673
4.2	480	.384
2.2	434	.347

TABLE VI.—Au-As.

T° K.	R (microhms).	R/R <sub>0</sub> .
300 <sup>o</sup>	291	1.067
273	273	1.000
85	147	.538
10	107	.392
4.2	100	.367
1.9	97	.355

TABLE VII.—Ag-Sb.

T° K.	R (microhms).	R/R <sub>0</sub> .
300 <sup>c</sup>	1354	1.080
273	1252	1.000
85	579	.451
4.2	324	.258
1.9	320	.255

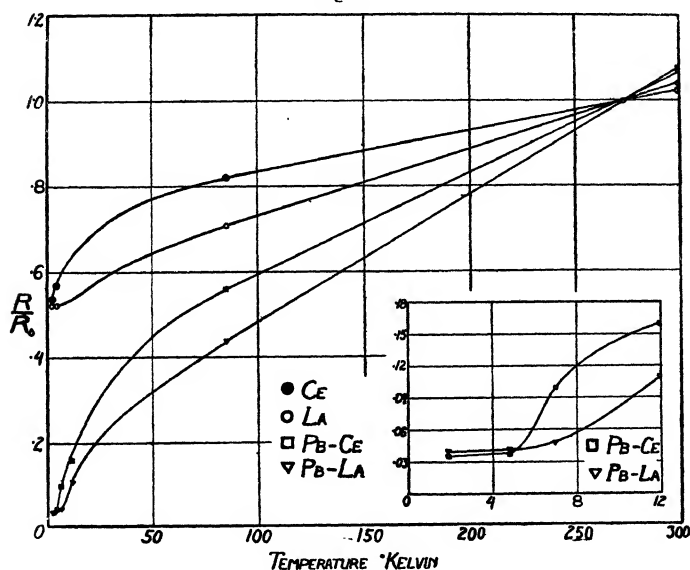
TABLE VIII.—Cd-Sb.

T° K.	R (microhms).	R/R <sub>0</sub> .
300 <sup>o</sup>	4690	1.096
273	4280	1.000
85	1192	.280
4.2	42	.0093
1.9	35	.0070

two metals Ce and La were pure samples obtained from Hopkin and Williams. Situated as they are in the periodic system surrounded by a group of superconductors it was hoped that they would prove to be superconductors. Neither one showed this property down to 1°·9 K., although

the curve for Ce takes a considerable drop at that temperature. Having made this test we desired to know the effect of alloying these metals with lead. Accordingly, the constituents were melted together in a pyrex tube. Difficulty was encountered in obtaining the alloys, since a violent exothermic reaction took place on fusion. However, fairly good samples were finally obtained and measurements made. The resistance-curves for the alloys were much the same as those for the pure metals, except that they had a greater slope. Also in the region

Fig. 3.



of the superconducting point of lead, both alloys and especially the Pb-Ce showed pronounced drops in resistance. This, however, might be due to a certain amount of free lead in the alloy.

#### IV.—FeS, AgS, Bi<sub>2</sub>S<sub>3</sub>.

The fact that CuS becomes superconducting is very peculiar, since Cu on being alloyed with a superconductor in nearly every case has the property of rendering the alloy non-superconducting. However, as it was our purpose to test other common sulphides for this phenomenon, AgS and FeS being easily made came under our

TABLE IX.—AgCl<sub>2</sub>.

T° K.	R (microhms).	R/R <sub>0</sub> .
300°	1837	1.114
273	1649	1.000
84	375	.228
4.2	66	.040
1.9	65	.0395

TABLE X.—Ce.

T° K.	R (microhms).	R/R <sub>0</sub> .
300°	2860	1.025
273	2792	1.000
85	2295	.820
4.2	1590	.568
2.0	1493	.535

TABLE XI.—La.

T° K.	R (microhms).	R/R <sub>0</sub> .
300°	4200	1.040
273	4015	1.000
85	2825	.706
4.2	2095	.522
1.9	2093	.520

TABLE XII.—Pb—Ce.

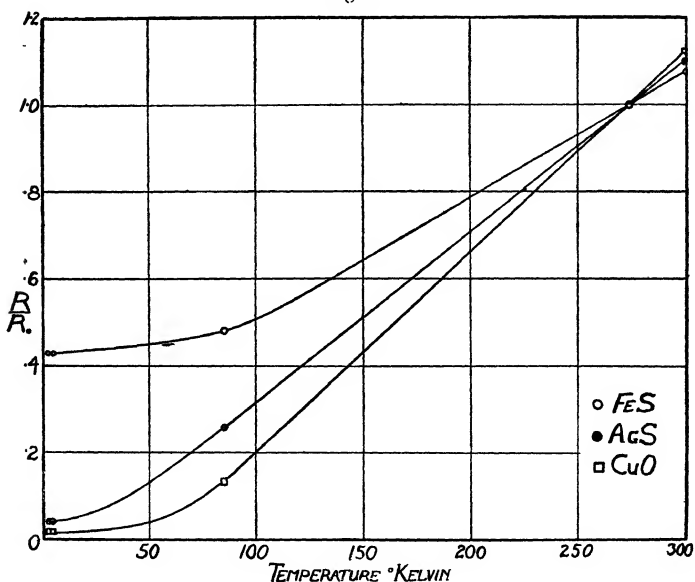
T° K.	R (microhms).	R/R <sub>0</sub> .
300°	1139	1.075
273	1060	1.000
85	593	.559
12	169.5	.160
7	105	.099
5	42	.0396
1.9	41	.0387

TABLE XIII.—Pb—La.

T° K.	R (microhms).	R/R <sub>0</sub> .
300°	488	1.077
273	453	1.000
85	198	.437
12	50	.1102
7	22	.0485
4.8	19	.0419
1.9	18	.0398

scrutiny. The sulphide in both cases consisted of a coating on the surface of a wire (and was formed by heating the wire) in a vapour of sulphur. From the measurements given in Tables XIV. and XV. and plotted in fig. 4, it can be seen that neither compound became superconducting above  $1^{\circ}9\text{K}$ . A single crystal of  $\text{Bi}_2\text{S}_3$ , a naturally occurring mineral known as Bismuthenite, was also examined, but no irregularities were observed in the resistance-curve, which is given in fig. 5 from data in Table XX.

Fig. 4.



## V.—CuO.

We desired in this case to find out if oxygen, which is the first member of the sixth group, had the effect of rendering Cu superconducting. The oxide was in the form of a film coated on the surface of copper ribbon. The curve which is shown in fig. 4 and Table XVI. shows no irregular features.

VI.—AgCl<sub>2</sub>.

A film of the chloride was coated on a silver wire by allowing the wire to stand in a vapour of chlorine for

several hours. The curve obtained is given in Table IX. and fig. 2 and shows no peculiarities. The curve, instead, followed the usual silver temperature resistance curve.

TABLE XIV.—FeS.

T° K.	R (microhms).	R/R <sub>0</sub> .
300	2531	1.083
273	2365	1.00
85	1140	.481
4.2	1016	.428
1.9	1000	.422

TABLE XV.—AgS.

T° K.	R (microhms).	R/R <sub>0</sub> .
300	1915	1.102
273	1740	1.000
85	450	.258
4.2	73	.042
1.9	70	.04

TABLE XVI.—CuO.

T° K.	R (microhms).	R/R <sub>0</sub> .
300	2765	1.130
273	2445	1.000
85	328	.134
4.2	34	.0138
1.9	33	.0135

TABLE XVII.—Heusler Alloy.

T° K.	R (microhms).	R/R <sub>0</sub> .
300	725	1.075
273	696	1.000
85	311	.447
4.2	208	.299
2.0	203	.292

## VII.—Heusler Alloy.

A rod sawn from a sample of this alloy which possesses marked magnetic properties was subjected to measurement at very low temperatures. Nothing abnormal was observed. The measurements are given in Table XVII.

## VIII.—Cd-Zn.

The eutectic alloy of these two metals was formed in the usual way in a pyrex tube. Aside from having an extremely small residual resistance, no irregularities were observed. The curve is shown in fig. 5 and the data given in Table XVIII.

Fig. 5.

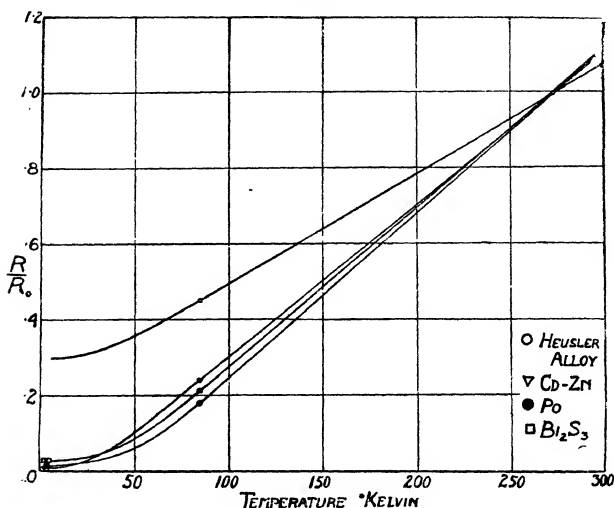


TABLE XVIII.—Cd-Zn.

T° K.	R (microhms).	R/R <sub>0</sub> .
300	1208	1.113
273	1085	1.000
86	254	.234
4.2	10.5	.0096
2.0	8.76	.0081

TABLE XIX.—Po.

T° K.	R (microhms).	R/R <sub>0</sub> .
300	510	1.118
273	456	1.000
85	81	.178
4.2	6	.0132

TABLE XX.— $\text{Bi}_2\text{S}_3$ .

T° K.	R (microhms).	R/R <sub>0</sub> .
300°	530	1.126
273	472	1.000
85	100	.212
4.2	11	.0233
2.0	11	.0233

IX.—Po.

This was a sample precipitated in 1922 and plated on copper. It was expected that since Po degenerates into an isotope of lead and has a half life of 136 days, it would become superconducting. This was not the case, however, the resistance-curve being the characteristic curve for copper. The surface of the Po, however, appeared badly oxidized, so that quite possibly there was no metallic lead on the plate. The curve is given in fig. 5 from data in Table XIX.

The Physical Laboratory,  
University of Toronto,  
June 18, 1930.

XLVIII. *Reducing Observations by the Method of Minimum Deviations.*

*To the Editors of the Philosophical Magazine.*

GENTLEMEN,—

IN your journal for May 1930 there is a paper by Dr. Rhodes on reducing observations by the method of Minimum Deviations, on which I should like to make some remarks.

(1) In practice it is often necessary to draw smooth curves through the plotted observations of two variables where there is a good deal of scatter of the plotted points and the exact theoretical relation between the variables is not known. The experience of the Physical Department is that in these cases it is rarely worth the labour of fitting algebraic curves, and it is usually enough to draw free-hand curves through the points. In some cases the drawing of the curves is assisted by dividing the observations into groups and finding the centre of gravity of each group.

(2) The first example given in Dr. Rhodes's paper seems

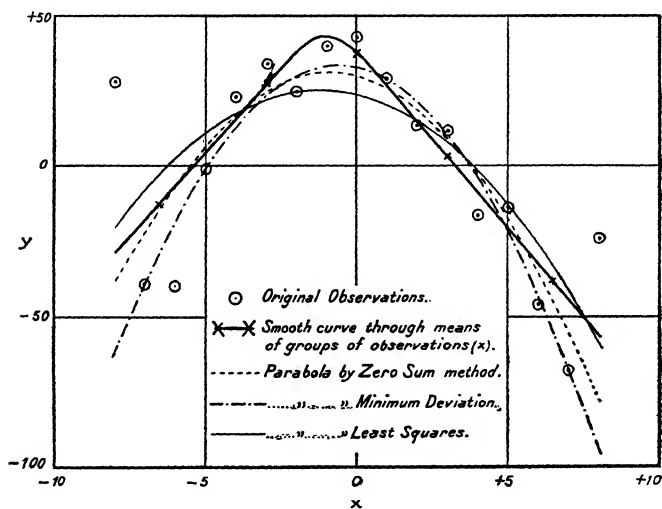


to be of the above type, as the observations show considerable variations.

Dividing the observations into five groups of 4, 3, 3, 3, 4 observations, the curve shown in the attached diagram is obtained, and is a good fit.

(3) If it is desired to fit a curve of particular algebraic type, *i.e.*, a parabola, the quickest way to do this is the method of Zero Sum described by Dr. Norman Campbell in the *Philosophical Magazine*, 1920, vol. xxxix. p. 177, and 1924, vol. xlvii. p. 816.

By this method the problem is reduced in a few minutes to the solution of three normal equations. The method of



least squares only arrives at its normal equations after much computation, and Dr. Rhodes's method of minimum deviations requires still more computation to arrive at the normal equations. In fact the amount of labour is prohibitive.

The parabola obtained by the method of Zero Sum is given in the diagram, as well as those obtained by Dr. Rhodes from Least Squares and Minimum Deviations. The most commonly occurring case in practice is the fitting of a straight line, and this is very quickly done by the method of Zero Sum. A justification of the method is given by Dr. Norman Campbell in the above papers.

Ministry of Public Works,  
Physical Department, Cairo.  
June 14th, 1930.

Yours faithfully,  
H. E. HURST.  
Director General, Physical Department.

XLIX. *The Effect of Stratification on the Gravity Gradient and the Curvature of the Level Surface.* By EDITH A. NELSON, M.A., M.Sc., *Natural Philosophy Laboratory, University of Melbourne*.\*

IT is found, on examination of the values of the gravity gradient and of the curvature of the level surface obtained in a gravity survey with the Eötvös balance, that in certain instances the curvature changes sign when the gradient is a maximum, while in other cases this does not hold. It will be shown that there is no general relation between these quantities, and that this phenomenon is evidence of the stratification of the earth's crust in the region under survey.

Let  $V$  be the gravity potential. The equation to the level surface is then  $V(xyz) = 0$ .

Since the plane XOY is a tangent plane at the origin,

$$\frac{\partial V}{\partial x} = \frac{\partial V}{\partial y} = 0, \quad \frac{\partial z}{\partial x} = \frac{\partial z}{\partial y} = 0.$$

Let A, B, F, G, H, respectively, denote the values at the origin of the quantities

$$\frac{\partial^2 V}{\partial x^2}, \quad \frac{\partial^2 V}{\partial y^2}, \quad \frac{\partial^2 V}{\partial y \partial z}, \quad \frac{\partial^2 V}{\partial z \partial x}, \quad \frac{\partial^2 V}{\partial x \partial y};$$

then 
$$g = \frac{\partial V}{\partial z}.$$

$$\text{Gradient along OX} = \frac{\partial g}{\partial x} = \frac{\partial^2 V}{\partial x \partial z} = G.$$

$$\text{Gradient along OY} = \frac{\partial g}{\partial y} = \frac{\partial^2 V}{\partial y \partial z} = F.$$

$$\therefore \text{Gradient} = (F^2 + G^2)^{\frac{1}{2}} = \Gamma.$$

If  $k_1, k_2$ , respectively, denote the maximum and minimum curvatures of the level surface at O, and  $\phi$  the angle between the section of minimum curvature and OX, then

$$\tan 2\phi = -2 \frac{\partial^2 V}{\partial x \partial y} / \left( \frac{\partial^2 V}{\partial y^2} - \frac{\partial^2 V}{\partial x^2} \right) = -2H/(B-A),$$

$$g(k_1 - k_2) = - \left( \frac{\partial^2 V}{\partial y^2} - \frac{\partial^2 V}{\partial x^2} \right) \sec 2\phi = - \{ (B-A)^2 + 4H^2 \}^{\frac{1}{2}} = T.$$

T is called the Curvature Vector of the level surface.

\* Communicated by Prof. T. H. Laby.

It is desired to find the nature of the relation, if any, between  $\Gamma$  and  $T$ .

Differentiating  $V(xyz) = 0$  with respect to the independent variables  $x$  and  $y$ , and substituting the values of the differential coefficients at the origin, we have

$$A + g \frac{\partial^2 z}{\partial x^2} = 0, \dots \dots \dots (1)$$

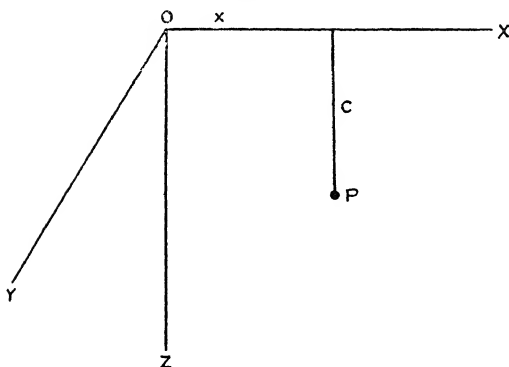
$$H + g \frac{\partial^2 z}{\partial x \partial y} = 0, \dots \dots \dots (2)$$

$$B + g \frac{\partial^2 z}{\partial y^2} = 0, \dots \dots \dots (3)$$

$$\Gamma = (F^2 + G^2)^{\frac{1}{2}}, \dots \dots \dots (4)$$

$$T = \{(B - A)^2 + 4H^2\}^{\frac{1}{2}}. \dots \dots \dots (5)$$

Fig. 1.



In order to obtain a relation between  $\Gamma$  and  $T$  it is necessary to eliminate the quantities  $A, B, F, G, H, \frac{\partial^2 z}{\partial x^2}, \frac{\partial^2 z}{\partial x \partial y}, \frac{\partial^2 z}{\partial y^2}$  from the above equations. This is clearly impossible without a knowledge either of the form of the function  $V$  or of the values of  $A, B, F, G, H$ . Each case must therefore be treated as an individual problem.

Two special cases will be considered :—

1. The disturbing body a sphere with centre at  $P(x, o, c)$ .

Let  $\gamma$  = constant of gravitation,

$M$  = mass of sphere ;

then  $B-A = -3\gamma Mx^2/(x^2+c^2)^{5/2},$

$$H = F = 0,$$

$$G = 3\gamma Mcx/(x^2+c^2)^{5/2},$$

whence

$$T = 3\gamma Mx^2/(x^2+c^2)^{5/2},$$

$$\Gamma = 3\gamma Mcx/(x^2+c^2)^{5/2}.$$

Fig. 2.

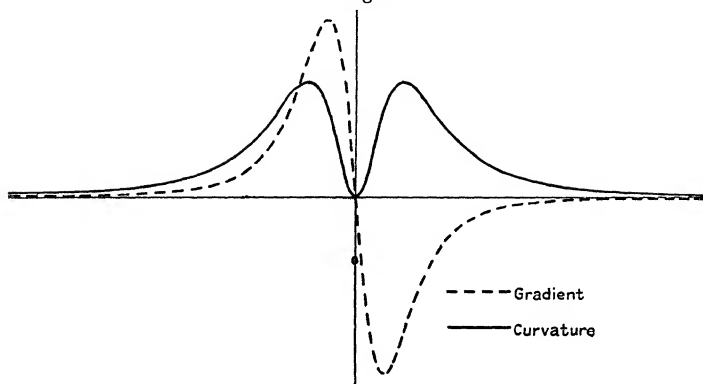
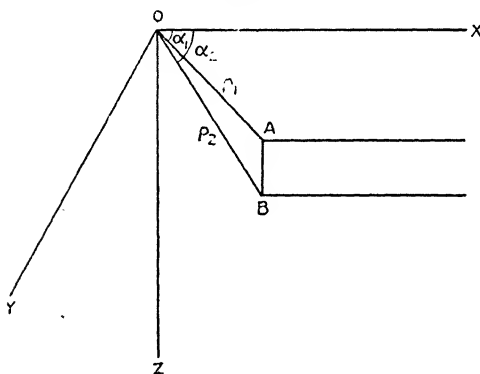


Fig. 3.



If, in a gravity survey in which  $T$  and  $\Gamma$  are determined, a traverse be taken in the direction  $OX$ , the values obtained are given by the curves in fig. 2. The gradient and the curvature vanish together above the centre of the sphere. The maximum value of the gradient is given at  $x=0.5c$ , and that of the curvature vector at  $x=0.82c$ .

## 2. The disturbing body a semi-infinite slab.

Let  $\sigma$  = density of the material of the slab,

$$OA = \rho_1, \quad OB = \rho_2,$$

$$XOA = \alpha_1, \quad XOB = \alpha_2;$$

then  $B - A = 2\gamma\sigma(\alpha_1 - \alpha_2),$

$$F = H = 0,$$

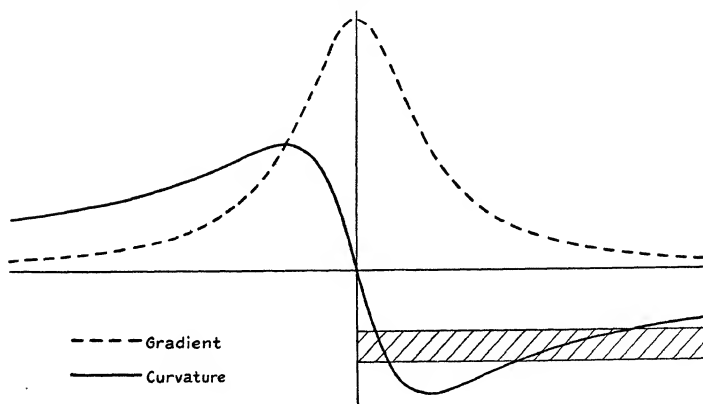
$$G = 2\gamma\sigma \log_e \rho_2/\rho_1,$$

whence

$$T = 2\gamma\sigma(\alpha_2 - \alpha_1),$$

$$\sigma = 2\gamma\sigma \log \rho_2/\rho_1.$$

Fig. 4.



The curves corresponding to a transverse in the direction OX are given in fig. 4. The curvature vector changes sign immediately over the edge of the slab, while the gradient has a maximum at the same point.

It may be concluded that when, in a survey of a region with the Eötvös balance, the curvature vector changes sign where the gradient is a maximum, the earth's crust in that region is stratified, the edge of the stratum being situated below the point of the maximum gradient.

In conclusion, I desire to express my thanks to Professor T. H. Laby, who suggested this problem.

Melbourne,  
November 1929.

*L. Notices respecting New Books.*

*Statistical Methods for Research Workers.* By R. A. FISHER, Sc.D., F.R.S. (Biological Monographs and Manuals, No. V.). Third Edition. [Pp. xv + 284, with tables.] (Edinburgh : Oliver and Boyd, 1930. Price 15s. net.)

THE need for a new edition of this book, at an interval of only two years after the publication of the previous edition, is an indication—if such were needed, in view of the excellence of the work—that it has met a real want. The present edition differs only slightly from the second edition, which was reviewed in these pages, and detailed notice is therefore unnecessary. The chapter on the principles of statistical estimation, added to the second edition to provide practical illustrations of a subject which had received only general discussion in the first edition, has been enlarged by the addition of two new sections illustrating the applicability of the method of maximum likelihood and of the quantitative evaluation of information. The principal other addition is the generalized expression for the series of orthogonal polynomials used in connexion with the fitting of curved regression lines ; these expressions are useful in cases in which polynomials of a high order require to be employed.

It may be mentioned that the numbers of sections, tables, and examples have been unaltered by the addition of fresh material in the later editions, so that references to them (but not to pages) are valid for any edition.

The book can be strongly recommended to all those who have occasion to use statistical methods but are not concerned with the theoretical foundations upon which these methods are based.

*The Acoustics of Orchestral Instruments and of the Organ.* By E. G. RICHARDSON, B.A., D.Sc., Ph. D. [Pp. 158 and 20 plates.] (London : Edward Arnold & Co., 1929. Price 10s. 6d. net.)

THE development of musical instruments has been to a large extent of an empirical nature and their design has been influenced to a very small extent by theoretical considerations. In this book, which is founded on the 1929 Martin White lectures given at the Northern Polytechnic, London, Dr. Richardson has given an essentially popular treatment of the acoustics of the orchestra and of the organ. Apart from an appendix which deals mathematically with the theory of fingering and cross-fingering on the wood-wind, the book is free from mathematics. It should therefore prove of interest

and help both to musical instrument makers and to players. Separate chapters are devoted to the flute, reed instruments, brass instruments, percussion instruments, and strings. A chapter is devoted to ensemble playing and questions of architectural acoustics. Some space might have been given in this connexion to the acoustic properties of the ear, which play an important part in listening to an orchestra. It may be remarked that, though the organ and church bells are included, the piano is omitted—a somewhat surprising omission.

The book is well illustrated and gives an attractive presentation of the theory underlying the instruments considered. Any one who frequents orchestral performances will find his interest increased by a reading of this book, which will give him a fuller realisation of the many problems involved in design and use of the instruments employed.

*Ondes et Corpuscules.* By LOUIS DE BROGLIE. Price 20 fr.  
*Mécanique Ondulatoire.* By the same author. Price 85 fr.  
 (Paris : Librairie Scientifique, Hermann et C<sup>ie</sup>, Rue de la Sorbonne.)

*Wave Mechanics.* Translated by H. T. FLINT, D.Sc., Ph.D.  
 Price 12s. 6d. net. (London : Methuen & Co., 36 Essex Street, W.C. 2.)

IN the papers contributed to scientific journals during the last two or three years, the author gives an historical account of the development of the undulatory theory of matter and of the corpuscular theory of light. The photo-electric and Compton effects required for their explanation, the hypothesis that light has a granular structure : in the theory of matter, the same duality appears, the expressions for energy and momentum being equally applicable to radiation and matter. The probability interpretation of the wave theory of matter leads to the result that physical measurements are only capable of finite precision, the quantum uncertainty principle of Heisenberg, a principle which has been claimed to be of equal importance with the principle of relativity.

The German edition, *Wellenmechanik*, was recently noticed in the pages of this Magazine, and the suggestion made that an English translation would be welcomed. The publishers are to be congratulated on undertaking this task and Dr. Flint for the able translation of de Broglie's standard work. The detailed account of the experimental verification of the wave theory by G. P. Thomson and Rupp was a notable feature of this work ; the author has taken advantage of the appearance of the French edition to include a description of the beautiful experiments of M. Ponte on the diffraction of electrons by

zinc oxide, which show a remarkable agreement between the observed and the theoretical values. Some photographs of diffraction rings, taken from this paper, are here reproduced.

*X-rays.* By B. L. WORSNOP, B.Sc., Ph.D. Price 2s. 6d. net.  
*X-ray Crystallography.* By R. W. JAMES, M.A., B.Sc. Price 2s. 6d. net. (London: Methuen & Co. Ltd., 36, Essex Street, W.C. 2.)

A USEFUL introduction to the study of X-rays, their properties and application to crystal structure is provided in these two monographs on physical subjects. Dr. Worsnop traces the development of the researches during the last twenty years, on the scattering, emission, and absorption of X-rays and the measurement of wave-lengths and gives in the concluding chapter a brief summary of the experimental results of Siegbahn on the refraction of X-rays by prisms, and of Compton and Doan on the use of reflexion gratings in the direct determination of wave-lengths and lattice constants.

In X-ray Crystallography, the author sets out the elementary principles of crystallography and of the methods employed in the observation of X-ray spectra by von Laue, Sir Wm. Bragg, and Debye and Scherrer, the measurement of crystal spacing and a number of important results in the analysis of organic and inorganic compounds. In the short bibliographies, references are given to advanced treatises for the more detailed and intensive study of the subject.

*Matter and Radiation, with particular reference to the Detection and Uses of the Infra-Red Rays.* By JOHN BUCKINGHAM, M.A. [Pp. xii + 144, with 15 diagrams and illustrations.] (London: Humphrey Milford. 1930. Price 7s. 6d. net.)

THE subject-matter of this volume falls into two parts which do not bear a very close relationship to one another. The first three chapters are concerned with modern theories of radiation and the electrical structure of matter, and give the main title to the book. These subjects are discussed in a pleasant discursive manner and with an avoidance of technical terms, suitable for the general non-scientific reader. The remaining two chapters deal with the detection and use of infra-red rays, and give the sub-title to the book; many of the applications which are dealt with are hypothetical to the extent that they have not received serious practical trial, and many difficulties would need to be overcome before they could be considered feasible. Other and more important applications are dismissed in very summary fashion. Thus, the important investigations into planetary atmospheres, carried out at the Lick Observatory, based upon the comparison of photographs



secured by ultra-violet, visual, and infra-red rays, is dealt with in two sentences, one of which is ambiguous, if not misleading:—"Fig. 13 is a photograph of Mars taken half on an ordinary and half on a special plate. The planet, which stands out clearly in one half, cannot be seen at all in the other." These chapters will serve, however, to make clear to the layman that the radiation which is termed infra-red rays possesses practical applications, as well as rays of shorter and longer wave-lengths.

*The Mechanism of Nature : Being a simple approach to Modern Views on the Structure of Matter and Radiation.* By Professor E. N. DA C. ANDRADE, D.Sc., Ph.D. [Pp. xii + 170.] (London : G. Bell & Sons, Ltd., 1930. Price 6s. net.)

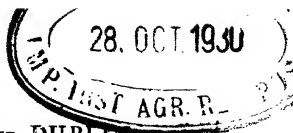
PROFESSOR ANDRADE is one of the few men of science who have the gift of expounding modern scientific work and theories in a manner which will appeal to a layman. This volume was written as a holiday-task in response to requests to make plain the achievements of modern physics. The requirements of such a book cannot be better expressed than in the author's own words, from the preface:—" 'It must,' they say, 'be short, for we are men of the age, and cannot long give our attention to one subject: it must be plain, for we have no inclination to struggle with a new jargon, who have to do with jargon enough in our own professions: it must not smell too much of the schoolroom, for we have neither the patience nor the compulsion which render schoolbooks read. Set to.' "

The volume under review fulfils these requirements. It can be read in a couple of hours; it is written in a literary style such as is possessed by few men of science, with clear and simple phraseology, and is accurate and authoritative. After an introductory chapter dealing with the scope of physics and the purpose of physical theories, succeeding chapters deal with heat and energy, sound and vibrations, light and radiation, electricity and magnetism, the quantum theory, and the atom. Many practical applications of the theories are referred to.

Too frequently the popular exposition of scientific development and achievement has been left, with deplorable results, to the journalistic type of writer, with no scientific qualification. In order that scientific work may receive its due recognition, and that its importance to modern civilization may be appraised at its proper value, the duty devolves upon men of science themselves to supply popular expositions which are accurate and authoritative. Not many have the requisite literary gift. Professor Andrade is to be congratulated upon this volume; in the interests of science the hope may be expressed that it will be very widely circulated.

---

[The Editors do not hold themselves responsible for the views expressed by their correspondents.]



THE  
LONDON, EDINBURGH, AND DUBLIN  
PHILOSOPHICAL MAGAZINE  
AND  
JOURNAL OF SCIENCE.

[SEVENTH SERIES.]

OCTOBER 1930.

LI. *Some Remarks on the Analogy of certain Cases of Propagation of Electromagnetic Waves and the Motion of a Particle in a Potential Field.* By W. DE GROOT, D.Sc.\*

§ 1. *Summary.*

IN §§ 2-6 the conditions are investigated for which a wave-equation of the type

$$\Delta\phi + \frac{\omega^2}{u^2}\phi = 0$$

may be such that a group of waves moves as a mass-point in a field of force which is independent of the frequency of the group. This leads to either the relativistic or the non-relativistic Schrödinger-equation for the dependence of  $u$  on  $\omega$ .

In the case of the propagation of electromagnetic waves in a medium containing charged particles, the movement of a group of waves may also be made to correspond to that of a particle in a potential field of force; in this case the potential, however, depends on  $\omega$  (§§ 7, 8).

In §§ 9-12 the formulæ derived in the foregoing paragraphs are applied to the case of radio-waves reflected by the Heaviside-Kennelly layer, and it is shown that the problem of finding the height of the layer, *i. e.* the determination of the concentration  $n$  of the electrons as a function of the height  $z$  from group-time measurements, is related to the

\* Communicated by Prof. E. V. Appleton, F.R.S.

integral-equation of the "tautochrone" as solved by Abel (1829).

In § 13 it is shown that if  $z$  is a multivalued function of  $n$  the problem becomes indefinite.

In § 14 the bending of the rays round the earth and the calculation of the "effective height" is treated.

In § 15 possible objections to the calculations contained in this article are anticipated.

§ 2. **I**N the next paragraphs we investigate the conditions which allow us to replace a problem of wave-propagation by that of the motion of a particle in a potential-field\*.

It is known that under certain restrictions the differential equation which governs the propagation of a disturbance in a non-homogeneous medium can be solved by an expression of the form

$$\phi(x, y, z)e^{j\omega t} = A(x, y, z)e^{j\{\omega t - S(x, y, z)\}} \quad (1)$$

Equation (1) represents a monochromatic wave of frequency  $\omega$  and amplitude  $A$ , whilst the surfaces

$$S = \text{const.}$$

are surfaces of equal phase. We will, however, limit our considerations to the cases in which the differential equation just mentioned, after substitution of the left-hand part of equation (1), changes into an "amplitude equation" of the form

$$\Delta\phi + \frac{\omega^2}{u^2}\phi = 0 \quad (2)$$

where  $u$ , the phase velocity, may depend on  $x, y, z$ †.

The restrictions alluded to may then be put in the form : The variations of the quantities  $A$  and  $S$ , as a function of  $x$ ,

\* I am indebted to Dr. B. van der Pol, Eindhoven, and to Prof. E. V. Appleton, London, who, in discussions on the propagation of radio-waves in the upper atmosphere, stimulated the investigations contained in this article. Prof. Appleton proposed the problem of the determination of the true height reached by wireless waves in a recent lecture at Eindhoven. The idea that the Schrödinger wave-equation might be of any use in this respect was suggested to us by Prof. G. Manneback (Leuven).

† A review of the questions referred to in this section, from a much broader point of view, is to be found in a series of lectures by A. D. Fokker (Dutch) entitled: "Inleiding tot de golvings- en quantum-mechanica" (i. e., "Introduction to the Wave- and Quantum-mechanics"), Haarlem (Holland), De Erven Loosjes, 1928 (Chap. I.), and, further, in A. Sommerfeld "Atombau," *Ergänzungsband*, Braunschweig, Vieweg-Sohn (Chap. III., Section 1).

$y, z$ , must be "slow." This leads to the following two conditions:

- (a) The radius of curvature of the surfaces  $S = \text{const.}$  must be large with respect to the local wave-length

$$R \gg \lambda.$$

- (b) The relative variation of the quantity  $u$ , when proceeding in the direction of its gradient along a distance equal to the local wave-length, must be small—

$$\frac{\lambda}{u} \left| \text{grad } u \right| \ll 1.$$

§ 3. Supposing the conditions (a) and (b) to be fulfilled, it is generally possible to consider a portion of space where the surfaces

$$u(\omega, x, y, z) = \text{const.} \quad (\omega = \text{const.})$$

are to be considered as parallel planes.

In this portion of space Snell's law is valid, so that

$$\frac{u}{\sin \theta} = \text{const.}, \quad . \quad . \quad . \quad . \quad . \quad (3)$$

where  $\theta$  is the angle between the normal of the surfaces of equal phase (ray) and the gradient of  $u$ . If, now, we wish to construct a potential distribution

$$V(x, y, z),$$

so that the motion of a particle imitates the motion of the waves, it is clear that the surfaces  $u = \text{const.}$  must also be the surfaces  $V = \text{const.}$  If this were not the case, a particle starting along the gradient of  $u$  would not follow the corresponding ray. Since  $\theta$  is also the angle between the direction of motion of the particle and the potential gradient,

$$v \sin \theta = \text{const.}, \quad . \quad . \quad . \quad . \quad . \quad (4)$$

where  $v$  is the velocity of the particle. It follows, therefore, from (4) and (5) that

$$u \cdot v = \text{const.} \quad (\text{K say}). \quad . \quad . \quad . \quad . \quad . \quad (5)$$

§ 4. The actual properties of  $V$  depend on the kind of mechanics we wish to adopt for the particle. We consider first non-relativistic classical mechanics, for which

$$E = V + \frac{1}{2} M v^2 = \text{const.} \quad . \quad . \quad . \quad . \quad . \quad (6)$$

It follows from (5) and (6)

$$V = E - \frac{1}{2} M v^2 = E - \frac{M K^2}{2 u^2} \quad . \quad . \quad . \quad . \quad . \quad (7)$$

We consider first the specifications necessary to make the function  $V$  independent of the frequency (condition I.).

It will be understood that this limits the form of the function  $u$ , because a surface  $u = \text{const.}$  must remain the same in changing over from one frequency to another. At the same time we attempt to fulfil a condition of quite another type, namely, that the velocity of a "group" of waves shall coincide with the velocity of the particle (condition II.). In order to fulfil the conditions I. and II. we make  $E$  and  $K$  depend on  $\omega$ .

Then condition II. leads to

$$\frac{\partial}{\partial \omega} \left( \frac{\omega}{u} \right) = \frac{1}{v} = \sqrt{\frac{M}{2\{E(\omega) - V(x, y, z)\}}}, \quad \dots (8)$$

whilst

$$u \cdot v = u; \quad \frac{\partial}{\partial \omega} \left( \frac{\omega}{u} \right) = K(\omega). \quad \dots (9)$$

From (9) it is seen immediately that it will be in general impossible to fulfil the conditions I. and II.

§ 5. From (8) and (9) the special kind of dispersion-law, for which it is possible to fulfil (I.) and (II.) (§ 4), may be derived; according to (9)

$$\frac{1}{u} \frac{\partial}{\partial \omega} \left( \frac{\omega}{u} \right) = \frac{1}{K(\omega)}.$$

Thus

$$\left( \frac{\omega}{u} \right)^2 = \int \frac{2\omega}{K(\omega)} d\omega = H(\omega) + F(x, y, z), \quad \dots (10)$$

so that

$$\frac{\omega}{u} = \sqrt{H(\omega) + F(x, y, z)} \quad \dots (11)$$

and

$$\frac{\partial}{\partial \omega} \left( \frac{\omega}{u} \right) = \frac{\frac{1}{2} \partial H / \partial \omega}{\sqrt{H(\omega) + F(x, y, z)}} \quad \dots (12)$$

Comparing this last expression with (8), it is seen that we are compelled to take

$$\frac{\partial H}{\partial \omega} = \text{const.}$$

and

$$H = a\omega + b;$$

and, as  $E$  must be proportional to  $H$ ,

$$E = h\omega - k.$$

Putting  $H = \gamma E$  and  $F = -\gamma V$  one easily finds that  $\gamma$  must be equal to  $2M/h^2$ , which reduces (11) to

$$\frac{\omega}{u} = \frac{1}{h} \sqrt{2M(h\omega - k - V)} = \frac{1}{h} \sqrt{2M(E - V)} \quad (13)$$

$$u = \frac{h\omega}{\sqrt{2M(h\omega - k - V)}} = \frac{E + k}{\sqrt{2M(E - V)}} \quad (14)$$

From (13) it follows that the amplitude equation (2) reduces to the form

$$\Delta\phi + \frac{2M}{h^2}(E - V)\phi = 0. \quad (15)$$

We see, therefore, that conditions I. and II. lead to the special form of amplitude-equation introduced into physics by Schrödinger\*.

In the case of Schrödinger's equation a special value is attributed to the constant  $h$ , namely,  $\frac{1}{2}\pi$  times the Planck constant  $= (6.55 : 2\pi) \cdot 10^{-27}$ . It will be clear that this value is of no interest for us now.

§ 6 We will derive now the equation corresponding to the conditions I. and II. in the case of the particle being subjected to relativistic mechanics. It is sufficient to replace in the equation

$$\frac{d}{dt} Mv_x = - \frac{\partial V}{\partial x} \quad (16)$$

the constant  $M$  by  $M/\sqrt{1-v^2/c^2}$ , where  $M$  is again a constant and represents the mass of the particle at rest. It follows, when  $x$  is the projection of the ray on the planes of equal potential, that instead of equation (4) we get

$$\frac{v \sin \theta}{\sqrt{1-v^2/c^2}} = \text{const.}, \quad (17)$$

so that instead of (5) we get

$$u \cdot v = \text{const.} \sqrt{1-v^2/c^2}, \quad (18)$$

where the constant may be a function of  $\omega$ . On the other hand, we have to consider the total energy  $E + Mc^2$  (where

\* E. Schrödinger: Four Lectures on Wave Mechanics (London, Blackie & Son, 1928). In the first of these lectures the equation (14) is derived with the constant  $k$  equal to zero. As will be seen further on, it proves better not to cancel the constant  $k$ , because when one tries to derive equation (14) from the corresponding relativistic equation supposing the particle velocity small, one finds  $k = Mc^2$ .

E is the sum of kinetic and potential energies) as being a function of  $\omega$  ( $f(\omega)$ , say), so that the kinetic energy proves to be

$$\frac{Mc^2}{\sqrt{1-v^2/c^2}} - Mc^2 = E - V = f(\omega) - Mc^2 - V, \quad (19)$$

from which follows

$$\frac{v}{c} = \frac{\sqrt{(f-V)^2 - M^2c^4}}{f-V} \quad (20)$$

Combining with (18) and (19), we get :

$$u = \frac{g(\omega)}{\sqrt{(f-v)^2 - M^2c^4}}, \quad (21)$$

$$\frac{\omega}{u} = j(\omega)\sqrt{(f-v)^2 - M^2c^4}, \quad (22)$$

where  $j(\omega) = \omega : g(\omega)$ , and

$$\frac{d}{d\omega}\left(\frac{\omega}{u}\right) = \frac{j \cdot f'(f-v)}{\sqrt{(f-v)^2 - M^2c^4}} + j' \sqrt{(f-v)^2 - M^2c^4} \quad (23)$$

(where the dot denotes derivation with respect to  $\omega$ ). Comparing this with (20), it follows that  $j'$  must be zero, so that  $j$  is a constant ( $p$  say) and  $f' = 1/cp = h$ . It follows that

$$Mc^2 + E = h\omega - k,$$

where  $k$  is arbitrary. If  $k$  is put equal to zero,

$$E + Mc^2 = h\omega, \quad (24)$$

so that from (21) we find for  $u$  :

$$u = \frac{ch}{\sqrt{(h\omega - V)^2 - M^2c^4}}, \quad (25)$$

$$\frac{\omega}{u} = \frac{1}{h} \sqrt{\frac{(h\omega - V)^2}{c^2} - M^2c^2}; \quad (26)$$

from (26) it follows that the amplitude equation is now

$$\Delta\phi + \frac{1}{h^2} \left\{ \frac{(h\omega - V)^2}{c^2} - M^2c^2 \right\} \phi = 0, \quad (27)$$

or

$$\Delta\phi + \frac{1}{h^2} \left\{ \frac{(E + Mc^2 - V)^2}{c^2} - M^2c^2 \right\} \phi = 0, \quad (27a)$$

which is the relativistic form of the Schrödinger equation for a particle.

From (20) and (25) it follows that

$$u.v = \frac{c^2 h \omega}{h \omega - V} = \frac{h \omega}{M} \sqrt{1 - v^2/c^2}, \quad . \quad . \quad (28)$$

in accordance with (18).

§ 7. We now turn to various wave-propagation problems which lead to a dispersion law conforming either to (25) or to (14). Let us begin with equation (25) in the special case for which  $V$  is zero throughout.

Then it follows from (25) that

$$u = \frac{c}{\sqrt{1 - \frac{M^2 c^4}{h^2 \omega^2}}}, \quad . \quad . \quad . \quad (29)$$

from which we see at once that our dispersion formula is identical in form with the well-known dispersion law for electromagnetic waves propagated in a medium containing charged particles. Let the number of these particles per c.c. be  $n$ , their charge  $e$ , and mass  $m$ ; then

$$u = \frac{c}{\sqrt{1 - \frac{4\pi n e^2}{m \omega^2}}}, \quad . \quad . \quad . \quad (30)$$

It was this accidental coincidence which led Sir J. J. Thomson \* to a somewhat obscure interpretation of the interference-phenomena of electron-beams investigated since 1927 by Davisson and Germer, G. P. Thomson, and Rupp.

From (28) it follows that when  $V = 0$

$$u.v = c^2. \quad . \quad . \quad . \quad (31)$$

§ 8. In the case where the quantity  $n$  of § 7 is not a constant, but depends on  $x$ ,  $y$ , and  $z$ , the analogy with either formulæ (14) or (25) vanishes.

Now, as this case is specially interesting for some problems concerning the propagation of radio-waves, especially for the questions arising in connexion with the reflexion of these waves by the Heaviside-Kennelly layer, we will indicate in this paragraph a procedure which allows us nevertheless to treat this problem by the methods indicated previously. For this purpose we first show that it is always possible to expand the expression for  $u$  in such a way that in a small

\* J. J. Thomson, 'Beyond the Electron.' London: Camb. Univ. Press (1928).



interval of frequencies it coincides with formula (14). We write down

$$u = \frac{\omega}{\sqrt{\omega^2/u^2}} = \frac{\omega}{\sqrt{\frac{\omega_0^2}{u_0^2} + 2(\omega - \omega_0)\frac{\omega_0}{u_0} \frac{\partial}{\partial u} \left( \frac{\omega}{u} \right)_0}},$$

where  $u_0$  is the value  $u$  assumes for  $\omega = \omega_0$ . It will be possible to bring it in the form (14) if it happens that  $2\omega_0/u_0 \cdot \partial/\partial \omega (\omega/u)_0$  proves to be a constant, which may be put equal then to  $2M/h$ . In this case we have

$$2 \frac{\omega_0}{u_0} \frac{\partial}{\partial \omega} \left( \frac{\omega}{u} \right)_0 = \frac{2M}{h}, \quad . \quad . \quad . \quad (32)$$

$$\frac{2\omega_0^2}{u_0} \frac{\partial}{\partial \omega} \left( \frac{\omega}{u} \right)_0 - \frac{\omega_0^2}{u_0^2} = \frac{2M(V+k)}{h^2}, \quad . \quad . \quad (33)$$

$$k + E = h\omega = h\omega_0 \cdot \frac{\omega}{\omega_0}. \quad . \quad . \quad . \quad (34)$$

Now in our case we have

$$u = \frac{c}{\sqrt{1 - \frac{4\pi ne^2}{m\omega^2}}} = \frac{c}{\sqrt{1 - N/\omega^2}}, \quad . \quad . \quad (35)$$

where  $N$  is written for  $4\pi ne^2/m$ , and

$$\frac{\partial}{\partial \omega} \left( \frac{\omega}{u} \right) = 1 : c \sqrt{1 - N/\omega^2}; \quad . \quad . \quad . \quad (36)$$

so that

$$\frac{\omega_0}{u_0} \frac{\partial}{\partial \omega} \left( \frac{\omega}{u} \right)_0 = \frac{\omega_0}{c^2}$$

proves to be independent of  $x, y, z$ .

According to (32), (33), and (34) we have

$$\frac{\omega_0}{c^2} = \frac{M}{h}, \quad h\omega_0 = Mc^2, \quad . \quad . \quad . \quad (37)$$

and putting  $k = \frac{1}{2}Mc^2$ , as is most convenient for our present purpose,

$$V = \frac{Mc^2}{2} \cdot \frac{N}{\omega_0^2}, \quad . \quad . \quad . \quad (38)$$

$$E = Mc^2 \cdot \frac{\omega}{\omega_0} - \frac{1}{2}Mc^2 = \frac{1}{2}Mc^2, \quad . \quad . \quad . \quad (39)$$

the difference between  $\omega$  and  $\omega_0$  being neglected in the last expression.

So we see that a group of waves, in the case considered, behaves as a particle of mass  $M$  subject to the non-relativistic mechanical law, so that

$$E - V = \frac{1}{2}Mv^2 \quad . \quad . \quad . \quad (40)$$

whatever the value of  $v$ , if only the potential-field is assumed according to (38).

From (40) it follows that

$$v = c \sqrt{1 - N/\omega_0^2}, \quad . \quad . \quad . \quad . \quad (41)$$

in accordance with (5).

The simplicity of this result suggests that we might have arrived at it in a simpler way. It is, indeed, seen from (35) and (36) that the product of  $u$  and  $v$  is independent of  $x, y, z$  (if  $1/v$  is put equal to  $\partial/\partial\omega(\omega/u)$ ); so condition II., § 4, is fulfilled by our dispersion law (30). If we disregard condition I., § 4, it follows immediately from (7) that

$$V = \frac{1}{2}Mc^2 \frac{N}{\omega^2}$$

if  $E$  be chosen arbitrarily equal to  $\frac{1}{2}Mc^2$ . So, if our sole purpose had been to study formula (30), we could have started here with the omission of §§ 5-8.

§ 9. We now come to the practical problem in which  $N$  is proportional to the concentration of the electrons in the Heaviside-layer. Treating first the surface of the earth as flat, we may assume that  $N$  only depends on  $z$ . Now there exists for a particular frequency  $\omega$  (the index zero being omitted) a particular value of  $z$  ( $z(\omega)$  say), for which

$$N(z) = \omega^2. \quad . \quad . \quad . \quad . \quad . \quad (42)$$

For this value of  $z$   $V = E$ . So we see that  $z(\omega)$  is the largest value of  $z$  that may be reached by the particle whose movement represents that of a group of waves. This value is only reached when the particle starts vertically, *i. e.* when the initial direction of the beam is vertical. In other cases a lower maximal value of  $z$  is reached.

After having reached its maximal height, the particle returns to the earth, which means reflexion of the corresponding beam. In many experiments \* the time for a group of waves to travel upwards and come down again is measured

\* E. V. Appleton and M. A. F. Barnett, 'Nature,' cxv. p. 333 (1925); Proc. Roy. Soc. A, cix. p. 621 (1925), cxiii. p. 450 (1926).

E. V. Appleton and J. A. Ratcliffe, *ibid.* cxv. pp. 291, 305 (1927); cxvii. p. 576 (1927).

G. Breit and M. A. Tuve, Phys. Rev. xxviii. p. 554 (1926).

L. R. Hafstad and M. A. Tuve, Proc. Inst. Rad. Eng. xvii. pp. 1513, 1786 (1929).

G. W. Kenrick and K. C. Jen, *ibid.*, xvii. 711 (1929).

Useful surveys by G. W. Kenrick and G. W. Pickard, Proc. Inst. Rad. Eng. xviii. p. 649 (1930); E. V. Appleton, Proc. Phys. Soc. xli. p. 43 (1928), xlii. p. 321 (1930).

directly or indirectly. This time, of course, will depend on the frequency  $\omega$  of the group and on the angle  $\theta$  which the initial direction of the beam makes with the vertical. To avoid duplication of expression let us not speak further of the group, but only of a particle. In case the particle starts vertically, the time needed to travel upwards to its maximal height will be

$$t = \int_0^{(z)\omega} \frac{dz}{V} = \frac{1}{c} \int_0^{z(\omega)} \frac{dz}{\sqrt{1 - N/\omega^2}}; \quad \dots \quad (42)$$

when starting under an angle  $\theta$  the velocity will retain a component  $c \sin \theta$  parallel to the earth, to which corresponds a portion

$$\frac{1}{2} Mc^2 \sin^2 \theta$$

of the kinetic energy which remains unaffected.

The particle now will reach a height such that

$$\frac{1}{2} Mc^2 \cos^2 \theta = V = \frac{1}{2} Mc^2 \frac{N}{\omega^2},$$

or

$$N = \omega^2 \cos^2 \theta;$$

and as

$$\frac{1}{2} M \dot{z}^2 = \frac{1}{2} Mc^2 \left( \cos^2 \theta - \frac{N}{\omega^2} \right), \quad \dots \quad (43)$$

$$t = \int \frac{dz}{\dot{z}} = \frac{1}{c \cos \theta} \int_0^{z(\omega \cos \theta)} \frac{dz}{\sqrt{1 - N/\omega^2 \cos^2 \theta}}, \quad \dots \quad (44)$$

so

$$t(\theta, \omega) = \frac{1}{\cos \theta} t(0, \omega \cos \theta). \quad \dots \quad (45)$$

So the case  $\theta \neq 0$  is reduced to the case  $\theta = 0$ , and we further need only to consider the latter.

§ 10. The chief problem involved in measurements of this kind is to determine how  $N$  depends on the height  $z$  when  $t$  as a function of  $\omega$  is determined experimentally. In this case equation (42) is to be considered as an integral equation for  $N$ .

Now we may make the formal analogy with a mechanical problem closer in assuming

$$V = M \cdot g \cdot y, \quad \dots \quad (46)$$

where  $y = N$  and  $g = c^2/2\omega^2$ .

Then putting

$$\frac{1}{2}Mc^2 = M \cdot g \cdot a \quad (a = \omega^2), \quad \dots \quad (47)$$

we get

$$v = \sqrt{\frac{2}{M}(E - V)} = \sqrt{2g(a - y)},$$

and

$$t(a) = \int_0^{z(a)} \frac{dz}{\sqrt{2g(a - y)}}, \quad \dots \quad (48)$$

where  $z(a)$  means the particular value of  $z$  for which  $y = a$ , so that  $t(a)$  is the time a particle starting with velocity  $c$  at  $z = 0$  needs to travel up a hill  $y = \text{function}(z)$ \* when the gravity-acceleration is chosen so that the maximum height reached is  $a$ .

This problem is easily reduced to one of constant gravity-acceleration by multiplying at both sides with

$$2g = c/\omega = c/\sqrt{a}.$$

$$\frac{ct(a)}{\sqrt{a}} = T(a) = \int_0^{z(a)} \frac{dz}{\sqrt{a - y}}. \quad \dots \quad (49)$$

This is a famous integral equation which was first solved by Abel in 1829 and, in a more elaborated way, by Liouville in 1839. Considering  $z$  as a function of  $y$ , it reduces to

$$T(a) = \int_0^a \frac{z' dy}{\sqrt{a - y}}, \quad \dots \quad (50)$$

which is a linear equation of the Volterra type. Its solution is

$$z = \frac{1}{\pi} \int_0^a \frac{T(x) dx}{\sqrt{a - x}}. \quad \dots \quad (51)$$

Replacing  $a$  by  $\omega^2$  and  $x$  by  $\xi^2$ , we get

$$z = \frac{2c}{\pi} \int_0^\omega \frac{t(\xi) d\xi}{\sqrt{\omega^2 - \xi^2}}, \quad \dots \quad (52a)$$

$$N(z) = \omega^2. \quad \dots \quad (52b)$$

\* The  $z$ -axis is now thought of as "horizontal," the  $y$ -axis as "vertical."

So by formulæ (52) we get  $z$  as a function of  $N$  instead of  $N$  as a function of  $z$ .

§ 11. We now consider a number of examples in connexion with equations (42) and (52).

*Case 1.* Let  $N$  be zero throughout. In this case the time for the group to travel from  $Z_A$  to  $Z_B$  is

$$t(AB) = \frac{1}{c} \int_A^B dz,$$

$$ct(AB) = Z_B - Z_A. \quad . \quad . \quad . \quad . \quad (53)$$

*Case 2.* Let  $N$  be a linear function of  $Z$ ,

$$N = a + bz;$$

as  $N$  is essentially positive, it will be sufficient to consider positive values of  $a$ .

Then

$$ct(AB) = \int_A^B \frac{dz}{\sqrt{1 - \frac{a+bz}{\omega^2}}}$$

$$= \frac{1}{\sqrt{1 - \frac{a}{\omega^2}}} \int_A^B \frac{dz}{\sqrt{1 - \gamma z}} \quad \left( \gamma = \frac{b}{\omega^2 - a} \right).$$

Hence

$$ct(AB) = \frac{2\omega \sqrt{\omega^2 - a}}{b} \left[ - \sqrt{1 - \gamma z} \right]_A^B. \quad . \quad . \quad (54)$$

Let us call  $t(AB) = t(\omega)$  if  $Z_A = 0$ ,  $Z_B = Z(\omega)$ ,  $N(Z_B) = \omega^2$ , so that  $\gamma Z_B = 1$ .

Then (fig. 1)

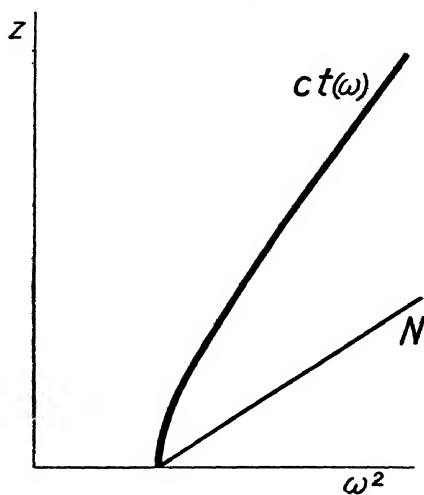
$$ct(\omega) = \frac{2\omega}{b} \sqrt{\omega^2 - a}. \quad . \quad . \quad . \quad . \quad (55)$$

And in the special case that  $a = 0$ ,

$$ct(\omega) = \frac{z\omega^2}{b} = 2z(\omega). \quad . \quad . \quad . \quad . \quad (56)$$

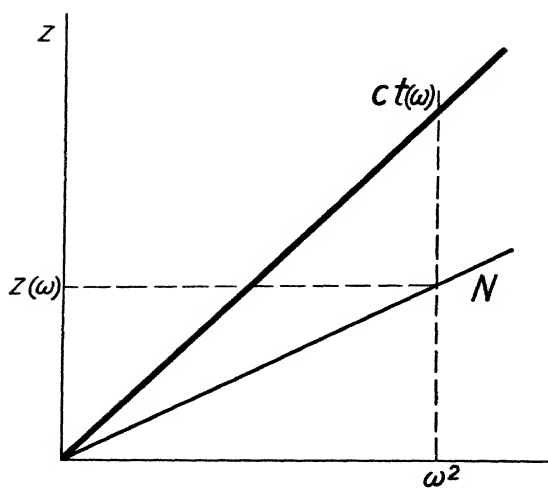
So in this case the time for the group to reach its maximal height is exactly twice the time to travel the same distance *in vacuo* (fig. 2).

Fig. 1.



$$N = a + bz.$$

Fig. 2.



$$N = bz.$$

It is easy in this case to verify formula (52), for

$$\frac{2}{\pi} \int_0^{\omega} \frac{2\xi^2}{b} \frac{d\xi}{\sqrt{\omega^2 - \xi^2}} = \frac{4\omega^2}{\pi b} \int_0^1 \sin^2 \phi d\phi = \omega^2/b = z(\omega)$$

$$(\xi = \omega \sin \phi).$$

We need not make the same test in the following cases, as this may be done by simple integration, and involves no particular difficulties.

*Case 3.* Let  $N$  be a quadratic function of  $z$ , which is nowhere negative:

$$N = a + pz + qz^2.$$

First, let  $a$ ,  $p$ , and  $q$  be positive; then

$$\begin{aligned} ct(AB) &= \int_A^B \frac{dz}{\sqrt{1 - \frac{a + pz + qz^2}{\omega^2}}} \\ &= \omega \int_A^B \frac{dz}{\sqrt{\omega^2 - a - pz - qz^2}} \\ &= \frac{\omega}{\sqrt{q}} \left[ \sin^{-1} \frac{2qz + p}{\sqrt{p^2 + 4q(\omega^2 - a)}} \right]_A^B. \end{aligned}$$

When especially  $Z_A = 0$ ,

$$a + pZ_B + qZ_B^2 = \omega^2, \quad Z_B = Z(\omega),$$

$$ct(\omega) = \frac{\pi}{2} \frac{\omega}{\sqrt{q}} \left\{ 1 - \sin^{-1} \frac{p}{\sqrt{p^2 + 4q(\omega^2 - a)}} \right\}. \quad (58)$$

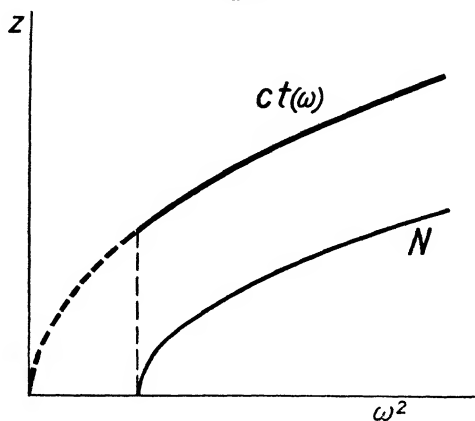
If  $p = 0$  (fig. 3),

$$ct(\omega) = \frac{\pi}{2} \frac{\omega}{\sqrt{q}}, \quad \dots \dots \dots (59)$$

which, of course, applies only for  $\omega^2 > a$ . If  $\omega^2 = a$ ,  $z(\omega) = 0$ ,  $ct(\omega) = \frac{\pi}{2} \sqrt{\frac{a}{q}}$ , so in this case the group requires a finite time for a distance zero, as a result of the group velocity being zero.

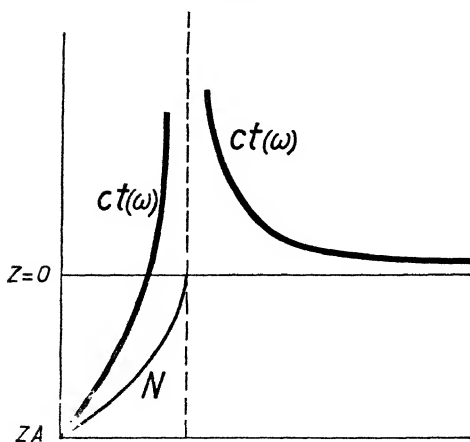
It is remarkable that formula (59) holds independent of the value of  $a$ . If  $a = 0$ , the group-time is exactly  $\frac{\pi}{2}$  times the vacuum time.

Fig. 3.



$$N = a + qz^2.$$

Fig. 4.



$$N = a - q'z^2.$$

If  $q$  is negative, it is sufficient to consider the case in which  $p = 0$  (fig. 4).



Then, if  $q' = -q$ ,

$$ct(AB) = \frac{\omega}{2\sqrt{q'}} \left[ \ln \left| \frac{q'z + \sqrt{q'(\omega^2 - a + q'z^2)}}{q'z - \sqrt{q'(\omega^2 - a + q'z^2)}} \right| \right] \Big|_A^B. \quad (60)$$

First, let  $\omega^2 < a$ . Then, if  $z_A$  be taken such that  $N(z_A) = a - qz_A^2 = 0$ ,  $N(z_B) = a - qz_B^2 = \omega^2$ ,  $z_B = z(\omega)$ ,  $t(AB) = t(\omega)$ .

$$ct(\omega) = \frac{\omega}{2\sqrt{q'}} \ln \frac{\sqrt{a} + \omega}{\sqrt{a} - \omega} \dots \dots \dots (61)$$

If  $\omega^2 > a$ , let  $z_B = 0$ ,  $t(AB) = t(\omega)$ .

$$ct(\omega) = \frac{\omega}{2\sqrt{q'}} \ln \frac{\omega + \sqrt{a}}{\omega - \sqrt{a}} \dots \dots \dots (62)$$

If  $\omega^2 \rightarrow a$ ,  $ct(\omega) \rightarrow \infty$  in both cases.

§ 12. Formula (61) gives an interesting example of a group-time tending to infinity for a special value of  $\omega$ . As Professor Appleton has pointed out, in the discussion of his lecture at Eindhoven, this may be of interest in connexion with some particular phenomenon observed since 1928, namely, that of abnormally retarded echoes\*.

When (as is suggested by Professor E. V. Appleton) the Heaviside layer consists of two ionized regions (E and F regions) at heights of about 100 and 200 km, it is possible that the quantity  $N$  reaches a maximum for a certain value of  $z$ , then a minimum and then increases again, so that to a certain value of  $N$  may correspond three values of  $z$ . In this case the dependence of  $t(\omega)$  on  $\omega^2$  may be as depicted in fig. 5.

§ 13. The question arises whether in the case of  $z$  being a multivalued function of  $N$  it is possible to reconstruct this function from the data available. That this is generally impossible may be shown in the following way. For values of  $\omega^2$  superior to  $N(E)$  the function  $t(\omega)$  may be considered as the sum of  $t(OE)$ ,  $t(EF)$ , and  $t(FP)$ , the height of  $P$  being  $z(\omega)$ . From these three parts  $t(OE)$  may be deduced

\* C. Störmer, 'Nature,' cxxii. pp. 681, 945 (1928).

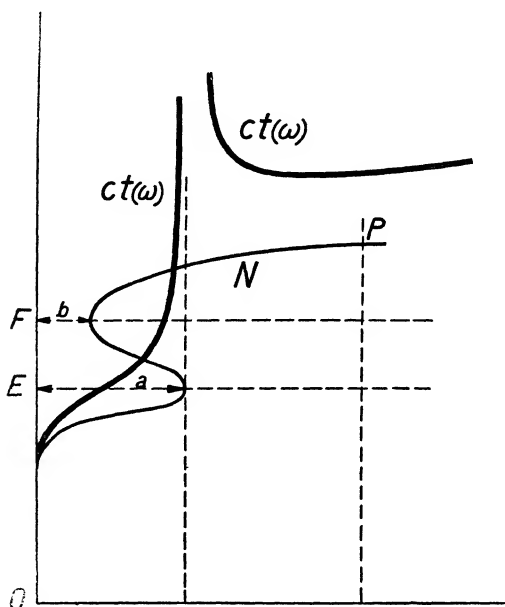
B. van der Pol, 'Nature,' cxxii. p. 878 (1928), and E. V. Appleton, 'Nature,' cxxii. p. 879 (1928), suggested the idea that this phenomenon might be connected with zero group-velocity; the explanation given by Prof. Störmer is based on widely different assumptions. A general survey of observed facts is given by C. Störmer (*Nat. wiss.* xvii. p. 643 (1929)).

directly from the values of  $N$  for  $z < z_E$  as found by solving the integral-equation. As may be seen from formula (62)  $t(OE)$  will behave as

$$-\log(\omega - \sqrt{a}) \cdot \text{const.}$$

for  $\omega^2 - a \ll a$  ( $a = N(E)$ ).

Fig. 5.



Subtracting  $t(OE)$  from  $t(\omega)$  we retain  $t(EF) + t(FP)$ . Of these two functions the latter will behave quite regularly in the neighbourhood of  $\omega^2 = a$ , while the former becomes infinite as

$$-\log(\omega - \sqrt{a}) \cdot \text{const.}$$

probably with the same constant, namely, if  $N$  as a function of  $z$  behaves as a parabola in the immediate neighbourhood of  $z = z(E)$ . If  $t(EP)$  as a function of  $\omega$  is accurately known in the region indicated, the constant may be derived experimentally, for

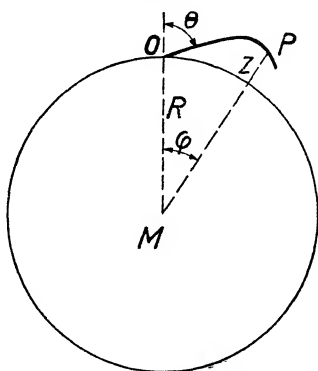
$$\rho^{-ct(EP)}$$

will be proportional to  $\omega - \sqrt{a}$ .

Now, it will be possible to draw an *arbitrary* curve which has the exact curvature in E and has a minimum in F, the height of F being arbitrary also. Assuming this curve for N between  $z_E$  and  $z_F$ , it is possible to calculate the corresponding  $t(EF)$ . Subtracting this from  $t(EP)$ , we retain a function which behaves regularly for  $\omega^2 = a$ , and we may interpret this function as  $t(FP)$ . Now, as this function is only fixed for  $\omega^2 > a$ , we may extrapolate it in quite an arbitrary way for smaller values of  $\omega^2$ . Then, beginning at F we may construct the curve FP by means of formula (52), so that

$$z_P - z_F = \int_{\sqrt{b}}^{\omega} ct(\xi) d\xi / \sqrt{\omega^2 - \xi^2}, \text{ where } t(\xi) = t(PF), b = N(F).$$

Fig. 6.



So the result is shown to be dependent on an infinity of voluntary assumptions, and it will be quite impossible to find out the true dependence of N on  $z$  in this way. This indeterminedness is already foreshadowed in the example to which formula (59) refers. In this example different functions N give the same  $t(\omega)$ , so it is impossible to find  $N(Z)$  from  $t(\omega)$  if the point of beginning is unknown. On the other hand, the assumptions about F and about  $t(FP)$  for  $\omega > a$  are limited, because  $t(FP)$  may not turn out negative, and because a very peculiar form of these curves must be rejected as unnatural. So it may turn out that in practice the function  $N(z)$  is to be fixed with a certain degree of probability.

§ 14. It may be shown that the bending of rays round the earth by a spherical layer may be treated by the same methods. In this case (fig. 6) the concentration  $n$ , and thus  $N$ , depend on the radius vector  $r$ . Let the ray be supposed to start at 0 with an angle  $\theta$  to the vertical. Let

$$MP = r = R + z, \quad MO = R, \quad \angle OMP = \phi.$$

Then we have to apply the mechanics of a point moving in a central field of force.

In this case we have

$$\frac{1}{2}M(\dot{r}^2 + r^2\dot{\phi}^2) + V = E, \quad . \quad . \quad . \quad (63)$$

where

$$E = \frac{1}{2}Mc^2, \quad V = \frac{1}{2}Mc^2 \frac{N}{\omega^2};$$

so

$$\dot{r}^2 + r^2\dot{\phi}^2 = \left(1 - \frac{N}{\omega^2}\right)c^2 \quad . \quad . \quad . \quad (64)$$

Now, because the field is a central one,

$$r^2\dot{\phi} = \text{const.} = Rc \sin \theta, \quad . \quad . \quad . \quad (65)$$

so that

$$\dot{r}^2 = c^2 \left(1 - \frac{N}{\omega^2} - \frac{R^2}{r^2} \sin^2 \theta\right), \quad . \quad . \quad . \quad (66)$$

Now, as  $r - R = z \ll R$ ,

$$1 - \frac{R^2}{r^2} = \frac{2z}{R}; \quad . \quad . \quad . \quad (67)$$

thus

$$cdt = \frac{dr}{\sqrt{\cos^2 \theta + \frac{2z}{R} \sin^2 \theta - \frac{N}{\omega^2}}}, \quad . \quad . \quad . \quad (68)$$

$$d\phi = \frac{\sin \theta}{R} \frac{\left(1 - \frac{2z}{R}\right) dz}{\sqrt{\cos^2 \theta + \frac{2z}{R} \sin^2 \theta - \frac{N}{\omega^2}}} \quad . \quad . \quad . \quad (69)$$

From this the time and the place of the point P may be derived by mere integration. In the special case that  $\theta = 90^\circ$

$$R\phi = \int \frac{\left(1 - \frac{2z}{R}\right) dz}{\sqrt{\frac{2z}{R} - \frac{N}{\omega^2}}}.$$

The maximal value of  $z$  is reached when the denominator is zero. As

$$\frac{2z}{R}$$

is of the order of magnitude of  $\frac{1}{30}$ , it is seen that the returning of the wave-group to the earth begins at a point where the concentration is only  $\frac{1}{30}$  of the corresponding concentration in the case of vertical ascent.

Further, putting

$$(R + z_e)\phi = ct,$$

it is possible to calculate the effective height  $z_e$  at which the waves have to travel, neglecting dispersion, to arrive in the same time. For  $\theta = 90^\circ$  approximately

$$z_e = \frac{\int 2z \, dz / \sqrt{2z/R - N/\omega^2}}{\int dz / \sqrt{2z/R - N/\omega^2}} \quad \cdot \quad \cdot \quad \cdot \quad (70)$$

§ 15. In the foregoing paragraphs I have tried to present some results which may be of use to those who work in the field of radio-wave propagation. There are, perhaps, two practical objections to my results which I should like to point out myself: first, absorption is never accounted for\*, and in the second place, we always assumed the condition (b) § 2 to be valid. Now this condition, translated into the quantities belonging to the mechanical image, becomes

$$(b') - \dots \frac{h}{M} \left| \text{grad } V \right| < < (E - \dot{V})^{3/2},$$

so it no longer holds when  $E = V$ . Thus, especially in the case of vertical ascent, something may happen at the maximal height which affects our results. This would require a careful examination of the original wave-equation, containing the time,  $\omega$  being eliminated.

\* P. Epstein (Proc. Nat. Ac. Sc. xvi. p. 37, 1930) recently proved that absorption may have a large influence on the behaviour of the rays.

LII. *Further Experiments on the Cohesion of Quartz Fibres.* By G. A. TOMLINSON, B.Sc. (from the National Physical Laboratory) \*.

**I**N a recent paper on "Some Phenomena of the Contact of Solids"† some very interesting experiments were described by Mr. W. Stone, who finds the adhesion of fused glass beads to be due to the presence of a water film on the surface of the glass. The adhesion invariably vanished in an atmosphere of dry air, and reappeared on renewing the film by breathing on the beads.

Mr. Stone made reference to my paper‡ on "Molecular Cohesion," remarking that his experiments lead to somewhat different conclusions. My principal conclusions were based on a study of the adhesion of quartz fibres, and it would certainly be necessary to revise these conclusions considerably if Mr. Stone's explanation of the adhesion of glass beads should apply also to the case of quartz fibres. I gave reasons in the paper for believing that the attraction of the fibres was a case of true cohesion, and was not an electrical force or a surface tension effect, my reason for excluding the latter being that the fibres immediately before an experiment were heated in a flame almost to the softening point of fused silica. The publication of Stone's interesting work, however, made it very advisable to test the adhesion of quartz fibres in a similar way, and a brief account of some further experiments follows.

Two quartz fibres were placed in a thick-walled brass cylinder, attached to metal rods passing through rubber bungs with enough flexibility to allow them to be manipulated from outside, to move them into contact or separate them. The fibres were heated in a flame, and the vessel immediately sealed up with a glass plate at each end. The fibres were now tested, and exhibited their usual property of adhesion. Dried air was then circulated through the vessel, having passed on its way through sulphuric acid, two calcium chloride towers, a tube containing a mixture of phosphorus pentoxide and powdered ignited pumice, and, finally, a cotton-wool

\* Communicated by the Author.

† *Phil. Mag.* ix. p. 610 (1930).

‡ *Loc. cit.* vi. p. 695 (1928).

filter. The air emerging from the vessel was not passed into the atmosphere, but was returned in a closed circuit through the drying system.

The result of this experiment was that I could detect no change in the adhesion of the fibres after circulating the dried air continuously for about six hours. After this the vessel was left in open communication with the drying tubes, and I have examined the adhesion at frequent intervals. Although the present experiments are largely qualitative, the strength of adhesion can be judged fairly well by the elastic deflexion of the fibres, and at the end of seven weeks in a dry atmosphere there was little, if any, diminution in the observed adhesion. On the other hand, fibres left exposed to the atmosphere lose most of their adhesion in a few hours, due to the slow accumulation of contaminating matter from the air.

To verify these results further, I have made another experiment, using two fibres in a different vessel that was exhausted by a mercury condensation pump. At the same time the fibres were heated by means of two grids of nichrome wire wound on mica frames, the fibres being situated between the two grids. This time the fibres were manipulated by deflecting a flexible magnetic needle suitably disposed inside the vessel. After subjecting the fibres to this treatment for the whole of a day, there was no change noticeable in the adhesion. A thermo-couple was afterwards substituted for the fibres, the temperature of which under the same conditions was found to be  $140^{\circ}$  C., which is probably lower than the corresponding temperature of the fibres owing to the higher thermal conductivity of the metal wires.

My experiments thus show that the adhesion of quartz fibres is not due to a film of water, as Stone found in the case of the glass beads. I find that in a dry and dust-free atmosphere the adhesion of quartz, instead of vanishing, persists for an unprecedented length of time. As regards the adhesion of glass in general, in my earlier experiments the behaviour of glass was found to be very fickle, and for this reason quartz was a preferable material to work with. For example, in working with glass one pair of blown bulbs might exhibit no tendency at all to adhere, like the dried glass beads in Stone's investigation. A different pair, on the other hand, may behave in a

way which leaves little doubt that the surfaces unite in true cohesion. The severance of the two can sometimes actually be heard as a faint musical clink, and the making of contact is frequently audible as a rather harsh rasping sound, probably caused by slight tremors in the tangential direction at the instant of contact.

An experiment I have described elsewhere\* may be referred to, as affording independent evidence that this condition of solid cohesion can be realized experimentally. In this experiment a light disk having 3 feet of clean lead is placed on a plate of clean glass (or steel), and the plate is carefully inverted. This can be done leaving the disk clinging to the underside of the plate.

Another experiment, not described hitherto, leads to the same conclusion, and perhaps has some interest in the present connexion. If a clean piece of glass is stroked repeatedly with a clean piece of metal, a faint film gradually forms on the surface of the glass. The first appearance resembles a dirty mark on the glass, but it is impossible to remove the film by hard rubbing or any ordinary mechanical means. On continuing the stroking the film increases in thickness and begins to assume the characteristic colour of the metal used. Its attachment to the glass remains very tenacious, and even hard scraping with the tip of a knife only results in removing the upper layers of the film. The layer in contact with the glass persists after prolonged scraping, although it has been reduced in thickness so far as to lose its characteristic colour altogether and become semi-transparent. Various metals, including copper, aluminium, nickel, lead, iron, and tin can be deposited upon glass in this way, and also upon polished hardened steel. A peculiarity of the film, in the case of a soft metal such as lead, is that when scraping it with a knife it feels considerably harder than the metal would be normally, giving the impression that some of the hardness of the surface layer of the glass is imparted by the bonding forces to the film of metal atoms. There can be little doubt that these films are united to the glass by cohesion bonds comparable in tenacity with those existing in the interior of a solid.

I have mentioned these other undoubted cases of solid cohesion because it is in some respects surprising

\* *Loc. cit.* vii, p. 905 (1929).



that cohesive attraction so largely eludes direct observation. The phenomena of solid friction and wear strongly suggest that cohesive combination is always an accompaniment of contact, a view also advocated recently by P. E. Shaw\* in connexion with tribo-electric phenomena and friction. It is probably the comparative coarseness of most solid surfaces, when considered in units of atomic dimensions, that renders the cohesive attraction generally imperceptible.

---

LIII. *A Micromanometer of High Sensitivity.* By E. OWER, A.C.G.I., B.Sc, National Physical Laboratory †.

OF the various types of instruments yet devised for air speed measurement, undoubtedly the most reliable and satisfactory is the combined pitot-static tube, which forms the accepted standard for speeds of the order of 15 feet per second and upwards. In view of the increased attention paid in recent years to the measurement of low air speeds, it is desirable to extend the calibration and use of the pitot-static tube to much lower speeds. Unfortunately, however, the differential pressures set up at such speeds are so small that considerable difficulty is experienced in measuring them with sufficient accuracy. The lowest speed for which the velocity head can be measured with an accuracy of  $\pm 1$  per cent. by the use of the standard 13-inch Chattock gauge is about 6 feet per second; but this degree of precision can only be achieved, at this speed, under the best conditions, and by taking the mean of numerous observations.

Attempts to increase the sensitivity of the Chattock gauge have not met with appreciable success, and the writer has therefore spent much time in a search for a means of measuring pressure differences that shall be capable of considerably greater sensitivity than the Chattock gauge and yet be as simple as possible. In this work he has borne in mind the desirability of the retention of one of the great advantages of the Chattock

\* *Loc. cit.* ix. pp. 577, 628 (1930).

† Communicated by E. F. Relf, Superintendent, National Aerodynamics Department.

gauge—that its calibration can be determined purely from measurements of length and of the density of the manometric liquid.

Many different devices were examined before a solution was found, but they all failed to give satisfaction, either on account of their extreme sluggishness of action under very small differential pressures, or because their zero readings were indefinite. Finally, the writer came across references to papers by B. J. P. Roberts\* and A. Henry† describing proposals for manometers consisting, in effect, of U-tubes having their two vertical limbs connected by a length of horizontal capillary tubing in which a small air-bubble separates the two columns of liquid. In both cases the applied pressure difference was to be measured in terms of the displacement of the bubble along the capillary tube. An instrument of this type possessing both the necessary sensitivity and a reasonable range would require a capillary of considerable length, and there would be a possibility that the bubble might not return exactly to its zero position after a large movement; the latter effect was, in fact, noticed by Henry. It appeared possible, however, that a null reading instrument based on these lines and using the Chattock principle, in which the movement of the liquid levels under pressure is balanced by tilting the cups, might be successful, and this proved to be the case.

Preliminary experiments with two cups, similar to those ordinarily used in the Chattock gauge, and connected by means of capillary tubing, showed that by a suitable choice of dimensions and manometric liquid an instrument sensitive to pressure differences of the order of 0.00001 inch of water could be designed without difficulty. This sensitivity was attained with the experimental rig-up with cups about 100 mm. diameter and capillary of 3 mm. bore and with xylol as the manometric liquid, and the rate of response to pressure changes was satisfactorily rapid. A number of liquids was tried, but none seemed as good as xylol in respect of mobility of the air-bubble in the capillary. Xylol is suitable also in other ways, as it is not excessively volatile and has a specific gravity less than that of water (about 0.86). Among other facts

\* "On a Compensated Micromanometer," *Proc. Roy. Soc. A*, lxxviii. p. 410 (1906).

† "A Micromanometer," *Comptes Rendus*, clv. p. 1078 (1912).

established by these preliminary experiments was the need to maintain steady and uniform temperature conditions over the whole instrument and the necessity for keeping the capillary horizontal. In the latter connexion, it was observed that when the capillary was inclined the bubble drifted under gravity towards the higher end, although the rate of movement was exceedingly slow for small inclinations.

The fact that the bubble can drift in an inclined capillary tube indicates that liquid can pass between its boundaries and the walls of the tube. It might, therefore, be feared that, even if the tube be horizontal, after the bubble has moved under an applied pressure difference it may fail to return to its original zero position upon removal of the pressure. However, this effect was found to be imperceptible; nor has it been observed under the more refined observations that can be carried out on the finished instrument. In practice, moreover, excessive motion of the bubble will be prevented by the use of a tap as in the Chattock manometer. All that is, in fact, necessary is to ensure that the capillary always remains horizontal irrespective of the movement of the cups. This can be done either by providing flexible rubber connexions between the capillary and the tubes leading from the cups and clamping the capillary to a fixed support, or by arranging the axis of the capillary to be parallel to the axis about which the cups tilt. From the following description of the finished instrument it will be seen that the latter alternative was preferred, as it was thought that difficulties might arise from small volume changes consequent on the movement that would have to be allowed to flexible connexions.

*Description of the Instrument.* (See figs. 1-3.)

As will have been gathered from the foregoing remarks, the instrument embodies the Chattock tilting principle with, however, a much more sensitive means of indication. In order to maintain the two cups at as nearly the same temperature as possible they are bored out of a single gun-metal casting and have thick walls; their internal diameter is 4 inches. To the underside of the cup casting are soldered three small steel balls which engage with a cone H, a lateral groove (not shown), and a horizontal

plane K carried by the upper lever D; the plane is provided with vertical screw adjustment. In this way the cups are geometrically located on the lever D, but can be lifted off if required. This lever is hinged to a

Fig. 1.

Fig. 2.

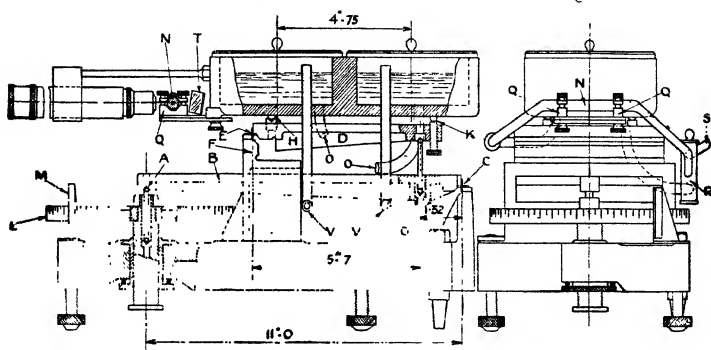
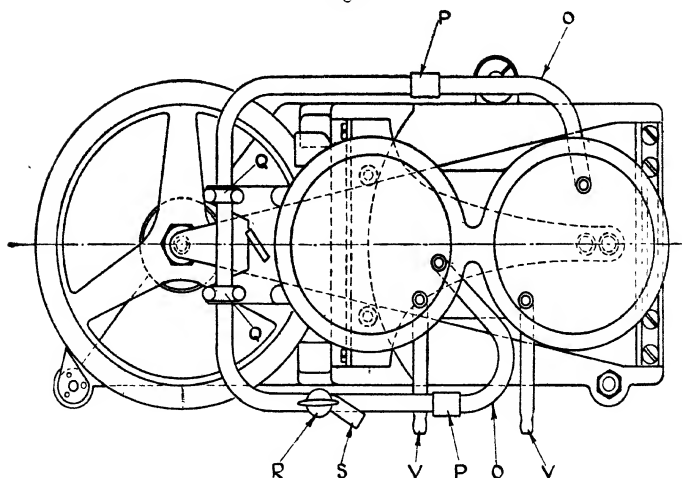


Fig. 3.



bridge piece F, which is securely bolted to the main base casting by means of crossed strips of spring steel, as shown at E, the axis of rotation being the intersection of the horizontal and vertical strips. Frictionless motion

is thus secured. The free end of D carries an inverted conical cup which engages with the upper end of a ball-ended strut whose lower end works in a similar cup G, fixed in the intermediate lever B near the fulcrum of the latter. This intermediate lever is hinged in the same manner to the base casting by spring hinges at C, while its free end A is moved, by means of a ball-ended strut-and-cup arrangement exactly similar to that already described, by the main micrometer screw, which is partially bored out as shown, to accommodate the strut. The micrometer screw works in the base casting which rests on three supports, two of which are adjustable for levelling purposes and are arranged so that the capillary can be levelled without affecting the tilt of the cups.

The function of the intermediate lever between the cup casting and the micrometer screw is to provide a mechanical reduction of the motion of the cups, so that the relative vertical motion of two points, one on each cup axis, is only  $1/10$  of the corresponding movement of the screw. How this is effected will be clear from the figures. Thus it is possible to ensure that, as far as the mechanical construction of the instrument is concerned, readings can be repeated to the desired degree of accuracy, viz., 0.00001 inch, without demanding a screw thread cut to limits outside those possible with normal workmanship.

The motion of the cups is read by means of the graduated rim of the wheel L attached to the micrometer screw and moving over the fixed vertical scale M. Slightly over an inch of total travel is permitted for the screw, whose buttress thread has a pitch of 0.05 inch. The diameter of the screw is 1 inch, and a spring nut is provided to prevent possible back-lash. The periphery of the wheel is divided into 500 parts, each of which represents 0.00001 inch change of liquid level in the cups, and is actually rather more than 0.04 inch long.

The capillary tube N forms part of a circuit of tubing (not shown completely in fig. 1; best seen in fig. 3) providing free communication between the liquid in the two cups. Of this circuit the parts OO soldered to the cups consist of "compo" tubing of about  $\frac{1}{4}$ -inch bore leading to lengths of glass tubing of the same bore. The capillary tube, of 3 mm. bore and about 3 inch long, is fixed at each end of these portions of glass tube. Connexion between the latter and the compo tubes is made

by means of corks PP impregnated with gelatine solution to render them leak-tight. Rubber joints are precluded, as they are soon destroyed by the xylol. The component tubing, while being amply stiff, still has sufficient flexibility to enable it to be bent with ease, so that its ends butt accurately in line against the ends of the glass tubes to which it is connected. Undue strains on the glass-work, which is independently held by rigid clamps, are thus avoided when the corks are in place. The horizontal capillary forms the highest part of the tubing circuit, so that there is no risk of loss of the bubble. The capillary is gripped in two V-blocks QQ carried by a brass plate supported from the cup casting and provided with a certain amount of adjustment, so that the axis of the capillary can be set horizontal and parallel to the axis of tilt of the cups.

Once in the glass tube the air-bubble rises into the capillary. The bubble is easily introduced through the two-way tap R, by means of which one of the cups can be connected either to the other cup or to a short open-ended branch tube S. After all the tubing connecting the cups has been filled with liquid the tap is turned so as to connect one of the cups with the open branch, and the bubble is forced in under a small head of liquid. A further function of the tap, which is performed by means of a quarter turn, is to stop all movement of the bubble as in the Chattock gauge.

The bubble is viewed through a microscope of about 30 magnifying power, carried by a bracket from the cup casting, and is illuminated by light reflected from the small adjustable mirror T. As source an ordinary 4-volt flash-lamp bulb is used, which at first was carried by a bracket from the microscope holder, but in this position, although the filament was over 2 inches from the capillary and above it, the minute quantity of radiant heat reaching the capillary was sufficient to disturb the zero reading seriously each time the bubble was allowed to move. The lamp is now fixed to the outside of the temperature insulation box in which the manometer is enclosed. Light from the lamp passes through a glass cell let into the wall of the box, and containing a solution of cupric chloride to filter the heat rays. The box itself is of wood, double-walled, with broken cork packing in the wall space, and lined with copper sheet. The microscope passes

through a hole in the front wall, while a claw projects through the roof for operation of the tap R. A universal joint is included in the claw spindle, and the claw is fairly slack on the head of the tap, so that the main action applied by the claw is a torque with little bending. Of the manometer itself only the front of the rim of the graduated micrometer wheel protrudes from the box, the necessary aperture being covered by a velvet curtain. Even so, it is essential to lag the capillary tube with cotton wool, to screen it from the heat of the hand of the operator adjusting the wheel.

Copper tubes VV, passing up through the bottoms of the cups and projecting above the levels of the liquid, serve to connect the instrument to the sources of pressure whose difference is to be measured. The cups are sealed by means of glass desiccator lids with ground rims resting on the tops of the cup walls, which are machined and polished. The joints are made good in the ordinary manner, except that instead of grease, which is attacked by xylol, soft soap is used. A viscous mixture of treacle and glycerine is used as a lubricant for the two-way tap.

With the somewhat extensive protection against temperature changes described, the performance of the instrument is entirely satisfactory, and it responds quite readily to changes of the applied pressure difference. The total vertical range of the cup movement is just over 0.1 inch, so that velocity heads corresponding to air speeds from 20 feet per second downwards can be measured. On the assumption of a sensitivity of 0.00001 inch of water, the lowest velocity head that can be measured to one per cent. accuracy corresponds to a speed of 2.1 feet per second. Actually, the sensitivity of the instrument is better than this: it is possible over short intervals of time (two or three minutes) to repeat the zero reading to at least 0.000005 inch. But whether conditions will remain steady long enough for this accuracy always to be achieved in practice is doubtful. Certain measurements already made of the differential pressure set up by a pitot-static tube moving through air at about 1.6 feet per second indicate that generally the zero for a single reading will not be certain to finer limits than 0.00001 inch. By taking the mean of several readings, however, the accuracy can probably be improved somewhat. It is, then, safe to say that the manometer is capable of

measuring the velocity head for a speed of 2 feet per second with an accuracy of  $\pm 1$  per cent., and that, under favourable conditions, this accuracy can be extended to a somewhat lower speed. On speed itself the accuracy is, of course, double that on velocity head; so that, provided a reliable source of velocity head is available, a speed of about 1.5 feet per second can be measured to  $\pm 1$  per cent.

It should be pointed out that no claim is advanced that this instrument is suitable for the measurement of low air speeds in mines or engineering works, although in certain conditions it may be possible to use it for such purposes. The accurate measurement of low speeds is a difficult operation which is best carried out in the laboratory. This manometer is intended to be chiefly a laboratory standard against which other instruments, such as vane, torsion, or hot-wire anemometers, better adapted for general use, can be calibrated.

Valuable advice was given during the design of the instrument by Dr. G. Barr, of the Chemistry Department, N.P.L., in connexion with the chemical problems that arose, and by Mr. J. E. Sears, Jr., of the Metrology Department, on certain important mechanical details; and the writer wishes to express his indebtedness to both these gentlemen.

---

LIV. *Crystal Structure in the System Copper-Bismuth.*  
By WILLIAM F. EHRET, *Ph.D.*, and RAY D. FINE, *M.Sc.*\*

[Plate II.]

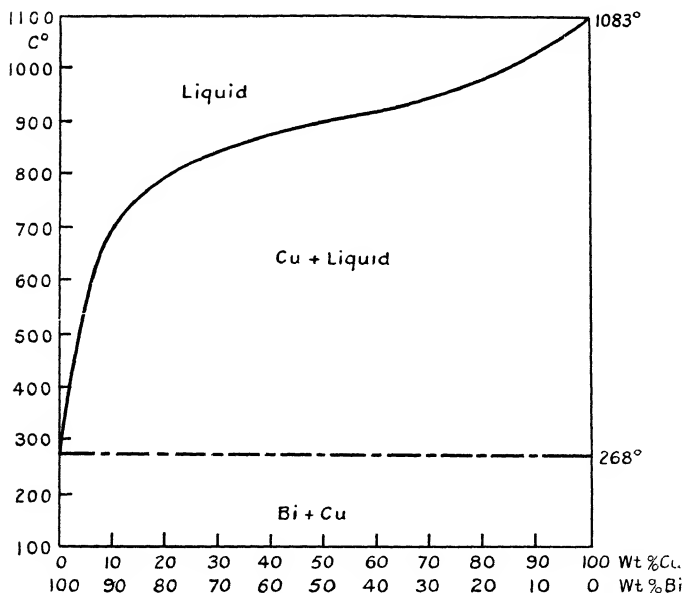
CRYSTAL structure in the system Cu-Bi was determined in connexion with a plan to study the relation between structure and composition in systems of the type A-B, in which A is Cu, Ag, or Au and B is As, Sb, Bi, or P. Since this work was begun the results of a crystal-structure analysis of the systems Cu-Sb and Ag-Sb have been published by Westgren, Hägg, and Eriksson<sup>(1)</sup>. The preliminary results obtained in our laboratory on the alloys of Cu and Sb were in complete accord with those of the Swedish workers, and nothing further has been done with this system. We hope to report our findings in some of the other systems shortly.

\* Communicated by the Authors.



The earliest systematic investigation of the alloys of Cu and Bi was probably that by Roland-Gosselin<sup>(2)</sup>. This and the work of later investigators—Heycock and Neville<sup>(3)</sup>, Gautier<sup>(4)</sup> and Jeriomin<sup>(5)</sup>—established the thermal diagram for the system (fig. 1). It is one of the simplest possible, no compound formation or solid solution being indicated. The eutectic temperature apparently lies very close to the melting-point of pure Bi. This in itself is an indication of very low solubility of Cu in liquid Bi at its melting-point. Tammann<sup>(6)</sup>

Fig. 1.



Equilibrium Diagram of the System Cu-Bi according to Jeriomin.

mentions this system as one of the very few binary metallic systems in which, as far as thermal analysis can discern, no solid solution or compound formation takes place.

For several reasons it might be suspected that the equilibrium diagram is not as simple as the thermal analysis indicates. They are as follows:—(i.) Sb and Bi are known to form a continuous series of solid solutions. The Cu-Sb system<sup>(1)</sup> involves both solid solution and compound formation. Likewise Cu and Ag form a broken series of solid solutions, and

solid Ag dissolves Bi to the extent of 5.3 per cent.\* Also, Au and Cu form an unbroken series of solid solutions and Au dissolves 4.5 per cent. Bi<sup>(7)</sup>. These facts readily lead to the inference of an appreciable solubility of Bi in Cu. (ii.) In all the systems mentioned above there is appreciable solubility of the lower melting in the higher melting solid †. (iii.) Bernal<sup>(8)</sup> places Cu fourth on his approximate scale of dissolving power of the metals. On the average, only Pd, Pt, and Ag show greater dissolving power. (iv.) Although it might be argued that solid solution is not to be expected between two metals so different in atomic volume as Cu ( $=11.8$ ) and Bi ( $=34.0 \text{ c.c.} \times 10^{-24}$ )<sup>(9)</sup>, it is well known that Bi is soluble in Ni in the solid state to the extent of 5.0 per cent. even though the atomic volumes of the latter elements show a greater divergence than Cu and Bi.

Several investigations of the solubility of Bi in Cu have been carried out. Jeriomin<sup>(5)</sup>, using the microscopic method, placed the solubility between 0.25 and 0.5 per cent. Portevin<sup>(10)</sup> found Bi insoluble. Recently, Hanson and Ford<sup>(11)</sup> concluded, from microscopic observations, that the solubility is approximately 0.001 per cent. Bernal<sup>(8)</sup> reports the solubility as nil. The deleterious effect of small quantities of Bi upon the rolling properties of Cu, a fact well known to metal workers, points to a very limited solubility of Bi in Cu. This particular phase of the subject has been discussed in several publications recently<sup>(12)</sup>.

Due to certain limitations inherent in the method of X-ray analysis employed, it is only possible to say, as the result of the work described below, that the solid solubility of Bi in Cu, and *vice versa*, is less than approximately 0.5 atomic per cent. Between these limits Cu and Bi form a series of heterogeneous alloys, the characteristic diffraction pattern of both metals being present on all the X-ray photograms.

### *Preparation and Composition of Alloys.*

A series of alloys, covering the whole range, was prepared from electrolytic Cu and from Bi of a high degree of purity supplied by Eimer and Amend. of New York City. Cu was determined electrolytically and Bi by the oxychloride method, after the basic nitrate and the phosphate methods had been

\* From results, soon to be published, obtained by S. J. Broderick in this laboratory.

† With the exception of Au-Sb. No information is available concerning the equilibrium diagrams of Au-P and Ag-P.

tried and found less reliable. The compositions were as follows:—

TABLE I.

Sample No.	1.	2.	3.	4.	5.	6.	7.	8.	9.	10.	11.	12.
Per cent. Bi ..	0.0	8.0	15.4	23.7	28.6	48.4	60.8	62.0	86.8	93.1	95.5	100
Per cent. Cu...	100	92.0	84.6	76.3	71.4	51.6	39.2	38.0	13.2	6.9	4.5	0.0

The melts were made in unglazed porcelain crucibles in an electrically heated furnace. The temperature was controlled with the aid of a previously determined temperature-current curve for the furnace. The melting was carried on under a thin layer of powdered charcoal and in an atmosphere of illuminating gas. It is believed that oxygen was thus effectively excluded. The melts were cooled rapidly, and samples for X-ray analysis taken by filing. The filings were annealed to remove stains set up during the cooling and cold working. Microscopic examination revealed all alloys heterogeneous and a complete absence of  $\text{Cu}_2\text{O}$ .

#### *Method of Working.*

Powder photograms of the pure metals and alloys were taken on the standard Davey apparatus<sup>(13)</sup>. The diffraction pattern of pure NaCl was taken simultaneously with each of the metal powders, the latter being diluted with corn-starch to reduce their absorptivity to that of the standardizing substance. In order to measure the positions of the diffraction lines accurately, a correction curve, using the known interplanar spacings for NaCl, was drawn for each photogram. The error in the measurements is thereby reduced to about 0.1 per cent. To arrive at the most probable value of the edge-length of the unit cells, the method of plotting the calculated values of  $\log a_0$  on arithmetic probability paper<sup>(14)</sup> was chosen. The mean error of the parameter values given may be estimated at 0.004 Å.

#### *Experimental Results.*

*Pure Cu.*—A large number of determinations of  $a_0$  for the face-centred unit cube of Cu are now available. It may be well to survey the field before giving the results of the present investigation. It is interesting to note that values as

diverse as 3.59 and 3.68 Å. have been reported. Wyckoff<sup>(15)</sup> summarizes the work previous to 1926 and gives an average value of 3.60(3) Å. Jung<sup>(16)</sup>, in the same year, summarizes the previous work and obtains an average of about 3.60(6) Å., although his own experiments lead to a value of 3.620 Å. Since 1926 a number of careful redeterminations of  $a_0$  for Cu have been made, chiefly in the laboratory of Professor Westgren at Stockholm. They leave little doubt that the most probable value is  $3.608 \pm 0.003$  Å.

In Table II. the results of the present investigation are given. The values of the interplanar distances are, in the case of pure Cu, the averages of readings taken from two photograms.

TABLE II.

Indices of planes.	Cu, <i>d</i> <sub>hkl</sub> .	Cu, log <i>a</i> <sub>0</sub> .	Cu, <i>a</i> <sub>0</sub> .	No. 2, <i>d</i> <sub>hkl</sub> .	No. 2, log <i>a</i> <sub>0</sub> .	No. 2, <i>a</i> <sub>0</sub> .
111	2.081 Å.	.5567	3.603 Å.	2.081 Å.	.5567	3.603 Å.
100(2)	1.089	.5585	3.618	1.806	.5577	3.612
110(2)	1.281	.5589	3.622	1.282	.5594	3.626
113	1.087	.5570	3.606	1.086	.5566	3.603
111(2)	1.039	.5561	3.598	1.039	.5561	3.598
133	0.828	.5575	3.610	0.829	.5580	3.614
120(2)	0.805	.5566	3.603	0.806	.5568	3.604
<i>a</i> <sub>0</sub> = 3.607 Å.			<i>a</i> <sub>0</sub> = 3.604 Å.			

The most probable value of  $a_0$  for pure Cu as obtained by plotting  $\log a_0$  on probability paper is 3.607 Å. If the average of the values of  $a_0$  is taken we get 3.608 Å. The density of Cu, calculated from the foregoing, is 8.94 as compared with the experimental value 8.89 (International Critical Tables). The value of  $a_0$  as obtained from the diffraction lines due to Cu in photograms of alloy No. 2 (Table I.) is 3.604 Å. If the average is taken in this case, we get 3.608 Å. These variations lie within the limits of experimental error, and indicate that any distortion in the lattice of Cu, due to dissolved Bi, is beyond detection by our method. In order to verify the foregoing statement, and at the same time eliminate any errors that might be due to differences in absorptivity, readings taken from two different films, etc., a comparison photogram was made in which the diffraction patterns of Cu and alloy No. 2 were recorded side by side on the same film and under

identical conditions. The average difference between the radii of corresponding diffraction rings on the two spectra is 9.1 per cent. This is the same as the average difference between two sets of measurements of the same spectrum taken at two different times. The two spectra are therefore identical within these limits.

In accordance with what was to be expected, as the result of the microscopic examination, all the alloys produce two superimposed diffraction patterns analogous to Cu and Bi. Pl. II., in which an attempt has been made to reproduce the photograms, shows the parent patterns in each of the alloys.

*Pure Bi.*—In so far as the authors are aware, no new values for the lattice constants of Bi have appeared since the summary of previous values by Wyckoff in 1926<sup>(15)</sup>. The parameter values depend upon the axes of reference chosen. When rhombohedral axes mutually inclined at  $87^{\circ}34'$  are employed, the average of previously obtained values is 6.549 Å. for the length of the side of the unit rhombohedron containing 8 atoms. With this choice of axes the unit of structure contains two interpenetrating face-centred rhombohedral lattices so situated with respect to one another that the whole lattice appears to be one of slightly distorted simple cubes. If the simpler primitive rhombohedron containing two Bi atoms is chosen as the elementary cell, the axes are mutually inclined at  $57^{\circ}16'$ , and the average of previous values of the edge of the elementary rhombohedron is 4.731 Å. Davey<sup>(17)</sup> used hexagonal axes of reference, and obtained  $4.539 \pm 0.005$  Å. for the side of the elementary triangular prism, the axial ratio being 2.606.

Table III. summarizes the results of our measurements on pure Bi and the corresponding diffraction lines of alloy No. 8. They are based on the simple primitive rhombohedron containing two atoms in the unit cell.

The appended values for  $a_1$  were obtained by the method of graphical solution from the values calculated for the various planes. If averages had been taken, the corresponding values would have been 4.749 and 4.757 Å. respectively. Similar measurements of the photogram for alloy No. 9 give a value of  $a_1$  identical with that of alloy No. 8. Since the difference between  $a_1$  for pure Bi and that for Bi supposedly saturated with Cu is just beyond the limits of experimental error, it is not possible to conclude from these measurements that any solid solution with consequent change in lattice has occurred. This opinion is further supported by one of our photograms in which the diffraction patterns of Bi and alloy

No. 11 were recorded simultaneously and under identical conditions. Measurements of the radii of the diffraction rings due to Bi on the two spectra agreed with one another to within 0.1 per cent.

In order to facilitate comparison of our results with former ones sometimes calculated on the basis of different axes, Table IV. has been constructed. The axial ratio has been established both crystallographically and by X-ray analysis.

TABLE III.

Indices of planes (87° 34').	Indices of planes (57° 16').	Bi, $d_{hkl}$ .	Bi, $\log a_1$ .	Bi, $a_1$ (57° 16').	No. 8, $d_{hkl}$ .	No. 8, $\log a_1$ .	No. 8, $a_1$ (57° 16').
200	110	3.29 Å.	.6775	4.759 Å	3.33 Å )	(.6827)	(4.817 Å.)
220	211	(2.354)	(.6737)	(4.718)	2.372	.6770	4.753
202	101	2.274	.6763	4.745	2.283	.6780	4.764
222	222	—	—	—	1.973	.6756	4.738
222	200	1.870	.6765	4.748	1.873	.6772	4.755
200	220	1.637	.6754	4.736	1.647	.6780	4.764
420	321	1.495	.6774	4.758	1.496	.6777	4.761
402	211	1.445	.6767	4.750	1.447	.6773	4.757
422	310	1.332	.6768	4.751	1.336	.6781	4.765
$a_1 = 4.749 \text{ Å.}$				$a_1 = 4.758 \text{ Å.}$			

TABLE IV.

System of axes chosen.	(Bi) $a$ .	Axial ratio.
Rhombohedral, $a = 87^\circ 34'$ .....	6.577 Å.	—
Rhombohedral, $a = 57^\circ 16'$ .....	4.749	—
Hexagonal .....	4.551	2.606

The intensities of the reflexions for Bi are in agreement with those previously observed<sup>(19)</sup>. No new light is shed on the question of the amount of displacement of the two face-centred rhombohedral lattices in the direction of the trigonal axis. The calculated density of Bi is 9.72 as compared with the experimental which is 9.67 (International Critical Tables). Our value of  $a_1$  is higher than any previously reported. It corresponds closely to that found by Hassel and Mark<sup>(19)</sup>, viz. 4.74 Å.

There remains to be considered the question of the amount of solid solubility that can be detected by our method. If we make the simplifying assumptions that the atomic radii are equal to one-half the distance of closest approach of the atoms, and that the distance of closest approach is a linear function of the composition, it is possible to calculate, on the basis of the structures of Cu and Bi, that solid solution to the extent of approximately 0.5 atomic per cent. should be detectable. Very little importance can, however, be attached to this estimate, since we are dealing with two different types of structure, and also, as is well known, solid solution frequently occurs without change in lattice.

### *Summary.*

As part of a programme to determine crystal structure in binary alloys in which one component is Cu, Ag, or Au and the other As, Sb, Bi, or P, the structure of alloys of Cu and Bi was examined and is here reported.

All the alloys examined were heterogeneous, showing clearly the superimposed diffraction patterns of Cu and Bi. Within the limits of our experimental error the lattices of Cu and Bi remain unchanged in their alloys. This is indicative of a very low mutual solubility.

The lattice constant of the face-centred unit cube of Cu is redetermined,  $a_0 = 3.607 \pm 0.004 \text{ \AA}$ . This is in very close agreement with several recent determinations.

Employing rhombohedral axes, mutually inclined at  $57^\circ 16'$ , the length of the edge of the elementary rhombohedron of the Bi structure is found to be  $4.749 \pm 0.005 \text{ \AA}$ . This is slightly higher than previously determined values.

### *References.*

- (1) Westgren, Hägg, and Eriksson, *Zeitschr. f. physik. Chemie*, B, iv. (6), p. 453 (1929).
- (2) Roland-Gosselin, *Bull. Soc. d'Encour.* (5) i. p. 1300 (1896).
- (3) Heycock and Neville, *Phil. Trans. A*, clxxxix. p. 25 (1897).
- (4) Gautier, 'Contribution à l'étude des alliages,' p. 110 (1901).
- (5) Jeriomin, *Zeitschr. anorg. Chemie*, lv. p. 413 (1907).
- (6) Tammann, *ibid.* liii. p. 454 (1907).
- (7) Nowack, *Zeitschr. Metallkunde*, xix. p. 238 (1927).
- (8) Bernal, *Trans. Faraday Soc.* xxxv. p. 372 (1929).
- (9) Goldschmidt, *Zeitschr. f. physik. Chemie*, cxxxiii. p. 397 (1928).
- (10) Portevin, *Rev. Mét.* iv. p. 1077 (1907).
- (11) Hanson and Ford, *Metal Industry* (London), xxx. p. 314 (1927).
- (12) Meissner, *J. Inst. Metals*, xxxii. p. 530 (1922); Schreiber, *Metal Industry* (London), xxi. p. 362 (1922); Stahl, *Metall u. Erz*, xxii. p. 421 (1925); Hanson and Ford, *loc. cit.*; Freude, *Metallbörse*, xviii. pp. 818, 874, 1043, 1099 (1928).

- (13) Davey, General Electric Rev. xxv. p. 565 (1922); J. Opt. Soc. Am. v. p. 479 (1921).  
(14) Davey, General Electric Rev. xxix. p. 118 (1926).  
(15) Wyckoff, International Critical Tables, i. p. 347 (1923).  
(16) Jung, *Zeitschr. f. Krist.* lxiv. p. 413 (1926).  
(17) Davey, Phys. Rev. xxv. p. 753 (1925).  
(18) McKeehan, J. Franklin Inst. cxcv. p. 59 (1923).  
(19) Hassel and Mark, *Zeitschr. f. Physik*, xxiii. p. 269 (1924).

Washington Square College,  
New York University.

---

LV. *The Interaction of Molecules with the Silver Ion*.\*

By FREDERICK KARL VICTOR KOCH†.

IT has been shown by Fajans and Joos (*Zeit. Physik*, xxiii. p. 1, 1924) both on the basis of refractometric data and on theoretical grounds that ions cannot be adequately represented as rigid electronic structures, but that they undergo a certain degree of polarization or "deformation" (Fajans) when subjected to the electrical fields of other neighbouring ions. That such a deformation takes place has been confirmed experimentally both for the crystalline state (Fajans and Joos, *l. c.*) and for concentrated electrolyte solutions in water (Fajans, Kohner, and Geffcken, *Z. Electrochem.* xxxiv. p. 1, 1928). On these lines Fajans (*Z. Elektrochem.* xxxiv. p. 502, 1928) has concluded that the transition from an electrovalent to a covalent linkage is continuous, and that the covalent bond may be regarded as having its origin in the extreme mutual deformation of the electron orbits of the constituent ions.

A parallelism to the above may be predicted for the interaction of ions and molecules, and solvation (the ionic molecular electrovalency) may be regarded as merging gradually into complex formation (the ionic-molecular covalency).

It is therefore to be expected that the refraction of an ion will vary with the solvent in a manner analogous to that with which it varies in the proximity of other neighbouring ions. The refractometric data relating to electrolytes in non-aqueous solvents (see Walden, 'Elektrochemie

\* Communicated by Prof. J. C. Philip.

† Feit Scientific Research Fellow.



nichtwässrige Lösungen,' 1924, p. 276) are, unfortunately, so scanty, and the effects to be expected in general are so small, that practically no conclusions can be drawn from this source. Schreiner (*Z. Physikal. Chem.* cxxxv. p. 461, 1928) did, however, find a change in the refraction (extrapolated to infinite dilution) of completely ionized hydrogen chloride and lithium chloride in water, methyl alcohol, and ethyl alcohol which must be ascribed to the effect of the solvent. The refractometric method has the inevitable disadvantage that the data always refer to at least two ions, and thus complicate the interpretation thereof.

Another possible line of approach, which is that attempted in this instance, is to compare the free energies of solvation of an ion which have been determined experimentally ( $A_E$ ) with those ( $A_T$ ) calculated by the method of Born (*Zeit. f. Physik*, i. p. 45, 1920) for the *ideal* case on the assumption that the ion is a rigid sphere located in a continuous medium of dielectric constant ( $\epsilon$ ). The differences  $A_C = A_E - A_T$  will represent the extra energy expended in the excess mutual deformation above that due to the induced moment (which is taken into account by the dielectric constant). This energy may therefore be termed the "Free Energy of Complex Formation" \* ( $A_C$ ). The experimental values of the free energies ( $A_E$ ) can be obtained from electrometric measurements of the variation of the electrode potential with the solvent.

The electrode potential of a metal represents the difference in the free energy of the ions in the metallic crystal and in the solvated state. The difference between the normal potential of a metal in two different solvents will therefore represent the difference in the free energies of solvation of the ion ( $\Delta A_E$ ). Thus

$$\Delta A_E = (A_E)_1 - (A_E)_2 = n \cdot F \cdot (E_1 - E_2) = R \cdot T \cdot \log_e P_1/P_2$$

$= R \cdot T \cdot \log_e \gamma_s$ , where  $(A_E)_1$ ,  $(A_E)_2$  are the free energies of solvation,  $E_1$ ,  $E_2$  the normal potentials,  $P_1$ ,  $P_2$  the Nernst solution tensions in the solvents 1 and 2 respectively, and  $\gamma_s$  is the specific distribution coefficient of the metal ion. The values of  $E_1$ ,  $E_2$ ,  $P_1/P_2$ , or  $\gamma_s$  can be determined experimentally, and hence  $\Delta A_E$  can be calculated. The

\* Under "complex formation" are grouped all those effects which deviate from the ideal state of Born, *e. g.*, (1) change in radius or shape of the ion or surrounding molecules, (2) electrical saturation effects in the medium surrounding the ion.

absolute free energy of solvation ( $A_E$ ) cannot be determined experimentally. By choosing  $A_E$  for a single solvent such that  $A_E = A_T$  it is, however, possible to calculate the remaining values of  $A_E$  by adding the differences  $\Delta A_E$ . This procedure will, of course, introduce a constant error into the values of  $A_E$ , since it is improbable that the ideal conditions are attained in any actual case. Thus the free energies of complex formation will all be too small by a constant amount ( $\chi$ ), and may more exactly be represented by ( $A_C - \chi$ ).

The free energies of solvation ( $A_E$ ) have been calculated for the silver ion in ten organic liquids from the experimental values of  $P_1/P_2$  determined by the author (J. Chem. Soc. 1928, p. 279). The assumption that  $A_E = A_T$  has been made in the case of acetone because the solution tension of silver and the solubility of silver nitrate are less in this than in any of the other solvents, and there is therefore reason to suppose that the tendency of the silver ion to form complexes is least in this case.

The ideal free energy of solvation ( $A_T$ ) of an ion, which represents the work obtained in transferring it from a vacuum into the solvent ( $\epsilon$ ), is given by the formula

$$A_T = 1.194 \times 10^{-11} \cdot e^2 \cdot z^2 \cdot N \cdot (1 - 1/\epsilon) / r_i \text{ kil. calories,}$$

where  $e = 4.774 \times 10^{-10}$  e.s.u. is the electronic charge,  $z$  is the valency, and  $r_i$  the radius of the ion, and  $N = 6.06 \times 10^{23}$  is the Avagadro Number. Using the experimental value of  $r_i = 1.13 \text{ \AA.U.}$  given by Goldschmidt (Trans. Faraday Soc. xxv. p. 282, 1929) deduced from X-ray analysis of crystal structure, the above equation reduces to

$$A_T = 146(1 - 1/\epsilon).$$

*Uncertainty due to  $r_i$ .*—The theoretical value for the radius of the silver ion calculated by Pauling (see Goldschmidt, *l.c.*) on the basis of the wave mechanics is  $r_i' = 1.26 \text{ \AA.U.}$ , and the value of the radius of the silver atom is  $r_a = 1.44 \text{ \AA.U.}$  The corresponding values of ( $A_C - \chi$ ) are included in the table in order to illustrate the effect which an error in  $r_i$  would have upon ( $A_C - \chi$ ). An error in  $r_i$  would, of course, cause an error in  $A_T$ , and hence part of ( $A_C - \chi$ ) would not be due to a deviation from the ideal state, but to the use of an incorrect ionic radius. The error due to this cause may be estimated as follows:—

$$A_C - \chi = A_E - A_T = A_E - 165 \times 10^{-8} (1 - 1/\epsilon) r_i.$$

By partial differentiation with respect to  $r_i$

$$\partial A_c = 165 \times 10^{-8} (1 - 1/\epsilon) \cdot \partial r_i / r_i^2.$$

This is the absolute error for all solvents. For acetone ( $\epsilon=21$ ) ( $A_c - \chi$ ) has, however, been taken arbitrarily as zero, and hence the absolute error also becomes zero. The error, referred to zero error for acetone, is therefore

$$\partial A_c' = 165 \times 10^{-8} (1/21 - 1/\epsilon) \cdot \partial r / r_i^2.$$

Taking  $r_i = 1.13 \text{ \AA.U.}$  and  $\partial r_i = \pm 0.3 \text{ \AA.U.}$ , i. e., a 30 per cent. error in the ionic radius—

For aniline.....	$\epsilon = 6.9$	$\partial A_c = \pm 3.8$
„ water .....	$\epsilon = 81.7$	„ $= \pm 1.4$
„ acetonitrile .....	$\epsilon = 36.4$	„ $= \pm 0.8$

*Uncertainty due to  $\epsilon$ .*—The effect which an experimental error in the dielectric constant would have upon ( $A_c - \chi$ ) may be found by partial differentiation with respect to  $\epsilon$ .

Taking  $r_i = 1.13 \text{ \AA.U.}$ ,

$$\partial A_c = 146 \cdot \partial \epsilon / \epsilon^2.$$

### Nitrogen Bases.

SOLVENT.	$\epsilon$ .	$A_E$ .	$A_T$ .	$A_c - \chi$ .		
				$r_i = 1.13 \text{ \AA.U.}$ (Goldschmidt).	$r_i' = 1.26 \text{ \AA.U.}$ (Pauling).	$r_a = 1.44 \text{ \AA.U.}$ (atom).
Aniline .....	6.85	147.2	124.6	22.6	21.1	19.5
Pyridine .....	12.4	151.7	134.2	17.5	17.1	16.5

### Nitriles.

Phenylaceto- nitrile.....	15	142.8	136.2	6.6	6.6	6.0
Acetonitrile .....	36.4	145.8	142.0	3.8	3.8	4.5
Propionitrile.....	27.5	144.1	140.7	3.4	3.7	3.8
Benzonitrile .....	26.3	142.7	140.4	2.3	2.5	2.7
Ethylcyano- acetate .....	27.7	142.8	140.6	2.2	2.4	2.5

### Alcohols.

Water .....	81.7	144.0	144.2	(-0.2)	0.4	1.0
Methyl Alcohol	35.4	141.5	141.8	(-0.3)	(-1.3)	(-2.3)
Ethyl Alcohol .....	25.4	141.1	140.3	0.8	0.4	1.2
Acetone.....	21	(139.0)	139.0	0	0	0

For an error of 10 per cent. in the dielectric constant—

For aniline . . . .	$\epsilon = 6.9$	$\partial\epsilon = \pm 0.7$	$\partial A_c = \pm 0.21$
„ water . . . . .	$\epsilon = 81.7$	„ $= \pm 8.0$	„ $= \pm 0.17$
„ acetonitrile .	$\epsilon = 36.4$	„ $= \pm 4.0$	„ $= \pm 0.44$

It will be seen that none of these errors is sufficiently large to account for the observed regularities.

The values of  $(A_c - \chi)$  fall into three classes, which merge, however, into one another, showing that the transition from solvation to complex formation is gradual. The classification into (1) nitrogen bases, (2) nitriles, (3) alcohols is, moreover, independent of whether  $r_i$ ,  $r_i'$  or  $r_n$  be used, but the value  $r_i = 1.13$  Å.U. must, of course, be regarded as the most appropriate. It therefore appears that these differences have a real significance, and in fact they stand in good agreement with the well-known chemical properties of the silver ion. Complex ions of the type  $\text{Ag}(\text{C}_5\text{H}_5\text{N})_2^+$  etc. are known to exist, whereas the silver ion is not known to form definite complexes with water, the alcohols, or acetone. It might perhaps be concluded that the constant error ( $\chi$ ) is negligibly small. The increased activity of the nitrile group in phenylacetonitrile, due to the substitution of the phenyl group in acetonitrile, is paralleled by the author's observation that boiling phenylacetonitrile reacts with silver nitrate, giving silver cyanide, whereas acetonitrile does not. The results thus lend additional support to the above procedure.

Solvation may be defined as that state of ionic-molecular interaction in which the electronic configurations of the ions and molecules are quasi-rigid. In this ideal state the whole deformation effect may be ascribed to the moment induced in a continuous dielectric medium by a rigid ion, and is given by the Born formula (*l.c.*). In any natural case there is, however, a further deformation due to the change in shape of the ion and one or more orientated solvent molecules. In the most extreme cases, which are generally known as "complex formation," the changes are of a still more profound nature, as is evidenced by the well-known colour effects etc., and there is an exact stoichiometrical relationship between the constituent ions and molecules. It is further to be expected that the action of the ion will be localized at certain parts of the molecules, and in the above examples of the silver ion at the nitrogen

and oxygen atoms. Since the refraction of an electrical system is a measure of its deformability (*cf.* Debye, *Handb. der Radiologie*, Bd. vi. p. 605), it is of interest to note that the refraction of nitrogen in aniline (primary amine) is 2.32 of nitrogen in pyridine (mol. refract. pyridine—5/6 mol. refract. benzene) is 2.25; of nitrogen in the nitriles (including half the acetylene bond) is 1.92; of oxygen in hydroxyl 1.52; and of oxygen in ketones 1.62.

In conclusion, the author wishes to thank the Trustees of the Beit Fellowship for a Fellowship.

Physical Chemistry Department,  
Imperial College of Science and Technology,  
London, S. W. 7.  
19th May, 1930.

LVI. *A Theorem in Determinants.* By J. B. COLEMAN \*.

**THEOREM.**—If the signs of all the elements in the alternate diagonals of a determinant be changed, the value of the determinant will be unchanged, unless the determinant be of odd order and a principal diagonal be one of the diagonals whose elements are changed, in which case the value of the determinant will be changed in sign, and sign only.

The theorem is established directly from the following lemma:—

**Lemma.**—Let A and B be two sets of numbers, each consisting of the integers 1, 2, 3, 4, . . . ,  $n$ . Let  $n$  number pairs  $(i, j)$  be formed,  $i$  being a number of set A and  $j$  being a number of set B, so that each number in A, and likewise each number in B, occurs once and only once in a pair. In all cases there will be an even number of pairs the sum of whose integers,  $i+j$ , is odd.

**Proof of Lemma.**—We shall call a pair an even pair if the sum of the integers is even, and an odd pair if the sum of the integers is odd. Now  $i+j$  can be even only if both  $i$  and  $j$  are even, or both odd. Let  $A_1$  and  $B_1$  be the sets remaining after removing from A and B, respectively, the numbers used in forming even pairs, for any possible pairing according to the lemma. Let  $k$  be the number of even numbers in  $A_1$ . Then there will be  $k$  even numbers in  $B_1$ , since A and B are

\* Communicated by the Author.

identical, and the same number of evens are removed from each. Also since the numbers of  $A_1$  and  $B_1$  form odd pairs, the even numbers of  $A_1$  must be paired with the odd numbers of  $B_1$ , so that there must be  $k$  odd numbers in  $B_1$ . Hence  $B_1$ , and likewise  $A_1$ , must contain  $2k$  numbers. Consequently the number of odd pairs is always even.

*Corollary.*—For any set of  $n$  pairs formed according to the conditions of the lemma there will be an even number of even pairs if  $n$  be even, and an odd number of even pairs if  $n$  be odd.

This is a direct result of the lemma, in which it was shown that the number of odd pairs is always an even number.

*Proof of Theorem.*—The terms in the expansion of a determinant of order  $n$  each consist of  $n$  factors of the form,  $a$ , the row and column indices forming a number pair for each factor. By a familiar law of determinants these pairs occur in any term of the expansion exactly as the sets of number pairs in the lemma above. Now in a set of alternate diagonals which does not include a principal diagonal all of the elements are such that  $i+j$  is odd. These index pairs correspond to odd pairs in the lemma. Consequently there must be an even number of such pairs, *i. e.*, there must be an even number of factors from this set of diagonal elements in any term of the expansion of the determinant. Hence changing the signs of all these elements will not affect any term in the expansion, proving the first part of the theorem.

In a set of alternate diagonals which does include a principal diagonal, every element is such that  $i+j$  is even, corresponding to an even pair in the lemma. By the corollary there will be an even number or an odd number of such pairs, according as  $n$  is even or  $n$  is odd, *i. e.*, there will be in each term of the expansion of the determinant an even number or an odd number of factors from this set of elements, according as  $n$  is even or odd. Then, if the sign of each element in such a set of alternate diagonals be changed, the terms in the expansion of the determinant will be unchanged or else all changed in sign, according as  $n$  is even or  $n$  odd. Hence the theorem.

Though it furnishes nothing new, it might be noted that the theorem with reference to change of sign of elements in alternate diagonals is also true when stated for change of sign of elements in alternate rows (or columns), principal diagonal being replaced by middle row (or column).

This theorem will be found to have special application in

continuan's. Its application to determinants of the third and fourth orders is shown below :—

$$\begin{vmatrix} a_{11} & a_{12} & a_{13} \\ a_{21} & a_{22} & a_{23} \\ a_{31} & a_{32} & a_{33} \end{vmatrix} = \begin{vmatrix} a_{11} & -a_{12} & a_{13} \\ -a_{21} & a_{22} & -a_{23} \\ a_{31} & -a_{32} & a_{33} \end{vmatrix} = - \begin{vmatrix} -a_{11} & a_{12} & -a_{13} \\ a_{21} & -a_{22} & a_{23} \\ -a_{31} & a_{32} & -a_{33} \end{vmatrix}$$

$$\begin{vmatrix} a_{11} & a_{12} & a_{13} & a_{14} \\ a_{21} & a_{22} & a_{23} & a_{24} \\ a_{31} & a_{32} & a_{33} & a_{34} \\ a_{41} & a_{42} & a_{43} & a_{44} \end{vmatrix} = \begin{vmatrix} a_{11} & -a_{12} & a_{13} & -a_{14} \\ -a_{21} & a_{22} & -a_{23} & a_{24} \\ a_{31} & -a_{32} & a_{33} & -a_{34} \\ -a_{41} & a_{42} & -a_{43} & a_{44} \end{vmatrix} = \begin{vmatrix} -a_{11} & a_{12} & -a_{13} & a_{14} \\ a_{21} & -a_{22} & a_{23} & -a_{24} \\ -a_{31} & a_{32} & -a_{33} & a_{34} \\ a_{41} & -a_{42} & a_{43} & -a_{44} \end{vmatrix}$$

University of South Carolina,  
Columbia, S. C.,  
October, 1929.

## LVII. *Graphic Statistics : Per mille Paper.*

By A. F. DUFTON, M.A., D.I.C.\*

1. IT is convenient to represent a frequency-distribution by means of a curve or diagram, which conveys the general run of the observations to the eye better than a column of figures, and for this purpose Galton's ogive, the frequency-polygon and the histogram are commonly used.

Galton's method has the advantage that the meaning of the various percentiles is simple and readily understood. The ogive curve, however, does not bring out any asymmetry in the distribution so clearly as does the frequency-polygon. None of the methods shows at a glance whether the distribution is normal.

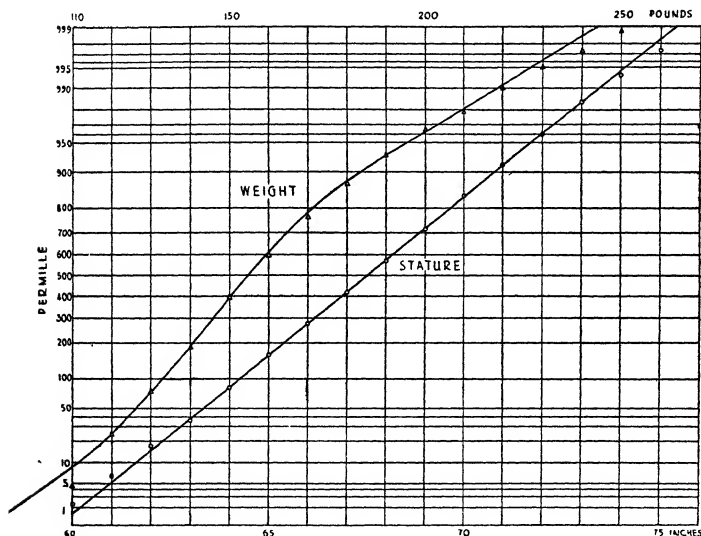
In the method of representation now proposed, the figures of the original table are added up step by step, so as to give the total frequency not exceeding the upper limit of each class interval, and ordinates are then erected to a horizontal base to represent, to a special scale, these integrated frequencies as parts permille; a smooth curve may be drawn through the tops of the ordinates. The special frequency scale is the scale of deviates of the

\* Communicated by the Author.

normal curve for each permille of frequency\*. When drawn to this scale a normal frequency-distribution is of course represented by a straight line.

2. In illustration of this method it is of interest to consider the curves obtained for two examples of vital statistics—the frequency-distribution of statures for adult males born in Great Britain and Ireland and the frequency-distribution of weights† (fig. 1). It is clear

Fig. 1.



that the frequency-distribution of stature is sensibly normal while that of weight is asymmetrical.

The weight-curve is not analytically simple. The smooth curve drawn, however, is of interest as it represents the normal distribution for a population of which two-thirds have an average weight of 152 pounds, with a standard deviation of 14 pounds, and one-third an average weight of 166 pounds, with a standard deviation of 28 pounds.

\* 'Tables for Statisticians and Biometricians,' p. 1.

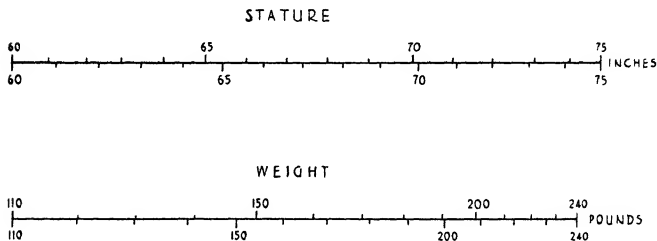
† Yule, 'Theory of Statistics,' pp. 88 & 95.



3. By an anamorphosis the curve can be transformed into a straight line, a scale of measurement being determined which makes the frequency-distribution normal: this may be of advantage when the functional scale so obtained is simple.

In a paper on "The Geometric Mean in Vital and Social Statistics" \* Galton states that the ordinary law of Frequency of Error, based on the arithmetic mean, corresponds sufficiently well with the observed facts of vital and social phenomena to be very serviceable to statisticians, but is far from satisfying their wants and may lead to absurdity when applied to wide deviations. Thus the law is very correct in respect to ordinary measurements of stature, although it asserts that the existence of giants, whose height is more than double the mean height of their race, implies the possibility of dwarfs

Fig. 2.



whose stature is less than nothing at all. Galton concludes that vital and sociological phenomena are, as a general rule, subject to the condition of the geometric mean and suggests that they are properly measured in logarithmic units.

In fig. 2 the functional scales for stature and weight are shown which make the frequency-distributions normal. Each is drawn above a logarithmic scale and it is clear that these two examples do not support Galton's contention.

4. It would appear desirable to have a name for the coordinate paper upon which the frequency curves are plotted: the name *Permille* is suggested.

Greenbank, Garston,  
Hertfordshire.

\* Proc. Roy. Soc. xxix. p. 365 (1879).

LVIII. *The Electrical Conductivities of Dilute Sodium Amalgams at various Temperatures.* By W. J. DAVIES, M.Sc., and Professor E. J. EVANS, D.Sc., *Physics Department, University College of Swansea* \*.

THE present research is a continuation of the systematic investigations carried out by several observers† in the Physical Laboratories of the University College of Swansea on the conductivities of dilute amalgams at various temperatures.

As the amalgams hitherto examined were those of metals belonging to Groups II., III., and IV. of the periodic table, it was decided to measure as accurately as possible the electrical conductivities of amalgams of sodium, a metal belonging to Group I. of the periodic table. Previous work carried out at Swansea and elsewhere has shown that the solution of metals in mercury causes an increase in conductivity, but this does not appear to be the case for alkali amalgams. These amalgams differ in other respects from the amalgams of other metals. Their formation is accompanied by the evolution of a great amount of heat, and their viscosity ‡ is greater than that of the amalgams of other metals.

Measurements of the electrical conductivities of sodium amalgams have been carried out by Batelli §, Grimaldi ||, Vanstone ¶, Müller \*\*, Bornemann and Rauschenplatt ††, Rogers ‡‡, Feninger §§, Lewis and Hine ||||, and Boohariwalla, Paranjpe and Prasad ¶¶.

\* Communicated by Prof. E. J. Evans, D.Sc.

† E. J. Williams, *Phil. Mag.* p. 589 (September 1925); T. I. Edwards, *Phil. Mag.* p. 1 (July 1926); A. L. Johns and E. J. Evans, *Phil. Mag.* p. 271 (February 1928); T. C. Williams and E. J. Evans, *Phil. Mag.* p. 1231 (December 1928).

‡ Feninger, 'Die Electriche Leitfähigkeit und innere Reibung Verdunter Amalgame,' Freiburg (1914).

§ *Atti Accad. Lincei*, [4] iii. p. 19 (1887).

|| *Atti Accad. Lincei*, [4] iii. p. 32 (1887).

¶ *Journ. Chem. Soc.* cv. p. 2617 (November 1914).

\*\* 'Metallurgie,' vii. p. 767 (1910).

†† 'Metallurgie,' ix. p. 510 (1910).

‡‡ *Phys. Rev.* [2] viii. p. 259 (1916).

§§ *Loc. cit.*

|||| *Nat. Accad. Sci. Proc.* ii. p. 634 (November 1916); *Journ. Amer. Chem. Soc.* [39] i. p. 882 (May 1917).

¶¶ *Indian Journ. Phys.* iv. pt. ii. p. 14 (April 1929).

Vanstone was chiefly concerned with the conductivities of solid amalgams and concentrated liquid amalgams; but Müller and Bornemann and Rauschenplatt determined the electrical conductivities of a few dilute sodium amalgams of different concentrations at temperatures varying from 50° C. to 350° C. Feninger, in addition to measuring the conductivities of dilute amalgams containing 0.201, 0.761, 1.192, 2.175, and 2.690 gram atoms per cent. of sodium, determined the viscosities of the amalgams at room temperature. The two most recent investigations of the electrical conductivities of sodium amalgams are due to Lewis and Hine\*, and Boohariwalla, Paranjpe and Prasad†.

The former investigators determined at a temperature of 20° C. the relative conductivities (*i. e.*, the conductivities with respect to mercury at the same temperature) of eleven sodium amalgams of concentrations ranging from 0.09 to 4.9 gram atoms per cent. of sodium, and the latter measured the electrical conductivities at 30° C. of eighteen sodium amalgams of concentrations ranging from 0.159 to 2.75 gram atoms per cent.

As the results of the above investigations are not in agreement, and comparatively few experiments had been carried out at temperatures above 80° C., it was hoped that the present investigation, which deals with the conductivities of dilute sodium amalgams of concentrations varying from 0.307 atom per cent. to 5.270 atoms per cent. at temperatures ranging from 0° C. to about 300° C., would throw further light on the problem.

The accurate determination of the electrical conductivities is difficult, especially at high temperatures, as sodium amalgams readily oxidize and react chemically with the glass or quartz of the containing vessel. From the experimental results are calculated certain quantities which are of importance in a theory of the conductivity of amalgams put forward by Skaupy‡. If  $L$  and  $\eta$  represent the conductivity and viscosity respectively of pure mercury, and  $\Delta L$ ,  $\Delta \eta$  the change in conductivity and viscosity due to a concentration  $C$  of the metal expressed in gram atoms dissolved in 100 gram atoms of mercury,

\* *Loc. cit.*

† *Loc. cit.*

‡ *Zeit. für Phys. Chem.* lxxviii. p. 560 (1907); *Verb. Deut. Phys. Ges.* xvi. p. 166 (1914); *ibid.* xviii. p. 252 (1916); *Phys. Zeit.* xxi. p. 597 (1920).

then, according to Skaupy, the value of  $\frac{1}{C} \frac{\Delta L}{L} + \frac{1}{C} \frac{\Delta \eta}{\eta}$  at infinite dilution is of the same order of magnitude for all metals dissolved in mercury.

If  $l$  is written for  $\frac{1}{C} \frac{\Delta L}{L}$  and  $r$  for  $\frac{1}{C} \frac{\Delta \eta}{\eta}$ ,

then 
$$H = \frac{1}{C} \frac{\Delta L}{L} + \frac{1}{C} \frac{\Delta \eta}{\eta} = l + r,$$

and

$$H_{\infty} = l_{\infty} + r_{\infty}.$$

Skaupy\* also considered the variation of  $H$  with concentration, and came to the conclusion that  $\frac{H_{\infty} - H}{C}$  should be constant. If the variation of viscosity with concentration can be neglected, it follows that  $l_{\infty}$  should be of the same order of magnitude for all metals dissolved in mercury, and that  $\frac{l_{\infty} - l}{C}$  should be constant.

The experiments carried out in this laboratory seem to lend support to these conclusions in the case of amalgams of metals belonging to Groups II., III., and IV. of the Periodic Table. For example, Williams and Evans† have shown that  $l_{\infty}$  has practically the same value for amalgams of copper, silver, and gold at the same temperature, and also that the relation between  $l_{\infty} - l$  and the concentration  $C$  is a linear one. The possible application of Skaupy's relations to the experimental results obtained for sodium amalgams will be discussed later.

### *Experimental Arrangement.*

#### *General Principle of Method.*

The general principle of the method of measurement is the same as that employed by other investigators working in this laboratory, but various modifications were made in the apparatus owing to the special properties of alkali amalgams.

The conductivity of mercury or an amalgam of given concentration was determined by measuring the electrical

\* *Loc. cit.*

† *Loc. cit.*

resistance of a fine column of the liquid conductor by means of a Callendar-Griffiths bridge in conjunction with a moving coil galvanometer of high sensitivity. The resistances of the bridge were all calibrated in terms of the largest resistance, and thus the relative values of the bridge resistances were accurately known. These relative values are sufficient for an accurate determination of the temperature coefficient of resistivity of pure mercury or of an amalgam, and the absolute value of the resistivity of an amalgam at any temperature can be deduced, if the resistivity of mercury at  $0^{\circ}\text{C.}$  is taken as  $94074 \times 10^{-9}$  ohm per cm.<sup>3</sup>

If  ${}_aR_t$  be the resistance of the amalgam column of length  $l$  and cross-section  $A$  at temperature  $t^{\circ}\text{C.}$ ,  ${}_a\rho_t$  its resistivity, and  ${}_mR_t$ ,  ${}_m\rho_t$  the corresponding quantities for mercury, it then follows that:—

$${}_a\rho_t = \frac{{}_aR_t}{{}_mR_t} \cdot {}_m\rho_t \cdot \dots \dots \dots (1)$$

From equation (1) it is easily seen that the resistivity and conductivity of an amalgam at a temperature  $t^{\circ}\text{C.}$  can be calculated from the resistivity of mercury at the same temperature, and the corresponding values of the resistances of the amalgam and mercury columns. The resistivity of pure mercury at any temperature can be calculated from the equation:—

$$\rho_t = 94074 \times 10^{-9} [1 + 0.38877t + 0.69777t^2 + 0.919t^3],$$

which represents the results of experiments carried out by Williams\* and Edwards† on the resistivity of mercury at temperatures up to  $300^{\circ}\text{C.}$  This equation also represents, within experimental error, the results for pure mercury obtained with the modified apparatus employed in the present research.

An amalgam of a given concentration was heated to a definite temperature by immersing the capillary tube in an iron bath containing a suitable liquid, which could be raised to the boiling point by a burner consisting of a long row of small flames protected from draughts. The liquids employed were methylated spirits, water, aniline, diethylaniline, engenol, and diphenylamine, and consequently measurements could be made at temperatures in the neighbourhood of  $20^{\circ}\text{C.}$  (room temperature),  $78^{\circ}\text{C.}$ ,

\* *Loc. cit.*

† *Loc. cit.*

100° C., 185° C., 225° C., 255° C., and 300° C. Since measurements were also carried out at the temperature of melting ice, it was possible to study the resistivity of an amalgam over a temperature range of 300° C., and measurements at a particular temperature were made under practically constant conditions, as the temperature of the boiling liquids only changed very gradually. The temperatures of the amalgam column were determined by a platinum resistance thermometer, which had been previously calibrated, and also by a suitable mercury thermometer. A set of mercury thermometers, which had been calibrated at the National Physical Laboratory, were used in these measurements. The degree of accuracy attained in the measurement of the bath temperature, when the liquid was boiling steadily, is indicated by the fact that the platinum and mercury thermometers agreed to within 0.1° C., even at 300° C. By taking a large number of observations, the resistance of the capillary column could be determined with an accuracy of about 0.00005 ohm, and since the resistance of the column at 0° C. was almost 0.29 ohm, it can be calculated from the observations that a change of resistance of 0.00005 ohm. corresponds to a change of temperature of 0.19° C. at 100° C., and to about 0.1° C. at 300° C. It is, therefore, seen that the measurement of temperature is of the required order of accuracy.

*Preparation of the Amalgam, and the Measurement of its Resistivity.*

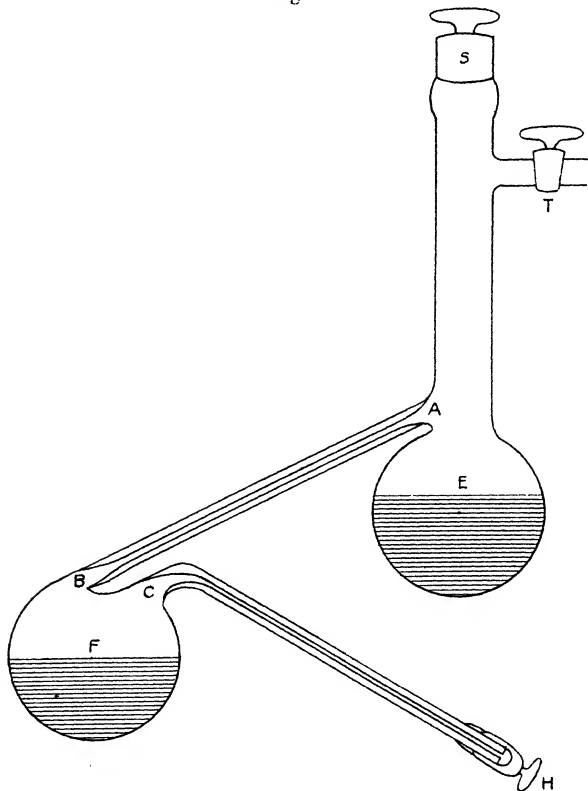
The special properties of the amalgam, such as its affinity for oxygen especially in presence of moisture and its chemical action on glass, necessitated certain modifications in methods previously employed \* for measuring the resistivities of other amalgams.

In the present experiments a quantity of concentrated liquid sodium amalgam was prepared by adding pure sodium contained in a sealed glass tube to a suitable quantity of pure redistilled mercury. The mercury was introduced into a conical flask, which was closed with a tightly fitting stopper, through which passed a bent glass tube connected to a glass tap by means of a short length of pressure tubing. The end of the bent tube outside the

\* T. I. Edwards, *loc. cit.*

flask had been drawn out to a fairly narrow bore. The flask was evacuated and then filled with pure dry nitrogen at atmospheric pressure; the stopper was then removed, and the sealed glass tube containing the sodium was broken and dropped into the mercury. The stopper was then quickly replaced, the flask evacuated, and the mercury

Fig. 1.



warmed until a uniform solution of amalgam was obtained. On cooling, nitrogen was again introduced into the flask, which contained a large quantity of concentrated amalgam, suitable for the preparation of dilute amalgams of various concentrations. This amalgam was, however, covered with oxide films, which were removed by the filtering apparatus sketched in fig. 1.

A large glass bulb E, provided with a tap T and a ground-glass stopper S, was connected with a similar bulb F by means of a coarse capillary tube AB. The bulb F was also provided with a fine capillary tube CH, the end of which was closed by a tightly fitting cap H. The apparatus was evacuated and filled with nitrogen through the tap T. The pressure tubing and tap were removed from the conical flask, and also the stopper S from the filtering apparatus, so that the amalgam could be poured into the bulb E, which was immediately sealed up by replacing the stopper. The apparatus was evacuated, to remove any air which had possibly diffused into the nitrogen during the operation of pouring, and was again filled with pure dry nitrogen. The amalgam contained in the bulb E was bright and clean, as most of the oxide films were removed when it passed through the constricted portion of the bent glass tube attached to the conical flask. The films remaining were almost completely removed by tilting the filtering apparatus so that the amalgam passed through the capillary tube AB into the bulb F. The concentrated liquid amalgam was kept in this bulb in an atmosphere of pure dry nitrogen until required for the preparation of a dilute amalgam of given concentration in the four-electrode resistance tube.

The four-electrode pyrex-glass tube which was employed in measuring the resistances of the amalgams is shown in fig. 2.

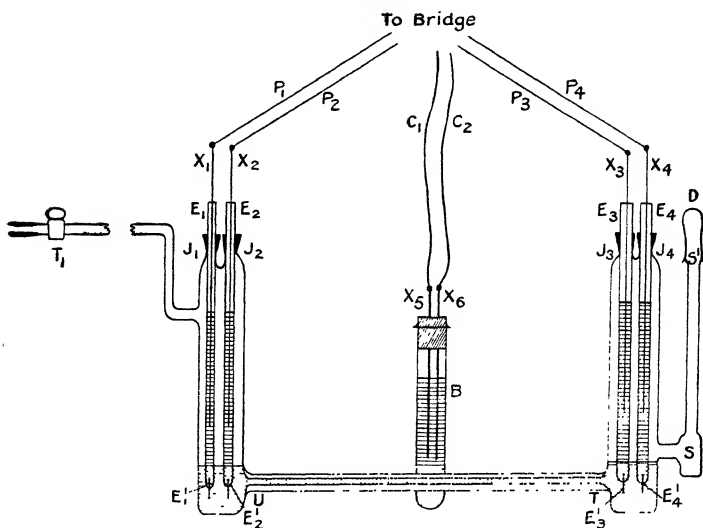
The four electrodes consisted of similar glass tubes,  $E_1E_1^1$ ,  $E_2E_2^1$ ,  $E_3E_3^1$ , and  $E_4E_4^1$ , through the lower ends of which platinum wires were sealed. The tubes were half-filled with mercury into which dipped stout copper wires,  $X_1$ ,  $X_2$ ,  $X_3$ , and  $X_4$ , which could be connected to the Callendar-Griffiths bridge through a specially constructed mercury key by means of flexible leads,  $P_1$ ,  $P_2$ ,  $P_3$ , and  $P_4$ . The compensating leads,  $C_1$  and  $C_2$ , were soldered to copper wires,  $X_5$  and  $X_6$ , which dipped into mercury contained in the test-tube B. This test-tube was placed in the bath near the centre of the capillary, UT, and the compensating leads were also permanently connected to the bridge through the mercury key.

As the amalgam oxidizes readily, it was necessary to work in an atmosphere of an inert gas, and with this end in view the apparatus was in the first place made gas-tight. This was accomplished by painting the ground electrode



joints,  $J_1$ ,  $J_2$ ,  $J_3$ , and  $J_4$ , with cellulose cement, and by sealing the dome D on the ground end of the vertical tube  $SS'$  with white wax. The apparatus could be connected to a pump or a cylinder containing nitrogen through the tap  $T$ , which was lubricated with ordinary tap grease. The tap was placed at a sufficient distance from the bath for the grease to be not affected by the bath, and the amalgam was not contaminated by grease films. A dilute amalgam of the required concentration was now prepared as follows :—

Fig. 2.



A known-weight of pure re-distilled mercury was introduced into the resistance tube through the upright limb  $SS'$ , and the dome D replaced. The tube was evacuated, and filled with nitrogen at atmospheric pressure. The nitrogen was freed from oxygen by passing over red-hot copper, and was also carefully dried. The concentration of the amalgam contained in the bulb F of the filtering apparatus was determined by running out a known-weight through the fine capillary CH into a conical flask, and adding a known volume of standard HCL solution until there was an excess of acid present, when all the sodium had come out of solution in mercury. The excess of acid

was then titrated with a standard solution of sodium carbonate, and from the results the weight of sodium contained in 100 grams of mercury could be calculated in the usual manner. The concentration of the amalgam having thus been determined, it was possible, after experience, to run into the resistance tube approximately the correct amount of concentrated amalgam to produce on admixture with pure mercury a dilute amalgam of the desired concentration. For this purpose the dome D was removed, and the concentrated amalgam run into the tube from the filtering apparatus. This operation was carried out quickly, and both the resistance tube and, filtering apparatus were immediately sealed up again. The resistance tube was then evacuated to a pressure of 1/100 mm. of mercury, to get rid of air which may have diffused into the nitrogen on removing the dome, and, finally, a sufficient quantity of pure dry nitrogen was allowed to enter the tube to produce a pressure of one atmosphere at 300° C. After the resistivities of the dilute amalgam had been measured at various temperatures from 0° C. to 300° C., the amalgam was run out into a conical flask, and its concentration again determined by the method previously described.

The method adopted for measuring the resistance of the amalgam column can be readily understood from fig. 2.

The resistances of the copper wires  $X_1 \dots X_6$  were equal, and the flexible copper leads  $P_1 \dots P_4$ ,  $C_1$ , and  $C_2$ , which also had equal resistances, were placed side by side close together, so that changes of temperature would affect their resistances equally. The following measurements were carried out with the Callendar-Griffiths bridge :—

- (1)  $P_1$  and  $P_4$  were connected to the bridge and the resistance measured. Let  $R_1$  be the resistance.
- (2)  $P_2$  and  $P_3$  were connected to the bridge. Let  $R_2$  be the resistance.
- (3)  $P_1$  and  $P_2$  were connected to the bridge. Let  $R_3$  be the resistance.
- (4)  $P_3$  and  $P_4$  were connected to the bridge. Let  $R_4$  be the resistance.

If  $R$  be the resistance of the amalgam column UT between the two inner electrodes, it can be shown that

$$R = \frac{1}{2}[(R_1 + R_2) - (R_3 + R_4)].$$

In this way the resistances of the various amalgam columns were determined and the electrode resistances eliminated.

### *Experimental Difficulties.*

The pyrex-glass resistance tube employed in the present investigation, after exposure to high temperatures for several hours, showed evidence of having been slightly attacked by the sodium amalgam. It was also noticed that the formation of bubbles in the capillary, at temperatures above  $100^{\circ}\text{C.}$ , was far more prevalent with sodium amalgams than with the other amalgams examined in this laboratory. It is therefore probable that the formation of bubbles is partly due to the chemical action of the amalgam on the glass. These bubbles were removed by placing the tube containing the amalgam in a metal air-bath, which could be tilted in a vertical plane about a fulcrum, and also heated to a temperature above that at which the resistance of the amalgam was measured. By gradually tilting the tube the amalgam was slowly passed through the capillary, and the operation was repeated until the capillary, when examined by a lens, showed no trace of bubbles. Even when bubbles had been removed in this way they frequently reappeared if the tube was kept at a temperature between  $250^{\circ}\text{C.}$  and  $300^{\circ}\text{C.}$  for an interval of one hour. After the resistance of the amalgam had been determined at a temperature above  $100^{\circ}\text{C.}$ , it was removed from the liquid heating bath and the capillary carefully examined for bubbles. If there were no bubbles present, and if the resistance determined at room temperature agreed with the value previously obtained, the high temperature measurement was considered satisfactory.

The analysis of the amalgam, after a set of observations, always indicated a slight loss of concentration as compared with that expected on mixing the amalgam from the filtering apparatus with the pure mercury in the tube. The concentrations given in Tables I. to VIII. are the ones obtained by analysing the amalgams, run out of the tube at the end of each set of experiments with an amalgam of given concentration. It is considered that the concentrations corresponding to the resistivities and conductivities given in these tables are correct to within  $\frac{1}{2}$  per cent. for the more concentrated amalgams, and to within 2 per cent.

for the very dilute amalgams. An inspection of the experimental results, however, shows that the concentration measurements are of sufficient accuracy as compared with the resistivity measurements.

The slight loss in the concentration of the sodium amalgam was also accompanied by a small increase in the diameter of the tube. The tube was cleaned and calibrated with pure mercury at 0° C. and 100° C. after each set of experiments with an amalgam of definite concentration. It was found, after the first set of experiments, that the resistance of the mercury column had diminished by about 1 in 3000 as compared with its original value. A similar decrease was observed after each set of amalgam determinations, but its magnitude diminished progressively. This effect of the amalgam on the diameter of the resistance tube was taken into account in calculating the resistivities and conductivities of the various amalgams.

Although this loss in the concentration of the amalgam was in all probability mainly due to the chemical action of the amalgam on the glass, a small part may possibly be due to oxidation as a consequence of (i.) a small leak of air into the apparatus on removal of the dome when introducing the concentrated amalgam into the tube, and of (ii.) the presence of air films adhering firmly to the glass surface.

At high temperatures, the effect of thermoelectric currents was very noticeable, but it was overcome by first closing the galvanometer circuit and adjusting the bridge resistance until there was no change in the deflexion on completing the battery circuit. Under these conditions, in virtue of the properties of conjugate conductors, the bridge resistance is equal to the resistance being measured. The very small inductance of the amalgam column caused no trouble.

It is estimated that the average error in the measurements of the resistivities and conductivities is not greater than about 1 in 7000, and that the possible error in the calculated values of  $\frac{\Delta L}{L}$  and  $\frac{1}{C} \frac{\Delta L}{L}$  is about 8 per cent.

for the lowest concentrations and about 2 per cent. for the high concentrations. The average temperature coefficient of resistance is estimated to be correct within 0.9 per cent. over the temperature range 0° C. to 20° C., and within about 0.06 per cent. over the range 0° C. to 300° C.

TABLE I.

Results for Eleven Sodium Amalgams of different Concentrations at a Constant Temperature of 0°C.

No. of Amalgam.	Concentration.		Resistance in ohms.		Relative resistivity $\frac{R_t}{m R_t}$ .	Average temperature coefficient of resistivity of Hg from 0° to t° C., $\frac{a_t}{m a_t}$ .		Average temperature coefficient of resistivity of Amalgam from 0° to t° C., $\frac{a_t}{m a_t}$ .		Resistivity of Hg at 0° C., $m \rho_t \times 10^8$ .	Resistivity of Sodium Amalgam at 0° C., $\rho_t \times 10^8$ .	Conduc- tivity of Hg at 0° C., $\frac{1}{m L_t}$ .	Conduc- tivity of Sodium Amalgam at 0° C., $\frac{1}{a_t}$ .	$\frac{\Delta L}{L} \times 10^3$ .	$\frac{1}{C} \cdot \frac{\Delta L}{L} \times 10^3$ .
	% "η,"	Atomic % "C."	$\frac{R_t}{m}$	$\frac{R_t}{a_t}$											
1	·035 <sub>2</sub>	·30 <sub>7</sub>	·2891 <sub>8</sub>	·2898 <sub>5</sub>	1·0023 <sub>3</sub>	—	—	—	—	9407	9429	10630	10605	—·23 <sub>5</sub>	—·77
2	·052 <sub>1</sub>	·45 <sub>4</sub>	·2891 <sub>5</sub>	·2901 <sub>0</sub>	1·0032 <sub>9</sub>	—	—	—	—	9407	9438	10630	10595	—·32 <sub>9</sub>	—·72
3	·076 <sub>2</sub>	·66 <sub>4</sub>	·2891 <sub>7</sub>	·2904 <sub>3</sub>	1·0043 <sub>4</sub>	—	—	—	—	9407	9448	10630	10584	—·43 <sub>3</sub>	—·65
4	·106	·92 <sub>2</sub>	·2716 <sub>6</sub>	·2731 <sub>3</sub>	1·0053 <sub>9</sub>	—	—	—	—	9407	9457	10630	10574	—·52 <sub>7</sub>	—·57
5	·136	1·18 <sub>4</sub>	·2715 <sub>5</sub>	·2734 <sub>0</sub>	1·0068 <sub>1</sub>	—	—	—	—	9407	9471	10630	10558	—·67 <sub>7</sub>	—·57
6	·212	1·84 <sub>9</sub>	·2714 <sub>3</sub>	·2735 <sub>4</sub>	1·0077 <sub>7</sub>	—	—	—	—	9407	9480	10630	10548	—·77 <sub>1</sub>	—·42
7	·262	2·29	·2713 <sub>8</sub>	·2735 <sub>0</sub>	1·0078 <sub>1</sub>	—	—	—	—	9407	9481	10630	10548	—·77 <sub>1</sub>	—·33
8	·297	2·59	·2713 <sub>8</sub>	·2734 <sub>3</sub>	1·0075 <sub>5</sub>	—	—	—	—	9407	9478	10630	10551	—·74 <sub>3</sub>	—·29
9	·354	3·08	·2893 <sub>5</sub>	·2917 <sub>1</sub>	1·0081 <sub>6</sub>	—	—	—	—	9407	9484	10630	10544	—·80 <sub>9</sub>	—·26
10	·458	3·99	·2893 <sub>0</sub>	·2911 <sub>0</sub>	1·0062 <sub>3</sub>	—	—	—	—	9407	9466	10630	10564	—·62 <sub>1</sub>	—·15 <sub>5</sub>
11	·604	5·27	·2891 <sub>5</sub>	·2881 <sub>0</sub>	·9965 <sub>5</sub>	—	—	—	—	9407	9375	10630	10666	+·34 <sub>0</sub>	+·06

TABLE II.

Results for Eleven Dilute Sodium Amalgams at a Constant Temperature of 20° C.

No. of Amalgam.	Concentration.		Resistance in ohms.		Relative resistivity $\frac{R_{20^\circ}}{R_{m, 20^\circ}}$ .	Average temperature coefficient of resistivity of Mercury from 0° to 20° C., = $m^{\alpha_f}$	Average temperature coefficient of resistivity of Amalgam from 0° to 20° C., = $a^{\alpha_f}$		Resistivity of Mercury at 20° C., $m^{\rho_{20^\circ}} \times 10^4$ .	Resistivity of Amalgam at 20° C., $a^{\rho_{20^\circ}} \times 10^4$ .	Conduc- tivity of Mercury at 20° C., $m^{\sigma_{20^\circ}}$	Conduc- tivity of Amalgam at 20° C., $a^{\sigma_{20^\circ}}$	$\frac{1}{\sigma} \cdot \frac{\Delta L}{L} \times 10^3$ .	$\frac{1}{\sigma} \cdot \frac{\Delta L}{L} \times 10^2$ .
	% weight "η."	Atomic % "C."	$\frac{R_{20^\circ}}{m}$	$\frac{R_{20^\circ}}{a}$										
1	·035 <sub>2</sub>	·30 <sub>7</sub>	·2944 <sub>1</sub>	·2951 <sub>2</sub>	1·0024 <sub>1</sub>	·0 <sub>3</sub> 907	·0 <sub>3</sub> 912	9578	9601	10440	10415	—24	—78	
2	·052 <sub>1</sub>	·45 <sub>3</sub>	·2948 <sub>8</sub>	·2954 <sub>8</sub>	1·0037 <sub>3</sub>	·0 <sub>3</sub> 907	·0 <sub>3</sub> 932	9578	9614	10440	10402	—36 <sub>4</sub>	—80	
3	·076 <sub>3</sub>	·66 <sub>4</sub>	·2944 <sub>0</sub>	·2957 <sub>6</sub>	1·0046 <sub>2</sub>	·0 <sub>3</sub> 907	·0 <sub>3</sub> 921	9578	9622	10440	10392	—45 <sub>9</sub>	—69	
4	·106	·92 <sub>2</sub>	·2765 <sub>9</sub>	·2781 <sub>7</sub>	1·0057 <sub>1</sub>	·0 <sub>3</sub> 907	·0 <sub>3</sub> 930	9578	9633	10440	10381	—56 <sub>6</sub>	—61	
5	·136	1·18 <sub>4</sub>	·2764 <sub>6</sub>	·2784 <sub>7</sub>	1·0072 <sub>7</sub>	·0 <sub>3</sub> 907	·0 <sub>3</sub> 934	9578	9648	10440	10365	—71 <sub>9</sub>	—61	
6	·212	1·84 <sub>6</sub>	·2763 <sub>4</sub>	·2789 <sub>2</sub>	1·0093 <sub>4</sub>	·0 <sub>3</sub> 907	·0 <sub>3</sub> 986	9578	9667	10440	10344	—92 <sub>0</sub>	—50	
7	·262	2·29	·2762 <sub>9</sub>	·2787 <sub>7</sub>	1·0089 <sub>8</sub>	·0 <sub>3</sub> 907	·0 <sub>3</sub> 965	9578	9684	10440	10348	—88 <sub>1</sub>	—38	
8	·297	2·59	·2762 <sub>9</sub>	·2786 <sub>3</sub>	1·0084 <sub>7</sub>	·0 <sub>3</sub> 907	·0 <sub>3</sub> 955	9578	9659	10440	10353	—83 <sub>3</sub>	—32	
9	·351	3·08	·2945 <sub>6</sub>	·2973 <sub>8</sub>	1·0094 <sub>6</sub>	·0 <sub>3</sub> 907	·0 <sub>3</sub> 970	9578	9668	10440	10343	—92 <sub>6</sub>	—30	
10	·458	3·99	·2945 <sub>3</sub>	·2967 <sub>2</sub>	1·0074 <sub>4</sub>	·0 <sub>3</sub> 907	·0 <sub>3</sub> 972	9578	9650	10440	10363	—73 <sub>8</sub>	—18 <sub>6</sub>	
11	·604	5·27	·2943 <sub>6</sub>	·2957 <sub>2</sub>	1·0046 <sub>2</sub>	·0 <sub>3</sub> 907	—	9578	9622	10440	10393	—45 <sub>0</sub>	—08 <sub>6</sub>	

TABLE III.

Results for Eleven Dilute Liquid Sodium Amalgams at a Constant Temperature of 78.4° C.

No. of Amalgam.	Concentration.		Resistance in ohms.		Relative resistivity or ratio $\frac{R_t}{R_m}$	Average temperature coefficient of increase of resistivity of Amalgam Mercury from 0° to 78.4° C., $\frac{R_t}{R_m}$		Resistivity of Mercury at 78.4° C., $\frac{R_t}{R_m} \times 10^3$	Resistivity of Amalgam at 78.4° C., $\frac{R_t}{R_m} \times 10^3$	Conduc- tivity of Mercury at 78.4° C., $\frac{L}{\rho_t}$	Conduc- tivity of Amalgam at 78.4° C., $\frac{L}{\rho_t}$	$\frac{\Delta L}{L} \times 10^3$	$\frac{1}{\bar{C}} \cdot \frac{\Delta L}{L} \times 10^3$
	% weight "η."	Atomic % "C."	$\frac{R_t}{m}$	$\frac{R_t}{a}$		$\frac{R_t}{m}$	$\frac{R_t}{a}$						
1	0.35 <sub>2</sub>	0.30 <sub>7</sub>	.3110 <sub>6</sub>	.3121 <sub>0</sub>	1.0035 <sub>0</sub>	0.965	0.982	10119	10155	9882	9848	— .34 <sub>4</sub>	— 1.12
2	0.52 <sub>1</sub>	0.45 <sub>1</sub>	.3109 <sub>6</sub>	.3124 <sub>0</sub>	1.0046 <sub>3</sub>	0.965	0.984	10119	10166	9882	9837	— .45 <sub>6</sub>	— 1.00
3	0.76 <sub>2</sub>	0.66 <sub>4</sub>	.3109 <sub>8</sub>	.3123 <sub>9</sub>	1.0061 <sub>4</sub>	0.965	0.990	10119	10181	9882	9822	— .61	— .92
4	1.06	0.92 <sub>2</sub>	.2921 <sub>8</sub>	.2944 <sub>2</sub>	1.0076 <sub>6</sub>	0.965	0.998	10119	10197	9882	9807	— .75 <sub>9</sub>	— .82
5	1.36	1.18 <sub>4</sub>	.2920 <sub>3</sub>	.2947 <sub>2</sub>	1.0092 <sub>1</sub>	0.965	0.998	10119	10212	9882	9792	— .91 <sub>1</sub>	— .77
6	2.12	1.84 <sub>9</sub>	.2919 <sub>1</sub>	.2952 <sub>7</sub>	1.0115 <sub>1</sub>	0.965	0.1017	10119	10236	9882	9770	— 1.13 <sub>3</sub>	— .61
7	2.62	2.29	.2918 <sub>6</sub>	.2951 <sub>8</sub>	1.0113 <sub>8</sub>	0.965	0.1013	10119	10234	9882	9771	— 1.12 <sub>3</sub>	— .49
8	2.97	2.59	.2918 <sub>6</sub>	.2951 <sub>9</sub>	1.0114 <sub>4</sub>	0.965	0.1016	10119	10235	9882	9771	— 1.12 <sub>3</sub>	— .43
9	3.54	3.08	.3111 <sub>8</sub>	.3150 <sub>6</sub>	1.0122 <sub>7</sub>	0.965	0.1021	10119	10243	9882	9763	— 1.20 <sub>4</sub>	— .39
10	4.58	3.99	.3111 <sub>2</sub>	.3142 <sub>7</sub>	1.0101 <sub>2</sub>	0.965	0.1019	10119	10222	9882	9783	— 1.00 <sub>2</sub>	— .25
11	6.04	5.27	.3109 <sub>6</sub>	.3129 <sub>8</sub>	1.0064 <sub>9</sub>	0.965	—	10119	10185	9882	9818	— .65 <sub>2</sub>	— .12 <sub>4</sub>

TABLE IV.

Results for Eleven Dilute Sodium Amalgams at a Constant Temperature  $t=100^{\circ}\text{C}$ 

No. of Amalgam.	Concentration.		Resistance in ohms.		Relative resistivity or ratio $\frac{R_t}{a}$ $\frac{R_t}{m \cdot K_t}$	Average temperature coefficient of resistivity of Hg from 0° to 100° C. $\frac{m \cdot \alpha_t}{m \cdot \alpha_t}$	Average temperature coefficient of resistivity of Amalgam from 0° to 100° C. $\frac{m \cdot \alpha_t}{m \cdot \alpha_t}$	Resistivity of		Conduc- tivity of Mercury at 100° C., $\frac{L}{m \cdot L_t}$	Conduc- tivity of Amalgam at 100° C., $\frac{L}{a \cdot L_t}$	$\frac{\Delta L}{L} \times 10^3$ .	$\frac{1}{\bar{O} \cdot \bar{L}} \times 10^2$		
	% weight "η."	Atomic % "C."	$\frac{R_t}{m}$	$\frac{R_t}{a}$				Mercury at 100° C., $\frac{\rho_t}{m \cdot \rho_t} \times 10^8$ .	Amalgam at 100° C., $\frac{\rho_t}{a \cdot \rho_t} \times 10^3$ .						
1	.035 <sub>2</sub>	0.30 <sub>7</sub>	.3176 <sub>4</sub>	.3187 <sub>9</sub>	1.0036 <sub>2</sub>	.0 <sub>3</sub> 987	.0 <sub>3</sub> 1001	10336	10373	9675	9640	—	.36 <sub>2</sub>	—	1.17
2	.052 <sub>1</sub>	0.45 <sub>4</sub>	.3176 <sub>0</sub>	.3191 <sub>8</sub>	1.0049 <sub>7</sub>	.0 <sub>3</sub> 987	.0 <sub>3</sub> 1006	10336	10387	9675	9627	—	.49 <sub>6</sub>	—	1.09
3	.076 <sub>2</sub>	0.66 <sub>4</sub>	.3176 <sub>3</sub>	.3197 <sub>4</sub>	1.0066 <sub>4</sub>	.0 <sub>3</sub> 987	.0 <sub>3</sub> 1013	10336	10405	9675	9611	—	.66	—	.99
4	.106	0.92 <sub>3</sub>	.2984 <sub>1</sub>	.3008 <sub>6</sub>	1.0082 <sub>1</sub>	.0 <sub>3</sub> 987	.0 <sub>3</sub> 1019	10336	10421	9675	9596	—	.81 <sub>6</sub>	—	.88
5	.136	1.18 <sub>4</sub>	.2982 <sub>6</sub>	.3012 <sub>7</sub>	1.0100 <sub>9</sub>	.0 <sub>3</sub> 987	.0 <sub>3</sub> 1023	10336	10440	9675	9578	—	1.00 <sub>2</sub>	—	.84
6	.212	1.84 <sub>9</sub>	.2981 <sub>4</sub>	.3017 <sub>3</sub>	1.0120 <sub>4</sub>	.0 <sub>3</sub> 987	.0 <sub>3</sub> 1035	10336	10461	9675	9560	—	1.19	—	.64
7	.262	2.29	.2980 <sub>8</sub>	.3015 <sub>4</sub>	1.0116 <sub>1</sub>	.0 <sub>3</sub> 987	.0 <sub>3</sub> 1028	10336	10456	9675	9564	—	1.14 <sub>7</sub>	—	.50
8	.297	2.59	.2980 <sub>8</sub>	.3016 <sub>8</sub>	1.0120 <sub>8</sub>	.0 <sub>3</sub> 987	.0 <sub>3</sub> 1037	10336	10461	9675	9559	—	1.19 <sub>8</sub>	—	.46
9	.354	3.08	.3178 <sub>2</sub>	.3218 <sub>8</sub>	1.0127 <sub>7</sub>	.0 <sub>3</sub> 987	.0 <sub>3</sub> 1038	10336	10468	9675	9553	—	1.26 <sub>1</sub>	—	.41
10	.458	3.99	.3177 <sub>7</sub>	.3212 <sub>1</sub>	1.0108 <sub>3</sub>	.0 <sub>3</sub> 987	.0 <sub>3</sub> 1037	10336	10448	9675	9571	—	1.07 <sub>4</sub>	—	.27
11	.604	5.27	.3176 <sub>0</sub>	.3198 <sub>8</sub>	1.0071 <sub>8</sub>	$\left\{ \begin{array}{l} .03993 \\ 78.4^{\circ} \text{ to} \\ 100^{\circ} \text{ C.} \end{array} \right.$		10336	10410	9675	9606	—	.71 <sub>3</sub>	—	.13 <sub>5</sub>



TABLE III.

Results for Eleven Dilute Sodium Amalgams at a Constant Temperature of 78.4° C.

No. of Amalgam.	Concentration.		Resistance in ohms.		Relative resistivity or ratio $\frac{R_t}{R_t}$	Average temperature coefficient of increase of resistivity of Amalgam Mercury from 0° to 78.4° C., $\frac{m}{m} \times 10^3$		Resistivity of Mercury at 78.4° C., $\frac{m}{m} \times 10^3$		Conduc- tivity of Mercury at 78.4° C., $\frac{m}{m} \times 10^3$		Conduc- tivity of Amalgam at 78.4° C., $\frac{m}{m} \times 10^3$		$\frac{1}{\bar{O}} \cdot \frac{\Delta L}{L} \times 10^3$
	% "η."	Atomic weight "C."	$\frac{R_t}{m}$	$\frac{R_t}{a}$		$\frac{m}{m} \times 10^3$	$\frac{m}{m} \times 10^3$	$\frac{m}{m} \times 10^3$	$\frac{m}{m} \times 10^3$	$\frac{m}{m} \times 10^3$	$\frac{m}{m} \times 10^3$	$\frac{m}{m} \times 10^3$	$\frac{m}{m} \times 10^3$	
1	0.35 <sub>2</sub>	0.30 <sub>7</sub>	3110 <sub>0</sub>	3121 <sub>0</sub>	1.0035 <sub>0</sub>	0.965	0.982	10119	10155	9882	9848	—	34 <sub>4</sub>	—1.12
2	0.52 <sub>1</sub>	0.45 <sub>4</sub>	3109 <sub>6</sub>	3124 <sub>0</sub>	1.0046 <sub>3</sub>	0.965	0.984	10119	10166	9882	9837	—	45 <sub>6</sub>	—1.00
3	0.76 <sub>3</sub>	0.66 <sub>4</sub>	3109 <sub>8</sub>	3128 <sub>9</sub>	1.0061 <sub>4</sub>	0.965	0.990	10119	10181	9882	9822	—	61	— .92
4	1.06	0.92 <sub>2</sub>	2921 <sub>8</sub>	2944 <sub>3</sub>	1.0076 <sub>6</sub>	0.965	0.998	10119	10197	9882	9807	—	75 <sub>9</sub>	— .82
5	1.36	1.18 <sub>4</sub>	2920 <sub>8</sub>	2947 <sub>2</sub>	1.0092 <sub>1</sub>	0.965	0.998	10119	10212	9882	9792	—	91 <sub>1</sub>	— .77
6	2.12	1.84 <sub>9</sub>	2919 <sub>1</sub>	2952 <sub>7</sub>	1.0115 <sub>1</sub>	0.965	0.1017	10119	10236	9882	9770	—	113 <sub>3</sub>	— .61
7	2.62	2.29	2918 <sub>6</sub>	2951 <sub>8</sub>	1.0113 <sub>9</sub>	0.965	0.1013	10119	10234	9882	9771	—	112 <sub>3</sub>	— .49
8	2.97	2.59	2918 <sub>5</sub>	2951 <sub>9</sub>	1.0114 <sub>4</sub>	0.965	0.1016	10119	10255	9882	9771	—	112 <sub>3</sub>	— .43
9	3.54	3.08	3111 <sub>8</sub>	3150 <sub>0</sub>	1.0122 <sub>7</sub>	0.965	0.1021	10119	10243	9882	9763	—	120 <sub>4</sub>	— .39
10	4.58	3.99	3111 <sub>2</sub>	3142 <sub>7</sub>	1.0101 <sub>2</sub>	0.965	0.1019	10119	10222	9882	9783	—	100 <sub>3</sub>	— .25
11	6.04	5.27	3109 <sub>6</sub>	3129 <sub>8</sub>	1.0064 <sub>9</sub>	0.965	—	10119	10185	9882	9818	—	65 <sub>3</sub>	— .12 <sub>4</sub>

TABLE IV.

Results for Eleven Dilute Sodium Amalgams at a Constant Temperature  $t=100^{\circ}\text{C}$ 

No. of Amalgam.	Concentration.		Resistance in ohms.		Relative resistivity or ratio $\frac{R_t}{m R_t}$	Average temperature coefficient of resistivity of Hg from $0^{\circ}$ to $100^{\circ}\text{C}$ , $0^{\circ}$ to $100^{\circ}\text{C}$ , $= m^{\alpha}_t$	Average coefficient of resistivity of Amalgam from $0^{\circ}$ to $100^{\circ}\text{C}$ , $0^{\circ}$ to $100^{\circ}\text{C}$ , $= a^{\alpha}_t$	Resistivity of Mercury at $100^{\circ}\text{C}$ , $100^{\circ}\text{C}$ , $m^{\rho}_t \times 10^8$	Resistivity of Amalgam at $100^{\circ}\text{C}$ , $100^{\circ}\text{C}$ , $a^{\rho}_t \times 10^8$	Conduc- tivity of Mercury at $100^{\circ}\text{C}$ , $100^{\circ}\text{C}$ , $m^{\sigma}_t$	Conduc- tivity of Amalgam at $100^{\circ}\text{C}$ , $100^{\circ}\text{C}$ , $a^{\sigma}_t$	$\frac{\Delta L}{L} \times 10^3$	$\frac{1}{\bar{O}} \cdot \frac{\Delta L}{\bar{L}} \times 10^2$
	$\frac{\%}{\text{weight}}$	Atomic "C."	$\frac{R_t}{m}$	$\frac{R_t}{a}$									
1 .....	.035 <sub>2</sub>	0.30 <sub>7</sub>	.3176 <sub>4</sub>	.3187 <sub>9</sub>	1.0036 <sub>2</sub>	.0 <sub>3</sub> 987	.0 <sub>3</sub> 1001	10336	10373	9675	9640	— .35 <sub>3</sub>	— 1.17
2 .....	.052 <sub>1</sub>	0.45 <sub>4</sub>	.3176 <sub>0</sub>	.3191 <sub>8</sub>	1.0049 <sub>7</sub>	.0 <sub>3</sub> 987	.0 <sub>3</sub> 1006	10336	10387	9675	9627	— .49 <sub>6</sub>	— 1.09
3 .....	.076 <sub>3</sub>	0.66 <sub>4</sub>	.3176 <sub>3</sub>	.3197 <sub>4</sub>	1.0066 <sub>4</sub>	.0 <sub>3</sub> 987	.0 <sub>3</sub> 1013	10336	10405	9675	9611	— .66	— .99
4 .....	.106	0.92 <sub>2</sub>	.2984 <sub>1</sub>	.3008 <sub>6</sub>	1.0082 <sub>1</sub>	.0 <sub>3</sub> 987	.0 <sub>3</sub> 1019	10336	10421	9675	9596	— .81 <sub>6</sub>	— .88
5 .....	.136	1.18 <sub>4</sub>	.2982 <sub>6</sub>	.3012 <sub>7</sub>	1.0100 <sub>9</sub>	.0 <sub>3</sub> 987	.0 <sub>3</sub> 1023	10336	10440	9675	9578	— 1.00 <sub>3</sub>	— .84
6 .....	.212	1.84 <sub>9</sub>	.2981 <sub>4</sub>	.3017 <sub>3</sub>	1.0120 <sub>4</sub>	.0 <sub>3</sub> 987	.0 <sub>3</sub> 1035	10336	10461	9675	9560	— 1.19	— .64
7 .....	.262	2.29	.2980 <sub>8</sub>	.3015 <sub>4</sub>	1.0116 <sub>1</sub>	.0 <sub>3</sub> 987	.0 <sub>3</sub> 1028	10336	10456	9675	9564	— 1.14 <sub>7</sub>	— .50
8 .....	.297	2.59	.2980 <sub>8</sub>	.3016 <sub>8</sub>	1.0120 <sub>6</sub>	.0 <sub>3</sub> 987	.0 <sub>3</sub> 1037	10336	10461	9675	9559	— 1.19 <sub>8</sub>	— .46
9 .....	.354	3.08	.3178 <sub>2</sub>	.3218 <sub>8</sub>	1.0127 <sub>7</sub>	.0 <sub>3</sub> 987	.0 <sub>3</sub> 1038	10336	10468	9675	9553	— 1.26 <sub>1</sub>	— .41
10 .....	.458	3.99	.3177 <sub>7</sub>	.3212 <sub>1</sub>	1.0108 <sub>3</sub>	.0 <sub>3</sub> 987	.0 <sub>3</sub> 1037	10336	10448	9675	9571	— 1.07 <sub>4</sub>	— .27
11 .....	.604	5.27	.3176 <sub>0</sub>	.3198 <sub>8</sub>	1.0071 <sub>8</sub>	{ .0 <sub>3</sub> 993 78.4° to 100° C.		10336	10410	9675	9606	— .71 <sub>3</sub>	— .13 <sub>8</sub>

TABLE V.

Results for Eleven Dilute Liquid Sodium Amalgams at Constant Temperature 185° C.

No. of Amalgam.	Concentration. % weight "η."	Resistance in ohms. $\left\{ \begin{array}{l} R_t \\ R_{t'} \end{array} \right\}$	Relative resistivity or ratio $\frac{R_t}{m R_{t'}}$	Average temperature coefficient of Mercury from 0° to 185° C., $= m^u t'$	Average temperature coefficient of Amalgam from 0° to 185° C., $= a^u t'$	Resistivity of Mercury at 185° C., $m^o t'$	Resistivity of Amalgam at 185° C., $a^o t'$	Conduc- tivity of Mercury at 185° C., $\frac{1}{m^o t'}$	Conduc- tivity of Amalgam at 185° C., $\frac{1}{a^o t'}$	$\frac{\Delta L}{L} \times 10^2$	$\frac{1}{\bar{C} \cdot \bar{L}} \times 10^2$
1	0.35 <sub>2</sub>	3465 <sub>0</sub>	1.0040 <sub>2</sub>	0.31075	0.31086	11278	11323	8867	8831	-40 <sub>6</sub>	-1.32
2	0.52 <sub>1</sub>	3464 <sub>6</sub>	1.0051 <sub>5</sub>	0.31075	0.31089	11278	11340	8867	8819	-54 <sub>1</sub>	-1.19
3	0.76 <sub>2</sub>	3464 <sub>8</sub>	1.0073 <sub>6</sub>	0.31075	0.31094	11278	11361	8867	8802	-73 <sub>3</sub>	-1.10
4	1.05 <sub>7</sub>	3455 <sub>3</sub>	1.0097 <sub>4</sub>	0.31075	0.31104	11287	11388	8867	8781	-93 <sub>9</sub>	-1.05
5	1.35 <sub>7</sub>	3453 <sub>7</sub>	1.0123 <sub>2</sub>	0.31075	0.31111	11278	11417	8867	8759	-121 <sub>8</sub>	-1.03
6	2.12	3452 <sub>3</sub>	1.0138 <sub>6</sub>	0.31075	0.31114	11278	11434	8867	8746	-136 <sub>4</sub>	-74
7	2.62	3451 <sub>7</sub>	1.0144 <sub>2</sub>	0.31075	0.31117	11278	11441	8867	8741	-142 <sub>1</sub>	-62
8	2.97	3451 <sub>7</sub>	1.0140 <sub>6</sub>	0.31075	0.31117	11278	11436	8867	8744	-138 <sub>7</sub>	-58
9	3.54	3467 <sub>0</sub>	1.0141 <sub>3</sub>	0.31075	0.31113	11278	11437	8867	8743	-139 <sub>8</sub>	-45
10	4.56	3466 <sub>6</sub>	1.0103 <sub>8</sub>	0.31075	0.31102	11278	11395	8867	8776	-102 <sub>6</sub>	-26
11	5.27	3461 <sub>6</sub>	1.0054 <sub>3</sub>	$\left\{ \begin{array}{l} 0.31074 \\ 78.4^\circ \text{ to } 185^\circ \text{ C.} \end{array} \right\}$	$\left\{ \begin{array}{l} 0.31063 \\ 78.4^\circ \text{ to } 185^\circ \text{ C.} \end{array} \right\}$	11278	11339	8867	8819	-54 <sub>1</sub>	-10 <sub>9</sub>

TABLE VI.

Dilute Sodium Amalgams at a Constant Temperature of 225.8° C.

No. of Amalgam.	Concentration. % Atonic weight "η," "C."	Resistance in ohms.			Relative resistivity or ratio $\frac{aR_t}{mR_t}$	Average temperature coefficient of resistivity of Hg from 0° to 225.8° C., = $m\alpha_t$	Average temperature coefficient of resistivity of Amalgam from 0° to 225.8° C., = $a\alpha_t$	Resistivity of		Conduc- tivity of Mercury at 225.8° C., $m\rho_t \times 10^9$	Conduc- tivity of Amalgam at 225.8° C., $a\rho_t$	$\frac{\Delta L}{L} \times 10^3$	$\frac{1}{\bar{O}} \cdot \frac{\Delta L}{L} \times 10^3$
		$\frac{R_t}{m}$	$\frac{R_t}{a}$	$\frac{R_t}{aR_t}$				Mercury at 225.8° C., $m\rho_t \times 10^9$	of Amalgam at 225.8° C., $a\rho_t \times 10^9$				
1	..... 035 <sub>2</sub>	30 <sub>7</sub>	3619 <sub>4</sub>	3637 <sub>4</sub>	1.0049 <sub>7</sub>	0.21118	0.21133	11782	11841	8488	8446	-49 <sub>6</sub>	-1.61
2	..... 052 <sub>1</sub>	15 <sub>4</sub>	3619 <sub>6</sub>	3642 <sub>6</sub>	1.0063 <sub>3</sub>	0.21118	0.21135	11782	11857	8488	8434	-63 <sub>6</sub>	-1.40
3	..... 076 <sub>2</sub>	66 <sub>4</sub>	3619 <sub>2</sub>	3647 <sub>7</sub>	1.0078 <sub>7</sub>	0.21118	0.21138	11782	11875	8488	8421	-78 <sub>6</sub>	-1.19
11	..... 604	5.27	3619 <sub>6</sub>	3630 <sub>2</sub>	1.0031 <sub>6</sub>	$\left\{ \begin{array}{l} 0.21115 \\ 78.4^\circ \text{ to} \\ 225.8^\circ \text{ C} \end{array} \right\}$		11782	11819	8488	8461	-31 <sub>6</sub>	-0.60

TABLE VII.

## Dilute Sodium Amalgams at a Constant Temperature of 255.2° C.

No. of Amalgam.	Concentration. % weight "η." "C."	Resistance in ohms.		Relative resistivity or ratio $\frac{aR_t}{mR_t}$	Average temperature coefficient of resistivity of Hg from 0° to 255.2° C., $=$ $\frac{a_t}{m}$		Average temperature coefficient of resistivity of Amalgam from 0° to 255.2° C., $=$ $\frac{a_t}{m}$		Resistivity of Mercury at 255.2° C., $m^o_t \times 10^8$ ,		Resistivity of Amalgam at 255.2° C., $a^o_t \times 10^8$ .		Conduc- tivity of Mercury at 255.2° C., $\frac{L_t}{m}$		Conduc- tivity of Amalgam at 255.2° C., $\frac{L_t}{a_t}$ .		$\frac{\Delta L}{L} \times 10^3$ .		$\frac{1}{C} \cdot \frac{\Delta L}{L} \times 10^3$ .	
		$\frac{R_t}{m}$	$\frac{R_t}{a}$																	
1 .....	.035 <sub>2</sub>	.30 <sub>7</sub>	.3737 <sub>3</sub>	.3759 <sub>6</sub>	1.0050 <sub>7</sub>	.0 <sub>2</sub> 1149	.0 <sub>2</sub> 1168	12167	12240	8219	8170	—	.59 <sub>6</sub>	—	1.94					
2 .....	.052 <sub>1</sub>	.45 <sub>4</sub>	.3736 <sub>8</sub>	.3766 <sub>9</sub>	1.0080 <sub>6</sub>	.0 <sub>2</sub> 1149	.0 <sub>2</sub> 1174	12167	12265	8219	8153	—	.80 <sub>9</sub>	—	1.77					
3 .....	.076 <sub>2</sub>	.66 <sub>4</sub>	.3737 <sub>1</sub>	.3775 <sub>9</sub>	1.0103 <sub>8</sub>	.0 <sub>2</sub> 1149	.0 <sub>2</sub> 1180	12167	12293	8219	8134	—	1.03 <sub>4</sub>	—	1.56					
11 .....	.604	5.27	.3936 <sub>9</sub>	.3765 <sub>0</sub>	1.0075 <sub>2</sub>	$\left\{ \begin{array}{l} .021145 \\ 78.4^\circ \text{ to } 255.2^\circ \text{ C.} \end{array} \right.$		12167	12259	8219	8158	—	.74 <sub>3</sub>	—	.14					

TABLE VIII.

## Dilute Sodium Amalgams at a Constant Temperature of 302.2° C.

No. of Amalgam.	Concentration — % Atomic weight "η." "C."	Resistance in ohms. $\left\{ \begin{array}{l} R_t \\ m \end{array} \right.$	Relative resistivity or ratio $\frac{R_t}{m}$ $\frac{R_t}{m_t}$	Average temperature coefficient of resistivity of Hg from 0° to 302.2° C., $=$ $m_t^{a_t}$		Average coefficient of resistivity of Amalgam from 0° to 302.2° C., $=$ $m_t^{a_t}$		Resistivity of Mercury at 302.2° C., $m_t^{a_t} \times 10^8$	Resistivity of Amalgam at 302.2° C., $a_t^{a_t} \times 10^8$	Conduc- tivity of Mercury at 302.2° C., $\frac{L_t}{m}$	Conduc- tivity of Amalgam at 302.2° C., $\frac{L_t}{a_t}$	$\frac{\Delta L}{L} \times 10^2$	$\frac{1}{O} \cdot \frac{\Delta L}{L} \times 10^2$
10	.....	458	3.99	3939 <sub>0</sub>	4001 <sub>0</sub>	1.0157 <sub>4</sub>	0.1200	0.1243	12819	13021	7680	-1.55	-39
11	.....	604	5.27	3936 <sub>7</sub>	4001 <sub>1</sub>	1.0163 <sub>6</sub>	$\left\{ \begin{array}{l} 0.1192 \\ 78.2^\circ \text{ to } 302.2^\circ \text{ C.} \end{array} \right.$	$\left\{ \begin{array}{l} 0.1248 \\ 78.4^\circ \text{ to } 302.2^\circ \text{ C.} \end{array} \right.$	12819 <sub>6</sub>	13029	7675	-1.61 <sub>5</sub>	-30 <sub>7</sub>

*Experimental Results.*

The electrical resistances of pure mercury and eleven dilute sodium amalgams were measured at various temperatures, and the results are given in Tables I. to VIII.

The relative resistivity  $\left(\frac{{}_aR_t}{{}_mR_t}\right)$  of an amalgam of a given concentration is readily obtained from measurements of the resistances of the amalgam and mercury columns under identical conditions. From the relative resistivity, the absolute resistivity  ${}_a\rho_t$  and the absolute conductivity  ${}_aL_t$  of the amalgam can be calculated as previously explained. The values of  ${}_a\bar{\alpha}_t$ , the average temperature coefficient over the temperature range 0 to  $t^\circ$  C., and of  $\frac{{}_aL}{L} \times 10^2$  and  $\frac{1}{C} \frac{{}_aL}{L} \times 10^2$ , have been calculated, and are included in the Tables.

The resistances were measured by means of two pyrex four-electrode tubes, and before one of the tubes was broken measurements of the resistances of mercury and amalgams 9, 10, 1, 2, 3, and 11 were completed in the order named. The second tube was then employed to measure the resistances of mercury and of amalgams 4, 5, 6, 7, and 8, in the order named. Since, as previously mentioned, the resistance of mercury was determined before and after each amalgam determination, the mercury resistances as recorded in the Tables show the effect of the chemical action of the amalgam on the diameter of the capillary tube.

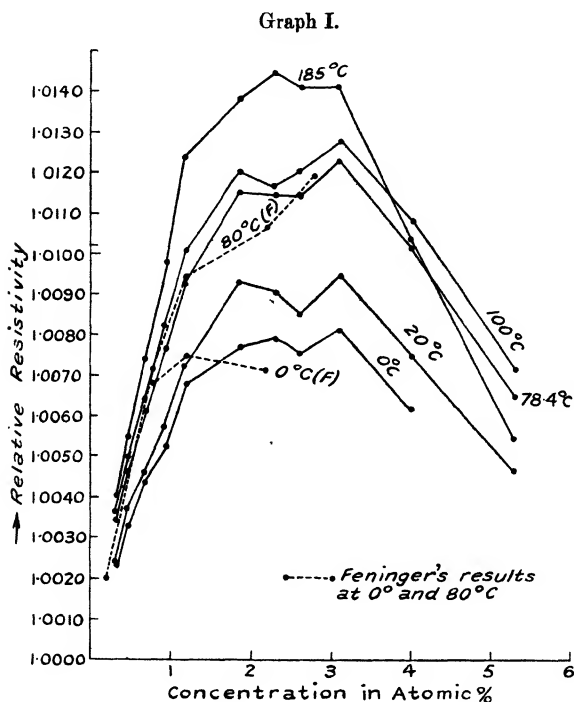
*Discussion of Results.*

- (a) The variation of relative resistivity at constant concentration with temperature.

This problem can be studied by reference to Graph I. It is seen that over the temperature range  $0^\circ$ — $185^\circ$  C., when the concentration is less than 3.6 atoms per cent., the relative resistivity increases with temperature. This result, however, does not hold for a sodium amalgam of concentration above 3.6 atoms per cent. at a temperature of  $185^\circ$  C.

(b) The variation of relative resistivity at constant temperature with concentration.

An inspection of the curves in Graph I. shows that all of them possess the same general characteristics. The value of the relative resistivity at first increases with the concentration, then remains fairly constant over a certain range of concentration, and finally diminishes with



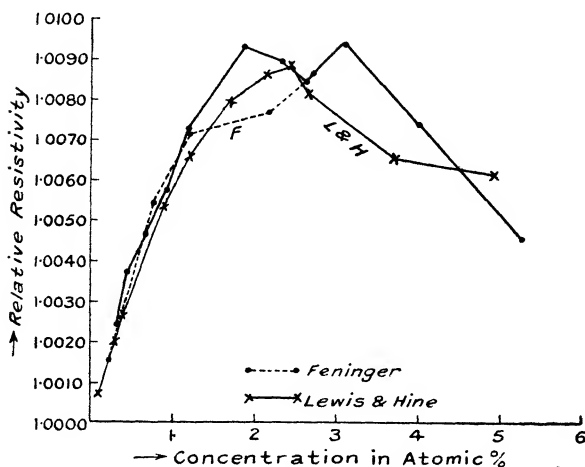
Relative resistivity-concentration curves at 0°, 20°, 78.4°, 100°, and 185°C.

further increase of concentration. The initial rise of the relative resistivity-concentration curve is steeper than the final fall. The results at higher temperatures are incomplete, but an examination of Tables VI., VII., and VIII. indicates that the general shape of the curves is, in all probability, very similar to those shown in Graph I.



Another interesting feature of these curves is the presence of discontinuities, which are specially noticeable at concentrations of 1.18, 1.85, 2.3, 2.6, and 3.08 atoms per cent. of sodium. It is difficult to decide with certainty whether these discontinuities in the curves are real, owing to the experimental difficulties encountered in the measurements, but their appearance in all the curves at practically the same concentrations seems to support the view that

Graph II.



Relative resistivity-concentration curve at 20° C. compared with results of Feninger and Lewis and Hine.

they are not altogether due to experimental errors. The results obtained in the present investigation can be compared with those of Lewis and Hine\* at 20° C. and those of Feninger† at 0°, 20°, and 80° C. by reference to Graphs I. and II.

It is seen that, on the whole, the results are in fairly good agreement, and Lewis and Hine's\* curve shows the same initial rise to a maximum followed by a more gradual fall.

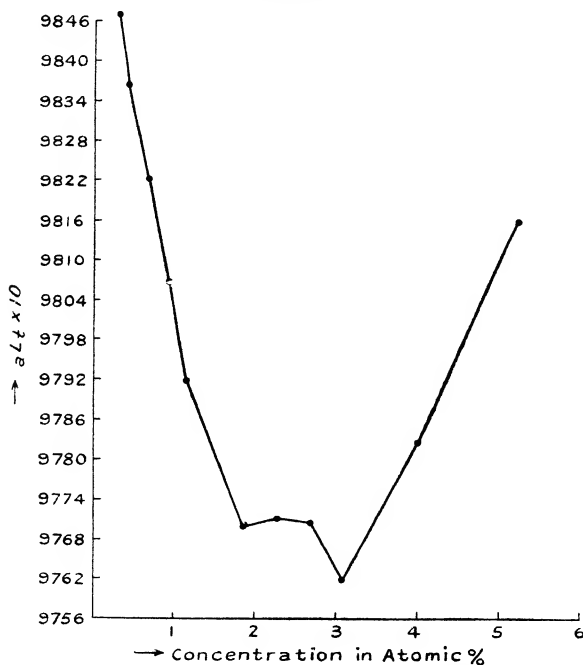
\* *Loc. cit.*

† *Loc. cit.*

*The Variation of Resistivity and Conductivity with Concentration at Constant Temperature, and a Comparison with Mercury.*

The experimental work has shown that the resistivities of all the amalgams examined, with one exception, are greater than that of mercury at the same temperature. The exception referred to is that of an amalgam of

Graph III.



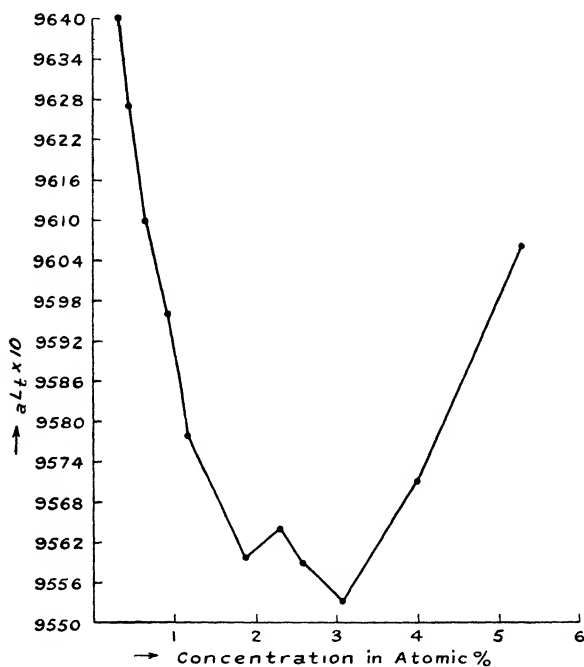
Conductivity-concentration curve at 78.4° C.

concentration 0.604 per cent. by weight (5.27 atoms per cent.) at 0° C., and its resistivity is  $9376 \times 10^{-8}$ , as compared with  $9407 \times 10^{-8}$  for pure mercury. It is, however, important to note that in the neighbourhood of 0° C. a solid mass, which seemed to possess a crystalline structure, separated from the liquid amalgam, and the measured resistivity is therefore not that of a pure liquid amalgam.

The solubility of the alkali metals in mercury increases with increasing temperature, and according to W. Kerp\* and his co-workers the percentage solubility of sodium in mercury at 0°, 25°, 65°, and 100° C. is given by 0.54, 0.65, 0.86, and 1.11 respectively.

The amalgam of concentration 0.604 per cent. by weight

Graph IV.



Conductivity-concentration curve at 100° C.

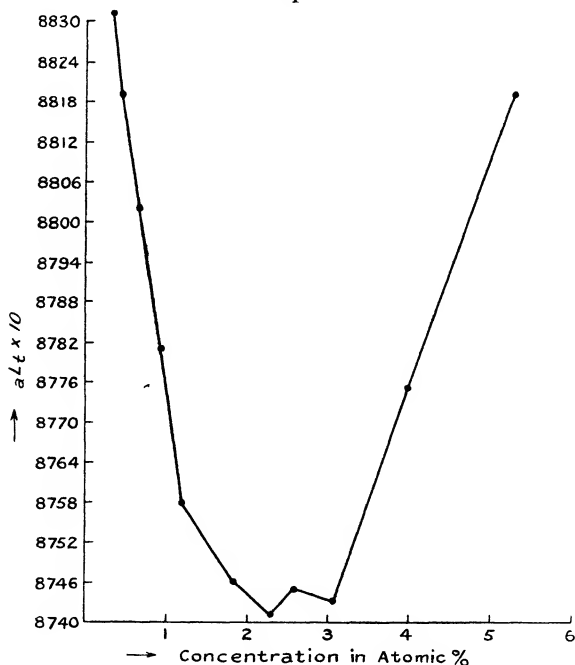
is, therefore, a liquid amalgam at all the other temperatures employed in this investigation.

An examination of Tables I.-VIII. shows that the difference between the resistivity of a sodium amalgam and mercury at the same temperature increases to a maximum as the concentration increases, and finally

\* Mellor, 'Inorganic & Theoretical Chem.,' iv. p. 1010.

diminishes at the highest concentrations. A curve showing the relation between the difference of resistivity and the concentration of the sodium would be similar to the relative resistivity-concentration curve at the same temperature. The relation between the absolute conductivity and concentration is shown in Graphs III., IV., and V. which represent the experimental results at 78.4° 100°, and 185° C. respectively.

Graph V.



Conductivity-concentration curve at 185°C.

and 185° C. respectively. The three curves have the same form, and show at first a diminution in conductivity with increase of concentration until a minimum is reached, and a further increase of concentration is accompanied by an increase in the conductivity. The initial and final portions of the curves are approximately straight lines, but the middle portions in the neighbourhood of the minima show the presence of discontinuities.

Booharwalla, Paranjpe and Prasad\*, in their experiments on the conductivities of sodium amalgams at 30° C., found two distinct discontinuities in the conductivity-concentration curve corresponding to concentrations of 0.079 and 0.272 per cent. by weight. They also found that a sodium amalgam of concentration 0.272 per cent. by weight was a better conductor than pure mercury. The present experiments also indicate the presence of a discontinuity for a concentration of 0.262 per cent. by weight (2.29 atoms per cent.) at a temperature of 20° C.; but there is no evidence of a definite discontinuity at a concentration of 0.079 per cent. by weight.

Although in the present investigation no experiments were carried out at 30° C., an examination of the relative resistivity-concentration curves at 0°, 20°, and 78.4° C. (graph I.) seems to indicate that the conductivity of the 0.272 per cent. amalgam is less than that of mercury at the same temperature.

### *Resistivity and Temperature.*

An examination of the experimental results given in Tables I. to VIII. shows that the average temperature coefficient of resistivity of an amalgam is, in almost all cases, greater than the average temperature coefficient of pure mercury over the same range of temperature, and also that the average temperature coefficient of an amalgam of given concentration increases with the range of temperature†. The variation of the average temperature coefficient of resistivity with concentration, when the interval of temperature is kept constant, is somewhat irregular; but the general tendency is for the average temperature coefficient to increase with concentration.

In the case of amalgams of metals not belonging to Group I. of the Periodic Table the average temperature coefficient of resistivity is less than that of mercury over the same temperature range, and diminishes with increase of concentration.

Müller‡, and later Bornemann and Rauschenplatt§, determined the resistivities of a sodium amalgam of

\* *Loc. cit.*

† Mellor, 'Inorganic & Theoretical Chem.,' iv. p. 1017.

‡ *Loc. cit.*

§ The only exception is the amalgam of concentration 5.27 gram atoms per cent.

concentration 0.96 atom per cent. at temperatures up to 300° C., and the latter investigators found that the resistivity of the amalgam increased from  $9976 \times 10^{-8}$  at 50° C. to  $13142 \times 10^{-8}$  at 300° C.

The value obtained by them at 100° C. was  $10274 \times 10^{-8}$ , which is lower than their value for pure mercury. The resistivities of this amalgam at other temperatures is, according to their measurements, greater than the corresponding values for mercury. The resistivities obtained in the present investigation for amalgams of concentrations 0.922 and 1.184 atoms per cent. were  $10421 \times 10^{-8}$  and  $10440 \times 10^{-8}$  respectively at 100° C., and were greater than the corresponding value for mercury ( $10336 \times 10^{-8}$ )).

*The Variation of  $\frac{1}{C} \frac{\Delta L}{L}$  with Temperature  
and Concentration.*

As already indicated, the resistivity of all the amalgams examined, with one exception, is greater than that of mercury at the same temperature, and it therefore follows that  $\frac{\Delta L}{L}$  and  $\frac{1}{C} \frac{\Delta L}{L}$  are negative quantities. In the case of amalgams of metals not belonging to Group I. of the Periodic Table  $\frac{1}{C} \frac{\Delta L}{L}$  is positive, and increases with increase of temperature (concentration constant), but diminishes with increase of concentration (temperature constant) especially at high temperatures. An examination of Tables I. to VIII. shows that the negative value of  $\frac{1}{C} \frac{\Delta L}{L}$  (concentration constant) increases with increase of temperature\*. The Tables also show that the negative value of  $\frac{1}{C} \frac{\Delta L}{L}$  (temperature constant) diminishes with increase of concentration. The values of  $\frac{1}{C} \frac{\Delta L}{L}$  at infinite dilution or  $l_{\infty}$  are more difficult to calculate, owing to the somewhat irregular nature of the curves connecting  $l$  with concentration at constant temperature.

\* The behaviour of the sodium amalgam of concentration 5.27 gram atoms per cent. is, however, rather irregular.

However, by plotting  $\frac{1}{C} \frac{\Delta L}{L}$  against the concentration  $C$  at  $0^\circ$ ,  $20^\circ$ ,  $100^\circ$ ,  $225.8^\circ$ , and  $252.2^\circ$  C. for the three or four lowest concentrations, it is found that the points lie approximately on straight lines, and the values of  $l_\infty$  as determined from the graphs are :—

$-0.88 \times 10^{-2}$ ,  $-0.92 \times 10^{-2}$ ,  $-1.28 \times 10^{-2}$ ,  $1.91 \times 10^{-2}$ , and  $-2.265 \times 10^{-2}$  respectively.

The values of  $l_\infty - l$  and  $\frac{l_\infty - l}{C}$  have also been calculated for the three temperatures  $100^\circ$ ,  $225.8^\circ$ , and  $255.2^\circ$  C., and the results are given in the following tables :—

*Temperature  $100^\circ$  C.*

$(l_\infty - l) \times 10^{-2}$ .	C.	$\frac{(l_\infty - l)}{C} \times 10^{-2}$ .
-0.11	0.307	-0.36
-0.19	0.454	-0.42
-0.29	0.664	-0.44
-0.40	0.922	-0.43
-0.44	1.184	-0.38
-0.64	1.849	-0.34
-0.78	2.29	-0.34
-0.82	2.59	-0.32
-0.87	3.03	-0.28
-1.01	3.99	-0.25
-1.14	5.27	-0.22

*Temperature  $225.8^\circ$  C.*

$(l_\infty - l) \times 10^{-2}$ .	C.	$\frac{(l_\infty - l)}{C} \times 10^{-2}$ .
-0.30	0.307	-0.98
-0.51	0.454	-1.12
-0.72	0.664	-1.08

*Temperature  $255.2^\circ$  C.*

$(l_\infty - l) \times 10^{-2}$ .	C.	$\frac{(l_\infty - l)}{C} \times 10^{-2}$ .
-0.32 <sub>5</sub>	0.307	-1.06
-0.49 <sub>5</sub>	0.454	-1.09
-0.70 <sub>5</sub>	0.664	-1.07

The above tables indicate that, in the case of the most dilute solutions, the value of  $\frac{l_{\infty} - l}{C}$  is approximately constant at each of the three temperatures. The figures given in the first table (100° C.) also show that for concentrations greater than about 1.0 atom per cent. the negative value of  $\frac{l_{\infty} - l}{C}$  diminishes continuously with increase of concentration, and it is interesting to note that the discontinuities in the conductivity-concentration curves commence at a concentration of about 1 atom per cent.

According to Skaupy's\* hypothesis the value of  $H_{\infty} = l_{\infty} + r_{\infty}$ , where  $r = \frac{1}{C} \frac{\Delta \eta}{\eta}$ , should be constant for all metals dissolved in mercury, and also  $H_{\infty} - H$  should vary linearly with the concentration  $C$ .

Feninger† gives the values of the viscosity at 18° C. of two sodium amalgams of concentrations 0.311 and 0.482 atoms per cent. Assuming that  $\frac{1}{C} \frac{\Delta \eta}{\eta}$  varies linearly with concentration, the calculated value of  $\frac{1}{C} \cdot \frac{\Delta \eta}{\eta}$  at infinite dilution for a temperature of 18° C. is  $9.3 \times 10^{-2}$ .

Since the value of  $\frac{1}{C} \frac{\Delta L}{L}$  at infinite dilution (temperature 20° C.) is  $-0.92 \times 10^{-2}$ , it follows that  $H_{\infty}$  has the value  $8.4 \times 10^{-2}$ , which is of the same order of magnitude as the value of  $H$  ( $9.8 \times 10^{-2}$ ) for gold amalgams at room temperature.

This latter value was calculated from Feninger's viscosity measurements and Williams and Evan's‡ conductivity measurements. It is, however, impossible to consider the problem further, owing to lack of data on the viscosity of sodium amalgams over a wide range of temperature.

In the relation  $\frac{H_{\infty} - H}{C} = \text{constant}$ ,  $H$  is the value of  $l + r$  at concentration  $C$ . From Feninger's§ results for sodium amalgams of concentrations 0.311 and 0.482 at

\* *Loc. cit.*

† *Loc. cit.*

‡ *Loc. cit.*

§ *Loc. cit.*



18° C. the calculated values of  $r$  are  $10.3 \times 10^{-2}$  and  $11.1 \times 10^{-2}$  respectively.

The values of  $l$  at 20° C. for the same concentrations can be obtained by plotting the first four values of  $\frac{1}{C} \frac{\Delta L}{L}$  in Table II. against the concentration. The values thus obtained for the two concentrations 0.311 and 0.482 are  $-0.82 \times 10^{-2}$  and  $-0.77 \times 10^{-2}$  respectively. Since  $H_{\infty} = 8.4 \times 10^{-2}$ , it follows that the values of  $\frac{H_{\infty} - H}{C}$  for the sodium amalgams of the above concentrations are  $-3.5 \times 10^{-2}$  and  $-4.0 \times 10^{-2}$  respectively.

Although the values are in fair agreement, considering the possible experimental errors, more experimental data relating to the viscosities of sodium amalgams at various temperatures must be available before the truth of the equation  $\frac{H_{\infty} - H}{C} = \text{constant}$  can be verified.

The physical properties of alkali amalgams have been studied by a large number of chemists\*, and the general results seem to indicate that in all probability amalgams are solutions of compounds of the dissolved metal with definite proportions of the solvent mercury in excess of mercury. Several compounds of sodium with mercury are supposed to exist, and some of them are considered to have been isolated. A comparison of the experimental results obtained for the conductivities of sodium amalgams with those obtained by Williams and Evans† for the amalgams of copper, silver, and gold show that the sodium amalgams behave in a more complicated manner than the latter. The small discontinuities in the conductivity-concentration curves are not unlike the discontinuities in similar curves obtained with alloys due to the production of intermetallic compounds, but the magnitudes of the changes in conductivity are much less.

The discontinuities, together with the fact that large amounts of heat are evolved during the production of sodium amalgams, may possibly be regarded as lending support to the view that compounds of mercury and sodium exist even in moderately dilute sodium amalgams.

\* Mellor, 'Inorganic and Theoretical Chemistry,' iv. p. 1017.

† *Loc. cit.*

*Summary of Results.*

1. The electrical resistivities of eleven liquid sodium amalgams of concentrations ranging from 0.307 to 5.27 atoms per cent. were measured at 0°, 20°, 78.4°, 100°, and 185° C. In the case of a few of these amalgams, measurements were also carried out at 225.8°, 255.2°, and 302.2° C.

2. It was found that the relative resistivity of an amalgam (*i. e.*, its resistivity relative to mercury) at constant temperature at first increases with increase in the concentration of the sodium, then remains practically constant over a certain range of concentration, and finally diminishes with further increase of concentration. The relative resistivity-concentration curves in the neighbourhood of the maxima are somewhat irregular, and seem to show the presence of small discontinuities.

3. The absolute conductivity of an amalgam at constant temperature at first diminishes with increase in the concentration of the sodium, then remains fairly constant over a certain range of concentration, and finally increases with further increase of concentration. Discontinuities also appear on the conductivity-concentration curves in the neighbourhood of the minima.

4. The average temperature coefficient of resistivity of the sodium amalgams examined in this investigation is generally greater than the average temperature coefficient of resistivity of pure mercury over the same range of temperature.

For an amalgam of a given concentration the average temperature coefficient increases with the temperature range.

5. The variation of the average temperature coefficient of resistivity with concentration is somewhat irregular, but the general tendency is for the average temperature coefficient to increase with concentration.

6. The variation of  $\frac{1}{C} \frac{\Delta L}{L}$  with temperature and concentration has been considered, and the results examined in relation to a theory put forward by Skaupy\*.

\* *Loc. cit.*

LIX. *Some Precision Measurements in the Soft X-ray Region.* By M. SÖDERMAN \*.

[Plates III. & IV.]

**D**URING the last ten years a great many researches have been made in order to join the ultra-violet and the soft X-ray region. Millikan and his assistants †, working from the ultra-violet side and using concave gratings, succeeded in registering wave-lengths down to 136 Å. Later researches in this region have been carried out by Léon and Eugène Bloch, Lyman, Wood, and others. Last year Edlén and Ericson ‡, of this laboratory, reached down to 75 Å., and this record was recently surpassed by Ekefors §, also working here, who found spark-lines from aluminium below 50 Å.

*Indirect Methods.*

The first attempts to attain greater wave-lengths from the X-ray side were made by indirect methods. Their aim is to determine the critical potentials of the elements. This is done by placing the element to be examined on the anode and bombarding it with an electron current from a tungsten filament. The accelerating potential is raised by steps, and the excited radiation is measured by the photoelectric effect produced upon an electrode, which is protected from the corpuscular radiation. In order to estimate where the discontinuities are to be found, the authors plot the photoelectric current as a function of the tension. Along the row of points thus obtained they place straight lines, and from the points of intersection of these lines they purport to be able to estimate the values of critical potentials with rather high accuracy. A great many researches have been carried out by this method ||,

\* Communicated by Dr. Manne Siegbahn.

† R. A. Millikan, I. S. Bowen, and R. A. Sawyer, *Astrophys. Journ.* liii. p. 150 (1921); R. A. Millikan and I. S. Bowen, *Phys. Rev.* xxiii. p. 1 (1924).

‡ Bengt Edlén and Algot Ericson, *Zs. für Physik*, lix. p. 656 (1930).

§ E. Ekefors, *Phys. Zs.* xxxi. p. 737 (1930).

|| E. H. Kurth, *Phys. Rev.* (2) xviii. p. 99 (1921); A. L. Hughes, *Phil. Mag.* xliii. p. 145 (1922); J. Holtmark, *Phys. Zs.* xxiii. p. 252 (1922); J. C. McLennan and M. L. Clark, *Proc. Roy. Soc. (A)*, cii. p. 389 (1923); M. Levi, *Roy. Soc. Canada*, xviii. p. 159 (1924); Charles Thomas, *Phys. Rev.* xxv. p. 322 (1925); G. K. Rollefson, *Phys. Rev.* xxv. p. 740 (1925).

but the agreement among the results obtained by different observers is very bad. Moreover, when repeated the investigations in this region would give new discontinuities besides those already observed, and a comparison of all the discontinuities that have been found shows that they are practically evenly distributed over the whole region examined, except possibly the value at about 290 volts, which has been obtained by most observers and is regarded as the K-absorption limit of carbon, due to the presence of hydrocarbon vapours from the vacuum grease. The other results of the examinations made by this method are so doubtful that a comparison of them with the results obtained by more reliable methods would hardly be of any interest.

A method that is better in principle has been worked out by Mohler and Foote\*. The element to be examined is in its gaseous state, and, as in the experiments described above, the variation of the photo-electric current is used for the determination of the critical potentials. The values obtained for the K-limit are given in Table I.

TABLE I.

Element.	4 Be.	5 B.	6 C.	7 N.	8 O.
K-limit (volts) .....	116	186	272	374	478

A comparison with the results obtained by the grating method (Table IX., p. 616) shows that the critical potentials for boron and beryllium might be rather good, but the values found for carbon, nitrogen, and oxygen must be too low, their energies being even less than those of the  $K_{\alpha}$  radiation.

According to the method introduced by Richardson and Bazzoni † the radiation that is to be examined produces photo-electrons, and their velocity is determined by their deviation in a magnetic field. A somewhat modified application of this method has been made by Lukirsky ‡, who, instead of deflecting the photo-electrons, determines

\* F. L. Mohler and P. D. Foote; *Scient. Pap. Bur. of Stand.* xvii. p. 471 (1922).

† O. W. Richardson and C. B. Bazzoni, *Phil. Mag.* xlii. p. 1015 (1921).

‡ P. Lukirsky, *Phil. Mag.* xlvii. p. 466 (1924).

their stopping potentials by means of an electric field. The most complete investigation by this method was carried out by Rudberg\*, who found the values shown in Table II.

TABLE II.

Element.	4 Be.	5 B.	6 C.
K <sub>α</sub> (volts) .....	96	178	273

It is to be observed that this method gives the energy of the K<sub>α</sub>-radiation, and not, like the two other methods, the K-limit. The critical values are determined, however, by the same plotting method, which is by no means objective and able to give reliable results. The agreement with the results obtained by the grating method is not very good, Rudberg's values being evidently too low.

The one of the indirect methods that seems to have given the best and most reliable results is the absorption method used by Holweck†. The values obtained by him, representing the K-limit, are given in Table III.

TABLE III.

Element.	5 B.	6 C.	7 N.	8 O.	9 F.	13 Al.
K-limit (volts) ...	192	280.5	397	528	684	1555

These results seem to agree well with those obtained in this research (Table IX., p. 616).

Among other indirect methods for studying the radiation in the intermediate region that of Rollefson and Poth|| is worth mentioning. Its aim is to determine the ionization potentials for the elements in the photographic emulsion. This is done by making a magnetically spread continuous cathode ray spectrum fall upon a photographic plate, and observing the places where the blackening shows irregularities.

\* E. Rudberg, *Kungl. Sv. Vetenskapsakad. Handl.* ser. 3, band 7 (1929).

† F. Holweck, "De la lumière aux rayons X" (Conf. Rapp. 1927).

‡ G. K. Rollefson and E. J. Poth, 'Science,' n. s. lxii. p. 497 (1925).

*Crystal Measurements.*

In 1923 and 1924 the first successful attempts to extend the region of crystal spectroscopy in the direction of greater wave-lengths were made by Siegbahn and Thoræus\*, who constructed a vacuum spectrograph for these wave-lengths. With this apparatus Thoræus† registered wave-lengths in the L-series up to about 25 Å. and the K-radiation from fluorine and oxygen. Some years later Dauvillier‡ succeeded in extending the region of crystal spectroscopy to about 120 Å. His results, however, are somewhat different from those obtained with better methods. A research upon the crystal method for soft X-rays, recently carried out in this laboratory by A. Karlsson§, shows that the grating constants of the complex fatty acids used by Dauvillier are very difficult to determine, and the values obtained differ a good deal from one another. The best spectrograms in this region have been obtained with crystals of palmitic acid. Karlsson also registered some wave-lengths in the K-series, and found the values shown in Table IV.

TABLE IV.

Element.	Na.	F.	O.	N.
K <sub>α</sub> (Å) .....	11.88	18.27	23.66	31.54

Greater wave-lengths than that of nitrogen proved to be impossible to measure with sufficient accuracy.

*Grating Methods.*

Compton and Doan|| were the first who used plane gratings for X-ray purposes. Their measurements, however, are limited to wave-lengths between 1 and 2 Å. After them several investigators have used the method for

\* M. Siegbahn and Thoræus, *Arkiv. för Mat. Astr. o. Fys.* Bd. xviii. no. 24, 1924, and Bd. xix. no. 12, 1925.

† R. Thoræus, *Phil. Mag.* (7) i. p. 312 (1926).

‡ A. Dauvillier, *Journ. de Phys.* viii. p. 1 (1927).

§ A. Karlsson, *Arkiv. för Mat. Astr. o. Fys.* Bd. xxii. A, no. 9.

|| A. H. Compton and R. L. Doan, *Proc. Nat. Acad. Amer.* ii. p. 598 (1925).

exploring the intermediate region. Thus Thibaud\* registered several lines in the soft X-ray region as well as in ultra-violet by means of a plane grating with grazing incidence. Further, the method has been used by Bäcklin† for a precision measurement of the Al- $K_{\alpha}$  wave-length referred to absolute dimensions. For the wave-length just mentioned he finds  $\lambda=8.333 \text{ \AA}$ , while Larsson's precision measurement‡ with a crystal gives  $\lambda=8.323 \text{ \AA}$ . Thus a certain wave-length referred to absolute dimensions becomes about 0.1 per cent. higher than when it is referred to the crystal scale, a fact which was rather unimportant as long as the accuracy of the grating measurements was about 1 per cent., but which must now be taken into consideration on a comparison between the wave-lengths found at different researches in the soft X-ray region, where both scales are used side by side. Some American investigators§ have also been busy with the same problem as Bäcklin, but their results are rather different. For the electron charge which can be calculated if the relation between absolute scale and crystal scale is known the authors obtain the following values:—

Wadlund:  $e=4.774 \text{ E.S.U.}$

Bäcklin:  $e=4.793.$

Bearden:  $e=4.835, 4.824, 4.804, 4.809$  (found at different times).

Among other absolute measurements of X-ray wave-lengths those carried out by Howe|| should be mentioned. He has examined several lines in the L-series and the  $K_{\alpha}$ -line of carbon, which he has found to be  $44.60 \pm 0.04 \text{ \AA}$ . Considering the fact that this wave-length is referred to the absolute scale and the one obtained by myself (Table IX.) to the crystal scale, the two results are to be regarded as well agreeing. A statement published by Bazzoni, Faust, and Weatherby¶ is specially interesting. The

\* J. Thibaud, *Journ. de Phys.* viii. p. 13 (1927), and *Phys. Zs.* xxix. p. 241 (1928).

† E. Bäcklin, "Abs. Wellenlängenbest. der Röntgenstrahlen," *Upps. Univ. Årsskr.* (1928).

‡ Not yet published.

§ A. P. R. Wadlund, *Phys. Rev.* xxxii. p. 841 (1928); J. A. Bearden, *Bull. Amer. Phys. Soc.* (April 1929).

|| C. E. Howe, *Phys. Rev.* xxxv. p. 717 (1930).

¶ C. B. Bazzoni, L. Y. Faust, and B. B. Weatherby, *Phys. Rev.* xxxiii. p. 1101 (1929).

authors claim to have found several components in the diffuse lines C  $K_\alpha$  and B  $K_\alpha$  by a densitometric method. The hypothesis that the diffuseness of these lines could be explained as a fine structure was mentioned by the author in an earlier paper \*, but the research that has been carried out now proves that, even when great dispersion and narrow slits are used, one single but broad line appears, the blackening curve of which varies without discontinuities, rather steep on the short wave-length side and less inclined on the other (see fig. 9, Pl. IV.), and this progress becomes finer and more uniform with improvement in the quality of the grating. The diffuseness of the K-lines from these lightest elements could possibly be explained by the assumption that the influence of the neighbouring atoms is proportionately greater than in heavier elements, or, in other words, that distinct X-ray levels do not exist in the lightest elements when they are in the solid state. Besides that it seems possible that the thermal motion of the emitting atoms could be of some influence. The observed resolution into components is probably explained in the simplest manner by the existence of focal defects in the grating.

Relative measurements with plane gratings have been carried out by Hunt †, who determined the wave-lengths of Al  $K_\alpha$  and C  $K_\alpha$  referred to Cu  $L_\gamma$ . Much greater accuracy was reached by Kellström ‡, who measured the L-series of the elements 29 Cu–20 Ca referred to Al  $K_\alpha$ , the wave-length of which has been determined by crystal precision measurement as was mentioned above §.

The investigation of the K-series of the light elements carried out by the author was begun in the summer of 1928 as a relative measurement referred to Al  $K_\alpha$ . A preliminary report on this work was published in January 1929 ||. Using an apparatus which permits greater accuracy in adjusting and by means of the new gratings made in this laboratory ¶ I have succeeded in increasing the accuracy of the values obtained. Also the examinations have been carried out with different angles of incidence

\* M. Söderman, *Zs. für Physik*, lii. p. 795 (1929).

† F. L. Hunt, *Phys. Rev.* xxx. p. 227 (1927).

‡ G. Kellström, *Zs. für Physik*, lviii. p. 511 (1929).

§ Page 604.

|| *Zs. für Physik*, lii. p. 795 (1929).

¶ M. Siegbahn and T. Magnusson, *Zs. für Physik*, lxii. p. 435 (1930).



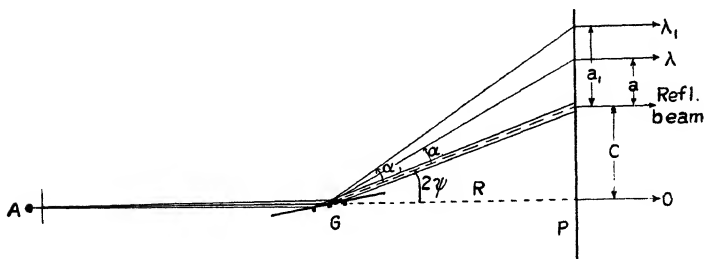
and with several gratings, ruled with 300, 900, and 1800 lines per millimetre respectively, so as to make the results more reliable. Further it has turned out to be practical to exchange the Al  $K_\alpha$ -line for Cu  $L_\alpha$  as reference line, the latter reaching nearly the same wave-length in its third order as the former in its fifth.

For the study of soft X-rays also concave gratings have been used. The concave grating method was tried by Osgood \*, who has published some results in the region 50–200 Å. He has also given a complete synopsis of the spectroscopic methods in the region between ultra-violet and X-radiation †. It seems, however, as if the few results hitherto obtained with concave gratings in the X-ray region are rather doubtful.

### *The Apparatus.*

The horizontal section through the apparatus, given schematically in fig. 1, shows the principle on which it is

Fig. 1.



constructed. The X-rays from the anode (A) pass a slit and fall upon the grating (G). The spectrogram is photographed on the plate (P).

The apparatus was constructed in this laboratory in the summer of 1929. Its exterior is shown in fig. 2, Pl. III. The X-ray tube is of the type usually employed here, and fitted with water-cooling both in the tube itself and in the electrodes, which permits a heavy current (250 milliamps at 4000 volts). It proved, however, to be very difficult to get good focussing when the tension was so low as in

\* T. H. Osgood, *Phys. Rev.* (2) xxx. p. 567 (1927).

† T. H. Osgood, *Phys. Rev.*, Suppl. (October 1929).

this investigation. This problem was solved in a simple but effective manner by means of the arrangement sketched in fig. 5. A diaphragm with a hole 2 or 3 millimetres in diameter was placed between the hot cathode and the anode, and connected with the earth. In order

Fig. 5.

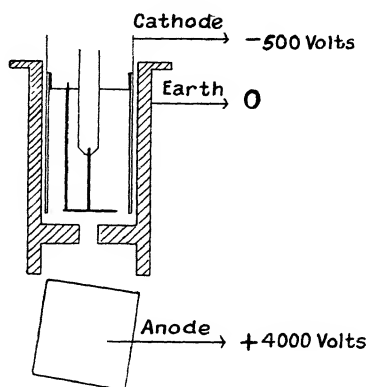
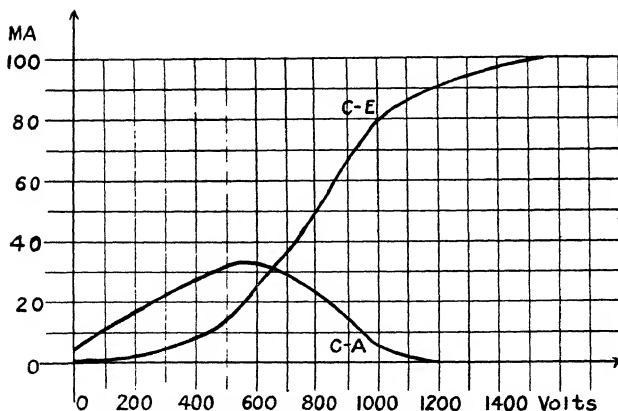


Fig. 6.



to make an electron current pass to the anode it was necessary to apply an accelerating negative auxiliary tension at the cathode. The currents in the two circuits cathode-anode (C-A) and cathode-earth (C-E) are plotted in fig. 6 as functions of the applied auxiliary

tension. The values used in this diagram are found in Table V. It is evident from the diagram that the anode current, which produces the X-radiation, could not be higher than about 35 milliamps, but of course it could have been raised by increasing the current through the hot cathode. The focus, however, was so sharp and the effect upon each superficial element so great that the current could hardly be increased further without melting the anode metal at the point of focus. The intensity of the X-radiation that passes the slit at 30 milliamps with this arrangement is greater than that procured by 250 milliamps falling upon a spread focus spot. Another great advantage is that the sputtering from the tungsten filament becomes a minimum and practically disappears when the vacuum is good.

The slit was made of tempered steel. Its width could be varied by putting in metal foils. The slit-widths used in

TABLE V.

Aux. tension (volts) ....	0	220	500	1000	1500
Current C-A (MA) ....	5	18	33	5	—
Current C-E (MA) ....	0	3	15	80	90

this investigation were between  $15\ \mu$  and  $50\ \mu$ . The slit could be turned in a plane at right angles to the direction of the X-ray beam by means of a lever (fig. 4, Pl. III.). A protecting slit between this slit and the grating, seen on the same figure, screened the optical beams diffracted from the first slit.

The gratings, which, as already mentioned, were produced in this laboratory, were ruled on plane glass plates. Since the ruled surface was only about 2 millimetres wide, there was no need of the usual second slit to limit the width of the diffracted beam, which was now equal to the projection of the width of the ruled surface on a plane at right angles to the beam. Also the position of the reflected beam could be easily determined, since the ruled part of the surface reflected less than the polished part on both sides, so the region on the plate corresponding to the reflected beam from the ruled surface appeared as a sharply limited

white line (C on fig. 8, Pl. IV.) upon the background, blackened by the radiation reflected from the unruled surface. In order to limit the background an edge was applied some tenth of a millimetre before the centre of the ruled surface. It is to be observed, however, that this edge serves only as a protecting screen, and does not screen off any of the lines on the grating nor the beams coming from it. In this manner the screening correction, calculated by Bäcklin\* for ordinary gratings, becomes unnecessary. The best contrast between illuminated and unilluminated field on this part of the plate was obtained with very short exposures; so a steel screen was placed in the path of the reflected beam. Near the end of each exposure the screen was removed by an electromagnet and the exposure continued for about 15 or 20 seconds, after which the circuit was disconnected. The appearance of the grating-table is shown in fig. 4, Pl. III. The grating is mounted in a holder which can be placed under the microscope for adjustment. Further, the whole grating-table can be turned about a conical joint, whose position is carefully fixed in the apparatus.

The plate-holder can be adjusted by means of three screws. Its position is particularly firm, since it is connected to the apparatus with two balks, shown in fig. 3, Pl. III. Both Imperial Eclipse and Agfa Contrast plates were used. The Contrast plates required somewhat longer exposure, especially for long wave-lengths; but the lines became sharper, which aided their measurement. In particular some of the sharpest lines had to be exposed on Contrast plates, since their whole width was of the same magnitude as the grains of the Eclipse plates. Fig. 8, Pl. IV., gives a comparison between an Eclipse plate and a Schumann plate, exposed under the same conditions. The Schumann plate is evidently less sensitive for the rather short wave-lengths (continuous radiation and Cu  $L_{\alpha}$ ), while the soft O  $K_{\alpha}$  and C  $K_{\alpha}$  lines appear with nearly the same intensity on both plates.

The whole apparatus can be hermetically shut by a steel cylinder, which rests upon a rubber gasket in the brass plate (figs. 3 and 4, Pl. III.). Though the volume amounts to 12 litres, it can be evacuated in 5 minutes by means of an oil-pump and a Siegbahn disk-pump of the smallest type.

\* E. Bäcklin, *l. c.* p. 36.

The generator was capable of producing 250 milliamps at 5000 volts. For the accelerating tension (see p. 607) another high-tension generator was first used, but, as there proved to be no use in making this tension higher than about 500 volts, the second generator was replaced by a battery connected in series with the municipal direct-current lighting-system. The hot-filament current was obtained from a step-down transformer.

### *Adjustments and Measurements.*

The grating to be used was mounted in an optical spectrometer and its grating constant determined in the usual manner. The gratings being ruled on plane parallel glass plates, they could be used for either reflexion or transmission. The determination of the dispersion for the grating with 1800 lines per millimetre is of special interest. Used as a transmitting grating, and illuminated by sunlight falling normally upon it, it gives a spectrum with very great dispersion. The beams deviated the least, *i. e.*, the violet rays in the first order, leave the grating at an angle of deviation of about  $50^\circ$ . The blue and green regions of the spectrum are also well visible, but in the yellowish green it makes a sudden stop, the angle of deviation being  $90^\circ$ . The position of this limit can be estimated by means of the absorption lines in the spectrum. The wave-length, corresponding to it, is evidently equal to the grating constant. By this method it is possible to estimate the value of the grating constant with rather high accuracy even without using the scale of the spectrometer—that is, the determination can as well be made with a spectroscope. To determine the grating constant by means of a microscope would be very difficult in this case, the distance between the ruled lines being less than the resolving power of the microscope. The only possibility for such a measurement would be the method suggested by Grossmuller and Lakemann\* to observe the phenomena of interference produced by a fine fibre stretched obliquely across the ruled surface.

When the grating constant had been determined the grating was mounted in its holder and adjusted under the microscope, so that the protecting edge became parallel to

\* J. Th. Grossmuller and C. Lakemann, *Zs. für Physik*, lix. p. 215 (1929).

the lines and before the middle of the ruled surface. In order to make this adjustment easy the middle of each grating ruled in this laboratory is marked by a line some millimetres longer than the others. The grating holder was fixed upon the table and its position adjusted parallel to the axis of rotation by means of a telescope and scale. Part of the surface outside the ruling was silvered, in order to make the readings easier. A surface-silvered plane glass plate was laid against the plane polished surface of the edge before the grating, and by readings in this glass the edge, and at the same time the ruled lines, could be made parallel to the axis of rotation of the grating table. After that the edge was screwed up to the grating. Then it evidently coincides with the middle line. This line had to be brought into the true axis of rotation, which was done by observing the edge through a microscope from above and adjusting by the two screws (fig. 4, Pl. III.) until the edge was stationary, when the grating table was rotated. After that the position of the whole apparatus was adjusted by its base screws, so that the axis of rotation was vertical. This was observed through a telescope, whose rotation axis could be carefully adjusted vertical, by comparing the direction of the edge with that of two plumb-lines hanging at the same distance from the telescope as the edge. In the same manner the first slit was made vertical, *i. e.*, parallel to the second.

The position of the plate-holder was adjusted by putting in a surface-silvered glass plate in the place of the photographic plate. The grating was rotated until the angle of incidence became  $0^\circ$ , when a beam from the first slit, which was illuminated, passed the second slit without deviation, thus marking the middle line of the apparatus. That part of the beam which came from the middle, vertically, of the ruled surface was screened off, and the position of the plate-holder adjusted until the edge of the screened beam was reflected into its own path. In order to make it possible to vary the position of the point of focus, the hole in the diaphragm, described on p. 607 was eccentrically drilled, and it could be decided by trial exposures at what position of the focus spot the emitted X-radiation reached a maximum. The distance between the grating and the plate was measured with an iron rod, whose length could be varied by a micrometer screw.

Indicating the angle of incidence by  $\psi$ , the wave-length

to be referred by  $\lambda$ , and the wave-length to be measured by  $\lambda_1$ , we obtain, according to the grating formula,

$$\lambda = 2e \sin \frac{2\psi + \alpha}{2} \sin \frac{\alpha}{2},$$

$$\lambda_1 = 2e \sin \frac{2\psi + \alpha_1}{2} \sin \frac{\alpha_1}{2},$$

where  $e$  denotes the grating constant,  $2\psi + \alpha$  and  $2\psi + \alpha_1$  the angles of deviation (fig. 1, p. 606). If the distance between the grating and the plate is denoted by  $R$ , the distance from the point  $O$  (fig. 1) to the reflected beam by  $C$ , and the distance from this to the reference line and to the unknown line by  $a$  and  $a_1$  respectively, it is evident that

$$\tan (2\psi + \alpha) = \frac{C + a}{R},$$

$$\tan (2\psi + \alpha_1) = \frac{C + a_1}{R},$$

$$\tan 2\psi = \frac{C}{R}.$$

The exact solution of this system leads to a very complicated expression for  $\lambda_1$ , but, the angles in question being small, several approximations can be made. In this investigation the wave-lengths were calculated according to the approximate formula

$$\lambda_1 = \frac{a_1}{a} \cdot \lambda + \frac{e}{2R^2} a_1(a_1 - a),$$

which gives too small values for the wave-lengths below the reference-line and too great for the others. In order to make the results coincide a correction is applied, determined by means of a graph for each dispersion, so that the value of the reference wave-length, calculated from different orders, is always the same. The total amount of this correction in no case exceeds 0.6 per cent., and the uncertainty for this greatest value of the correction is only about 0.02 per cent. Thus the errors arising from the approximation in the mathematical treatment may be neglected.

For some plates, where the reference-line appears in three orders or more, also another method of calculation

has been used. Supposing that the wave-length ( $\lambda$ ) depends upon the line's distance ( $a$ ) from the reflected beam according to the function

$$\lambda = A \cdot a + B \cdot a^2 + C \cdot a^3,$$

one may calculate the constants A, B, and C, and thus determinate the wave-length  $\lambda_1$ . Terms containing higher powers than  $a^3$  can be neglected, even the term  $Ca^3$  being very small compared with the two other terms. The advantage of this method is its purely empirical character, i. e., it is not based upon any questionable assumptions about the reflexion at grazing incidence and about the constants included in the formula, but it gives directly one wave-length referred to another.

The plates have been treated one by one, and the angle of incidence has been varied between most exposures. The following values have been obtained :—

	Grating constant.	Lines/mm.
Grating 47....	$e=33367 \pm 3 \text{ \AA.}$	299.70
„ 15....	$e=10984 \pm 1.5$	910.4
„ 29....	$e=5601.1 \pm 1$	1785.4

Distance between grating and plate :  $R=271.3 \pm 0.1 \text{ mm.}$

TABLE VI.

O K $\alpha$ .		N K $\alpha$ .		C K $\alpha$ .	B K $\alpha$ .	Be K $\alpha$ .
I.	II.	I.	II.	I.	I.	I.
23.57	23.58	31.56	31.63	44.61	67.79	115.54
55	60	54	64	50	71	84
57	58	52	59	50	63	
57	56	54		55		
	56	52		51		
	57	52		58		
	60	51		54		
	57					
23.57		31.56		44.54	67.71	115.7

The lowest dispersion (900/3) has been used only for the elements O, N, C, B, and Be. The results calculated from different orders and different plates are shown in Table VI. All values except that for Be K have been



referred to Cu  $L_{\alpha}$  = 13.306 Å.\*, and exposed with angles of incidence between 1° and 1°·5. For the beryllium line one maximum had earlier † been found at 113.4 and one at 119 Å. It was then suspected that this maximum depended upon the line OK $_{\alpha}$ v. In order to determine whether this was the case I have now worked with greater angles of incidence, 3°·5 and 4°. At these angles the intensity of the reflected O  $K_{\alpha}$ -radiation becomes negligible, though no sharp "angle of total reflexion" seems to exist, a fact noticed by many other observers‡. At these great angles

TABLE VII.

Al $K_{\alpha}$ .		Mg $K_{\alpha}$ .		Na $K_{\alpha}$ . F $K_{\alpha}$ .		O $K_{\alpha}$ .	N $K_{\alpha}$ .	
I.	II.	I.	II.	III.	I.	I.	I.	I.
8.321	8.323	9.888	9.873	9.876	11.884	18.276	23.572	31.553
322	325	879	871		885	270	545	554
324	324	869			885	268	540	567
		876					555	550
		872					572	569
		874					572	559
		892					555	
		875					549	
8.323		9.877			11.885	18.271	23.557	31.553

of incidence, however, no Cu  $L_{\alpha}$ -lines appear, and the beryllium line had to be referred to C  $K_{\alpha}$ , which appeared in four orders on both plates, and whose wave-length was taken as 44.54 Å. On these plates the blackening curve of the beryllium line proved wholly smooth, analogous to that of the carbon, but spread over a yet greater region of wave-length (see Table IX.). The fact that the value which has now been obtained for the beryllium line is greater than that found earlier is probably due to a simply physiological phenomenon. Experience has proved that

\* Recently determined in this laboratory by A. Larsson.

† M. Söderman, *l. c.* p. 803.

‡ El. Laird, *Phys. Rev.* (2) xxvii. p. 510 (1926); H. E. Strauss, *Phys. Rev.* (2) xxxi. p. 491 (1928); M. Valouch, *Journ. de Phys.* (6) x. p. 109 S. (1929); J. A. Prins, 'Nature,' cxxiv. p. 370 (1929).

in comparator measurements on a diffuse line with unsymmetric blackening the comparator is set between the maximum and the middle of the line, the flatter blackening curve the nearer the middle. If a second maximum appears the two settings are made too far apart—that is, in this case the real maximum was given too short a wave-length.

The angles of incidence which were used for grating 15 (1800/2) were  $0^{\circ}.8$ ,  $1^{\circ}.0$ , and  $1^{\circ}.5$ . The values obtained are shown in Table VII.

The greatest dispersion (1800/1) was used only for the wave-lengths of the elements Al–O. Table VIII. gives the values obtained.

TABLE VIII.

Al $K_{\alpha_{1,2}}$			Mg $K_{\alpha_{1,2}}$		Na $K_{\alpha}$	F $K_{\alpha}$	O $K_{\alpha}$
I.	II.	III.	I.	II.	I.	I.	I.
8.321	8.325	8.320	9.868	9.874	11.887	18.287	23.549
322	321	320	873	873	885	284	562
320	324		871		885	274	569
320	324		874		883		580
321	325		869		887		576
326							578
321							
324							
8.322			9.872		11.885	18.282	23.569

With this dispersion also some other lines than the  $K_{\alpha_{1,2}}$  could be measured. Thus in Al and Mg it was possible to distinguish between a strong line corresponding to  $K_{\alpha_{1,2}}$  and a faint line partly overlapping the other and probably due to  $K_{\alpha_{3,4}}$ . The lines could be measured one by one and their separation was found to be  $0.060 \text{ \AA}$  for Al and  $0.075 \text{ \AA}$  for Mg, in good agreement with the results obtained by crystal methods. Further, the  $K_{\beta}$ -line of aluminium appeared after sufficient exposure, and could be measured. Its distance from the  $K_{\alpha_{1,2}}$ -line was  $0.370 \text{ \AA}$ .

Table IX. gives a summary of the results of this research. The mean errors of the values obtained from different orders and different plates are between  $0.02$  and  $0.03$  per

cent. for the elements Al-F, and increase gradually with increasing wave-lengths from 0.06 per cent. for O to 0.15 per cent. for Be. It might be possible to raise the accuracy a little for the wave-lengths of the first elements of the table, especially by using narrower slits, but for the lightest elements this is of no interest. The flatness of the blackening curves for these elements makes a specific indication of its maximum hardly possible; nor is it suitable to state the middle of the unsymmetric blackening as the wave-length. Taking this into consideration, there

TABLE IX.

Line.	$\lambda$ (referred to $\text{CuL}\alpha = 13.306 \text{ \AA.}$ )	E (volts).	Appr. width of the lines.
Al $\text{K}\beta$ .....	7.952	1552	
Al $\text{K}\alpha_{3,4}$ ...	8.262	1494	
Al $\text{K}\alpha_{1,2}$ ...	8.323	1483	
Mg $\text{K}\alpha_{3,4}$ ...	9.799	1260	
Mg $\text{K}_{1,2}$ ...	9.874	1250	
Na $\text{K}\alpha$ .....	$11.885 \pm 0.004 \text{ \AA.}$	1038	
F $\text{K}_I$ .....	$18.275 \pm 0.007 \text{ \AA.}$	675.5	
O $\text{K}_I$ .....	$23.567 \pm 0.02 \text{ \AA.}$	523.8	
N $\text{K}_I$ .....	$31.557 \pm 0.03 \text{ \AA.}$	391.2	0.5 $\text{\AA.}$
C $\text{K}_I$ .....	$44.54 \pm 0.04 \text{ \AA.}$	277.2	1 $\text{\AA.}$
B $\text{K}\alpha$ .....	$67.71 \pm 0.1 \text{ \AA.}$	182.3	2 $\text{\AA.}$
Be $\text{K}\alpha$ .....	$115.7 \pm 0.15 \text{ \AA.}$	106.7	10 $\text{\AA.}$

would be no meaning in indicating the wave-lengths of the lightest elements with the accuracy obtained in this research. Instead Table IX. gives the range within which the wave-lengths might be indicated. The range is of the order of the interval between the maximum and the middle of the blackening.

I am greatly indebted to Professor Siegbahn, who suggested the research, and whose friendly encouragement and fruitful advice were essential to its successful completion. Mr. Ivar Lindell, instrument maker for the University, was responsible for the painstaking construction of the apparatus.

Upsala,  
Physics Laboratory of the University,  
June 1930.

LX. (i.) *The End-corrections of an Open Organ Flue-pipe ;*  
 and (ii.) *The Acoustical Conductance of Orifices.* By  
 A. E. BATE, M.Sc., Northern Polytechnic, London \*.

# ABSTRACT.

(i.) THE end-correction at the mouth of an organ flue-pipe is shown to be independent of the frequency, but to depend on the dimensions of the mouth and on the sectional area of the pipe. The correction has the same value whether the pipe be open or closed, and is unaffected by the motion of the air-jet. It is shown that the correction  $\alpha$ , in terms of  $A$ , the area of the pipe, and  $\omega$ , the area of the mouth, may be represented by

$$\alpha = \frac{A}{k \cdot 2 \sqrt{\omega/\pi}},$$

where  $k$  is a constant. This is of linear dimension, as is to be expected.

The correction  $\beta$  at the open end is found to be independent both of the dimensions of the mouth and of the frequency. It is somewhat larger than the usually accepted value, being given by

$$\beta = 0.66R.$$

$R$  is the radius of the pipe.

(ii.) The conductance  $C$  of a circular orifice in the otherwise closed end of a cylindrical resonator is shown to be closely represented by the expression

$$C = 2^{d/D} \cdot d,$$

$d$  being the diameter of the orifice and  $D$  that of the pipe. This formula is also applicable to square orifices if  $d$  represents the diameter of a circle equal in area to the square. In a similar manner the conductance of a rectangular orifice may be determined when almost square, but for narrow rectangles the conductance must be treated as that of an ellipse of equal area, the ratio between the axes being the same as the ratio between the sides of the rectangle.

\* Communicated by Dr. Reg. S. Clay.

## PART I.

§ 1. **I**N the two papers already published, the effect of wind-pressure and of the height of the mouth on the frequency of an organ pipe\* and upon the end-correction at the mouth of a stopped pipe† have been dealt with. These will be referred to as the first and second papers respectively in this communication.

In the present paper it is shown that the results of the second paper are applicable to the mouth of an open pipe ; the corrections at the open end are also included. In addition, the gap in the second paper between the results for frequencies of 128 and 256 has been bridged by including a frequency of 192 vibrations per second, which was obtained by comparison with a specially constructed fork.

The expression  $\frac{V}{nh} = 6.17$  was established in the first paper as the relationship between  $V$ , the velocity of the air-jet ;  $n$ , the frequency of the pipe ; and  $h$ , the distance from the lip to the slit from which the air issues when the pipe is speaking its most stable note, the slit being 0.12 cm. wide. This relationship was used to determine the air-pressures required for the different heights of the mouth at the different frequencies.

§ 2. The apparatus described in the former papers has been again used for these further experiments. The pipe has a movable lip, which was adjusted so that the height of the mouth was 1.5 cm. The pipe was then blown with the pressure that has been found to be required to give a particular jet-frequency. The frequencies used were 132, 196, 260, 292, and 324 ; these were obtained by adjusting the length of the pipe to be approximately in tune with forks vibrating 128, 192, 256, 288, and 320 times per second respectively ; the length was then decreased until there were four beats per second between the fork and the pipe, the beats being timed with a metronome. This method admits of very close adjustment, whereas true unison is very difficult to detect by ear.

The length of the pipe was obtained by placing a measuring rod inside the mouth and adjusting it so that the zero end coincided with the end of the pipe ; an index sliding

\* Phil. Mag. viii. p. 750 (Nov. 1929).

† Phil. Mag. ix. p. 23 (Jan. 1930).

on the rod was then brought into contact with the mouth and clamped to the rod; the position of this index thus indicated the length of the pipe. These measurements were taken both with the pipe open and closed at each frequency.

The whole procedure was then repeated with the height of the mouth altered to 1.25 cm., and again with it altered to 1.0 cm.

The difference between the lengths of the open pipe and of the corresponding closed pipe was taken as the length of the open pipe above the node, *i. e.*, the nodes in both cases were assumed to be at the same distance from the mouth. The amount by which the length above the node falls short of the quarter-wave-length is the open end-correction, and the amount by which the closed pipe falls short of the same quantity is the mouth end-correction.

§ 3. In § 9 of the second paper the end-corrections at the mouth for each height of the mouth were shown to remain practically constant when the length of the pipe is increased by one or by two half-wave-lengths. This also holds for the open pipe, so that the wave-lengths can be measured by lengthening the pipe until it recovers its initial frequency. One result will illustrate this, the frequency being 260 :—

	1st length.	2nd length.	Half-wave-length.
Closed pipe .....	25.1	90.0	64.9
Open pipe .....	55.8	120.6	64.8

The length of the half-wave calculated from the velocity of sound at this temperature is 65.0 cm.

### Results.

§ 4. The actual readings obtained, and the resulting corrections, are set out in the following tables. The lengths of the pipe are all given in cm.

TABLE I.

Corrections when height of mouth = 1.5 cm.

Frequency .....	132	196	260	292	324
Closed pipe (i.) .....	56.8	36.1	25.1	21.7	19.2
Open pipe .....	119.7	77.6	55.8	49.1	43.7
Closed pipe (ii.) .....	185.7	122.6	90.0	79.9	72.0
$\lambda/4$ .....	64.45	43.25	32.45	29.1	26.4
Correc- tions. {	Open-end .....	1.55	1.75	1.75	1.8
	Mouth .....	7.65	7.25	7.35	7.2
	Total .....	9.2	9.0	9.1	9.0

TABLE II.

Corrections when height of mouth = 1.25 cm.

Frequency .....	132	196	260	292	320	
Closed pipe (i.).....	56.1	35.4	24.5	21.1	18.4	
Open pipe .....	119.2	77.0	55.3	48.4	43.1	
Closed pipe (ii.) .....	184.7	122.2	89.5	79.2	71.1	
$\lambda/4$ .....	64.3	43.4	32.5	29.05	26.35	
Correc- tions. {	Open-end .....	1.2	1.8	1.7	1.75	1.65
	Mouth .....	8.2	8.0	8.0	7.95	7.95
	Total .....	9.4	9.8	9.7	9.7	9.6

TABLE III.

Corrections when height of mouth = 1.0 cm.

Frequency .....	132	196	260	292	320	
Closed pipe (i.).....	54.8	34.2	23.5	20.1	17.5	
Open pipe .....	117.7	75.9	54.1	47.3	42.05	
Closed pipe (ii.) .....	182.9	121.3	88.1	78.1	70.2	
$\lambda/4$ .....	64.05	43.55	32.3	29.0	26.35	
Correc- tions. {	Open-end .....	1.15	1.9	1.7	1.8	1.8
	Mouth .....	9.25	9.35	8.8	8.9	8.85
	Total .....	10.4	11.2	10.5	10.7	10.65

These measurements were read to the nearest 0.5 mm., and are believed to be correct to within 1 mm. up to 100 cm.; hence the end-corrections should be accurate to within 2 mm. for all frequencies other than 132, and to within 4 mm. for that frequency. Discrepancies arise owing to changes in temperature; this accounts for the different values of the half-wave-lengths given above for a particular frequency, which were obtained at different times. To avoid errors due to this cause, the readings in any one series were taken as rapidly as possible. The poor agreement of the end-corrections for the lower frequencies in Tables II. and III. is probably due to the fact that the low pressures required were not far above the minimum values necessary to elicit notes of these frequencies.

§ 5. It has been assumed that the node in the open pipe occupies the same position as the closed end of the closed pipe when the pipe is giving the same note under identical conditions of blowing. This is not necessarily true, as the energy is being transmitted through the node for the maintenance of the vibrations in the upper portion, and to supply the energy that is being dissipated from its open or partially open end when the pipe is not closed.

Results, however, justify the assumption, for the difference between the lengths of the open pipe and of the corresponding closed pipe is the same at all intensities within the limits of experimental error; hence the transmission of energy by the node does not cause a noticeable alteration in its position.

### § 6. *Discussion of Results.*

After an alteration has been made in the height of the mouth, the alteration in the length of the open pipe which is necessary in order to maintain a note of given frequency is seen from the above tables to be due to an alteration in the end-correction at the mouth; it follows that the open-end correction is independent of the intensity of the note over the range of the pressure used, this intensity being governed by the jet-velocity. The pressure did not exceed 10 cm. of water. The results also prove that the open-end correction is independent of the height of the mouth and of the frequency. The mean value of the open-correction, omitting the doubtful values for the lowest frequency in Tables II. and III., is 1.74 cm. This is somewhat larger than the value of the end-correction of a resonance tube as determined by the usual tuning-fork method, which, for a tube of this diameter, would amount to 1.53 cm. Irons\* draws attention to the fact that this method of obtaining the end-correction is untrustworthy, and quotes Boehm†: "A maximum of intensity outside the tube may not indicate that the resonator is nearest to unison with the pitch produced." In the present experiments forks are used as standards of comparison, and are, of course, independent of the exciting agent, the jet. Boehm gives the mean value of the end-correction as 0.656R. The corresponding figure obtained from the present results is 0.657R. The presence of a large flange increases this to about 0.84R (see § 12).

§ 7. On reference to the tables, it will be seen that the end-corrections at the mouth are, within reasonable limits, constant for each height of the mouth, and are independent of the frequency and (except for very low pressures) of the velocity of the air. The mean values of these corrections are 7.4, 8.0, and 9.0 cm. when the heights of the mouth are respectively 1.5, 1.25, and 1.0 cm. The

\* Phil. Mag. v. p. 592 (Mar. 1928).

† Phys. Rev. xxxi. p 341 (1910).



diameters of circles that would have areas equal to the areas of the mouth when it has these heights are 2.70, 2.46, and 2.20 cm. respectively; these were called the "equivalent diameters" in the second paper, and are approximately equal to the conductance of the mouth in each case. In that paper the relationship between the end-corrections  $\alpha$  and the conductances  $C$  was expressed by

$C = \frac{A}{\alpha}$ , in which  $A$  stands for the area of the cross-section

of the pipe. This formula would give the three values of  $C$  as 2.98, 2.76, and 2.45 cm. respectively. The difference between these theoretical values and the practical results is partly attributable to the shape of the mouth, the formula being strictly applicable only when the mouth is a circular orifice. This point is further dealt with in Part II. (§ 16).

§ 8. The ratio between the conductances and the equivalent diameters is 1.1 nearly in all three cases, so that

$$\alpha = \frac{A}{C} = \frac{A}{1.1 \text{ (equivalent diameter)}}.$$

Since the equivalent diameter  $= 2\sqrt{\omega/\pi}$ , where  $\omega$  stands for the area of the mouth, the formula for the mouth-correction may be written generally

$$\alpha = \frac{A}{k \cdot 2 \sqrt{\omega/\pi}},$$

in which  $k$  is a numerical value depending on the shape and size of the mouth and on the presence of obstructions such as the "ears" which are usually fixed to each side of the mouth of an organ pipe, for these factors vary the conductance. For pipes in the same stop—an open diapason, for example—the value of  $k$  should be constant; in any case, it probably lies between 1.0 and 1.5, so that for such a set of similar pipes the mouth-correction is proportional to the sectional area of the pipe, and is inversely proportional to the square-root of the area of the mouth.

§ 9. An ordinary open cylindrical organ pipe of diameter 5.8 cm., designed to give 256 vibrations per second, was tuned at the correct wind pressure by means of the sleeve ("tuning top") fitted for that purpose. It was then found to measure 56.9 cm. from languid to open end. The half-wave-length at the temperature of the room was 66.3 cm.;

hence the total correction was equal to 9.4 cm. Allowing 1.9 cm. for the open end-correction, the mouth-correction was 7.5 cm. The dimensions of the mouth were : width, 4.45 cm. ; height, 1.8 cm. Substituting these values in the formula, we find that  $k=1.10$ . The close agreement with the results obtained with the experimental pipe probably comes about because the presence of the ears in the ordinary organ pipe compensates for the unusual position of the mouth of the experimental pipe.

The open diapason pipe is usually made with a mouth of which the breadth is equal to one-quarter of the circumference, and the height to one-quarter of the diameter. Such a mouth will have an equivalent diameter equal to the radius of the pipe ; in this case the formula reduces

to  $\alpha = \frac{\pi}{k} \cdot R$ . If  $k$  is taken as 1.1, this becomes  $2.85R$ , so

that the total correction is then about  $3.5R$ .

In delicate stops (Dulciana, Gamba, etc.) the area of the mouth of a pipe varies from one-fifth to one-sixth of the sectional area of the pipe ; this increases the mouth-correction for such stops. On the other hand, the mouth of a pipe of a flute stop is usually made equal to about one-third of the area of the pipe, and in this case the mouth-correction is less.

(Organ builders usually make their open pipes about  $3.3R$  short of the half-wave-length, and then trim them down as required ; final tuning is accomplished by means of the tuning-top.)

## PART II.

§ 10. Lord Rayleigh\* gave the conductance of an extremely short cylindrical pipe as\* with infinite flanges at the ends as

$$\frac{\pi R^2}{L + \frac{1}{2}\pi R},$$

in which  $R$  is the radius and  $L$  the length of the pipe ; the second term in the denominator is the sum of the two end-corrections. He proceeds to show that if the two flanges approach until  $L=0$ , the conductance becomes  $2R$  ; i. e., the conductance of a circular orifice in an infinite plane of negligible thickness is equal to the diameter.

\* 'Sound,' ii. p. 181.

If, now, a cylinder whose dimensions are large compared with those of the orifice is supposed to be fixed to one side of the flange, with its axis concentric with the orifice, the conductance of the latter will remain practically unaltered. On decreasing the diameter of the cylinder (which is supposed closed at its unattached end), the conductance of the orifice alters, and eventually, when the diameters are equal, we have a pipe closed at one end and fitted with an infinite flange at the other. The correction at one end will now be eliminated, and the conductance becomes

$$\frac{\pi R^2}{\frac{1}{4}\pi R} = 4R,$$

*i.e.*, the conductance of the open end of a pipe fitted with an infinite flange is equal to twice the diameter.

Thus the limiting values of the conductance of a concentric circular orifice on the end of a circular pipe are  $d$  and  $2d$ ,  $d$  being the diameter of the orifice. A simple formula, which fits both extreme cases, is  $C = 2^{d/D} \cdot d$ , where  $D$  is the diameter of the pipe and  $C$  the conductance, for when  $d=0$ ,  $C=0$ ; and when  $d=D$ ,  $C=2D$  \*.

Substituting this expression for the conductance in the equation  $\alpha = \frac{A}{C}$ , we get

$$\alpha = \frac{A}{2^{d/D} \cdot d}.$$

The truth of this formula for values between the two limiting values can be readily tested by the method employed in Part I. For this purpose nine caps were constructed to fit over the open end of the open pipe. In the centre of the plane-face of five of these caps circular holes were drilled, the diameters being 1, 2, 3, 4, and 5 cm. respectively. In the four remaining caps square holes were cut, the sides being 1, 2, 3, and 4 cm. long respectively.

Subsequently six additional caps were used, the apertures being rectangular and of dimensions (in cm.):

$$4 \times 3, 4 \times 2, 4 \times 1.5, 4 \times 1, 3 \times 2, \text{ and } 3 \times 1.$$

§ 11. The end-corrections were found for the capped end of the pipe with the five frequencies previously used, each of the caps being used in turn. The results obtained with

\* [Note.—This limit is probably somewhat smaller than  $2D$ , as  $\frac{1}{4}\pi R$  is the lower limit of the end-correction of a flanged tube.]

the circular orifices are given in Table IV. The upper part of the table gives the difference between the lengths of the closed pipe and the complete pipe in each case, the lengths being measured from the inside of the caps. The wave-lengths were obtained by the method previously used. (Different values for a particular frequency were due, as before, to variation in temperature.)

The corrections are set out in the second part of the table; they were obtained by subtracting the length above

TABLE IV.

End-corrections for circular orifices of various diameters.

Height of mouth	.....	1.5	1.25	1.5	1.25	1.5	1.25	1.5	1.25	1.5
Frequency	.....	132	196	260	292	324				
Length of pipe above node when diams. of orifices were	1 cm.	44.0	24.1	24.8	16.2	16.7	13.1	13.7	10.7	11.7
	2	54.9	34.1	34.1	24.0	24.1	20.5	20.7	17.4	18.1
	3	59.4	38.2	38.2	27.7	27.5	24.3	24.4	21.4	21.4
	4	61.4	40.05	40.0	29.5	29.5	26.0	26.1	23.3	23.2
	5	62.5	41.0	41.0	30.5	30.3	27.0	27.1	24.25	24.1
Open pipe ....	5.3	62.9	41.6	41.5	30.8	30.7	27.3	27.4	24.7	24.6
$\lambda/4$ .....		64.45	43.4	43.25	32.5	33.45	29.05	29.1	26.35	26.3
Corrections for orifices of diams.	1 cm.	20.45	19.3	18.45	16.3	15.75	15.95	15.4	15.65	14.6
	2	9.55	9.3	9.15	8.5	8.35	8.55	8.4	8.95	8.2
	3	5.05	5.2	5.05	4.8	4.95	4.75	4.7	4.95	4.9
	4	3.05	3.35	3.25	3.0	2.95	3.05	3.0	3.05	3.1
	5	1.95	2.4	2.25	2.0	2.15	2.05	2.0	2.1	2.2
Open pipe ....	5.3	1.55	1.8	1.75	1.7	1.75	1.75	1.7	1.65	1.7

the node from the quarter-wave-length. Two heights of the mouth were used except for the first frequency (132),

so that, in conformity with the formula  $\frac{V}{nh} = 6.17$ , two

different values of  $V$ , the velocity of the air-jet, were necessary at each of the remaining frequencies. Any alteration in velocity is accompanied by an alteration in the intensity of the note produced, as stated in § 6.

It will be seen that the corrections for the larger orifices are independent of the wave-length and of the intensity, within reasonable limits. For the smaller orifices, however, the correction varies both with the frequency and with the intensity. The intensity variation may be due to the flow of air from the jet which travels through the pipe and

issues from the orifice ; at low pressures and with large orifices this flow has no appreciable effect on the correction. The variation with frequency may be due to the short length of the pipe that becomes necessary when the orifice is small, for then the diameter can no longer be neglected in comparison with the length. For this reason the values obtained with the lower frequencies and longer pipes should more nearly agree with the values obtained with the formula.

§ 12. The means of the above corrections are respectively : 1·7, 2·1, 3·2, 4·9, 8·8, and 16·9 cm. for orifices of diameter 5·3, 5·0, 4·0, 3·0, 2·0, and 1·0 cm. For such orifices in an infinite flange the calculated corrections would be 2·1, 2·3, 3·3, 5·0, 8·5, and 19·4 cm. A flange about 1 metre square was found to increase the corrections by 0·5, 0·5, 0·4, 0·4, 0·35, and 0·35 cm. respectively, *i. e.*, the pipe had to be shortened by these lengths to maintain the original frequencies when the flange was added. Thus the corrections with the flange become 2·2, 2·6, 3·6, 5·3, 9·15, and 17·25 cm.

These results are roughly 0·3 cm. larger than the calculated values ; this is to be accounted for by the fact that the thickness of the plate containing the orifice has been ignored, for the thickness reduces the conductance, and therefore increases the end-correction. The smaller discrepancy between the calculated and measured values of the open end-correction, amounting to 0·1 cm., where the thickness of the orifice does not arise, supports this view.

The end-corrections, with and without the flange, are shown in the graph (fig. 1). The curve gives the relationship between the diameters of the orifices and the corrections calculated from the proposed formula.

§ 13. The means of the experimental results obtained with square orifices are given in Table V. :—

TABLE V.

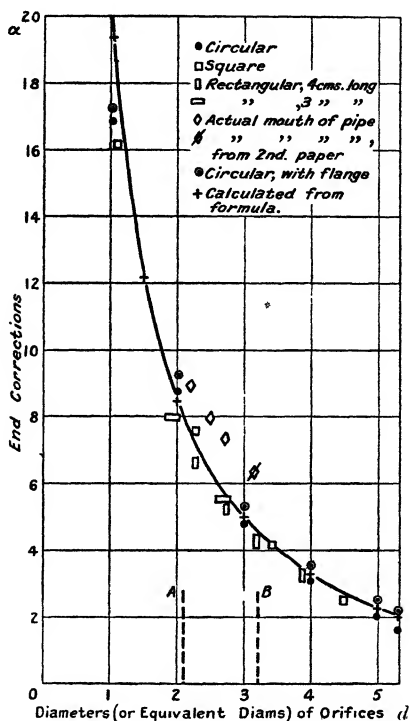
End-corrections with square orifices (unflanged).

Length of side of orifice in cm. ....	4	3	2	1
End-correction .....	2·6	4·2	7·6	16·2
Equivalent diameter.....	4·5	3·4	2·25	1·1

The relationship between the correction and the equivalent diameter is shown on the graph (fig. 1), from which it is seen that the correction for a square orifice is the same as that of a circular orifice of equal area.

§ 14. The end-corrections were next obtained with the rectangular apertures. The dimensions, equivalent dia-

Fig. 1.



meters, and mean values of the corrections are shown in the following table :—

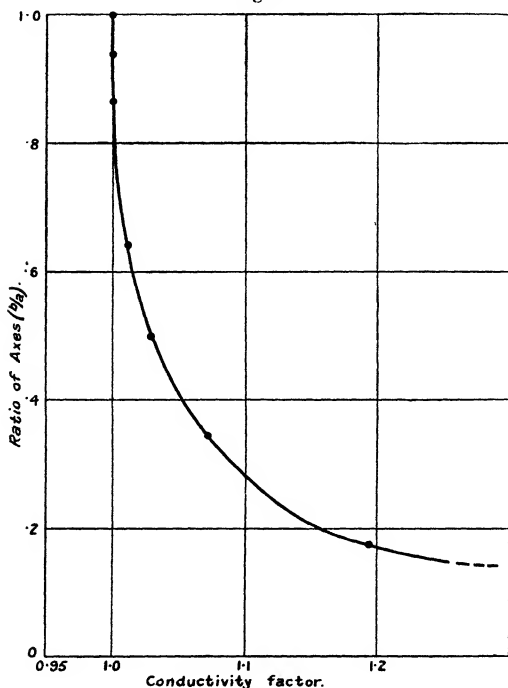
TABLE VI.

End-corrections with rectangular orifices (unflanged).

Dimensions in cm...	4×3	4×2	4×1.5	4×1	3×2	3×1
End-corrections ..	3.3	4.4	5.35	6.7	5.5	8.0
Equivalent diameters	3.9	3.2	2.75	2.25	2.75	1.95

The first four results, together with that for the square orifice of side 4 cm. (§ 13) resemble the end-corrections at a variable mouth of corresponding dimensions, and may be compared with the results recorded in Tables I., II., and III. On reference to the graph it will be seen that the first four results given in Table VI. deviate from the calculated curve as the ratio length/breadth is increased. The same applies to the orifices of length 3 cm. Thus the end-correction

Fig. 2.



for the orifice measuring  $3 \times 2$  cm. is greater than that for the orifice measuring  $4 \times 1.5$  cm., although these have equal areas. It follows that the conductance of a rectangular orifice of constant area increases with increase in the ratio length/breadth.

§ 15. In this connexion it is interesting to recall that Rayleigh\* has shown, from theoretical considerations, that

\* 'Sound,' ii. p. 179.

the conductance of an elliptical orifice of a fixed area increases as the eccentricity is increased. He calculated the ratios of the conductivity of ellipses to those of circles of equal area, the ratio of the axes of the former varying from 0 to 1.

It appeared probable that the same factors would hold in the comparison of the conductivity of a rectangle with that of a square of equal area, when the ratio of the sides of the rectangle replaced those of the axes of the ellipse. To determine these factors of conductivity the results which Rayleigh had calculated were plotted in a graph (fig. 2), and the conductance factors for the ellipses whose axes are in the same ratio as the sides of the rectangular orifices were read off from the curve. These factors are entered in the second row of Table VII.

The end-corrections of the square orifices (unflanged) which would have apertures equal in area to the rectangular apertures used were next read from the graph (fig. 1). Since the end-corrections are inversely proportional to the conductances, the end-corrections thus found must be divided by the conductivity factors to obtain the true end-corrections. The results are shown in Table VII. :—

TABLE VII.

Calculated corrections for rectangular apertures.

Dimensions in cm. . .	4×3	4×2	4×1·5	4×1	3×2	3×1
Conductivity factors.	1·00	1·03	1·06	1·12	1·01	1·08
End-corrections for square orifices of equal areas. }	3·4	4·4	5·6	7·6	5·5	8·8
Calculated end-corrections for rectangular orifices. }	3·4	4·3	5·3	6·8	5·4	8·1
Actual corrections for rectangular orifices. }	3·3	4·4	5·35	6·7	5·5	8·0

These readings are in excellent agreement with those given in Table VI., which are included above for comparison. It follows that, just as a square orifice has practically the same conductance as a circular orifice of equal area used under similar conditions, so a rectangular orifice has approximately the same conductance as an elliptical orifice of equal area, providing the ratio of the



axes of the ellipse is the same as the ratio of the sides of the rectangle.

These results extend Rayleigh's suggestion that any orifice may be treated as circular if it does not differ too much from a circle, to the case of a rectangle, which may be treated as an ellipse of equal area.

§ 16. Reverting to the question of the mouth correction which was discussed in Part I. (§ 7), the coefficient  $k$  in the equation  $\alpha = \frac{A}{k \cdot d}$  has been found to be practically constant.

The ratios of the equivalent diameters of the openings of the mouth to the actual diameters of organ pipes range from 0.4 to 0.6 (Dulciana to Flute). This range is represented by that portion of the graph (fig. 1) between the ordinates marked A and B; the curve in this region is nearly straight, and, since the end-correction for a rectangular orifice is smaller than that for a square one of equal area, the curve connecting the correction with the height of the mouth (the width remaining constant) will deviate from the calculated curve as the mouth decreases in height, and tend to become more nearly straight. This explains why  $k$  is practically constant. The mean values of  $k$  which were obtained with the experimental pipe are shown in the graph (fig. 1). They are above the curve, but this is probably due to the thickness of the lower lip, which forms a projection on the outside of the pipe and therefore decreases the conductance.

§ 17. The formula proposed for the conductance of an orifice fits the experimental results of two other experimenters. Richardson \* obtained by measurement the lengths of a resonance tube when the open end of the latter was covered with caps containing circular apertures of various diameters. He then proceeded to calculate the lengths by means of the formula

$$\tan \frac{\pi L}{\lambda/2} = \frac{\lambda}{2\pi} \cdot \frac{C}{A},$$

$C$  being the conductance of the orifice, which he assumed to be equal to the diameter, and  $A$  the sectional area of the tube. The other terms have their usual meanings. The tube was 4.3 cm. in diameter, and the frequencies

\* Proc. Phys. Soc. xl. p. 206 (1928).

ranged from 1000 to 224 v.p.s. The calculated and actual lengths were plotted on the same graph, from which he concluded that "... the theoretical and experimental curves are similar, but that there is lack of agreement when  $r$  (radius of orifice) is large. This, one may judge, is due to a change in the dependence of  $C$  upon  $r$ . It is evident that some such change must take place as resonator conditions are approached. . . ."

Repetition with a tube 2.2 cm. in diameter resulted in similar curves.

The writer repeated Richardson's calculations with the conductances obtained from the expression  $C=2^{d/D} \cdot d$ , and these gave much closer agreement with the measured values. (Allowance must be made for the absence of infinite flange, and also for the fact that resonance was obtained by holding tuning-forks over the orifices).

Again, Irons \*, by fitting similar caps over the end of a Kundt's tube 4.7 cm. in diameter, found experimentally that the products of the conductances and the corresponding end-corrections,  $C \cdot \alpha$ , were roughly 14.3 cm. when orifices of from 1 to 2 cm. diameter were used; the capped end was fitted with a large flange. The product of the diameters of the orifices and the corresponding end-corrections he found to be 11.0 cm.; so "... to reconcile theory with practice, the conductances of the orifices in question must be assumed to be somewhat larger than their diameters. . . ."

From these values the approximate ratio of  $\frac{C}{d}$  equals 1.3; if, however, we substitute 4.7 for  $D$ , and 1.0 and 2.0 for  $d$  in each case in the formula, the values of  $\frac{C}{d}$  become 1.16 and 1.34 respectively.

### Conclusions.

§ 18. The end-correction at the mouth of an organ flue-pipe has the same value whether the pipe be open or stopped, and may be obtained from the formula

$$\alpha = \frac{A}{k \cdot 2 \sqrt{\omega/\pi}},$$

\* Phil. Mag. vii. p. 873 (May 1929).

in which  $A$  stands for the sectional area of the pipe,  $\omega$  for the area of the mouth, and  $\alpha$  the correction at the mouth-end of the pipe;  $k$  is a numerical coefficient, and is constant for a particular type of pipe.

The end-correction  $\beta$  at the open end of an unstopped pipe is shown to be represented by the expression  $\beta = 0.66R$ . This is higher than the usually accepted value.

Both end-corrections are, within experimental limits, independent of the intensity of the note and of the frequency. For low pressures the results are unreliable.

The conductance  $C$  of a circular orifice in an infinite flange at the end of a cylindrical pipe is closely represented by

$$C = 2^{d/D} \cdot d,$$

in which  $d$  is the diameter of the orifice and  $D$  that of the pipe. This is approximately true for unflanged orifices, particularly when the orifices are small. When the orifice is square, or nearly so, the formula will give very close results if the aperture is regarded as circular and of the same area. For a rectangular orifice, as the ratio length/breadth is increased, the conductance increases beyond the value given in the formula. However, the factor which Rayleigh calculated to be the ratio between the conductivity of an elliptical aperture to that of a circular aperture of equal area is shown, experimentally, to be the same as the ratio between the conductivity of a rectangular aperture and that of a square aperture of equal area, provided the ratio of the axes of the ellipse is the same as the ratio of the sides of the rectangle.

This extends Rayleigh's suggestion that any orifice may be treated as circular if it does not differ too much from a circle, to the case of the rectangle which may similarly be treated as an ellipse of equal area.

The author wishes to acknowledge his indebtedness to Dr. R. S. Clay for much helpful criticism during the course of this work.

LXI. *The Expansion of Metals at High Temperatures.*  
 By FDK. L. UFFELMANN, B.Sc., *East London College* \*.

ABSTRACT.

AN optical interference method, for measurements in three perpendicular directions on the same specimen, and for use up to  $800^{\circ}\text{C.}$ , is described. The use of continuous temperature variation is made possible by a device for equalizing the temperature-lag of the platinum resistance thermometer and the specimen. Observations were taken during both heating and cooling of the specimen.

Results are given for tin, cadmium, zinc, lead, aluminium, copper, brass, cobalt, nickel, and steel, and, where possible, the quadratic and Thiesen's relations are fitted. Tin, cadmium, and zinc show pronounced anisotropic properties; while for cobalt, nickel, and steel the coefficient of expansion curve during heating is different from that during cooling, cobalt showing a sharp peak at  $450^{\circ}\text{C.}$  on heating and at  $330^{\circ}\text{C.}$  on cooling.

THIS work was undertaken at the suggestion of Professor C. H. Lees to provide more reliable information on the expansion of the metals tin, cadmium, zinc, lead, aluminium, copper, brass, cobalt, nickel, and steel from air temperature up to  $700^{\circ}\text{C.}$  A modified Fizeau method was used, as it requires a small specimen only to be kept at uniform temperature, and is sufficiently sensitive. The apparatus in its early form was designed by Mr. Madge, B.Sc., in consultation with Prof. Lees.

The specimens were cubes of side 4 mm. Expansion measurements were made in three perpendicular directions on the specimen, and the cubical expansion of the specimen was deduced.

The length of the specimen was found with a standard screw gauge, and could be estimated to 0.0001 cm. or to  $1/4000$  of the length of the cube.

The passage of a fringe could be estimated to from  $1/20$ – $1/40$  fringe. This, over a range of 20–40 fringes, gives an error to the expansion coefficient varying from  $1/400$ – $1/1600$ .

\* Communicated by Prof. C. H. Lees, F.R.S.

In the earlier experiments the temperature was measured by means of a platinum wire wound round a silica core, in a silica tube of about 4 mm. diameter, with its axis at the same level as the specimen. This method was found not to give the temperature of the specimen with sufficient accuracy. In the later form used in the following work a winding of asbestos string replaced the silica tube, and the whole was inserted in a block of brass of mass so determined that the lag of temperature of the brass and the metal specimen should be the same.

The error of measurement of the temperature interval was of the order of  $1/40$  degree Centigrade. This, over the average temperature interval of 40 to 60 degrees, results in an error of  $1/1600$  to  $1/2400$  to the expansion coefficient.

The maximum total error to the expansion coefficient varies from  $1/400 + 1/1600 + 1/4000 = 0.003$ , or .3 per cent., to  $1/1600 + 1/2400 + 1/4000 = 0.001$ , or 0.1 per cent. This means that in the majority of cases there is doubt over the fourth significant figure of the expansion coefficient.

### *The Apparatus.*

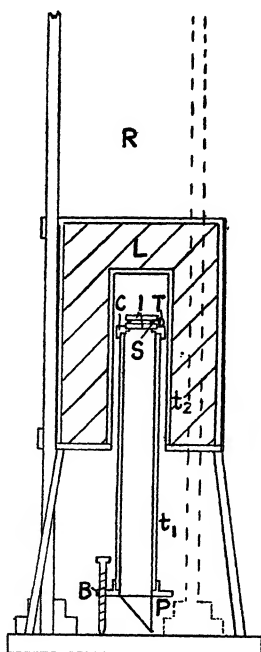
*The Interference Plates.*—The apparatus consists essentially of two fused quartz interference plates (I, fig. 1)  $2\frac{1}{2}$  cm. in diameter, separated by the specimen under test. In the early experiments the specimen was placed on the middle of the lower plate and formed the sole support of the upper interference plate, the interference pattern being visible around the specimen. Later, however, two supplementary supports of the same material and of equal length were introduced to reduce tilting of the upper plate, caused by non-uniform extension of the specimen. The lower surface of the upper interference plate is lightly platinized, while the lower interference plate is uncoated\*. The interference plates are ground with their two surfaces making an angle of about 7 minutes, just sufficient to prevent confusion of the fringes used in the measurements. The lower interference plate is supported at the top of a

\* Theoretically the best fringes are obtained when the upper plate is heavily coated while the lower plate is lightly coated. A palladium surface on the upper interference plate was found to be not durable at high temperatures. Messrs. Hilger undertook to coat the plate with platinum by the "liquid" process. The limit of durability of this coating was stated to be  $800^{\circ}\text{C}$ .

silica tube ( $t_1$ ), 4 cm. diameter, by a Steatite cap (C) cemented to the tube. The lower end of the silica tube is cemented into a brass holder (B) standing upon three massive brass screws and supporting a 45 degree prism (P).

*The Furnace.*—The heating is performed by an electric furnace having an inner tube of silica ( $t_2$ ), which gives from 2–3 mm. clearance when lowered over the tube ( $t_1$ ). To reduce convection currents this tube is only open at the

Fig. 1.



bottom. It is wound with two heating coils—one uniformly along the whole length, the second a small coil at its lower end to make up for loss of heat at the mouth of the furnace.

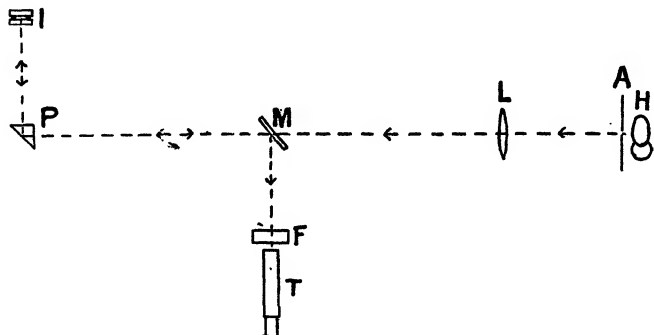
The outside of the furnace is of compressed asbestos sheet bound with steel right-angle strips. The space between the silica tube and the outside walls is packed with asbestos wool (L). The lagging was so good that, even when the furnace had an interior temperature of 800° C. or more,

the outside of the furnace was only in the neighbourhood of  $50^{\circ}\text{C}$ .

To admit of adjustment of the interference plates the furnace slides vertically upwards on three steel bars (R), rigidly connected together at the top, and screwed firmly to a base-board, which is in turn screwed to the bench.

*The Optical System* (see fig. 2).—Light from a mercury-vapour lamp (H) passes through an adjustable aperture (A), is rendered parallel by a lens (L), and passes through the semi-silvered piece of plane glass (M) to the 45 degree prism (P) at the bottom of the tube  $t_1$ , and up the tube to the interference plates (I). The reflected light returns down the silica tube through the

Fig. 2.



prism, and is reflected by the semi-silvered plate into the mercury green filter (F) and the telescope (T). The aperture, the lens, the reflecting mirror, the filter, and the telescope were all clamped firmly to substantial stands screwed to the benches.

For stability the whole apparatus was set up in the basement, and to reduce vibration the bench supporting the interference apparatus was mounted on rubber blocks.

*The Thermometer*.—The thermometer was of gauge 40 platinum wire, having a resistance of about 1 ohm at air temperatures. In the early experiments the platinum wire was welded to a pair of 22 gauge copper leads. To act as a compensator a short piece of 40 gauge platinum wire was welded between the ends of another pair of copper leads. The copper leads, however, deteriorated rapidly,

and it was found necessary to insert lengths of 22 gauge platinum wire to extend about 5 cm. out of the furnace, where they were silver-soldered to the copper leads. The leads were kept in position by passing through four holes in small pieces of slate, and at intervals were bound to the silica tube with pieces of nickel wire, insulated from the platinum with mica. The resistance of the thermometer was measured with a Callendar and Griffiths bridge made by the Cambridge Instrument Co.

### *The Adjustment of the Apparatus.*

The three specimens are placed in position on the lower interference plate, and the cover plate is lowered gently on to them. If the specimens have been accurately ground, the reflected images of the aperture (A) from the facing surfaces of the two interference plates, as seen in the telescope (T, fig. 2), will almost coincide. The lengths of the specimens are adjusted, by lightly rubbing on the finest emery paper, until a definite degree of overlap of the images is obtained which is known by experience to correspond, on re-focussing, to fringes of the most convenient width. The aperture (A) is then adjusted to give the correct degree of illumination for the production of distinct fringes.

Before observations are commenced the light beam is made a parallel one and normal to the plates.

### *Methods of Observation.*

The furnace currents are adjusted so that one fringe passes about every 20 seconds at the steepest part of the heating curve.

The time of passage of every fringe is noted to the nearest second. In between the passage of consecutive fringes the Callendar and Griffiths bridge is balanced, and the time of balance is noted correct to the nearest second.

The resistances are adjusted periodically to keep the heating currents constant, and in experiments taken above 300° C. the currents are increased during the experiment. Just before the proposed maximum temperature for an experiment is reached the heating currents are reduced or cut off. Observations are continued, great care being taken not to miscount the fringes at the point where the cooling of the furnace commences. The experiment is

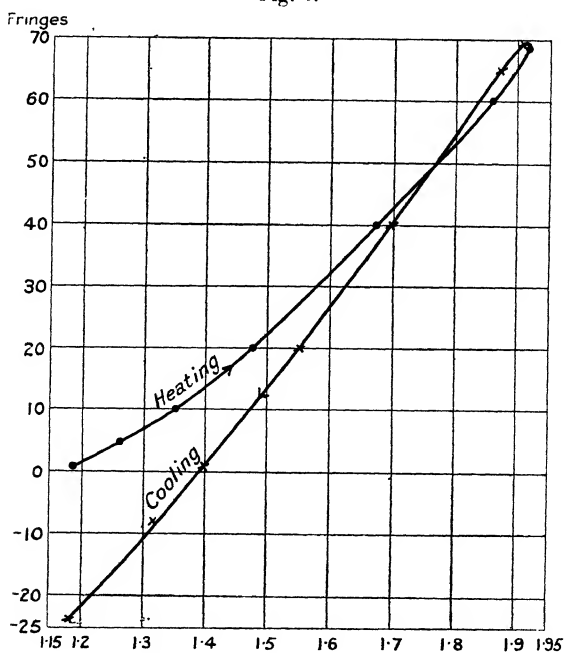


continued down to a temperature of  $30-60^{\circ}\text{C.}$ , where the fringes pass at the rate of one every 5–10 minutes. A complete experiment takes from 4–7 hours.

### *Errors and Corrections.*

*Stress.*—Before the experiment was performed the furnace, containing the specimens in adjustment, was heated to a temperature slightly greater than it was proposed to

Fig. 3.



Resistance of thermometer in ohms.

Results with badly annealed specimen of tin.

reach during the experiment, and then was allowed to cool slowly to relieve any stress in the specimens. In some cases a single heating was not sufficient. The graph (fig. 3) shows the results obtained with a specimen of tin after two previous heatings. It will be noticed that the rate of extension and the rate of contraction have entirely different values, but in the later heatings the two curves almost coincide.

*Oxidation of Specimen.*—In most cases this preliminary heating forms a skin of oxide round the specimen which, provided the specimen is not subsequently heated to an unduly high temperature, prevents further oxidation. In addition, the brass cubes were lightly nickel-plated and the copper cubes lightly gold-plated.

*Error of Lag.*—When the temperature of the furnace is changing the temperature of the specimen lags behind that of the thermometer, and on plotting the number of fringes passed against the temperature, the curve for heating does not coincide with that for cooling. This difference could also be produced by (1) relief of stress during the experiment, (2) oxidation of the specimen during the experiment, (3) a difference between the expansion and contraction coefficient (this was found for cobalt and nickel).

(1) and (2) can be overcome as explained above, while (3) is very pronounced when it occurs, and not easily confused with lag separation.

To prove in the case of a specimen of well annealed tin that (1) and (2) had been overcome observations were taken down to air temperature by gently lifting the furnace from over the specimens when the rate of cooling got unduly slow. It was found the specimen had the same length as at the start (see fig. 4).

It should be noted here that the distance between the curves for heating and cooling increased considerably when the furnace was lifted from the specimen, proving that the lag depends upon the rate of change of temperature (see fig. 4).

*Reduction of Lag.*—The introduction of a heavy copper cover \* to enclose the specimen, interference plates, and thermometer failed to reduce the lag.

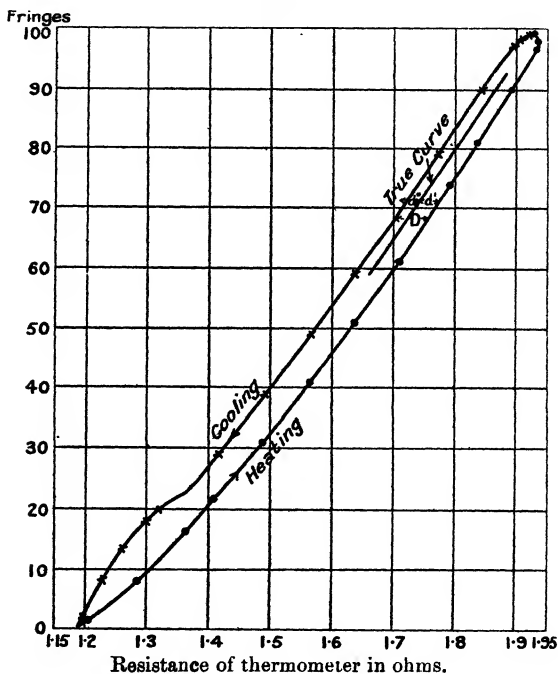
A piece of brass, having a water equivalent equal to the excess water equivalent of the two interference plates over that of the thermometer, was made to fit over the thermometer. The distance (D) (fig. 4) gives the sum of the deviations of the thermometer from the temperature of the specimen upon heating ( $d'$ ), and upon cooling ( $d''$ ), and was noted at a definite temperature in experiments taken over about 20 fringes, (1) without, and (2) with the piece of brass in position ((2) was found to reverse the lag). Then

\* See W. Gray, Bull. Bur. Stand. p. 450 (1914-15).

a piece of brass was cut off, and the value of (D) again found, and the process repeated.

A graph was plotted with the weights of the "compensator" as abscissa, and the values of D as ordinate. The intersection of the curve with the abscissa gives the weight of the "compensator" when D is zero. The "compensator" was reduced to this weight, and upon trial it was

Fig. 4.



Extension curve obtained without "Lag Compensator."

found that the lag was now very small; the improvement is illustrated by the two curves for tin (figs. 4 & 5).

A fresh "compensator" was needed for every material tested.

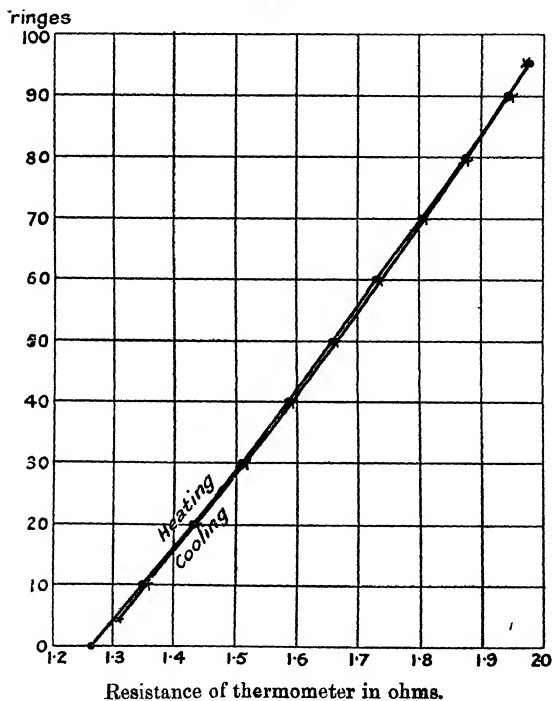
*Correction for Lag.*—The remaining lag was corrected for by taking it proportional to the rate of heating  $\frac{dv}{dt}$ .

During heating

$$v_1 = v_0 + b \frac{dv_0}{dt}, \quad . . . . . (1)$$

where  $v_1$  is the temperature of the specimen,  $v_0$  is the temperature registered by the thermometer, and  $b$  is a constant.

Fig. 5.



Extension curve obtained with "Lag Compensators."

During cooling

$$v_1 = v_0' + b \frac{dv_0'}{dt}, \quad . . . . . (2)$$

Hence

$$v_0 + b \frac{dv_0}{dt} = v_0' + b \frac{dv_0'}{dt},$$

and

$$v_1 = v_0 - (v_0 - v_0') \frac{\frac{dv_0}{dt}}{\frac{dv_0}{dt} - \frac{dv_0'}{dt}}, \quad . \quad . \quad . \quad (3)$$

$$v_1 = v_0' - (v_0 - v_0') \frac{\frac{dv_0'}{dt}}{\frac{dv_0}{dt} - \frac{dv_0'}{dt}}. \quad . \quad . \quad . \quad (4)$$

The two expressions (3) and (4) give the true temperature of the specimen for any particular fringe, in terms of the temperature recorded at the passage of this fringe upon heating and upon cooling, and of the rates of heating and cooling.

No error is introduced, and a great deal of labour is saved if the formula

$$r_1 = r_0' - (r_0 - r_0') \frac{\frac{dr_0'}{dt}}{\frac{dr_0}{dt} - \frac{dr_0'}{dt}} \quad . \quad . \quad . \quad (6)$$

is used in place of (4).  $r$  is the resistance corresponding to the temperature  $v$ .

*The Error Introduced by the Use of Three Supports.*—The two auxiliary specimens were made in the shape of cubes of 4 mm. side, with the top cut away to leave a square of 2 mm. side, and both were cut, together with the actual specimen, in the same direction from the same block of material, so that they should expand equally.

The two auxiliary supports were put in line at one end of the interference plate, while the actual specimen was placed as accurately as possible on the perpendicular bisector of the line joining the two supports, in a position very close to the thermometer.

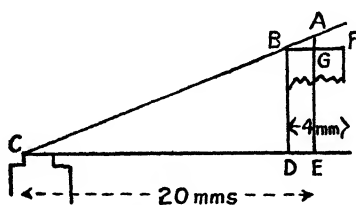
When all three specimens were arranged in the same relative positions, it was found on heating that very little tilt of the plate occurred. If the actual specimen expands differently from the auxiliary supports, the plate will tilt. No error is introduced by this tilt provided the cross-wires of the telescope are focussed in the line of contact of the specimen with the interference plate (see fig. 6). The line

of contact is through B or F, and is parallel to the line joining the two auxiliary specimens. Suppose they are focussed midway along the length of the specimen at the point A. The perpendicular distance of the centre of the specimen from the supports (C) is about 20 mm. The error is represented by the length  $AG = AE \cdot \frac{BG}{CE} = \frac{AE}{10}$ . If AG

is required in terms of fringes, then AE represents the excess number of fringes passed at A over the number which have passed at C.

It is only in the case of tin, cadmium, and zinc that any appreciable tilting of the interference plate was noticed. In the case of zinc the error was eliminated by cutting away the specimen to leave knife-edges on three perpendicular sides. The specimen was arranged so that the knife-

Fig. 6.



edge in use was parallel to the line joining the two support specimens. The cross-wires were focussed in the line of the knife-edge at a point just beside the specimen.

*Correction for the Change in the Refractive Index of Air with Variation of Temperature and Pressure.*—The number of fringes passed on heating from  $T_1^\circ\text{A}$  to  $T_2^\circ\text{A}$  is given by

$$N = \frac{2}{\lambda} [\mu_2(L + \Delta L) - \mu_1 L],$$

where  $\lambda$  is the wave-length of the light,  $\mu_1, \mu_2$  are the refractive indices of air for the wave-length  $\lambda$  at the temperatures  $T_1, T_2$  and the pressures  $p_1$  and  $p_2$  respectively,  $L$  is the length and  $\Delta L$  the increase in length of the specimen. Assuming the pressure is constant

during the experiment, and that  $\frac{\mu - 1}{\rho}$  is constant, we get

to an accuracy of 0.001 per cent. that

$$\frac{1}{L} \cdot \frac{\Delta L}{\Delta T} = \frac{1}{L} \cdot \frac{N \cdot \lambda}{2 \cdot \Delta T} + (\mu_0 - 1) \cdot \frac{273}{760} \cdot \frac{p}{T_1 \cdot T_2},$$

where  $\mu_0$  is the index at N.T.P., i. e.,

$$\alpha \text{ (corrected)} = \alpha \text{ (uncorrected)} + (\mu_0 - 1) \cdot \frac{273}{760} \cdot \frac{p}{T_1 \cdot T_2}.$$

For the mercury green line  $\mu_0$  has the value 1.0002933  
Hence the correction is

$$0.0001052 \cdot \frac{p}{T_1 \cdot T_2}.$$

This is required to one significant figure only, and is easily applied with the aid of a graph, in which the correction for equal temperature intervals is plotted against the mean temperature of the interval.

#### *The Calibration of the Thermometer.*

In all, four different thermometers were calibrated. The fixed points used for the calibration were

- (1) The melting point of ice.
- (2) The boiling point of water.
- (3) The freezing point of tin..... 231.8(5)° C.
- (4) The freezing point of cadmium ..... 320.9° C.
- (5) The freezing point of zinc ..... 419.4(5)° C.
- (6) The freezing point of NaCl ..... 801° C.

*The Calibration at the Melting Point of Ice and at the Boiling Point of Water.*—The usual type of apparatus was used for these determinations. In both cases the thermometer was enclosed in a long glass tube with the mouth plugged with asbestos wool.

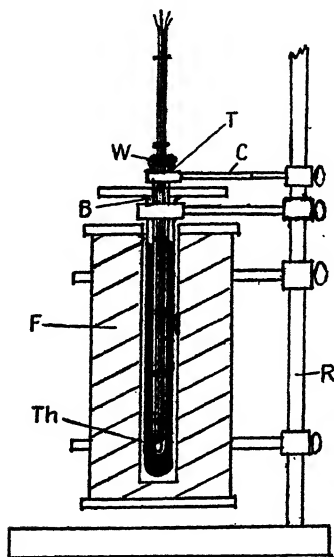
*The Calibration at the Freezing Points of the Metals.*—The apparatus used is shown in fig. 7. It consists of a small electric furnace (F) with a central opening just large enough to hold a hard glass boiling tube (B). The furnace is supported vertically by a retort stand (R).

The thermometer (Th) was enclosed in a long hard glass tube (T) plugged with asbestos wool (W). The joints

between the platinum and copper leads were screened from the furnace to avoid the production of varying e.m.fs. by unsteady heating.

After melting the calibration metal in the tube (B), the tube (T) was forced down into it and held in position by the clamp (C). The furnace was allowed to cool slowly, and resistance-time observations were made so as to obtain a freezing point curve.

Fig. 7.



Apparatus for thermometer calibration.

*Calibration at the Freezing Point of NaCl.*—The thermometer was enclosed in a silica tube about 15 cm. long, while the salt was placed in a tall fireclay crucible cemented into a muffle furnace.

*Calculation of Thermometer Constants.*—For a platinum resistance thermometer

$$r = r_0(1 + \alpha v + \beta v^2),$$

where  $r$  is the resistance of the thermometer at the temperature  $v^\circ\text{C.}$ , and  $r_0$  is the resistance at  $0^\circ\text{C.}$   $\alpha$  and  $\beta$  are the



required constants, and were calculated, by the method of least squares, from the calibration values of  $r$  and the corresponding values of  $v$ .

The temperature in terms of the thermometer resistance is given by

$$v = -\frac{\alpha}{2\beta} - \sqrt{\frac{1}{r_0\beta} \cdot \sqrt{\frac{\alpha^2 r_0}{4\beta} + (r - r_0)}}.$$

An example of a thermometer calibration is given below :—

Calibration Points.	Temperature $v$ .	Resistance $r$ .
(1) The melting point of ice.....	0 °C.	1.1275 ohms.
(2) The boiling point of water at 77.41 cm. pressure .....	100.51°C.	1.5146 „
(3) The freezing point of tin .....	231.85°C.	1.9968 „
(4) The freezing point of cadmium ...	320.9°C.	2.3154 „
(5) The freezing point of zinc .....	419.45°C.	2.6612
(6) The freezing point of NaCl .....	801°C.	3.8524 „

This gives

$$\alpha = 0.0034696; \quad \beta = -0.000\,000\,56391;$$

and

$$v = 3076.37 - 1254.1\sqrt{7.1448 - r}.$$

### *The Calculation of Results.*

The resistance of the thermometer at the time of passage of a fringe is first found by interpolation at intervals of 10–20 fringes. A curve is then plotted with the resistance of the thermometer as abscissa and the number of fringes passed as ordinate. Any necessary correction for lag is applied, and the temperature calculated. The expansion coefficients are then worked out, usually over ranges of 10–40 fringes, but when changes in the coefficient are rapid over smaller ranges. Finally, the correction for the change of refractive index of air with temperature is applied.

The final values for the three linear coefficients  $\alpha_1, \alpha_2, \alpha_3$ , are plotted against the mean temperature. Wherever any systematic difference in  $\alpha_1, \alpha_2, \alpha_3$  occurs, the cubical coefficient ( $\alpha_c$ ) curve is plotted from the  $\alpha_1, \alpha_2, \alpha_3$  curves; otherwise the mean linear coefficient ( $\alpha_l$ ) curve is plotted.

*Calculation of the Constants A and B in the relation*

$$V = V_0(1 + Av + Bv^2),$$

where V is the volume at the temperature v, and V<sub>0</sub> is the volume at 0° C.

If the points plotted for the cubical expansion coefficient fall on a straight line, then the relation holds good, and A is the intercept on the axis of  $\alpha_c$ , while B is half the slope of the straight line.

Similarly the constants A<sub>l</sub>, B<sub>l</sub>, in the relation

$$L = L_0(1 + A_lv + B_lv^2)$$

are determined from straight line  $\alpha_l$  curves.

*Calculation of the Constants in Thiesen's Formula*

$$\frac{dV}{dT} = K \cdot T^n.$$

T is the absolute temperature,

V is the volume,

K and n are constants.

We may write the formula

$$\alpha_c = \frac{K}{V} \cdot T^n, \text{ or for unit volume } \alpha_c = K T^n.$$

If this formula holds, on plotting log  $\alpha_c$  against log T we should get a straight line graph, whose intercept with the (log  $\alpha_c$ ) axis is log K, and whose slope is n.

*The Constants of the Relation*  $\frac{dL}{dT} = K_l T^n.$

L is the length of the specimen.

For unit length the constant n has the same value as in the relation  $\frac{dV}{dT} = K \cdot T^n$ , while  $K_l = K/3$ .

*The Results.*

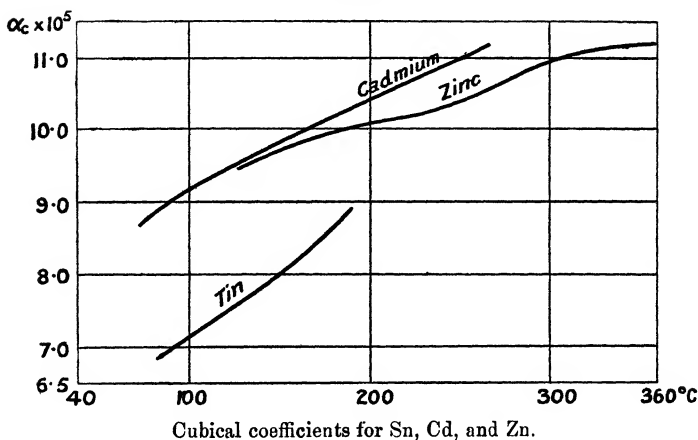
The linear coefficient of expansion for side 1 of the cube ( $\alpha_1$ ) was found to be much greater than the coefficients for the other two sides ( $\alpha_2, \alpha_3$ ), e. g., at 120° C.  $\alpha_1 = 3.38 \times 10^{-5}$ ,  $\alpha_2 = 1.92 \times 10^{-5}$ ,  $\alpha_3 = 2.18 \times 10^{-5}$ . This seems to indicate that the axis of the crystal lies approximately perpendicular to the face side 1.

\* See *Deuts. Phys. Ges. Verh.* x. pp. 410-415 (1908).

The values for the cubical coefficient are given below (see fig. 8).

Temperature $v$ .	$\alpha_c$ .
80° C. ....	6.84(7) . $10^{-5}$ .
100° C. ....	7.14(5) „
120° C. ....	7.47(2) „
140° C. ....	7.82(6) „
160° C. ....	8.21(4) „
180° C. ....	8.65(5) „
190° C. ....	8.90(5) „

Fig. 8.



Neither the Quadratic nor Thiesen's relation seems to fit the results, since both plots  $\alpha_c$  against  $v$ , and  $\log \alpha_c$  against  $\log v$ , have a definite curvature upwards. For the region 120–190° C. the mean values for the Quadratic constants are

$$A = 5.05 \cdot 10^{-5} \quad \text{and} \quad B = 9.9 \cdot 10^{-8}.$$

#### *Cadmium.*

The three linear coefficients were found different at air temperatures (e.g., at 60° C.  $\alpha_1 = 2.37 \cdot 10^{-5}$ ,  $\alpha_2 = 2.54 \cdot 10^{-5}$ ,  $\alpha_3 = 3.50 \cdot 10^{-5}$ ), but to approach each other towards the melting point of the metal.

The final values for the cubical expansion coefficient are as follows (see fig. 8):—

Temperature $v$ .	$\alpha_l$ .
70° C. ....	8.62(1) . $10^{-5}$ .
80° C. ....	8.81(4) „
90° C. ....	8.98(3) „
100° C. ....	9.14(3) „
110° C. ....	9.30(0) „
120° C. ....	9.44(3) „
130° C. ....	9.58(5) „
140° C. ....	9.71(4) „
150° C. ....	9.84(4) „
170° C. ....	10.07(3) „
190° C. ....	10.29(7) „
210° C. ....	10.52(7) „
230° C. ....	10.76(2) „
250° C. ....	10.99(1) „
268° C. ....	11.21(8) „

*Thiesen's Constants.*—The logarithmic plot gives two sets of constants :—

$$(1) \quad 90\text{--}130^\circ \text{ C.} \dots\dots n=0.626; K=2.25 \cdot 10^{-6}.$$

$$(2) \quad 130\text{--}270^\circ \text{ C.} \dots\dots n=0.519; K=4.27 \cdot 10^{-6}.$$

*Constants of the Quadratic Relation.*—This relation holds for the range 130–270° C. The constants have the value

$$A=8.04(8) \cdot 10^{-5}; \quad B=5.9 \cdot 10^{-8}.$$

### Zinc.

The three linear coefficients were found to be very different, *e. g.*, at 200° C.  $\alpha_1=4.12 \cdot 10^{-5}$ ,  $\alpha_2=3.67 \cdot 10^{-5}$ ,  $\alpha_3=2.29 \cdot 10^{-5}$ .

The values found for the cubical expansion coefficient are :—

Temperature $v$ .	$\alpha_c$ .
120° C. ....	9.40(1) . $10^{-5}$ .
140° C. ....	9.59(9) „
160° C. ....	9.78(1) „
180° C. ....	9.95(8) „
190° C. ....	10.03(5) „
200° C. ....	10.10(2) „
220° C. ....	10.20(0) „
240° C. ....	10.30(6) „
260° C. ....	10.51(3) „
280° C. ....	10.75(1) „
300° C. ....	10.94(8) „
320° C. ....	11.09(7) „
340° C. ....	11.17(2) „
360° C. ....	11.18(7) „

Above 180° C. the results are irregular (see fig. 8).

*Thiesen's Constants.*—The logarithmic plot gives a straight line for the region 120–180° C., which, when produced, meets the curve again as a tangent over the region 300–320° C. From this straight line we get :—

$$n=0.402; K=8.54.10^{-6}.$$

*The Constants of the Quadratic Relation.*—The mean values for the range 120–360° C. are :—

$$A=8.50.10^{-5}; B=3.9.10^{-8}.$$

Allotropic changes in zinc have been found by E. Cohen to occur at 64.9° C., 170° C., and 310° C.\*. The decided change in the slope of the coefficient of expansion curve over the range 300–360° C. may correspond to the upper transition point. Similarly the change in the slope over the range 180–240° C. may correspond to the allotropic change which has been found at 170° C.

### *Lead.*

The results given below are the mean linear coefficients (see fig. 9).

Temperature <i>v.</i>	<i>α</i> <i>l.</i>
80° C. ....	2.89(6) . 10 <sup>-5</sup> .
100° C. ....	2.91(2) „
120° C. ....	2.95(0) „
140° C. ....	2.99(2) „
160° C. ....	3.02(1) „
170° C. ....	3.03(4) „
180° C. ....	3.05(9) „
190° C. ....	3.09(1) „
200° C. ....	3.12(1) „
220° C. ....	3.16(2) „
240° C. ....	3.20(0) „
250° C. ....	3.23(7) „
260° C. ....	3.30(2) „
280° C. ....	3.43(3) „

These results for lead divide themselves into four different sections :—(1) below 95° C.; (2) from 95–170° C.; (3) from 170–245° C.; (4) from 245–280° C. An allotropic change occurs in lead at 50° C. according to

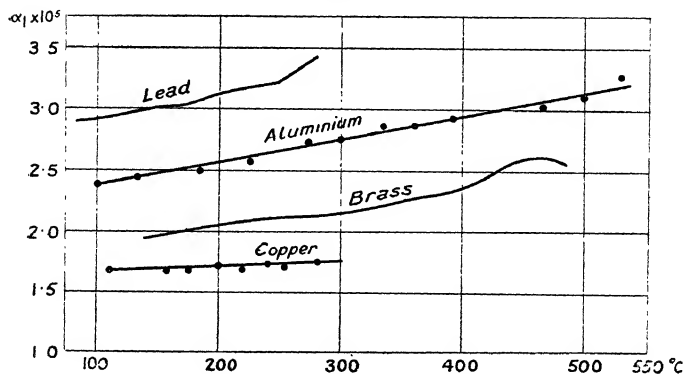
\* See Mellor, 'A Treatise on Inorganic Chemistry,' iv. p. 430.

E. Cohen and W. D. Helderman, and at 59–62° C. according to E. Jänecke\* ; the change in the slope of the expansion coefficient curve in the region of 95° C. may correspond to this transition point. No allotropic changes have been found which would explain the changes in the slope of the curve at 170° C. and 245° C.

*Thiesen's Constants.*—If we neglect the depression from 150–190° C., the logarithmic plot falls into two straight lines, which give :—

- (1) 100–240° C. ....  $n=0.306$  ;  $K_l=4.74 \cdot 10^{-6}$ .
- (2) 250–280° C. ....  $n=1.054$  ;  $K_l=4.44 \cdot 10^{-8}$ .

Fig. 9.



Linear coefficients for Pb, Al, brass, and Cu.

*The Constants of the Quadratic Relation.*—Neglecting the depression from 150–190° C., we get :—

- (1) 100–240° C. ....  $A_l=2.69 \cdot 10^{-5}$  ;  $B_l=1.1 \cdot 10^{-8}$ .
- (2) 250–280° C. ....  $A_l=1.60(4) \cdot 10^{-5}$  ;  $B_l=3.2(7) \cdot 10^{-8}$ .

### Aluminium.

The results obtained at different times for aluminium, especially over the range 340–540° C., are somewhat at variance (e.g., at 400° C.  $\alpha \cdot 10^{-5}=2.855, 2.894, 2.910$ , and,

\* See Mellor, 'A Treatise on Inorganic Chemistry,' vii. p. 520.

several months later, 3·027, 3·196), but no systematic difference is found for the three separate sides of the cube. An explanation may lie in the fact that cold-worked aluminium recrystallizes slowly in a manner depending upon the temperature\*.

The values given below are the mean linear coefficients of selected sets of results (see fig. 9) :—

Temperature <i>v.</i>	<i>α<sub>l</sub></i>
100° C. ....	2·35(6) . 10 <sup>-5</sup> .
140° C. ....	2·43(6) „
180° C. ....	2·50(3) „
220° C. ....	2·57(3) „
260° C. ....	2·65(8) „
300° C. ....	2·74(4) „
340° C. ....	2·83(7) „
380° C. ....	2·88(9) „
420° C. ....	2·96(1) „
460° C. ....	3·01(7) „
500° C. ....	3·11(4) „
530° C. ....	3·23(3) „

*Thiesen's Constants.*—As an average for the whole range 100–530° C. we get :—

$$n = 0·384 ; \quad K_l = 2·40 \cdot 10^{-6}.$$

*The Constants of the Quadratic Relation.*—For the range 100–530° C.,

$$A_l = 2·16(5) \cdot 10^{-5} ; \quad B_l = 9·5 \cdot 10^{-9}.$$

Commercial aluminium was used for these measurements.

### *Brass.*

Observations were taken up to 500° C. Up to 400° C. the maximum divergence from the mean values is about 1 per cent., but above 400 a 4 per cent. divergence is reached. The values given below are the mean linear coefficients :—

\* See Mellor, 'A Treatise on Inorganic Chemistry,' v. p. 176.

Temperature $v$ .	$\alpha_l$ .
140° C. ....	1.93(0) . $10^{-5}$ .
160° C. ....	1.97(1) „
180° C. ....	2.00(9) „
200° C. ....	2.04(2) „
220° C. ....	2.06(6) „
240° C. ....	2.08(8) „
260° C. ....	2.10(6) „
280° C. ....	2.12(8) „
300° C. ....	2.15(2) „
320° C. ....	2.18(0) „
340° C. ....	2.21(4) „
360° C. ....	2.25(1) „
380° C. ....	2.29(5) „
400° C. ....	2.35(4) „
420° C. ....	2.4(4) „
440° C. ....	2.5(6) „
460° C. ....	2.6(0) „
480° C. ....	2.5(6) „

These results do not fit either Thiesen's or the Quadratic formula. The rate of increase of  $\alpha_l$  with temperature decreases until about 270–280° C., after which it increases, at first gradually, and later very rapidly. A maximum value for  $\alpha_l$  occurs at about 460° C. (see fig. 9).

Common brass of 62 per cent. copper was used.

### Copper.

Observations were taken up to 340–350° C. only. The mean results for the linear coefficients are (see fig. 9):—

Temperature $v$ .	$\alpha_l$ .
110° C. ....	1.66(3) . $10^{-5}$ .
120° C. ....	1.66(8) „
140° C. ....	1.68(0) „
160° C. ....	1.68(7) „
180° C. ....	1.69(3) „
200° C. ....	1.69(9) „
220° C. ....	1.70(7) „
240° C. ....	1.71(8) „
250° C. ....	1.72(2) „
260° C. ....	1.73(5) „
280° C. ....	1.74(0) „
300° C. ....	1.75(2) „

*Thiesen's Constants.*—For the range 110–300° C.,

$$n=0.112; K_l=8.53.10^{-6}.$$

*The Constants of the Quadratic Relation.*—For the range 110–300° C.,

$$A_l=1.62(3).10^{-5}; B_l=2.0.10^{-9}.$$



*Cobalt.*

In the experiments with cobalt observations were taken from air temperature to about 730° C., and down again to about 100° C.

It was found that the coefficient of expansion during heating is different from that during cooling. Upon heating the coefficient increases slowly and regularly from air temperature to 390° C. At this temperature the coefficient increases rapidly to form a sharp peak with a maximum in the region of 450° C., where the coefficient is over twice that at the bottom of the peak. The base of the peak extends for 70–130° C. Above the region of the peak the curve continues sometimes with little variation in the coefficient, and sometimes with a small peak. The general characteristic of the expansion coefficient during cooling is that it decreases gradually down to about 360° C., where a peak commences. This peak has a height equal to about half that of the peak in the heating curve, and has its maximum in the neighbourhood of 330° C., *i. e.*, at a full 120 degrees below the maximum in the heating curve.

So far as can be ascertained, the peaks in the coefficient of expansion curves for cobalt have not previously been noted. They indicate the point at which some molecular change takes place. Honda and Shimizu\* concluded that annealed cobalt undergoes a molecular change at 464° C., as the magneto-striction effect was then zero.

The results given below are the values for the volume coefficient from 100–380° C., during heating.

Temperature <i>v.</i>	<i>α<sub>c</sub>.</i>
100° C. ....	3·55(6) . 10 <sup>-5</sup> .
120° C. ....	3·59(1) „
140° C. ....	3·62(6) „
160° C. ....	3·66(1) „
180° C. ....	3·69(6) „
200° C. ....	3·73(5) „
220° C. ....	3·77(5) „
240° C. ....	3·81(4) „
260° C. ....	3·85(3) „
280° C. ....	3·89(5) „
300° C. ....	3·94(2) „
320° C. ....	3·99(3) „
340° C. ....	4·04(3) „
360° C. ....	4·09(8) „
380° C. ....	4·15(0) „

---

\* Phil. Mag. [6] vi. p. 392 (1903).

These results when plotted (see fig. 10) fall into three different straight lines. The points at which the changes of slope occur are (1) at about 190° C. and (2) from 260–300° C. Since the error of lag could not be completely

Fig. 10.

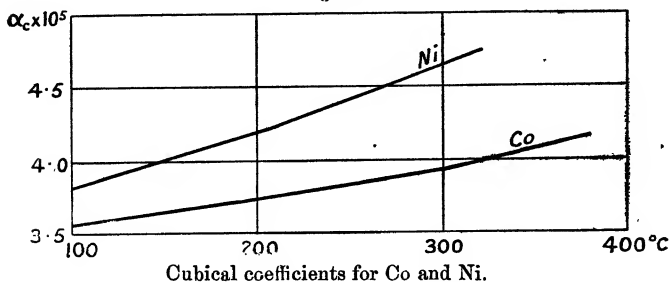
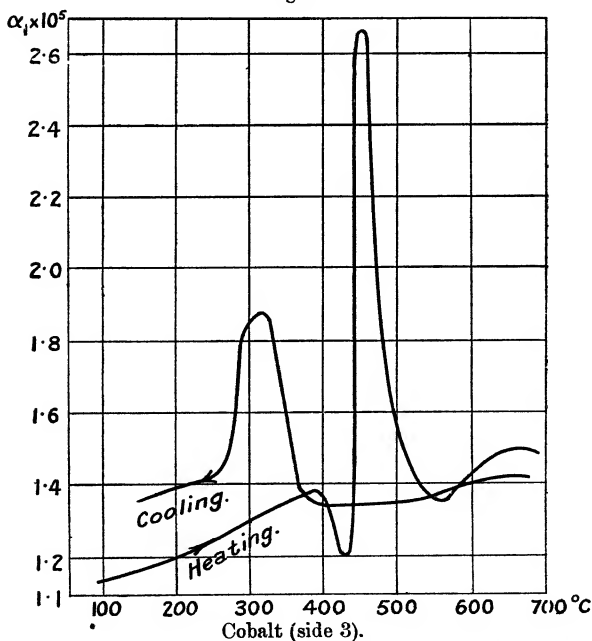


Fig. 11.



allowed for, however, these results are not so reliable as those for other metals.

The specimen set of results for cobalt given below is shown plotted in fig. 11.

Cobalt (side 3).— $L=0.3990$  cm.

Heating.				Cooling.			
N.	$v, ^\circ\text{C.}$	$v$ (mean), $^\circ\text{C.}$	$\alpha$ .	N.	$v, ^\circ\text{C.}$	$v$ (mean), $^\circ\text{C.}$	$\alpha$ .
0	29.62	90	$1.14(1) \cdot 10^{-5}$	141	723.54	676	$1.42(7) \cdot 10^{-5}$
10	92.40			131	675.01		
20	150.20			121	627.57		
30	209.36			111	578.64		
40	263.10			101	529.65		
50	317.52	315	$1.32(2)$	91	478.11	479	$1.35(7)$
60	366.79	367	$1.37(6)$	81	428.74	406	$1.34(9)$
70	417.15	426	$1.20(7)$	72	383.03		
73	434.18						
75	443.21	439	$1.51(8)$	66	353.21	343	$1.63(8)$
		445	$3.20(7)$	61	332.30	323	$1.87(4)$
77	447.48						
		450	$2.65(7)$	56	314.02	305	$1.87(7)$
80	455.09	451	$2.69(9)$	51	295.77	286	$1.80(4)$
85	469.35	462	$2.40(0)$	46	276.77	265	$1.49(3)$
90	488.43	478	$1.79(4)$	41	253.78	230	$1.41(1)$
95	510.64	500	$1.54(1)$	31	205.19	181	$1.38(8)$
100	535.16	525	$1.39(6)$	21	155.74	133	$1.35(1)$
111	591.23	586	$1.41(4)$	12	100.00		
121	636.84	637	$1.49(6)$				
131	682.75	683	$1.49(5)$				
141	728.43						

*Nickel.*

Observations were taken up to  $710$ – $720^\circ\text{C.}$ , with the exception of some early work, in which  $770^\circ\text{C.}$  was reached.

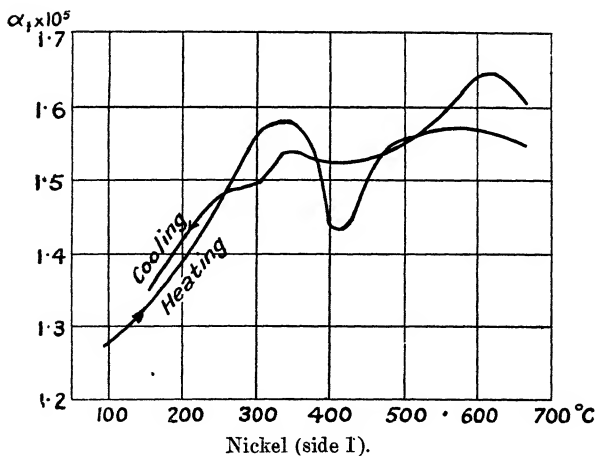
As in the case of cobalt, the rate of expansion is different from the rate of contraction for any definite temperature. During heating the coefficient increases fairly regularly from air temperature to form a shallow peak with its maximum at  $340$ – $360^\circ\text{C.}$ , above which the coefficient falls to form a minimum at about  $420^\circ\text{C.}$ , and continues in an indefinite manner until the maximum temperature of the experiment is reached. In experiments in which the temperature of  $770^\circ\text{C.}$  was reached the coefficient increased regularly with temperature over this extended range both upon heating and upon cooling; this indicates

that nickel reaches a stable state above 700° C. The general characteristics of the cooling curve are, very approximately, that of the heating curve. Individual sets of observations vary greatly beyond the first minimum of the heating curve. The first maximum in the heating curve corresponds to the point at which nickel loses its ferro-magnetic properties.

The results for nickel during heating from 100–320° C. are :—

Temperature $t$ .	$\alpha_c$ .
100° C. ....	3·81(7) $\cdot 10^{-5}$ .
120° C. ....	3·88(9) „
140° C. ....	3·96(0) „
160° C. ....	4·03(2) „
180° C. ....	4·10(7) „
200° C. ....	4·18(7) „
220° C. ....	4·27(4) „
240° C. ....	4·36(8) „
260° C. ....	4·46(1) „
280° C. ....	4·55(3) „
300° C. ....	4·64(7) „
320° C. ....	4·74(9) „

Fig. 12.



These values for  $\alpha_c$ , when plotted against the temperature (see fig. 10), form two straight lines meeting just below 200° C. The error due to lag renders these results, like those for cobalt, less reliable than those for other metals.

The specimen set of results given below is shown plotted in fig. 12.

Nickel (side 1).— $L=0.4060$  cm.

Heating.				Cooling.			
N.	$v, ^\circ\text{C.}$	$v$ (mean), $^\circ\text{C.}$	$\alpha.$	N.	$v, ^\circ\text{C.}$	$v$ (mean), $^\circ\text{C.}$	$\alpha.$
3	42.92			150	707.59		
10	81.11	88	$1.26(3) \cdot 10^{-5}$ .	140	664.98	666	$1.60(7) \cdot 10^{-5}$ .
20	133.96	133	$1.30(6)$ „	130	623.85	624	$1.64(3)$ „
30	184.10	181	$1.36(1)$ „	120	583.05	582	$1.62(4)$ „
39	227.82	231	$1.43(7)$ „	110	540.95	540	$1.57(5)$ „
50	277.73	275	$1.51(0)$ „	100	497.62		
60	321.34			90	453.98	476	$1.54(2)$ „
		343	$1.58(2)$ „			432	$1.52(4)$ „
70	363.86			80	409.79		
		379	$1.54(8)$ „			388	$1.52(8)$ „
77	394.27			70	365.71		
						344	$1.54(1)$ „
78	397.26	425	$1.43(7)$ „	60	322.00		
		475	$1.54(2)$ „			297	$1.49(4)$ „
90	453.41			49	272.42		
						252	$1.48(1)$ „
100	497.01	540	$1.56(6)$ „	40	231.47		
		532	$1.57(1)$ „			210	$1.43(3)$ „
120	582.89			31	189.08		
		626	$1.56(6)$ „			154	$1.35(3)$ „
130	624.97			17	119.21		
		668	$1.54(8)$ „				
140	668.80						
150	711.88						

### *Steel.*

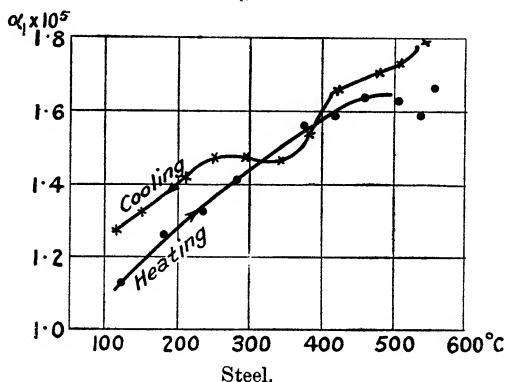
Fig. 13 is an example of the results obtained for a sample of steel which acted as the sole support of the upper interference plate. Frequent discontinuities in the extension curve make the results unreliable, but they serve to show a difference in the expansion coefficient during heating and cooling.

### *Summary of Results.*

Tin, cadmium, and zinc show pronounced anisotropic properties, and over extended temperature ranges the cubical expansion coefficient curves fit neither the Quadratic nor Thiesen's formula. The expansion coefficient curve for lead has definite changes in slope at  $170^\circ$  and  $245^\circ$  C. ; the mean aluminium and copper curves fit

the Quadratic relation, while that for brass with a maximum at 460° C. does not fit. For cobalt, nickel, and steel the expansion coefficient curve during heating is different from that during cooling, cobalt showing a sharp peak at 450° C. on heating, and at 330° C. on cooling; nickel has a maximum in the heating curve at 340–360° C. (the Curie point).

Fig. 13.



### Acknowledgment.

I wish to thank Professor C. H. Lees for much help and advice given throughout these measurements.

## LXII. X-Ray Study of some Tungsten Magnet Steel Residues.

By W. A. WOOD, M.Sc., *Physics Department, The National Physical Laboratory, Teddington, Middlesex* \*.

[Plate V.]

### Introduction.

THE nature of the carbide and other constituents of tungsten magnet steels has been the subject of much research. Thus Arnold and Read <sup>(1)</sup> isolated these constituents by dissolving away the iron electrolytically in dilute acid and collecting the insoluble remainder. From chemical analysis of the residues they inferred the presence of tungsten carbide, cementite, and free carbon, but found

\* Communicated by G. W. C. Kaye, O.B.E., D.Sc.

no indication of a mixed carbide. Honda and Murakami<sup>(2)</sup>, using their method of magnetic analysis, came to the conclusion that, in addition to those carbides in this type of steel, a mixed carbide,  $4\text{Fe}_3\text{C} \cdot \text{WC}$ , also formed after certain heat treatments. Evershed<sup>(3)</sup> has published a very full survey of the problems arising in the manufacture of tungsten magnet steels. In it he states that the substances normally to be found in such steels are tungsten carbide and cementite, and that these compounds may decompose, apparently into their constituent atoms, when the steel has been "spoiled" by having been heated at about  $950^\circ\text{C}$ . Swinden<sup>(4)</sup>, working on 3 per cent. tungsten steels, adduced evidence for the formation in normal steels of a compound of composition  $\text{Fe}_3\text{W}$ . In the case of high speed tool steels containing a large proportion of tungsten Westgren and Phragmén<sup>(5)</sup>, by using the method of X-ray analysis, proved that the carbide constituent consisted mainly of a mixed carbide, to which they assign the formula  $\text{Fe}_4\text{W}_2\text{C}$ , the metal atoms being to a slight extent mutually replaceable. The general lack of agreement concerning the nature of the constituents of magnet steels containing about 6 per cent. of tungsten is very evident, and is probably largely due to difficulties of interpretation inherent in the methods used.

X-ray analysis in this type of problem provides the most direct method of attack. It is possible by a straightforward photograph of the steel to obtain an X-ray diffraction spectrum of the carbide constituents superposed on the spectrum due to the iron. A difficulty appears, however, in the case of steels such as those investigated in the present work, because the proportion of any carbides will be small in comparison with the amount of iron present. Consequently an increase in exposure, made with a view to intensifying the carbide spectrum, merely results in such an increase of general X-ray scattering by the iron atoms that the weaker carbide lines are masked by the background of the photograph. It is therefore preferable to follow the process of Arnold and Read, and isolate the carbides by dissolving away the iron. The question then arises as to what extent the constituents of the residues as revealed by X-ray analysis are representative of the corresponding substances in the untreated steel. The degree of correspondence can be tested, however, by comparing the spectra of the residues, obtained under various conditions of

electrolysis, with the spectrum of the untreated steel. This latter, though less complete, is quite sufficient for the purpose. Evidence on this point is discussed in the paper.

### *Identification of the Residues.*

The residues from some twenty steels were examined. Each had approximately the same composition as the following typical specimen: by weight, tungsten 6 per cent., carbon 0.72 per cent., nickel 0.19 per cent., manganese 0.28 per cent., silicon 0.14 per cent., sulphur 0.023 per cent., and phosphorus 0.027 per cent. Different steels had received different heat treatments. The residues from the steels gave diffraction spectra which were, with the reservations discussed below, very similar. For purpose of complete measurement two steels were chosen. They will be referred to as C1 and C3. The former had been heated for one hour and the latter for six hours at 900° C., and then allowed to cool in air. The surface of each was ground in order to remove the decarbonized layers. To obtain X-ray photographs of the residues a Debye camera was used. The radiation employed throughout is the iron  $K\alpha$  wave-length.

The problem then presents itself of identifying the carbides from the complicated spectrum arising from the probable presence of more than one constituent. Fortunately, advantage can here be taken of work by Dr. G. Shearer and the author—that, it is hoped, will soon be published—in which it was noted that variations in heat treatment of these steels resulted in large differences in the distribution of intensity amongst the lines of the spectra without alteration in their position. The same effect was reproduced in the spectra of the corresponding residues. The point is illustrated in Pl. V. figs. 1 and 2, which show the powder photographs of the residues C1 and C3 respectively. The measurements made from them are given in the table (p. 662). The lines are specified by the diffraction angle  $\theta$  at which they occur. When a resolution of the  $K\alpha$  and  $\alpha'$  doublet appears the angle for the  $\alpha$  radiation alone is recorded. Column 1 gives the values of  $\theta$  for the residue C1, and column 2 for C3. Here, again, the aforementioned point is illustrated. Nearly all lines, except very weak ones, are common to both; but while the positions are the same, the intensities of the lines do not correspond. Practically all the lines marked strong in the one are weaker when



Residue C1 $\theta$ (in degrees).	Residue C3 $\theta$ (in degrees).	WC $\theta$ (in degrees) (calc.)	$\text{Fe}_4\text{W}_2\text{C}$ $\theta$ (in degrees). (calc.)
16.7 v.w.	—	—	16.9 v.w.
—	17.9 w.	18.0 w.	—
18.2 v.w.	—	—	18.2 w.
19.8 w.	19.8 s.	20.0 s.	—
20.3 v.w.	20.3 m.	20.4 m.	20.2 w.
20.5 w.	—	—	20.5 m.
22.4 m.	—	—	22.4 s.
22.6 w.	22.6 s.	22.6 s.	—
22.9 w.	—	—	22.9 m.
24.3 m.	24.3 w.	—	24.3 m.
25.3 s.	25.4 m.	—	25.4 s.
26.7 v.w.	—	—	26.7 w.
27.1 s.	27.1 m.	—	27.1 s.
27.8 v.w.	27.9 m.	27.8 s.	—
28.5 m.	28.5 w.	—	28.4 v.w.
29.7 s.	29.7 w.	—	29.7 s.
31.1 w.	31.1 s.	31.0 s.	—
33.0 w.	—	—	—
33.5 v.w.	—	—	33.7 v.w.
34.6 v.w.	—	—	34.6 w.
—	37.0 v.w.	36.7 w.	—
37.8 v.w.	—	—	37.7 w.
—	38.5 v.w.	38.2 v.w.	—
38.7 s.	38.8 w.	—	38.7 w.
40.5 v.w.	—	—	40.5 w.
42.2 w.	42.2 m.	41.8 s.	—
42.4 s.	42.4 v.w.	—	42.3 s.
—	43.0 v.w.	42.8 w.	—
43.3 v.w.	43.4 m.	43.2 m.	—
43.5 v.w.	—	—	43.5 v.w.
44.6 v.w.	44.6 v.w.	44.3 w.	44.5 v.w.
—	45.5 v.w.	45.3 m.	—
45.9 s.	—	45.8 v.w.	45.9 s.
48.0 s.	} 48.1 m.	—	48.0 s.
48.2 s.		—	—
48.8 w.		48.5 s.	—
49.3 s.	48.8 m.	—	49.3, 49.4 m.
—	49.3 w.	—	—
50.6 v.w.	50.0 w.	49.8 w.	—
51.4 w.	50.6 m.	50.4 m.	—
51.9 w.	—	—	—
52.3 v.w.	51.9 s.	51.6 s.	—
53.0 w.	—	—	52.3 w.
54.0 w.	—	—	52.8, 53.0 w.
55.3 m.	—	—	54.1 w.
57.8 w.	55.2 v.w.	—	55.2 m, 55.4 w.
60.6 s.	57.8 m.	57.2 w.	—
60.8 s.	60.5 m.	—	60.5 s.
63.2 s.	60.8 m.	—	60.7 s.
63.4 s.	63.1 w.	—	63.1 s.
64.3 w.	63.4 w.	—	63.4 s.
65.0 s.	—	—	—
66.3 w.	65.0 m.	—	65.0, 65.1 s.
67.8 w.	—	—	—
73.2 m.	67.8 w.	67.5 w.	67.8 w.
—	73.2 s.	72.4 s.	—

v.w.=very weak intensity, w=weak, m=medium, s=strong.

they occur in the other. It is therefore possible to isolate a set of lines, belonging presumably to one substance, which on going from C1 to C3 increase in intensity. These lines correspond to the known spectrum of tungsten carbide. This is shown in column 3, which is arranged so that opposite these lines are placed the values of the diffraction angles for tungsten carbide as given by Westgren and Phragmén <sup>(6)</sup> in their research on the tungsten-carbon system. A comparison of the columns shows definitely the presence of tungsten carbide in both residues with a preponderance in C3. A closer examination of the diffraction angles observed for tungsten carbide is made below. First we proceed to isolate a second set of lines, namely, those which on going from C1 to C3 decrease in intensity. Here, again, a correspondence was obtained with the diffraction angles of a substance the crystal structure of which has been determined. The values of the angles for this substance, the mixed carbide  $\text{Fe}_4\text{W}_2\text{C}$ , are given in column 4. They are arranged, for ease of comparison, so as to be on the same row as the lines in the residues to which they correspond. In order not to confuse this arrangement a few of the calculated values of the angles for the mixed carbide, which correspond to lines which are very weak and were not observed, are omitted. The agreement of the large number of lines in column 4 with those isolated in the above procedure proves definitely the presence of the compound  $\text{Fe}_4\text{W}_2\text{C}$ . That the residues consist, therefore, of a mixture of the double carbide  $\text{Fe}_4\text{W}_2\text{C}$  and tungsten carbide in varying proportions would accord with the observed spectra. There are, however, five lines unaccounted for in the C1 residue. One, at  $\theta = 28^\circ.5$ , is too strong for the known spectrum of  $\text{Fe}_4\text{W}_2\text{C}$ . The others, at  $\theta = 33^\circ.0$ ,  $51^\circ.4$ ,  $64^\circ.3$ , and  $66^\circ.3$ , do not occur at all in the above carbides. These lines do not fit on a simple structure, and are too few to afford information about a complicated one. They do not correspond to lines which would be produced by the presence of cementite, of the compound  $\text{W}_2\text{C}$ , or of free carbon. The residue of a steel containing an enhanced proportion of silicon (1.05 per cent.) also gave these lines, and they were stronger in proportion, thus suggesting that they are due to a silicon compound as yet unidentified.

Closer examination of the carbides reveals interesting information. In the case of tungsten carbide a definite

discrepancy is evident between the values of the larger glancing angles observed and those published by Westgren and Phragmén. That this difference exceeded experimental error was shown thus:—A section of the magnet bar C3 was sawn, and filed into the form of a thin rod, and then reduced by dissolving away the surface electrolytically in dilute hydrochloric acid until a very thin wire remained. The diameter of this wire was made as nearly as possible the same as that of the powder which was used in the Debye camera, so that a photograph of the wire could be secured under the same conditions as those obtaining in the case of the residue photographs. A reproduction is shown in Pl. V. fig. 3. Measurements of the positions of the iron lines then afforded an accurate means of checking the spacings of the tungsten carbide lines which occurred on the same photograph. It was found that the latter, like the corresponding lines in the residues, still exhibited the small deviation in spacing from the results given by Westgren and Phragmén. On the other hand, a comparison photograph of tungsten carbide obtained from other sources gave results agreeing with those of Westgren and Phragmén. Moreover, it was observed that in certain residues, generally those in which the mixed carbide lines were weak, the intensity of one or two lines was increased disproportionately when compared with a photograph of the normal tungsten carbide. In consequence, one is led to conclude that the tungsten in the tungsten carbide is to some extent replaceable, probably by iron, a smaller atom. This would then explain the slight decrease in the size of the tungsten carbide lattice.

In the case of the mixed carbide,  $\text{Fe}_4\text{W}_2\text{C}$ , it was found that, on comparing the photographs of residues from differently heat-treated steels, definite variations in the relative intensities of the lines were noticeable. This suggests the possibility of a slight disturbance of the arrangement of the atoms in the unit-cell, due either to atomic replacement or the interpenetration of a foreign atom.

#### *The Validity of the Residue Method.*

Photographs of steels C1, C3, and others, reduced to the form of wires in the manner described above, were obtained in the Debye camera, together with comparison-photographs of residues from the same steels. Preliminary

work showed that the spectrum was not affected by reducing the steels to this shape. A set of residues from each steel was prepared by the use of current densities of 0.4, 0.1, 0.05, and 0.001 amp. per sq. cm. respectively passed through hydrochloric acid of specific gravity 1.014. A comparison of the residue and the steel photographs was carried out, and the following conclusions were arrived at:—

Firstly, a few lines often occurred on the residue photographs which were absent from the corresponding steel photograph, despite the fact that they were of sufficient intensity in the former to warrant their appearance in the latter. They are, therefore, presumably due to spurious products formed in the process of electrolysis. In order to secure sufficient residue for purpose of chemical analysis, the conditions would appear to be such as to permit of the formation of foreign products, which would invalidate conclusions based on such analysis. The method of X-ray analysis, however, has the advantage that a spectrum from the source of the residues can be used to check the residue spectrum, and thus extraneous effects can be eliminated.

Secondly, it was found that the relative proportions of tungsten carbide and the double carbide present in the residue from a given steel varied with different electrolysis conditions. A chemical analysis was made of two such residues, which showed a slight difference in proportion of the carbides present. The results of the analysis of each residue were very different. This, suggests, again, that the results obtained by the chemical method are much more difficult to interpret than X-ray results.

Thirdly, it was found that the breadth of the carbide lines, which depends on the average particle size, as observed in a steel spectrum and in the corresponding residue spectrum, is the same. As an extreme case it was observed that in some steels no carbide spectrum at all appeared, from which one concludes that the carbide crystals are so small as to be practically amorphous. In such cases it appeared that the corresponding residue also yielded no X-ray pattern. Here, of course, the X-ray method can give no clue to the chemical nature of substances present, but it does illustrate the state of carbide subdivision in a region inaccessible to optical microscopy. When steels in which the carbides are amorphous are heated at 900° C. there is a tendency for the carbide particles to grow. Invariably in such steels the carbide

spectra gave strong sharp lines. But similar heating of the amorphous residues *in vacuo*, in air, or in argon, with a view to crystallizing them, did not produce these carbides. Instead, other substances formed, as yet unidentified. This would suggest that the amorphous residues do not contain the same compounds as the crystalline ones; but further work on this point is needed and will be undertaken.

The above results would seem to indicate that the method of chemical analysis of residues as a guide to the nature of steel constituents is of doubtful value. The method of X-ray analysis, on the other hand, appears to be quite reliable provided that control photographs of the untreated steel are utilized in determining the correct conditions of electrolytic separation and the choice of electrolyte.

In conclusion, the author wishes to express his thanks to Mr. J. R. Clarkson for help in the preparation of many residues. He is also indebted to Dr. G. Shearer for his helpful interest in the work, and to Dr. G. W. C. Kaye for his interest and the facilities which have made the work possible. The steels were supplied by Dr. W. H. Hatfield in connexion with a wider research on the magnetic spoiling of tungsten steels.

### *Summary.*

1. The carbide constituents of tungsten magnetic steels are identified from the X-ray spectra of the residues. They are tungsten carbide, the mixed carbide  $\text{Fe}_4\text{W}_2\text{C}$ , and a third compound probably due to the silicon content. No cementite is found.

2. The tungsten carbide spacings are found to be slightly smaller than the normal values. In this, as well as in the mixed carbide, it is suggested that atomic replacement occurs.

3. Chemical analysis of the residues as an indication of steel constituents is found to be of doubtful value. X-ray analysis is shown to be reliable when controlled by photographs of the untreated steel.

### *References.*

- (1) Arnold and Read, Proc. Inst. Mech. Eng. (1914).
- (2) Honda and Murakami, Tok. Sci. Rep. vi. no. 2 (1917); no. 5 (1918).

- (3) Evershed, Journ. Inst. Elec. Eng. lxiii, p. 725 (1925).  
(4) Swinden, Journ. Iron & Steel Inst. i. p. 291 (1907); ii. p. 223 (1909).  
(5) Westgren and Phragmén, Trans. Am. Soc. Steel Treat. xiii. p. 539 (1928).  
(6) Westgren and Phragmén, Z. anorg. Chem. clvi, p. 27 (1926).
- 

LXIII. *The Electrical Properties of the Soil at Radio Frequencies.* By J. A. RATCLIFFE, M.A., and F. W. G. WHITE, M.Sc. (Strathcona Research Student, St. John's College, Cambridge), Cavendish Laboratory, Cambridge\*.

### I. Introduction.

RECENTLY two methods have been developed by means of which the influence of the earth on wireless waves may be investigated. In one of these the attenuation of the waves is measured as they pass over the surface of the earth, while in the other the tilt of the wave-front is measured. The results of both classes of experiment have always been expressed in terms of a conductivity ( $\sigma$ ) and a dielectric constant ( $\epsilon$ ) for the soil considered. In this paper it is pointed out that, on theoretical grounds, we should not expect the quantities  $\sigma$  and  $\epsilon$  to be constant, but we should expect them to vary with the frequency of the waves used.

In order to investigate how serious this variation may be, samples of soil have been investigated, in the laboratory, by two methods. The results of these experiments show that the variations may be considerable as we pass from one wave-length to another. We shall show, in paragraph II., that the fact that  $\sigma$  and  $\epsilon$  are not constant leads to difficulties in the interpretation of the attenuation experiments. After describing the laboratory experiments in paragraphs III., IV., and V., we shall, in paragraph VI., apply our results to a fuller discussion of these difficulties.

### II. Difficulties resulting from the Variation of the Ground Constants.

The purpose of experiments in which the attenuation of wireless waves is measured has been twofold. Firstly,

\* Communicated by Professor E. V. Appleton, F.R.S.

they were carried out in order to verify the theories of propagation over the earth, which have been worked out by Zenneck \* and Sommerfeld †; and, secondly, they were made to determine the electrical properties of the ground, so that its behaviour might be foretold in the future. The fact that the effective dielectric constant and conductivity of the ground may change with the frequency of the applied e.m.f. leads to considerable difficulties in the interpretation of attenuation experiments in the following three ways.

1. In the attempted verification of Sommerfeld's theory the method which has sometimes been used is that of making attenuation measurements on two different wave-lengths, and from them deducing the values of  $\sigma$  and  $\epsilon$  in the two cases. If the results were the same in the two cases, it has been thought that the theory is verified. We now see, however, that we should not necessarily expect to obtain the same values of  $\sigma$  and  $\epsilon$  on two different wave-lengths, so that this method of verification is not satisfactory.

2. It has often been assumed that if  $\sigma$  and  $\epsilon$  have been measured for a certain wave-length then the attenuation of waves of different wave-length may be foretold by the applications of Sommerfeld's calculations. Thus Rolf ‡, working on this assumption, has drawn up a series of curves to show how it is possible, given the attenuation of waves at one frequency, to deduce that at all other frequencies. It is interesting in this connexion to note that Rolf says that "Measurements known to the author [Rolf] give no evident reason for further complicating the theory by introducing variable constants of the soil." He also says that "The main task in the near future is to show by comparison between theory and experiments that these characteristic constants of the earth's surface are really constant, and not dependent upon wave-length." If the "constants" do, in fact, vary with frequency, curves of the kind mentioned above must be used with great care, and extrapolations to very different wave-lengths must not be made.

3. It has also been pointed out recently § that an explanation of the anomalous "negative attenuation"

\* *Ann. der Phys.* xxiii. p. 846 (1907).

† *Ann. der Phys.* xxviii. p. 665 (1908).

‡ *Proc. Inst. Radio Eng.* xviii. p. 391 (1930).

§ 'Nature,' p. 926 (June 21, 1930).

effect noticed by Ratcliffe and Barnett\* can be given if we may assume that  $\sigma = 7 \times 10^{-15}$  e.m.u. and  $\epsilon = 80$  e.s.u. for the ground considered. These values differ widely from those to be expected as a result of measurements on other frequencies. How are we to know whether or not these apparently "abnormal" values are the correct deduction from the attenuation experiments, or whether some other disturbing factor is influencing the propagation? We shall be helped to a decision by a laboratory investigation of how the properties of the ground change with frequency.

### III. *Theoretical Considerations.*

Before describing the experimental procedure in detail we will discuss a few fundamental points underlying the theoretical work of Zenneck and Sommerfeld.

When a wave passes over the ground it induces in it currents which are due to all or any of the following causes:—

- (a) a displacement current in the æther between the soil molecules;
- (b) movements of bound charges in the soil molecules;
- (c) orientation of polar molecules;
- (d) movements of free "electrolytic" ions in crystals, moving under a frictional force, as shown by Joffe†;
- (e) movements of electrolytic ions in solution.

The resultant current will not necessarily be in phase with the e.m.f. producing it, and, on account of the complicated nature of the conduction, the magnitude of the current and its phase relation to the e.m.f. will depend on the frequency.

At any given frequency we can resolve the current into a component  $I_R$  in phase with the e.m.f. and a component  $I_C$  in quadrature with the e.m.f. (fig. 1). The in-phase component is called the conduction component and the quadrature component is called the capacitative component. Considering only  $I_R$ , we should say that the soil acted like a substance with conductivity  $\sigma$  where  $\sigma = \frac{I_R}{E}$ ,

\* Proc. Camb. Phil. Soc. xxiii. p. 288 (1926).

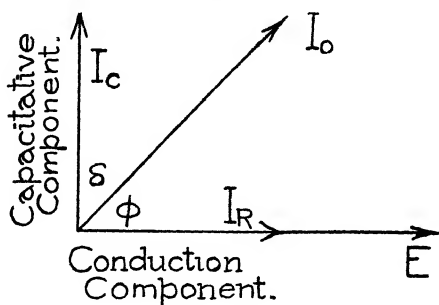
† 'The Physics of Crystals.'



while if we consider  $I_C$  alone we should say that it acted like a substance with dielectric constant  $\epsilon$ , where  $\epsilon$  is defined by  $I_C = \frac{\epsilon}{4\pi} \frac{\partial E}{\partial t}$ . In this way we are led to think

of the current flowing in the soil at any given frequency as made up of these two components, although the physically important fact is that a current of magnitude  $I_0$  flows and makes a phase angle of  $\phi$  with the e.m.f. The results of experiments described in this paper show that the phase and magnitude of the current in a given sample of soil change with frequency, so that the "conductivity"  $\sigma$  and the "dielectric constant"  $\epsilon$  are functions of the frequency of the applied e.m.f. and are not constant.

Fig. 1.



If, therefore, we still wish to describe the electrical properties of the soil in terms of  $\sigma$  and  $\epsilon$ , it is more satisfactory to speak of these quantities as the "effective conductivity" and "effective dielectric constant" respectively. It often happens, however, that it is more convenient to describe the electrical properties of the soil in terms of the phase angle  $\phi$  and the effective dielectric constant  $\epsilon$ . This is more particularly the case since the publication of Rolf's valuable series of attenuation curves, which he expresses in terms of  $\epsilon$  and a quantity  $\tan b$ , where  $\tan b = \frac{n(\epsilon+1)}{2\sigma}$  ( $n$ =frequency of the wave). If  $\epsilon$

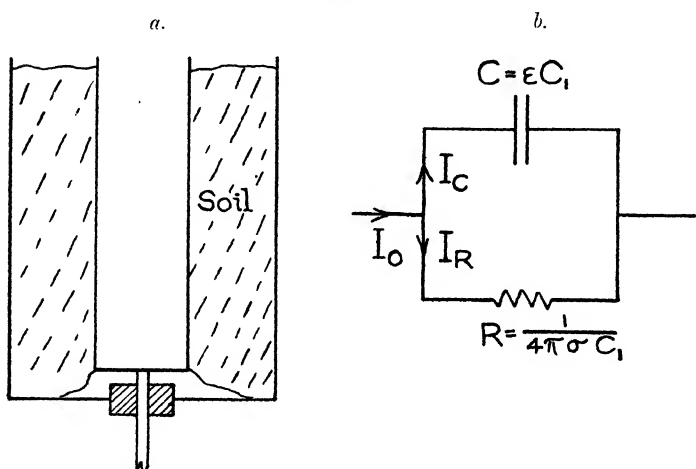
is large, as it is in the case under consideration, we have the approximate relation  $\tan b = \tan \phi$ . We shall see that

$\tan \phi$  is a quantity which is directly measured in one of our experiments, and we have expressed our results in terms of  $\epsilon$  and  $\tan \phi$ . For comparison with previously determined values of  $\sigma$  we have also given the values of  $\sigma$  for the different frequencies.

#### IV. *Experimental Arrangements.*

The soil was used as the dielectric between the plates of a cylindrical condenser, as shown in section in fig. 2, *a*. This

Fig. 2.



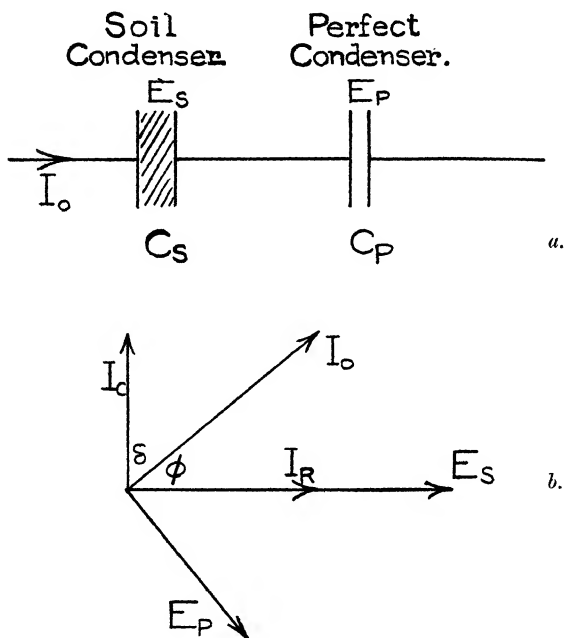
soil condenser may be replaced, for the purpose of explanation, by a perfect condenser with a dielectric of effective dielectric constant  $\epsilon$ , in parallel with a resistance of effective value  $R$  (fig. 2, *b*). A knowledge of  $R$  will give the effective value of  $\sigma$  if we know  $C_1$ , the geometric capacity of the cylindrical condenser, since  $R = \frac{1}{4\pi\sigma C_1}$ . If  $C_s$  is the capacity of the soil condenser, we then have

$$\tan \phi = \frac{I_C}{I_R} = R\omega C_s = \frac{\epsilon\omega}{4\pi\sigma} \quad \text{and} \quad \epsilon = \frac{C_s}{C_1}.$$

Two methods of investigation were used, and will be described separately.

If the soil condenser is placed in series with a perfect condenser (capacity  $C_P$ ) and an alternating current  $I_0$  passed through both (fig. 3, *a*) the vector diagram will be as in fig. 3, *b*. The e.m.f.  $E_s$  across the soil condenser will be in phase with the resistance component of the current  $I_R$ , while  $I_0$  will be ahead of  $E_s$  by the angle  $\phi$ . The e.m.f.

Fig. 3.

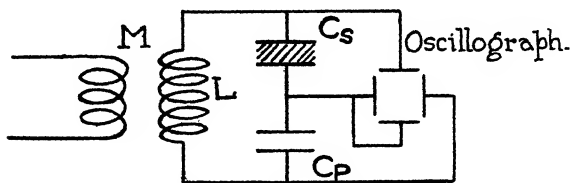


across the perfect condenser will be  $90^\circ$  behind  $I_0$ , and will lag behind  $E_s$  by the angle  $\delta$ , which is also the angle between  $I_0$  and  $I_C$ . Thus, we can find  $\delta$  and hence  $\phi$  by investigating the phase difference between the e.m.f. across the soil condenser and that across the perfect condenser. This measurement is made by means of a cathode-ray oscillograph as shown in fig. 4. Current is caused to flow through the two condensers by loosely coupling the circuit

$L C_P C_S$  to a source of radio-frequency current. The amplitudes of  $E_S$  and  $E_P$  can be made approximately the same by adjusting  $C_P$ . Precautions were taken to see that everything was working as expected. Substitution of other components, such as resistances and inductances, for  $C_S$  gave the correct oscillograph figure. Stray effects were eliminated by keeping the leads to the oscillograph as short as possible, while the coupling coils were placed at a sufficient distance to prevent magnetic deflexions of the cathode ray beam. It was demonstrated that any good mica condenser was sufficiently perfect to be used as the comparison condenser at  $C_P$ . Values of  $\tan \phi = \tan (90 - \delta)$  are obtained simply by tracing the elliptic pattern on the oscillograph screen and measuring it.

The advantage of this method lies in the fact that  $\tan \phi$  can be obtained directly from the oscillograph trace. In

Fig. 4.



order to obtain values for the effective conductivity and the effective dielectric constant it would be necessary to measure the current through, and the e.m.f. across, the soil condenser at the same time as  $\tan \phi$  was measured. Several values were determined and found to be of the same order as those found by the resonance method to be described below. The accuracy with which  $\tan \phi$  can be obtained was limited by the method of tracing the ellipse on tissue paper in a dark room. Probably better results would be obtained by photographing the trace, but the accuracy obtained was sufficient for the present purpose.

### *Resonance Method.*

The circuit used in the resonance method is shown in fig. 5. It is a tuned resonance circuit in which the capacity consists of a calibrated variable air condenser  $C_A$  in

674 Messrs. J. A. Ratcliffe and F. W. G. White on the  
parallel with the soil condenser  $C_s$ . An e.m.f. is induced  
from a radio-frequency source by way of the mutual

Fig. 5.

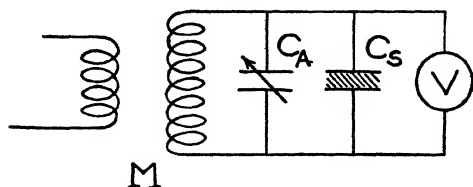
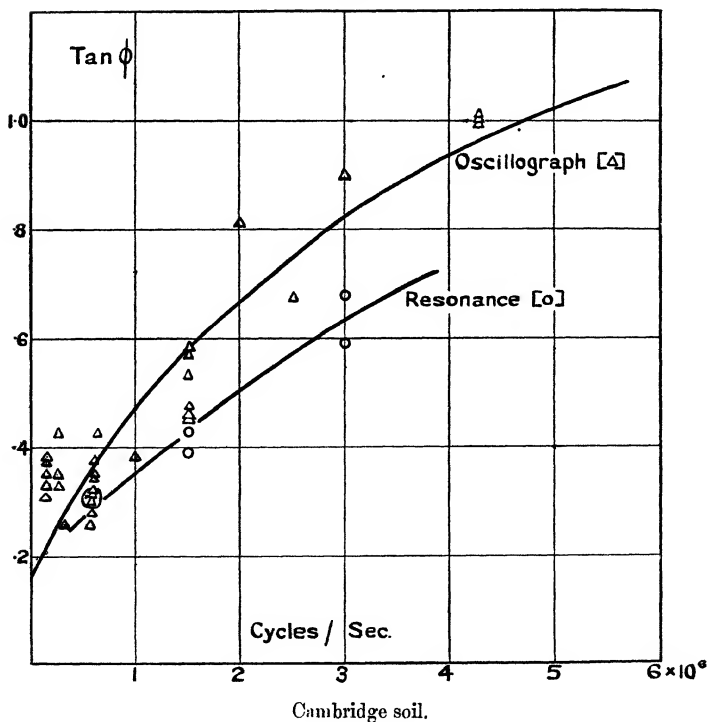


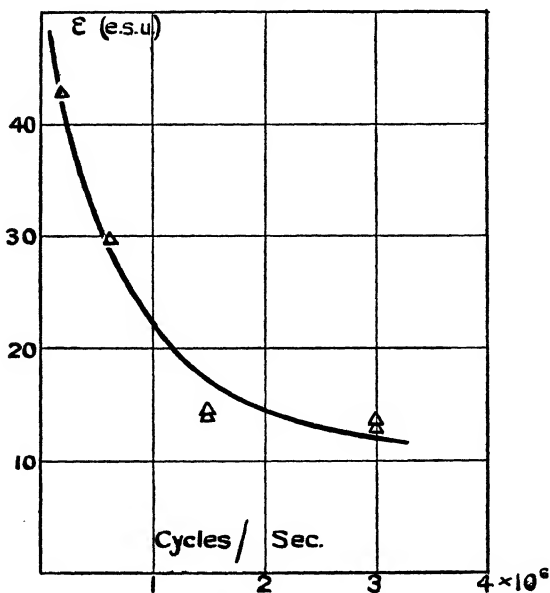
Fig. 6 a.



inductance  $M$ . A Moullin voltmeter  $V$  measures the radio-frequency e.m.f. across the soil condenser.

To make a measurement the source is adjusted to provide an e.m.f. of the required frequency, the soil condenser is removed, and the air condenser is adjusted to give voltage resonance, as shown by the voltmeter. The soil condenser is now placed in parallel with the air condenser, and the latter is again adjusted to give voltage resonance. The difference between the two readings of the air condenser gives the effective capacity of the soil condenser.

Fig. 6 b.



Cambridge soil.

From a knowledge of the geometric capacity of the soil condenser the effective dielectric constant  $\epsilon$  can be found.

A voltage resonance curve is now plotted, with the soil condenser in position, by varying the capacity  $C_A$ . If  $C_a$  and  $C_b$  are the values of  $C_A$  at the points where the e.m.f. across the condenser is  $1/\sqrt{2}$  times the maximum e.m.f., and if we write  $\Delta C = (C_a - C_b)$ , then it can be shown that

$$\tan \phi = R\omega C_s = \frac{2C_s}{\Delta C} \quad \text{and} \quad \epsilon = \frac{C_s}{C_1}.$$

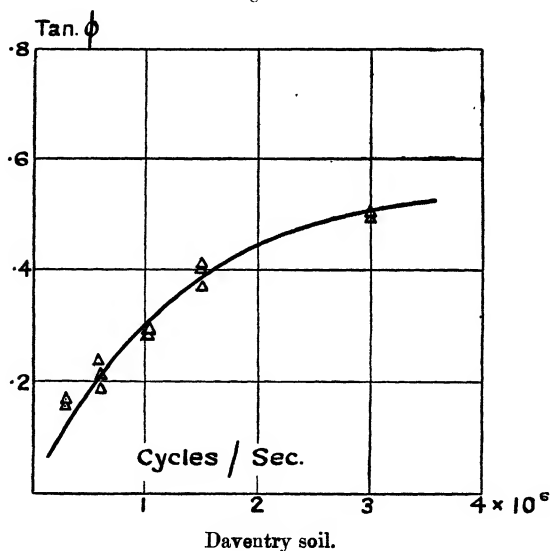
In this way  $\epsilon$  and  $\tan \phi$  are found.

There are certain limitations to the use of this method. At low frequencies the decrement becomes too high to allow a good resonance curve to be obtained, while at very high frequencies the magnitudes of  $\Delta C$  and  $C_s$  become small. It has proved useful for frequencies between  $0.2 \times 10^6$  and  $5 \times 10^6$  cycles per second.

### V. Experimental Results.

Two types of soil were experimented upon, these being garden soil from Cambridge and surface soil from near

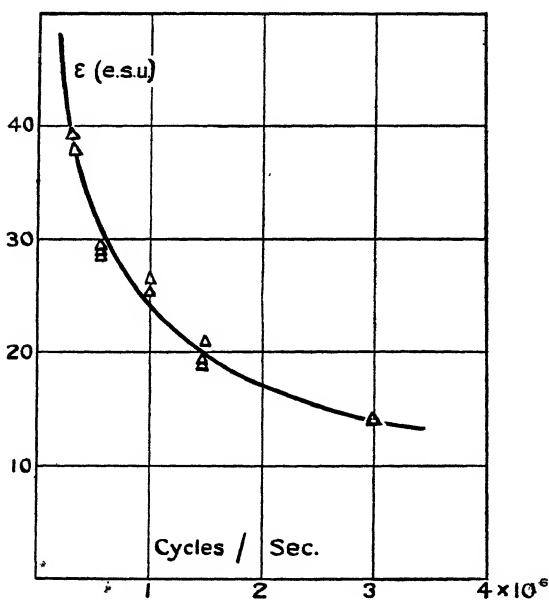
Fig. 7 a.



the Daventry Broadcasting Station. Figs. 6 a and 6 b show how the values of  $\tan \phi$  and  $\epsilon$  for the Cambridge soil vary with frequency, while figs. 7 a and 7 b show the results for the Daventry soil. At high frequencies  $\epsilon$  assumes a low limiting value which remains approximately the same up to a frequency of  $10 \times 10^6$  cycles per second—a value not shown on the curves. For lower frequencies, however, the value of  $\epsilon$  increases, becoming three or four times its value at the higher frequency. Although the two specimens

appear to be of very different physical and chemical constitution, the results obtained are similar. This is probably due to the fact that the moisture content of the soil plays a large part in determining its electrical properties. In order to investigate this point the same specimen of Daventry soil which was used to obtain fig. 7 was dried and again used as the dielectric. It was found that  $\epsilon$  (at

Fig. 7 b.



Daventry soil.

$0.2 \times 10^6$  cycles per second) had decreased from 48.5 to 5.3, while  $\tan \phi$  increased from 0.14 to 1.25. A similar change was also found as the amount of solid rock in the soil was increased.

Although  $\tan \phi$  and  $\epsilon$  are of primary importance from the point of view of attenuation experiments, it is interesting to note the variation that takes place in the effective conductivity  $\sigma$ . The curves (figs. 8 a and 8 b) have been



678 Messrs. J. A. Ratcliffe and F. W. G. White on the  
calculated from the smoothed curves of  $\tan \phi$  and  $\varepsilon$ , by  
writing

$$\sigma = \frac{\varepsilon \omega}{4\pi \tan \phi}.$$

Fig. 8 a.

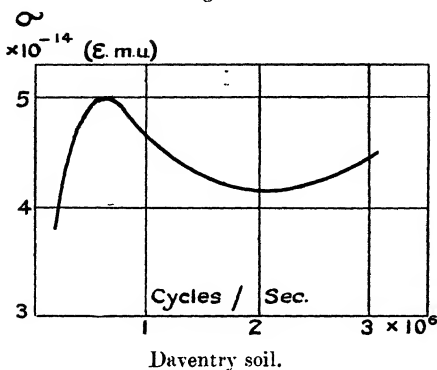
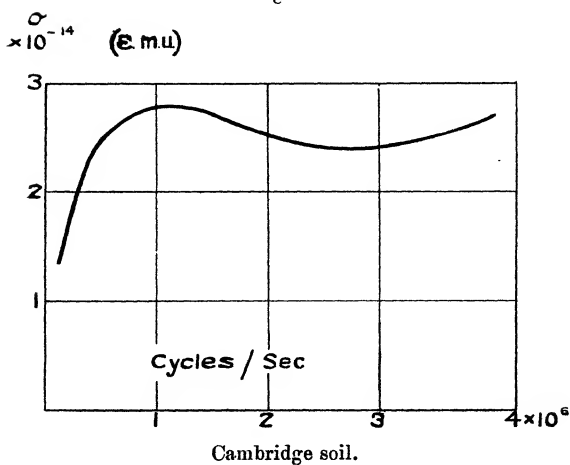


Fig. 8 b.



## VI. Discussion of Results.

The measurements have shown that the values of  $\varepsilon$  and  $\sigma$  change very considerably as the frequency of the

wave is changed. We will now apply this experimental result to a consideration of the three fundamental difficulties mentioned in paragraph II.

(1) In the confirmation of Sommerfeld's theory we now see that it is not sufficient to obtain attenuation curves on two different wave-lengths and expect to arrive at the same values of  $\sigma$  and  $\epsilon$ . Since also  $\sigma$  and  $\epsilon$  are different for different samples of soil, it is not possible to attempt a verification of Sommerfeld's expression by deducing the values of these quantities from an attenuation curve and then comparing them with the values found for a specimen of soil in the laboratory. The values of  $\sigma$  and  $\epsilon$  found from the attenuation curve are undoubtedly average values for a layer of soil the thickness of which is of the order of one wave-length. It appears that the only possible method of verification is to measure the effective values of  $\sigma$  and  $\epsilon$  for the ground *in situ* at the same frequency, and under conditions where the penetration of the wave is of the same order as in the attenuation experiments. The only method available for this determination is that of measuring the tilt of the wave-front as developed by Barfield.

(2) The method of predicting the attenuation of waves of one frequency from a knowledge of the attenuation at another frequency, assuming  $\sigma$  and  $\epsilon$  to remain constant, now appears to be fundamentally incorrect. As an example of the kind of errors into which the procedure will lead us we will suppose that  $\sigma$  and  $\epsilon$  have been measured at a wave-length of 100 metres, and have been found to be  $10^{-14}$  e.m.u. and 10 e.s.u. respectively. If we then assume that the quantities remain constant as we change the wave-length to 1600 metres, we deduce an attenuation factor at a distance of 100 wave-lengths from the transmitter of 0.32 at the new wave-length. If, however, we take the value of  $\epsilon$  to be 45 on the new wave-length, we deduce a value of 0.5 for this attenuation factor. This illustrates the kind of error into which we may be led if we neglect the variation of  $\epsilon$  with frequency.

(3) The values of  $\sigma = 7 \times 10^{-15}$  e.m.u. and  $\epsilon = 80$  e.s.u. required for an explanation of the "negative attenuation" effect on 1600 metres are not very far removed from those obtained in the present experiments,  $\sigma = 4 \times 10^{-14}$ ,  $\epsilon = 45$ . Considering the possible variations of soil properties with depth, it appears reasonable to suppose that the values

$\sigma = 7 \times 10^{-15}$  e.m.u. and  $\epsilon = 80$  e.s.u. are the correct deductions from the attenuation experiments. Experiments are being carried out to test this conclusion further.

The value of the effective dielectric constant  $\epsilon$  has been found previously by Ratcliffe and Shaw \* by means of attenuation measurements made at Cambridge using a wave-length of 30 metres. They found  $\epsilon = 20$  e.s.u. The present results for the Cambridge surface soil give a value  $\epsilon = 13$  e.s.u. In view of the probable variation of  $\epsilon$  with depth, this is considered to be as close a confirmation as could be expected by this method. It is interesting to note that the value for  $\epsilon$  deduced from the attenuation curve is higher than that deduced from the surface sample of soil both for 1600 and for the 30 metre measurements. This is possibly due to the fact that the deeper layers of soil may have a higher water content than the superficial layers.

In view of the very large values which have been obtained for the effective dielectric constant of the soil at the lower frequencies, it is of interest to inquire whether other investigators have noticed this effect. Bairsto† has investigated the dielectric constant and conductivity of slate at different frequencies, and has found values very similar to those which we find for soil. His values for  $\epsilon$  are 10 e.s.u. at a frequency of  $10^6$  cycles per second, 16 e.s.u. at 100,000 cycles per second, and 40 e.s.u. at 3000 cycles per second. The variation in conductivity is also in the same direction as that observed by Bairsto.

## VII. *Summary.*

Laboratory experiments have been made at radio-frequencies to investigate the way in which the effective conductivity  $\sigma$  and the effective dielectric constant  $\epsilon$  of the soil vary with frequency. The results of the experiments are shown in figs. 7 and 8. The bearing of these results on some problems of the propagation of wireless waves is discussed, and the conclusion is reached that the only satisfactory way of measuring these quantities is to measure them for ground *in situ* and at the frequency required, either by the tilt method or by means of attenuation curves.

\* 'Nature,' cxxiv. p. 617 (1929).

† Proc. Roy. Soc. xcvi. p. 363 (1912).

LXIV. *The Relations of the Magnetic and Thermal Constants of Ferromagnetic Substances.* By J. R. ASHWORTH, D.Sc.\*

INDEX TO PARAGRAPHS.

1. The object of the paper.
2. Curie's Law and Constant.
3. Development of the ferromagnetic equation and its constants.
4. Energy equation to ferromagnetism.
5. Relations of  $a'$  to  $R'$  and  $\theta$  to  $I_0$ .
6. The specific heat  $C_\theta$  and its discontinuity  $\Delta c$  at the critical temperature, and their relations to the ferromagnetic constants.
7. Relation of  $\Delta c$  to  $C_\theta$ .
8. Remarks on these relations.
9. Ratios of constants in groups of the ferromagnetics.
10. Table of fundamental quantities and constants.
11. Summary of equations.

1. **I**N the general equation to ferromagnetism, which treats intensity of magnetization as a function of field-strength and temperature, three fundamental constants appear. If the equation is written in terms of energy it is at once allied to certain thermal quantities, and is amenable to thermal considerations. It is the object of this paper to present some relations which exist between the ferromagnetic constants themselves and between their allied thermal constants amongst the available substances which exhibit magnetic properties in a high degree. The ferromagnetic substances here considered are iron, cobalt, nickel, Heusler's alloy, and magnetite.

2. Curie's investigation † of the magnetic behaviour of diamagnetic, paramagnetic, and ferromagnetic substances under the influence of high temperatures laid the foundation for the modern theory of the relation of magnetism to temperature and led to the law and the constant which goes by his name. His researches at temperatures above the magnetic critical temperatures showed that the product of the susceptibility and the absolute temperature was constant for each ferromagnetic substance, but different for different substances. Calling this constant  $A$ , we have

$$A = kT, \quad . \quad . \quad . \quad . \quad . \quad . \quad (1)$$

where  $k$  is the magnetic susceptibility and  $T$  the absolute

\* Communicated by the Author.

† 'Œuvres' de P. Curie, 1908.

temperature. If  $I$  is the intensity of magnetization, that is, magnetic moment per unit volume, and  $H$  is field-strength, the equation can be put

$$\frac{H}{I} = \frac{T}{A} \quad \text{or} \quad \frac{H}{I} = R'T, \quad . . . . \quad (2)$$

where  $R'$  is the reciprocal of Curie's constant  $A$ . This is the paramagnetic equation. Curie pointed out that this equation is analogous to the gas-equation

$$PV = RT \quad \text{or} \quad \frac{P}{\rho} = RT, \quad . . . . \quad (3)$$

where  $\rho$  is the density, which is inversely as the volume  $V$ ,  $P$  is the pressure, and  $R$  is the well-known gas-constant. Thus  $H$ ,  $I$ , and  $R'$  correspond respectively to  $P$ ,  $\rho$ , and  $R$ , while in both  $T$  is the absolute temperature.

3. Curie further pointed out that the passage of a ferromagnetic from paramagnetism to strong magnetism through the critical temperature is like the passage of a fluid from a gas to a liquid through its critical temperature, so that it is an obvious step to extend the paramagnetic equation into a more general equation to include ferromagnetism, just as van der Waals extended the gas equation to include liquids. Van der Waals's equation takes account of the mutual attraction of the molecules, which acts like an internal pressure, and of the finite size of the molecules which sets a limit to the density; and as ferromagnetism is distinguished from paramagnetism by the mutual action of the magnetic molecules, and the fact that the intensity has a limiting value, it follows that the ferromagnetic equation may be written on the model of the fluid equation, thus:

$$(H + a'I^2)\left(\frac{1}{I} - \frac{1}{I_0}\right) = R'T. \quad . . . . \quad (4)$$

Here  $a'$  is the intrinsic field constant analogous to van der Waals's  $a$ , and  $I_0$  is the limiting intensity of magnetization, so that  $\frac{1}{I_0}$  is analogous to van der Waals's  $b^*$ .

This equation is a cubic in  $I$ , and we can proceed to treat it after the manner of van der Waals's equation. For example, the critical values of  $H$ ,  $I$ , and  $T$  can be written

$$H_c = \frac{a'I_0^2}{27}, \quad . . . . \quad (5)$$

$$I_c = \frac{1}{3} I_0, \quad . \quad . \quad . \quad . \quad . \quad . \quad (6)$$

$$\theta = \frac{8}{27} \frac{a' I_0}{R'}. \quad . \quad . \quad . \quad . \quad . \quad (7)$$

For the evaluation of  $a'$  the equation to the critical temperature is most suitable. The two other constants  $I_0$  and  $R'$  can be obtained by direct experiment. Values for the constants  $a'$ ,  $I_0$ , and  $R'$ , with others, will be found at the end of this paper for all the ferromagnetics.

4. The equations to paramagnetism and to ferromagnetism are susceptibility equations, whilst the gas and fluid equations are energy equations. It is easy, however, to pass from a susceptibility equation to an energy equation for magnetism. In the paramagnetic state, where the mutual action of the molecular magnets is absent, we have

$$\frac{1}{k} = R'T, \quad . \quad . \quad . \quad . \quad . \quad (8)$$

which becomes

$$\frac{I_0^2}{k} = R'I_0^2 T \quad . \quad . \quad . \quad . \quad . \quad (9)$$

on multiplying throughout by  $I_0^2$ .

The left side is an expression for maximum work when  $H$  is constant and  $T$  variable. The equivalent thermal energy is that of two degrees of freedom of kinetic energy, which may be written  $RT$ , and consequently

$$\frac{I_0^2}{k} = R'I_0^2 T = RT,$$

from which we get

$$R'I_0^2 = R, \quad . \quad . \quad . \quad . \quad . \quad (10)$$

where  $R$  is in mechanical units and is referred to unit volume.

Thus by multiplying by  $I_0^2$  we can pass from a susceptibility equation to an energy equation. We can then write for the ferromagnetic energy equation

$$I_0^2(H + a'I^2) \left( \frac{1}{I} - \frac{1}{I_0} \right) = R'I_0^2 T, \quad . \quad . \quad (11)$$

or more conveniently,

$$(HI_0 + a'I_0 I^2) \left( \frac{I_0}{I} - 1 \right) = RT, \quad . \quad . \quad (12)$$

where the first bracket represents energy in terms of

magnetism and the second bracket has only numerical significance. The equation to the absolute critical temperature ( $\theta$ ) becomes

$$\theta = \frac{8}{27} \frac{a'I_0^3}{R} \quad . \quad . \quad . \quad . \quad . \quad (13)$$

or

$$R\theta = \frac{8}{27} a'I_0^3. \quad . \quad . \quad . \quad . \quad . \quad (14)$$

Equation (10), namely,

$$R'I_0^2 = R,$$

is one connecting constants which can be separately determined, and its truth can thus be readily tested. It can, however, be used in turn for the evaluation of any of the constants, and is convenient for the determination of  $I_0$ . The values of  $I_0$  in the table at the end of this paper have been so determined, except those for Heusler's alloy and for magnetite.

The constant  $R$  as used above refers to the kinetic energy per degree centigrade in mechanical units for two degrees of freedom per cubic centimetre. If the gas constant has the usually accepted meaning of  $83.15 \times 10^6$  ergs per degree centigrade for a gram molecule, then we must substitute for  $R$  in the formula the term  $\frac{R}{an}$  to make it apply to one gram, and  $\frac{R}{an}\rho$  for one cubic centimetre of volume, where  $a$  is the atomic mass,  $n$  the number of atoms in the molecule, and  $\rho$  the density of the material. Thus

$$R'I_0^2 = R \frac{\rho}{an} \quad . \quad . \quad . \quad . \quad . \quad (15)$$

The application of this equation for the evaluation of  $I$  involves a knowledge of  $n$ , but this presents no difficulty, as  $n$  must be a small number, and can be determined by inspection. Thus for iron we have

$$I_0^2 = \frac{R}{an} \frac{\rho}{R'} = \frac{83.15 \times 10^6}{55.85n} \frac{7.8}{3.56} = \frac{3.3 \times 10^6}{n},$$

which gives  $I_0 = 1817$  when  $n = 1$ . Any other value of  $n$  greater than unity would make  $I$  much less than it is known to be from experiment\*.

\* Ashworth, "Magnetic and Electric Saturation Values," *Phil. Mag.*, October 1918.

We may now proceed to consider certain relations which exist between the constants  $a'$ ,  $I_0$ , and  $R'$  amongst themselves and in connexion with the specific heat, both in the same and in different ferromagnetics.

5. Relations of  $a'$  to  $R'$  and  $I_0$  to  $\theta$ .

Equation (7) to the critical temperature for ferromagnetism discloses a simple and interesting relation between the maximum intensity of magnetization and the critical temperature. Writing the equation

$$\frac{\theta}{I_0} = \frac{8}{27} \frac{a'}{R'}, \quad \dots \dots \dots (16)$$

we find the ratio of  $\frac{a'}{R'}$  is very approximately a whole number beginning with 2 for iron and increasing by successive units to 6 for magnetite. This is shown in Table I.

TABLE I.

Ferromagnetic.	$\frac{a'}{R'}$ .	$q$ .	Percentage difference from whole number.
Iron .....	7.0/3.56	2	+2
Cobalt .....	19.2/6.0	3	-6
Nickel ....	83.7/20.8	4	-0.6
Heusler's alloy .....	173/34	5	-1.7
Magnetite .....	203/35	6	+3

The departure from a whole number is largest with cobalt. There is some uncertainty in the values of the constants of cobalt, and the discrepancies here, and in what follows, are always larger with cobalt than with other ferromagnetics.

If we put

$$\frac{\theta}{I_0} = \frac{8}{27} q, \quad \dots \dots \dots (17)$$

$q$  being  $\frac{a'}{R'}$ , then we may say that  $q$  has values which to a first approximation are whole numbers from 2 to 6, in consecutive order. There is apparently no ferromagnetic substance with  $q=1$ . If such should be found its critical temperature would probably be low unless the intensity of magnetization were very large.

The following table gives values of  $\frac{\theta}{I_0}$  and the corresponding values of  $q$ .



TABLE II.

Ferromagnetic.	$\frac{\theta}{I_0}$ .	$\frac{8}{q \cdot 27}$ .	$q$ .
Iron .....	0.58	0.59	2
Cobalt .....	0.95	0.89	3
Nickel.....	1.20	1.19	4
Heusler's alloy .....	1.50	1.48	5
Magnetite .....	1.79	1.78	6

The progressive increase by unit steps from 2 to 6 which  $q$  assumes from one to another of the ferromagnetics may be treated as an experimental fact apart from any theory, although it was first observed in connexion with the constants  $a'$  and  $R'$  which are fundamental in the theory of ferromagnetism.

#### 6. Specific Heat and Ferromagnetism.

The magnitude of the intrinsic field,  $a'I^2$ , of a magnet can be calculated when  $a'$  is known, and  $a'$  can be most easily determined from the equation to the critical temperature.

The maximum intrinsic field calculated in this way is of enormous magnitude regarded as a magnetic field, although it would be more correct to treat it as thermal rather than magnetic energy per unit of intensity of magnetization. With iron the intrinsic field at its maximum is  $2.31 \times 10^7$  gaussess, and is as much as  $4.63 \times 10^7$  gaussess with magnetite. At the critical temperature this enormous field vanishes, as the result of thermal action, and the energy associated with it which disappears is large enough to affect prominently the specific heat of the ferromagnetics at the critical temperature. Thus with nickel the specific heat at ordinary temperatures is about 0.109. It increases progressively up to 0.154, the true specific heat at the critical temperature ( $C_0$ ), and immediately above this temperature abruptly falls to 0.125, the discontinuity ( $\Delta c$ ) of the specific heat being 0.029. The discontinuity is larger with other ferromagnetics, and is as much as 0.120 with iron. Weiss\*, who has made careful and detailed experiments on this subject, treats the discontinuity of the specific heat as the equivalent of the loss of intrinsic magnetic energy which takes place when the temperature is raised to the critical point. According to the formula used by him, the intrinsic field is equal to  $NI$ , where  $N$  is a constant, and the magnetic

\* P. Weiss and P. N. Beck, *J. de Phys.* (4) vii. p. 279 (1908).

energy associated with this field is then  $\frac{1}{2}NI^2$ . The calculation, even when revised and amended by H. A. Lorentz \*, does not agree very well with experimental results, as will be seen in the table here given:—

TABLE III.

Ferromagnetic.	$\Delta c$ .	
	By Lorentz's formula (1).	By experiment.
Iron .....	0.089	0.120
Nickel.....	0.282	0.285
Magnetite .....	0.064	0.079

(1) Bulletin of the National Research Council, iii. pt. 3, no. 18, p. 123.

According to Lorentz,  $\Delta c = \frac{4.97}{m}$ , where  $m$  is the molecular mass, and in order to arrive at the calculated result given above it is supposed that the magnetic carrier of iron is one atom, that of nickel three atoms, and that of magnetite  $\frac{1}{3}(\text{Fe}_3\text{O}_4)$ .

The discrepancy between calculation and experiment does not prove the connexion to be false between the intrinsic field energy and the discontinuity of the specific heat at the critical temperature; it points rather to some defect in the formula which has been used in the calculation.

If, instead of the formula used by Weiss, we employ a formula in which the value of the intrinsic energy of magnetization is derived from the ferromagnetic equation, then it is possible to arrive at calculated results which are in very good agreement with the facts of experiment.

If the thermal energy of the discontinuity at the critical temperature,  $\Delta c\theta$ , is equated to the product of the maximum intrinsic field and the maximum intensity of magnetization, we get

$$f\Delta c\theta = a'I_0^3 \quad . \quad . \quad . \quad . \quad . \quad (18)$$

$f$  being a numerical factor. To express the thermal energy of the discontinuity in mechanical and in volume units we must multiply by  $J$  the mechanical equivalent of heat and by  $\rho$  the density. We have also to multiply by the factor  $n$ , which is the same in magnitude as in equation (15). We then have  $f=nJ\rho$ , and we get

$$n \cdot \Delta c \cdot \theta J \rho = a'I_0^3, \quad . \quad . \quad . \quad . \quad . \quad (19)$$

\* Lorentz, *Revue Scientifique*, 1912, p. 1.

from which we obtain the value of  $\Delta c$ , thus :

$$\Delta c = \frac{a'I_0^3}{n\rho J\theta} \quad . \quad . \quad . \quad . \quad . \quad (20)$$

The truth of these equations is seen in the following table :—

TABLE IV.

Ferromagnetic.	n.	$n\Delta c\theta J\rho \times 10^{-10}$ .	$a'I_0^3 \times 10^{-10}$ .	$\Delta c$
				observed and used in the calculation.
Iron .....	1	4.26	4.20	0.120 <sup>(1)</sup>
Cobalt .....	1	4.75	5.52	0.098 <sup>(2)</sup>
Nickel .....	2	1.40	1.41	0.029 <sup>(3)</sup>
Heusler's alloy...	2	1.26	1.28	0.036 <sup>(4)</sup>
Magnetite.....	3/2	2.19	2.21	0.079 <sup>(5)</sup>

(1), (3), (5) Weiss, Piccard, and Carrard, *Arch. des Sc.* xlii. p. 378, and xliii. pp. 22, 113, and 199.

(2) A. Göbl, Thesis, Zurich University, 1911.

(4) Ashworth (unpublished).

Throughout the agreement is satisfactory, with the exception of cobalt.

In the equation which has been constructed we may replace  $a'I_0^3$ , by means of equation (14), with  $\frac{27}{8} \frac{R\theta}{an} \rho$ , and we get

$$n\Delta cJ = \frac{27}{8} \frac{R}{an}, \quad . \quad . \quad . \quad . \quad . \quad (21)$$

and writing  $R/I_0^2/\rho$  for  $R/an$ , by equation (15), we obtain

$$n\Delta cJ\rho = \frac{27}{8} R/I_0^2. \quad . \quad . \quad . \quad . \quad . \quad (22)$$

Either equation (21) or (22) allows  $\Delta c$  to be calculated, as all the other quantities are known by experiment with the exception of  $n$ , which may be obtained from (15) or (26).

We can put equation (21) thus :

$$\Delta c = \frac{27}{8} \frac{R}{Jan^2}, \quad . \quad . \quad . \quad . \quad . \quad (23)$$

and since  $\frac{27}{8} \frac{R}{J} = 6.683$ , we get

$$\Delta c = \frac{6.683}{an^2}, \quad . \quad . \quad . \quad . \quad . \quad (24)$$

which applies to iron, cobalt, and nickel.

The calculation of  $\Delta c$  may be made from equation (22) instead of (21), and it is preferable to do so in the case of an alloy like Heusler's alloy and a compound such as magnetite, as the quantity  $\rho R/an$  is replaced by the experimentally-determined product  $R'I_0^2$ , the reciprocal of Curie's constant and the intensity of magnetization, and this avoids a knowledge of  $a$  for the alloy and the chemical compound magnetite.

The following table gives the calculated and experimental values of  $\Delta c$  :—

TABLE V.

Ferromagnetic.	$n$ .	$\Delta c$ .	$\Delta c$ by experiment.	Percentage difference.
		as $\frac{27}{8} \frac{R'I_0^2}{J\rho n}$ .		
Iron .....	1	0.120	0.120 <sup>(1)</sup>	$\pm 0$
Cobalt .....	1	0.114	0.098	+16
Nickel .....	2	0.029	0.029	$\pm 0$
Heusler's alloy ...	2	0.037	0.036	+ 2
Magnetite .....	3/2	0.079	0.079	$\pm 0$

<sup>(1)</sup> *Loc. cit.*

In the calculation there are no adjustable quantities, as  $n$  may be derived from other equations.

### 7. Relation of $\Delta c$ , the discontinuity, to $C_\theta$ , the specific heat, at the critical temperature.

It has already been mentioned that a characteristic of ferromagnetic substances is the abnormal increase of the specific heat, which attains at the critical temperature very high values before the abrupt fall occurs which we have been considering. The specific heat  $C_\theta$  at the critical temperature has the following values :—

Iron.	Cobalt.	Nickel.	Heusler's alloy.	Magnetite.
$C_\theta$ <sup>(1)</sup> = 0.309	0.270	0.154	0.179	0.299

<sup>(1)</sup> *Loc. cit., vide  $\Delta c$ .*

These are true specific heats, and they have been obtained by applying a correction to the mean specific heat between the critical temperature and a temperature of about 15° C. The values for iron and nickel have been determined with considerable precision, and are better known than the others.

These true specific heats have a simple relation to the discontinuity  $\Delta c$ . In general terms for elementary metals the relation may be expressed by the equation

$$maC_\theta = 5na\Delta c, \dots \dots \dots (25)$$

in which  $ma$  may be regarded as the molecular weight of the magnetic carriers much below the critical temperature and  $na$  the molecular weight just above the critical temperature. As  $m$  appears to have the value 2 for all the ferromagnetics when  $n$  has the numbers given above to it, and  $a$  is the same on both sides of the equation, we have

$$C_\theta = \frac{5}{2}n\Delta c. \quad (26)$$

The verification of this is as follows :—

TABLE VI.

Ferromagnetic.	$n$ .	$5 \frac{n}{2} \Delta c$ .	$C_\theta$ by experiment <sup>(1)</sup> .	Percentage difference.
Iron.....	1	0.300	0.309	—3.0
Cobalt .....	1	0.245	0.270	—9.2
Nickel .....	2	0.145	0.154	—7.1
Heusler alloy .....	2	0.180	0.179	+0.5
Magnetite .....	3/2	0.296	0.289	—1.0

<sup>(1)</sup> *Loc. cit.*, *vide*  $\Delta c$ .

Cobalt and nickel yield the least satisfactory results. Cobalt, according to A. Göbl, \* has two discontinuities, one about 500° to 600° C., of magnitude 0.02, and the other at the critical temperature, of magnitude 0.098. It is the latter which appears in Tables IV. and V. If it is allowable to use the total discontinuity, which is 0.118, and to employ a corrected true specific heat at the critical temperature of 0.290, then cobalt has an error no larger than the other ferromagnetics. Thus in Tables IV. and V. the experimental and calculated values of  $\Delta c$  do not differ by more than 4 per cent., and in Table VI.  $C_\theta$ , equal to 0.290, differs from the calculated value, 0.295, by less than 2 per cent.

With regard to nickel a very recent determination of  $C_\theta$  and  $\Delta c$  by an electrical method puts  $C_\theta = 0.1577$  and  $\Delta c = 0.0325$ , and the formula above would therefore give  $C_\theta$  by calculation as 0.1625, with an error now of only +3 per cent. †

We can now obtain a formula for  $C_\theta$  in terms of magnetic or thermal constants by substituting for  $\Delta c$  its equivalents. Thus we get

$$C_\theta = \frac{5}{2} \frac{27}{8} R I_0^2 \frac{1}{J\rho} \text{ in magnetic units} \quad (25)$$

\* *Loc. cit.*, Table IV.

† Lapp, *C. R.* clxxxvi. pp. 1104–1106 (April 1928).

and 
$$C_\theta = \frac{5}{2} \frac{27}{8} \frac{R}{J} \frac{1}{na} \text{ in thermal units . . . (26)}$$

The latter reduces to

$$C_\theta = \frac{16.79}{na}, \text{ . . . . . (27)}$$

which applies satisfactorily to iron, cobalt and nickel, where  $a$ , the atomic weight, has a single definite value. With Heusler's alloy and magnetite we can substitute for  $R/aJ$  in the formula one-third of the specific heat at ordinary temperatures, in conformity with the law for pure metals that  $3R/aJ$  is equal to the specific heat. Formulæ (23) and (26) may then be applied to Heusler's alloy and magnetite as with the other ferromagnetics.

8. (a) In all the formulæ where  $n$  appears it has, for any ferromagnetic, one and the same value, as may be seen in the tables given previously, and it means the number of atoms in the molecule above the critical temperature, that is, in the paramagnetic state.

The number of magnetic atoms in the molecule at ordinary temperatures in the ferromagnetic state is signified by  $m$ .

Now with nickel and Heusler's alloy  $n$  and  $m$  are alike, each being equal to 2, and therefore these metals show no change in the number of atoms to the molecule on passing through the critical temperature, but with iron and cobalt  $m = 2$  and  $n = 1$ , and so in passing from the ferromagnetic to the paramagnetic state through the critical temperature there is a change in the constitution of the molecule, and the molecule of these metals becomes apparently monatomic in the paramagnetic condition.

(b) In the formula  $maC_\theta = 5na\Delta c$  the number 5 is inserted arbitrarily, but it may be given a rational interpretation. The specific heat of a metal is by theory  $3R/aJ$ , in which  $R$  refers to the sum of the kinetic and potential energies for one degree of freedom. With metals generally there is an increase of specific heat with rise of temperature, which has been attributed to the progressive acquisition of rotational energy by the molecules, and this, in the case of the ferromagnetic metals, would be facilitated in virtue of the magnetic ties existing between the molecules. As these ties impose constraints to rotational motion, the energy acquired will be both potential and kinetic. The two degrees of rotational freedom thus added to the three degrees of translatory freedom give a total of five degrees of freedom, which would account for the number 5 in the formula.

At the critical temperature, the thermal agitation is assumed to be violent enough to rupture the magnetic or other molecular ties affecting rotation and, whilst the kinetic energy is preserved, the potential energy of rotations of two degrees of freedom vanishes, and its loss accounts for the discontinuity of the specific heat. If the potential and kinetic energies are equal, the discontinuity will be one-fifth of the whole specific heat, provided no change of molecular structure has taken place. With nickel and Heusler's alloy, in which there is no change in the molecule,  $\Delta c$  is very closely one-fifth of  $C_\theta$ . Where there is a change from two atoms to one,  $\Delta c$  is two-fifths of  $C_\theta$ .

(c) In a former paper (Phil. Mag. xlvii. p. 848, May 1924) reasons were given for considering the energy change on passing through the critical temperature as  $\rho R\theta/an$ , and this is not inconsistent with the values of the discontinuity of the specific heat if we understand  $R/an$  to apply to the equation,

$$\frac{\rho R\theta}{an} = \frac{8}{27} a' I_0^3,$$

whilst  $\Delta c$  applies to

$$J\rho n\Delta c\theta = a' I_0^3.$$

The first of these equations might be written

$$\frac{\rho R\theta}{an} = a' \left(\frac{2}{3} I_0\right)^3 = a' (I_0 - I_c)^3$$

since  $I_c$ , the critical intensity, is  $\frac{1}{3} I_0$ , and from this it appears that  $R/an$  refers to an energy change measured by loss of intensity of magnetization from  $I_0$  to  $I_c$ , while  $\Delta c$  is measuring the whole loss of  $I_0$ .

#### 9. Ratios of the principal magnetic and thermal constants in groups of ferromagnetics.

When the constants  $a'$ ,  $R'$ ,  $I_0$ ,  $\theta$ ,  $\Delta c$ , and  $C_\theta$  are compared in pairs of ferromagnetics, it is found that iron and nickel fall into one group and cobalt and magnetite fall into another group. A comparison of these groups is set out in Table VII.

TABLE VII.

	$a'$ .	$R'$ .	$I_0$ .	$\theta$ .	$\Delta c$ .	Increment of specific heat. ( $C_\theta - C_{15}$ )	$C_\theta$ .
I. { Iron Nickel }	·085	·17	3·3	1·6	4·0	4·0	2·0
II. { Cobalt Magnetite }	·09	·17	3·0	1·6	1·23	1·25	0·9

Table of Fundamental Quantities and Constants.

	Iron.	Cobalt.	Nickel.	Heusler alloy.	Magnetite.
$a$ ...	55.85	58.97	58.68	—	—
$\rho$ ...	7.85	8.6	8.9	6.6	5.1
$\theta$ ...	1058° <sup>(1)</sup>	1349° <sup>(2)</sup>	661° <sup>(3)</sup>	633° <sup>(4)</sup>	853° <sup>(5)</sup>
$I_0$ ...	1817 <sup>(6)</sup>	1422 <sup>(7)</sup>	522 <sup>(8)</sup>	420 <sup>(9)</sup>	477 <sup>(10)</sup>
$R'$ ...	3.56 <sup>(11)</sup>	6.0 <sup>(12)</sup>	20.8 <sup>(13)</sup>	34 <sup>(14)</sup>	35 <sup>(15)</sup>
$a'$ ...	7.0	19.2	83.7	173	204
$n$ ...	1	1	2	2	3/2
$q$ ...	2	3.2	4	5	6
$\rho R/a$ ..	$11.70 \times 10^6$	$12.14 \times 10^6$	$12.6 \times 10^6$	$10.7 \times 10^6$	$11.75 \times 10^6$
$R'I_0^2$ ..	$11.76 \times 10^6$	$12.13 \times 10^6$	$6.34 \times 10^6$	$6.00 \times 10^6$	$7.67 \times 10^6$
$R/aJ$ ...	0.0356	0.0338	0.0339	(116/3 = .0387)	(165/3 = .055)
$a'I_0^3$ ...	$4.197 \times 10^{10}$	$5.52 \times 10^{10}$	$1.41 \times 10^{10}$	$1.28 \times 10^{10}$	$2.21 \times 10^{10}$
$\Delta c$ ...	0.120	0.098	0.029	0.036	0.079
$C\theta$ ...	0.309	0.270	0.154	0.179	0.299
$C_{15}$ ...	0.112	0.107	0.109	0.116	0.165

(1) and (3) Ashworth, Phil. Mag., Jan. 1912.

(2) Stiffler, Phys. Rev. ix p. 373 (1910).

(4) Ashworth.

(5) Weiss, Piccard, and Carrard, *Arch. des Sc.* xlii. p. 378; xliii. p. 22.

(6), (7), and (8) Ashworth, Phil. Mag. xxxvi. p. 351 (Oct. 1918).

(9) Ashworth (unpublished).

(10) Weiss, Piccard, and Carrard, *Arch. des Sc.* xlii. p. 378.

(11) Curie, 'Œuvres,' p. 227.

(12) Weiss and Bloch, *Arch. des Sc.* xxxiii. p. 293.

(13) Weiss and Foëx, *Arch. des Sc.* xxxi. pp. 5 and 89.

(14) Ashworth (unpublished).

(15) Weiss and Foëx, *Arch. des Sc.* xxxi. pp. 5 to 161.

$A$  = Curie's constant.

$J$  = Mechanical equivalent of heat =  $4.18 \times 10^7$ .

$R$  = Gas constant =  $83.2 \times 10^5$  ergs per degree C. for a gram molecule.

$a$  = Atomic weight.

$\rho$  = Density in grams per cubic centimetre.

$\theta$  = Critical temperature on the absolute scale.

$I_0$  = Maximum intensity of magnetization.

$R' = 1/kT$  = the reciprocal of Curie's constant.

$a'$  = Intrinsic field constant =  $H/I^2$ .

$n$  = Number of atoms in molecule above the critical temperature.

$q$  = Ratio  $a'/R'$ .

$\Delta c$  = Discontinuity of the specific heat.

$C\theta$  = True specific heat at the critical temperature.



Some of the correspondences observed in Table VII. must necessarily follow from the fact that the  $q$  values of iron and nickel have a ratio (2/4) the same as the  $q$  values of cobalt and magnetite (3/6). This applies to  $a'$  and  $R'$  and to  $I_0$  and  $\theta$ . The explanation of the observed value of any one of these ratios is, however, obscure. Nevertheless it is clear that the several ferromagnetics are intimately related, and the meaning of these simple ratios will probably throw light on ferromagnetism and the structure of ferromagnetic bodies.

10. The table on p. 693 gives a list of some principal and useful quantities in ferromagnetism. Iron and nickel have been investigated more thoroughly than the other ferromagnetics, and the values given for their constants are probably not far from the truth; but with magnetite, and more particularly cobalt and Heusler's alloy, our knowledge of the constants is less precise. A complete revision of all would be of great use in the development of magnetic theory.

11. *Summary of Equations.*

$$\text{I. } \begin{cases} A = kT. \\ R' = 1/A. \end{cases}$$

$$\text{II. } R'I_0^2 = \rho R/an.$$

$$\text{III. } \begin{cases} (HI_0 + a'I_0 I^2) \left( \frac{I_0}{I} - 1 \right) = \frac{\rho RT}{an}. \\ \frac{\rho R_\theta}{an} = \frac{8}{27} a' I_0^3; \quad I_c = \frac{I_0}{3}; \quad H_c = \frac{a' I_0^2}{27}. \end{cases}$$

$$\text{IV. } \theta/I_0 = \frac{8}{27} q; \quad q = \frac{a'}{R'}.$$

$$\text{V. } \begin{cases} n\Delta c\theta J\rho = a' I_0^3. \\ n\Delta cJ = \frac{27}{8} R/an. \end{cases}$$

$$\text{VI. } C_\theta = \frac{5}{2} n\Delta c.$$

**LXV. A Note on Approximation Curves for a Fourier Series.**  
*By H. V. LOWRY, The College of Technology, Manchester\*.*

IF  $S_n(x)$  is the sum of the first  $n$  terms of the Fourier series for  $f(x)$ , the curve  $y=S_n(x)$  is usually called an "approximation curve," and it nearly coincides with  $y=f(x)$ , when  $n$  is large enough.

We can devise other functions which approximate to the Fourier series. The object of this paper is to show one such way of approximating to the series

$$2(\sin x - \frac{1}{2} \sin 2x + \frac{1}{3} \sin 3x - \dots). \quad (1)$$

The method used also gives an insight into the origin of the discontinuities in the sum of this series.

When  $n$  is an integer

$$\sin^{2n}(\frac{1}{2}x) = \frac{2n!}{2^{2n-1}(n!)^2} \left\{ 1 - \frac{n}{n+1} \cos x + \frac{n(n-1)}{(n+1)(n+2)} \cos 2x - \dots + (-1)^n \frac{n(n-1)\dots 1}{(n+1)\dots 2n} \cos nx \right\},$$

whence, integrating from 0 to  $x$ ,

$$\int_0^x \sin^{2n} \frac{1}{2} u du = \frac{2n!}{2^{2n-1}(n!)^2} \left\{ x - \frac{n}{n+1} \sin x + \frac{n(n-1)}{(n+1)(n+2)} \frac{\sin 2x}{2} - \dots + (-1)^n \frac{n(n-1)\dots 1}{(n+1)\dots 2n} \frac{\sin nx}{n} \right\}.$$

This equation can be written

$$\begin{aligned} & 2 \left[ \frac{n}{n+1} \sin x - \frac{n(n-1)}{(n+1)(n+2)} \frac{\sin 2x}{2} \right. \\ & \quad \left. + \frac{n(n-1)(n-2)}{(n+1)(n+2)(n+3)} \frac{\sin 3x}{3} - \dots \right] \\ & \quad = x - \frac{2^{2n}(n!)^2}{2n!} \int_0^x \sin^{2n}(\frac{1}{2}u) du. \quad (2) \end{aligned}$$

When  $n \rightarrow \infty$  the left-hand side of (2) approaches the

\* Communicated by the Author.

series (1). Hence the behaviour of (1) can be deduced from the limiting form of the right-hand side of (2).

Now

$$\frac{2^{2n}(n!)^2}{2n!} \int_0^x \sin^{2n}(\tfrac{1}{2}u) du < \frac{2^{2n}(n!)^2 \sin^{2n}(\tfrac{1}{2}x)\pi}{2n!}, \quad (3)$$

when  $0 < x < \pi$ ; but, by Stirling's theorem,

$$\frac{2^{2n}(n!)^2}{2n!} = \sqrt{\pi n} \quad \text{nearly,}$$

when  $n$  is large, and hence by (3)

$$\lim_{n \rightarrow \infty} \frac{2^{2n}(n!)^2}{2n!} \int_0^x \sin^{2n}(\tfrac{1}{2}u) du = 0,$$

provided  $0 < x < \pi$ .

On the other hand, whatever the value of  $x$ ,

$$\frac{2^{2n}(n!)^2}{2n!} \int_0^\pi \sin^{2n}(\tfrac{1}{2}u) du = \pi. \quad (4)$$

From (3) and (4) it follows that

$$\lim_{n \rightarrow \infty} \frac{2^{2n}(n!)^2}{2n!} \int_x^\pi \sin^{2n}(\tfrac{1}{2}u) du = \pi, \quad (5)$$

and by changing the variable to  $2\pi - u$  we find that

$$\lim_{n \rightarrow \infty} \frac{2^{2n}(n!)^2}{2n!} \int_\pi^x \sin^{2n}(\tfrac{1}{2}u) du = \pi, \quad (6)$$

when  $\pi < x < 2\pi$ , however near  $x$  is to  $\pi$ .

From (3), (5), and (6) we deduce that

$$\begin{aligned} \lim_{n \rightarrow \infty} \frac{2^{2n}(n!)^2}{2n!} \int_0^x \sin^{2n}(\tfrac{1}{2}u) du \\ = 0 \quad \text{when } 0 < x < \pi, \\ = \pi \quad \text{when } x = \pi, \\ = 2\pi \quad \text{when } \pi < x < 3\pi, \end{aligned}$$

and generally

$$= 2r\pi \quad \text{when } (2r-1)\pi < x < (2r+1)\pi.$$

Therefore, when  $n \rightarrow \infty$ , (2) takes the form

$$\begin{aligned} 2[\sin x - \tfrac{1}{2} \sin 2x + \tfrac{1}{3} \sin 3x - \dots] = x - 2r\pi, \\ \text{when } (2r-1)\pi < x < (2r+1)\pi. \end{aligned}$$

Thus we have seen, in an elementary way, how the discontinuities arise in the Fourier series (1).

When  $n$  is large (3) is still very nearly true, and hence we may take

$$y = 2 \left[ \frac{n}{n+1} \sin x - \frac{n(n-1)}{(n+1)(n+2)} \frac{\sin 2x}{2} + \frac{n(n-1)(n-2)}{(n+1)(n+2)(n+3)} \frac{\sin 3x}{3} - \dots \right] \quad (7)$$

as an approximating curve to the Fourier series.

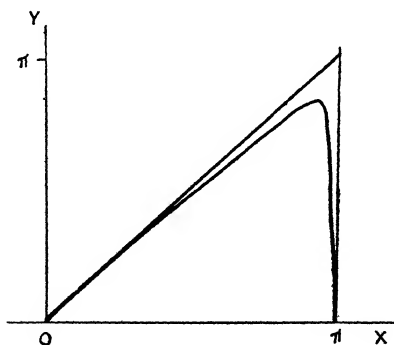
(2) shows that  $y$  is always less than  $x$ , when  $0 < x < \pi$ , and hence there can be no Gibbs's phenomenon for such approximation curves. Moreover, by (2)

$$\frac{dy}{dx} = 1 - \frac{2^{2n}(n!)^2}{2n!} \sin^{2n}(\tfrac{1}{2}x),$$

whence we deduce that  $y$  has only one turning value, namely, a maximum, given by

$$\sin(\tfrac{1}{2}x) = \left( \frac{2n!}{2^{2n}(n!)^2} \right)^{\frac{1}{2n}} = \left( \frac{1}{\pi n} \right)^{\frac{1}{4n}} \text{ nearly,}$$

which is close to 1 for all values of  $n$ . Therefore  $y$  has a maximum value near  $x = \pi$ . Moreover,  $\frac{d^2y}{dx^2}$  is negative for all values of  $x$ , and therefore gradient decreases continuously from  $x=0$  to  $x=\pi$ . Therefore the general shape of the approximation curve (7) is



LXVI. *The Statistical Theory of Para- and Diamagnetism.*  
*By* EMRYS HOWELLS, M.Sc. \*.

THE foundations of the statistical theory of the magnetic properties of matter were laid by Langevin in 1905 †, and the main features of his work have permeated molecular theories since that time. The molecules were assumed to have orbital electrons which were equivalent to the molecular currents of Ampère and Weber and the consequent magnetism observed; this conception was applied by Langevin to the simple case of a gaseous medium.

One effect of the application of a magnetic field is the acceleration of the electrons in their orbits; diamagnetism is then ascribed to the resulting deformation of the electronic orbits, and the effect, being an affair of the internal constitution of the molecules, is practically independent of temperature. This occurs whether the molecules have a resultant magnetic moment or not.

When the molecular magnetic moments are not zero a paramagnetic effect is superimposed. Under the action of an applied magnetic field the molecules tend to orientate themselves in positions of lower potential energy—that is, with their axes in the direction of the field; this tendency is counteracted by the mutual collisions of the molecules which re-distribute the kinetic energy obtained from the field partly as kinetic energy of rotation and partly as kinetic energy of translation with a consequent conversion into heat. The condition of equilibrium is finally attained when the tendency to alignment with the field is balanced by the attempts of the collisions to turn the axes in all directions. The problem then yields to statistical treatment in the determination of the equilibrium distribution function and the calculation of the relation between the intensity of magnetization and the magnetic field.

It is clear that the problem reduces (on the basis of equipartition and classical statistics) to the determination of the distribution function for the final equilibrium state of magnetization; this analysis depends essentially on the assumptions made as to what is conserved during the collisions and interaction of the molecules. Langevin assumed that the molecules of a paramagnetic gas have equal and constant magnetic moments, and effects due to rotations about other

\* Communicated by Prof. G. H. Livens.

† *Ann. de Chim. et Phys.* (8) v. p. 70 (1905).

axes together with intra-molecular forces were ignored, with the result that many experimental facts are not in accord with his form of the theory.

Among the attempts made to improve on Langevin's theory of para- and diamagnetism may be mentioned the work of Gans \*, who assumed that substances are constituted of rigid axial magnetons which consist of negative electrons within a uniformly charged positive sphere. As pointed out by Livens †, the evaluation of the energy expression in the distribution formula, however, contains a series of errors which seriously influence his final results. This form of the theory, with certain modifications, can, however, be retained in seeking a generalization of the Langevin analysis to embrace both para- and diamagnetism.

We assume that the rotation of a molecule about an axis with angular momentum  $\Psi$  is equivalent to a magnetic moment  $\mu\Psi$ , where

$$\mu = \frac{e}{2mc} \text{ (electromagnetic units)}$$

is the equivalent magnetic moment of a single orbital electron having unit angular momentum,  $e$  being the electric charge on the electron measured in electromagnetic units,  $m$  its mass, and  $c$  the ratio of the electromagnetic measure of charge to the electrostatic ‡. If, then, we assume an axis of symmetry, and use the Eulerian coordinates  $(\theta, \phi, \psi)$  for the axes of principal inertia with corresponding moments  $A, A, C$ , the kinetic energy of the rotatory motions which are dynamically independent of the translatory motion is of the form

$$T = \frac{1}{2} [A(\dot{\theta}^2 + \sin^2 \theta \dot{\psi}^2) + C(\dot{\psi} + \dot{\phi} \cos \theta)^2].$$

In addition, there is the magnetic potential energy, which, if the applied magnetic force  $B$  is along the polar axis of the coordinates, is

$$V = -\mu B [A\dot{\phi} \sin^2 \theta + C \cos \theta (\dot{\psi} + \dot{\phi} \cos \theta)],$$

the term in the square brackets representing the component of the resultant momentum in the direction of  $B$ .

According to the general theory, the distribution function defining the number of molecules with their space and

\* Gans, *Ann. d. Phys.* xl. p. 149 (1916); l. p. 163 (1916).

† Livens, *Ann. d. Phys.* lxxv. p. 822 (1924).

‡ Livens, 'Theory of Electricity,' ed. 2, p. 391.

velocity coordinates in the usual differential range is  $e^{-\frac{E}{R\theta}}$ , where  $E$  is the total energy. In the Gans \* analysis this is taken to be the sum of the kinetic and potential energies of the axial magneton; this quantity, however, is not necessarily conserved on interaction of the molecules, and the correct expression must be sought in a more general way. In dynamical theory it is shown that for a general system defined by coordinates  $q_1, q_2, \dots, q_n$ , the quantity

$$E = -L + \sum_{i=1}^n \frac{\partial L}{\partial \dot{q}_i} \dot{q}_i$$

(where  $L = T - V$ ) is such a function. When  $L$  involves the velocities  $\dot{q}_i$  only as a homogeneous quadratic function the expression  $E$  reduces to  $T + V$ , but in other cases, as the present, where  $L$  contains terms linear in the velocities, no such reduction is possible. Then

$$L = \frac{1}{2}[A(\dot{\theta}^2 + \sin^2 \theta \dot{\phi}^2) + C(\dot{\psi} + \dot{\phi} \cos \theta)^2] \\ + \mu B[A\dot{\phi} \sin^2 \theta + C \cos \theta(\dot{\psi} + \dot{\phi} \cos \theta)],$$

and

$$E = \frac{1}{2}A(\dot{\theta}^2 + \sin^2 \theta \dot{\phi}^2) + \frac{1}{2}C(\dot{\psi} + \dot{\phi} \cos \theta)^2.$$

The momenta are defined generally from the Lagrangian function  $L$  by the equations

$$\Theta = \frac{\partial L}{\partial \dot{\theta}} = A\dot{\theta},$$

$$\Phi = \frac{\partial L}{\partial \dot{\phi}} = A \sin^2 \theta \dot{\phi} + C \cos \theta(\dot{\psi} + \dot{\phi} \cos \theta) \\ + \mu B[A \sin^2 \theta + C \cos \theta],$$

$$\Psi = \frac{\partial L}{\partial \dot{\psi}} = C(\dot{\psi} + \dot{\phi} \cos \theta) + \mu B C \cos \theta,$$

so that  $E$  can be written in the form

$$E = \frac{\Theta^2}{2A} + \frac{(\Phi - \Psi \cos \theta - \mu B A \sin^2 \theta)^2}{2A \sin^2 \theta} + \frac{(\Psi - \mu B C \cos \theta)^2}{2C}.$$

The number of elements per unit-volume for which the variables  $\Theta, \Phi, \Psi, \theta, \phi, \psi$  lie within the differential range  $d\Omega$  is

$$dn = ae^{-\frac{E}{R\theta}} d\Omega,$$

\* Gans, *Ann. d. Phys.* xlix. p. 154 (1916); see also Lennard-Jones, *Proc. Phys. Soc.* xl. [5] (1928).

where

$$d\Omega = \sin \theta \, d\theta \, d\phi \, d\psi \, d\Theta \, d\Phi \, d\Psi.$$

The constant  $a$  is determined from the fact that the total number  $n$  of the molecules per unit-volume is specified, so that

$$n = a \int_{-\infty}^{\infty} e^{-\frac{E}{kT}} d\Omega.$$

Now each of the molecules in  $d\Omega$  contributes to the magnetization along the direction of  $B$  an amount

$$\mu [A\dot{\theta} \sin^2 \theta + C \cos \theta (\dot{\psi} + \dot{\phi} \cos \theta)],$$

so that on the whole

$$\begin{aligned} I &= a\mu \int_{-\infty}^{\infty} [A\dot{\phi} \sin^2 \theta + C \cos \theta (\dot{\psi} + \dot{\phi} \cos \theta)] e^{-\frac{E}{kT}} d\Omega, \\ &= a\mu \int_{-\infty}^{\infty} [\Phi - \mu B (A \sin^2 \theta + C \cos^2 \theta)] e^{-\frac{E}{kT}} d\Omega, \\ &= n\mu \frac{\int_{-\infty}^{\infty} [\Phi - \mu B (A \sin^2 \theta + C \cos^2 \theta)] e^{-\frac{E}{kT}} d\Omega}{\int_{-\infty}^{\infty} e^{-\frac{E}{kT}} d\Omega} \end{aligned}$$

If, as assumed by Gans, the limits for  $\Phi$  and  $\Psi$  are from  $-\infty$  to  $+\infty$  the integration yields a zero result—that is, if the range of variation of the motion in the rotatory coordinates is unrestricted, the resultant effect of the magnetic field is zero, no resultant polarity either of diamagnetic or paramagnetic character will be induced. If, then, a definite result is to be obtained, it is necessary to restrict the variation of at least one of the rotation momenta  $\Phi$  and  $\Psi$ . It is difficult to say what limitations should be imposed, but in view of modern theories as to the structure of the atom, it is at least reasonable to suppose that  $\Psi$  is restricted to one or more definite constant values, the same for all molecules. We will first try one single value for  $\Psi$ , and also, as a further simplification and to make the expressions tractable, we shall assume that  $A$  is negligibly small; for an electronic orbit this approximation is probably also justifiable, but in any case it enables us to obtain some idea of the form of the ultimate results.



Under these conditions we have then \*

$$I = \frac{n\mu \int_0^\pi (\Psi - \mu BC \cos \theta) e^{-\frac{E}{R\theta}} \sin \theta \cos \theta d\theta}{\int_0^\pi e^{-\frac{E}{R\theta}} \sin \theta d\theta},$$

where

$$E = \frac{(\Psi - \mu BC \cos \theta)^2}{2C},$$

or, putting  $x = \Psi - \mu BC \cos \theta$ ,

$$I = \frac{\int_{\Psi - \mu BC}^{\Psi + \mu BC} x(\Psi - x) e^{-\frac{x^2}{2RC\theta}} dx}{\int_{\Psi - \mu BC}^{\Psi + \mu BC} e^{-\frac{x^2}{2RC\theta}} dx}$$

The polarization is therefore in part paramagnetic and in part diamagnetic, the former arising from the permanent angular momentum  $\Psi$  and the latter from the induced angular momentum  $-\mu BC \cos \theta$ . That these effects co-exist was pointed out by Gans †; the paramagnetism is caused by the thermal agitation of the molecules, so that the diamagnetism, which is an internal phenomenon, can predominate at sufficiently high temperatures. It is conceivable that in certain circumstances the two effects may just balance with the result that the medium appears to be non-magnetic.

Integration of the numerator leads to

$$I = \frac{nR\theta}{B} \frac{\left[ \mu BC \left\{ e^{-\frac{(\Psi + \mu BC)^2}{2RC\theta}} + e^{-\frac{(\Psi - \mu BC)^2}{2RC\theta}} \right\} - \int_{\Psi - \mu BC}^{\Psi + \mu BC} e^{-\frac{x^2}{2RC\theta}} dx \right]}{\int_{\Psi - \mu BC}^{\Psi + \mu BC} e^{-\frac{x^2}{2RC\theta}} dx}$$

$$= \frac{nR\theta}{B} \frac{\left[ 2\mu BC e^{-\frac{\Psi^2 + \mu^2 B^2 C^2}{2RC\theta}} \cosh \frac{\mu B \Psi}{R\theta} - \int_{\Psi - \mu BC}^{\Psi + \mu BC} e^{-\frac{x^2}{2RC\theta}} dx \right]}{\int_{\Psi - \mu BC}^{\Psi + \mu BC} e^{-\frac{x^2}{2RC\theta}} dx}.$$

\* These formulæ were given by Livens, 'Theory of Electricity,' ed. 2, pp. 393-394.

† *Gött. Nachr.* p. 197 (1910).

The complete integration gives difficulty, but under ordinary conditions of temperature and magnetic inducing force the numerator and denominator can be expanded, and only a few terms are required. The resultant magnetic intensity then becomes

$$I = \frac{n\mu^2\Psi^2B}{3R\mathfrak{S}} - \frac{n\mu^2CB}{3},$$

and susceptibility

$$\chi = \frac{n\mu^2\Psi^2}{3R\mathfrak{S}} - \frac{n\mu^2C}{3}.$$

The first term represents the paramagnetism varying inversely as the absolute temperature in accordance with Curie's law \*, which is well verified for paramagnetic gases and is in good agreement with observations for certain paramagnetic solutions and for some solid salts.

The second term stands for the diamagnetism, which, as expected, is independent of the temperature. Generally speaking the two types will be present; the one or the other will predominate according to temperature—a rise in temperature being favourable to diamagnetism.

The condition for a resultant diamagnetic effect is

$$\frac{\Psi^2}{C} < R\mathfrak{S},$$

or

$$\frac{1}{2}C\omega^2 < \frac{1}{2}R\mathfrak{S},$$

where  $\omega$  is the angular velocity of a molecule about its axis. In other words, the kinetic energy of the rotatory motion of a molecule must be less than the energy of translation. If the particular temperature at which this change of magnetism is observed for a substance, an estimate of  $\frac{\Psi^2}{C}$  can be made.

The first term in the magnetic intensity is the outcome of the view that paramagnetism arises from the effort of the magnetic field to orientate the molecules which are spinning about as the result of gaseous encounters. If, therefore, the whole of the internal energy of the medium associated with its magnetization is to be regarded as added thermal energy, then Curie's law is a natural result,

$$\chi = \frac{\Delta}{\mathfrak{S}}.$$

\* Curie, *Ann. de Chim. et Phys.* (7) v. pp. 289-405 (1895); see also Auerbach, 'Modern Magnetism,' ch. viii.-ix.

If only the proportion  $\frac{S}{S+\Delta}$  of the internal energy is converted into heat, we shall have a modified law of the form

$$\chi = \frac{\Delta}{S+K}.$$

There are a number of substances, including paramagnetic solids, which obey this form of variation with temperature\*.

### *The Internal Field.*

In the case of a gas the mutual magnetic influence of the neighbouring molecules can be neglected, but when the molecules are very close together, as in a solid body, the local interaction field may assume large proportions†. The nature of the field is unknown; it is not necessarily electric or magnetic in character, but progress is not impossible.

It is evident that we cannot deal with the highly irregular field of the individual molecules, and therefore we take an average estimate of this variable magnitude, which is regarded as constant over the physically small element of volume on account of the enormous number of molecules contained in it.

Weiss postulates that, on an average, the molecular field is proportional to the intensity of magnetization, so that the complete magnetic force is

$$B + \alpha I.$$

Following Weiss, we can obtain a theory for solid bodies by substituting this complete value instead of  $B$  in the general expression which still retains its form. In particular, if there is no applied magnetic inducing force,  $B = 0$ , and we have, if  $I_s = n\mu\Psi$ ,

$$I = \frac{I_s \left[ \frac{nR\bar{S}}{\alpha II_s} \left\{ 2\mu C\alpha I e^{-\frac{1}{2RC\bar{S}} \left( \frac{I_s^2}{\mu^2 n^2} + \mu^2 \alpha^2 I^2 C^2 \right)} \cosh \frac{\alpha II_s}{nR\bar{S}} - \int_{\frac{I_s}{\mu n} - \mu C\alpha I}^{\frac{I_s}{\mu n} + \mu C\alpha I} e^{-\frac{x^2}{2RC\bar{S}}} dx \right\} \right]}{\int_{\frac{I_s}{\mu n} - \mu C\alpha I}^{\frac{I_s}{\mu n} + \mu C\alpha I} e^{-\frac{x^2}{2RC\bar{S}}} dx}.$$

Besides‡ the zero solution,  $I = 0$ , there is another solution,

\* Livens, 'Theory of Electricity,' Appendix i.; See also Weiss, *Journal d. Phys.* (4) vi. p. 661 (1907).

† Bull. Nat. Research Council, iii. pt. 3 (1922); Heisenberg, *Zeit. für Phys.* xlix. p. 619 (1928).

‡ Livens, 'Theory of Electricity,' ed. 2, p. 400; see also Peddie, 'Molecular Magnetism,' chap. iv.

and this accounts for permanent magnetization. Moreover, this non-zero solution, when it exists, represents the stable condition of the medium, because the magnetic potential energy in it is a minimum. The zero solution corresponds to a maximum value of the potential energy, and is therefore in general unstable.

At ordinary temperatures the approximate form is sufficiently accurate even for high values of the magnetic field. This gives

$$I = \frac{\alpha I_s^2 I}{3nR\mathfrak{S}},$$

and indicates a limiting temperature,

$$\mathfrak{S}_s = \frac{\alpha I_s^2}{3nR},$$

at which spontaneous magnetization becomes possible. If we introduce this critical temperature into the relation

$$I = \frac{I_s^2 (B + \alpha I)}{3nR\mathfrak{S}}$$

we have

$$I = \frac{B\mathfrak{S}_s}{\alpha(\mathfrak{S} - \mathfrak{S}_s)}.$$

This is Weiss's modification of the Curie law already mentioned; the expression retains its form, but the temperature is now measured from the critical point  $\mathfrak{S}_s$ . Many substances obey the modified law, and determinations of  $\alpha$  have been made\*. Values of the order  $10^6$  absolute units have been obtained, so that it is not surprising that the intensity of magnetization does not sometimes appear to be affected by the external applied field.

### *Low Temperature Considerations.*

The investigation of the magnetic behaviour of substances at low temperatures has caused considerable difficulty both experimentally and theoretically. It is now of interest to examine how far the present theory, based on classical statistical mechanics, can account for the peculiar deviations from the simple linear laws.

\* Stoner, 'Magnetism and Atomic Structure,' chap. iv.; *vide* Bull. Nat. Res. Council, p. 119.

The general expression for the magnetic intensity can be written

$$I = nR\vartheta \frac{\partial}{\partial B} \log \left\{ \frac{1}{\mu BC} \int_{\Psi - \mu BC}^{\Psi + \mu BC} e^{-\frac{x^2}{2RC\vartheta}} dx \right\}$$

$$= nR\vartheta \frac{\partial}{\partial B} \log \left[ 2e^{-\frac{\Psi^2}{2RC\vartheta}} \left\{ 1 + \frac{\mu^2 B^2 C^2}{3!} \left( \frac{\Psi^2}{R^2 C^2 \vartheta^2} - \frac{1}{RC\vartheta} \right) \right. \right.$$

$$\left. \left. + \frac{\mu^4 B^4 C^4}{5!} \left( \frac{\Psi^4}{R^4 C^4 \vartheta^4} - \frac{6\Psi^2}{R^3 C^3 \vartheta^3} + \frac{3}{R^2 C^2 \vartheta^2} \right) + \dots \right\} \right],$$

giving

$$\frac{I}{n\mu\Psi} = \left( \frac{\mu\Psi B}{3R\vartheta} - \frac{\mu CB}{3\Psi} \right) - \left( \frac{\mu^3 \Psi^3 B^3}{45R^3 \vartheta^3} + \frac{4\mu^3 \Psi CB^3}{45R^2 \vartheta^2} - \frac{2\mu^3 B^3 C^2}{45R\vartheta\Psi} \right) + \dots$$

Taking  $\mu = \frac{e}{2mC} = .89.10^7$  electromagnetic units, and for the magnetic moment \*

$$\mu\Psi = 3.6.10^{-21},$$

we have for the angular momentum

$$\Psi = 4.10^{-28}.$$

Moreover, if  $B = 10^3$  gauss,

$R$  = Boltzmann's gas constant for single molecule,

$$= 1.36.10^{-16} \text{ erg per degree,}$$

moment of inertia  $C = 10^{-41}$  gram cm.<sup>2</sup>,

$$\vartheta = 300^\circ,$$

we have, for order of terms,

$$\frac{I}{n\mu\Psi} = (10^{-5}) - (10^{-11}) + \text{smaller quantities.}$$

Under ordinary conditions the first bracket is sufficient; it is clear that fall of temperature to (say)  $10^\circ$  will not demonstrate any material variation from the usual law. The additional terms will not assert themselves until  $\vartheta$  is below  $1^\circ$ . Variations, however, are known to occur at  $70^\circ$  for some substances. To explain this it is necessary to assume that the extra terms hitherto neglected become large by a

\* These values are taken from the work of Reiche, Von Weyssenhoff, and Oosterhuis, Bull. Nat. Res. Council, pp. 101-102.

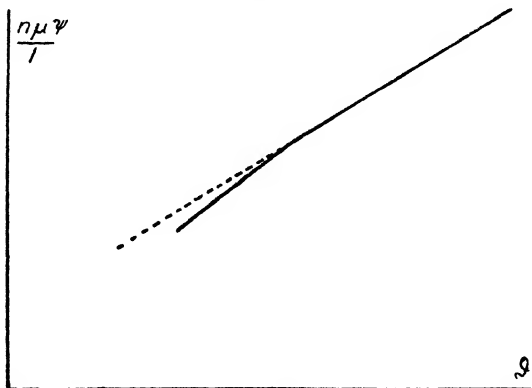
substantial increase in the force  $B$ , which is here taken quite generally to include any local field, if necessary; this is not an unreasonable assumption, as powerful intra-molecular fields are known to exist and must be expected to become effective in the regions of temperature where the molecules come much closer together, finally leading to the domination of crystal structure.

If, for example, we insert the value  $10^6$  for  $B$ , which is of the order determined experimentally by Oxley and others\*,

$$\frac{I}{n\mu\Psi} = (0.029 - 0.074) - (0.01),$$

the modifying term being negative. In the graph of  $\frac{n\mu\Psi}{I}$

Fig. 1.



against  $\Theta$  this would indicate a deviation from the straight line. This term may also be positive; in fact, it is at first at very low temperatures positive, and becomes negative with decreasing temperature. The positive deviation is shown in fig. 1.

This is followed by the opposite deviation, shown in the lower part of fig. 2.

If the new term gains supremacy there arises the possibility of maximum and minimum positions indicated in fig. 3. At the very lowest temperatures the temperature factor

$e^{-\frac{x^2}{2RC\Theta}}$  in the integrals becomes exceedingly small, and the

\* *Journ. d. Phys.* (4) vi. p. 661 (1907); Stoner, 'Magnetism and Atomic Structure,' chap. iv.

integration gives the saturation value  $n\mu\Psi$ . This accounts for the result that the intensity becomes practically independent of temperature just above absolute zero.

An extensive series of experiments has been conducted by Jackson \* on paramagnetism at low temperatures. A few

Fig. 2.

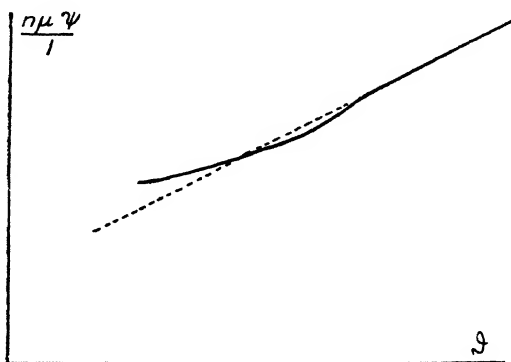
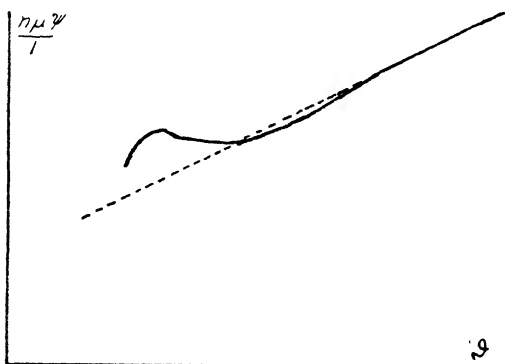


Fig. 3.



substances obey the Curie law down to the lowest temperatures; others conform to Weiss's modification of the same law, still retaining the linear relationship. However, it was found that deviations occur. Considering double sulphates, a curve similar to that of fig. 1 was obtained, the intensity

\* Phil. Trans. A, cciv. pp. 1-48 (1923).

increasing more rapidly with fall of temperature than is indicated by the linear law. The effect was considerable in the case of cobalt ammonium sulphate, less with nickel ammonium sulphate, and too small for measurement with ferrous ammonium sulphate. Jackson also obtained the cryomagnetic effect illustrated by the lower portion of the curve in fig. 2; in this case the intensity increases less rapidly with fall in temperature than is demanded by the usual relation. Certain salts also exhibited a maximum or minimum at the lowest temperatures.

We have succeeded in showing the character of the deviations by postulating a large local field; the magnitude of the effects depends on the strength of the field and on how it grows and gains dominance with falling temperature. The increasing field and decreasing temperature assist in magnifying the effects as we proceed down the temperature scale.

### Quantum Modifications.

It may be objected that the analysis is based on classical equipartition ideas; according to Planck's First Quantum Theory the mean energy of an oscillator of frequency  $\nu$  is

$$\bar{\epsilon} = \frac{h\nu}{e^{R\theta} - 1},$$

where  $h = 6.558 \cdot 10^{-27}$  erg-secs. (Planck's constant). At ordinary temperatures the expansion of the expression gives  $R\theta$ , but at low temperatures this is inaccurate. Since the new value is smaller than  $R\theta$ , the introduction of Planck's form simply serves to increase the deviations (particularly at the lower part of the scale) without affecting their character. The saturation point would be reached sooner, and complete magnetic saturation would prevail over a certain range of temperature.

On the classical theory the law of distribution is a continuous one, and integration is taken over all values. According to the orientation law of quantization only certain positions are possible. If  $\theta$  is the angle between the direction of the effective moment of the magnet and the field  $B$ , the values are determined by

$$\cos \theta = \frac{1}{m}, \frac{2}{m}, \frac{3}{m}, \frac{4}{m}, \dots, \frac{m}{m},$$

where  $m$  is an integer.



## 710 *The Statistical Theory of Para- and Diamagnetism.*

Acting on this assumption the general expression becomes

$$I = nR\vartheta \frac{\partial}{\partial B} \log \sum e^{-\frac{(\Psi - \mu BC \cos \theta)^2}{2RC\vartheta}}$$

or \*

$$I = nR\vartheta \frac{\partial}{\partial B} \log \sum_1^n e^{-\frac{\Psi^2}{2RC\vartheta} + \frac{\mu B\Psi}{R\vartheta} \left(\frac{P}{m}\right) - \frac{B^2 C}{2R\vartheta} \left(\frac{P}{m}\right)^2}.$$

If  $m = 1$ ,

$$\frac{I}{n\mu\Psi} = 1 - \frac{\mu BC}{\Psi}.$$

Since  $\cos \theta = 1$ , all the axes are orientated parallel to the field direction, and we expect the saturation value indicated.

If  $m = \infty, \dots, -\infty$ ,

$$\frac{I}{I_s} = -\frac{\mu BC}{3\Psi} + \frac{\mu B\Psi}{3R\vartheta}.$$

If we therefore regard the saturation value obtained for the case  $m = 1$  as what we expect at absolute zero, and the other value as the result for usual conditions, it seems that the restricting forces accounting for the quantized positions lose their power as the temperature rises, this being a parallel to the classical theory.

If it is assumed that the molecules can have other momenta values which are integral multiples of  $\Psi$ , it is found that the additional terms due to the factors  $e^{-\frac{2\Psi^2}{RC\vartheta}}, e^{-\frac{9\Psi^2}{2RC\vartheta}}, e^{-\frac{8\Psi^2}{RC\vartheta}}, \dots$  are negligible. From this it appears that when higher values are ascribed to the angular momenta the dominating terms are those corresponding to the smaller values, and the tendency to increase the magnetic intensity is almost negligible. The reason for this lies in the character of the distribution function—there being less tendency to alignment with the field direction under these conditions.

### *Summary and Conclusion.*

A generalization of Langevin's statistical theory of magnetization is developed somewhat on the lines laid down by Gans by assuming that the magnetization of the molecules arises from their angular motions and is influenced by the magnetic force. By making certain simple assumptions and developing the theory on classical lines it proves to be more

\* *Vide* R. H. Fowler, 'Statistical Mechanics,' chap. xii.

than adequate enough for giving a general description of the trend of magnetization. The paramagnetism appears as the Curie term, varying inversely with absolute temperature, and is the outcome of the permanent molecular angular momentum. The diamagnetism is constant, being independent of the temperature, and is ascribed to the induced angular momentum. With the introduction of a molecular field permanent magnetization is accounted for.

Even at low temperatures, where its failure is most to be expected, the theory succeeds in demonstrating the character of the typical deviations. On introducing a large local field the peculiarities become more pronounced and resemble those observed experimentally below  $70^{\circ}$ .

The effect of substituting Planck's function  $f(R\theta)$  for  $R\theta$  is to magnify the deviations, and indicates the probability of saturation over a range of temperature just above absolute zero; this is borne out by empirical evidence.

Quantum orientation corresponds to the general classical result for  $m = \infty$  and to the saturation value of zero temperature for  $m = 1$ , indicating greater freedom from restricting forces with rise of temperature.

The problem seems to turn about the term

$$\frac{\mu\Psi B}{f(R\theta)},$$

powers of which play an important rôle at low temperature and with strong fields. It becomes necessary to have a further knowledge of how and when the intra-molecular forces assert themselves with falling temperature, and this involves an acquaintance with the structural form of the medium.

---

LXVII. *Some Series in the Extreme Ultra-Violet Spark Spectra of Copper.* By F. C. CHALKLIN, Ph.D., University of Sheffield\*.

§1. IT has been found by Prof. O. W. Richardson and the writer† that many of the numerous critical potentials found for iron, cobalt, nickel, and copper in the soft, X-ray region could be arranged in series of the type

\* Communicated by Prof. O. W. Richardson, F.R.S.

† Proc. Roy. Soc. A, cxix. p. 64 (1928); cxxi. p. 218 (1928).

$A - \frac{b}{n^2}$ . More recently the writer\* has found that some of

his results for manganese could be treated in the same way.

The series scheme appears to be capable of extension to cover the low voltage effects found by Thomas† for iron, cobalt, nickel, and copper, using the same value of  $b$  as in the higher voltage series of the element concerned, but choosing a new value of  $A$ .

For copper, using the original value of  $b$ , 2360, and choosing for  $A$  the value 39.7 volts, the results given in Table I. are obtained. To conform with the previous notation, the initial energy level  $A$  has been called  $X_4$ .

TABLE I.

$b=2360$ ,  $X_4=39.7$  volts.

$n$ .	9.	10.	11.	12.	13.
$X - \frac{b}{n^2}$ ... ..	10.6	16.1	20.2	23.3	25.7
Experimental value...	$\overline{10.3}$	15.7	20.7	23.8	25.5

Values with a bar have also been used elsewhere.

The agreement shown between experimental results and the values from the series is quite good. The experimental effects obtained by Thomas at 12.3, 14.2, and 19.0 volts are left unexplained, but, apart from these, we are now able to account for all the discontinuities up to 40 volts. (The critical potentials at 33.7 and 35.5 volts are probably unresolved higher members of the series.)

TABLE II.

$n$ .	9.	10.	11.	12.	13.
$X_4 - \frac{b}{n^2}$ .. ..	13.9	19.6	23.8	27.0	29.5
Experimental break..	14.1	19.4	24.3	—	28.8

The weakness of this series lies in the smallness of the number of terms. The same difficulty applies to the corresponding series for iron, cobalt, and nickel. For these elements the series are further weakened by the absence of the critical potential for  $n=12$ . We venture to give this doubtful series for iron in Table II., firstly because it seems

\* Phil. Mag. ix. p. 847 (1930).

† Phys. Rev. xxv. p. 322 (1925); xxvi. p. 744 (1925).

to correspond to the more secure series just given for copper, and, secondly, because of the completeness with which the series scheme, thus extended, explains the critical potentials given by Thomas for iron. We find that, for this element, 36 out of 45 of Thomas's discontinuities are explained on the basis of the series scheme, with the same value of " $b$ " employed throughout. The value of  $X_4$  chosen is 43.8 volts, and the value of  $b$  used in all the iron series is 2420. Corresponding series can be applied to the low voltage effects for cobalt and nickel, with  $X_4=40.3$  and 41.3 volts respectively, and with  $b=2357$  volts in each case.

§ 2. Returning to the more secure series for copper, it is observed that it extends over a spectral region examined by Millikan and Bowen\* in their ultra-violet spark experiments. It is of obvious importance to discover whether or not the series suggested to account for the critical potentials have their counterpart in the spectroscopic work. The conditions are very different in the two types of experiment; in the former case the critical potentials are observed as a result of the excitation of radiations from a solid under electronic bombardment, and, in the second case, the spectral lines are excited in a probably ionized vapour by a spark discharge. It would, therefore, be surprising if we were to find identical series in the two cases, and a similarity is all that we can hope for. In the event of such a similarity being found, it will suggest that there is some common factor in the two modes of excitation.

It is found, however, that the Millikan results contain a series very nearly identical with the critical potential series. Using the series formula  $A_1 - \frac{b}{n^2}$  and putting  $A_1=39.62$  volts as compared with  $A=39.7$  volts in the critical potential case, and giving to  $b$  the value 2395, instead of 2360, we obtain the values shown in Table III.

In the table, and in succeeding tables, I have taken the liberty of changing Millikan and Bowen's wave-lengths into volts by the formula  $V = \frac{12345}{\lambda}$ . The series starts apparently for  $n=10$ , but the line for  $n=9$  would be

\* Phys. Rev. xxiii. p. 1 (1924).

outside the Millikan region. The term  $n=9$  is later shown to be present. The writer proposes to defer the discussion of the intensities until later in the paper. It is necessary to make sure that the apparent agreement between the lines and the series formula is not due to the lines being so close together that an agreement was bound to occur. We find that, between 700 and 600 Å., the average distance apart of lines is .15 volt; between 600 and 500 Å., .20 volt; between 500 and 400 Å., .25 volt; and between 400 and 300 Å., .40 volt. In Series 1 the greatest error was .03 volt for the line 484.5 Å., *i.e.*, in a region where the average distance apart of lines is .25 volt. From this standpoint the series seems to be satisfactory. The writer

TABLE III.—Series 1.

$$A_1 = 39.62 \text{ volts}; \quad b = 2395.1.$$

$n$ .	10.	11.	12.	13.	14.	15.
$A_1 - \frac{b}{n^2}$ (volts) .....	15.67	19.83	22.99	25.45	27.40	28.98
Millikan & Bowen (volts)	15.66	19.81	23.00	25.48	27.40	28.97
$\lambda$ in Å. ... ..	788.3	623.1	536.8	484.5	450.5	426.1
Intensity ... ..	6	0	0	4	2	1
Estimated intensity...	5	3	2	2	1	1

has found no mention of the probable error in the measurement of the spectral lines, but, in a previous paper, Millikan, Bowen, and Sawyer \* say "wave-lengths accurate to about .2 Å."

An attempt was next made to see if there were more series of this type capable of fitting the copper data. It was found that there was another series employing the same final level but involving a new system of initial levels. These were again of the form  $\frac{b}{n^2}$  and involved a value of  $b$  equal to 230.14 volts.

Whilst there are only five lines in series 2, it must be borne in mind that in choosing the series formula, only the value of  $b$  was arbitrary. The numerical agreement is decidedly good. No line appears for  $n=4$ .

\* Astrophysical Journal, liii. p. 150 (1921).

The value of  $b$  (230.14) corresponds to an effective nucleus of  $4.13e$ .

As there are now two sets of  $\frac{b}{n^2}$  terms, we will differentiate between them by calling those for which  $b=2395.1$ ,  $\alpha(n)$ , and those for which  $b=230.14$ ,  $\beta(n)$ .

It is found that there are lines corresponding to transitions from the  $\beta(n)$  terms to  $\alpha(10)$ . These combination lines are given in Table V.

TABLE IV.—Series 2.

$A_1=39.62$ .  $b=230.14$  volts.

$A - \frac{b}{n^2}$ ...	$n$ ...	5.	6.	7.	8.	9.
30.41	...	30.41	33.23	34.92	36.02	36.78
Millikan & Bowen (volts).	...	30.41	33.24	34.91	36.03	36.76
$\lambda$ in Å.	...	405.9	371.4	353.6	$\overline{342.6}$	335.8
Intensity	...	2	2	1	3	4
Estimated intensity	...	3	2	1	1	0

TABLE V.—Series 3.

$n$ ...	5.	6.	7.	8.	9.
$\alpha(10) - \beta(n)$ from series...	14.74	17.56	19.25	20.35	21.11
$\alpha(10) - \beta(n)$ from actual lines.	14.75	17.58	19.25	20.37	21.10
Millikan & Bowen (volts)	14.77	17.63	19.22	20.37	21.12
$\lambda$ in Å.	836.0	700.1	642.3	$\overline{606.0}$	584.6
Intensity	2	3	0	1	1
Estimated intensity	3	2	1	1	0

Row 2 has been obtained by taking  $\frac{2395.1}{10^2} - \frac{230.14}{n^2}$ .

Row 3 is obtained by subtracting the actual line  $A_1 - \alpha(10)$  from the line  $A_1 - \beta(n)$ . It is to be noted that in these combinations three errors are involved; an error in each of the lines or terms from which the combination is calculated and an error in the line with which comparison is made. In the circumstances the agreement seems to be good, and greatly strengthens the scheme. The range of Millikan and Bowen's work has only allowed the  $\alpha(n)$

terms to be extended down to  $n=10$ . If a term of this type exists for  $n=9$ , then we should expect to find transitions  $\alpha(9)-\beta(n)$ . These transitions are found. We get

$$\alpha(9) = \frac{2395.1}{n^2} = 29.57 \text{ volts.} \quad \text{Since } A_1 - \alpha(9) = 39.62 - 29.57$$

$= 10.05$  volts, the combination lines should be 10.05 volts less than the corresponding  $A_1 - \beta(n)$  lines. This method has been employed in the second row of Table VI.; the

$$\text{first row is calculated from } \frac{2395.1}{9^2} - \frac{230.14}{n^2}.$$

TABLE VI.—Series 4.

$n$ .	5.	6.	7.	8.	9.
$\alpha(9)-\beta(n)$ Calculated ...	20.36	23.18	24.87	25.97	26.73
$\alpha(9)-\beta(n)$ Using actual line to get $\beta(n)$ .	20.36	23.19	24.86	25.98	26.71
Millikan line in volts ...	20.37	23.21	24.84	25.92	26.59
Millikan line in Å. ...	606.0	531.8	496.9	476.2	464.3
Intensity ...	1	0	3	3	5
Estimated intensity ...	3	2	1	1	0

TABLE VII.—Series 5.

$$A_2 = 53.71 \text{ volts.}$$

$n$ .	11.	12.	13.	14.	15.
$A_2 - \frac{b}{n^2}$ ...	33.92	37.08	39.54	41.49	43.07
Millikan & Bower (volts)	33.91	37.05	39.51	41.54	43.09
$\lambda$ in Å. ...	364.0	333.2	312.4	297.2	286.5
Intensity ...	2	4	1	0	0
Estimated intensity ...	4	3	2	2	1

The first three terms agree well with our expectations, and the fourth fairly well, but the fifth seems to be too far out. Once again, however, we may regard this combination series as solidifying the scheme that we have built up.

There are no combination lines for  $\alpha(8)$  and it may be taken that this term is not present. Similarly there are no combinations for  $\alpha(11)$ .

It is found that there is another series of lines employing the  $\alpha(n)$  terms and a new final level  $A_2$ . This series is given in Table VII. and seems to fit reasonably well.

Again, the  $\alpha(n)$  terms may be employed with another final level  $A_3$  at 38.335 volts to give another series of Millikan lines. These are shown in Table VIII.

TABLE VIII.—Series 6.

$A_3=38.335$  volts.

$n$ .	10.	11.	12.	13.	14.	15.	16.	17.
$A_3 - \frac{b}{n^2}$ ...	14.39	18.54	21.70	—	26.12	27.69	28.98	30.04
Millikan & Bowen (volts).	14.39	18.52	21.73	—	26.13	27.64	28.97	30.03
$\lambda$ in Å. ...	858.1	666.4	568.1	—	472.5	466.6	426.1	411.2
Intensity ...	2	1	0	—	3	4	1	0
Estimated intensity	6	4	3	2	2	1	1	0

It is observed that the line for  $n=13$  is missing. This will receive explanation when the intensities are dealt with.

There appear to be no lines indicating transitions from the  $\beta(n)$  terms to the  $A_3$  level given by Series 6, until the terms for  $n=7$  is reached. From  $n=7$  to  $n=10$  we find lines with the correct wave-length for transitions of this type. These are shown in Table IX. Until the  $A_3$  level

TABLE IX.—Series 7.

$n$ .	7.	8.	9.	10.
$A_3 - \beta(n)$ ...	33.64	34.74	35.49	36.03
Millikan & Bowen (volts)	33.64	34.75	35.45	36.03
$\lambda$ in Å. ...	367.0	355.3	348.2	342.6
Intensity ...	1	1	3	3
Estimated intensity	2	1	1	0

was found, none of the series obtained showed an overlapping of  $\alpha(n)$  and  $\beta(n)$  terms; the  $\alpha(n)$  terms failed beyond  $n=15$ , at a depth of 10.64 volts, whilst the  $\beta(n)$  terms started at  $n=5$ , at a depth of 9.21 volts. In Series 6, however, in dealing with the transitions to the  $A_3$  level, it was found that the  $\alpha(n)$  terms persisted up to  $n=17$ , at a depth of 8.29 volts, and so it is rather interesting that the  $\beta(n)$  terms giving transitions to the  $A_3$  level do not start until  $\beta(n)=7$ , at a depth of 4.70 volts.



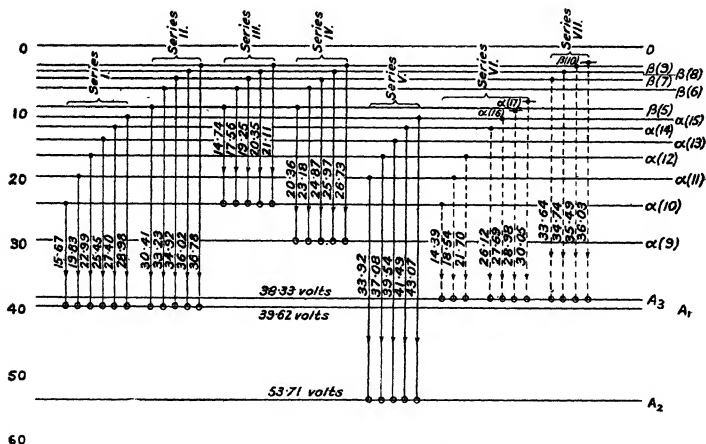
Hence, if the series involving  $A_3$  are regarded apart from the previous series, the  $\alpha(n)$  and  $\beta(n)$  terms never overlap.

The energy levels involved in the series are represented in fig. 1. The arrows indicate the experimental results of Millikan and Bowen. The diagram shows that the series scheme fits together rather well.

### § 3. Intensities.

In the tables giving the series, the fourth row gives the intensities found by Millikan and Bowen. It is at once seen that they are not at all what one would expect for

Fig. 1.



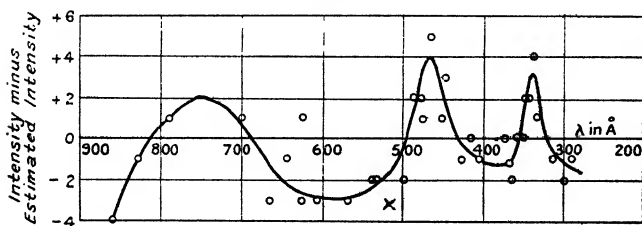
Energy diagram for Copper.

genuine series. This was regarded as a very serious difficulty. If the peculiar arrangement of intensities in the series were due to actual differences in the probabilities of the initial levels, then it would be expected that, in comparing two series originating in the same set of initial levels, we should find a similar arrangement of intensities. We do not find this.

It is, however, to be expected that the intensities will depend to some extent on the experimental conditions and it is also to be expected that the intensities may be modified by uneven sensitiveness of the photographic plate. If this be the case, then it will be found that in a sensitive region

all the lines will be stronger than their position in the series scheme would lead one to expect, and in an insensitive region all the lines should be too weak. Assuming the series scheme to be true, the intensity to be expected for each line was estimated. Subtracting this value from the actual intensity obtained by Millikan and Bowen, the error due to the photographic sensitiveness and other causes should be obtained. This should be a function of the wave-length, and hence, if we plot it against the latter, a curve should be obtained. Such a curve is shown in fig. 2. With one exception (possibly due to two lines being coincident) every point falls reasonably well on a smooth curve. Moreover, it is seen that peaks appear—peaks very suggestive of the absorption bands found in the optical region. From X-ray data it is found that bromine

Fig. 2.



is predicted to have an  $N_7$  edge at 410 Å., and an  $N_{5,6}$  edge at 1100 Å., whilst silver should have an  $N_{5,6}$  absorption edge at 280 Å.\* Going in the direction of shorter wave-lengths, Thoriaeus's† measurements predict the bromine  $M_{1,2}$  edge at 175 Å., and the other M levels will occur at still shorter wave-lengths. The determination of the edges from the X-ray data is not likely to be very accurate in this long wave-length region. It is to be perceived, however, that absorption edges are to be expected in the neighbourhood of the wave-lengths at which we have found intensity peaks, and that the description of the sensitiveness of the plate is a reasonable one.

In Series 6 it was observed that the line  $A_3-\alpha(13)$  was missing. This is explained by the sensitiveness curve, for the line would be expected at a little under 510 Å. and

\* Taken from A. H. Compton's 'X-Rays and Electrons,' p. 190.

† Phil. Mag. ii. p. 1015 (1926).

would be in a region of low sensitiveness. The line is indicated by a cross in fig. 2.

Only a small fraction of the lines tabulated by Millikan and Bowen has so far been dealt with, and it is not improbable that the scheme is capable of considerable extension. In these circumstances it seems inadvisable to advance any theory to account for the phenomena dealt with. We have therefore contented ourselves with summarising the salient features arising from the series classification.

- (1) Just as Rydberg series can be fitted to the critical potentials of soft X-ray excitation for iron, nickel, cobalt, manganese, and copper, so can series of the same type be fitted to the vacuum spark lines of copper.
- (2) The  $A_1$  level for the spectra agrees exactly with the  $X_4$  level for the critical potentials. Of the two values for " $b$ " occurring in the  $\frac{b}{n^2}$  terms, one, at 2395.1, is very close to the critical potential value at 2360.
- (3) The scheme so far embraces three arbitrary final levels,  $A_1$ ,  $A_2$  and  $A_3$ , and two sets of levels of the form  $\frac{b}{n^2}$ , described as  $\alpha(n)$  and  $\beta(n)$ .
- (4) The  $A_1$  level has transitions from both the  $\alpha(n)$  and the  $\beta(n)$  levels. The  $A_2$  level only receives transitions from the  $\alpha(n)$  levels.  $A_3$  receives jumps from the  $\alpha(n)$  levels and also from the  $\beta(n)$  levels. There are transitions from the  $\beta(n)$  levels to the  $\alpha(n)$  levels.
- (5) The effective nucleus involved in the  $\alpha(n)$  terms is  $13.3e$ . This corresponds to the critical potential value of  $13.2e$ . The effective nucleus for the  $\beta(n)$  terms is  $4.13e$ .
- (6) The intensities of the lines lead to a reasonable curve for the sensitiveness of the photographic plate as a function of the wave-length.

Points (1) and (2) give rise to the suggestion that there is, in those portions which emit radiations between 300 Å.

and 1000 Å., something in common between the excitation of the copper in Millikan and Bowen's vacuum sparks and the excitation of solid copper by electronic bombardment in the soft X-ray experiments. It may be, therefore, that a more complete analysis of the Millikan lines will throw light on the problem of the origin of the numerous critical potentials found for solids in the soft X-ray region, thus giving information on the state of the periphery of the atom in solids.

Recently Ericson and Edlén\* have published a brief account of some experiments on copper using a vacuum spectrograph designed by Siegbahn, with a considerably greater dispersion than that of Millikan and Bowen. Their published plates extend from a little over 100 Å. to 550 Å., and they obtain far more lines than did Millikan and Bowen. Ericson and Edlén have not yet published their numerical results, but, from a study of their photographs, these are not expected to invalidate our series.

In conclusion, the writer would like to express his gratitude to Prof. O. W. Richardson for his kind interest and advice.

---

#### LXVIII. *The Effect of Temperature on the Viscosity of Air.*

By W. G. SHILLING, M.C., D.Sc., and A. E. LAXTON, M.Sc., A.I.C.†

THE experiments described below were undertaken as a result of Rankine's criticism‡ of Williams's measurements§ on the effect of temperature on the viscosity of air from room-temperature up to 1000° C. Some of the objections raised have already been answered by Williams||. Since this work was completed¶, Edwards\*\* has completed a series of experiments, the results of which do not agree with those obtained by Williams.

\* Nature, cxxiv. p. 688 (1929); *Zeits. für Physik*, lix. p. 665 (1930).

† Communicated by the Authors.

‡ Proc. Roy. Soc. A, cxi. p. 219 (1927).

§ *Loc. cit.* cx. p. 141 (1926).

|| *Loc. cit.* cxiii. p. 233 (1927).

¶ *Loc. cit.* cxvii. p. 245 (1928).

\*\* In the summer of 1927.

In principle the method is exactly that used by Williams. Modifications have been introduced where necessary to ensure that the doubts raised by Rankine's criticisms should be covered.

The first serious criticism raised concerns the temperature measurements in Williams's work, with particular reference to the fact that only one thermoelement was used for the whole of the temperature measurements. Our experience with a method of heating such as that used by Williams is that the central portion of the furnace is extremely uniform in temperature and is very easily controlled. Moreover, the efficient lagging permissible and the constancy of heat supply enable the temperature to be maintained to  $\pm 1^\circ \text{C.}$  for several hours. In addition, the central portion of the furnace containing the pre-heating bulb and spiral was shut off by fire-clay stoppers, thus enabling conditions approximating to black-body radiation to be maintained, especially at the higher temperatures used. One thermocouple will then presumably give the correct temperature reading for the whole of the enclosure. To test this point, five thermocouples were used throughout the present work. The furnace used by Williams was again employed. One thermocouple, No. 5, was placed exactly as in Williams's experiments. The other four were evenly distributed, with their hot junctions near the capillary and placed as shown in the subsidiary sketch of fig. 1. Their positions longitudinally are shown in the main diagram. Each thermocouple was separately calibrated using the fixed points employed by Williams, and, in addition, were checked from  $700^\circ \text{C.}$  upwards by a disappearing filament type of pyrometer reading to  $\pm 1^\circ \text{C.}$  The cold junctions of Nos. 1 to 4 were immersed in a water-box placed near the furnace and fed from a tap with cold water. For No. 5 thermocouple the cold junction was immersed in the thermostat. The cold-junction corrections were made by means of the experimentally-determined equation

$$y = 6.16t - 8.6,$$

where  $y$  is the number of microvolts correction to be applied and  $t$  is the temperature of the cold junction in degrees centigrade. Table I. shows the type of result obtained. The figures give the temperature of each thermocouple for a definite furnace temperature.

Readings in Table I. are taken to the nearest  $0.5^{\circ}\text{C}$ ., the limit to which the higher temperatures could be taken with certainty.

From Table I. it can be seen that had the temperatures been measured only by No. 5 thermocouple little difference would be made. It is doubtful whether the vapour-bath method of heating, used by Edwards, has any advantage over an electric furnace for such work. The temperatures obtainable by vapour baths are limited both in range and in number.

TABLE I.  
Comparison of Thermocouple Readings.

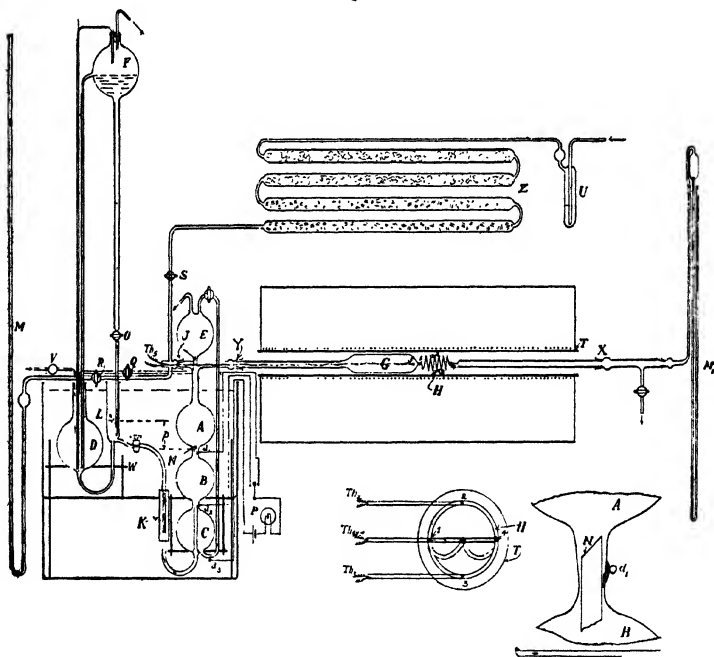
Thermocouple.				Mean 1-4.	5.	Mean temp.
1.	2.	3.	4.			
123.5	124.5	124.0	124.0	124.0	124.0	124.0
124.0	124.0	123.0	124.5	124.0	124.5	124.0
181.5	182.5	182.0	182.0	182.0	181.5	182.0
189.5	188.5	189.0	188.5	189.0	189.5	189.0
258.0	258.5	257.5	258.0	258.0	257.5	258.0
359.0	359.5	358.5	358.5	359.0	359.0	359.0
431.5	430.5	431.0	431.0	431.5	430.0	431.0
537.5	537.0	536.5	536.5	537.0	538.0	537.0
699.5	700.0	700.5	701.5	701.0	700.0	701.0
847.0	847.5	846.5	847.5	847.0	847.0	847.0

The principal modification of Williams's apparatus was made as a result of the next point raised by Rankine, namely, the pressure control.

This criticism has already been fully answered by Williams. To remove any possibility of error caused by personal fatigue, the pressure feed shown in fig. 1 was designed to be automatic when once started. Each of the bulbs A, B, and C has a capacity of about 300 c.c. At the commencement of an experiment the tube leading from C up to E is filled with mercury, and a little mercury remains in C. The latter bulb has the same function as the first bulb in Williams's apparatus. It is of sufficient size to ensure equilibrium by the time the mercury has risen to the point  $d_2$ , which is the beginning of the calibrated

volume between the points  $d_1$  and  $d_2$ . The subsidiary sketch in fig. 1 shows the form of the top contact  $d_1$  and also the end of the tube N. The bottom contact  $d_2$  is similar. The bulb A is inserted to steady the flow and to ensure that the volume of the gas leaving B is at the measured thermostat temperature. From A the gas goes directly into the furnace to the preheater G.

Fig. 1.



The remainder of the apparatus shown in the thermostat is the device for feeding mercury into the bulbs at constant pressure. An overflow head L is fixed at a height indicated by  $p$  above the overflow tube N, which terminates between the bulbs A and B. The overflow L is fed by a stream of mercury controlled by a sensitive tap O from the flask F, secured by stout brackets to the wall at a little more than barometric height vertically above L. The flask F is kept filled to the overflow side-tube from the flask D by means of suction and a con-

trolled air-inlet V. The overflow from L returns to the flask D. It was found necessary to maintain a constant level in F, otherwise the stream flowing into L gradually diminished, giving a slight decrease in the driving pressure due to lowering of the meniscus at L. Also the stands holding the apparatus had to be constructed of stout L-iron, rigidly connected, with the feet firmly placed on a thick base. If rigidity is not thus ensured, the transfer of about 700 c.c. of mercury from one side of the stand to the other during an experiment caused changes of pressure amounting to as much as 0.1 mm. of mercury.

The main platform of the stand carried bulb B, which rested in a carefully-shaped cup cut in a crossbar of teak. The four corner posts of the stand were of  $\frac{3}{4}$  in. diameter brass rod, and passed through heavy adjusting collars fixed to the platform. The height of each platform was adjustable. The weight in bulb C was supported by a teak stand slung from the main platform. Two of the corner posts were extended so that clamps could be affixed to support the glass apparatus above bulbs A and D respectively.

The height of the bulb D is adjustable relative to bulbs A, B, and C. Connexion is made by a length of glass tubing inside a piece of rubber pressure-tubing as shown at K. This connecting piece could be made of any convenient length, thus enabling the driving pressure to be varied. The height of stand W could be separately adjusted to suit the pressure required.

By applying suction at E, the mercury filling bulbs B and C at the end of each experiment could be raised into E by opening the stopcock connecting C to E.

Then, by opening the stopcock Q, the mercury was allowed to run back by gravity into D ready for the next experiment.

The mercury was periodically withdrawn from bulb E for cleaning, although most of the oxide collected in the bulbs D and F, and gave no trouble in the experimental bulbs C or B. As the mercury left the bulbs B and C, fresh gas was allowed to enter through the purifying train by opening the stopcock S. The stopcock R, connecting the oil manometer M, was closed during this process to avoid undue disturbance of the oil-levels. Until bulb C was about one-third full in the next experiment the stopcock R was not reopened. The working of this apparatus was



extremely smooth and the pressure very constant throughout the longest experiments. Deviations from the mean pressure never exceeded 0.5 mm. pressure of oil having a density given by

$$d_{4^{\circ}\text{C.}}^{20^{\circ}\text{C.}} = 0.9072 - 0.00064t.$$

This equation was determined experimentally for the oil used.

The remaining criticism raised by Rankine concerns the calibration and testing of the capillary used. For our experiments The Thermal Syndicate, Ltd., kindly sent us a selection of tubes to be calibrated throughout their length. Calibration was done by the mercury-pellet method, and the tubes were rotated at each point so that their mean diameters at angles of  $60^{\circ}$  could be estimated, thus checking uniformity of cross-section. The best tube for our purpose had a bore of about 0.4 mm. and a length of 100 cm. The maximum difference in bore did not exceed 10 per cent. of the bore, and deviations were much less than this over the greater part of the length. All cross-sections seemed to be perfectly circular, although, unless the tube is broken, these measurements are admittedly difficult to make. The calibrated tube was then returned to the makers, who undertook to coil it into a spiral without any risk of flattening of cross-section. The resulting spiral had six turns with a pitch of 8 mm. and an outside diameter of 5.2 cm. Great care was taken to avoid any sudden bends, especially near the ends. The whole of the transpiratory apparatus was of transparent silica. The spiral was connected directly to the preheating vessel C on one side and to a length of 1.3 cm. bore tubing terminating in half of a ground joint X on the other. Connexion of the glass apparatus to the preheater was made by a further length of wide tubing reaching out of the furnace and also terminating in half of a ground joint Y. The other half of this joint was of ordinary soda glass for direct connexion to the top of bulb A. The dimensions of the preheater (6.4 cm. diameter and 19.5 cm. long) were proved sufficient by the fact that no variation was observed in the temperature recorded by thermocouple No. 5 when the first rush of gas took place in each experiment before equilibrium was reached in filling the bulb C.

The final test of the suitability of the capillary was then made. Experiments were made with the driving pressures

roughly in the ratios 1 : 2 : 3, all other conditions remaining the same. If Meyer's formula holds, the time taken will be inversely proportional to the pressure used. The suggestion made by Rankine that this test should be made on Williams's capillary could not be carried out, since the

TABLE II.

$\frac{p_1 - p_2}{\text{dynes/cm.}^2}$	$p_2$ dynes/cm. <sup>2</sup>	$V_1$ c.c.	$t_1$ ° C.	$\eta_1 \times 10^4$ .	$\tau_1$ .	$\kappa(1 + 4\xi_1/R) \times 10^{10}$ .
36,710	1,014,100	286.90	22.9	1.8235	1833.6	3.9558
36,600	1,014,300	286.90	22.9	1.8235	1847.4	3.9370
36,400	1,017,700	287.29	23.3	1.8255	1852.6	3.9140
36,530	1,018,100	287.29	23.3	1.8255	1851.2	3.9461
36,570	1,014,700	286.90	22.9	1.8235	1848.2	3.9205
36,620	1,014,500	287.00	23.0	1.8240	1849.0	3.9340
36,740	1,013,900	287.44	23.45	1.8262	1837.6	3.9566
36,670	1,017,100	286.90	22.9	1.8235	1842.0	3.9407
Mean .....						3.9380

TABLE III.

$\frac{p_1 - p_2}{\text{dynes/cm.}^2}$	$p_2$ dynes/cm. <sup>2</sup>	$V_1$ c.c.	$t_1$ ° C.	$\eta_1 \times 10^4$ .	$\tau_1$ .	$\kappa(1 + 4\xi_1/R) \times 10^{10}$ .
71,800	1,015,200	287.29	23.3	1.8255	955.2	3.9539
72,010	1,015,200	286.81	22.8	1.8230	952.8	3.9407
72,140	1,015,200	287.19	23.2	1.8250	955.2	3.9334
71,450	1,015,200	287.23	23.24	1.8252	960.0	3.9511
71,720	1,015,200	286.90	22.9	1.8235	955.0	3.9487
71,900	1,015,200	286.56	22.55	1.8218	950.8	3.9488
72,070	1,022,300	287.27	23.28	1.8254	956.0	3.9345
71,940	1,022,100	286.90	22.9	1.8235	950.0	3.9575
Mean .....						3.9461

tube was unfortunately broken by workmen during a summer vacation. But, in spite of the difficult nature of the work, all the capillaries sent us by The Thermal Syndicate compared well with the best glass capillaries

available. The results of the tests on the capillary are set out in Tables II. to IV. below, the symbols used in these and in subsequent tables having the same meaning as in the corresponding tables in Williams's communication. The last column of each table gives the capillary constant uncorrected for slip. The values found for this constant under different driving pressures show that Meyer's formula holds to the limits of experimental error.

TABLE IV.

$\frac{p_1 - p_2}{\text{dynes/cm.}^2}$	$p_2$ dynes/cm. <sup>2</sup>	$V_1$ c.c.	$t_1^\circ \text{C.}$	$\eta_1 \times 10^4.$	$\tau_1.$	$\kappa(1 + 4\xi_1/R) \times 10^{10}.$
107,780	1,005,100	288.90	24.3	1.8304	655.0	3.9357
107,970	1,005,200	287.63	23.65	1.8271	650.8	3.9303
108,130	1,005,200	287.29	23.3	1.8255	649.0	3.9275
108,130	1,005,100	287.10	23.1	1.8245	647.0	3.9347
108,040	1,005,000	286.61	22.6	1.8221	647.0	3.9262
108,020	1,005,200	286.71	22.7	1.8225	645.6	3.9375
107,930	1,005,400	286.90	22.9	1.8235	647.2	3.9360
107,760	1,006,600	286.90	22.9	1.8235	648.2	3.9257
107,780	1,006,600	287.15	23.15	1.8247	646.4	3.9424
Mean .....						3.9329

The results of Tables II. to IV. are conveniently summarized in Table V. :—

TABLE V.

Driving pressure (dynes/cm. <sup>2</sup> ).	Mean value of $\kappa(1 + 4\xi_1/R) \times 10^{10}.$
36,600	3.9380
72,000	3.9461
108,000	3.9329
Mean value .....	3.9390

From the mean value of  $\kappa(1 + 4\xi_1/R) \times 10^{10}$  the true value of  $\kappa$ , corrected for slip, was calculated exactly as described by Williams. Using the values  $\kappa = 0.0.93939$  (Table V.) and  $L = 100$  cm., the value of  $R$  is 0.02116 cm.

The corrected values of  $\kappa$  and  $R$  are 0.03932 and 0.02115 cm. respectively.

Since the lower half of Williams's temperature range seems to be more open to criticism than the upper half, particular attention was paid to the region below 200° C. Measurements were then made at higher temperatures up to 850° C., at which point the work had to be discontinued.

Gas volumes at the temperature of each experiment were calculated from the calibrated volume of bulb B and the known pressure at 23° C. by using Berthelot's Equation of State. The critical pressure for air was taken as 39.3 atm., and a value of 132.6° abs. was used for the critical temperature. For the main series of experiments the highest of the three calibration pressures, namely ca. 108,000 dynes/cm.<sup>2</sup>, was used as being the most convenient. The air was purified by the train of reagent tubes shown in fig. 1. The rate of flow was indicated by the wash-bottle U, containing sulphuric acid, which also served to dry the air. From this wash-bottle the air passed through a tube containing broken stick potassium hydroxide to remove carbon dioxide, a tube of calcium chloride for the initial drying, followed by two tubes containing phosphorus pentoxide. All these tubes were of liberal dimensions. Before commencing experiments the whole apparatus was tested under a pressure of 1 mm. of mercury by evacuating at the end normally forming the gas-exit. No leakage greater than that corresponding to a rise in pressure of 1 mm. on standing overnight was tolerated. To obviate any possibility of back-pressure the manometer and fittings were removed at X for all experiments.

The calibrated volume of bulb B between the contact points  $d_1$  and  $d_2$  was 287.0 c.c. at 23° C. All times were measured to  $\pm 0.2$  sec. by an accurate stop-watch, the daily rate of which was checked against wireless time-signals. Times of experiments varied from 650 sec. at room-temperature to 6000 sec. at the highest temperature measured.

In Table VI. are given the experimental results. Table VII. gives the experimental values of  $\eta$  with the corresponding values of  $T^{3/2}/\eta$ .

When the values of  $T^{3/2}/\eta$  are plotted against temperature the resulting line is almost straight, but shows a

TABLE VI.

$\frac{p_3 - p_4}{\text{dynes/cm.}^2}$	$p_4$ dynes/cm. <sup>2</sup>	$V_2$	$\tau_2$	$t_2$ °C.	$\frac{\eta_2 \times 10^4}{1 + 4\xi_2/R}$
107,070	1,007,500	331.68	832.6	69	2.0146
107,290	1,007,200	332.65	834.2	70	2.0138
107,340	1,006,800	332.65	834.8	70	2.0164
107,440	1,001,900	383.13	1068.0	122	2.2415
107,420	1,001,800	385.08	1069.2	124	2.2375
107,060	1,002,500	385.08	1075.4	124	2.2380
107,220	1,003,100	385.08	1074.8	124	2.2421
107,910	1,005,400	441.36	1376.8	182	2.5193
107,970	1,005,800	443.30	1368.6	184	2.4945
107,660	1,006,100	447.18	1371.0	188	2.4705
107,770	1,005,100	448.15	1367.8	189	2.4615
107,590	1,007,600	513.16	1742.0	256	2.7339
107,640	1,007,900	515.10	1748.8	258	2.7353
108,030	1,008,400	514.13	1756.0	257	2.7615
107,760	1,008,700	518.98	1777.4	262	2.7623
107,220	1,011,400	615.01	2371.6	361	3.0959
107,590	1,011,400	613.07	2348.4	359	3.0855
107,800	1,010,800	607.25	2344.6	359	3.0861
107,940	1,010,600	613.07	2344.8	359	3.0901
108,100	1,000,500	683.71	2802.6	430	3.3136
107,900	992,100	684.84	2829.6	433	3.3328
107,600	999,700	684.84	2838.4	433	3.3270
108,080	992,600	684.84	2826.2	433	3.3355
108,320	1,005,500	776.01	3429.0	527	3.5813
107,730	1,005,600	773.10	3455.0	524	3.6032
107,480	1,007,400	780.86	3504.6	532	3.6107
108,060	1,007,900	785.71	3508.8	537	3.6116
107,540	1,012,500	844.87	3980.0	598	3.7929
107,990	1,011,000	844.87	3970.0	598	3.7982
108,300	1,008,100	942.83	4711.4	699	4.0498
107,640	1,007,700	944.77	4764.4	701	4.0629
108,240	1,006,500	929.25	4616.8	685	4.0241
107,690	1,008,400	1009.7	5327.2	768	4.2527
107,650	1,007,600	1013.6	5325.0	772	4.2329
108,180	1,015,100	1067.9	5792.2	828	4.4025
107,660	1,014,900	1086.4	5979.2	847	4.4516

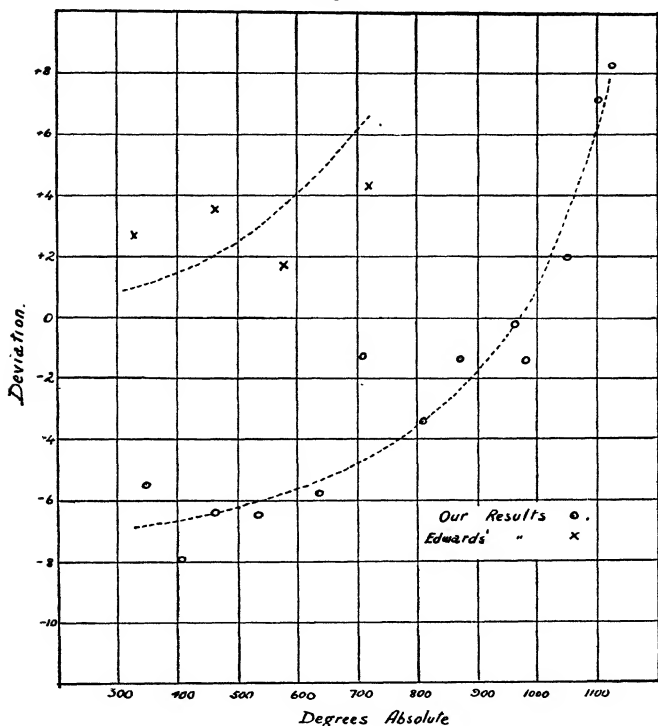
TABLE VII.  
Experimental Results.

Temp. ° C.	Temp. ° abs.	$\eta_2 \times 10^4$ .	$T^{3/2}/\eta \times 10^{-7}$ .
69	342	2.019	3.140
70	343	2.018	3.148
70	343	2.021	3.144
122	395	2.247	3.494
124	397	2.243	3.527
124	397	2.243	3.527
124	397	2.247	3.520
182	455	2.527	3.841
184	457	2.502	3.905
188	461	2.478	3.995
189	462	2.469	4.023
256	529	2.743	4.435
257	530	2.771	4.403
258	531	2.745	4.458
262	535	2.772	4.464
359	632	3.099	5.127
359	632	3.099	5.127
359	632	3.103	5.120
361	634	3.109	5.135
430	703	3.330	5.598
433	706	3.349	5.601
433	706	3.343	5.611
433	706	3.352	5.597
524	797	3.623	6.210
527	800	3.601	6.284
532	805	3.631	6.291
537	810	3.632	6.348
598	871	3.816	6.736
598	871	3.821	6.727
685	958	4.051	7.319
699	972	4.078	7.432
701	974	4.091	7.431
768	1041	4.284	7.840
772	1045	4.264	7.922
828	1101	4.438	8.233
847	1120	4.488	8.353

distinct tendency to curve. On the assumption that this curvature might be due to experimental errors, a straight line was drawn as nearly as possible through the results. The intercept with the temperature axis gave a numerical value of 116 for the Sutherland Constant.

Using this value for the constant, the actual divergences from the "true" value were plotted from the

Fig. 2.



results given in Table VII. The "true" value is that calculated for the temperature in question on the assumption that Sutherland's law is obeyed. The four values obtained by Edwards\* were similarly treated, using his experimental value for the constant, viz.,  $C = 118$ . In fig. 2 the divergences from the "true" values are shown as parts per thousand on the true value of  $\eta$ . The trend of

\* *Loc. cit.*

these experimental errors (indicated by the broken lines) both in the case of our own work and in that of Edwards, indicates that there is a small but steady deviation from Sutherland's law over the temperature range observed.

There is no indication of the sudden break which Williams obtained by joining his results on to those of other workers at the low temperature end. The experimental method used by Williams is considered to be completely vindicated against all criticism made against it by Rankine. It is suggested that the peculiar results which Williams found were due to his method of smoothing his experimental results.

After this work was completed, a publication by Braune, Basch, and Wentzel \* gives results supporting the above conclusions. In addition, they agree † with some of Williams's replies to Rankine's criticisms.

#### SUMMARY.

1. The coefficient of viscosity of air has been measured by the comparative transpiration method over the temperature range  $23^{\circ}$ – $850^{\circ}$  C. Particular attention has been paid to points raised in criticisms of Williams's work, and the method which he used has been completely vindicated.

2. The results show that there is a small but steady deviation from Sutherland's law over the range considered.

3. It is suggested that the peculiar results obtained by Williams are due to his method of smoothing experimental values.

In conclusion, the authors desire to thank Prof. J. R. Partington, M.B.E., D.Sc., for his interest and helpful suggestions throughout the course of the work. They wish also to thank the Department of Scientific and Industrial Research and the London County Council for maintenance grants. Thanks are also due to the Chemical Society for a grant which defrayed part of the cost of the apparatus.

Chemistry Department,  
East London College,  
University of London.

---

\* *Z. Phys. Chem.* cxxxvii. p. 176 (1928).

† *Ibid.* p. 187.



LXIX. *The Multistage Valve Amplifier.* By A. C. BARTLETT, B.A. (Communication from the Staff of the Research Laboratories of the General Electric Company, Limited, Wembley.)

### SUMMARY.

THE  $n$ th power of a second order square matrix is first obtained, and then from this the equations of the multistage amplifier.

#### 1. Preliminary.

IF  $I_1$  is the current flowing into the input terminals of a passive four-terminal network,  $I_2$  is the current flowing from the output terminals, while  $V_1$  and  $V_2$  are the voltages across the input and output respectively, then it is known that

$$V_1 = aV_2 + bI_2,$$

$$I_1 = cV_2 + dI_2,$$

where  $(ad - bc) = 1,$

and  $a, b, c,$  and  $d$  are constants depending on the particular structure of the network.

Thus  $V_1$  and  $I_1$  are obtained from  $V_2$  and  $I_2$  by a homogeneous linear substitution, of which the matrix is

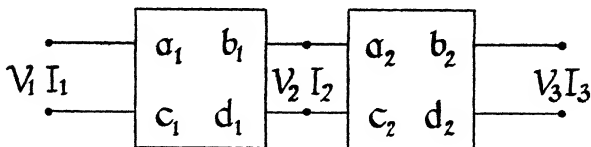
$$\begin{vmatrix} a & b \\ c & d \end{vmatrix},$$

of which the determinant

$$ad - bc = 1.$$

If there are two networks, as in fig. 1, of which the

Fig. 1.



matrices are

$$\begin{vmatrix} a_1 & b_1 \\ c_1 & d_1 \end{vmatrix} \quad \text{and} \quad \begin{vmatrix} a_2 & b_2 \\ c_2 & d_2 \end{vmatrix},$$

then

$$V_2 = a_2 V_3 + b_2 I_3,$$

$$I_2 = c_2 V_3 + d_2 I_3,$$

$$V_1 = a_1 V_2 + b_1 I_2,$$

$$I_1 = c_1 V_2 + d_1 I_2.$$

Thus  $V_1$  and  $I_1$  are obtained from  $V_3$  and  $I_3$  by the successive application of the two substitutions \*. Therefore  $V_1$  and  $I_1$  are obtained from  $V_3$  and  $I_3$  by a linear substitution, of which the matrix is

$$\begin{vmatrix} a_1 & b_1 \\ c_1 & d_1 \end{vmatrix} \times \begin{vmatrix} a_2 & b_2 \\ c_2 & d_2 \end{vmatrix} = \begin{vmatrix} a_1 a_2 + b_1 c_2 & a_1 b_2 + b_1 d_2 \\ c_1 a_2 + d_1 c_2 & c_1 b_2 + d_1 d_2 \end{vmatrix}.$$

This process can be continued for a chain of any number of networks, the matrix of the substitution for the whole chain being the product in order of the matrices of the constituents. In particular, if the chain consists of  $n$  successive identical members, the matrix of the whole chain is the  $n$ th power of the matrix of one element. A network having a pair of output and a pair of input terminals may be specified by three constants,  $Z$ ,  $\theta$ , and  $\phi$  †, and then the equations relating  $V_1$  and  $I_1$  with  $V_2$  and  $I_2$  are

$$V_1 = \frac{\cosh(\theta + \phi)}{\cosh \phi} \cdot V_2 + \frac{Z \sinh \theta}{\cosh \phi} \cdot I_2,$$

$$I_1 = \frac{\sinh \theta}{Z \cosh \phi} \cdot V_2 + \frac{\cosh(\theta - \phi)}{\cosh \phi} \cdot I_2.$$

But it is also known that if there is a chain of  $n$  identical networks, and if  $V_1$  and  $I_1$  are the input volts and current, and  $V_{n+1}$  and  $I_{n+1}$  are the output volts and currents, then

$$V_1 = \frac{\cosh(n\theta + \phi)}{\cosh \phi} \cdot V_{n+1} + \frac{Z \sinh n\theta}{\cosh \phi} \cdot I_{n+1},$$

$$I_1 = \frac{\sinh n\theta}{\cosh \phi} \cdot V_{n+1} + \frac{\cosh(n\theta - \phi)}{\cosh \phi} \cdot I_{n+1}.$$

But the matrix of this substitution is the  $n$ th power of the matrix of the preceding substitution. Hence the following theorem: given a matrix

$$\begin{vmatrix} a & b \\ c & d \end{vmatrix},$$

\* Cf. M. Vaultot, *Revue Générale d'Electricité*, p. 493 (1927).

† J. I. E. E. 1927, p. 223.

of which the determinant is unity, its  $n$ th power is

$$\begin{vmatrix} \frac{\cosh(n\theta + \phi)}{\cosh \phi}, & \frac{Z \sinh n\theta}{\cosh \phi} \\ \frac{\sinh n\theta}{Z \cosh \phi}, & \frac{\cosh(n\theta - \phi)}{\cosh \phi} \end{vmatrix},$$

where  $Z$ ,  $\theta$ , and  $\phi$  are chosen so that

$$\cosh(\theta + \phi)/\cosh \phi = a,$$

$$Z \sinh \theta/\cosh \phi = b,$$

$$\sinh \theta/Z \cosh \phi = c,$$

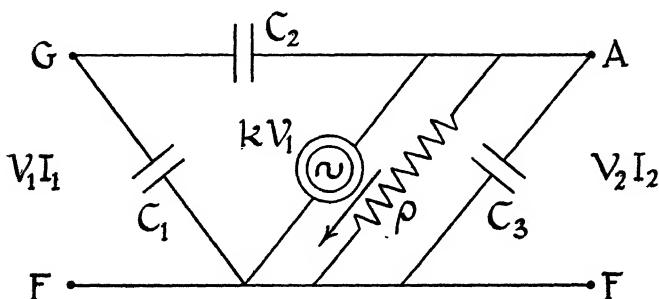
$$\cosh(\theta - \phi)/\cosh \phi = d.$$

This result can be easily verified by induction.

## 2. The Thermionic Valve.

A thermionic valve has the equivalent circuit shown in fig. 2, where  $\rho$  is the internal resistance and  $k$  the mutual

Fig. 2.



conductance of the valve, while the sine wave within two circles is a constant current generator giving a constant current  $kV_1$ . If  $u$  is the impedance of  $C_1$ ,  $v$  of  $C_2$ , and  $w$  the impedance of  $\rho$  and  $C_3$  in parallel, then it is readily shown that

$$V_1 = \frac{w + v}{w(1 - vk)} \cdot V_2 + \frac{v}{1 - vk} \cdot I_2,$$

$$I_1 = \frac{w + u + v + ukw}{wu(1 - vk)} \cdot V_2 + \frac{u + v}{u(1 - vk)} \cdot I_2.$$

This, again, is a homogeneous linear substitution, but differs

from that of a passive network in that its determinant is not unity but is  $1/(1-vk)$ .

Let

$$1/(1-vk) = \sigma^2.$$

Then the matrix of this substitution may be written as

$$\sigma \begin{vmatrix} a, & b \\ c, & d \end{vmatrix},$$

where

$$a = \frac{\sigma}{w}(w+v),$$

$$b = \sigma v,$$

$$c = \frac{\sigma}{wu}(w+u+v+uwk),$$

$$d = \frac{\sigma}{u}(u+v),$$

and

$$ad - bc = 1.$$

### 3. The Multistage Valve Amplifier.

Now consider a multistage valve amplifier made up of  $n$  stages. Let each stage consist of a valve whose matrix is

$$\sigma \begin{vmatrix} a, & b \\ c, & d \end{vmatrix},$$

followed by a passive coupling network whose matrix is

$$\begin{vmatrix} a', & b' \\ c', & d' \end{vmatrix}.$$

Then the matrix of a single stage will be

$$\sigma \begin{vmatrix} a, & b \\ c, & d \end{vmatrix} \times \begin{vmatrix} a', & b' \\ c', & d' \end{vmatrix} = \sigma \begin{vmatrix} A, & B \\ C, & D \end{vmatrix},$$

where

$$(AD - BC) = 1.$$

Hence, if we chose three constants,  $Z$ ,  $\theta$ , and  $\phi$ , corresponding to  $A$ ,  $B$ ,  $C$ , and  $D$ , the matrix of a multistage amplifier of  $n$  such stages will be

$$\left\{ \sigma \begin{vmatrix} A, & B \\ C, & D \end{vmatrix} \right\}^n = \sigma^n \begin{vmatrix} \frac{\cosh(n\theta + \phi)}{\cosh \phi}, & \frac{Z \sinh n\theta}{\cosh \phi} \\ \frac{\sinh n\theta}{Z \cosh \phi}, & \frac{\cosh(n\theta - \phi)}{\cosh \phi} \end{vmatrix},$$

and thus, if  $V_{n+1}$  and  $I_{n+1}$  are the output volts and current of the  $n$  stage amplifier,

$$V_1 = \frac{\sigma^n \cosh (n\theta + \phi)}{\cosh \phi} \cdot V_{n+1} + \frac{\sigma^n Z \sinh n\theta}{\cosh \phi} \cdot I_{n+1},$$

$$I_1 = \frac{\sigma^n \sinh n\theta}{Z \cosh \phi} \cdot V_{n+1} + \frac{\sigma^n \cosh (n\theta - \phi)}{\cosh \phi} \cdot I_{n+1}.$$

If the amplifier is terminated by an impedance  $z$ , then  $V_{n+1}/I_{n+1} = z$ , and if  $z_n$  is the sending-end impedance of the  $n$  stage amplifier terminated by  $z$

$$z_n = \frac{V_1}{I_1} = Z \cdot \frac{z \cosh (n\theta + \phi) + Z \sinh n\theta}{z \sinh n\theta + Z \cosh (n\theta - \phi)}.$$

If  $y_n$  is the receiving-end impedance of the  $n$  stage amplifier terminated by  $z$ ,

$$y_n = \frac{V_1}{I_{n+1}} = \sigma^n \cdot \frac{z \cosh (n\theta + \phi) + Z \sinh n\theta}{\cosh \phi}.$$

The voltage amplification will be

$$\frac{V_{n+1}}{V_1} \doteq \frac{z I_{n+1}}{V_1} = \frac{z \cosh \phi}{\sigma^n \{ z \cosh (n\theta + \phi) + Z \sinh n\theta \}}.$$

## LXX. Notices respecting New Books.

*Index Generalis: Annuaire général des Universités, Grandes Ecoles, Bibliothèques, Instituts Scientifiques, Jardins Botaniques et Zoologiques, Musées, Observatoires, Sociétés Savantes.*  
Published under the direction of Dr. R. DE MONTESSUS DE BALLORE. [Pp. 2320.] (Paris: Editions Spes. 1929-30.)  
Price not stated.

THE current volume of the 'Index Generalis' is the tenth of the series, which was commenced in 1919. It is now well-known as a comprehensive directory of the learned world. The present volume comprises: (1) Directories of universities, colleges, and professional schools, arranged according to countries, 1161 pages; (2) astronomical observatories, 86 pages; (3) libraries and archives, 276 pages; (4) scientific institutes and museums, 118 pages; (5) learned societies and academies, 190 pages; (6) list of exchanges, 7 pages; (7) index of names (60,000 persons), 423 pages; (8) geographical and other indices, 50 pages.

In addition to the names of professors, lecturers, teachers, scientific staff, and administrative officers, much miscellaneous

information is given, such as dates of foundation and number of students of universities, etc., instrumental equipment and programmes of observatories, lists of fellows and foreign members of the principal scientific societies, etc.

A proof of each entry is sent annually to the contributor in order to ensure that the Index is accurate and up-to-date.

A careful examination leads to the conclusion that the entries are reasonably complete. There are, however, a comparatively large number of errors in the extensive name-index—names spelt incorrectly, wrong initials, incorrect page stated, &c. The entries referring to Sir J. J. Thomson may be instanced : there are two separate entries "Thomson, J. J.," and two other entries "Thomson, Sir J. J.," all referring to the same person, though apparently to four separate persons ; a third entry "Thomson, J. J." is an error for "Thompson, J. J." Immediately preceding, under "Thomson, J. G.," are three entries, one of which refers to a J. H. Thomson. Many errors of such and similar natures were found, and it would appear that more careful editing and proof-reading of the index is required.

In spite of such defects, the volume provides an invaluable work of reference, the editing of which must have been a heavy task. The Index is published in two editions, the one French, the other English.

*A Course of Analysis.* By E. G. PHILLIPS, M.A., M.Sc. [Pp. viii + 362, with 35 figures.] (Cambridge : at the University Press, 1930. Price 16s. net.)

A REAL need has been met by this book, which is intended for First Year Honour Students. There has not hitherto been any text-book in English which covers the same ground. The author, in his preface, remarks that "Since modern analysis requires great precision of statement and demands from the student a very clear understanding of its fundamental principles, I have aimed at presenting the subject in such a way as to make every important concept clearly understood." In this aim he has undoubtedly succeeded ; the explanations of fundamental principles are very clear, and the essential steps in the logical arguments are carefully emphasized.

A brief account of the definition of number is given in Chapter I., including Russell's modification of Dedekind's method of defining an irrational number. Chapter II. is devoted to bounds and limits of sequences, and is followed by chapters on limits and continuity and on the differential calculus. Prominence is given to "differentials," a feature to be commended and one which has not been widely adopted in English text-books. The chapter on Inequalities is a

valuable one, and contains proofs of both Hölder's and Minkowski's inequalities, which have not been given previously in any English book. Two chapters deal with the integral calculus and its applications. Functions of more than one variable are next dealt with; here the conception of differentials leads to clarity and conciseness. The remaining chapters deal with implicit functions, double integrals, triple and surface integrals, and power series.

A student who works through this book intelligently and conscientiously cannot fail to have a thorough grounding in the subject, paving the way for the more advanced standard treatises. At the end of each chapter a series of examples have been given; these have been carefully selected to illustrate the fundamental concepts, and will prove of great value to teachers and lecturers.

*An Introduction to Surface Chemistry.* By E. K. RIDEAL. Second Edition. [Pp. xii + 460.] (Cambridge: at the University Press, 1930. Price 21s. net.)

THE increasing importance of the study of the properties of interfacial phases, and the development of the subject as well on the theoretical as on the experimental side, have been responsible for a considerable increase—124 pages—in the new edition of this book, as compared with the first edition published nearly four years previously. The present edition gives full consideration to recent work, but, in addition, a thorough revision has been made and errors noted in the first edition have been corrected.

Dr. Rideal has given a masterly survey of the many and varied phenomena which depend ultimately upon the cohesive forces which hold solid and liquid masses together. To students of physical chemistry the book will prove invaluable; other scientific readers will find much of interest in the discussions of the phenomena dealt with and of their theoretical foundations. The arrangement of the material is logical and satisfactory. The surface energy and surface tension of liquids is dealt with in the first chapter, which is followed by others devoted to the surface tension of solutions and to phenomena dependent upon surface films. The properties of liquid-liquid interfaces are then discussed, including a full treatment of spreading and of emulsions. Chapters on gas-solid interfaces and liquid-solid interfaces follow. Electrical phenomena at interfaces are fully dealt with in the next chapter. The two remaining chapters are devoted to the theory and properties of colloids, including the theory of the Brownian movement and the structure of gels. Detailed name and subject indices are given; some errors in references to pages in these have been noticed.

*Contributions to the History of Determinants, 1900-1920.* By Sir THOMAS MUIR. (London: Blackie & Son, Ltd., 50 Old Bailey. Price 30s. net.)

THE original plan to write a history of determinants to the end of the nineteenth century was completed by the publication of the fourth volume, seven years ago. The supplementary volume continues the history of the subject, and gives a record of the researches during the first two decades of the twentieth century on determinants in general, compound determinants, alternants, recurrences, and wronskians. The author's contributions to this volume include over a hundred papers on these special determinants.

Historical papers on other special forms\*, which do not appear in this volume however, have been contributed by Sir Thomas Muir to the 'Proceedings' of the Royal Societies of Edinburgh and South Africa. Each paper is carefully reviewed, and points of historical interest recorded in the introductory remarks. The work of Kostka on symmetric functions and determinants, extending over a period of forty years, receives notice, in particular, his final memoir embodying his life's work on the subject. Unfortunately, no reference is made to the investigations of other workers in this field.

One chapter is devoted to notices of text-books, and a complete subject-index of the contributions reviewed in this volume and its predecessors is provided in an appendix.

It is a matter of congratulation that Sir Thomas Muir has had the opportunity of bringing his *History of Determinants* to recent times, and all students of mathematics, specialists or not, will recognize their indebtedness to him on this great achievement.

*The Theory of Approximation.* By DUNHAM JACKSON, American Mathematical Society Colloquium Publications. Vol. XI. (New York: published by the American Mathematical Society, 501 West 116th Street.)

THE *Theory of Approximation* has formed the subject of two important monographs by De la Vallée Poussin and S. Bernstein, with which Prof. Jackson's work has some points of contact. The approximate representation of continuous functions in terms of polynomials and trigonometric sums, and the convergence of Fourier and Legendre series are considered in the introductory chapter, followed by a discussion of the corresponding theorems for discontinuous functions, the degree of convergence of Fourier and Legendre series under the hypothesis of limited variation, and the convergence and degree of convergence of Fejér's arithmetic mean. Atten-

\* Eleven in all—circulants, continuants, hessians, jacobians, etc.



tion is drawn to the relation between Fourier series and the principle of least squares, and to the remarkable theorems of Bernstein on the derivatives of trigonometric sums and polynomials. The polynomial theorem has been generalized in the case of developments in terms of characteristic functions of differential systems and in the polynomial approximation over an infinite interval. The next section deals with trigonometric interpolation, in which reference is made to the work of Faber and the extensions of Jensen to the case of Sturm-Liouville sums. In the final chapter the author gives an introductory exposition on the geometry of function space, and adds a list of all the important theorems which appear in the text.

*The Quarterly Journal of Mathematics : Oxford Series.* Vol. I. No. 1. April 1930. [Pp. 76.] (Oxford : at the Clarendon Press, 1930. Price 7s. 6d. net. Annual Subscription 27s. 6d. post free.)

THE 'Quarterly Journal of Mathematics (Oxford Series)' is the successor to the 'Quarterly Journal of Mathematics' and 'The Messenger of Mathematics.' It is edited by T. W. Chaundy, W. L. Ferrar, and E. G. C. Poole, with the cooperation of A. L. Dixon, E. B. Elliott, G. H. Hardy, A. E. H. Love, E. A. Milne, F. B. Pidduck, E. C. Titchmarsh. These names should ensure the future success of the Journal, of which there will be no doubt if the standard of the first number is maintained. This contains important papers by E. A. Milne on "The Motion of a Fluid in a Field of Radiation," by O. Veblen on "A Generalization of the Quadratic Differential Form," by G. Pólya on "Some Problems connected with Fourier's Work on Transcendental Equations," and by Mary L. Cartwright on "The Zeros of Certain Integral Functions." The Journal in its new form is well printed on good paper, and we wish it a successful future.

*The Material Culture and Social Institutions of the Simpler Peoples. An Essay in Correlation.* By L. T. HOBHOUSE, G. C. WHEELER, and M. GINSBERG. [Pp. viii + 299.] (London : Chapman and Hall, Ltd., 1930. Price 10s. 6d. net.)

THIS work, which appeared originally in 1915, has long been out of print. The present republication, by the Replika Process, is necessarily identical with the original edition, so that it has not been possible to incorporate the results of the considerable amount of field-work in social anthropology which has been carried out in the intervening years. Nevertheless, the republication—summarizing as it does an enormous amount of data bearing on material culture and social institutions

of the more primitive races and tribes—will be welcomed by students of sociology and anthropology.

In the introduction the general problem of classifying such data is discussed and the various difficulties inherent in such a process are pointed out. The investigation itself is divided into four chapters. In the first the methods of classifying the simpler peoples according to their economic level are explained, and some 600 peoples or tribes are grouped into the following categories:—Lower Hunters, Higher Hunters, Incipient Agriculturals, Pure Agriculturals, Higher Agriculturals, and two forms of Pastorals. In the remaining chapters a tabulated morphology is provided of the institutions of these peoples, including government and justice, the family—embracing marriage, divorce, and the position and status of women—war, social structure, and property. The classifications given in each chapter are treated statistically, in order to discover the relations between economic growth and the development of the social order. The general correlation between social development and economic level are clearly brought out. The data are exhibited in a form which permits of ready verification, and extensive notes are given to each table of classification. The volume is of great value both as a summary of a mass of anthropological data and as a contribution to theories of social development.

*Advanced Trigonometry.* By C. V. DURELL, M.A., and A. ROBSON, M.A. [Pp. viii + 336, with 79 figures.] (London : G. Bell and Sons, Ltd., 1930. Price 8s. 6d.)

THE need of suitable school text-books in mathematics, in which the subjects are presented from the modern point of view, has been felt by many teachers. The volume under review is the first of a series by the same authors, which will include parallel volumes on advanced algebra, on calculus, and a companion volume on analysis, and which attempt to meet this need. The basic idea underlying the treatment is that advanced trigonometry should serve as an introduction to modern analysis ; thus the methods for expanding functions in series are used to draw attention to remainders and limits ; the idea of convergence is introduced at an early stage ; the reality of complex numbers is emphasized, etc. The proposed companion volume on analysis is intended to be used in conjunction with the present volume and to deal more fully with such matters as limits, continuity, convergence, etc.

The present volume has been carefully planned, and represents a serious attempt to provide a course which will not merely train the student in the manipulation of symbols, but which will give him also a real insight into the subject. Difficult points are not shirked, but are carefully explained.

There are many illustrative examples, some of which are worked out by three or four different methods. Each chapter contains a series of easy and a series of harder examples to be worked by the student. A key for the convenience of teachers is published (price 15s. net) in which solutions are given in considerable detail. The volume can be strongly recommended as an advanced text-book for schools.

*La Planète Mars, 1659-1929.* Par E. M. ANTONIADI.  
[Pp. 240, with 150 figures and 10 plates.] (Paris : Hermann et C<sup>ie</sup>, 1930. Price 80 fr.)

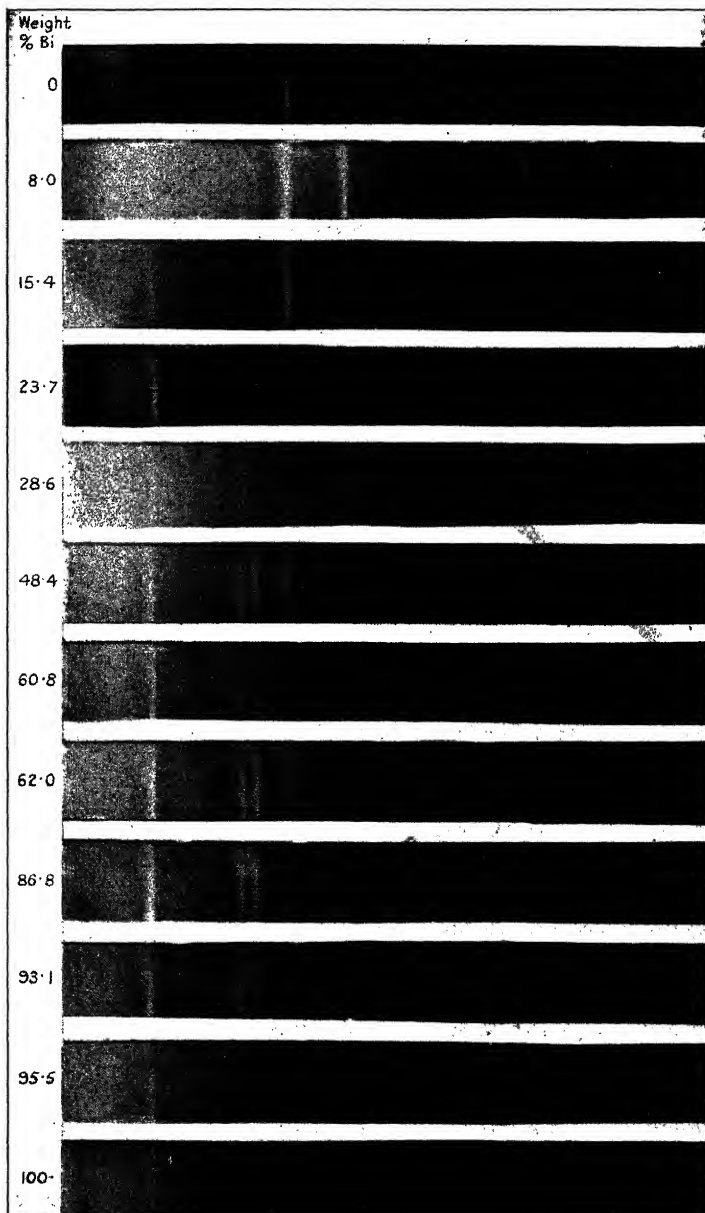
M. ANTONIADI has been an assiduous observer of Mars for many years, and for more than twenty years has had the use of the large 83 cm. refractor at Meudon for such observations. His observations are summarized and discussed in the present monograph ; in addition he has summarized all the observations of the various topographical features obtained since the first sketches of Mars by Huyghens in 1659. These collected observations form the second and main portion of the monograph, which constitutes in effect a dictionary of Mars, which will be found indispensable by all observers of the planet.

The first portion is devoted to more general matter : old observations, methods of observation, numerical data, the surface spots, the canals, the polar caps, the atmosphere of Mars, its physical conditions and habitability, its satellites. M. Antoniadi is strongly convinced that the canals have no objective reality ; his own careful observations have failed to reveal them even under the best conditions, and he cites statements by many other acute observers who, with large instruments and under favourable conditions, have not been able to observe them. He considers, however, that they have a basis of reality, in irregular lines, more or less continuous and spotted, or in other irregular surface markings. M. Antoniadi rejects the temperatures found for Mars and other planets by bolometric methods as illusory ; although these run counter to the preconceived ideas of most planetary observers, it seems that they must be accepted. The agreement between modern observations made by different methods is surprisingly good, and Jeffreys has shown that they are in accordance with what would be anticipated theoretically.

The volume is well illustrated with figures showing various details ; several composite drawings of the surface of the planet and of different regions are given in the form of plates. A large majority of the drawings are by the author himself. The volume forms an excellent summary of his own observations and of those of other observers of Mars.

---

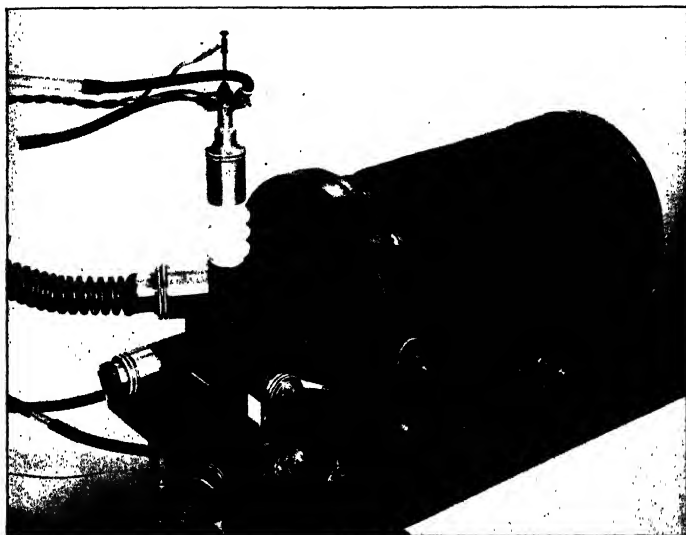
[*The Editors do not hold themselves responsible for the views expressed by their correspondents.*]



Powder Photograms of the System Cu-Bi. Mo-K Radiation.



FIG. 2.



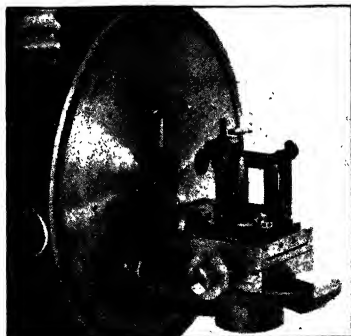
Vacuum Spectrometer for plane gratings.

FIG. 3.



Plate-holder and grating table.

FIG. 4.



The grating, mounted in its holder.



FIG. 7.

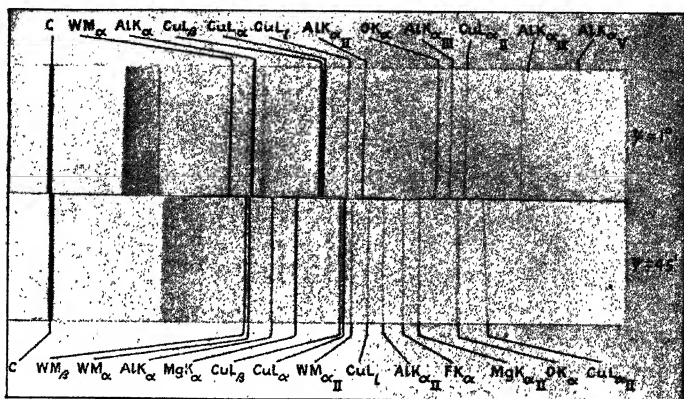
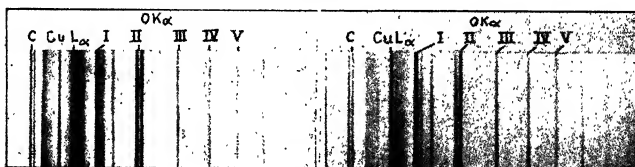


FIG. 8.

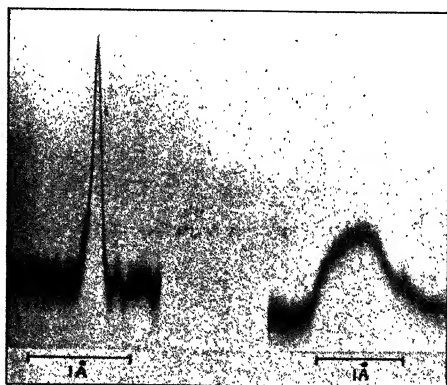


Eclipse plate.

Schumann plate.

Exposed under the same conditions.

FIG. 9.

 $AlK_{\alpha}$  $CK_{\alpha}$ 

Blackening curves from  $AlK_{\alpha II}$  and  $CK_{\alpha I}$ . The small variations in the  $CK_{\alpha}$ -curve are apparently due to irregularities in the emulsion. They do not reappear when different parts of the line are micro-photometered.





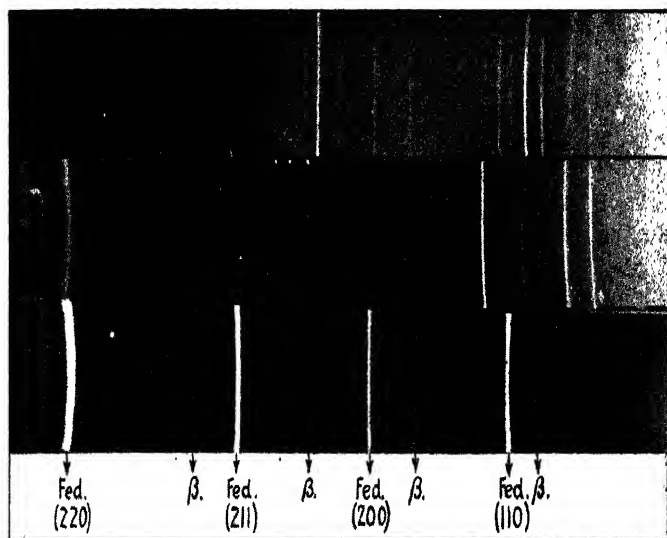


FIG. 1.

FIG. 2.

FIG. 3.



THE  
LONDON, EDINBURGH, AND DUBLIN  
PHILOSOPHICAL MAGAZINE  
AND  
JOURNAL OF SCIENCE.

---

[SEVENTH SERIES.]

---

NOVEMBER 1930.

---

LXXI. *Fitting Observations to a Curve.*  
By NORMAN CAMPBELL, *Sc.D.* \*

SUMMARY.

THE simplified method of curve-fitting described by Condon, Birge, and Shea with reference to the method of least squares is applied to the method of zero sum. The relative advantages of the two methods are unchanged by the simplification of both of them. Tables are given, applicable to zero sum, similar to those given by Birge and Shea for least squares.

Some general considerations of the problem of curve-fitting are offered, suggested by the simplified method.

---

1. **I**N the University of California Publications in Mathematics (ii. pp. 55-118 (1927)) Condon, Birge, and Shea (hereafter called C.B.S.) describe a greatly simplified method of fitting observations to a curve by means of least squares. The primary object of this paper is to point out that their simplified method is equally applicable to the method of zero sum, and that the relative advantages of the two methods are unchanged when the same simplification is applied to both. But I want to take the opportunity to make

\* Communicated by the Author.

some general observations on curve-fitting that are suggested by C.B.S.'s work.

The proposition on which the simplified method depends is this. We desire to fit by least squares a series of correlated observations  $(x, y)$  to a curve

$$y = \sum a_r x^r, \quad . \quad . \quad . \quad . \quad . \quad . \quad (1)$$

where  $r$  is the set of positive integers from 0 to  $n$ —that is to say, we desire to determine the constants  $a_r$  so that the “smoothed” values of  $y$ , calculated from (1), may be used in substitution for the observed values. If we subject (1) to any linear transformation

$$x' = ax + b \quad . \quad . \quad . \quad . \quad . \quad . \quad (2)$$

and fit the observations to the curve

$$y = \sum a_r' x'^r, \quad . \quad . \quad . \quad . \quad . \quad . \quad (1.1)$$

then, although we shall, of course, arrive at different constants  $a_r'$ , we shall arrive at precisely the same smoothed values of  $y$ . This proposition is useful when the  $x$ 's (supposed free from all experimental error) are given at equal intervals, so that  $x$  is of the form

$$x = x_0 + p\lambda, \quad . \quad . \quad . \quad . \quad . \quad . \quad (3)$$

where  $p$  is the series of integers. For now the transformation (2) may be made to give (1.1) the form

$$y = \sum a_r' p^r \quad . \quad . \quad . \quad . \quad . \quad . \quad (1.2)$$

independent of  $x_0$  and  $\lambda$ . The numerical work is greatly simplified by the substitution of integers for the  $x$ 's; moreover, tables can be worked out, once and for all, whereby any series of equidistant observations can be fitted to any polynomial by entering the observed  $y$ 's on a simple standard form.

2. The truth of the proposition may seem to follow immediately from the fact that the linear transformation (2) corresponds in graphical smoothing to a change in zero and a change of scale; such changes ought not to affect the result of a graphical smoothing. But the matter is not quite so simple as that; for, if this were all, the proposition ought to remain true if any other form of curve were substituted for the polynomial (1). Actually it does not; it remains true only if the curve (1) is such that its form remains unchanged by the substitution, its form being determined by the number of adjustable constants  $a_r$  and their

dimensions in terms of  $x, y$  \*. Thus it remains true, if the curve has the form  $y = Ae^{ax}$ , but not if it has the form (1), and  $r$  includes negative or fractional values. It might be suggested, therefore, that there was something less arbitrary in fitting to a curve for which the proposition is true than in fitting to one for which it is not true, so that the smoothed values depend on the choice of zero (but not on the choice of scale).

But further reflexion shows that this suggestion is false. Curve-fitting may have one of two objects: (a) The constants  $a, r$  may be true secondary magnitudes †; the form of the curve is then absolutely determined, and the object is to determine those constants. If the curve is not of the form for which the proposition is true, the zero will then have physical significance—choice of zero is not arbitrary at all. (b) The object is mere smoothing with a view to interpolation, differentiation, etc. Then any choice of form of curve is arbitrary. It is no more arbitrary to select a particular zero in fitting to a form of curve for which the proposition is true than to select one out of the many forms of curve for which it is true (*e.g.*, to select a particular degree  $n$  for the polynomial (1)). Accordingly there is no greater arbitrariness in fitting to one form of curve than to another. Smoothing must always involve some arbitrariness; there would be no such thing as smoothing if there were not certain limits within which there is nothing to decide between one arbitrary choice and another.

3. The choice between equally permissible methods of smoothing must be made on the grounds of convenience. The graphical method is usually the most convenient; it has, moreover, the advantage in principle that smoothing is an essentially graphical conception; it should therefore always be adopted if its sensitivity is sufficient ‡. Its sensitivity is most likely to be insufficient when the object of smoothing is not merely interpolation, but some analytical

\* I am indebted to Mr. R. H. Fowler for pointing out to me this condition. A general proof seems not to be very easy, but there is no doubt that the condition is necessary and sufficient in all relevant instances.

† See my 'Measurement and Calculation,' chap. vi.

‡ Since the preference expressed here for a graphical method is directly contrary to that expressed in Whittaker and Robinson's standard treatise, it may be well to point out that they are concerned throughout with statistics, while I am concerned with physics. The word *accuracy* has entirely different meanings in the two sciences. To a statistician observations are accurate if the greatest possible care has been expended in obtaining them, whatever the result obtained. To a physicist (etymologically less correct) they are accurate only if

operation such as differentiation. It is only then that algebraic smoothing is desirable. Among the algebraic methods the choice of a polynomial (1) is again preferable on the score of convenience to the choice of other forms of curve, if it is permissible, and so is the choice of zero sum to least squares. It would be utterly inconsistent to adopt the polynomial rather than a curve to which the simplified C.B.S. method is inapplicable, and then to adopt a less rather than a more convenient method of smoothing to it, so long as there is no evidence that one method gives a result within the prescribed limits and the other gives a result outside them.

4. The strictest limits that can be set are defined by the rule that the residuals must be wholly irregular and that no smoothed point must diverge from an observed point by more than the maximum error determined by repetition \*. However, less strict limits are often assigned; systematic residuals, exceeding the maximum error, are sometimes tolerated, especially at the ends of the curve. There may be good reason for such toleration, but once more it must be applied consistently. There is no reason to prefer one method to another, because it gives smaller residuals, unless it is clear that the larger residuals exceed some limit, assignable *à priori*, within which the smaller residuals are found to lie; if both sets of residuals are systematic, such a limit is unlikely to be found; then both methods of smoothing are usually justifiable or neither of them.

The decision whether any proposed choice of curve and any proposed method of smoothing to it are justifiable can be determined in the last resort only by an examination of the residuals; but it is one of the advantages of choosing the curves (1) that there is a simple method of deciding whether any such curve is permissible, and, if so, what must be the degree of the polynomial, which will nearly always give the right answer. It is this: take the successive diffe-

---

they fulfil certain conditions, of which one is always that the observations shall be so regular that graphical smoothing does not increase the error. The observations that Whittaker and Robinson take as their example in chap. xi. are doubtless highly accurate to a statistician; but if they were presented to a physicist as the result of an experiment he would reject them as so hopelessly irregular that no important conclusion could be based on them. He would say that the experiment on which they were based did not prove what it was intended to prove, and would devise another experiment. This difference in the meaning of the word accuracy is the main reason why the computational methods worked out by statisticians are so seldom applicable to physics.

\* See 'Measurement and Calculation,' chap. x.

rences (divided differences, if the  $x$ 's are not equidistant) of the observations, arranged in order of  $x$ . It will often be found that the differences remain regular and decrease generally in arithmetic magnitude, as the order of the difference is increased, until the  $n$ th order is reached; thereafter they become irregular and tend to increase in arithmetic magnitude. If this is not so, no curve of the form (1) is satisfactory for smoothing. If it is so, smoothing to a polynomial of degree  $(n+1)$  is likely to be satisfactory, and no improvement is likely to result from choosing a polynomial of degree greater than  $(n+1)$  \*.

5. We now proceed to the method of smoothing to a polynomial (1) of degree  $n$  by zero sum. Since there are  $n+1$  constants to be determined, we require  $n+1$  equations and  $m(n+1)$  observations at equal intervals of  $x$ , where  $m$  is some integer. Let  $N$  be the number of observations; whatever is  $N$ , the observations will not usually be equidistant; whether we use least squares or zero sum, the conversion of the original observations to equidistant observations will usually be necessary. A preliminary graphical smoothing is the best plan; the sensitivity can always be made great enough by taking the differences of the observations from some very rough smoothed curve—*e.g.*, a straight line. For  $m$  the integer equal to or next greater than  $N/(n+1)$  should be chosen.

The general rule of zero sum is to place in order of increasing  $x$  the observational equations that result from substituting corresponding values of  $x$  and  $y$  in (1), and to form the required  $(n+1)$  equations by summing the first  $m$ , the second  $m$ , ... equations. This procedure is to be modified, in virtue of C.B.S.'s principle, only by substituting the series of integers 0, 1, 2, ... for the equidistant  $x$ 's †. The resulting  $(n+1)$  equations for the  $a_r$ 's in (1.2) are then

\* It should be observed that  $x$  and  $y$  in (1) need not be the actual observations; they may be functions of the observations, such as  $\log y$  or  $x^2$ . The range of sets of observations that can be fitted to curves of the form (1) is therefore much greater than might appear at first sight. Indeed, periodic observations are the only large and important class resulting from physical experiments that cannot be fitted to this form.

† In virtue of their principle the result is precisely the same if the order of the observations is reversed, and the highest, instead of the lowest,  $x$  replaced by 0. C.B.S. work with central differences, whereas we use differences from one end. The disadvantage of central differences is that different tables are required according as  $N$  or  $(n+1)$  is even or odd; the advantage is that a given accuracy can be obtained by retaining a smaller number of figures. But, as will appear presently, this advantage is less with zero sum than with least squares; with the former, therefore, differences from one end seem preferable.



$$Y_s = a_0' \cdot S_{sm}^0 + \dots + a_r' \cdot S_{sm}^r + \dots + a_n' \cdot S_{sm}^n, \quad (4)$$

( $s = 0$  to  $n$ )

where  $Y_s$  is the sum of the  $(s+1)$ th set of  $m$   $y$ 's and  $S_{sm}^r$  is the sum of the  $r$ th powers of the integers from  $sm$  to  $(s+1)m-1$  inclusive ( $S_{0m}^0 = m$ ). If the successive differences of these equations are taken, the coefficient of  $a_r'$  is zero in the difference of  $(r+1)$ th order. Accordingly, if we write

$$\left. \begin{aligned} \Delta^q Y_0 &= q\text{th order difference of } Y_0, \\ D_r^q &= \Delta^q S_{0m}^r = q\text{th order difference of } S_{0m}^r, \end{aligned} \right\} \quad (5)$$

we have

$$\left. \begin{aligned} Y_0 &= a_0' \cdot S_{0m}^0 + a_1' \cdot S_{0m}^1 + \dots + a_n' \cdot S_{0m}^n, \\ \Delta^1 Y_0 &= a_1' \cdot D_1^1 + \dots + a_n' \cdot D_n^1, \\ &\vdots \\ \Delta^{n-1} Y_0 &= a_{n-1}' \cdot D_{n-1}^{n-1} + a_n' \cdot D_n^{n-1}, \\ \Delta^n Y_0 &= a_n' \cdot D_n^n. \end{aligned} \right\} \quad (6)$$

$Y_0$  and  $\Delta^q Y_0$  are taken from a difference table of the  $Y$ 's, the coefficients  $S_{0m}^r$  and  $D_r^q$  from tables given in the Appendix. The last equation then gives  $a_n'$ ; when the value so obtained is substituted in the remainder, the last but one gives  $a_{n-1}'$ , and so on. During the solution it is convenient at the same time to insert the values of the  $a_r'$  in equations (7, 8) below.

If the problem is one of curve-fitting, the values of  $a_r$  in (1) will be required. They are obtained from

$$a_r = \sum_q \frac{a_q'}{\lambda^q} \cdot (x_0)^{q-r} \cdot {}^q C_r \dots (q=r \text{ to } n). \quad (7)$$

If, on the other hand, the problem is one of smoothing, the smoothed values of  $y$  will be required. These are best obtained from a difference table, using the leading differences obtained from the  $a_r'$  by the equations

$$\left. \begin{aligned} y_0 &= a_0', \\ \Delta^r y_0 &= \sum_q \Delta^r 0^q a_q' \dots (q=r \text{ to } n), \end{aligned} \right\} \quad (8)$$

where  $\Delta^r 0^q$  is the  $r$ th order "difference of zero" of degree  $q$ . Forms for solving (7) and (8) are given in the Appendix.

The table built up from these differences will, of course, give interpolated values of  $y$  and also the derivatives  $\frac{d^r y}{dp^r}$

by the usual formulæ ; from these last  $\frac{d^r y}{dx^r}$  can be obtained by means of

$$\frac{d^r y}{dx^r} = \frac{1}{\lambda^r} \cdot \frac{d y}{dp^r} \cdot \cdot \cdot \cdot \cdot \cdot \quad (9)$$

All this is the same as with C.B.S.'s method, but there is one important difference in the building-up of the table of calculated  $y$ 's. If the arithmetic is correct the residuals of any group of  $y$ 's summed to form a single  $Y$  must sum to zero. This proposition, characteristic of zero sum but not of least squares, is very convenient. An error of 1 in  $\Delta^2 y_0$  produces an error  $N^{-1}C_q$  in the last calculated  $y$  ; accordingly, if perfect accuracy is required, many more places must be retained in  $\Delta^2 y_0$  than are required in  $y$ . But if too few places are retained in zero sum, the sums of the residuals corresponding to any  $Y$  will diverge from zero progressively and regularly as  $q$  increases. By examining this divergence, if it is not too large, a correction to the calculated  $y$ 's may readily be found which reduces it to zero and makes the last place correct ; for this reason it is permissible to omit at least one more figure from  $\Delta^2 y_0$  when using zero sum than when using least squares\*.

6. It remains only to apply the method to an example ; that used by C.B.S. will be taken. In Table I. the column headed  $y$  gives the observed values of  $y$  ;  $x$  increases by steps of  $-1$  from  $-1\frac{1}{2}$  for the first  $y$  to  $-25\frac{1}{2}$  for the last. The columns headed  $\Delta^3 y$  and  $\Delta^4 y$  on the left give the third and fourth order differences of the unsmoothed  $y$ 's (the first and second orders are omitted to save space). These differences are used, in accordance with the rule on p. 749, to determine the value of  $n$  in (1) that is to be adopted. It will be seen that the third order differences show some regularity, being predominantly positive, while the fourth order differences are chaotic and are tending to increase in arithmetic magnitude. Accordingly we take  $n=4$ , which is the value taken by C.B.S. Since the observations are equidistant in  $x$ , and since  $N$  (by a coincidence) is a multiple of  $(n+1)$ , we can proceed at once with the original observations, and

\* It may occur to the reader that, if all these operations subsidiary to the main computation have to be performed, the "simplified" method will actually turn out to be more laborious than the direct method ; but many of them are mere substitutions for operations that are required equally in the direct method. There is no doubt whatever that, if  $n$  is as great as 3, the simplified method is a great saving.

TABLE I.

$$x_0 = -1\frac{1}{2}; \lambda = -1.$$

$\Delta^4 y.$	$\Delta^3 y.$	$y.$	Y.	$\Delta' Y.$	$\Delta^2 Y.$	$\Delta^3.$	$\Delta^4 Y.$
		3295.47					
		277.79					
-0.39	+0.27	257.86	16279.01 (=Y <sub>0</sub> )				
+0.14	-0.12	235.95					
+0.01	+0.02	211.94					
-0.01	+0.03	185.85		- 651.25 (= $\Delta' Y_0$ )			
+0.03	+0.02	157.71					
-0.04	+0.05	127.54	15627.76		- 249.61 (= $\Delta^2 Y_0$ )		
-0.04	+0.01	095.39					
+0.15	-0.03	061.27					
-0.10	+0.12	025.15		- 900.86		+16.27 (= $\Delta^3 Y_0$ )	
-0.11	+0.02	2987.15					
+0.18	-0.09	947.29	14726.90				
-0.01	+0.09	905.48		- 233.34		+0.58 (= $\Delta^4 Y_0$ )	
-0.11	+0.08	861.83					
+0.09	-0.03	816.42		-1134.20		+16.85	
-0.09	+0.06	769.22					
+0.03	-0.03	720.29	13592.70		-216.49		
+0.08	+0.00	669.60					
-0.01	+0.08	617.17					
-0.28	+0.07	563.06		- 1350.69			
+0.46	-0.21	507.40					
-0.34	+0.25	449.98	12242.01				
	-0.09	391.05					
		330.52					

can omit the step of obtaining  $m(n+1)$  equidistant observations. In the column headed Y the observations are

TABLE II.

(m=5).

$\Delta^4 Y_0 = 75000 a_4'$ (+0.58)	$a_4' = +0.000007733$
$\Delta^3 Y_0 - 142500 a_4' = 3750 a_3'$ (+16.27) (-1.102)	$a_3' = +0.00404480$
$\Delta^2 Y_0 - 82750 a_4' - 5250 a_3' = 250 a_2'$ (-249.61) (-0.640) (-21.235)	$a_2' = -1.085940$
$\Delta Y_0 - 14625 a_4' - 1825 a_3' - 225 a_2' = 25 a_1'$ (-651.25) (-0.1131) (-7.3818) (+244.3365)	$a_1' = -16.57634$
$Y_0 - 354 a_4' - 100 a_3' - 30 a_2' - 10 a_1' = 5 a_0'$ (+16279.01) (-0.003) (-0.404) (+32.578) (+165.764)	$a_0' = +3295.389$
$(a_r'/\lambda^r = (-1)^r a_r'; x_0 = -1.5, x_0^2 = +2.25; x_0^3 = -3.375;$ $x_0^4 = +5.0625).$	
$a_4 = a_4'/\lambda^4$	$= +0.000007733$
$a_3 = -4x_0 \cdot a_4'/\lambda^4 + a_3'/\lambda^3$ (+0.0000464) (-0.0040448)	$= -0.0039984$
$a_2 = +6x_0^2 \cdot a_4'/\lambda^4 - 3x_0 \cdot a_3'/\lambda^3 + a_2'/\lambda^2$ (+0.000104) (-0.018202) (-1.085940)	$= -1.104038$
$a_1 = -4x_0^3 \cdot a_4'/\lambda^4 + 3x_0^2 \cdot a_3'/\lambda^3 - 2x_0 \cdot a_2'/\lambda^2 + a_1'/\lambda$ (+0.00010) (-0.02730) (-3.25782) (+16.57634)	$= +13.29132$
$a_0 = +x_0^4 \cdot a_4'/\lambda^4 - x_0^3 \cdot a_3'/\lambda^3 + x_0^2 \cdot a_2'/\lambda^2 - x_0 \cdot a_1'/\lambda + a_0'$ (0.000) (-0.0137) (-2.443) (+24.865) (+3295.389)	$= +3317.797$
$\Delta^4 y_0 = 24 a_4'$	$= +0.0001856$
$\Delta^3 y_0 = 36 a_4' + 6 a_3'$ (+0.0002784) (+0.0242688)	$= +0.024547$
$\Delta^2 y_0 = 14 a_4' + 6 a_3' + 2 a_2'$ (+0.000108) (+0.024269) (-2.171880)	$= -2.14750$
$\Delta y_0 = a_4' + a_3' + a_2' + a_1'$ (+0.00001) (+0.00404) (-1.08594) (-16.57634)	$= -17.6583$

summed in sets of five; in the remaining columns on the right these sums are differenced and the values of  $\Delta^r Y_0$  obtained.

In Table II. the equations (6), (7), and (8) are set up by means of the tables in the Appendix and solved. No further

explanation of the procedure should be necessary, but it will be observed that the order of the equations has been reversed for convenience.

In Table III. the smoothed or calculated  $y$ 's are obtained from a difference table, using the values of  $\Delta^2 y_0$  found in Table II. To save space only the first part of the Table is given; it is to be observed that the residuals for each of the first two sets of five  $y$ 's add to zero, as they should.

Finally, the accompanying figure shows the residuals obtained by zero sum and by least squares. In the first few values of  $x$  the residuals show an obvious trend (there is some

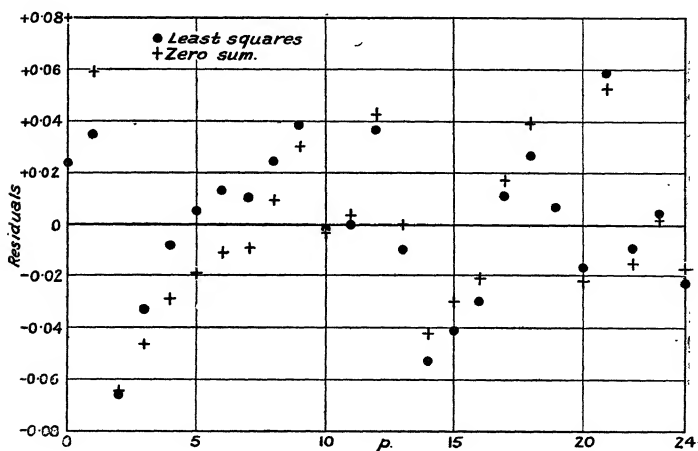
TABLE III.

$\Delta^4 y.$	$\Delta^3 y.$	$\Delta^2 y.$	$\Delta^1 y.$	$y(\text{calc.}).$	$y(\text{obs.}) - y(\text{calc.}).$	
				3295.389	+0.081	} sum =0.000
			-17.6583	277.731	+0.059	
+0.001856	+0.024547	-2.14750	-19.8058	257.925	-0.065	
	+0.024733	-2.12295	-21.9287	235.996	-0.046	
	+0.024918	-2.09822	-24.0269	211.969	-0.029	
	+0.025104	-2.07330	-26.1002	185.869	-0.019	} sum =0.000
	+0.025290	-2.04819	-28.1484	157.721	-0.011	
	+0.025475	-2.02290	-30.1713	127.549	-0.009	
	+0.025661	-1.99743	-32.1687	095.381	+0.009	
		-1.97177	-34.1405	061.240	+0.030	

sign of a repetition of the same trend for later values of  $x$ ); neither method of smoothing satisfies the strict criterion of p. 748, both import something that is not justified by the observations themselves. Further, the trend of the residuals cannot be removed by adopting a larger value of  $n$ , unless  $n$  becomes comparable with  $N$  and there is no smoothing. Whether, in these circumstances, smoothing to a polynomial is justified at all is a question that cannot be answered without a thorough inquiry into the meaning and origin of the observations; but it is most unlikely that such an inquiry would show that the difference between the two methods of smoothing (which is marked only in the first two values of  $x$ ) is such that one is justifiable and the other is not.

As usual, it turns out that, when there is any justification for adjusting observations by either least squares or by zero sum, the two methods yield physically indistinguishable results.

Once more, then, I would plead with the adherents of least squares. Physicists generally do not study computational methods deeply; when they are forced to use them, they accept what they are told by those who have made them their special study. Such persons are accepting a very heavy responsibility if they induce their colleagues to waste unnecessary labour without offering any evidence that the traditional methods are superior.



### Appendix.

Table IV. gives the coefficients of  $a_r'$  in equations (6) sufficient to fit to any polynomial of degree not greater than 6. A different set of coefficients is required for each value of  $m$ , but the coefficient of any  $a_r'$  is the same whatever the value of  $n$ . Accordingly the values for equations of lower degree than the sixth are obtained by simply omitting the higher terms (see example, where the terms  $a_5'$  and  $a_6'$  are simply omitted from the table for  $m=5$ ). Values for  $m > 10$  are not likely to be required, for accuracy is very seldom gained by having more than ten observations in each group.

The coefficients can be calculated either by forming the

sums  $S_{sm}^r$  and differencing them, or, more conveniently, by using the formula

$$\Delta^q S_{0m}^r = \sum_t {}^r C_t \cdot S_{0m}^t \cdot m^{r-t} \cdot \Delta^q 0^{r-t} \quad (t=0 \text{ to } r-q).$$

TABLE IV.

$m=2.$	$a_0'.$	$a_1'.$	$a_2'.$	$a_3'.$	$a_4'.$	$a_5'.$	$a_6'.$
$Y_0 =$	2	1	1	1	1	1	1
$\Delta^1 Y_0 =$		4	12	34	96	274	792
$\Delta^2 Y_0 =$			16	120	688	3600	18,136
$\Delta^3 Y_0 =$				96	1344	12,960	107,520
$\Delta^4 Y_0 =$					768	17,280	251,520
$\Delta^5 Y_0 =$						7680	253,440
$\Delta^6 Y_0 =$							92,160

$m=3.$	$a_0'.$	$a_1'.$	$a_2'.$	$a_3'.$	$a_4'.$	$a_5'.$	$a_6'.$
$Y_0 =$	3	3	5	9	17	33	65
$\Delta^1 Y_0 =$		9	45	207	945	4359	20,385
$\Delta^2 Y_0 =$			54	648	5886	48,600	385,614
$\Delta^3 Y_0 =$				486	10,692	161,190	2,084,940
$\Delta^4 Y_0 =$					5832	204,120	4,607,280
$\Delta^5 Y_0 =$						87,480	4,461,480
$\Delta^6 Y_0 =$							1,574,640

$m=4.$	$a_0'.$	$a_1'.$	$a_2'.$	$a_3'.$	$a_4'.$	$a_5'.$	$a_6'.$
$Y_0 =$	4	6	14	36	98	276	794
$\Delta^1 Y_0 =$		16	112	712	4480	28,456	183,232
$\Delta^2 Y_0 =$			128	2112	26,240	295,680	3,197,888
$\Delta^3 Y_0 =$				1536	46,080	944,640	16,588,800
$\Delta^4 Y_0 =$					24,576	1,167,360	35,696,640
$\Delta^5 Y_0 =$						491,520	33,914,880
$\Delta^6 Y_0 =$							11,796,480

$m=5.$	$a_0'.$	$a_1'.$	$a_2'.$	$a_3'.$	$a_4'.$	$a_5'.$	$a_6'.$
$Y_0 =$	5	10	30	100	354	1300	4890
$\Delta^1 Y_0 =$		25	225	1825	14,625	118,225	968,625
$\Delta^2 Y_0 =$			250	5250	82,750	1,181,250	16,171,750
$\Delta^3 Y_0 =$				3750	142,500	3,693,750	81,937,500
$\Delta^4 Y_0 =$					75,000	4,500,000	173,625,000
$\Delta^5 Y_0 =$						1,875,000	163,125,000
$\Delta^6 Y_0 =$							56,250,000

TABLE IV. (cont.).

$m=6.$	$a_0'.$	$a_1'.$	$a_2'.$	$a_3'.$	$a_4'.$	$a_5'.$	$a_6'.$
$Y_0 = 6$	15	55	225	979	4425	20,515	
$\Delta^1 Y_0 =$	36	396	3906	38,016	373,026	3,708,936	
$\Delta^2 Y_0 =$		432	11,016	210,384	3,635,280	60,209,352	
$\Delta^3 Y_0 =$			7776	357,696	11,210,400	300,464,640	
$\Delta^4 Y_0 =$				186,624	13,530,240	630,322,560	
$\Delta^5 Y_0 =$					5,598,720	587,865,600	
$\Delta^6 Y_0 =$						201,553,920	
$m=7.$	$a_0'.$	$a_1'.$	$a_2'.$	$a_3'.$	$a_4'.$	$a_5'.$	$a_6'.$
$Y_0 = 7$	21	91	441	2275	12,201	67,171	
$\Delta^1 Y_0 =$	49	637	7399	84,721	977,599	11,428,417	
$\Delta^2 Y_0 =$		686	20,580	461,678	9,363,900	181,969,046	
$\Delta^3 Y_0 =$			14,406	777,924	28,595,910	898,502,220	
$\Delta^4 Y_0 =$				403,363	34,286,280	1,871,627,520	
$\Delta^5 Y_0 =$					14,117,880	1,736,499,240	
$\Delta^6 Y_0 =$						592,950,960	
$m=8.$	$a_0'.$	$a_1'.$	$a_2'.$	$a_3'.$	$a_4'.$	$a_5'.$	$a_6'.$
$Y_0 = 8$	28	140	784	4676	29,008	184,820	
$\Delta^1 Y_0 =$	64	960	12,832	168,960	2,241,184	30,113,280	
$\Delta^2 Y_0 =$		1024	35,328	910,336	21,196,800	472,743,424	
$\Delta^3 Y_0 =$			24,576	1,523,712	64,266,240	2,316,042,240	
$\Delta^4 Y_0 =$				786,432	76,677,120	4,799,201,280	
$\Delta^5 Y_0 =$					31,457,280	4,435,476,480	
$\Delta^6 Y_0 =$						1,509,949,440	
$m=9.$	$a_0'.$	$a_1'.$	$a_2'.$	$a_3'.$	$a_4'.$	$a_5'.$	$a_6'.$
$Y_0 = 9$	36	204	1296	8772	61,776	446,964	
$\Delta^1 Y_0 =$	81	1377	20,817	309,825	4,644,081	70,503,777	
$\Delta^2 Y_0 =$		1458	56,862	1,654,830	43,499,430	1,094,944,878	
$\Delta^3 Y_0 =$			39,366	2,755,620	131,154,390	5,332,124,700	
$\Delta^4 Y_0 =$				1,417,176	155,889,360	11,004,371,640	
$\Delta^5 Y_0 =$					63,772,920	10,139,894,280	
$\Delta^6 Y_0 =$						3,443,737,680	



TABLE IV. (cont.).

$m=10.$	$a_0'.$	$a_1'.$	$a_2'.$	$a_3'.$	$a_4'.$	$a_5'.$	$a_6'.$
$Y_0 = 10$	45	285	2025	15,333	120,825	978,405	
$\Delta^1 Y_0 =$	100	1900	32,050	532,000	8,891,650	150,499,000	
$\Delta^2 Y_0 =$		2000	87,000	2,822,000	82,650,000	2,317,499,000	
$\Delta^3 Y_0 =$			60,000	4,680,000	248,100,000	11,232,000,000	
$\Delta^4 Y_0 =$				2,400,000	294,000,000	23,106,000,000	
$\Delta^5 Y_0 =$					120,000,000	21,240,000,000	
$\Delta^6 Y_0 =$						7,200,000,000	

Table V. gives the coefficients of  $a_q/\lambda^q$  in the equation for  $a_r$  according to (7). Table VI. gives the coefficients of  $a_q$  in the equation for  $\Delta^r y_0$  according to (8).

TABLE V.

$a_0'.$	$a_1'/\lambda.$	$a_2'/\lambda^2.$	$a_3'/\lambda^3.$	$a_4'/\lambda^4.$	$a_5'/\lambda^5.$	$a_6'/\lambda^6.$
$a_0 = 1$	$-x_0$	$+x_0^2$	$-x_0^3$	$+x_0^4$	$-x_0^5$	$+x_0^6$
$a_1 =$	1	$-2x_0$	$+3x_0^2$	$-4x_0^3$	$+5x_0^4$	$-6x_0^5$
$a_2 =$		1	$-3x_0$	$+6x_0^2$	$-10x_0^3$	$+15x_0^4$
$a_3 =$			1	$-4x_0$	$+10x_0^2$	$-20x_0^3$
$a_4 =$				1	$-5x_0$	$+15x_0^2$
$a_5 =$					1	$-6x_0$
$a_6 =$						1

TABLE VI.

$a_0'.$	$a_1'.$	$a_2'.$	$a_3'.$	$a_4'.$	$a_5'.$	$a_6'.$
$y_0 = 1$	0	0	0	0	0	0
$\Delta^1 y_0 =$	1	1	1	1	1	1
$\Delta^2 y_0 =$		2	6	14	30	62
$\Delta^3 y_0 =$			6	36	150	540
$\Delta^4 y_0 =$				24	240	1560
$\Delta^5 y_0 =$					120	1800
$\Delta^6 y_0 =$						720

LXXII. *The Magneto-Optical Dispersion of Organic Liquids.*  
 Part I. *The Magneto-Optical Dispersion of Normal Butyl Alcohol, Isobutyl Alcohol, and Propionic Acid.* By EMLYN STEPHENS, M.Sc., and Prof. E. J. EVANS, D.Sc., *Physics Department, University College of Swansea* \*.

INTRODUCTION.

A STUDY of the magneto-optical rotations of organic liquids provides valuable information concerning the nature and properties of molecules. The problem has been investigated from this point of view by Perkin†, who determined the molecular rotations for sodium light of a large number of organic liquids belonging to various homologous series. The rotation, however, depends upon the wave-length, and although Lowry‡ and others have examined the magneto-optical dispersion of many organic liquids, our information on this aspect of the problem is still very incomplete. The present investigation is a continuation of previous work carried out by Stephens and Evans§ etc. on the magneto-optical dispersion of organic liquids in the ultra-violet region of the spectrum. The problem of magneto-optical rotation has been considered from the theoretical side by Larmor||, Richardson¶, and others, and the experimental results of the present investigation have been considered in relation to their work.

According to Larmor the magneto-optical rotation is a kinetic phenomenon related to the free periods of the resonators in the molecule. If the natural dispersion of a substance is known, it is possible from the measurements of its magneto-optical dispersion to deduce important information with regard to the nature and number of resonators present in the molecule, together with their free periods.

For regions of the spectrum not too near an absorption band the natural dispersion of a substance can be represented accurately by the following equation of the Ketteler-Helmholtz type :—

$$n^2 - 1 = b_0 + \frac{b_1}{\lambda^2 - \lambda_1^2} + \frac{b_2}{\lambda^2 - \lambda_2^2} + \dots \quad (1)$$

\* Communicated by the Authors.

† Journ. Chem. Soc. p. 468 (1884).

‡ Journ. Chem. Soc. p. 1067 (1913).

§ Phil. Mag. iii. (March 1927): Jones & Evans, Phil. Mag. v. (March 1928); Evans & Evans, Phil. Mag. viii. (August 1929).

|| 'Æther and Matter,' Appendix F, p. 352.

¶ Phil. Mag. xxxi. pp. 232 & 454.

where  $n$  is the refractive index for wave-length  $\lambda$ ;  $b_0, b_1, b_2$ , &c., are constants; and  $\lambda_1, \lambda_2 \dots$  are the wave-lengths of the absorption bands of the substance.

According to Larmor the value of Verdet's constant,  $\delta$ , is given by the equation

$$\delta = \frac{e}{2mC^2} \lambda \frac{dn}{d\lambda}, \dots \dots \dots (2)$$

where  $C$  is the velocity of light, and  $\frac{e}{m}$  is the ratio of charge to mass for all the resonators. In deducing this equation the charge  $e$  is measured in electrostatic units and the field in electromagnetic units.

If the value of  $\frac{dn}{d\lambda}$  obtained from equation (1) is now put into equation (2), it can be shown\* that

$$\phi = n\delta\lambda^2 = K_1 \left\{ \frac{\lambda^2}{\lambda^2 - \lambda_1^2} \right\}^2 + K_2 \left\{ \frac{\lambda^2}{\lambda^2 - \lambda_2^2} \right\}^2 + \dots, \quad (3)$$

where  $K_1, K_2$ , &c. are constants, and  $\lambda_1, \lambda_2$ , &c. are wave-lengths corresponding to the free periods of the resonators.

For substances which are transparent in the visible and infra-red,  $\lambda_1, \lambda_2$ , &c., represent wave-lengths corresponding to ultra-violet free periods, and when a substance possesses only one absorption band in the ultra-violet contributing to the magnetic rotation, the equation takes the form

$$\phi = K_1 \left\{ \frac{\lambda^2}{\lambda^2 - \lambda_1^2} \right\}^2 \dots \dots \dots (4)$$

From the two values of  $\phi$  corresponding to two values of  $\lambda$  it is possible to determine  $K_1$  and  $\lambda_1$  for the region of the spectrum between the two wave-lengths chosen. If the experimental results lead to different values of  $\lambda_1$ , depending on the wave-lengths chosen, and if the values change progressively when the chosen wave-lengths are taken in regions of shorter and shorter wave-lengths, it is presumed that the substance has more than one free period. If, however, the values of  $\lambda_1$  are constant within experimental error, the values of  $\phi$  are given by equation (4).

#### EXPERIMENTAL ARRANGEMENT.

A parallel beam of light was obtained by placing a tungsten arc at the focus of a quartz lens. This lens, together with the modified Jellett prism † immediately behind it, formed

\* Richardson, *loc. cit.*

† 'Dictionary of Applied Physics,' iv p. 476.

the polarizing unit of the Bellingham-Stanley polarimeter. This polarimeter had been specially designed for work in the ultra-violet region of the spectrum, as the components of the polarizer were assembled without any intervening film which may cause absorption in that region. The beam of light, after emerging from the polarizer, consisted of two semicircular beams, the vibrations in one half being polarized at a slight angle with those in the other, the line of demarcation between them being horizontal. The beam then traversed the liquid contained in a tube which was fixed in position inside a solenoid. On emerging from the liquid the beam falls on the analyser and is brought to a focus on the slit of a quartz spectrograph by a quartz-fluorite lens, which formed part of the Bellingham-Stanley analyser unit. The analyser was of the usual type, its component parts being assembled with a thin film of glycerine. Both the analyser and the quartz-fluorite lens behind it were mounted in the same brass tube, and the lens could be independently adjusted so that the beam of light passed axially through the apparatus. The analyser unit, which could be rotated, had a vernier scale fixed to it, and the rotation could be measured on a fixed circular scale to  $1'$  of arc.

The same polarimeter tube was used throughout the investigation. It was made of clear fused quartz, having an external diameter of about 1 cm., and could contain a column of liquid 30.5 cm. long. The two ends of the tube were closed by fusing on disks of polished fused quartz. The disks were fused along the outside circumference of the tube, and there was no distortion of light by the central portions of the disks. These disks rotate polarized light in a magnetic field, so that a correction has to be applied when measuring magneto-optical rotations of liquids. The value of the actual correction to be applied at any wave-length could be read off from a curve obtained by the experimental determination of the rotations of the disks corresponding to several wave-lengths.

The solenoid, which was wound on a brass tube 47.3 cm. long and 4.27 cm. diameter, was connected in series with a battery of accumulators, two variable resistances, a Weston ammeter and a standard ammeter made by the Cambridge Instrument Company. One of these resistances was fitted with a fine adjustment, and the current of 2 amperes employed could be kept constant to within 1 part in 1000. One ammeter served as a check on the other, so that any change in the behaviour of one of the instruments during

the progress of the work could be easily detected. The ammeters were also periodically calibrated by comparison with a large standard Weston ammeter. By passing water through the jacket between the coil and the polarimeter tube the temperature of the liquid in the tube could be kept constant to within  $0.2^{\circ}\text{C}$ . for long intervals of time, and the variation of temperature during an exposure of only fifteen minutes was less than  $0.1^{\circ}\text{C}$ .

The magnetic field\* at various points inside the solenoid had been previously measured by means of a delicate ballistic galvanometer and an accurately constructed search-coil, and the value of  $\Sigma Hl$  for the polarimeter tube found to be 12,270 cm. gauss when a current of 2 amperes passed through the solenoid. In the expression  $\Sigma Hl$ ,  $l$  represents the length of liquid over which  $H$  can be assumed to be constant. In previous experiments Stephens and Evans† had determined the values of Verdet's constant for conductivity-water at different wave-lengths. During the present investigation experiments on the rotation of conductivity-water at different wave-lengths were periodically carried out in order to check the value obtained for  $\Sigma Hl$  when a current of 2 amperes passed through the solenoid. In all cases the value was found to be 12,270 cm. gauss within experimental error.

The spectrograph employed was of the usual type, and consisted of a Cornu quartz prism, together with quartz lenses. The glycerine films employed in assembling the components of the analyser and the Cornu prism absorbed practically no light in the region of the spectrum investigated, since with the three liquids examined it was found impossible to measure Verdet's constant for wave-lengths below  $0.32\mu$ , even with such a powerful source of ultra-violet radiation as the tungsten arc.

Wellington special rapid plates were used, and the exposures, two of which were taken on each plate, varied from about 4 minutes at  $0.43\mu$  to about 30 minutes at  $0.32\mu$ .

### *Mode of Experiment.*

The two beams of plane polarized light, after emerging from the polarimeter, appear at the camera end of the spectroscope as two spectra, one on top of the other, separated by a fine horizontal gap. These spectra are in general of different intensity, but in the absence of the

\* Evans & Evans, *loc. cit.*

† *Loc. cit.*

magnetic field, and with no liquid in the tube, it is always possible, by rotating the analyser, to make the two spectra have the same intensity throughout their length. They are only equally intense for four definite positions of the analyser, with an angle of  $90^\circ$  separating one position from the next. Two of these positions, separated from one another by  $180^\circ$ , correspond to the maximum intensity, and the other two to the minimum intensity. In this latter position the instrument is very sensitive, and one of these positions is used as the zero reading of the analyser.

The position of the zero could be determined within a few minutes of arc by direct observation in the visible, but a series of photographs corresponding to different settings of the analyser near the position of minimum intensity were necessary for determining the exact position. With the liquid in the tube and the magnetic field not excited a few photographs near the zero position would be sufficient to show whether the liquids contained a small percentage of an optically active impurity. The presence of a very small percentage can be detected, as the column of liquid is 30.5 cm. long, and the rotation can be examined in the ultra-violet region of the spectrum.

With these preliminaries over, the determination of the magnetic rotation could be commenced. The magnetic field was applied, and a stream of water allowed to flow through the jacket. It generally required an interval of about one hour to adjust the flow of water so that the polarimeter tube was at the required temperature and for the conditions to become steady. When the temperature of the liquid in the tube was not steady the image of the two semicircular half-fields produced by the quartz-fluorite lens on the slit of the spectroscope was distorted. The analyser was then rotated through a known angle  $\theta_1$  from the zero, and a photograph taken. It is important to note that in measuring angles of rotation the readings on both verniers were taken. During the exposure a constant watch was kept over the reading of the ammeters, the temperature of the water, and the position of the arc light. With the magnetic field reversed, and a rotation of  $\theta_1$  on the opposite side of the zero, a second photograph was then taken on the same plate.

An examination of the plate shows that whilst the upper and lower halves of each spectrum are of very different intensities, there is a line of definite wave-length which has the same intensity in both halves. When the zero position had been accurately determined the wave-length of this line

is very nearly the same for each direction of the magnetic field. The reversal of the magnetic field supplies a means of eliminating certain sources of error, such as a slight mistake in the location of the zero position and an error in the centring of the circular scale of the analyser.

If  $\lambda$  is the mean wave-length of the lines which give equality of intensity in the two spectra, and  $\theta_2$  the magnetic rotation of the quartz disks at wave-length  $\lambda$ , then the rotation produced by the liquid at wave-length  $\lambda$  is  $(\theta_1 - \theta_2)$ . Then, Verdet's constant  $\delta$  is given by

$$\delta \cdot \Sigma Hl = \theta = (\theta_1 - \theta_2) = \delta \times 12,270.$$

A series of determinations of  $\delta$  were made for each liquid, corresponding to increasing values of  $\theta$ , until the point of equality had shifted to the limit in the ultra-violet.

The accuracy of the experimental results is chiefly affected by the difficulties involved in measuring the value of  $\Sigma Hl$  for the tube, and in estimating the wave-lengths of the lines of equal intensities on the photographic plate. The measurement of  $\Sigma Hl$  had been previously carried out by Evans and Evans\*, who found that the experimental value agreed with that calculated from the dimensions of the coil to within one in a thousand. Taking all factors into consideration it is considered that the experimental results are correct to within one part in three hundred on the average. This conclusion is supported by the fact that the values of  $\lambda$  for sodium light deduced from the equation connecting  $\delta$  with  $\lambda$  are in good agreement with those obtained experimentally by Perkin†. It is, however, important to remember that the positions of the absorption bands as calculated from the measured rotations for two wave-lengths are not affected by an inaccuracy in the determination of the absolute value of  $\Sigma Hl$  for the tube.

The three liquids employed in this work were the purest obtainable from Dr. Schuchardt, of Görlitz, and the specimen of butyl alcohol was marked exceptionally pure. However, each liquid was subjected to a process of fractional distillation before using, and the fraction retained which came over at the boiling point given in the most recent literature. The process of fractional distillation showed that propionic acid and isobutyl alcohol were reasonably pure, and the special purity of the butyl alcohol was indicated by the fact that all the liquid distilled over at a constant temperature.

\* *Loc. cit.*

† *Loc. cit.*

*The Measurement of Natural Dispersion.*

As one of the main objects of the present investigation was to test the application of equation (4) and calculate the positions of the absorption bands, it was necessary to obtain the values of the refractive indices of the three liquids for wave-lengths in the visible and ultra-violet. These values could not, however, be obtained from existing tables, and consequently the ordinary dispersion of the three liquids was investigated.

The same spectrograph was used in these determinations as for the magneto-optical dispersion, but the Cornu prism was replaced by a hollow prism closed by plates of polished fused quartz. The prism was first filled with a standard liquid whose refractive indices are known over a wide range of wave-lengths. Light from a copper arc, after passing through a quartz lens, was brought to a focus on the slit, immediately in front of which was supported a metal plate perforated with three holes slightly overlapping. A photograph was taken with the top portion of the slit illuminated. The liquid was then completely removed from the prism by evaporation caused by an air current, care being taken not to shift the prism, which had been rigidly fixed in position. The prism was then filled with the liquid whose dispersion was required, and a second photograph was taken on the same plate with the middle portion of the slit illuminated. With the standard liquid again placed in the prism, a third photograph was taken on the same plate with the bottom portion of the slit illuminated. In this way three spectra slightly overlapping were obtained on the photographic plate, and by observation of the top and bottom spectra any displacement of the prism or photographic plate, and any displacement of the spectra due to slight changes of temperature, could be observed. The temperature was observed on a thermometer placed inside the spectrograph near the prism, and an interval of time was allowed to elapse between successive photographs in order that the liquid should attain the temperature of the air inside the spectrograph.

To find the refractive indices at various wave-lengths for the substances examined, it is only necessary to identify a line of wave-length  $\lambda_1$ , say, in the spectrum due to refraction through the standard liquid which is superposed upon a line of wave-length  $\lambda_2$  due to refraction through the substance. The refractive index of the substance for wave-length  $\lambda_2$  is then equal to the refractive index of the



standard liquid for wave-length  $\lambda_1$ . The standard liquid employed in these experiments was propyl alcohol, and the values of its refractive indices over a wide range of wave-lengths have been accurately measured by Victor Henri\*. The chief difficulty encountered in accurate determinations of refractive indices is the variation in the values caused by small changes of temperature of one or two degrees, and the small shifts found on some of the plates were in all probability due to this cause. It is claimed, however, that on the average the refractive indices are correct to within

TABLE I. (a).  
Normal Butyl Alcohol.

SPECTROMETER DETERMINATIONS.		PHOTOGRAPHIC DETERMINATIONS.	
Wave-length (microns).	Refractive index.]	Wave-length (microns).	Refractive index.
·6678	1·400 <sub>2</sub>	·5105	1·405 <sub>8</sub>
·5876	1·402 <sub>4</sub>	·4545	1·409 <sub>2</sub>
·5016	1·406 <sub>2</sub>	·4375	1·410 <sub>3</sub>
·4922	1·406 <sub>8</sub>	·4275	1·411 <sub>6</sub>
·4713	1·408 <sub>2</sub>	·4022	1·414 <sub>8</sub>
·4472	1·409 <sub>6</sub>	·3861	1·416 <sub>4</sub>
		·3688	1·418 <sub>6</sub>
		·3600	1·420 <sub>0</sub>
		·3454	1·423 <sub>0</sub>
		·3339	1·425 <sub>5</sub>
		·3247	1·427 <sub>5</sub>
		·2997	1·434 <sub>2</sub>
		·2805	1·441 <sub>2</sub>

Temperature..... 13·0° C.

one part in 1400, and this degree of accuracy is more than sufficient for evaluating the wave-lengths of the absorption bands from the magneto-optical dispersion experiments. The refractive indices of the three liquids in the region of the visible spectrum, extending from ·6678  $\mu$  to ·4472  $\mu$ , were determined accurately at a known temperature by means of a spectrometer with a circular scale reading to 10". The slit of the spectrometer was illuminated by the capillary of a helium spectrum tube, and the angles of minimum deviation

\* 'Études de Photochemie,' p. 61.

were measured for the strong helium lines when the prism was filled with each liquid in turn. The values of the refractive indices obtained by the photographic method overlapped those obtained by the visual method over a certain region of the spectrum, and the effect of slight shifts visible on some of the plates could thus be adjusted.

## EXPERIMENTAL RESULTS.

### *Natural Dispersion.*

The refractive indices of normal butyl alcohol, isobutyl alcohol, and propionic acid in the visible and ultra-violet

TABLE I. (b).  
Isobutyl Alcohol.

SPECTROMETER DETERMINATIONS.		PHOTOGRAPHIC DETERMINATIONS.	
Wave-length (microns).	Refractive index.	Wave-length (microns).	Refractive index.
·6678	1·396 <sub>8</sub>	·4545	1·405 <sub>4</sub>
·5876	1·398 <sub>6</sub>	·4375	1·406 <sub>6</sub>
·5016	1·402 <sub>4</sub>	·4275	1·407 <sub>7</sub>
·4922	1·403 <sub>0</sub>	·4022	1·410 <sub>4</sub>
·4713	1·404 <sub>2</sub>	·3860	1·412 <sub>5</sub>
·4472	1·406 <sub>1</sub>	·3655	1·415 <sub>5</sub>
		·3530	1·417 <sub>4</sub>
		·3415	1·419 <sub>5</sub>
		·3337	1·421 <sub>1</sub>
		·3247	1·423 <sub>5</sub>
		·2961	1·431 <sub>9</sub>
		·2883	1·434 <sub>2</sub>
		·2825	1·436 <sub>3</sub>
		·2766	1·438 <sub>7</sub>

Temperature..... 13·0° C.

regions of the spectrum are given in Tables I. (a), I. (b), and I. (c) respectively, and plotted in fig. 1.

### *Magneto-Optical Dispersion.*

#### *Normal Butyl Alcohol.*

The experimental results for the magneto-optical dispersion of butyl alcohol are given in Tables II. (a) and fig. 2.

TABLE I. (c).  
Propionic Acid.

SPECTROMETER DETERMINATIONS.		PHOTOGRAPHIC DETERMINATIONS.	
Wave-length (microns).	Refractive index.	Wave-length (microns).	Refractive index.
6678	1.387 <sub>3</sub>	5105	1.392 <sub>5</sub>
5876	1.389 <sub>4</sub>	4507	1.396 <sub>2</sub>
5016	1.393 <sub>0</sub>	4275	1.398 <sub>0</sub>
4922	1.393 <sub>5</sub>	4062	1.400 <sub>1</sub>
4713	1.394 <sub>9</sub>	3861	1.402 <sub>6</sub>
4472	1.396 <sub>6</sub>	3600	1.406 <sub>3</sub>
		3238	1.413 <sub>2</sub>
		3118	1.416 <sub>3</sub>
		3039	1.418 <sub>5</sub>
		3008	1.419 <sub>6</sub>

Temperature..... 13.4° C.

Fig. 1.

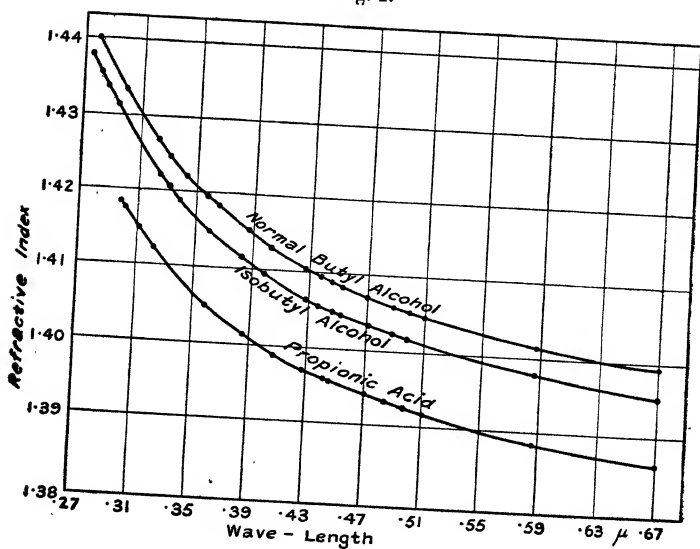


TABLE II. (a).

Temp. in degrees Cent.	Wave-length in microns ( $10^{-4}$ cm.).	Verdet's constant in mins. per cm. gauss.
12.9	.4545	.0216 <sub>6</sub>
13.0	.4437	.0228 <sub>6</sub>
13.0	.4335	.0240 <sub>7</sub>
12.8	.4250	.0252 <sub>7</sub>
12.8	.4162	.0264 <sub>7</sub>
13.0	.4079	.0276 <sub>8</sub>
12.8	.4007	.0288 <sub>8</sub>
13.0	.3933	.0300 <sub>8</sub>
12.8	.3870	.0312 <sub>8</sub>
13.0	.3808	.0324 <sub>9</sub>
13.0	.3750	.0337 <sub>9</sub>
13.0	.3700	.0349 <sub>9</sub>
13.0	.3646	.0361 <sub>1</sub>
13.0	.3597	.0372 <sub>9</sub>
13.0	.3550	.0385 <sub>1</sub>
12.8	.3503	.0397 <sub>2</sub>
13.2	.3457	.0409 <sub>2</sub>
13.1	.3417	.0421 <sub>3</sub>
13.2	.3380	.0433 <sub>3</sub>
12.8	.3344	.0445 <sub>4</sub>
13.0	.3308	.0457 <sub>4</sub>
13.0	.3272	.0469 <sub>6</sub>
13.0	.3240	.0481 <sub>5</sub>

Table II. (b) gives a series of values of  $n$ , the refractive index, and  $\delta$  Verdet's constant for butyl alcohol taken from fig. 1 and Table II. (a) respectively. These were made use of in testing the results in relation to Larmor's theory, and it was found that the experimental results could be represented by a formula of the type

$$\phi = n\delta\lambda^2 = K \left\{ \frac{\lambda^2}{\lambda^2 - \lambda_1^2} \right\}^2.$$

TABLE II. (b).

	$\lambda$ .	$n$ .	$\delta$ .
(a).....	.4335	1.411 <sub>2</sub>	.0240 <sub>7</sub>
(b).....	.4079	1.413 <sub>7</sub>	.0276 <sub>8</sub>
(c).....	.3750	1.417 <sub>8</sub>	.0337 <sub>9</sub>
(d).....	.3503	1.422 <sub>1</sub>	.0397 <sub>2</sub>
(e).....	.3240	1.427 <sub>6</sub>	.0481 <sub>5</sub>

The values of the function  $\phi$  were calculated for each wave-length, and from several pairs of these a set of values of  $\lambda_1$  and  $K$  was obtained.

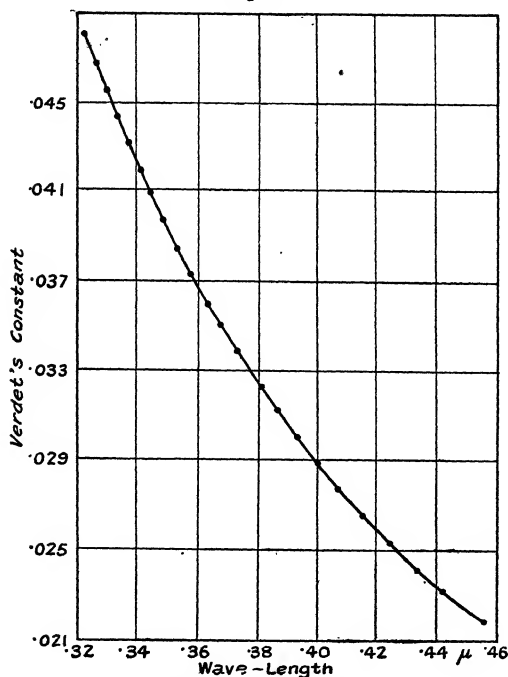
From (a) and (b)  $\lambda_1 = .1152 \mu$  and  $K = 5.513 \times 10^{-3}$ .

„ (b) „ (d)  $\lambda_1 = .1151 \mu$  „  $K = 5.514 \times 10^{-3}$ .

„ (c) „ (e)  $\lambda_1 = .1147 \mu$  „  $K = 5.520 \times 10^{-3}$ .

„ (a) „ (e)  $\lambda_1 = .1148 \mu$  „  $K = 5.519 \times 10^{-3}$

Fig. 2.



Normal butyl alcohol.

The mean values of  $\lambda_1$  and  $K$  are  $.1149 \mu$  and  $5.516 \times 10^{-3}$  respectively,  $\delta$  being measured in minutes per cm. gauss, and  $\lambda$  in microns.

Thus the magneto-optical dispersion of normal butyl alcohol for the region of the spectrum investigated ( $.4545 \mu$  to  $.3240 \mu$ ) can be represented by

$$n\delta = 5.516 \times 10^{-3} \frac{\lambda^2}{\{\lambda^2 - (.1149)^2\}^2} \quad \dots (A)$$

With values of  $n$  read off from fig. 1  $\delta$  was calculated for a few wave-lengths where experimental determinations had been carried out. The observed and calculated values of  $\delta$  are shown in Table II. (c).

TABLE II. (c).

$\lambda$ .	$\delta$ (calculated).	$\delta$ (observed).
·4545 $\mu$	·0216 <sub>2</sub>	·0216 <sub>8</sub>
·4250 $\mu$	·0251 <sub>8</sub>	·0252 <sub>7</sub>
·3933 $\mu$	·0301 <sub>2</sub>	·0300 <sub>8</sub>
·3700 $\mu$	·0348	·0349
·3550 $\mu$	·0384 <sub>3</sub>	·0385 <sub>1</sub>
·3417 $\mu$	·0421 <sub>8</sub>	·0421 <sub>3</sub>
·3344 $\mu$	·0444 <sub>9</sub>	·0445 <sub>4</sub>

Lowry and Dickson\*, who determined the magnetic rotations of normal butyl alcohol for a number of wave-lengths in the visible spectrum, compare the rotary powers at various wave-lengths with that at  $\lambda = \cdot 5461 \mu$ .

Using values of  $n$  obtained from fig. 1  $\delta$  was calculated for each of these wave-lengths from equation (A), and a comparison of the results thus obtained with those of Lowry and Dickson is given as follows:—

Wave-length (microns).	Magnetic rotary power relative to that at $\cdot 5461 \mu$ .	
	Lowry & Dickson.	Present results.
·6708	·649	·644
·6438	·707	·703
·5993	·849	·849
·5086	1·168	1·167
·4800	1·328	1·327
·4359	1·637	1·648

The value of  $\delta$ , calculated from equation (A), for sodium light ( $n = 1·402_4$ ) is  $\cdot 01224$  at  $13·0^\circ \text{C}$ ., and assuming  $\cdot 0131$  as the value of Verdet's constant for water at  $\cdot 5893 \mu$ , the specific rotation of normal butyl alcohol relative to water is therefore  $\cdot 935$ .

#### *Isobutyl Alcohol.*

The magneto-optical dispersion of isobutyl alcohol has been investigated from  $\cdot 4610 \mu$  to  $\cdot 3465 \mu$ . Table III. (a)

\* Journ. Chem. Soc. i. p. 1072 (1913).

gives the results for the sample which had been subjected to a process of fractional distillation, and Table III. (b) the

TABLE III. (a).

Temperature (degrees Cent.).	$\lambda$ (microns).	$\delta$ (minutes per cm. gauss).
13.0	.4610	.0216 <sub>6</sub>
13.0	.4495	.0228 <sub>7</sub>
13.1	.4397	.0240 <sub>8</sub>
13.2	.4220	.0264 <sub>8</sub>
13.0	.4133	.0276 <sub>9</sub>
13.2	.3804	.0337 <sub>2</sub>
13.2	.3690	.0361 <sub>2</sub>
13.2	.3640	.0373 <sub>8</sub>
13.1	.3594	.0385 <sub>4</sub>
13.2	.3512	.0409 <sub>5</sub>

TABLE III. (b).

Temperature (degrees Cent.).	$\lambda$ (microns).	$\delta$ (minutes per cm. gauss).
13.2	.4610	.0216 <sub>6</sub>
13.2	.4500	.0228 <sub>7</sub>
12.8	.4397	.0240 <sub>8</sub>
13.2	.4307	.0252 <sub>8</sub>
13.2	.4220	.0264 <sub>8</sub>
13.2	.4139	.0276 <sub>9</sub>
12.8	.4063	.0288 <sub>9</sub>
13.0	.3988	.0301 <sub>0</sub>
13.2	.3926	.0313 <sub>0</sub>
13.0	.3864	.0325 <sub>1</sub>
12.8	.3804	.0337 <sub>2</sub>
13.0	.3743	.0349 <sub>2</sub>
12.8	.3693	.0361 <sub>2</sub>
13.2	.3645	.0373 <sub>3</sub>
12.8	.3594	.0385 <sub>4</sub>
12.8	.3551	.0397 <sub>4</sub>
13.2	.3503	.0409 <sub>5</sub>
13.2	.3465	.0421 <sub>5</sub>

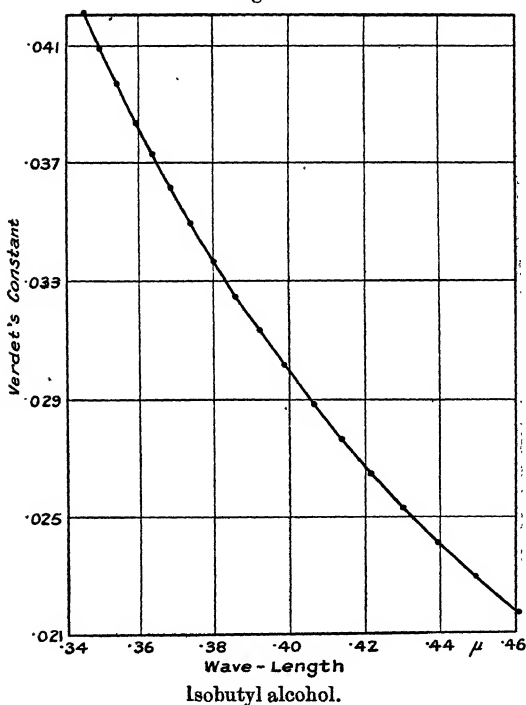
results for the same sample after it had been subjected to further fractional distillation. The results are plotted in fig. 3.

In Table III. (c) values of Verdet's constants and the refractive indices corresponding to certain wave-lengths are given, and these values were utilized to calculate the constants of the equation for isobutyl alcohol.

TABLE III. (c).

	$\lambda$ (microns).	$n$ (refractive index).	$\delta$ (minutes per cm. gauss).
(a).....	·4610	1·404 <sub>9</sub>	·0216 <sub>6</sub>
(b).....	·4397	1·406 <sub>4</sub>	·0240 <sub>8</sub>
(c).....	·3864	1·412 <sub>3</sub>	·0325 <sub>1</sub>
(d).....	·3594	1·416 <sub>3</sub>	·0385 <sub>4</sub>
(e).....	·3551	1·417 <sub>1</sub>	·0397 <sub>4</sub>

Fig. 3.



From (a) and (c)  $\lambda_1 = \cdot 1162 \mu$  and  $K = 5 \cdot 671 \times 10^{-3}$ .  
 „ (b) „ (d)  $\lambda_1 = \cdot 1148 \mu$  „  $K = 5 \cdot 686 \times 10^{-3}$ .  
 „ (c) „ (e)  $\lambda_1 = \cdot 1138 \mu$  „  $K = 5 \cdot 718 \times 10^{-3}$ .  
 „ (a) „ (e)  $\lambda_1 = \cdot 1152 \mu$  „  $K = 5 \cdot 684 \times 10^{-3}$ .



The mean values of  $\lambda_1$  and  $K$  are  $\cdot 1150 \mu$  and  $5\cdot69 \times 10^{-3}$  respectively, and the relation between Verdet's constant and wave-length for isobutyl alcohol is represented by

$$n\delta = 5\cdot69 \times 10^{-3} \frac{\lambda^2}{\{\lambda^2 - (\cdot 1150)^2\}^2} \quad \dots (B)$$

This equation was used to evaluate  $\delta$  for a few wave-lengths at which determinations have been carried out. The result of the comparison between the calculated and experimental values is shown in Table III. (d).

TABLE III. (d).

Temperature (degrees Cent.).	$n$ .	$\lambda$ (microns).	$\delta$ (observed).	$\delta$ (calculated).
13·1	1·405 <sub>7</sub>	·4498	·0228 <sub>7</sub>	·0229 <sub>0</sub>
13·2	1·408 <sub>0</sub>	·4220	·0264 <sub>8</sub>	·0264 <sub>8</sub>
13·1	1·408 <sub>9</sub>	·4136	·0276 <sub>9</sub>	·0277 <sub>3</sub>
13·2	1·411 <sub>5</sub>	·3926	·0313 <sub>0</sub>	·0312 <sub>9</sub>
13·2	1·415 <sub>5</sub>	·3643	·0373 <sub>8</sub>	·0373 <sub>8</sub>
13·2	1·417 <sub>9</sub>	·3507	·0409 <sub>5</sub>	·0409 <sub>6</sub>

TABLE III. (e).

$\lambda$ (microns).	Magnetic rotary power relative to that at $\cdot 5461 \mu$ .	
	Lowry & Dickson.	Present results.
·6708	·648	·644
·6438	·699	·703
·5893	·846	·848
·5086	1·162	1·167
·4800	1·321	1·327
·4359	1·635	1·647

The equation was also employed to calculate Verdet's constant for the wave-length of sodium light, and the value obtained is  $\cdot 01266$  at  $13\cdot2^\circ \text{C}$ . According to Perkin the specific rotation of isobutyl alcohol for sodium light at a mean temperature of  $17\cdot7^\circ \text{C}$ . is  $0\cdot9663$ . Thus, assuming  $\cdot 0131$  as the value of Verdet's constant for water, the value calculated for isobutyl alcohol at  $17\cdot7^\circ \text{C}$ . is  $\cdot 01265$ . Shwers \* obtained  $\cdot 01266$  as the value of Verdet's constant for sodium light at  $16^\circ \text{C}$ ., and  $\cdot 01203$  at  $55\cdot3^\circ \text{C}$ .

\* 'Bulletin de la classe des sciences, Académie Royale de Belgique,' p. 719 (1912).

A comparison of Lowry and Dickson's results with the values of the magnetic rotary power relative to that at  $5461\mu$ , calculated from equation (B), is given in Table III. (e).

*Propionic Acid.*

The magnetic rotations of propionic acid have been examined in the present work from  $4560\mu$  to  $3170\mu$ , and

TABLE IV. (a).

Temperature (degrees Cent.).	$\lambda$ (microns).	$n$ (refractive index).	$\delta$ (minutes per cm. gauss).
12.9	4560	1.395 <sub>7</sub>	0192 <sub>2</sub>
12.8	4437	1.396 <sub>5</sub>	0204 <sub>2</sub>
13.1	4326	1.397 <sub>3</sub>	0216 <sub>2</sub>
12.8	4274	1.397 <sub>7</sub>	0222 <sub>2</sub>
12.9	4225	1.398 <sub>2</sub>	0228 <sub>1</sub>
13.0	4128	1.399 <sub>2</sub>	0240 <sub>2</sub>
13.1	4037	1.400 <sub>1</sub>	0252 <sub>2</sub>
12.9	3958	1.401 <sub>1</sub>	0264 <sub>2</sub>
13.2	3883	1.402 <sub>0</sub>	0276 <sub>2</sub>
13.0	3811	1.402 <sub>9</sub>	0288 <sub>3</sub>
12.8	3739	1.404 <sub>0</sub>	0300 <sub>3</sub>
13.0	3680	1.405 <sub>0</sub>	0312 <sub>3</sub>
13.0	3618	1.405 <sub>9</sub>	0324 <sub>3</sub>
12.8	3568	1.406 <sub>3</sub>	0336 <sub>4</sub>
12.8	3513	1.407 <sub>8</sub>	0348 <sub>3</sub>
13.0	3458	1.409 <sub>0</sub>	0360 <sub>3</sub>
12.8	3411	1.409 <sub>9</sub>	0372 <sub>4</sub>
13.0	3391	1.410 <sub>3</sub>	0378 <sub>4</sub>
12.8	3370	1.410 <sub>3</sub>	0384 <sub>4</sub>
13.0	3324	1.411 <sub>8</sub>	0396 <sub>4</sub>
12.8	3285	1.412 <sub>7</sub>	0408 <sub>3</sub>
12.8	3247	1.413 <sub>3</sub>	0420 <sub>5</sub>
13.1	3205	1.414 <sub>8</sub>	0432 <sub>4</sub>
12.8	3170	1.415 <sub>4</sub>	0444 <sub>5</sub>

the experimental results are given in Table IV. (a) and fig. 4. As in the case of the other two organic liquids examined, it was found possible to explain these results by the presence of one strong ultra-violet absorption band.

Table IV. (b) contains results read off from fig. 1 and

Table IV. (a), and these were made use of in solving the dispersion equation.

Fig. 4.

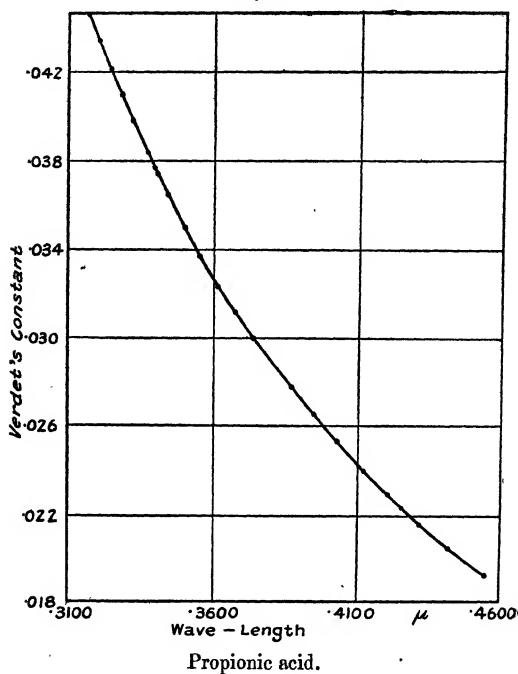


TABLE IV. (b).

	$\lambda$ .	$n$ .	$\delta$ .
(a) .....	$\cdot 4326 \mu$	$1\cdot 397_3$	$\cdot 0216_2$
(b) .....	$\cdot 4037 \mu$	$1\cdot 400_1$	$\cdot 0252_2$
(c) .....	$\cdot 3811 \mu$	$1\cdot 402_9$	$\cdot 0288_3$
(d) .....	$\cdot 3458 \mu$	$1\cdot 409_0$	$\cdot 0360_3$
(e) ..	$\cdot 3205 \mu$	$1\cdot 414_6$	$\cdot 0432_4$

From (a) and (c)  $\lambda_1 = \cdot 1074$  and  $K = 4\cdot 978 \times 10^{-3}$ .

„ (b) „ (d)  $\lambda_1 = \cdot 1051$  „  $K = 5\cdot 002 \times 10^{-3}$ .

„ (c) „ (e)  $\lambda_1 = \cdot 1037$  „  $K = 5\cdot 037 \times 10^{-3}$ .

„ (a) „ (d)  $\lambda_1 = \cdot 1044$  „  $K = 5\cdot 014 \times 10^{-3}$ .

„ (a) „ (e)  $\lambda_1 = \cdot 1050$  „  $K = 5\cdot 007 \times 10^{-3}$ .

The mean values of  $\lambda_1$  and  $K$  are  $\cdot 1051$  and  $5\cdot 00_8 \times 10^{-3}$  respectively, and the equation relating Verdet's constant with wave-length is

$$n\delta = 5\cdot 00_8 \times 10^{-3} \frac{\lambda^2}{\{\lambda^2 - (\cdot 1051)^2\}^2} \quad \text{. . . (C)}$$

The accuracy of the representation of the results by the formula (C) is shown in Table IV. (c), where the values of Verdet's constant calculated from the formula are compared with the values obtained experimentally.

TABLE IV. (c)

$\lambda$ (microns).	$\delta$ (observed).	$\delta$ (calculated).
$\cdot 4560$	$\cdot 0192_2$	$\cdot 0192_8$
$\cdot 4225$	$\cdot 0228_1$	$\cdot 0228_3$
$\cdot 4128$	$\cdot 0240_2$	$\cdot 0240_2$
$\cdot 3958$	$\cdot 0264_2$	$\cdot 0264_1$
$\cdot 3883$	$\cdot 0276_2$	$\cdot 0275_9$
$\cdot 3739$	$\cdot 0300_2$	$\cdot 0300_8$
$\cdot 3680$	$\cdot 0312_3$	$\cdot 0312_1$
$\cdot 3568$	$\cdot 0336_4$	$\cdot 0335_9$
$\cdot 3513$	$\cdot 0348_3$	$\cdot 0347_7$
$\cdot 3411$	$\cdot 0372_1$	$\cdot 0372_7$
$\cdot 3370$	$\cdot 0384_4$	$\cdot 0383_5$
$\cdot 3285$	$\cdot 0408_3$	$\cdot 0408_6$
$\cdot 3170$	$\cdot 0444_5$	$\cdot 0444_3$

The value of Verdet's constant for the wave-length of sodium light, calculated from formula (C), is  $\cdot 0110_7$ . This is in good agreement with that deduced from Perkin's results for propionic acid at various temperatures, after making the temperature correction and assuming  $\cdot 0131$  as the value of Verdet's constant for water. The value thus obtained for Verdet's constant of propionic acid at  $13\cdot 0^\circ \text{C}$ . for sodium light is  $\cdot 0110_6$ .

A comparison of Lowry and Dickson's results for propionic acid, with the values of the magnetic rotary power relative to that at  $\lambda = \cdot 5461 \mu$ , calculated from equation (C), is given in Table IV. (d).

TABLE IV. (d).

$\lambda$ (microns).	Magnetic rotary power relative to that at $5461 \mu$ .	
	Lowry & Dickson.	Present results.
6708	648	648
6438	711	706
5893	856	850
5086	1165	1165
4800	1320	1321
4359	1635	1633

*The Natural Dispersion Equations.*

The experimental results have shown that the magneto-optical dispersion of each liquid over the range of spectrum investigated can be explained by the presence of only one absorption band. If the assumption is now made that the natural dispersion over the same range of wave-length can be explained by the presence of the same band, the equation for the natural dispersion now becomes

$$n^2 - 1 = b_0 + \frac{b_1}{\lambda^2 - \lambda_1^2} \cdot \cdot \cdot \cdot \cdot \quad (D)$$

As will be seen later, the refractive indices of normal butyl alcohol, isobutyl alcohol, and propionic acid can be represented within experimental error by equations of the above type, where  $\lambda_1$  is the wave-length of the absorption band for each liquid as determined from the magneto-optical experiments. The values of  $b_0$  and  $b_1$  can be determined from two values of the refractive index,  $n_x$  and  $n_y$ , corresponding to wave-lengths  $\lambda_x$  and  $\lambda_y$ .

*Normal Butyl Alcohol.*

The pairs of values of the refractive indices utilized to calculate  $b_0$  and  $b_1$  are given in Table V. (a).

TABLE V. (a).

$\lambda$ (cm. $\times 10^5$ ).	$n$ .	$\lambda$ (cm. $\times 10^5$ ).	$n$ .
(A) $\begin{cases} 6.678 \\ 6.688 \end{cases}$	$\begin{cases} 1.400_2 \\ 1.418_6 \end{cases}$	(B) $\begin{cases} 5.876 \\ 3.454 \end{cases}$	$\begin{cases} 1.402_4 \\ 1.423_0 \end{cases}$
(C) $\begin{cases} 5.016 \\ 3.247 \end{cases}$	$\begin{cases} 1.406_2 \\ 1.427_5 \end{cases}$	(D) $\begin{cases} 4.922 \\ 2.997 \end{cases}$	$\begin{cases} 1.406_8 \\ 1.434_2 \end{cases}$
(E) $\begin{cases} 4.472 \\ 2.805 \end{cases}$	$\begin{cases} 1.409_9 \\ 1.441_2 \end{cases}$		

From (A)  $b_1 = .888_1 \times 10^{-10}$  and  $b_0 = .9400_3$ .

„ (B)  $b_1 = .907_4 \times 10^{-10}$  „  $b_0 = .9393_3$ .

„ (C)  $b_1 = .908_0 \times 10^{-10}$  „  $b_0 = .9393_0$ .

„ (D)  $b_1 = .895_7 \times 10^{-10}$  „  $b_0 = .9400_0$ .

„ (E)  $b_1 = .900_3 \times 10^{-10}$  „  $b_0 = .9396_3$ .

The mean values of  $b_1$  and  $b_0$  are  $.899_5 \times 10^{-10}$  and  $.9396_3$ , respectively, and the natural dispersion equation for normal butyl alcohol is

$$n^2 = 1.9396_6 + \frac{.899_5 \times 10^{-10}}{\lambda^2 - (1.149 \times 10^{-6})^2}.$$

This equation was used to calculate  $n$  for a number of wave-lengths in the region of the spectrum investigated, and the calculated and observed results are given below :—

$\lambda$ .	$n$ (observed).	$n$ (calculated).
.6678 $\mu$	1.400 <sub>2</sub>	1.400 <sub>2</sub>
*.6563 $\mu$	1.4002 <sub>7</sub>	1.4004 <sub>3</sub>
*.5892 $\mu$	1.4023 <sub>2</sub>	1.4023 <sub>6</sub>
.5106 $\mu$	1.405 <sub>8</sub>	1.405 <sub>7</sub>
*.4861 $\mu$	1.4071 <sub>4</sub>	1.4071 <sub>2</sub>
.4713 $\mu$	1.408 <sub>2</sub>	1.408 <sub>1</sub>
*.4340 $\mu$	1.4110 <sub>8</sub>	1.4110 <sub>4</sub>
.3688 $\mu$	1.418 <sub>6</sub>	1.418 <sub>7</sub>
.2805 $\mu$	1.441 <sub>2</sub>	1.441 <sub>2</sub>

The observed values of  $n$ , which have been corrected to 13° C., are taken from Landolt and Börnstein, ii. p. 975.

### Isobutyl Alcohol.

The constants of the equation for isobutyl alcohol have been calculated from the following pairs of values of the refractive index, taken from fig. 1 :—

TABLE V. (*b*)

$\lambda$ (cm. $\times 10^5$ ).	$n$ .	$\lambda$ (cm. $\times 10^5$ ).	$n$ .
(A) { 6.678	1.396 <sub>3</sub>	(B) { 5.876	1.398 <sub>6</sub>
{ 3.337	1.421 <sub>1</sub>	{ 2.961	1.431 <sub>9</sub>
(C) { 4.922	1.403 <sub>0</sub>	(D) { 4.472	1.406 <sub>1</sub>
{ 2.825	1.436 <sub>3</sub>	{ 2.766	1.438 <sub>7</sub>

From (A)  $b_1 = .886_3 \times 10^{-10}$  and  $b_0 = .9291_7$ .

„ (B)  $b_1 = .904_5 \times 10^{-10}$  „  $b_0 = .9288_4$ .

„ (C)  $b_1 = .887_5 \times 10^{-10}$  „  $b_0 = .9296_6$ .

„ (D)  $b_1 = .887_6 \times 10^{-10}$  „  $b_0 = .9295_9$ .

The mean value of  $b_1 = .892 \times 10^{-10}$  and of  $b_0 = .9293_2$ , and the equation for the natural dispersion for isobutyl alcohol is

$$n^2 = 1.9293_2 + \frac{.892 \times 10^{-10}}{\lambda^2 - (1.150 \times 10^{-5})^2}.$$

The value of  $n$  has been calculated from this equation for various wave-lengths, and a comparison of the observed and calculated results is given below:—

$\lambda$ .	$n$ (observed).	$n$ (calculated).
.6678 $\mu$	1.396 <sub>3</sub>	1.396 <sub>4</sub>
*.6563 $\mu$	1.3963 <sub>9</sub>	1.3966 <sub>7</sub>
*.5893 $\mu$	1.3983 <sub>8</sub>	1.3985 <sub>9</sub>
.5016 $\mu$	1.402 <sub>4</sub>	1.402 <sub>4</sub>
*.4861 $\mu$	1.403 <sub>2</sub>	1.4033 <sub>2</sub>
.4472 $\mu$	1.406 <sub>1</sub>	1.406 <sub>1</sub>
*.4340 $\mu$	1.4071 <sub>2</sub>	1.4072 <sub>1</sub>
.4022 $\mu$	1.410 <sub>4</sub>	1.410 <sub>4</sub>
.3415 $\mu$	1.419 <sub>5</sub>	1.419 <sub>7</sub>
.2883 $\mu$	1.434 <sub>2</sub>	1.434 <sub>2</sub>
.2766 $\mu$	1.438 <sub>7</sub>	1.438 <sub>8</sub>

\* Landolt and Börnstein, ii. p. 975.

### Propionic Acid.

The following pairs of values of the refractive indices, taken from fig. 1, were used in calculating the constants of the equation for propionic acid:—

TABLE V. (c).

$\lambda$ (cm. $\times 10^6$ ).	$n$ .	$\lambda$ (cm. $\times 10^6$ ).	$n$ .
(A) { 6.678 4.062	1.387 <sub>3</sub> 1.400 <sub>1</sub>	(B) { 5.876 3.861	1.389 <sub>4</sub> 1.402 <sub>6</sub>
(C) { 5.016 3.600	1.393 <sub>0</sub> 1.406 <sub>3</sub>	(D) { 4.922 3.039	1.393 <sub>6</sub> 1.418 <sub>5</sub>
(F) { 4.507 3.008	1.396 <sub>2</sub> 1.419 <sub>6</sub>		

From (A)  $b_1 = .850_3 \times 10^{-10}$  and  $b_0 = .9050_5$ .

„ (B)  $b_1 = .866_5 \times 10^{-10}$  „  $b_0 = .9045_0$ .

„ (C)  $b_1 = .870_5 \times 10^{-10}$  „  $b_0 = .9042_6$ .

„ (D)  $b_1 = .878_2 \times 10^{-10}$  „  $b_0 = .9041_4$ .

„ (E)  $b_1 = .892_5 \times 10^{-10}$  „  $b_0 = .9029_1$ .

# Magneto-Optical Dispersion of Organic Liquids. 781

The mean value of  $b_1$  is  $\cdot 871_6 \times 10^{-10}$  and of  $b_0$   $\cdot 9041_7$ , and the equation for the natural dispersion is given by

$$n^2 = 1\cdot 9041_7 + \frac{\cdot 8716 \times 10^{-10}}{\lambda^2 - (1\cdot 051 \times 10^{-5})^2}.$$

The value of  $n$  has been calculated from this equation for various wave-lengths, and a comparison of the observed and calculated values is given below :—

$\lambda$ .	$n$ (observed).	$n$ (calculated).
$\cdot 6678 \mu$	1·387 <sub>3</sub>	1·387 <sub>1</sub>
* $\cdot 6563 \mu$	1·3874	1·3874
* $\cdot 5893 \mu$	1·3894 <sub>8</sub>	1·3892 <sub>8</sub>
$\cdot 5106 \mu$	1·392 <sub>5</sub>	1·392 <sub>5</sub>
* $\cdot 4861 \mu$	1·3942	1·3939
$\cdot 4472 \mu$	1·396 <sub>8</sub>	1·396 <sub>8</sub>
* $\cdot 4340 \mu$	1·3980	1·3976 <sub>1</sub>
$\cdot 4275 \mu$	1·398 <sub>6</sub>	1·398 <sub>2</sub>
$\cdot 3118 \mu$	1·416 <sub>3</sub>	1·416 <sub>1</sub>

\* Landolt and Börnstein, p. 974, values corrected to 13·4° C. from values at 0° C. and 20° C.

## THE CALCULATION OF $\frac{e}{m}$ .

The values of  $\frac{e}{m}$  for each of the three liquids can be deduced from the experimental results given in the present paper.

According to Larmor's theory :

$$\delta = \frac{e}{2m \cdot c^2} \cdot \lambda \cdot \frac{dn}{d\lambda} \quad \dots \quad (E)$$

It has been shown that the magneto-optical and natural dispersion, over the range of spectrum investigated, can be explained by the presence of the same absorption band, and that the facts can be represented by the following equations:—

$$n \cdot \delta = K \cdot \frac{\lambda^2}{(\lambda^2 - \lambda_1^2)^2} \quad \dots \quad (F)$$

and

$$n^2 - 1 = b_0 + \frac{b_1}{\lambda^2 - \lambda_1^2} \quad \dots \quad (G)$$

Differentiating (G),

$$n \cdot \frac{dn}{d\lambda} = - \frac{b_1 \lambda}{(\lambda^2 - \lambda_1^2)^2},$$



782 Mr. E. Stephens and Prof. E. J. Evans on the  
and making use of (E),

$$n\delta = -\frac{e}{2mC^2} \cdot \frac{b_1 \lambda^2}{(\lambda^2 - \lambda_1^2)^2} \cdot \cdot \cdot \cdot \cdot \quad (\text{H})$$

Therefore, since from equation (F)

$$n\delta = K \cdot \frac{\lambda^2}{(\lambda^2 - \lambda_1^2)^2},$$

it follows from equation (H) that

$$\frac{e}{m} = -\frac{2KC^2}{b_1}.$$

K and  $b_1$  have already been determined,<sup>1</sup> so that a value of the ratio  $\frac{e}{m}$  may be obtained.

The value of K for butyl alcohol, when  $\delta$  is expressed in minutes per cm. gauss and the wave-length in microns, is  $5.516 \times 10^{-3}$ . When, however, the value of  $\delta$  is expressed in radians per cm. gauss, and  $\lambda$  in cm., the value of K is  $1.604 \times 10^{-14}$ .

Then

$$\begin{aligned} \frac{e}{m} &= \frac{2KC^2}{b_1} = \frac{2 \times 1.604 \times 10^{-14} \times 9 \times 10^{20}}{.8995 \times 10^{-10}} \\ &= 3.21 \times 10^{17} \text{ e.s.u.} \\ &= 1.07 \times 10^7 \text{ e.m.u.} \end{aligned}$$

The absolute values of K for isobutyl alcohol and propionic acid are  $1.655 \times 10^{-14}$  and  $1.456_7 \times 10^{-14}$  respectively.

The value determined for  $\frac{e}{m}$  for isobutyl alcohol =  $1.11 \times 10^7$  e.m.u., and for propionic acid  $\frac{e}{m} = 1.00 \times 10^7$  e.m.u.

#### DISCUSSION OF RESULTS.

The experimental results for the magneto-optical dispersion of normal butyl alcohol, isobutyl alcohol, and propionic acid can be represented by equations of the type

$$n\delta = K \frac{\lambda^2}{(\lambda^2 - \lambda_1^2)^2}$$

where  $n$  is the refractive index,  $\delta$  the value of Verdet's constant,  $\lambda_1$  the wave-length corresponding to the free period of the resonators, and K a constant whose value

varies from one liquid to another. The values of  $\lambda_1$  for the three liquids referred to above are  $\cdot 1149 \mu$ ,  $\cdot 1150 \mu$ , and  $\cdot 1051 \mu$  respectively.

The values of Verdet's constant for isobutyl alcohol are about 3 per cent. higher than the corresponding values for normal butyl alcohol, but it is interesting to note, in spite of differences in their structural formulæ, that the absorption band responsible for the magneto-optical dispersion of isobutyl alcohol has practically the same wave-length as that for normal butyl alcohol. It is also seen from the experimental results of Jones & Evans and Evans & Evans that the magneto-optical dispersions of propyl and isopropyl alcohols are controlled by absorption bands of practically the same wave-lengths. The results hitherto obtained for the alcohols are collected in Table VI.

TABLE VI.

	$\lambda_1$ (microns).	K.	$\delta$ for $\lambda$ = $\cdot 5893 \mu$ .	Temp. degrees Cent.
CH <sub>4</sub> O Methyl alcohol *.....	$\cdot 1100$	$4\cdot 090 \times 10^{-3}$	$\cdot 00956$	9.0
C <sub>2</sub> H <sub>6</sub> O Ethyl alcohol † .....	$\cdot 1114$	$4\cdot 96_4 \times 10^{-3}$	$\cdot 0113_1$	12.8
C <sub>3</sub> H <sub>8</sub> O { Normal propyl alcohol*.	$\cdot 1138$	$5\cdot 34 \times 10^{-3}$	$\cdot 0119_7$	16.0
{ Isopropyl alcohol †.....	$\cdot 1137$	$5\cdot 552_6 \times 10^{-3}$	$\cdot 0125_2$	13.0
C <sub>4</sub> H <sub>10</sub> O { Normal butyl alcohol .	$\cdot 1149$	$5\cdot 516 \times 10^{-3}$	$\cdot 0122_4$	13.0
{ Isobutyl alcohol .....	$\cdot 1150$	$5\cdot 69 \times 10^{-3}$	$\cdot 0126_6$	13.2

\* Jones & Evans, Phil. Mag. v. (March 1928).

† Stephens & Evans, *loc. cit.*

† Evans & Evans, Phil. Mag. viii. (August 1929).

The Table shows that the values of  $\lambda_1$  and K increase as molecular weight of the alcohol increases, and the position of the absorption band is displaced on the average about  $\cdot 0016 \mu$  towards the red by the addition of CH<sub>2</sub> to the molecular weight.

The experimental results also indicate that the refractive indices of normal butyl alcohol, isobutyl alcohol, and propionic acid can be represented within experimental error by equations of the type

$$n^2 - 1 = b_0 + \frac{b_1}{\lambda^2 - \lambda_1^2},$$

where the constants  $b_0$  and  $b_1$  depend on the nature of the liquid, and  $\lambda_1$  is the wave-length calculated for a particular liquid from the magnetic rotation experiments.

Evidence as to the nature of the resonators controlling the magneto-optical and ordinary dispersion in the visible

## 784 *Magneto-Optical Dispersion of Organic Liquids.*

and ultra-violet regions of the spectrum was obtained by combining the results of the magnetic rotation experiments with those relating to ordinary dispersion. The calculations show, in conformity with the results of other investigators, that the electron is the resonator, but the values of  $\frac{e}{m}$  [ $1.07 \times 10^7$  e.m.u. for normal butyl alcohol,  $1.11 \times 10^7$  e.m.u. for isobutyl alcohol, and  $1.00 \times 10^7$  e.m.u. for propionic acid] are decidedly lower than the accepted value  $1.77 \times 10^7$  e.m.u. The calculations of Drude, Victor Henri, and S. S. Richardson indicate that the number of electrons per molecule is practically equal to the sum of the valencies of all the atoms in the molecule, and it seems as if the interactions between these vibrating electrons are equivalent to an increase in the effective mass of the electron.

### SUMMARY.

*a.* The magneto-optical rotations and refractive indices of butyl alcohol, isobutyl alcohol, and propionic acid have been determined for various wave-lengths in the visible and ultra-violet regions of the spectrum.

*b* (1). The magneto-rotary dispersion of butyl alcohol and of isobutyl alcohol for the ranges of wave-length investigated can be represented by the equations

$$n \delta = 5.516 \times 10^{-3} \frac{\lambda^2}{\{\lambda^2 - (\cdot 1149)^2\}^2}$$

and

$$n \delta = 5.69 \times 10^{-3} \frac{\lambda^2}{\{\lambda^2 - (\cdot 1150)^2\}^2}$$

respectively, where  $n$  is the refractive index and  $\delta$  Verdet's constant in minutes per cm. gauss for wave-length  $\lambda$ . The absorption bands which control the magnetic rotation for these two liquids have practically the same wave-length, about  $\cdot 1150 \mu$ .

*b* (2). The natural dispersion of butyl and isobutyl alcohols for the ranges of wave-length investigated can be represented by the equations

$$n^2 = 1.9396_6 + \frac{\cdot 899_6 \times 10^{-10}}{\lambda^2 - (1.149 \times 10^{-5})^2}$$

and

$$n^2 = 1.9293_2 + \frac{\cdot 892 \times 10^{-10}}{\lambda^2 - (1.150 \times 10^{-5})^2}$$

respectively, where  $n$  is the refractive index and  $\lambda$  the wave-length measured in cm. The wave-lengths of the absorption bands are the same as in the corresponding magneto-optical equations.

c. The magneto-rotary and natural dispersions of propionic acid for the range of wave-length investigated can be represented by the equations

$$n \delta = 5.00_8 \times 10^{-3} \frac{\lambda^2}{\{\lambda^2 - (1.051)^2\}^2}$$

and

$$n^2 = 1.9041_7 + \frac{.871_6 \times 10^{-10}}{\lambda^2 - (1.051 \times 10^{-5})^2}$$

respectively, the wave-length of the absorption band being  $1.051 \mu$  in each case.

d. From the experimental results for the magneto-optical and natural dispersions of normal butyl alcohol, isobutyl alcohol, and of propionic acid the value of  $\frac{e}{m}$  has been determined for each liquid:

For butyl alcohol  $\frac{e}{m} = 1.07 \times 10^7$  e.m.u.; for isobutyl alcohol  $\frac{e}{m} = 1.11 \times 10^7$  e.m.u.; and for propionic acid

$$\frac{e}{m} = 1.00 \times 10^7 \text{ e.m.u.}$$

May 1930.

LXXIII. *The Lateral Bending of Bars, limited by Surfaces of Second Order.* By Prof. A. N. DINNIK, Member of Academy of Sciences in Ukraina, and Prof. A. S. LOKSHIN, Mining Institute, Dnepropetrowsk\*.

### § 1. Preface.

THE lateral bending of bars of variable cross-section presents a very interesting problem. These bars are often used in engineering constructions, on account of their lightness in comparison with uniform bars. The calculation of such bars is not sufficiently understood—as is, for instance, seen from the last edition of ‘Hütte’†.

\* Communicated by R. V. Southwell, F.R.S.

† ‘Hütte,’ vol. i. pp. 630–631 (Moscow, 1929).

Mathematically this problem requires the integration of a differential equation of the second order with variable coefficients, by obtaining a transcendental equation to define the critical force in terms of the boundary conditions, and by calculating the roots of the last equation. We have several solutions for special cases of different form of bars. It is desirable here to make a more general investigation ; to take a sufficiently general law of varying cross-section, solve this problem, obtain numerical results, and examine the cases which may be useful for technics. It has been performed in cases where the moment of inertia of the section varies along the axis according to a power or exponential law \*.

In this paper we consider the question of the lateral bending of bars limited by second order surfaces, when the line of action of the compressive force coincides with the axis of the surface.

The problem of stability of bars limited by a surface of revolution of the second order has been solved by Lagrange † in a very original way. Lagrange considered only the case in which the ends are supported, and he has not calculated any table of stability coefficients. We examine a general case of second order surfaces, and solve this problem by direct integration of the bending equations. Using the boundary conditions we get in every case the equation for calculating the critical force, and solve it. It is evident that in all cases the critical force may be expressed by a simple formula

$$P = \frac{K \cdot E \cdot I}{l^2},$$

where K is the coefficient of stability, which depends upon the law of variable moment of inertia and upon the means of fastening the ends of the bar,

E, modulus of elasticity,

I, moment of inertia of the largest cross-section of the bar about the bending axis ‡,

l, length of the bar.

\* A. Dinnik, "The Lateral Bending of Bars, the Stiffness of which varies by the Binomial Law," 'Isvestia Gornogo Instituta,' 1914 ; "The Lateral Bending of Bars by the Exponential Law," 'Westnik Ingenerow,' 1916 ; "Calculation of Compressed Bars of Variable Section," 'Westnik Ingenerow,' 1929.

† Lagrange, 'Sur la figure des colonnes.'

‡ Excepting the case of a hyperboloid of one sheet, § 5, where I is the moment of inertia of its smallest cross-section.

We calculate the roots of the equations, form tables of stability coefficients "K," and, finally, give applications of the results obtained.

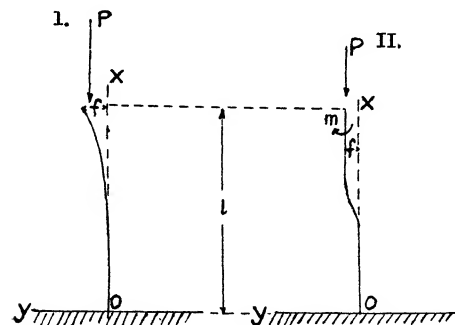
It is evident that the results obtained will be satisfactory provided that the stresses do not surpass the limit of elasticity; this will be true provided that the transverse dimensions of the bar are small in comparison with its length\*.

## § 2. Cylindrical Bar.

### Case I.

The lower end of a vertical uniform bar (for instance, an elliptical cylinder), of length  $l$ , is built-in and at the upper free end a vertical force  $P$  is applied (fig. 1).

Fig. 1.



The bending-moment of the bar at a cross-section distant  $x$  from the lower end is

$$M = P(f - y), \quad . \quad . \quad . \quad . \quad . \quad (2)$$

where  $f$  is the deflexion on the upper end. The differential bending equation is

$$EIy'' + P(y - f) = 0, \quad . \quad . \quad . \quad . \quad . \quad (3)$$

and its integral is

$$y = A \cos nx + B \sin nx, \quad . \quad . \quad . \quad . \quad . \quad (4)$$

$$n^2 = \frac{P}{EI} \quad . \quad . \quad . \quad . \quad . \quad . \quad . \quad . \quad . \quad (5)$$

\* In the case of iron or wooden bars, the length " $l$ " must exceed at least 100 times the smallest radius of inertia of the bar's cross-section. Cf. Timoshenko, 'Resistance of Materials,' § 175 (1929).

The boundary conditions of the lower and upper ends of the bar,

$$x = 0, \quad y = 0, \quad y' = 0, \quad . \quad . \quad . \quad (6)$$

$$x = l, \quad y = f, \quad . \quad . \quad . \quad . \quad . \quad (7)$$

lead to the following equation for determining the critical force :

$$\cos nl = 0,$$

from which

$$P_k = \frac{\pi^2 EI}{4l^2} = 2.4674 \frac{EI}{l^2}. \quad . \quad . \quad . \quad (8)$$

### Case II.

*The lower end of the bar is built-in, the upper end is free to move, but cannot turn (fig. 1, II.).*

The bending-moment, the differential equation of the bent bar, and its integral are :

$$M = P(y - f) - m, \quad . \quad . \quad . \quad . \quad . \quad (9)$$

$$EIy'' + P(y - f) = m, \quad . \quad . \quad . \quad . \quad . \quad (10)$$

$$y = A \cos nx + B \sin nx + f + \frac{m}{P}, \quad . \quad . \quad . \quad (11)$$

where  $m$  is the reaction moment which prevents the upper end from turning.

The boundary conditions,

$$x = 0, \quad y = 0, \quad y' = 0, \quad . \quad . \quad . \quad (12)$$

$$x = l, \quad y = f, \quad y' = 0, \quad . \quad . \quad . \quad (13)$$

give the following equation for determining the critical force :

$$\sin nl = 0, \quad . \quad . \quad . \quad . \quad . \quad (14)$$

from (14) and (4),

$$P_{cr.} = \frac{\pi^2 EI}{l^2} = 4.8696 \frac{EI}{l^2}. \quad . \quad . \quad . \quad . \quad (15)$$

### § 3. Ellipsoidal Bar.

Let a bar have the form of a triaxial ellipsoid (fig. 2), the equation of which is

$$\frac{x^2}{a^2} + \frac{y^2}{b^2} + \frac{z^2}{c^2} = 1. \quad . \quad . \quad . \quad . \quad (16)$$

The moment of inertia of the largest section in the middle of the bent ellipsoid (in the plane  $zOy$ ) is

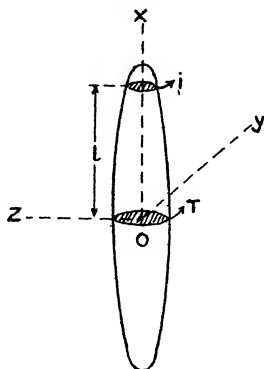
$$\dots \dots \dots I = \frac{\pi b^3 c}{4} \dots \dots \dots (17)$$

The moment of inertia of a section distant  $x$  from the centre of the ellipsoid is

$$I(x) = \frac{\pi \beta^3 \gamma}{4}, \dots \dots \dots (18)$$

where  $\beta, \gamma$  denote the semiaxis of the ellipse which we get by intersection of the ellipsoid by a plane  $x = \text{const.}$

Fig. 2.



From (16), (17), (18)

$$I(x) = \frac{\pi b^3 c}{4a^4} (a^2 - x^2)^2 = I \cdot \left(1 - \frac{x^2}{a^2}\right)^2 \dots \dots (19)$$

The differential bending equation, by (2) and (19), is

$$EI \left(1 - \frac{x^2}{a^2}\right)^2 y'' + P(y - f) = 0. \dots \dots (20)$$

Integrating, we get

$$y = \sqrt{a^2 - x^2} \{A \cos u + B \sin u\} + f, \dots \dots (21)$$

$$y' = (a^2 - x^2)^{-1/2} \{A[-x \cdot \cos u + \sqrt{n^2 - a^2} \sin u] - B[x \sin u + \sqrt{n^2 - a^2} \cos u]\}, \quad (22)$$



where 
$$u = \frac{\sqrt{n^2 - a^2}}{2a} \log \frac{a-x}{a+x} \quad (23)$$

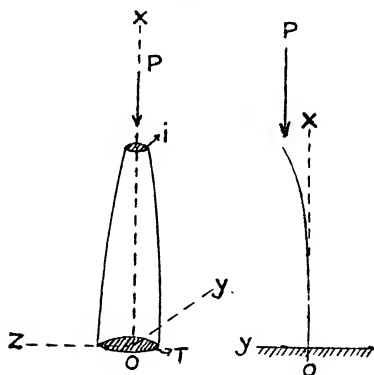
$$\eta^2 = \frac{Pa^4}{EI}, \quad (24)$$

as may be verified by inserting (22)–(24) in (20).

We shall consider only the upper half of the truncated ellipsoid. The moment of inertia of the upper section at the distance  $l$  from the ellipsoid centre is  $i$ ; then the ratio

$$\frac{i}{I} = k^2; \quad (25)$$

Fig. .



by  $k = 0$  we get an entire ellipsoid,  
 $k < 1$  „ „ truncated ellipsoid,  
 $k = 1$  „ „ elliptical cylinder,  
 $k > 1$  „ „ hyperboloid of one sheet.

#### Case I.

The lower end is built-in, the upper is free (fig. 3, and fig. 1, I.).

The boundary conditions (5) require that in (21)  $B=0$ ; condition (6) gives

$$A \cos U = 0,$$

$$U = \frac{\sqrt{n^2 - a^2}}{2a} \log \frac{a-l}{a+l} = \frac{\sqrt{n^2 - a^2}}{2a} \log \frac{1 - \sqrt{1-k}}{1 + \sqrt{1-k}}, \quad (26)$$

from which or  $A=0$ , i. e., rectilinear form of equilibrium, or

$$\cos U = 0. \quad . \quad . \quad . \quad . \quad . \quad (27)$$

The smallest root of this equation is  $U=\pi/2$ . Then, from (24) and (26), we get

$$P_k = (1-k) \left\{ 1 + \left[ \frac{\pi}{\log \frac{1-\sqrt{1-k}}{1+\sqrt{1-k}}} \right]^2 \right\} \frac{ET}{l^2} = \frac{KEI}{l^2}. \quad (28)$$

The stability coefficient  $K$  calculated from (28) is given for different values of  $i/I$  in Table I.

TABLE I.

$i/I$ .	$K$ .	$i/I$ .	$K$ .	$i/I$ .	$K$ .
0	1	0.3	2.131	0.7	2.357
0.0001	1.262	0.4	2.203	0.8	2.397
0.01	1.571	0.5	2.262	0.9	2.434
0.1	1.899	0.6	2.313	1	2.467
0.2	2.038				

Taking the second, third, and other roots of the equation (27), we get the second, third, and other values of the critical force.

### Case II.

The lower end of the bar is built-in, the upper is free to move but cannot turn (fig. 1, II.).

In this case in (20) we add the term  $m$ , and in (21) the term  $m/P$  (see § 2 (9)-(11)). The boundary condition (12) gives  $A=0$ ; the condition (13) gives  $B=0$  (rectilinear form of equilibrium) or

$$U \tan U = \frac{1}{2} \sqrt{1-k} \log \frac{1-\sqrt{1-k}}{1+\sqrt{1-k}}, \quad . \quad . \quad (29)$$

where, calculating  $U$ , we find from (24)-(26)

$$P_k = (1-k) \left\{ 1 + \left[ \frac{2U}{\log \frac{1-\sqrt{1-k}}{1+\sqrt{1-k}}} \right]^2 \right\} \frac{EI}{l^2}. \quad (30)$$

The critical force is found in the following way :—

- (1) We have the ratio of  $i/I$ , and from (21) we find  $k$  ;
- (2) this value of  $k$  we put into (19), and calculate the first root  $U$  of the equation (26) ;
- (3) this value of  $U$  we insert in (27), and find the critical force.

In Table II. are given the roots of the equation (29) and the stability coefficients  $K$ .

TABLE II.

$i/I$ .	$U$ .	$K$ .	$i/I$ .	$U$ .	$K$ .
0.0001	2.2088	1.5285	0.5	—	8.1532
0.01	2.5460	2.6637	0.6	3.0617	8.1532
0.1	2.8076	4.5664	0.7	—	8.625
0.2	2.9007	5.6176	0.8	3.1063	9.0643
0.3	—	6.655	0.9	—	9.8700
0.4	3.0004	7.0446	1	3.1416	

#### § 4. *Hyperboloid of One Sheet.*

Replacing in (16)–(30) the semiaxis  $a$  by  $ai$ , we get the solution for a bar having the form of a hyperboloid of one sheet (fig. 4).

Since  $i > I$  and  $k > 1$ , we must substitute in all formulas, § 3,  $\sqrt{1-k}$  by  $i\sqrt{k-1}$  \*. Using the known relation between the logarithmical and circular function

$$\log \frac{1-ix}{1+ix} = -2i \tan^{-1} x,$$

we get for the first case, when the lower end is built-in and the upper free, in place of (28),

$$P_k = (k-1) \left\{ \left[ \frac{\pi}{\tan^{-1} \sqrt{k-1}} \right]^2 - 1 \right\}.$$

The stability coefficient calculated from (21) is given in Table III.

\* We denote by  $i\sqrt{-1}$ , and the moment of inertia of the end section too. We think that this will not cause any confusion.

For the second case (fig. 1, II.), after a not complicated transformation, the equation (29) gives

$$U \tan U = \sqrt{k-1} \tan^{-1} \sqrt{k-1}, \quad . \quad . \quad . \quad (32)$$

$$P_k = (k-1) \left\{ \left[ \frac{U}{\tan^{-1} \sqrt{k-1}} \right]^2 - 1 \right\}. \quad . \quad . \quad (33)$$

Fig. 4.

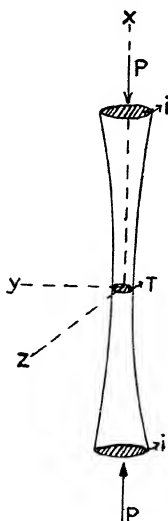


TABLE III.

$i/L$	$K$	$i/L$	$K$
1	$\pi^2/4$	3	2.879
1.2	2.527	4	3.000
1.4	2.578	5	3.1024
1.6	2.625	10	3.620
1.8	2.674	100	5.233
2	2.724	10000	13.919

The equation (32) has an evident root

$$U_0 = \tan^{-1} \sqrt{k-1},$$

but to this corresponds  $P_k=0$ . By calculating the next root of the equation (32), and putting it in (33), we obtain Table IV.

TABLE IV.

$i/L$	U.	K.	$i/L$	U.	K.	$i/L$	U.	K.
1	$\pi$	$\pi^2$	2	3.254	13.03	10	3.528	26.23
1.2	3.171	10.59	3	3.322	15.40	100	3.906	79.03
1.4	3.196	11.26	4	3.370	17.42	1000	4.212	249.8
1.6	3.217	11.87	5	3.408	20	10000	4.419	795.0
1.8	3.237	12.45						

If we consider  $K$  as depending upon the ratio  $I/i$ , *i. e.*, the ratio of the moment of inertia  $I$  of the middle smallest section of the one sheet hyperboloid (fig. 4) to the moment  $i$  of the largest end section, then we get from the equations (32)–(34) the values in the second column of Table V.

TABLE V.

$I/i$	K.	K.	$I/i$	K.	K.
0.0001	0.079	0.030	0.5	6.50	1.79
0.01	0.790	0.284	0.6	7.24	1.95
0.1	2.62	0.856	0.7	7.94	2.09
0.2	3.84	1.17	0.8	8.59	2.22
0.3	4.83	1.41	0.9	9.24	2.35
0.4	5.70	1.61	1		

By using this table we have to substitute in the fundamental formula (1), instead of  $I$ ,  $i$ , *i. e.*, the moment of inertia of the end section. Table V. shows how much the stability of a compressed bar diminishes when it is made thinner in its middle part.

### Case III.

*The lower end of the bar is supported, the upper end is free to move but cannot turn* (fig. 5).

These conditions obtain for each half of a bar which is narrowed at its supported ends and has as boundary a hyperboloid of one sheet (see § 9, fig. 5).

We get the differential equation and its integrals from (19)–(24) by substituting  $ai$  instead of  $a$ .

$$\left. \begin{aligned} y &= \sqrt{a^2 + x^2} \{A \cos u + B \sin u\} + f + \frac{m}{P}, \\ u &= \frac{\sqrt{a^2 + n^2}}{a} \tan^{-1} \frac{x}{a}. \end{aligned} \right\} \quad (34)$$

The boundary conditions are

$$x = 0, \quad y = 0, \quad y'' = 0, \quad . \quad . \quad . \quad (35)$$

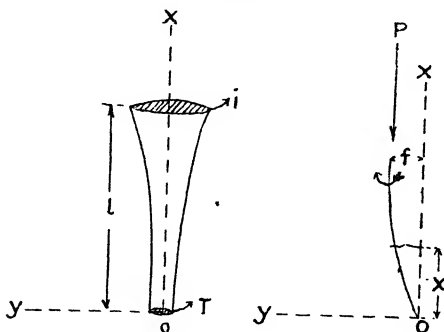
$$x = l, \quad y = f, \quad y' = 0; \quad . \quad . \quad . \quad (36)$$

(35) gives  $A=0$ ; (36) gives

$$U \cot U + \sqrt{k-1} \tan^{-1} \sqrt{k-1} = 0. \quad . \quad . \quad (37)$$

The stability coefficients calculated from (33) and (37) are given in the third column of Table V.

Fig. 5.



### § 5. Hyperboloid of Two Sheets.

The bar is limited by a hyperboloid of two sheets (fig. 6), the equation of which is

$$\frac{x^2}{a^2} - \frac{y^2}{b^2} - \frac{z^2}{c^2} = 1. \quad . \quad . \quad . \quad (38)$$

The moment of inertia of a section at a distance  $x$  from the origin of the coordinates is

$$I(x) = \frac{\pi b^3 c}{4a^4} (x^2 - a^2)^2. \quad . \quad . \quad . \quad (39)$$

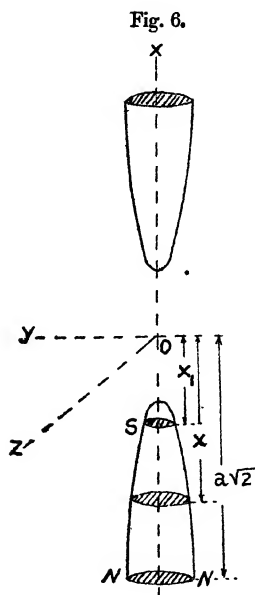
Substituting (39) in (3), we get

$$(x^2 - a^2)^2 y'' + n^2 y = 0, \quad . \quad . \quad . \quad (40)$$

$$n^2 = \frac{4Pa^4}{\pi E b^3 c}. \quad . \quad . \quad . \quad (41)$$

The integral of this equation is

$$\left. \begin{aligned} y &= \sqrt{x^2 - a^2} \{ A \cos u + B \sin u \}, \\ y' &= (x^2 - a^2)^{-1/2} \{ A [x \cos u - \sqrt{n^2 - a^2} \sin u] \\ &\quad + B [x \sin u + \sqrt{n^2 - a^2} \cos u] \}, \\ u &= \frac{\sqrt{n^2 - a^2}}{2a} \log \frac{x - a}{x + a}. \end{aligned} \right\} \quad \dots (42)$$



The boundary conditions yield relations by which we can calculate the critical force.

We will consider, for instance, the stability of a part cut off from a one-sheet hyperboloid, where the lower base NN is at a distance  $x_0 = a\sqrt{2}$  from the centre of the surface O and the upper SS at a distance  $X_1$ . Then

$$I(x_0) = I = \frac{\pi b^3 c}{4}, \quad \dots (43)$$

which coincides with the moment of inertia of the largest section of the ellipsoid (17).

Case I. (fig. 1, I.).

Here the boundary conditions (6)-(7) give the following equation for calculating the critical force

$$\left. \begin{aligned} \tan U &= \frac{1}{\sqrt{2} \cdot c} U, \\ c &= \log \frac{\sqrt{1+k}-1}{\sqrt{k}(\sqrt{2}-1)}, \end{aligned} \right\} \dots \dots \dots (44)$$

$$P_k = \frac{(c^2 + U^2)(\sqrt{2} - \sqrt{1+k})}{c^2} \frac{EI}{l^3} \dots \dots (45)$$

The roots of equation (44) and the values of the stability coefficients are given in Table VI.

TABLE VI.

$i/l$ .	U.	K.	$i/l$ .	U.	K.
0.0001	2.2646	0.3941	0.4	1.7110	1.8834
0.01	2.1474	0.7646	0.6	1.6507	2.1122
0.1	1.8995	1.2593	0.8	1.6066	2.3181
0.2	1.8043	1.5540	1	$\pi/2$	$\pi^2/4$

Case II. (fig. 1, II.).

The boundary conditions (12)-(13) give the equation

$$c \left[ \sqrt{2(1+k)} + \frac{U^2}{c^2} \right] \tan U = (\sqrt{1+k} - \sqrt{2}) U, \quad (46)$$

where

$$c = \frac{1}{2} \log \frac{(\sqrt{1+k}-1)(\sqrt{2}+1)}{(\sqrt{1+k}+1)(\sqrt{2}-1)},$$

and  $P^k$  is obtained from formula (45).

TABLE VII.

$i/l$ .	U.	K.	$i/l$ .	U.	K.
0.0001	3.3056	0.5756	0.4	3.1440	6.3410
0.01	3.2428	1.4382	0.6	3.1440	7.6044
0.1	3.1780	3.4996	0.8	3.1421	8.8259
0.2	3.1620	4.6550	1	$\pi$	$\pi^2$

In Table VII. are calculated the roots of (46) and the corresponding stability coefficients.



§ 6. *Elliptical Paraboloid* (fig. 7).

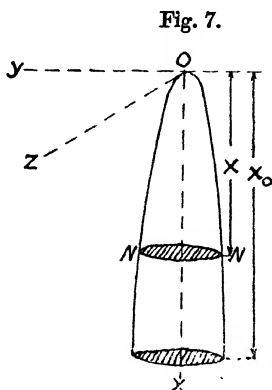
The equation is

$$\frac{y^2}{2q} + \frac{z^2}{2r} = x. \quad (47)$$

By (18) and (47) the moment of inertia of the cross-section at a distance  $x$  from the paraboloid's top is

$$I(x) = \pi \sqrt{qr^3} x^2, \quad (48)$$

i. e., it changes by the square law.



The differential equation of bending and its integral are

$$\left. \begin{aligned} EI \left( \frac{x}{l} \right)^2 y'' + Py &= 0, \\ y &= \sqrt{x} \{ A \cos \mu \log x + B \sin \mu \log x \}, \end{aligned} \right\} \quad (49)$$

where

$$\mu^2 = \frac{Pl^2}{EI} - \frac{1}{4}, \quad i = k^4.$$

The boundary conditions for the first case give \*

$$\tan 2\mu \log k = 2\mu, \quad (50)$$

and for the second case

$$2\mu \log k = \pi. \quad (50a)$$

\* The integral has a form (49) when  $\mu$  is real and different from 0. When  $\mu$  is imaginary and  $\mu=0$ , the integral has another form. For detail see the work of A. Dinnik mentioned in § 1.

In both cases

$$P_k = \frac{(1 + 4\mu^2)(1 - k^2)^2 EI}{4l^2} = \frac{KEI}{l^2} \dots (50b)$$

In Table VIII. are given the roots of equation (50) and the stability coefficients for cases I. and II.

TABLE VIII.

$i/I.$	U.	K.	K.
0	0	0.25	0.25
0.1	3.25	1.35	3.60
0.2	4.46	1.59	4.73
0.3	5.79	1.76	5.62
0.4	7.44	1.90	6.39
0.5	9.66	2.02	7.07
0.6	12.90	2.13	7.70
0.7	13.23	2.22	8.29
0.8	28.78	2.31	8.88
0.9	60.27	2.39	9.37
1	$\infty$	$\pi^2/4$	$\pi^2$

### § 7. Elliptical Cone.

When the top of the cone is at the origin of the co-ordinates the equation is

$$\frac{y^2}{b^2} + \frac{z^2}{c^2} = \frac{x^2}{a^2} \dots (51)$$

By (18) and (51) the moment of inertia of the section at distance  $x$  from the top is

$$I(x) = \frac{\pi b^3 c}{a^4} x = I \frac{x^4}{h^4} \dots (52)$$

It varies by the law of fourth power. Here  $I$  is the moment of inertia of the section at the distance  $h$  from the top.

The differential equation of bending and its integral are

$$\left. \begin{aligned} EI \left( \frac{x}{h} \right)^4 y'' + Py &= 0, \\ y &= x \left\{ A \cos \frac{Uh}{x} + B \sin \frac{Uh}{x} \right\} \end{aligned} \right\} \dots (53)$$

where

$$U^2 = \frac{Ph}{EI}, \quad \frac{i}{I} = k^2.$$

The boundary conditions give for the first case

$$\tan \frac{(1-k^2)U}{k^2} = -U, \quad . \quad . \quad . \quad (54)$$

and for the second case

$$(k^2 + U^2) \tan \frac{1-k^2}{k^2} U = (1-k^2)U, \quad . \quad . \quad . \quad (55)$$

where in both cases

$$P_k = (1-k^2)^2 U^2 \frac{EI}{k^2} = \frac{KEI}{l^2}. \quad . \quad . \quad . \quad (56)$$

The roots of equations (54) and (55), with the corresponding  $K^*$ , are given in Table IX.

TABLE IX.

$i/l$	U.	K.	U.	K.
0	0	0	0	0
0.1	2.51	1.20	4.18	3.32
0.2	3.70	1.50	6.44	4.56
0.3	5.03	1.71	9.03	5.50
0.4	6.68	1.87	12.27	6.31
0.5	8.89	2.00	16.65	7.02
0.6	12.13	2.12	23.10	7.67
0.7	17.46	2.22	33.71	8.27
0.8	28.00	2.31	54.77	8.83
0.9	54.47	2.39	117.7	9.36
1	$\infty$	$\pi^2/4$	$\infty$	$\pi^2$

### § 8. Hyperbolical Paraboloid.

There is no question of the lateral bending of an elastic body, limited by such a surface, because of its form. It is, of course, possible to study the stability of a bar partly limited by a surface of a hyperbolic paraboloid

$$\frac{y^2}{q} - \frac{z^2}{r} = 2x,$$

and partly by another surface; for instance, by two planes  $y = \pm h$ . But this problem is out of our consideration.

\* For other cases of fastening the ends see the work of A. Dinnik mentioned in § I.

### § 9. Symmetrical Column.

Let us consider a column symmetrical in relation to its middle and narrowed at both ends. Let each half of this column be a part of a body limited by a surface of second order, as mentioned above. The axis of the surface coincides with the axis of the column.

When both its ends are supported (fig. 8, *b*), half of it is in the conditions of the first case; with the ends built-in

Fig. 8.

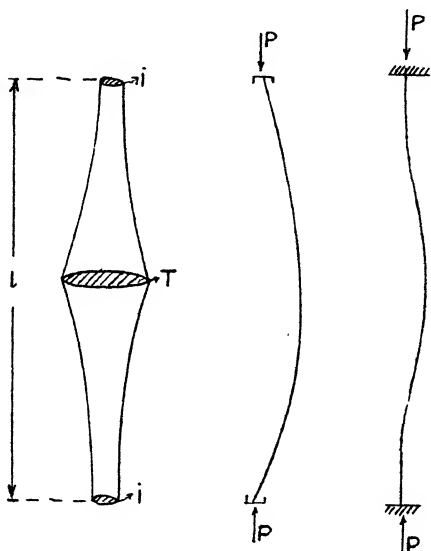


(fig. 8, *c*), it is in the conditions of the second case. Hence the critical force for this kind of column is given by formula (1), where  $I$  is the moment of inertia of the column's middle section,  $l$  = the length of it,  $K$  = stability coefficient.

For the ellipsoid and hyperboloid of one sheet  $K$  is given in Table X.

When  $\frac{i}{I} < 1$  we have an ellipsoid. In particular, when  $i=0$  the ellipsoid is entire (not truncated); when  $i=I$  it is an elliptical cylinder; when  $i>I$  it is a hyperboloid of one sheet.

For the columns of which each half is a part of a hyperboloid of one or two sheets, or an elliptical paraboloid, or a cone, the coefficients are given for the case of supported ends in Table XI., and for the case of built-in ends in Table XII.

TABLE X.

$i/l$ .	K ends support.	K ends built-in.	Remark.
0	4.00	—	} Triaxial ellipsoid.
0.0001	5.10	6.11	
0.01	6.28	10.65	
0.1	7.60	18.27	
0.2	8.15	22.47	
0.3	8.52	—	
0.4	8.81	28.18	
0.5	9.00	—	
0.6	9.25	32.61	
0.7	9.43	—	
0.8	9.59	32.26	} Elliptical cylinder.
0.9	9.73	—	
1	$\pi^2$	$4\pi^2$	
1.2	—	42.36	
1.4	10.32	45.03	
1.6	10.51	47.49	
1.8	10.69	49.81	
2	10.85	52.13	
3	11.50	61.59	
4	12.00	69.66	
5	12.41	76.80	} Triaxial hyperboloid of one sheet.
10	13.87	104.9	
100	20.94	316.1	
1000	33.52	—	

### § 10. Applications.

We very often meet in engineering compressed columns of varying section, for instance, in cranes, connecting-rods, and the details of aeroplane construction. Columns of varying cross-section having the stability of uniform columns are much lighter, and are therefore used in practice.

Let us consider some examples.

Example 1.

The lateral bending of an aeroplane pine strut of elliptical form is to be examined. The length  $l=200$  cm., the largest middle cross-section is an ellipse with semiaxis  $C=6$ ,

TABLE XI.

$i/l$ .	K ellipt. parabol.	Hyperboloid of two sheets.	Elliptical cone.	Hyperboloid of one sheet.
0	1.00	—	—	—
0.0001	2.00	1.57	0.32	0.12
0.01	3.45	3.06	2.15	1.35
0.1	5.40	5.18	4.81	3.42
0.2	6.37	6.21	6.20	4.67
0.3	7.05	—	6.84	5.64
0.4	7.61	7.53	7.48	6.45
0.5	8.09	—	8.01	7.17
0.6	8.51	8.45	8.47	7.79
0.7	8.89	—	8.87	8.36
0.8	9.26	9.26	9.23	8.90
0.9	9.57	—	9.56	9.40
	$\pi^2$	$\pi^2$	$\pi^2$	$\pi^2$

TABLE XII.

$i/l$ .	Elliptical paraboloid.	Hyperboloid of two sheets.	Elliptical cone.	Hyperboloid of one sheet.
0	1.00	—	—	—
0.0001	2.80	2.30	0.66	0.32
0.01	5.84	5.75	4.90	3.16
0.1	14.39	14.00	13.30	10.49
0.2	18.93	18.62	18.23	15.36
0.3	22.49	—	22.02	19.32
0.4	25.54	25.36	25.23	22.80
0.5	28.28	—	28.08	26.00
0.6	30.79	30.44	30.68	28.97
0.7	33.14	—	33.08	31.76
0.8	35.35	35.30	35.33	34.36
0.9	37.47	—	37.46	36.96
1	$4\pi^2$	$4\pi^2$	$4\pi^2$	$4\pi^2$

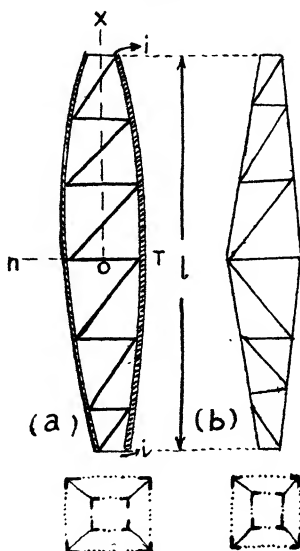
$b=3$  cm. The end sections are ellipses with semiaxes  $c_0=4$ ,  $b_0=2$  cm. Young's modulus  $E=100000$ . Tensile strength, 100 kg./cm.<sup>2</sup>.

Here the moment of inertia of the middle cross-section about the axis of the smallest stiffness is

$$I = \frac{\pi b^3 c}{4} = 40.5 \pi,$$

and for the end sections  $i = 8\pi$ , where  $i/I = 0.198$ , or 0.2 approximately. Using Table VIII. for an ellipsoid with supported ends when  $i/I = 0.2$ , we have the stability coefficient  $K = 8.15$ , whence, from (1),  $P = 2600$  kg.

Fig. 9.



The compressive stress in the end sections is 103 kg./cm.<sup>2</sup>, *i. e.*, exceeds a little the permissible stress. The stress in the middle cross-section will evidently be smaller.

If the strut had the form of an elliptical cone, we should get from Table IX.  $K = 6.20$  and  $P = 1980$  kg.

### Example 2.

#### *Lattice column of parabolic form.*

Let a column be constituted of four angle-irons of constant sections joint with a sufficiently solid lattice (fig. 9). The

moment of inertia of a section at the distance  $x$  from the middle of the column is

$$I(x) = 4I_c + 4S\eta^2, \quad . \quad . \quad . \quad . \quad . \quad (57)$$

where  $I_c$  is the moment of inertia of the angle-iron relatively to its centre of gravity,  $S$  the area of every angle-iron,  $\eta$  the distance of the centre of gravity from the neutral plane of the bent column.

It frequently happens that the first term in (57) is very small in comparison with the second. Neglecting it, we have

$$I(x) = 4S\eta^2. \quad . \quad . \quad . \quad . \quad . \quad (58)$$

The angle-irons are curved in the form of a parabola

$$\eta = A \frac{a^2 - x^2}{a^2}. \quad . \quad . \quad . \quad . \quad . \quad (59)$$

Hence the largest moment of inertia (at the middle of the column) is

$$I = 4SA^2.$$

The moment of inertia at any other section is

$$I(x) = I \cdot \left(1 - \frac{x^2}{a^2}\right)^2, \quad . \quad . \quad . \quad . \quad (60)$$

*i. e.*, it varies by the same law as the ellipsoid; so we can calculate this column, using Table X.

### Example 3.

A crossbar of 7 m. long consists of 2 U-irons, no. 12, curved in the form of a parabola. The distance between the U-irons is in the middle 10 cm. and at the ends 1 cm. A sheet of 1 cm. is pressed between the U-irons.

The moment of inertia of the middle section\* is

$$I = 2(92 + 17 \cdot 3 \cdot 6 \cdot 65^2) = 1710.$$

For the end sections

$$i = 2(92 + 17 \cdot 3 \cdot 2 \cdot 15^2) = 344.$$

\* The dimensions are taken by the U.S.S.R. standards by 'Hütte,' i. p. 855 (1929).



Hence

$$i/I = 0.2.$$

From Table VIII. we have

$$K = 8.15,$$

and the critical force from (1)

$$P_k = \frac{8.15 \cdot 2 \cdot 10^6 \cdot 1710}{490000} = 5700.$$

The compressive stress is 1670 kg./cm.<sup>2</sup>, which is smaller than the elastic limit.

#### Example 4.

##### *Pyramidal column latticed.*

A very important case in practice is when the edges of the column have a rectilinear form (fig. 9, b). In this case the moment of inertia varies according to the same law as the elliptical paraboloid, § 7. Hence, in calculating this column we may use the values of the second column of Tables XI. and XII.\*

#### Example 5.

A supporting leg of an overshaft pile-driver of 20 m. long is compressed by a force of 30 t. The piped section is of four equilateral angle-irons tied together by a lattice. The allowed intensity of compressive stress is 500 kg./cm.<sup>2</sup>. The reserve of stability in lateral bending is to be 4. The dimensions of the angle-irons and the distance between them have to be found.

At first we calculate the simple compression of the leg, and find that the area of every angle-iron is 15 cm.<sup>2</sup>. From the standard tables it is seen that this corresponds to the angle-irons no. 8, i. e., 80, 80, 10 mm.; its area, 15.11 cm.<sup>2</sup>. The intensity of compression is 496 kg./cm.<sup>2</sup>. Now we have to get the distance between the angle-irons so that the leg should be sufficiently stable. If we take the width of the leg as 30 cm., the moment of inertia of the cross-section of the leg, from (57), is

$$I = 4 \cdot 87 \cdot 2 + 4 \cdot 15 \cdot 11 \cdot 12 \cdot 66^2 = 10000,$$

\* We neglect the value  $I_0$  with comparison  $S\eta^2$ . The calculations made by student D. B. Volper show that, even in a most unfavourable case, when at the ends of the column the angle-irons touch one another with their shelves, the error attains only a few per cent.

where the moment of inertia of the angle-iron about the axis passing through its centre of gravity is 87.2. The distance of the centre of gravity of the angle-iron from its edge is  $12.66 = 15 - 2.34$ .

All values are taken from the standard tables.

If the section is constant, the critical force by Euler's formula is  $P = 49500$ , *i. e.*, the stability reserve is less than twice.

To increase the stability the leg must be made larger in the middle, the end sections being kept the same. We place the angle-irons on the half-length of the leg at a distance of 50 cm. Then the moment of inertia of this section, constituted from four angle-irons no. 8 at a distance of 50 cm., is

$$I = 4 \cdot [87.2 + 15 \cdot 11.22 \cdot 66^2] = 31400.$$

The ratio  $i/I = 0.31$ .

In our case the moment of inertia varies along the leg by a law sufficiently near to the square law. The stability coefficient from Table IX., when  $i/I = 0.3$ ,  $K = 7.05$ , and the critical force by (1),

$$P_k = 110000 \text{ kg.},$$

that is, by widening the leg in the middle while the angle-irons no. 8 remain the same its stability increases more than twice, and we get the reserve stability in more than three times.

But that is not enough; we put the width of the leg in the middle 52 cm.; then, by (51),

$$I = 4 \cdot 87.2 + 4 \cdot 15 \cdot 11.25 \cdot 68 = 34200.$$

The ratio  $i/I = 0.29$ , or approximately 0.3, which corresponds with Table XI,  $K = 7.05$ . Hence, by (1),  $P = 120000$  kg., *i. e.*, the required reserve of stability.

If the strut's flanges are curved in the form of a parabola (59), or of a broken line the tops of which lie on the parabola (59), then the moment of inertia  $I(x)$  of the strut varies by the law (60). From Table X., when  $i/I = 0.3$ , the stability coefficient  $K = 8.52$ ;

$$\text{by } I = 31000 \text{ the critical force} = 133000,$$

$$I = 34200 \quad \text{,,} \quad \text{,,} \quad \text{,,} = 14500,$$

*i. e.*, increases approximately about 20 per cent.

*Example 6.*

A connecting-rod of a low-speed steam engine has a length of  $l=554$  cm. It is narrowed to the ends like a cone; the largest diameter of the connecting-rod is 22 cm., the smallest is 18 cm. The critical force has to be found. Here the moment of inertia  $i=5150$ ,  $I=11500$ , where  $i/I=0.45$ . From Table IX.  $K=7.75$  (average between 7.48 and 8.01), and by (1)  $P=582000$ . The critical compression in the narrowest place is 2280 kg., *i. e.*, it does not exceed the elastic limit for steel \*.

§ 11. *Conclusion.*

We have examined in this paper the question of lateral bending of bars of varying cross-section which have the form of one of the surfaces of second order when the axis coincides with the axis of the surface.

We have considered the elliptical cylinder, elliptical cone, triaxial ellipsoid, hyperboloid of one and of two sheets, and elliptical paraboloid. The hyperbolical paraboloid and the sphere are out of the question, because of the form of their surface. We have integrated the differential equations of bending, and from the boundary conditions we have obtained transcendental equations, from which we have determined the critical forces.

It appears that in all these cases the critical force may be expressed by a simple formula,

$$P_{cr.} = \frac{KEI}{l^2}.$$

The stability coefficient  $K$  depends only upon the form of the bar and upon the means of fastening it.

We have given tables for the coefficients  $K$ .

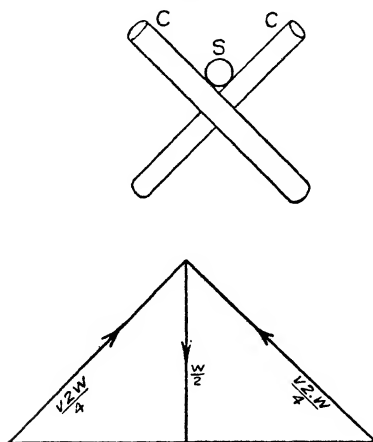
At the end we have given several examples dealing with the practical applications of the results obtained.

\* The dimensions are taken for a lift of one of the mines of Donbass. We neglect the influence of the heads of the connecting-rod because they are small. The diameter of the cylinder of the lift is 107 cm.; the steam-pressure is 7 atm., which corresponds with a loading on the connecting-rod about 65 T., *i. e.*, the stability reserve is about 9.

LXXIV. *Friction of Dry Solids in vacuo.* By Prof. P. E. SHAW, M.A., D.Sc., and E. W. L. LEAVEY, M.Sc., University College, Nottingham\*.

THE relation of the friction of dry solids to their elastic constants or other characteristic properties may prove of great theoretical interest. Recently experiments in this connexion have been published by G. A. Tomlinson (Phil. Mag., Suppl., June 1929). We shall endeavour to show in this paper that further relations can be established.

Fig. 1.



To measure the coefficient of friction of dry clean solids we place them in a vacuum tube on which is threaded a heating coil, so that by exhaustion and repeated heating to  $350^{\circ}$  C. all lubricants as well as all surface strain can be removed from the rubbing surfaces.

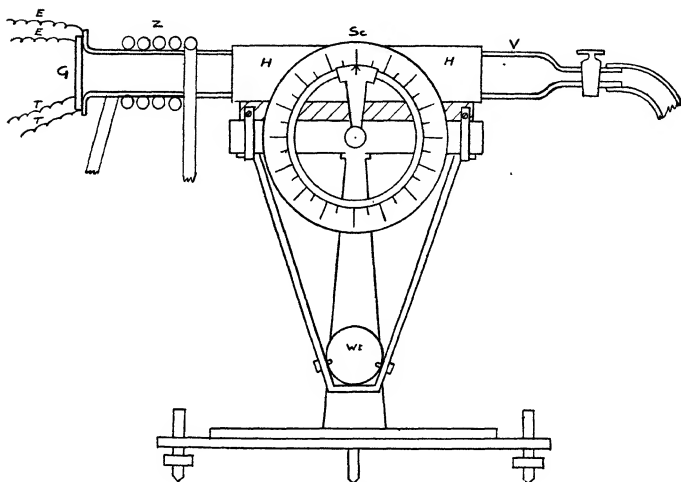
The friction apparatus is a development of that described by one of us (Shaw, Journ. Sci. Inst. iv. April 1927). The general view is shown in fig. 2, and a perspective view showing details inside the vacuum tube is given in fig. 3.

A cylinder of the material is cut into five lengths; one forms a sliding rod, S, 12 cm. long, the others, each 4 cm.

\* Communicated by the Authors.

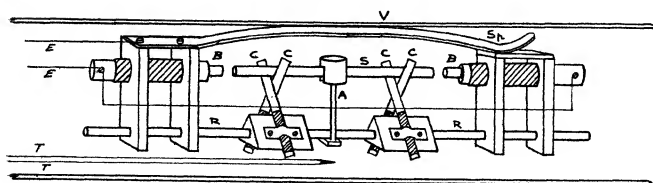
long, are arranged in two crutches, C, C, whose arms are each at  $45^\circ$  to the vertical (fig. 1). The slider rests on the two crutches, and slips when the vacuum tube V (figs. 2 and 3), which turns on a horizontal axis, is tilted to the angle of repose  $\theta$  of the materials. By reversing the angle

Fig. 2.



The Apparatus.

Fig. 3.



Inside the vacuum tube.

of slope the slider moves the other way, and the true angle of repose is taken as half the difference of the two angular readings. The total weight,  $W$ , of the slider is supported equally at four contacts, and as the system is symmetrical the weight supported by one crutch is  $\frac{W}{2}$ . The reaction

of each arm of the crutch is normal to its length and equal to  $\frac{\sqrt{2}W}{4}$  (see fig. 1). As there are four of these reactions the total normal thrust when the slider is tilted through angle  $\theta$  is  $\sqrt{2}W \cdot \cos \theta$ . The total component force urging the rod to slip being  $W \cdot \sin \theta$ , we have, by the law of friction,

$$W \sin \theta = \mu(\sqrt{2}W \cdot \cos \theta);$$

hence

$$\mu = \frac{\tan \theta}{\sqrt{2}},$$

where  $\mu$  = coefficient of friction.

Since friction may depend on surface strain, and so on previous rubbing, it is clearly an advantage to insure that the same parts of slider and crutches are rubbed throughout an experiment, otherwise readings would not progress regularly. For this reason only one degree of freedom—that along its length—is allowed to the slider. This is arranged by attaching to the slider an arm, A, weighted, to rub *lightly* against the fixed rod, RR, which is parallel to the axis of the tube, and to which all the working parts except the slider are attached. The crutches are shown insulated by mica sheets from the rest of the apparatus. During the experiments the sliding is not watched, but is registered by electric contact. At each end of the sliding rod, and free of it, is a stop B; and when the slider strikes B at either end it completes a circuit and excites a current indicator outside the vacuum tube. There are advantages in this electric touch method, especially as the heating coil H is usually in place and obscures the view of the inside of the tube. Thus the observer does not need to observe the actual movement of the slider. Each of the stops BB is a buffer having a bar sliding in a tube with a steel spring attached behind it. It is important to have BB yielding, not rigid, for two reasons: (a) If the slider meets a rigid stop when moving down a slope it jumps and falls again, and so the surfaces are bruised and their friction modified just where the friction is to be tested. But the buffers bring the slider slowly to rest and obviate shock. (b) To obtain a true coefficient of friction the slider should touch the crutches, and no other solid such

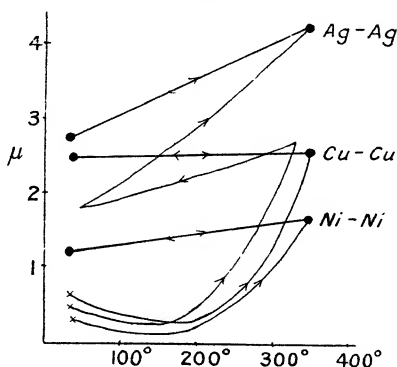
as the stops, at the moment when friction begins ; for any such contact may admit some spurious stress normal to the surfaces. This would introduce error in the coefficient of friction. To explain the action of the buffer, suppose the apparatus is tilted and the slider is compressing a buffer spring. When the tilt of the apparatus is slowly reversed the buffer recovers from the compression and drives the slider out of contact with it. The indicator reveals that contact is broken, and when the apparatus is further tilted to the angle of repose on the reverse side the rod slides again and moves to the lower buffer, where electric contact again occurs. Thus we insure free friction for the slider with one degree of freedom only.

Alternating current is used in the heating coil to avoid magnetization of the iron or nickel rods, and consequent error in  $\mu$ . As a further precaution demagnetization was secured by reducing the A.C. gradually to zero, in the usual way. The results were then checked by repeating the whole experiment, using Bunsen burners in place of the heating coil. The temperature is recorded by a thermocouple, insulated in the vacuum tube, and connected to a calibrated galvanometer outside. The leads for the contact arrangement are E E, and those for the thermocouple T T. These all leave the tube where it is sealed to the glass plate G, sealing-wax being used. As the temperature of the seal must be kept low, a few turns of rubber tube Z carrying cold water are coiled on the vacuum tube. Vacuum to about  $10^{-6}$  mm. is used. A tap and rubber tube connexion to a pump are shown on the right. The tube and its connexions are free to swing either way  $90^\circ$  to the horizontal, and the angle is read on the scale Sc. To attain balance on the tilting apparatus a counterpoise Wt is attached below. The frame carrying the components inside the vacuum tube is fitted tight by the steel spring Sp, so that even when the tube is set vertical nothing but the slider can move.

The metals used (Fe, Ni, Cu, Ag, Al) are cleaned by finest sand-paper and then by a clean blade. The soda-glass rods used are given a preliminary cleaning in a Bunsen flame. The friction between each of the various combinations of these materials is found first at ordinary temperature and pressure. Then vacuum is attained, and temperature raised to the upper limit and lowered again repeatedly, the values of the angle of repose being recorded

throughout until readings at any temperature are constant. Before the first heating the coefficient of friction is invariably low, between 0.1 and 0.3, and remains low after prolonged evacuation and sliding to and fro. Fig. 4 shows, for three cases, how  $\mu$  changes as heating and sliding proceed. When heating commences  $\mu$  falls to a minimum at about  $150^{\circ}\text{C}$ . (see fig. 4). Then, as temperature rises, it rises slowly till about  $250^{\circ}$ , then rapidly to the limiting temperature  $350^{\circ}$ . After repeated heating and cooling  $\mu$  attains a constant high value. Some of our values point to the failure of the law of friction at high temperatures. Thus, for Ag-Ag and Ni-Al at  $320^{\circ}$ ,  $\mu$  is about 4, so that the angle

Fig. 4.



Variation in  $\mu$  as the heat treatment proceeds for three like pairs. Initial readings shown by star. Final values for the temperature range shown between circles.

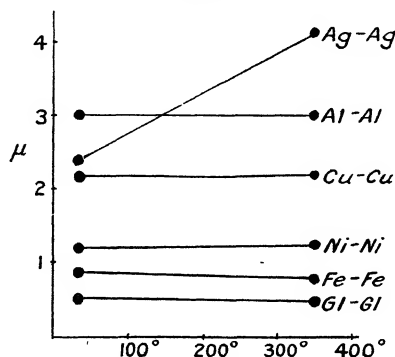
of repose is about  $80^{\circ}$ . In some cases we find the slider even becomes vertical without sliding, so that here the tangential force is finite and the normal force vanishes and  $\mu = \infty$ . This corresponds to Tomlinson's experience with lead (*loc. cit.* p. 936), and indicates that the two surfaces are strongly combined. Even steel, which normally has a low coefficient of friction, behaves in the same way in some circumstances; for when two Johansson gauges are "wrung" together the force required to pull them apart may amount to several kilograms to the square centimetre. Under such conditions the law of friction could not be applied.



Fig. 5 shows the values of  $\mu$  for like materials depending on temperature, and fig. 6 shows the results when the rubbing materials are unlike. The curves show a large temperature coefficient with Ag-Ag, Ag-Al, Ag-Ni, Al-Fe, and Al-Ni; other combinations of the metals used have little or no temperature coefficient when once the full values of  $\mu$  have been attained by vacuum heat.

Direct comparison can be made between our results at ordinary temperature and those given by G. A. Tomlinson (*loc. cit.*) for Cu, Al, Fe, Ni, and glass. He scours the metals with fine emery, then polishes, and cleans with ammonia, alcohol, and ether. In experimenting on glass he uses

Fig. 5.



Final values for like materials. Silver alone has marked temperature coefficient.

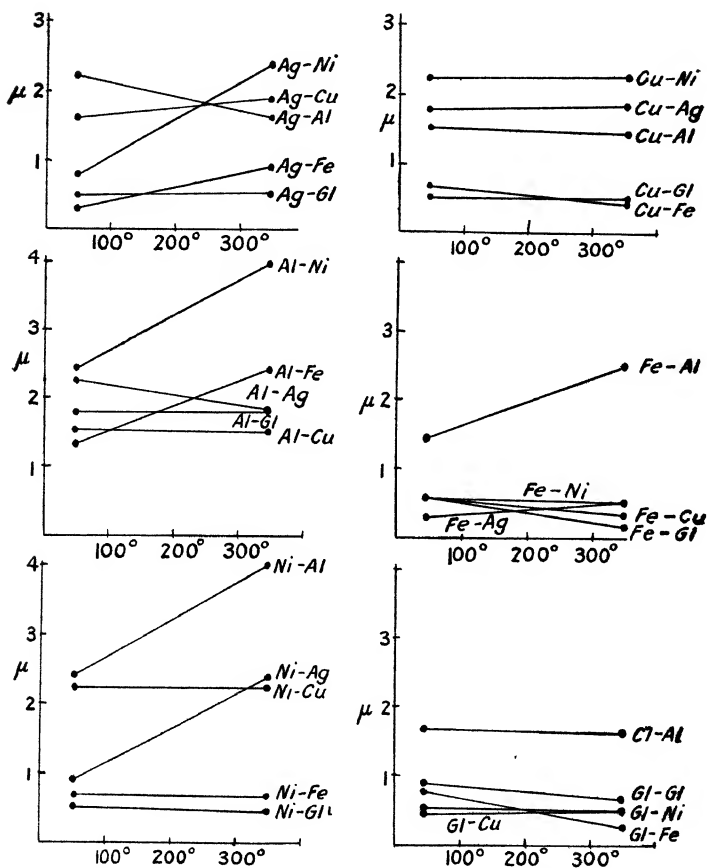
a fused bead on a plate of glass. Friction is then measured in the usual way by applying an increasing horizontal load to the upper solid till it slides on the lower. No heat is applied, and the operation is performed in open air.

Thus the methods employed in this research differ markedly from ours; the great disparity between his results and ours is shown in fig. 7, though it will be observed that in both sets of results soft metals have large friction\*.

\* It may be noted, as a practical issue of our results, that in bearings which become hot after lubricant has failed, friction increases rapidly when the temperature rises above the temperature of relaxation; for then the low values of  $\mu$  usually found rapidly increase about three-fold to our values. This would precipitate "seizing."

For metals our results are higher, for glass lower, than his. In the case of glass this is not surprising; for the value of  $\mu$  changes from say 0.3 for recently heated glass, to, say, 1.0 or more after prolonged treatment with boiling

Fig. 6.



Final values for the five metals and glass.

chromic acid, which roughens and disintegrates the surface. Various glasses vary enormously in composition. Unless therefore glass of the same composition and treatment be used, it is useless to compare the results. But in the case

of the metals, which would all be approximately pure, and are in each case treated not chemically but mechanically by clean emery or knife, the difference between the results of the two researches is striking.

We attribute the disparity primarily to the fact that the vacuum-heat treatment is very drastic. It not only at 350° removes adsorbed layers or adherent impurity, but, what seems much more important, fundamentally modifies

Fig. 7.

3.0	Al-Al		
	Ag-Ag		
	Al-Ni		
	Cu-Cu		
2.0	Al-Ag		
	Cu-Ni		
	Ag-Cu		
	Al-Cu		
	Al-Fe		
1.0	Ni-Ni		Al-Al
	Ag-Ni		Al-Ni
	Fe-Fe		Al-Cu
$\mu$	Ni-Fe & Cu-Fe		Al-Fe & Cu-Cu
			Cu-Fe & Cu-Ni
			Fe-Fe & Ni-Ni
	Ag-Fe		
Shaw & Leavey.		Tomlinson.	

First column.—Our values of  $\mu$ , at ordinary temperature, after heat treatment.

Second column.—Tomlinson's values of  $\mu$ .

the metal surfaces, relaxing surface strain and leaving the surfaces annealed\*.

There are good grounds for considering that at or below 300° C. surface relaxation occurs; Sir. G. Beilby (see 'Aggregation and Flow of Solids') found that at some

\* It might be suggested that at high temperature oxides may form on the metals, even in the good vacuum used, and modify the friction. But close observation in every case tried by us revealed no oxide, the rubbing surface after the experiments being quite bright.

temperature below  $300^{\circ}$  "vitreous" metal surfaces change to the crystalline state, and that any peculiar thermoelectric quality produced by surface strain is destroyed. Again, in a research by one of us (Shaw, Proc. Roy. Soc. A, xciv. 1917) it is shown that the surfaces of many metals (Pb, Al, Zn, Fe, Ni, Au, Pt) undergo triboelectric transformation at some temperature, between  $100^{\circ}$  and  $300^{\circ}$ , peculiar to the material.

The difference between cold-worked and annealed metals is seen in a variety of ways; mercury wets silver and copper better when hardened than when annealed; also iron is more soluble in acids in the former state than in the latter.

We have applied various tests to our theory—

1. The surfaces have been heated to  $300^{\circ}$  in contact with one another and values of the coefficient of friction taken at successive temperatures rising and falling. In this way the surfaces would press one another over the whole range of temperature. This is the standard method, whose results are shown above.

2. The surfaces are heated when out of contact and allowed to cool before friction is measured. The coefficients in this method are slightly higher than in the former. Thus for the metals tried the value of  $\mu$  is about 10 per cent. higher than by method 1. This we expected, as the rubbing of the surfaces when warm would impose some strain on them and harden them.

3. The surfaces having been annealed in vacuum, giving the high values shown above, are then removed from the vacuum, treated with finest emery, then polished and cleaned as in Tomlinson's experiment. The values of  $\mu$  are now found as low as his.

4. The results so far are for light loads (say 15–25 gm.), *i. e.*, the rod and slider combined (see fig. 3).

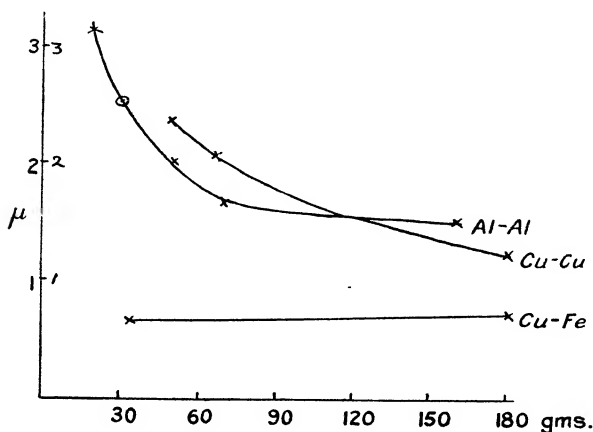
To vary the conditions, larger, and even smaller, loads than these are now tried. In fig. 8 is shown the effect on  $\mu$  of varying load from 20 gm. to 180 gm. for Al-Al, Cu-Cu, Cu-Fe.

Great reduction of  $\mu$  occurs for the like metals. For the case of Cu-Fe the value is not materially affected by greater loads. Enough has been done even with these

cases to demonstrate that an annealed surface is liable to change in character when friction occurs under heavy loads. On comparing these results with those of fig. 7 it is seen that, even now, our values are considerably higher than Tomlinson's.

This is not surprising. Tomlinson uses abrasives which cut into the material, dislodging some masses and straining other parts; he next polishes under pressure, and, as we know from Rayleigh's work, polish connotes surface flow. In contrast, friction without previous straining between two metals, as in our work, is a continued process of

Fig. 8.



Values for heavy loads. Commercial metal used except in one case marked C, which is 99.65 per cent. pure.

combination and sundering under pressure, and such actions are quite unlike those of abrading or polishing.

Tomlinson established the following remarkable relation between friction and the elastic constants at ordinary temperatures:—

$$\frac{(\mathfrak{S}_A + \mathfrak{S}_B)^{\frac{2}{3}}}{\mu} \cdot 10^8 = \text{const. K.}$$

The bracket term involves rigidity and compressibility for the metals A and B used. The dimensions of the bracket term are the inverse of elasticity. This means

that friction is greatest for yielding materials such as lead and tin, and least for strong metals Fe and Ni, because the area of contact, other things being equal, would be greater for the softer materials.

Thus the coefficient of friction depends directly on the area of contact. Tomlinson observed values of  $\mu$  for 10 materials in every combination, 55 results in all. The mean value found for K is 5.47, and 42 results are within 10 per cent. of this mean. This concurrence is all the more remarkable as the range in elasticity is so great—from  $3 \times 10^{11}$  for lead to  $8.9 \times 10^{11}$  for iron—and the range in melting-points from  $200^\circ \text{C.}$  to  $1500^\circ \text{C.}$

The above equation, which we call Tomlinson's law, holds for the nine metals used and glass, and may prove universal. Accepting the law, the general principle follows that the elastic body-properties of these materials when polished hold good *right up to the outermost layer of molecules*. This is unexpected, for the surface of a solid is a peculiar region, normally possessing a large field of force, as shown by adsorption and other properties. Yet according to these experiments, coupled with the foregoing theory, the surface retains the full elasticity of the body of the solid and is for frictional purposes identical with it.

To account for the result we put forward the suggestion that the cleaning processes adopted by Tomlinson, in which he scours the surface with emery and then cleans and polishes, leaves that surface strained and hardened, and that the surface thus hardened is so well held by underlying layers that it possesses the full elastic strength of the whole solid mass. In contradistinction, our surfaces we take to be well annealed, and consequently softer and more frictional.

In the following Table are shown in the second column the values of  $\mu$  after heat treatment for the unlike metals of the first column. In the third column are the mean values for the metals. Thus, for Ag-Fe we have 1.7, the mean of Ag-Ag (2.6), and of Fe-Fe (.8) (see foot of the Table). The fourth column shows how the actual values are, in all but two cases, below the mean values. In the last column are shown the affinities of the crossed metals for one another, as given by metallurgical data (see 'International Critical Tables,' vol. ii.).

It seems clear that affinity has an influence on friction, for when, as at the head of the Table, the metals have

small affinity the friction for the crossed metals is greatly reduced below the mean values, whereas, when further down the Table the affinity is great, the friction is less reduced, or in two cases, Cu-Ni, Al-Ni, is actually above the mean value.

These metallurgical data are obtained when temperatures are much higher than those of our experiments; but we seem forced to admit from the Table that the affinities found at high temperatures hold good, in part, and affect our results even down to ordinary temperatures. By contrast with our results Tomlinson obtains results for unlike metals which are intermediate between those of the

Metals.	$\mu$ .	Mean values, $\mu_1$ .	$\mu - \mu_1$ .	Affinities.
Ag-Fe ....	·3	1·7	-1·40	Two immiscible liquids, when melted.
Cu-Fe ....	·69	1·5	-·80	
Ni-Fe ....	·69	·9	-·20	
Ag-Ni ....	·86	2·1	-1·30	
				Two immiscible liquid solutions at Ni end.
Al-Fe ....	1·28	2·0	-·72	One compound
Al-Cu ....	1·47	2·7	-1·23	Four „
Ag-Cu ....	1·72	2·2	-·48	No „
Cu-Ni ....	2·01	1·7	+·31	No „
Al-Ag ....	2·20	2·8	-·60	Two „
Al-Ni ....	2·36	2·1	+·26	Three „
				and solid solutions form.
Fe-Fe ....	0·8			
Ni-Ni ....	1·1			
Cu-Cu ....	2·3			
Ag-Ag ....	2·6			
Al-Al ....	3·1			

two individuals (*loc. cit.* p. 928); and so his values would seem to depend on elasticity chiefly, and slightly, or not at all, on affinity.

We will endeavour to account for this singularity in our results. We have already suggested that the strained surfaces of metals are annealed, and so are fundamentally changed by heat treatment. When in the annealed state we suppose that the natural affinities of the metals operate even at room temperatures. When the affinity is small the strength of the attachment of the surfaces is small and the friction is below that to be expected from the elastic moduli; and when affinity is high the friction is thereby raised.

As an example take again the case of Ag-Fe. The friction of Ag-Ag is very great (2.6), of Fe-Fe small (.8), but the affinity of silver for silver and of iron for iron is greater than that of one metal for the other, alien, metal, and the resulting coefficient is only 0.3. It is well known that when two metals alloy with one another the distortion of the lattice structure and the consequent hardness of the alloy is greater, as the affinity between the metals is less. The affinity itself is small as the range of solubility is small. In pursuance of this idea the alloys formed at the head of the table would be harder than those further down, and if the alloying were deep enough in the lattice structure the hardening of the material would cause reduction in the area of contact and in  $\mu$ , in accordance with Tomlinson's theory. But we do not consider this effect would influence results, since for metals in contact only a short time the alloying cannot be expected to be so deep-seated as to affect the general lattice strength.

If our views are correct, then as regards our experiments friction depends on the elastic moduli and affinity jointly.

### *Previous Researches.*

Two investigators have adopted methods somewhat like ours :

1. C. Jacob (*Ann. d. Phys.* xxxviii. May, 1912) used a tilting method in a vacuum tube, and raised temperature by a heating coil outside it. Her results, so far as they bear on the present work, are :—

- (a) Rise of temperature causes a small decrease in  $\mu$ , with a minimum value between 150° and 200° C.
- (b) At higher temperature there is a great increase in  $\mu$ .

Definite values for  $\mu$  are not given, but in both the above points there is general agreement with our results.

2. R. B. Dow (*Phys. Rev.* xxxiii. Feb. 1929) also used a tilting method. The metals used—brass, copper, zinc, aluminium—are enclosed in a vacuum into which various gases were introduced in turn. No heating coil was used,



so the results are not comparable with ours. The values of  $\mu$  were all low, 0.1 to 0.5.

We wish to thank the National Physical Laboratory, and particularly Mr. S. L. Archbutt, of the Metallurgical Department, for kindly supplying pure metals and for advice in our work.

### *Summary.*

1. Friction is performed in a vacuum chamber surrounded by a heating coil, so that the materials—aluminium, silver, copper, nickel, iron, and soda-glass—can be heated to 350° C. and exhausted. Every combination of the materials, like and unlike, is investigated. The tilt method of measuring friction is adopted.

2. After repeated heating and cooling in vacuum, the friction rises and finally settles to values which are, in general, practically constant between 15° and 350°. But for two or three cases there is a pronounced plus or minus temperature-coefficient of friction.

3. The coefficient of friction is much higher, especially for light loads, than when the materials are treated in open air. The suggestion is put forward that, for the metals, the heat treatment causes thorough surface relaxation of the material, and the surface is thus not only softened but is radically different in character from one ground and polished. The ground and polished surface possesses the elastic characteristics of the general body of the metal; the relaxed surface is not only softer, but is more free to assert its natural affinity for other metals. The result of the heat treatment is that friction is increased by increase of softness and increase of affinity.

4. As the load on the surface is increased up to about 180 gm.  $\mu$  decreases, but reaches limiting values which are, even then, considerably higher than those for fully strained surfaces.

5. It is clear that the term "coefficient of friction" has to be defined in terms of the history and physical condition of the reacting surfaces.

LXXV. *A Note on the Representation of Crystal Structure by Fourier Series.* By Prof. W. L. BRAGG, F.R.S., Langworthy Professor of Physics, Manchester University, and J. WEST, Moseley Research Student (Royal Society)\*.

### 1. Introduction.

IN a former paper<sup>(1)</sup> an account has been given of the use of a double Fourier series to represent the projection of a crystal structure on a given plane. If measurements of X-ray diffraction are made for all planes round a given zone in a crystal, and certain further information about "phase" is available, a projection can be made by summing a Fourier series with two variables. It was shown that such projections give a vivid picture of the atomic arrangement in the crystal.

In the present paper we wish to discuss the extent to which the representation is a faithful image of the actual crystal structure. It will be seen that the term "image" is appropriate, for it suffers from defects precisely analogous to those caused by diffraction in an optical image. It is interesting to see how close the analogy is and how constants of X-ray analysis can be defined which have exactly the same significance as the "resolving power" and "numerical aperture" of a microscope.

### 2. The Fourier Representation.

The use of a Fourier series to represent the results of X-ray analysis was first suggested by W. H. Bragg<sup>(2)</sup>, and developed by Duane<sup>(3)</sup>, Compton<sup>(5)</sup>, and Havighurst<sup>(4)</sup>. The method employed in the previous paper in the 'Proceedings of the Royal Society' was based on the same principle as their work, but is more extended in its scope. If the crystal structure, when projected parallel to a zone on any given plane, has a two-dimensional unit cell of area  $A$  and sides  $b$  and  $c$ , then the density of scattering matter (number of electrons per unit area) at a point  $y, z$  referred to the cell sides as axes is given by

$$\rho(y, z) = (1/A) \cdot \sum_{-\infty}^{\infty} \sum_{-\infty}^{\infty} F(okl) \cos 2\pi(ky/b + lz/c).$$

\* Communicated by the Authors.

$F(okl)$  measures the reflecting power of the plane ( $okl$ ) as previously defined, and the projection in this case is supposed to be parallel to the  $a$  axis of the crystal.

If the series is calculated for points distributed throughout the unit cell the atoms appear as concentrations of greater density. Though they sometimes overlap each other in the projection, certain of them often stand out clear of their neighbours. In such cases it is possible to sum

TABLE I.

$\sin \theta/\lambda$ .	F values. Room-temperature.		F values. Atoms at rest.	
	Na+.	Cl-.	Na+.	Cl-.
0 .....	10.0	18.0	10.0	18.0
0.05 .....	9.82	17.05	9.86	17.12
.10 .....	9.35	15.02	9.50	15.23
.15 .....	8.61	12.80	8.93	13.18
.20 .....	7.71	10.93	8.21	11.50
.25 .....	6.76	9.48	7.45	10.24
.30 .....	5.81	8.44	6.67	9.30
.35 .....	4.90	7.37	5.93	8.60
.40 .....	4.10	6.58	5.25	8.05
.45 .....	3.29	5.83	4.51	7.63
.50 .....	2.76	5.30	4.07	7.24
.60 .....	1.83	4.14	3.22	6.49
.70 .....	1.23	3.13	2.63	5.76
.80 .....	0.83	2.28	2.23	5.06
.90 .....	0.57	1.62	1.97	4.42
1.00 .....	0.37	1.10	1.73	3.84
1.1 .....	0.25	0.74	1.59	3.34

up the total amount of scattering matter, and so to obtain a direct count of the number of electrons in the atom.

There are many problems of crystal structure which it would be interesting to solve in this way. Havighurst and Compton have used Fourier series with a single variable to test such questions as the ionization of sodium and chlorine in sodium chloride. The Fourier series with two variables is on the face of it a more powerful method, because it separates the atoms more from each other. Further, the series is just as easy to manipulate for large

unit cells containing many atoms as for small cells of a simple type such as that of sodium chloride. A cell of large dimensions yields measurements of scattering at small glancing angles, and these are essential in finding out the positions of the outer electrons in the atoms. An instance of a problem on which light may be cast by the Fourier representation is the distribution of electrons between silicon and oxygen in silicates.

The difficulty of such investigations arises partly from errors in the experimental measurement of diffraction (values of  $F$ ), and partly from the termination of the Fourier series before its coefficients have become very small.

TABLE II.

Values of  $F(okl)$  for Crystal at Room-temperature.

	0.	1.	2.	3.	4.	5.	6.	7.	8. $\rightarrow k$
0 ....	28.00	—	16.14	—	7.94	—	3.64	—	1.40
1 ....	—	4.09	—	2.44	—	2.15	—	1.12	—
2 ....	19.90	—	13.94	—	7.31	—	3.39	—	1.32
3 ....	—	2.47	—	2.55	—	1.94	—	1.00	—
4 ....	12.15	—	9.56	—	5.73	—	2.75	—	1.14
5 ....	—	2.58	—	2.32	—	1.57	—	0.78	
6 ....	7.32	—	6.19	—	3.93	—	1.97	—	
7 ....	—	2.16	—	1.78	—	1.11	—	0.55	
8 ....	4.21	—	3.64	—	2.42	—	1.27		
9 ....	—	1.40	—	1.11	—	0.70			
10 ....	2.29	—	1.95	—	1.34				
11 ....	—	0.76	—	0.62					
$l \downarrow$ 12 ....	1.14	—	1.00						

The series is terminated because it is impossible to measure more than a certain number of reflexions with a given X-ray wave-length, and its effect is precisely like that which limits the resolving power of an optical instrument. In the present paper we wish to examine the question of resolving power alone, and will take an ideal case where we suppose no experimental errors to have been made.

### 3. Diffraction Effects in the Image.

It has been shown by James Waller and Hartree<sup>(6)</sup> that the observed X-ray diffraction by sodium chloride corresponds very closely with that to be expected from the

Hartree model of atomic structure. We have therefore tested the Fourier representation by taking an ideal crystal of sodium chloride composed of such Hartree atom-models, calculating its diffraction as if observations were being made experimentally for a limited range of crystal planes, expressing these results in the form of a double Fourier series, and then seeing with what faithfulness the projection represents the original model\*.

The most convenient projection which separates the sodium and chlorine atoms is that upon the plane (110);

TABLE III.

Values of  $F(okl)$  for Crystal when Atoms are at rest.

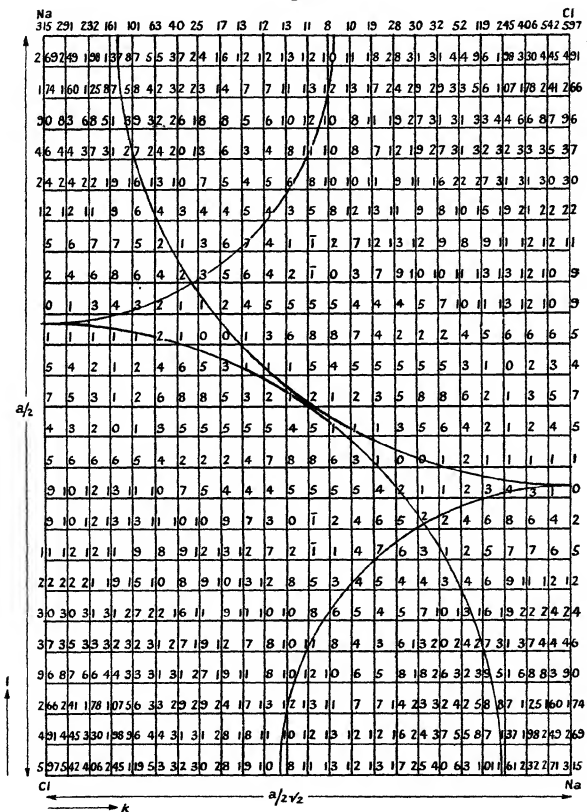
	0.	1.	2.	3.	4.	5.	6.	7.	$\rightarrow k$ 8.
0 ....	28.00	—	17.58	—	11.23	—	7.76	—	5.53
1 ....	—	4.12	—	2.77	—	3.24	—	2.51	—
2 ....	20.67	—	15.76	—	10.74	—	7.53	—	5.44
3 ....	—	2.64	—	3.05	—	3.16	—	2.39	—
4 ....	14.38	—	12.52	—	9.49	—	6.94	—	5.12
5 ....	—	3.04	—	3.28	—	2.93	—	2.15	
6 ....	10.74	—	9.87	—	7.99	—	6.18	—	
7 ....	—	3.24	—	3.05	—	2.51	—	1.81	
8 ....	8.25	—	7.76	—	6.63	—	5.34		
9 ....	—	2.79	—	2.51	—	2.06			
10 ....	6.49	—	6.18	—	5.44				
11 ....	—	2.16	—	1.94					
$\downarrow$ 12 ....	5.11	—	4.93						

the unit cell then has the dimensions  $a$  by  $a/\sqrt{2}$ , and contains two atoms of each kind. It is only necessary to represent one quarter of such a cell in order to see the pattern.

\* Havighurst (Phys. Rev. xxix. p. 1, 1927) has made a precisely similar examination with a single Fourier series and a model of the sodium atom, and comes to the conclusion that "the value of the retention of the temperature factor in the experimental F-curves as a means of securing a rapidly convergent series and therefore of obtaining a more trustworthy Fourier analysis is clearly demonstrated." As will be seen, we arrive at the same conclusion about a temperature factor for the double Fourier series. It is interesting to examine this series in detail, however, because it is so widely applicable to complex crystals, where the single Fourier series is helpless, and, further, because the optical analogies are so striking.

We have supposed the measurements to be made up to a glancing angle  $\theta_0$  equal to  $\pi/6$  ( $\sin \theta_0 = 0.5$ ), and for a wave-length of  $0.615 \text{ \AA}$ . ( $Rh K_{\alpha}$  radiation). The series has been calculated for values of  $F$  at room-temperature ( $290^\circ$  absolute) and for an ideal crystal of atom-models

**Fig. 1.**



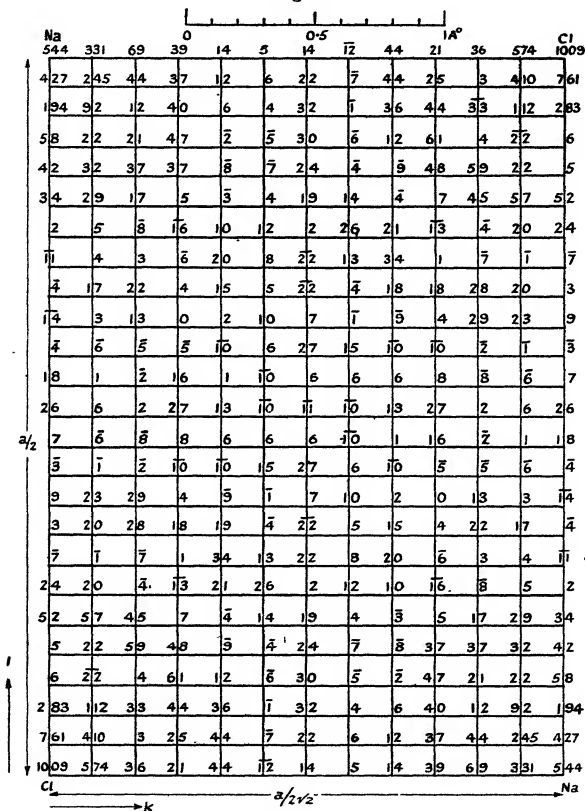
Projection on (100) [i.e., (110) true cell of side  $a=5.628 \text{ \AA}$ ].  
Crystal at room-temperature.

unaffected by any movement or by the so-called zero-point energy. The  $F$  values adopted for each atom in the two cases are given in Table I.; they are taken or deduced from those given by James, Waller, and Hartree.

The F values for the unit cell used in the projection and appropriate to each crystal plane are given in Tables II. and III.\* These values are normally found by experiment. Planes (*okl*) in our adopted unit cell correspond to planes (*kkl*) in the *true* unit cell of rock-salt.

In the case of the crystal at room-temperature the

**Fig. 2.**



**Projection on (100).** Crystal with atoms at rest. The number of points taken here is less than in fig. 1, but a more detailed analysis is given in figs. 4 and 5.

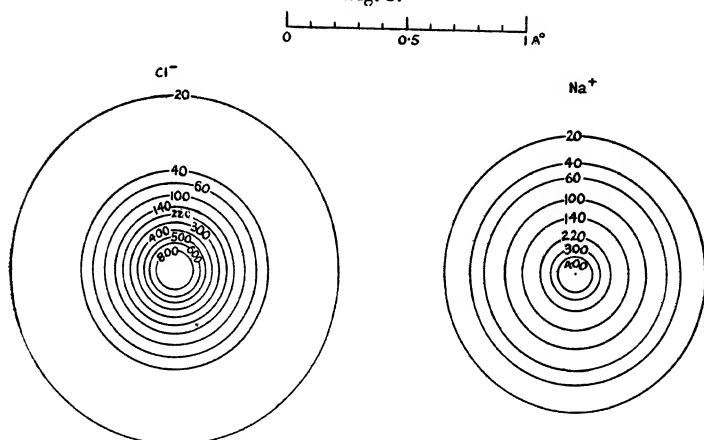
\* The numbers given in Tables II. and III. in the figs. 1-5 should strictly be doubled, since there are two molecules in the unit cell adopted. It is necessary to note this when estimating the distribution of scattering matter in the diagrams concerned.

calculated electron density throughout the unit cell is shown in fig. 1. The numbers represent the summation of the Fourier series

$$\sum_{-\infty}^{\infty} \sum_{-\infty}^{\infty} F(okl) \cos 2\pi(ky/b + lz/c),$$

and, after being doubled (see note above), must be divided by the area of the cell (22.40 Å.) in order to get the actual density. It is convenient to use the Ångström as a unit of length in such a projection. Although the coefficients of the series are still appreciable when the series terminates, they are small compared with the initial coefficients.

Fig. 3.



Projection on plane of atom-models used in calculations. The scale is the same as that for figs. 1 and 2. The numbers on all three diagrams have the same meaning.

The corresponding projection for the ideal crystal composed of atoms unaffected by movement is shown in fig. 2. In fig. 3 we give to the same scale as the two previous diagrams the projections on a diametral plane of the two kinds of atom-models. The contour lines in all three diagrams are drawn through points of corresponding density.

#### 4. Discussion of Fig. 1.

In regions widely removed from the centres of the atoms the density is very small, and it nowhere has an



appreciable negative value. Although sodium and chlorine overlap in the direction of the short axis (perpendicular to the (110) plane in the normal unit cell) they are fairly well separated elsewhere. The image reproduces correctly the spherical symmetry of the atom-models, and an attempt can be made to separate the one atom from the other, apportioning the density between the two atoms in the part where they overlap, so that the components are in accord with the values found elsewhere at corresponding distances. The result of an electron count gave 17.5 for chlorine and 10.5 for sodium, and is close to the values 18 and 10 for the ionized atoms.

The count does not, however, decide definitely the question as to whether the atoms are ionized or not, although the figures on which the projection is based were appropriate to ionized atoms. At first sight this may seem to be due to an error in drawing the boundary between the two atoms. Such an error could arise from the presence of irregularities in the projection—discussed below as “diffraction effects”—caused by terminating the Fourier series whilst the coefficients are still appreciable. These irregularities, as we shall see later, can seriously affect an electron count, and although in fig. 1, by making use of a temperature factor, they are by no means so marked as in fig. 2, they are still present.

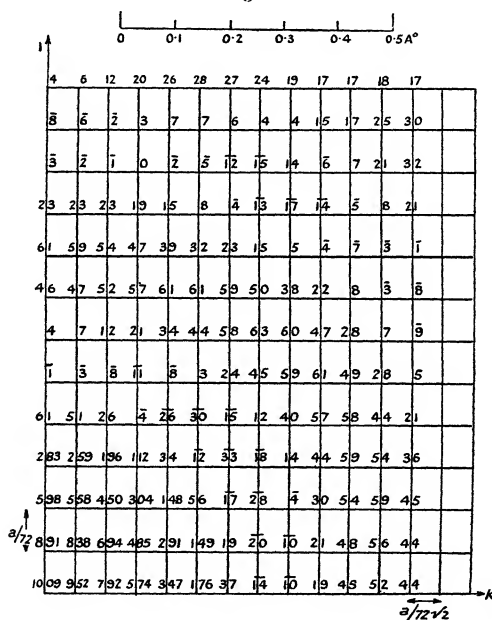
A consideration of Table IV. will, however, show that the defect is more fundamental, and that the count would still be incorrect even if the irregularities just mentioned were removed by the use of a higher temperature coefficient. The boundaries chosen for the two atoms are indicated by the arcs in fig. 1, which have radii 1.73 Å. for  $\text{Cl}^-$  and 1.08 Å. for  $\text{Na}^+$ . Table IV. shows that whereas the latter radius includes in effect all the electrons of  $\text{Na}^+$ , the former only includes about 17.4 electrons of  $\text{Cl}^-$ . The remainder falls within the boundary of the sodium atom, and being automatically included in the count for  $\text{Na}^+$  in the projection, is wrongly ascribed to it. This seems to suggest that a correct electron count is not possible. However, we have to remember that the original F curves used were calculated for free ions, and since presumably F values measured experimentally will correspond to ions whose electrons are compressed into a smaller region by the mutual approach of the atoms, it would seem possible that a correct count might be made

in an actual experiment provided the difficulties of obtaining accurate  $F$  values are successfully overcome. At the same time it is clear that considerable caution should be exercised in interpreting the results and that rigorous conditions must be satisfied before they can be relied upon.

### 5. Discussion of Fig. 2.

In this case the numbers show oscillations between positive and negative values all over the unit cell. The

Fig. 4.

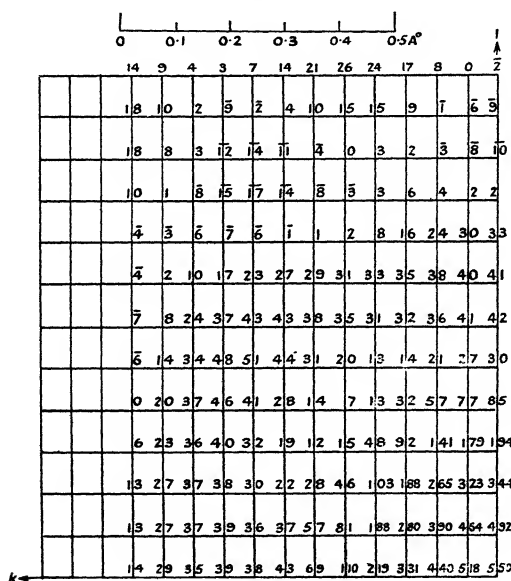


Portion of fig. 2 (neighbourhood of chlorine atom) magnified and calculated for closer points.

centres of atoms are marked by higher peaks than in fig. 1 but they are surrounded by concentric rings of positive and negative density which, by overlapping, produce the complicated aspect of the projection. *These irregularities have no counterpart in the atomic structure.* They are due to the termination of the Fourier series whilst the coefficients are still large, and are precisely

analogous to the diffraction effects produced by an optical instrument. The atomic model has a large concentration of scattering matter at its centre, and an effect is produced like the diffraction rings around the image of a luminous point. In the present case it is *amplitude* and not *intensity* which is plotted, so that the diffraction rings give both positive and negative contributions and are more important as compared with the central maxi-

Fig. 5.



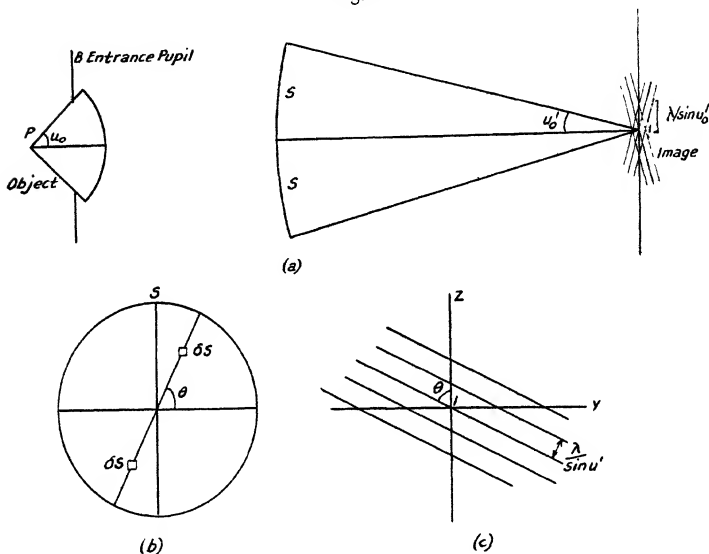
Portion of fig. 2 (neighbourhood of sodium atom) magnified and calculated for closer points.

mum. A negative value for the density has no physical significance in this case, and its existence shows that the picture is artificial.

In figs. 4 and 5 the electron density around atoms of either kind is shown plotted on a larger scale and calculated for closer points. Electron counting is much more difficult here than in fig. 1. If, for instance, we count merely the number of electrons in the central region of positive density for chlorine we obtain 11.3, whereas we

should have 18. Clearly the scattering matter represented by the outer rings must be included in the count, but it is difficult to know where to draw the boundary between the atoms, since the oscillations overlap in all directions. The precise point at which counting stops influences considerably the total number obtained, whereas in fig. 1 it matters little where the boundary is placed, since the region between the atoms has a vanishing density.

Fig. 6.



### 6. The Optical Analogy.

The origin of these circular bands of positive and negative density is clear if we treat the projection as analogous to an image formed by an optical instrument with a circular stop.

Consider the image  $I$  of a luminous point  $P$  (fig. 6). The rays from  $P$  which traverse the instrument are limited by a circular stop at some point in the system which is equivalent in its effect to the "entrance pupil"  $B$ . After traversing the system a wave coming originally from  $P$  converges to build up the image at  $I$ . The angular aperture is measured by  $2u_0$  and the angle of projection by  $2u'_0$ .

The customary treatment of diffraction divides a wave front such as S into elements, the secondary waves from which combine to form the image at I. A pair of elements of area  $\delta S$  symmetrically placed at opposite sides of the wave centre contributes an amplitude proportional to

$$\delta S \cos(2\pi t/T) \cos 2\pi(\cos \theta \sin u' \cdot y/\lambda + \sin \theta \sin u' \cdot z/\lambda),$$

where  $2u'$  is the angle the elements subtend at I. The elements and the wave system they produce are shown in fig. 6 (*b* and *c*). The resultant amplitude of vibration for a given point  $yz$  in the image plane is got by integrating this expression over the whole wave surface. The pattern has circular symmetry, the amplitude of vibration at a distance  $r$  from the centre of the image being given by

$$\begin{aligned} & \text{constant} \cdot J_1(2m)/m \\ &= \text{constant} \left( 1 - \frac{1}{2} \left( \frac{m}{1} \right)^2 + \frac{1}{3} \left( \frac{m^2}{2} \right)^2 - \frac{1}{4} \left( \frac{m^3}{3 \cdot 2} \right)^2 + \dots \right), \end{aligned}$$

where  $m/\pi = r(\sin u'_0)/\lambda$ .

The square of this expression yields the familiar diffraction pattern for a circular aperture, but we are here concerned with amplitude and not intensity.

The curve for the amplitude  $J_1(2m)/m$  is plotted in fig. 7. Its maxima, minima, and points where it crosses the axis occur as follows:—

	Magnitude.	$m/\pi$ .
Central maximum .....	1.0	0
Zero value .....	—	0.61
Minimum (first diffraction ring) .....	0.132	0.81
Zero value .....	—	1.116
Second maximum (second diffraction ring)....	0.064	1.333
Zero value .....	—	1.619

In the same figure the amplitude for a slit whose width is equal to the diameter of the stop is shown for comparison, the expression in this case being

$$(\sin 2m)/2m.$$

Each pair of equal and opposite elements in the wave converging to form the image builds up in the image plane a contribution to the amplitude like that of a set of standing waves. Elements close to the centre give standing waves of long wave-length, whilst those farther apart give waves of short wave-length because the wavelets from those elements cross at a greater angle. The

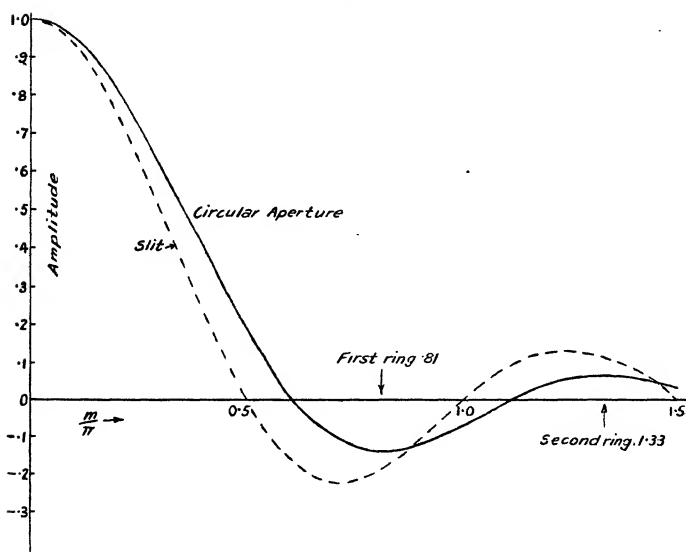
shortest wave-lengths which go to compose the image have a length  $\lambda/\sin u_0'$ , as shown in the figure. This corresponds to a distance in the object of

$$\lambda/n \sin u_0 = \lambda/a,$$

where  $a$  is the numerical aperture of the instrument,  $n$  being the refractive index of the medium in which the object is placed.

To sum up, the diffraction image at I is built up by integrating these standing waves, which cross each other

Fig. 7.



Optical diffraction rings for circular aperture and slit.

in all directions and have wave-lengths varying from infinitely great to a minimum value corresponding to a distance  $\lambda/a$  in the object. These waves are all in phase at the centre of the image where the effect is greatest.

Suppose now that the projection of a crystal structure is being found which for simplicity we take to consist of a simple network of single electrons. The image of such a structure is given by the Fourier series

$$\rho(y, z) = (1/A) \sum_{-\infty}^{\infty} \sum_{-\infty}^{\infty} F(okl) \cos 2\pi(ky/b + lz/c),$$

in which all values of  $F$  are unity. All spectra are measured for planes whose spacings are not less than a given amount  $d_0$ , thus imposing limitations on possible values of  $k$  and  $l$ . The smaller  $d_0$ , and the larger the dimensions of the unit cell, the greater will be the number of spectra. It is easy by considering the reciprocal net to show that the number of spectra approximates to

$$\pi A/d_0^2.$$

The image of each electron is formed by sets of cosine waves crossing in all directions, as in the optical case, only now their number is finite, and we are dealing with a Fourier series instead of the integral over the wave surface in the optical case. Nevertheless, when the number of spectra is very large, the form of the image will be like that due to optical diffraction. The electron density at each point in the image at a distance  $r$  from a corner of the net is given by

$$\begin{aligned}\rho(r) &= \frac{1}{A} \cdot \frac{\pi A}{d_0^2} \sum_{-\infty}^{\infty} \sum_{-\infty}^{\infty} \cos 2\pi(ky/b + lz/c) \\ &\approx \frac{\pi}{d_0^2} \cdot J_1(2m)/m,\end{aligned}$$

where  $m/\pi = r/d_0$ .

The size and shape of the unit cell of the network do not affect this last expression. When the number of spectra is very large, the image of each net point approximates to what it would be if it were the only point in the field of view; expressed otherwise, the diffraction patterns are only slightly affected by overlapping. It is as if we were looking through the microscope at a regular two-dimensional array of luminous points producing cross spectra in the region  $S$  (fig. 6). Waves from these spectra recombine in the image plane to reproduce an array of images, each of which is surrounded by diffraction rings, much as it would be if it were the only point in the field.

Now, the shortest wave which goes to build up the image of our network corresponds to the shortest distance  $d_0$  between reflecting planes. If all spectra are measured up to a glancing angle  $\theta_0$ , then

$$d_0 = \lambda/2 \sin \theta_0.$$

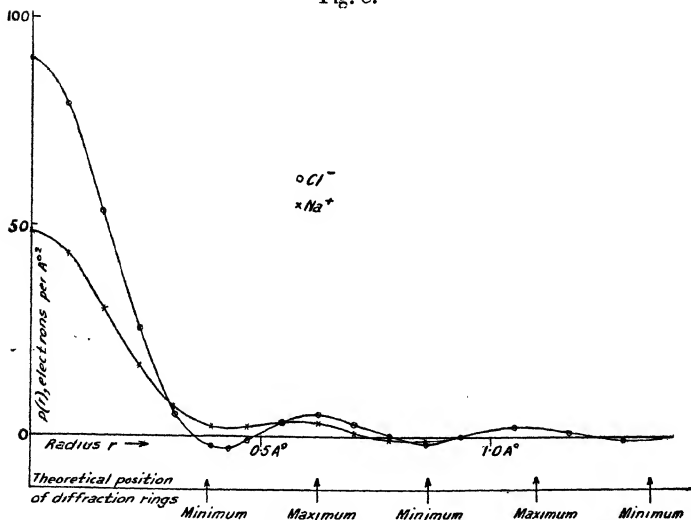
In the optical image the corresponding distance is  $\lambda/a$ . Thus, *the numerical aperture in X-ray analysis must be*

defined as  $2\sin\theta_0$ . In the microscope points cannot be resolved unless their distance apart is greater than  $0.6\lambda/a$ . Similarly in X-ray analysis detail cannot be distinguished unless it is on a coarser scale than  $0.6d_0$  or  $0.6\lambda/2\sin\theta_0$ .

### 7. Diffraction Effects in the Fourier Projections.

In the Hartree atom-models there is a strong concentration of scattering matter at the centre of the atom. This gives rise to diffraction rings on the projection like

Fig. 8.



those due to a bright point at the atom centre. The first diffraction ring has its greatest negative value at  $0.81d_0$ , the next its greatest positive value at  $1.33d_0$ , and so forth. In the present case the maximum value of  $\theta$  is  $\pi/6$ , so that the "angular aperture,"  $2\sin\theta_0$ , is unity, and  $d_0$  is equal to  $\lambda$ , i. e.,  $0.615\text{ \AA}$ .

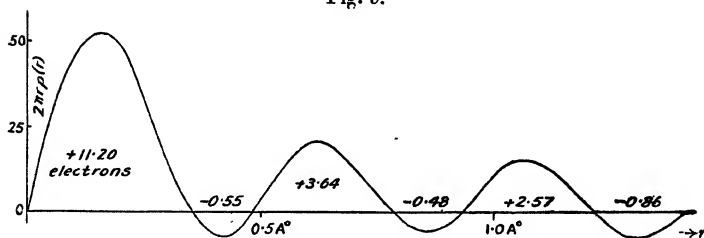
In fig. 8,  $\rho(r)$  is plotted against  $r$  for sodium and chlorine, using the data of figs. 2, 4, and 5, and disentangling as far as possible the overlapping system of rings. The corresponding positions of the maxima and minima due to the diffraction rings of a luminous point are marked in the



diagram. It is obvious that the rings of positive and negative density in the projection correspond precisely to optical diffraction rings. They have no counterpart in the atomic structure, and are merely due to the termination of the Fourier series whilst the coefficients are still large. The image of either atom consists of a faithful representation of the more diffused outer parts, together with a system of diffraction rings, due to the large concentration at the centre, superimposed upon it.

By plotting  $\rho(r) \cdot 2\pi r$  against  $r$  (fig. 9) it can be seen why the electron count for the central diffraction maximum is so small. Owing to their larger radius the outer rings contribute considerably to the total number of electrons. The contributions of the successive rings to the total number of electrons in the chlorine atoms are

Fig. 9.

Distribution of electrons in projection of  $\text{Cl}^-$  derived from fig. 4.

shown in fig. 9. The central maximum gives 11.2, a sum which is raised to 15.2 by the rings shown in the figure. The count is not yet complete, but beyond this point it is impossible to separate the diffraction effects of neighbouring atoms.

The concentration of scattering matter at the centres of the sodium and chlorine atom-models, which causes these diffraction effects, is shown in Table IV. The Hartree model atoms have been projected on a diametral plane. The figures in the Table give the radii of circles within which successive integral numbers of electrons are contained in the projection. Fig. 3 was based on this table.

### 8. Conclusions.

The use of a Fourier series which is incomplete, in that the coefficients are still large when it is terminated, leads

to an image of the crystal structure which has defects like those produced by optical diffraction. Such defects are strongly marked in fig. 2, whereas in fig. 1 they are much less apparent. The coefficients fall to a much smaller value in this latter case, because a "temperature factor"  $e^{-B \sin^2 \theta}$  has been added to allow for thermal agitation. Although this agitation will increase the overlapping of the atoms to a certain extent, the effect is more than

TABLE IV.

Cl <sup>-</sup> .		Na <sup>+</sup> .	
Radius of circle.	Number of electrons within circle.	Radius of circle.	Number of electrons within circle.
3.19 A. ....	17.96	1.06 A. ....	9.96
2.40 ....	17.8	0.575 ....	9
1.55 ....	17	0.446 ....	8
1.14 ....	16	0.367 ....	7
0.936 ....	15	0.298 ....	6
0.772 ....	14	0.239 ....	5
0.692 ....	13	0.186 ....	4
0.522 ....	12	0.128 ....	3
0.440 ....	11	0.074 ....	2
0.314 ....	10	0.027 ....	1
0.256 ....	9	0 ....	0
0.213 ....	8		
0.181 ....	7		
0.149 ....	6		
0.117 ....	5		
0.096 ....	4		
0.064 ....	3		
0.043 ....	2		
0.027 ....	1		
0 ....	0		

compensated for by the disappearance of the diffraction effects, and the line of demarcation between the atoms is actually much more evident. An electron count in fig. 1 can be made with considerable accuracy, whereas in fig. 2 it is impossible.

This suggests that it would be desirable in all cases to multiply the coefficients by an arbitrary factor  $e^{-B \sin^2 \theta}$ , choosing a value of  $B$  which makes the final coefficients very small. If, for instance, the maximum value of

$\sin \theta_0$  is 0.5, a value of 2.3 for B gives the following factors:—

$\sin \theta.$	$e^{-B \sin^2 \theta}.$
0.1	0.912
0.2	0.692
0.3	0.437
0.4	0.229
0.5	0.100

It is somewhat surprising to see to what a small value of the average amplitude of thermal agitation this value of B corresponds. The factor in terms of the average mean square of the amplitude,  $\overline{u_x^2}$ , is

$$e^{-\frac{8\pi^2 \sin^2 \theta}{\lambda^2} \cdot \overline{u_x^2}}.$$

For  $\lambda = 0.615 \text{ \AA}$ , and  $\frac{8\pi^2 \overline{u_x^2}}{\lambda^2} = 2.3$  as above, we have

$$\overline{u_x^2} = (0.21 \text{ \AA})^2.$$

Such an amplitude hardly affects the extent to which the atoms overlap. The Fourier series will give a very faithful picture of the actual crystal structure with this assumed thermal agitation. Electron counting should therefore be more reliable, and one can be sure that no false detail due to diffraction will appear.

Compton ('X-rays and Electrons,' p. 164) develops a formula for the amount of scattering matter  $U_r dr$  between radii  $r$  and  $r + dr$  in the atom

$$U_r dr = \frac{8\pi r}{D^2} \sum_1^\infty n F_n \sin\left(\frac{2\pi n r}{D}\right) dr,$$

where each F value is measured or deduced for an order of reflexion  $n$  from a simple crystal of spacing  $D$  composed of the one kind of atom. This series converges very slowly. Using experimental determinations of F, Compton obtained a curve for chlorine, for instance, with a series of "humps." By comparing the curve with the Hartree model (with which we know the experimental measurements to be in accord) it is clear that the humps are similar to the diffraction effects treated above, and do not correspond to the actual distribution in the chlorine atom. Havighurst used the same formula (Phys. Rev. *loc. cit.*)

and pointed out the importance of a temperature coefficient in making the series converge. Even in Havighurst's results for chlorine, however, humps appear which have no counterpart in the Hartree model, and, indeed, Havighurst expresses doubts of their reality. It seems clear that we can only trust details of structure indicated by the Fourier analysis when the actual or applied temperature coefficient causes the series to converge so fast that the last terms are vanishingly small. Unless this is the case, many real-looking features appearing in the representation must be distrusted.

By making the final coefficients of the Fourier series vanishingly small in this artificial way we are sacrificing a part of the information about the crystal structure which the experimental determinations have provided. A comparison of figs. 1 and 2 shows what is being lost. The higher terms define more sharply the positions of the atomic centres by making the peaks in the density higher and more concentrated. They give, in fact, more exact information about the positions of the atomic centres in more complicated crystals where these are not fixed by symmetry considerations. The electron count, on the other hand, is mainly determined by the earlier terms in the series. The higher terms "trim" the crude picture of the structure given by the earlier terms, and in order to make this trimming effective and to cut out false detail it is quite justifiable to multiply the coefficients by an arbitrary temperature factor. The introduction in an optical instrument of a screen with a graded absorption increasing towards the edge would cut out false detail due to diffraction in just the same way.

In a further paper we hope to apply these results to experimental measurements on crystal diffraction.

### *References.*

- (1) W. L. Bragg, *Proc. Roy. Soc. A*, cxxiii. p. 538 (1929).
- (2) W. H. Bragg, *Phil. Trans. Roy. Soc. A*, ccxv. p. 253 (1915).
- (3) W. Duane, *Proc. Nat. Acad. Sci.* xi. p. 489 (1925).
- (4) R. J. Havighurst, *Ibid.* xi. p. 502 (1925).
- (5) A. H. Compton, 'X-rays and Electrons,' p. 151
- (6) R. W. James, I. Waller, and D. R. Hartree, *Proc. Roy. Soc. A*, cxviii. p. 334 (1928).

Manchester University,  
July 28, 1930.

LXXVI. *The Conduction of Electricity in Liquid Dielectrics.*  
 By D. H. BLACK, *Ph.D.*, and R. H. NISBET, *B.Sc.*  
 (*International Telephone and Telegraph Laboratories,*  
*Incorporated*) \*.

[Plates VI. & VII.]

**A**LTHOUGH a considerable amount of work has been carried out in recent years on the electrical properties of solid insulating materials, there do not appear to have been many investigations of any great value published on the phenomena associated with liquid dielectrics. As is known to all who have attempted the subject, the experimental difficulties encountered when dealing with such liquids are very great, being greater in many respects than those associated with solid dielectrics. Consequently the experimental data are somewhat meagre, and it has not been possible to draw any very conclusive deductions from them, although it seems to be generally assumed that the direct current conductivity of liquid dielectrics is similar in nature to the electrical conductivity of ionized gases. It is therefore the more regrettable that some writers, while making no attempt to explain some of the more well-known experimental facts, do not seem to appreciate fully some of the consequences to which the theory of conduction in gases leads.

Such well-known facts as the decrease in current with time and variations of resistance with voltage are often attributed to the action of counter E.M.F.'s formed by the accumulation of space-charges; but no attempt is made to account for the absence of the residual discharge currents which these space-charges would seem to entail. Largely on account of the absence of such discharge currents one of us <sup>(1)</sup> put forward the hypothesis that the formation of a contact resistance at one or both of the electrodes was responsible for the observed facts; and the simple mathematical relationships derived were found to agree with the bulk of the experimental data obtained up to that time. In this paper we give the results of further experiments on direct current conduction in insulating oils, and discuss their bearing on the nature of the processes involved.

\* Communicated by the Authors.

*Experimental Methods.*

Measurements on the steady value of the resistance of oil films have been extended to higher and to lower potential gradients. The same testing vessel as mentioned in the previous paper has been used throughout, the electrode area being 240 sq. cm., and the same attention has been paid to the control of temperature. When possible the resistances were measured with a moving-coil galvanometer in conjunction with a standard megohm, and when the currents were too small for this method a null electrometer system of measurement was used <sup>(2), (3)</sup>.

An Einthoven string galvanometer has been used for taking measurements at short time intervals after the application, reversal, or removal of the potential. The deflexions were recorded on a moving bromide paper strip, and time intervals were marked on the record by means of a toothed wheel which interrupted the beam of light, the wheel being controlled by an electrically driven tuning-fork. Owing to the progressive tightening of the galvanometer fibre with increasing deflexion the readings were not proportional to the current, and it was therefore necessary to take calibration deflexions for every observation. These calibrations were carried out by applying the potential across the megohm, and recording the deflexions due to the resulting current at three or more settings of a universal shunt connected across the galvanometer. On account of the large capacity currents involved, the galvanometer was shunted by a low resistance when the applied potential was changed, and a small fraction of a second later the shunt was disconnected and the full current allowed to flow through the galvanometer. The value of the shunt resistance was so chosen that the flow of the capacity current produced a small kick in the galvanometer, thus indicating the exact moment at which the change in the potential took place. When recording the current flowing through an oil it was necessary to short-circuit the megohm, as, if it was in series with the film, its presence was found to alter the shape of the curve, the effect probably being due to inductance since the resistance was wire wound.

The liquids used in the experiments quoted in the paper were oils of the paraffin class; and for the majority of the tests two grades of liquid paraffin were used.

Liquid paraffin "A" was a highly purified medicinal paraffin, and liquid paraffin "B" an oil supplied as extra high viscosity liquid paraffin. Both these oils were supplied in sealed glass bottles and received no further treatment other than de-gassing under vacuum for several hours. In the experiments with the special apparatus for the detection of contact resistances, which is described later, a light mineral oil supplied for turbine lubrication was employed.

### *Steady Current Phenomena.*

Many writers on the subject have assumed that conduction of electricity in liquid dielectrics is very similar in nature to conduction in ionized gases, and in many instances they attribute the decrease in the current with time\* to the gradual formation of space-charges in the liquids†. In the case of solid dielectrics also the accumulation of charges in the material is generally assumed to be the cause of the decrease in current with time; and in this case it is assumed that the disappearance of such charges on removal of the applied potential gives rise to the observed residual discharge currents. In the case of liquid dielectrics, however, residual discharge currents of appreciable magnitude are seldom observed, and therefore it did not seem reasonable to attempt to explain the decreases in current by the same mechanism for both solids and liquids. It was mainly on account of the absence of such discharge currents in oils that the attempt was made to explain the observed effects in some other manner, namely, by the formation of contact resistances.

In the previous paper a simple expression was obtained connecting the final resistance,  $R_s$ , of an oil film with the final value of the current,  $I$ , flowing across it. This was

$$R = R_0 + nI, \quad . . . . . (1)$$

$n$  being a constant at any particular temperature, while  $R_0$ , which was considered to be the true resistance of the

\* On account of the apparent similarity to the phenomena observed with solid dielectrics this decrease is sometimes referred to as an "absorption current," but we do not consider the term satisfactory when referring to liquids.

† A decrease in current with time would presumably take place in gases, but the final steady conditions would be attained so rapidly that such a charge has not yet been recorded.

oil, was proportional to the film thickness. This can be written in the form

$$V = R_0 I + n I^2, \quad . \quad . \quad . \quad . \quad . \quad (2)$$

where  $V$  is the applied potential, and is then identical with that obtained for the relationship between current and voltage for conduction in gases under certain conditions, more particularly for conduction in flames <sup>(4), (5)</sup>. According to the gas theory, from which the above formula can be derived, there are sudden drops of potential at the electrodes, and the distribution of ions in the central region is the same as that existing before the application of the potential. Since the current flowing is the same throughout the space between the electrodes, these drops of potential can only occur in regions where the specific resistance is higher than in the body of the liquid. Deficits in the numbers of both kinds of ions in these regions are the cause of the increased resistance, and the space-charges arise through there being fewer positive than negative ions near the positive electrode, and fewer negative than positive near the negative electrode.

In the theory of contact resistances previously outlined the form in which these resistances existed was not stipulated\*; and such a general resistance theory may perhaps be regarded as including the gas theory with its concentration of resistances at the electrodes. It is, however, difficult to trace any connexion between the methods by which the results are obtained in the two cases.

It seems to have been assumed by some writers† on this subject that under low stresses the resistance of a film of liquid dielectric remains constant as the potential is increased, Curtis mentioning a value of 300 volts/cm. as the upper limit to the range over which Ohm's law is found to hold. However, the theories discussed above require that there should be a linear relationship between resistance and current even for small values of the current, and our experimental results definitely support

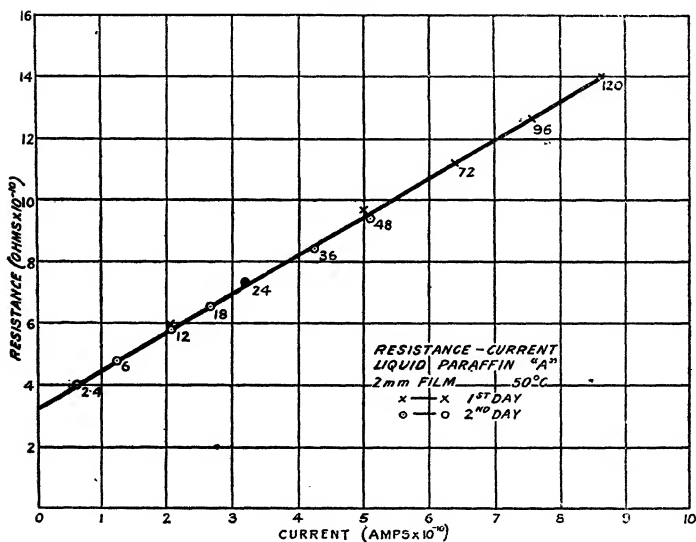
\* It was suggested that these resistances might possibly be due to the formation of gas films on the electrodes, but it has since been found that the experimental facts upon which this suggestion was based arose through the presence of occluded gases in the oils, and were not directly due to the passage of the current.

† See, for example, Curtis <sup>(6)</sup> and Nikuradse <sup>(7)</sup>.



this conclusion. We have extended the measurement of resistance to stresses lower than those mentioned in the previous paper, and one set of results is shown in fig. 1, where the linear relationship is seen to hold within very close limits\*. The actual voltage applied at each point is indicated on the graph, and the values cover a variation in stress of from 600 to 12 volts/cm. Incidentally it may be mentioned that in some instances steady conditions were not attained until five or six hours after

Fig. 1.



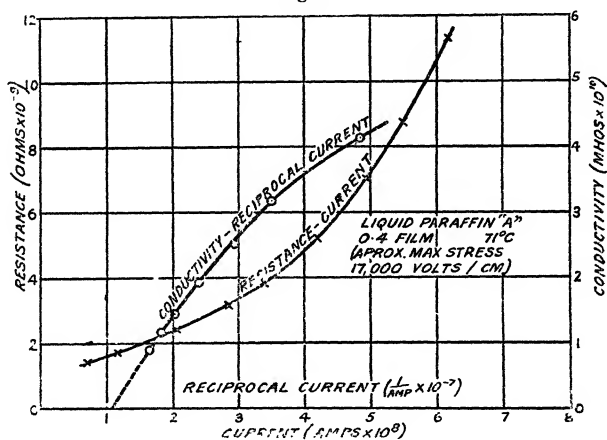
changing the applied potential, and this fact must be borne in mind if misleading results are to be avoided.

Our further experiments show that in general the resistance-current relationship is linear, thus supporting the evidence of the previous paper. This cannot, however, be expected to be always the case, for both the gas theory

\* In expressing results of this kind I is usually graphed against  $V$ , but this is not such a satisfactory method as graphing  $R$  against  $I$ , for in the former case the curve is parabolic, and this can give, and has in some instances apparently given, an impression that a saturation current is being approached, when such is far from being the case.

and a contact-layer theory conclude that a straight line relationship holds only so long as the region of higher potential gradient at the electrodes extends over a distance which is small in comparison with the distance between them. We have been able to observe such departures from the linear law by applying sufficiently high stresses to *sufficiently thin films*. Fig. 2 shows some results obtained on a film of 0.4 mm. thickness, the maximum stress being 17,000 volts/cm. The possible existence of saturation currents is best seen by graphing the conductivity against the reciprocal of the current, as has been

Fig. 2.



done in the same figure. Assuming that extrapolation is justifiable, the form of the curve shows clearly that the maximum possible value of the current in this case is approximately  $10^{-7}$  amp.

According to both the gas theory and a contact-layer theory, in all cases where the resistance-current relationship is linear the liquid between the electrodes remains unchanged except in the comparatively thin regions adjacent to the electrodes; and in the gas theory it is the changes in the concentration of the "ions" at the electrodes which alters the total resistance between them. Some writers <sup>(6), (7)</sup>, while basing their statements on the gas theory, make the assumption that the potential gradient is approximately constant throughout the

volume between the electrodes, and they apparently consider that the decrease in current on applying the potential is caused by a diminution in the number of ions everywhere within the film. It is clear that, given the withdrawal of a certain number of ions, the increase in resistance is much greater if they are all drawn from regions close to the electrodes than if they are withdrawn uniformly throughout the whole volume.

By making the assumption that the gradient is constant Nikuradse<sup>(7)</sup> obtains a formula which may be written in the form

$$I = a - b/R^2. \quad . \quad . \quad . \quad . \quad . \quad (3)$$

As can be seen by making  $R$  infinite,  $a$  is the value of the saturation current, and thus, if two values of  $R$  and  $I$  are known, the saturation current can be calculated. If the values of  $I$  in fig. 1 when  $R$  is equal to  $4 \times 10^{10}$  and  $8 \times 10^{10}$  ohms are inserted in the formula, the value of the saturation current obtained is  $5 \times 10^{-10}$  amp. As seen from the figure a value of  $I = 8.5 \times 10^{-10}$  amp. was measured in this instance, and the fact that the linear relationship still holds at this point shows that we were not even approaching a saturation value. Therefore we may state that our experimental results give no support to such an assumption\*.

#### *Absence of Residual Discharge Currents.*

In the previous paper it was pointed out that charges would be expected to accumulate at the boundaries of any resistance layers, although, on account of the apparent absence of any residual discharge currents, it was considered that any effects due to such charges must be small in comparison with the actual changes in resistance. Since all resisting layer theories, including the gas theory, require the existence of space-charges, it was important to see whether this apparent absence of discharge currents was due to the space-charges disappearing in so short a period of time that they had previously escaped detection.

Measurements were therefore taken with the string galvanometer in which a potential was applied across a

\* The values of mobility etc. mentioned in the article concerned are not invalidated by the assumption, since the necessary value of the saturation current is obtained by extrapolation from the experimental results, and not by means of the equation.

film until steady conditions had been reached, when the potential was then removed and the film short-circuited through the galvanometer. The usual practice of allowing the capacity discharge current to make a deflexion to indicate the moment of switching was not followed, as such a deflexion might have confused any other discharge effects. Accordingly the galvanometer was completely short-circuited during the capacity-discharge interval, but it was known from other experiments that this period was not greater than 0.05 sec. Curve 1, fig. 3 (Pl. VI.), shows the results of such an experiment. The initial value of the current in this case was  $19 \times 10^{-8}$  amp., and the steady value, which gave the deflexion shown on the left, was  $5.1 \times 10^{-9}$  amp. It is seen that any discharge effects existing after 0.05 sec. are extremely small, even in comparison with the final conduction current, which is itself less than one-thirtieth of the initial current. Therefore we conclude that any residual discharge effects which may exist disappear in a time of the same order as that of the capacity discharge, and that the law of superposition does not hold for liquid dielectrics.

*Residual Effects observed after Removal of Potential.*

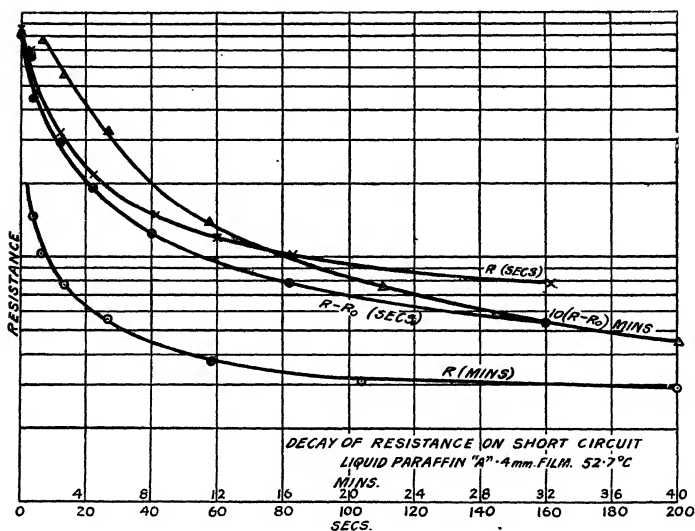
It is generally considered that, if after removing the applied potential a film of oil is short-circuited, it will regain its original conductivity \*. In the previous paper these facts were accounted for by supposing that the contact resistances at the electrodes gradually disappeared, and a point in the theory was the assumption that the rate at which a contact resistance at an electrode disappears is proportional to that resistance. Thus, if resistances are formed at both electrodes, the curve connecting the total increase of resistance above the initial value with the time of short-circuit would be expected to be the sum of two exponentials.

Attempts were made to measure the rate at which the resistance disappeared on short-circuiting the film for definite intervals of time after steady conditions had been attained, and then reapplying the potential in the usual way. Intervals of short-circuit up to about 10 secs. were measured on the string galvanometer record and

\* But see Bruninghaus®).

longer intervals by means of a stop-watch. A typical result is shown in fig. 4, where both the total resistance,  $R$ , and the increase in resistance above the initial value,  $R - R_0 = r$ , are graphed against the time of short-circuit; but we have not been able to find a simple formula to express the relationship between them. In our experiments the period of short-circuit necessary for  $r$  to fall to  $1/\epsilon$  of its value,  $r$ , at the beginning of the period was found to vary from 10 secs. to 7 mins., its value depending on the nature and condition of the oil.

Fig. 4.

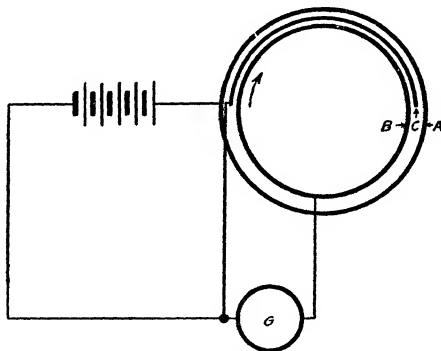


That the recovery of the initial conditions in a short-circuited film is not as simple as might at first be imagined is shown by the shape of the current-time records obtained on reapplying the potential. In fig. 3 (Pl. VI.), curve 2, is shown a record obtained on reapplying the potential across a film of liquid paraffin "B" after a short-circuit of 20.4 secs. These irregularities are not noticeable after very short intervals of short-circuit, but appear as the period is lengthened, and on further increasing the time the irregularities flatten out once more into a uniform curve.

gradually approaching the form of the curve observed when a potential is first applied (see curve 3, fig. 3 (Pl. VI.)). We have so far been unable to obtain a satisfactory explanation of these irregularities, but their existence is so marked that they must be considered when attempting to form any complete theory of the subject.

In an attempt to prove the existence or otherwise of contact resistances a special piece of apparatus was constructed. It consisted of two accurately concentric cylinders, A and B, the inner one, B, being capable of rotation through  $180^\circ$  and being shielded over one-half of its surface by a guard C as shown in fig. 5. This guard was placed close to B, but was insulated

Fig. 5.



Apparatus for detecting contact resistances and space-charges.

from it. Owing to constructional difficulties the distance between the cylinders could not be made particularly small, the actual value being approximately an eighth of an inch. The cylinders were placed in a jar of oil and connected to a battery and a galvanometer as shown. It was hoped that if, after a steady current value had been reached, B was rotated through  $180^\circ$ , any contact layer which had been formed upon its exposed half would be carried around behind the guard and a clean surface exposed, thus causing a decrease in resistance. On rotating B increases in current were observed, but such increases were masked in their initial stages by a discharge through the galvanometer in the opposite direction to the conduction current. Some typical results are given in

the following Table, where the change in resistance on rotation, with B negative and positive in turn, is expressed as a fraction of the total increase in resistance obtained from the final and initial current values.

Detection of Contact Resistances. Light Mineral Oil.

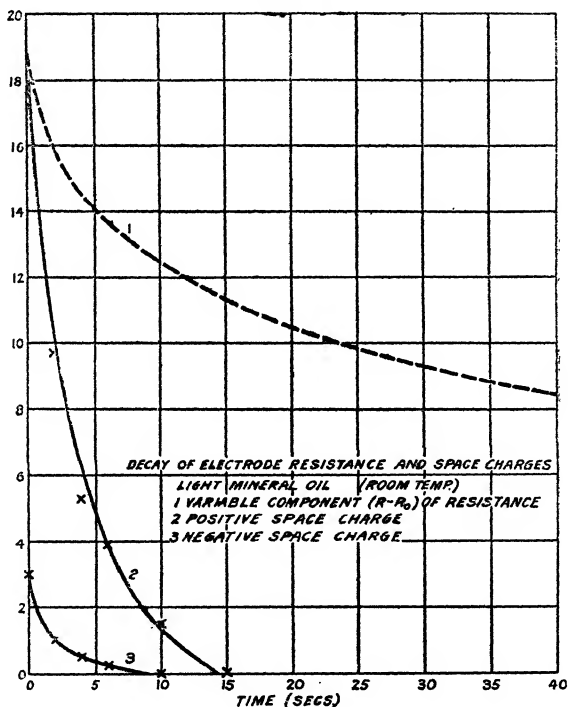
Temp.	Voltage.	$\frac{r}{R_0}$	$\frac{r+}{r}$	$\frac{r-}{r}$
25° C. ....	350	0.81	0.29	0.14
34 ....	350	0.44	0.34	0.22
34 ....	240	0.70	0.43	—
38.7 ....	240	0.34	0.28	0.09
48.9 ....	240	0.24	0.32	0.22

It will be observed that the sum of the last two columns is always less than unity, which means that the sum of the resistances swept out was not great enough to account for the total resistance built up by the current.

The fact that a discharge took place through the galvanometer on rotating the inner cylinder of the above apparatus, shows that charges do accumulate in a liquid dielectric when a potential is applied across it. The presence of such charges seems to be required by the theories put forward, but, as we have seen, no discharge currents are observed under normal circumstances. Although no residual discharge currents are observed, we have shown that an oil film regains its conductivity at a measurable rate when it is short-circuited, and it is therefore, important to know whether the charge which we have shown to accumulate also decreases at a measurable rate, or whether it disappears with great rapidity. By rotating the inner cylinder after definite periods of short-circuit it was discovered that accumulated charges were still present after measurable intervals of time. In fig. 6 the magnitudes of the charges measured by means of a ballistic galvanometer are shown as a function of the time of short-circuit when the inner electrode was positive and negative respectively. The rate of decrease of  $r$  is shown on the same diagram for purposes of comparison, and it will be noticed that the decrease in  $r$  takes place at a slower

rate than the decrease in the charges. These experiments are of the greatest importance, as they show that resistance changes can exist in an oil film after the disappearance of the space-charges, and consequently any treatment which considers that the phenomena encountered in liquid dielectrics can be explained by changes in space-charges alone may lead to quite erroneous results.

Fig. 6.



We are also faced with the problem of accounting for the fact that space-charges can disappear within the body of a liquid between two electrodes when they are short-circuited without causing any effect in the external circuit. If we assume, in contrast to the assumption of material-resisting layers on the electrodes, that conduction in dielectrics is similar to that in gases, then the mobility of the "ions" is the same everywhere within the liquid.



as is also the dielectric constant. It is, then, not unreasonable to expect that on short-circuit the portion of an accumulated space-charge which will be attracted to an electrode would be just sufficient to neutralize the induced charge on it, and, such being the case, no residual discharge currents would flow in the external circuit. If there are two space charges of opposite sign they will partially neutralize each other on short-circuit, but the above argument is practically unaffected. If such a hypothesis is correct the objections previously raised to the gas theory are removed, and, in fact, it appears that, where no residual discharge currents occur, the increases in resistance due to the mechanism supposed for conduction in gases are more likely to be the kind involved than those due to layers of resisting material on the electrodes.

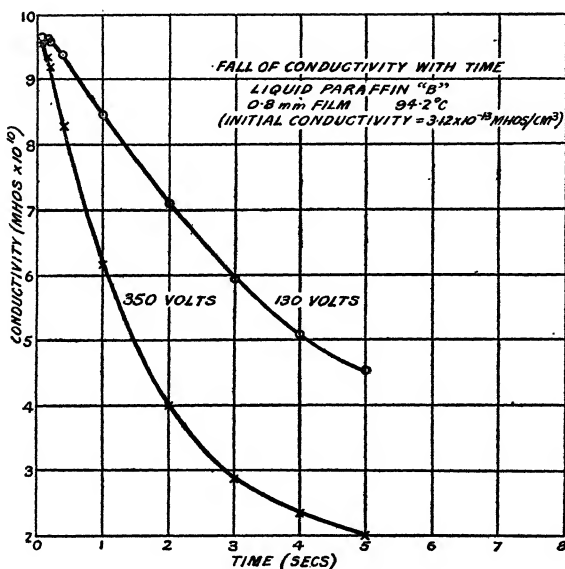
We have already pointed out that, according to the gas theory, regions of increased resistance occur near the electrodes owing to deficits in the total number of "ions" present, while space-charges occur through unequal deficits in the number of each sign. Upon short-circuit the space-charges will tend to disappear under the electrical forces involved, but the deficit in the total number can only be made up by the production of fresh "ions," and hence the decay of the additional resistance may take place at a much slower rate than the disappearance of the space-charges, as we have shown experimentally to be the case.

#### *Initial Current Values.*

We have taken numerous records with the string galvanometer of the decay of current with time from the moment of application of the potential across an oil film. A typical result is shown in fig. 3 (Pl. VI.), curve 3. In every case the shape of the curve indicates that the current is not the continuation of a capacity charging current such as would be obtained from a system of fixed capacities and resistances, but rather that it is due to the conductivity of the oil film decreasing with time from a definite initial value. Further, for a short space of time the curves are concave downwards, suggesting that at the moment of application of the potential the curves, apart from the true capacity current, would be practically horizontal. Fig. 7 shows the values of the conductivity calculated from two records with applied potentials of 350 and 130 volts, and from this

it is seen that the conductivity tends to the same initial value for both voltages. These results support the contention which has been put forward in the past\*, that a film of liquid dielectric has a definite initial conductivity which is independent of the applied potential†. This initial value obviously corresponds to the true resistance,  $R_0$ , of the oil, as mentioned previously. The agreement between the initial values of the conductivity obtained from the string galvanometer records and the values of

Fig. 7.



$R_0$  obtained by extrapolation of the resistance-current curves for steady conditions is usually as good as can be expected, *e.g.*, from a record taken a few days after those giving the results in fig. 7, a value of  $R_0 = 0.93 \times 10^9$  ohms was obtained, while the value obtained by extrapolation of the resistance current curve was  $1.00 \times 10^9$

\* *E.g.*, Tank<sup>(9)</sup>.

† These results, together with those pointing to the absence of discharge currents, are quite different from those obtained by Whitehead<sup>(10)</sup> when dealing with solid and impregnated paper dielectrics.

ohms. In some cases, however, the agreement has not been satisfactory, and we hope to make further investigations on this point.

If, as our records indicate, the rate of decrease in conduction current is practically zero at the moment of application of the potential, the conductivity would not be expected to vary appreciably during a cycle of alternating current of a frequency of 50 or more. No variation of dielectric loss with frequency would therefore be expected, provided that the causes of such loss were the same as in direct current conduction. In general such losses are far from constant with changes in frequency, and therefore additional causes must be looked for. As shown by some workers<sup>(10)</sup> the presence of permanent dipoles in the liquid is a possible cause, but one would not expect its effects to be noticeable at comparatively low frequencies in non-viscous oils. The subject is of great theoretical importance, and we contemplate carrying out a series of measurements on the alternating current losses in oils over a range of frequencies from 500 cycles to 1,000 kilocycles.

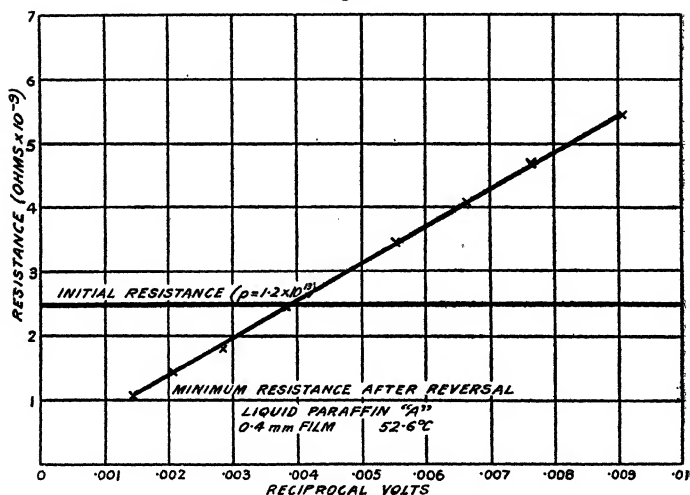
### *Reversal of Applied Potential.*

It was previously thought that the value of the current immediately after the reversal of the applied potential was the same as that preceding the reversal. Results obtained with the string galvanometer show, however, that the current flowing after the reversal of the potential is always greater than that immediately before it, an example being shown in curve 1, fig. 8 (Pl. VII.). To check the obvious interpretations of these effects, as being due to a polarization potential having been set up or to some kind of rectifying action, a double reversal was made, the duration of the first reversal being less than one second. Curve 2, fig. 8 (Pl. VII.), shows a record of such an experiment, the duration of the first reversal being 0.33 sec., and it can be seen that the deflexion after the second reversal is greater than that due to the previous steady value of the current. Owing to switching complications it was found simpler to obtain the values of the current for the first reversal from a separate record. The values obtained from one experiment gave the following results :—

Steady current before reversal . . . .	$3.50 \times 10^{-8}$ amp.
Extrapolated value of current at instant of second reversal . . . . .	$5.5 \times 10^{-8}$ amp.
Duration of first reversal . . . . .	0.8 sec.
Current after 0.8 sec. on a single reversal . . . . .	$5.6 \times 10^{-8}$ amp.

If the sudden increase in current on reversal had been due to either of the causes mentioned above then the value of the current immediately after a second reversal would have been less than that observed for the first reversal. That such was not the case shows that some

Fig. 9.

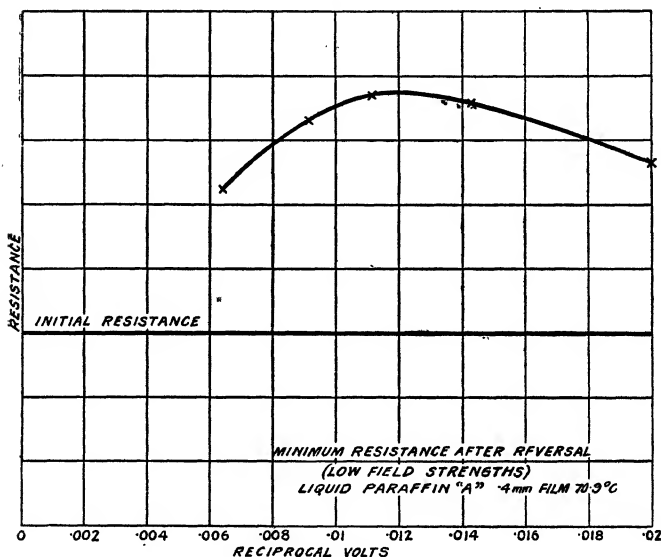


other explanation of the phenomena is required, and further investigation is called for.

In the previous paper were shown results obtained by the reversal of the applied potential, and it was seen that the current rose gradually to a maximum and then fell to a final steady value, two maxima being noted in some instances. The times to rise to the maximum values were usually of the order of minutes, but by suitably increasing the temperature and the applied stresses it was possible to record the changes by means of the string galvanometer without having to use too long a strip of bromide paper,

curve 3, fig. 8 (Pl. VII.), showing a typical result. From such curves it was noticed that the maximum value of the current was sometimes greater than the current on the initial application of the voltage, and from fig. 9, where the minimum values of the effective resistance are graphed against the reciprocals of the applied voltage, it can be seen that this maximum current may be more than twice the initial value. This shows that the increase in current is not simply due to a polarization potential assisting the

Fig. 10.



applied potential on reversal, for in that case the maximum current could not be greater than twice the initial current.

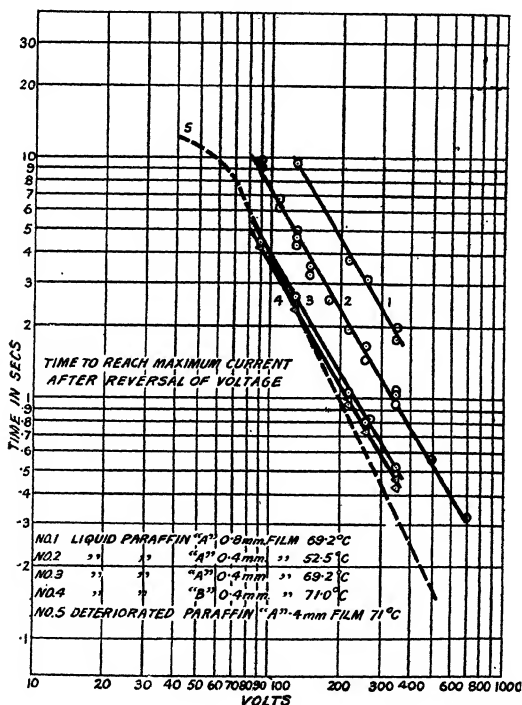
It is seen from fig. 9 that the relationship connecting the minimum values of the resistance,  $R_m$ , obtained from the reversal curves and the applied voltage,  $V$ , can be very well expressed by the formula

$$R_m = A + \frac{B}{V}, \quad \dots \dots \dots (4)$$

where  $A$  and  $B$  are constants. This linear relationship cannot, however, be expected to hold for low values

of  $V$ , for the proportionate changes in the current are small for such values, and therefore the value of  $R_m$  cannot continue to increase as  $\frac{1}{V}$  is increased, but must gradually approach the initial value of the resistance,  $R_0$ . On account of the smallness of the currents and the length

Fig. 11.



of time involved it is difficult to obtain satisfactory records for the lower potentials. We have, however, obtained evidence that the linear relationship breaks down for low voltages, as is shown in fig. 10.

The earliest experiments showed that the time,  $t$ , taken for the current to reach its maximum value on reversal varied with the voltage,  $V$ . A formula has been found

expressing the relationship between them over the range of voltages from 130 to 700. This is

$$t = aV^{-n}, \quad . \quad . \quad . \quad . \quad . \quad . \quad (5)$$

where  $a$  is a constant depending on the condition of the oil, and  $n$  is a constant which was found to have the value  $\frac{5}{3}$  for two different oils and for several ranges of temperature and film thickness, as seen in fig. 11. That the value of  $n$  is not always equal to  $\frac{5}{3}$  was indicated by the results obtained when one of the two oils mentioned had become deteriorated. These are shown by the broken curve in fig. 11, where it can be seen that, over the voltage range mentioned, the curve is linear but that the value of  $n$  is greater than  $\frac{5}{3}$ .

The relationships expressed in formulæ (4) and (5) are of great interest, because they represent experimental laws which must be capable of explanation by any theory of the processes occurring in liquid dielectrics. It is easy to show that the more obvious methods of attempting to account for the phenomena are incapable of doing so. Up to the present we have been unable to find any satisfactory explanation.

### *Factors affecting Conductivity.*

Examination of the mathematical treatment of the theory of conduction of electricity in gases leads to the following conclusions:—the relative absorption\* increases as the rate of ionization decreases, it increases with the voltage, and it decreases as the mobility increases up to a certain critical value. Our experimental results lead to similar conclusions for conduction in oils, for it has been observed that (1) the relative absorption is greater the purer the oil (as judged by the initial conductivity), (2) the relative absorption becomes greater as the voltage is increased, and (3) absorption effects become less marked as the temperature is increased—that is, as the mobility increases—although no evidence has been obtained of any critical value. The agreement between these theoretical and experimental results affords considerable further support to the hypothesis that the process of conduction in liquids is of the same type as that in gases.

\* Relative absorption is taken to be the ratio of the initial current to the final steady current.

So far we have not discussed the probable nature of the carriers by means of which an electrical current is conveyed through liquid dielectrics. It is well known that progressive purification of an insulating liquid effects large decreases in its conductivity, leading to the conclusion that the presence of impurities is in general the predominating factor in the conductivity of such liquids. The theory of conduction in gases assumes that ions are produced by the ionization of the molecules of the gas itself by some external source, and it is known that such ionizing agents as  $\gamma$ - and X-rays will increase the conductivity of liquid dielectrics. It does not seem reasonable, however, to assume that the normal conductivity of such liquids is due to an external source, such as some penetrating radiation, for in this case the majority of the ions would be produced from the molecules of the liquid itself, and the comparatively minute quantities of impurities present would not exert their predominating effect. Consequently any experiments carried out with external sources of ionization can only give information on the properties of the ions produced from the molecules of the liquid itself, and can have no bearing on the carriers normally involved. So far we have not obtained any direct evidence as to the nature of these carriers, but it seems clear that they must be produced mainly by internal causes.

### *Summary.*

The possibility of applying the theory of conduction in gases to conduction in liquid dielectrics is investigated. The gas theory is considered as leading to a distribution of internal resistances, and is shown to be a special case of a general theory advanced in a previous paper which attributed the fall of current usually known as "absorption" to the formation of internal resistances.

Experimental proof is obtained that in liquid dielectrics of the paraffin oil class space-charges are formed during the passage of the current and disappear slowly when the current is cut off. Nevertheless, discharge currents are found to be absent—an apparent contradiction which is resolved. Further residual effects are found which are quite independent of the space-charges, and are due only to the resistances set up by the current.



It is shown that the gas theory is able to account for all these facts, and is in some respects more capable of doing so than other theories. The law  $R=R_0+nI$ , arrived at by gas theory for final steady currents, is checked for a wide range of field strengths. Further agreements with gas theory are noted.

It is pointed out that some customary "approximate" treatments of gas theory lead to widely erroneous results, and cannot be used as tests of the gas theory. The cause of the failure of the "approximation" is elucidated.

Measurements have also been made at short time intervals after the initial application and after the reversal of the voltage. New phenomena have been discovered which do not appear susceptible of a simple explanation, although simple empirical laws have been found governing them.

*Note.*—Since this paper was written an article has appeared by Whitehead and Marvin<sup>(12)</sup> which deals with many of the points set out above. Many of their results are in good agreement with ours, but in some cases they differ somewhat sharply; and they do not attempt to give any explanation of some of the processes involved.

In conclusion, we wish to thank the International Telephone and Telegraph Laboratories Incorporated, for permission to publish the results set out in this paper.

### *References.*

- (1) Black, *Phil. Mag.* vi. p. 369 (1928).
- (2) Hartshorn, *Journ. Sci. Inst.* iii. p. 303 (1926).
- (3) Race, *Trans. Am. Inst. Elect. Engin.* xlvii. p. 1044 (1928).
- (4) Thomson, 'Conduction of Electricity Through Gases' (3rd ed.), p. 183 *et seq.*
- (5) Wilson, 'Modern Physics,' p. 250 *et seq.*
- (6) Curtis, *Journ. Am. Inst. Elect. Engin.* xlvi. p. 1095 (1927).
- (7) Nikuradse, *Archiv. f. Elek.* xxii. p. 305 (1929).
- (8) Brünninghaus, *Journ. de Physique*, vii. 1, p. 11 (1930).
- (9) Tank, *Ann. der Physik*, xlviii. p. 307 (1925).
- (10) Whitehead, *Journ. Frank. Inst.* ccviii. p. 453 (1929); and Whitehead and Marvin, *Journ. Am. Inst. Elect. Engin.* xlviii. p. 186 (1929).
- (11) Kitchin and Müller, *Phys. Rev.* xxxii. p. 979 (1928).
- (12) Whitehead and Marvin, *Journ. Am. Inst. Elect. Engin.* xlix. p. 182 (1930).

LXXVII. *An Acoustical Interpretation of the Schrödinger Wave Equation.* By R. B. LINDSAY, Associate Professor of Theoretical Physics, Brown University, Providence, Rhode Island, U.S.A.\*

ABSTRACT.

INVESTIGATION is made of the one-dimensional compressional vibrations of an ideal fluid of variable density (in equilibrium under the action of an external force) confined in an infinite tube of bounded but variable cross-section. The non-homogeneity, is so chosen that the wave velocity is everywhere the same. It is assumed that the ordinary acoustic equations are applicable except as modified by the non-homogeneity and that the cross-section is small enough so that transverse motions may be neglected. It is then found that the problem of determining the stationary wave-pattern in such a tube satisfying the boundary condition that the condensation  $s = \delta\rho/\rho_0$  (where  $\rho_0$  is the equilibrium density at any point and  $\delta\rho$  the excess density) shall remain analytic, everywhere  $\ll 1$  and vanish at infinity, is formally equivalent to the problem of solving a one-dimensional Schrödinger wave equation subject to the usual boundary condition. The appropriate density variation and the shape of the tube are related to the potential energy of the particle whose motion is described by the Schrödinger equation. As illustrations the free particle, the simple harmonic oscillator, and the one-dimensional hydrogen atom are investigated. The motion of the first corresponds to the oscillations of a homogeneous fluid in an infinite tube of uniform cross-section. For the simple harmonic oscillator the corresponding tube is a surface of revolution obtained by revolving the curve representing the error function about the  $x$  axis. A method of generalizing the results to the case of three degrees of freedom is indicated.

---

RECENT atomic physics is marked by the tendency to place less emphasis on a mechanical picture of atomic phenomena, and the use of models in describing atomic structure seems to be passing out of fashion, yielding place to more or less complicated mathematical algorithms based

\* Communicated by the Author. This work was done while the writer was a member of the Department of Physics at Yale University.

on postulates which do not lend themselves easily to visualization in the mechanical sense. The logical validity of the methods employed in quantum mechanics is undoubted, and the success they have met with affords considerable justification. Nevertheless, many physicists continue to think in terms of pictures, generally mechanical, for this is the kind they have learned to understand best. The writer will not undertake to defend this attitude, for it is doubtless philosophically indefensible. Nevertheless, it is of interest to observe that a mechanical interpretation of Schrödinger's wave equation is perfectly possible, and, indeed, in many ways, though doubtless most of these will be unduly complicated to be of any utility. One such interpretation is due to Madelung\*, who showed that the "time" wave equation can be put into the form of the hydrodynamical equation for the irrotational flow of a fluid. So far as the writer is aware this suggestion has never been followed up further. The recent work of A. Press (Phil. Mag. iv. p. 1248 (1927), and vi. p. 33 (1928)) should also be mentioned in this connexion. The present paper suggests a somewhat similar and rather simple interpretation based on the equations of acoustics.

We shall approach the matter by investigating approximately the vibratory motion of a compressible non-homogeneous fluid confined in an infinitely long rigid tube of bounded but varying cross-section. The non-homogeneity is assumed (for reasons which will appear presently) to be of such a character that

$$c = \sqrt{E(x)/\rho_0(x)}$$

is a constant. The quantity  $c$  is, of course, the velocity of the compressional waves in the tube, and the volume elasticity  $E(x)$  and the equilibrium density  $\rho_0(x)$  are now supposed functions of distance along the tube. We shall confine our attention at first to one-dimensional flow, choosing the diameter of the tube small enough so that transverse motions may be neglected (as in the horn theory of A. G. Webster†). We shall also assume that the ordinary equations of acoustics are applicable except as modified by the lack of homogeneity.

The equation of continuity for one-dimensional motion is

$$S\dot{\rho} = -\frac{\partial}{\partial x}(\rho S\xi), \quad . . . . . (1)$$

\* E. Madelung, *Zs. f. Phys.* xl. p. 322 (1926).

† A. G. Webster, *Proc. Nat. Acad. Sci.* v. p. 275 (1919).

where  $\rho$  is the density,  $S$  the cross-sectional area, and  $\xi$  the particle velocity. Introducing the condensation  $s$ , i. e., placing  $\rho = \rho_0(1 + s)$ , where  $\rho_0(x)$  is the equilibrium density at any point, and assuming that everywhere  $s \ll 1$  at all times, we may write in place of (1)

$$\rho_0 S \ddot{s} = - \frac{\partial}{\partial x} (\rho_0 S \xi), \quad . . . . . (2)$$

wherein  $\frac{\partial}{\partial x} (\rho_0 s S \xi)$  has been neglected.

We must next write the equation of motion. In order to assure equilibrium for the undisturbed fluid in the tube it is essential that an external force act on the fluid in the  $x$  direction (consider as an illustration a fluid in equilibrium under gravity in which density and pressure increase downward). We may represent this force per unit volume as the gradient of the equilibrium pressure, viz.,  $\frac{\partial p_0}{\partial x}$ . The equation of motion for small disturbances is then

$$\rho \ddot{\xi} = - \frac{\partial (p - p_0)}{\partial x}, \quad . . . . . (3)$$

where  $p$  is the absolute pressure. The difference  $p - p_0$  is then the acoustic excess pressure  $\delta p$ , which we shall more conveniently denote by  $p_e$ . With the same convention as above regarding  $s$ , (3) may then be written

$$\rho_0 S \ddot{\xi} = - S \frac{\partial p_e}{\partial x}. \quad . . . . . (4)$$

If we differentiate (2) with respect to the time and substitute from (4), the result is

$$\rho_0 S \ddot{s} = S \frac{\partial^2 p_e}{\partial x^2} + \frac{\partial S}{\partial x} \cdot \frac{\partial p_e}{\partial x}. \quad . . . . . (5)$$

As usual, we assume a relation between excess pressure  $p_e = \delta p$  and the corresponding density alteration  $\delta \rho$  in the form

$$\delta p = c^2 \delta \rho, \quad . . . . . (6)$$

where, in accordance with our previous assumption,  $c$  is to remain constant. Since by definition  $s = \delta \rho / \rho_0$ , it follows that

$$s = p_e / \rho_0 c^2, \quad . . . . . (7)$$

and hence equation (5) becomes

$$\frac{\partial^2 p_e}{\partial x^2} + \frac{1}{S} \cdot \frac{\partial S}{\partial x} \cdot \frac{\partial p_e}{\partial x} = \ddot{p}_e / c^2, \quad . . . . . (8)$$

or, if  $p_e$  is a harmonic function of the time with frequency  $\nu = \omega/2\pi$ , the excess pressure equation takes the form (reverting to ordinary derivatives)

$$\frac{d^2 p_e}{dx^2} + \frac{1}{S} \cdot \frac{dS}{dx} \cdot \frac{dp_e}{dx} + \frac{\omega^2}{c^2} p_e = 0. \quad (9)$$

For any particular form of tube and any given type of variation in  $\rho_0$  we are restricted to solutions of (9), for which  $s$  is very small compared with unity no matter how long the tube may be.

Let us now consider the Schrödinger wave equation for one degree of freedom, viz.,

$$\frac{\partial^2 \psi}{\partial x^2} + (\alpha - \mu V) \psi = 0, \quad (10)$$

where  $\alpha = 8\pi^2 m_0 / h^2 \cdot E$  and  $\mu = 8\pi^2 m_0 / h^2$ ,  $E$  being the total energy of the particle whose motion is being considered, and  $V$  the potential energy. To establish an acoustical analogy whereby equation (10) may be looked upon as an acoustic wave equation, let us consider  $\psi$  as made up of two parts, i. e.,

$$\psi = \sqrt{S} \cdot p_e, \quad (11)$$

where  $S$  is the area of cross-section of a tube such as has been earlier described and  $p_e$  is the excess pressure due to acoustic propagation through this fluid. On substitution into (10) and reversion to ordinary derivatives, we have

$$\frac{d^2 p_e}{dx^2} + \frac{1}{S} \cdot \frac{dS}{dx} \cdot \frac{dp_e}{dx} + \frac{1}{\sqrt{S}} \frac{d^2 \sqrt{S}}{dx^2} \cdot p_e + (\alpha - \mu V) p_e = 0. \quad (12)$$

We shall now suppose that  $\sqrt{S}$  is given as the first eigenfunction of the equation

$$\frac{d^2 \sqrt{S}}{dx^2} + [f(\mu) - \mu V] \sqrt{S} = 0, \quad (13)$$

where  $f(\mu)$  is the first eigenwert\*. This step is dictated by the fact that the acoustical analogy demands that  $S$  shall be finite, continuous, and single-valued everywhere, and vanish at infinity. Furthermore, the first eigenwert is chosen in order to secure a tube which has no knots between  $x=0$  and

\* We are applying the analysis to problems in which *discrete* eigenwerte exist, though it will probably prove unnecessary to make this restriction general.

$x = \infty$ . With this assumption, the original equation now becomes

$$\frac{d^2 p_e}{dx^2} + \frac{1}{S} \cdot \frac{dS}{dx} \cdot \frac{dp_e}{dx} + [\alpha - f(\mu)] p_e = 0, \quad (14)$$

which is identical with equation (9) if  $\alpha - f(\mu) = \omega^2/c^2$ . The problem of solving the one-dimensional Schrödinger equation is thus shown to be equivalent to the study of the small acoustic harmonic oscillations in a non-homogeneous fluid confined in an infinitely long tube with variable cross-sectional area given by equation (13). In particular we are restricted to those oscillations for which  $s \ll 1$ , and for which both  $s$  and  $\xi$  vanish at  $\infty$ . The choice of variation in density  $\rho_0$  is naturally somewhat arbitrary, but in the cases so far studied (see below) it has been found most simple analytically to choose  $\rho_0$  so that  $\rho_0 \sqrt{S} = \text{constant}$ . In this case we are at once restricted to solutions of (14) which correspond to the eigenwerte of the corresponding Schrödinger equation, for it makes  $\psi$  proportional to the condensation  $s$ . This is an appropriate place to point out that, while the introduction of two varying factors (*i.e.*, both  $S$  and  $\rho_0$ ) may seem to involve an unduly artificial construction, simple calculations indicate that no simple interpretation of the Schrödinger equation is possible from the acoustic point of view if (1)  $\rho_0$  is kept constant and  $S$  varies, or (2) if  $S$  is kept constant and  $\rho_0$  varies. The point of view chosen in the present paper is thus not quite so arbitrary as might at first be thought.

Proceeding to special problems, consider first the trivial case of a free particle. Here  $V = 0$ , and the equation (13) becomes, since the first eigenwert may here be considered zero (they are not discrete),

$$\frac{d^2 \sqrt{S}}{dx^2} = 0, \quad (14a)$$

leading at once to  $S = \text{constant}$ . Thus, free motion corresponds to the oscillations of a homogeneous fluid in an infinite tube of *uniform* cross-section.

Next, consider the more important problem of the simple harmonic oscillator. Here  $V = Kx^2$ , and the equation (13) becomes

$$\frac{d^2 \sqrt{S}}{dx^2} + [f(\mu) - \mu K x^2] \sqrt{S} = 0, \quad (15)$$

of which the first eigenwert\* is  $f(\mu) = \sqrt{\mu K}$ , and the

\* A. Sommerfeld, *Wellenmechanischer Ergänzungsband*, pp. 18, 19.

corresponding eigenfunction is  $\sqrt{S} = Ce^{-\sqrt{\mu K}x^2/2}$ , so that for the shape of the tube we have

$$S = C^2 e^{-\sqrt{\mu K}x^2}. \quad (16)$$

The equation (14) becomes

$$\frac{d^2 p_e}{dx^2} - 2\sqrt{\mu K}x \cdot \frac{dp_e}{dx} + [\alpha - \sqrt{\mu K}]p_e = 0. \quad (17)$$

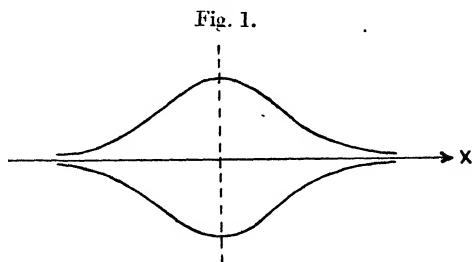
Assuming now  $\rho_0 \sqrt{S} = \text{const.}$ , we have

$$\rho_0 = \rho_{01} e^{\sqrt{\mu K}x^2/2}. \quad (18)$$

From equation (7) it is evident that we must restrict ourselves to polynomial solutions of (17). That is, we have

$$(p_e)_n = A_n H_n(\sqrt[4]{\mu K}x), \quad (19)$$

where  $H_n$  is the Hermite polynomial of order  $n$  and  $A_n$



a normalized constant. For the condensation we have consequently

$$s_n = \frac{A}{\rho_{01}c^2} H_n(\sqrt[4]{\mu K}x) e^{-\sqrt{\mu K}x^2/2}, \quad (20)$$

which, of course, has the same form as the Schrödinger  $\psi_n$  aside from a constant multiplier. From (16) the tube is seen to be a surface of revolution obtained by revolving the curve representing the error function about the axis of  $x$  (fig. 1). The solution given by (19) and (20) represents a standing wave-pattern in the infinite tube resulting from the imposed boundary conditions. There will be points of zero condensation (or loops) at the zeros of  $H_n(\sqrt[4]{\mu K}x)$  and nodes (maximum condensation) at the maxima of the polynomials. The eigenwerte (see Sommerfeld, *loc. cit.*) for this problem are given by

$$\alpha / \sqrt{\mu K} = 2n + 1, \quad (21)$$

where  $n$  is an integer, and the corresponding characteristic wave-lengths of the vibrations in the tube are given by

$$\omega^2/c^2 = 4\pi^2/\lambda^2 = \alpha - \sqrt{\mu K}. \quad (22)$$

For  $n=0$  we have  $\omega/c=0$ , corresponding to infinite wave-length or zero frequency (for  $c$  finite); this corresponds to the ground state of the oscillator. For  $n=1$ , we have

$$\lambda^2 = \frac{\pi}{\sqrt{\mu K}} = \frac{h}{4\pi m_0 \nu_0}, \quad (23)$$

since (Sommerfeld, *loc. cit.*)  $\sqrt{\mu K} = 4\pi^2 m_0 \nu_0 / h$ , where  $m_0$  is the mass of the oscillator and  $\nu_0$  is the fundamental mechanical frequency. For an intra-atomic frequency ( $m_0$  being the mass of the electron)  $\nu_0 = 10^{16}$ , we get  $\lambda$  of the order of  $10^{-8}$  cm. In this case the medium must be extremely fine-grained. Knowledge of the corresponding frequency will depend on the value assigned to  $c$ . If the latter is given the value of the velocity of light, the above, of course, corresponds roughly to hard X-rays or gamma radiation.

As another illustration, let us consider the one-dimensional hydrogen atom, for which  $V = -Ze^2/x$ ,  $Z$  being the number of positive charges on the nucleus. The equation (13) now becomes

$$\frac{d^2 \sqrt{S}}{dx^2} + [f(\mu) + \mu Ze^2/x] \sqrt{S} = 0. \quad (24)$$

The first eigenwert is  $f(\mu) = -(\mu Ze^2/2)^2$ , and the corresponding eigen-function is

$$\sqrt{S} = C x e^{-\frac{\mu Ze^2 x}{2}},$$

so that for the cross-sectional area of the tube we have

$$S = C^2 x^2 e^{-\mu Ze^2 x}, \quad (25)$$

where negative values of  $x$  have here no significance. The tube is a surface of revolution obtained by revolving the curve given by  $\sqrt{S}$  about the  $x$  axis, the appearance of the cross-section being shown in fig. 2. The maximum cross-section occurs for  $x = 2/\mu Ze^2$ . The equation (14) becomes for this case

$$\frac{d^2 p_e}{dx^2} + (2/x - \mu Ze^2) \frac{dp_e}{dx} + [\alpha + (\mu Ze^2/2)^2] p_e = 0. \quad (26)$$

Assuming now, as before,  $\rho_0 \sqrt{S} = \text{const.}$ ,

$$\rho_0 = \frac{\rho_{01}}{x} \cdot e^{\frac{\mu Ze^2 x}{2}}. \quad (27)$$



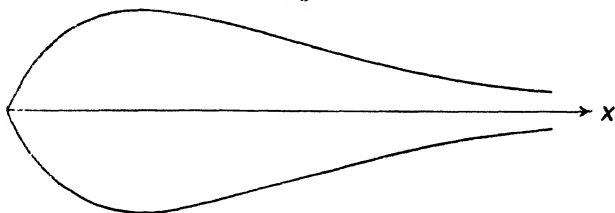
The solutions of (26), which correspond to the eigenwerte of the Schrödinger equation and which assure that  $s$  and  $\xi$  shall vanish at infinity, are found to be

$$(p_e)_n = \frac{A_n}{x} \cdot e^{\frac{n-1}{2n} \mu Z e^2 x} B_n(x), \quad . . . \quad (28)$$

where the  $B_n(x)$  form a set of polynomials, the solutions of the equation

$$\frac{d^2 v}{dx^2} - 2\sqrt{-\alpha} \cdot \frac{dv}{dx} + \frac{\mu Z e^2}{x} v = 0, \quad . . . \quad (29)$$

Fig. 2.



corresponding to the values of  $\alpha$  which are eigenwerte of the original Schrödinger equation. Thus we have

$$\left. \begin{aligned} B_1(x) &= x, \\ B_2(x) &= x \left[ 1 - \frac{\mu Z e^2}{4} x \right], \\ B_3(x) &= x \left[ 1 - \frac{\mu Z e^2}{3} x + \frac{1}{6} \left( \frac{\mu Z e^2}{3} \right)^2 x^2 \right], \\ &\dots \end{aligned} \right\} . . . \quad (30)$$

The characteristic wave-lengths for this case are given by

$$x = \frac{2\pi}{\sqrt{\alpha + \left( \frac{\mu Z e^2}{2} \right)^2}} . . . . . \quad (31)$$

For the electron  $\mu Z e^2/2$  is of the order of  $10^8 Z$ , and hence, since the eigenwerte are given by

$$\alpha = - \left( \frac{\mu Z e^2}{2n} \right)^2, \quad . . . . . \quad (32)$$

the first finite wave-length is again of the order of  $10^{-8}$  cm.

We may now suggest the following generalization to three degrees of freedom. For this case the equation of continuity may be written

$$\dot{\rho} + \frac{\partial(\rho_0 \dot{\xi})}{\partial x} + \frac{\partial(\rho_0 \dot{\eta})}{\partial y} + \frac{\partial(\rho_0 \dot{\zeta})}{\partial z} = 0, \quad . \quad . \quad (33)$$

where the component displacements along the three coordinate axes are  $\xi$ ,  $\eta$ , and  $\zeta$  respectively, and we are, as usual, assuming that  $s \ll 1$ . Now the component equations of motion are to the same approximation,

$$\left. \begin{aligned} \rho_0 \ddot{\xi} &= -\frac{\partial p_e}{\partial x}, \\ \rho_0 \ddot{\eta} &= -\frac{\partial p_e}{\partial y}, \\ \rho_0 \ddot{\zeta} &= -\frac{\partial p_e}{\partial z}, \end{aligned} \right\} \quad . \quad . \quad . \quad (34)$$

if we neglect terms of the order of  $\dot{\xi} \frac{\partial \xi}{\partial x}$ , etc. The continuity equation then becomes

$$\rho_0 \ddot{s} = \nabla^2 p_e,$$

or, since  $p_e = \rho_0 c^2 s$  and  $c$  is still assumed to be constant we have

$$\nabla^2 p_e + \frac{\omega^2}{c^2} p_e = 0 \quad . \quad . \quad . \quad (35)$$

for the excess pressure equation ( $p_e$  being harmonic in time with frequency  $\omega/2\pi$ ). To this must be added a statement of the condition that there must be zero velocity normal to the confining surface at every point. If we denote the direction cosines of the normal at any point by  $n_x$ ,  $n_y$ ,  $n_z$  respectively, the condition becomes

$$n_x \dot{\xi} + n_y \dot{\eta} + n_z \dot{\zeta} = 0 \quad . \quad . \quad . \quad (36)$$

at the bounding surface.

From the equations of motion (34) it follows that (36) can be written

$$n_x \frac{\partial p_e}{\partial x} + n_y \frac{\partial p_e}{\partial y} + n_z \frac{\partial p_e}{\partial z} = 0. \quad . \quad . \quad (37)$$

# 872 *Interpretation of the Schrödinger Wave Equation.*

Now consider the Schrödinger equation for three degrees of freedom, namely,

$$\nabla^2\psi + (\alpha - \mu V(x, y, z))\psi = 0. \quad (38)$$

As before, let us introduce the substitution of the form

$$\psi = F(x, y, z) \cdot p_e, \quad (39)$$

where the significance of  $F$  will appear in a moment. The equation (38) now becomes

$$\nabla^2 p_e + (\alpha - \mu V) p_e + \frac{\nabla^2 F}{F} \cdot p_e + \frac{2}{F} \cdot \sum_{x, y, z} \frac{\partial F}{\partial x} \cdot \frac{\partial p_e}{\partial x} = 0. \quad (40)$$

Now let  $F(x, y, z) = \text{const.}$  be the equation of the surface within which the fluid is confined. Then, since  $n_x \propto \frac{\partial F}{\partial x}$ , etc.,

$$\sum_{x, y, z} \frac{\partial F}{\partial x} \cdot \frac{\partial p_e}{\partial x} = 0$$

is precisely the condition that there shall be no motion normal to the confining surface. We shall suppose that  $F$  is determined as the first eigenfunction of the equation

$$\nabla^2 F + [f(\mu) - \mu V] F = 0, \quad (41)$$

where  $f(\mu)$  is the first eigenwert of the problem. The equation (40) then becomes

$$\nabla^2 p_e + [\alpha - f(\mu)] p_e = 0, \quad (42)$$

which, if  $\alpha - f(\mu) = \omega^2/c^2$ , is precisely the equation (35) for the excess pressure in the fluid vibrations within the surface. The solutions of (42) are to be taken as those which correspond to the eigenwerte of the original Schrödinger equation (38). In the acoustical problem these assure the vanishing of  $s$  and the component velocities at infinity, as well as their analytic nature everywhere else.

LXXVIII. *Interference Methods and Stellar Parallax.*

By E. H. SYNGE \*.

THERE is no difficulty in seeing that the methods of stellar interferometry should afford a means of determining parallax with a refinement comparable with the resolving power of the interferometer. If the images of the field provided by the two sets of mirrors of a stellar interferometer, whether in the original form of Michelson or in that proposed by the writer in a recent paper †, are exactly superposed in the focal plane of the telescope, and if, for any one star S, the path-lengths of the two beams are made equal, there will generally be inequality of path-lengths for any other star S'. If  $\phi$  (supposed small) is the component of the angular distance between S and S' along the axis of the interferometer, then, if the path-lengths are equal for S, the relative retardation between the beams in the case of S' will be proportional to  $\phi$ , and if this retardation is known  $\phi$  will be known. This obviously involves a method of determining parallax. For if we have some convenient means of finding this retardation we shall know  $\phi$ , and from a number of observations, at different times and with different pairs of stars, the parallaxes can be calculated. This idea, in a somewhat modified form, will be applied to the design of an apparatus in the present paper.

First, however, a method will be suggested for obtaining interference between two beams from a star which differs from Michelson's, and which seems to possess great advantages over it. The interference fringes used by Michelson are diffraction phenomena, but the principle ‡, which shows how different fringes are formed by different points of light, is one of geometrical optics. And as this is the vital factor, it is clear that the method does not essentially depend upon diffraction at all. Interference of the two beams can be obtained independently of diffraction by means of a half-silvered plate, the two

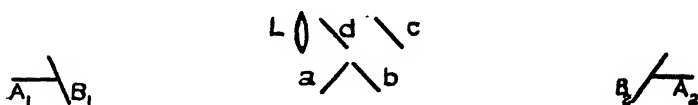
\* Communicated by the Author.

† "A Modification of Michelson's Beam Interferometer." *Phil. Mag.* (August 1930).‡ Schuster and Nicholson, 'Theory of Optics,' 3rd ed. pp. 167 F, G.  
*Phil. Mag.* S. 7. Vol. 10. No. 66. Nov. 1930. 3 M

beams being completely superposed on one another, as in Michelson's ordinary interferometer for measuring wave-lengths; and in that form the interference is adapted to measurement by a photo-electric cell.

It was for this reason that the writer was led to consider this form of interference as an alternative to the diffraction fringes used by Michelson. But other advantages soon became apparent which suggested that the method might well supersede Michelson's for every purpose. The diagram shows an arrangement by which this direct interference could be effected.

$A_1, A_2$  are the axes of two siderostats, these axes being collinear.  $B_1, B_2$ , the mirrors of the siderostats, are set so that the two beams from a certain star are reflected in opposite directions along the common polar axis.  $a, b, c$  are fully silvered mirrors, and  $d$  is a half-silvered mirror. The beam from  $B_1$  is first reflected by  $a$ , and then, in part, by  $d$ , into a telescope  $L$ . The beam from  $B_2$  is reflected by  $b$  to  $c$ , and then passes, in part, through  $d$ , entering  $L$  in



the same direction as the beam from  $B_1$ , upon which it is exactly superposed. Since the beam from  $B_2$  passes through the thickness of the glass of  $d$ , a plate of glass  $e$  (not shown) of similar thickness should be interposed at the same angle in the path of the beam from  $B_1$ .

Disregarding, for the present, the dispersion of the atmosphere, as is usually but unjustifiably done, the phenomena will be the following.

If the path lengths of these two beams, as measured from any arbitrary wave-front in space, are equal as they enter  $L$ , the two beams will reinforce one another, and all the light energy of both will pass into  $L$ . But if the beams differ by a half wave-length they will cancel one another, and an observer looking through the telescope will not perceive anything. Under good atmospheric conditions an observer will perceive an image of the star constantly vanishing and re-appearing, as the optical path-lengths of the two beams keep varying slightly. If, however, one

path-length becomes longer than the other by more than a few wave-lengths the different colours, for ordinary mixed light, will produce an overlapping, and the fluctuations will diminish and finally cease altogether, the star then appearing of an unvarying brightness, which is half the brightness when the two path-lengths are exactly equal.

It has been assumed that the star in question is sufficiently beyond the limit of resolution of the interferometer. For as the star approaches resolution, the maxima and minima will become less and less marked, even in the immediate neighbourhood of path-length equality. The optical principle here is essentially the same as in the case of the fringes used by Michelson. For if we consider two very close stars, the difference between whose declinations

is equal to  $\frac{\lambda}{2D \cos \theta}$ , where  $D$  is the distance between the

central points of the two siderostats,  $\theta$  the declination of one of the stars, and  $\lambda$  a wave-length, the same general law which determines the phenomena exhibited by Michelson's fringes in the case of a double star\* shows that if there is exact equality of path-lengths in the case of one of the stars, and thus mutual reinforcement of the two beams

from it as they enter  $L$ , there will be a difference of  $\frac{\lambda}{2}$

between the path-lengths of the beams from the other star, and therefore no light from it will enter  $L$ . It is merely a matter of integration to extend the case of a double star to that of a stellar diameter, and to find the decreasing sharpness of fluctuation as resolution is approached. When resolution is complete no fluctuation at all will be observed. This corresponds to the vanishing of Michelson's fringes.

In the case of a star bright enough to give a graphical record with a photo-electric cell, the recording apparatus should show a series of maxima and minima readings, of which several hundreds would be registered in a few minutes. The highest maxima would correspond to path-equality, and their difference from the mean would indicate with quantitative exactness the approach to resolution.

The method suggested for the equalization of path-

\* Schuster and Nicholson, *loc. cit.*

lengths, by means of the mirrors in the diagram, is the following. The four mirrors  $a, b, c, d$ , with the telescope  $L$ , are mounted on a carriage, which can travel on rails laid down between the two siderostats, the rails following a polar axis. A first approximation to equality of path-lengths is obtained by moving the carriage. To effect and maintain exact equality,  $a$  and  $d$  are rigidly connected and movable together relative to the carriage in the direction of a polar axis, while  $b$  and  $c$  are rigidly connected and capable of receiving slight rotations together, about an axis perpendicular to the plane of the paper, which represents a vertical section. Equality of path-lengths is obtained by moving  $a, d$  to the proper position, and maintained by very small rotations given to  $b, c$ , such rotations changing slightly the path-length of the beam from  $B_2$ , while not altering its direction, as it leaves  $c$ . This, for instance, will always remain parallel to its direction as it leaves  $B_2$ , if  $b$  and  $c$  are parallel to one another.

These methods of equalizing the path-lengths do not, however, by any means cover the question. Owing to the different refraction by the atmosphere of light of different wave-lengths the rays of different wave-lengths from a star reach the surface of the earth at slightly different angles, and in all forms of the interferometer this translates itself into a difference in relative retardation when the two beams unite. Thus, if there is equality of path-length at  $L$  for light of one wave-length, there will in general not be equality for light of a different wave-length. In amount the effect depends upon the altitude of the star, being zero at the zenith. It also increases with the length of the base-line, and the consideration of it is vital in any form of the stellar interferometer, although it is not referred to at all in most accounts of Michelson's Beam Interferometer. In that apparatus the crossed glass wedges and tilted plates set in the paths of the two beams can supply compensation and produce tolerable achromatism for the short base-lines used; and the writer fancies that this is usually done in an empirical way by skilful manipulation. The compensation is, of course, produced by one beam having a greater air-path and a less glass-path than the other. Equality of path-length can thus in general be obtained for any two different wave-lengths, and this implies an approximate achromatism.

For the much longer path-lengths feasible by the use of two siderostats it is, however, necessary to go into the question more closely, and to provide means by which the proper compensation may be given for any case by a calculated adjustment. A consideration of the question will also lead us to the recognition of a system of interference bands or fringes, which have many advantages over Michelson's fringes, and which seem to afford the only means of extending the method to those very long base-lines whose employment the writer, in his previous paper, suggested was conceivable.

The simplest method to secure chromatic compensation is to rotate  $e$  from its standard position, through a calculated angle. If the dispersion of  $e$  (with  $d$ ) is well chosen, quite good compensation should be obtained in this way. But a better compensation could be obtained by the following arrangement of crossed wedges. We will suppose that a plate of glass  $v_1$  and a pair of crossed wedges  $w_1$  are set at right angles in the path of the beam from  $B_1$ , while a plate  $v_2$  and crossed wedges  $w_2$  are similarly set in the path of the beam from  $B_2$ .  $v_1$  and  $w_2$  are constructed of one variety of glass, and  $v_2$  and  $w_1$  of another variety having a different dispersion. When the thickness of  $w_2$  is adjusted so as to be equal to that of  $v_1$ , and the thickness of  $w_1$  to be equal to that of  $v_2$ , the systems affect both beams equally, and there is no compensating effect. This is the proper adjustment for a star in the zenith. We may now select some wave-length  $\lambda$  as a standard, and suppose that one wedge of the pair  $w_1$  and one of  $w_2$  are moved transversely in such a way that the path-lengths of the rays of wave-length  $\lambda$  vary equally, and thus remain equal. The angles of the wedges can be made so that this effect is produced by an equal transverse motion of the two wedges in question.  $w_1$  and  $w_2$  might be conveniently set in the paths of the respective beams, just before each of them reaches  $d$ , and it would then be easy to make the turning of a single screw  $T$  impart the proper relative motion to both wedges at the same time.

If now we consider a star which is not in the zenith, and suppose that the system is adjusted so that the rays of wave-length  $\lambda$  unite in  $L$  with equality of path-lengths, then, if the achromatizing system  $v_1, w_1, v_2, w_2$  were absent, there would be a certain relative retardation  $r$  between



the rays of any other wave-length  $\nu$ . But, owing to the different dispersions of  $w_1$  and  $w_2$ , there will be one adjustment of  $w_1$  and  $w_2$ , which, while preserving equality of path-lengths for  $\lambda$ , will produce a compensating retardation ( $-\tau$ ) for  $\nu$ . The rays of both wave-lengths  $\lambda$  and  $\nu$  will then unite with equality of path-lengths, and if the dispersions of the two glasses are appropriately chosen, there will be practical achromatism over a considerable part of the spectrum, provided the base-line is not too long and the star is not too far from the zenith. A more complicated achromatizing system, with several crossed wedges, would provide a more perfect achromatism, but we need not consider this here.

Even if perfect achromatism were secured for one instant it would not, however, persist without continual adjustment of the screw T, for the distance of the star from the zenith and the effect in the interferometer will be continually changing. The rate of this change will be a minimum for the proposed apparatus when the star is on the meridian, and stars can therefore be best examined when they are in the immediate neighbourhood of the meridian. During a few minutes while they are crossing the meridian no readjustment of T should usually be needed. The screw would be set, by calculation, for this passage, the calculation being based on the altitude of the star during the passage and on the actual refraction of the atmosphere, which, of course, will not always remain constant. The correctness of the adjustment could be tested with great simplicity by converting the image of the star into a short spectrum which will be traversed with bands if the adjustment is not correct. These are the bands or fringes which have been referred to as a substitute for Michelson's diffraction fringes.

In the method suggested above for the use of a photo-electric cell to determine stellar diameters the achromatism should be provided for the photo-electrically active portion of the spectrum, and only that part of the spectrum admitted to the cell for which the achromatism is good. This method of measuring stellar diameters should succeed best when the interferometer has about one-half the full resolving power of the star, and should give the diameter correctly to at least 1 part in 100 if a sufficiently broad beam is used and only the highest of the maxima

considered. When a photo-electric cell is employed, the complementary beam issuing from  $d$  in the direction of  $ad$  produced could be used by an observer for purposes of control.

We will now turn to the spectrum bands or fringes, the simplicity and importance of which may not be immediately apparent. The existence of these bands does not essentially depend upon refraction or defects in achromatism, for if we suppose that the system is perfectly achromatic, but that one beam has a retardation of  $r$  upon the other, then there will be a dark band across the spectrum at every wave-length which has the value

$$\frac{r}{n + \frac{1}{2}}, \text{ where } n \text{ is any integer.}$$

To recognize the importance of these bands it is only necessary to observe that the same general law \* which governs the phenomena of the Michelson fringes in the case of a double star operates equally here. If we consider the spectra given by a double star, the north-south component of the angular distance between whose members

is equal to  $\frac{\lambda}{2D \cos \theta}$ , then, assuming that the spectra are

ordinarily continuous, if one spectrum exhibits a dark interference band having its centre at the wave-length  $\lambda$ , the other spectrum will have  $\lambda$  as the centre of a bright band. And since these two spectra are superposed we shall have the same kind of phenomena as is shown by Michelson's fringes in a similar case. But everything will be exhibited more clearly here, because a double star will, in general, only be exactly resolved for a single wave-length, and for accurate results this wave-length must be known. In Michelson's fringes all the wave-lengths are confounded together. Here, on the other hand, the exact wave-length can be immediately picked out. The passage from a double star to stellar diameters is, as before, only a matter of integration, the resolution being complete when the bands vanish; and here again there is superiority to Michelson's fringes, for the completeness of the resolution should differ, according to a definite law, for different wave-lengths, and by any non-correspondence of the

\* Schuster and Nicholson, *loc. cit.*

observed difference with theory, effects such as the reddening of the limbs of a star, due to the stellar atmosphere, should be immediately indicated.

In the case of a star whose spectrum is itself made up of noticeable lines an ordinary spectrum of the star (not exhibiting interference) should be obtained, and brought for comparison into the field of vision, side by side with the interference spectrum. Such a comparison spectrum would, indeed, be useful in any case. The question of the slits is not of great importance. No slit at all may be used, or a slit sufficient to delimit the star from the rest of the field, or a slit as in ordinary stellar spectroscopy; the choice depends upon the particular case and the amount of light available.

It is in regard to the amount of light available that we have one of the greatest advantages of the spectrum bands over Michelson's fringes; for in the case of the latter the light is wastefully spread over the area of a circle and enormous magnification has to be employed. Using the spectrum bands the light is, on the other hand, concentrated along a narrow line which need appear little broader than the limit of ocular resolution, and if the star is faint only two or three bands are necessary. The bands will of course move about very much like Michelson's fringes, but they will not become confused in the same way when one of the two beams is a few wave-lengths longer than the other. In such a case they will simply increase in number, and not very rapidly, so that the apparatus should be far easier to control by means of them. On the whole, after allowing for the loss of half the light at the half-silvered plate, there should be an advantage of about 100 to 1 over Michelson's fringes in the matter of light, which means that about 1000 times as many stars could be dealt with by the spectrum bands.

There is a similar advantage in regard to achromatism. It would be almost impossible to secure perfect achromatism when the base-line was very long, and an almost perfect achromatism is needed to obtain good results from Michelson's fringes. But in the case of the spectrum bands it is quite unnecessary that the system should be perfectly achromatic. Indeed, for several purposes it is even desirable that it should not be so. The exact degree and manner in which there is departure from achromatism

can be known from the adjustment of  $w_1$  and  $w_2$  and the refraction and dispersion of the atmosphere at the time; but for the evaluation of stellar diameters in the manner indicated it is quite unnecessary that these should be known. Nothing more is needed than that there should be interference bands and that these should not be too numerous.

We will now discuss the determination of parallax, for which also these bands should prove of service. For parallax we shall suppose that two pairs of siderostats are set up: a siderostat  $A_1'B_1'$  side by side with  $A_1B_1$ , and another  $A_2'B_2'$  side by side with  $A_2B_2$ . Let  $P_1, P_2$  be the points where the reflecting surfaces of  $B_1, B_2$  cut the common axis of the siderostats  $A_1B_1$  and  $A_2B_2$ , and let  $P_1', P_2'$  be the points where the reflecting surfaces of  $B_1', B_2'$  cut the common axis of  $A_1'B_1'$  and  $A_2'B_2'$ . Then we shall suppose that the points  $P_1, P_2, P_1', P_2'$  remain unchanged for all angular adjustments of the respective mirrors, and that the line joining  $P_1, P_2$  is exactly perpendicular to the polar axes, and similarly for the line joining  $P_1', P_2'$ . It might not be easy to satisfy these conditions exactly in practice; but the apparatus can be calibrated to show the departure from them for any adjustment and equivalent corrections introduced in the calculations. We shall assume that these conditions are exactly satisfied and that the distances between  $P_1P_2$  and between  $P_1'P_2'$  are each equal to  $D$ .

The pair of siderostats,  $A_1B_1, A_2B_2$ , which, with their subsidiary apparatus, we may call  $\sigma$ , has that system of mirrors, wedges, telescope, etc. which we have already described. The other pair of siderostats, which we may similarly call  $\sigma'$ , has a corresponding set  $a', d', e', v_1', v_2', w_1', w_2', L', b, c$ .  $b$  and  $c$  are common to  $\sigma$  and  $\sigma'$ , these two mirrors extending completely across the paths of both  $\sigma$  and  $\sigma'$ . But  $a', d', w_1', w_2'$ , and the telescope  $L'$  are independent for  $\sigma'$ , and the adjustments of  $a', d', w_1', w_2'$  will in general be different from the adjustments of  $a, d, w_1, w_2$ . It is the difference between these adjustments which will serve for the determination of parallax.

Let us now consider two near stars,  $S$  of declination  $\theta$ , and  $S'$  of declination  $\theta'$ .  $\sigma$  and  $\sigma'$  are adjusted so that the beams from  $S$  travel along the axis of  $\sigma$ , coming together in  $L$  with equality of path-lengths, while the beams from

$S'$  travel along the axis of  $\sigma'$ , and come together in  $L'$  with equality of path-lengths. For simplicity we are disregarding refraction and aberration. If, now, we consider the two rays from  $S$  which pass through  $P_1$  and  $P_2$ , these rays, considered at these two points, have a relative retardation of  $D \sin \theta$ , and since they meet with equality of path-lengths in  $L$ , there must be an optical difference of path-lengths, as measured from  $P_1, P_2$  to  $L$ , equal to  $D \sin \theta$ . Similarly in the case of  $S'$  and  $\sigma'$ , there is an optical difference of path-lengths, as measured from  $P_1', P_2'$  to  $L'$ , equal to  $D \sin \theta'$ . But the difference between these two differences, and therefore between  $D \sin \theta$  and  $D \sin \theta'$ , is made up by the difference in the adjustments of  $a, d$ , and  $a', d'$ , and of  $w_1, w_2$  and  $w_1', w_2'$ , and can be evaluated, if desired, to nearly a hundredth part of a wavelength. We have therefore  $D(\sin \theta - \sin \theta')$  with very great accuracy, and the adjustment of  $a, d, w_1, w_2$  necessary to give equality of path-lengths for  $S$ , as compared with some standard adjustment, and confirmed by similar observations on stars of different altitudes, will give the necessary correction for refraction with very great accuracy. If it proved possible to use a sufficiently long base-line, we should have  $\sin \theta - \sin \theta'$  to beyond

$\frac{1}{100,000}$  of a second of arc, assuming of course that the

stars we are dealing with are beyond the limit of resolution for the base-line used. By taking similar observations at different seasons and on a number of stars we shall have the north-south component of parallax to a similar degree of accuracy. This, of course, will be combined with the north-south component of the proper motion, but can be easily separated from it; and, knowing the north-south component of the parallax, we know the parallax.

We have assumed, however, a perfectly calm atmosphere, and have still to consider the effect of atmospheric disturbances, through which any given adjustment of  $\sigma, \sigma'$  only establishes a path equality for  $S, S'$  for a single instant. We desire to find correct mean values for these adjustments, or, rather, for the difference between the adjustments, for it is with  $D \sin \theta - D \sin \theta'$  that we are concerned rather than with  $D \sin \theta$  and  $D \sin \theta'$  separately. It is here that the spectrum bands will prove of service. For let us set  $w_1, w_2$  so that if, for a state of the

atmosphere which is believed to represent the true mean of the disturbances, there is equality of path-lengths for some one wave-length  $\lambda$  of the star S, and at the same time a retardation of  $\frac{\nu}{2}$  at some other wave-length  $\nu$ . Then

there will be a different configuration of the bands for every different retardation of one beam on the other. The configuration at any one instant will mark the exact retardation (for  $\lambda$ ) and will show also which beam is in retardation. A similar adjustment is made for  $\sigma'$ , S'.

Let us now imagine that two observers watch the spectra of S and S' respectively for a few minutes as the stars are crossing the meridian, during which time the chromatic conditions will not vary appreciably. A certain configuration of bands will indicate a retardation  $\kappa\lambda$  for wave-length  $\lambda$  of the beam from B<sub>2</sub> with respect to that from B<sub>1</sub>, and another configuration will indicate a retardation in the opposite sense  $-\kappa\lambda$ ,  $\kappa$  being a selected small number, 3 or 4 perhaps. The observer counts the number of times in which the two configurations present themselves, say N<sub>1</sub> and N<sub>2</sub> respectively. The other observer does similarly during the same time for  $\sigma'$ , S', obtaining N<sub>1</sub>' , N<sub>2</sub>'. If the adjustments for path-length equality for  $\lambda$  represent true means, we shall have N<sub>1</sub>=N<sub>2</sub> and also N<sub>1</sub>'=N<sub>2</sub>' if the average is taken over a large enough number of cases. But even if the adjustments for path-length equality for  $\lambda$  do not represent true means, yet if the *relative* adjustments of  $\sigma$  and  $\sigma'$  are correct, which is what we are really concerned with, since they give  $\sin\theta - \sin\theta'$ , we shall have N<sub>1</sub> : N<sub>2</sub> = N<sub>1</sub>' : N<sub>2</sub>'. If we obtain this relation over a wide enough average we may measure the difference of path represented by the relative adjustments of  $a, d$ ;  $a', d'$  and of  $w_1, w_2$ ;  $w_1', w_2'$ , and set this difference equal to D( $\sin\theta - \sin\theta'$ ). If the relation is not quite satisfied there will be a correction to which we can approximate.

This assumes that there are not large movements in the atmosphere. To deal with such one of the observers should be able to control  $b, c$ , a rotation of  $b, c$  affecting equally  $\sigma$  and  $\sigma'$ , and counteracting broader atmospheric effects. When a configuration of the spectrum bands showed that one beam had a retardation upon the other exceeding a certain definite amount, say 6 or 7 wave-lengths, the observer would impose a correcting motion on  $b, c$ . This

motion might be one of invariable magnitude, so as to avoid the personal factor. The control might also be interchanged between the observers from time to time.

A different, and, with good seeing, possibly a better method would be the following.  $b, c$  do not extend across  $\sigma'$ , which has separate mirrors  $b', c'$ .  $b, c$  are parallel to one another, and likewise  $b', c'$ . A parallel beam of light is thrown obliquely upon  $b$ , so as to be reflected to  $c'$ , and then focussed by a telescope—or, better, after  $c'$ , reflected by a fixed mirror back, nearly, but not quite, along its former path, into the telescope from which it issued—forming a spot of light,  $O$ . When there is any angular difference between  $b, c$  and  $b', c'$ ,  $O$  is displaced. Two observers, by controlling  $b, c$  and  $b', c'$ , now endeavour to hold certain spectrum interference bands of  $S$  and  $S'$  at positions which represent path-equality. In the process,  $O$  shifts back and forwards, and if it is received on a photographic plate, the centre, or position of maximum intensity of the track made by  $O$ , will indicate the *average* angular difference between  $b, c$  and  $b', c'$ , which, of course, represents a difference in path-length to be added to that due to  $a, d$  and  $a', d'$ . The personal factor can be eliminated by photographing portion of the spectra at the same time. This can be done by using the blue end of the spectra for photography and the other end for vision, or by photographing spectra of the complementary beams found. The exact positions of the centres or maxima in the averaged spectra bands in the photographs, together with that of the  $O$  track, should supply data giving a result to very nearly a hundredth part of a fringe. A single observer could probably control both  $\sigma$  and  $\sigma'$ , if the images of the two spectra were brought by mirrors into the same field of vision. It would be an advantage to have several pairs of siderostats, with a suitable number of observers, and thus to deal with a number of stars at the same time.

The apparatus suggested seems, so far as one can judge from theoretical considerations, to afford a means of measuring both the angular diameters of stars and their parallaxes with an accuracy in suitable cases approaching one-millionth of a second of arc. Since the knowledge of the parallax and the angular diameter together gives the absolute diameter, the apparatus would actually measure

the stars ; and one might perhaps suggest the name of *siderometer* for it, confining that of interferometer, as would seem convenient, to an instrument designed to measure wave-lengths. It may be remarked that the increase of accuracy which interference methods should give to a large body of astronomical data ought to be quite comparable to the increase of accuracy which interference methods brought to the measurement of wave-lengths, that is, an increase of 100 to 1000 times.

The apparatus described, with a north-south arrangement of siderostats, could, however, only increase the accuracy of the data of position ; but a similar refinement might be introduced into time measurements, as determined or tested by the passages of stars across the meridian, by an east-west arrangement of two siderostats. Mirrors would be placed to conduct the beams of any star, which both siderostats reflected along their respective axes, to ultimate union in a telescope by means of a half-silvered plate, the arrangements of the mirrors being such that there was equality of path-lengths as measured from the siderostats to the telescope. As an irresolvable star crossed the meridian there would now be equality of path-lengths, as measured from any arbitrary wave-front in space to the telescope ; and an observer, if his eye were sensitive to a sufficiently short time interval, would suddenly see a maximum, twice the average brightness, flash out, accompanied by dark minima before and after it. The duration of this maximum would, however, be far too brief in general to be observed by the eye.

In the case of a sufficiently bright star the maximum might be recorded by photo-electric apparatus. It could also be made accessible to the eye by means of some device—such as a moving mirror—which would continuously change the path-length of one of the beams at an appropriate rate for a few seconds as the star was crossing the meridian. This would incidentally afford a means of determining the east-west diameters of stars. But the east-west method as a whole would require, at the same time as it would supply a test for, a great increase in the accuracy of astronomical clocks.



LXXIX. *On an Application of the New Methods of the Calculus of Variations to some Problems in the Theory of Elasticity.* By N. M. BASU, D.Sc.\*

1. **M**OST problems of the mechanics of continuous media reduce ultimately to the solution of boundary-value problems associated with certain partial differential equations. The solution of such partial differential equations satisfying given boundary conditions can be effected in only a limited number of cases for which the boundaries are very simple curves. The success of the solution depends in general on the knowledge *à priori* of a complete set of particular solutions of the differential equation in question and the expansibility of an arbitrary function in terms of these functions in the manner of Fourier's Series. In 1908 Walter Ritz † proposed a new method which is applicable to a wider class of problems, and by which numerical values can in general be obtained to any desired degree of approximation in a comparatively simple manner. His method consists in treating the problem as one of the Calculus of Variations, into which it can easily be translated, since the differential equations of most mechanical problems can be derived from Hamilton's Principle. The problem is thus reduced to the determination of a function which, while satisfying certain boundary conditions and conditions of differentiability, renders a certain Integral expression minimum. But although Ritz's method gives a solution where the classical method fails, it does not afford any means of testing the measure of exactness realized in any particular case, and one has to be satisfied that the error must be small when further approximations do not give any appreciable variation in the value of the Integral. Recently, however, a method has been indicated by K. Friedrichs ‡ by means of which in certain cases it may be possible to associate with the given problem another Integral of which the maximum is exactly equal to the minimum of the given Integral, so that by considering the two extremum-problems we have a means of estimating the error involved in the solution obtained.

In the present paper the deflexion of a uniformly loaded square membrane has been worked out by Ritz's method, and the result tested by the consideration of an associated

\* Communicated by the Author.

† See Crelle's *Journal*, Bd. cxxxv. pp. 1-61.

‡ See *Göttinger Nachrichten*, 1929.

problem set up by elementary reasoning. The result seems to be very satisfactory, inasmuch as a second approximation shows the error to be less than 1 in 400. The twisting couple of an elastic prism with square section, when subjected to torsion, has also been calculated, and compared with the result obtained by Saint Venant.

*The Problem.*

2. We know that the equilibrium position of a loaded membrane is determined by the equations

$$T\left(\frac{\partial^2 u}{\partial x^2} + \frac{\partial^2 u}{\partial y^2}\right) + p = 0 \quad \text{at inner points,} \quad . \quad . \quad (1)$$

$$u = 0 \quad \text{at the boundary,} \quad . \quad (2)$$

where  $u$  is the vertical displacement at the point  $(x, y)$ ,  $T$  is the uniform tension with which the membrane is stretched, and  $p(x, y)$  is the load per unit area at the point  $(x, y)$ . If we write  $\frac{p}{2T}u$  for  $u$  in the above equations, they reduce, when  $p$  is constant, to

$$\nabla^2 u + 2 = 0 \quad \text{at all inner points,} \quad . \quad . \quad (3)$$

$$u = 0 \quad \text{at the boundary} \quad . \quad . \quad . \quad (4)$$

It is now easily seen that the problem under consideration is equivalent to the following problem of the Calculus of Variations (*Problem I.*):

*“Of all functions  $u$  which vanish on the boundary and which together with their first and second derivatives are finite and continuous at all inner points, to determine that one which makes the Integral*

$$I[u] = \frac{1}{2} \iint \left[ \left( \frac{\partial u}{\partial x} \right)^2 + \left( \frac{\partial u}{\partial y} \right)^2 - 4u \right] dx dy \quad . \quad (5)$$

*a minimum.”*

The integral extends over the whole of the area under consideration.

That the minimum-problem enunciated above is *not meaningless* is easily seen, for certainly there are functions of the specified class for which  $I[u]$  exists, and secondly  $I[u]$  is bounded below. To prove this second point we note that by virtue of Schwarz's inequality

$$\left( \iint u dx dy \right)^2 \leq A \iint u^2 dx dy,$$

where  $A$  is the area of the region under consideration.

Further, as is well known\*, since  $u$  vanishes on the boundary

$$\iint u^2 dx dy \leq c \iint \left[ \left( \frac{\partial u}{\partial x} \right)^2 + \left( \frac{\partial u}{\partial y} \right)^2 \right] dx dy,$$

where  $c$  is a positive constant. Thus we have

$$\left| \iint u dx dy \right| \leq c' \sqrt{\iint \left[ \left( \frac{\partial u}{\partial x} \right)^2 + \left( \frac{\partial u}{\partial y} \right)^2 \right] dx dy},$$

from which the truth of the above assertion follows at once,  $c'$  being a positive constant.

3. We now consider a little more general problem, and shall come back to our original problem later. We consider the following problem (*Problem II.*):

“Of all functions  $u(x, y)$ , having a given value  $\bar{u}$  on the boundary which together with their first and second derivatives are finite and continuous at all inner points, to find that one which makes the Integral

$$M[u] \equiv \frac{1}{2} \iint \left[ \left( \frac{\partial u}{\partial x} \right)^2 + \left( \frac{\partial u}{\partial y} \right)^2 - 4uf(x, y) \right] dx dy \quad (6)$$

a minimum,  $f(x, y)$  being a given function.”

It is easily seen that under suitable assumptions in regard to the functions  $u$  and  $f$ , the above problem has a sense. The Eulerian differential equation of this problem is obviously

$$\nabla_1^2 u + 2f(x, y) = 0. \quad (7)$$

Let us write

$$\frac{\partial u}{\partial x} = \xi, \quad \frac{\partial u}{\partial y} = \eta.$$

If  $p$  and  $q$  are any two functions of  $x$  and  $y$ , we have

$$\begin{aligned} & \left[ \frac{1}{2}(\xi^2 + \eta^2) - 2uf \right] + \left[ \frac{1}{2}(p^2 + q^2) - p\xi - q\eta + 2uf \right] \\ & = \frac{1}{2}[(\xi - p)^2 + (\eta - q)^2] \geq 0, \end{aligned}$$

for any values of  $\xi, \eta, u, p$ , and  $q$ , the sign of equality holding only when

$$\xi = p \quad \text{and} \quad \eta = q$$

simultaneously. Reintroducing the values of  $\xi$  and  $\eta$ , integrating over the area under consideration— $p$  and  $q$  must,

\* See, for instance, Courant, “Über die Eigenwerte bei den Differentialgleichungen der Mathematischen Physik,” *Math. Zsft.* vii. pp. 13-16.

of course, be integrable functions—and partially transforming one of the area integrals into a boundary integral, we have

$$M[u] + \frac{1}{2} \iint (p^2 + q^2) dx dy - \int (lp + mq) \bar{u} ds + \iint \left( \frac{\partial p}{\partial x} + \frac{\partial q}{\partial y} + 2f \right) u dx dy \geq 0,$$

where  $ds$  is an elementary arc of the boundary and  $(l, m)$  are the usual direction-cosines of the outward-drawn normal at  $ds$ .

Since  $p$  and  $q$  are arbitrary functions, we can impose any conditions on them at pleasure. We make them satisfy the condition

$$\frac{\partial p}{\partial x} + \frac{\partial q}{\partial y} + 2f(x, y) = 0 \quad . \quad . \quad . \quad (8)$$

Then we have

$$-\frac{1}{2} \iint (p^2 + q^2) dx dy + \int (lp + mq) \bar{u} ds \leq M[u]$$

for all admissible functions  $p, q$ , and  $u$ . If Problem II. has a solution  $v(x, y)$  for which  $M[v] = d$ , then, taking  $u = v$  and writing

$$N[p, q] \equiv -\frac{1}{2} \iint (p^2 + q^2) dx dy + \int (lp + mq) \bar{u} ds,$$

we must have

$$N[p, q] \leq d$$

for all functions  $p, q$  satisfying the equation (8). But since  $v$  satisfies the equation (7),  $p = \frac{\partial v}{\partial x}$ ,  $q = \frac{\partial v}{\partial y}$  satisfy the equation (8). Moreover, for these values of  $p$  and  $q$  the sign of equality must hold, as we have already remarked, so that we have

$$N\left[\frac{\partial v}{\partial x}, \frac{\partial v}{\partial y}\right] = d = M[v].$$

Thus we see that when the Problem II. has a solution, the expression  $N[p, q]$  does indeed attain its maximum value, and we have

$$\text{Max. } N[p, q] = d = \text{Min. } M[u].$$

We thus associate with Problem II. a new problem, namely, that of finding the maximum value of  $N[p, q]$ , where  $p, q$  are subject to the condition (8), and we have, for all admissible  $p, q$  and  $u$ ,

$$N[p, q] \leq d \leq M[u],$$

which furnishes the means for determining the degree of exactness to which the calculated value of  $M[u]$  approximates its true minimum value.

To satisfy the equation (8) we proceed as follows:—

We notice that the condition may be written as

$$\frac{\partial}{\partial x}(p + F) + \frac{\partial q}{\partial y} = 0,$$

where

$$F(x, y) = 2 \int f(x, y) dx.$$

We must therefore have

$$p + F = \frac{\partial w}{\partial y}$$

$$q = -\frac{\partial w}{\partial x}$$

where  $w$  is an undetermined function. Substituting these expressions for  $p$  and  $q$  in  $N(p, q)$ , the associated problem is defined in terms of only one unknown function  $w$ , which, on account of its connexion with the solution of Problem II., must possess continuous first and second derivatives in the region under consideration.

4. Returning now to our original problem (Problem I.), we see that it is only a special case of Problem II. with  $\bar{u}=0$  and  $f(x, y)=1$ . Thus the associated problem becomes:

*“To find the maximum value of the integral*

$$J[w] = -\frac{1}{2} \iint \left[ \left( \frac{\partial w}{\partial x} \right)^2 + \left( \frac{\partial w}{\partial y} \right)^2 - 4x \frac{\partial w}{\partial y} + 4x^2 \right] dx dy \quad (9)$$

*where the admissible functions  $w$  are such as are continuous and have continuous first and second derivatives in the region under consideration.”*

Taking the sides of the square to be given by the equations  $x=\pm 1$ ,  $y=\pm 1$ , we have

$$J[w] = -\frac{8}{3} + L[w], \quad . . . . . (10)$$

where

$$L[w] = -\frac{1}{2} \iint \left[ \left( \frac{\partial w}{\partial x} \right)^2 + \left( \frac{\partial w}{\partial y} \right)^2 - 4x \frac{\partial w}{\partial y} \right] dx dy. \quad (11)$$

The problem therefore resolves itself into finding the maximum value of  $L[w]$ .

For the purpose of numerical calculations we note that if  $\psi_1, \psi_2, \dots, \psi_n, \dots$  are given functions, all vanishing on

the boundary, and  $a_1, a_2, \dots$  are arbitrary constants, and if  $u_n$  be that function of the type  $a_1\psi_1 + a_2\psi_2 + \dots + a_n\psi_n$  (which we shall hereafter call a function of class  $C_n$ ) which makes  $I[u]$  a minimum, then this minimum value  $I[u_n]$  is given by

$$I[u_n] = - \iint u_n dx dy. \quad . \quad . \quad . \quad (12)$$

This easily follows from the consideration that the first variation of  $I[u_n]$ ; namely

$$\iint \left[ \frac{\partial u_n}{\partial x} \frac{\partial}{\partial x} (\delta u_n) + \frac{\partial u_n}{\partial y} \frac{\partial}{\partial y} (\delta u_n) - 2\delta u_n \right] dx dy, \quad (13)$$

must be zero, where  $\delta u_n$ , the small variation of  $u_n$ , is such that  $u_n + \delta u_n$  also belongs to the class  $C_n$ . This is obviously satisfied by taking  $\delta u_n = \epsilon \cdot u_n$ , where  $\epsilon$  is a small constant. Substituting this value of  $\delta u_n$  in (13), and equating the result to zero, we derive the equation (12). In a similar manner, if  $w_n$  be that function of class  $C'_n$ \* which makes  $L[w]$  a maximum, then this maximum is given by

$$L[w_n] = \iint x \frac{\partial w_n}{\partial y} dx dy. \quad . \quad . \quad . \quad (14)$$

*Choice of the  $\psi$ -functions for  $I[u]$ .*

5. We know from a theorem due to Weierstrass that an arbitrary function which, together with its derivatives up to a given order, is finite and continuous, can always be represented by a series of polynomials which converge uniformly and can be differentiated the required number of times. Having regard to the form of the boundary and the conditions to be satisfied by the  $\psi$ -functions employed in Ritz's method †, we choose them to be given by

$$\psi_{mn} = (1-x^2)(1-y^2)x^m y^n, \quad m, n = 0, 1, 2, \dots$$

These functions satisfy all the required conditions.

*The Integral  $I[u_n]$ .*

6. The nature of the problem shows that the solution must be symmetrical in  $x$  and  $y$  and contain only their even powers. We therefore give to  $m, n$  the values  $0, 2, 4, \dots$

\* We call this class  $C'_n$  instead of  $C_n$  as in general we shall use different  $\psi$ -functions for the integral  $L[w]$ .

† *Loc. cit.* p. 10. The conditions to be satisfied for the problem under consideration are slightly different—e. g., the boundary condition  $\frac{\partial \psi}{\partial n} = 0$  is no longer required, and the “Hauptableitungen” include only derivatives up to the second order.

Thus, as a first approximation we take

$$u_1 = a\psi_{00} = a(1-x^2)(1-y^2).$$

Substituting this value of  $u$  in  $I[u]$ , and putting  $\frac{\partial I}{\partial a} = 0$ , we get  $a = \frac{5}{8}$ .

Thus, as a first approximation we get

$$u_1 = \frac{5}{8}(1-x^2)(1-y^2), \dots \dots \dots (15)$$

and from (12)

$$I[u_1] = - \iint u_1 dx dy = -\frac{10}{9} \dots \dots \dots (16)$$

As a second approximation we take, remembering that the solution must be symmetrical in  $x$  and  $y$ ,

$$u_2 = a\psi_{00} + b(\psi_{02} + \psi_{20}) + c\psi_{22}.$$

Substituting  $u = u_2$  in  $I[u]$ , evaluating the integrals and putting

$$\frac{\partial I}{\partial a} = \frac{\partial I}{\partial b} = \frac{\partial I}{\partial c} = 0,$$

we get the following three equations:

$$280a + 96b + 8c - 175 = 0.$$

$$2016a + 2464b + 295c - 1470 = 0.$$

$$168a + 295b + 2788c - 147 = 0.$$

Solving these equations, and retaining only five places of decimals, we obtain as a second approximation

$$u_2 = (1-x^2)(1-y^2) [\cdot 58453 + \cdot 11733(x^2 + y^2) + \cdot 00846x^2y^2] \dots (17)$$

and

$$I[u_2] = -252 \cdot 72016 / 225 \dots \dots \dots (18)$$

We observe that the coefficients diminish rapidly, indicating rapid convergence.

*The Associated Integral J[w].*

7. We now determine the approximations to the maximum value of the associated integral. We observe that  $w$  is not subject to any other condition except the conditions of continuity and differentiability two times, but on forming the Eulerian differential equation for this variation problem it is found to be

$$\nabla_1^2 w = 0.$$

We therefore take \* for the functions  $\psi$ , in this case, the plane harmonic polynomials, namely,  $1, x, y, x^2 - y^2, xy, x^3 - 3xy^2, 3x^2y - y^3$ , etc. Simple considerations, into the details of which we need not enter here, show that the constant term and harmonics of odd degree, as well as those harmonics of even degree which contain only even powers of the variables, drop out of consideration. We therefore have to consider functions of the type

$$w = axy + b(x^3y - xy^3) + c(3x^5y - 10x^3y^3 + 3xy^5) + \dots$$

As a first approximation we take

$$w = w_1 = axy.$$

Substituting this value in  $L[w]$ , and putting  $\frac{\partial L}{\partial a} = 0$ , we get  $a = 1$ ; so that

$$\left. \begin{aligned} w_1 &= xy, \\ L[w_1] &= \frac{4}{3}, \end{aligned} \right\} \cdot \cdot \cdot \cdot \cdot \quad (19)$$

and from (10)

$$J[w_1] = -\frac{8}{3} + \frac{4}{3} = -\frac{4}{3} \cdot \cdot \cdot \cdot \cdot \quad (20)$$

As a second approximation we take

$$w = w_2 = a'xy + b(x^3y - xy^3).$$

We then find

$$\left. \begin{aligned} w_2 &= xy - \frac{7}{18}(x^3y - xy^3), \\ L[w_2] &= \frac{208}{135}, \end{aligned} \right\} \cdot \cdot \cdot \cdot \cdot \quad (21)$$

and

$$J[w_2] = -\frac{8}{3} + \frac{208}{135} = -\frac{152}{135} \cdot \cdot \cdot \cdot \cdot \quad (22)$$

### The Estimation of the Error.

8. If  $d$  denotes the true minimum value of  $I[u]$ , then, in accordance with the conclusions of Art. 3, we must have for every  $u$  and  $w$

$$J[w] \leq d \leq I[u].$$

\* We are here concerned only with finding approximations to the maximum value of  $J[w]$ , and not with  $w$  itself, and it is therefore not necessary to examine whether the functions  $\psi$  used here satisfy the conditions required in Ritz's method. All that is required is that  $J[w]$  should have an upper limit, which is obviously true in the present case, since  $J[w] < 0$ , and then whatever function may be substituted for  $w$  we shall get a value not greater than this upper limit.



Using the first approximate solution  $u_1$ , we get

$$-\frac{152}{135} \leq d \leq -\frac{10}{9}.$$

Hence, if  $\delta_1$  denotes the error (i. e.  $-\frac{10}{9} - d$ ),

$$|\delta_1| \leq \frac{152}{135} - \frac{10}{9} = \frac{2}{135}.$$

Since

$$|d| \geq \frac{10}{9},$$

the error is less than  $\left(\frac{2}{135} \div \frac{10}{9}\right)$  100 per cent., that is less than  $1\frac{1}{3}$  per cent.

Using the second approximate solution  $u_2$ , we have similarly

$$-\frac{152}{135} \leq d \leq -\frac{252.72016}{225}$$

and

$$|\delta_2| \leq \frac{152}{135} - \frac{252.72016}{225} = .002725.$$

Hence the error is less than  $.02725 \times 9 = .2453$  per cent., which is less than 1 in 400.

If the deviation of the value of the integral  $I[w_2]$  from the true minimum value of  $I[u]$  be taken as a measure of the degree of exactness of the approximation, we must come to the conclusion that the solution  $u_2$  obtained above must be a very good approximation indeed. Thus for all practical purposes the deflexion of a square membrane subjected to a uniform load  $p$  per unit area and a uniform tension  $T$  is given by the simple formula

$$u = \frac{p}{2T} u_2,$$

where  $u_2$  is given by (17).

### *The Torsion Problem.*

9. The results obtained above can be utilized in calculating the twisting couple of an elastic prism whose cross-section is a square and which is subjected to torsion about its axis. It is well known that the solution of the Torsion Problem consists in the determination of the *torsion-function*  $\phi$ , and that

if  $\psi$  denotes the conjugate of the torsion-function then  $\psi$  satisfies the following conditions:—

$$\nabla^2 \psi = 0 \text{ at all inner points,}$$

$$\psi = \frac{1}{2}(x^2 + y^2) + \text{constant, on the boundary.}$$

Putting

$$\psi = u + \frac{1}{2}(x^2 + y^2) + \text{constant,}$$

we see that  $u$  satisfies the equations (3) and (4), so that for all practical purposes  $u$  is given by the equation (17). If  $\mu$  denotes the rigidity of the material,  $\tau$  the twist,  $\phi$  the torsion-function, and  $\psi$  its conjugate, the twisting couple  $M$  is given by\*

$$\begin{aligned} M &= \mu\tau \iint \left( x^2 + y^2 + x \frac{\partial \phi}{\partial y} - y \frac{\partial \phi}{\partial x} \right) dx dy \\ &= \mu\tau \iint \left( x^2 + y^2 - x \frac{\partial \psi}{\partial x} - y \frac{\partial \psi}{\partial y} \right) dx dy \\ &= -\mu\tau \iint \left( x \frac{\partial u}{\partial x} + y \frac{\partial u}{\partial y} \right) dx dy, \end{aligned} \quad (23)$$

whence, on effecting Green's transformation, and remembering that  $u$  vanishes on the boundary,

$$M = 2\mu\tau \iint u dx dy \quad . \quad . \quad . \quad (24)$$

For the first approximation we have

$$M_1 = \frac{20}{9} \mu\tau = 2.2222 \mu\tau.$$

Saint Venant's† result is  $2.2492 \mu\tau$ . The difference is  $.027 \mu\tau$ , *i. e.*, approximately 1.2 per cent.

Using the second approximation ( $u_2$ ) we get

$$\begin{aligned} M_2 &= 2\mu\tau \times 252.72016/225 \} \quad . \quad . \quad . \quad (25) \\ &= 2.2464 \mu\tau. \end{aligned}$$

The difference is  $.0028 \mu\tau$ , *i. e.*, approximately .124 per cent., which is less than 1 in 800. Thus we see that, using the value  $u_2$ , we obtain very close agreement with Saint Venant's result. The deviation is negligible for all practical purposes.

It may be noted that even without knowing Saint Venant's result it is possible to obtain an estimate of the error in the calculated value of  $M$ . For this purpose we observe from the equations (12) and (24) that

$$M = -2\mu\tau I[u],$$

\* See Love's 'Theory of Elasticity,' 4th ed. p. 312.

† *Ibid.* p. 324.

where  $u$  is the function which makes  $I[u]$  minimum, and therefore with successive approximations the calculated value of  $M$  must increase and approach its true value, the error percentage being the same as for  $I[u]$ . Hence, in accordance with the result of Art. 8, the error in the value of  $M$  given by (25) is certainly less than 1 in 400.

10. From the results obtained above it is clear that the deflexion of a membrane or the twisting couple of a prism can be determined by the above method to a fairly high degree of approximation. In the case of the torsion problem, however, it must be remembered that in order to determine the displacement or the state of strain and stress at any point it is necessary to know the torsion-function itself, and not its conjugate function. The above method determines the conjugate function to any desired degree of approximation, but it is not possible to construct the torsion-function from it, as it does not satisfy the potential equation. It will, however, be shown in a subsequent paper how the method of the calculus of variations leads to a direct determination of the torsion-function.

LXXX. *On the Torsion Problem of the Theory of Elasticity.*  
By Dr. N. M. BASU \*.

1. **T**HE solution of the torsion problem of the Theory of Elasticity consists in the determination of a function  $\phi(x, y)$ , called the *torsion-function*, which at all inner points of a plane area  $T$  satisfies the potential equation

$$\nabla_1^2 \phi \equiv \frac{\partial^2 \phi}{\partial x^2} + \frac{\partial^2 \phi}{\partial y^2} = 0, \quad . \quad . \quad . \quad . \quad . \quad (1)$$

while at the boundary  $S$  has the outward normal derivative given by

$$\frac{\partial \phi}{\partial n} = ly - mx, \quad . \quad . \quad . \quad . \quad . \quad (2)$$

$l, m$  being the direction-cosines of the outward-drawn normal.

The usual method of determination of  $\phi$  consists in solving the boundary value problem for the conjugate function

\* Communicated by the Author.

$\psi(x, y)$ , i. e., a function which at all inner points of  $T$  satisfies the equation

$$\nabla_1^2 \psi = 0, \quad . \quad . \quad . \quad . \quad . \quad (3)$$

while at the boundary  $S$

$$\psi = \frac{1}{2}(x^2 + y^2) + \text{a constant.} \quad . \quad . \quad . \quad . \quad (4)$$

Although the existence of the solution in all cases where the boundary is suitable is known from the usual Potential Theory, it is not an easy matter to construct the solution except when the boundary consists of one or more very simple curves. In the present paper it is proposed to give a general method of solving the problem which is applicable to a wide class of problems, and is specially suitable for numerical computations.

2. Let the area under consideration be a singly-connected region  $T$ , of which the boundary  $S$  is an analytic curve possessing continuous tangent and curvature. In these circumstances we are assured by the usual potential theory of the existence of a regular potential function  $\psi$  satisfying the equations (3) and (4), and therefore also of the torsion-function  $\phi$  satisfying the equations (1) and (2). It is obvious that the solution contains an arbitrary constant and is otherwise unique. Since, however, the addition of an arbitrary constant implies a rigid body displacement, we shall suppose  $\phi$  uniquely determined by adjusting the constant in such a manner that  $\phi$  vanishes at a given point, say the origin of coordinates. Let  $\phi = u(x, y)$  denote this unique solution of the boundary value problem for  $\phi$ . We now consider the following problem in the calculus of variations :

*"Of all functions  $w$  vanishing at the origin which together with their first derivatives are continuous in  $T + S$  and have continuous or piecewise continuous second derivatives in  $T$  to determine that one which makes the Integral*

$$I[w] \equiv \iint_T \left[ \left( \frac{\partial w}{\partial x} - y \right)^2 + \left( \frac{\partial w}{\partial y} + x \right)^2 \right] dx \, dy$$

*taken over the area  $T$ , a minimum."*

It is clear that there are functions of the specified class for which  $I[w]$  exists and that  $I[w]$  is bounded below, so that the minimum problem formulated above has a sense. We shall first show that if the problem has a solution this solution must be unique. For, if possible, let  $v_1$  and  $v_2$  be two independent solutions each furnishing the same minimum value, say  $d$ , so that

$$I[v_1] = I[v_2] = d.$$

Writing  $v_1 - v_2 = \zeta$ , we have

$$\begin{aligned} I[v_1] &= I[v_2 + \zeta] \\ &= I[v_2] + D[\zeta] + 2K[v_2, \zeta], \end{aligned}$$

where

$$D[\zeta] = \iint_T \left[ \left( \frac{\partial \zeta}{\partial x} \right)^2 + \left( \frac{\partial \zeta}{\partial y} \right)^2 \right] dx dy$$

and

$$K[v_2, \zeta] = \iint_T \left[ \left( \frac{\partial v_2}{\partial x} - y \right) \frac{\partial \zeta}{\partial x} + \left( \frac{\partial v_2}{\partial y} + x \right) \frac{\partial \zeta}{\partial y} \right] dx dy.$$

Since  $v_1$  and  $v_2$  belong to the class of admissible functions,  $\zeta$  also belongs to the same class. Hence, in accordance with well-known principles of the calculus of variations;

$$K[v, \zeta] = 0.$$

Thus we must have

$$D[\zeta] = 0,$$

whence, on account of the continuity of  $\zeta$  and its first derivatives,  $\zeta$  must be a constant, which, again, must be zero, as  $\zeta$  is zero at the origin. Thus the solution, if it exists, must be unique.

We shall now show that the function  $u$  mentioned above does actually solve the minimum-problem. Let us consider any admissible function  $w$ , and let  $w - u = \eta$ . Then, in accordance with the notation used above,

$$I[w] = I[u] + D[\eta] + 2K[u, \eta].$$

Using Green's transformation formula, we have

$$\begin{aligned} K[u, \eta] &= - \iint_T \eta \nabla_1^2 u \, dx dy + \int_S \eta \left( \frac{\partial u}{\partial n} - ly + mx \right) ds \\ &= 0, \end{aligned}$$

since  $u$  is the torsion-function and satisfies the equations (1) and (2). Thus

$$I[w] \geq I[u],$$

and the sign of equality holds only when

$$D[\eta] = 0,$$

i. e., when

$$\eta = \text{a constant} = 0,$$

since  $\eta$  must be 0 at the origin. We thus conclude that *the solutions of both problems exist and that they are identical.*

3. We shall now show that for the class of problems under consideration the torsion-function  $u$ , together with its first derivatives, can be approximated as closely as we please in the closed region  $T+S$  by means of a series in the harmonic polynomials

$$1, x, y, x^2 - y^2, xy, \dots$$

If we denote the conjugate function of  $u$  by  $v$ , then

$$u + iv = f(z),$$

where  $f(z)$  stands for a regular analytic function of the complex variable  $z$  in the region  $T$ . Now, since on  $S$   $v = \frac{1}{2}(x^2 + y^2) + \text{a constant}$ ,  $v$  is analytic on the boundary  $S$ , which is an analytic curve and is a regular potential function inside the region  $T$ . Hence  $v$  can be analytically continued\* over the boundary  $S$ , that is, there exists a regular potential function  $V$  in a region  $T'$  of which  $T+S$  is a partial region, and such that  $V=v$  in  $T+S$ . It follows that there exists a regular analytic function  $F(z)$  in  $T'$  such that  $F(z)=f(z)$  in  $T+S$ . Now, in accordance with Runge's Theorem† we can approximate  $F(z)$  in every partial region of  $T'$ , and therefore in  $T+S$ , as closely as we please by means of a polynomial in  $z$ . Since  $u(x, y)$  is the real part of  $F(z)$  in  $T+S$ , the assertion made above is established, since the harmonic polynomials are nothing but the real and imaginary parts of powers of  $z$ .

4. We now restrict the admissible functions  $w$  to only such functions as are regular potential functions in  $T$ , and can, together with their first derivatives, be approximated as closely as we please in  $T+S$  by a series of harmonic polynomials. This does not imply any real limitation, nor is the minimum value thereby altered, as the solution of the problem is now known to belong to this restricted class of functions.

Let  $\psi_1, \psi_2, \psi_3, \psi_4, \dots$  stand for the harmonic polynomials  $x, y, x^2 - y^2, xy, \dots$ , the constant 1 being left out of consideration as  $w$  is to be zero at the origin. Let  $u_n$  be the  $n$ th approximation to  $u$  according to Runge's Theorem, so that  $u_n$  is of the form

$$u_n = c_1\psi_1 + c_2\psi_2 + \dots + c_n\psi_n,$$

\* See Goursat, 'Cours d'Analyse Mathématique,' tome iii.

† See Bieberbach, 'Funktionentheorie,' Bd. I.

where  $c_1, c_2, \dots c_n$  are constants. If  $w_n$  be that function of the class  $C_n^\dagger$  which makes  $I[w]$  a minimum, then

$$I[u_n] \geq I[w_n] \geq d.$$

But since when  $n$  increases indefinitely  $u_n$  tends to  $u$  and the first derivatives of  $u_n$  tend to those of  $u$ , it follows that

$$\lim_{n \rightarrow \infty} I[u_n] = I[u] = d.$$

Hence

$$\lim_{n \rightarrow \infty} I[w_n] = d.$$

Thus  $w_1, w_2, \dots w_n, \dots$  form a minimal sequence. If we can now show that the sequence  $w_1, w_2, \dots$  does tend to a limiting function  $w$ , which vanishes at the origin and which, together with its derivatives, is continuous in  $T$  and such that

$$I[w] = d,$$

then  $w$  will be the required solution.

5. To prove the convergence of the sequence we shall require the following convergence theorem :

*“If  $\phi_1, \phi_2, \dots$  denote a sequence of regular potential functions having a given value at a fixed point in a given region  $T$ , such that*

$$\lim_{\substack{m \rightarrow \infty \\ n \rightarrow \infty}} D[\phi_m - \phi_n] = 0,$$

*then the sequence converges uniformly towards a regular potential function  $\phi$ , and the partial derivatives of the sequence converge towards the corresponding partial derivatives of  $\phi$  in every partial region  $T^*$  of  $T$ .*

We prove the theorem in the following way. Without loss of generality we take the given value as 0 and the given point as the origin. Put

$$\frac{\partial \phi_m}{\partial x} = \theta_m, \quad \frac{\partial \phi_m}{\partial y} = \chi_m.$$

Then it follows that  $\theta_m$  and  $\chi_m$  are regular potential functions in  $T$ , and that

$$\lim_{\substack{m \rightarrow \infty \\ n \rightarrow \infty}} \iint (\theta_m - \theta_n)^2 dx dy = 0, \quad \lim_{\substack{m \rightarrow \infty \\ n \rightarrow \infty}} \iint (\chi_m - \chi_n)^2 dx dy = 0,$$

$\dagger$  A function of the type  $a_1\psi_1 + a_2\psi_2 + \dots + a_n\psi_n$  where,  $a_1, a_2, \dots a_n$  are constants, will be called a function of the class  $C_n$ .

the integrals being taken over  $T$  or any partial region of the same. Hence by a well-known theorem\* the sequences  $\theta_1, \theta_2, \dots$  and  $\chi_1, \chi_2, \dots$  converge uniformly to regular potential functions, and so also do their partial derivatives. Let these limiting functions be denoted by  $p$  and  $q$ . Then  $\frac{\partial \theta_m}{\partial y}$  and  $\frac{\partial \chi_m}{\partial x}$  also converge uniformly to  $\frac{\partial p}{\partial y}$  and  $\frac{\partial q}{\partial x}$  respectively. But

$$\frac{\partial \theta_m}{\partial y} - \frac{\partial \chi_m}{\partial x} = 0 \text{ for all } m.$$

Hence

$$\frac{\partial p}{\partial y} - \frac{\partial q}{\partial x} = \lim \left( \frac{\partial \theta_m}{\partial y} - \frac{\partial \chi_m}{\partial x} \right) = 0.$$

Thus there exists a function  $\phi$  such that

$$\frac{\partial \phi}{\partial x} = p = \lim_{m \rightarrow \infty} \frac{\partial \phi_m}{\partial x},$$

and

$$\frac{\partial \phi}{\partial y} = q = \lim_{m \rightarrow \infty} \frac{\partial \phi_m}{\partial y}.$$

Now

$$\begin{aligned} \lim \phi_m(P) &= \lim \int_0^P \left( \frac{\partial \phi_m}{\partial x} dx + \frac{\partial \phi_m}{\partial y} dy \right) \\ &= \int_0^P \left( \frac{\partial \phi}{\partial x} dx + \frac{\partial \phi}{\partial y} dy \right) \\ &= \phi(P), \end{aligned}$$

$\phi(0)$  being chosen to be zero. It is easily seen that  $\phi(P)$  is a potential function, and the convergence of the partial derivatives follow without difficulty. Thus the theorem is proved.

6. Since  $w_n$  is that function of the class  $C_n$  for which  $I[w]$  has its minimum value, it follows by the usual principles of the calculus of variations and with the notations of Art. 2 that

$$K[w_n, \zeta_n] = 0$$

for every admissible function  $\zeta_n$  of class  $C_n$ . Now, if  $m < n$ ,  $\zeta_n = w_n - w_m$  is obviously a function of the class  $C_n$ , hence

$$K[w_n, w_n - w_m] = 0.$$

\* See Kellogg, 'Foundations of Potential Theory,' p. 268, Theorem X.



On the other hand,

$$\begin{aligned} I[w_m] &= I[w_n + w_m - w_n] \\ &= I[w_n] + D[w_m - w_n] + 2K[w_n, w_m - w_n] \\ &= I[w_n] + D[w_m - w_n]. \end{aligned}$$

But

$$\lim I[w_m] = \lim I[w_n] = d.$$

Hence

$$\lim D[w_m - w_n] = 0.$$

In accordance with the convergence theorem proved in the preceding article, it follows that the sequence  $w_1, w_2, \dots, w_n, \dots$  converges uniformly to a regular potential function  $w$  in every partial region  $T^*$  of  $T$ . The same is also true in regard to the sequence of the derivatives which converges to the derivative of  $w$ . It then follows that

$$\lim_{n \rightarrow \infty} I_{T^*}[w_n] = I_{T^*}[w].$$

If we define the integral over the region  $T$  as the limit of the integral over the region  $T^*$  as  $T^*$  approaches  $T$  as a limit, we have

$$I_T[w_n] \geq I_{T^*}[w_n].$$

Therefore

$$\lim_{n \rightarrow \infty} I_T[w_n] \geq \lim_{n \rightarrow \infty} I_{T^*}[w_n] = I_{T^*}[w] \text{ for every } T^*,$$

or

$$d = \lim I_T[w_n] \geq I_T[w].$$

But since  $d$  is the minimum value of the integral, we must have

$$I_T[w] \geq d$$

Hence

$$\lim I_T[w_n] = I_T[w] = d.$$

Thus the function  $w$  is a solution of the minimum problem, and, as explained in Art. 2, must be identical with the torsion-function  $u$ .

We have thus a method for constructing the torsion-function in a convergent infinite series of simple polynomials applicable to all cases where the region under consideration is of the kind considered in this paper.

7. If the boundary of the area, instead of being a single analytic curve, consists of a finite number of pieces of analytic curves cutting at definite angles, then the arguments of Art. 3 are not wholly applicable, for in this case the larger region  $T'$  referred to there will not necessarily contain

the angular points as inner points. If, however, we assume that the torsion-function is such that it admits of analytical continuation also at these angular points, then the subsequent arguments hold *in toto*, and we can construct the torsion-function exactly as before. Having regard to the physical nature of the problem, it seems quite reasonable to make this assumption. To test the validity of the assumption and the power of the method detailed above the case of the prism with square section has been worked out, and the result compared with the known result due to Saint Venant, with which it is found to agree very closely. The details of the calculations are given in the following paragraph.

8. We shall find successive approximations to the function  $w$  which makes the integral  $I[w]$  defined in Art. 2 a minimum—that is, we shall construct the sequence  $w_1, w_2, \dots$ . To avoid unnecessary troubles of calculation we shall make use of the results obtained in the previous paper\*. For this purpose we put

$$w = xy - v(x, y).$$

Then we have  $I[w] = -2J[v]$ ,

where  $J$  is the integral defined in Art. 4 of the paper referred to above. Thus the problem is to find the function  $v$  which makes the integral  $J[v]$  a maximum, the co-ordinate functions being the plane harmonic polynomials  $\psi_1, \psi_2, \psi_3, \dots$  of Art. 4. To determine the  $n$ th approximation we assume

$$v = a_1\psi_1 + a_2\psi_2 + \dots + a_n\psi_n,$$

and substituting in  $J$ , determine the values of  $a_1, a_2, \dots, a_n$  which make  $J$  a maximum. It will be found that the equations fall into two groups, one of these groups being a group of homogeneous linear equations in those members of the constants  $a_1, a_2, \dots, a_n$  which are associated with the polynomials of odd degree and those polynomials of even degree in which the variables  $x, y$  occur in their even powers. These constants are therefore 0. We have therefore to consider only the polynomials of the following type:—

$$xy, x^2y - xy^3, 3x^5y - 10x^3y^3 + 3xy^5, \dots$$

As a first approximation we have already found in the paper mentioned

$$v = xy - \frac{7}{18}(x^3y - xy^3),$$

whence

$$w_1 = \frac{7}{18}(x^3y - xy^3).$$

\* "On an Application of the New Methods of the Calculus of Variations to some Problems in the Theory of Elasticity," *suprà*, p. 886.

### 904 *The Torsion Problem of the Theory of Elasticity.*

To determine a second approximation we assume

$$v = axy + b(x^3y - xy^3) + c(3x^5y - 10x^3y^3 + 3xy^5) \\ + d(x^7y - 7x^5y^3 + 7x^3y^5 - xy^7).$$

We find, retaining five decimal places,

$$a=1, b=-.36255, c=0, d=.02147.$$

Hence, as a second approximation we get

$$w_2 = .36255(x^3y - xy^3) - .02147(x^7y - 7x^5y^3 + 7x^3y^5 - xy^7).$$

Following the method of the paper mentioned, it is easy to show that, if  $w_n$  denotes the  $n$ th approximation for  $w$ , then

$$I[w_n] = \iint \left[ x^2 + y^2 + x \frac{\partial w_n}{\partial y} - y \frac{\partial w_n}{\partial x} \right] dx dy.$$

Hence if  $M[w_n]$  denotes the value of the twisting couple calculated with the  $n$ th approximation  $w_n$ , we have

$$M[w_n] = \mu\tau I[w_n] = -2\mu\tau J[v_n],$$

so that, calculating for the second approximation, we get

$$M[w_2] = 2.2494\mu\tau.$$

Again, in the paper under reference it has been shown that the maximum value of  $J[v]$  is exactly equal to the minimum value of the integral (there denoted by  $I[u]$ )

$$I'[u] = \frac{1}{2} \iint \left[ \left( \frac{\partial u}{\partial x} \right)^2 + \left( \frac{\partial u}{\partial y} \right)^2 - 4u \right] dx dy,$$

and that the minimum value of  $I'[u]$  is less than or equal to

$$I'[u_2] = -\frac{252.72016}{225} = -1.1232.$$

Thus if  $M$  denotes the true value of the twisting couple we must have

$$2.2494\mu\tau \geq M \geq -2\mu\tau(-1.1232) = 2.2464\mu\tau.$$

This shows that the error in taking  $2.2494\mu\tau$  as the value of the twisting couple as calculated with the second approximation  $w_2$  does not exceed about 1 in 750. The deviation from Saint Venant's result ( $2.2492\mu\tau$ ) is only  $.0002\mu\tau$ , which is about 1 in 12,000. The agreement is extraordinarily good.

We thus conclude that the expression  $w_2$  obtained above may be used as the required torsion-function for all practical purposes. If greater exactness be required higher approximations may be calculated without difficulty.

LXXXI. *Early Developments in A.C. Circuit Theory. Some Notes on the Application of Complex Methods to the Solution of A.C. Circuit Problems.* By G. WINDRED\*.

(1) *Neglect of the Theory in England.*

THE first application, in America more than thirty years ago, of the method of complex numbers to the solution of problems in alternating-current circuit theory was a highly important step—one which has, however, received very much less subsequent attention than is warranted by its extreme practical importance.

This circumstance applies particularly to England, which has contributed practically nothing to the furtherance of the subject, although, strangely enough, the names of many English mathematicians are encountered in the history of the purely mathematical applications of complex numbers †.

Relatively few English text-books of electrical theory contain any reference to the use of complex methods, and where such reference does occur the bare fundamentals are stated; their development and application are left to the reader's unpracticed imagination.

It must here be remarked that such extension of elementary principles is not so simple as is conveniently assumed in these text-books. The application of complex methods to subjects in which any degree of complexity is reached may be attended with considerable mathematical difficulty.

Under these conditions progress is of necessity slow, as is amply attested by the almost complete neglect of the subject in this country.

Perhaps the most notable exception to this general tendency of English text-books is Dr. Alexander Russell's 'Treatise on the Theory of Alternating Currents,' 2nd ed. Cambridge, i. (1914), in chapter vii. of which the theory is developed in sufficient mathematical detail to give a clear insight into the fundamentals of its application.

Some of the more advanced parts of the theory are touched upon in arts. 522, 537, and 583*a* of Sir J. H. Jeans's 'Mathematical Theory of Electricity and Magnetism,' 5th ed. Cambridge (1927), which presupposes a previous

\* Communicated by the Author.

† See the author's paper "History of the Theory of Imaginary and Complex Quantities," 'Mathematical Gazette,' xiv. pp. 533-541 (Oct. 1929).

reading of the theory of complex numbers, although an outline of the theory is given in arts. 309 *et seqq.*, introductory to conjugate functions and problems in two dimensions.

These last two subjects are somewhat outside the scope of the present inquiry, but a recent paper by Dr. F. W. Carter, making use thereof, has given rise to an interesting (even if somewhat heated) discussion which has a bearing on our present considerations. This paper, entitled "The Magnetic Field of the Dynamo-Electric Machine," Journ. I. E. E. lxiv. pp. 1115-1138, sets forth in an admirable manner the applications of the theory of conjugate functions to the solution of such two-dimensional problems as occur in connexion with the magnetic circuits of dynamo-electric machinery. In the discussion of this paper—which will well repay the careful attention of the student of mathematical physics—several papers and books of a fundamental nature are quoted. In general the discussion affords an excellent perspective of the confused state of the theory, and the misapprehension which exists concerning its first applications.

## (2) *Systematic Use in America and Germany.*

Among American and German theorists full use has been made of the theory of complex numbers in its applications to electrical circuit theory, with a consequent simplification of the attendant calculations, together with a more elegant means of exposition.

It must be evident that more elegant methods of analysis inevitably tend to simplify operations, and it is further obvious that such methods are not attended with such risks of error as exist with the more cumbersome methods of working.

With reference to the introduction of vector analysis into electrical calculations, Oliver Heaviside, whose opinion on such matters is far above question, has written:—

"The notorious difficulty of understanding and working Quaternions will always be a bar to their serious practical use by any but mathematical experts. But, on the other hand, a vector algebra and analysis of a simple kind, independent of the quaternion, and readily understandable and workable, can with great advantage take the place of much of the usual cumbrous Cartesian investigations, and be made generally useful in all physical mathematics concerning vectors, and be employed, comparatively speaking, by the multitude" \*.

\* Page xi of the Preface to his 'Collected Papers,' i. (1892).

The general method of complex numbers is such a method as Heaviside here describes.

It is a significant fact that this accomplished investigator employed complex methods frequently in his calculations; his work is an example of mathematical exposition, and it is evident that he clearly recognized the scope afforded by such methods in the solution of many of his original and difficult problems.

It appears that Heaviside was the first to apply imaginary Bessel functions to the problem of oscillatory induced currents in cores. This application is found in §10 of a series of papers contributed to 'The Electrician' \* in 1884 and 1885, in which the mathematical side of the problem is treated exhaustively. The subject has also received the attention of Lord Kelvin †, who introduced his "bei" and "ber" functions ‡ in this connexion.

Apart from these isolated examples of the use of complex methods in applied mathematics, we find little else of importance in English scientific literature. This applies in particular to electrical circuit theory, with which we are at present concerned; no effort has been made in this branch of electrical theory to obtain the benefits of complex representation.

In Germany the method has been freely adopted in electrical circuit theory, and has found its way into standard electrical text-books. Thus, in Dr. Adolf Thomälen's well-known treatise on 'Electrical Engineering' (Eng. trans. by A. W. O. Howe; Arnold) we find, on pp. 467 *et seqq.*, a lucid exposition suited to direct use in practical problems.

In America the development has been perhaps greater than in Germany, mainly on account of the efforts of Dr. Steinmetz in this direction. Practically all of his published works contain extensive applications of complex numbers, which, as we shall see later, he did much to develop in connexion with electrical circuit theory. In point of fact the present state of development of this part of the subject is almost entirely due to the efforts of Steinmetz, although it appears that he was not, as is generally supposed, responsible for the first inception of these methods. A true perspective of this development is afforded by a brief historical retrospect, to which we now proceed.

\* 'The Electrician,' xiii, pp. 583 *et seqq.*

† Journ. I. E. E. xviii, p. 4 (Jan. 1889); also British Association Report, p. 736 (1890).

‡ See also Russell, 'Alternating Currents,' ch. xvi.

(3) *Analytical Methods of Oliver Heaviside.*

Oliver Heaviside's electrical papers abound with original mathematical methods. In view of the facility with which he devised and applied these methods it is to be expected that in the mathematical branches of electrical theory he was considerably ahead of his contemporaries. This fact is proved by the long period which elapsed before the proper appreciation of this part of his work.

Examination of his numerous papers makes it evident that Heaviside never failed to obtain a solution to his problem on account of unsuitable mathematical methods. In this respect he was quite independent of convention, but at the same time highly conscious of the necessity for mathematical rigour. Thus his works bear the mark of accurate analysis from logically founded principles.

We have previously remarked upon Heaviside's use of imaginary Bessel functions. In other instances he made extensive use of the properties of imaginary functions, but from the present viewpoint the most important piece of analysis is contained in part v.\* of a series of papers contributed to the 'Philosophical Magazine' in the years 1886 and 1887, "On the Self-Induction of Wires."

The problem concerns the circuit conditions in a homogeneous line of length  $l$ , resistance  $R$ , and inductance  $L$ , acted upon at one end by an impressed force  $V_0 \sin nt$ .

With a current  $C$  in the line, and a potential-difference  $V$  at distance  $z$  from the transmission end of the line, the fundamental line-equations are

$$\left. \begin{aligned} -\frac{dC}{dz} &= \left( K + S \frac{d}{dt} \right) V, \\ -\frac{dV}{dz} &= R''C, \end{aligned} \right\} \dots \dots (1)$$

where  $K$  and  $S$  are the conductance of the insulator and the electric capacity respectively, and  $R'' = R' + L'(d/dt)$  in the periodic case,  $R'$  and  $L'$  being the ultimate values of  $R$  and  $L$  at the given frequency.

If the terminal conditions be represented by

$$\left. \begin{aligned} V &= Z_1 C \text{ in the case where } z=l, \\ -V_0 \sin nt + V &= Z_0 C \text{ in the case where } z=0, \end{aligned} \right\} (2)$$

\* Phil. Mag. p. 10 (Jan. 1887). Heaviside's operational methods have recently received considerable attention; see, e.g., Ernst J. Berg, 'Heaviside's Operational Calculus,' New York, 1920. The theory we are at present using has also received the attention of Lord Rayleigh, cf. 'Theory of Sound,' Cambridge, i. 1894, arts. 235p, 235u, 235x.

then  $V = Z_0 C$  is the terminal condition when  $z = 0$  if there be no impressed force.

To obtain the solution Heaviside takes the equation \*

$$C_1 = (\cos mz + q_1 \sin mz) \frac{\cos mz_2 + q_0 \sin mz_2}{(m/S'')(q_0 - q_1)} e_2,$$

of which the required solution is a special case. In the above equation  $\cos mz$  and  $\sin mz$  are the normal current-functions in a homogeneous line, neglecting variability of electrical constants†,  $m$  is the function of  $p$  given by  $-m^2 = R''S''$ , and  $q_0$  and  $q_1$  are respectively

$$q_0 = -\frac{S''}{m} Z_0,$$

$$q_1 = \frac{(m/S'') \sin ml - Z_1 \cos ml}{(m/S'') \cos ml + Z_1 \sin ml}.$$

If in the given equation we take

$$S'' = K + S \frac{d}{dt},$$

$$R'' = R' + L' \frac{d}{dt},$$

and put  $F^2$  for  $-m^2 = R''S'' = (K + Sp)(R' + L'p)$ , we obtain, by taking  $z_2 = 0$ ,  $e_2 = V_0 \sin nt$ , and putting the equation in the exponential form,

$$C = \frac{\left(\frac{F}{S''} + Z_1\right) e^{F(l-z)} + \left(\frac{F}{S''} - Z_1\right) e^{-F(l-z)}}{e^{Fl} \left(\frac{F}{S''} + Z_1\right) \left(\frac{F}{S''} - Z_0\right) - e^{-Fl} \left(\frac{F}{S''} - Z_1\right) \left(\frac{F}{S''} + Z_0\right)} V_0 \sin nt. \quad \dots (5)$$

If now in  $F$ ,  $S''$ ,  $Z_0$ , and  $Z_1$  we take  $d^2/dt^2 = -n^2$ , we can put

$$C = \frac{P' + Q' \frac{d}{dt}}{A' + B' \frac{d}{dt}} V_0 \sin nt = \frac{(A'P' + B'Q'n^2) + (A'Q' - B'P') \frac{d}{dt}}{A'^2 + B'^2 n^2} V_0 \sin nt, \quad (6)$$

\* Phil. Mag. p. 419 (Nov. 1886), *vide* equations (162 b).

† *Ibid.* equations (174), (160 b).



which is the complete expression for the amplitude and phase difference at any point. For the amplitude we have

$$C_0 = V_0(A'^2 + B'^2 n^2)^{-\frac{1}{2}}(P'^2 + Q'^2 n^2)^{-\frac{1}{2}}, \quad \dots \quad (7)$$

in which expression  $A'$  and  $B'$  are constant and  $P'$  and  $Q'$  are functions of  $z$ .

We come now to the most important part of this analysis from the present viewpoint. Heaviside puts

$$\left. \begin{aligned} F &= P + Qi, \\ Z_1 &= R_1' + L_1' ni, \\ -Z_0 &= R_0' + L_0' ni, \end{aligned} \right\} \dots \dots \dots (8)$$

where  $ni = p \quad \text{and} \quad i = \sqrt{-1},$

and obtains

$$P = (\frac{1}{2})^{\frac{1}{2}} \{ (R'^2 + L'^2 n^2)^{\frac{1}{2}} (K^2 + S^2 n^2)^{\frac{1}{2}} + (KR' - L'Sn^2) \}^{\frac{1}{2}},$$

$$Q = (\frac{1}{2})^{\frac{1}{2}} \{ (R'^2 + L'^2 n^2)^{\frac{1}{2}} (K^2 + S^2 n^2)^{\frac{1}{2}} - (KR' - L'Sn^2) \}^{\frac{1}{2}}.$$

The complex form of the expressions in (8) for the impedances should be particularly noted, although it must be remarked that up to the end of the investigation we are now using Heaviside makes no direct application of this form of the impedance equation.

#### (4) *Early Papers of Dr. A. E. Kennelly.*

In the 'Transactions of the American Institute of Electrical Engineers' for April 1893, x. pp. 175-216, we find what is evidently the first application of complex quantities to problems in electrical technology, contained in a paper on "Impedance" by A. E. Kennelly. This paper, which was read on 18th April, 1893, is of fundamental importance on account of its treatment of practical problems by the method of complex quantities. It is also the first paper to give a consistent account of this method in its application to alternating-current circuit theory.

On page 186 of the paper Dr. Kennelly points out that all continuous-current corollaries from Ohm's law become applicable to harmonic currents when the admittances and impedances are treated vectorially, and that Kirchhoff's laws, while true of instantaneous conditions in alternating-current circuits, can only be applied when the currents are all in phase, and arithmetical operations with the circuit constants are permissible. In any other circumstances vectorial methods are necessary, and some form of vectorial algebra is required for the complete analysis of the circuit conditions.

Referring to these observations Dr. Kennelly makes the following important statement :—

“Any combination of resistances, non-ferric inductances, and capacities, carrying harmonically alternating currents, may be treated by the rules of unvarying currents, if the inductances are considered as resistances of the form  $pl\sqrt{-1}$ , and the capacities as resistances of the form  $-\frac{1}{kp}\sqrt{-1}$ , the algebraic operations being then performed according to the laws controlling ‘complex quantities.’”

In the expressions mentioned,  $p=\omega=2\pi f$ , where  $f$  is the frequency,  $l$  the inductance, and  $k$  the capacity of the circuit. These forms are identical with modern practice ; they have been applied extensively by their inventor and by the late Dr. C. P. Steinmetz, whose work we consider hereafter.

A further paper by Dr. Kennelly, “On the Fall of Pressure in Long Distance Alternating Current Conductors,” published in the ‘Electrical World,’ New York, Jan. 6th, 1894, xxiii. pp. 17-19, introduces the system of vectorial notation developed by this author, in which the disposition of an angle with respect to its components is indicated by one of the forms  $\angle\theta$ ,  $\sqrt{\theta}$ ,  $\overline{\theta}$ . In electrical work this system has evident advantages over the algebraical forms, since it indicates at once the nature of the angular component of any expression.

The paper is concerned with the rigorous computation of the fall of pressure in alternating-current lines of known constants. The author makes use of the two fundamental relations

$$U = u \cosh Lz + yi \sinh Lz,$$

$$I = i \cosh Lz + \frac{u}{y} \sinh Lz,$$

which are based on Oliver Heaviside’s solution\* of the differential equations of an alternating current line, and which represent respectively the pressure and current at any point of the line, where  $u$  is the pressure at the receiving end,  $L$  is the distance between the supply end and the receiving end,  $i$  is the load current, and  $y$  and  $z$  are given by the expressions

$$y = \left[ \frac{r + j\omega l}{g + j\omega c} \right]^{\frac{1}{2}}, \quad z = [(r + j\omega l)(g + j\omega c)]^{\frac{1}{2}},$$

\* Vide ‘Electromagnetic Theory,’ i. pp. 451-452 (1893).

where  $r$  = resistance of line per unit length,  
 $l$  = inductance of line per unit length,  
 $g$  = leakage conductance of line per unit length,  
 $c$  = capacity of line per unit length,  
 $\omega = 2\pi f$ ,  
 and  $j = \sqrt{-1}$ .

The values of the necessary constants are worked by vectorial analysis, and applied to the solution of a typical transmission line problem with arbitrarily assigned circuit constants, a comparison being made between two specimen lines from which the effects of high pressure on the neutralizing electrostatic action are made evident.

In the foregoing investigation the forms of the expressions for  $y$  and  $z$  should be particularly noted. They represent a practical extension of the same author's preliminary statement which we have already quoted.

The practical application of complex quantities is further extended by Dr. Kennelly in his treatise on 'The Application of Hyperbolic Functions to Electrical Engineering Problems,' University of London Press, 3rd ed. (1925), in chapter v. of which the subject is exhaustively treated in its relation to the types of electrical problems with which this work is concerned.

#### (5) *Development by Dr. C. P. Steinmetz.*

Since the appearance of Dr. Kennelly's papers of 1893 and 1894 the subject has received considerable extension, notably, as we have already observed, in America, where the contributions of the late Dr. C. P. Steinmetz are the most outstanding in this connexion. His extensive paper on "Complex Quantities and their Use in Electrical Engineering,"\* before the International Electrical Congress of Chicago in August 1893, contains an extension of Dr. Kennelly's work, and gives, for the first time, a generalization of Kirchhoff's laws to the inclusion of alternating-current phenomena. The majority of Dr. Steinmetz's works† on alternating-current theory contain applications of complex methods, which are also to be found in many of his electrical papers.

\* Proc. Int. El. Congress, A.I.E.E., pp. 33-74, also pp. 24, 25 (1894).

† A demonstration of complex quantities is contained in his 'Theoretical Elements of Electrical Engineering,' 3rd ed. New York, 1909, art. 14, pp. 83 *et seqq.* Cf. also 'Theory and Calculation of Alternating-Current Phenomena,' New York, 1897.

This circumstance has resulted in a general opinion that the inception of these methods is due to him, but, as we have shown above and as Dr. Kennelly has already pointed out\*, their origin rests elsewhere.

The priority of Dr. Kennelly is acknowledged by Steinmetz himself in his discussion† of Dr. Kennelly's paper on "Impedance," wherein he remarks, with reference to the mathematical treatment of vector quantities:—"It is, however, the first instance here, so far as I know, that attention is drawn by Mr. Kennelly to the correspondence between the electrical term 'impedance' and the complex numbers." Steinmetz also adds:—"The importance hereof lies in the following: the analysis of the complex plane is very well worked out, hence, by reducing the electrical problems to the analysis of complex quantities they are brought within the scope of a known and well understood science."

At the hands of Steinmetz the method of complex quantities has received considerable development in its application to electrical engineering problems. The present state of development is, however, also due to many of his contemporaries, as well as more recent exponents of electrical theory, a circumstance which makes the bibliography of the subject very extensive.

In the course of its application to alternating-current problems the method of complex quantities has become closely related to circular trigonometry. The theory of circular and hyperbolic functions of a complex angle is of considerable importance in electrical theory‡, and has been applied to numerous problems in this connexion; thus it may be regarded as an extension of complex methods, and must be included in our bibliography of the subject.

In the appended bibliography, arranged in historical order, are given the most important relevant papers and

\* In a letter addressed to Dr. E. W. Rice, Jr., discussing this writer's article on "Charles Proteus Steinmetz" in the 'General Electric Review,' xxvi. no. 12, pp. 796-799 (Dec. 1923). *Vide* Gen. El. Rev. xxvii. no. 2, pp. 132-133 (Feb. 1924).

† *Vide* Trans. A.I. E. E. x. p. 227 *et seqq.* (April 1893).

‡ The 'Tables of Complex Hyperbolic and Circular Functions,' by A. E. Kennelly, Harvard University Press, contains functions of  $p/8$  to  $p=3.0$  by steps of 0.1 and to  $\delta=45^\circ$  to  $90^\circ$ , together with functions of  $x+iq$  to  $x=10$ , by steps of 0.05, and to  $q=\text{inf.}$  (virtually) by steps of 0.05.

The same author's 'Chart Atlas of Complex Hyperbolic and Circular Functions,' Harvard University Press, contains curves of the above-mentioned calculations, to facilitate graphical computation.

works concerning both pure and applied theory. It must, however, be pointed out that the list is of necessity incomplete on account of the dissociated nature of the majority of these publications and the consequent difficulty of obtaining references thereto.

### *Bibliography.*

Many of the papers and works quoted below are concerned with subjects other than electrical circuit theory. All, however, are related thereto either on account of the similarity of their subject-matter or of the mathematical methods employed therein.

- (1) A. B. Strehlke, "Über Periodische Kettenbrüche," *Grunert's Archiv der Mathematik und Physik*, xlii. p. 341 (1864).
- (2) W. Ligowski, 'Tafeln der Hyperbelfunctionen' (Berlin, 1890).
- (3) J. J. Thomson, "On the Heat produced by Eddy Currents in an Iron Plate exposed to an Alternating Magnetic Field," 'The Electrician,' xxviii. p. 599 (1891).
- (4) O. Heaviside, 'Electrical Papers,' 2 vols. (London, 1892).
- (5) O. Heaviside, 'Electromagnetic Theory,' 3 vols. (London, 1893-1912).
- (6) F. Bedell and A. C. Crehore, 'Alternating Currents' (New York, 1893).
- (7) A. E. Kennelly, "Impedance," *Trans. A. I. E. E.* x. p. 175 (April 1893).
- (8) C. P. Steinmetz, "Complex Quantities and their Use in Electrical Engineering," *Proc. of the International Electrical Congress, Chicago*, pp. 33-76 (Aug. 1893).
- (9) A. Macfarlane, "On the Analytical Treatment of Alternating Currents," *ibid.* pp. 24-32.
- (10) A. E. Kennelly, "Impedance of Mutually Inductive Circuits," 'The Electrician,' xxxi. pp. 699-700 (Oct. 27, 1893).
- (11) Lord Rayleigh, 'The Theory of Sound,' Cambridge, i. (1894), ii. (1896).
- (12) A. E. Kennelly, "On the Fall of Pressure in Long Distance Alternating-Current Conductors," 'Electrical World,' xxiii. no. 1, p. 17 (Jan. 1894).
- (13) C. P. Steinmetz, 'Theory and Calculation of Alternating Current Phenomena' (New York, 1897).
- (14) A. Macfarlane, "Application of Hyperbolic Analysis to the Discharge of a Condenser," *Trans. A. I. E. E.*, xiv. p. 163 (1897).
- (15) J. Hertzog and C. Feldman, 'Die Berechnung Elektrischer Leitungsnetze,' Berlin, i. (1903), ii. (1904).
- (16) A. Russell, 'A Treatise on the Theory of Alternating Currents' (Cambridge, 1904).
- (17) A. E. Kennelly, "The Alternating Current Theory of Transmission Speed over Submarine Telephone Cables," *Proc. Int. Elec. Congress, St. Louis, Sec. A*, i. pp. 68-105 (1904).
- (18) A. E. Kennelly, "Two Elementary Constructions in Complex Trigonometry," *Am. Annals of Maths.* 2nd ser. v. no. 4, pp. 181-184 (July, 1904).
- (19) A. Roessler, 'Die Fernleitung von Wechselströmen' (Berlin, 1905).

- (20) A. E. Kennelly, "The Expression of Constant and of Alternating Continued Fractions in Hyperbolic Functions," *Am. Annals of Maths.* ix. no. 2, pp. 85-96 (Jan. 1908).
- (21) W. Cramp and C. F. Smith, 'Vectors and Vector Diagrams Applied to the Alternating Current Circuit' (London, 1909).
- (22) Gáti Béla, "Wechselstrom als Träger von Telephonströmen," *E. T. Z.* Heft 39 (1909).
- (23) A. Russell, "The Coefficients of Capacity and the Mutual Attractions or Repulsions of Two Electrified Spherical Conductors when Close Together," *Proc. Roy. Soc. A*, lxxxii. (June, 1909).
- (24) F. Rusch, "Über die Wirbelstromverluste in Leitungskupfer der Wechselstromarmaturen," *Elek. und Maschinenbau* (Jan. 23 and 30, 1910).
- (25) Gáti Béla, "Über die Anwendung hyperbolischer Functionen auf weite Entfernungen wirkenden Telegraphen und Telephonströmen," *ibid.* Heft 33 (1910).
- (26) K. W. Wagner, "Über die Frequenz der Fernsprechröme," *Phys. Zeitschrift*, pp. 11122-27 (1910).
- (27) W. E. Miller, "Formulæ, Constants, and Hyperbolic Functions or Transmission Line Problems," *Gen. Elec. Rev.*, Suppl. (New York, May 1910).
- (28) A. E. Kennelly, "Vector Power in Alternating Current Circuits," *Proc. A. I. E. E.* pp. 1023-1025 (June 27, 1910).
- (29) F. Breisig, "Über die Energieverstellung in Fernsprechkreisen," *E. T. Z.* Heft 23, pp. 558-561; Heft 24, pp. 590-593 (June 1911).
- (30) A. E. Kennelly, "Tables of Hyperbolic Functions in Reference to Long Alternating Current Transmission Lines," *Proc. A. I. E. E.* pp. 2481-2492 (Dec. 1911).
- (31) A. E. Kennelly, "Tables of Sines, Cosines, Tangents, Cosecants, Secants, and Cotangents of Real and Complex Hyperbolic Angles," *Harvard Eng. Journal*, x. (Jan. 1912).
- (32) K. W. Wagner, "Eine neue künstliche Leitung zur untersuchung von Telegraphenströmen und Schaltvorgängen," *E. T. Z.* i. and ii. (1912).
- (33) D. C. and J. P. Jackson, 'Alternating Currents and Alternating Current Machinery' (New York, 1913).
- (34) J. H. Morecroft, "Hyperbolic Functions and their Application to Problems in Electrical Engineering," *The School of Mines Quarterly*, xxxiv. no. 3 (April 1913).
- (35) A. E. Kennelly, 'Tables of Complex Hyperbolic and Circular Functions,' Harvard University Press (1914).
- (36) A. E. Kennelly, 'Chart Atlas of Complex Hyperbolic and Circular Functions,' Harvard University Press (1914).
- (37) K. W. Wagner, "Über eine Formel von Heaviside zur Berechnung von Einschaltvorgängen," *Archiv für Elek.* iv. p. 159 (1916).
- (38) A. E. Kennelly, "A New Geometrical Model for the Orthogonal Projection of the Cosines and Sines of Complex Angles," *Proc. Amer. Acad. Arts and Sci.* liv. no. 5 (April 1919).
- (39) G. W. Pierce, "A Table and Method of Computation of Electrical Wave Propagation, Transmission Line Phenomena, Optical Refraction, and Inverse Hyperbolic Functions of a Complex Variable," *ibid.* lvii. no. 7 (April 1922).
- (40) J. R. Carson, "The Heaviside Operational Calculus," *Bell. Syst. Tech. Journ.* (Nov. 1922).

- (41) A. Boyajian, "Physical Interpretation of Complex Angles and their Functions," *Trans. A. I. E. E.* (Feb. 1923).
- (42) J. B. Pomey, "Le Calcul Symbolique d'Heaviside," *Rev. Gén. élec.* xiii. pp. 813-815 and 860-863 (May 1923).
- (43) A. E. Kennelly, "Hyperbolic Function Series of Integral Numbers and the Occasions for their Occurrence in Electrical Engineering," *Proc. Int. Math. Cong., Toronto, Sec. IVa* (Aug. 1924).
- (44) E. J. Berg, "Heaviside's Operators in Engineering and Physics," *Journ. Franklin Inst.* cxviii. pp. 647-702 (Nov. 1924).
- (45) A. E. Kennelly, "The Application of Hyperbolic Functions to Electrical Engineering Problems," 3rd ed. (London, 1925).
- (46) L. Casper, "Zur Formel von Heaviside für Einschaltvorgänge," *Archiv für Elek.* xv. p. 95 (1925).
- (47) H. Salinger, "Die Heavisidesche Operatorenrechnung," *E. N. T. ii.* pp. 365-376 (Nov. 1925).
- (48) J. J. Smith, "An Analogy between Pure Mathematics and Operational Mathematics of Heaviside by Means of the Theory of H-Functions," *Journ. Franklin Inst.* pp. 519-534 (Oct. 1925); pp. 635-672 (Nov. 1925); pp. 775-814 (Dec. 1925).
- (49) J. R. Carson, "The Heaviside Operational Calculus," *Bull. Am. Math. Soc.* xxxi. no. 1 (Jan.-Feb. 1926).
- (50) J. H. Jeans, "Mathematical Theory of Electricity and Magnetism," 5th ed. (Cambridge, 1927).
- (51) G. Windred, "Complex Numbers in Engineering," *The Electrician*, xcviii. pp. 142-145 (Feb. 1927).
- (52) G. Windred, "The Complex Number and its Use in Electrical Theory," *ibid.* ci. pp. 173-174 and 201-203 (Aug. 1928).
- (53) E. J. Berg, "Heaviside's Operational Calculus" (New York, 1929).
- (54) L. Cohen, "Heaviside's Electrical Circuit Theory" (New York, 1929).
- (55) G. Windred, "Electrical Circuit Theory based on the Method of Complex Numbers," *The Electrician*, cii. pp. 409-411 and 437-438 (April 1929).

LXXXII. *Fine Structure of Zinc Lines in the Visible and the Ultra-Violet Regions.* By WALI MOHAMMAD, M.A. (Punjab), B.A. (Cantab.), Ph.D. (Göttingen), Professor of Physics, Lucknow University, and PREM NATH SHARMA, M.Sc., Fellow, Lucknow University\*.

### I. Introduction.

IN earlier papers published in the *Philosophical Magazine* one of the authors has investigated the fine structure of arc lines in vacuum of cadmium and thallium<sup>(1,2)</sup> in the ultra-violet. The following is the extension of the same work to zinc.

### II. Previous Work.

Michelson<sup>(1)</sup>, Houston<sup>(2)</sup>, Hamy<sup>(3)</sup>, Janicki,<sup>(4,5)</sup> Gehrcke and von Baeyer<sup>(5)</sup>, Lunelund<sup>(6,10)</sup>, and Wali Mohammad<sup>(7)</sup> also

\* Communicated by the Authors.

have worked on the same element, but they have confined their attention to the visible region only.

As will be seen later on, there is hardly any information available on the fine structure of zinc lines in the ultra-violet.

### III. *Apparatus Used.*

The apparatus used was the same as was described in the previous papers. Briefly speaking, the light from a special vacuum arc lamp consisting of a Wehnelt oxy-cathode of platinum and a zinc anode, after having been rendered parallel by a quartz lens, was made to fall on a quartz Lummer-Gehrcke plate, after passing which the beam was accurately focussed by a quartz-fluorite achromat on the slit of the spectrograph. Two quartz Lummer-Gehrcke plates were available for use, and had the following dimensions:—

Small plate :—Length 13·0 cm.

Thickness 0·4597 cm.

Large plate :—Length 19·5 cm.

Thickness 0·365 cm.

The spectrograph used was the new 3-metre type with interchangeable optical system introduced recently by Hilger, and had a quartz prism and a quartz lens of 7·5 cm. aperture. This gave a very good dispersion in the regions investigated, and was a much more satisfactory arrangement than the Hilger  $E_3$  spectrograph used in previous investigations. A Wollaston prism was placed in front of the Lummer plate in order to transmit the beam polarized with the electric vector parallel to the parallel surfaces of the Lummer plate. The fringes were photographed in the usual way in the spectrograph. The region from 8000 Å.U. to 2680 Å.U. was covered by three plates each 10 cm. long. Ilford Panchromatic plates for the visible region and Wellington Iso-and Anti-screen plates for the ultra-violet region were used. The time of exposure was generally about 5 minutes except in the case of faint lines, when the exposure had to be made longer. The oxy-cathode in the lamp was heated to incandescence by a current of about 15 amperes, and a voltage of 220 was applied between the cathode and the anode made of zinc. The thermionic current varied from ·3 to ·6 amp.

### IV. *Calculation of Wave-lengths.*

Measurements were taken upon the fringe system from the upper face of the Lummer plate, and the fringes of the lowest



orders were measured and the mean of several observations taken. In this way the distance between two main-line fringes and between a main-line fringe and the satellites was determined.

The distance  $\Delta\lambda$  max in Å.U. between the orders of the fringe system of spectrum lines was calculated from the constants of the Lummer plate with the help of von Baeyer's formula,

$$\Delta\lambda \text{ max.} = \frac{n\lambda^2}{n^2\lambda - 4t^2\mu \frac{d\mu}{d\lambda}},$$

where

$\mu$  = the refractive index of quartz with respect to the ray under investigation,

$n$  = order of the fringe system given by

$$n\lambda = 2t\sqrt{\mu^2 - 1};$$

$t$  = thickness of the Lummer plate;

$\lambda$  = wave-length of the ray; and

$\frac{d\mu}{d\lambda}$  is the dispersion of quartz about  $\lambda$ .

The position of the satellites was determined in the following manner:—

If  $a$  is the distance between two successive main-line fringes, and  $b$  is the distance between the satellite and the lower-order fringe, then the wave-length of the satellite is

$$\frac{b}{a} \Delta\lambda \text{ max.}$$

If  $b < a/2$ , the satellite is positive and if  $b > a/2$  the satellite is negative.

## V. Measurement on Zinc Lines.

### 1. $\lambda$ 6362.58.

Michelson<sup>(1)</sup>, Houstoun<sup>(2)</sup>, Janicki<sup>(4, 9)</sup>, Lunelund<sup>(6, 10)</sup>, Gehrccke and von Baeyer<sup>(5, 8)</sup>, and Wali Mohammad<sup>(7)</sup> all find this line to be sharp and simple. Nutting<sup>(11)</sup> obtained this line simple only when extremely sharp. He found it triple with diffuse components separated by about 0.80 t.m. from the central primary.

We find this line to be extremely sharp and simple.

### 2. $\lambda$ 5182.17.

Janicki<sup>(4, 9)</sup> and Wali Mohammad<sup>(7)</sup> found this line to be sharp and simple.

We also find this line to be sharp and simple.

3.  $\lambda$  4810·71.

Houstoun<sup>(2)</sup>, Lunelund<sup>(6, 10)</sup>, Gehrcke and von Baeyer<sup>(5, 8)</sup>, Janicki<sup>(4, 9)</sup>, and Wali Mohammad<sup>(7)</sup> find this line to be sharp and simple. Michelson<sup>(1)</sup> found that it possessed one satellite, and Nutting<sup>(11)</sup> found it to possess a trace of structure on reversal.

We find this line to be sharp and simple.

4.  $\lambda$  4722·26

Gehrcke and von Baeyer<sup>(5, 8)</sup>, Janicki<sup>(4, 9)</sup>, and Wali Mohammad<sup>(7)</sup> find this line to be sharp and simple. Houstoun<sup>(2)</sup> found this line to be double. Nutting<sup>(11)</sup> found that, like  $\lambda$  4810·71, this line also showed a trace of structure on reversal.

We find that this line possesses one satellite :—

$$\begin{array}{r} +0\cdot070 \\ 0\cdot000. \end{array}$$

5.  $\lambda$  4680·38.

Gehrcke and von Baeyer<sup>(5, 8)</sup>, Janicki<sup>(4, 9)</sup>, and Wali Mohammad<sup>(7)</sup> find this line to be sharp and simple. Houstoun<sup>(2)</sup> found it to be double, and Nutting<sup>(11)</sup> noticed a trace of structure on reversal, as in the case of  $\lambda$  4810·71 and  $\lambda$  4722·96.

We find this line to be sharp and simple.

6.  $\lambda$  4298·54.

This line is found to possess two satellites. One of these is strong while the other is very faint and diffuse, appearing only on certain plates. The following structure is obtained :—

$$\begin{array}{r} +0\cdot067 \text{ (very faint),} \\ +0\cdot042 \\ 0\cdot000. \end{array}$$

Sometimes the faint line appears at  $-0\cdot046$ . Consequently the position of the faint satellite is doubtful.

7 & 8.  $\lambda\lambda$  3345·62 and 3345·13.

According to Kayser and Runge, there are two lines near each other and having the wave-lengths

$$\begin{array}{r} 3345\cdot62, \\ 3345\cdot13. \end{array}$$

We find that the line 3345·62 is simple, while the line 3345·13 possesses one satellite :

$$\begin{array}{r} +0\cdot033 \\ 0\cdot000. \end{array}$$

# 920 *Zinc Lines in the Visible and Ultra-Violet Regions.*

9 & 10.  $\lambda\lambda$  3303.03 and 3302.67.

Kayser and Runge have found two lines close to each other and of the wave-lengths

$$\begin{array}{r} 3303.03, \\ 3302.67. \end{array}$$

and of equal intensity.

We find that the line 3303.03 has one satellite :

$$\begin{array}{r} 0.000 \\ -0.051. \end{array}$$

The other line, 3302.67, is found to be simple.

11.  $\lambda$  3282.42.

This line is sharp and simple.

12.  $\lambda$  3075.99.

Wood <sup>(12)</sup> has found this line to be simple.

We find this line to possess one satellite which is quite sharp.

$$\begin{array}{r} +0.033 \\ 0.000. \end{array}$$

13.  $\lambda$  3072.19.

This line appears simple.

14.  $\lambda$  3035.93.

This line appears to have one satellite:

$$\begin{array}{r} 0.000 \\ -0.056. \end{array}$$

15.  $\lambda$  3018.90.

This line appears to be sharp and simple.

16.  $\lambda$  2800.90.

This line also appears sharp and simple.

17.  $\lambda$  2770.94.

This line is found to have one satellite :

$$\begin{array}{r} +0.042 \\ 0.000. \end{array}$$

18.  $\lambda$  2756.53.

This line is sharp and simple.

## *References.*

(1) Michelson, *Phil. Mag.* xxxiv. p. 280 (1892).

(2) Houstoun, *ibid.* vii. p. 456 (1904).

(3) Hamy, *Comptes Rendus*, cxxviii. p. 959 (1904).

(4) Janicki, *Ann. d. Physik*, xix. p. 36 (1906); *ibid.* xxix. p. 845 (1909).

- (5) Gehreke and von Baeyer, *ibid.* xx. p. 269 (1906).
- (6) Lunelund, *ibid.* xxxiv. p. 505 (1911).
- (7) Wali Mohammad, *Astrophys. Jour.* xxxix. p. 185 (1914).
- (8) O. V. Baeyer, *Verh. d. Deutsch. Phys. Ges.* xx. p. 733 (1908).
- (9) Janicki, *Diss. Halle* (1905).
- (10) Lunelund, *Diss., Helsingfors* (1910).
- (11) Nutting, *Astrophys. Jour.* xix. p. 190 (1904).
- (12) Wood, *Phil. Mag.* ii. p. 611 (1926).
- (13) Wali Mohammad and S. B. L. Mathur, *ibid.* v. p. 1112 (1928);  
*ibid.* iv. p. 112 (1927).

LXXXIII. *Discharges in Neon.* By P. JOHNSON, M.A.,  
Fellow of Magdalen College, Oxford\*.

1. **F**OLLOWING on researches which have been made at the Electrical Laboratory, Oxford, on the electric forces required to maintain high-frequency discharges in certain gases, I have undertaken the measurement of these forces in neon.

For these investigations it is necessary to have the gas very pure, and the precautions which were taken in order to obtain pure neon were the same as those used in other experiments which have been made in the laboratory and have already been published. Each specimen of the gas was tested for impurities by observing the spectrum of a high-frequency discharge in a wide tube containing the gas at high pressure. It has been found that this method of detecting impurities is much more sensitive than the ordinary method of examining the spectrum of a discharge in a narrow tube.

The discharge-tubes were cleaned by repeatedly admitting clean gas, heating with a blowpipe, and pumping the gas out again. After the process had been repeated several times, there were no impurities observed in the spectrum of the high-frequency discharge.

2. The arrangement first used for measuring the high-frequency currents in the tubes was exactly similar to one that was employed by Townsend and Nethercot † in their experiments on nitrogen. A continuous wave generator, maintained by two 30-watt valves, was used to induce

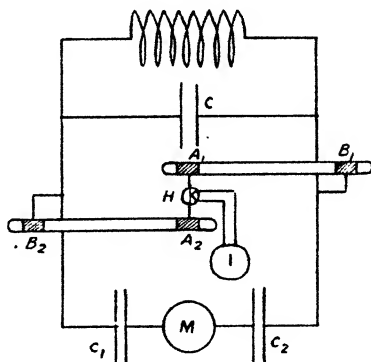
\* Communicated by Prof. J. S. Townsend, F.R.S.

† J. S. Townsend and W. Nethercot, *Phil. Mag.* vii. p. 600 (March 1929).

oscillations in a secondary circuit, which is shown in fig. 1. It consisted of a symmetrical arrangement of two discharge-tubes fitted with external sleeve electrodes  $A_1$ ,  $B_1$ , and  $A_2$ ,  $B_2$ , the current, being measured by a thermocouple  $H$  situated between the two sleeves  $A_1$ ,  $A_2$ . The currents in the tubes were adjusted by a rheostat in the filament circuit of the generator.

The distance  $x$  between the sleeves  $A_1$  and  $B_1$  was the same as the distance between  $A_2$  and  $B_2$ , and the force was measured by observing the mean potential difference between the two sleeves  $B_1$  and  $B_2$  for a given current and different distances  $x$  between the sleeves. The potentials were measured by means of a thermoammeter  $M$  connected

Fig. 1.



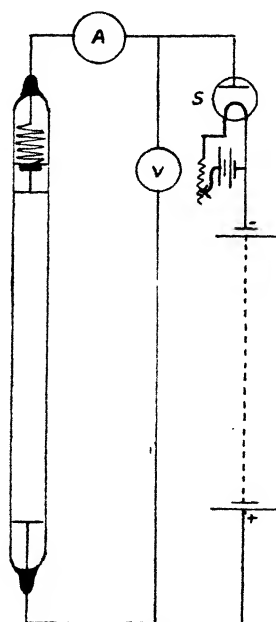
between two exactly similar variable condensers  $C_1$  and  $C_2$  in the secondary circuit, to which the sleeves were connected. The tubes were of pyrex of internal diameter 3.1 cm.

The results of these experiments showed that, as in the case of nitrogen, the mean force in the luminous column of a high-frequency discharge in neon was independent of the current in the tube from 1 to 10 milliamps, and of the wave-length of the oscillator from 30 to 120 metres.

3. In order to ascertain whether the force in the uniform positive column of a direct-current discharge is the same as the mean force in the luminous column of a high-frequency discharge, a pyrex tube of internal diameter 3.1 cm. was made up with internal aluminium electrodes, one of which

was fixed and the other movable along the axis of the tube. Electrical connexion was made to the movable electrode by a long strip of aluminium foil, and a piece of soft iron was fixed to the electrode so that it was possible to adjust the distance between the two electrodes by altering the position of the movable electrode with an electromagnet. A discharge was maintained by a battery of cells, and the current and the potential difference between the electrodes

Fig. 2.



were measured directly by means of a milliammeter A and a voltmeter V as shown in fig. 2.

The current in the tube was controlled by the two electrode valves S. The forces obtained were substantially the same as those found in the tubes with external electrodes with the same gas-pressures.

4. As this method of investigation, involving the use of three tubes, is rather complicated, it was considered desirable to make the measurements of the forces in the

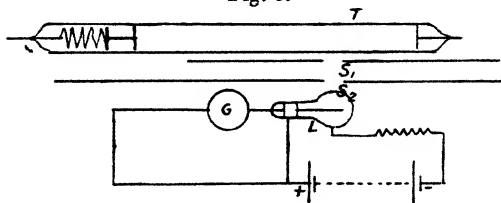
direct-current discharges and the high-frequency discharges with the same sample of the gas in the same tube. In order to do this, it became necessary to alter the method of measuring the currents in the high-frequency discharges so as to be able to use one discharge-tube only.

As there are some difficulties in obtaining accurate results by the method used by Townsend and Nethercot to measure currents in a single tube, another method was adopted which was found to be very convenient.

The current in the gas was indicated by a photoelectric cell on which the light from a small section of the discharge was allowed to fall. Since practically all the light from a neon discharge is confined to the red end of the spectrum, the photoelectric effect was small, and a sensitive galvanometer was required to indicate the photoelectric currents.

The discharge-tube T and the photoelectric cell L are arranged as shown in fig. 3, so that the light from the tube

Fig. 3.



which passes through the slits S<sub>1</sub> and S<sub>2</sub> falls on the cell. The internal electrodes of the tube could be connected as desired to the same sources of steady or high-frequency potentials as those used in the first experiments, and the methods of measuring these potentials were identical with those already described. It was also possible to maintain a high-frequency discharge in the tube T with external sleeves as electrodes, and in a preliminary set of experiments it was ascertained that the forces in the high-frequency discharges were the same whether the internal electrodes or the external sleeves were used.

The cell was calibrated by observing the deflexions of the galvanometer G when direct-current discharges were maintained in the tube T. The current in the galvanometer depended on the intensity I of the current in the tube and on the pressure *p* of the gas. It might be assumed that similar photoelectric currents would be obtained when

high-frequency discharges of similar intensities are maintained in the tube, but it is not necessary to make this assumption in order to measure the force in the luminous column of the high-frequency discharge. The mean potential difference  $E$  between the electrodes depends on the intensity  $I$  of the current through the gas; and the force  $X$  in the uniform luminous column is obtained by finding the potentials  $E_1$  and  $E_2$  corresponding to two different distances  $x_1$  and  $x_2$  between the electrodes. The force  $X$  in the luminous column is  $(E_1 - E_2)/(x_1 - x_2)$ , and experiments have shown that the force is independent of the current. Any current may therefore be used to determine  $X$ , provided the intensity  $I$  is the same when  $E_1$  and  $E_2$  are being measured. Since there are changes in the photoelectric current accompanying changes in the current in the discharge-tube, the latter may be maintained constant by adjusting the intensity of the oscillations so that the same photoelectric current is obtained when  $E_1$  and  $E_2$  are being measured for two distances  $x_1$  and  $x_2$  between the electrodes.

5. Table I. gives the values in volts per cm. of the forces  $x_1$  in the uniform positive column of the direct-current discharge, and the mean forces  $X_2$  in the uniform column of the high-frequency discharge of wave-length 35 metres, for different values of the pressures ( $p$ ), which are given in millimetres of mercury. (The ratio of the mean force  $X_2$  to the amplitude of the high-frequency force is  $2/\pi$ .) The currents in the tube were from 3 to 20 milliamps.

It is clear from the second and third columns that the forces in the two cases are practically identical until low pressures are reached. Below 2 mm. pressure the force in the high-frequency discharge remains steady at about 3 volts per cm. until striations set in at about .5 mm. pressure.

The force in the positive column of the direct-current discharge decreases as the pressure decreases below 5 mm. and the column itself begins to lose its uniform appearance. At .5 mm. pressure the force becomes very small, and it is difficult to measure since the total potential between the electrodes becomes very large at the lower pressures.

The variation of the mean force  $X$  in the high-frequency discharge with the pressure  $p$  is shown by curve I. (fig. 4),  $X$  being the ordinate in volts per cm., and  $p$  the abscissa in millimetres of mercury. The straight part of the curve

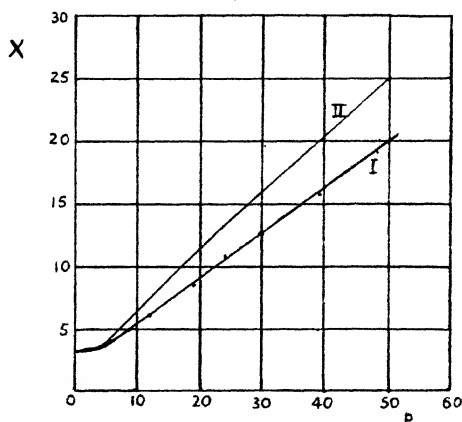


from  $p=10$  to  $p=50$  does not pass through the origin, and it is clear that the ratio  $X/p$  increases progressively as the pressure falls.

6. Values of the force in the luminous column of a high-frequency discharge in neon at different pressures have been determined by Hayman\*, and for comparison his results are given in curve II. (fig. 4).

In his investigations the forces were not measured for different currents through the gas, but for the smallest current which gave a uniform glow in the tube, and he had no direct means of measuring this current. The accuracy of his measurement of the force depends on the fact that

Fig. 4.



this current is approximately the same for different distances between the electrodes, but it is clearly better to have a direct means of measuring the current and to find the values of  $X$  for different currents.

His values are greater than mine except at the lowest pressures, and this to a small extent is accounted for by the fact that the diameter of his tube was 2.9 cm. while that which I used was 3.1 cm. in diameter, but there are possible sources of error which may account for the difference between his results and mine.

The principal cause of the difference between the two sets of results is probably due to the fact that it is not

\* R. L. Hayman, *Phil. Mag.* vii. p. 586 (March 1929).

possible to obtain neon which is absolutely free of helium, and the presence of the latter would have the effect of increasing the force.

The mean energy of agitation  $E_1$  of electrons in gases has been determined in terms of  $X/p$  from the experiments on the diffusion of electrons in gases that have been made in the laboratory. The curves\* giving the values of  $E_1$  in helium and neon corresponding to the range of  $X/p$  given in Table I. show that for these values of  $X/p$  the mean energy of agitation is controlled to a great extent by the small losses of energy of the electrons in their collisions with atoms of the gas. These losses are greater in the collisions with atoms of helium than in the collisions with atoms of neon, so that a small amount of helium in the neon would have a comparatively large effect in reducing the energy of agitation. This effect is emphasized by the fact that the mean free paths between the collisions in which these small losses occur are smaller in helium than in neon. Taking these effects into consideration, it is to be expected that for a given value of the ratio  $X/p$  the energy of agitation of electrons in pure neon would be reduced by about 6 or 7 per cent. by introducing 1 per cent. of helium. Thus, in order that the supply of electrons by the process of ionization by collision may be sufficient to maintain a current in a discharge through neon containing 1 per cent. of helium, it would be necessary to have the electric force 6 or 7 per cent. greater than the force in pure neon.

7. In the process of purification the gas was stored at high pressure in a reservoir containing charcoal cooled with liquid air. Neon at high pressure is absorbed by the charcoal to a much greater extent than helium, but is given off again as the pressure is reduced. Small quantities of gas could be admitted to the discharge-tube from the reservoir, and it is clear that if there were any helium in the gas originally, the first samples so removed would contain a higher percentage of helium than the later samples. It was found that the force when measured in a discharge in one of the first samples of gas was invariably greater than that measured in a later sample.

The values given in Table I. and represented by curve I. (fig. 4) were obtained from what were considered to be the

\* J. S. Townsend, *Phil. Mag.* ix. p. 1145 (June 1930).

purest specimens of the gas; but forces as much as 15 per cent. greater than these were sometimes obtained with the first specimens of the gas taken from the reservoir.

The average partial pressure of the helium in the various samples was about 1 per cent. of that of the neon. In the purest samples the partial pressure of the helium was considerably less.

8. In general the impurities in helium and neon are more easily detected by the radiation from discharges in wide tubes containing the gases at high pressures, but there is an exception to this rule in the case of neon when the impurity

TABLE I.

Forces  $X$  in luminous columns of discharges in neon at pressure  $p$  in a tube 3.1 cm. internal diameter.

$p$ .	$X_1$ .	$X_2$ .	$X/p$ .
48.0	19.5	19.0	.40
39.5	16.5	15.5	.40
30.0	12.5	12.7	.42
19.5	9.0	8.8	.46
13.0	7.0	6.8	.53
8.8	5.1	5.05	.58
6.4	4.3	4.1	.66
4.1	2.8	3.6	—

consists of a small quantity of helium. In this case the helium is more easily detected when the gas-pressure is low. This may be attributed to the fact that the energy of agitation of the electrons in the gas, which increases with the ratio  $X/p$ , is greater at low pressures than at high pressures. (The figures in Table I. show that the ratio  $X/p$  is greater for small pressures than for large pressures.)

I have examined mixtures of helium and neon spectroscopically, using a high-frequency discharge of wave-length 35 metres. In a mixture where the partial pressure of helium was three times that of the neon, it was not possible to detect the lines due to helium by a direct-vision spectroscope when the total pressure in the discharge-tubes was greater than 5 mm. In fact, the radiation from the discharges at the higher pressures appeared to be the same as that from a discharge in pure neon. When the pressure

was reduced to 3 mm. the principal blue line of the helium spectrum could be seen.

In another mixture of about equal parts of helium and neon the helium lines were faintly discernible at a pressure of 1.5 mm. It follows from the results of these experiments that a small trace of helium in neon could not be detected except at a very low pressure, but here a further difficulty would arise, namely that the intensity of the light emitted from the discharge would be so small that no impurities could be identified.

9. When calibrating the photoelectric cell by means of the radiation from the positive column of a direct-current discharge in which a known current was flowing, the photoelectric current through the cell was found to be proportional to the current in the tube. This means that

TABLE II.

Photoelectric current  $d$  in arbitrary units for a discharge current  $I$  in milliamps. in neon at 10 mm. pressure.

$I.$	$d.$	$I/d.$
14.0	4.5	3.1
10.7	3.5	3.05
7.6	2.5	3.05

the intensity of light emitted is proportional to the current, as was found by Gill\* for the ultra-violet light which is emitted by a discharge in air. This result is in accordance with the theory of the positive column, which shows that the effect of recombination is negligible†. Since the electric force is independent of the current, the energy of agitation of the electrons is also independent of the current, and all effects due to collisions of electrons with molecules of the gas are proportional to the current.

The calibration of the photoelectric cell by means of the direct-current discharge in neon at 10 mm. pressure is shown in Table II., where  $I$  is the current in the discharge-tube in milliamps., and  $d$  the deflexion of the galvanometer

\* E. W. B. Gill, *Phil. Mag.* p. 412 (Sept. 1911).

† J. S. Townsend, 'Electricity in Gases,' pp. 441 and 442; *Comptes Rendus*, p. 55 (Jan. 1928).

measuring the photoelectric current in centimetres; the third column gives the ratio  $I/d$ , which is seen to be constant and equal to 3.1 when the gas-pressure is constant at 10 mm. This ratio fell to 2.5 when the pressure in the tube was 20 mm., and had about that value at all higher pressures, the behaviour of the cell varying a little from day to day. As the pressure was decreased from 10 mm. the ratio increased and was about 7 at 2 mm. pressure. It appears from this that the intensity of light for a given current emitted from a direct-current discharge is practically constant at high pressures, but at lower pressures the intensity decreases as the pressure decreases. The colour also changes, and the proportion of red light to yellow light diminishes as the pressure is reduced. Further experiments on the intensity of the light in different parts of the spectrum are in progress.

10. A selenium cell has since been tried in place of the photoelectric cell, and was found to be far more sensitive to red light, giving a current of the order of  $\frac{1}{10}$  milliamp. when 10 milliamps. were flowing in the discharge-tube. It has the minor disadvantages that a considerable current flows through the selenium when no light is falling on it, and that the increase of the current in the cell is not exactly proportional to the current in the discharge-tube.

11. In a tube 3.1 cm. in diameter the luminous column of the high-frequency discharge in neon begins to break up into striations at a pressure of .4 mm. The striations take the form of a series of regions of high and low luminosity along the length of the luminous column. The number of these regions depends on the distance between the electrodes, and the relative brightness of the different sections of the luminous column increases as the pressure is diminished.

At pressures in the neighbourhood of 5 mm., using external sleeve electrodes, spiral striations of the form described by MacCullum\* were obtained. They appeared after the gas had been rendered impure by strongly heating the discharge-tube and then allowing the high-frequency discharge to carry away most of the impurity. They were never obtained in pure neon.

\* S. P. MacCullum and W. T. Perry, 'Nature,' cxxiv. p. 984, (Dec. 28, 1929).

12. It was observed when the current in the high-frequency discharge in neon was measured by means of the thermocouple, that at low pressures there was always a certain minimum value of the current that would flow. The value of this current increased as the pressure decreased. Thus at a pressure of  $\cdot 4$  mm. the current could not be reduced below 2.5 milliamps. without the discharge ceasing altogether; at  $\cdot 15$  mm. pressure the minimum current was 4 milliamp. The wave-length of the oscillations in these experiments was 35 metres.

My best thanks are due to Professor Townsend for his advice and help throughout this research.

---

LXXXIV. *On the Principle of the Inaccessibility of the Absolute Zero.* By HEINRICH MACHE, Ph.D., Professor of Physics at the Technical High School, Vienna \*.

PROF. N. A. KOLOSSOWSKY has recently observed † that Clausius gave expression to this principle as early as 1862, and objects that Nernst and all other authors who have been concerned with this problem at a later date have not given him sufficient credit. He writes: "It is strange enough that nobody has up to date mentioned the circumstance, so much the more that, if one occupies oneself in researches in the domain of these questions, a deep study of Clausius' classical works is absolutely indispensable." As one of the authors referred to by Prof. Kolossowsky perhaps I may be allowed to point out that what he says is not justified, since to-day one recognizes a new postulate in the said principle, and no longer a simple deduction from the second law as it appeared to Clausius. Actually the principle can only be deduced from the second law when it is assumed that the specific heat remains finite at the absolute zero, or, if it vanishes, it does so at a lower order than  $T$ . This is shown ‡ by the following consideration:

Let us consider a substance which passes through a reversed Carnot cycle, i. e., which behaves as a refrigerating machine, in that it extracts the amount of heat  $q$  from the

\* Communicated by Dr. Robert W. Lawson.

† Phil. Mag. (7) ix p. 208 (1930).

‡ Cf. also *Ber. Wien. Akad. Wiss.* (II. a) cxxxvi. p. 75 (1927).

heat container at lower temperature by the expenditure of work  $q' - q$ . Then  $q/q' - q = T/T' - T$  is a measure of the efficiency for each cycle. As heat container at the lower temperature we consider the body which is to be cooled, so that  $T$  is variable; on the other hand, the upper isotherm we keep unchanged at the temperature  $T'$ . The efficiency per cycle decreases with  $T$  and converges towards zero as the absolute zero is approached. Nevertheless, the absolute zero might be attainable with finite expenditure of work, provided that the specific heat of the body being cooled decreased also towards the value zero.

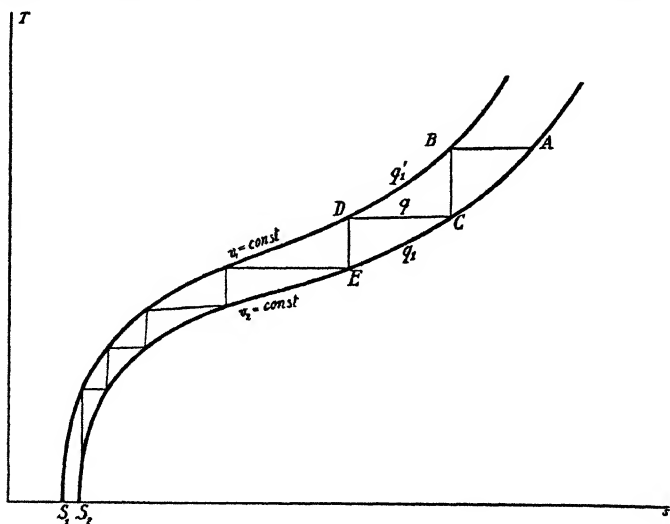
In order that the removal of heat in each cycle may occur at a definite temperature, and the cycle may remain perfectly reversible also with respect to the transfer of heat, let us make the assumption that the cooling body during the removal of heat is simultaneously subjected to an isothermal compression, whereby the quantity of heat  $q$  is given up to the working substance in the Carnot process, and that it is then expanded again adiabatically to the original volume. In this way its temperature falls in stages from cycle to cycle, but does not change so long as it is in contact with the working substance. The isothermal compression and adiabatic expansion occur in this way at each cycle between the same limits of volume, let us say from  $v_1$  to  $v_2$ . The heat of compression  $q$ , developed and taken up by the working substance, will be different at each cycle, and in accordance with the relation  $q = q' \cdot T/T'$  will decrease towards zero with decrease in  $T$ .

We can represent the changes which the cooling body experiences in this way in a Gibbs diagram, after Grumbach\*. If the curves represent lines of constant volume, between which the body is alternately isothermally compressed (AB, CD, etc.) and adiabatically expanded (BC, DE, etc.), a series of steps of decreasing height is obtained, provided that at higher temperatures  $c_v$  remains approximately constant, and the lines of constant volume are represented fairly well by logarithmic curves. If however  $c_v$  is small at low temperatures and finally zero, so that the curves meet the  $s$ -axis normally, the height of the steps will again increase, and it no longer appears

\* *L'Enseignement scientifique*, i. p. 139 (1928).

impossible that, despite the simultaneous decrease in efficiency of the Carnot process, the absolute zero can be reached\*.

If we denote by  $q_1$  that quantity of heat which must be removed from the body to bring it from C to E on the curve  $v_2 = \text{const.}$ , and by  $c_v$  the mean value of its specific heat on this path, then  $q_1$  is smaller than  $q$  by the area DCE, and the cooling resulting from the adiabatic expansion of the body  $q_1/c_v$  is smaller than  $q/c_v$ . If  $q/c_v$  disappears as the absolute zero is approached, then the cooling obtained by adiabatic expansion to the initial volume after each cycle of the Carnot process



will decrease still more towards zero. Since, however, the diminution of  $q = q'$ ,  $T/T'$  is of the same order as  $T$ , the quotient  $q/c_v$  will disappear if  $c_v$  is finite or decreases more slowly than  $T$  towards zero†. Thus an infinite expan-

\* According to Nernst's theorem  $S_1$  and  $S_2$  will coincide, but from the second law alone we must consider  $s$  as a function of  $v$ .

† It is obvious that  $q'$  must remain finite. Otherwise two adiabats starting from two points on an isotherm as far apart as  $v_2 - v_1$  would meet at the temperature  $T'$  and trace a cycle of finite area without consumption of heat.

The same can be shown in the  $T-s$  diagram. As long as  $S_1$  and  $S_2$  do not coincide the area over each of the isothermal lines (e. g., CD) up to the temperature  $T'$ , representing  $q'$ , will be finite. It is only from Nernst's theorem that we know that  $S_1$  and  $S_2$  coincide, and the area can become infinitely small.



dition of work is required in order to cool the body to the absolute zero, and its unattainability is a consequence of the second law alone, or, more exactly, a consequence of the assumption that the second law still holds, however closely we approach the absolute zero.

The proof is convincing, since the reversible Carnot cycle represents the most efficient refrigerating machine. One might perhaps raise the criticism that the expansion occurs always from the volume  $v_1$  to the volume  $v_2$ , and maintain that at the lowest temperatures use should be made of larger expansions. However, since nothing more has been said regarding the difference  $v_2 - v_1$  than that it is neither infinitely small nor infinitely large, nothing prevents our assuming the largest possible expansion during the whole cooling process.

If we admit that the specific heats vanish at a higher order than  $T$  the case is quite different, and the absolute zero appears attainable. To show this we make the assumption that now the cooling body expands at first adiabatically along BC, comes in contact with the working substance of the Carnot cycle, and is then compressed at constant temperature (CD) till the original volume is again reached. If  $q_1'$  denotes the quantity of heat which we must remove from the body on the curve  $v_1 = \text{const.}$  from B to D and  $c_v'$  the mean value of its specific heat on this path, then  $q_1'$  is greater than  $q$  by the area BCD, and the cooling produced by the adiabatic expansion  $q_1'/c_v' > q/c_v'$ . As now  $q/c_v'$  rises to infinitely large values,  $q_1'/c_v'$  will do so *a fortiori*.

Clausius did not hesitate to express the principle that the absolute zero was unreachable, since in his time one could not foresee that specific heats decrease towards zero as the absolute zero is approached. In the paper quoted by Kolossowsky, which Clausius did not retain, moreover, in the second and third editions of his 'Mechanische Wärmetheorie,' a proof is given which is characterized by the introduction of the concept of "disgregation" ( $z$ ). By this is understood the quotient of the work performed against external and internal forces for a change of state, and the temperature. On a reversible adiabatic the increase in disgregation on expansion from the temperature  $T_0$  to  $T$  is given by the expression

$$z - z_0 = \int_{T_0}^T \frac{h dT}{T},$$

where  $k$  is what Clausius calls the "true heat capacity." It denotes by how much the kinetic energy per unit-mass of the substance under consideration increases per degree, and should be independent of the temperature and the state of aggregation, which, as we know to-day, is only the case when the number of degrees of freedom remains unchanged and the principle of equipartition remains valid. If from the fact that when  $T=0$  the change of disgregation becomes infinitely large it is concluded that the absolute zero is unattainable, then it must be assumed that the true heat capacity  $k$  either remains finite or disappears at a slower rate than  $T$ . But  $k$  is only a part of  $c_v$  or  $c_p$ , and if these quantities disappear then  $k$  must also disappear.

What has been so far considered may be summarised as follows:—If it is assumed that the second law still holds at the absolute zero, then the absolute zero is unattainable *only* for the case when the specific heat remains finite or disappears at a slower rate than  $T$ . If it disappears according to an expression of higher order than the first, then the zero appears to be attainable.

The original conception of Nernst's heat theorem requires that at the absolute zero the specific heat remains unaltered for every change. Planck goes somewhat further in his hypothesis, which requires that the heat capacity disappears at the absolute zero, as had been confirmed by Nernst. Not much has been said here of the order in which the specific heat disappears. A finite zero-point value for the entropy only presupposes

that when  $T=0$ ,  $\int_0^T \frac{cdT}{T}$  converges towards zero. If we take  $c=aT^n$ , then  $\int_0^T \frac{cdT}{T} = \frac{a}{n} T^n$ , and this expression disappears for all positive values of  $n$ , and also for values of  $n$  less than one.

It is, however, to be assumed on the basis of experimental work and of Debye's theory of specific heats that  $c$  disappears more rapidly than  $T$ . If we bring this into consideration, we can with Nernst extend the heat theorem in the following words:—"In the neighbourhood of the absolute zero every process takes place without change in the entropy"\*. Thus for  $T=0$ , and for every change taking

\* W. Nernst, 'Die theoret. u. exper. Grundlagen des neuen Wärmesatzes,' I. Aufl. p. 71 (1918).

place there or starting off from there, we have  $ds=0$ , where  $ds$  represents the *total differential* of the entropy. In actual fact it follows conversely from  $ds=dq/T=cdT/T=0$ , and  $ds/dT=c/T=0$ , for  $T=0$ , that  $c$  disappears more rapidly than  $T$ . This means that not only every change of pressure, density, or chemical union occurring on the zero isotherm, but also an infinitely small rise of temperature taking place on it, leaves the value of the entropy unchanged. Not only is the zero isotherm itself an adiabetic, but also every change of state starting from any point on the zero isotherm proceeds at first adiabatically. Herein, however, is revealed the contradiction in which the behaviour of this region lying on the zero isotherm stands to the second law; adiabetic curves will actually intersect there in a finite range. The principle of Caratheodory\* can also be utilized, according to which, in the region of validity of the second law, there must exist, in arbitrary proximity to every state, neighbouring states which cannot be reached from the first state on an adiabetic path. On the other hand, from the zero-point isotherm all neighbouring states can be reached solely by an adiabetic path. One can say, therefore, that in the immediate neighbourhood of the absolute zero the second law loses its validity for every body. *Only as a result of this does it appear possible that, in spite of the disappearance of specific heats in an order higher than the first, the zero nevertheless remains unreach-able.* The proof given above, according to which the zero was attainable in this case, assumed the validity of the second law also at the absolute zero, and now appears untenable.

If the unattainability of the zero-point is also postulated, with Nernst, for the case in which the specific heats disappear with  $T$  in higher order than the first, then this postulate demands conversely the invalidity of the second law, and with it the constancy of the entropy in the region lying near the zero isotherm. It is therefore a necessary consequence of this postulate that for  $T=0$ ,  $ds=0$ .

From the previous considerations one is led to the conviction that it would have been inexpedient to describe the principle of the unattainability of the absolute zero

\* Cf. M. Bor.a, *Phys. Ze'its.* xxii. p. 282 (1921).

as a special principle as long as it appeared wholly contained in the second law, and in the "Clausius-Carnot principle," from which this second law was developed. It is the experiments of Nernst on specific heats at the lowest attainable temperatures, and the related theoretical investigations of Einstein and of Debye, which have raised the principle of the inaccessibility of the absolute zero to an independent postulate, with a wider physical meaning than hitherto. It would therefore be unjust not to name this new knowledge after Nernst, but to attach to it the name of Clausius, the more so as to-day it is generally accepted that ultimately all the essentials of the new thermodynamics depend on the fundamentals which were laid down by Clausius.

---

*LXXXV. The Effect of Systematic Surface Treatment on the Photoelectric Emission from Metals. By R. F. HANSTOCK, B.Sc., University College, Nottingham \*.*

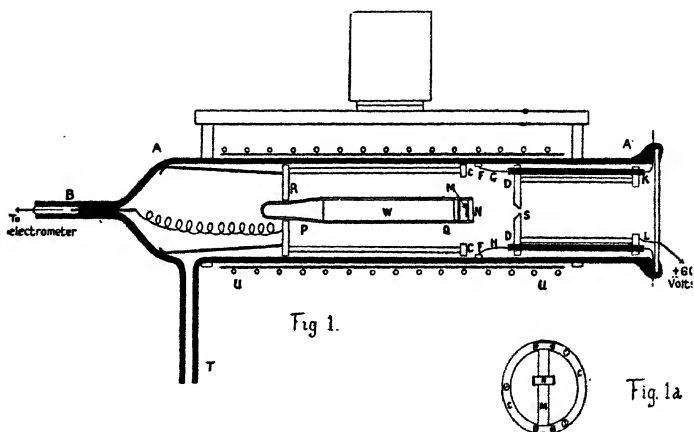
THERE is evidence to show that †, when an annealed metal surface is polished, a change takes place in the physical nature of the surface. This research is undertaken to examine the photoelectric emission from metal surfaces in a vacuum at intervals during the process of polishing, the surface being initially in an annealed state.

The following is a description of the apparatus used for this purpose:—Treatment of the metal surface is done in a vacuum tube AA (fig. 1) of "Vitreosil" (fused quartz). This tube is found to provide good insulation for the metal parts and can easily be heated to the temperature required to anneal the metal under examination. The end of the tube is closed by a transparent quartz plate attached by sealing-wax. During the heating of the tube the wax is kept cool by a current of cold air from a fan-motor. The metal to be tested is shown at M. This is a flexible strip, 5 cm. long, 5 mm. broad, and 0.07 mm. thick. The strip is fixed to a brass ring CC, held in a plane perpendicular to

\* Communicated by Prof. P. E. Shaw, M.A., D.Sc.

† Beilby, 'Aggregation and Flow of Solids.' Shaw, Proc. Roy. Soc. A, xciv. p. 16 (1917); Proc. Phys. Soc. xxxix. p. 449 (1927). Shaw and Jex, Proc. Roy. Soc. A, cxi. p. 349 (1926).

the axis of the tube by means of the framework shown. *M* is connected through the lead-quartz seal *B* to the quadrant electrometer. Fig. 1*a* shows a front view of the ring *C*. The anode of the photoelectric cell is the plate *DD*, having a slit *S*, 9 mm. long and 1 mm. wide, through which U.V. radiation falls on the specimen *M*. The distance between *D* and *C* is 4 cm., and the potential applied to *D* is +60 volts. To obtain good insulation between the high potential plate and the electrometer system an earthed metal ring, *F*, is placed round the tube near to *C*. Wires, *G* of copper, *H* of eureka, are connected by *F*, and pass through the insulating tubes *K* and *L* to the outside. This arrangement forms one junction of a thermo-couple, the



other junction being kept in a bath of water outside the tube, and hence provides a means of measuring the temperature near the specimen. The thermoelectric circuit is earthed at one point.

To polish the specimen the metal cylinder *N* is used. This is held fixed at one end of the bar *PQ*, the other end of which fits loosely into a hole in the plate *R*. This bar is weighted by a mass of brass, *W*, weighing 200 gms. When the tube is held vertically, with the quartz window upwards, the weight is supported by the cylinder resting on the strip. If the tube is now rocked from side to side in the vertical plane containing the strip, *N* slides over *M* and polishes the latter. The strip, being very thin and

flexible, adjusts itself to maximum contact with the cylinder. The tube is mounted so that it can easily be oscillated to produce the polishing. In presenting the results obtained, a slide of the polishing cylinder from one end of the strip to the other is called 1 rub. The side tube T is connected to a vacuum pump, drying tubes, and McLeod gauge by means of a short length of pressure tubing, this being necessary to allow for the movement of the apparatus. The apparatus is heated by the coil U, the leads to which are earthed during electrometer readings. The whole apparatus and lead to the electrometer are electrostatically shielded.

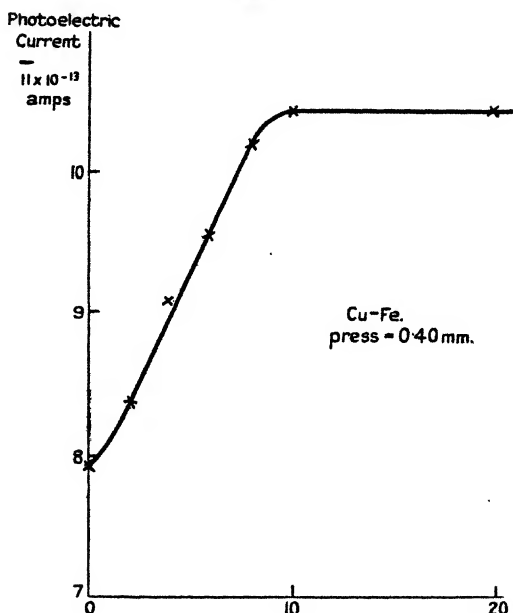
When exposing the metal to the U.V. radiation the tube is held horizontally, so that M falls to one end of the strip, which is thus left freely exposed to the light. As the source of U.V. radiation a parallel arc is used, the electrodes being made of an alloy of Ni and Cr silicates. This produces radiation of wave-length down to 1900 Å, and is an intense source. The arc is housed in an earthed metal case with a shutter, and is at a distance of 50 cm. from the specimen.

The following is a description of the preparation of the specimens and the method of taking readings. The specimen is cleaned with a fine glass-paper, wiped with clean filter-paper, and then washed in benzene. The cylinder is kept highly polished by means of rouge, and is washed in benzene before fixing in the tube. When sealed up the tube is heated to 300° C. and then allowed to cool slowly, remaining above the temperature 200° C. for approximately one hour, the tube being evacuated during heating. Further prolongation of the heating is not found to influence the results. After the tube has cooled down the photoelectric readings are taken. These consist in a measurement of the P.E. current when the surface is annealed, followed by measurement of the current as the surface is rubbed by increasing amounts. After rubbing, the apparatus is allowed to stand for a short time before taking readings, so that any frictional charge developed (indicated by the electrometer) may leak away. The method employed in measuring the current is to observe the time for the spot of light from the electrometer to drift through a 100 mm. on the scale, after the rate of drift has become constant. These measurements thus give a curve showing how the photoelectric current changes on

rubbing the surface. Examination of the surface after rubbing shows, for the material used, that it is polished and not simply scratched.

The materials used for the strips are Cu, Ag, Au, and Pt, and for the polishing cylinder steel and Ni. These are chosen because both steel and Ni polish the other metals easily without scratching, and are not likely to form alloys with them. It is not possible to use a polishing cylinder

Fig. 2.



made of the same metal as the strip, since it is found that a tearing and scratching of the surface results.

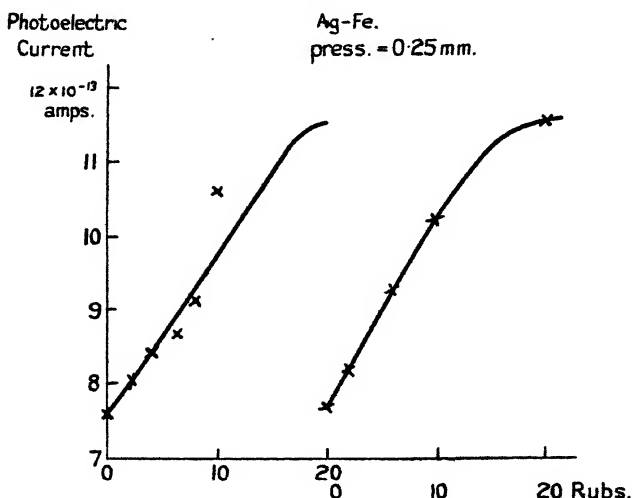
### Results.

Fig. 2 is the curve for Cu rubbed with steel, the readings being taken at a pressure of 0.40 mm. All the metals tested give curves of similar shape. There is an increase of the photoelectric current as the metal is changed from an annealed to a polished state. The relation between photoelectric current and number of rubs is almost linear

for the first eight rubs, and then quickly reaches a stationary value.

In fig. 3 are shown curves for Ag rubbed with steel. The first curve is obtained in the usual way. The specimen is then heated again to the annealing temperature, and, on cooling, the readings are repeated, producing the second curve. It is found that the photoelectric current can always be increased by rubbing, decreased by heating, and then increased by rubbing, and so on for any number of times. As a result of experiments using Ag rubbed by

Fig. 3.



steel, it is found that unless the specimen is heated to more than  $150^{\circ}\text{C}$ . there is no change to the annealed state from the polished state as indicated by the photoelectric current.

There seems to be no definite relation between the pressure in the tube and the ratio of the current for the polished to the current for the annealed state. Calling the current from the surface in the polished state  $i_m$ , and the current from the annealed surface  $i_0$ , it is found that 23 curves taken for Ag, Pt, Cu, Au, rubbed with steel, and Ag rubbed with Ni, give values of  $i_m/i_0$  between 1.85 and 1.15, but of these 23 curves 20 give values of  $i_m/i_0$  between 1.51 and 1.15. The range of pressure used is from



0.001 mm. to 1 mm. The following are the mean values of  $i_m/i_0$  for the various metal combinations :—

Ag/Steel.....	1.41
Au/Steel.....	1.45
Pt/Steel .....	1.33
Cu/Steel.....	1.23
Ag/Ni.....	1.38

The experiment is also repeated for a more limited range of the exciting radiation. For this purpose a filter consisting of a solution of potassium chromate in water is used. The solution is contained in a Baly tube with quartz ends, so that the thickness of the absorbing solution can be varied. The sensitivity of the electrometer is increased to about ten times its previous value, and the thickness of the solution adjusted to the greatest value consistent with a measurable photoelectric current. Photographs of the arc spectrum taken through the solution show transmission between 2260 and 2330 Å., the limiting lines being very faint. Transmission begins again above 3000 Å., but since the long-wave limits for the metals used are probably not greater than 3000 Å., this should have little effect. With this limited range of wave-length the curve shown in fig. 4 is obtained for Ag rubbed with steel, the pressure being 0.15 mm.

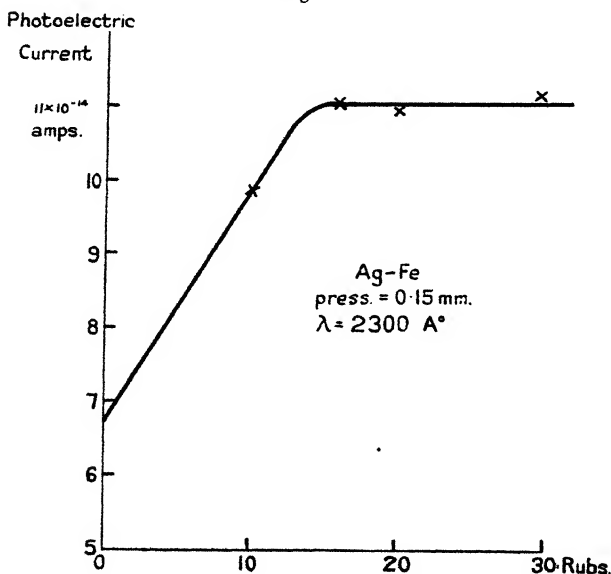
The main characteristics of the curves may be summarized as follows :—

1. The photoelectric current is increased when the metal surface is polished.
2. The increase of the photoelectric current with rubbing is approximately a linear function of the number of rubs until just before the maximum value is reached.
3. The ratio  $i_m/i_0$  shows no regular dependence on the pressure of the gas in the tube.
4. The effect appears for radiation of a restricted range of wave-length as well as for the full spectrum.
5. By heating to above 150° C. the metal can be reduced to its less active state.

The following are some of the possible causes of the effect observed requiring consideration:—

- (a) A change in the adsorbed gas layer at the metal surface, brought about by the rubbing.
- (b) Transfer of metal from the polishing cylinder to the specimen.
- (c) The formation of oxide films by heating, and removal or transfer on rubbing.
- (d) The formation of a layer of a modified form of the annealed metal, corresponding to Beilby's "vitreous" layer, produced by polishing.

Fig. 4.



While it is impossible to eliminate definitely any of the above possibilities, the results obtained make some more probable than others.

Since there is no definite dependence of  $i_m/i_0$  on the pressure throughout the range used (0.001 to 1 mm.), and as also the increased activity produced by rubbing does not disappear even after several days, the effect does not seem to be due chiefly to a removal of part of the adsorbed layer. It is possible, however, that a change in the form of the metal surface itself, either geometrical or physical,

might alter its adsorbed layer, and thus increase the emission. If the change were due solely to a smoothing out of surface irregularities the reproducibility obtainable by successive heating and polishing would not be expected.

The possibility of transfer of metal from the polishing cylinder to the specimen is always present, but it should be noted that it would be a transfer from a harder metal to a softer one in all the experiments undertaken. Even if transfer takes place the reproducibility obtained by successive heating and polishing requires more than this to explain it, since heating to a temperature of  $150^{\circ}\text{C.}$  would not remove the transferred metal.

Formation of thin oxide films on the surfaces during heating is very probable, although no visible signs of oxidation are noticed. Also the values of  $i_m/i_0$  are nearly the same for the easily oxidizing metals Cu and Ag as for Pt and Au.

The remaining possible cause is worthy of consideration, since it will explain the results obtained, and since there is other experimental evidence indicating that a modified layer exists on the surface of a polished metal. Beilby has shown that such a layer can be produced to a depth of 50 to  $500\ \mu$  on the surface of a metal by polishing. By heating to about one-third of the absolute melting-point of the metal this layer returns to its original state. The minimum temperature required to change the metal from the more to the less active photoelectric state is shown to be greater than  $150^{\circ}\text{C.}$ , which is approximately one-third of the melting-points for the metals considered.

There are other physical properties of metals considered by Beilby which show a sudden change at this "annealing" temperature, namely, the electrical conductivity, thermal E.M.F., and elasticity. It has also been shown\* that the tribo-electric charge developed when a metal is rubbed on an insulator depends on the state of the metal. Hence it is probable that the change observed for the photoelectric effect arises from the same cause as that producing change in these other physical properties.

In conclusion, I wish to thank Prof. P. E. Shaw, M.A., D.Sc., of the Physics Department, University College, Nottingham, for the facilities provided for this research and for advice in experimental details.

\* Shaw, Proc. Roy. Soc. A, xciv. p. 16 (1917).

LXXXVI. *On the Effect of Constrictions in Organ Pipes.*  
By ERIC J. IRONS, Ph.D.\*

1. *Introductory.*

THE work described in this paper is a sequel to two previous investigations. The first of these<sup>(1)</sup> was designed to determine the effect on the distribution of nodes and antinodes of introducing diaphragm constrictions into a Kundt's sound tube, and was, in consequence, concerned with the adjustment of "tube lengths" for resonance to a note of fixed frequency. The second investigation<sup>(2)</sup> was on the effect of side-holes in wind instruments, and the present problem of determining the frequency variation of an organ pipe of fixed length when diaphragm constrictions are placed at various points along its axis is in theory similar to it. The theory of the problem has already been treated in part<sup>(3)</sup>, and on it the present work was founded, originally with a view to designing an organ pipe capable of emitting a lower note than an ordinary stopped pipe of the same length. During the progress of the experiments Dr. E. G. Richardson drew my attention to a description of a patent in *Musique et Instruments*, and on investigation I found that the idea of realizing a bass organ pipe on this principle was the subject of French patent No. 621,719 (1927) granted to M. de Mons. I have accordingly restricted this report to the more complete theory proposed in the next paragraph, and experimental data to verify it.

2. *Theoretical.*

In a former paper<sup>(3)</sup> simple proofs were given of Webster's formulæ<sup>(4)</sup>

$$(A) \quad Z_1 = \frac{\beta}{\sigma} \cdot \frac{Z_2 \cos kl - (\beta/\sigma) \sin kl}{Z_2 \sin kl + (\beta/\sigma) \cos kl}, \quad \dots \quad (1)$$

for the impedance,  $Z_1$ , at one end of a tube of length  $l$  † and area of cross-section  $\sigma$  in terms of the impedance,  $Z_2$ , at the other end, and  $\beta$  the product of the elasticity of the gas into  $k$  ( $= 2\pi n/a$  with the usual notation) ;

$$\text{and (B)} \quad Z_1' = -\beta k/c, \quad \dots \quad (2)$$

for the impedance of an orifice of conductance  $c$ .

\* Communicated by the Author.

† Throughout the paper the "length" of a pipe is to be considered as its geometrical length together with any end correction or corrections.

By the use of these formulæ it is easy to write down an expression for the resonant frequencies of the system shown in fig. 1. For, by (1), the impedance at Q due to the gas column of length  $l_2$  being

$$\frac{Z_P - (\beta/\sigma) \tan kl_2}{1 + Z_P(\sigma/\beta) \tan kl_2},$$

$$Z_Q = -\beta k/c + \frac{Z_P - (\beta/\sigma) \tan kl_2}{1 + Z_P(\sigma/\beta) \tan kl_2}, \quad \dots (3)$$

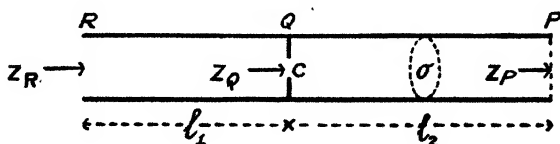
and similarly

$$Z_R = \frac{Z_Q - (\beta/\sigma) \tan kl_1}{1 + Z_Q(\sigma/\beta) \tan kl_1}.$$

If the system is resonating to a source at R (such that R is an antinode), then, neglecting friction,  $Z_R = 0$ , or

$$Z_Q = (\beta/\sigma) \tan kl_1. \quad \dots (4)$$

Fig. 1.



If the tube be open at P,  $Z_P = 0$ , and from (3) and (4)

$$\tan kl_1 + \tan kl_2 = -k\sigma/c, \quad \dots (5)$$

or, if it be closed,  $Z_P = \infty$ , and

$$\tan kl_1 - \cot kl_2 = -k\sigma/c. \quad \dots (6)$$

Formulæ (5) and (6) lend themselves to a graphical treatment (due to Paris<sup>(6)</sup>) which has been used by the present author to demonstrate the effect of side-holes on the frequency of a wind instrument<sup>(2)</sup>. Put

$$f = \frac{l_1}{l_1 + l_2} = \frac{l_1}{L},$$

so that

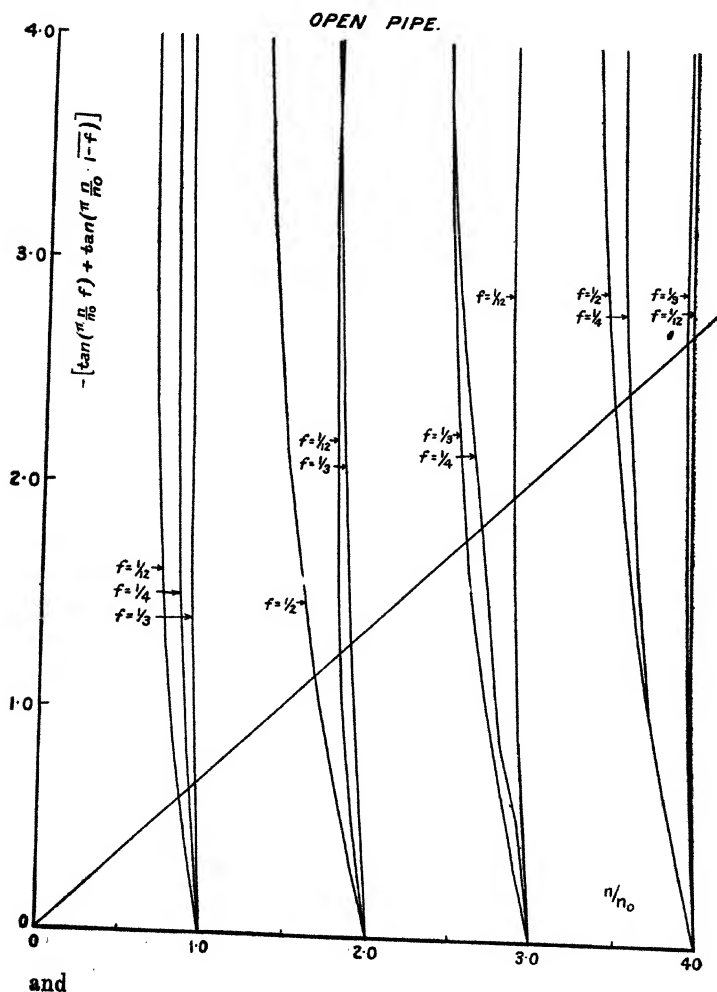
$$(1-f) = \frac{l_2}{L},$$

and let the frequency of the pipe when there is no constriction present be  $n_0$ . We then have  $a = 2Ln_0 = 2\pi n/k$  or

$k = (\pi/L) \cdot (n/n_0)$  for an open tube, and  $k = (\pi/2L) \cdot (n/n_0)$  for a closed tube. Equations (5) and (6) then become

$$-\left(\tan \pi \cdot \frac{n}{n_0} \cdot f + \tan \pi \cdot \frac{n}{n_0} \cdot \overline{1-f}\right) = \frac{\pi}{L} \cdot \frac{n}{n_0} \cdot \frac{\sigma}{c}, \dots (5.1)$$

Fig. 2.

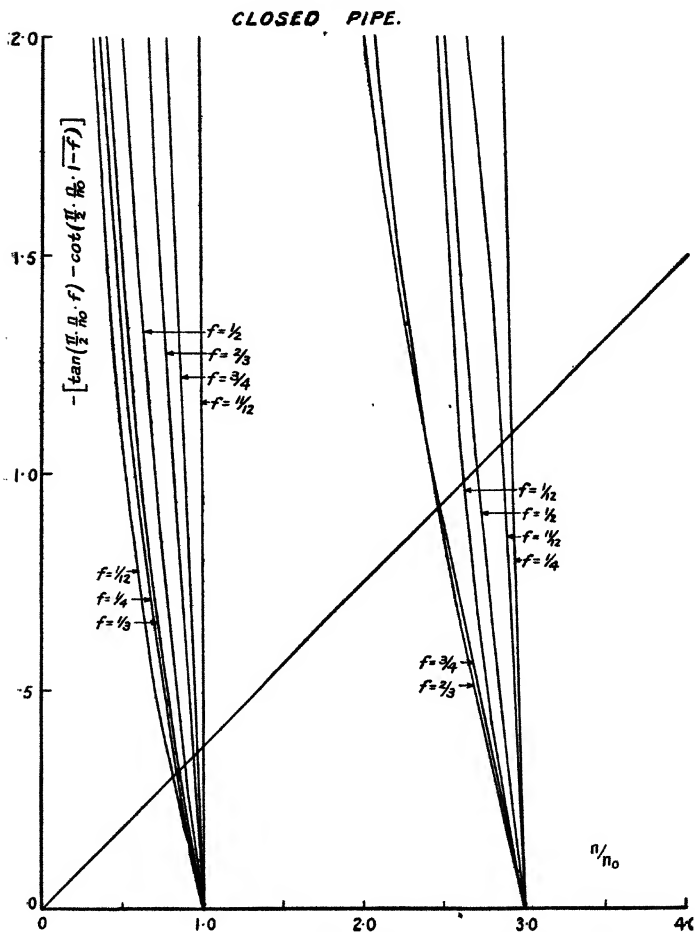


and

$$-\left(\tan \frac{\pi}{2} \cdot \frac{n}{n_0} \cdot f - \cot \frac{\pi}{2} \cdot \frac{n}{n_0} \cdot \overline{1-f}\right) = \frac{\pi}{2L} \cdot \frac{n}{n_0} \cdot \frac{\sigma}{c}, \dots (6.1)$$

Plotting values of the left-hand sides of these equations against  $n/n_0$  for various values of  $f$  gives rise to the curves of figs. 2 and 3 respectively. Plotting values of the right-hand sides

Fig. 3.



for given constrictions in pipes of known length and cross-section against  $n/n_0$  gives rise to a series of straight lines on the same figures. It is to be noted that the curves, as distinct from the straight lines, will serve for any pipe for which the value of  $n_0$  is known.

It is of *theoretical* interest to note from figs. 2 and 3 the values of the frequencies indicated for the cases in which  $c$  is very large (equivalent to removing the constriction) and very small (equivalent to blocking the tube), and to compare them with the corresponding "stationary wave diagrams" of the pipe. The values of  $n/n_0$  in these instances are set out in Table I.

TABLE I.

f.	Open Tube.		Closed Tube.	
	$c=0.$ (Gradient $\neq \infty$ .)	$c=\infty.$ (Gradient $=0$ .)	$c=0.$ (Gradient $=\infty$ .)	$c=\infty.$ (Gradient $=0$ .)
1/12.....	6/11	1	0	1
	18/11	2	24/11	3
	30/11	3		
	42/11	4		
1/4 .....	2/3	1	0	1
	6/3	3	8/3	3
	10/3	4		
1/3 ....	3/4	1	0	1
	6/4	2	3	
	9/4	3		
	15/4	4		
1/2 .....	1	2	0	1
	3	4	2	3
2/3 .....	3/4	1	0	1
	6/4	2	3/2	3
	9/4	3		
	15/4	4		
3/4 .....	2/3	1	0	1
	6/3	3	4/3	3
	10/3	4		
11/12.....	6/11	1	0	1
	18/11	2	12/11	3
	30/11	3		
	42/11	4		

\* The gradient referred to is that of the straight lines.

It is to be noted that :

1. In the columns for  $c = \infty$  are to be found the overtones proper to the tube without any constriction, except in those instances in which a node would occur at the position of the constriction were it present when these overtones appear under the column  $c = 0$ .

2. The values under  $c = 0$  are, as might be expected from energy considerations, associated with that part of the tube



which, if sounded by itself, would yield the lower frequencies (*i. e.*, in general, the longer part).

3. The values  $n/n_0 = 0$  for  $c = 0$  in a closed tube may be interpreted as the note associated with a tube of infinite length.

The value of the "conductance" of a hole in a disk perpendicular to the axis of a tube has not yet received theoretical treatment. In consequence  $c$  was determined experimentally by plotting the observed values of  $n/n_0$  for various values of  $f$  on figs. 2 and 3, drawing the best straight line from the origin through the points so obtained, and measuring the gradient of this line. This is in some measure tantamount to assuming the validity of formulæ which it is the object of experiment to test. The justification for this procedure is that the experimental values of the frequencies do not differ greatly from those calculated assuming throughout the same value of  $c$  for the constriction used. It is, however, possible that  $c$  may vary slightly with the frequency and the proximity of the constriction to the mouth of the tube, and this may account to a certain extent for the existing discrepancies.

### 3. *Experimental.*

The "boot" of an open cylindrical flue organ pipe designed to emit E (= 320 cycles/sec.) was severed from the rest of the pipe and fitted with a collar to carry one of three brass tubes of length 100, 60, and 35 cm. respectively, and of internal diameter approximately equal to that of the original pipe (4.7 cm.). The constriction used was of brass of thickness 0.2 cm., having a circular aperture, of diameter .84 cm., coaxial with the pipe.

As a preliminary it was necessary to determine the end correction of the pipe and its variation (if any) with frequency. To this end the 100 cm. pipe was furnished with a closely fitting piston, and the pipe lengths corresponding to the normal tones or harmonics of a series of tuning-forks were determined. If  $L$ ,  $n$ , and  $C$  are the length, frequency, and mouth correction (supposed constant) of the pipe, then

$$L = (a/4) \cdot 1/n - C, \quad . \quad . \quad . \quad . \quad (7)$$

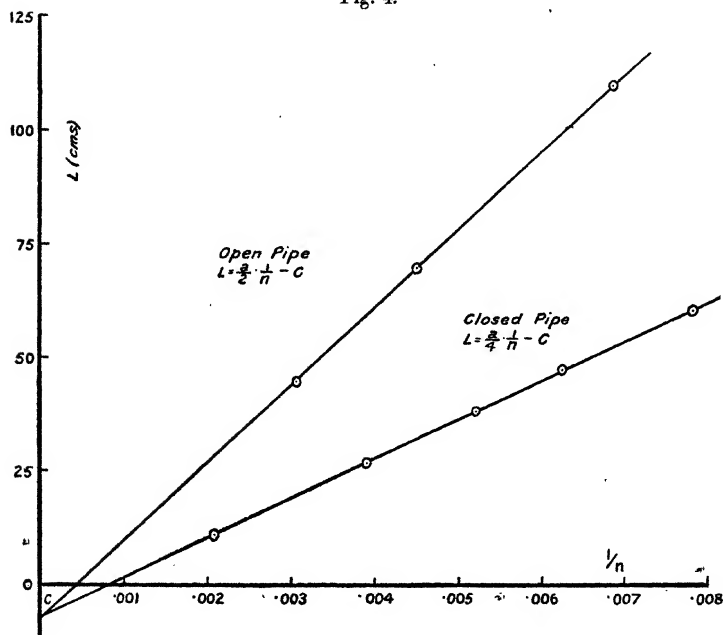
where  $a$  is the velocity of sound. The frequencies obtained by using the mouthpiece in conjunction with the three unstopped brass pipes were also determined (by a sonometer), and in these instances

$$L = (a/2) \cdot 1/n - C, \quad . \quad . \quad . \quad . \quad (8)$$

where  $L$  is now to be interpreted as the geometrical length of the pipe increased by 0.58 times its radius. Plots of  $L$  against  $1/n$  (fig. 4) are sensibly rectilinear, and indicate that the mouth correction 6.9 cm. (= 2.9 times tube radius\*), may, for the purposes of this work, be taken as the same whether the pipe be closed or open and also as independent of the frequency  $\dagger$ .

In making these measurements care was taken to ensure that the pipe was neither over- nor under-blown for the particular note under test, and it was found that, with the

Fig. 4.



\* This value is in agreement with that obtained for a flageolet <sup>(2)</sup>.

$\dagger$  If it be assumed that the mouth correction is a linear function of  $L$  ( $= C + bL$ , say), then

$$L = \frac{a}{4n(1+b)} - \frac{C}{(1+b)}$$

for a closed pipe, and a straight line is, for this particular function, still obtained by plotting  $L$  against  $1/n$ . The measured gradients of the lines of fig. 4 yielded values of the velocity of sound equal to 342 and 343 metres per sec. for an open and closed pipe respectively, so that, having regard to the temperature of the air in the pipes ( $19^\circ\text{C}$ ), it appears safe to assume that  $b = 0$ .

aid of a water manometer, consistent results could be obtained after a little practice.

Another and similar pipe was calibrated in the same manner as the experimental pipe and a satisfactory value of the velocity of sound was deduced from the gradient of a plot of  $L$  against  $1/n$ . This pipe was then ready for use to determine the frequencies of the notes emitted by the experimental pipe with a constriction in position: these comparisons were facilitated by the counting of beats.

In Table II. are shown the frequencies (expressed as  $n/n_0$  in those instances for which  $n/n_0 < 3$ ) obtained experimentally,

TABLE II.

$f$ .	Open Pipe.		Closed Pipe.	
	Calc.	Obs.	Calc.	Obs.
1/12.....	.85 1.82	*	.82 2.63	*
1/4 .....	.92 2.64	.93 2.69	.84 2.93	.81 2.93
1/3 .....	.95 1.88	.97 1.90	.86	.84
1/2 .....	1.67	1.66	.89 2.71	.87 2.75
2/3 .....	.95 1.88	.94 1.96	.93 2.46	.94 2.56
3/4 .....	.92 2.64	.91 2.63	.97 2.47	.97 2.58
11/12.....	.85 1.82	.83 1.83	1.00 2.86	.99 2.90

\* Due to a slight tapering of the pipe "boot" it was not possible to place the constriction in the place corresponding to  $f=1/12$ .

In some instances other notes, normal overtones of the pipe without a constriction and tones to be expected if the diaphragm formed a node, were elicited by appropriate blowing.

and from figs. 2 and 3 for the fundamental and first overtone of the 60 cm. brass pipe †. The conductance of the hole in the diaphragm, determined in the manner described above, was 1.02 cm. ‡ With the kind assistance of Mr. W. Lethersich, B.Sc., the results were verified approximately by means of a sonometer.

† The corrected length of (a) the open pipe (including end corrections and "boot" length) was 76.5 cm., and (b) the pipe when closed by a 3.2 cm. thick brass stop was 71.9 cm.

‡ With a smaller wave-length than any used in these experiments a smaller value for the conductance of a hole of this size has been determined.

It is considered that the agreement between the "theoretical" and actual results is sufficient to substantiate the correctness of the theory proposed.

It is of interest to note that M. de Mons places his constriction near the mouth of a stopped pipe and also decreases the conductance of the orifice by making it in the form of a short tube instead of a simple hole in a diaphragm: the present theory shows that both these procedures tend to minimize the frequency of the note.

I have pleasure in tendering my thanks to Professor Lees for placing the resources of his laboratory at my disposal for the purposes of this work, and to Messrs. Spurden Rutt & Co., of Leytonstone, for supplying the pipe "boots."

#### References.

- (1) Irons, *Phil. Mag.* v. p. 580 (1928).
- (2) Irons, *Phil. Mag.* x. p. 16 (1930).
- (3) Irons, *Phil. Mag.* ix. p. 346 (1930).
- (4) Webster, *Proc. Nat. Acad. Sci.* v. p. 275 (1919).
- (5) Paris, *Phil. Mag.* xlviii. p. 769 (1924).
- (6) Irons, *Phil. Mag.* vii. p. 873 (1929).

---

LXXXVII. *The Orientation of Rolled Aluminium.* By J. THEWLIS, *M.Sc.*, *Physics Department, National Physical Laboratory, Teddington, Middlesex* \*.

[Plates VIII.-X.]

THE present investigation on the rolling of aluminium is divided into two parts. The first part deals with the flat-rolling of aluminium, which has been the subject of divergent opinion, and the second part deals with the square-rolling of aluminium, which has not previously been investigated. The latter refers to a specimen which has been rolled in such a way as to preserve a square cross-section throughout the rolling process.

#### 1. *The Orientation of Flat-rolled Aluminium.*

The results of previous investigations on the flat-rolling of aluminium, with the exception of those of Göler and Sachs†,

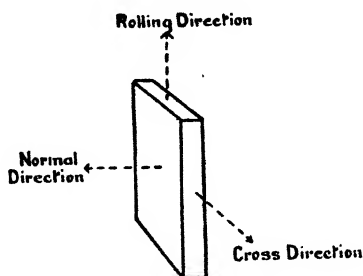
\* Communicated by Dr. G. W. C. Kaye, Superintendent.

† v. Göler and G. Sachs, *Z. f. Phys.* xli. p. 873 (1927).

may be divided into two groups. In one \* the direction of rolling is given as a  $[111]$  direction and the normal direction as a  $[211]$ , and in the other † the rolling direction is given as a  $[211]$  direction and the normal direction as a  $[01\bar{1}]$ . Göler and Sachs find that the rolling direction is in the neighbourhood of a  $[335]$  direction and the normal direction is in that of a  $[\bar{5}31]$ .

In the present investigation two series of photographs were taken of a specimen of flat-rolled aluminium, the X-ray beam making various angles with the normal direction (fig. 1). The rolling direction was vertical in one series and the cross direction was vertical in the other. The X-rays (from a molybdenum target) passed straight through the specimen, a photographic plate being set up at

Fig. 1.



right angles to the beam. The photographs consisted of spots lying on powder rings. The intensity and position of each spot varied from photograph to photograph. Each plane reflected to some extent in almost every position of the specimen, indicating a somewhat incomplete selective orientation.

Fig. 2 (Pl. VIII.) and fig. 3 (Pl. IX.) illustrate the kind of photograph obtained.

If it could be decided in what position of the specimen a given spot had its maximum intensity on the photograph, it would be easy to determine the predominating orientation. Unfortunately the spots appear to be of the same intensity in some cases for a range of  $20^\circ$  or  $30^\circ$  in the

\* F. Wever, *Z. f. Phys.* xxviii. p. 69 (1924); Owen and Preston, *Proc. Phys. Soc.* xxxviii. p. 132 (1926).

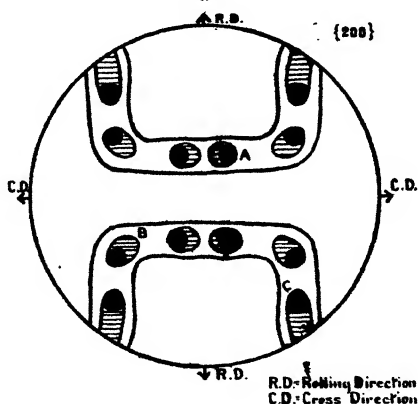
† Uspenski and Konobejewski, *Z. f. Phys.* xvi. p. 215 (1923); Mark and Weissenberg, *Z. f. Phys.* xiv. p. 328 (1923).

position of the specimen. This is due partly to the difficulty of comparing relative intensities on separate negatives, and partly to the incompleteness of the selective orientation. It is therefore necessary to devise a method for finding the mean position of maximum reflexion, for each plane.

The method adopted will be illustrated by considering its application to the  $\{200\}$  planes, these being the easiest to discuss.

Corresponding to each spot on any photograph there must be a certain "reflexion plane" of the specimen in a definite position. This position was determined for each of the  $\{200\}$  spots in both series of photographs, and the

Fig. 4.



poles of the various "reflexion planes" were plotted on a stereographic projection of the specimen. The projection is shown in fig. 4, and maps out the areas in which the  $\{200\}$  poles lie.

The shaded portions correspond to intense spots on the photographs, and therefore to concentrations of  $\{200\}$  poles. The problem is to find positions of maximum preference in these portions.

Consider the area A (fig. 4). One of the required poles is within this area, and there must be two other corresponding poles  $90^\circ$  away from it and from one another. The only areas in which these can lie are those marked B and C. Owing to the difficulty mentioned above of comparing relative intensities on separate negatives the areas

A, B, and C are larger than they would have been if their extent had been entirely due to incomplete selective orientation. These additions to the true areas may be detected by their having no corresponding areas  $90^\circ$  away from them. Thus it is obvious that some of the points in

Fig. 5.

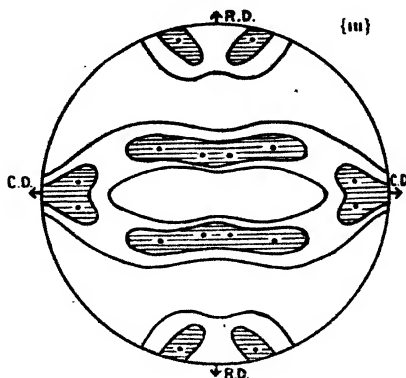
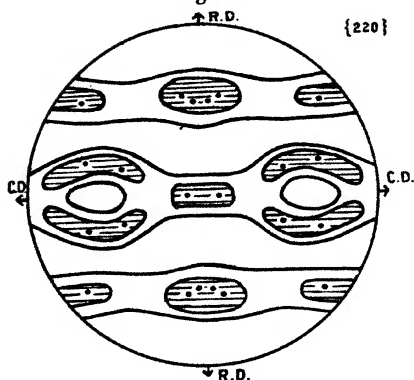


Fig. 6.



B have no corresponding points  $90^\circ$  away from them in A, so that the area of B which need be considered can be reduced. Similarly, by taking the areas in pairs portions of A and C can be eliminated, enabling B to be cut down still more. The process can be continued until all portions of the areas not having corresponding parts  $90^\circ$  away from them have been eliminated. The areas left as a result of

this process are represented by black areas in the diagrams. A maximum has been taken to be at the middle of each black area. It will be noticed that there are twelve such areas; hence four sets of crystals occur.

Figs. 5 and 6 show corresponding diagrams for the  $\{111\}$  and  $\{220\}$  poles respectively. The final black areas have been omitted for simplicity, the positions of maximum preference being indicated by dots. Fig. 7 shows the maxima of the poles of all three types of plane, for one set of crystals, plotted on the same diagram. From the angles which the poles of fig. 7 make with the rolling direction and the normal direction, the direction cosines of these two directions with respect to the cube axes  $[100]$ ,  $[010]$ , and  $[001]$  may be calculated. These (expressed as angles) are shown in Table I.

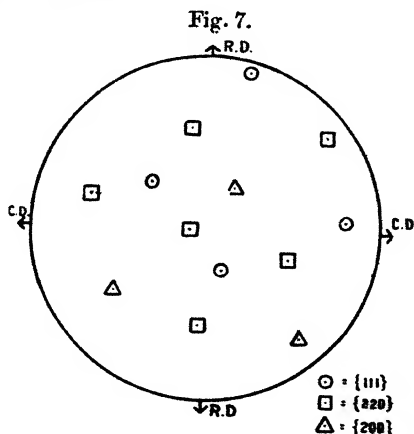


TABLE I.

Angle between :	[100].		[010].		[001].	
	and :					
	R.D.	N.D.	R.D.	N.D.	R.D.	N.D.
Calc. from $\{111\}$ planes.	62°·9	123°·0	40°·0	98°·9	62°·5	35°·6
Calc. from $\{200\}$ planes.	59°·0	118°·0	44°·5	103°·0	62°·0	31°·0
Calc. from $\{220\}$ planes.	64°·0	127°·0	38°·6	96°·2	63°·8	38°·2
Mean .....	62°·0	122°·7	41°·0	99°·4	62°·8	34°·9
Direction cosines ..	0·470	-0·540	0·755	-0·163	0·457	0·820

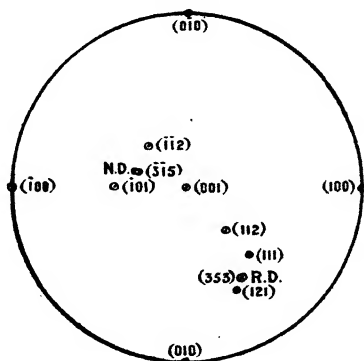


The direction cosines of the rolling direction are seen to be very nearly in the ratio 3 : 5 : 3, and those of the normal direction to be very nearly in the ratio - 3 : - 1 : 5.

From Table I. the positions of the rolling direction and normal direction were plotted on a stereographic projection of the crystal, the plane of projection being the (001). This is shown in fig. 8.

It can be seen that the rolling and normal directions are not far from  $[353]$  and  $[\bar{3}15]$  directions respectively. It must be remembered, however, that the rolling and normal directions occur within appreciable ranges, and must not be associated with definite directions, crystallographic or non-crystallographic.

Fig. 8.



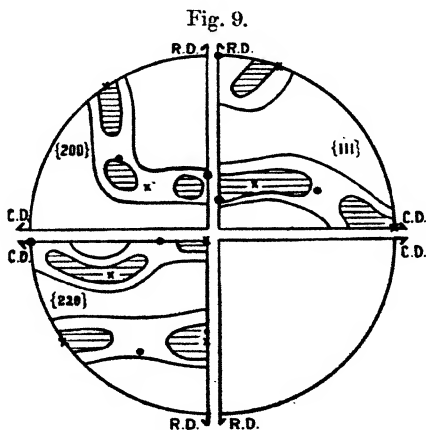
It has already been mentioned that investigations previous to that of Göler and Sachs gave either a  $[111]$  or a  $[211]$  as the direction of rolling, with a  $[\bar{2}11]$  and a  $[01\bar{1}]$  as normal direction respectively. Göler and Sachs \* suggest that these two orientations might exist together, and by overlapping give a result similar to that found. In this case one would expect the areas in figs. 4, 5, and 6, corresponding to strong reflexions, to contain the positions of poles which would occur if the two orientations in question existed. Accordingly the positions of these poles were marked on figs. 4, 5, and 6, and collected on one diagram (fig. 9). The points refer to the orientation with a  $[111]$  as direction of rolling, and the crosses refer to that with a  $[211]$  as rolling direction.

\* *Loc. cit.*; *Zeit. f. Phys.* lvi. p. 477 (1929).

It will be seen that the areas of strong reflexion lie in general between the poles. If the result is to be explained by the overlapping of the two orientations, then it must be assumed that these orientations are very indefinite. This is equivalent to the statement that the rolling direction and normal direction can each occur within a big range. There seems to be no reason for assuming the existence of these two orientations as such.

## 2. The Orientation of Square-rolled Aluminium.

The specimen (which before square-rolling had been carefully annealed, and on examination by X-rays had



given no sign of selective orientation) was mounted on a goniometer. As before, a fine beam of X-rays from a molybdenum target was passed straight through the specimen, a photographic plate being set up at right angles to the beam.

The rod was mounted with the direction of rolling vertical, and a series of photographs was taken in which the X-ray beam made different angles with a face of the specimen. In each case the photograph was the same as that obtained when the specimen was rotated about the rolling direction. This photograph is reproduced in fig. 10 (Pl. X.). Such a result suggested that the crystals of which the rod was composed had one crystallographic direction in common, but were otherwise randomly oriented, the common direction being parallel to the direction of rolling.

This was confirmed by taking photographs in which the direction of rolling was horizontal, the specimen being rotated about a vertical axis. The same picture was obtained whatever the inclination of the specimen faces to the vertical. Such a photograph is reproduced in fig. 11 (Pl. X.).

The direction of rolling may be determined from fig. 10 (Pl. X.). It is found to coincide with a  $[111]$  direction. There is also evidence of the presence of a second orientation with a  $[100]$  direction in the direction of rolling. Table II. gives the angles between the normals to the various planes and the rolling direction as observed and as calculated for a  $[111]$  as rolling direction and a  $[100]$  as rolling direction.

TABLE II.

Plane (h. k. l.)	Angle between normal to plane and rolling direction.		
	Observed.	Calculated.	
		$[111]$ as R.D.	$[100]$ as R.D.
111	$\begin{cases} 54^{\circ}.9 \\ 70^{\circ}.7 \end{cases}$	—	$54^{\circ}.8$
200	$\begin{cases} 55^{\circ}.1 \\ 35^{\circ}.4 \end{cases}$	$70^{\circ}.6$	$90^{\circ}.0$
220	$\begin{cases} 35^{\circ}.4 \\ 90^{\circ}.0 \end{cases}$	$54^{\circ}.8$	$45^{\circ}.0$
		$90^{\circ}.0$	$90^{\circ}.0$

Thus a square-rolled aluminium rod has the same orientation as a cold-drawn aluminium wire\*.

In addition to the above, observations were made on the square-rolling of a rod which had previously been flat-rolled. The orientation of the rod before square-rolling was found to be the same as that described in Part I. After square-rolling it was found that the direction of rolling was a  $[111]$  direction, the normal to one pair of faces a  $[110]$ , and the normal to the other pair a  $[11\bar{2}]$ . It is hoped to pursue this investigation at a subsequent date.

The author is indebted to Dr. G. Shearer for his continued interest and helpful criticism, and to Prof. G. I. Taylor, who kindly furnished the specimens.

\* Ettisch, Polanyi, and Weissenberg, *Z. f. Phys. Chem.* xcix. p. 332 (1921); Schmid and Wassermann, *Z. f. Phys.* xlii. p. 779 (1927).

*Summary.*

The orientation of a flat-rolled aluminium sheet has been determined by a graphical method. It has been found to be such that no definite direction in the crystal can be identified with the rolling direction or the normal direction. The mean position of the rolling direction is near a  $[353]$  direction, and that of the normal direction is near a  $[\bar{3}15]$  direction. Four sets of crystals occur, the plane of the rolling and normal directions and the plane of the cross and normal directions behaving like mirror planes. This result confirms that of Göler and Sachs.

The effect of the square-rolling of aluminium has been investigated. It has been found that a square-rolled rod, if rolled from an aluminium rod possessing random orientation, has the same orientation as a cold-drawn aluminium wire.

It has been found that the square-rolling of an aluminium rod which has previously been flat-rolled produces an orientation in which the rolling direction is a  $[111]$  direction, the normal to one pair of faces a  $[1\bar{1}0]$  direction, and the normal to the other pair a  $[11\bar{2}]$  direction.

LXXXVIII. *Notices respecting New Books.*

*The Zeta-Function of Riemann.* By E. C. TITCHMARSH, M.A. (Cambridge Tracts in Mathematics and Mathematical Physics, No. 26.) [Pp. vii + 104.] (Cambridge: At the University Press, 1930. Price 6s. 6d. net.)

IN this tract an account is given of the theory of the zeta-function, without regard to its applications in the theory of numbers, which is to form the subject of a companion tract. The better-known properties of the function are briefly sketched in an introductory chapter. The first chapter is devoted mainly to inequality theorems, with a view to the study of the asymptotic behaviour of  $\zeta(\sigma + it)$ , as  $t \rightarrow \infty$  for given values of  $\sigma$ . It is shown that there is a critical strip within which the problem of the order of the function is unsolved. The second chapter deals with mean value theorems, and it is shown that the problem of the average order or mean value of the function in the critical strip is much easier. The important problem of the distribution of the zeros of the function is discussed in the third chapter,

along with the famous "Riemann hypothesis," that all the complex zeros of  $\zeta(\sigma + it)$  lie on the line  $\sigma = \frac{1}{2}$ . This is followed in the next chapter by the wider problem of the general distribution of the values of the zeta-function; this chapter is in part adapted from a manuscript prepared by Professors Bohr and Littlewood. In Chapter V. some of the consequences of the improved Riemann hypothesis are investigated; if the hypothesis is false, it might be hoped that in this way a contradiction would sooner or later be met with, but so far the theory based on the hypothesis has proved perfectly coherent. The hypothesis enables more precise results to be deduced about the vertical distribution of the zeros and about order problems. In a final chapter some consequences of Lindelöf's hypothesis are considered. This hypothesis is more restricted than Riemann's, and does not necessarily involve the truth of the latter, although, on the other hand, if Riemann's hypothesis is true, Lindelöf's hypothesis is also true.

The tract provides an excellent summary of zeta-function theory, clearly though concisely expressed. The most recent investigations are incorporated. An extensive bibliography is added at the end, to which references are given throughout the text.

*A Comprehensive Treatise on Inorganic and Theoretical Chemistry.* By J. W. MELLOR, D.Sc., F.R.S. Vol. x. S, Se. [Pp. x + 958, with 66 figures.] (London: Longmans, Green & Co., 1930. Price £3 3s. net.)

THE publication of Dr. Mellor's "magnum opus" is proceeding at the rate of one volume per year. Three further volumes have yet to be published. The new volume is devoted to the allied elements, sulphur and selenium: 692 pages are given to sulphur and 266 to selenium. Both of these elements have physical properties of considerable interest, and emphasise the advantages of Dr. Mellor's arrangement, which deals in some detail with both physical and chemical problems. The sections which deal with the history, occurrence, methods of extraction, and use contain much of general interest. Under compounds of sulphur, sulphuric acid naturally occupies a prominent place and receives very full treatment.

With the progress of the publication of this great work, one becomes more and more amazed at the industry of the author, at the manner in which the standard of the initial volumes has been maintained, and at the thoroughness with which not only chemical but also physical literature has been combed almost up to the date of publication. The work is remarkably complete, and fullest references to original papers are given. There are doubtless some omissions, but

a careful search through the present volume has failed to reveal any of importance. Each volume contains a detailed subject-index. No chemical library can afford to be without Dr. Mellor's 'Comprehensive Treatise.'

*An Outline of Wave Mechanics.* By N. F. MOTT, Lecturer in Theoretical Physics, The University, Manchester. (Cambridge University Press, 1930. Price 8s. 6d.)

THIS interesting book is based on a course of lectures given by Mr. Mott in the University of Manchester in 1929-30.

Mr. Mott's aim has been to give an account of the New Quantum Theory which should be intelligible to the advanced student of experimental physics and to the research worker.

The author presupposes an acquaintance with Fourier analysis and with the elementary principles of wave-motion, but so excellent is the exposition that the intelligent student—to whom it is addressed—should have no difficulty in following any mathematical argument which is introduced.

The reviewer would like specially to recommend this volume not only to students of physics, but also to the applied mathematicians.

*A History of Science.* By WM. CECIL DAMPIER-WHETHAM, M.A., F.R.S., Fellow and sometime Senior Tutor of Trinity College, Cambridge; Fellow of Winchester College. (Cambridge University Press, 1929. Price 18s.)

IN this interesting volume Mr. Dampier-Whetham makes an attempt to give a complete outline of the development of scientific thought. The general plan is based on a book entitled 'Science and the Human Mind,' published by Mr. Dampier-Whetham as long ago as 1912. The present volume also contains many of the ideas in the chapter on the "Scientific Age" of the Cambridge Modern History and the article "Science" in the eleventh edition of the 'Encyclopædia Britannica.'

It is of great value to the general reader to have this important material welded together in one compact volume.

Mr. Dampier-Whetham has also, of course, published a number of other essays on the subject, including an interesting chapter in Harmsworth's Universal History.

The volume is notable for the large number of references which would enable the student of the subject to read more and more deeply in this important branch of history.

At the present time, when fundamental advances are being made in so many different directions, there is a danger that the history of science may not be sufficiently studied by the young student. This fascinating and interesting work should certainly do something to counteract this tendency.

*Optics.* By B. K. JOHNSON, F.R.M.S., Demonstrator in the Technical Optics Dept. of the Imperial College of Science and Technology, Lecturer in the Applied Optics Dept. of the Northampton Polytechnic Institute (London). (London: Edward Arnold & Co., 1930. Price 8s. 6d.)

THIS interesting and useful book serves as a convenient reference book for a course of lectures and experiments in optics.

There appears to be a modern tendency for mathematical students to study optics without sufficient experimental background. To the present reviewer it would seem an admirable plan if the ordinary theoretical reading of the mathematical student were supplemented by a course of experiments. In such a scheme the present book would prove of the greatest value.

This book, however, has no doubt as its primary purpose the education of the students of physics, and the author has certainly succeeded admirably if this is his aim.

It is a feature of the book that there is a detailed description of all the apparatus required, so it should prove exceedingly handy for the assistant who is responsible prior to the lecture for seeing that everything is ready to hand.

A word must be added about the diagrams, which seem specially successful.

*Traité de Polarimétrie.* Par Prof. GEORGES BRUHAT. [Pp. xvi + with 250 figures.] (Paris: Éditions de la *Revue d'Optique théorique et instrumentale*, 1930. Price 65 frs.)

PROFESSOR BRUHAT has defined, in his introduction, the subject of this book as the study of the phenomena of rotatory polarization and of the apparatus used for their measurement. With subject-matter so defined, the book naturally falls into two sections, one dealing with the instrumental equipment and the methods of making the measurements, and the other concerned with the observed phenomena and their applications.

The phenomena associated with the radiation of the plane of polarization are of interest to the physicist, to the laboratory chemist, and to the industrial chemist in certain industries. The author has had all three classes in mind in writing this book, and has aimed at producing a volume which shall be self-contained, in the sense that a chemist, for instance, using the book will not need to turn to another book to find the meaning of a physical term. The physical principles involved in polarization and double refraction are therefore developed at some length. The book suffers to some extent from over elaboration in this respect, though this is an error on the right side. The instruments described and their use are explained

with great care, and all who use such apparatus will undoubtedly derive much benefit from the study of this book. The author remarks that chemists will only use apparatus which is supplied in perfect order by the maker, but that he has deemed it necessary that they should know the defects and good points of different apparatus and why the most expensive apparatus is effectively the best.

In the second part the chief phenomena of rotatory polarization are discussed and theories of stereo-chemistry are considered. A considerable space is naturally devoted, both as illustrating the methods and also on account of its intrinsic importance, to the determination of sugar contents. The two final chapters deal with rotatory effects of crystals and magnetic rotatory polarization.

An extensive bibliography is given which will be found of great value, and a good index is provided. The bibliography emphasises the large amount of work which has been done in this subject and the rapid developments in recent years. The volume is well provided with illustrations of instruments and with numerous diagrams. The paper on which it is printed is of poor quality.

*La Topographie sans Topographes. Traité de Photogrammétrie.*  
Par F. OLLIVIER. [Pp. xviii + 301, with 158 figures.]  
(Paris : Éditions de la *Revue d'Optique théorique et instrumentale*, 1929. Price 42 fr.)

THE application of photographic methods to topographical surveying is becoming of rapidly increasing importance, particularly in the case of mountainous regions, in view of the great saving in field-work which it permits and of the high order of accuracy which it can attain. This volume, by Captain Ollivier, of the French Army, gives an excellent account of the methods of observation, of the instruments used, and the manner in which the photographs are measured and reduced. It deals only with vertical photographs taken from points on the surface of the earth. Aerial surveying is being rapidly developed, and a further volume is promised in which the restriction to vertical photographs will be removed and the use of photographs taken under any conditions and in particular from aeroplanes will be discussed.

The volume begins with an interesting historical retrospect, from which the interesting fact emerges that as early as 1860 the French Colonel Laussedat had developed all the principles which were embodied at a later date in the Zeiss phototheodolite. The author then considers the general principles embodied in the observation of relief; and deals with binocular and stereoscopic vision and stereoscopic instruments. This provides a basis for the appreciation of the principles involved



in stereophotograms. These principles, both geometrical and instrumental, are carefully and clearly explained. A chapter is devoted to the Zeiss phototheodolite, the Zeiss stereo-comparator and the stereoautograph. It is to be regretted that no account is given of the remarkable Wild phototheodolite, which the author would perhaps regard as not sufficiently tried out in practice. An interesting and important chapter deals with the question of the precision of the methods, and a comparison with the precision attainable by other methods of surveying is made; a detailed study of the various instrumental and other errors is given. This is followed by a further chapter dealing with the corrections required to take account of residual instrumental imperfections, with a view to obtaining the highest precision possible. The final section deals with observational procedure and methods of conducting surveys.

The volume provides not merely a very adequate account of the theory underlying the methods of photographic surveying, but deals with all the practical points involved from the time of securing the photographs to their final measurement and reduction. The author knows his subject thoroughly and has given an admirable exposition of it. The further volume, in which the limitation to vertical photographs is removed, will be awaited with much interest.

*Cours d'Analyse, professé à l'Ecole Polytechnique.* Tome II.  
Par J. HADAMAND. [Pp. vi + 721, with 72 figures.]  
(Paris: Librairie Scientifique, Hermann et C<sup>e</sup>, 1930. Price 140 frs.)

THE general subjects treated in the second and concluding volume of Professor Hadamand's 'Cours d'Analyse' include potential theory, calculus of variations, the properties of analytic functions, differential equations, partial differential equations, the theory of probabilities, and the error law of Gauss.

Whilst adhering to a vigorous treatment throughout, the author has endeavoured to bring into the foreground various applications to neighbouring branches of science; dynamics, hydrodynamics, wave-theory, electrical theory, astronomy, and optical theory supply illustrations. The course is thus particularly well adapted for physical students. The treatment is not advanced, but is very comprehensive, and difficult points are carefully and clearly expounded. The general properties of harmonic functions are dealt with under the section concerned with potential theory; those of elliptic functions are dealt with under analytic functions. The solution of differential equations by methods of successive approximation is given prominence, in view of its practical importance.

LXXXIX. *Proceedings of Learned Societies.*

## GEOLOGICAL SOCIETY.

[Continued from p. 368.]

June 11th, 1930.—Prof. E. J. Garwood, M.A., Sc.D., F.R.S.,  
President, in the Chair.

SLIDES illustrating frost stone-packing on the shores of Loch Lomond in relation to stone-polygons were exhibited by Prof. J. W. GREGORY. He remarked that the stone-polygons of the Arctic soils had been described by Dr. C. S. Elton in the *Quarterly Journal* (vol. lxxxiii, 1927, pp. 163–93), and are well known from an extensive literature. According to the chief alternative theories, they are due either to pebbles being pushed outwards from a freezing centre which is left as a stoneless core of clay, or to repeated freezing reducing the central material to dust (Nansen's theory). When the President and himself landed in Spitsbergen with Sir Martin Conway's Expedition in 1896, their interest was at once aroused in these structures, which they regarded as the effect of repeated frost and thaw. So far as he knew, the structures are not definitely known from the Glacial drifts; he had seen embryonic developments in the soil in several places in Scotland, and they are well developed on the summit of the Merrick, the highest mountain in Scotland south of the Highlands. A development of this frost stone-packing occupies some acres on the eastern shore of Loch Lomond, on the Ross Promontory, on a beach formed of waste-fragments from an old slate-quarry. The slate fragments are vertical or steeply inclined; they are arranged in concentric series, often around boulders of the Lennoxian grits, and in places around tree-trunks. They occur in groups ranging from a few inches to a few feet in diameter. They are simple or multiple, regular or irregular in shape, and in some cases occur in bands composed of polycentric groups around oval depressions as much as 12 yards long; these long bands resemble the arcuate series in the Arctic.

This stone-packing is an example of solifluxion. The remarkable development beside Loch Lomond is clearly due to the repeated freezing of ground composed of flat slate-fragments, and irregularly charged with water; the absence of the mud core is due to the lack of fine-grained sediment; the vertical position of the stones indicates their packing and arrangement by horizontal pressure.

The slate-quarry was last worked 51 years ago, and the stone mosaic has probably been developed gradually during that interval.

June 25th, 1930.—Prof. E. J. Garwood, M.A., Sc.D., F.R.S.,  
President, in the Chair.

A LECTURE on the Tertiary Igneous Complex of Ardnamurchan was delivered by JAMES ERNEST RICHEY, M.C., B.A., F.R.S.E., F.G.S. The Lecturer said that Ardnamurchan is the

last of the well-known igneous complexes of Western Scotland to be studied in detail by the Geological Survey, and illustrates in a comparatively simple manner many of the remarkable features of Tertiary igneous activity in Britain. The mapping was carried out by Prof. E. B. Bailey, Mr. Simpson, and the Lecturer, and Dr. Herbert H. Thomas had been responsible for the petrology.

The district measures some 9 miles from east to west and 5 miles from north to south. It is chiefly noteworthy on account of its intrusive rocks, and only small outliers of the widespread Tertiary plateau basalt-lavas are preserved. The types of intrusion include volcanic vents piercing the basalt-lavas, and largely filled with acid and trachytic fragmental materials; minor intrusions, including cone-sheets, chiefly quartz-dolerite, and dykes; and plutonic masses, nearly all gabbro or dolerite, occurring mainly as ring-dykes. The above, excepting the dykes, are arranged in concentric series around three different centres, marking three foci of igneous activity which functioned successively.

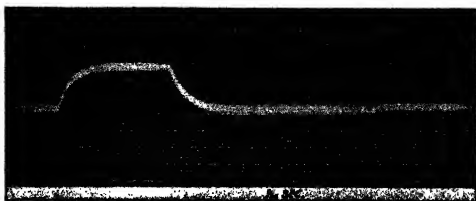
Around Centre 1, situated on the east, there are extensive volcanic vents, a few major intrusions, and a set of massive cone-sheets. In relation to Centre 2, on the west, periods of cone-sheet and ring-dyke intrusion alternated, and there is only one small elongate vent. Country-rocks were first domed around this centre and then copiously injected by cone-sheets, including many of composite habit, with acid centres. These cone-sheets form an outer set around the succeeding ring-dykes. The intrusion of the ring-dykes was interrupted by a second, inner, suite of cone-sheets. Although only a single vent is developed, explosive brecciation of the walls of ring-dykes, or of entire ring-dykes themselves, is a recurring feature. The complex of Centre 3, situated midway between the two earlier centres, has obliterated large portions of those of earlier date. It consists of ring-dykes, with only a few cone-sheets cutting the outermost and earliest ring-dyke. The ring-dykes are, on the whole, successively younger as the centre is approached, and the more centrally situated include rock-types of rare occurrence in the British Tertiary province—biotite-bearing gabbros, tonalite, and quartz-monzonite. No vents are met with, and brecciation of the walls of ring-dykes is rarely seen. It is suggested that the three complexes are successively more deep-seated, due, presumably, to the growth of an overlying volcanic pile. The regular ring-patterns marked by the intrusions are, however, of more especial interest. They constitute evidence of the formation of annular or arcuate fissures that are considered here, as in Mull, to have resulted from localized stresses set up in the roof of an underlying magma-reservoir.

North-west dykes are numerous, and were intruded at various times during the period of localized activity, as well as after its close. The more westerly belong, in part at least, to the great Mull swarm.

---

*[The Editors do not hold themselves responsible for the views expressed by their correspondents.]*

FIG. 3.



CURVE 1.—Steady deflexion. Discharge.  
Liquid paraffin "A," 52.5° C. Film thickness 0.4 mm.



CURVE 2.—Effect of 20.4 sec. short-circuit on liquid paraffin "B," 94° C.  
(Steady deflexion before short-circuit shown on left.)



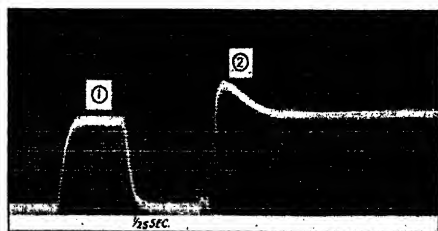
CURVE 3.—Liquid paraffin "B" initial current, 350 v., 94° C.  
(Time indication of moment of application omitted).



FIG. 8.



CURVE 1.—Deflexion before reversal. Reversal.  
Liquid paraffin "A," 91° C. Film thickness 0.8 mm.



CURVE 2.—Increase in deflexion on double reversal: 1. Steady deflexion;  
2. After second reversal. (Deflexion due to first reversal not shown.) Liquid Paraffin "A," 71° C. 0.4 mm. film.



CURVE 3.—Liquid paraffin "B" reversal current, 350 v., 86° C.



FIG 2.

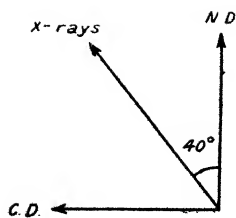
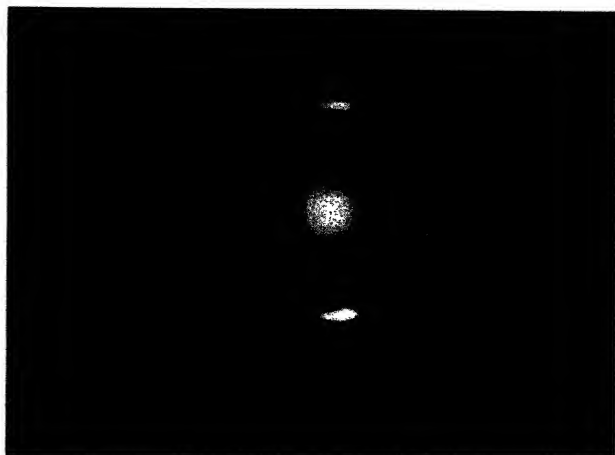






FIG. 3.

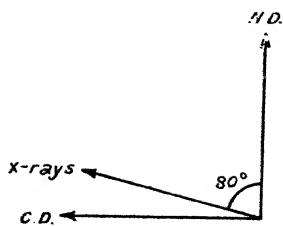
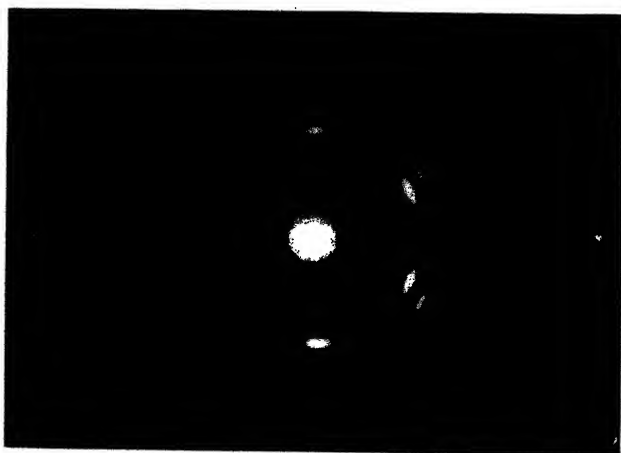




FIG. 10.

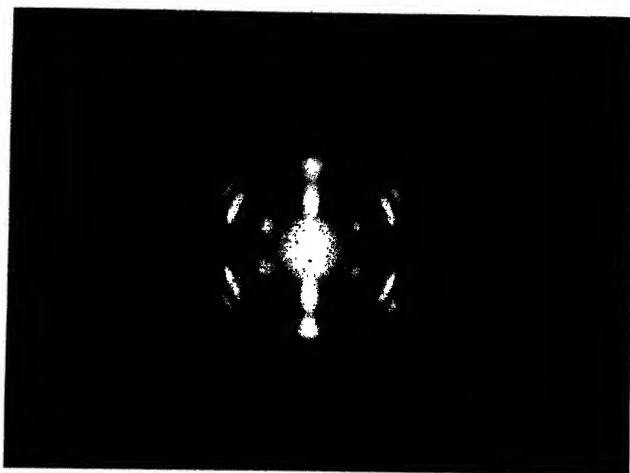
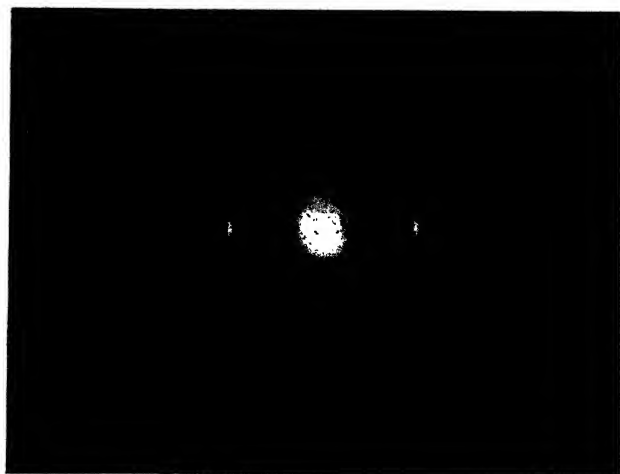


FIG. 11.





THE  
LONDON, EDINBURGH, AND DUBLIN  
PHILOSOPHICAL MAGAZINE  
AND  
JOURNAL OF SCIENCE.

---

[SEVENTH SERIES.]

---

DECEMBER 1930.

---

XC. *On some Radio-Frequency Properties of Ionized Air.*  
By E. V. APPLETON, F.R.S., and E. C. CHILDS, B.Sc.\*

1. *Introduction.*

THE experimental investigations described in the present paper were carried out with the aim of elucidating by laboratory experiments the rôle played by ionized air in wireless-wave propagation. Interest in such experiments dates back to the British Association discussion of 1912, in which Dr. Eccles gave an account of his ionic refraction theory †, according to which the bending of wireless waves round the earth is attributed to an increased phase velocity brought about in the upper atmosphere by the presence of ions. As a result of the discussion the late Professor E. H. Barton, at the suggestion of Professor J. A. Fleming, began an experimental investigation of the effect of ionization on the conductivity and dielectric constant of ionized gas for high frequency electromotive forces. Theory indicates that, for conditions under which the phase velocity of electric waves of a particular frequency is increased by the presence of ions, the dielectric constant of the medium should be less than unity for alternating electromotive forces of the same frequency.

\* Communicated by the Authors.

† *Vide* Proc. Roy. Soc. A, lxxxvii, pp. 79-89 (1912).

Barton and Kilby\*, using gaseous ionization produced at atmospheric pressure by X-rays or radium bromide, were able to detect, by high frequency methods, the effect of the conductivity of the gas; but they did not consider that their results indicated a diminution of the dielectric constant of the gas. Their experimental apparatus included an oscillatory circuit in which the condenser consisted of two plates between which the ionization was produced. Variations of apparent capacity were found, which were attributed to the effects of the conductance of the gas acting as a leak in parallel with the condenser. It was shown that the effect of such a leak would be to alter the natural frequency of an oscillatory circuit, and the variations of apparent capacity were attributed to this effect. But the experimental arrangement used by Barton and Kilby was such that *forced* and not *free* vibrations were produced in the oscillatory circuit, and we think their work requires another interpretation. When this is done it will be seen that these authors probably did detect experimentally the reduction of the dielectric constant below unity—in other words, it is possible that their experiment was more successful than they thought.

The same problem of the dielectric constant of ionized gas was later attacked by van der Pol†, who used very short damped waves to energize a Lecher wire system. The effect of introducing the ionized gas of a glow discharge between two small electrodes at the end of the Lecher wire system was compared with the effect of introducing common salt solution of the same conductivity. The apparent dielectric constant of the ionized gas was examined at different pressures, and found to be sometimes greater than unity, sometimes indistinguishable from unity, and at very low pressures definite evidence of a dielectric constant less than unity was found. Van der Pol attributed the increase of the dielectric constant beyond unity to inhomogeneity in the gas between the condenser plates. In this connexion it may be mentioned that Barton and Kilby had previously found an apparent increase of the dielectric constant but they had regarded the effect as spurious and due to the effect of the conductance of the gas on the circuit tuning.

The present series of investigations was begun in 1922 at Cambridge by Captain A. G. D. West and one of the authors. It had been found theoretically that by tuning an oscillatory circuit to *potential* resonance and not to *current* resonance the difficulties usually introduced by shunting the oscillatory

\* Phil. Mag. [6] xxvi. p. 567 (1913).

† Thesis, University of Utrecht (1920).

circuit condenser by a resistance could be entirely avoided, so that the problem of measuring the dielectric constant could be attacked in a new way.

In the experiments carried out at Cambridge in 1922, which are described briefly below, a definite diminution of the dielectric constant was found, confirming van der Pol's result, although the wave-lengths used were of quite a different order of magnitude. This effect was found chiefly at low pressures and very low ionic concentrations. With higher concentrations the dielectric constant assumed values greater than unity, so that the discrepancy of theory and experiment still remained although the experimental conditions were widely different from those of Barton and Kilby, on the one hand, and from those of van der Pol on the other. In this connexion it should be mentioned that the theoretical expression for the dielectric constant of ionized gas does not permit values greater than unity whatever the ionic concentration may be.

The experiments were resumed again in London in 1925 with the aim of elucidating the above-mentioned discrepancy and also of testing various modifications of the ionic theory of refraction that had been proposed in the meantime. For example, Sir Joseph Larmor\* had then just published a theory in which free electrons with long mean free paths were considered as the effective electrical agents in the process of atmospheric wave deviation, while it had been shown by one of the writers† that, if this were so, the earth's magnetic field would produce the magneto-optic phenomena of double refraction and rotary polarization. If the effective carriers are ions of molecular mass no such magnetic effects are to be expected for wave-lengths within the wireless spectrum. In the experiments carried out to test this point, which are described below, magneto-optic resonance corresponding to the Inverse Zeeman effect has been found, thus demonstrating that we must regard free electrons as producing the reduction of dielectric constant. An account is also given of experiments which explain the increase of apparent dielectric constant quantitatively as well as qualitatively.

Within the last few years papers on the subject of the dielectric constant of ionized gas have been published by Gutton‡, Bergmann and Düring§, Szekely||, and Benner¶.

\* Larmor, *Phil. Mag.* [6] *xlvi*. no. 228, p. 1025 (1924).

† Appleton, *Proc. Phys. Soc.* *xxxvii*. part 2 (Feb. 15th, 1925).

‡ *Annales de Physique*, *xiii*. p. 62 (1930).

§ *Annalen der Physik*, v. Bd. i. no. 8, p. 1041 (1929).

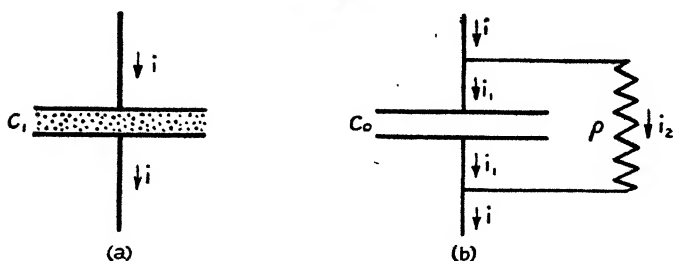
|| *Annalen der Physik*, v. Bd. iii. no. 1, p. 112 (1929).

¶ *Die Naturwissenschaften*, *xvii*. p. 120 (1929).



Gutton found a diminution of the dielectric constant for low ionic concentrations, but at higher concentrations he found an apparent increase of dielectric constant. From his results Gutton has concluded that the electrical carriers in ionized gas cannot be regarded as free, and that they possess a natural frequency, due to the existence of quasi-electric forces, which is proportional to  $N^{3/8}$ , where  $N$  is the number of electric charges per c.c. This result, if true, would completely revolutionize our ideas as to the mechanism of the atmospheric deviation of wireless waves, and therefore demands a careful examination. Bergmann and Düring have demonstrated the important and significant result that when there are only electrons between the condenser plates an increase in the dielectric constant is not observed, complete agreement with the simple theory (which predicts a

Fig. 1.



dielectric constant decreasing steadily with increase of  $N$ ) being found. Szekely, in an experiment mainly devoted to the measurements of absorptive effects, found evidence of an increase of apparent dielectric constant.

## 2. *The Measurement of the Dielectric Constant of a Conducting Ionized Medium.*

The effect of ionizing the air between the plates of a condenser is equivalent to altering the values of the capacity of the condenser and at the same time inserting a high resistance leak in parallel. In order to obtain the relationship between the dielectric constant and the degree of ionization of the medium (air) let us consider the equivalent circuits (figs. 1 *a* and 1 *b*).  $C_1$  is the capacitance of the leaky condenser, whose dielectric is ionized air, which may be considered as being electrically equivalent to a perfect condenser of capacitance  $C_0$  in parallel with a resistance  $\rho$ .

Let  $A$  be the area of the condenser plates in both cases and  $d$  the distance between them. Let  $V$  be the instantaneous value of the alternating potential difference across the plates. The electric field in both cases is given by  $V/d$ . We now consider each case separately.

*Circuit 1 a.*

Let us assume that the ionized medium contains  $N$  electrons per c.c. each of charge  $e$  and mass  $m$ . If  $x$  is the displacement of the electrons under the influence of the alternating electric field  $E$ , we have

$$m \frac{d^2 x}{dt^2} + g \frac{dx}{dt} = Ee, \quad \dots \quad (1)$$

where  $g$  is a frictional constant. If  $E$  is sinusoidal in form (*e. g.*,  $E_0 \sin pt$ ) we find that

$$\frac{dx}{dt} = v = \left( \frac{eg}{m^2 p^2 + g^2} \right) E - \left( \frac{me}{m^2 p^2 + g^2} \right) \frac{dE}{dt} \quad \dots \quad (2)$$

Now for the current through  $A$  units of area of cross-section we have, generally,

$$i = A \left( Nev + \frac{1}{4\pi} \frac{dE}{dt} \right), \quad \dots \quad (3)$$

so that, on substituting for  $v$  from (2), we have

$$i = \left( \frac{ANe^2 g}{m^2 p^2 + g^2} \right) E + \frac{A}{4\pi} \left( 1 - \frac{4\pi Ne^2 m}{m^2 p^2 + g^2} \right) \frac{dE}{dt} \quad \dots \quad (4)$$

*Circuit 1 b.*

Here we have (see figure)

$$i = i_1 + i_2 = \frac{V}{\rho} + C_1 \frac{dV}{dt},$$

or

$$i = \frac{d}{\rho} E + C_1 d \frac{dE}{dt} \quad \dots \quad (5)$$

Now, since the two systems are to be considered as electrically equivalent, we may equate the coefficients of  $E$  and  $\frac{dE}{dt}$  in (4) and (5). We then get

$$\frac{d}{\rho} = \frac{ANe^2 g}{m^2 p^2 + g^2}, \quad \dots \quad (6)$$

and

$$C_1 d = \frac{A}{4\pi} \left( 1 - \frac{4\pi Ne^2 m}{m^2 p^2 + g^2} \right), \quad \dots \quad (7)$$

But  $\frac{A}{4\pi d} = C_0$ , and  $\rho = \frac{d}{A\sigma}$ , where  $\sigma$  is the conductivity of the medium, so that we have from (6) and (7)

$$C_1 = C_0 \left( 1 - \frac{4\pi N e^2 m}{m^2 p^2 + g^2} \right), \quad . . . . (8)$$

$$\sigma = \frac{d}{\rho A} = \frac{N e^2 g}{m^2 p^2 + g^2} . . . . . (9)$$

We thus see that the introduction of the ionized gas between the plates of a given condenser is equivalent to diminishing the dielectric constant by  $\frac{4\pi N e^2 m}{m^2 p^2 + g^2}$ , at the same time adding a leak in parallel of magnitude given by  $\rho$  in (9) \*. The problem of investigating the high-frequency behaviour of ionized gas, then, resolves itself into the measurement of the dielectric constant of a conducting medium obeying Ohm's law.

### 3. *The Elimination of the Conductance Effect.*

In his experiments on the dielectric constant of a glow discharge van der Pol allowed for the effect of leakage on the conditions of resonance by a series of check experiments, using salt solution in place of ionized gas. In this case it had to be assumed that the dielectric constant of the salt solution was constant when the concentration and therefore the conductivity was varied. In the experiments described here the effect of the conductance of the gas on the "tuning" of the oscillatory circuit, of which the experimental condenser formed a part, has been eliminated. This was found to be possible by using an electrostatic voltmeter to determine the value of capacity for which the resonance voltage is obtained. The theory of this method is outlined very briefly below.

Let us consider the effect of the impression of an electromotive force  $E_0 \sin pt$  on the oscillatory circuit represented diagrammatically in fig. 2. We assume that reaction from the oscillatory circuit on the generator is negligible.

\* In the above calculation the ionization has been assumed small and the usual Lorentz local polarization term has not been introduced.

To introduce this term, however, it is only necessary to replace  $m$  in (8) and (9) by  $\left( m + \frac{4\pi N e^2}{3 p^2} \right)$ .

As the expression for Kirchhoff's laws for the oscillatory circuit we have

$$L \frac{di_1}{dt} + Ri_1 - E_0 \sin pt = \int \frac{i_2 dt}{C} = -v,$$

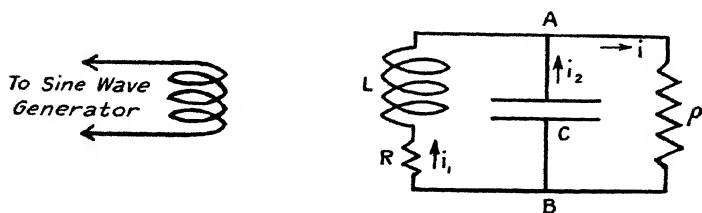
and

$$i = i_1 + i_2 = \frac{v}{\rho},$$

where  $R$  is the ohmic resistance of the coil  $L$ ,  $\rho$  the non-inductive resistance (*e.g.*, of ionized gas) in parallel with the condenser  $C$ , and  $v$  the instantaneous voltage between the points  $A$  and  $B$ . These equations may be combined in the representative differential equation

$$\frac{d^2v}{dt^2} + \left( \frac{R}{L} + \frac{1}{\rho C} \right) \frac{dv}{dt} + \frac{1}{LC} \left( 1 + \frac{R}{\rho} \right) v = \frac{E_0}{LC} \sin pt, \quad (10)$$

Fig. 2.



the particular integral of which is given by

$$v = A \sin (pt - \theta),$$

where

$$A = \frac{E_0}{LC \sqrt{\left( \frac{R}{L} + \frac{1}{\rho C} \right)^2 p^2 + \left( \frac{1}{LC} \left( 1 + \frac{R}{\rho} \right) - p^2 \right)^2}}. \quad (11)$$

The value of  $A$  is a maximum for a value of  $C$  given by

$$C = \frac{L}{p^2 L^2 + R^2}, \quad (12)$$

a value independent of  $\rho$ . For this condition of resonance we have

$$A = \frac{E}{R \sqrt{\frac{C}{L} + \frac{1}{\rho} \sqrt{\frac{L}{C}}}}. \quad (13)$$

Moreover, for a given value of  $p$  the particular amplitude obtained at resonance will depend on the relation of the circuit constants. When  $p$  is infinite the value of  $A$  increases steadily with increase of the ratio  $\frac{L}{C}$ , but when  $p$  is finite this is not so. For this case, to get maximum amplitude we must have

$$\frac{L}{C} = R\rho, \quad . \quad . \quad . \quad . \quad . \quad (14)$$

a condition mentioned previously\*.

The result demonstrated above may be summarized by saying that if by resonance obtained by capacity variation we mean that the voltage across the circuit condenser, and not the current in the coil, is a maximum, the value of the capacity necessary for resonance is independent of the leak resistance  $p$ †. Thus any alteration of capacity necessary to restore such voltage resonance when a leaky dielectric is introduced between the plates of the condenser  $C$  must be attributed to the effective dielectric constant of the dielectric and not to its conductivity.

#### 4. *Experimental Results.*

The first series of experiments on the dielectric constant of ionized air were carried out by Captain A. G. D. West and one of the writers at Cambridge during 1922-3. In these experiments alternating electromotive forces of frequencies varying from  $10^5$  to  $10^6$  cycles per second were used. In one form of apparatus used the experimental condenser consisted of two tin-foil sheets, pasted opposite each other on the walls of a discharge tube of simple type. The discharge was produced either by means of a cold cathode and a 4000 volt Evershed-Vignolles generator, or by means of a hot cathode (incandescent oxide-coated platinum) and a battery

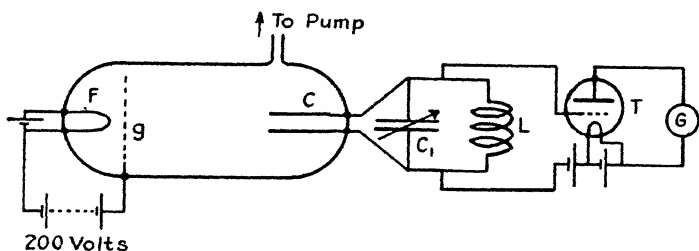
\* Appleton, Phil. Mag. xxxvii. p. 129 (1919).

† This result was communicated to Dr. D. Dye in 1927, who informed us that this property of an oscillatory circuit was well known at the National Physical Laboratory. More recently Mr. Albert Campbell has brought to our notice the interesting fact that, when the exciting electromotive force is applied to the oscillatory circuit between points A and B (see fig. 2), and not *via* the coil, one must use current resonance and not voltage resonance to make the appropriate value of the capacity independent of the leak. See Orlich, 'Kapazität und Induktivität,' 1909, p. 120; Jezewski, *Zeit. für Phys.* Bd. xlviii. p. 123 (1928); Doborzynski, *Zeit. für Hochfrequenz*, Bd. xxxi. p. 15 (1928); Lattey and Gatty, Phil. Mag. [7] ii. p. 985 (1929).

of cells. By means of a saturated diode in the circuit the amount of current passing through the diode, and thus through the discharge-tube, could be varied if necessary.

In another form of apparatus the experimental condenser was not situated midway between the anode and cathode, but was arranged as illustrated in fig. 3. Here the tube-current was varied by varying the current through the filament F. The grid G acted as anode and, because of its perforations, permitted the discharge to fill the tube. The experimental condenser C was connected in parallel with a variable calibrated condenser  $C_1$  connected to a coil L. The oscillatory potential across  $C_1$  and C was measured by means of a triode voltmeter T. The galvanometer used in this voltmeter was very sensitive, so that the triode generator supplying the impressed electromotive force could be used some metres away.

Fig. 3.



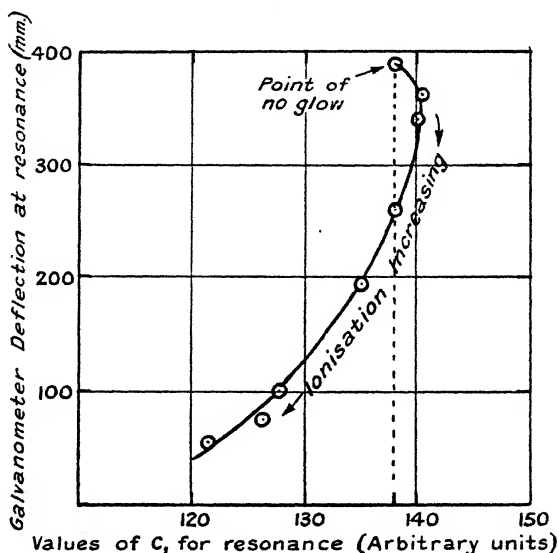
With such arrangements the experimental procedure was to plot a resonance curve of galvanometer deflexion against the readings of  $C_1$  with and without the discharge. If the value of  $C_1$  required for resonance was greater with the discharge than without a diminution of the dielectric constant was indicated. Very often a check on the theory outlined above was obtained by replacing a leak of extremely high resistance, connected across  $C_1$ , by one of similar pattern but of sufficiently low resistance to bring about the same damping as that produced by the glow discharge.

For the majority of combinations of tube-current and pressure the apparent dielectric constant was found to be greater than one. Only for the particular conditions of very low pressure and very small tube-current was the diminution of the dielectric constant below unity obtained. This result is illustrated in fig. 4, in which the value of the resonance amplitude is plotted against the value of  $C_1$  to give resonance.

To obtain these figures the value of the ionization current through the tube was steadily increased from a very low value.

From fig. 4 it will be seen that, as the ionization was increased, the effective dielectric constant at first became steadily less than unity, but reached a minimum value, and on increasing finally became greater than unity. It is interesting to note that the galvanometer deflexion at resonance steadily decreases as the ionization increases.

Fig. 4.



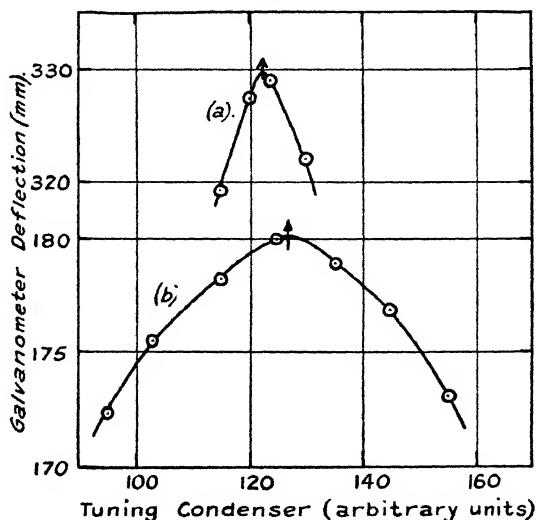
This is characteristic of all similar curves which we have obtained subsequently. In fig. 5 are shown resonance curves with and without the glow. The curve (a) shows the relation between galvanometer deflexion and tuning capacity with unionized air between the plates of the experimental condenser. The curve (b), taken with the glow present, shows much greater damping and a shift illustrating a dielectric constant less than unity.

The results described above were obtained at pressures of 0.01 to 0.06 mm. of mercury, and they were obtained only for conditions under which the discharge was somewhat difficult to maintain. In all runs carried out at high pressures

evidence of an increase of dielectric constant was always found. It was clear therefore that since, according to the theory outlined above, the dielectric constant of the ionized medium must be less than unity at all pressures and for all values of  $N$ , the apparent increase of dielectric constant, found experimentally, must most probably be a spurious effect of the discharge-tube.

Before passing to the second series of experiments carried out at King's College, London, in which the nature of this spurious influence was found, it may be of interest to note

Fig. 5.



that in the experiments carried out by Barton and Kilby in 1913 the criterion of resonance was maximum voltage amplitude across the oscillating circuit, as measured by an electrometer. Although Barton and Kilby applied a theory of free vibration to their results, it seems clear that the theory of forced vibration given above should more properly apply. The shift of Barton and Kilby's cymometer scale should therefore correspond to the readings of  $C_1$  in fig. 4. An examination of Barton and Kilby's paper in the light of this interpretation reveals the fact that their results, if plotted as in fig. 4, would give a curve very similar to that actually shown here. It therefore seems to us probable that Barton and Kilby, in their original experimental work on this



subject, obtained evidence of a dielectric constant less than unity.

The second series of experiments, begun at King's College in 1926, was carried out with the aim of elucidating the phenomenon, experienced in the earlier measurements, of an apparent increase in the capacity of the experimental condenser when dense ionization was introduced, whereas theoretical considerations predicted a decrease. It was also considered desirable to extend the observations on the dielectric constant and absorption of ionized air to cases in which a steady magnetic field was applied, since it had been pointed out\* that, if the effective electrical carriers in the atmospheric ionized layer were of electronic mass, the earth's magnetic field would have an influence on the phase velocity and absorption of waves passing through it.

In the first experimental tube used the source of ionization was a cold cathode electric discharge in air at low pressure. The length of the tube was 40 cm., the diameter was 7 cm., and that of both the anode and cathode 3 cm. Midway between these electrodes were sealed four subsidiary electrodes as in fig. 6, the tube having been designed originally for an experiment requiring a rotating electric field. In using the tube for observations on the dielectric constant of ionized gas these plates were connected, so that adjacent pairs formed the two plates of the experimental condenser, which, together with a tuning coil and a finely-adjustable variable condenser, formed an oscillatory circuit, in which forced vibrations were produced by a local valve generator. The discharge was maintained by means of a 6000 volt Evershed-Vignolles motor-generator, the discharge current being maintained constant by the inclusion of a saturated diode in the discharge circuit. The amplitude of the forced vibrations produced in the oscillatory circuit was measured by means of a Cambridge Thermionic Voltmeter.

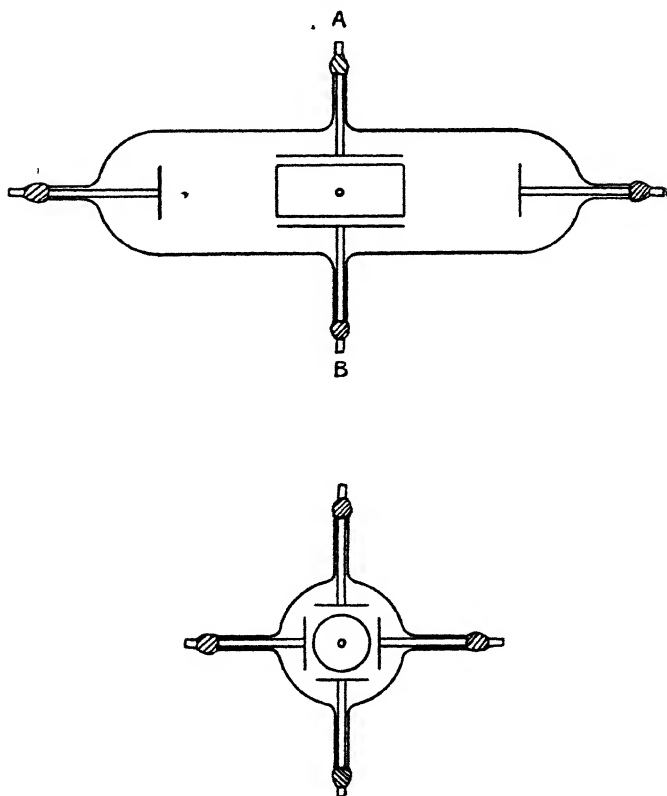
It was realized very early in the course of these experiments that a possible cause of the apparent increase of dielectric constant for cases of intense ionization was the formation of positive ion sheaths on the plates of the experimental condenser. Such sheaths had been recently investigated by Langmuir and Mott-Smith †, and may briefly be described as follows:—When a subsidiary electrode is inserted in a gas discharge it becomes surrounded by a sheath of positive ions or electrons, according to whether it

\* Proc. Phys. Soc. xxxvii. part 2, p. 21 D (Feb. 15th, 1925).

† 'General Electric Review,' xxvii. p. 449 (1924).

is at a negative or positive potential with respect to the space potential at that point. If the electrode is insulated from the rest of the apparatus the total current to it is zero, but it assumes a potential which in general differs from the space potential. The velocity of the positive ions is much lower than that of the electrons, and hence the electrode at

Fig. 6.



first collects more electrons per second than positive ions. This state of affairs causes the electrode to acquire a negative potential, some slow electrons consequently failing, from lack of energy, to be collected. Finally, a state of equilibrium is reached, when the positive ion current and the current due to the fastest electrons become equal, the electrode potential reaching a constant value. The acquired negative potential,

as stated above, produces a positive ion sheath around the electrode, and its thickness may be calculated from space-charge equations\*.

The potential fall between an auxiliary electrode and the neighbouring part of the main discharge is localized in a sheath, so that, in a problem such as ours, the effect of the sheath is to cause an increase of the effective capacity of the experimental condenser. In other words, the main body of the discharge can be regarded, when sheaths are present, as a conductor which reduces the effective distance between the condenser plates. To investigate this question quantitatively we assume, with Langmuir and Mott-Smith, the space-charge equation for the positive ion current in a sheath, namely

$$i_+ = \frac{AV^{3/2}}{x^2}, \quad . \quad . \quad . \quad . \quad . \quad (15)$$

$i_+$  being the positive ion current,  $V$  the potential fall across the sheath of thickness  $x$ , and  $A$  a constant involving the ratio of the charge to the mass of the carrier and the area of the electrodes. Allowing for the effect of the space-charge, each sheath will form a condenser of capacity per unit area  $C'$  where

$$C' = \frac{K}{3\pi x} \cdot . \quad . \quad . \quad . \quad . \quad (16)$$

In this expression  $K$  is the effective dielectric constant of the sheath. If we consider the general body of the discharge as joining in series the two condensers formed by the sheath, we have for the combined capacity per unit area

$$C'' = \frac{K}{6\pi x} \cdot . \quad . \quad . \quad . \quad . \quad (17)$$

The change of capacity per unit area, due to the introduction of ionization, is  $C'' - C$ , where  $C$  is the capacity between the plates, separated by distance  $D$ , before the gas is ionized.

\* It should be mentioned here that, as Wilson and Gold (Phil. Mag. [6] xi. p. 484, 1906) have shown in their work on the high-frequency properties of flames, the difference in the mobilities of positive and negative ions gives rise to the formation of ionic sheaths near the electrodes when an oscillatory potential is applied. Ionic sheaths of this type, however, would cause variations of apparent capacity of the experimental condenser which would be dependent on the amplitude of the applied oscillatory potential. No variations of apparent capacity with voltage were found in our experiments, so that we conclude that the effect of this type of sheath, although possibly present, has been masked by the effect of sheaths of the Langmuir type.

$C'' - C$  is the quantity which is measured experimentally. If  $x$  is small compared with  $D$ ,  $C'' - C$  is equal to  $\frac{K}{6\pi x}$ .

The validity of (17) was verified by finding the change in the effective capacity of the experimental condenser when the potential fall across the sheath was varied. In the case under consideration (*i. e.*, with plane collectors), if we neglect "edge effects" the ions cannot move in orbits which do not intersect the collector, so that the positive ion current is determined solely by the rate at which ions cross the boundary between the sheath and the main discharge. It is therefore independent of the potential of the condenser plates, and remains constant provided the conditions in the tube remain unaltered. We may write (15) as

$$x^2 \propto V^{3/2}, \quad . \quad . \quad . \quad . \quad . \quad (18)$$

so that using (17)

$$C'' = V^{-3/4} \times \text{const.},$$

or

$$\log C'' = \text{const.} - \frac{3}{4} \log V. \quad . \quad . \quad . \quad . \quad (19)$$

Since the value of  $C''$  is usually large compared with the original capacity of the experimental condenser, in the absence of ionization, it is clear that the reduction in the value of the subsidiary condenser of the oscillatory circuit necessary to restore resonance after the discharge is started is a measure of  $C''$ .

The relation (19) was tested by means of the tube shown in fig. 6 with a circuit arrangement as shown in fig. 7, where the assembly is as described above except that a potentiometer is included for varying the mean potential of the condenser relative to the anode. The potential difference between the condenser and the anode was read on the voltmeter  $V$ . The amplitude of oscillation was measured by means of the thermionic voltmeter  $T$ , the circuit  $L_1 C_1$  being brought to resonance by varying  $C_1$ . The change of  $C_1$  required to restore resonance was a measure of  $C''$ .

In fig. 8 is shown the relation obtained experimentally between  $C''$  and  $V$ . It will be observed that the points lie, within the limits of experimental error, on a straight line, of slope  $-\frac{3}{4}$ , as (19) would suggest. It should, of course, be stated that  $V$  does not measure the potential between the electrode and the discharge in that region, but the space potential in the discharge was only about  $-7$  volts with respect to the anode, as found by Langmuir's method, and this correction was applied to  $V$  in order to obtain fig. 8.

Fig. 7.

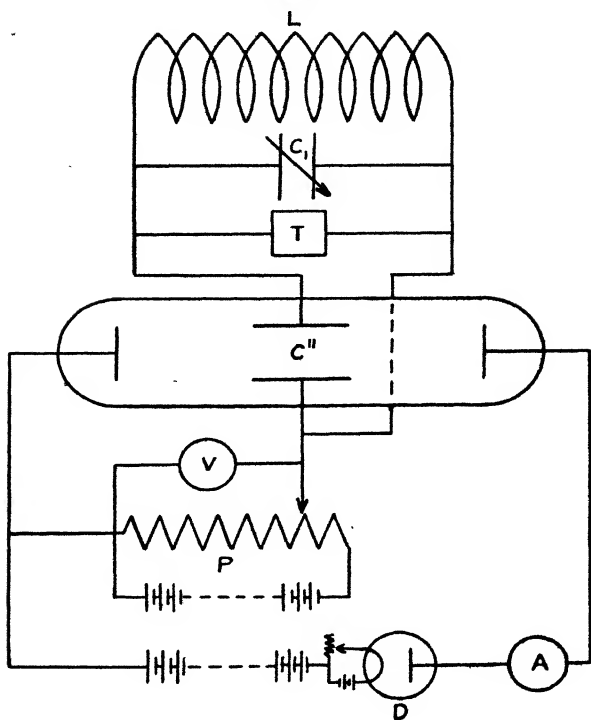
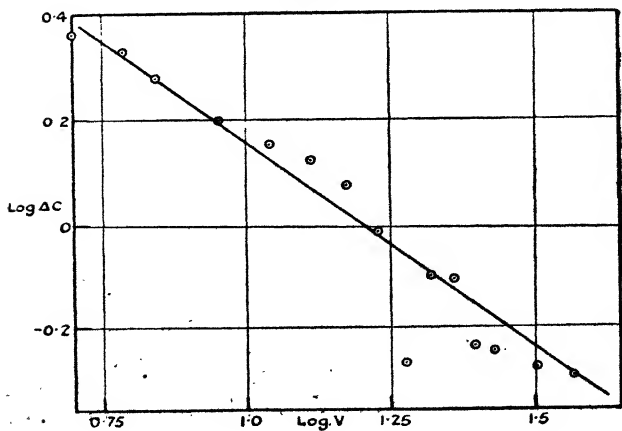


Fig. 8.



In order to examine the behaviour of the condenser when both the effects mentioned above are operative, equations (8), (15), and (17) may be combined. The positive ion current,  $i$ , of (15) is proportional to the ion density,  $N$ , in the discharge; hence (15) may be rewritten

$$N \propto \frac{1}{x^2}, \quad . \quad . \quad . \quad . \quad . \quad . \quad (20)$$

provided that  $V$  is constant. The value of  $x$  obtained, when substituted in (17), and using the value of  $K$  from (8), yields

$$C'' \propto \left(1 - \frac{4\pi N e^2 m}{m^2 p^2 + g^2}\right) N^{\frac{1}{2}}. \quad . \quad . \quad . \quad . \quad (21)$$

An examination of the behaviour of (21) reveals that  $C'' = 0$  when  $N = 0$ , whereas experimentally, of course,  $C'' = C$ , the original capacity of the condenser. The explanation of this is to be found in (20), according to which  $x = \infty$  when  $N = 0$ , regardless of the fact that the experimental tube is of limited dimensions; the value of  $x$  having, in fact, an upper limit of  $D/2$ , where  $D$  is the distance between the condenser plates. Let  $N'$  be the ionic density corresponding to  $x = D/2$  in (20). Then, for all values of  $N$  between 0 and  $N'$  the sheath occupies the whole of the dielectric space, and the variations of capacity depend only on the dielectric constant as given by (8); in other words, between  $N=0$  and  $N=N'$  the capacity of the condenser steadily decreases. For  $N=N'$  the sheaths can form according to (20), and the expression (21) is now valid for the capacity  $C''$ . It is easily seen that this function increases rapidly at first, with increase of  $N$ , then reaches a maximum, and finally assumes negative values. Thus we see that, as the ionization is increased, the value of  $C''$  should at first fall, and then, at the critical value of  $N$ , should start to increase. For further increase of  $N$  it should reach a maximum, and then should steadily fall.

With the wave-length first used (about 300 m.) no diminution of capacity was observed. A calculation of the amplitude of vibration of the ions in the tube, assuming a friction coefficient of  $\frac{m}{\tau}$  ( $\tau$  = time between collision of ions), revealed that this was comparable with the dimensions of the tube, and consequently ions suffered interference by collisions with the condenser plates and the walls of the tube. This indicated that a much higher frequency was necessary for the success of the experiment.

For work with lower pressures and higher frequencies a new experimental arrangement was used, with which the effect of an imposed magnetic field could also be studied. The cathode of the tube was a tungsten filament taking a current of 2 amps, the anode being an aluminium disk 2 cm. in diameter situated about 12 cm. from the cathode. Between these were sealed two condenser plates, 5 cm. long and 2 cm. wide, separated by a distance of 2 cm. The long sides were parallel with the axis of the discharge-tube, which was about 5 cm. in diameter.

The tube A of fig. 9 was mounted in a vertical position, and the condenser plates were connected to the ends of a pair of parallel brass rods 216 cm. in length, which, with a short-circuiting bar, constituted a Lecher wire system suitable for a wave-length of about 5 m. The amplitude of oscillation was measured in arbitrary units by means of a triode detector, T, coupled to the ends of the Lecher wires by two small condensers, CC, consisting of short brass tubes, which were insulated from the rods by thin mica. The steady current through the galvanometer, G, was balanced out by that from a single cell controlled by a high variable resistance, R. On tuning this circuit, it was found that the short-circuiting bar B was approximately at the mid-point of the Lecher wires, and thus the pick-up could be taken from the ends CC, which was very convenient. In order to be sure that it was the part BA, and not BC, that was in resonance with the oscillator, the condenser plates were disconnected at A, and the expected detuning effect was observed.

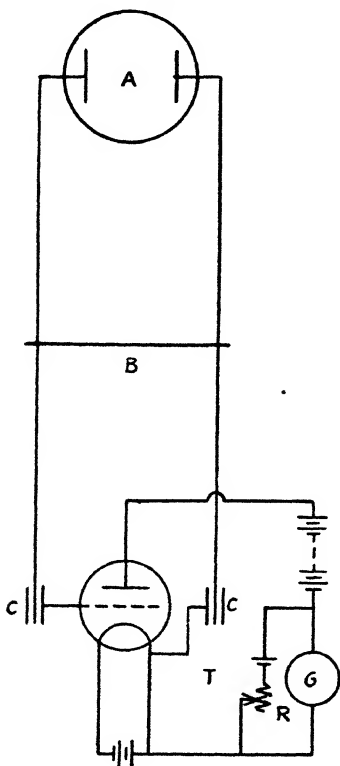
A pair of Helmholtz coils was mounted concentrically with the tube, so that a uniform magnetic field could be applied parallel to the condenser plates. The disposition of these coils relative to the tube is shown in fig. 10.

A triode generator of waves 5.46 metres in length was used to induce oscillations in the Lecher wire system. In the experiments without an applied magnetic field the relation between the ionization and the tuning of the Lecher wire system was studied. The ionic density was increased by raising the temperature of the filament of the diode in the discharge circuit, thus causing an increase of current through the tube. An attempt was made to measure the ion density in the discharge by means of plotting current-potential characteristics for the condenser plates, as described by Langmuir\*. The attempt failed because the negative potential

\* *Loc. cit.*

necessary to obtain the straight positive ion current part of the curve was so large that the discharge was very badly distorted long before this condition was reached, the plates showing a tendency to become the cathode. In the absence of any knowledge of the positive ion current, the corrected

Fig. 9.



electron current at any part of the curve could not be ascertained ; hence neither the space potential nor the ion density were calculable. It was noticed that, at the pressures used, the discharge was not striated, the negative glow just filling the space between the condenser plates. This is an important point, as it had been observed in previous experiments that spurious results may be obtained owing to the

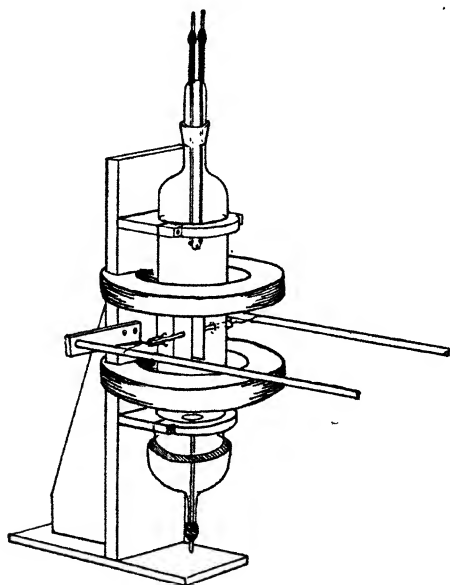


striations moving along the tube as the pressure or discharge current is varied.

The experimental curve shown in fig. 11 shows the change of position of the short-circuiting bar of the Lecher wire system plotted against the current passing through the discharge-tube, the former being approximately proportional to the change of capacity of the condenser.

The experimental curve (fig. 11) shows very definitely

Fig. 10.

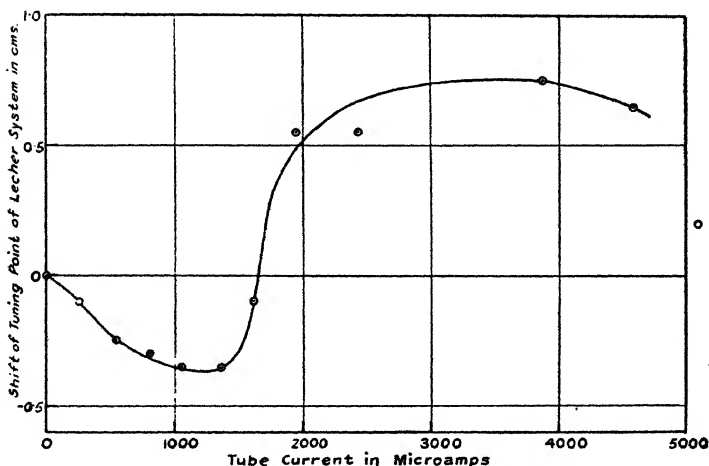


that for small ionization densities the dielectric constant of the gas is less than unity, but that, as the ionization is increased, the apparent dielectric constant increases and becomes greater than unity. Our previous experiments enable us to explain this result as being due to the combined action of the true reduction in the dielectric constant and the formation of ionic sheaths round the electrodes. For very low ionization densities such sheaths do not form, so that the effect sought is not masked. At high densities the formation

of the sheaths increases the apparent capacity of the system, and the effective dielectric constant is found to be greater than unity.

An examination of (21) leads us to the conclusion that when  $N$  becomes very large  $C''$  ultimately approaches zero and then assumes negative values, in which case it is equivalent to a self-inductance. This effect was not observed in practice, owing to instability of the discharge for large values of  $N$ , but fig. 11 shows that there is evidence at least of a maximum value of  $C''$ .

Fig. 11.



### 5. Experimental Results (continued).

#### *The Influence of an Imposed Magnetic Field.*

As mentioned above, particular interest in connexion with theories of wireless propagation centres round the question as to whether the electrical carriers in ionized gas are negative particles of electronic mass or ions of molecular mass. The particular point can, perhaps, best be seen by comparing the equations for the refractive index  $\mu$  of ionized gas for wireless waves with and without an applied magnetic field. We consider, for simplicity, collisional friction suffered by the electrical carriers to be negligible, and consider a case of propagation along the lines of magnetic force. For the

case of no imposed magnetic field and small ionization, we have

$$\mu^2 = 1 - \frac{4\pi N e^2 / m}{p^2} \dots \dots \dots (22)$$

For the case of propagation along a magnetic field of strength  $H_0$  we have

$$\mu^2 = 1 - \frac{4\pi N e^2 / m}{p^2 \pm p p_0}, \dots \dots \dots (23)$$

where

$$p_0 = \frac{H_0 e}{mc} \dots \dots \dots (24)$$

If the electrical carriers are electrons the upper and lower signs in (23) refer to the left-handed and right-handed circularly polarized components which travel along the lines of magnetic force. For one of these components there is a kind of resonance when  $p$  is equal to  $p_0$ , which is the angular frequency with which free electrons spiral round the lines of force. The value of the critical frequency evidently depends on  $H_0$  and  $m$ . For the earth's field of 0.5 gauss and carriers of electronic mass it is  $1.4 \times 10^6$  cycles per second, a frequency well within the wireless spectrum, while for the same field and molecules of, say, nitrogen, which gas probably predominated in the discharge-tube, it is 28 cycles per second.

The experiments to be described were carried out with the idea of establishing whether or not this magneto-ionic resonance existed. At first experiments were made using a discharge-tube oriented along the lines of total force of the earth, but these were unsuccessful as the tube was constructed with a cold cathode, and it was impossible with it to maintain a discharge current small enough and with pressures low enough to prevent the formation of sheaths round the electrodes.

In designing a new tube with a hot cathode it was felt that, for a number of reasons, a better way of testing the theory would be to use an imposed magnetic field which would be much stronger than that due to the discharge current itself. This necessitated the use of very high frequencies (of the order of  $10^8$  cycles per second) in order to test for resonance phenomena due to the gyric motion of electrons. As has been shown above, the necessity of preventing the formation of sheaths also required small ionization densities.

The experimental assembly has been already shown in fig. 9. The magnetic field was applied in the direction of

the discharge current, and its effect on the absorption in the experimental condenser studied. To do this the variation of the amplitude of the forced oscillations maintained in the Lecher wire system was noted as the current through the Helmholtz coils was increased. Three different wave-lengths were used and in each case it was found that at one particular value of the magnetic field a pronounced absorption took place.

Before describing the results further it is, however, necessary to examine more closely the relation of the experimental conditions to those contemplated in wave propagation theories. In our experiments the electric forces acting on the electrons made them vibrate at right angles to the direction of the magnetic field, and we consider that this state of affairs is comparable with the case examined by Lorentz\* for propagation of waves at right angles to an imposed magnetic field, the electric vector being also at right angles to the field. In such a case, as Lorentz points out, the formulæ for the phase velocity and absorption coefficient of the waves become so complicated as to be intractable except in special cases, which, fortunately, are the only ones arising in practice. The same remarks will obviously apply equally to the formulæ for dielectric constant and conductivity of the gas for applied electromotive forces of the same frequency as that of the waves. We consider here the special conditions which seem applicable to our problem, and assume that the number of collisions per second ( $f$ ) between an electron and gas molecules is small compared with  $p$ . Remembering that, although the electric displacement in a direction perpendicular both to the magnetic field and the alternating electric forces is zero, there is a definite polarization, and therefore a field in that direction, we may deduce that the conductivity of the gas ( $\sigma$ ) is given by

$$\sigma = \frac{p\beta\{(4\pi - \alpha)^2 + \gamma^2\}}{\{\alpha^2 - 4\pi\alpha - \gamma^2\}^2}, \dots \dots (25)$$

where  $\alpha = \frac{mp^2}{Ne^2} + \frac{4\pi}{3}$ ,  $\beta = \frac{mpf}{Ne^2}$ , and  $\gamma = \frac{mpp_0}{Ne^2} \dagger$ .

By using a small ionization it is possible to reduce  $N$  so that  $\alpha$  is large compared with unity, in which case (24) becomes

$$\sigma = \frac{p\beta(\alpha^2 + \gamma^2)}{(\alpha^2 - \gamma^2)^2}, \dots \dots \dots (26)$$

\* 'Theory of Electrons,' p. 160 (Leipzig, 1916).

† The notation is here slightly different from that used by Lorentz.

or

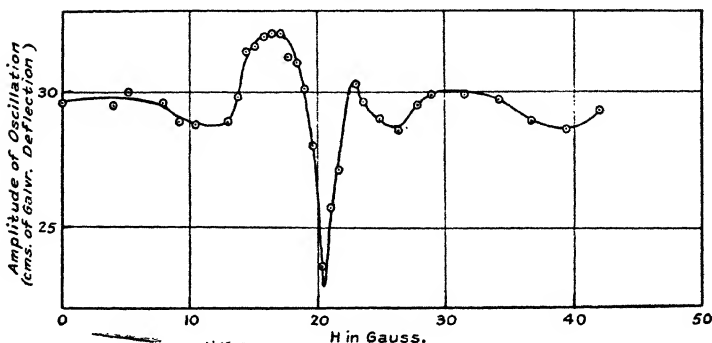
$$\sigma = \frac{Ne^2 f(p^2 + p_0^2)}{m(p^2 - p_0^2)^2} \dots \dots \dots (27)$$

The value of  $\sigma$  is therefore a maximum when

$$p = p_0 = \frac{H_0 e}{mc}, \dots \dots \dots (28)$$

We thus see that in the case in which the ionization is small we should expect the critical value of the magnetic field producing maximum absorption to be proportional to the excitation frequency, and to be given by (28), but, if the ionization is appreciable, the relation is not so simple.

Fig. 12.



For a wave-length of 5.46 metres (corresponding to an angular frequency  $p = 3.45 \times 10^8$  cycles per second) the relation between the potential amplitude produced in the Lecher wire system and the current through the Helmholtz coils was as exhibited in fig. 12, where a pronounced absorption is noted for a current of 0.78 ampere, which corresponds to a magnetic field of 20.5 gauss.

It will be seen that other variations take place, but the maxima and minima are not marked and they are not sharp. They may be due to imperfect screening of the Lecher wire system from the observer, it being a matter of difficulty to ensure that the capacity to the observer is exactly the same after each adjustment of the magnetic field current.

Experiments were made with two other wave-lengths which yielded similar results. In the following Table are shown the frequencies used, the critical values of  $H_0$  producing

maximum absorption, and also the critical value of  $H_0$  calculated from (28):—

Angular frequency (cycles per sec.).	Critical Field (gauss). Exp. observed.	Critical Field (gauss). Calc. from (28):
$2.96 \times 10^8$	16.5	16.7
$3.45 \times 10^8$	20.5	19.4
$5.48 \times 10^8$	31.5	31.0

In all three cases it will be seen that the observed values of  $H_0$  are not very different from the calculated values, so that we conclude that the effective electrical carriers in the ionized air are electrons.

In a recent note Benner \* has demonstrated the quasi-resonance phenomena of free electrons in a magnetic field. Benner used a wireless vacuum valve, the electrons being emitted by a hot filament in the usual way. As the tube used was a transmitting valve, and therefore one of extreme exhaustion, the conditions are different from those in our experiments, where the problem was to find the nature of the electrical carriers in ionized gas at low pressures. It is of interest to note that complete agreement between the calculated and observed values of the critical value of  $H_0$  was not observed by Benner, his observed values being 12 per cent. higher than the theoretical value. This may be due to the fact that the wireless valve used most probably had an anode of nickel, which, being magnetic, would effectively reduce the imposed field.

## 6. Summary.

The experiments described above confirm earlier work on the subject of the dielectric constant of ionized gases for radio-frequency electromotive forces, in that a dielectric constant less than unity has been observed under certain conditions. This result was obtained only with very low ionization densities and low pressures. The existence of an apparent dielectric constant greater than unity at higher ionization densities, which appears to have been observed by all workers on the subject, has been the subject of special study, and has been shown to be due to the formation of ionic sheaths round the experimental electrodes, which effectively increase the capacity of the experimental condenser, and so

\* *Loc. cit.*

mask the true effect sought. The variation in the thickness of these sheaths with the potential across them has been examined by a wireless method, the result being in agreement with the theory of collectors developed by Langmuir and Mott-Smith.

The influence of an imposed magnetic field on the radio-frequency properties of ionized air has been studied, and the existence of an Inverse Zeeman effect for free electrons demonstrated. This effect was predicted in connexion with the magneto-ionic theory\* of the atmospheric deviation of wireless waves. For a particular value of the imposed magnetic field a critical frequency is found for which pronounced absorption occurs. The relative magnitudes of the imposed magnetic field and the critical frequency yield

a value of  $\frac{e}{m}$  of  $1.74 \times 10^7$  e.m.u. for the electric carriers, so

that there is therefore no doubt that they are electrons.

The experiments therefore support the theory of Sir Joseph Larmor, according to which the refractive deviation of wireless waves in the upper atmosphere is due to the influence of free electrons.

#### 7. Acknowledgment.

In conclusion, we wish to express our thanks to Captain A. G. D. West for his assistance in the earlier series of these experiments, which were carried out as part of the programme of the Radio Research Board of the Department of Scientific and Industrial Research.

XCI. *The Values and Inter-relationships of  $c$ ,  $e$ ,  $h$ ,  $M_p$ ,  $m_o$ ,  $G$ , and  $R$ .* By W. N. BOND, M.A., D.Sc., F.Inst.P., Lecturer in Physics in the University of Reading †.

#### Introduction.

OF the universal constants with which we are concerned in Physics, probably the most important are :—

$c$ , the velocity of light ;

$e$ , the electronic (or protonic) charge ;

$h$ , Planck's constant ;

\* See Proc. Phys. Soc. xxxvii. part 2, p. 21 D (Feb. 15th, 1925).

† Communicated by the Author.

$M_p$ , and  $m_o$ , the masses of proton and electron ; and  $G$ , the gravitational constant.

With suitable definitions these have all been measured in terms of our three primary units of mass, length, and time, and hence their dimensions are expressible in terms of  $[M]$ ,  $[L]$ , and  $[T]$ . It is well known that for six quantities, expressible in terms of three primary units, there are (in general) three independent non-dimensional products, the numerical values of which will be independent of the size of our primary units. In the present instance three independent products are found, such as

$$hc/e^2, M_p/m_o, \text{ and } hc/M_p^2 G. \quad (1)$$

These products are rather simpler in form than if the six quantities had been any six physical quantities chosen at random. Moreover, the numerical values of the first two (860 and 1840 approximately) are nearer in magnitude to unity than might be expected by chance (where the individual quantities range numerically from  $3 \times 10^{10}$  to  $9 \times 10^{-28}$ ). Hence we might expect the first two products to have physical significance. It might at first be thought that the third non-dimensional product was certainly not of significance, as its numerical value is about  $10^{89}$ . But, on the other hand, it must be borne in mind that we continue to have evidence of the inter-relatedness of natural phenomena, and that it is unlikely that  $G$  should form an exception.

Apart from experimental measurement, various suggestions have been made as to the values of these non-dimensional products. Thus Lewis and Adams \* suggested

$$\frac{hc}{2\pi e^2} = 8\pi \left( \frac{8\pi^5}{15} \right)^{1/3} \quad (2)$$

and Eddington †

$$\frac{hc}{2\pi e^2} = 137. \quad (3)$$

Perles ‡ suggested

$$\frac{hc}{e^2} = \frac{M_p/m_o}{\pi - 1} \quad (4)$$

and Fürth §

$$\frac{hc}{e^2} = \frac{15}{32} \frac{(M_p + m_o)^2}{M_p m_o}, \quad (5)$$

\* Lewis and Adams, *Phys. Rev.* (2) iii. p. 92 (1914).

† Eddington, 'Nature,' Aug. 24, 1929, p. 320; *Proc. Roy. Soc. A*, cxxvi. p. 696 (1930).

‡ Perles, *Naturwiss.* xvi. p. 1094 (1928).

§ Fürth, *Phys. Zeit.* xxx. p. 895 (1929).



and

$$\frac{hc}{2(M_p + m_o)^2 G} = \frac{\pi}{2} (16)^{32}. \quad . \quad . \quad . \quad (6)$$

It is the purpose of this paper to discuss the evidence supporting any of these suggestions or theories. It is concluded that two, and possibly three, relationships are significant; and incidentally the numerical values here suggested for the six universal constants differ slightly from those recently given \* (with the exception of the value of the velocity of light).

*The Values of  $c$ ,  $e$ ,  $h$ ,  $hc/e^2$  and  $e/m$ .*

The value of  $c$  we may consider known to a very high degree of accuracy (Birge, *loc. cit.*). The values Birge attributes to  $h$  and  $hc/e^2$  are chiefly in doubt owing to the uncertainty of the value to be assumed for  $e$ . Before discussing the values obtained experimentally for  $e$ , we will consider another method of estimating  $e$  and  $h$ .

In any method of measuring  $h$ , experiments are performed resulting in the estimate of a number,  $A$ , that occurs in an equation of the form

$$h = Ae^n, \quad . \quad . \quad . \quad . \quad . \quad (7)$$

where  $n$  has values 1,  $1\frac{1}{2}$ ,  $1\frac{2}{3}$ , according to the method used. If a second method were used involving a different power of  $e$ , we should have, similarly,

$$h = A'e^{n'}. \quad . \quad . \quad . \quad . \quad . \quad (7^*)$$

Apart from errors of experiment or theory, these two equations would together yield values of  $e$  and  $h$ . To minimise the effects of errors, all the accurate experiments should be used, and not only a pair as described above.

To illustrate the calculation I show in the figure the values of  $h$  collected by Birge (*loc. cit.*) plotted against the values of the index  $n$  to which  $e$  occurs in the estimation of  $h$ . All the values here plotted are based on the assumed value (Birge) of

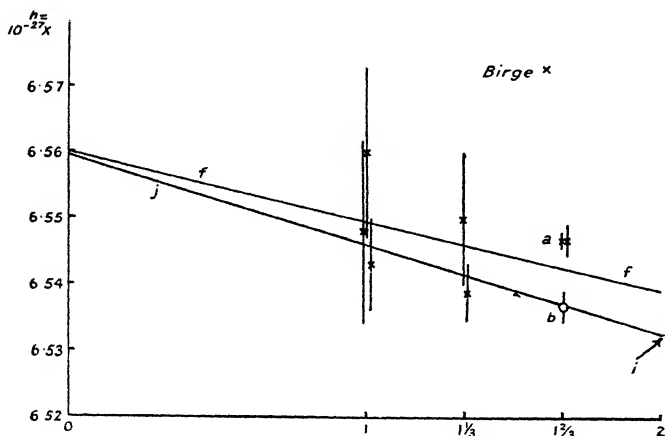
$$e = (4.770 \pm 0.005) \times 10^{-10} \text{ abs-es-unit.}$$

If this value of  $e$  be correct, the values of  $h$  deduced from experiment should not vary systematically with the index  $n$ . On the other hand, if this assumed value of  $e$  be too small by a small percentage  $E$ , the deduced values of  $h$  will also be on this account too small, and by an amount very nearly equal

\* Birge, Phys. Rev. Supp. i. No. 1, pp. 1-73 (July 1929).

to  $nE$  per cent. In other words, the straight line best fitting the points in the figure would not be horizontal but inclined, intersecting the  $h$ -axis nearly at the true value of  $h$ , and having an ordinate where  $n = 1$  of about  $E$  per cent. less.

Before finding the best straight line to fit these values, a digression will be made. A noticeable feature of Prof. Birge's paper is that he attributes to  $e/m$  two values—the "spectroscopic" and the "deflexion." He decides that the values of  $e/m$  estimated from a comparison of the Hydrogen and Helium spectra, and from the Zeeman effect, agree very closely, but differ (for some unexplained reason) from the value deduced from deflexion experiments by more than can



Values of the power  $n$  to which  $e$  is raised in deducing  $h$ .

be accounted for by experimental errors. Now the method of estimating  $h$  by means of Rydberg's constant necessitates a knowledge of  $e/m$ . Prof. Birge in this case makes use of the "spectroscopic" value of  $e/m$  ( $a$  in figure). As there is no definite evidence requiring the rejection of the "deflexion" value, I have at first used *three* estimates of  $h$ , those based on the two spectroscopic methods being at  $a$  and that based on the deflexion value of  $e/m$  at  $b$  (see figure).

In proceeding to find the straight line that best fits the points in the figure, account might be taken of the estimated probable errors of the different points. These errors are, however, only estimates, and I feel that it is more satisfactory at first to attribute equal weight to each of the points in the

diagram. Doing this, and using the ordinary method of least squares, I obtain the values ( $ff$  in figure) :—

$$\left. \begin{aligned} e &= (4.777_4 \pm 0.003_9) \times 10^{-10} \text{ abs-es-unit,} \\ h &= (6.560 \pm 0.007) \times 10^{-27} \text{ erg. sec.,} \\ \text{which do not depend on any direct determination} \\ &\text{of } e. \end{aligned} \right\} \dots (8)$$

Together with the value of  $c$  given by Birge, and using his method of estimating the probable error, we then obtain

$$ch/2\pi e^2 = 137.14 \pm 0.11.$$

Before discussing this result, let us consider the results of direct determinations of  $e$  (by oil-drop and ruled-grating methods). Birge considers values due to Millikan, Bäcklin and Wadlund (and at the end of his paper mentions an unpublished value due to Bearden). He rejects Bäcklin's value, partly because it does not agree with a calculation involving Rydberg's constant and the "spectroscopic" value of  $e/m$ , and also because Bäcklin's pioneer work may contain unsuspected errors.

Considering the results now, I know of no definite reason for rejecting any of the four, even though their estimated probable errors are little more than a half of what would be required to account for the differences between their results. (We may note that Bearden's published results do not appear as abnormal as the values mentioned, before publication, by Birge.) Thus we have:—

$$\left. \begin{aligned} \text{Millikan} &\dots\dots 4.768 \pm 0.005 \\ \text{Bäcklin} &\dots\dots 4.794 \pm 0.006 \\ \text{Wadlund} &\dots\dots 4.775_7 \pm 0.0076 \\ \text{Bearden} &\dots\dots 4.809_5 \end{aligned} \right\} \times 10^{-10} \text{ abs-es-unit.}$$

As the estimated probable errors are all of the same order, but appear to be underestimates, I take the unweighted mean :

$$\left. \begin{aligned} e &= (4.787 \pm 0.007) \times 10^{-10} \text{ abs-es-unit.} \\ \text{Using this estimate of } e, \text{ but otherwise following} \\ \text{Birge as to data and method of calculation, we} \\ \text{obtain} \\ h &= (6.576 \pm 0.012) \times 10^{-27} \text{ erg. sec.} \\ \text{and} \\ hc/2\pi e^2 &= 136.94 \pm 0.15. \end{aligned} \right\} \dots (9)$$

The estimated values of  $hc/2\pi e^2$  given in (8) and (9) may be compared with Birge's estimate of  $137.29 \pm 0.11$ . The new estimates are further from the suggestion of Lewis and Adams, 137.348 (equation (2)), but nearer to that of Eddington, 137 (equation (3)). Prof. Birge's estimate differs from 137 by 2.6 times his probable error, which, if due to chance, has only a probability of  $\frac{1}{2}$ . My less accurate estimate (equation (9)) differs from 137 by only 0.4 times the probable error; and my more accurate (equation (8)) by 1.27 times the probable error.

I conclude, therefore, that the new estimates given above form definite evidence for Professor Sir A. Eddington's suggestion. At this stage I think we may safely *assume* as correct Eddington's equation:

$$\frac{hc}{2\pi e^2} = 137. \quad . \quad . \quad . \quad . \quad . \quad (3)$$

(This equation appears to have a much better theoretical basis than that of Lewis and Adams.)

Equation (3) can now be used with the measurements of  $A$  of equation (7) to obtain a more accurate estimate of  $e$ . This is equivalent to fitting to the points in the figure a straight line through the fixed point  $i$ . The probable errors of the points (apart from error in the assumed value of  $e = 4.770 \times 10^{-10}$ ) I have deduced from Birge's data, and have indicated by the vertical lines in the figure. It is evident that if the points are to fit on a straight line through  $i$ , the point  $a$  (based on Rydberg's constant and the "spectroscopic" value\* of  $e/m$ ) must be discarded, but that the point  $b$  (based on Rydberg and the "deflexion" value of  $e/m$ ) may be retained. This is the reverse of Birge's procedure. I then fitted the line ( $ij$  in figure) by the usual methods, weighting in accordance with the probable errors of the points. The result shows the errors to have been overestimated, as judged by internal consistency, so I base the estimate of the final probable error on the residuals. Finally,

$$e = (4.779_2 \pm 0.0017) \times 10^{-10}.$$

Taking the weighted mean of this value and the mean direct estimate of equation (9) I get

$$\left. \begin{aligned} e &= (4.779_7 \pm 0.0017) \times 10^{-10} \text{ abs-es-unit,} \\ \text{and from equation (3),} \\ h &= (6.559_8 \pm 0.0046) \times 10^{-27} \text{ erg. sec.} \end{aligned} \right\} . \quad . \quad (10)$$

\* This value is smaller than *all* the final values given in Geiger and Scheel's 'Handbuch der Physik,' xxii. p. 81.

This value for  $e$  could be used together with Rydberg's constant to estimate  $e/m$  were it not that the point  $b$  (see figure) assumed a value of  $e/m$ . The determination of  $e$  was therefore repeated, not using point  $b$  (nor point  $a$ ), and this slightly different estimate of  $e$ , together with Rydberg's constant, gave

$$e/m = (1.7688_0 \pm 0.0007_1) \times 10^7 \text{ abs-em-unit} \cdot \text{g}^{-1}.$$

This agrees well with Birge's "deflexion" value of

$$1.7689 \pm 0.0018,$$

but disagrees with his "spectroscopic" value

$$1.761 \pm 0.001.$$

The disagreement is now not between "deflexion" and "spectroscopic," but between "deflexion" and "Rydberg" on the one hand and methods depending on small spectroscopic differences on the other hand. This appears less difficult to account for, and may suggest that the results Birge gives, depending on the spectroscopic differences are not quite accurate.

Taking the weighted mean of the "deflexion" and "Rydberg" values we obtain:--

$$\underline{e/m = (1.7688_2 \pm 0.0006_2) \times 10^7 \text{ abs-em-unit} \cdot \text{g}^{-1} \cdot (11)}$$

This may be compared with the estimate of the International Critical Tables,  $1.769 \pm 0.003$ , and with that of the *Handbuch der Physik*,  $1.766$ ; from the data given in the latter book I estimate  $1.767_7 \pm 0.001$ .

The results of this part of the paper are now contained in equations (3), (10), and (11).

### *The Value of $M_p/m_o$ .*

Using the value of  $e/m$  given in equation (11), and following Birge as to other data and as to method of calculation, we obtain directly

$$\left. \begin{aligned} \frac{M_H}{m_o} &= 1847.43 \pm 0.65, \\ \frac{M_p}{m_o} = \frac{M_H - m_o}{m_o} &= 1846.43 \pm 0.65, \\ \frac{(M_p + m_o)^2}{M_p m_o} &= 1848.43 \pm 0.65, \end{aligned} \right\} \dots (12)$$

Testing the suggestions contained in equations (4) and (5) by means of data of (3) and (12), we find that

$$\pi - 1 = 2.14159, \quad \frac{M_p/m_o}{hc/e^2} = 2.1450 \pm 0.0007_5$$

and

$$\frac{32}{15} = 2.1333, \quad \frac{(M_p + m_o)^2/M_p m_o}{hc/e^2} = 2.1472 \pm 0.0007_5.$$

The differences between my estimates and the suggested values are in the two cases 4.5 and 18.5 times the probable errors. Moreover, it is only the latter equation, (5), that has a theoretical basis. Hence neither of the equations (4) and (5) seems tenable.

If the values of equation (12) be divided by  $2\pi$ , we obtain

$$294.02 \pm 0.10,$$

$$293.86 \pm 0.10,$$

$$294.18 \pm 0.10,$$

and I should like to suggest that one of these should, perhaps, be exactly 294.

*The Values of  $\frac{hc}{2(M_p + m_o)^2 G}$  and  $G$ .*

Fürth (*loc. cit.*), in putting forward the theoretical suggestion (equation (6)), takes the values of the quantities as given by Birge (*loc. cit.*) and obtains for the two sides of the suggested equality the values

$$(5.33 \pm 0.03) \times 10^{38} \quad \text{and} \quad 5.34 \times 10^{38}.$$

If we assume that we have now enough theoretical and experimental evidence for Eddington's suggestion (equation (3)), we can make a more rigorous test of Fürth's suggestion. Thus equation (6) can be transformed into

$$\frac{hc}{2\pi e^2} = \frac{16^{32}}{2} \left( \frac{H}{Fc} \right)^2 \cdot G,$$

where  $H$  denotes the atomic weight (relative to  $O = 16$ ) of Hydrogen, and  $F$  is the Faraday constant. Taking the values of  $H$ ,  $F$ , and  $c$  given by Birge, we get

$$137 = \frac{16^{32}}{2} \left\{ \frac{1.00777 \pm 0.00002}{(2.8927 \pm 0.0002) \times 10^{14}} \right\}^2 G.$$

Hence

$$G = (6.635 \pm 0.001) \times 10^{-8} \text{ dyne} \cdot \text{cm}^2 \cdot \text{g}^{-2}. \quad (13)$$

This does not agree at all well with the value Birge (*loc. cit.*) adopts,

$$(6.664 \pm 0.002) \times 10^{-8},$$

but it is in moderate agreement with the values adopted in Geiger and Scheel's 'Handbuch der Physik' (ii. p. 491),

$$6.6_s \times 10^{-8},$$

and in the 'International Critical Tables' (i. p. 17),

$$(6.66 \pm 0.01) \times 10^{-8}.$$

As Prof. Birge's final estimate of G is based entirely on the work of Heyl, I undertook a fresh analysis of all the estimates I could find, deducing an *experimental* value

$$\underline{G = (6.65 \pm 0.01) \times 10^{-8} \text{ dyne.cm}^2.\text{g}^{-2}. \dots (14)}$$

This again is in reasonable agreement with the value given by Fürth's suggestion (equation (13)). I conclude that this agreement is significant, and that Prof. Birge's adoption of a value for G entirely based on the results of one experimenter has resulted in his considerably underestimating the probable error.

We may notice that, according to Fürth's suggestion, an experimental number of the order  $10^{39}$  is expressed in the comparatively simple form of  $\pi(16)^{32}$ , with an error that appears to be certainly less than  $\frac{1}{2}$  per cent., and is probably of the order  $\frac{1}{4}$  per cent. or less. This agreement can hardly be considered fortuitous, even if we make allowance for possible choice of variables, etc.

If we accept the evidence for Fürth's suggestion (equation (6)), it then appears that the indirect estimate of G (equation (13)), based on equation (6), is more accurate than the direct estimates such as (14). It is, however, still possible that Fürth's suggested equation might be subject to some small correction term.

The results of this part of the paper are then contained in equations (6), (13), and (14).

#### *Conclusion and the Value of M<sub>p</sub>cR/h.*

I believe that there is sufficient experimental evidence to support the suggested relationships

$$\text{(Eddington)} \quad hc/2\pi e^2 = 137, \dots \dots \dots (3)$$

$$\text{(Fürth)} \quad hc/\pi(M_p + m_o)^2 G = (16)^{32}. \dots \dots \dots (6)$$

Assuming these, I obtain

$$e = (4.779_7 \pm 0.0017) \times 10^{-10} \text{ abs-es-unit,}$$

$$h = (6.559_6 \pm 0.0046) \times 10^{-27} \text{ erg.sec.,}$$

$$e/m = (1.7688_2 \pm 0.0006_3) \times 10^7 \text{ abs-em-unit} \cdot g^{-1},$$

$$M_p/m_o = 1846.43 \pm 0.65,$$

$$G = (6.635 \pm 0.001) \times 10^{-8} \text{ dyne} \cdot \text{cm}^2 \cdot g^{-2}.$$

I further suggest that there may be significance in the fact that the values of

$$M_H/2\pi m_o, \quad M_P/2\pi m_o, \quad \text{and} \quad (M_p + m_o)^2/2\pi M_p m_o,$$

are within experimental error of 294.

Finally, we may notice that the universal constant "the radius of curvature of space-time" may also prove to be related to the universal constants considered above.

Thus, taking the estimate given by Silberstein ('Nature,' Aug. 3, 1929, p. 179) of  $R = 5.74 \times 10^6$  light-years, with an uncertainty of about  $2\frac{1}{2}$  per cent., I find

$$M_p c R / h = (0.121 \pm 0.003) \times (16)^{32},$$

which suggests to me  $M_p c R / h = \frac{1}{8}(16)^{32}$ .

This may have some bearing on the fact that, according to Weyl (*Annalen der Physik*, lix. p. 129), the radius of curvature of space-time, the electrical radius of the electron, and the gravitational radius of the electron should form approximately a geometric progression.

Department of Physics,  
University of Reading,  
July 28th, 1930.

**XCII.** *On the Glow Discharge at the Active Electrode of an Electrolytic Rectifier.* By JOHN S. FORREST, M.A.,  
*Mackay-Smith Scholar in the University of Glasgow* \*.

[Plate XI.]

### 1. Introduction.

**T**HE mode of action of the electrolytic rectifier has been the subject of many investigations since 1905, but, owing to the large number of variables involved, the problem is a difficult one. and, so far, no satisfactory theory has been propounded. The present paper, however, does not deal primarily with the rectifying action of these cells, but an interesting subsidiary phenomenon is discussed, namely, the luminosity which, under certain conditions, appears on

\* Communicated by E. Taylor Jones, D.Sc.



the surface of the active electrode. It is probable that a close study of this luminosity might lead to a more complete theory of the rectifying action of the electrolytic cell. In the following sections an account is given of some experiments which were made in order to find out something about the nature of the luminosity.

## 2. *Description of the Electrolytic Cells used in the Experiments.*

As has been remarked above, the properties of electrolytic cells are functions of a large number of variables, and therefore a fairly exact description of the cells used will be given. For the purposes of the present investigation only three types of cell were found to be at all suitable, namely, cells with active electrodes of aluminium, tantalum, and tungsten.

In the aluminium cell the active electrode was of commercial sheet aluminium immersed in an electrolyte of ammonium phosphate solution

(124 gm.  $(\text{NH}_4)_2\text{HPO}_4 \cdot 12\text{H}_2\text{O}$  per litre).

Tantalum foil was used for the active electrode in the tantalum cell, while the electrolyte was dilute sulphuric acid (sp. gr. = 1.2) with some ferrous sulphate added to prevent disintegration of the tantalum <sup>(1)</sup>.

In the tungsten cell a tungsten wire (diam. = 1 mm.) was immersed in dilute sulphuric acid (sp. gr. = 1.2).

The immersed area of the active electrode in all cases was 1-2 sq. cm. Sheet lead (commercial) immersed to about the same area was always used for the inactive electrode.

Asymmetric conductivity (or rectification) does not occur unless the active electrode is "formed." To "form" an electrode it may be connected to the positive terminal of a D.C. supply of suitable voltage until the large current which flows initially has diminished to a very small value owing to the insulating oxide film which forms on the electrode surface. With this oxide film there is associated a gas film, and these two films seem to be responsible for the rectifying effect.

## 3. *General Observations on the Luminosity.*

If the potential difference across the electrodes (active electrode positive) of one of the formed cells described in

the preceding section be gradually increased, the following phenomena are observed. When the P.D. is about 60 v. a faint uniform glow may be seen on the active electrode surface in a dark room. As the P.D. is further increased, the intensity of the glow increases, and then small random scintillations of a violet colour appear on the electrode in addition to the uniform glow. These small sparks give rise to more violent sparks, until, ultimately, the insulating layer breaks down completely and very large currents pass. In this last stage the sparks are often replaced by "arcs" of a reddish colour; this is well shown with tantalum.

Fig. 1.

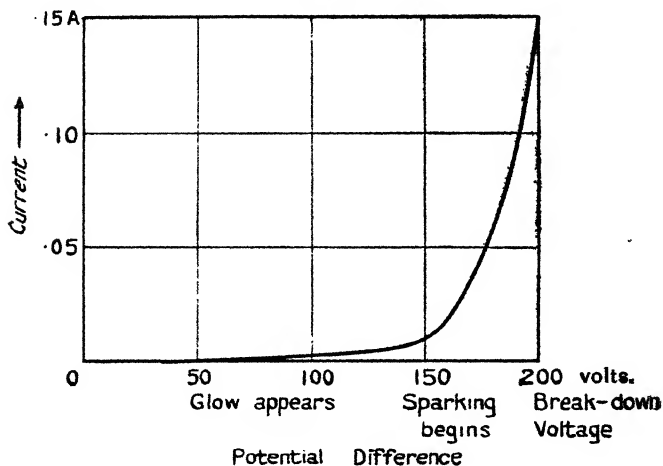


Fig. 1 shows the P.D.-current characteristic for aluminium. For the tantalum and tungsten cells similar curves are obtained, except that the breakdown voltage is about 115 for the tungsten cell and about 90 for the tantalum cell.

The aluminium cell gives the brightest glow, and all subsequent remarks refer to it unless otherwise stated. The tantalum cell gives a faint glow, but it behaves very consistently. The tungsten electrode glows quite brightly, but the insulating layer is rather unstable. It is worth while noting that the oxidation and reduction of the tungsten electrode can be seen easily, as the oxide is white and the reduced metal black.

The glow appears (if the voltage is high enough) and disappears simultaneously with the switching on and off of the current.

If the surface of a glowing electrode is touched with a glass rod, and gentle pressure is applied, bright flashes appear at the point of contact of the rod and the electrode.

Moreover, figures scratched on the surface of a formed electrode shine brightly for some seconds when the electrode is used again.

The glow is usually distributed continuously over the surface of the electrode, but some parts of the electrode, especially at the surface of the electrolyte, may glow more brightly than others. When examined with a microscope ( $\times 300$ ) the luminosity still appeared to be uniform.

The above experiments strongly suggest that the luminosity is a glow discharge between the metal electrode and the electrolyte, through the layer of gas on the electrode surface. In the following sections the various characteristics of this glow discharge will be described.

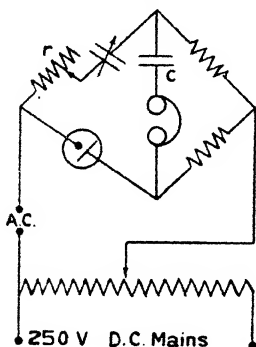
#### 4. *Thickness of the Gas Layer.*

When a P.D. is maintained across a cell, the cell is found to possess a large capacity owing to the active electrode and the electrolyte acting as the plates of a condenser, with the oxide and gas layer for dielectric. The presence of this capacity may be demonstrated by discharging through a galvanometer a cell which has just been disconnected from the current supply; sometimes it is even possible to obtain a small spark on discharge.

In order to measure the capacity in question the bridge shown in fig. 2 was used. This bridge enables the capacity to be measured while a P.D. is maintained across the cell. (Another method of accomplishing the same object has been given by E. M. Dunham <sup>(1)</sup>). The purpose of condenser C is to safeguard the telephones. The resistance  $r$  is used to balance the power factors of the cell and the variable condenser. A source of audio-frequency alternating current is shown at A.C., but the commutator ripple in the mains may be sufficient to work the bridge. By means of this bridge it was found that trustworthy results could be obtained with an ordinary capacity bridge if the measurements were made immediately after the cell was disconnected from the mains.

The laws regarding the capacity of electrolytic cells are fairly well known <sup>(2)</sup> <sup>(3)</sup>, and need not be repeated here. For the present purpose it is sufficient to state that in these experiments the capacity of the aluminium electrode was about  $\cdot 1\mu\text{F}/\text{cm}^2$ , and that of the tantalum electrode about  $\cdot 2\mu\text{F}/\text{cm}^2$ . These figures correspond to a thickness of the order of  $10^{-6}$  cm. if the dielectric constant is taken to be unity. Now, although the manner in which the oxide and gas layers are associated with each other is not known, it is probably reasonable to take the above figure as the thickness of the *gas* layer. That the oxide layer is at least ten times as thick as the gas layer is indicated by the

Fig. 2.



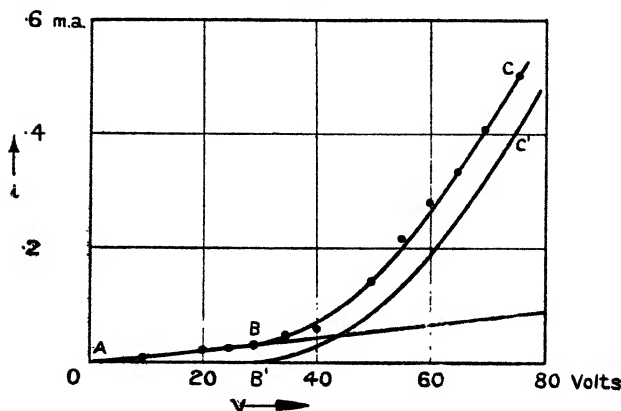
interference colours seen on formed electrodes. Tantalum electrodes show these colours particularly well. In addition, if a formed and dried aluminium electrode be immersed in mercury the capacity between the electrode and the mercury can usually be measured, and it is found to correspond to a thickness of at least  $10^{-5}$  cm. In the following, therefore, the thickness of the gas layer will be taken to be of the order of  $10^{-6}$  cm.

##### 5. The Potential Difference-Current Characteristic in Rectifying Cells.

The general form of the P.D.-current curve has been dealt with in section 3, but a more detailed examination brings out some interesting features. The curve of fig. 1 does not show much evidence of the production of a glow

discharge at about 60 v. If, however, the small currents in the region 0–80 v. be measured with a more sensitive instrument, and the graph redrawn to a larger current scale, then the curve ABC of fig. 3 is obtained. This curve seems to indicate that Ohm's law conduction (leakage) takes place alone up to about 30 v., when ionization by collision begins and the current increases more rapidly. If AB is produced, and the leakage current subtracted from the total current, the ionization current is found. B' C' gives the glow discharge current through the

Fig. 3.



gas. Tantalum gives a similar curve, but the leakage currents are smaller. The equation of B' C' is found to be

$$V - E = k\sqrt{i}, \quad \dots \dots \dots (A)$$

where  $V$  is the applied P.D. and  $i$  the current through the cell.

$E = 30\text{--}40$  v. for both aluminium and tantalum.

$k = 3000$  approx. for aluminium, and

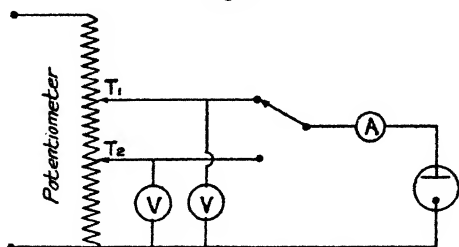
$= 10,000$  approx. for tantalum in volt ampere units.

The experimental curves agree very closely with equation (A) if certain precautions are taken. The main difficulty is that the thicknesses of the gas and oxide layers vary with the applied voltage. Now, in the present experiments,

it is desirable to keep the thickness of the gas layer constant—the current through the gas and the applied voltage should be the only variables. This leads to the adoption of the arrangement shown in fig. 4. The cell is connected to a fixed tapping  $T_1$  (at 100 v., say) on a potentiometer until a stable state is reached. The voltage (and current) readings in the range 0–80 v. are then obtained by switching over to the variable tapping  $T_2$ , and reading the instruments as quickly as possible. Between readings the cell should be connected to  $T_1$ . Thus, throughout the experiment the gas layer will be of a nearly constant thickness, namely, the thickness corresponding to 100 v.

At voltages greater than 80 the current increases according to higher powers than the square of the voltage, and it does not appear to be possible to find a simple expression for it which holds over a reasonably large range.

Fig. 4.



### 6. Pressure of the Gas.

In order to obtain an idea of the magnitude of the pressure of the gas in the gas layer a rectifying cell was subjected to external pressures varying from  $\frac{1}{40}$  to 4 atmos. Owing to the aqueous electrolyte it was not possible to reduce the pressure (at room temperature) much below 2 cm. of mercury. At this pressure there is very little change in the characteristics of the cell. The scintillations become slightly less violent with the reduction of pressure, but the capacity and breakdown voltage appear to be unaltered. Likewise, when the external pressure was increased to 4 atmos. no change could be detected in the capacity etc. It seems reasonable to suppose, therefore, that the pressure in the gas layer is high, probably amounting to many atmospheres.

### 7. *The Spectrum of the Glow.*

On account of its faintness the spectrum of the glow is difficult to observe. However, little information is to be gleaned from the spectrum, as it is a continuous one. As the photograph (fig. 6, Pl. XI.) shows it is brightest in the green at about  $555\text{ }\mu\mu$ . This appears to be the spectrum of oxygen under weak excitation <sup>(4)</sup>. [The diffuse band in the blue is due to stray light.] The photograph was taken on an Ilford "Golden Iso-zenith" plate (1400 H. & D.), and an exposure of 50 hours was necessary. In order to obtain a brighter glow and shorten the time of exposure as much as possible the cell was supplied with alternating current (see section 10), but the spectrum is the same as that observed visually with direct current.

### 8. *Influence of Magnetic Fields.*

As the application of a magnetic field sometimes produces large variations in the current flowing through an ordinary discharge-tube, it was thought worth while to try the effect of a magnetic field on an electrolytic cell. Fields up to 4000 gauss, applied both transversely and longitudinally, were used, but the current through the cell and the appearance of the glow were quite unaffected.

### 9. *Relation between Intensity of Glow and Current.*

Some measurements were made of the intensity of the glow by means of a visual photometer. The results are only roughly accurate, as the intensity of the glow is of the order of  $\cdot 0001\text{ C.P./cm.}^2$ . Such weak intensities are perceived by so-called scotopic vision, and the discriminating power of the scotopic eye is very poor.

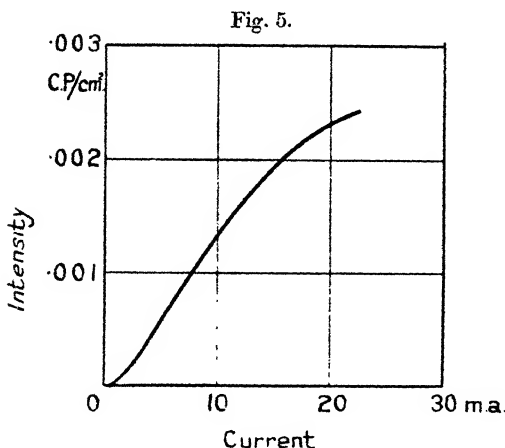
An extremely simple form of photometer was used. Outside the cell a comparison surface was supported adjacent to the glowing electrode. The comparison surface was illuminated by a faint green source, while the glowing electrode was screened from this source. The source was set at various distances from the comparison surface, and in each case the current through the cell was adjusted until the electrode and the comparison surface appeared equally bright. The general nature of the results obtained is shown in fig. 5.

While it is dangerous to draw definite conclusions from results of such a rough character, the following facts seem to emerge :—

(1) The intensity is primarily a function of the current, being over a considerable range approximately proportional to the current.

(2) The curve is, at small values of the current, slightly concave upwards. This may be due to the increase in thickness of the gas layer as the current (and voltage) increase. In this case it was not possible to keep the thickness constant by the method described in section 5, as the readings could not be taken quickly.

(3) A "saturation" value of the intensity seems to be suggested. This may be due to saturation in the usual sense of the term, or it may be due to leakage currents,



which become very large as the breakdown voltage is approached.

More satisfactory measurements of the intensity of the glow could probably be made photographically. Fairly long exposures (about 1 hour) would have to be made of the glow for various currents, and the images on the negatives compared with some form of densitometer.

### 10. The Cathode Glow.

In all the above experiments the active electrode was used as the anode, and the resulting glow may be called the "anode glow." If the connexions to a cell which is showing the anode glow are reversed only a momentary glow—the "cathode glow"—is seen, and then the resistance of the cell falls to a low value. This momentary



cathode glow appears even if the cell stands idle for some minutes before the reversed current is applied. Thus, the gas layer persists for some time after the cell is disconnected; capacity measurements (section 4) also demonstrate this fact.

It appears to be impossible, then, to investigate the cathode glow by means of direct current, as the oxide and oxygen layers are speedily reduced when the active electrode is made the cathode. If a cell is supplied with alternating current of suitable voltage and frequency, and if the circuit resistance is not too high, the anode and the cathode glows are produced alternately, and the frequency of the glow is twice the frequency of the alternating current. If the circuit resistance is high the voltage across the cell may be insufficient to produce the cathode glow; the anode glow is then produced alone, and the frequency of the glow is the same as the frequency of the alternating current. The photograph of the spectrum was taken under such conditions, the peak voltages of alternate half-cycles being 180 and 60; the mean current was .04 amp. and the frequency 25 cycles per second. The greater brightness of the glow on alternating current is probably due to the increased current which flows during the "positive half-cycle" (*i. e.*, the half-cycle which makes the active electrode the anode) after the film has been reduced by the preceding "negative half-cycle."

In order to observe the cathode glow alone it is necessary to view the electrode through a stroboscope disk driven off the alternating current which supplies the rectifier. By means of the stroboscope either the anode or the cathode glow may be examined separately. Moreover, if the slots on one half of the disk are "180° out of phase" with those on the other half, then the anode glow will be seen through one half and the cathode glow through the other. This is a useful arrangement for detecting differences between the anode and cathode glows.

With the help of the stroboscope, it was found that:

- (1) the cathode glow becomes visible at about the same voltage (about 60 v.) as the anode glow;
- (2) the intensity of the cathode glow appears to be about equal to that of the anode glow at the same voltage; and
- (3) the distribution of the cathode glow over the surface of the electrode is sometimes different from that of the anode glow.

25-cycle A.C. was used in these experiments, and the mean current through the rectifier was .3–.5 amp.

### 11. *Discussion of the Results.*

One of the most interesting features of the glow discharge in the electrolytic rectifier is that it takes place between electrodes which are about  $10^{-6}$  cm. apart (section 4). This results in an abnormally strong electric field—about  $10^8$  v./cm.,—and, consequently, the application of a relatively weak magnetic field produces no observable effect (section 8).

This glow discharge also differs from the ordinary glow discharge in that the oxygen is probably at a pressure of many atmospheres (section 6). The electrostatic attraction between the electrolyte and the electrode might account for this high pressure. Moreover, the mean free path of an electron in oxygen is about .00005 cm. at atmospheric pressure so that at this pressure about 98 per cent. of the electrons would cross the oxygen layer without colliding with oxygen molecules. This percentage seems much too high, and provides an additional reason for supposing that the pressure of the oxygen is greater than 1 atmos.

It is interesting to note that equation (A) (section 5) is of the same *form* as the well-known parabolic relation between the P.D. and current for an ordinary glow discharge between parallel plate electrodes <sup>(5)</sup>. The values of the constants for this case do not apply to the rectifier discharge, but this is not surprising as the conditions of the two discharges are so different.

It is difficult to say precisely how the glow is produced. In the oxygen layer the oxygen may be in the atomic or molecular state, and the electrons may be free or associated with oxygen atoms forming negative ions. Negative ions are usually found at high pressures, but in this case they may not be formed owing to the thinness of the layer. The relation between intensity of glow and current ought to give some information about the mechanism of the discharge <sup>(6)</sup>, but the experimental curves are rather inconclusive, although they suggest a linear relation. It is probable that the glow is produced by the ionization of oxygen molecules by collision with electrons, and the subsequent recombination of the electrons with the

ionized molecules; but complete experimental evidence cannot be given for this statement at present.

Some of the facts mentioned in section 11 are of interest in connexion with the electrochemical and electron theories of the rectifying action. To put the matter very briefly, rectification, on the electrochemical theory, is due to oxidation and reduction. The positive half-cycle forms a high-resistance layer of oxide and oxygen, while the negative half-cycle reduces this layer and a large current passes. On the electron theory, rectification occurs because the gas layer is bounded by a metal on one side and by an electrolyte on the other. The metal has a plentiful supply of free electrons, while the electrolyte contains only ions. The positive half-cycle is unable to drive the relatively massive negative ions of the electrolyte through the gas, but the negative half-cycle acts on the mobile electrons of the metal and a large current flows through the gas. Now, the glow is seen during the negative half-cycle, so that the oxygen layer does not disappear as it is supposed to do in the electrochemical theory. The electron theory also does not seem to be entirely satisfactory. If the whole current passes through the oxygen layer, a difference in the intensity of the anode and cathode glows might reasonably be expected, as the current during the negative half-cycle may be hundreds of times as great as that during the positive half-cycle. In order to account for all the facts a new theory of the rectifying action is required, probably involving both the electrochemical and electron hypotheses, but it is not proposed to attempt to formulate such a theory here.

In conclusion, the author wishes to express his gratitude to Professor Taylor Jones for his kind assistance, which has proved invaluable. The work was performed in the Research Laboratories of the Natural Philosophy Department of Glasgow University.

#### *References.*

- (1) E. H. Robinson, *Exp. Wir.* pp. 889-892 (Nov. 1925).
- (2) E. M. Dunham, *Phys. Rev.* pp. 819-822 (May 1929).
- (3) Jolley, 'Alternating Current Rectification'; Guntherschulze, 'Electric Rectifiers and Valves.'
- (4) W. M. Hicks, 'The Analysis of Spectra,' p. 77.
- (5) Aston and Watson, *Proc. Roy. Soc. A*, lxxxvi. p. 168 (1912).
- (6) J. Thomson, *Phil. Mag.* p. 988 (Dec. 1929).

July 1930.

**XCIII. Rates and Temperature Coefficients of the Catalytic Decomposition of Ammonia over Molybdenum, Tungsten, and Promoted Iron.** By C. H. KUNSMAN, E. S. LAMAR, and W. EDWARDS DEMING\*.

**T**HE decomposition of ammonia on hot surfaces can be treated kinetically, since it is a reaction of the simpler form, the reacting substance and the products being gases. The results herein described should be of interest in the study of catalysts for the ammonia reaction. The applicability to surface reactions of concepts commonly accepted in homogeneous reactions is considered.

Perman and Atkinson†, and Bodenstein and Kranendieck‡, studying the decomposition of ammonia in porcelain and quartz vessels from 677° to 1111° C., concluded that the observed rate could be accounted for by a wall or surface reaction.

We are indebted to Sir William Hardy for establishing the chemistry and physics of a fourth state, surfaces, in comparison with gases, liquids, and solids. The present method of investigating heterogeneous reactions and interpreting their results is an outgrowth of work carried on by Hinshelwood§ and his collaborators. Burk|| and Schwab¶ have studied the ammonia reaction with the object of determining the order of the reaction and the effect of the products of reaction. Reports of similar tests have been reported by Kunsman\*\*.

*Apparatus.*

The essential parts of the apparatus that was used for these catalytic studies are shown in fig. 1. The arrangement consists essentially of a decomposition chamber of about 1 litre capacity, containing and supporting the surfaces upon which the kinetics of the decomposition of ammonia

\* Communicated by the Authors.

† Perman and Atkinson, Proc. Roy. Soc. lxxiv. p. 110 (1904).

‡ Bodenstein and Kranendieck, 'Nerst Festschrift,' Wilhelm Knapp (1912).

§ Hinshelwood, "Kinetics of Chemical Changes in Gaseous Systems," Oxford University Press (1926), hereafter referred to as Hinshelwood, 'Kinetics.'

|| Burk, Proc. Nat. Acad. Sci. xiii. p. 67 (1927).

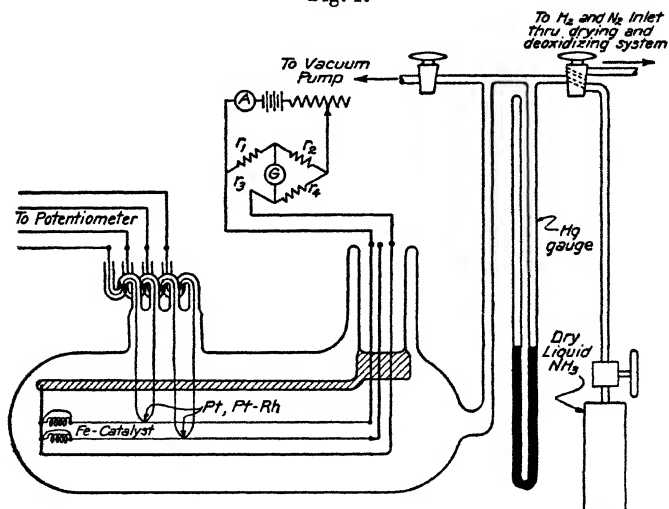
¶ Schwab, Zs. Physik. Chem. cxxviii. p. 161 (1927).

\*\* Kunsman, J. Am. Chem. Soc. l. p. 2100 (1928); li. p. 688 (1929); J. Frank, Inst. cciii. p. 635 (1927); J. Chem. Education, vi. p. 623 (1929).

were investigated. Three chambers were actually employed, identical in construction except that one contained drawn filaments of molybdenum, one contained a tungsten filament, and the other, as illustrated, contained platinum strips coated with iron catalysts. The molybdenum wires were 0.0308 cm. in diameter, and were furnished by the Fansteel Products Company. The tungsten filament was 0.254 mm. in diameter, and was furnished by the General Electric Company. The cross-section of the platinum strips was  $0.46 \times 0.10$  mm.

The apparatus was constructed of pyrex with heavy tungsten wires leading into the decomposition chamber. The tungsten leads formed a part of the support of the

Fig. 1.



Apparatus for the study of the decomposition of ammonia on hot surfaces.

surfaces, and enabled the catalyst surface to be heated to a desired temperature from a storage battery. The filaments or coated strips were kept taut by means of molybdenum springs. The shunted platinum strip carried most of the current, so that no part of the apparatus was sufficiently hot to decompose ammonia except the filaments or coated strips.

As the rate of a chemical reaction and the corresponding kinetics are so vitally dependent on the temperature, every precaution was taken to determine the temperature of the hot surface and keep it constant throughout a test.

Three methods were used to determine the temperature: (1) direct observation with a Leeds and Northrup optical pyrometer, calibrated at the Bureau of Standards, and corrected for the emissivity of the surface and absorption by the glass; (2) employing the temperature coefficient of the resistance of tungsten or molybdenum; and (3) using a thermocouple welded to the filament or coated strip. In the last method 0.005 cm. diameter Pt, Pt-Rh wire was used, the juncture being located at the hot surface in the middle of its length. As some difficulty is experienced in making the thermocouple lead seals through pyrex, the form of the seal was modified as shown in fig. 1 to form a small cup about each wire. This cup may be filled with mercury or deKhotinsky wax, either of which will stop any leak that may result from an imperfect metal to pyrex seal.

Since the hydrogen formed as a decomposition product is a better conductor of heat than ammonia or nitrogen, it is necessary to increase the current through the filament or coated strip as the decomposition progresses, in order to keep the resistance and temperature of the filament constant. The Wheatstone bridge arrangement shown in fig. 1 enables this to be done quickly and easily. The coated strip is made one resistance  $r_3$  of the bridge, comparable with  $r_4$ , but small in comparison with  $r_1$  and with  $r_2$ .

A minimum number of stopcocks was used. A mercury trap, which is not shown in fig. 1, separated the decomposition chamber and manometer from the rest of the apparatus during a decomposition run. The decomposition chamber and connecting parts were first thoroughly heated in an oven and evacuated to a low pressure. Very pure dry ammonia was then admitted to a pressure of about one-third of an atmosphere, and the rate of decomposition was measured for a given temperature by the increase of pressure noted on the manometer at various moments as the reaction progressed. Thus the pressure in the tube is obtained as a function of the time.

The coated strips were much more active catalysts than the drawn filaments, and it may be well to describe in detail their preparation. Incidentally these catalysts are among the better ones developed for the commercial synthesis of ammonia. They are made from fused pure artificial magnetite, to which about 1 per cent. of aluminium oxide and 1 per cent. of an alkali oxide, usually of potassium, has been added in the fusion process. Very uniform coated surfaces can be obtained from the oxide mixture when ground to 300 mesh or finer, reduced by hydrogen, and

mixed with paraffin. This is applied to the electrically heated twisted platinum strip with a glass rod. The strip should be only hot enough to vaporize the paraffin. After obtaining a uniform layer over the entire length of the strip it should be raised to a dull red temperature in air. A bright hot spot will develop, due to the rapid oxidation of the finely divided iron particles, and will spread over the entire surface. A temperature sufficiently high to sinter or fuse the coating to the strip is thus reached. This procedure may be repeated until the desired thickness has been obtained. Such a coating, after being reduced in hydrogen, is very stable, and is uniform in thickness throughout its length, but it does not furnish as active a catalytic surface as one obtained by coating with the unreduced mixture, for in the latter case the particles are not as firmly attached. The procedure for coating the strips with the unreduced oxides is similar to that just described, but the coating is not subjected to the sintering process. In either case the coating of oxides must be reduced in order that it may serve as a catalyst. The reduction should be carried on at a dull red temperature for about twelve hours in hydrogen. The coated platinum strips used in these experiments were in every case covered originally with the unreduced mixture. There was about 1 gram of oxides on each strip.

By means of the very active coated strips, on the one hand, and the relatively inactive molybdenum and tungsten filaments on the other, decomposition runs were made from 475° to 1295° C.

### *Theory of Surface Kinetics.*

In this discussion let  $E$  denote  $-Rd \ln k : dT^{-1}$ , where  $k$  is the reaction velocity at temperature  $T$ . Arrhenius found the plot of  $\ln k$  vs.  $T^{-1}$  to be a straight line with many homogeneous reactions, and he called  $E$  the "heat of activation." With a heterogeneous reaction the plot often has some curvature, and Hinshelwood\* calls  $E$  at any point the "apparent heat of activation" for that temperature. One cause of this curvature, mentioned by Hinshelwood†, may be that the observed reaction is a composite one made up of two or more concurrent reactions differently influenced by temperature. Another cause may be that the fractions of the active surface that are covered by the reactants and

\* Hinshelwood, 'Kinetics,' p. 176.

† Hinshelwood, 'Kinetics,' p. 46.

products may vary with temperature. In this paper the second cause is treated.

The "true heat of activation" is the value of  $E$  that would be observed in a simple reaction where the fraction of the active surface covered by each product and reactant, and consequently where the inhibition by the products, is independent of the temperature.

Hinshelwood\* discusses two special cases of inhibition by the adsorbed products. By treating it in a more general way we arrive at the second explanation of curvature, and also are enabled to compute the true heat of activation when the reaction is a simple one (not composite).

In this paper we shall give this more general treatment, and then use the results to find the true heat of activation for the decomposition of ammonia on different catalysts, and to estimate the difference in the heats of adsorption for ammonia and hydrogen.

We shall use the following symbols, with the subscripts 0 for the reactant, and 1, 2, ...,  $n$  for the  $n$  products of the decomposition:—

$a_i$  = rate of condensation of gas  $i$  onto unit uncovered area of the catalytic surface.  $a_i$  may vary with pressure, but scarcely with temperature †.

$\sigma_i$  = fraction of the active surface covered by gas  $i$ , averaged with respect to time.

$b_i e^{-\lambda_i/RT}$  = rate of evaporation of gas  $i$  from unit area completely covered at temperature  $T$ .

$\lambda_i$  = heat of desorption for gas  $i$ , here treated as being constant.

$$B_i = b_i a_i^{-1} e^{-\lambda_i/RT}, \quad dB_i/dT^{-1} = -\lambda_i B_i/R.$$

We shall assume that the establishment of adsorption equilibrium is rapid compared with the rate of removal or deposition of molecules by chemical change, and we shall neglect the back reaction.

At adsorption equilibrium, while the partial pressures are constant,

$$\left(1 - \sum_0^n \sigma_i\right) a_i = \sigma_i b_i e^{-\lambda_i/RT}, \quad i=0, 1, 2, \dots, n; \quad (1)$$

\* Hinshelwood, 'Kinetics,' pp. 176-178.

† Hinshelwood, 'Kinetics,' p. 144.





If  $\sigma_2$  is practically zero, and if  $\sigma_0 + \sigma_1$  remains practically unity, then  $\sigma_0/\sigma_1 = B_1/B_0$  (from eq. 3) becomes

$$\sigma_0/(1-\sigma_0) = B_1/B_0;$$

whence

$$\frac{a_0}{a_1} = \frac{\sigma_0}{1-\sigma_0} \cdot \frac{b_0}{b_1} e^{(\lambda_1 - \lambda_0)/RT} \equiv \frac{\sigma_0}{1-\sigma_0} g(T). \quad (8)$$

By making use of Langmuir's conclusion that practically every molecule that strikes a surface condenses,  $a_i$  is the number of molecules of gas  $i$  that strike unit area of the catalyst surface per second. Consequently, from kinetic theory and from eq. (8),

$$\frac{a_0}{a_1} = \frac{p_0}{p_1} \left( \frac{M_1}{M_0} \right)^{\frac{1}{2}} = \frac{\sigma_0}{1-\sigma_0} g(T); \quad (9)$$

whence

$$\sigma_0 = \left[ \frac{p_1}{p_0} \left( \frac{M_0}{M_1} \right)^{\frac{1}{2}} \cdot g(T) + 1 \right]^{-1}. \quad (10)$$

At constant temperature,  $k \propto \sigma_0$  (eq. 5), so we may write

$$k \equiv c(T) \left[ \frac{p_1}{p_0} \left( \frac{M_0}{M_1} \right)^{\frac{1}{2}} g(T) + 1 \right]^{-1},$$

or

$$1/k = \frac{g(T)}{c(T)} \cdot \left( \frac{M_0}{M_1} \right)^{\frac{1}{2}} \frac{p_1}{p_0} + 1/c(T). \quad (11)$$

So if  $1/k$  is plotted against  $\frac{p_1}{p_0} \left( \frac{M_0}{M_1} \right)^{\frac{1}{2}}$  as abscissas, there should result a straight line whose intercept on the  $1/k$  axis is  $1/c(T)$ , and whose slope is  $g(T)/c(T)$ . Thus one can find  $g(T)$  and  $c(T)$ .  $\sigma_0$  as a function of  $T$  can then be found from eq. (10).

$c(T) = k/\sigma_0$  is the rate of decomposition on unit area covered with ammonia.  $-R d \ln c(T) : dT^{-1}$  should be the true heat of activation  $Q$ . If  $\sigma_2 = 0$  and  $\sigma_0 + \sigma_1 = 1$  in (7),

$$E = Q + (\lambda_1 - \lambda_0) (1 - \sigma_0). \quad (12)$$

Knowing  $E$  and  $\sigma_0$  at particular values of  $T$  and of  $p_1/p_0$ , and knowing  $Q$ , we can easily find  $\lambda_1 - \lambda_0$  from eq. (12). But this is not a very accurate method, because  $\lambda_1 - \lambda_0$  is thus made the small difference between two relatively large quantities.

Another method of getting  $\lambda_1 - \lambda_0$  comes from the definition of  $g(T)$  in eq. (8). If  $\ln g(T)$  vs.  $T^{-1}$  be plotted,  $R d \ln g(T) : dT^{-1} = \lambda_1 - \lambda_0$ .

*End Correction for the Heated Filament.*

The correction for cooling at the ends of an 18 cm. molybdenum filament while being used as a catalyst has been investigated\*. The equivalent length effective at the maximum temperature  $T_{\max}$ , which is the temperature in the middle, was computed by averaging the rate of reaction along the full length; thus, if  $k$  is the reaction rate over an element  $\Delta x$  at a distance  $x$  from one end, and  $\bar{k}$  the reaction rate at  $T_{\max}$ , the equivalent length is  $\Sigma k \Delta x / \bar{k}$ . The results follow closely the law  $y = ax^n$ , with  $a = .099448$  and  $n = 1.5464$ ,  $x$  being  $(10^4/T_{\max})$  and  $y$  being the end correction (for both ends) in cm.,  $y = 18$  cm. minus equivalent length. One can expect the end correction to be independent of the length of the filament provided it is not too short. A different filament would have new constants on account of having different heat conductivity, resistivity, and catalytic action, but the equation for molybdenum could probably be used for tungsten with some confidence, because the characteristics of molybdenum and tungsten are not too far different.

A portion of the increase in reaction rate observed with increase in temperature is due to the decrease in end correction. It was thought best to present the experimental results and deductions for molybdenum and tungsten as if there were no end correction, and then to introduce the refinement. It was not necessary to correct the figures for the promoted iron catalysts, because the platinum strips were coated so that the whole coated length when heated appeared to be of uniform redness.

The end correction for this work is very easily applied. If  $c'(T)$  and  $Q'$  are the uncorrected values of  $c(T)$  and  $Q$ , and if  $L$  is the total measured length of filament, then

$$c(T) = c'(T)L/(L - y) = c'(T)L/(L - ax^n),$$

$$\frac{d}{dx} \ln c(T) = \frac{d}{dx} \ln c'(T) + nax^{n-1}L^{-1};$$

80

$$Q = Q' - 10^4 R n a x^{n-1} L^{-1}. \quad . \quad . \quad . \quad (13)$$

Here  $n - 1 = .5464$  and the range of  $x$  is never great, so the end correction term is considered to be independent of  $x$ , which would make  $Q$  and  $Q'$  differ by a constant; in other words, if the plot of  $\ln c(T)$  vs.  $T^{-1}$  is a straight line, the plot of  $\ln c'(T)$  vs.  $T^{-1}$  would also be straight. In practice

\* E. S. Lamar and W. E. Deming, "Temperature Distribution along a Heated Filament used as a Catalyst," *Phil. Mag.* p. 28 (Jan. 1930).

the average value of  $x$  for a set of decomposition runs was used in the correction term.

The quantity  $g(T)$  as defined in eq. (8) is dimensionless, and is not affected by the end correction.

*Evaluation of  $Q$  and of  $\lambda_0 - \lambda_1$  on Molybdenum.*

Two sets of data were taken using two different molybdenum filaments. One (a), 18 cm. long, had been used as a catalyst several months, and the other (b), 12 cm. long, was new.

In a previous article \* it was shown by one of the authors that an initial excess of nitrogen has little or no effect on the time for half decomposition. His experiments have been repeated, and this conclusion corroborated; so it appears that nitrogen is adsorbed only slightly in the presence of hydrogen and ammonia. Therefore we feel justified in putting  $\sigma_2 = 0$ . But an initial excess of hydrogen lengthens the time for half decomposition, so  $\sigma_1 \neq 0$ .

We found that if the temperature of the filament is kept constant, then over quite a wide range of initial pressures of ammonia (from 12 to 30 cm.) the time for half decomposition is proportional to the initial pressure of ammonia. This means that the average rate of decomposition over the half-time is independent of the initial pressure of ammonia. Since  $k \propto \sigma_0$ , and since  $k$  does not increase with initial ammonia pressure, the maximum available surface must remain covered with hydrogen and ammonia, i. e.,  $\sigma_0 + \sigma_1 = 1$  and  $\sigma_2 = 0$ . Still another proof of this point was obtained by testing the data by means of eq. (10), from which it can be seen that if the original assumptions are correct, at a particular temperature  $k$  should be a function of  $p_1/p_0$  only, regardless of the initial ammonia pressure. This was found to hold over the pressure range mentioned above.

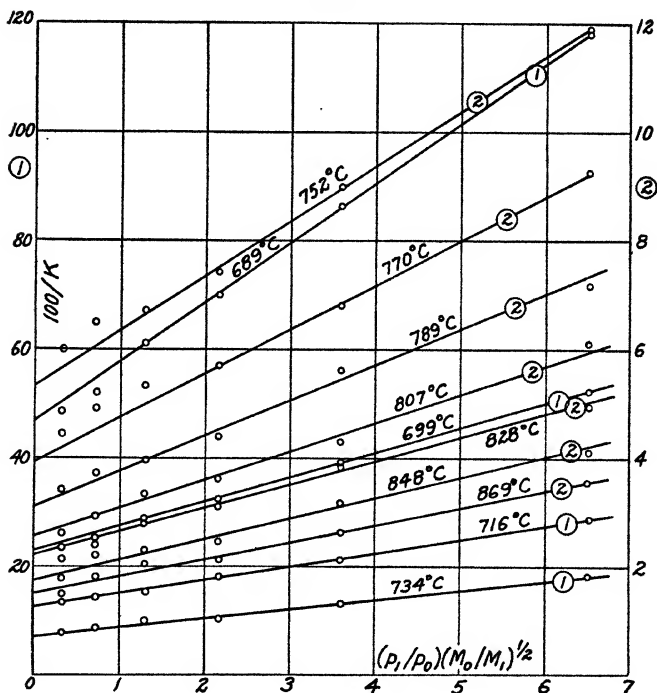
$k$ , which represents the speed of decomposition at any instant, is proportional to  $dp:dt$ , the time rate of increase of pressure in the tube. We put  $k = dp:dt$ , the slope of a pressure vs. time plot of the original data. In our work  $k$  and  $dp:dt$  refer to unit area of catalyst surface as determined by the geometrical dimensions of the filament.

Figs. 2 and 3 show the  $1/k$  vs.  $(p_1/p_0)(M_0/M_1)^{\frac{1}{2}}$  isotherms. Each point is the average of two runs, taken one after another, beginning with the highest temperature and

\* Kunsman, J. Amer. Chem. Soc. 1. p. 2100 (1928); li. p. 688 (1929); J. Frank, Inst. cciii. p. 365 (1927); J. Chem. Education, vi. p. 623 (1929).

working down to the lowest, then working back up again to the highest. Nine different temperatures, ranging from 681° to 926° C., were used for filament *b*, and twelve, ranging from 689° to 891° C., for filament *a*. Over the time interval used for the entire set of observations the activities of neither catalyst decreased a measurable amount. The curve for 891° C. is omitted from fig. 2 because it happens almost to coincide with another one plotted to a different scale.

Fig. 2.



$k^{-1}$  vs.  $(p_1/p_0)(M_0/M_1)^{1/2}$  for used molybdenum filament (*a*).

$k$  = reaction rate in cm. Hg per minute per square centimetre of catalyst surface.

$p_0, p_1$  = partial pressure of ammonia, hydrogen.

$M_0, M_1$  = molecular weight of ammonia, hydrogen.

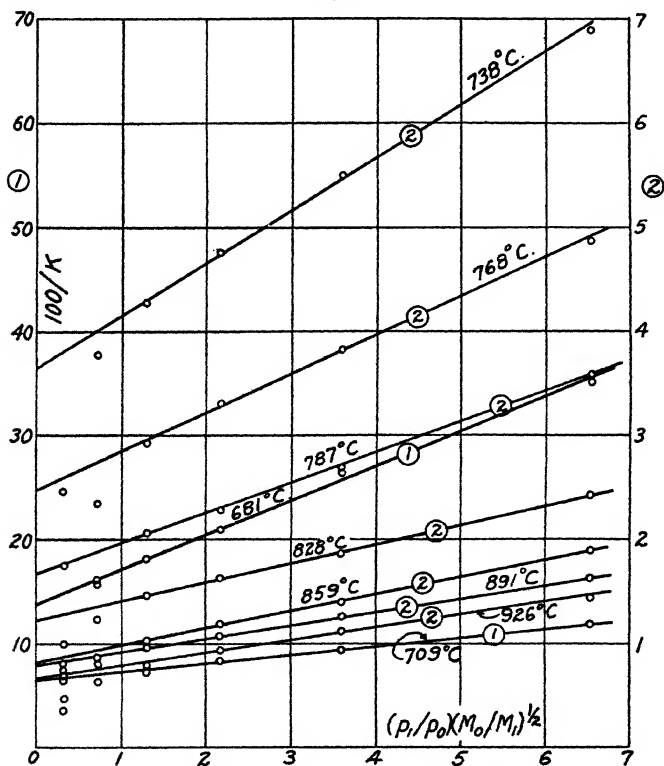
The numbers in the circles designate the scale for the ordinates.

The temperature of the filament, as measured by its resistance, was held constant to within three degrees during a run. The initial ammonia pressure was 26.6 cm. Hg for all runs.

From the isotherms of figs. 2 and 3 we find  $g(T)$  and  $c'(T)$  by the method previously explained.

Near the beginning of a run, where  $(p_1/p_0)(M_0/M_1)^{1/2}$  is small, there is superimposed upon the rate of reaction an apparent rate (an increase in pressure) due to the heating of the gas in the tube immediately after the filament is

Fig. 3.



$k^{-1}$  vs.  $(p_1/p_0)(M_0/M_1)^{1/2}$  for new molybdenum filament (b).

$k$ =reaction rate in cm. Hg per minute per square centimetre of catalyst surface.

$p_0, p_1$ =partial pressure of ammonia, hydrogen.

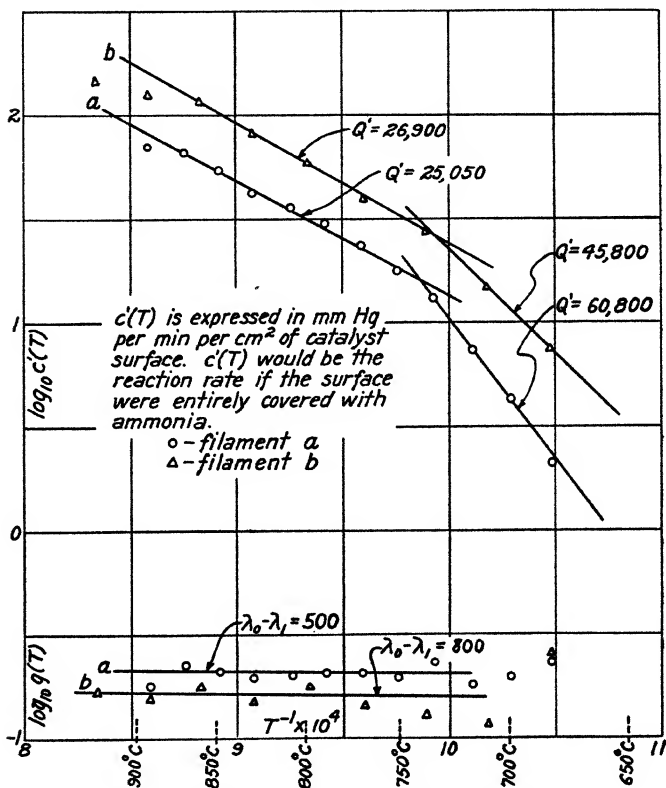
$M_0, M_1$ =molecular weight of ammonia, hydrogen.

The numbers in the circles designate the scale for the ordinates.

turned on. At the lower temperatures this source of error is noticeable only at the beginning of a run. At the highest temperatures half decomposition is completed before the gas

in the tube has reached temperature equilibrium. Since it takes time for the products of the reaction to diffuse away from the filament, the value of  $p_1/p_0$  near the filament is not the value of  $p_1/p_0$  in the tube. This difference is negligible except at the highest temperatures, when the reaction is very fast. In getting  $c'(T)$  and  $g(T)$  from figs. 2 and 3 the

Fig. 4.

Evaluation of  $Q^1$  and of  $\lambda_0 - \lambda_1$  for molybdenum.

right-hand portions only of the curves were considered, because the errors are least effective there.

$c(T)$  is the value that  $k$  would have at temperature  $T$  if the filament were entirely covered with ammonia. The  $\ln c'(T)$  vs.  $T^{-1}$  and the  $\ln g(T)$  vs.  $T^{-1}$  curves are shown in fig. 4. The  $c'(T)$  points for each filament determine two

straight lines, which break at about  $1013^{\circ}\text{K}$ . ( $740^{\circ}\text{C}$ .) for  $a$  and at about  $1008^{\circ}\text{K}$  ( $735^{\circ}\text{C}$ .) for  $b$ . The portions on the low temperature sides of the breaks seem to indicate the existence of molybdenum nitride, probably formed from the ammonia. We conclude that at temperatures above the breaks the nitride ceases to exist in the presence of hydrogen. The deviations of the extreme high-temperature points from the straight line are due to the second source of error mentioned in the preceding paragraph, since at these temperatures the reaction is very fast and the products do not have a chance to diffuse from the filament as fast as they are formed. There are no perceptible breaks in the  $q(T)$  curves.

The following tabulation is derived from fig. 4:—

L.	Mo. Fil. <i>a</i> . 18 cm.	Mo. Fil. <i>b</i> . 12 cm.
Q uncorrected :		
High temperature.....	25,050	26,900
Low temperature .....	60,800	45,800
Average $10^4/T$ :		
High temperature.....	9.2	9.2
Low temperature .....	10.4	10.4
Q corrected (eq. 13) :		
High temperature .....	24,500	26,050
Low temperature .....	60,200	44,900
$\lambda_0 - \lambda_1$ .....	500	800

Filament  $b$ , the new one, was more active than  $a$ , and had a higher heat of activation. The metal composing a filament tends to form larger and larger crystals as it is used, and this lowers its activity, probably because its available surface area is thus decreased.

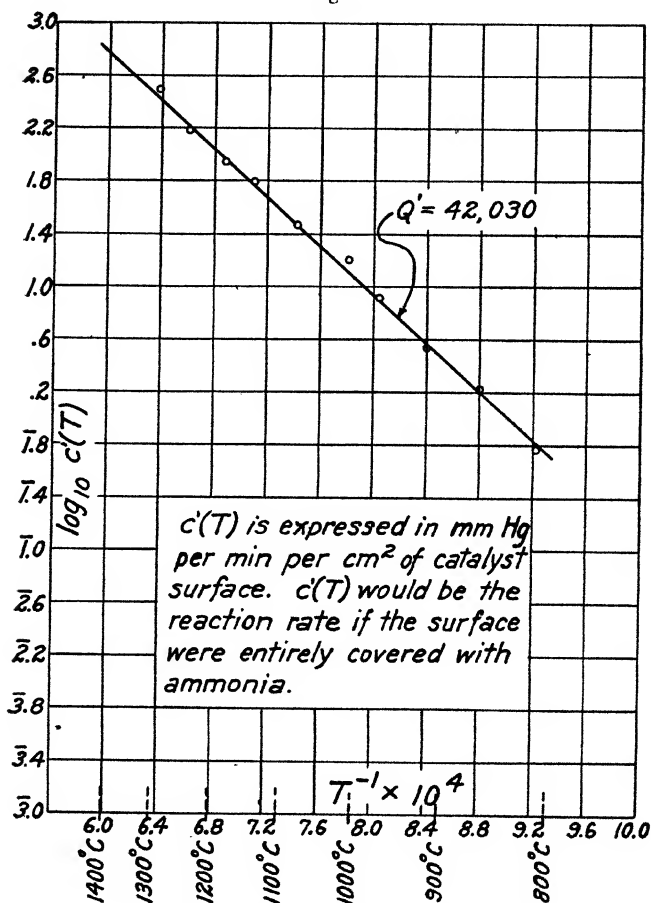
#### *Evaluation of Q for a Tungsten Filament.*

The best available data for tungsten were treated in the same manner as the data on molybdenum. The same arguments that were used to show that nitrogen is only slightly adsorbed, if at all, and that the active surface remains entirely covered by hydrogen and ammonia for the molybdenum filament, hold good for tungsten. The ten decomposition runs were made, beginning with the highest temperature ( $1295^{\circ}\text{C}$ .) and working down to the lowest ( $810^{\circ}\text{C}$ .). A check-back on the highest temperature showed that there had been no measurable change in activity. The  $1/k$  vs.  $(p_1/p_0)(M_0/M_1)^{1/2}$  plot is omitted because it is a series of straight lines similar to those for molybdenum. The



$\log c'(T)$  vs.  $T^{-1}$  curve is fig. 5, whose slope gives  $Q$  (uncorrected) = 42,030 calories per mol. The length of the tungsten filament was 18 cm., and the average of  $10^4/T$  is easily estimated from the figure to be about 7.8, whence

Fig. 5.

Evaluation of  $Q^1$  for tungsten.

by eq. (13)  $Q$  (corrected) = 41,500. An attempt was made to evaluate  $\lambda_0 - \lambda_1$ , but the curvature of the  $p$  vs.  $t$  curves was so small that  $g(T)$  could not be determined accurately. Furthermore, there was only one run at each temperature,

and this fact lessened the precision. As far as we could tell,  $\lambda_0 - \lambda_1$  is small, probably not greater than 1500.

*Evaluation of  $Q$  and of  $\lambda_0 - \lambda_1$  for Iron Catalyst no. 1.*

The promoted iron catalyst mixture no. 1 in the unreduced form consisted of a mixture of the oxides of iron, aluminium, and potassium, in the ratio 98.69 : 1.05 : 0.26 by weight. The coated strip, 19 cm. in length, was reduced in hydrogen at dull red heat. The activity of such a catalyst is highest immediately following reduction, after which it decreases, rapidly at first, and then more and more slowly. With our catalyst a temperature calibration was taken immediately after reduction, so by the time the decomposition runs were made it was in fairly stable condition, but its activity was somewhat lower than it was initially.

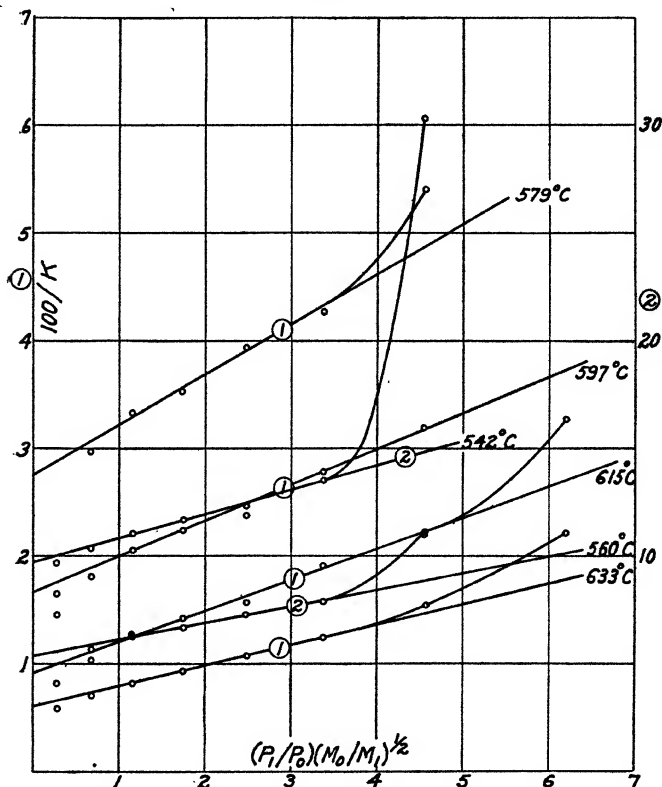
The processes that take place on an iron mixture may be more complicated than those encountered on the surface of a drawn metal wire, such as the molybdenum and tungsten filaments already discussed. On the latter the surface conditions remain very uniform, but on the former the thermal conduction from the surface increases with the progress of the reaction, and the temperature of the entire surface decreases slightly while the resistance and temperature of the platinum strip remain constant. The upward curvature in figs. 6 and 9 is thus attributed to a physical change in surface conditions rather than to a change in  $\sigma_0 + \sigma_1$ . It is to be remembered that  $g(T)$  is dimensionless, and is thus independent of the amount of surface covered, so values of  $g(T)$  obtained from slopes and intercepts of tangents taken at different points along a single  $1/k \propto v/s_0 \cdot p_1/p_0 (MM_1)^{\frac{1}{2}}$  would be the same if the curvature were due to a change in  $\sigma_0 + \sigma_1$ . But the values of  $g(T)$  obtained from figs. 6 and 9 do depend on the point of tangency, so it seems certain that the departure of these curves from linearity is due to a change in surface conditions, and not to a change in  $\sigma_0 + \sigma_1$ .

The curves in fig. 6 have well-defined straight portions, which indicate constant surface conditions over part of each run. The  $c(T)$  and  $g(T)$  determined from these straight portions refer to the surface in its constant state.

The runs on catalyst no. 1 were taken at six different filament temperatures, one after another, over  $91^\circ$  range, beginning with the highest temperature and working down to the lowest, then working back to the highest. Thus two runs were taken at each temperature. Over the interval of time required for these runs the activity at the highest

temperature decreased about 1.5 per cent., which is barely outside the experimental error. The effect of this gradual shift in activity was eliminated by taking the average of the two runs at each temperature. As before, the temperature of the filament was held constant to within several degrees during a run. The initial ammonia pressure was 26.6 cm.

Fig. 6.



$k^{-1}$  vs.  $(p_1/p_0)(M_0/M_1)^{1/2}$  for promoted iron catalyst no. 1.

$k$  = reaction rate in cm. Hg per minute per square centimetre of catalyst surface.

$p_0, p_1$  = partial pressure of ammonia, hydrogen.

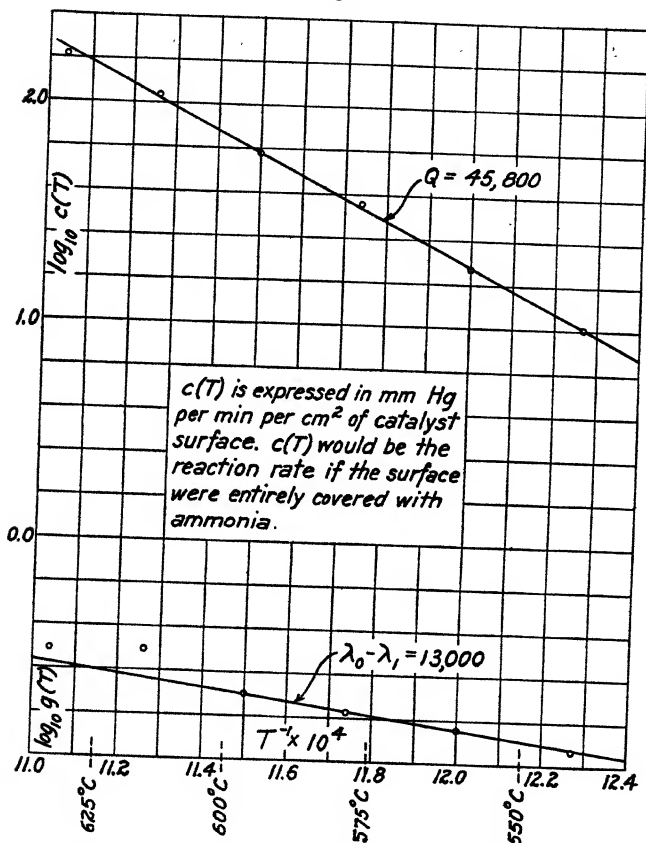
$M_0, M_1$  = molecular weight of ammonia, hydrogen.

The numbers in the circles designate the scale for the ordinates.

Hg for all runs. All the data were taken in exactly the same manner.

The results are shown graphically in fig. 6. The straight portions of these curves determine  $c(T)$  and  $g(T)$ , whose logarithms are plotted as functions of  $T^{-1}$  in fig. 7. The slopes of the straight lines determined by these points give

Fig. 7.



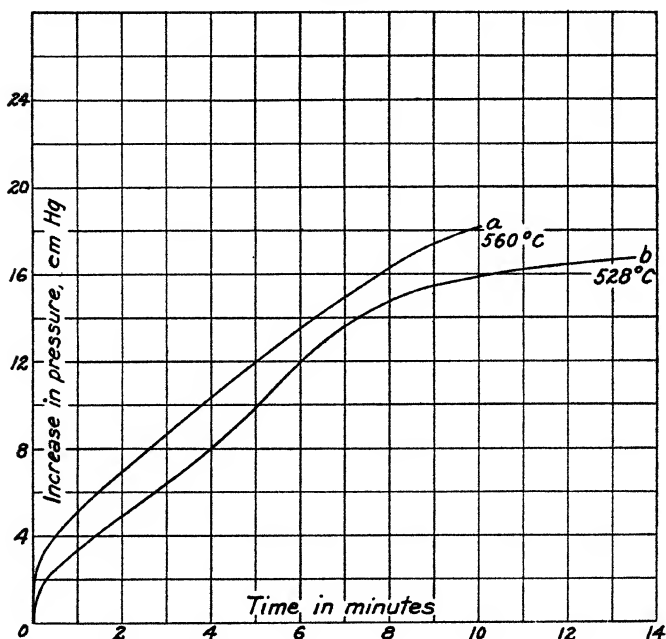
Evaluation of  $Q$  and of  $\lambda_0 - \lambda_1$  for promoted iron catalyst no. 1.

$Q = 45,800$  calories per mol., and  $\lambda_0 - \lambda_1 = 13,000$ . As mentioned before, it is not necessary to make an end correction for  $Q$  for the iron catalysts.

Since the temperatures were comparatively low, it was suspected that the decomposition may have taken place on a nitride rather than on an iron surface. An attempt was

made to test for such a nitride at each of the temperatures used in the decomposition runs. The procedure at a particular temperature was as follows:—A decomposition run was allowed to go halfway to completion, then the filament was turned off and the products were pumped out. Hydrogen was then admitted, and the filament heated to  $633^{\circ}\text{C}$ ., the highest temperature used. It was expected that the hydrogen would reduce the nitride to form ammonia, and that the

Fig. 8.



Pressure vs. time curves.

(a) Typical for promoted iron after some use. \*

(b) Typical for promoted iron immediately after reduction, its most active condition.

The ordinates are the increase in pressure in the tube above the initial 26.6 cm. Hg.

ammonia would decompose catalytically. There should result, then, an increase in pressure equal to the partial pressure of the nitrogen liberated. Such an increase was observed and measured with a manometer. The above procedure was repeated, stopping the decomposition runs at smaller degrees of completion, and as near as could be

determined the partial pressure of nitrogen was the same in each case. This means that the nitride is probably formed near the beginning of the decomposition run, and that during the remainder the entire active surface is covered with nitride. This conclusion is further substantiated by the fact that within the limits of experimental error the nitride content was the same at each of the different temperatures investigated. The results given in fig. 7, therefore, are probably those for an iron nitride surface as a catalyst.

Fig. 8 shows two pressure vs. time curves: (a) is a typical one for the promoted iron just discussed; (b) is one for a promoted iron catalyst in its most active condition, immediately after reduction. An interesting phenomenon is apparent in curve (b). The first rapid rise in pressure is the temperature effect previously mentioned, but after that it will be observed that there is actually an increase in decomposition rate as the run progresses, which finally levels off fairly sharply. Near the beginning of the run the surface may become covered with a nitride of iron, and, further, the activity of the nitride as a catalyst may be less than the activity of the iron itself. As the run progresses more hydrogen is liberated, which begins to reduce the nitride. As the nitride is reduced, more and more of the iron surface becomes available, and the rate increases until a point is reached at which the hydrogen as a thermal conductor becomes effective in reducing the temperature of the surface. At this point the  $p$  vs.  $t$  curve begins to level off.

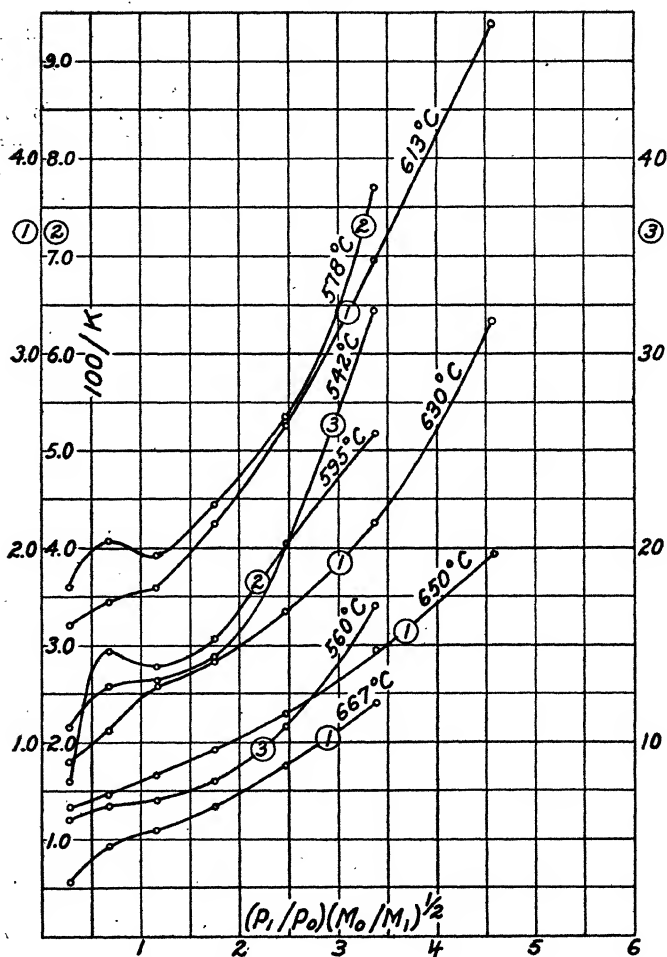
If the above analysis is the correct one, the iron nitride is more readily removed by hydrogen from the more active form of the catalyst than from the less active form.

#### *Evaluation of $Q$ and of $\lambda_0 - \lambda_1$ for Iron Catalyst no. 2.*

Application of the theory that was developed in the first part of this paper was made by placing  $\sigma_0 + \sigma_1 = 1$  and  $\sigma_2 = 0$ —that is, by assuming that the entire active surface remains covered with ammonia and hydrogen. When the  $1/k$  vs.  $(p_1/p_0) (M_0/M_1)^{1/2}$  curves are straight lines the condition of the surface remains invariable. When one of these curves yields varying values of  $g(T)$  the surface conditions vary during a decomposition run, and values of  $Q$  and of  $\lambda_0 - \lambda_1$  for the *average* surface are desired. When these curves are replaced by straight lines that best approximate the points along the curves, the slopes and intercepts of these straight lines determine the  $Q$  and  $\lambda_0 - \lambda_1$  that refer to the average surface conditions.

The iron catalyst mixture no. 2 in the unreduced form consisted of the oxides of iron, aluminium, potassium, and molybdenum in the ratio 94.11 : 2.00 : 0.25 : 3.64 by weight.

Fig. 9.



$k^{-1}$  vs.  $(p_1/p_0)(M_0/M_1)^{1/2}$  for promoted iron catalyst no. 2.

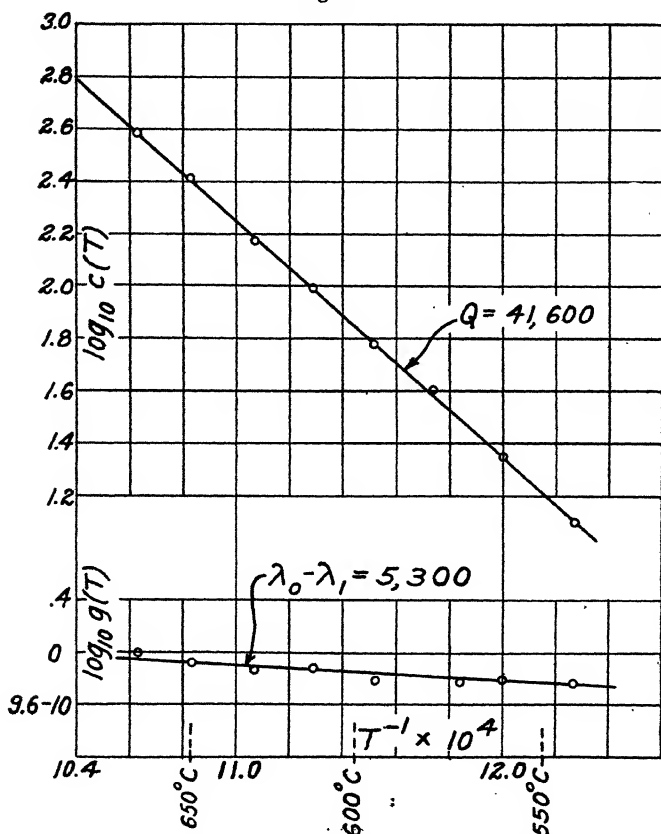
$k$  = reaction rate in cm. Hg per minute per square centimetre of catalyst surface.

$p_0, p_1$  = partial pressure of ammonia, hydrogen.

$M_0, M_1$  = molecular weight of ammonia, hydrogen.

Runs were taken at eight different filament temperatures, one after another over  $125^\circ$  range, beginning with the highest temperature ( $667^\circ\text{C.}$ ) and working down to the lowest ( $542^\circ\text{C.}$ ), then working back to the highest. Thus, two runs were taken at each temperature. Over this interval the activity at the highest temperature decreased 1.5 per

Fig. 10.



Evaluation of  $Q$  and of  $\lambda_0 - \lambda_1$  for promoted iron catalyst no. 2.

cent., which is barely outside the experimental error. The length of the platinum strip was again 19 cm., and the runs were made in the same manner as those for no. 1.

The  $1/k$  vs.  $(p_1/p_0)(M_0/M_1)^{1/2}$  curves are shown in fig. 9. The straight lines that replace these curves are not shown,



because they confuse the figure. The slopes and intercepts of these lines determine  $c(T)$  and  $g(T)$ , shown in fig. 10.  $Q$  turns out to be 41,600 and  $\lambda_0 - \lambda_1$  to be 5300.

The authors wish to acknowledge the continual support of Dr. F. G. Cottrell, the director of this laboratory, and the cooperation of other members of the staff in the course of this work.

### *Summary.*

The writers have taken into consideration the condensation on to the catalyst surface and the evaporation therefrom of the products of a catalytic decomposition, and have derived a formula (neglecting the back reaction) for the so-called "true heat of activation,"  $Q$ , in terms of the temperature coefficient  $E$ , and the heats of desorption of the reactant and products. The formula is

$$E = Q - \lambda_0 + \sum_0^n \lambda_i \sigma_i,$$

in which  $\lambda_0, \lambda_1, \dots, \lambda_n$  are the heats of desorption for the reactant and  $n$  products, and  $\sigma_0, \sigma_1, \dots, \sigma_n$  are the fractions of the surface covered by the reactant and  $n$  products.

They have decomposed ammonia on molybdenum and on tungsten in the form of filaments electrically heated, and on promoted iron catalysts applied on electrically heated platinum strips, and have shown that the adsorption of nitrogen from the gas phase is negligible, but that the active surface remains entirely covered with hydrogen and ammonia during a run within the temperature ranges studied. From theoretical considerations they are able to compute the heat of activation  $Q$  and the heat of desorption of ammonia less that of hydrogen,  $\lambda_0 - \lambda_1$ , tabulated below.  $Q$  and  $\lambda_0 - \lambda_1$  are in calories per mol.

Catalyst.	$Q$ .	$\lambda_0 - \lambda_1$ .
Used molybdenum (a):		
High temperature.....	24,500	500
Low temperature .....	60,200	500
New molybdenum (b):		
High temperature.....	26,050	800
Low temperature .....	44,900	800
Tungsten .....	41,500	—
Iron catalyst no. 1 .....	45,800	13,000
Iron catalyst no. 2 .....	41,600	5300

A break in the curves of fig. 4 for molybdenum, they interpret, determines a temperature ( $740^\circ \text{C.}$ ) above which any nitride ceases to exist in the presence of hydrogen.

They infer that the decomposition on the two iron catalysts may actually take place on nitrides formed from the nitrogen in the ammonia.

Bureau of Chemistry and Soils,  
U. S. Department of Agriculture,  
Washington, D. C.,  
August 10th, 1929.

**XCIV.** *On some Integrals involving Legendre Polynomials.*  
By DOROTHY WRINCH, M. A., D.Sc., Hertha Ayrton Fellow,  
Girton College, Cambridge\*.

*Introduction and Summary.*

**I**N the course of an investigation into the pressure on a spheroidal obstacle in the presence of a source of fluid at a point on its axis, it became necessary to evaluate the integral

$$\int_{-1}^{+1} \frac{\mu(1-\mu^2)}{\nu^2-\mu^2} P_m'(\mu) P_n'(\mu) d\mu$$

when  $\nu^2$  is greater than unity and  $m$  and  $n$  are positive integers. This integral, evidently zero when  $m+n$  is even, at once directs attention when  $m+n$  is odd to the integral

$$\frac{1}{2} \int_{-1}^{+1} (1-\mu^2) P_m'(\mu) P_n'(\mu) \frac{d\mu}{\nu-\mu},$$

to which it is then equal. Since the characteristic properties of the Legendre functions allow the product

$$(1-\mu^2) P_m'(\mu) P_n'(\mu)$$

to be expressed in the form

$$a_{m+n} P^{m+n}(\mu) + a_{m+n-2} P_{m+n-2}(\mu) + \dots$$

with appropriate values of the constant coefficients, the key integral is

$$\frac{1}{2} \int_{-1}^{+1} P_n(\mu) \frac{d\mu}{\nu-\mu}.$$

Now this integral has been shown by Neumann† to be equal to  $Q_n(\nu)$ , when  $n$  is a positive integer, provided that

\* Communicated by the Author.

† See Whittaker and Watson, 'Modern Analysis,' p. 320 (1927).

$\nu$  is not a real number between  $-1$  and  $+1$ . In view of the recurrence relations possessed by the Legendre functions, an argument based on induction offered an elementary and yet elegant method of evaluation of the integral first required, since such a relation is in all cases involved when induction is used. It was found that by this method the evaluation of a wide class of integrals could readily be effected, and further, that the line of argument could be admirably demonstrated by evaluating the key integral. For this reason a proof of Neumann's result is first given.

On the basis of this result are quickly established the formulæ

$$\left. \begin{aligned} \frac{1}{2} \int_{-1}^{+1} P_n(\mu) P_m(\mu) \frac{d\mu}{\nu - \mu} &= P_n(\nu) Q_m(\nu), & n \leq m; \\ \frac{1}{2} \int_{-1}^{+1} P_n'(\mu) P_m(\mu) \frac{d\mu}{\nu - \mu} \\ &= P_n'(\nu) Q_m(\nu), & n \leq m+1 \\ &= Q_n'(\nu) P_m(\nu) + \frac{1}{2} \left( \frac{1}{\nu-1} - \frac{(-1)^{n-m}}{\nu+1} \right), & n \geq m+1 \end{aligned} \right\};$$

$$\frac{1}{2} \int_{-1}^{+1} (\mu^2 - 1) P_n'(\mu) P_m'(\mu) \frac{d\mu}{\nu - \mu} = (\nu^2 - 1) P_n'(\nu) Q_m'(\nu), \quad n \leq m.$$

It should be remarked that it proves necessary only to exclude real values of  $\nu$  between  $-1$  and  $+1$  and not (as in the application for which the original integral was first required) to make  $\nu$  a real number such that  $\nu^2$  is greater than  $1$ . By the adoption of a cross-cut in the  $\nu$ -plane from  $-1$  to  $+1$ ,  $Q_m(\nu)$  becomes a one-valued function of  $\nu$ .

§ 1. Let

$$\alpha_n(\nu) = \frac{1}{2} \int_{-1}^{+1} P_n(\mu) \frac{d\mu}{\nu - \mu},$$

$$a_n(\nu) = \frac{1}{2} \int_{-1}^{+1} \mu P_n(\mu) \frac{d\mu}{\nu - \mu}.$$

Since the Legendre function  $P_n(z)$  (as also the associated function  $Q_n(z)$ ) satisfies the recurrence relation

$$(n+1)\chi_{n+1}(z) - (2n+1)z\chi_n(z) + n\chi_{n-1}(z) = 0, \quad (1)$$

it follows that

$$(n+1)\alpha_{n+1}(z) - (2n+1)a_n(z) + n\alpha_{n-1}(z) = 0.$$

But so long as  $n$  is not zero,

$$\int_{-1}^{+1} P_n(\mu) d\mu = 0,$$

and therefore  $\alpha_n(\nu) = \nu \alpha_n(\nu)$ . Hence, not only the two Legendre functions but also the function  $\alpha_n(z)$  satisfies the recurrence relation.

Consider, now, the values of  $\alpha_0(\nu)$  and  $\alpha_1(\nu)$ . We have

$$\alpha_0(\nu) = \frac{1}{2} \int_{-1}^{+1} \frac{d\mu}{\nu - \mu} = \frac{1}{2} \log \frac{\nu + 1}{\nu - 1} = Q_0(\nu),$$

$$\alpha_1(\nu) = \frac{1}{2} \int_{-1}^{+1} \mu \frac{d\mu}{\nu - \mu} = \nu Q_0(\nu) - 1 = Q_1(\nu),$$

and since the  $\nu$ -plane is cut from  $-1$  to  $+1$ ,  $Q_0(\nu)$  and  $Q_1(\nu)$  are one-valued functions of  $\nu$ . Thus  $\alpha_n(\nu)$  is a function which is equal to the Legendre function  $Q_n(\nu)$  when  $n=0$  and when  $n=1$ , and shares with this function a recurrence relation of the second order. It follows that when  $n$  is an integer

$$\alpha_n(\nu) = Q_n(\nu), \quad . \quad . \quad . \quad . \quad . \quad (2)$$

and that

$$a_n(\nu) = \nu Q_n(\nu) \quad . \quad . \quad . \quad . \quad . \quad (3)$$

except in the case when  $n$  is zero, when  $a_n(\nu) = Q_1(\nu)$ .

§ 2. The next integrals to be discussed are

$$\beta_{n,m} = \frac{1}{2} \int_{-1}^{+1} P_n(\mu) P_m(\mu) \frac{d\mu}{\nu - \mu},$$

$$b_{n,m} = \frac{1}{2} \int_{-1}^{+1} \mu P_n(\mu) P_m(\mu) \frac{d\mu}{\nu - \mu}.$$

We have at once

$$\left. \begin{aligned} \nu \beta_{n,m}(\nu) - b_{n,m}(\nu) &= \frac{1}{2} \int_{-1}^{+1} P_n(\mu) P_m(\mu) d\mu = \frac{1}{2m+1}, & n=m \\ &= 0, & n \neq m \end{aligned} \right\} \quad . \quad . \quad . \quad (4)$$

The application of the recurrence relation (1) to the function  $P_n(\mu)$  in the integrand of  $\beta_{n,m}(\nu)$  yields now the result that  $\beta_{n,m}(z)$  qua function of  $n$ , also shares this recurrence relation for all values of  $n$ , with the one exception that when  $n=m$  the relation becomes

$$(m+1)\beta_{m+1,m}(z) - (2m+1)z\beta_{m,m}(z) + m\beta_{m-1,m}(z) = -1. \quad (5)$$

But

$$\beta_{0,m}(\nu) = \alpha_m(\nu) = Q_m(\nu) = P_0(\nu)Q_m(\nu),$$

$$\beta_{1,m}(\nu) = \alpha_m(\nu) = \nu Q_m(\nu) = P_1(\nu)Q_m(\nu).$$

The inductive argument establishes the result

$$\beta_{n,m}(\nu) = P_n(\nu)Q_m(\nu), \quad n \leq m, \quad . \quad . \quad (6)$$

and from (4) we deduce

$$\left. \begin{aligned} b_{n,m}(\nu) &= \nu P_n(\nu)Q_m(\nu), & n < m \\ b_{m,m}(\nu) &= \nu P_m(\nu)Q_m(\nu) - 1/(2m+1) \end{aligned} \right\} \quad . \quad (7)$$

Since any polynomial of degree  $n$  can be expressed in the form

$$a_0P_0 + a_1P_1 + \dots + a_nP_n,$$

we have as an immediate corollary to (6) the theorem :

*If  $\phi(z)$  is any polynomial of degree not greater than  $m$ , then*

$$\frac{1}{2} \int_{-1}^{+1} \phi(\mu) P_m(\mu) \frac{d\mu}{\nu - \mu} = \phi(\nu) Q_m(\nu).$$

§ 3. Since  $\beta_{n,m}(\nu)$  and  $b_{n,m}(\nu)$  are functions symmetric in the two parameters  $m$  and  $n$ , it is not necessary to attempt an independent evaluation when  $n$  is greater than  $m$ . However, for the sake of studying this type of argument, it is worth while to exhibit the fashion in which the interchange of the  $P$  and  $Q$  functions is accomplished.

Since for  $n > m$  as for  $n < m$  the function  $\beta_{n,m}(z)$  satisfies the recurrence relation (1), the equality

$$\beta_{n,m}(\nu) = Q_n(\nu)P_m(\nu), \quad n > m \quad . \quad (8)$$

at once follows if it is true for  $n=m$  and for  $n=m+1$ . Now when  $n=m$  the recurrence relation established for  $\beta_{n,m}(\nu)$  takes the special form (5), and the values of  $\beta_{n,m}(\nu)$  for  $n=m-1$  and  $n=m$  already found yield the consequence that

$$\beta_{m+1,m}(\nu) = P_{m+1}(\nu)Q_m(\nu) - 1/(m+1).$$

But, as is well known,

$$P_{m+1}(\nu)Q_m(\nu) - Q_{m+1}(\nu)P_m(\nu) = 1/(m+1).$$

Hence the result (8), established for  $n=m$  as a case of (6), is now established for  $n=m+1$  and so for all larger values of  $n$ .

For the function  $b_{n,m}(\nu)$  the corresponding result

$$b_{n,m}(\nu) = \nu Q_n(\nu) P_m(\nu), \quad n > m, \quad (9)$$

can now be based on (4) instead of being inferred by symmetry from (7).

§ 4. We consider next the integrals

$$\gamma_{n,m}(\nu) = \int_{-1}^{+1} P_n'(\mu) P_m(\mu) \frac{d\mu}{\nu - \mu},$$

$$c_{n,m}(\nu) = \int_{-1}^{+1} \mu P_n'(\mu) P_m(\mu) \frac{d\mu}{\nu - \mu}.$$

The derivative  $P_n'(z)$  being a polynomial of degree  $n-1$ , these integrals come, the former for  $n \leq m+1$  and the latter for  $n \leq m$ , within the theorem at the close of § 2, and we have

$$\gamma_{n,m}(\nu) = P_n'(\nu) Q_m(\nu), \quad n \leq m+1, \quad (10)$$

$$c_{n,m}(\nu) = \nu P_n'(\nu) Q_m(\nu), \quad n \leq m. \quad (11)$$

To evaluate the first integral when  $n$  takes larger values, we use the relation

$$\chi'_{n+1}(z) - \chi'_{n-1}(z) = (2n+1)\chi_n(z),$$

which is true for  $P_n(z)$  and  $Q_n(z)$ . Because this relation is true for  $P_n(z)$ ,

$$\begin{aligned} \gamma_{n+1,m}(\nu) - \gamma_{n-1,m}(\nu) &= (2n+1)\beta_{n,m}(\nu) \\ &= (2n+1)Q_n(\nu)P_m(\nu), \quad n \geq m, \end{aligned}$$

and because the same relation is true for  $Q_n(z)$ ,

$$(2n+1)Q_n(\nu)P_m(\nu) = Q'_{n+1}(\nu)P_m(\nu) - Q'_{n-1}(\nu)P_m(\nu).$$

Thus for  $n \geq m$ ,

$$\gamma_{n+1,m}(\nu) - Q'_{n+1}(\nu)P_m(\nu) = \gamma_{n-1,m}(\nu) - Q'_{n-1}(\nu)P_m(\nu),$$

and therefore, for  $n=m+2, m+4, m+6, \dots$ ,

$$\begin{aligned} \gamma_{n,m}(\nu) - Q_n'(\nu)P_m(\nu) &= \gamma_{m,m}(\nu) - Q_m'(\nu)P_m(\nu) \\ &= P_m'(\nu)Q_m(\nu) - Q_m'(\nu)P_m(\nu) \\ &= 1/(\nu^2-1), \end{aligned}$$

and for  $n=m+3, m+5, m+7, \dots$ ,

$$\begin{aligned} \gamma_{n,m}(\nu) - Q_n'(\nu)P_m(\nu) &= \gamma_{m+1,m}(\nu) - Q_{m+1}'(\nu)P_m(\nu) \\ &= P_{m+1}'(\nu)Q_m(\nu) - Q_{m+1}'(\nu)P_m(\nu) \\ &= \nu/(\nu^2-1). \end{aligned}$$

That is, for  $n > m$ ,

$$\left. \begin{aligned} \gamma_{n,m}(\nu) &= Q_n'(\nu)P_m(\nu) + 1/(\nu^2-1), & n-m \text{ even} \\ &= Q_n'(\nu)P_m(\nu) + \nu/(\nu^2-1), & n-m \text{ odd} \end{aligned} \right\}, \quad (12)$$

and the results for  $\gamma_{n,m}(\nu)$  may be stated as follows:

$$\left. \begin{aligned} \gamma_{n,m}(\nu) &= P_n'(\nu)Q_m(\nu), & n \leq m+1 \\ &= Q_n'(\nu)P_m(\nu) + \frac{1}{2} \left( \frac{1}{\nu-1} - \frac{(-1)^{n-m}}{\nu+1} \right), & n \geq m+1 \end{aligned} \right\}. \quad (13)$$

To complete the evaluation of  $c_{n,m}(\nu)$ , we notice that for  $n > m$

$$\left. \begin{aligned} \nu\gamma_{n,m}(\nu) - c_{n,m}(\nu) &= \frac{1}{2} \int_{-1}^{+1} P_n'(\mu)P_m(\mu) d\mu = 0, & n-m \text{ even} \\ &= 1, & n-m \text{ odd} \end{aligned} \right\},$$

whence

$$\left. \begin{aligned} c_{n,m}(\nu) &= \nu Q_n'(\nu)P_m(\nu) + \nu/(\nu^2-1), & n-m \text{ even} \\ &= \nu Q_n'(\nu)P_m(\nu) + 1/(\nu^2-1), & n-m \text{ odd} \end{aligned} \right\}, \quad (14)$$

and the results corresponding to (13) run

$$\left. \begin{aligned} c_{n,m}(\nu) &= \nu P_n'(\nu)Q_m(\nu), & n \leq m \\ &= \nu Q_n'(\nu)P_m(\nu) + \frac{1}{2} \left( \frac{1}{\nu-1} + \frac{(-1)^{n-m}}{\nu+1} \right), & n \geq m \end{aligned} \right\}. \quad (15)$$

### § 5. The evaluation of the original integral

$$\delta_{n,m}(\nu) = \frac{1}{2} \int_{-1}^{+1} (\mu^2-1)P_n'(\mu)P_m'(\mu) \frac{d\mu}{\nu-\mu}$$

may now be completed. Both  $P_m(z)$  and  $Q_m(z)$  satisfy the relation

$$(z^2-1)\chi_m'(z) = mz\chi_m(z) - m\chi_{m-1}(z).$$

Hence

$$\delta_{n,m}(\nu) = m \{ c_{n,m}(\nu) - \gamma_{n,m-1}(\nu) \}, \quad (16)$$

and for  $n \leq m$ ,

$$\begin{aligned} \delta_{n,m}(\nu) &= mP_n'(\nu) \{ \nu Q_m(\nu) - Q_{m-1}(\nu) \} \\ &= (\nu^2-1)P_n'(\nu)Q_m'(\nu). \end{aligned} \quad (17)$$

By symmetry we have for  $n \geq m$ ,

$$\delta_{n,m}(\nu) = (\nu^2-1)Q_n'(\nu)P_m'(\nu); \quad (18)$$

it is not necessary to discuss this case, but a glance will verify that the result is deducible alternatively by the application of (12) and (14) to (16).

Finally, it may be recorded that, since

$$\frac{1}{2} \int_{-1}^{+1} (\mu^2 - 1) P_n'(\mu) P_m'(\mu) \frac{d\mu}{\nu + \mu} = (-)^{m+n} \delta_{n,m}(\nu),$$

we have, if  $n \leq m$ ,

$$\frac{1}{2} \int_{-1}^{+1} \mu \frac{\mu^2 - 1}{\nu^2 - \mu^2} P_n'(\mu) P_m'(\mu) d\mu = (\nu^2 - 1) P_n'(\nu) Q_m'(\nu), \quad (19)$$

$m + n$  odd,

$$\frac{1}{2} \int_{-1}^{+1} \nu \frac{\mu^2 - 1}{\nu^2 - \mu^2} P_n'(\mu) P_m'(\mu) d\mu = (\nu^2 - 1) P_n'(\nu) Q_m'(\nu), \quad (20)$$

$m + n$  even,

whereas the former of these integrals is zero if  $m + n$  is even, as was remarked at the outset, and the latter is zero if  $m + n$  is odd.

XCV. *On the Elastic Extension of Metal Wires under Longitudinal Stress.*—Part I. *A New Method for Measuring the Deviation from Hooke's Law.* By L. C. TYTE, B.Sc., A.Inst.P., Research Student, East London College\*.

### *Introduction.*

THE object of the experiments was to examine the departure from Hooke's law when a wire was subjected to longitudinal stress, a method being devised by Professor Lees by which the deviation was obtained directly.

The principle of the method was to determine the difference between the extensions of two wires, of the same cross-sectional area and of the same material, one double the length of the other, the stretching force on the shorter being double that on the longer. If Hooke's law were strictly true both wires would extend by equal amounts, but any deviation from the law would cause one wire to extend more than the other, the excess being measured by the tilt of an optical lever.

### *Description of Apparatus.*

A diagram of the apparatus is shown in fig. 1. A steel bar A was screwed on to a stout wooden beam supported

\* Communicated by Prof. C. H. Lees, F.R.S.



between two iron girders. The bar was fitted at either end with steel lugs B, brazed on to the opposite edges of the bar in such a manner that the horizontal planes passing through their upper surfaces were one metre apart. Holes were drilled in these lugs to accommodate the metal chucks C (fig. 2). These chucks had a fine hole drilled along the axis

Fig. 1.

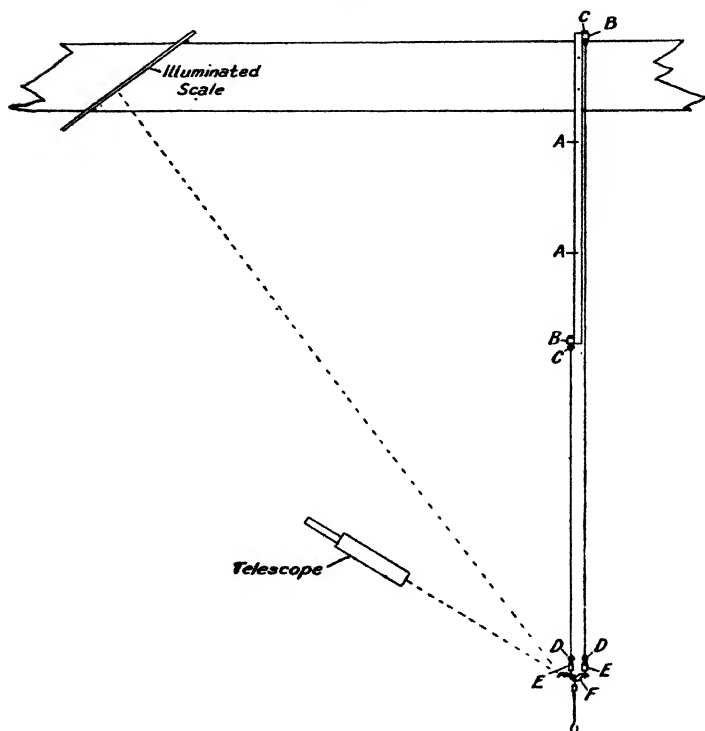


Diagram of Apparatus.

to accommodate the experimental wire, and one end was tapered, threaded, split with an axial saw-cut, and provided with a screw nut, thus gripping the wire, the other end being fitted with a nut to stop the chuck slipping through the hole in the lug. The lower ends of the wires supported chucks D (fig. 3), one end of which gripped the wire, and the other was fitted with a simple thread, on which the stirrup-shaped pieces E (shown in fig. 4) could be screwed.

Fig. 2.

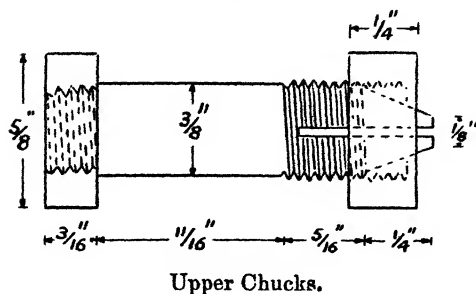


Fig. 3.

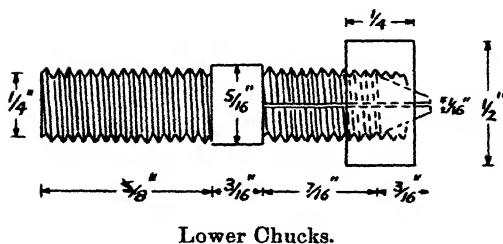
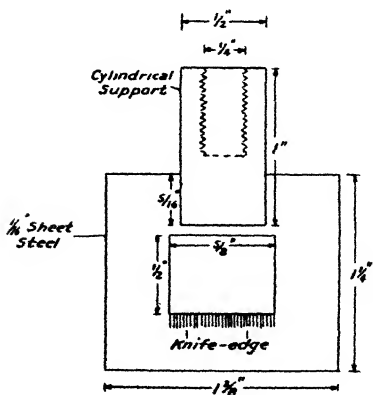


Fig. 4.



The aluminium ones were somewhat smaller and had a steel knife-edge set in the lower inner edge.

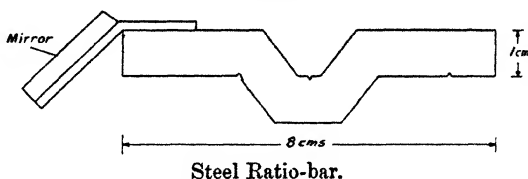
The lower inner edges of these stirrups formed knife-edges, on which rested a cranked bar F (fig. 5). This bar was provided with three V-shaped notches—one, in the centre of the bar, on the upper surface of the cranked portion, two on the lower surface of the bar, on opposite sides of the centre, and 1.5 cm. and 3.0 cm. respectively from it.

The knife-edges attached to the wires rested in the two outer notches, while a third stirrup-shaped piece fitted into the centre notch and supported the load.

Two ratio-bars and two sets of stirrups were used, a steel ratio-bar and stirrups for wires of high tensile strength, and an aluminium set for materials of small tensile strength. Two sets of chucks were also used, one set made of steel for the steel wires, and one of brass for the other materials.

The wires used were 1 and 2 metres long respectively, with their lower ends at the same level. At the commencement of an experiment, with sufficient load on the wires to

Fig. 5.



The aluminium one was exactly similar, but only 0.6 cm. square instead of 1 cm.

keep them taut, the ratio-bar was horizontal, any slight tilt being removed by screwing one of the knife-edges up or down. The ratio-bar ensures that any load put on it is divided in the ratio of 2 : 1 between the shorter and longer wires. Any inequality in the extensions will result in a tilt of the ratio-bar, measured by a beam of light reflected from a small mirror attached to the end of the ratio-bar on the side of the shorter wire. Light from a fixed illuminated scale about 240 cm. away from the mirror, and perpendicular to the line joining its zero-point to the mirror, is reflected from the mirror into an observing telescope.

It was found that the system swung too much for observations to be taken unless the motion was restricted by passing the cylindrical portions of the stirrups through two holes bored in a sheet of aluminium, which was placed so that the centres of the holes were accurately under the upper



2. *Error of Ratio in the Ratio-bar.*—Assume that the ratio of the lengths of the wires and of the arms of the ratio-bar should be in the ratio  $a : 1$ , but that an error in the latter case makes the ratio  $a(1+\delta) : 1$ . Hence, if  $L$  and  $b$  are the lengths of the shorter wire and ratio-arm respectively, a load  $M$  on the ratio-bar is divided into forces

$$a(1+\delta)M/[1+a(1+\delta)] \quad \text{and} \quad M/[1+a(1+\delta)],$$

causing extensions

$$e_1 = La(1+\delta)M/E_1A[1+a(1+\delta)]$$

and

$$e_2 = LaM/E_2A[1+a(1+\delta)]$$

of the shorter and longer wires respectively, where  $E_1$  and  $E_2$  are the values of Young's Modulus corresponding to the stress conditions, and  $A$  the cross-sectional area of the wires. Therefore

$$e_1/e_2 = [(1+\delta)E_2]/E_1,$$

and the difference of extensions caused by the error in the ratio-bar is

$$e_1 - e_2 = [\{(1+\delta)E_2\}/E_1 - 1]e_2.$$

Hence

$$\tan \phi_{\text{Expt.}} = [\{(1+\delta)E_2\}/E_1 - 1]e_2/b[1+a(1+\delta)], \quad (2)$$

and

$$\tan \phi_{\text{Theory}} = [E_2/E_1 - 1]e_2/b[1+a]; \quad \dots \quad (3)$$

$$\therefore \tan (\phi_{\text{Expt.}} - \phi_{\text{Theory}}) =$$

$$\frac{\frac{[\{(1+\delta)E_2\}/E_1 - 1]e_2}{b[1+a(1+\delta)]} - \frac{[E_2/E_1 - 1]e_2}{b[1+a]}}{1 + \frac{[\{(1+\delta)E_2\}/E_1 - 1][E_2/E_1 - 1]e_2^2}{b^2[1+a(1+\delta)][1+a]}}$$

which, neglecting the  $e_2^2$  term, reduces to

$$e_2\delta[E_2/E_1 + a]/b(1+a)[1+a(1+\delta)];$$

further, assuming Hooke's law to hold for consideration of this error,

$$\tan (\phi_{\text{Expt.}} - \phi_{\text{Theory}}) = e_2\delta/b[1+a(1+\delta)], \quad \dots \quad (4)$$

and the actual error of excess extension causing it is  $e_2\delta$  which is proportional to the load.

From the table,  $\delta_{\text{Steel}} = -0.0025$  and  $\delta_{\text{Aluminium}} = +0.00035$ , which means errors of  $-0.25$  per cent. and  $+0.35$  per cent. respectively {considering errors which increase the excess

extension of the shorter wire over the longer to be positive} of the Hooke's law extensions of the wires. Hence from equation (2) it is seen that for  $\delta$  negative the value of  $\tan \phi_{\text{Expt.}}$  starts by being negative, increases to a maximum value, then falls to zero and becomes positive, the maximum and zero values depending on the rate of increase of  $E_2/E_1$  and  $\delta$ .

The percentage error of the error with respect to the excess extension is given by

$$[\delta / \{(1 + \delta)E_2\} / E_1 - 1] \times 100 \text{ per cent.}$$

This, in the case of the steel bar, starts as being negative, and rapidly increases until the denominator is zero, when it changes sign and is a large positive quantity, which rapidly decreases. From the results it appears that this change of sign of the error occurs for very small stresses. In the other case, with  $\delta$  positive, it steadily decreases throughout.

3. *Error due to Knife-edges not being in the same Plane.*—Suppose that the three knife-edges are not in the same plane, but that the centre one is lower than the other two, thus forming the corners of a triangle ABC. Drop a perpendicular from C to AB at D, and call the distances AD, DB, and CD,  $b$ ,  $2b$ , and  $x$  respectively. When the ratio-bar is in its normal untilted position, the ratio of the arms is  $2b : b$ , but if it is deflected through a small angle  $\theta$  the ratio becomes

$$2b - x \tan \theta : b + x \tan \theta,$$

or

$$2\{1 - \frac{x}{2b} \tan \theta\} / \{1 + \frac{x}{b} \tan \theta\} : 1,$$

which can be written

$$2\{1 - \frac{x}{2b} \tan \theta\} \{1 - \frac{x}{b} \tan \theta\} : 1$$

as a first approximation, reducing to

$$2\{1 - \frac{3x}{2b} \tan \theta\} : 1.$$

For the steel ratio-bar  $x = 0.10$  cm., and for the aluminium bar  $x = 0.62$  cm.;  $b$  can be assumed to equal 1.5 cm. for both cases. Hence the ratio for the steel bar is

$$2\{1 - 0.1 \tan \theta\} : 1,$$

and for the aluminium one

$$2\{1 - 0.6 \tan \theta\} : 1.$$

When the ratio-bar is tilted, owing to the excess extension of the shorter wire the ratio of the lengths of the arms is changed, and consequently the shorter wire receives a greater load, which increases the total extension of the wire.  $\theta$  is a function of the load, and for the largest loads considered only amounts to  $1^\circ$ . Thus for the extreme cases the values of the ratio only become

1.9965 : 1 for steel, and

1.9790 : 1 for aluminium.

4. *Error in the Ratio of the Lengths of the Wires.*—Assuming Hooke's law for the consideration of this error, the error of the excess extension is proportional to the load, being positive if the shorter wire is more than half the longer and negative if less. Such an error would be small, for an error of 0.1 cm. in the length of the shorter wire makes a difference of 1 in 2000 in the ratio, and the error is more probably only a tenth of this. Further, there is no reason to believe that the error would always be in the same direction, and in the mean value it would largely cancel itself out.

5. *Error caused by Variation of the Distance from the Mirror to the Scale due to Extension of the Wires.*—When the wires extend they carry the mirror with them and increase the distance between the mirror and the illuminated scale. The actual excess extension of the wire  $\epsilon$  and the observed scale deflexion  $D$  are connected by the relation

$$D = 2\lambda\epsilon/d;$$

thus an increase in the value of  $\lambda$  makes the observed deflexion larger than it should be.  $\lambda$  is approximately 242 cm., and the greatest value of the total extension is 0.7 cm., being usually less than a tenth of this, and since the illuminated scale is inclined at an angle of  $35^\circ$  to the horizontal, the actual increase in  $\lambda$  is  $0.7 \cos 35^\circ$  or 0.57 cm. Therefore the error would be

$$\{0.57 \times 100/242\} \text{ per cent.} = \frac{1}{4} \text{ per cent. approx.}$$

This is not an error affecting the total extension of the wire, but merely an error of observation in the determination of the actual excess extension.

6. *Error in the Assumption that  $\tan \phi \equiv \phi$  and  $\tan 2\phi \equiv 2\phi$ .*—The important assumption is that  $\tan 2\phi \equiv 2\phi$ , for this includes the other. Now

$$\tan 2\phi = D/\lambda;$$

the largest deflexion observed was  $D = 5$  cm., and  $\lambda = 242$  cm. Thus

$$\tan 2\phi = 5/242 = 0.0207,$$

and

$$2\phi = 1^\circ 11'.$$

The value of  $1^\circ 11'$  in radians is 0.0207; and hence the assumption is perfectly justified within the limits of the experiments.

7. *Error due to the Initial Loads on the Wires not being in the Correct Ratio.*—If the initial loads, caused by the chucks and ratio-bar, on the two wires are not in the correct ratio, an error is introduced. In the case of the steel ratio-bar and accessories (with one exception) the load on the shorter wire was 152.6 gm., and that on the longer wire 68.7 gm. Thus there was a load of approximately 15 gm. too much on the shorter wire; but as the initial load in these cases was 1 kilogramme, this was only a very small error. For the aluminium ratio-bar and accessories the ratio between the loads was made exact by attaching a small piece of lead to the stirrup piece attached to the longer wire.

8. *Error due to Expansion of the Wires caused by Variations of the Room-temperature.*—The usual difficulties caused by the expansion of the experimental wire are eliminated by the use of two wires, but a new source of error is introduced when the material under examination has a coefficient of expansion different from that of the steel supporting bar. Then temperature fluctuations will cause differential expansion between the metre of steel supporting bar and one metre of the test wire. The values of these errors are only quite small, being negligible for steel, iron, and nickel, approximately  $6 \times 10^{-4}$  cm. per degree C. for copper and brass, and approximately  $14 \times 10^{-4}$  cm. per degree C. for aluminium, zinc, tin, and lead.

The experiments were performed in a basement laboratory, the temperature variations of which were small, the complete fluctuation for a day being usually less than a degree. Further, the change would sometimes be an increase and sometimes a decrease in temperature, and this source of error would tend to cancel out in the mean value.

### *Discussion of Method.*

This new method can claim many advantages, among which are the simplicity of design and manipulation, being quite free from mechanical devices introducing undesirable frictional forces.



To investigate deviations from Hooke's law for wires by the ordinary extension method specimens of 10 to 20 metres length are required; hence the present apparatus possesses the advantage of compactness and convenience for use in the ordinary laboratory, and requires much less material, which means greater uniformity over the specimen. Further, the sensitiveness, which in the present apparatus is 1 part in  $10^6$  in the excess extension, can be pushed to almost any limit by decreasing the length of the lever arm, *i.e.*, the distance between the wires, and increasing the optical path between the mirror and scale, thus surpassing as an instrument of precision the interference method due to Grüneisen. The chief disadvantage is that the actual extension of the specimens is not known, but it is hoped to construct a new extensometer capable of giving simultaneous observations of the extension and excess extension.

### *Conclusion.*

The instrument has been found to behave perfectly satisfactorily in use, and observations have been made on a large number of metals. The results of these investigations are to be published in a subsequent paper.

**XCVI.** *The Comparison of Molecular Ionizing Potentials in an Alternating Electric Wind.* By W. M. THORNTON. D.Sc., D.Eng., Armstrong College, Newcastle-on-Tyne\*.

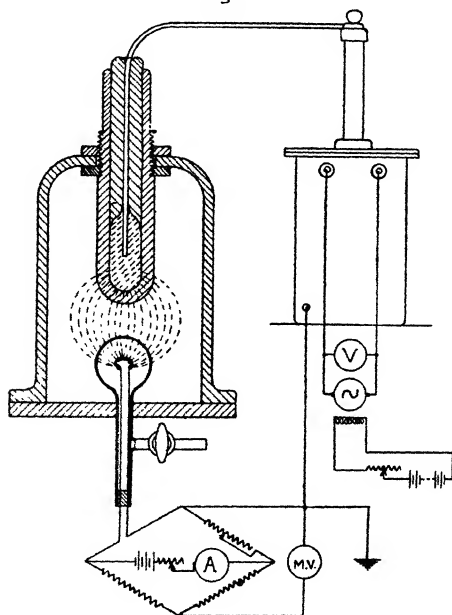
### 1. INTRODUCTION.

**T**HE intensity of the electric wind from a pole of a strong alternating field is proportional both to the velocity of molecular ions and to their number. When one pole is earthed there is still a wind to be observed from it, for the effect depends on the local gradient, not on the total voltage alone. If this earthed pole is made a hot wire the wind is much increased, and its cooling influence can be so great that a red-hot wire is reduced by it to blackness. This cooling is a linear function of the field over a wide range, and since the velocity of ions in gases at atmospheric pressure is proportional to the field, the number of ions is also proportional to it. By enclosing the hot wire in an insulating vessel, fig. 1, containing a gas at pressures from

\* Communicated by the Author.

10 cm. of mercury to atmospheric pressure, and insulating the high tension electrode, the other end of the secondary winding being earthed, the arrangement provides a new means of observing the behaviour of a gas in a strong electric field with only one electrode in the gas. This has certain advantages. High voltages can be used without risk of shock or electrical breakdown, and the wire being at earth potential can be made part of a bridge by which its change of resistance may be continuously observed.

Fig. 1.



The galvanometer deflexion of a bridge of which the hot wire is one arm is at the start proportional to the field, so that the steepest tangent drawn to the curves connecting deflexion and applied field voltage is a measure of the molecular ionization produced. For a given apparatus the product of maximum slope of curve and ionizing potential should therefore be approximately constant. This is shown below to be the case by the behaviour of the monatomic gases helium, neon, and argon. The slope of the observed curve for argon in a particular apparatus was 0.0133 bridge volts per volt of field, its ionizing potential is

11.5. The product of these is 0.153. Dividing this number by the slope of the curve for any other gas in the same apparatus gives a measure of its molecular ionizing potential, which should be inversely proportional to the tangent to the curve, and the following ionizing potentials of gases were found in this way. It is given as a new and convenient method of comparing ionization by which no current is passed *through* the gas, the ions being forced to move to and fro as the field reverses, the alternating molecular movement cooling the hot wire which forms the earthed pole.

## 2. MONATOMIC GASES.

The gases helium, neon, and argon have first ionizing potentials of 25.4, 21.5, and 11.5 volts respectively. These are sufficiently distinct to provide a test of the nature of the wind and of the validity of the method by finding whether the cooling of the wire in the three gases under the influence of an electric field is inversely proportional to these potentials. The tube enclosing the gas and the wire was placed near to an insulated high tension electrode, the other pole being the wire itself. The voltages given as abscissæ are those applied between the two electrodes, the hot wire being earthed. A simple bridge method was used, the initial current in the hot-wire circuit being constant at 0.4 ampere throughout. The gases were transferred by mercury displacement from the bulbs in which they were supplied by the British Oxygen Co., but not further dried, direct to the test vessel at a pressure of 10 centimetres of mercury.

*Argon* (I. P. 11.5 volts).

(Argon 99 per cent., nitrogen 0.7 per cent., oxygen 0.3 per cent.)

On the application of the field there was in the apparatus used no cooling of the wire until a voltage of 24 kV. had been reached. The slope of the curve, fig. 2, is 0.01328 bridge volts per volt. The product of slope and ionizing potential is 0.1530.

*Neon* (I. P. 21.5 volts).

(Neon 98 per cent., helium 2 per cent.)

Cooling started at 30 kV. Slope of curve 0.0080. The ionizing potential derived from the slope is 19.2.

*Helium* (I. P. 25.4 volts).

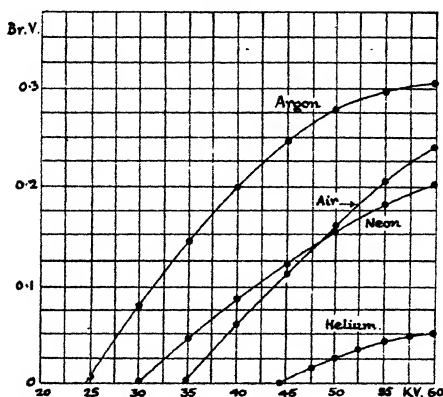
(Helium 98 per cent., neon 2 per cent.)

Starting voltage 45 kV. Slope of curve .0057. Derived ionizing potential 26.8.

From these we have :

	Ionizing Potential, P.	Slope of Curve, S.	P. $\times$ S.
Argon .....	11.5	0.01328	0.1530
Neon .....	21.5	0.0080	0.1720
Helium .....	25.4	0.0057	0.1445
			Mean .. 0.1565

Fig. 2.



Argon was taken as the standard gas for comparison in the tests on other gases.

The cooling effect of the wind therefore follows the same sequence as the reciprocals of the ionizing potentials. There is greater cooling in argon in a given field because of its lower ionizing potential. Having regard to the early state of the knowledge of the effect and to its possible dependence on the chemical purity of the gases, the above agreement may be considered satisfactory. It is only by extended trials that the degree of precision possible can be found, but the results given below show that the effect is regular and consistent. The behaviour of mixtures of gases will be given in a later paper.

## 3. DIATOMIC GASES.

*Hydrogen.*

Working at the same current 0.4 ampere in the wire the normal cooling was so great that that due to the field was not perceptible up to 50 kV. The temperature was therefore raised and the out-of-balance volts measured, while the field was maintained constant at 50 kilovolts. The results are given in Table I.

There is a rapid rise in the rate of cooling of the wire by the field as the temperature approaches redness. It reaches a sharp maximum at 1.0 ampere, after which corona begins and the maximum of cooling falls. The

TABLE I.

Hydrogen at 10 cm. Hg pressure.

Current in wire. Amperes.	Out-of-balance volts due to constant field.
0.5	0.00
0.6	0.006
0.7	0.02
0.8	0.04
0.9	0.07
1.0	0.074
1.03	0.055 unsteady.

surface conditions are in any case completely modified by corona when it occurs.

The curves of fig. 3 have all nearly the same initial slope of 0.00364 bridge volts per volt applied. The ionizing potential of molecular hydrogen is not a fixed quantity, but taking for comparison the products of the slope and ionizing potential for argon

$$(M. I. P.) \times 0.0036 = 11.5 \times 0.0133,$$

the value obtained for hydrogen = 42.4.

*Oxygen.*

The observed slope of the curve given in fig. 4 for oxygen was 0.0220, which corresponds to  $0.153/0.0220 = 6.9$  volts for the molecular ionizing potential, the atomic potential being 13.56, or double the molecular value.



*Nitrogen.*

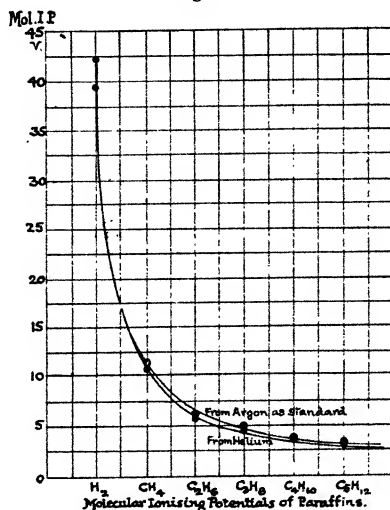
Observed slope 0.0133, corresponding to  $0.153/0.0133 = 11.5$ , the atomic potential being 14.49.

*Air.*

Observed slope 0.0133, molecular potential 11.50. Air was identical with nitrogen and argon in the cooling effect of the wind on a hot wire. It is remarkable that these three gases in air should have the same molecular ionizing potentials.

In hydrogen it will be noted that the M. I. potential as

Fig. 5.



interpreted here is much higher than the atomic. In oxygen and nitrogen it is less.

## 4. THE PARAFFIN SERIES.

The paraffin series of polyatomic gases is of special interest in engineering, methane being the most important factor in coal mining, and the higher members in internal combustion engines. It is the only regular series of gases available in convenient form. The methane was nearly pure, but contained a trace of nitrogen. Ethane was prepared from ethyl iodide by the zinc-copper couple, and passed through alcohol and strong sulphuric acid. Pro-

pane and butane were obtained from the Shell-Mex laboratories by the kindness of Mr. Kewley. Pentane was prepared from pure Karlbaum liquid. The molecular ionizing potentials were calculated in each case by dividing the product 0.153 of the slope and potential for argon by the observed slope of cooling of the wire in the gas under the action of the field.

The results gave for the ionizing potentials: methane 11.3 volts, ethane 6.32, propane 5, butane 3.77, pentane 3.49. These are shown in fig. 5 to form a regular curve with the number of methyl radicles or of carbon atoms as abscissæ. Its equation can be made to include hydrogen by writing it

$$(m-a)(n+b)=c,$$

where  $a=0.44$ ,  $b=0.326$ ,  $c=14.4$ ,  $m$  is the M. I. P., and  $n$  the number of carbon atoms.

The observed and calculated values are given below.

TABLE II.

	$n$ .	$m$ .	
		Obs.	Cal.
Hydrogen .....	0	42.4	43.8
Methane .....	1	11.3	11.29
Ethane .....	2	6.32	6.70
Propane .....	3	5.0	4.91
Butane .....	4	3.77	3.77
Pentane .....	5	3.49	3.14

The regularity of these figures supports the use of the method as an indicator of the behaviour of gases under electrification.

The results in Table II. are of interest in connexion with the suggestion that the ignition of gases and the propagation of flame might depend on ionization from the wave front or source. Ignition by unidirectional break-sparks \* of mixtures of the paraffins of maximum inflammability requires the same igniting current for each gas in the series. In the case of alternating currents † tested by the same method it actually becomes *more difficult* to ignite the higher paraffins by break-sparks of this kind, although the heat of combustion of the gas is so much greater. But the

\* "The Electrical Ignition of Gases," Proc. Roy. Soc. A, xc. fig. 2, p. 277 (1914).

† *Loc. cit.* fig. 12, p. 290.



present results show that ionization of the kind which might be expected in explosion—that is, molecular—takes less energy in the higher paraffins. There is no type of ignition of gases that becomes easier in the higher paraffins except that by hot wires. It is therefore improbable that molecular ionization such as is caused by collision of ions with molecules in an electric field plays any part in ignition, but that the whole effect is due to activation by radiation\*.

The special interest of fig. 5 is that each addition of a  $\text{CH}_2$  radicle lessens the energy required for ionization by collision in an electric field in a regular manner. Hydrogen itself has a high value, yet as the number of hydrogen atoms in the molecule is increased the critical ionizing potential diminishes. The presence of carbon atoms lowers the ionizing potential in close proportion to their number. The lower curve in fig. 5 is calculated from helium as a standard gas; the difference is small.

### 5. OTHER GASES.

In order to examine the relative influence of carbon and hydrogen atoms on the effect, acetylene and ethylene were tested under the same conditions as before, with the following results:—

	Slope of Curve.	M. I. Pot.
Acetylene, $\text{C}_2\text{H}_2$ ....	0.0243	6.29 volt.
Ethylene, $\text{C}_2\text{H}_4$ ....	0.0245	6.25 „
Ethane, $\text{C}_2\text{H}_6$ ....	0.0242	6.32 „

There is therefore evidence that the carbon atoms have a preponderating influence in ionization of hydrocarbons in strong fields. The influence of hydrogen would seem to be by comparison almost negligible, and it may be noted that the “atomic” ionizing potentials of ethane, acetylene, and ethylene are so nearly twice the present observed values of the molecular potentials. The ratios are 2.025, 1.96, 1.95 respectively.

The atomic ionizing potential of carbon is 11.3, not much different from atomic hydrogen (13.53), but molecular hydrogen is difficult to ionize in this manner.

Replacing three hydrogen atoms by chlorine, we have

	Slope.	M. I. P.
Chloroform, $\text{CHCl}_3$ .....	0.0200	7.65

\* *Vide*, “The Propagation of Flame in Gaseous Mixtures,” *Phil. Mag.* ix. p. 260 (Feb. 1930).

Adding an oxygen atom to butane,  $C_4H_{10}$ , whose M. I. P. is 3.77, gives

	Slope.	M. I. P.
Ethyl ether, $C_4H_{10}O$ .....	0.445	3.45

Thus, when there is hydrogen present in the molecule the addition of oxygen does not appear to have marked effect; but it is very marked when there are only carbon and oxygen present.

	Slope.	M. I. P.
Carbon dioxide, $CO_2$ .....	.0091	16.8
Carbon monoxide, $CO$ ....	.060	2.55

It is the oxygen atoms here that determine the ionic wind, and the fewer they are the greater the cooling.

In consideration of the meaning of these experimental results the energy of formation of the molecule may play some part, but does not appear to be sufficient to account for more than a small fraction of the observed differences, about 0.8 volt in the case of methane.

Nitrogen has been found to have a molecular ionizing potential of 11.5, and hydrogen about 40, yet ammonia  $NH_3$ , differs greatly from both, its M. I. P. being 4.02. A combination of nitrogen and oxygen, nitrous oxide, has the following value :—

	Slope.	M. I. P.
Nitrous oxide, $N_2O$ .....	0.0101	15.29
Ammonia, $NH_3$ .....	0.038	4.02

Thus the addition of an oxygen atom to a nitrogen molecule has scarcely any influence on the resultant molecular ionizing potential, but the addition of hydrogen to a nitrogen atom lowers it considerably.

There is clearly a regular and characteristic change in the relations of oxygen and hydrogen to carbon and nitrogen, as shown by the electric wind, which may be summarized as follows:—In compounds of carbon and hydrogen the degree of molecular ionization is apparently determined solely by the number of carbon atoms in the molecule of gas; the greater the number the more readily the gas is ionized. When hydrogen is present an added oxygen atom does not appear, in the case of ethyl ether, to have measurable influence. In compounds of carbon and oxygen it is the oxygen that determines the action, making it more difficult. In compounds of nitrogen and oxygen

1062 *Comparison of Ionizing Potentials in Electric Wind.*

or hydrogen oxygen has little influence, while hydrogen has a marked effect, in the latter case facilitating ionization. The examination of mixtures of gases by means of the electric wind, the technique of which is not difficult, might

TABLE III.

Gas.	Cooling starts at kv.	Slope of curves.	Relative slope.	Atomic ionizing potential.	Apparent molecular ionizing potential.	
						Volts.
Argon .....	24	-0133	1.0	11.5	11.5	A
Neon .....	30	-0080	0.6	21.5	19.2	N
Helium .....	45	-0057	0.429	25.4	26.8	He
Hydrogen .....	37.5	-00364	0.27	13.53	42.4	H <sub>2</sub>
Oxygen .....	22.5	-0220	1.65	13.56	6.9	O <sub>2</sub>
Nitrogen .....	19.5	-0133	1.00	14.49	11.5	N <sub>2</sub>
Air.....	19.5	-0133	1.00	—	11.5	4N <sub>2</sub> +O <sub>2</sub>
Methane .....	29.5	-0135	1.015	14.4	11.3	CH <sub>4</sub>
Ethane .....	32.5	-0242	1.82	12.8	6.32	C <sub>2</sub> H <sub>6</sub>
Propane .....	30.5	-0306	2.3	—	5.0	C <sub>3</sub> H <sub>8</sub>
Butane .....	33.4	-0406	3.05	—	3.77	C <sub>4</sub> H <sub>10</sub>
Pentane .....	39.0	-0440	3.3	—	3.49	C <sub>5</sub> H <sub>12</sub>
Acetylene .....	24.7	-0243	1.825	12.3	6.29	C <sub>2</sub> H <sub>2</sub>
Ethylene .....	31.2	-0245	1.84	12.2	6.25	C <sub>2</sub> H <sub>4</sub>
Chloroform .....	13.0	-0200	1.5	—	7.65	CHCl <sub>3</sub>
Ethyl ether ....	25.0	-0445	3.34	—	3.45	C <sub>4</sub> H <sub>10</sub> O
Carbon dioxide ..	17.5	-0091	0.685	—	16.8	CO <sub>2</sub>
Carbon monoxide .	22.1	-060	4.5	—	2.55	CO
Nitrous oxide ....	23.1	-0101	0.76	—	15.29	N <sub>2</sub> O
Ammonia .....	20.0	-038	2.85	—	4.02	NH <sub>3</sub>
Carbon disulphide .	32.5	-0133	1.0	—	11.5	CS <sub>2</sub>
Water vapour ..	17.5	-02	1.5	—	7.65	OH <sub>2</sub>

throw further light on the mechanism of ionization of complex molecules by collision in a field of force.

The results are collected in Table III. (See L. Rolla and G. Piccardi, *Phil. Mag.* Feb. 1929, no. 42, p. 296, for a recent list of ionizing potentials; and J. C. Morris, *Phys. Rev.* xxxiii., pp. 456-458, Sept. 1928.)

The observed figures given in Table III. refer to the apparatus in which the tests were made. They can be reduced to any other form of instrument by comparing in each the slopes of the curves of observation with that of any convenient standard gas.

The first column of figures is given for comparison of the relative voltages at which the cooling of the wire begins. These voltages, and to a less degree those of the second column, depend upon the dimensions of the apparatus. The relative values did not change in the various forms of experimental arrangement used.

XCVII. *The Psychophysical Law.—III. The Tactile Sense.*

By P. A. MACDONALD, *M.Sc., Ph.D., Hudson's Bay Fellow*, and D. M. ROBERTSON, *M.A., Department of Physics, University of Manitoba, Winnipeg, Canada* \*.

WEBER'S Law states that the magnitude of the differential threshold, that is, the strength of the just perceptible increment of a sensory stimulus, bears a constant ratio to the strength of the stimulus at which the differential threshold is determined. In the first part † of this paper it was shown that the law held exactly for the visual sense; it was further shown that abrupt changes in the value of the ratio occurred at some intensities of the stimulus, probably corresponding to the similar changes of slope observed in curves obtained by plotting the reciprocal of the critical duration of flicker against the logarithm of the stimulating intensity.

Investigations dealing with the behaviour of the differential threshold in the auditory sense ‡ were described in Part II. of the communication, in which it was shown that, while Weber's law did not hold, there was an exact law relating the increment to the total intensity by the equation

$$\Delta I \cdot \log I = C,$$

or, adopting Weber's form,

$$\frac{\frac{I}{\Delta I}}{\log I} = C',$$

\* Communicated by Prof. Frank Allen.

† "The Psychophysical Law.—I.", *Phil. Mag.* ix. p. 817 (1930).

‡ "The Psychophysical Law.—II.," *ibid.* p. 827.

where  $\Delta I$  is the differential threshold,  $I$  the intensity of the stimulus at which  $\Delta I$  is determined, and  $C$  and  $C'$  are constants.

The present paper deals with an extension to the tactile sense of the experimental procedure followed in the investigations in vision and audition, and it will be shown that an accurate law exists in the form

$$\Delta I \cdot \log I = C$$

which, as we have stated, seems to hold for the auditory sense.

In examining the tactile sense, the two fundamental principles employed in vision and audition were followed. First, an adequate stimulus was allowed to act on the receptors for a brief period; its intensity was then suddenly increased by a small amount, thus adding an increment of the stimulus to the same receptors. Second, care was taken to maintain the receptors at their normal sensitivity while successive readings were being made.

### *Experimental Procedure.*

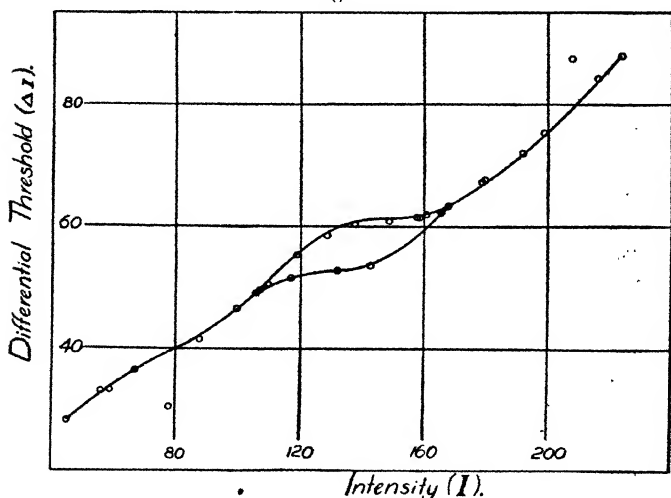
A jet of air was used as the adequate stimulus. The air collected over water in a constant-pressure tank was delivered by a suitable nozzle to the surface of the lower lip, which was kept in position by a chin-rest and a perforated metallic plate. The air-pressure, determined by a water-manometer connected in the air-circuit immediately behind the nozzle, was taken as the strength of the stimulus. Since an increase in pressure was directly proportional to the magnitude of the weight placed on the top of the tank, both the intensity and increment were controlled in this manner.

Air at a definite pressure was allowed to flow through the nozzle directly upon the lip, previously coated with a thin film of vaseline to prevent drying, for a period of approximately one second, after which, while the air was still playing on the lip, the observer suddenly, by a lever, added a small weight to the top of the tank and noted the presence or absence of an increase in sensation. The value of the small weight was taken as a direct measure of the magnitude of the increment, as the actual change in the numerical value of the pressure in this case was too small to be measured by the manometer.

In order that the receptors might return to their normal state of sensitivity, a rest-period of ten minutes was then allowed, following which another trial was made with a decrease or increase in the magnitude of the small weight, depending on whether or not the previous increment had been perceptible. Considerable experience is required to determine in this manner the differential threshold with a high degree of accuracy.

The data obtained for a number of pressures are shown graphically in fig. 1 and given numerically in Table I., where  $I$  and  $\Delta I$  are both expressed in millimetres of air-

Fig. 1.



Showing the behaviour of the differential threshold at different intensities of stimulation.

pressure, the measurements of the former being observed and of the latter computed from the values of the small

weights. In fig. 2 the same data are plotted,  $\frac{1}{\Delta I}$  against  $\log I$ , the resulting linear relation showing that the differential threshold is related to the intensity of the stimulus by the equation,

$$\frac{1}{\Delta I} = K \log I + C,$$

and that at certain magnitudes of the intensity the constants suddenly change in value, which is indicated by

TABLE I.—Data for figs. 1 and 2.

Intensity.	Log I.	$\Delta I.$	$\frac{1}{\Delta I} \times 1000.$
45 mm.	1.653	28.0	35.71
56	1.748	33.0	30.30
59	1.771	33.0	30.30
67	1.826	36.1	27.70
78	1.893	30.3	33.00
88	1.945	41.5	24.10
100	2.000	46.5	21.50
108	2.033	49.6	20.16
109	2.037	50.0	20.00
110	2.041	50.5	19.80
117	2.068	51.4	19.46
119	2.076	55.4	18.05
129	2.110	58.6	17.06
132	2.121	52.7	18.98
138	2.140	60.4	16.56
143	2.155	53.6	18.66
149	2.173	60.8	16.45
158	2.199	61.4	16.29
159	2.201	61.4	16.29
161	2.207	61.8	16.18
166	2.220	62.2	16.08
168	2.225	63.5	15.75
179	2.253	67.2	14.88
180	2.255	67.6	14.79
192	2.283	72.1	13.87
199	2.299	75.3	13.28
208	2.318	87.5	11.43
214	2.330	84.3	11.96
224	2.350	88.0	11.36

Intensity and differential threshold are both expressed in mm. of water pressure.

Diameter of air nozzle 0.7 mm.

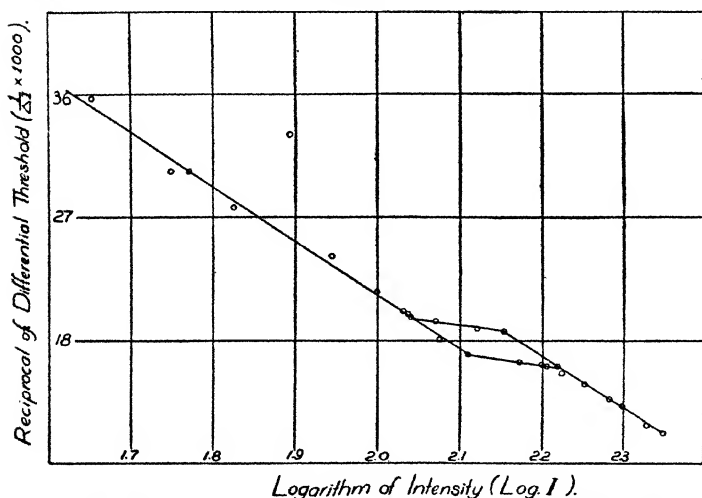
abrupt changes in the slope of the graph. The loop in the curve was obtained by taking readings on different days,

and indicates that the intensity at which changes of slope occur is not constant, but may vary from day to day, a phenomenon which we have observed in vision in both the Weber and Ferry-Porter graphs.

*Similarities between Flicker and Increment Phenomena.*

Allen and Hollenberg \*, by alternating equal periods of stimulation and rest in rapid succession, have succeeded in obtaining a flickering tactile sensation similar in nature to the flickering visual sensation obtained with the flicker photometer.

Fig. 2.



Showing the logarithmic relation existing between the differential threshold and the stimulating intensity.

On plotting the logarithm of the intensity of the stimulus against the critical duration of the stimulus, measured at the point where the sensation has become just continuous, they obtained a linear relation, reproduced here as fig. 3, showing the equation to be

$$D = K \log I + C,$$

where  $D$  is the critical duration of the stimulus and  $I$  its intensity.

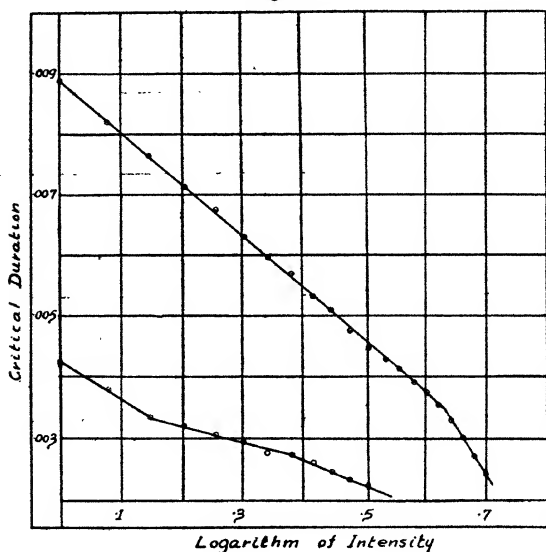
\* Quart. Journ. Exper. Physiol. xiv. No. 4, p. 351 (1924).



The similarity between this curve and that of fig. 2, together with the fact that both the critical duration and the differential threshold are probably closely related to sensation, led us to determine the two curves with the same apparatus over the same range of intensity.

In order to obtain the critical duration curve, the air playing on the lip was interrupted by a cardboard disk containing equal numbers of open and closed equiangular segments, the disk being rotated between the air-nozzle and

Fig. 3.



Critical duration of percussion curve obtained by Allen and Hollenberg.

the protecting plate by a low-velocity synchronous motor. The air-pressure was altered by a needle-valve until the sensations resulting from the individual pulses of air were fused into a just continuous sensation. The duration of a pulse was then computed from the velocity of the motor and the number of segments cut from the disk. Different values of the duration were obtained by substituting disks containing different numbers of segments, the corresponding pressure necessary to produce a continuous sensation being measured in each case. A ten-minute rest period

was observed between successive readings, as in determining the threshold curve. Considerable difficulty was experienced at first in obtaining consistent readings, and after some trials it was concluded that the air-nozzle was too small. A new nozzle of larger bore was substituted, whereupon accurate readings were obtained without difficulty. The resulting data are given in Table II. and shown graphically in fig. 4. It will be seen that two curves are obtained, similar to those found by Allen and Hollenberg, indicating the presence of two groups of tactile receptors.

The change in the size of the nozzle necessitated repetition of the differential threshold curve. Difficulty was

TABLE II.—Data for fig. 4.

Duration.	Upper graph.		Lower graph.	
	I.	Log I.	I.	Log I.
0.0222 sec.	140 mm.	2.146	108 mm.	2.033
0.0166	149	2.173	120	2.079
0.0133	156	2.193	—	—
0.0111	158	2.199	136	2.134
0.0095	171	2.233	143	2.155
0.0075	203	2.308	167	2.223
0.0060	221	2.344	186	2.270
0.0053	245	2.389	200	2.301
0.0044	260	2.415	219	2.340
0.0039	313	2.496	250	2.398
0.0035	354	2.549	297	2.473

Duration given in seconds.

Intensity given in mm. of water-pressure.

here experienced in making accurate increment readings because the nozzle was too large. Readings were obtained finally, however, with sufficient accuracy to enable the intensities at which the changes of slope occur to be located. A comparison of these intensities with those of the critical duration curves reveals close agreement, emphasizing a similarity in the two phenomena.

The intensities at which changes of slope occur in the differential threshold curve are

$$I=166 \text{ mm.}, I=246 \text{ mm.},$$

and the corresponding values in the critical duration curve are

$$I=160 \text{ mm.}, I=258 \text{ mm.}$$

Fig. 4.

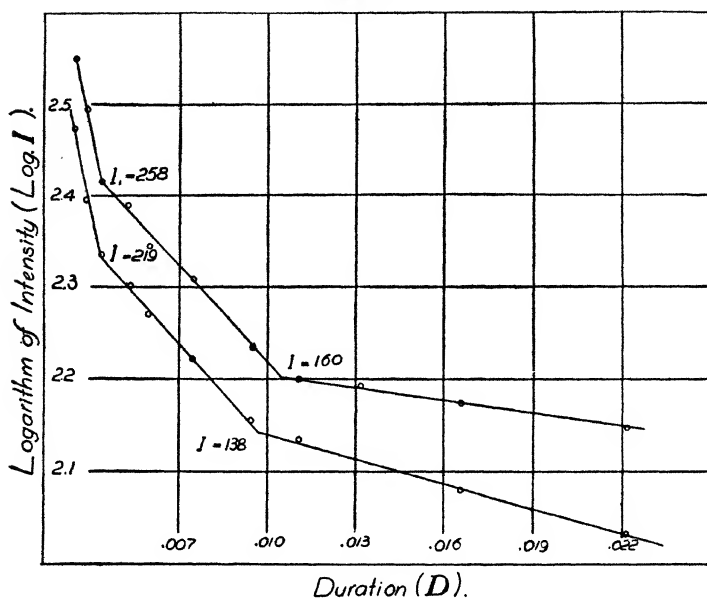
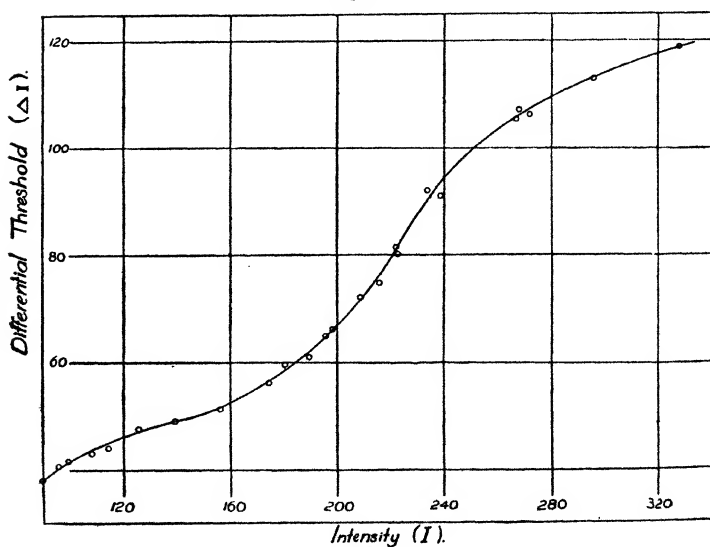


Fig. 5.



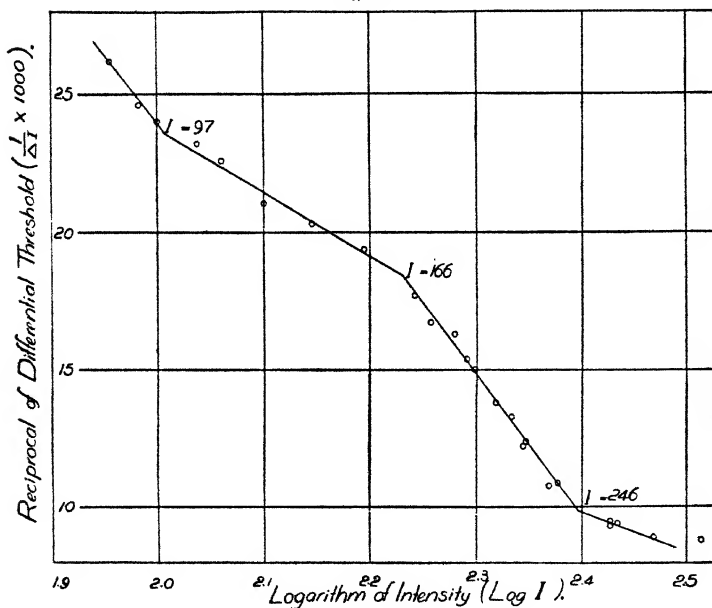
The complete curves are given graphically in figs. 5 and 6, and the corresponding numerical data in Table III.

From the work presented in this communication the authors draw three conclusions :—

- (1) Weber's law does not hold for the tactile sense.
- (2) A definite and accurately determinable relation exists between the differential threshold and the stimulating intensity expressed by the equation

$$\Delta I \cdot \log I = C.$$

Fig. 6.



- (3) There is some intimate relation, at present unknown, between the phenomenon of the critical duration of percussion and that of the least perceptible increment or differential threshold.

#### Recapitulation.

In the three senses studied, the authors feel confident in stating that the equations,

$$\frac{\Delta I}{I} = C, \text{ in vision,}$$

and

$$\frac{1}{\Delta I} = K \log I, \text{ in touch,}$$

TABLE III.—Data for figs. 5 and 6.

Intensity.	Log I.	$\Delta I$ .	$\frac{1}{\Delta I} \times 1000$ .
79 mm.	1.898	33.60 mm.	29.7
90	1.954	38.10	26.2
96	1.982	40.60	24.6
100	2.000	41.60	24.0
109	2.037	43.10	23.2
115	2.061	44.10	22.6
126	2.100	47.60	21.0
140	2.146	49.10	20.3
157	2.196	51.41	19.4
175	2.243	56.41	17.7
181	2.258	59.60	16.7
190	2.279	61.10	16.3
196	2.292	64.91	15.4
199	2.299	66.60	15.0
209	2.320	72.10	13.8
216	2.334	74.91	13.3
222	2.346	81.60	12.2
223	2.348	80.10	12.4
234	2.369	92.10	10.8
239	2.378	91.10	10.9
267	2.427	105.41	9.5
268	2.428	107.10	9.3
272	2.435	106.10	9.4
296	2.471	112.91	8.9
328	2.516	113.91	8.8

Intensity and differential threshold are both expressed in mm. of water-pressure.

Diameter of nozzle 1.5 mm.

starting from the threshold value, hold exactly over wide ranges of intensity, with suitable changes in constants, and that in the auditory sense the equation

$$\frac{1}{\Delta I} = K \log I,$$

holds exactly for the limited range of intensity obtainable from tonvariators, when employed as the sound-source.

Recent work by other observers in sound has been examined, but it was not possible to test with it the auditory equation, as complete numerical data have not been given.

Moreover, the linear relation with characteristic change of slope would probably be concealed by the practice of taking means not only of individual observer's results, but of the results of a number of different observers. This practice can hardly be considered legitimate for two reasons: first, changes in the state of adaptation of the individual alter the position of the change of slope; and second, means of a group of observers will merge together the individual sharp changes of slope into a curve, since these changes hardly ever occur at the same intensity for different individuals.

Weber's law has also been investigated in the gustatory sense, but owing to the physiological elements involved in such an investigation the results will be published elsewhere, probably in the 'Quarterly Journal of Experimental Physiology.'

---

XCVIII. *X-Ray Study of Grain Size in Steels of different Hardness Values.* By W. A. WOOD, M.Sc., *Physics Department, National Physical Laboratory, Teddington, Middlesex* \*.

*Introduction.*

THE particles which compose a solid may be either single crystals of more or less irregular shape or minute aggregates of single crystals. It is with the size of the ultimate single crystals that X-ray investigations are concerned. These may be so large, about  $10^{-3}$  cm. or greater, that the interference lines produced by a given volume illumined by an X-ray pencil are broken up into spots. Each spot is due to one crystal, and from the number of spots it is possible, under correct conditions, to deduce the number of crystals per unit volume and hence an average grain size. On the other hand, they may be so

\* Communicated by G. W. C. Kaye, O.B.E., M.A., D.Sc.

small that the interference lines are continuous. In this case, if they are small enough, about  $10^{-5}$  cm. or less, then the diminution in the number of diffracting planes in any one grain will affect the resolving power of the crystal. A measurable broadening of the interference lines may then occur. In the present work measurement of the broadening effect is made for a set of ten samples of stainless steel. The samples had the same chemical composition but differed widely in degree of hardness. The average grain size, which is of a sub-microscopic order of magnitude, is estimated. An account is also given of a relation found to hold between the measured grain size and the hardness of the steels.

A mathematical investigation of the connexion between grain size and the breadth of X-ray interference lines was first put forward by Scherrer\* and extended by Laue†. The latter gives a number  $n$  which is a measure of the relative breadth of an interference line so far as this breadth depends only on the size of the particles. It is

$$n_{(h_1 h_2 h_3)} = \frac{\lambda}{4\pi} \sqrt{\sum \left( \frac{b_i G}{m_i} \right)^2}, \quad G = \frac{\sum h_i b_i}{|\sum h_i b_i|}, \quad (1)$$

where the numbers  $h_i$  are integral and the quantities  $b_i$  are the usual reciprocal lattice vectors given by the relation

$$b_i = \frac{[a_k a_l]}{(a_i a_k a_l)},$$

in which  $a_i, a_k, a_l$  are the vectors defining the primitive translation triplet of a general crystal lattice. The number  $m_i$  measures the extent of the particles in the direction  $a_i$ .

In the case of a cubic lattice of side  $a$ , which holds for the steels investigated, equation (1) simplifies to

$$n = \frac{\lambda}{4\pi} \sqrt{\frac{1}{a^2} \frac{\sum \left( \frac{h_i}{m_i} \right)^2}{\sum (h_i)^2}} = \frac{\lambda}{4\pi m a}. \quad (2)$$

Thus we have a simple expression which, if  $n$  can be obtained in terms of a measurable quantity, will yield the estimated grain size  $ma$ .

The value of  $n$  was evaluated by Laue for the practical experimental case of a rod of powder of radius  $r$  placed at the centre of a circular camera, radius  $R$ . It is given in

\* P. Scherrer, *Göttingen Nachr.* xcvi. (1918).

† V. Laue, *Zeit. für Kryst.* lxiv. p. 115 (1926).

terms of the half-breadth  $B$  of the interference line for which the angle of reflexion is  $\theta$ . Thus

$$B = \frac{\frac{\pi\omega}{n_k} \left(\frac{r}{R}\right)^2 \cos^3 \theta}{\sqrt{1 + \left(\frac{\omega r \cos^2 \theta}{n_k R}\right)^2} - 1}, \quad \omega = \frac{1}{1.8} \quad (3)$$

By the half-breadth is meant the ratio of the total intensity of the interference line to the intensity at the maximum. It is usually estimated by measuring the distance between the two points on each side of the peak where the intensity is half the maximum.

From equation (3) we have, by transposition,

$$n_k = \frac{\omega}{2} \left[ \frac{B \cos \theta}{\pi} - \frac{\pi}{B} \left(\frac{r}{R}\right)^2 \cos^3 \theta \right]. \quad (4)$$

Since we know  $r$ ,  $R$ ,  $\theta$ , and can measure  $B$ , we are able from equations (2) and (4) to determine the grain size of the material under consideration.

Two main assumptions are made by Laue. First, the effect of absorption in the powder rod is neglected, and second, all the particles are taken to be of the same size and atomic arrangement. The effect of absorption is important. It means that since points inside the powder rod will reflect X-rays with less intensity than points on the surface, and some points not at all, the effective shape of the rod, as far as the X-rays are concerned, is not the geometric shape. A simple correction, however, has been described by Brill\*. It involves a multiplication of the measured half-breadth by a factor  $\frac{1}{\sin^2 \theta}$ . The

assumption that the particles are similar has probably less influence on the validity of the result. Patterson†, using a distribution function of the Maxwell type, concludes that the results given by Laue's equations would need correction by 35 per cent. But a symmetrical function of the Gaussian type  $s = ce^{-(\mu - \mu_0)^2 p}$  is a preferable assumption, and this leads to average grain size values practically the same as those calculated above (Mark).

#### *Measurement of the Half-breadth.*

The interference lines produced by the steels were photometered with the aid of a Moll microphotometer. The

\* R. Brill, *Zeit. für Kryst.* lxviii. p. 387 (1928).

† Patterson. Cf. Mark, *Far. Trans.* (March 1929).



screw and drum motions result in a magnification factor whose value was found to be 6.97, thus facilitating measurements of a high degree of accuracy. For the correct interpretation of the records it is essential to ensure, in the first instance, that the density of a line on the X-ray film is proportional to the intensity of the beam by which it is caused. This has been shown to be the case provided that the density is not too large\*. If  $I_0$  is the intensity of the photometer beam incident on a point of a film where the photographic density is  $D$ , and  $I$  the intensity of the transmitted beam, then  $D$  is defined by the relation

$$D = \log_{10} \frac{I_0}{I}.$$

The value of  $D$  in the experiments was always less than 2. This was brought about by suitable choice of exposures.

In the second instance, it is necessary to calibrate the microphotometer so that observed galvanometer deflexions can be interpreted in terms of the density of the film for which that deflexion occurs. For this purpose a wedge was utilized. This wedge consisted of seven steps of known relative photographic density. From the microphotometer record could be measured  $y_0$  and  $y$ , the galvanometer deflexions corresponding to an incident intensity  $I_0$  and a transmitted intensity  $I$ , for each step of the wedge. We have then

$$D = \log \frac{I_0}{I} = F\left(\frac{y_0}{y}\right),$$

and it is necessary to find the most useful way of writing the function  $F$ . It is preferable, of course, that the function should be linear. In fig. 1 the known values of  $D$  for

the wedge are plotted against  $\log \frac{y_0}{y}$ . It appears that from values of  $D = 0$  to  $D \simeq 0.5$ , and from values of  $D \simeq 0.7$  to  $D \simeq 1.8$  the graph is practically a straight line. The slope of the two portions is different and the intervening part is curved. Therefore, whilst a small density cannot be compared with a heavy one without the use of a separate calibration curve, densities of the same order, if they both lie in one of the above regions, may be compared with the aid of the relation  $D = \log \frac{y_0}{y}$ . The exposures and development times were such, in the actual experiments, as

\* Blunck und Koch, *Ann. Phys.* lxxvii. p. 483 (1925).

to bring the line densities in one linear region. Moreover, all ten steel photographs were simultaneously developed and

Fig. 1.

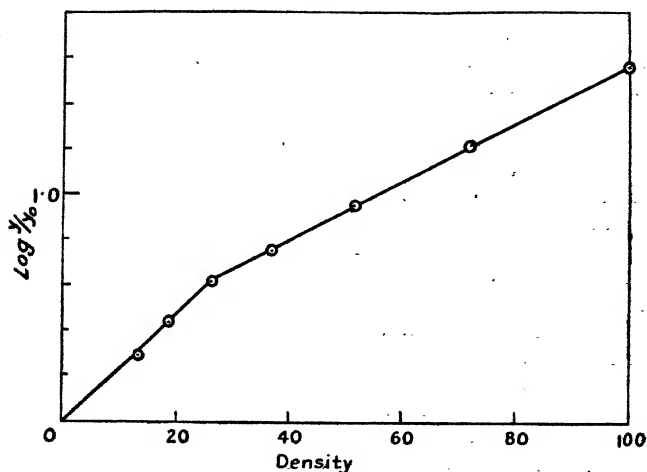
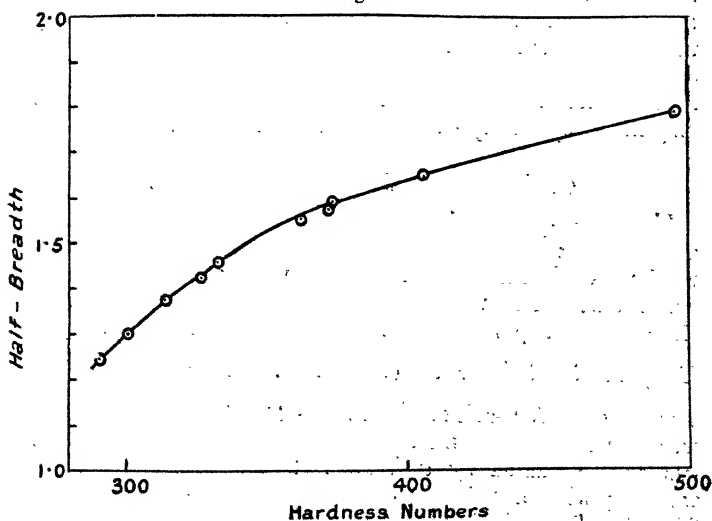


Fig. 2.



fixed for the same periods to avoid differences in photographic contrast.

*The Line Breadths and the Hardness Numbers.*

The half-breadths were measured on the (200) and (211) lines of the  $\alpha$ -iron spectrum produced by the steels. It was found that when the measured breadths were plotted against the hardness numbers a smooth continuous curve resulted. This is illustrated for the (211) by fig. 2. Now the steels were of the same composition, namely, 0.39 per cent. carbon, 0.51 per cent. silicon, 0.028 per cent. sulphur, 0.024 per cent. phosphorus, 0.17 per cent. nickel, 12.45 per cent. of chromium, and of manganese a trace. The variations of hardness were produced by heat treatment which from other data and from the appearance of the accompanying carbide lines does not appear to have greatly affected the nature of the carbides. The grain size might therefore have been expected to be the main factor influencing the hardness, and it is interesting to find that this is suggested by the continuity of the curve. Further, it must be pointed out that the continuity of the relation is independent of any theoretical assumptions about the broadening of the interference lines save the perfectly general and justifiable one that the effect is a function of the size of the diffracting grains. Since, too, it is safe to say that as the line broadens the grain size decreases, the slope of the curve shows that as the hardness increases the grain size decreases at first fairly rapidly and then very slowly. This extends previous results on the subject of grain size and hardness therefore into the region where the grain size is of a sub-microscopic order of magnitude by purely experimental observations.

*Grain Size and the Hardness Numbers.*

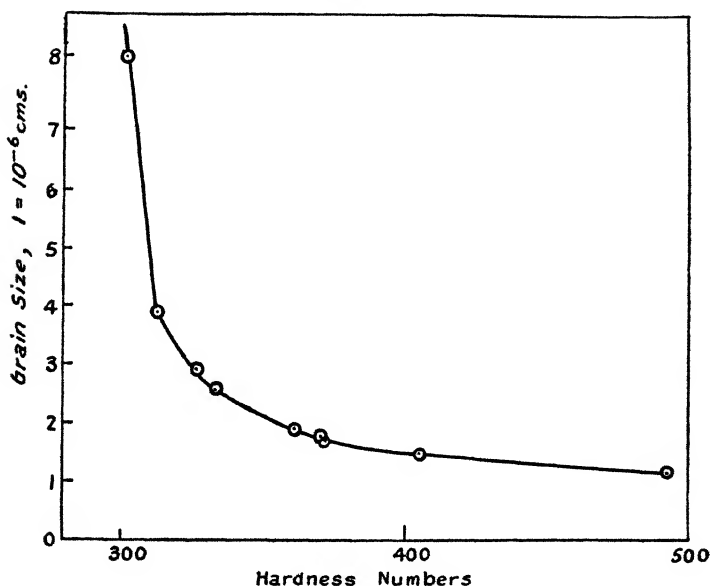
To give a quantitative aspect to the above observation we assume the validity of the equations of Laue and the corrections of Brill. The following were the experimental conditions. The radiation used was  $\text{FeK}_\alpha$  characteristic ( $\lambda = 1.932 \text{ \AA.}$ ) giving the value of  $\theta$  to be  $42^\circ 33'$  for the (200) and  $55^\circ 54'$  for the (211) line. The value of  $\left(\frac{r}{R}\right)^2$  was the same for each steel, namely  $4 \times 10^{-4}$ . The exposures were for  $1\frac{1}{2}$  hours in a Debye camera using a water-cooled gas tube actuated by a Watson 2 K. V. A. transformer working with a primary current of about 4 amperes at 80 volts. The calculation of the grain size based on either the (200) or (211) line gave practically the same result. Since the correction for absorption is much less in the case of the (211) line the values given by that line are

preferable to a mean of the two values. The (200) values are considered as a check. In Table I., column 1, are given

TABLE I.

Hardness.	Grain size.
290	$28.9 \times 10^{-6}$ cm.
300	8.3     "
313	3.9     "
326	3.0     "
333	2.6     "
361	1.9     "
370	1.8     "
371	1.7     "
404	1.5     "
495	1.1     "

Fig. 3.



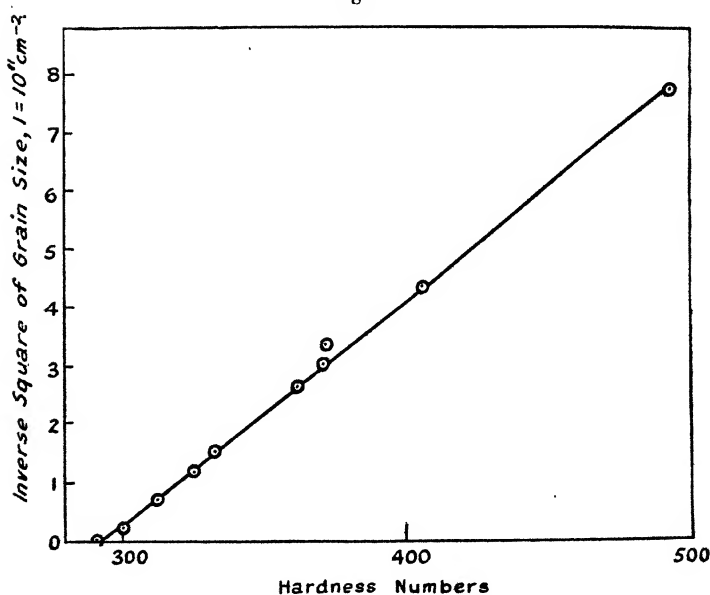
the hardness numbers of the steels, and in column 2 the calculated grain size values. The hardness numbers are expressed in kilogrammes per square millimetre. In fig. 3

the grain size is plotted against the hardness, and it is seen that a similar type of curve to that in fig. 2 is the result.

A physical interpretation of the curve and an indication of its type were next sought. It was found that if the hardness number were plotted against the inverse square of the grain size a definite linear relation appeared. The resulting straight line is depicted in fig. 4. Thus we have that if  $S$  is the average grain size in a steel of hardness  $H$ , then

$$H = \frac{k}{S^2}, \quad k = \text{constant}.$$

Fig. 4.



Now  $S$  is the diameter of the average grain and is of linear dimensions, so that  $S^2$  may be taken as being proportional to the area of surface of the grain. If  $A$  is the superficial area of the average grain, then

$$H = \frac{c}{A}, \quad c = \text{constant}.$$

Thus we would appear to have obtained by the application of Laue's equation to the observed broadenings of the interference lines an indication that, other things being equal,

the hardness of this type of steel is a function of the surface area of the grain in a region where the grain size is of the order of  $10^{-6}$  cm. It might be interpreted either as being due to the atomic layers, or possibly carbide material, coating the grain. Alternatively, it may mean that the force required to separate the grains must overcome a type of cohesion force of a definite magnitude per unit surface area and that the purpose of the carbides is mainly to interfere with grain growth. It must be remembered that the hardness numbers are usually determined by measuring the deformation produced by the impression of various loads, so that they are probably a measure of the force necessary to slide one crystal over another. In any case, the application of X-rays in this sphere contributes some data which should be of value to an understanding of the nature and cause of hardness. It is hoped to extend the work to other types of materials and also to cases in which the changes of grain size in steels are accompanied by physical and chemical carbide changes.

The thanks of the writer are due to Dr. G. Shearer for his discussion of the results and to Dr. G. W. C. Kaye, who provided the facilities for the research. The writer is, moreover, very deeply indebted to Mr. V. Stott for kindly loaning the specimens and supplying the hardness numbers determined by him.

### *Summary.*

1. The mathematical investigation of Laue of the effect of particle size on the breadth of X-ray interference lines is applied to the case of samples of steel of different hardness values.

2. The method of measuring the half-breadths of the iron lines by the Moll microphotometer is described. A relation is found to exist between the measured half-breadths and the hardness numbers of the respective steels.

3. From the half-breadths the grain size of the steels is determined with the aid of Laue's equations. The relation between the grain size and the hardness is discussed, the relation being found to agree with the assumption that the hardness varies inversely as the superficial area of the grains.

**XCIX. New Bands in the Secondary Spectrum of Hydrogen.**  
 Part III. By D. B. DEODHAR, M.Sc., Ph.D., Physics  
 Department, Lucknow University, Lucknow (India) \*.

**A**S indicated in the previous paper †, "New Bands, Part II.," a system of a new group of bands is discovered in the violet region of the spectrum, and I wish to deal with that group in the present communication.

The new group in the violet consists of seven bands, and the P(2)-lines of these bands approximately possess the same sequence of frequency differences as exists in the case of the P(2)-lines of the yellow ‡ and the blue bands. The vertical differences of the P, Q, and R branches of these bands are also similar to those in the yellow and the blue regions. This set of bands is weak as compared with the blue, and the set of bands in the blue previously described is weaker than the yellow bands. Like the yellow and the blue, the development of the violet bands also appears to be favoured by the special type of low voltage, low pressure discharge in hydrogen known as the first type discharge according to the nomenclature adopted by Prof. O. W. Richardson. A large mass of strong lines in the visible region first measured by Merton and Barratt §, and later resolved and measured by Gale, Monk, and Lee ||, have been further resolved and carefully measured recently by Finkelnburg ¶, in whose list many strong lines initially measured as singlets or doublets appear as resolved into many components whose number in certain cases is as large as six. The interpretation of the microphotograph of the first-type spectrogram of hydrogen made in the light of Finkelnburg's tables of wave-lengths offered a great facility in picking up relevant band-lines discussed in the present paper. Owing to the similarity of these bands to those published before, they are named as D bands, with the suffixes 1, 2, 3, etc., to distinguish one band of the group from the other. Further, the letter D is given two dashes for its index to distinguish the violet group from the

\* Communicated by the Author.

† Phil. Mag. ix. pp. 37-49 (1930).

‡ Phil. Mag. vii. pp. 466-479 (1928).

§ Phil. Trans. Roy. Soc. A, cccxii. pp. 369-400 (1922).

|| Astro-Phys. Journal, lxvii. pp. 89-113 (1928).

¶ Zeit. für Phys. Band. lii. Heft 1. & 2, pp. 27, 114 (1928).

blue group. Each of these bands possesses three branches, P, Q, and R, having a common null line.

The details of these bands are given in Table I. The band-lines are represented by their wave-numbers, the values of which are taken from Finkelburg's tables. The intensity estimates in Finkelburg's lists appear to be rather high, but this may be due to the strong current and the high voltage used in running the discharge-tube in his experiments. However, his intensity values are given in brackets which follow the frequencies of lines. These intensity estimates are next followed by the author's intensity estimates from the first-type plate. In certain cases of lines which are not given in Finkelburg's tables the frequencies are taken from tables of Gale, Monk, and Lee \*, Tanaka †, or Deodhar ‡. Such lines are indicated by the letters G., M., L., T., or D. put underneath the corresponding frequencies. The band-lines set forth here have got very few important claims by other series; but in those cases where such a claim exists the fact is indicated by giving the proper reference underneath such a line. The intensities and the first-type characters are followed by the first and second differences. The horizontal and the vertical differences are given in Tables II. and III. respectively.

The intensity of the line 25030.11 which figures as  $D''_1P(4)$  is not known definitely, as it is mixed up with 25031.45 M.B., which is broad on the first-type plate and whose intensity is one. 25319.33  $D''_1Q(4)$  is the resolved part of 25321.65 T, which comes up in the first-type spectrum.  $D''_3P(2)$  is identical with  $D''_2Q(2)$ . This double claim appears to be justifiable when we consider the intensity of the line 25551.39. Finkelburg gives the number 2 for its intensity, and on the whole there are very few strong lines in these bands. 25727.09 figures as  $D''_5P(2)$  and also as  $D''_2R(1)$ . It is the component of 25754.70 M.B.(0). which comes out in the first-type spectrum with much strength. However, its claim as  $D''_5P(2)$  seems to be superior to its allocation as  $D''_2R(1)$ . It may as well be remembered that this line is not claimed anywhere else. 25659.60  $D''_3Q(3)$  does not appear in the author's published list of new lines, but it is present in the unpublished

\* *Astro-Phys. Journal*, lxvii. pp. 89-113 (1928).

† *Proc. Roy. Soc. A*, cvii. pp. 592-606 (1925).

‡ *Proc. Roy. Soc. A*, cxiii. pp. 420-432 (1926).



TABLE I.

$D''_1P(m).$			$D''_1Q(m).$			$D''_1R(m).$		
$m.$	$\Delta_1.$	$\Delta_2.$	$m.$	$\Delta_1.$	$\Delta_2.$	$m.$	$\Delta_1.$	$\Delta_2.$
2.	25250.22(0)( $<0$ )	$>100.89$	1.	25448.74(0)( $<0$ )	$>29.99$	1.	25616.60(0)(0)	$>30.22$
3.	25149.33(00)(?)	$>119.22$	2.	25418.75(00)( $<0$ )	$>41.39$	2.	25646.82(0)(0)	$>10.83$
4.	25030.11(0)(?)	$>129.53$	3.	25377.36(00)( $<0$ )	$>58.03$	3.	25666.21(00)( $ab$ )	$>19.39$
5.	24900.58(00)( $ab$ )	$>131.88$	4.	25319.33(0)( $<0$ )	$>66.41$	4.	25673.16(0)( $ab$ )	$>6.95$
			5.	25253.92(0)( $ab$ )	$>56.94$			
$D''_2P(m).$			$D''_2Q(m).$			$D''_2R(m).$		
$m.$	$\Delta_1.$	$\Delta_2.$	$m.$	$\Delta_1.$	$\Delta_2.$	$m.$	$\Delta_1.$	$\Delta_2.$
2.	25401.95(00)( $<0$ )	$>105.40$	1.	25578.37(0)( $<0$ )	$>26.98$	1.	25727.09(00)( $<0$ )	$>41.47$
3.	25206.55(0)( $<0$ )	$>126.14$	2.	25551.39(2)( $<0$ )	$>38.10$	2.	$D''_2P(3)$ 25768.56(1)(1)	$>4.94$
4.	25170.41(00)( $<0$ )	$>131.88$	3.	25513.29(0)( $ab$ )	$>51.55$	3.	25805.09(0)( $<0$ )	$>36.53$
5.	25038.53(0)( $ab$ )	$>131.88$	4.	25461.74(00)( $<0$ )	$>56.94$	4.	25868.26(0)( $<0$ )	$>23.17$
			5.	25404.80(2)( $<0$ )	$>56.94$			

TABLE I. (*cont.*).

$D''P(m).$		$D''Q(m).$		$D''R(m).$	
<i>m.</i>	$\Delta_1, \Delta_2$	<i>m.</i>	$\Delta_1, \Delta_2$	<i>m.</i>	$\Delta_1, \Delta_2$
2.	25551.39(2)( $<0$ )	1.	25720.77(0)( <i>ab</i> )	1.	25864.55(1)( <i>ab</i> )
3.	25440.56( $\tau$ )( $\tau$ )	2.	25695.07(2)( $<0$ )	2.	25914.38(2)( $<0$ )
4.	25308.72(0)( $<0$ )	3.	25659.60( $\tau$ )( <i>rd</i> )	3.	25962.32(0)( <i>ab</i> )
5.	25172.62(0)( $<0$ )	4.	25612.08(0)( <i>ab</i> )	4.	25997.76( $<0$ )( <i>ab</i> )
		5.	25559.01(0)( <i>ab</i> )		
$D''P(m).$		$D''Q(m).$		$D''R(m).$	
<i>m.</i>	$\Delta_1, \Delta_2$	<i>m.</i>	$\Delta_1, \Delta_2$	<i>m.</i>	$\Delta_1, \Delta_2$
2.	25699.94(00)( $<0$ )	1.	25899.02( $<0$ )( <i>ab</i> )	1.	26072.76( $\tau$ )( $\tau$ )
3.	25594.71(2)( $<0$ )	2.	25873.84(0)( <i>ab</i> )	2.	26127.76(0)( <i>ab</i> )
4.	25448.74(4)( $<0$ )	3.	25838.13(4)( $<0$ )	3.	26183.08(1)( $<0$ )
5.	25311.15(00)( <i>ab</i> )	4.	25793.45(0)( <i>ab</i> )	4.	26224.34(0)(0)

TABLE I. (*cont.*).

$D''_6P(m).$			$D''_6Q(m).$			$D''_6R(m).$		
$m.$	$\Delta_1$	$\Delta_2$	$m.$	$\Delta_1$	$\Delta_2$	$m.$	$\Delta_1$	$\Delta_2$
2. 25848.05(1)(0)	> 120.96	> 17.25	1. 26114.38(0)(ab)	> 23.32	> 5.16	1. 26357.05(r)(r)	> 69.24	> 0.20
3. 25727.09(00)(<0)	> 138.21	> 7.20	2. 26091.06(0)(<0)	> 28.48	> 11.81	2. 26426.29(0)(<0)	> 69.04	> 11.81
4. 25588.88(0)(rd)	> 145.41		3. 26062.58(1)(<<0)	> 40.29	> 8.07	3. 26495.33(r)(r)	> 57.23	
5. 25443.47(0)(ab)			4. 26022.29(0)(<0)	> 48.36		4. 26552.56(00)(ab)		
			5. 25973.93(00)(ab) G.M.L.					
$D''_6P(m).$			$D''_6Q(m).$			$D''_6R(m).$		
$m.$	$\Delta_1$	$\Delta_2$	$m.$	$\Delta_1$	$\Delta_2$	$m.$	$\Delta_1$	$\Delta_2$
2. 25994.82(1)(0)	> 124.31	> 21.60	1. 26368.02(7)(0)	> 21.26	> 5.06	1. 26719.53(0)(<0)	> 77.63	> 0.10
3. 25870.51(2)(1)	> 145.81	> 10.86	2. 26346.76(4)(0)	> 26.32	> 14.06	2. 26797.16(0)(<0)	> 77.53	> 6.54
4. 25724.70(3)(1)	> 156.67		3. 26320.44(0)(ab)	> 40.38	> 6.54	3. 26874.69(0)(ab) G.M.L.	> 70.99	
5. 25568.03(2)(0)			4. 26280.06(0)(<0)	> 46.92		4. 26945.68(0)(prob. present)		
			5. 26233.14(1)(ab)					

TABLE I. (cont.).

$D''_7P(m).$			$D''_7Q(m).$			$D''_7R(m).$		
$m.$	$\Delta_1.$	$\Delta_2.$	$m.$	$\Delta_1.$	$\Delta_2.$	$m.$	$\Delta_1.$	$\Delta_2.$
2.	26136.88(2)(0)	> 130.01	1.	26714.37(1)(r)	> 20.66	1.	27270.71(5)(1)	> 83.68
3.	26006.87(1)(0)	> 147.77	2.	26693.71(0)(ab)	> 25.48	2.	27354.39(r)(r)	> 89.64
4.	25859.10(1)(ab)	> 9.26	3.	26668.23(0)(ab)	> 33.67	3.	27444.03(r)(r)	> 79.4
5.	25702.07(00)(<0)	> 157.03	4.	26634.56(rd)(ab)	> 43.98	4.	27523.37 (calculated)	> 10.30
			5.	26590.58(0)(0)				

TABLE II.

Horizontal Differences of P(*m*)'s, Q(*m*)'s, and R(*m*)'s.

P( <i>m</i> ).						
	$D''_2 - D''_1$ .	$D''_3 - D''_2$ .	$D''_4 - D''_3$ .	$D''_5 - D''_4$ .	$D''_6 - D''_5$ .	$D''_7 - D''_6$ .
P(2).....	151.73	149.44	148.55	148.11	146.77	142.06
P(3).....	147.22	144.01	144.15	142.38	143.42	136.36
P(4).....	140.30	138.31	140.02	140.14	135.82	134.40
P(5).....	137.95	134.09	138.53	132.32	134.56	134.04
Q( <i>m</i> ).						
Q(1).....	130.03	142.40	178.25	215.36	253.64	346.35
Q(2).....	132.64	143.68	178.77	217.22	255.70	346.95
Q(3).....	135.93	146.31	178.53	224.45	257.86	347.79
Q(4).....	142.41	150.34	181.37	228.84	257.37	354.50
Q(5).....	150.88	154.21	182.57	232.35	259.21	357.44
R( <i>m</i> ).						
R(1).....	110.49	137.46	208.21	284.29	362.48	551.18
R(2).....	121.74	145.82	213.38	298.53	370.87	557.23
R(3).....	138.88	157.23	220.76	312.25	381.00	567.69
R(4).....	155.10	169.50	226.58	328.22	393.12	577.39

TABLE III.

Vertical Differences of P(*m*), Q(*m*), and R(*m*) lines.

P( <i>m</i> )'s.				
Band.	P(2)—P(3).	P(3)—P(4).	P(4)—P(5).	
D' <sub>1</sub> .....	100·89	119·22	129·53	
D' <sub>2</sub> .....	105·40	126·14	131·88	
D' <sub>3</sub> .....	110·83	129·41	136·10	
D' <sub>4</sub> .....	115·23	135·97	137·59	
D' <sub>5</sub> .....	120·96	138·21	145·41	
D' <sub>6</sub> .....	124·31	145·81	156·67	
D' <sub>7</sub> .....	130·01	147·77	157·03	
Q( <i>m</i> )'s.				
	Q(1)—Q(2).	Q(2)—Q(3).	Q(3)—Q(4).	Q(4)—Q(5).
D' <sub>1</sub> .....	29·99	41·39	58·03	65·41
D' <sub>2</sub> .....	26·98	38·10	51·55	56·94
D' <sub>3</sub> .....	25·70	35·47	47·52	53·07
D' <sub>4</sub> .....	25·18	35·71	44·68	51·87
D' <sub>5</sub> .....	23·32	28·48	40·29	48·36
D' <sub>6</sub> .....	21·26	26·32	40·38	46·92
D' <sub>7</sub> .....	20·66	25·48	33·76	43·98

TABLE III. (cont.)

	R( <i>m</i> )'s.		
	R(1)–R(2).	R(3)–R(2).	R(4)–R(3).
D' <sub>1</sub> .....	30.22	19.39	6.95
D' <sub>2</sub> .....	41.47	36.53	23.17
D' <sub>3</sub> .....	49.83	47.94	35.44
D' <sub>4</sub> .....	55.00	55.32	41.26
D' <sub>5</sub> .....	69.24	69.04	57.23
D' <sub>6</sub> .....	77.63	77.53	70.99
D' <sub>7</sub> .....	83.68	89.63	79.05

list under the heading of doubtful lines on the first-type plate. The existence of this line is now confirmed by Finkelburg's observation; 25584.71, figuring as D'<sub>4</sub>P(3), is Tanaka's line, and its intensity as given by him is only *p*, though its intensity is 2 in Finkelburg's tables. 25448.74 D'<sub>4</sub>P(4) is very strong according to Finkelburg, but according to Tanaka its intensity is only *p*. On the first-type plate also its intensity is much less than zero. Similarly, 25838.13 is (4) in Finkelburg's table; but according to Merton and Barratt its intensity is zero. In the first-type spectrum its intensity is less than zero. 26062.58 D'<sub>5</sub>Q(3) given by Finkelburg was originally observed on the first-type plate, but it was not then published, as it was difficult to measure owing to its faintness. In Finkelburg's table it appears as a strong line. 26280.06 D'<sub>6</sub>Q(4) must be mixed up with 26275.27 D, which is wide on the first-type plate. This line seems to be probably resolved from 26275.37 D (*rw*). The calculated wave-number for D'<sub>6</sub>R(3) is 26875.80. The corresponding line in G., M., and L.'s tables is given by 26874.69. This line is difficult to measure according to G., M., and L. Finkelburg also finds it difficult to measure, and omits the fractional part of the wave-length value. This shows that the value of the wave-number in the tables is inaccurate. 25702.07 F. figures as D'<sub>7</sub>P(5), and it is resolved from 25704.34 M.B., whose intensity is 3 on the first-type plate. 27270.71 M.B. figures as D'<sub>7</sub>R(1); its intensity is 5 according to Finkelburg, but only 1 according to Merton and Barratt and also according to the first-type spectrum. 27523.37 D'<sub>7</sub>R(4) is a calculated wave-number which does not appear in published tables. A very faint line corresponding to the wave-number appears to be present on the

first-type plate. This portion of the spectrum is specially difficult to measure, on account of the diffuse nature of the lines and the superposition of a continuous background. This calculated line is not used in determining the band-constants.

The horizontal and the vertical differences of P's, Q's, and R's of all the bands are arranged in Tables II. and III. The fairly systematic run of the successive horizontal differences is evident from Table II. Table III. shows the systematic nature of variation of the vertical differences of P, Q, and R lines. The vertical differences of the band-lines in the present paper are very much like those in the yellow and the blue. The P(2)—P(3) differences of the yellow, the blue, and the violet bands gradually rise from 99, 98, and 100 for the first bands, and go up to 130, 132, and 130 respectively for the last bands. The Q(1)—Q(2) differences begin from 29, 30, and 30, and gradually go down to 21 for the last band in the yellow, the blue, and the violet alike. The R(2)—R(1) values for the yellow and blue start from 26 and 29 respectively for the first band, and they gradually ascend up to 82 and 83 for the seventh band. Also in the case of violet bands the R(2)—R(1) values gradually go up from 30 for the first band to 83 for the seventh band. All these differences clearly indicate the similarity of the bands in the yellow, the blue, and the violet.

All these bands consist of single P, Q, and R branches, amongst which the combination principle such as  $Q(m+1) + Q(m) = P(m+1) + R(m)$  is strictly obeyed. The initial and the final term-differences are tabulated in Tables IV. and V. From these term-differences one can easily evaluate the moments of inertia of the emitters of the bands. The values of the initial and the final term-differences can also serve as a check upon the correct agreement of the combination principle. The frequencies of the null lines, the moments of inertia, the correction terms due to the electronic angular moments, and other band constants are assembled in Table VI. The properties of lines and the systematic variation of the successive differences from the first band to the seventh band show that these bands are related. One observes the same systematic variations in the values of the null lines, which go on gradually increasing from one band to the other. The initial moment of inertia in each case is larger

TABLE IV.  
Initial Terms.

Band.	$m$ .	$R(m)$ $-Q(m)$ .	$Q(m-1)$ $-P(m-1)$ .	Means.	Term diff.	2nd diff.
$D'_1$	1 ...	167.86	166.53	168.18	$F(2)-F(1)$	
	2 ...	228.07	228.03	228.05	$F(3)-F(2)$	> 59.87
	3 ...	288.85	289.22	289.03	$F(4)-F(3)$	> 60.98
	4 ...	353.83	353.34	353.58	$F(5)-F(4)$	> 64.55
$D'_2$	1 ...	148.72	149.44	149.08	$F(2)-F(1)$	
	2 ...	217.17	216.74	216.95	$F(3)-F(2)$	> 67.87
	3 ...	291.80	291.33	291.56	$F(4)-F(3)$	> 74.61
	4 ...	366.52	366.27	366.39	$F(5)-F(4)$	> 74.83
$D'_3$	1 ...	143.78	143.68	143.74	$F(2)-F(1)$	
	2 ...	219.31	219.04	219.17	$F(3)-F(2)$	> 75.43
	3 ...	302.72	303.36	303.04	$F(4)-F(3)$	> 83.87
	4 ...	385.68	386.39	386.03	$F(5)-F(4)$	> 82.99
$D'_4$	1 ...	173.74	173.90	173.82	$F(2)-F(1)$	
	2 ...	253.92	253.42	253.67	$F(3)-F(2)$	> 79.85
	3 ...	344.95	344.71	344.83	$F(4)-F(3)$	> 91.16
	4 ...	430.89	430.43	430.66	$F(5)-F(4)$	> 85.83
$D'_5$	1 ...	242.67	243.01	242.84	$F(2)-F(1)$	
	2 ...	335.23	335.49	335.36	$F(3)-F(2)$	> 92.52
	3 ...	432.75	433.41	433.08	$F(4)-F(3)$	> 97.72
	4 ...	530.27	530.46	530.31	$F(5)-F(4)$	> 97.23
$D'_6$	1 ...	351.51	351.94	351.72	$F(2)-F(1)$	
	2 ...	450.40	449.93	450.17	$F(3)-F(2)$	> 98.45
	3 ...	555.84	555.36	555.60	$F(4)-F(3)$	> 105.43
	4 ...	665.62	665.11	665.36	$F(5)-F(4)$	> 109.76
$D'_7$	1 ...	556.34	556.83	556.58	$F(2)-F(1)$	
	2 ...	660.68	661.36	661.02	$F(3)-F(2)$	> 104.44
	3 ...	775.79	775.46	775.62	$F(4)-F(3)$	> 114.60
	4 ...	888.51	888.51	888.51	$F(5)-F(4)$	> 112.89



TABLE V.  
Final Terms.

Band.	<i>m</i> .	$\frac{R(m)}{-Q(m+1)}.$	$\frac{Q(m)}{-P(m+1)}.$	Means.	Term diff.	2nd diff.
$D'_1$	1 ...	197.85	198.52	198.18	$f(2)-f(1)$	
	2 ...	269.46	269.42	269.44	$f(3)-f(2)$	> 71.26
	3 ...	346.88	347.25	347.06	$f(4)-f(3)$	> 77.62
	4 ...	419.24	418.75	418.99	$f(5)-f(4)$	> 71.05
$D'_2$	1 ...	175.70	176.42	176.06	$f(2)-f(1)$	
	2 ...	255.27	254.84	255.05	$f(3)-f(2)$	> 78.99
	3 ...	343.35	342.68	343.11	$f(4)-f(3)$	> 88.06
	4 ...	423.46	423.21	423.33	$f(5)-f(4)$	> 80.22
$D'_3$	1 ...	169.48	169.38	169.43	$f(2)-f(1)$	
	2 ...	254.78	254.51	254.64	$f(3)-f(2)$	> 96.22
	3 ...	350.24	350.88	350.56	$f(4)-f(3)$	> 95.92
	4 ...	438.75	439.46	439.10	$f(5)-f(4)$	> 88.54
$D'_4$	1 ...	198.92	199.08	199.00	$f(2)-f(1)$	
	2 ...	289.63	289.15	289.38	$f(3)-f(2)$	> 90.38
	3 ...	389.63	389.39	389.51	$f(4)-f(3)$	> 100.13
	4 ...	482.76	482.30	482.53	$f(5)-f(4)$	> 93.02
$D'_5$	1 ...	265.99	266.33	266.16	$f(2)-f(1)$	
	2 ...	363.71	363.97	363.84	$f(3)-f(2)$	> 97.68
	3 ...	473.04	473.70	473.37	$f(4)-f(3)$	> 109.49
	4 ...	578.63	578.82	578.72	$f(5)-f(4)$	> 105.35
$D'_6$	1 ...	372.77	373.20	372.95	$f(2)-f(1)$	
	2 ...	476.72	476.25	476.48	$f(3)-f(2)$	> 103.53
	3 ...	596.27	595.74	596.00	$f(4)-f(3)$	> 119.52
	4 ...	712.54	712.03	712.28	$f(5)-f(4)$	> 115.28
$D'_7$	1 ...	577.00	577.49	577.24	$f(2)-f(1)$	
	2 ...	686.16	686.84	686.50	$f(3)-f(2)$	> 109.26
	3 ...	809.46	809.13	809.29	$f(4)-f(3)$	> 122.79
	4 ...	932.79	932.49	932.49	$f(5)-f(4)$	> 123.20

TABLE VI.—Band Constants.

Band.	$\nu_0$ From Q(1).	$\nu_0$ From P(2).	$\nu_0$ From R(1).	F(2).	F(1).	f(2).	f(1).	P.	$\rho$ .	Initial Moment of Inertia.	Final Moment of Inertia.
D <sub>1</sub> '...	25473.90	25473.83	25473.84	327.91	159.71	333.32	185.22	-1.31	-1.38	$9.39 \times 10^{-41}$ gm. cm. <sup>2</sup>	$7.76 \times 10^{-41}$ gm. cm. <sup>2</sup>
D <sub>2</sub> ' ..	25599.76	25599.36	25599.65	245.52	96.91	294.32	118.19	-0.69	-0.73	8.15	7.00
D <sub>3</sub> '...	25740.05	25740.52	25740.36	219.08	74.99	264.12	94.58	-0.41	-0.49	9.04	6.49
D <sub>4</sub> '...	25918.99	25919.75	25919.30	286.72	112.67	332.48	132.95	-0.68	-0.72	6.93	6.15
D <sub>5</sub> '...	26147.47	26146.53	26147.20	450.31	207.91	506.39	240.73	-1.22	-1.22	5.98	5.66
D <sub>6</sub> '...	26399.87	26399.91	26400.51	816.98	464.83	869.92	497.32	-2.07	-2.10	5.61	5.34
D <sub>7</sub> '...	26744.12	26743.74	26744.44	1774.90	1218.24	1825.10	1248.31	-3.83	-3.78	5.30	5.06

than the final moment of inertia, and the values of these moments of inertia gradually go on descending from a high value for the first band to a low value for the seventh band.

Remembering that  $R(m)$  line is due to a quantum jump  $m+1 \rightarrow m$ ,  $P(m)$  line due to a  $m-1 \rightarrow m$  jump, and the  $Q(m)$  line results when the quantum number stays unchanged, one can represent them in the usual equation form as :—

$$\left. \begin{aligned} R(m) &= \nu_0 + F(m+1) - f(m), \\ Q(m) &= \nu_0 + F(m) - f(m), \\ P(m) &= \nu_0 + F(m-1) - f(m). \end{aligned} \right\} (A)$$

Here  $\nu_0$  stands for the frequency of the null line and  $F$  and  $f$  represent the initial and the final state of the molecules. From these equations we can get expressions for term-differences. For instance, we have from (A) above,

$$\left. \begin{aligned} F(m+1) - F(m) &= R(m) - Q(m) = Q(m+1) - P(m+1) \\ &\text{initial term-differences, and} \\ f(m+1) - f(m) &= R(m) - Q(m+1) = Q(m) - P(m+1) \\ &\text{final term-differences.} \end{aligned} \right\} (B)$$

By giving suitable integral values to the quantum number  $m$  in (B), and substituting the values of relevant frequencies of lines, one can obtain successive differences, which are worked out and tabulated in Tables IV. and V. It is seen from (B) that these term-differences can be got in two ways. The means of such two values are tabulated in the fourth column of Tables IV. and V., and the successive differences of these means are placed in the sixth column of these tables. These differences, which are called second differences, are inversely proportional to the moments of inertia. The final and the initial second differences are known to be  $2b$  and  $2B$  respectively; and it is also known that  $I' = h/8\pi^2cB$  and  $I'' = h/8\pi^2cb$ , where  $I'$  is the initial moment of inertia and  $I''$  is the final moment of inertia of the molecule about the axis perpendicular to the line joining the nuclei,  $h$  is Planck's constant, and  $c$  the velocity of light.

In general the initial and the final terms may be represented by the following equations :—

$$\left. \begin{aligned} F(m) &= B(m-p)^2, \\ f(m) &= b(m-\rho)^2, \end{aligned} \right\} (C)$$

where  $P$  and  $\rho$  are Kratzer's correction terms. These correction terms can be evaluated by using the means in Tables IV. and V., and the second differences of the means. The null lines can hence be quickly calculated from any one of the three equations in (A). The frequencies of the null lines have been calculated by using  $Q(1)$ ,  $P(2)$ , and  $R(1)$  lines for each band, and the three values so obtained agree quite well with one another.

The values of moments of inertia for these bands are of the same order as those for the yellow and the blue band, and this fact, along with the other similarities, indicates that the emitter of these bands is an excited hydrogen molecule ( $H_2$ ). In deriving the values of moments of inertia use is made of only one of the three values of  $B$  or  $b$  for each band, but, by taking their average values into consideration, it appears that the final moment of inertia for the  $D_1$  bands in the yellow, the blue, and the violet possesses the same value, while the initial moments of inertia for  $D_1$  bands of yellow, blue, and violet colours are different from one another. The same is the case with  $D'_2$ 's,  $D'_3$ 's, and the others. This fact appears to suggest that the final excitation condition of the molecule is the same for all the three  $D_1$  bands, while their initial excitation conditions are different from one another. However, this question of interconnexion of these bands will be taken up later on, after the matter is thoroughly investigated.

Physics Department,  
Lucknow University, India.

---

C. *On Mutual Transference of Torsional and Pendulous Oscillations.* By G. SUBRAHMANYAM\*.

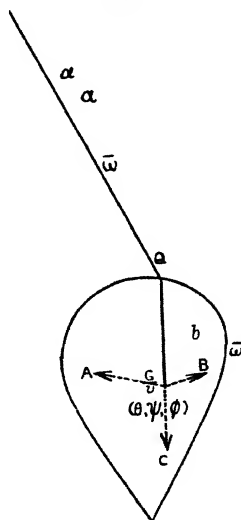
A FEW years ago, in connexion with my extensive study of the dependence of logarithmic decrement on the amplitude of torsional oscillations leading to the determination of the coefficients of viscosity of some metals (Phil. Mag. April 1925, October 1925, May 1926, and April 1927; also Landolt & Börnstein's tables), I had an occasion to observe closely the torsional oscillations of quite

\* Communicated by the Author.

a large number of wires, of lengths and of thicknesses varying over a wide range of values. In certain cases it was noticed (*l. c.* April 1925, p. 714) that there was a mutual transference of activity from torsional to pendulous states.

It is evident that such a transference is possible when the centre of gravity of the solid of revolution does not lie along the axis, or when the point of attachment of the wire to the solid is different from the extremity of an axis of the solid. The following solution of this problem affords an interesting application of the principle of moving axes and Eulerian coordinates.

Fig. 1.



Let a solid of revolution be suspended by a wire, the point of attachment  $Q$  being different from the extremity of an axis of the solid; let  $\bar{u}$  be the velocity of the free extremity of the wire,  $\bar{v}$  that of the c.g. of the body relative to the lower extremity of the wire, and  $\bar{w}$  the velocity of a particle  $m$  relative to the c.g. of the body.

The kinetic energy  $T$  of the body of total mass  $M$

$$\begin{aligned}
 &= \Sigma \frac{1}{2} m (\bar{u} + \bar{v} + \bar{w})^2 \\
 &= \frac{1}{2} \{ m (\bar{u}^2 + \bar{v}^2 + \bar{w}^2) + 2 \Sigma m (\bar{u} \bar{v}) + 2 \Sigma m (\bar{v} \bar{w}) + 2 \Sigma m (\bar{u} \bar{w}) \} \\
 &= \frac{1}{2} M (\bar{u}^2 + \bar{v}^2) + \frac{1}{2} \Sigma m \bar{w}^2 + M \bar{u} \bar{v} + \bar{v} (\Sigma m \bar{w}) + \bar{u} (\Sigma m \bar{w}) \\
 &= \frac{1}{2} M (\bar{u}^2 + \bar{v}^2) + \frac{1}{2} \Sigma m \bar{w}^2 + M \bar{u} \bar{v}.
 \end{aligned}$$

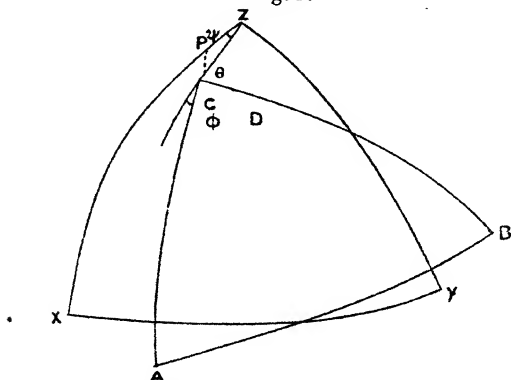
Let  $G$  be the c.g. of the solid,  $GQ=b$  and " $\alpha$ " be the length of the wire. Take axis  $GC$  in the direction of the wire produced,  $GB$  perpendicular to  $GC$  lying in the plane containing wire and axes of the solid of revolution. Let  $GA$  be perpendicular to  $GB$  and  $GC$ .

Let the Eulerian angles of  $QG$  be  $\theta, \psi, \phi$ , with respect to  $Gx, Gy, Gz$ , the positions of  $GA, GB, GC$  when the body is in equilibrium. Let  $GD$  be drawn in the direction of wire produced, and  $\alpha$  be the inclination of  $GD$  to vertical.

Now to find the twist of the wire. For small displacements the amount of twist depends on initial and final positions only, and is independent of path. Produce arc  $AC$  to meet  $zx$  in  $P$ . Then  $PCz$  may be considered to be a plane  $\Delta$ ,

$$\angle cPx = \angle Pcz + \angle Pzc = \phi + \psi.$$

Fig. 2.



The twist of wire is  $\angle cPx = \phi + \psi$  (same as that of the solid) :

$$\bar{u} = \bar{a}\bar{\alpha} \text{ along tangent at D to } zD,$$

$$\bar{v} = \bar{b}\bar{\theta} \text{ along tangent at C to } zC.$$

So,

$$T = \frac{1}{2}M(a^2\dot{\alpha}^2 + b^2\dot{\theta}^2 + 2ab\dot{\theta}\dot{\alpha}) + \frac{1}{2}(Ap^2 + Bq^2 + Cr^2 - 2Fqr),$$

where  $p, q, r$  are the angular velocities of the suspended body about the moving axes and  $A, B, C$  are the moments of inertia given by

$$A = \Sigma m(y^2 + z^2), \quad B = \Sigma m(x^2 + z^2), \quad \text{and} \quad C = \Sigma m(x^2 + y^2).$$

$$L = \frac{K}{2}(\phi + \psi)^2 + Mg\{a(1 - \cos \alpha) + b(1 - \cos \theta)\}.$$

$$\therefore T = \frac{1}{2}M(a^2\dot{\alpha}^2 + b^2\dot{\theta}^2 + 2ab\dot{\theta}\dot{\alpha}) \\ + \frac{1}{2}\{B\dot{\theta}^2 + C(\dot{\phi} + \dot{\psi})^2 - 2F\dot{\theta}(\dot{\phi} + \dot{\psi})\}.$$

So Lagrange's equations are :

$$(Mb^2 + B)\ddot{\theta} + Mab\ddot{\alpha} - F(\ddot{\phi} + \ddot{\psi}) = -Mgb\theta, \\ -F\ddot{\theta} + c(\ddot{\phi} + \ddot{\psi}) = -k(\phi + \psi), \\ Mab\ddot{\theta} + Ma^2\ddot{\alpha} = -Mga\alpha.$$

To solve the above equations we have to find the roots of the algebraic equation given by the following determinant :—

$$\begin{vmatrix} (Mb^2 + B)x^2 - Mgb & Mabx^2 & -Fx^2 \\ Mabx^2 & Ma^2x^2 - Mga & 0 \\ -Fx^2 & 0 & cx^2 - k \end{vmatrix} = 0.$$

This is of the form

$$\begin{vmatrix} a & h & g \\ h & b & 0 \\ g & 0 & c \end{vmatrix} = 0.$$

$\therefore abc - bg^2 - ch^2 = 0$  ; here  $g$  and  $h$  are small.

$$a = \frac{bg^2 + ch^2}{bc}, \quad b = \frac{ch^2}{ac - g^2} = \frac{h^2}{a'}, \quad c = \frac{bg^2}{ab - h^2} = \frac{g^2}{a''},$$

where  $a'$ ,  $a''$  are obtained by successive approximations.

$$(Mb^2 + B)x^2 - Mgb = \frac{g^2}{c'} + \frac{h^2}{b'} \\ = \frac{F^2 \left( \frac{Mgb}{Mb^2 + B} \right)}{c \frac{Mgb}{Mb^2 + B} - k} + \frac{(Mab)^2 \left\{ \frac{Mgb}{Mb^2 + B} \right\}^2}{\frac{Ma^2 \cdot Mgb}{Mb^2 + B} - Mga}, \\ Ma^2x^2 - Mga = \frac{h^2}{a'} = \frac{(Mgb)^2 \left( \frac{Mgb}{Mb^2 + B} \right)^2}{(Mb^2 + B) \frac{g}{a} - Mgb}, \\ cx^2 - k = \frac{g^2}{a''} = \frac{F^2 \left( \frac{Mgb}{Mb^2 + B} \right)^2}{(Mb^2 + B) \frac{k}{c} - Mgb},$$

and the approximate values of the roots are

$$\frac{Mgb}{Mb^2 + B}, \quad \frac{g}{a}, \quad \frac{k}{c}.$$

For sufficiently heavy solids and long wires the ratio of the torque ( $k$ ) per unit twist to the moment of inertia ( $c$ ) is very small and may be considered to be negligible, and the possibility of the mutual transference of torsional and pendulous oscillations therefore depends on the approximate equality of the two remaining roots, *i. e.*,

$$\frac{Mgb}{Mb^2 + B} \quad \text{and} \quad \frac{g}{a}.$$

In conclusion, I wish to thank Prof. S. Purushotham, Professor of Mathematics, Maharaja's College, Vizianagaram, for his kind help in solving the problem.

Vizianagaram, South India.

April 1930.

CI. *A Note on the Fracture of Discharge-Tubes.* By R. H. SLOANE, *M.Sc., Demonstrator in Physics, The Queen's University of Belfast* \*.

[Plate XII.]

WHILST investigating the conditions of excitation near the cathode of the glow discharge in argon inconvenience was experienced from frequent spontaneous failure of the tubes. This was rather surprising, as quite gentle discharges (*e. g.* 2 milliamps. at 400 volts) were being passed. Apparently it is due partly to the use of argon, which, as is well known, gives rise to heavy cathodic sputtering, but mainly to the fact that the design of the tubes involved contact of the cathode with the walls.

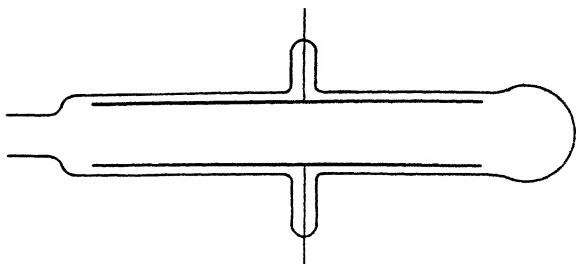
The form of discharge-tube in question consisted of a length of soda-glass tubing, 27 cm. long and 3 cm. in diameter, in which were mounted two parallel sheet-nickel electrodes  $22.5 \times 2$  cm., and 2 cm. apart, in close contact with the glass at their long edges. The design of the tube will be apparent from the accompanying figure. This tube contained pure argon at a pressure of 0.3 mm.

\* Communicated by Dr. K. G. Emeléus.



Fig., and was run from the 440 volt d.c. mains with a wire resistance of 1700 ohms in series, which limited the current to about 1 ma. Conditions were varied slightly from time to time, but the current density rarely exceeded 0.1 ma. per sq. cm.

After a run of the order of twelve hours the exposed glass walls were always heavily sputtered, but usually no sign of incipient fracture was visible at this stage. More prolonged use, approximately thirty hours, however, resulted in small pieces of the sputtered film peeling away from the glass close to the cathode. The first visible sign of this was the appearance of a small spot of yellow light at a point of contact between the cathode and wall. This had a scintillating appearance. The colour was due to the sodium of the glass. The spot grew brighter and larger, and small streamers were observed to shoot out



from it along the surface of the sputtered film, leaving permanent trails from which the sputtered metal had been removed. These trails were rather long and tortuous. Once this process started it became rapidly more intense, until a fracture through the bright spot terminated the life of the tube.

An examination of the tube after fracture revealed some interesting points. Microphotographs of a piece of the glass are shown in Pl. XII. Fig. 1 (Pl. XII.) is a full-size photograph, taken by transmitted light; the arrow points to the edge which was formed by the original fracture, the other edges being produced when the tube was opened up; the clear triangular piece at the top was behind the cathode. Fig. 2 of the same Plate is a microphotograph ( $\times 8.7$ ) of part of fig. 1; the arrow in this case points to the edge of the cathode at which the fracture originated. Fig. 3 is an extension of fig. 2 to the

left, and fig. 4 is part of fig. 2 under higher magnification ( $\times 21$ ), the central part of fig. 4 being that part of fig. 3 indicated by the arrow; the pattern towards the end of the streamers is very complicated and the curvature increases. Fig. 5 is an edge-on view ( $\times 8.8$ ) in the direction of the arrow in fig. 1; it shows how the glass was eaten away in a conical shaped hole; presumably the crack formed when the apex of the cone had penetrated the glass. A porcelain-like material, which was apparently a nickel glass, remained in the cavity so formed, and appears white in fig. 5. Examination of this and the adjoining leaf-pattern shown in figs. 2 and 3, under high magnification, showed that it consisted of small globules of fused glass; these do not photograph well.

It is difficult to give a satisfactory explanation of these observations. The most obvious one would seem to be that the film makes contact with the cathode, and then itself sputters, giving the pattern observed. Although perhaps explaining the trails, this fails to account for the bright spot or for the formation of the trails *subsequent* to the appearance of the bright spot. Patterns somewhat similar to these have been observed by K. G. Emeléus and F. M. Emeléus with an oxygen discharge-tube\*, and were attributed at the time to oxidation of the sputtered nickel. This could hardly explain the facts in the present case, as the argon was spectroscopically free from oxygen.

Another explanation has been suggested by Dr. Emeléus as the result of some work by him and Miss J. Beck in this laboratory on the potential of the walls in the dark space†. They have found that the walls of a slightly sputtered discharge-tube are strongly positive to the discharge close to the cathode, potential differences of 200 volts being frequently found. Taking 0.01 mm. as a reasonable spacing for a poor contact, an average field of  $2 \cdot 10^5$  volts per cm. would result between the cathode and wall. This might be large enough to draw an auto-electronic current from the cathode which would cause sufficient heating of the glass where it impinged on the latter to give the observed hot spot. Why this process should be aggravated by the formation of the sputtered film is not clear, except that it might increase the potential difference by increasing the conductivity of the walls

\* Phil. Mag. viii. p. 383 (1929).

† To be published shortly.

between the negative glow and cathode. The conditions when the walls were heavily sputtered were not investigated by Emeléus and Beck, their tubes being never more than slightly clouded.

The streamers could be accounted for by the release of strains in the film or underlying glass, or by the existence of irregularities in the surface of the glass itself. As already mentioned, the average curvature of these streamers increases towards their ends. Fine streamers were, however, sometimes observed, extending comparatively straight along the film perpendicular to the cathode, without bright spots at their origins. The curvature may thus be influenced by the presence of the bright spot and perhaps by its effect on strains.

It is not proposed to follow up these observations systematically. Rapid failure of a tube is readily avoided, as with tubes passing heavier discharges, by suitably spacing the cathode from the wall.

---

## *CII. Notices respecting New Books.*

*The Measurement of Hydrogen Ion Concentration.* By JULIUS GRANT, Ph.D., M.Sc., A.I.C. [Pp. viii + 159 with 40 figures.] (London: Longmans, Green & Co., 1930. Price 9s. net.)

THE measurement of hydrogen ion concentration is of importance to many branches of industry—to brewing and other industries, which depend upon fermentation, such as bakery and sugar manufacture; to the dyeing industry; to the leather industry; to the manufacture of paper; and to agriculture. It is also of importance to the metallurgist, to the biochemist and in chemical analysis. The technique for determining the pH value has to be used by many industrial workers who do not need to have much knowledge of the theories upon which the methods are based. It is primarily for such workers that the volume under review has been written. Hitherto the industrial worker who wished to undertake the study of hydrogen ion concentration only had available for consultation books which were written for the academic student. In the present volume the theory has been treated very briefly and the controversial points have not been discussed in any detail. No previous knowledge of

electrochemistry has been assumed, so that the beginner in a strange field may safely use this volume as a guide.

The methods for the estimation of the pH values, both the electrometric and the colorimetric methods, are explained. Full attention is given to all the practical details, and numerous pitfalls and sources of error are pointed out. Special modified methods in use for various purposes in different industries are described. A large number of selected references to the literature are given, which will be found of value by the research worker. At the end there are collected in tabular form all the data and information normally required in the estimation of pH values.

The volume undoubtedly fills a serious gap in the chemical literature, and cannot fail to prove of value to all who require to make determinations of hydrogen ion concentration.

*A Treatise on Light.* By R. A. HOUSTOUN, M.A., Ph.D., D.Sc.,  
Lecturer in Physical Optics, University of Glasgow. (Longmans, Green & Co.) Price 12s. 6d.

THIS book, intended for students who have been through a first-year's physics course, has now reached its sixth edition. In this edition there is some new material and a number of additional diagrams. These but enhance the value of the work which since 1915 in its various editions has held its own as one of the best text-books on Light, remarkable as much for its careful treatment of the whole range of the subject as for the systematic incorporation of the results of recent researches as they occur. We recommend the book heartily to the intelligent student.

*Etoiles et Atomes.* By A. S. EDDINGTON, M.A., D.Sc., LL.D.,  
F.R.S., Professor of Astronomy at Cambridge University.  
Translated by J. Rossignol, Professeur agrégé de l'Université. (Price 35 francs.) (Hermann et Cie, Paris.)

It is interesting to note the appearance in French of Sir Arthur Eddington's 'Stars and Atoms.'

The translation appears to lack nothing in clearness, and will no doubt ensure that this classical work is read by as wide a public in France as it has already reached in English-speaking countries.

---

[The Editors do not hold themselves responsible for the views expressed by their correspondents.]

## INDEX to VOL. X.

- ABSOLUTE** zero, on the inaccessibility of the, 931.
- Acoustical** conductance of orifices, on the, 623.
- Air**, on the absorption of X-rays in, 329; on the effect of temperature on the viscosity of, 721; on some radio-frequency properties of ionized, 969; on the ionizing potential in, 1058.
- Alcohols**, on the magneto-optical dispersion of the, 759.
- Alkali** metals, on the lattice constants of the, 224.
- Allen (J. F.)** on electrical conductivity measurements at low temperature, 500.
- Alpha-particles**, on the capture of electrons by swift, 401; on the photographic counting of, 413.
- Alternate** current circuit problems, on the application of complex method to the solution of, 905.
- Alternating** current bridge circuits, on inductive ratio arms in, 49.
- Aluminium**, on the expansion of, at high temperatures, 633; on the orientation of rolled, 953.
- Ammonia**, on the behaviour of electrons in molecules of, 145; on the catalytic decomposition of, over molybdenum, tungsten, and promoted iron, 1015; on the ionizing potential in, 1061.
- Ammoniates**, on ion, 77.
- Amplifier**, on the multistage, 734.
- Antimony**, on the lattice constants of, 230; on an X-ray investigation of the alloys of, and lead, 470; on the conductivity of alloys of, at low temperatures, 500.
- Appleton (Prof. E. V.)** on some radio-frequency properties of ionized air, 969.
- Argon**, on the ionizing potential in, 1054.
- Arsenic**, on the lattice constants of, 230; on the conductivity of alloys of, at low temperatures, 500.
- Ashworth (Dr. J. R.)** on the magnetic and thermal constants of ferromagnetic substances, 681.
- Atmosphere**, on the reflexion of electromagnetic waves from the upper, 1; on ozone and atomic oxygen in the upper, 345, 369.
- Azobenzene**, on an X-ray investigation of the crystals of, 306.
- Bailey (Prof. V. A.)** on the behaviour of electrons amongst the molecules  $\text{NH}_3$ ,  $\text{H}_2\text{O}$ , and  $\text{HCl}$ , 145.
- Banerji (A. C.)** on some problems of nuclear physics, 450.
- Bannister (F. A.)** on the identification of minerals in thin sections of rocks by X-ray methods, 368.
- Barium**, on the lattice constants of, 785.
- Bars**, on the lateral bending of, 785.
- Bartlett (A. C.)** on the multistage valve amplifier, 734.
- Basu (Dr. N. M.)** on an application of the calculus of variations to the theory of elasticity, 886; on the torsion problem of the theory of elasticity, 896.
- Bate (A. E.)** on the end-corrections of an open organ flue-pipe, and on the acoustical conductance of orifices, 617.
- Beam** interferometer, on a modification of Michelson's, 291.
- Bending** of bars, on the lateral, 785.
- Benzene**, on the dielectric polarization of mixtures of, and nitrobenzene, 265.

- Beryllium, on the lattice constants of, 225.
- Bhatnagar (Prof. S. S.) on magnetism and molecular structure, 101.
- Bismuth, on the lattice constants of, 230; on the conductivity of alloys of, at low temperatures, 500.
- Bismuth-copper, on the crystal structure in the system, 551.
- Black (Dr. D. H.) on the conduction of electricity in liquid dielectrics, 842.
- Bond (Dr. W. N.) on the values and inter-relationships of  $c$ ,  $e$ ,  $h$ ,  $M_p$ ,  $m_0$ ,  $G$ , and  $R$ , 994.
- Books, new: Deimel's *Mechanics of the Gyroscope*, 360; Jeans's *The Universe around Us*, 361; Lawrence's *Soap Films*, 361; Coles's *An Introduction to Modern Organic Chemistry*, 362; Coble's *Algebraic Geometry and Theta Functions*, 363; Crookall's *Coal Measure Plants*, 363; Haas & Hill's *An Introduction to the Chemistry of Plant Products*, 364; Smith's *The Effects of Moisture on Chemical and Physical Changes*, 364; Richard's *La Gamme—Introduction à l'étude de la musique*, 365; Lodge's *Beyond Physics*, 366; Fisher's *Statistical Methods for Research Workers*, 517; Richardson's *The Acoustics of Orchestral Instruments and of the Organ*, 517; de Broglie's *Ondes et Corpuscles, Mécanique Ondulatoire, Wave Mechanics*, 518; Worsnop's *X-rays*, 519; James's *X-ray Crystallography*, 519; Buckingham's *Matter and Radiation*, 519; Andrade's *The Mechanism of Nature*, 520; Index Generalis, 738; Phillips's *A Course of Analysis*, 739; Rideal's *An Introduction to Surface Chemistry*, 740; Muir's *Contributions to the History of Determinants*, 741; Jackson's *The Theory of Approximation*, 741; The *Quarterly Journal of Mathematics*; Oxford Series, 742; Hobhouse, Wheeler, & Ginsberg's *The Material Culture and Social Institutions of the Simpler Peoples*, 742; Durell & Robson's *Advanced Trigonometry*, 743; Antoniadi's *La Planète Mars*, 744; Titchmarsh's *The Zeta Function of Riemann*, 961; Mellor's *A Comprehensive Treatise on Inorganic and Theoretical Chemistry*, 962; Mott's *An Outline of Wave Mechanics*, 963; Dampier-Whetham's *A History of Science*, 963; Johnson's *Optics*, 964; Bruhat's *Traité de Polarimétrie*, 964; Ollivier's *La Topographie sans Topographes*, 965; Hadamand's *Cours d'Analyse*, 966; Grant's *The Measurement of Hydrogen Ion Concentration*, 1102; Houstoun's *A Treatise on Light*, 1103; Eddington's *Etoiles et Atomes*, 1103.
- Bradford (Dr. S. C.) on the kinetic theory of vaporization, 160.
- Bradley (R. S.) on polymolecular films, 323.
- Bragg (Prof. W. L.) on the representation of crystal structure by Fourier series, 823.
- Brass, on the expansion of, at high temperatures, 633.
- Bridge circuits, on inductive ratio arms in alternating current, 49.
- Bruce (J. H.) on the corona discharge in hydrogen, 476.
- Burnett (D.) on the reflexion of long electromagnetic waves from the upper atmosphere, 1.
- Butyl alcohol, on the magneto-optical dispersion of, 759.
- Cadmium, on the conductivity of alloys of, at low temperatures, 500; on the expansion of, at high temperatures, 633.
- Cæsium, on the lattice constants of, 224.
- Calcium, on the lattice constants of, 225.
- Campbell (Dr. N.) on fitting observations to a curve, 745.
- Carbon, on the lattice constants of, 226.
- compounds, on the ionizing potentials in, 1060.

- Carbon dioxide, on the absorption of X-rays in, 329.
- tetrachloride, on the dielectric polarization of mixtures of, and benzene, 265.
- Carpenter (L. G.) on the specific heat of mercury, 249.
- Cerium, on the conductivity of alloys of, at low temperatures, 500.
- Chalklin (F. C.) on some series in the ultra-violet spark spectra of copper, 711.
- Chapman (Prof. S.) on the annual variation of upper-atmospheric ozone, 345; on ozone and atomic oxygen in the upper atmosphere, 369.
- Chemical state, on the influence of, on X-ray absorption frequencies, 71.
- Childs (E. C.) on some radio-frequency properties of ionized air, 969.
- Chloroform, on the ionizing potential in, 1060.
- Chromium, on the lattice constants of, 227.
- Cobalt, on the lattice constants of, 229; on the expansion of, at high temperatures, 633; on the magnetic and thermal constants of, 681.
- Coleman (J. B.) on a theorem in determinants, 564.
- Colours, on the relative visibility of, 416.
- Conductivities, on the electrical, of dilute sodium amalgams, 569.
- Constants, on the values and interrelationships of, 994.
- Constrictions, on the effect of, in organ pipes, 945.
- Coordination, studies in, 76, 77.
- Copper, on the lattice constants of, 229; on the conductivity of alloys of, at low temperatures, 500; on the expansion of, at high temperatures, 633; on the ultra-violet spark spectra of, 711.
- Copper-bismuth, on the crystal structure in the system, 551.
- Cork-dust, on movements of, in a Kundt's tube, 139.
- Corona discharge in nitrogen, on the, 185; in hydrogen, on the, 476.
- Crowther (Prof. J. A.) on the absorption of X-rays in gases, 329.
- Crystal structure, on the, in the system copper-bismuth, 551; on the representation of, by Fourier series, 823.
- Curves, on approximation, for a Fourier series, 695; on fitting observations to, 746.
- Dark adaptation, on, 416.
- Davies (W. J.) on the electrical conductivities of dilute sodium amalgams, 569.
- Deming (W. E.) on the rates and temperature coefficients of the catalytic decomposition of ammonia, 1015.
- Deodhar (Dr. D. B.) on new bands in the secondary spectrum of hydrogen, 1082.
- Determinants, on a theorem in, 564.
- Diamagnetism and submolecular structure, on, 191; on the statistical theory of para- and, 698.
- Dielectric polarization of liquid mixtures, on the, 265.
- Dielectrics, on the conduction of electricity in, 812.
- Dinnik (Prof. A. N.) on the lateral bending of bars, 785.
- Discharge-tubes, on the fracture of, 1099.
- Dougall (Dr. J.) on Newton's law of gravitation in an infinite Euclidean space, 81.
- Drops, on the effect of the surrounding medium on the life of floating, 383.
- Dufton (A. F.) on the reduction of observations, 465; on graphic statistics, 566.
- Duncanson (W. E.) on the behaviour of electrons amongst the molecules  $\text{NH}_3$ ,  $\text{H}_2\text{O}$ , and  $\text{HCl}$ , 145.
- Earth's crust, on the effect of stratification on the curvature of the, 513.
- Ehret (Dr. W. F.) on the crystal structure in the system copper-bismuth, 551.
- Elastic extension of metal wires under longitudinal stress, on the, 1043.
- Elasticity, on the application of the calculus of variations to the theory of, 886; on the torsion problem of the theory of, 896.

- Electric forces, on the distribution of, in spaces traversed by electrons, 134.
- wind, on the ionizing potentials in an alternating, 1052.
- Electrical conductivity, on the, of dilute sodium amalgams, 569.
- — — measurements at low temperatures, on, 500.
- properties of the soil at radio frequencies, on the, 667.
- Electricity, on the conduction of, in liquid dielectrics, 812.
- Electrodeless discharge, on the mechanism of the, 280.
- Electrolytic rectifier, on the glow discharge at the active electrode of an, 1003.
- Electromagnetic waves, on the reflexion of, from the upper atmosphere, 1; on the propagation of, 521.
- Electrons, on the distribution of electric forces in spaces traversed by, 134; on the behaviour of, amongst the molecules  $\text{NH}_3$ ,  $\text{H}_2\text{O}$ , and  $\text{HCl}$ , 145; on the periodic orbits of, 314; on the capture of, by swift alpha-particles, 401.
- Elements, on the lattice constants of the, 217.
- End-corrections of an open flue-pipe, on the, 617.
- Ethylene, on the absorption of X-rays in, 320.
- Evans (Prof. E. J.) on the isotope effect in neon lines, 128; on the electrical conductivities of dilute sodium amalgams, 569; on the magnetic-optical dispersion of organic liquids, 759.
- Expansion of metals at high temperatures, on the, 633.
- Farquharson (Dr. J.) on diamagnetism and sub-molecular structure, 191.
- Ferromagnetic substances, on the magnetic and magneto-thermal properties of, 27; on the relations of the magnetic and thermal constants of, 681.
- Films, on polymolecular, 323.
- Fine (Prof. R. D.) on the crystal structure in the system copper-bismuth, 551.
- Fingering of wind instruments, on the, 16.
- Flageolet, on the frequencies of the notes of a, 16.
- Flue-pipe, on the end-corrections of an open organ, 617.
- Forrest (J. S.) on the glow discharge at the active electrode of an electrolytic rectifier, 1003.
- Fourier series, on approximation curves for a, 695; on the representation of crystal structures by, 823.
- Friction, on the, of dry solids *in vacuo*, 809.
- Garrick (F. J.) studies in coordination, 76, 77.
- Gases, on the absorption of X-rays in, 329.
- Geological Society, proceedings of the, 368, 967.
- Gill (E. W. B.) on the distribution of electric forces in spaces traversed by electrons, 134.
- Glow discharge in hydrogen, on the, 244; on the, at the active electrode of an electrolytic rectifier, 1003.
- Gold, on the lattice constants of, 229; on the conductivity of alloys of, at low temperatures, 500.
- Grain size in steels, on an X-ray study of the, 1073.
- Graphic statistics, on, 566.
- Graphical method for the reduction of observations, on a, 465.
- Gravitation, on Newton's law of, in an infinite Euclidean space, 81.
- Gravity gradient, on the effect of stratification on the, 513.
- Gray (Dr. F. W.) on diamagnetism and sub-molecular structure, 191.
- Gregory (Prof. J. W.) on frost stone-packing on the shores of Loch Lomond, 967.
- de Groot (Dr. W.) on the propagation of electromagnetic waves, 521.
- Hafnium, on the lattice constants of, 225.
- Hanstock (R. F.) on the effect of surface treatment on the photoelectric emission from metals, 937.
- Heat, on the loss of, from a plate embedded in an insulating wall, 480.



- Helium, on the ionizing potential in, 1055.
- Heusler alloy, on the conductivity of a, at low temperatures, 500; on the magnetic and thermal constants of, 681.
- Hodges (A. L.) on an automatic recording waterproof tester, 327.
- Hooke's law, on a method for measuring the deviations from, 1043.
- Houstoun (Dr. R. A.) on the visibility of radiation and dark adaptation, 416; on Weber's law and visual acuity, 433.
- Howells (E.) on the statistical theory of para- and diamagnetism, 698.
- Hume-Rothery (Dr. W.) on the lattice constants of the elements, 217.
- Hurst (H. E.) on reducing observations by the method of minimum deviations, 511.
- Huxley (Dr. L. G. H.) on the corona discharge in nitrogen, 185.
- Hydrates, on ion, 76.
- Hydrochloric acid, on the behaviour of electrons in molecules of, 145.
- Hydrogen, on the glow discharge in, 244; on the absorption in, of hydrogen positive rays, 297; on the corona discharge in, 476; on the ionizing potential in, 1056; on new bands in the secondary spectrum of, 1082.
- sulphide, on the absorption of X-rays in, 329.
- Inductive ratio arms in alternating current bridge circuits, on, 49.
- Integrals involving Legendre polynomials, on some, 1037.
- Interference methods and stellar parallax, on, 873.
- Interferometer, on a modification of Michelson's beam, 291.
- Ion ammoniates, on, 77.
- hydrates, on, 76.
- Ionizing potentials, on the, in an alternating electric wind, 1052.
- Iridium, on the lattice constants of, 229.
- Iron, on the lattice constants of, 228; on the conductivity of compounds of, at low temperatures, 500; on the magnetic and thermal constants of, 681; on the catalytic decomposition of ammonia over, 1015.
- Irons (Dr. E. J.) on the fingering of wind instruments, 16; on the effects of constrictions in organ pipes, 945.
- Isobutyl alcohol, on the magneto-optical dispersion of, 759.
- Isotope effect in neon lines, on the, 128.
- Jacobsen (J. C.) on the capture of electrons by swift alpha-particles, 401; on the photographic counting of alpha-particles, 413.
- Johnson (P.) on discharges in neon, 921.
- Kinetic theory of vaporization, on the, 160.
- Knowler (A. E.) on the measurement of the sound transmission of a partition, 342.
- Koch (F. K. V.) on the interaction of molecules with the silver ion, 559.
- Kundt's tube, on movements of particles in, 139.
- Kunsman (C. H.) on the rates and temperature coefficients of the catalytic decomposition of ammonia, 1015.
- Lamar (E. S.) on the rates and temperature coefficients of the catalytic decomposition of ammonia, 1015.
- Lanthanum, on the conductivity of alloys of, at low temperatures, 500.
- Lattice constants of the elements, on the, 217.
- Law (A. C.) on the absorption in hydrogen gas of hydrogen positive rays, 297.
- Laxton (A. E.) on the effect of temperature on the viscosity of air, 721.
- Lead, on an X-ray investigation of the alloys of, and antimony, 470; on the conductivity of alloys of, at low temperatures, 500; on the expansion of, at high temperatures, 633.
- Leavey (E. W. L.) on the friction of dry solids *in vacuo*, 809.
- Legendre polynomials, on some integrals involving, 1037.

- Lindsay (Prof. R. B.) on an acoustical interpretation of the Schrödinger wave equation, 863.
- Liquid drops, on the life of floating, 383.
- mixtures, on the dielectric polarization of, 265.
- Liquids, on the magneto-optical dispersion of organic, 759.
- Lithium, on the lattice constants of, 224.
- Lokshin (Prof. A. S.) on the lateral bending of bars, 785.
- Lowry (H. V.) on approximation curves for a Fourier series, 695.
- Macdonald (P. A.) on the psychophysical law, 1063.
- Mache (Prof. H.) on the inaccessibility of the absolute zero, 931.
- McLennan (Prof. J. C.) on electrical conductivity measurements at low temperatures, 500.
- Magnet steels, on the constitution of tungsten, 659.
- Magnetic and magneto-thermal properties, on the, of ferromagnetic substances, 27, 681.
- susceptibilities of some liquid organic isomers, on the, 101.
- Magnesium, on the lattice constants of, 225.
- Magnetite, on the magnetic and thermal constants of, 681.
- Magneto-optical dispersion of organic liquids, on the, 759.
- Mahajan (Prof. L. D.) on the effect of the surrounding medium on the life of floating drops, 383.
- Mal (R. S.) on magnetism and molecular structure, 101.
- Manganese, on the conductivity of alloys of, at low temperatures, 500.
- Mathur (R. N.) on magnetism and molecular structure, 101.
- Mercury, on the specific heat of, in the neighbourhood of the melting-point, 249.
- Metals, on the expansion of, at high temperatures, 633; on the effect of surface treatment on the photoelectric emission from, 937.
- Michelson's beam interferometer, on a modification of, 291.
- Micromanometer, on a, of high sensitivity, 544.
- Minimum deviations, on the reduction of observations by the method of, 511.
- Mohammad (Prof. W.) on the fine structure of zinc lines, 916.
- Molecular structure, on magnetism and, 101.
- Molecules, on the behaviour of electrons amongst, 145; on the interaction of, with the silver-ion, 559.
- Molybdenum, on the lattice constants of, 227; on the catalytic decomposition of ammonia over, 1015.
- Morris-Jones (W.) on an X-ray investigation of the lead-antimony alloys, 470.
- Mutch (G.) on the absorption in hydrogen gas of hydrogen positive rays, 297.
- Nelson (Miss E. A.) on the effect of stratification on the gravity gradient and the curvature of the level surface, 513.
- Neon, on discharges in, 921; on the ionizing potentials in, 1054.
- lines, on the isotope effect in, 128.
- Newton's law of gravitation in an infinite Euclidean space, on, 81.
- Nickel, on the lattice constants of, 229; on the expansion of, at high temperatures, 633; on the magnetic and thermal constants of, 681.
- Nisbet (R. H.) on the conduction of electricity in liquid dielectrics, 842.
- Nitrobenzene, on the dielectric polarization of mixtures of, and benzene and carbon tetrachloride, 265.
- Nitrogen, on the corona discharge in, 185; on the absorption of X-rays in, 329; on the ionizing potential in, 1058.
- Nuclear physics, on problems of, treated according to wave-mechanics, 450.
- Observations, on the reduction of, 465, 511; on fitting, to a curve, 746.
- Orbits, on periodic, in the field of a non-neutral dipole, 314.

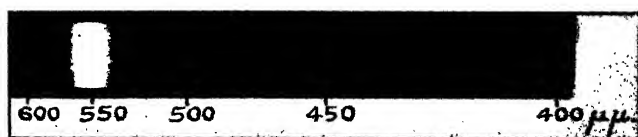
- Organ pipes, on the end-corrections of open, 617; on the effect of constrictions in, 945.
- Organic isomers, on the magnetic susceptibilities of some liquid, 101.
- Orifices, on the acoustical conductance of, 623.
- Orton (L. H. H.) on the absorption of X-rays in gases, 329.
- Oscillations, on mutual transference of torsional and pendulous, 1095.
- Osmium, on the lattice constants of, 228.
- Ower (E.) on a micromanometer of high sensitivity, 544.
- Oxygen, on the absorption of X-rays in, 329; on atomic, in the upper atmosphere, 369; on the ionizing potential in, 1056.
- Ozone, on, in the upper atmosphere, 345, 369.
- Page (Prof. L.) on three-dimensional periodic orbits in the field of a non-neutral dipole, 314.
- Pal (N. N.) on the dielectric polarization of liquid mixtures, 265.
- Palladium, on the lattice constants of, 229.
- Para- and diamagnetism, on the statistical theory of, 698.
- Paraffin series, on the ionizing potentials in the, 1058.
- Partition, on the sound transmission through a, 342.
- Permillé paper, note on, 566.
- Photoelectric emission from metals, on the effect of surface treatment on the, 937.
- Photoelectrons, on the space distribution of X-ray, 387.
- Photographic counting of alpha-particles, on the, 413.
- Physical constants, on the values and inter-relationships of, 994.
- Physics, on problems of nuclear, treated according to wave-mechanics, 450.
- Pipes, on the frequencies of stopped, 16.
- Plate, on the heat-loss from a rectangular, 480.
- Platinum, on the lattice constants of, 229.
- Polarization of liquid mixtures, on the, 265.
- Polymolecular films, on, 323.
- Positive rays, on the absorption in hydrogen of, 297.
- Potassium, on the lattice constants of, 224.
- Potential and attraction of rectangular bodies, on the, 110.
- field, on the motion of a particle in a, 521.
- Prasad (M.) on an X-ray investigation of the crystals of azobenzene, 306.
- Pringle (C. O.) on movements of particles in Kundt's tube, 139.
- Propionic acid, on the magneto-optical dispersion of, 759.
- Psychophysical law, on the, 1063.
- Quartz fibres, on the cohesion of, 541.
- Radiation, on the visibility of, 416.
- Radio-frequency properties of ionized air, on some, 969.
- Ratcliffe (J. A.) on the electrical properties of the soil at radio frequencies, 667.
- Rectangular bodies, on the potential and attraction of, 110.
- Rectifier, on the glow discharge at the active electrode of an electrolytic, 1003.
- Reduction of observations, on the, 465, 511.
- Rhodium, on the lattice constants of, 229.
- Richey (J. E.) on the tertiary igneous complex of Ardnamurchan, 967.
- Robertson (D. M.) on the psychophysical law, 1063.
- Robinson (Prof. H. R.) on the influence of chemical state on critical X-ray absorption frequencies, 71.
- Rubidium, on the lattice constants of, 224.
- Rusk (Dr. R. D.) on the glow discharge in hydrogen, 244.
- Ruthenium, on the lattice constants of, 228.
- Schofield (F. H.) on the heat-loss from a plate embedded in an insulating wall, 480.
- Schrödinger wave equation. on an acoustical interpretation of the, 863.

- Selenium, on the lattice constants of, 231.
- Sharma (P. N.) on the fine structure of zinc lines, 916.
- Shaw (Prof. P. E.) on the friction of dry solids *in vacuo*, 809.
- Shearer (J. F.) on Weber's law and visual acuity, 433.
- Shilling (Dr. W. G.) on the effect of temperature on the viscosity of air, 721.
- Silica, on movements of particles of, in a Kundt's tube, 139.
- Silicon, on the lattice constants of, 226.
- Silver, on the lattice constants of, 229; on the conductivity of alloys of, at low temperatures, 500.
- ion, on the interaction of molecules with the, 559.
- Simons (Dr. L.) on the space-distribution of X-ray photoelectrons from a solid film, 357.
- Sloane (R. H.) on the fracture of discharge-tubes, 1099.
- Söderman (M.) on precision measurements in the soft X-ray region, 600.
- Sodium, on the lattice constants of, 224.
- amalgams, on the electrical conductivities of dilute, 569.
- Soil, on the electrical properties of the, at radio frequencies, 667.
- Solids, on the friction of dry, *in vacuo*, 809.
- Solomon (D.) on an X-ray investigation of the lead-antimony alloys, 470.
- Solutions, on the vapour pressure of, 160.
- Sound transmission of a partition, on the measurement of the, 342.
- Specific heat, on the, of mercury, 249.
- Statistics, on graphic, 566.
- Steel, on the expansion of, at high temperatures, 633; on some tungsten magnet, residues, 659; on an X-ray study of grain size in, 1073.
- Stellar parallax, on interference methods and, 873.
- Stephens (E.) on the magneto-optical dispersion of organic liquids, 759.
- Stoner (Dr. E. C.) on the magnetic and magneto-thermal properties of ferromagnetics, 27.
- Stoodley (L. G.) on the specific heat of mercury in the neighbourhood of the melting-point, 249.
- Stratification, on the effect of, on the gravity gradient and the curvature of the level surface, 513.
- Strontium, on the lattice constants of, 225.
- Submolecular structure, on diamagnetism and, 191.
- Subrahmaniam (G.) on mutual transference of torsional and pendulous oscillations, 1095.
- Susceptibilities, on the magnetic, of some liquid organic isomers, 101.
- Synge (E. H.) on a modification of Michelson's beam interferometer, 291; on a design for a very large telescope, 353; on interference methods and stellar parallax, 873.
- Tactile sense, on the, 1063.
- Telescope, on a design for a very large, 353.
- Tellurium, on the lattice constants of, 231.
- Thermal and magnetic constants of ferromagnetic substances, on the relations of, 681.
- insulators, on an apparatus for testing, 480.
- Thewlis (J.) on the orientation of rolled aluminium, 953.
- Thomas (E.) on the isotope effect in neon lines, 128.
- Thomson (Dr. J.) on the mechanism of the electrodeless discharge, 280.
- Thorium, on the lattice constants of, 226.
- Thornton (Prof. W. M.) on the molecular ionizing potentials in an alternating electric wind, 1052.
- Tin, on the lattice constants of grey, 230; on the expansion of, at high temperatures, 633.
- Titanium, on the lattice constants of, 226.
- Tomlinson (G. A.) on the cohesion of quartz fibres, 541.
- Torsion problem of the theory of elasticity, on the, 896.
- Torsional and pendulous oscillations, on mutual transference of, 1095.

- Tungsten, on the lattice constants of, 227; on the catalytic decomposition of ammonia over, 1015.  
 — magnet steel residues, on some, 659.
- Tyte (L. C.) on the elastic extension of metal wires under longitudinal stress, 1043.
- Uffelmann (F. L.) on the expansion of metals at high temperatures, 633.
- Ultra-violet spark spectra of copper, on the, 711.
- Valve amplifier, on the multistage, 734.
- Vaporization, on the kinetic theory of, 160.
- Variations, on the application of the calculus of, to the theory of elasticity, 886.
- Visual acuity, on Weber's law and, 433.
- Walsh (R.) on inductive ratio arms in alternating current bridge circuits, 49.
- Water, on the behaviour of electrons in molecules of, 145.
- Waterproof tester, on an automatic recording, 327.
- Wave equation, on an acoustical interpretation of the Schrödinger, 863.  
 — mechanics, on problems of nuclear physics treated according to, 450.
- Weber's law and visual acuity, on, 433.
- West (J.) on the representation of crystal structure by Fourier series, 823.
- Whistle, on the frequencies of the notes of a, 16.
- White (F. W. G.) on the electrical properties of the soil at radio frequencies, 667.
- Wilhelm (J. O.) on electrical conductivity measurements at low temperatures, 500.
- Wind instruments, on the fingering of, 16.
- Windred (G.) on the application of complex methods to the solution of A.C. circuit problems, 905.
- Wireless waves, on the influence of the earth on, 687; on the role played by ionized air in the propagation of, 969.
- Wires, on the elastic expansion of, under longitudinal stress, 1043.
- Wood (W. A.) on an X-ray study of some tungsten magnet steel residues, 659; on an X-ray study of grain size in steels, 1073.
- Wright (C. E.) on the potential and attraction of rectangular bodies, 110.
- Wrinch (Dr. D.) on some integrals involving Legendre polynomials, 1037.
- X-ray absorption frequencies, on the influence of chemical state on, 71.  
 — investigation of the lead-antimony alloys, on an, 470.  
 — photoelectrons, on the space distribution of, 387.  
 — region, on precision measurements in the soft, 600.  
 — study of tungsten magnet steels, on an, 659; of grain size in steels, on an, 1073.
- X-rays, on the absorption of, in gases and vapours, 329.
- Young (C. L.) on the influence of chemical state on critical X-ray absorption frequencies, 71.
- Zero, on the inaccessibility of the absolute, 931.
- Zinc, on the expansion of, at high temperatures, 633.  
 — lines, on the fine structure of, 916.
- Zirconium, on the lattice constants of, 226.

END OF THE TENTH VOLUME.

Fig. 6



Spectrogram of glow.



FIG. 1.

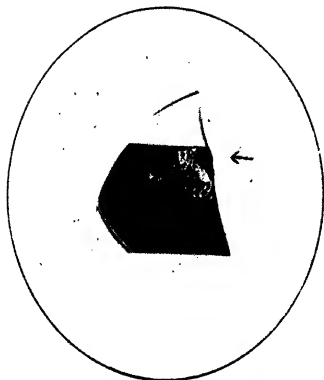


FIG. 2.



FIG. 3.



FIG. 4.



FIG. 5.



Fracture of Discharge-Tubes.





INDIAN AGRICULTURAL RESEARCH  
INSTITUTE LIBRARY, NEW DELHI.

[illegible]

GIPNLK—H-4) I.A.R.I.—29-4-55—15,000